

ABSTRACTS OF THE 37TH ANNUAL MIDWINTER MEETING OF THE



Dear Attendees:

Welcome back to San Diego for the ARO MidWinter Meeting. The Manchester Grand Hyatt has been a superb venue for us in the past, and we're looking forward to another great meeting in 2014. This year is the forty-first anniversary of the founding of the ARO and the 37th MidWinter Meeting. Since last year's meeting, auditory science has been honored by the Lasker Award, given to three luminaries in cochlear implant research and development, Graeme Clark, Ingeborg Hochmair and Blake Wilson. All have contributed greatly to our field and directly and indirectly to the ARO.

One of the highlights of the meeting, particularly for the President who gets to organize it, is the presidential symposium on Saturday Morning. The topic of this year's symposium is "First-in-Human Studies of Neurotechnology: Past, Present and Future." Jim Patrick from Cochlear, Ltd, an engineer central to the development of the first FDA approved multichannel cochlear implant will begin the session. Rob Greenberg from Second Sight, a physician, engineer and founder of that company will discuss the research and regulatory process leading to the FDA approval of the first retinal prosthesis. Matt Howard from the University of Iowa, a neurosurgeon, will discuss physiologic research in human auditory cortex. James Phillips from the University of Washington, a vestibular physiologist, will discuss human studies of the vestibular prosthesis. Dr Steven Cheung from the University of California, San Francisco, a neurotologist, will discuss studies of deep brain stimulation for tinnitus. Jeff Ojemann, a neurosurgeon, will discuss human studies of brain-computer interfaces. The symposium will explore the unique challenges and promise of first-in-human studies of these neurotechnologies.

Think about getting more involved in the ARO organization. There are many opportunities to serve on committees. The new committee members will be appointed shortly after the MidWinter Meeting by the new president, who will be Ruth Anne Eatock. If you are interested in serving on a committee, please indicate your interest on the post-meeting questionnaire. Also, consider speaking with or dropping an email to Ruth Anne or the chair of the committee of your choice.

Finally, don't miss a chance to let down your hair at the Hair Ball Tuesday evening with the popular band, Baytown Band. Here's a chance to see a side of your colleagues that you might have missed at the poster sessions.

It has been an extraordinary opportunity to serve the ARO as President this past year, and I wish you all a very stimulating and enjoyable conference.

Jay T. Rubinstein
ARO President, 2013-2014

CONFERENCE OBJECTIVES

At the conclusion of the MidWinter Meeting, participants should be better able to:

- Explain current concepts of the function of normal and diseased states of the ear and other head and neck structures
- Recognize current controversies in research questions in auditory neuroscience and otolaryngology
- Describe key research questions and promising areas of research in otolaryngology and auditory neuroscience

REGISTRATION

The 37th Annual MidWinter Meeting Registration Desk is located in the Harbor Ballroom Foyer and will be open and staffed during the following hours:

Friday, February 21	4:00 PM-7:00 PM
Saturday, February 22	6:30 AM-6:00 PM
Sunday, February 23	6:30 AM-7:00 PM
Monday, February 24	7:00 AM-7:00 PM
Tuesday, February 25	7:00 AM-6:00 PM
Wednesday, February 26	7:30 AM-12:00 PM

SPEAKER READY ROOM

The 37th Annual MidWinter Meeting Speaker Ready Room is located in the Cove Room and will be open and staffed during the following hours:

Friday, February 21	4:00 PM-7:00 PM
Saturday, February 22	7:00 AM-6:00 PM
Sunday, February 23	7:00 AM-6:00 PM
Monday, February 24	7:00 AM-6:00 PM
Tuesday, February 25	7:00 AM-6:00 PM
Wednesday, February 26	7:30 AM-11:30 AM

ADMISSION

Conference name badges are required for admission to all activities related to the 37th Annual MidWinter Meeting, including the Exhibit Hall and social events.

ABSTRACT BOOKS

A limited supply of the abstract book will be available for purchase at the ARO MidWinter Meeting Registration Desk. Electronic copies of the books are also available online at www.aro.org.

MOBILE DEVICES

As a courtesy to the speakers and your fellow attendees, please switch your mobile device(s) to silent while attending the sessions.

RECORDING POLICY

ARO does not permit audio or photographic recording of any research data presented at the meeting.

ASSISTED LISTENING DEVICES

A limited amount of assisted listening devices are available at the ARO MidWinter Meeting Registration Desk, courtesy of Phonak.

A SPECIAL NOTE FOR THE DISABLED

ARO wishes to take steps that are required to ensure that no individual with a disability is excluded, denied services, segregated or otherwise treated differently than other individuals because of the absence of auxiliary aids and services. If you need any auxiliary aids or services identified in the Americans with Disabilities Act or any assistance please see the ARO staff at the Registration Desk.

2014 ARO MIDWINTER MEETING

General Chair

Jay T. Rubinstein, MD, PhD (2013-2014)

PROGRAM COMMITTEE

Lawrence R. Lustig, MD, *Chair* (3/11-2/14)

Kumar Alagramam, PhD (3/13-2/16)

Jianxin Bao, Ph.D (3/12-2/15)

Julie Arenberg Bierer, PhD (3/11-2/14)

Alan Cheng, MD (3/13-2/16)

Yale E. Cohen, Ph.D. (3/11-2/14)

Richard Hallworth, PhD (3/12-2/15)

Gay R. Holstein, PhD (3/11-2/14)

Lisa L. Hunter, PhD (3/11-2/14)

Philip X. Joris, MD, PhD (3/13-2/16)

Jeff Lichtenhan, PhD (3/13-2/16)

Ruth Y. Litovsky, PhD (3/11-2/14)

Su-Hua Sha, MD (3/12-2/15)

Jenny Stone, PhD (3/13-2/16)

Xiaoquin Wang, PhD (3/13-2/16)

Council Liaison: Lawrence R. Lustig, MD

Program Publications

Linda J. Hood, PhD (2012-2015)

Animal Research Committee

Claus-Peter Richter, MD, PhD, *Chair* (3/13-2/16)

Esperanza Bas Infante, PhD (3/12-2/15)

Robert Keith Duncan, PhD (3/11-2/14)

Sherri Marie Jones, PhD (3/11-2/14)

Andrej Kral, MD, PhD (3/13-2/16)

Amanda Lauer, PhD (3/12-2/15)

Edward Lobarinas, PhD (3/11-2/14)

Karen S. Pawlowski, PhD (3/11-2/14)

Charidrakala Puligilla, PhD (3/13-2/16)

Soroush G. Sadeghi (3/11-2/14)

Maike Vollmer, MD, PhD (3/13-2/16)

Council Liaison: Ruth Y Litovsky, PhD

Award Of Merit Committee

Eric D. Young, PhD, *Chair* (3/13-2/16)

Karen B. Avraham, PhD (3/11-2/14)

David P. Corey, PhD (3/13-2/16)

Jeffrey T. Corwin, PhD (3/11-2/14)

Charley Della Santina, MD PhD (3/12-2/15)

Brian C. J. Moore, PhD (3/12-2/15)

Dan H. Sanes, PhD (3/11-2/14)

Karen P. Steel, PhD (3/13-2/16)

Steve D. Rauch, MD (3/13-2/16)

Council Liaison: David J. Lim, MD

Diversity & Minority Affairs Committee

Avril Genene Holt, PhD, *Chair* (3/13-2/16)

Deniz Baskent, PhD (3/13-2/16)

Gail S. Donaldson, PhD (3/12-2/15)

Frank Lin, M.D. PhD (3/11-2/14)

J Tilak Ratnanather, DPhil (3/13-2/16)

Shurud Rajguru, PhD (3/13-2/16)

Khaleel Razak, PhD (3/12-2/15)

Lina Reiss, PhD (3/13-2/16)

Dwayne D. Simmons, PhD (3/11-2/14)

Peter S. Steyger, PhD (3/11-2/14)

Council Liaison: Howard W. Francis

External Relations Committee

Carey D. Balaban, PhD, *Chair* (2012-2014)

Anne Luebke, PhD, *Chair* (2009-2014)

Julie Bierer, PhD (3/13-2/16)

Jonathan Fritz, PhD (3/13-2/16)

Corne Kros, PhD (3/12-2/15)

Hainan Lang, MD, PhD (3/12-2/15)

George Pollak, PhD (3/12-2/15)

Pamela Roehm, MD, PhD (3/12-2/15)

Beverly Wright, PhD (3/13-2/16)

Jinsheng Zhang, PhD (3/13-2/16)

Council Liaison: Ruth Y. Litovsky, PhD

Finance & Investment Committee

Dennis R. Trune, PhD, MBA, *Chair* (3/10-2/14)

Steven Wan Cheung, MD (3/10-2/14)

Paul Fuchs, PhD (3/13-2/16)

Sharon G. Kujawa, PhD (3/12-2/15)

Robert Raphael, PhD (3/12-2/15)

Ex-officio: John P. Carey, MD

International Committee

Robert K. Shepherd, PhD, Australia, *Chair* (3/12-2/14)

Karen Banai, PhD, U of Haifa, Israel (3/12-2/15)

Byung Yoon Choi, MD, Korea (3/12-2/15)

Alain Dabdoub, PhD, Canada (3/13-2/16)

Andy Forge, PhD, UK (3/13-2/16)

M'hamed Grati, Eng., PhD., USA (3/11-2/14)

Benedikt Grothe, PhD, Germany (3/12-2/15)

Bo Hong, Ph.D., China (3/12-2/15)

Andrej Kral, MD, PhD, Germany (3/13-2/16)

Christian Lorenzi, PhD, France (3/13-2/16)

Takayuki Nakagawa, MD, PhD, Japan (3/11-2/14)

Jan Wouters, PhD, Belgium (3/13-2/16)

Council Liaison: Robert K. Shepherd, PhD

Jaro Editorial Board

Paul B. Manis, PhD, *Editor-in-Chief* (2011-2016)
Christian Chabbertrand, PhD (2012-2015)
Bertrand Delqutte, PhD (2013-2016)
Nigel P. Cooper, PhD (2010-2014)
Ruth Anne Eatock, PhD (2011-2014)
Mark Eckert, PhD (2013-2016)
Donna Fekete, PhD (2012-2015)
Robert Funnell (2013-2016)
Andrew Griffith, MD, PhD (2011-2014)
Ruth Litovsky, PhD (2013-2016)
Manuel Malmierca, MD, PhD (2012-2015)
Shawn Newlands, MD, PhD (2012-2015)
Donata Oertel, PhD (2013-2016)
Dominik Oliver, PhD (2012-2015)
Christopher Plack, PhD (2013-2016)
Christoph Schreiner, MD, PhD (2012-2015)
Susan E. Shore, PhD (2012-2015)
Xiaorui Shi, MD, PhD (2013-2016)
Marianne Vater, PhD (2013-2016)

Long Range Planning Committee

Karina S. Cramer, PhD, *Chair* (3/12-4/14)
Steven H. Green, PhD (3/11-2/14)
Troy Hackett, PhD (3/12-2/15)
KC Lee, ScD (3/13-2/16)
Sunil Puria, PhD (3/13-2/16)
Edwin W. Rubel, PhD (3/11-2/14)
George Spirou, PhD (3/12-2/15)
Konstantina M. Stankovic, MD, PhD (3/11-2/14)
Doris Wu, PhD (3/12-2/15)
Amy Donahue, PhD - *NIDCD Rep.*
Council Liaison: Karina S. Cramer, PhD
President-Elect: Ruth Anne Eatock, PhD
International Cmte: Robert K. Shepherd, PhD

Membership Committee

Colleen Garbe Le Prell, PhD, *Chair* (3/12-2/14)
Eric Bielefeld, PhD (3/12-2/15)
Glenis R. Long, PhD (3/12-2/15)
Tianying Ren, MD (3/12-2/15)
Chris J. Sumner (3/12-2/15)

Nominating Committee

John C. Middlebrooks, PhD (3/13-2/14)
Paul Fuchs, PhD (3/13-2/14)
Donata Oertel, PhD (3/13-2/14)
Peter Santi, PhD (3/13-2/14)
Peter Steyger, PhD (3/13-2/14)

Publications Committee

Anil K. Lalwani, MD, *Chair* (3/13-2/16)
Yuri M. Agrawal, MD (3/13 – 2/16)
Thomas B. Friedman, PhD (3/11-2/14)
Charles J. Limb, MD (3/13-2/16)
Erick Xi Lin, PhD (3/12-2/15)

Xue Z. Liu, MD, PhD (3/12-2/15)
John S. Oghalai, MD (3/12-2/15)
Susan E. Shore, PhD (3/11-2/14)
Chris Stecker, PhD (3/13 – 2/16)
Daniel Tollin, PhD (3/12-2/15)
Kelly L. Tremblay, PhD (3/13 – 2/16)
JARO Editor: Paul B. Manis, PhD, *ex officio*
Springer Representative: Melissa Higgs, *ex officio*
Secretary/Treasurer: John P. Carey, MD
Council Liaison: Linda J. Hood , PhD

Travel Awards

Marlan R. Hansen, MD, *Chair* (3/08-2/14)
Jin Woong Bok, PhD (3/12-2/15)
Angelika Doetzlhofer, PhD (3/12-2/15)
Dianne Durham, PhD (3/11-2/14)
Robert Froemke, PhD (3/12-2/15)
Samuel Gubbels, MD (3/12-2/15)
Michael Hildebrand, PhD (3/12-2/15)
Avril Genene Holt, PhD (3/11-2/14)
Yunxia Wang Lundberg, PhD (3/11-2/14)
Yehoash Raphael, PhD (3/11-2/14)
Felipe Santos, MD (3/13 – 2/16)
Jong Ho Won, PhD (3/13 – 2/16)
Li Xu, MD, PhD (3/12-2/15)
James F. Battey, MD, PhD, *NIDCD Dir ex-officio*
Council Liaison: Linda J. Hood , PhD

Executive Offices

Association For Research In Otolaryngology

19 Mantua Road
Mt. Royal, New Jersey 08061
Phone: (856) 423-0041
Fax: (856) 423-3420
E-Mail: headquarters@aro.org
Meetings E-Mail: meetings@aro.org

AWARD OF MERIT



Award of Merit Recipient
H. Steven Colburn, PhD
Boston University

Award Lecture and Abstract

Shoulders of Giants: A Personal Walk through the Development of Ideas about Binaural Hearing

H. Steven Colburn
ARO 2014

The development of current understanding of binaural processing will be reviewed, including psychophysical and physiological data and concepts. More specifically, ideas related to the functional importance of binaural processing and the mechanisms of this processing will be discussed in the context of the people whose ideas shaped this field and who shaped my personal understanding, both about this field and about the nature of the scientific enterprise. I was strongly influenced by many people, including early personal and professional influences of Nat Durlach, Lloyd Jeffress, Nelson Kiang, Bill Siebert, Jay Goldberg, and Ed Rubel. This presentation will attempt to thread the development of thinking about binaural hearing over the last five decades together with my personal experiences in this enterprise. Some attempts at a summary of the current state of our ignorance and excitement will be included.

AWARD OF MERIT BIOSKETCH

H. Steven Colburn (or simply Steve to everyone who knows him) is being recognized today for his profound influence on hearing science, especially in the area of spatial and binaural hearing. Steve's tangible contributions in the form of creative scientific discovery, exemplary leadership, and selfless service are impressive by any measure. Yet, arguably the greater part of Steve's legacy to our field is how his spirit of warmth, generosity, intelligence, and playfulness infuses his every interaction, whether with a young, unknown student or a world-famous senior scientist.

When, at the advice of a relatively worldly uncle, Steve went to study at the Massachusetts Institute of Technology, he was only the second person from Clay Township Rural High School to attend college outside of the state of Ohio. Steve obtained both his S.B. (1963) and S.M. (1964) in electrical engineering at MIT, where he established his deep friendship and long-standing collaboration with Nat Durlach. Fortuitously for us all, after spending a year studying mathematics in Germany, he returned to MIT to study under Prof. William Siebert. He became a member of the faculty at MIT immediately after receiving his PhD., where he helped to make the Sensory Communications research group of the MIT Research Laboratory of Electronics a powerhouse in the areas of psychophysics, spatial and binaural hearing, and modeling. In 1980, Steve migrated across the Charles River to become Chair of Boston University's nascent Biomedical Engineering Department, which flourished under his capable guidance throughout the 80s. In the mid 90s, he founded the Boston University Hearing Research Center, which quickly became (and remains) a "must visit" Boston stop for auditory neuroscientists, psychoacousticians, and speech and hearing scientists from all over the world. He also is known within the tightknit binaural hearing community as the host of the annual "Binaural Bash," an informal (quintessential Steve-style) two-day meeting held each fall at Boston University that draws researchers from all over the world to argue, compare notes, and reach new insights—especially over wine at Steve's house.

Steve's main academic focus explores spatial and binaural hearing. While he spent the first portion of his career unraveling how spatial information in the signals reaching the ears is extracted by processing early in the auditory pathway, his more recent work explores how spatial auditory information is used to perform important everyday tasks. His work has led to over 100 publications, many of them key papers in the field. The two seminal articles resulting from his PhD work, published in the 70s, remain highly visible and relevant examples of how to relate physiological measures to perception through quantitative models. His efforts to extend the Jeffress model of binaural interaction to allow quantitative predictions of fundamental behavioral phenomena, including binaural unmasking and sound localization, have had a lasting influence not only on how we understand binaural processing in the brainstem, but on how to approach the herculean task of using physiological results to inform our understanding of perception. All of his work reflects a keen intellectual integrity, an ability to integrate information from disparate approaches and levels of description in order to gain a deep understanding of underlying mechanisms. It is Steve's openness, curiosity, and intelligence that helps explain why he is equally likely to be found talking deeply with an anatomist, a physiologist, a psychophysicist, a geneticist, a neuroimager, a computational modeler, or an audiologist; and why each of them is likely to come away from the conversation with some new insight into their own research (just follow him around at a poster session to see this magic in action).

His tremendous achievements have earned Steve numerous awards. For his scientific contributions, he received the Silver Medal from the Acoustical Society of America in 2005. He is a fellow both of the Acoustical Society of America and of the American Institute for Medical and Biological Engineering. His exceptional mentorship has led to the Boston University undergraduate student population electing him the Biomedical Engineering Professor of the Year on four separate occasions—a record without precedent. In addition to his leadership in the profession (e.g., serving on the editorial boards of various journals, serving on NIH study section), he has given of himself tirelessly to his department, college, and university.

Steve is a devoted husband to his wife Theo, unfailingly supportive father to his three sons and their partners, and adoring grandfather to his grandson and granddaughter. He extends this same love and encouragement to his students and colleagues, never failing to listen with empathy and provide heartfelt advice and comfort, even when he has pressing demands.

His energy and enthusiasm are infectious, whether discussing a scientific idea, going snowboarding or sailboarding, or enjoying the relative quiet of family time on Prince Edward Island. His love for science, and for life, inspires as much as do his impressive scientific contributions. It is this rare combination of virtues that make it an unparalleled pleasure to see Steve receive the 2014 Award of Merit.

Barbara Shinn-Cunningham

Past Presidents

1973-74	David L. Hilding, MD
1974-75	Jack Vernon, PhD
1975-76	Robert A. Butler, PhD
1976-77	David J. Lim, MD
1977-78	Vicente Honrubia, MD
1978-80	F. Owen Black, MD
1980-81	Barbara Bohne, PhD
1981-82	Robert H. Mathog, MD
1982-83	Josef M. Miller, PhD
1983-84	Maxwell Abramson, MD
1984-85	William C. Stebbins, PhD
1985-86	Robert J. Ruben, MD
1986-87	Donald W. Nielsen, PhD
1987-88	George A. Gates, MD
1988-89	William A. Yost, PhD
1989-90	Joseph B. Nadol, Jr., MD
1990-91	Ilsa R. Schwartz, PhD
1991-92	Jeffrey P. Harris, MD, PhD
1992-93	Peter Dallos, PhD
1993-94	Robert A. Dobie, MD
1994-95	Allen F. Ryan, PhD
1995-96	Bruce J. Gantz, MD
1996-97	M. Charles Liberman, PhD
1997-98	Leonard P. Rybak, MD, PhD
1998-99	Edwin W. Rubel, PhD
1999-00	Richard A. Chole, MD, PhD
2000-01	Judy R. Dubno, PhD
2001-02	Richard T. Miyamoto, MD
2002-03	Donata Oertel, PhD
2003-04	Edwin M. Monsell, MD, PhD
2004-05	William E. Brownell, PhD
2005-06	Lloyd B. Minor, MD
2006-07	Robert V. Shannon, PhD
2007-08	P. Ashley Wackym, MD
2008-09	Paul A. Fuchs, PhD
2009-10	Steven Rauch, MD
2011-12	Karen B. Avraham, PhD
2012-13	Debara L. Tucci, MD
2013-14	John C. Middlebrooks, PhD

Award Of Merit Recipients

1978	Harold Schuknecht, MD
1979	Merle Lawrence, PhD
1980	Juergen Tonndorf, MD
1981	Catherine Smith, PhD
1982	Hallowell Davis, MD
1983	Ernest Glen Wever, PhD
1984	Teruzo Konishi, MD
1985	Joseph Hawkins, PhD
1986	Raphel Lorente de Nó, MD
1987	Jerzy E. Rose, MD
1988	Josef Zwislocki, PhD
1989	Åke Flóck, PhD
1990	Robert Kimura, PhD
1991	William D. Neff, PhD
1992	Jan Wersäll, PhD
1993	David Lim, MD
1994	Peter Dallos, PhD
1995	Kirsten Osen, MD
1996	Ruediger Thalmann, MD & Isolde Thalmann, PhD
1997	Jay Goldberg, PhD
1998	Robert Galambos, MD, PhD
1999	Murray B. Sachs, PhD
2000	David M. Green, PhD
2001	William S. Rhode, PhD
2002	A. James Hudspeth, MD, PhD
2003	David T. Kemp, PhD
2004	Donata Oertel, PhD
2005	Edwin W. Rubel, PhD
2006	Robert Fettiplace, PhD
2007	Eric D. Young, PhD
2008	Brian C. J. Moore, PhD
2009	M. Charles Liberman, PhD
2011	Robert V. Shannon, PhD
2012	David P. Corey, PhD
2013	Karen P. Steel, PhD
2010	Ian Russell, PhD
2011	Robert V. Shannon, PhD
2012	David P. Corey, PhD
2013	Karen P. Steel, PhD
2014	H. Steven Colburn, PhD

2014 TRAVEL AWARD RECIPIENTS

Adrian Au, MD	Michael Pastore, PhD
Yoni Bhonker, BSc	Richard Penninger, DI(FH)
Jake Carpenter-Thompson, BS	Alessandro Presacco, MS
Collin Chen, MD	Dongdong Ren, MD
Jenny Chen, BA	Efrem Roberson, MS, BS
Ananthakrishna Chintanpalli, PhD	Nicole Rosskothén-Kuhl
Soyoun Cho, PhD	Elin Roverud, AuD
Inyong Choi, PhD	Francesca Yoshie Russo, MD
Yoojin Chung, PhD	Jefta Saija, MSc
Laura Corns, PhD	Zafar Sayed, MD
Scott Cronin, MD	Zahra Sayyid, BS
Alexander Ferber, BS	Tim Schoof, MRes
Katharine Fernandez, PhD	Nathan Schularick, MD
Eric Formeister, MS	Alison Seline, BA
Shimon Francis, PhD	Adam Sheppard, BA
Tom Franken, MD	Seiji Shibata, MD, PhD
Christina Fuller, MSc	Jae Hoon Sim, PhD
Stephanie Furrer, PhD	Katie Smith, BSc, PhD
Etienne Gaudrain, PhD	Ediz Sohoglu, PhD
Adele Goman, MRes	Yohan Song, BA
Owen Gross, PhD	Joris Soons, PhD
Yaa Haber, MBS	Greta Stamper, AuD
Sarah Hayes, BS	Morrison Steel, BSc
Ariel Hight, MS	Qudsia Tahmina, PhD
Chengcheng Huang, BS	Shikha Tarang, PhD
Salima Jiwani, MSc	Daniela Saderi Thorson, MS
Karl Koehler, BA	Ann Todd, MS
Elliott Kozin, MD	James Traer, PhD
Anisha Kumar, BA	Kristy Truong, MD
Karina Leal, PhD	Zachary Urdang, BS
Hee Yoon Lee	Phillip Uribe, BS
Daniel Lee, MD	Zachary Vandegriend, MD
Chang Liu, BS	Sebastian Alonso Vasquez Lopez, MSc
Vicente Lumbreras, PhD	A. Catalina Velez-Ortega
Ross Maddox, PhD	Gardiner von Trapp, BA
David Martel, BSE	Bin Wang, MD, PhD
Joseph McClellan, BS	Bryan Ward, MD
Will McLean, BS	Melissa Watts, MD
Richard McWalter, MSc	Alyssa Wheeler, BS
Xiangying Meng, PhD	Tanika Williamson, MS
Ian Mertes, AuD, PhD	Uzma Wilson, BS
Rahul Mittal, PhD	Nikolaus Wolter, MD
Takushi Miyoshi, MD	Kevin Woods, BS
Hideaki Moteki, MD, PhD	Yazhi Xing, MD, MS
Ala Mullangi, MS	Yingyue Xu, BS
Tenzin Ngodup, MS	Ofer Yizhar-Barnea, MSc
Hiroe Ohnishi, PhD	Lichun Zhang, MD, PhD
Catherine O'Leary, MD, MS	Nathaniel Zuk, BS
Carina Pals, MSc	

The *Abstracts of the Association for Research in Otolaryngology* is published annually and consists of abstracts presented at the Annual MidWinter Research Meeting. A limited number of copies of this book and previous books of abstracts (1978-2011) are available. Please address your order or inquiry to Association for Research in Otolaryngology Headquarters by calling (856) 423-0041 or emailing headquarters@aro.org.

This book was prepared from abstracts that were entered electronically by the authors. Authors submitted abstracts over the World Wide Web using Omnipress Abstract Management System. Any mistakes in spelling and grammar in the abstracts are the responsibility of the authors. The Program Committee performed the difficult task of reviewing and organizing the abstracts into sessions. The Program Committee; Program Committee Chair, Dr. Lawrence R. Lustig; the President, Dr. Jay T. Rubinstein; and the Editor, Dr. Linda J. Hood constructed the final program. Omnipress electronically scheduled the abstracts and prepared Adobe Acrobat pdf files of the Program and Abstract Books. These abstracts and previous years' abstracts are available at www.aro.org.

Citation of these abstracts in publications should be as follows: **Authors, year, title, Assoc. Res. Otolaryngol. Abs.: page number.**

Table of Contents

Abstract Number

Presidential Symposium

Symposium

First-in-Human Trials of Neurotechnology: Past, Present and Future..... 001-06

Podium

Structural and Physiological Development of Auditory Synapses..... 007-013

NIDCD Workshop 1

Inner Ear: Prestin and Outer Hair Cell Motility 001-014

NIDCD Workshop 2

Applying for NIDCD Training and Career Development Awards

NIDCD Workshop 3

Early Stage Investigators (ESI) and New Investigators (NI)

Poster

Applying for NIDCD SBIR and STTR Grand Awards

Aging I001-011

Aging II 013-025

Inner Ear: Damage and Protection I..... 026-043

Auditory Pathways: ERPs 044-057

Auditory Pathways: Midbrain..... 058-077

Auditory Pathways: Cortex and Thalamus I 094-848

Localization: Physiological 098-109

Otoacoustic Emissions.....110-129

Plasticity of Central Auditory System 130-140

Psychoacoustics I 141-151

Psychoacoustics: Masking, Noise and Reverberation 152-165

Psychoacoustics and Localization: Modeling 166-175

Development I 176-186

Regeneration I..... 187-201

Vestibular: Basic Research I 202-219

Tinnitus: Animal Models818

Symposium

Consider Bone Conducted Hearing 014-019

Central Vestibular Control of Essential Autonomic Functions 020-025

Podium

Auditory Nerve 015-022

Symposium

Auditory Neural Remodeling by Environmental Noise and Other Background Sounds..... 026-032

Neurotrophins: Their Function in Survival, Neurite Growth, Funtional Diversification and Maintenance 033-038

Podium

Cochlear Implant/Auditory Prostheses I 024-030

Regeneration I..... 031-038

Inner Ear: Hair Cell Transduction I 039-046

Vestibular: Basic Research 047-054

Regeneration II..... 055-062

Inner Ear: Hair Cell Transduction II 063-070

Otoacoustic Emissions..... 071-077

Poster

Auditory Nerve I 220-849

Auditory Nerve II 232-245

Auditory Prostheses I 246-498

Auditory Pathways: Cortex and Thalamus II 262-280

Genetics 281-303

	Development II	304-524
	Inner Ear: Anatomy and Physiology I	317-334
	Inner Ear: Anatomy and Physiology II	335-351
	Inner Ear - Hair Cell Physiology & Anatomy.....	352-357
	Inner Ear: Damage and Protection II.....	358-376
	Inner Ear Damage and Protection III.....	377-395
	Psychoacoustics and Localization: Binaural and Precedence	396-415
	Vestibular: Clinical and Basic	416-425
	Vestibular: Clinical.....	426-430
	Auditory Pathways: Midbrain.....	065
Symposium		
	Vestibular Related Traumatic Brain Injury (TBI)	039-043
	Macro to Micro: The Role of Spike Timing Dependent Plasticity and Neural Hypersynchrony in Disease	044-049
Podium		
	Cochlear Implant II	078-085
Symposium		
	Recent Developments in Cochlear Implant Research	050-054
	Cochlear Neurodegeneration in Noise and Aging – From Animal Models to Human Temporal Bones.....	055-059
Podium		
	Psychoacoustics	086-093
	Inner Ear: Genetics and Clinical Pathology.....	094-101
	Inner Ear: Synapses.....	102-108
	Drug Delivery	109-116
	Inner Ear: Anatomy and Physiology I	117-124
	Aging	125-131
Poster		
	Auditory Pathways: Cortex and Thalamus III	431-447
	Auditory Pathways: Binaural Circuits	448-467
	Auditory Prostheses II	468-495
	Clinical Otolaryngology	496-506
	Clinical Audiology	507-528
	Inner Ear: Hair Cells.....	529-538
	Inner Ear: Mechanics & Modeling	539-546
	Inner Ear – Prestin and OHC Motility	547-551
	Inner Ear Damage and Protection IV	552-569
	Inner Ear Damage and Protection V	570-587
	Psychoacoustics II	588-598
	Psychoacoustics: Multimodal and Attention	599-618
	Regeneration II.....	619-633
	Vestibular: Basic Research II	634-650
Symposium		
	Dynamics of Attention and Learning in the Auditory System.....	060-063
Podium		
	Inner Ear: Damage and Protection I - Ototoxic Drug	132-139
	Development	140-147
Symposium		
	Central Consequences of Deafness	064-071
Podium		
	Inner Ear: Damage and Protection II.....	148-155
	Development II	156-163
	Inner Ear: Damage and Protection III - Noise Damage.....	164-171
	Inner Ear: Mechanics & Modeling	172-179
	Psychoacoustics: Binaural	180-187

Young Investigator Symposium

Poster

Cochlear Mechanotransduction	072-079
Auditory Prostheses III	651-672
Auditory Pathways: Brainstem	673-687
Auditory Pathways: Cochlear Nucleus	688-707
Drug Delivery	708-719
External and Middle Ear Diagnosis & Treatment	720-727
External Middle Ear Microbiology.....	728-738
External Middle Ear Physiology	739-750
Inner Ear: Synapses.....	751-764
Inner Ear: Genetics and Clinical Pathology.....	765-774
Physiology: Inner Ear - Membranes and Fluids	775-783
Psychoacoustics: Pitch Perception	784-795
Clinical Otolaryngology	502-796
Speech	797-809
Plasticity of Central Auditory System	136
Tinnitus: Animal Models	810-829
Tinnitus: Human Patients	830-846
Auditory Pathways: Cochlear Nucleus	847

Podium

Auditory Pathways: Cortex and Thalamus	196-215
External and Middle Ear.....	188-195
Podium: Inner Ear: Anatomy and Physiology II.....	204-210
Inner Ear: Hair Cells Anatomy and Physiology	216-220

SY - 001

The Cochlear Implant: Past, Present, and Future

Jim Patrick

Cochlear Limited

The cochlear implant is the first medical treatment to successfully restore a human sense. Outcomes include normal language development for children and the use of the telephone for adults.

However early researchers worked in an environment of extreme scepticism, from both neurophysiologists and medical specialists, and this limited the funding of research. This presentation will describe early research, especially the multi-disciplinary program at the University of Melbourne, under Professor Graeme Clark. Prior to the first human implant, the team conducted a range of studies that illustrated the potential benefit of multiple intracochlear electrodes and that the use of these electrodes was safe.

It describes the research implant developed in Melbourne, why attempts to use an electrical model to mimic normal cochlear response failed, and how psychophysics experiments demonstrated that different stimulus dimensions (place and rate of stimulation) could be perceived independently. This vital observation was then used to develop coding strategies that transmitted different speech features, especially features that were not accessible through lip-reading. Our research volunteer was central to this work. He was very patient, an excellent reporter and he had been a singer before his deafness.

Our first speech coding strategy was the F0/F2 strategy. It provided significant help with lipreading, and was the Proof-of-Concept that led to the successful commercial development of the first multi-channel cochlear implant, the Nucleus22. Over the 30 years since this work, there have been advances in electronics technology, many of which have been integrated into a series of implants and external processors, providing improved outcomes and ease-of-use. Clever signal processing and the use of multiple microphones improves performance in noisy environments.

For people with severe to profound hearing loss, or a steeply sloping high frequency loss the cochlear implant can be combined with acoustic stimulation in Hybrid or Electro-acoustic devices. Studies also indicate a hearing benefit when people with single sided deafness use a cochlear implant in the deaf ear.

Two areas of future research and development opportunity are the electro-neural interface and the development of invisible hearing, or the totally implanted cochlear implant. If the stimulus currents could be localised to smaller groups of nerve cells then better simulation of normal neural function might be achieved, improving performance, while a totally implanted system would resolve any cosmetic concerns of the candidate while reducing the level of maintenance demanded by the current processor/coil/cable assembly.

SY - 002

The Development of Second Sight's Argus II Retinal Prosthesis

Robert Greenberg

Second Sight Medical Products, Inc.

SY - 003

Neurosurgical Studies of the Functional Organization of Human Auditory Cortex

Matthew Howard

University of Iowa

SY - 004

Human Trial of an Implantable Vestibular Prosthesis

Jim Phillips

University of California - San Francisco

SY - 005

Striatal Stimulation for Tinnitus Modulation

Steven Cheung

Background

Deep brain stimulation (DBS) of the basal ganglia is under Phase I clinical trial investigation to treat bothersome tinnitus, a phantom sensory disorder manifested by auditory percepts in the absence of external correlates. This approach is conceptually distinct from neuromodulatory treatments that aim to alter central auditory reorganization, dysfunctional hyperactivity or synchronized oscillations, changes implicated in tinnitus perception. The treatment target is a subsite of the dorsal striatum, area LC, a locus of the caudate positioned at the junction of the head and body of the nucleus.

Methods

Two acute, awake human electrical stimulation experiments in area LC on movement disorders patients with and without comorbid tinnitus undergoing DBS surgery were performed. The first experiment focused on tinnitus loudness modulation while the second experiment focused on tinnitus sound quality alteration and auditory phantom triggering. Seven interactive adult subjects participated. Tinnitus loudness was rated on a 0 to 10 scale (0 – none; 5 – conversation; 10 – jet engine), sound quality was described qualitatively, and spatial location was referenced to the ears.

Results

Short-term area LC stimulation suppressed tinnitus loudness to a nadir of at least 2 and controllably triggered new phantom tones, clicks, and frequency modulated sounds. Those results suggest the dorsal striatum may play an important role in gating potential auditory phantoms for perceptual awareness. A basal ganglia-centric model of phantom percept gate control emerges, and is under investigation.

Conclusions

Striatal dysfunction may be enabling bothersome tinnitus. DBS neuromodulation of area LC could confer healthy restrictive dorsal striatal gate function, thereby rejecting potential auditory phantoms.

Funding

NIDCD 1U01DC013029 and DoD CDMRP W81X-WH-13-1-0494.

SY - 006

Learning and Feedback for a Sensorimotor Brain-Computer Interface

Jeff Ojemann

University of Washington

SY - 007

Anatomical and Physiological Maturation of Inner Hair Cell Ribbon Synapses

Tobias Moser¹; Aaron B Wong²; Mark A Rutherford³; Zhizi Jing⁴; Mantas Gabrielaitis^{2,8}; Tina Pangrsic²; Thomas Frank²; Fabian Göttfert⁵; Susann Michanski⁶; Stefan Hell⁷; Fred Wolf⁸; Nicola Strenzke⁴; Carolin Wichmann⁹

¹University of Goettingen Medical School; ²InnerEarLab, Department of Otolaryngology, University of Goettingen Medical School; ³Department of Otolaryngology, Washington University School of Medicine; ⁴Auditory Systems Physiology Group, InnerEarLab, Department of Otolaryngology, University of Goettingen Medical School; ⁵MPI for Biophysical Chemistry; ⁶Molecular Architecture of Synapses group, InnerEarLab, Department of Otolaryngology, University of Goettingen Medical School; ⁷MPI for Biophysical Chemistry, Goettingen; ⁸MPI for Dynamics and Self-Organization; ⁹Molecular Architecture of Synapses Group, InnerEarLab, Department of Otolaryngology, University Medical Center Göttingen

Background

The role of cochlear inner hair cells (IHCs) changes from pre-sensory pacemaker to sensory transducer over development. This switch is accompanied by changes in structure and function of the ribbon synapses between IHCs and spiral ganglion neurons (SGNs) around the postnatal hearing onset in mice. Specifically, how the molecular anatomy and physiology of the IHC ribbon synapse matures and how this shapes sound coding properties of these synapses remain important questions.

Methods

Here we combined morphological (electron microscopy (EM), immunohistochemistry, confocal and stimulated emission depletion (STED) microscopy) and functional (electrophysiology, confocal Ca²⁺-imaging, and Ca²⁺-uncaging) techniques with biophysical modeling to study the IHC afferent synapse during postnatal maturation.

Results

Synapses matured from holding several small presynaptic active zones (AZs) and apposed postsynaptic densities (PSDs) to one large AZ/PSD complex per SGN bouton. Upon the onset of hearing (1) IHC had fewer and larger ribbons; (2) Ca_v1.3-channels formed stripe-like clusters rather than the smaller and round clusters observed before; (3) active zones with a large number of Ca_v1.3-channels and strong Ca²⁺ signaling co-emerged with SGNs with higher spontaneous firing rate (4) extrasynaptic Ca_v1.3-channels were selectively

pruned; and (5) the fast exocytic component was regularly observed upon Ca²⁺ uncaging. In parallel, the apparent Ca²⁺-dependence of exocytosis linearized when manipulating the number of open Ca²⁺-channels. Biophysical modeling revealed that this is consistent with one of the few contributing Ca²⁺ channels to dominate the [Ca²⁺] at each mature release site.

Conclusion

We conclude that IHC synapses undergo a major developmental refinement and thereby tighten the spatial coupling of Ca²⁺-influx to exocytosis. The resulting Ca²⁺ nanodomain control of exocytosis likely enables temporal precision of coding already for weak stimuli. We hypothesize that the number of Ca²⁺ channels at each IHC AZ critically determines the firing properties of its corresponding SGN and propose that AZ heterogeneity enables IHCs to decompose auditory information into functionally diverse SGNs.

SY - 008

Ribbon Development and Function in Zebrafish Hair Cells

Teresa Nicolson

SY - 009

Development of Spiral Ganglion Neurons and Their Synaptic Connections

Lisa Goodrich¹; Wei-Ming Yu¹; Jessica Appler¹; Ye-Hyun Kim²; Jeffrey Holt²

¹Harvard Medical School; ²Boston Children's Hospital

All acoustic stimuli are encoded by the electrical activity of spiral ganglion neurons, which receive signals from hair cells and transmit this information to target neurons in the cochlear nucleus. Synaptic transmission must be unusually fast and precise in order to capture the tiny differences in timing and intensity that underlie sound localization. Hence, hair cells develop structurally and physiologically distinct pre-synaptic zones, characterized by the presence of an elongated, electron dense ribbon. The ribbon tethers synaptic vesicles close to the active zone, enabling sustained release that accurately reflects the pattern of stimulation even at high frequencies. Similarly, spiral ganglion neurons must elaborate specialized post-synaptic densities (PSD) in order to respond to hair cell-released glutamate quickly and repeatedly, without losing sensitivity. Hence, AMPA-type glutamate receptors are clustered abundantly in a large PSD that extends beyond the boundaries of the active zone. We found that the transcription factor MafB acts in spiral ganglion neurons to drive differentiation of the post-synaptic density in the ribbon synapse. In mice lacking MafB, PSDs are defective, leading to secondary effects on the number, morphology, and localization of pre-synaptic ribbons in the hair cells. As a result, synapse number is reduced and hearing is impaired in mutant mice. Conversely, early overexpression of MafB is sufficient to trigger PSD differentiation, even in mutant backgrounds with severely disrupted spiral ganglion neuron development. These findings raise the intriguing possibility that MafB might offer a useful molecular tool for restoration of synapses lost as a result of aging or acoustic overexposure.

SY - 010

Differential Plasticity at Developing Afferent Synapses

Johanna Montgomery¹; Meagan Barclay¹; Lin-Chien Huang¹; Gary Housley²; Peter Thorne³

¹University of Auckland; ²University of New South Wales;

³University of Auckland

SY - 011

Activity and Endbulb Development

David Ryugo¹; Connelly Catherine¹; Amanda Lauer²

¹Garvan Institute and University of New South Wales;

²Johns Hopkins University School of Medicine

Background

Hearing loss is accompanied by a notable difficulty in speech comprehension in noisy backgrounds. We hypothesize that abnormalities in the central auditory system caused by hearing loss underlie this impairment. Such abnormalities would be consistent with the conclusion that impaired auditory perception cannot be attributed solely to the inner ear pathology and so must involve the brain.

Methods

CBA/CaH, DBA/2, and Shaker-2 mice show that congenital and acquired hearing loss results in abnormal brain development affecting bushy cells of the cochlear nucleus, endbulbs of Held, which are the large axosomatic synaptic endings of auditory nerve fibers, and inhibitory endings of unknown origin onto bushy cells. CBA/CaH mice are a strain that has good hearing throughout most of their life; DBA/2 mice have adolescent onset, progressive hearing loss due to pathology affecting the organ of Corti; Shaker-2 mice have congenital deafness and never hear as result of defective stereocilia in the auditory receptor cells. Analysis utilized ABR recordings, staining of auditory nerve fibers using neuroanatomical tracers (e.g., HRP and neurobiotin), antibodies against vesicular glutamate transporter-1 and glycine transporter-2, and electron microscopy.

Results

Results to date reveal central abnormalities are directly correlated to hearing sensitivity. Compared to normal hearing CBA/CaH mice, hearing loss has the greatest effect on brain structure in congenitally deaf Shaker-2 mice and an intermediate effect in DBA/2 mice. Cell body size of bushy cells is smaller, the complexity and number of endbulb components are reduced, endbulb synapses can be pathologically flattened and hypertrophied, and the density of axosomatic inhibitory endings is lowered. These data suggest that inner ear pathology produces a cascade of synaptic change in the central auditory pathways.

Conclusion

Abnormalities within auditory circuits following hearing loss are more dramatic and far-reaching than previously anticipated. The changes imply that peripheral hearing loss does more than create a need for amplified sounds. The reduction of auditory input diminishes the detail and clarity of sound input by pixelating the acoustic environment. The synaptic pa-

thology will impair timing in signal transmission and uncouple neural activity to acoustic events, creating perceptual sound ambiguities. We are planning studies aimed at preserving and/or restoring hearing function through the use of amplification and/or auditory enrichment environments.

SY - 012

Structural Dynamics of Neurons and Glia During Rapid Growth of the Calyx of Held

George Spirou¹; Paul Holcomb¹; Dakota Jackson¹; Kartik Motwani¹; Brian Chen¹; Cody Mullins¹; Jessica Patterson¹; Tom Deerinck²; Mark Ellisman²

¹West Virginia University; ²University of California San Diego

Background

Formation of neural circuits during early brain development is a dynamic process of assembly and disassembly, coordinated with functional maturation of constituent cells. Although typically considered to be an interaction between pre and postsynaptic partners, increasingly the roles for glia in synapse formation are being revealed. Understanding structural features of glia/neuron interactions is limited when using light microscopic techniques that inherently lack sufficient resolution and which selectively label cellular subpopulations and not all cellular compartments.

Methods

To reveal glia/neuron interactions and structural dynamics at high resolution, we used electron microscopy, which labels all cells and subcellular organelles in an unbiased fashion. To obtain large image volumes in 3D, we used the new technology of serial blockface scanning electron microscopy (SBEM). We focused on the formation of calyx of Held (CH) innervation of principal cells of the medial nucleus of the trapezoid body (MNTB), which we have shown to exhibit hallmark features of neural circuit formation including early exuberant innervation and competition to yield monoinnervation.

Results

Both neurons and glia reposition themselves in coordinated fashion as growth of synaptic inputs begins. Prior to growth of the CH, MNTB neurons are tightly packed and large regions of the cell body are coated by glial processes. This tight structure unfolds as calyciform (calyx forming) inputs begin to contact the MNTB cell body. The MNTB cell body is polarized by the position of its nucleus. Glia maintain contact with one pole of the cell body and may play roles in determining the region of the cell surface that is innervated by the CH. Glia also contact competing calyciform inputs by wrapping their axons and intervene between growing nerve terminals and the postsynaptic surface. These glial "incursions" can affect the size of competing terminals by preventing formation of new synaptic contacts.

Conclusion

These multiple modes of glia/neuron contact provide substrates for possible new mechanisms in selection of "winning", competitive inputs.

SY - 013

Activity of Neuronal Ensembles During Hearing Development: Clusters of co-Active Neurons or Propagating Waves?

Adrian Rodriguez-Contreras

PD - 001

Prestin and Heterologously Expressed Membrane Proteins Are Constrained by the Trilaminar Lateral Wall of Outer Hair Cells

Tetsuji Yamashita¹; Pierre Hakizimana²; Stefan Jacob³; Temirov Jamshid¹; Jie Fang¹; Marcia Mellado-Lagarde¹; Barbara Leibiger³; Sara Leijon³; Per-Olof Berggren³; William E. Brownell⁴; Anders Fridberger²; Jian Zuo¹

¹St. Jude Children's Research Hospital; ²Linköping University; ³Karolinska Institutet; ⁴Baylor College of Medicine

Background

The outer hair cell (OHC) lateral wall contains nature's fastest motor protein, prestin, in a cytoskeletal matrix sandwiched between membranes. Prestin can undergo voltage-dependent conformational changes associated with the rapid OHC length changes that are critical for high frequency mammalian hearing. Additionally, prestin endows OHCs the proper passive mechanical stiffness for optimal cochlear amplification. Previous studies indicate that prestin is freely mobile in the plasma membrane, calling into question its association with the laminated structures and the existence of a supra-molecular motor complex.

Methods

We created a knockin mouse expressing a prestin-YFP fusion protein and measured prestin's dynamics in OHCs using fluorescent recovery after photobleaching in isolated OHCs for 3 min and using bright and number analysis in temporal bone preparations. Four membrane fluorescent proteins were heterologously expressed in OHCs of knockin mice and their dynamics were also examined in the OHC lateral wall as well as in OHC hair bundle and neighboring supporting cell membranes. Co-treatments of salicylate and methyl- β -cyclodextrin (MbCD) were assessed for effects on protein's dynamics in isolated OHCs.

Results

Prestin-YFP recapitulates endogenous prestin expression during development and in adults. No lateral diffusion of prestin was observed in the OHC lateral wall. Furthermore, lateral diffusion of other heterologously expressed membrane fluorescent proteins was also relatively minimal but much greater in membranes of OHC stereocilia and neighboring supporting cells. Co-treatments of salicylate and MbCD increased the mobility of prestin and all the other membrane proteins studied.

Conclusion

Prestin is not so tightly packed that the OHC lateral wall has no extra space for other membrane proteins. Prestin and other membrane proteins are constrained by trilaminar structures and likely microdomains specifically in the OHC lateral

wall. The efficient motor complex of the OHC lateral wall incorporates prestin and other membrane proteins with minimized lateral diffusion into the highly specialized laminated organization to endow OHC's passive and active mechanical capabilities for mammalian-specific high frequency hearing. Similar laminated organization is found in gliding bacteria, plant cells, skeletal muscles and axon initial segments, most of which also have relatively minimized lateral mobility of membrane proteins, thus suggesting that the laminated structures with minimized lateral diffusion of membrane proteins represent convergent evolution across the entire spectrum of life to coordinate force generation of cellular motors.

PD - 002

Prestin Activity Contributes to the Stereocilia Deflection Phase

Pierre Hakizimana; Anders Fridberger
Linköping University

Background

Inner hair cells (IHC) rely on the stereocilia deflection for detecting sound stimuli, which are converted into electrical impulses in the auditory nerve. It is well accepted that comparison of the IHC and outer hair cells (OHC) response phases is a reliable approach for investigating IHC stimulation mechanism. However, published phase data vary from one study to another, casting some doubt about the true IHC stimulation mechanism.

Methods

The stereocilia deflection phase was quantified in IHC and OHC by time-resolved confocal imaging and optical flow computation techniques in the apical turn of the cochlea in temporal bone preparations from guinea pigs. To investigate the effect of prestin activity on the stereocilia movement, salicylate was added in the perfusion system.

Results

Here we quantified the deflection phase in same-location IHC and OHC from the apical turn of guinea pig cochlea directly at the stereocilia level at the best frequency. In 11 different measurements, IHC stereocilia phase-lead OHC stereocilia by 86°, indicating that IHC are primarily stimulated by the viscous drag of the endolymph. To investigate possible effect of prestin activity on the stereocilia movements, we investigated the phase behaviour in presence of salicylate, which blocks prestin. Salicylate induced a significant positive phase shift in OHC stereocilia motion relative to the situation before salicylate treatment, indicating that prestin contributes to the stereocilia movement. A similar positive shift was seen in IHC after salicylate treatment relative to the control, suggesting that the IHC can sense changes in the OHC phase, most likely through endolymph motion.

Conclusion

Our results show that IHCs are stimulated by the endolymph viscous drag and that the stereocilia get an input from prestin activity.

PD - 003

Intracellular Chloride Level Affects Nonlinear Capacitance but Neither Frequency Response nor Magnitude of Electromotility in Outer Hair Cells

Joseph Santos-Sacchi; Lei Song

Yale University

Background

Prestin is a protein motor within the lateral membrane of OHCs that drives electromotility and cochlear amplification. During the last decade the interaction of chloride with the motor has been a major focus of study. It is known that the magnitude of nonlinear capacitance (NLC), representing associated charge movement during conformational changes in the motor, is susceptible to intracellular chloride concentration. Electromotility and NLC have been considered tightly coupled, though we recently showed that this coupling is chloride level dependent (PNAS 110(10):3883-8, 2013). Here we further evaluate effects of chloride on NLC and both steady state and high frequency measures of electromotility.

Methods

Isolated OHCs were studied under whole cell voltage clamp with altered levels of intracellular (with matched extracellular) chloride substituted with gluconate. Chloride levels were varied from 140 mM to 0.1 mM. NLC was measured with admittance techniques, and simultaneously electromotility was measured with high speed video or photodiode techniques.

Results

NLC presents a Cl^- $K_{1/2}$ of 1 mM, with about 1/3 of the NLC insensitive to chloride. Changes in Boltzmann characteristics of the NLC occur as chloride levels decrease. There is a depolarizing shift of the motor's voltage dependence (V_h) and a reduction in the voltage sensitivity (z). On the other hand, steady-state electromotility magnitude is unaffected by changes in chloride levels, and indeed there is no difference in the voltage-driven mechanical frequency response (measured up to 6 kHz) between low and high chloride conditions.

Conclusion

Chloride has no effect on electromotility but does have great effects on NLC. If chloride were reducing NLC because of slowed motor kinetics this should have evidenced itself in the mechanical frequency response. Either chloride affects NLC magnitude independent of altered kinetics or NLC and electromotility are not causally related.

PD - 004

Voltage Under Fire: IR Laser-Induced Perturbations of the Voltage-Dependent Solute Carrier Protein, SLC26a5

Oluwarotimi Okunade; Joseph Santos-Sacchi

Yale University

Background

Alterations in membrane capacitance can arise from linear and nonlinear sources. For example, changes in membrane surface area or dielectric properties can modify capacitance linearly, whereas sensor residues of voltage-dependent proteins

can modify capacitance nonlinearly. Here, we examined the effects of fast temperature jumps induced by an IR laser in control and prestin (SLC26a5)-transfected HEK cells under whole cell voltage clamp.

Methods

Here, we examined the effects of fast temperature jumps induced by an IR laser in control and prestin (SLC26a5)-transfected HEK cells under whole cell voltage clamp. Nonlinear capacitance (NLC) was measured with admittance techniques.

Results

Prestin's voltage sensor imparts a characteristic bell-shaped, voltage-dependent nonlinear capacitance (NLC). Temperature jumps in control HEK cells cause a monophasic increase in membrane capacitance (C_m) regardless of holding voltage due to double layer effects. Prestin-transfected HEK cells, however, additionally show a biphasic increase/decrease in C_m with a reversal potential corresponding to the voltage at peak NLC of prestin (V_h), attributable to a rapid temperature-following shift in V_h , with shift rates up to 14 V/s over the course of a 5 ms IR pulse. Treatment with salicylate, a known inhibitor of NLC, re-establishes control cell behavior. A simple kinetic model recapitulates our biophysical observations.

Conclusion

These results verify a voltage-dependent protein's ability to respond to fast temperature perturbations on par with double layer susceptibility, likely arising from prestin's unique ability to move sensor charge at kilohertz rates, a requirement for the OHC's role as cochlear amplifier.

PD - 005

Effect of General Anesthetics and Alcohols on Prestin Function

Guillaume Duret¹; Fred Pereira²; Robert Raphael¹

¹Rice University; ²Baylor College of Medicine

Background

The membrane protein prestin, localized in the membrane of outer-hair cells, has proven to be particularly sensitive to perturbations in the lipid bilayer. Changes in cholesterol concentration, the presence of lipophilic ions and NSAIDs impact the electrophysiological signature of prestin. However, the functional interaction between prestin and the membrane physical properties is not fully understood.

The alteration by anesthetics and alcohols of the lipid bilayer has been proposed to be in part or fully responsible for their effects on ligand-gated ion channels, through an alteration of the conformational free-energy landscape of the protein. We decided to put this theory to the test on prestin, and monitor the changes on the various electrophysiological parameters of prestin in the presence of alcohols with various C-chains (C2 to C10) and some general anesthetics (GA: propofol, isoflurane, halothane, chloroform, etomidate and xylazine).

Methods

To measure the non linear capacitance of prestin, we use HEK-cells stably transfected with a plasmid containing the

prestin gene. The NLC is measured from these cells after 48 hours of induction. For each cell, a control NLC in the absence of drug is obtained. The appropriate alcohol or GA is then perfused in the recording chamber and a second NLC is measured.

Results

All the alcohols tested trigger a dose-dependent shift in the characteristic voltage at half-maximal charge transfer ($V_{1/2}$), with the sensitivity increasing as the alcohols' carbon-chain is longer. The direction of the shift changes with concentration, the lower concentration cause a negative shift while higher concentrations shift $V_{1/2}$ closer to 0mV. These shift are correlated with changes in the linear capacitance of the cell. All of the GA we tested caused a dose-dependent increase in charge density at sub-millimolar concentrations as well as a shift of $V_{1/2}$ toward hyperpolarized voltages. The sensitivity of prestin to these molecules seems to follow the Meyer/Overton correlation.

Conclusion

General anesthetics as well as alcohols induce alterations in the function of prestin which could in turn impact hearing. The shift in the NLC as well as the increase in charge density could modify the function of the OHC at resting potential and alter cochlear amplification.

PD - 006

LPA Activation of a RhoA/cPKC α -Mediated Signaling Pathway Regulates Outer Hair Cell Motility by Phosphorylating the Cytoskeletal Protein Adducin

Channy Park; Federico Kalinec

House Research Institute and David Geffen School of Medicine, UCLA

Background

In prior studies on outer hair cells (OHC) we demonstrated that LPA was able to induce RhoA/ROCK-mediated adducin phosphorylation at Thr445, and RhoA/PKC-mediated adducin phosphorylation at Ser726 (Zhang et al, *J Biol Chem* 278:35644-50, 2003). Adducin, together with actin and spectrin, is a major component of the OHC's cortical cytoskeleton. Thus, activation of RhoA/PKC pathway could induce changes in OHC length and motility associated with structural modifications in this cytoskeletal structure. In this study, we aimed at determining if PKC inhibitors were able to regulate RhoA/PKC-adducin mediated effects on OHC motility.

Methods

Actin-dependent changes in cell length (slow motility) and the amplitude of electrically induced changes in cell length (fast motility) were measured in isolated guinea pig OHC, patch clamped in whole-cell mode and internally perfused through the patch pipette with inhibitor of PKC while being externally stimulated with LPA. OHC motility was monitored by high-speed video microscopy, whereas confocal microscopy was used to investigate effects of PKC inhibitor on RhoA/PKC-Adducin signaling pathway.

Results

We found that LPA induced expression of cPKC α and nPKC ζ , with cPKC α but not nPKC ζ phosphorylating adducin both of Ser725 and Thr445. However, treatment with specific pharmacological inhibitors of PKC α reduced adducin phosphorylation only at Ser726. Also, we determined that activation of the RhoA/PKC α -mediated signaling pathway by LPA induced OHC shortening and a simultaneous increase in the amplitude of fast motility.

Conclusion

Our results support a positive role for cPKC α in OHC motility and strongly suggest a link between cPKC α , adducin phosphorylation and the regulation of OHC motility.

PD - 007

Gene Discovery by Next Generation

Sequencing: Which is the Real Mutation?

Ofer Yizhar-Barnea¹; Zippora Brownstein¹; Amal Abu Rayyan²; Orly Yaron³; Moshe Frydman⁴; Stavit Shalev⁵; Hagit Baris⁶; Noam Shomron⁷; Moien Kanaan²; Karen B. Avraham¹

¹Department of Human Molecular Genetics and Biochemistry, Sackler Faculty of Medicine and Sagol School of Neuroscience, Tel Aviv University, Tel Aviv, Israel;

²Department of Biological Sciences, Bethlehem University, Bethlehem, Palestine; ³Functional Genomics Laboratory, Tel Aviv University, Tel Aviv, Israel; ⁴Danek Gartner Institute of Human Genetics, Sheba Medical Center, Tel Hashomer; Sackler School of Medicine, Tel Aviv University, Tel Aviv, Israel; ⁵Genetics Institute, Ha'Emek Medical Center, Afula, Israel; ⁶Raphael Recanati Genetic Institute, Rabin Medical Center, Petach Tikva, Israel; ⁷Department of Cell and Developmental Biology, Sackler Faculty of Medicine, Tel Aviv University, Tel Aviv, Israel

Background

Hundreds of mutations in more than 70 genes are associated with hearing loss, yet for the majority of individuals with hereditary defects, the etiology remains unknown. In many cases, the causative mutation might be in a known gene that is not screened routinely due to practical limitations. Until recently, the large reservoir of known deafness genes, as well as their large size, precluded comprehensive genetic diagnosis. The combination of targeted genomic capture and massively parallel sequencing (MPS) has become a promising tool for detecting novel and known mutations involved in hereditary hearing loss and for solving many cases in a rapid and cost-effective manner. Alternatively, the mutation may be in an as yet undiscovered gene with respect to deafness, which can be solved by whole exome sequencing (WES).

Methods

We first performed MPS using a targeted genomic capture approach with 284 genes, including 121 human genes and 163 human orthologues of mouse deafness genes in 107 hearing impaired unrelated individuals from Israeli Jewish and Palestinian Arab families. Four families underwent WES. Mutations were validated by Sanger sequencing.

Results

Targeted genomic capture and MPS resulted in the doubling of the number of deafness genes in the Middle East population. This approach solved about a third of the deafness. Four of the unsolved families underwent WES, which led to intriguing results in two out of the participating four families. In one large family, with several consanguineous marriages, two causative mutations in two different genes, *OTOF* and *SLC25A21*, were found in different branches of the family. In the second family, two candidates were identified. Both are promising in terms of the auditory system, both segregate with hearing loss in the family and both have high damaging prediction scores. Functional assays are ongoing to determine the pathogenicity of each and contribution to hearing impairment.

Conclusion

These results emphasize the need for WES for resolving the genetic basis of hearing loss. However, the work also emphasizes the complexity of deep sequencing results and the difficulty in determining the causative mutation. Functional assays to compare the wild type and mutant proteins will hopefully solve the puzzle: which is the real mutation?

PD - 008

The Use of Different NGS Protocols to Study Inherited Forms of Hereditary Hearing Loss (HHL)

Paolo Gasparini; Diego Vozzi; Anna Morgan; Dragana Vuckovic; Elisa Rubinato; Mariateresa Di Stazio; Flavio Faletra; Stefania Lenarduzzi; Giorgia Giroto
Institute for Maternal and Child Health-IRCCS "Burlo Garofolo", University of Trieste, Italy

Background

The presence of a large genetic heterogeneity and the need to identify new HHL genes prompted us to design an extremely powerful algorithm characterized by 3 steps: 1) screening of 96 HHL genes by targeted re-sequencing (TS). In negative cases: 2) linkage studies (LS) to filter 3) whole exome sequencing (WES) data for the identification of new genes.

Methods

TS analyses 96 different HHL genes using Ion Torrent PGM™ (LifeTechnologies) and 3487 amplicons ensuring approximately 92% coverage of the target region (a total of 411.420 bp). Resulting genomic variants are annotated by ANNOVAR and filtered according to: a) pedigree pattern of inheritance b) linkage data c) NCBI dbSNP v137, 1000 Genomes Project, ESP6500 databases, c) pathogenicity evaluation by *in silico* predictors tools, d) evolutionary amino-acid conservation (PhyloP, GERP++). LS are performed using High-density SNP arrays. As regards WES, after exome enrichment step, library construction, sample sequencing and reads mapping, nucleotide variants and INDELS are called by GATK and annotated/filtered as above.

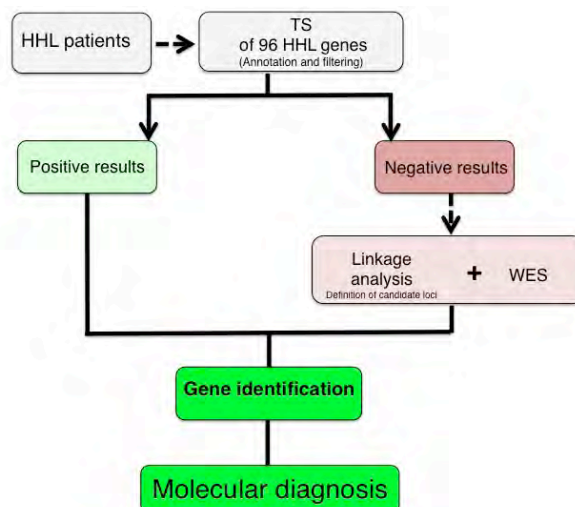
Results

This algorithm has been applied to an overall number of 47 families/patients leading to the identification of several new

HHL genes as well as to the solution of a series of cases (mainly small pedigrees) so far not solved with conventional approaches. In particular, Step 1 (TS) allowed us to characterize several families with mutations in known genes (i.e. *GJB2*, *TECTA*, *USH2A*, etc.). In TS negative cases, the combination of LS and WES led to the identification of the following new genes: 1) *BDP1*, in which a mutation (c.7873 T>G; p.*2625Gluext*11) results in an elongation of 11 residues of the BDP1 protein. Immunohistochemistry in the mouse inner ear showed a clear expression of Bdp1 gene; 2) *P2X2*, in which a new missense mutation (c.1057G>C; p.G353R) leading to the substitution of the hydrophobic Gly with a charged residue as the Arg, is expected to destabilize the protein folding; 3) *TBL1Y*, in a pedigree resembling a Y-linked form of HHL a missense mutation (c.A206T; p.D69V) was identified. *In silico* prediction analysis reported this mutation as disease causing. Functional studies are now in progress to confirm the pathogenic role of this variation. Two additional strong candidate HHL genes are now under final validation step. Up-to-date data will be presented and discussed.

Conclusion

These findings clearly demonstrate the usefulness of our molecular diagnostic algorithm for HHL disease gene identification.



PD - 009

Copy Number Variation of Deafness Genes Analyzed With the Next-Generation Sequencing Method

Haiting Ji¹; Jingqiao Lu¹; Huawei Li²; Xi Erick Lin¹

¹Emory University School of Medicine; ²EENT hospital of Fudan University

Background

It is known that structural variations have a much higher incidence than the single nucleotide polymorphism in the human genome. Copy Number variation (CNV) is one type of structural variation, which has been associated with many types of complex diseases. Large numbers of studies have demonstrated that hereditary hearing loss is caused by various types of DNA mutations, including frameshift mutations, nonsense mutations or missense mutations. However, currently little is

known about the role of CNV in causing deafness. Here we detected CNVs in 129 deafness genes in 79 Chinese patients clinically diagnosed with sensorineural hearing loss by using next-generation sequencing (NGS) technologies.

Methods

Coding regions of 129 deafness genes were captured by a hybridization based method from the genomic DNA of patients (N=79) and normal-hearing subjects (N=100). Captured DNA fragments were processed through the standard NGS and analysis steps. After alignment to the reference human genome, we deducted the CNVs from the relative changes in average-coverage between patient and control samples processed together during the hybridization step.

Results

We identified a total of 95 CNV events, among them 71 CNV gains in the ratio between 1.5 and 6 when compared to controls, and 24 CNV losses (ratio of 0.5 and 0 comparing to controls). In the 79 samples, we found 16 with disease-causing mutations, 22 heterozygous recessive mutations. We could not find disease-causing DNA sequence mutations in 41 samples. In the 63 patient samples that no disease-causing mutations could be identified, we found 31 samples with CNVs. The 24 affected genes are DIAPH1, COL11A2, SLC4A11, MYO1C, OTOA, MYO3A, STRC, ERCC2, USH1C, MYO6, GRHL2, MYO7A, MYO15A, MYH14, CDH23, SOX2, EYA4, TMPRSS5, SLC26A4, COCH, COL9A3, DFNA5, DFNB59 and MTAP. Five of them were found to have corresponding pseudogenes (MTAP, MYO15A, OTOA, SOX2 and STRC). We are still conducting analysis on the effect of these pseudogenes on our CNV findings. We validated the CNV findings obtained by the NGS approach by quantitative PCR (qPCR) method. Results showed that 14 of the 15 CNVs could be confirmed by the independent qPCR method.

Conclusion

Our studies provided experimental data that serve as a basis to explain how CNVs may disrupt normal functions of genes known to be critical for the normal operation of the cochlea. These results may significantly expand our understanding about how various types of genetic mutations cause deafness in humans.

PD - 010

Sequential Utilization of Custom Targeted Capture Platforms in Non-Syndromic Hearing Loss: Impacts on Diagnosis and Novel Gene Discovery

Christina Sloan¹; Diana Kolbe²; Hela Azaiez²; David J. Eisenman³; Lorna Silipino³; Ran Elkon⁴; A. Eliot Shearer¹; Ronna Hertzano³; Richard JH Smith¹

¹Molecular Otolaryngology and Renal Research Laboratories, Department of Otolaryngology, University of Iowa, Iowa City, Iowa; Department of Molecular Physiology and Biophysics, University of Iowa Carver College of Medicine, Iowa City, Iowa; ²Molecular Otolaryngology and Renal Research Laboratories, Department of Otolaryngology, University of Iowa; ³Department of Otorhinolaryngology-Head and Neck Surgery, University of Maryland School of Medicine, Baltimore, Maryland; ⁴Division of Gene Regulation, The Netherlands Cancer Institute, Amsterdam, The Netherlands

Background

Targeted genomic enrichment and massively parallel sequencing (TGE + MPS) have revolutionized the diagnosis of non-syndromic hearing loss (NSHL) and made genetic testing the most cost-effective clinical investigation after an audiogram in the evaluation of the deaf and hard-of-hearing patients. Using OtoSCOPE®, for example, we can interrogate all genes currently known to cause NSHL, but even with this breadth, the diagnostic rate of only ~50% indicates that many genetic causes of NSHL await discovery. Whole exome sequencing (WES) has been used to identify novel NSHL genes but it has failed to close the gap between known loci (164) and known genes (68), is expensive and time consuming, and is typically used on a family-by-family basis. These constraints support the need for a high-throughput strategy for novel gene discovery.

Methods

Sequential Workflow: 96 probands from Iranian families segregating NSHL were recruited. TGE + MPS using OtoSCOPE®v5 was performed. OtoSCOPE®-negative probands advanced for testing on a custom-developed candidate-gene panel.

Candidate Panel Design: Advanced cell sorting and RNA-Seq analysis of mouse inner ears were used to characterize expression and localization of currently known NSHL genes and to identify 268 candidate genes for the NSHL gene-discovery panel (GDP).

Results

Tiered screening using OtoSCOPE® and then the GDP offer an efficient and effective method to identify novel genetic causes of NSHL. The initial OtoSCOPE® screen provides a front-end filter to preselect an enriched population of probands highly likely to segregate novel causes of hearing loss for further testing. And the subsequent screen against 268 candidate genes with expression enriched in cochlear sensory cells and/or more specifically cochlear hair cells affords

an excellent down-stream filter against highly plausible candidate genes.

Conclusion

The utilization of a sequential workflow for deafness diagnosis and novel gene discovery increases sample throughput, is efficient and cost effective, and is highly likely to increase novel NSHL gene discovery in carefully selected probands from families segregating deafness.

PD - 011

The Newborn Mouse Inner Ear Hair Cell-Specific Transcriptome – Lessons From Microarray and RNA-Seq, and a Critical Comparative Analysis of Both Methods

Ran Elkon¹; Laura Morrison²; Lorna Silipino²; David Eisenman²; **Ronna Hertzano²**

¹The Netherlands Cancer Institute; ²University of Maryland School of Medicine

Background

Hair cells are the sensory cells of the mouse inner ear. Recent advances in cell separation techniques allowed us to isolate the different inner ear cell types of newborn mouse inner ear, hair cells included. In this presentation we critically compare the auditory and vestibular hair cell transcriptomes, as obtained via microarray and RNA-Seq analyses. We further discuss new and unique findings of hair cell-specific gene expression profiles.

Methods

Auditory and vestibular epithelia from newborn Math1/nGFP mice were dissociated and separated into Hair Cells (HC), Epithelial Non-Sensory Cells (ENSC) and Non-Epithelial Cells (NEC) using flow cytometry. Cell purity was greater than 94% for all sorted populations. We recorded gene expression from the sorted cells using (a) the Illumina MouseWG-6 v2.0 microarrays, and (b) RNA-Seq. Array data were analyzed using Bioconductor beadarray package; RNA-Seq data were aligned to the mouse genome (mm9) using TopHat. Only uniquely mapped reads were used in the analysis.

Results

Both methods detected ~11k-12k expressed genes, with an overall high concordance between the two techniques. RNA-seq measurements showed a greater dynamic range and improved sensitivity in detecting differential expression, especially for genes with a low level of expression. The improved dynamic range was primarily due to relatively high background signal in microarray measurements. As a set, the expression of mouse orthologues of human deafness genes was enriched in HCs. Importantly, as RNA-Seq does not rely on gene annotation it can be used to detect novel genes. We subsequently identified 32 long non-coding RNA (Lnc-RNA) genes whose expression is enriched in HCs. We also identified several dozen HC-enriched genes which map to known deafness loci, which were not detected by microarray analysis.

Conclusion

We present the first comparative analysis of the mouse inner ear hair cell-specific transcriptome using microarray and RNA-Seq, obtained from identical samples. RNA-Seq provides a much wider dynamic range in gene expression levels resulting in greater sensitivity for detecting differential gene expression. Mouse hair cells express a variety of hair cell-enriched Lnc-RNA whose role is yet to be explored. While some hair cell-unique transcripts are detected by RNA-Seq others transcripts may or may not be detected depending on the selected depth of sequencing. The decision of which approach to use for a given experiment depends on the specific goals of the experiment as well as budget-related concerns.

PD - 012

CHD7 and SOX11 Contributions to Inner Ear and Craniofacial Development

Ethan Sperry¹; Elizabeth Hurd²; Joseph Micucci¹; Nicole Corsten-Janssen³; Conny van Ravenswaaij-Arts³; Glenn Green¹; Donna Martin¹

¹The University of Michigan; ²University of Edinburgh;

³University of Groningen

Background

Tight regulation of gene expression is dependent on interactions of transcription and chromatin architecture. CHD7, a chromatin remodeling protein, is required for proper development of tissues affected in CHARGE syndrome, a multiple anomaly condition associated with craniofacial dysmorphisms and inner ear dysfunction. While mutations in *CHD7* occur in the majority of individuals with CHARGE, other genetic lesion(s) in the remaining patients have not been well defined. We identified a child with CHARGE syndrome and a chromosomal gain including *SOX11*. Mutations in *Sox11* (and the family member *Sox4*) result in severe CHARGE-like malformations in mice. Further, recent evidence suggests that CHD7 is necessary for proper expression of both *SOX4* and *SOX11* and for neurogenesis. While direct interaction between CHD7 and *SOX4/11* has not yet been defined, CHD7 interacts with *SOX2* in neural progenitor cells. Based on these observations, we hypothesized that CHD7 and *SOX4/11* may cooperate to promote proper development of CHARGE-related tissues.

Methods

We performed quantitative PCR on genomic DNA to test whether other *CHD7*-mutation negative CHARGE individuals also have altered dosage of *SOX11*. Changes in *Sox11* expression were assayed using RNA-seq, qRT-PCR, and *in situ* hybridization on microdissected otocysts or sections from E10.5 wild type and *Chd7* mutant embryos. Co-localization between CHD7 and *SOX11* was assayed by immunofluorescence on embryonic and adult mouse tissues. Finally, overexpression of *Sox11* in zebrafish was performed to assess for CHARGE-like phenotypes.

Results

No *SOX11* duplications were found in 28 unrelated, CHD7-mutation-negative CHARGE individuals. Interestingly, *Sox11* mRNA was significantly reduced in *Chd7* null otocysts

relative to wild type and heterozygous mice. Consistent with this result, SOX11 protein co-localized with CHD7 in neural, nasal, inner ear, and ocular tissues. Surprisingly, *Sox11* mRNA was reduced in the E10.5 *Chd7* null otocyst. Zebrafish injected with high dose (100 ng/uL), but not lower dose (1 or 10 ng/uL) of *Sox11* mRNA demonstrated body axis, neurologic, otologic, and cardiac phenotypes consistent with previous reports in *chd7*-deficient zebrafish.

Conclusion

We provide several lines of evidence from zebrafish, mouse, and human that proper dosage of SOX11 is critical for development of CHARGE-relevant organs and tissues. Further functional studies are underway to help clarify the molecular relationships between SOX11 and CHD7, which may be tissue and developmental-stage specific.

PD - 013

A Common Lipase: The Role of the Poorly Annotated Gene *C2orf43* in Hearing Loss, Obesity and Prostate Cancer

Benjamin Currall¹; Yanbo Yin²; Tatiana Hoyos³; Kristen Wong⁴; Eric Liao³; Charles Liberman²; Cynthia Morton¹

¹Brigham and Women's Hospital and Harvard Medical School; ²Massachusetts Eye and Ear Infirmary and Harvard Medical School; ³Massachusetts General Hospital and Harvard Medical School; ⁴Brigham and Women's Hospital

Background

Hearing loss is an extremely heterogeneous disorder. Currently, over a hundred genes have been associated with hearing loss and it is estimated that hundreds more may yet be identified. The Developmental Genome Anatomy Project (DGAP, www.dgap.harvard.edu) seeks to identify genes involved in disorders such as hearing loss by examining human subjects with chromosomal rearrangements. In DGAP056, a subject with a constellation of non-inherited phenotypes including various craniofacial anomalies, congenital profound sensorineural hearing loss and early onset prostate cancer (age 38), a *de novo* translocation between chromosomes 2 and 13 was detected disrupting the poorly annotated gene *C2orf43*.

Methods

Several standard methods are used including G-banded karyotyping, Sanger sequencing, fluorescence *in situ* hybridization (FISH), PCR, qPCR, 3' RACE, *in situ* hybridization, Western blot, H&E staining, auditory brainstem response (ABR) and distortion product otoacoustic emission (DPOAE).

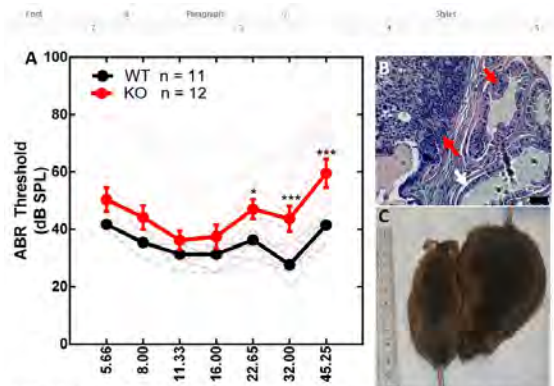
Results

Bioinformatic analyses suggest that *C2orf43* functions as a lipase and is associated with several diseases including lipodystrophy, type 2 diabetes and prostate cancer. *In vitro* analysis shows subcellular targeting of the protein product to lipid droplets. Embryonic expression of *C2orf43* is seen in the developing zebrafish and mouse inner ear. When *C2orf43* is knocked out in a mouse model, hearing thresholds, as measured by ABR and DPOAE, are elevated at high frequencies. Between the ages of 6 and 18 months, several knockout (KO, 2 out of 12) and heterozygous (Het, 3 out of 10) mice have

developed signs of prostate tumors, a finding not found in their wild-type (WT, 0 out of 9) littermates. Female KO mice have accelerated weight gain compared to their WT littermates and are morbidly obese by 18 months.

Conclusion

C2orf43 is involved in hearing loss. Furthermore, reduction of *C2orf43* leads to prostate tumors in males and obesity in female mice. While its biological mechanism is yet to be elucidated, *C2orf43* appears to act as a lipase and disruption of *C2orf43*'s function in lipid metabolism has consequences in diverse organ systems ranging from the prostate and adipose tissue to the inner ear.



C2orf43 KO mice have abnormalities in common with DGAP056 including (A) hearing loss as measured by auditory brainstem response (ABR) at 1 year and (B) the development of prostate cancer as seen in H&E staining of prostate tissue. Female KO mice also show increased (C) weight accumulation compared to their WT littermates as can be seen in gross photographic images (WT is on the left and KO on the right). Error bars represent S.E.M., * p<0.05, ** p<0.01 and *** p<0.001. White arrow indicates hyperplasia, red arrow indicates normal growth.

PD - 014

Death of a Hair Cell: How is the Auditory Apoptosis That Causes Acquired Hearing Loss Regulated?

Rachel Burt

Murdoch Childrens Research Institute

Background

Acquired hearing loss is a significant public health issue with 3 out of 4 people over the age of 70 years suffering a measurable degree of hearing impairment. Noise, and drug-induced hearing-loss are also common. The molecular mechanisms resulting in this condition are poorly understood. However, it is clear that programmed death (apoptosis) of sensory cells within the cochlea is often involved. **Objectives:** To understand the molecular regulation of sensory cell death in the ear so as to identify drug targets for prevention and treatment of acquired hearing loss.

Methods

A panel of engineered mouse strains harbouring mutations in apoptotic regulators is being assessed for hearing loss, to better understand apoptosis in the ear.

Results

Mutations in the intrinsic pathway of apoptosis have a profound effect on the auditory system. Deficiencies of certain apoptotic regulators can disrupt development of the ear, or result in progressive hearing loss in the adult.

Conclusion

Our work suggests that tightly regulated apoptosis is required for both development and maintenance of hearing. Targeting of apoptotic regulators may prove useful in prevention of auditory cell death and resultant hearing loss.

PS - 001

Age-Related Changes in Subcortical-Cortical Encoding and Categorical Perception of Speech

Gavin Bidelman¹; Joshua Villafuerte²; Sylvain Moreno²; Claude Alain²

¹University of Memphis; ²University of Toronto, Rotman Research Institute, Baycrest Centre for Geriatric Care

Background

Aging is associated with declines in a wide range of perceptual and cognitive abilities including decreased speech understanding. While speech processing deficits are partially peripheral (i.e. cochlear) in origin, difficulties can persist in the absence of measurable hearing loss suggesting that central brain processes play a critical role in governing auditory abilities late into life.

Methods

To elucidate the neurobiological basis of these perceptual speech listening deficits, we compared cortical and brainstem neuroelectric responses (ERPs) elicited by a categorical speech continuum in younger and older adults. Comparing multiple ERPs generated from different levels of the auditory system allows us to examine the interplay between brainstem and cortical representations of speech sounds and the effects of age on subcortical/cortical processing. Older adults had no worse than mild (< 35 dB) hearing loss at pure tone audiometric frequencies. All younger adults had normal hearing (better than 25 dB HL). Stimuli were presented at equal sensation level to control for audibility.

Results

Older adults showed reduced speech classification performance (slower and more variable identification) than younger adults. Behavioral deficits coincided with weaker onset and sustained brainstem phase-locking to speech cues (voice pitch and formants) concomitant with increased but delayed cortical ERPs. Neurophysiological responses were predicted by listeners' hearing sensitivity which showed negative (brainstem) and positive (cortical) correlations with evoked response amplitudes, respectively; brainstem responses were weaker and cortical responses stronger in older adults with more hearing loss. Additionally, older adults showed increased non-evoked EEG activity (i.e., "neural noise"), implying that speech representations undergo a decrease in signal-to-noise ratio with advancing age.

Conclusion

Collectively, our results show that normal aging produces decreased brainstem excitation and increased cortical dysinhibition to yield a differential impact on brain processing between subcortical/cortical levels of the central auditory nervous system. We conclude that age-related changes in speech

processing ultimately weaken the hierarchy of speech representations along the auditory pathway, consequently reducing the internal quality of phonemic templates necessary for robust speech understanding.

PS - 002

Aldosterone Augments Pre-Pulse Inhibition but not Startle Amplitude in Middle-Aged CBA Mice

Joshua Halonen; Ashley Hinton; Xiao Xia Zhu; Joseph Walton

University of South Florida

Background

The mineralocorticoid aldosterone (ALD) is released from the adrenal cortex and regulates Na⁺ and K⁺ flow across cell membranes. Previous research has demonstrated in humans that ALD serum levels correlates significantly with pure-tone thresholds. Furthermore, ALD treatment has been shown to significantly improve cochlear function, as measured by the auditory brainstem response, in autoimmune deficient mice. This experiment was designed to investigate if ALD treatment improves behavioral measures of hearing using pre-pulse inhibition (PPI) of the acoustic startle response (ASR).

Methods

Animals were placed on top of a platform connected to piezoelectric transducers located inside sound attenuated chambers. Prior to the presentation of the acoustic stimuli, animals were allowed 5 minutes to acclimate to the testing context. Acoustic stimuli were presented through Fostex speakers located 30 cm directly above the transducer platform. ASR input-output functions were collected by presenting the startle elicitor (20 ms wideband noise) at random inter-trial intervals between 10 to 20 seconds at intensities ranging from 55-115 dB, in 10 dB increments. Each level of stimulus intensity was presented 10 times for a total of 70 trials. Approximately 30 minutes after startle testing noise pre-pulse inhibition (PPI) testing occurred. PPI testing consisted of random inter-trial intervals of 15 to 30 secs. Pre-pulse stimuli were wideband noise, 50 ms in duration, and were presented at 20 and 40-70 dB SPL in 10 dB steps. The 20 ms startle eliciting stimulus was presented 30 ms after the pre-pulse at 100 dB, with 20 trials at stimulus each intensity. Baseline tests were followed by tests at 4 and 8 weeks post aldosterone pellet treatment. After baseline ASR testing, animals were randomly assigned to receive either placebo or a dose of 1.67 µg per day of D-aldosterone (Innovative Research of America, Sarasota, FL) administered by extended release pellets, implanted subcutaneously via syringe injection in a pocket of skin behind the shoulders.

Results

No significant differences were found in startle at baseline, 4 or 8 weeks post treatment. However, a significant difference at 8 weeks post treatment from baseline in PPI ($1 - \frac{PPI_{test}}{PPI_{baseline}}$) was found. ALD treated animals were found to have approximately 30% greater inhibition as compared to the control group at 40 dB and a 35% increase at 70 dB. The increased inhibition at 40dB indicates increased salience for

low level noise signals and indicates improvement in hearing sensitivity.

Conclusion

These results are the first we are aware of to demonstrate a behavioral effect on pre-pulse inhibition in CBA mice treated with aldosterone. The implications of these results, together with those of the accompanied poster, suggest that aldosterone treatment could be an effective way to rescue hearing function.

PS - 003

The Role of Age-Related Auditory and Cognitive Declines in Understanding Speech in Noise

Tim Schoof; Stuart Rosen

UCL

Background

Older adults often experience increased difficulties understanding speech in noise even in the absence of hearing impairment. This may be attributed to an auditory temporal processing deficit, although a decline in cognitive processing abilities likely also plays an important role. This study set out to examine the relative contribution of declines in both low-level auditory and higher-level cognitive processing to the difficulties older adults experience when perceiving speech in noise.

Methods

Participants included 19 older (60 - 72 yrs) and 19 younger (19 - 29 yrs) adults with normal hearing (thresholds <25 dB HL up to 6 kHz). Speech Reception Thresholds (SRTs) were measured for IEEE sentences in steady-state speech-shaped noise (SSN), 10-Hz amplitude-modulated speech-shaped noise (AMN), and two-talker babble. In addition, frequency following responses (FFR), reflecting neural encoding at the brainstem, were recorded to the vowel /a/ in quiet, SSN, and AMN. Temporal processing abilities were assessed by measuring thresholds for gap, amplitude-modulation, and frequency-modulation detection. Additionally, measures of processing speed, attention, working memory, and Text Reception Threshold were also obtained. Of primary interest is the extent to which the various measures correlate with listeners' abilities to perceive speech in SSN, AMN, and babble.

Results

Contrary to expectations, SRTs did not differ between the young and older adults. However, the FFRs of older adults were significantly degraded both in quiet and noise (SSN and AMN). In addition, older adults showed some cognitive processing declines (working memory and processing speed) although no declines in temporal processing.

Conclusion

The data suggest that central auditory processing declines with age even when peripheral hearing is normal. However, given the claim that the FFR primarily results from neural activity at more basal sites along the cochlea (Dau, 2003) the group differences may in fact be due to slight hearing losses at higher frequencies in the older adults.

The results furthermore show that despite declines in auditory and cognitive processing, normal hearing older adults do not necessarily have problems understanding speech in noise.

PS - 004

The Roles of Mitochondrial Isocitrate Dehydrogenase in Age-Related Hearing Loss

Mi-Jung Kim; Logan Walker; Chul Han; Paul Linser;

Shinichi Someya

University of Florida

Background

Mitochondrial isocitrate dehydrogenase 2 (IDH2) plays a critical role in the TCA (tricarboxylic acid) cycle in the mitochondrial matrix through converting isocitrate to α -ketoglutarate and reducing NADP⁺ to NADPH. IDH2 also plays a central role in regeneration of mitochondrial glutathione and thioredoxin by supplying NADPH to mitochondrial NADPH-dependent glutathione reductase and thioredoxin reductase. Evidence indicates that decreased expression of *Idh2* results in elevated levels of hydrogen peroxide and oxidative damage, while overexpression of *Idh2* protects the cells from ROS-induced cell death in mouse fibroblasts. Our preliminary evidence indicates that CR (calorie restriction) delays the onset of AHL (age-related hearing loss), reduces oxidative DNA damage and cochlear cell loss, and increases the activities of glutathione reductase and thioredoxin reductase, NADPH levels, and IDH2 activity in the mitochondria of mouse cochlea. Therefore, we hypothesized that mitochondrial IDH2 plays an essential role in the CR-mediated prevention of AHL, the most common sensory disorder.

Methods

To investigate whether *Idh2* is expressed in the mitochondria, cytosol, or nuclei in mouse cochlea, we performed colocalization analysis in the cochlear sections from wild-type mice using immunofluorescence confocal microscopy. To investigate whether *Idh2* knockdown promotes oxidative stress-induced cell death, we are currently conducting *in vitro* oxidative stress tests using H₂O₂, followed by cell viability tests in mouse inner ear cells (HEI-OC1) or human neuroblastoma cells (SHSY-SY) that are transfected with siRNA targeted to *Idh2*.

Results

We show that *Idh2* is present in the mitochondria of the hair cells, spiral ganglion neurons, and stria vascularis in the cochlea of mice.

Conclusion

We are currently investigating the roles of mitochondrial *Idh2* in protecting the cochlear cells from oxidative stress and/or slowing the progression of AHL under calorie restriction using *Idh2* KO mice. The results of this project will provide an enhanced understanding of the fundamental molecular mechanisms underlying AHL.

Fatty Acid-Binding Protein 7 Deficiency Slows the Progression of Age-Related Hearing Loss in Mice by Modulating Metabolic Pathways

Jun Suzuki¹; Takeshi Oshima¹; Ryuichi Kimura¹; Naohiro Yoshida²; Kaichi Yoshizaki¹; Yusuke Takata¹; Yuji Owada³; Tetsuaki Kawase¹; Toshimitsu Kobayashi¹; Yukio Katori¹; Noriko Osumi¹

¹Tohoku University Graduate School of Medicine; ²Jichi Medical University Saitama Medical Center; ³Yamaguchi University Graduate School of Medicine

Background

The fatty acid-binding proteins (Fabps) bind to fatty acids and mediate their uptake and transport, thereby regulating metabolic pathways and gene expression. In the mouse cochlea, Fabp3 and Fabp7 have been identified. Fabp3 has been reported to localize in spiral ganglion (SG) neurons and supporting cells in the organ of Corti (OC), and Fabp7 has been reported to localize in satellite cells in the SG, supporting cells in the OC, and fibrocytes in the spiral limbus and spiral ligament. However, the role of Fabps in the cochlea remains unknown. Here, we analyzed the role of Fabps, focusing on age-related hearing loss (AHL) and noise-induced hearing loss (NIHL).

Methods

Fabp3 (+/+), *Fabp3* (-/-), *Fabp7* (+/+), *Fabp7* (+/-), and *Fabp7* (-/-) mice on the C57BL/6 background were used. Auditory thresholds were measured by the ABR at several time points from young adulthood to old age and after acoustic overexposure. Cochlear morphology was assessed via HE staining, immunostaining, surface preparation method, and electron microscopy. Transcriptome analysis using DNA microarray was performed using *Fabp7* (+/+) and *Fabp7* (-/-) mice at 7 months. The results of the DNA microarray analysis were verified by quantitative RT-PCR.

Results

Fabp3 (-/-) mice exhibited no auditory phenotypes, both after aging and after acoustic overexposure. In contrast, the ABR thresholds of *Fabp7* (-/-) mice were significantly reduced at every frequency (4, 8, 12, 16, and 32 kHz) compared to *Fabp7* (+/+) mice at 12 months. *Fabp7* (+/-) mice showed milder levels of the phenotype. The ABR threshold of *Fabp7* (-/-) mice at 32 kHz was significantly decreased compared to *Fabp7* (+/+) mice at 2, 7, and 15-20 months. The numbers of SG neurons and fibrocytes were remarkably preserved in *Fabp7* (-/-) mice at 12 and 15 months. It also seemed that the numbers of OHCs were retained in *Fabp7* (-/-) mice at 7 and 12 months. Mitochondrial morphology in fibrocytes tended to be preserved in aged *Fabp7* (-/-) mice. *Fabp7* (-/-) mice were more resistant to the acoustic overexposure that causes TTS than *Fabp7* (+/+) mice. Transcriptome analysis indicated that Fabp7 deficiency caused up-regulation of carbohydrate metabolism-related genes and energy reservation-related genes and conversely caused down-regulation of lipid metabolism-related genes.

Conclusion

The lack of Fabp7 delayed AHL progression and caused NIHL reduction. The results of this study offer new insights into the functions of Fabp7 and reveal novel mechanisms of hearing preservation.

PS - 006

Morphological Predictors of Cortical Theta Band Desynchronization for Younger and Older Adults

Kelly C Harris; Mark A. Eckert; Judy R Dubno

Medical University of South Carolina

Background

Age-related changes in encoding of acoustic features are hypothesized to originate from neural desynchronization throughout the auditory system. Cortical neural synchrony can be estimated by measuring across-trial consistency of phase at specific frequencies of interest. Theta band activity has been shown to entrain to temporally modulated stimuli and these phase-locked oscillations are, in turn, associated with stimulus perception. Here, we examined age-related changes in cortical theta band phase locking. We used quantitative neuroimaging methods to examine the extent to which age-related differences in phase locking are associated with morphological differences in auditory cortex and temporal processing.

Methods

Gap detection thresholds were measured and EEGs were recorded from 24 younger adults and 24 older adults with normal hearing through 4.0 kHz. Age-related differences in theta phase locking values (PLVs) were assessed by averaging PLVs from 0 to 250 ms following gap onset from a cluster of electrodes where EEGs showed maximal activity and phase locking. Diffusion metrics of mean diffusivity (MD) and magnetic resonance spectroscopy [N-acetyl aspartate (NAA)] were acquired from a subset of 30 participants (15 older adults).

Results

PLVs were significantly lower for older than younger adults, and lower PLVs were associated with poorer gap detection. Moreover, individual and age-related differences in MD and NAA significantly predicted PLVs. Multiple regression demonstrated that the association between PLV, MD, and NAA remained significant after controlling for individual differences in total brain volume and pure-tone thresholds.

Conclusion

Neural synchrony is crucial for encoding time-varying acoustic cues, both for gap detection and speech recognition. Desynchronization of theta oscillations may limit the neural encoding for temporal features of auditory stimuli, thereby contributing to deficits in auditory processing. Associations between MD and NAA suggest that age-related differences in phase locking may be attributed to neuronal loss or changes in myelination, as increases in MD and decreases in NAA have been attributed to changes in white matter with neuropathology and aging. The current study was designed to tar-

get phase locking and morphological differences at the level of the cortex. Nevertheless, the results likely reflect the accrual of age-related changes in phase locking and morphometry throughout the auditory system, given that evidence consistent with neural desynchronization in older adults has been observed at the level of the brainstem.

PS - 007

Cortical Spectrotemporal Responses and Parvalbumin Expression in Aging Mice

Dustin Brewton; Khaleel Razak; Michael Trujillo
University of California, Riverside

Background

Presbycusis (age-related hearing loss) is the most common form of hearing impairment in humans and contributes to speech processing deficits in the elderly. Presbycusis affects 35% of people over 65 years old and 45% of those over 75. It is a major priority to understand the underlying neural deficits leading to speech processing impairment, so that proper treatment can be engineered. Presbycusis involves changes in the peripheral and central auditory systems. Human studies suggest that impairment in spectrotemporal processing may underlie speech processing deficits. Research has begun to tease out the neural correlates of altered spectrotemporal processing in mouse models, but the relative contributions of age and hearing loss remains unknown. The mouse strain C57BL/6 is homozygous for the accelerated hearing loss gene, which leads to significant hearing loss with age, while the CBA strain exhibits a reduced form of hearing loss with age. We utilize these two strains to distinguish the contributions of aging (CBA) and presbycusis (C57BL/6) to auditory cortex response property deficits and parvalbumin (PV) staining reductions.

Methods

Extracellular single unit electrophysiology is used to record neural response properties elicited by frequency-modulated (FM) sweeps of variable rates (0.14-11.667 kHz/ms) and directions (up/down) in young (1-3 mo) and old (12-16 mo) CBA and C57 mice.

Results

The profile of primary auditory cortical neurons is altered with age in the C57 strain, such that neurons are less selective for FM sweep rate, selectivity shifts to slower FM sweep rates, and there is increased variability in responses. Immunohistochemistry shows a reduction in the number of PV inhibitory interneurons in old cortex. Preliminary data also suggests increased bursting in the old cortex. We report a comparison of FM responses and PV expression between young and old CBA and C57 mice.

Conclusion

These data indicate a deficit in fast FM sweep processing as C57 mice age, and suggest a reduction in PV inhibitory interneuron as a possible basis. The comparison of CBA and C57 mice will provide a way to determine relative contributions of central aging and peripheral hearing loss to presbycusis-related cortical plasticity.

PS - 008

Aldosterone Reduces Spiral Ganglion Neuron Loss in Middle-Aged CBA/CaJ Mice

Xiaoxia Zhu; Bo Ding; Joseph P. Walton; Robert D. Frisina
University of South Florida

Background

Spiral ganglion neuron (SGN) degeneration with age is the one of the etiologies of presbycusis – age-related hearing loss (ARHL). We previously discovered that higher serum aldosterone (ALD) levels correlate with lower hearing thresholds in older human subjects [Tadros et al., *Hear. Res.* 2005]. In addition, SGN density declines 30% ~ 60%, from apex to base in old CBA/CaJ mice compared to the young adults [Tang et al. ARO Abstract# 632, 2013]. In our current study, CBA/CaJ mouse serum ALD levels declined with age, but were still within the normal range. In addition, we investigated how treatments with ALD affect mouse inner ear auditory function.

Methods

Four months (mon) ALD treatment mice (N=5), and same-age control mice (N=5) mice started treatments and testing at 16~17mon. Auditory brainstem responses (ABRs) were measured pre-treatment and post-treatment at 2 and 4 mon. Serum ALD level were quantitatively measured by ELISA. Cochlear sections were stained with Hematoxylin and eosin (H&E) and the SGN cells counted by Metamorph imaging software and data analyzed by GraphPad Prism.

Results

ABR thresholds elevated significantly in the control group at 4 mon of treatment relative to the ALD group at 24, 32 and 36 kHz. Serum ALD levels were higher in the ALD group. H&E staining showed that for the ALD treatment group, SGN density was higher than the untreated control mice throughout the cochlea and was correlated with ABR thresholds shifts in the same mice.

Conclusion

In closing, ALD may play a key role in preserving hearing and for modulating SGN degeneration in the aging cochlea, and ALD could be a component in developing treatments to prevent or slow the progression of ARHL.

PS - 009

Isoform Selectivity and Age-Related Expression of Na, K-ATPase in the Cochlear Stria Vascularis

Bo Ding; Xiaoxia Zhu; Robert D. Frisina; Joseph P. Walton
University of South Florida

Background

The endocochlear potential (EP) is critical for normal hearing and its dysfunction has been implicated in a number of types of hearing loss and deafness. Na,K-ATPase is one of the key ion channels responsible for generating the EP and is composed of four α subunits and three β subunits. Alteration of subunit isoforms in the cochlear lateral wall could contribute to hearing dysfunction, and age-related changes in Na,K-ATPase have not been previously investigated. The purpose of

the present report was to examine subunit alterations with age in the mouse cochlear lateral wall.

Methods

To avoid inconsistent and non-specific detection we combined RT-PCR, western blot and immunocytochemistry methodologies to assay subunit expression levels. Expression levels of $\alpha 1$, $\beta 1$ and $\beta 2$ subunit isoforms were detected in the lateral wall of young adult and old CBA/CaJ mice.

Results

We found that aging led to the down-regulation of all three Na,K-ATPase isoforms, and H&E staining revealed an atrophy of the cochlear stria vascularis (SV), suggesting that there is a combination of changes involving morphology and ion channel functional expression in the ageing cochlea. Specifically, immunoprecipitation assays showed that the $\alpha 1$ - $\beta 1$ heterodimer is the selective preferential heterodimer over the $\alpha 1$ - $\beta 2$ subunit isoform heterodimer. Interestingly, *in vitro* pathway studies utilizing cultured SV-K1 cells (cochlear marginal cells of SV), indicated that decreased mRNA and protein expression of $\alpha 1$, $\beta 2$ and $\beta 3$ subunit isoforms are not associated with Na,K-ATPase activity inhibition, as induced by ouabain, but this ouabain did disrupt the $\alpha 1$ - $\beta 1$ heterodimer activity. Lastly, the association between the $\alpha 1$ and $\beta 1$ subunit isoforms was present in the cochlea of young adult mice, but this interaction could not be detected in the old mice.

Conclusion

Taken together, these data suggest that there is a specific, functionally-selective assembly of Na, K-ATPase subunit isoforms in SV, which is disrupted and down-regulated with age. This age-related alteration in isozyme function as revealed by changes in inhibition may play a role in regulation of the $\alpha 1$ - $\beta 2$ heterodimer in the aged cochlea. Prevention of this age-linked ion channel dysfunction may serve as a target of biotherapeutic intervention for the treatment of age-related hearing loss.

PS - 010

Musical Experience and Hearing Loss: Perceptual, Cognitive and Neural Benefits

Alexandra Parbery-Clark¹; Samira Anderson²; Nina Kraus¹
¹Northwestern University; ²University of Maryland

Background

With age, understanding speech - especially in noisy environments, becomes more difficult. Findings from several research groups have recently showed that older adult musicians both with normal hearing and hearing loss have perceptual advantages for hearing in noise that are underscored by enhanced cognitive and neural speech-sound processing relative to age- and hearing- matched controls. While these findings highlight the positive effects of musical training for both normal-hearing and hearing-impaired older adults, musical experience is rarely considered in a clinical setting. Given that a musician's occupation puts him or her at risk for hearing loss, understanding how musicianship in a hearing-impaired population promotes hearing abilities relative to normal-hearing nonmusicians may improve clinical services to this population. Additionally, determining whether musical

experience minimizes the effects of hearing loss on biological, perceptual and cognitive processes would further support the use of music as a rehabilitative tool for individuals with hearing loss.

Methods

We recorded neural responses to a speech sound /da/ in 62 normal hearing and hearing impaired musicians and non-musicians (45-65 years) matched for age, IQ and sex; we focused our analyses on measures of neural response fidelity and variability. In addition to behavioural tests of auditory perception (i.e., frequency and temporal discrimination) and cognitive skills (i.e., auditory and visual memory), we also quantified subjective and objective clinical measures of speech-in-noise perception by administering a self-report questionnaire on which each individual rated their ability to hear in noise as well as QuickSIN and the Hearing in Noise Test.

Results

Older musicians with hearing loss outperformed age-matched nonmusicians with normal hearing on all perceptual, auditory-based cognitive and neural measures, highlighting the positive role of musical training in offsetting the negative effects of hearing loss. Musicians with hearing loss, however, did not rate their perceptual abilities higher than nonmusicians with normal hearing, suggesting a disconnect between their actual and self-perceived hearing ability.

Conclusion

Together, these results provide biological evidence for music promoting those mechanisms that support hearing in noise in an adult population, with implications for overcoming hearing loss. As such, we propose music training as a potential strategy for minimizing the widespread biological, cognitive and perceptual impacts of hearing loss on the human nervous system.

PS - 011

Estrogen Improves ABR Gap Responses Following Hormone Treatment in Middle Age Mice

Tanika Williamson; Xiaoxia Zhu; Joseph P. Walton; Robert D. Frisina

University of South Florida

Background

Previous studies have shown that gonadal hormones, such as estrogen and progesterone, have an impact on the auditory system. During middle age, the depletion of these hormones can contribute to age related hearing loss (ARHL), also known as presbycusis. For the present study, middle age CBA/CaJ mice, a strain that has been shown to lose their hearing similarly to that of many humans, were used to investigate how various hormone treatments can affect auditory temporal processing abilities. Auditory brainstem responses (ABR) and ABR gap-in-noise (GIN) responses were compared between each of the treatment groups to study the effects of sex hormones on the progression of ARHL.

Methods

For this particular study, 23 CBA/CaJ middle-aged mice were used; 18 female and 5 male (15-18 months old). The female mice were randomly placed into 4 groups that were based upon treatment: estradiol (E), progesterin (P), estradiol and progesterin (E+P) and placebo (Pb) via slow-released hormone pellets. A male mouse group served as an untreated comparison group. After being anesthetized, the mice underwent ABR GIN testing, which involved a wide band noise stimulus at 80 dB SPL, with gap-in-noise ranging from 0.1 to 48.1 msec. The amplitude of the response to the second noise duration (NB2) onset at the termination of the gap was measured (P1). Recovery ratios compared the P1 response for NB2 to the P1 response for the first noise burst (NB1). ABR testing was also performed on the mice, using a span of frequencies: 3 to 48 kHz.

Results

At 1 month after treatment began, recovery ratios for P1 amplitude levels significantly increased for animals treated with E. P1 recovery ratios for amplitude levels remained the same for the other subject groups. On the contrary, amplitude levels for treatment groups P and Pb *began to decline following treatment*. Meanwhile, ABR threshold shifts for subject groups, and results for later times post-treatment are under study.

Conclusion

The present study findings coincide with previous studies where estrogen had a positive effect on the auditory system; whereas, progesterone was shown to exacerbate ARHL. In conclusion, temporal processing measures can be used to show the effects of various gonadal hormones on the auditory system, and how they may interact with ARHL.

PS - 012

Age-Related Changes in the Stria Vascularis in C57BL/6 Mice

Mitsuya Suzuki

Toho University, Faculty of Medicine

Background

Previous studies have shown a failure of the basement membrane (BM) structure of the stria capillaries in 6- and 12-month-old C57BL/6 mice. The purpose of this study was to examine age-related changes in the stria vascularis of C57BL/6 mice.

Methods

C57BL/6 mice were grouped according to age as follows: 3 days, 8 weeks, 6 months, 12 months, and 15 months. Cationic polyethyleneimine (PEI) was used to examine age-related changes in the anionic sites of the BM of the stria vessels. After decapitation, the left bony labyrinths of 3-day-old, 4- and 8-week-old, and 6- and 12-month-old mice were immersed in a 0.5% PEI solution and embedded in epoxy resin. Ultra-thin sections of the cochlear lateral wall were examined using a transmission electron microscope. In 3-day-old, 4- and 8-week-old, and 6-, 12-, and 15- month-old mice, the right bony labyrinths were embedded in paraffin. Serial mid-modiolar 5-µm-thick sections were obtained to measure the

widths of the stria vascularis and were then incubated with anti-mouse IgG antibody.

Results

In 3-day-old mice, PEI particles were evenly distributed on the capillary BM of the stria vascularis and spiral ligament. The area of distribution of the PEI particles in the capillary BM of the stria vascularis in 8-week-old mice was smaller than that in 3-day-old mice. In 6- and 12-month-old mice, PEI particles were barely detected on the BM capillaries. A statistically significant difference was observed in the distribution of PEI particles between 3-day-old mice and 8-week-, 6-, and 12-month-old mice. The width of the stria vascularis tended to be greater in 4-week-old mice than in 3-day-old mice; however, the difference was not significant. In addition, the stria vascularis was narrower in 6-month-old mice than in 4-week-old mice; however, the difference was not significant. A significant difference in the width of the stria vascularis was observed between the 4-week-old and 12-month-old mice. The 3-day-old and 4-week-old mice barely showed any anti-IgG staining in either the stria vascularis or in the spiral ligament. IgG deposition was detected in the stria capillary BM in 8-week-, 6-, 12- and 15-month-old mice.

Conclusion

1. Age-related changes in the BM anionic sites begin before age-related atrophic changes in the stria vascularis.
2. The appearance of IgG deposition in the stria vascularis may reduce the anionic sites on the BM of the stria capillaries.

PS - 013

The Roles of Glutathione Reductase in Age-Related Hearing Loss

Chul Han¹; Hyo-Jin Park¹; Mi-Jung Kim¹; Logan Walker¹; Diego Rielo¹; Paul Linser²; Shinichi Someya¹

¹University of Florida; ²Whitney Laboratory, University of Florida

Background

Glutathione acts as the major small molecule antioxidant and is found mostly in the reduced form (GSH) in healthy cells. During aging, oxidized glutathione (GSSG) accumulates, and hence an altered ratio of GSH:GSSG is thought to be a marker of both oxidative stress and aging. Glutathione reductase (GSR) plays a critical role in preventing accumulation of GSSG and maintaining the appropriate redox environment in cells through regeneration of GSH, thereby enhancing the glutathione antioxidant defense system. We have previously shown that CR (calorie restriction) delays the onset of AHL (age-related hearing loss), reduces oxidative DNA damage and cochlear cell loss, and increases the activity of glutathione reductase and the GSH/GSSG ratio in mouse cochlea. Therefore, we hypothesized that Gsr plays an essential role in protecting the inner ear cells from oxidative stress and slowing the development of AHL.

Methods

To investigate whether Gsr knockdown promotes oxidative stress-induced cell death, we conducted *in vitro* oxida-

tive stress tests using H₂O₂, followed by cell viability tests in mouse inner ear cells (HEI-OC1) or human neuroblastoma cells (SHSY-SY) that are transfected with siRNA targeted to Gsr (knockdown of Gsr). To investigate whether Gsr is expressed in the mitochondria, cytosol, or nuclei in mouse cochlea, we performed colocalization analysis in the cochlear sections from wild-type and Gsr knockout (KO) mice using immunofluorescence confocal microscopy.

Results

We show that Gsr is present in the nuclei of the hair cells, spiral ganglion neurons, and stria vascularis in the cochlea of mice. Knockdown of Gsr increased susceptibility to oxidative stress-induced cell death in cultured mouse inner ear cells and human neuroblastoma cells.

Conclusion

These results suggest that GSR may play a key role in protecting nuclear macromolecules in cochlear cells against oxidative stress. Currently, we are investigating whether Gsr deficiency promotes AHL. Knowledge of these molecular mechanisms has enormous potential for improving health outcomes through the discovery/development of novel therapeutics for human AHL.

PS - 014

TrkB Mediated Protection Against Circadian Sensitivity to Noise Trauma in the Murine Cochlea

Inna Meltser; Christopher Cederroth; Vasiliki Basinou; Sergey Savelyev Savelyev; Gabriella Schmitz Lundkvist; Barbara Canlon

Karolinska Institute

Background

Noise-induced hearing loss is a permanent impairment affecting 10-15% of the population and there is no cure for this debilitating disorder. New innovative strategies are therefore needed. The identification of a robust circadian expression of *Period 2* mRNA transcripts in the mouse cochlea prompted us to evaluate if there is a functional response to this audio clock.

Methods

A battery of electrophysiological, morphological and molecular techniques were used in this study.

Results

Different recovery patterns were found in response to noise trauma delivered during day or night. Complete recovery was found 2 weeks after day trauma, whereas a permanent loss persisted after night trauma. Recovery from day noise trauma coincided with a greater induction of brain-derived neurotrophic factor (BDNF) mRNA transcripts in the cochlea compared to night trauma. *In vivo* administration of the selective TrkB receptor agonist 7,8-dihydroxyflavone (DHF) in the night, but not in the day, lead to a complete auditory recovery after noise and maintenance of inner hair cell synaptic integrity. *In vitro* application of DHF phase shifted and boosted the amplitude of cochlear PER2::LUC rhythms.

Conclusion

We report for the first time that noise trauma during the night contributes to more severe consequences compared to noise exposure given during the day and that this daily variance in noise sensitivity is adjusted by a self-sustained circadian cochlear clock gating the protective functions of TrkB on synaptic integrity. These findings highlight the coupling of circadian rhythmicity and TrkB receptor for the successful prevention and treatment of noise-induced hearing loss.

PS - 015

High-Fat Diets Delay the Progression of Age-Related Hearing Loss in C57BL/6J Mice.

Takeshi Fujita¹; Daisuke Yamashita²; Shingo Hasegawa²; Ken-ichi Nibu²

¹Nishi Kobe Medical Center; ²Kobe University Graduate School of Medicine

Background

Age-related hearing loss, known as presbycusis, is the most common sensory disorder in the elderly population. We used C57BL/6J mice as an age-related hearing loss model in this study to clarify the interaction between age-related hearing loss and high-fat diet (HFD).

Methods

Forty C57BL/6J mice were randomly assigned to control or HFD groups. They were then divided into the following subgroups: 1-month group, 3-month group, 5-month group, and 12-month group (HFD, n = 5; control, n = 5; each). Nine CBA/N-slc mice were also assigned to 12-month control (n = 5) or 12-month HFD (n = 4) group. Hearing function was evaluated at 1, 3, 5 and 12 months using auditory evoked brainstem responses (ABR). Spiral ganglion cells (SGCs) were counted.

Results

At 3 and 5 months, compared to the baseline, auditory brain stem response (ABR) threshold shifts were significantly decreased in the HFD group (at 32 kHz) compared with controls, in the C57BL/6J mice. After 12 months, ABR thresholds were significantly decreased in the HFD group at all frequencies, in the C57BL/6J mice. On the other hand, CBA/N-slc mice showed the opposite outcome in that, ABR thresholds were significantly increased in the HFD group compared with controls at all frequencies, at 12 months. These results in CBA mice showed similar findings to some previous reports. The numbers of SGCs in the 12-month group were significantly preserved in all portions of the cochlea in the HFD group in comparison with the control group.

Conclusion

C57BL/6J mice in the HFD group showed that the ABR threshold's elevation by aging and the loss of spiral ganglion cells were significantly suppressed compared with that in the normal-diet group. These results suggest that high-fat diets delay the progression of age related hearing loss in C57BL/6J mice.

PS - 017

Effects of Age on the ABR Wave I Latency and Amplitude in HET4 Mice

David Dolan; Karin Halsey; Jennifer Eberle; Lisa Kabara;
Ariane Kanicki; Richard Altschuler
KHRI

Background

Auditory processing problems are a common condition in the elderly. These processing disorders can occur in the absence of hearing loss. Kajawa and Liberman (2006) showed that early noise exposure, which does not cause PTS, can cause late life changes in neural structures leading to reduced Wave I amplitude of the ABR in older CBA/CaJ mice. These changes were associated with neural degeneration throughout the cochlea and loss of spiral ganglion cells. The same lab (Sergeyenko et al., 2013) showed evidence of synaptic loss below the IHC in unexposed older mice. This loss also occurred in the absence of hearing loss. In these mice (CBA/CaJ) the synaptic loss was correlated to a reduction in Wave I amplitude.

Here we describe changes in ABR waveform (Wave I) in an outbred mouse strain bred through a group of genetically heterogeneous mice (UM-HET4 stock) whose grandparents were from inbred stocks (MOLF/Ei, 129/S1/SvImJ, C3H/HeJ and FVB/NJ). Longitudinal ABRs were acquired at 8, 18 and 22 months of age. In addition to the ABR analysis, 25 animals were processed using CTBP2 immunostaining to measure the presence of synaptic ribbons at the base of the IHC as a marker for inner hair cell-auditory nerve (IHC-AN) connections.

Methods

The ABR was measured using TDT System III. Waveform latency and amplitude were measured using a software program provided by Joseph Walton, Ph.D. Histology: Mice were terminated with an injection of sodium pentobarbitol. The cochleae were placed in fixative, rinsed in PBS, and decalcified. The cochleae were pre-treated in phosphate buffered saline with calcium and magnesium, triton-100 and donkey serum. The cochleae were then placed in mouse anti-CTBP2 antibody. They received co-labeling with both goat anti-mouse immunoglobulin with an Alexafluor 568 fluorescent label and phalloidin with an Alexafluor 488 fluorescent label. Cochleae were then microdissected into three segments.

Results

Aged HET4 mice show significant (ANOVA, Systat) increases in Wave I latency by 18 months of age with further significant increases by 22 months. The increases in latency were present at threshold and suprathreshold stimulus levels. Wave I amplitude changes were less evident. However, there was a trend for reduced amplitude.

Analysis of CTBP2 in 26 month old mice showed a large variation at each location throughout the length of the cochlea. Values ranged from ~9 to 16 IHC-AN connections per inner hair cell. There was little correlation between Wave I latency and the number of CTBP2 markers.

Conclusion

The change in Wave I latency may be attributed to post synaptic events in the HET4 mouse.

PS - 018

Age-Related Structural Change in Blood-Labyrinth Barrier of the Stria Vascularis

Xiaorui Shi; Lingling Neng; Fei Zhang; Jinhui Zhang
Oregon Health & Science University

Background

A tightly controlled blood-labyrinth barrier (BLB) in the stria vascularis is critical for maintaining the ionic, fluid, and energy balance necessary for hearing function. Disruption of the BLB has long been considered a major etiologic factor in a variety of hearing disorders.

Methods

In this study, using confocal microscopy combined with fluorescence immunohistochemistry approach, auditory brainstem response (ABR) and endocochlear potential (EP) measurement, structural change in the blood-labyrinth barrier (BLB) of the stria vascularis was examined in an experimental set of age-graded C57BL/6 mice (1 month to 21 months).

Results

We found capillary density was significantly reduced in 6-month-old compared to 3-month-old mice ($p < 0.05$) and in 9-month-old mice ($p < 0.001$). Density of stria with normal capillaries varied greatly in aged animals, ranging from 0.0617 to 0.0548 mm capillary/mm² stria. Blood barrier accessory cells, including pericytes (PCs) and perivascular resident macrophages (PVMs), were also significantly reduced with aging (density of PCs dropped from 21/mm capillary at 1 month to 12/mm capillary at 21 months; density of PVMs from 352/mm² stria area to 247/mm² stria area.) Loss of PCs/PVMs is highly correlated with reduced capillary density. Hearing thresholds evaluated by auditory brainstem response shows a significant drop at all measured frequencies in aged animals, and the resting endocochlear potential (EP) also varied markedly, ranging from 76 to 104 mV.

Conclusion

Our results indicate significant correlation between capillary density and population of PCs and PVMs in the BLB. The results highlight the importance of PCs and PVM for maintaining stria vascularization and sustaining the EP and hearing function.

PS - 019**Methionine Sulfoxide Reductase A (MsrA) Expression in the Mouse Cochlea**

Marcello Peppi¹; Dianne Durham²; Mark Chertoff³; Jakob Moskovitz⁴; Hinrich Staecker²

¹University of Kansas Medical Center; ²University of Kansas Medical Center, Department of Otolaryngology/Head and Neck Surgery; ³University of Kansas Medical Center, Department of Hearing and Speech; ⁴University of Kansas-Lawrence, Department of Pharmacology and Toxicology

Background

Methionine sulfoxide reductases (Msrs), enzymes that protect the biological activity of proteins from oxidative modifications, are considered major players in preventing the biological effects of aging and the onset of age-dependent neurodegenerative diseases. Although two types of methionine sulfoxide reductase (MsrA and MsrB) have been identified, little information is known about the presence, distribution, and role of these proteins in the cochlea and in hearing. A previous study (Riazuddin et al, Am J Hum Genetics 2011) localized MsrB to the organ of Corti and spiral ganglion neurons and linked this protein to human deafness DFN74. In this study, we investigated the age-related expression and distribution of the MsrA protein in mouse cochlea, using quantitative qRT-PCR and confocal microscopy.

Methods

To examine the distribution of MsrA in the cochlea, mid-modiolar paraffin sections were prepared from cochleae of 6 to 90 days old B6/129F2 mice. Sections were incubated overnight with primary antibodies to MsrA and analyzed with a confocal microscope. Real-time quantitative PCR was used to assess MsrA mRNA levels in the cochlea. For each sample, the spiral ganglion and organ of Corti from both ears of B6/129F2 mice were pooled, dissected, and the RNA extracted. Real time amplification included a SYBER green super mix and a probe for mouse MsrA. 18S rRNA was used as an internal control.

Results

By P6, high levels of MsrA mRNA was detected by qPCR in the cochlea, and from P16 it declined rapidly followed by further decline reaching the lowest level at P60. Confocal microscopy analysis showed that MsrA expressed throughout the vestibule and the cochlea. At P6, MsrA staining appeared in the crista ampullaris, semicircular canals, vestibular ganglion neurons, lateral wall, spiral limbus, organ of corti, and spiral ganglion neurons. In the adult cochlea (P60), MsrA localized predominantly in the cytoplasm of spiral ganglion neurons and in inner and outer hair cells.

Conclusion

The age-related changes in MsrA expression that we observed support the idea that MsrA might also play a role in the biological effects of aging in hearing.

PS - 020**Effect of Aging on Parameter of Distortion Product Otoacoustic Emission**

Jae-Hun Lee; Ki-Hyeon Jang; Su-Jin Kim; Hey-Su Kim; Ji-Yeon Woo; Chul-Hee Choi

Catholic University of Daegu

Background

Since the first measurement of distortion product otoacoustic emissions (DPOAEs), DPOAEs have been thought to reflect the active mechanisms of the outer hair cells (OHCs) within the cochlea responsible for the presence of cochlear amplification which substantially increases hearing sensitivity, frequency selectivity, and wide dynamic range of the normal hearing in mammals. To check the function of OHCs, many researchers have used the similar parameters ($f1/f2$ ratio=1.2 and $L1-L2=0$ or 10) for DPOAEs ($2f1-f2$). However, these parameters do not optimize or maximize the response levels of DPOAEs. Therefore, this study investigated how different parameter values of DPOAEs affect DPOAE magnitude in aging. This study provides optimal parameters to maximize the DPOAE response in different aging groups.

Methods

Six college students aging from 21 to 25 years old were randomly participated as young subjects while other 6 elders aging above 55 years old were participated as old subjects. DPOAEs were measured with the OAE software [GSI AUD-ERA, Grason-Stadler Inc(GSI), Eden Prairie, MM, USA]. DPOAE recordings were acquired with a 10B+ microphone (Etymotic Research, Elk Grove Village, IL) placed 5mm from the tympanic membrane. In this study, $L1-L2$ was used from 0 to 20 in 5 step and $f1/f2$ ratio was used from 1.10 to 1.30 in 0.05 step. DPOAEs with different parameters in different aging groups were analyzed with ANOVA.

Results

When $L1-L2$ is 15, the differences of DPOAE between young and old subjects were observed. When $f1/f2$ ratio is 1.30, the differences of DPOAE between young and old subjects were observed. The optimal parameters of DPOAE were different for the different groups.

Conclusion

These results provide significant and important information to differentiate young adults with normal hearing from elders with normal hearing.

PS - 021**Decoding the Locus of Attention to Visual, Auditory, and Audiovisual Stimuli from Single-Trial EEG Data**

Lenny Varghese; Samantha W Michalka; Arash Yazdanbakhsh; David C Somers; Cara E Stepp; Frank H Guenther; Barbara G Shinn-Cunningham

Boston University

Background

Methods to decode the locus of spatial attention in real-time are of great interest to researchers working on brain-computer interfaces and auditory prostheses, as knowledge of

where attention is focused could be used by paralyzed individuals to control devices, or by hearing-impaired listeners to “intelligently” steer an advanced assistive listening device. Previous studies have decoded the focus of attention from either visual or auditory stimuli; here, we investigated changes in electroencephalography (EEG) signal strength associated with covert and overt attention shifts for audiovisual stimuli, as well as unimodal visual and auditory inputs. We applied pattern-classification techniques to decode the locus of spatial attention on single trials.

Methods

Participants were presented with 1) two polarity-reversing checkerboards (one per hemifield), 2) streams of consonant-vowel syllables (spatialized +/- 90 degrees), or 3) both. On each two-second trial, participants attended to one location to detect brief changes in contrast and/or intensity from stimuli in that direction. Polarity reversal and syllable onset timings were engineered to ensure that events from competing locations were uncorrelated. EEG data were recorded over two sessions: one with gaze fixated center-screen (covert attention), and one where eyes were directed to the attended location (overt attention). EEG data were preprocessed by filtering and removing eyeblink artifacts. Data dimensionality was reduced using spatial and temporal principal component analyses (PCA). PCA scores were used as features to train a linear support-vector machine, which then classified the direction of attention on a subset of trials not used for training.

Results

Average attend-left and attend-right trials differed significantly for all presentation modalities. Differences were strongest over parietal/occipital locations in visual conditions, and over central/parietal locations in auditory and audiovisual conditions. On covert trials, single-trial classification accuracy was slightly better than chance (approximately 60-70% for the best subjects), with no improvement for audiovisual presentation. Overt attention generally improved classifier performance, particularly in visual and audiovisual conditions (with near-perfect decoding accuracy in the best subject).

Conclusion

Work is underway to understand effects of attention on single-trial auditory EEG responses, and to determine the feasibility of our approach for decoding the locus of attention to auditory and audiovisual stimuli in real-time.

PS - 022

In Vivo and Modeling Study of Age Related Changes in Frequency Tuning and Spontaneous Activity in the Inferior Colliculus

Brandon Coventry; Emily Han; Aravindakshan Parthasarathy; Edward Bartlett

Purdue University

Background

The Inferior Colliculus (IC) is a major integrative auditory center, with converging excitatory and inhibitory inputs from several nuclei, each with different response patterns to changes

in tone frequency or noise center frequency. Frequency preferences and their sensitivities are described by frequency tuning curves (FTCs). Synaptic inhibition is a major factor in the tuning of these neurons, and previous studies have shown that changes in inhibitory input in IC have been associated with changes in the IC responses of aged animals, compounding age-related changes observed in inputs to IC. However, aging changes in FTCs observed in previous unit studies have been relatively small. The goal of this study is to better understand how neuronal FTCs are generated and how that may change with aging.

Methods

Simulating spike trains and frequency tuning properties provides a powerful tool to analyze factors that contribute to IC tuning changes under pathological conditions such as age related hearing loss. A biophysical, conductance based single compartment IC neuron model was constructed using NEURON and Matlab software. compared its response to the spike trains and tuning curves generated from *in vivo* recording of single unit responses obtained from young (3-5 months old) and aged (20-22 months old) rat ICs. Responses are evoked by sinusoidal tone stimuli with frequencies varying between 0.500 and 40 kHz in ≤ 0.1 octave steps 20-40 dB above threshold. In addition, band-passed noise stimuli with center frequencies from 1-36 kHz, 0.5 octave bandwidth were also presented.

Results

Consistent with a reduction in GABAergic inhibition, we found raised level of spontaneous activities in aged IC neurons, which has been repeated in the conductance model. Our preliminary data suggest that FTCs exhibit narrower tuning (in octaves) for higher best frequencies, with no clear differences in tuning between young and aged. As expected, tuning is much broader for noise stimuli in young and aged.

Conclusion

The study provides a working model to simulate, describe, and eventually predict synaptic activities regarding latency and frequency tuning with varying synaptic inputs and noises in young and aged animals. This model provides the ability to further probe the biophysical mechanisms of age related hearing decline. The IC frequency tuning model is highly flexible and can be used to investigate other mechanisms implicated in age related hearing loss.

PS - 023

Comparative Measurements of Distortion Product Otoacoustic Emissions and Frequency-Following Responses Evoked by Amplitude Modulated Tones in Young and Aged Rats

Jesyin Lai; Edward Bartlett

Purdue University

Background

Speech and natural sounds are dynamic signals with multiple time-varying modulations in amplitude and frequency. Temporal cue provided by amplitude modulation (AM) is crucial

for speech recognition. Even elderly listeners with normal hearing thresholds have difficulties to understand speech, especially in background noise. This study aims to identify the relationship of the cochlear gain modulation in AM processing compared with neural measures of central temporal processing.

Methods

Distortion product otoacoustic emissions (DPOAEs), evoked by AM tone/pure tone combinations, and frequency following responses (FFRs), evoked by the same stimuli as DPOAEs or by simple two-tone stimuli, were obtained from young (3-5 months) and aged (20-22 months) Fischer-344 rats. For DPOAE stimuli, either the lower tone (f1) or the higher tone (f2) was the AM tone. The ratio of f2/f1 was always fixed at 1.2 and f1 levels were 55-75 dB (f2 levels were 10 dB lower). The AM frequency was set at 45 or 128 Hz while the AM depths varied from 3 to 100 %. For simple two-tone stimuli, both tones were pure tones and the ratio of f2/f1 was not fixed. The values of Δf (f2-f1) were 0, 25, 50, 75, 100, 150, 250, 350 and 500 Hz. The carrier-frequencies of all the tones were in the range of 6.5-9.6 kHz.

Results

The young generally had larger amplitudes in their 2f1-f2 peaks than the aged in all conditions. The 2f1-f2 peak had multiple sidebands in AM evoked DPOAEs. When f1 pure tone/f2 AM tone combinations were used, the average amplitudes of the first lower and upper sidebands increased relatively linearly with increasing stimulus AM depth. The young had larger amplitudes in their first lower and upper sidebands than the aged. This coincides with our previous studies where the young exhibited higher FFR amplitudes for modulation frequencies at 128 Hz and 256 Hz. FFRs to the Δf were detected consistently in the young and their Δf thresholds were lower.

Conclusion

The 2f1-f2 modulation patterns measured in DPOAEs evoked by AM tones may serve as a predictor for peripheral AM detection. The FFRs evoked by the same AM tones or simple two-tone stimuli reflect the central temporal processing abilities. By comparing the responses of DPOAEs and FFRs, the relationship of the cochlear gain modulation in AM processing with the central temporal processing can be established. This will allow us to identify the relative contributions for age related temporal processing deficits.

PS - 024

Mapping the Call Perception Circuit in Awake-Behaving Wild Type Mice and Genetic Models of Speech and Language Disorders

Gregg Castellucci¹; Matthew McGinley²; Justus Verhagen³; David McCormick²

¹Yale University, Haskins Laboratories; ²Yale University;

³John B. Pierce Laboratory, Yale University

Background

The perception of speech is thought to rely on rapid and precise interactions between an array of brain regions (Acker-

mann, Trends in Neuroscience 31 (6): 265-72, 2008; Hickok & Poeppel Nature Reviews Neuroscience 8: 393-402, 2007). We hypothesize that a similar network underlies the perception of conspecific calls in mice, and we aim to elucidate its functional anatomy in awake-behaving mice. To test this hypothesis, we will use GCaMP population calcium imaging and electrophysiological recording to examine neuronal activity in the auditory cortex and other areas such as motor cortex and the cerebellum during call perception, as these regions are noted to be important in speech perception (Ackerman, 2008; Meister *et al.*, Current Biology 17: 1692-6, 2007).

Methods

Functional mapping will be performed in mice that have been exposed to vocalizations as well as age-matched controls with no vocalization exposure in order to determine the role of experience in circuit development. A final test group will consist of mice that have been socially isolated but exposed to sound in the frequency range of mouse vocalizations. Mice in each group will be imaged while being presented with excerpts of male mouse courtship song recorded in our laboratory, as well as pitch-matched tone pips and/or modulation-spectrum matched noise stimuli. These experiments will elucidate the role of exposure to and production of vocalizations in development of the call perception circuit.

The underlying causes of speech and languages disorders remains largely unexplored, particularly at the cellular and circuit level. Therefore, we will compare functional maps of the call perception circuit of wild type mice and genetic models of speech and language disorders. We will conduct parallel experiments to the above physiological studies in mice with a single functional copy of Foxp2 – a gene implicated in Specific Language Impairment. In addition, we also hope to conduct the same studies in Dcdc2 in Kiaa0319 knock-out mice, as these genes are associated with dyslexia (Gibson & Gruen, Journal of Communication Disorders 41: 409-420, 2008).

Results

No results are available for reporting at the time of this submission, but data will be collected in the following months.

Conclusion

In sum, we hope these studies will provide insight into the proper development of the mouse call perception circuit while providing circuit-level data about the function of genes known to be associated with speech and language disorders.

PS - 025

Hearing Loss in C57BL6/J Mice Is Not Influenced by Dietary Supplement With ACEMg or CEMg

Colleen Le Prell; Karessa White; Caitlin Simmons; Thomas Babcock; Yunea Park; Christopher Spankovich
University of Florida

Background

The use of nutritional supplements to modify hearing loss during aging has had mixed success. Across studies, species, strain, and active agents have varied. Here, we assessed the combination of β -carotene, vitamins C and E and

magnesium ("ACEMg"), as well as a combination in which β -carotene was omitted ("__CEMg"), for potential benefit in a mouse that experiences rapidly progressive high-frequency hearing loss. ACEMg has been shown to reduce hearing loss after noise insult by attenuating free radical formation in the inner ear, and daily supplement use to prevent slowly progressive changes in hearing after occupational noise might one day be possible. Free radical formation likely contributes to age-related hearing loss; it is therefore worthwhile to establish the effects of long-term supplement use on the aging ear in the absence of noise insult.

Methods

Female C57BL/6J mice were maintained on nutritionally complete control diets (TD. 07123) or one of two experimental diets (ACEMg: TD. 120071; __CEMg: TD. 120072). Mice arrived at 6-weeks of age, acclimated, and underwent baseline threshold assessment at 8 weeks of age using sound-evoked auditory brainstem response (ABR) measurements at frequencies of 5, 10 20, and 28.3 kHz. Complete input-output functions were collected (1026 averages per frequency x level combination, with tone levels presented from 90 dB SPL to 0 dB SPL, in 10-dB step sizes). Subjects were randomly assigned to study diets at 8 weeks of age after baseline tests. ABR measurements were repeated at 4-, 5-, and 8- months of age.

Results

Maintenance on the supplemented diets did not alter effects of aging on hearing loss as measured using ABR threshold. In addition, there was no difference in amplitude of ABR wave I as a function of maintenance on supplemented diets from 8 weeks to 8 months of age compared to age-matched controls.

Conclusion

Dietary antioxidant therapy has been suggested to have the potential to deliver a safe and cost-effective strategy for prevention of acquired hearing loss, including hearing loss secondary to noise, aminoglycoside insult, and perhaps even aging. While age-related hearing loss has been attenuated in some studies, including studies using the C57BL6/J mice used here, the current data provided no evidence of benefit for prevention of age-related hearing loss. Threshold shift and changes in ABR Wave I amplitude were equivalent across groups assigned to different dietary conditions. Additional investigation is needed to resolve discrepancies across studies.

PS - 026

ERK2 Mediates Hair Cell Survival and Protects Noise-Induced Hearing Loss in Mice

Takaomi Kurioka¹; Takeshi Matsunobu¹; Yasushi Satoh²; Katsuki Niwa¹; Atsushi Tamura¹; Akihiro Shiotani¹

¹Department of Otolaryngology, National Defense Medical College, Tokorozawa, Saitama, Japan; ²Department of Anesthesiology, National Defense Medical College, Tokorozawa, Saitama, Japan

Background

Noise-induced hearing loss (NIHL) is a major form of acute sensorineural hearing loss. The audiological features and cochlear morphology of NIHL are well characterized, but the molecular process in the development of NIHL is not well-elucidated. The extracellular signal-regulated kinase 2 (ERK2) is one of a family of mitogen-activated protein kinases (MAPKs) and coordinately regulate gene expression, mitosis, metabolism, motility, cell survival, apoptosis, and differentiation. ERK2 is activated by phosphorylation of both threonine and tyrosine residues in response to a variety of extracellular stimuli such as acoustic trauma. However, the specific role of ERK2 in the auditory function is not fully understood. Here we show that ERK2 play an important role in regulating hair cell survival and NIHL in mice.

Methods

Erk2 knockout mouse is embryonically lethal (Satoh et al.,2007). We created conditional *Erk2* knockout mice to delete the *Erk2* gene primarily in the inner ear using Cre/loxP system. *Erk2*^{fllox /fllox} mice were bred to transgenic mice with cre recombinase under the control of the promoter of Pou4f3 (Pou4f3-cre), a hair cell-specific transcription factor. Resultant hair cell-specific *Erk2* knockout (h*Erk2* KO) and control mice were viable and fertile with normal appearance. For this experiment 8 weeks old mice were used. These h*Erk2* KO and control mice were exposed to 126dB SPL 4-kHz octave band noise for 5 hours. Animals in each group underwent measurements for auditory brainstem response (ABR) before and immediately after noise exposure, and 1, 2, 4 weeks after noise exposure. Furthermore outer hair cells (OHCs) and inner hair cells (IHCs) loss of the cochlea was examined using surface preparation technique at 4weeks after noise exposure.

Results

Immunohistochemical staining revealed that ERK2 is expressed in supporting and hair cells of control mice but not in h*Erk2* KO mice. After noise exposure control mice demonstrated a moderate recovery of ABR threshold shifts, however, no significant recovery was found for h*Erk2* KO mice. There was significant difference in ABR threshold shifts between h*Erk2* KO and control mice. Furthermore a significant lower survival rate of OHCs and IHCs were observed of h*Erk2* KO mice as compared to control mice.

Conclusion

We found that h*Erk2* KO mice exhibited an increased sensitivity to noise exposure, suggesting that ERK2 plays an important role in protecting the organ of Corti from noise ex-

posure. The results of this study will make clear the cellular mechanisms underlying NIHL.

PS - 027

Maxipost, a Potassium Channel Modulator Demonstrates High-Frequency Protection Against Salicylate-Induced Hearing Loss

Adam Sheppard; Guang-Di Chen; Richard Salvi
University at Buffalo

Background

It is well known that salicylate induces a peripheral hearing loss by reduction of the prestin-mediated amplification in outer hair cells (OHCs). However, more recent studies indicate that salicylate can influence cochlear KCNQ4 channels, which regulate the flow of potassium ions and membrane potential in sensory cells. Thus, in addition to modifying prestin, salicylate could alter the membrane potential of hair cells and reduce the transduction currents responsible for OHC electromotility and inner hair cell synaptic function. Potassium channels within the cochlea show a frequency-dependent distribution with the highest expression in the basal high-frequency region of the cochlea. Maxipost, a potassium modulator originally developed as a treatment for stroke, has been shown to be neuroprotective and suppress salicylate-induced tinnitus. Since KCNQ channels are abundantly expressed in the cochlea, we hypothesized that Maxipost might affect the cochlear potentials alone or in combination with sodium salicylate (SS), a well known ototoxic drug that induces tinnitus and hearing loss.

Methods

To test this hypothesis, we measured the cochlear microphonic (CM) and the compound action potential (CAP) amplitude from the cochlea of rats treated with saline (control), sodium salicylate (SS) (200mg/kg), Maxipost (10mg/kg), or a combination of SS and Maxipost. Recording were made from the round window of the cochlea using a silver wire electrode and responses were elicited with tone bursts.

Results

Maxipost alone and SS alone had little or no effects on the CM. Likewise, Maxipost alone had little or no effect on the CAP. By contrast, salicylate alone caused a significant reduction in CAP amplitude and an elevation in thresholds. Interestingly, CAP amplitudes elicited by high frequency tone bursts (>24 kHz) were significantly greater in rats treated with Maxipost plus SS than SS alone. These results suggest that Maxipost partially blocked the ototoxic effects of SS at the high frequency, but did not demonstrate protective influence at the mid and low frequencies (2-16 kHz).

Conclusion

Our CAP data demonstrate that Maxipost blocks the ototoxic effects of SS in the high frequency region of the cochlea. This frequency-dependent protective effect may be related to base-to-apex distribution of KCNQ along the cochlea.

PS - 028

D-Methionine Reduces Tobramycin-Induced Ototoxicity Without Antimicrobial Interference

Kathleen Campbell; Daniel Fox; Melissa Roberts; Susan Yanik; Robert Meech; Tim Hargrove; Steven Verhulst; Leonard Rybak; Morris Cooper
Southern Illinois University School of Medicine

Background

Tobramycin is a highly efficacious aminoglycoside whose clinical use is restricted by adverse side effects; including hearing loss. If tobramycin-induced toxicities could be reduced or alleviated without compromising antimicrobial efficacy, then aminoglycosides would become critical combatant tools against resistant gram negative infections without detrimental side effects. D-methionine (D-met) has demonstrated safe protection from a variety of ototoxic agents and noise exposures. However, D-met otoprotective dose response from tobramycin-induced ototoxicity and potential antimicrobial interference has not yet been tested with D-met/tobramycin combinations. This study has tested D-met otoprotection from tobramycin-induced ototoxicity and potential antimicrobial interference.

Methods

Electrophysiological studies included six guinea pig groups (n = 10) treated with tobramycin and D-met doses ranging from 0 (saline control) to 480 mg/kg/day D-met in 60 mg/kg/day increments. Two, 4, and 6-week post-drug induction ABR threshold shifts and post-6-week ABR assessment outer hair cell (OHC) quantifications were analyzed.

Antimicrobial interference studies comprised *in vitro* and *in vivo* studies. *In vitro* tested inhibition assays at and above minimum inhibitory concentration (MIC), and post antibiotic effect (PAE) at and above MIC. *In vivo* analysis tested for D-met-induced antimicrobial interference with *E. coli* murine model survival studies and intraperitoneal (ip) lavage bacterial counts.

Results

D-met conferred highly significant dose-sensitive permanent ABR threshold shift reductions ($p \leq 0.01$) relative to controls. Optimal otoprotective D-met dose occurred in the 360 to 420 mg/kg/day range. OHC quantification measured increases in percent OHC present; with post-hoc analysis indicating significant OHC increases at 20 kHz in the 420 mg/kg/day D-met dosing group.

Time course and PAE studies did not detect antimicrobial interference between D-met and aminoglycosides. *E. coli*-infected murine model survival and ip lavage bacterial counts confirmed *In vitro* study observations; indicating no D-met-induced antimicrobial interference.

Conclusion

Overall results indicate significant D-met protection from tobramycin-induced ototoxicity and no significant antimicrobial interference in D-met/tobramycin combinations. These findings and previous otoprotective studies suggest concurrent D-met administration with an aminoglycoside will not interfere

with antimicrobial activity and also protect from aminoglycoside-induced hearing loss. The study results may impact future clinical use; particularly in vulnerable patient populations who are prescribed tobramycin for acute and chronic bacterial infections who may incur permanent hearing loss.

PS - 029

Protective Effect of Silymarin Against Cisplatin-Induced Ototoxicity

Sung-II Cho; Jun Han Lee; Hun Jae Oh
Chosun University

Background

Silymarin is a plant extract with strong antioxidant properties in addition to anti-inflammatory and anticarcinogenic actions. Anti-oxidant and anti-apoptotic properties of silymarin may have protective role against cisplatin-induced ototoxicity. The aim of this study was to investigate the potential preventive effect of silymarin on cisplatin ototoxicity in an auditory cell line, HEI-OC1 cells.

Methods

Cultured HEI-OC1 cells were exposed to cisplatin (30 μ M) with or without pre-treatment with silymarin (50 μ M). Cell viability was evaluated using MTT assay. Hoechst 33258 staining was used to identify cells undergoing apoptosis. Western blot analysis was done to evaluate whether silymarin inhibits cisplatin-induced caspase and PARP activation. Cell-cycle analysis was done by flow cytometry to investigate whether silymarin is capable of protecting cisplatin-induced cell cycle arrest.

Results

Cell viability significantly increased in cells pretreated with silymarin compared with cells exposed to cisplatin alone. Pre-treatment of silymarin appeared to protect against cisplatin-induced apoptotic features on Hoechst 33258 staining. Cisplatin increased cleaved caspase-3 and PARP on western blot analysis. However, pre-treatment with silymarin inhibited the expression of cleaved caspase-3 and PARP. Silymarin did attenuate cell cycle arrest and apoptosis in HEI-OC1 cells.

Conclusion

Our results demonstrate that silymarin treatment inhibited cisplatin-induced cytotoxicity in the auditory cell line, HEI-OC1. Silymarin may be a potential candidate drug to eliminate cisplatin-induced ototoxicity.

PS - 030

The Potential of Human Induced Pluripotent Stem Cells for Spiral Ganglion Neuron Replacement in the Deaf Cochlea

Niliksha Gunewardene¹; Mirella Dottori²; Karina Needham¹; Bryony Nayagam³

¹Department of Otolaryngology, University of Melbourne;

²Centre for Neural Engineering, University of Melbourne;

³Department of Audiology and Speech Pathology, University of Melbourne

Background

The irreversible loss of spiral ganglion neurons (SGNs) that occurs due to deafness may compromise performance with a cochlear implant. Therefore investigations in our laboratory are focused on using human stem cells to substitute lost SGNs. The aim of this project is to examine the potential of human induced pluripotent stem cells (hiPSCs) for SGN replacement. As these cells can be obtained directly from the patient, they offer the possibility of using patient-matched SGNs combined with a cochlear implant for the treatment of hearing loss.

Methods

An established neural induction protocol was used to differentiate two hiPSC lines (hiPS1 and hiPS2) and one human embryonic stem cell (hESC; H9; control) line towards a neurosensory lineage *in vitro*. Immunocytochemistry and qPCR were used to examine the expression of a cohort of SGN developmental markers at defined time points of differentiation. The hiPSC and hESC-derived neural progenitors were then co-cultured with cochlear explants obtained from P3/P4 rat pups for up to 10 days *in vitro* (DIV).

Results

Both hiPSCs and hESCs expressed the SGN markers, Pax7, Pax2, Sox2, NeuroD1, Islet1, Brn3a, GATA3, Neurofilament 160kDa, β III-tubulin, Peripherin and VGLUT1 over the time-course examined. The highest expression levels of these markers were observed after four weeks of differentiation (28 DIV). Interestingly, the differentiation potential of the hiPSC lines was variable when compared with other hiPSC lines and to hESC controls. These results were supported using qPCR. In co-cultures, the hiPSC- and hESC-derived neural progenitors extended processes towards and along the rows of hair cells in cochlear explants. The hiPSC and hESCs were capable of making direct contact with both inner and outer hair cells. However, the hiPSCs (n=16) made contact with fewer hair cells compared to the hESCs (n=12).

Conclusion

These findings suggest that hiPSCs can differentiate into SGN-like neurons and form direct connections with hair cells *in vitro* but with a lower efficiency compared to hESCs.

Temporal Bone Histopathology in Drug Addiction and the Expression of Mu Opioid Receptor in the Human Inner Ear

Kimanh Nguyen; Ivan Lopez; Gail Ishiyama; Akira Ishiyama

UCLA Medical Center

Background

Within the past forty years, there have been multiple reports of patients experiencing both reversible and irreversible, profound or rapidly-progressive sensorineural hearing loss secondary to opioid use. These opioids have included heroin, cocaine, methadone, hydrocodone/acetaminophen, oxycodone/acetaminophen, and codeine, among others. Opioid receptors have recently been found in the inner ear of the rat and guinea pig, but the etiology of opioid-associated hearing loss remains unknown and opioid receptors have yet to be identified in the human ear. One leading theory explaining this hearing loss involves opioid-induced vasospasm leading to cochlear ischemia and subsequent hearing loss. Herein we demonstrate the presence of Mu opioid receptor within the human inner ear, and examine temporal bone histopathology in heroin addicts with particular attention to inner ear vasculature.

Methods

Four temporal bones from two adults (ages 37 and 40) with longstanding heroin addiction encompassing 18-22 years were examined under light microscopy and compared with that of an adult with no otologic history. Temporal bone removal, inner ear tissue processing, and immunocytochemistry methods have been described in detail (Balaker AE et al., *Anat Rec*, 296:326-332, 2013). Formalin fixed frozen and celloidin embedded sections of the cochlea and vestibular endorgans were immunoreacted with antibodies against rabbit polyclonal antibodies for Mu opioid receptor.

Results

Mild atrophy of the stria vascularis adjacent to the spiral prominence was found in one patient with heroin addiction, while the other patient had thickening of the basement membrane of the stria vascularis. However, no significant differences were found in the appearance or the blood vessel diameter of the modiolous, spiral ligament, organ of Corti, basilar membrane, spiral lamina, or spiral prominence in either the basal, middle, or apical turns of the cochlea. The saccule and crista ampullaris also appeared normal. Immunocytochemistry demonstrated the existence of Mu opioid receptor in the cytoplasm of the spiral ganglion neurons of the cochlea and in the nerve terminals that surrounded the type I hair cells of the macula utricule.

Conclusion

Examination of temporal bones from two heroin addicts showed evidence of mild atrophy of the stria vascularis and thickening of the stria vascularis basement membrane. However, no differences in vessel diameter were noted when compared to normal temporal bones. Mu opioid receptor was found in the cochlea and macula utricule, corroborating recent

animal studies, and also pinpointing the likely site of insult and suggesting a possible mechanism of opioid-associated sensorineural hearing loss.

Proteomic Analysis of the Mouse Cochlea in Lipopolysaccharide Induced Endotoxemia Model

Jae Hong Park¹; Ah-Nam Choi¹; Yoon Chan Rah¹; Kyung Tae Park¹; Ki Soon Dan²; Yang Sun Choi²; Sang Hoon Song²; Ja-Won Koo¹

¹Seoul National University Bundang Hospital; ²Seoul National University Hospital

Background

Bacterial sepsis had been shown to potentiate inner ear uptake of aminoglycoside not only by increased serum level of aminoglycoside secondary to poor renal function, but also by increased permeation of aminoglycoside across the blood-labyrinthine barrier into the stria. In the present study, we investigated protein expression profiles of the organ of Corti (OC) and the lateral wall (LW) of murine cochlea in lipopolysaccharide (LPS) induced endotoxemia model to explore the mechanisms related to increase the permeability of blood-labyrinth barrier.

Methods

LPS (10 mg/kg) was injected intraperitoneally in C57BL/6 mice (15~20g, 5 weeks old, N=10) to induce endotoxemia models. Same volume of phosphate-buffered saline (PBS) was injected for control (N=10). The OC and LW were separately harvested 24 hours after injection. Samples were prepared and loaded into 2-dimentional nanoUPLC/Q-tof mass spectrometer. ProteinlynxGlobalServer 2.4 with Identity^E informatics and Swiss-prot mouse database were utilized for data processing and searching, and gene ontology analysis.

Results

256 and 352 proteins were identified from the OC and the LW, respectively, and a total of proteins were 409. In the OC, 6 proteins were up-regulated two-folds or more, 19 down-regulated half or less, 65 newly expressed after LPS injection, 37 newly expressed after saline injection, while 4 up-regulated, 8 down-regulated, 131 newly expressed after LPS injection, and 14 newly developed after saline injection in the LW. Alpha-tectorin and carcinoembryonic antigen-related cell adhesion molecule 16 were down-regulated in the OC, while cochlin and Myosin IX, most widely expressed in both the OC and the LW and expressed only in the LW, respectively, remained constant. Macrophage migration inhibitory factor, known as a pro-inflammatory cytokine, was up-regulated in the LW with constant in the OC, indicating the LW seems to response to bacterial pathogens more sensitively than the OC by systemic LPS injection. Potassium-transporting ATPase alpha chain 2, essential for ion homeostasis and hair cell polarization, was significantly down-regulated in the LW with constant in the OC.

Conclusion

Gene ontology for the up/down regulated proteins in the OC and LW was established, and biological processes, cellular components and molecular functions were revealed. Investigating the role of modulated proteins in sepsis is necessary to unveil the mechanism of sepsis induced aminoglycoside ototoxicity.

PS - 033

DNA Repair Adjuvant Therapy Regenerates Neural Sensitivity When Administered After Noise Trauma

O'neil Guthrie¹; Jinwei Hu²; Helen Xu²

¹Loma Linda Veterans Affairs Medical Center; ²Loma Linda University Medical Center

Background

Previous research has demonstrated the existence of an inducible DNA repair pathway within spiral ganglion neurons (Guthrie et al, *Hear Res* 239, 79-91, 2008; Guthrie and Xu, *Hear Res* 294, 21-30, 2012). After noise exposure or cisplatin intoxication, there is active transcription and intracellular translocation of DNA repair enzymes within a distinct population of neurons. Recent experiments have shown that carboxy alkyl esters (CAEs) that have been standardized to increase intracellular DNA repair can augment the capacity of spiral ganglion neurons to mobilize DNA repair enzymes (Guthrie, *Int J Neurosci* 122, 757-766, 2001). However, it is unclear whether such mobilization of DNA repair enzymes would restore neural sensitivity after trauma. Therefore in this study, we investigated whether or not adjuvant therapy with CAEs that begins after noise trauma could restore neural sensitivity.

Methods

Long-Evans rats were used as subjects and they were randomly divided into four experimental groups: vehicle-control, noise, CAE and noise+CAE. Hair cell and neural sensitivity were monitored with distortion product otoacoustic emissions and auditory brainstem responses.

Results

The noise trauma was severe enough to cause a permanent and complete loss of both hair cell and neural sensitivity. However, treatment with CAEs starting 1 day after the noise trauma, resulted in statistically significant ($p < 0.5$) recovery in neural sensitivity with just 7 days of post-trauma treatment. At 28 days of post-trauma treatment with CAEs, neural sensitivity was restored to approximate baseline sensitivity and the sensitivity of the control group.

Conclusion

These results suggest that DNA repair adjuvant therapy may rescue neural functions when administered after injury.

PS - 034

Diametric Effect of "Localized" Thermal Exposure on Cisplatin Induced Ototoxicity

Christopher Spankovich; Edward Lobarinas; Colleen Le Prell

University of Florida

Background

Hyper- and Hypothermic exposure has been demonstrated to provide protection from acoustic trauma, transient cochlear ischemia, and surgical trauma to the cochlea. Here we examined the effects of thermal treatment on cisplatin induced ototoxicity.

Methods

Guinea pigs were exposed to a local thermal manipulation either using cool (hypothermic), body temperature (euthermic), or warm water (hyperthermic) irrigation of the external ear canal and compared to non-treated controls (i.e., no thermal exposure). The animals were then injected with cisplatin (12 mg/kg, i.p.). Auditory brainstem responses (ABR) were performed (2 to 24 kHz) pre-treatment and 3-days post cisplatin injection. Animals were sacrificed after physiological testing and prepared for histological assays. The tissue was washed, stained, surface preparations created, and mounted on glass slides for view under fluorescence microscopy.

Results

The physiological and histological findings demonstrated that the euthermic exposure group had elevated ABR thresholds and loss of hair cells consistent with the cisplatin only condition (control animals). The hyperthermic exposure exacerbated cisplatin induced ototoxicity, with significantly elevated ABR thresholds, and greater hair cell loss compared to the cisplatin only condition and euthermic condition. However, the hypothermic condition provided robust protection with no significant ABR threshold shift from pre-test and minimized hair cell loss.

Conclusion

The findings are consistent with a diametric effect of thermal exposure on cisplatin induced ototoxicity, where hypothermia provides protection and hyperthermia exacerbated ototoxicity. These findings provide evidence for a non-invasive and "localized" treatment for prevention of cisplatin ototoxicity with high potential for translation to human clinical application.

PS - 035

Auditory Sensory Cells Potentiate TNF- α -Induced ROS Generation in Response to IFN- γ Through NOX1 Activation

Jeong-Im Woo¹; Sejo Oh²; Yoojin Lee¹; Raekil Park³; David Lim¹; Sung Moon¹

¹David Geffen School of Medicine at UCLA; ²House Research Institute; ³Wonkwang University School of Medicine

Background

Among various causes of acquired sensorineural hearing loss (SNHL), drug-induced ototoxicity is clinically important because it is frequently preventable and manageable. Inflam-

matory reactions are importantly involved in the pathogenesis of ototoxicity induced by cisplatin, but we poorly understand the molecular mechanism involved in inflammation-mediated hair cell damage. Pro-inflammatory cytokines are known to be critically involved in cisplatin ototoxicity. Previously, we have demonstrated that IFN- γ augments TNF- α -induced cytotoxicity of the auditory sensory cells. Since ROS production plays an important role in cell death, we aimed to determine if IFN- γ affects TNF- α -induced ROS generation in the auditory sensory cells.

Methods

For observing morphologic change of hair cell by ototoxicity, the organ of Corti was isolated from the Math-1-EGFP mice and fluorescence microscopic image analysis was performed. Superoxide generation was monitored using flow cytometric analysis with hydroethidine staining. qRT-PCR analysis was conducted to determine NOX1 regulation.

Results

We found that IFN- γ potentiates TNF- α -induced ROS generation in the HEI-OC1 cells. IFN- γ was also noted to augment TNF- α -induced NADPH-dependent superoxide generation. Particularly, NOX1 appeared to be significantly involved in TNF- α and IFN- γ -induced generation of superoxide. The HEI-OC1 cells were found to enhance TNF- α -induced up-regulation of NOX1 expression. IFN- γ -mediated augmentation of TNF- α -induced superoxide generation appeared to be inhibited by ML171 (a NOX1-specific inhibitor), not by apocynin (a NOX family inhibitor). ML171 also inhibited IFN- γ -sensitized TNF- α -mediated cytotoxicity of the auditory sensory cells in our *ex vivo* model. In contrast, both apocynin and ML171 appeared to attenuate TNF- α and IFN- γ -induced potentiation of cytotoxicity when exposed to a suboptimal dose of cisplatin.

Conclusion

Taken together, it is suggested that IFN- γ sensitizes the auditory sensory cells to TNF- α -induced cytotoxicity through NOX1-mediated ROS generation.

PS - 036

Pyrroloquinoline Quinone Protect Vestibular Hair Cells Against the Neomycin Ototoxicity

Kazuma Sugahara; Yoshinobu Hirose; Takeshi Hori; Hironori Fujii; Makoto Hashimoto; Hiroaki Shimogori; Hiroshi Yamashita

Yamaguchi University Graduate School of Medicine

Background

Pyrroloquinoline quinone (PQQ) is an organic molecule that was discovered as a redox cofactor. The molecule was reported as the new vitamins (Nature 2003). It is to be involved in mitochondrial function, and the animals with PQQ deficiency showed development disorder, immunodeficiency and infertility. In addition, the animals which received the molecules showed myocardial protective effect and neuroprotective effect from ischemia for a strong antioxidant activity. In the present study, we evaluated the protective effect on the inner ear sensory cells against neomycin ototoxicity.

Methods

Cultured utricles of CBA/N mice were used. Cultured utricles were divided to three groups (Control group, Neomycin group, Neomycin + PQQ group). In the Neomycin group, utricles were cultured with neomycin (2 mM) to induce hair cell death. In Neomycin + PQQ group, utricles were cultured with neomycin and PQQ (100 – 1 μ M). Twenty-four hours after exposure to neomycin, the cultured tissues were fixed with 4% paraformaldehyde. To label hair cells, immunohistochemistry were performed using anti-calmodulin antibody. The rate of survival vestibular hair cells was evaluated with the fluorescence microscope. In addition, immunohistochemistry against 4-hydroxy-2-nonenal was performed to evaluate the product of hydroxy radical.

Results

The survival rate of hair cells in Neomycin + PQQ group was significantly more than that in Neomycin group. The signals of 4-hydroxy-2-nonenal were inhibited in neomycin + PQQ group.

Conclusion

The results indicated that PQQ protects sensory hair cells against neomycin-induced death in mammalian vestibular epithelium. PQQ can be used as the protective drug in the inner ear.

PS - 037

Survey Of Current Auditory Monitoring For Ototoxicity In Oncology, Audiology And Cystic Fibrosis Services In The UK

Ghada Al-Malky¹; Miranda De Jongh²; Merijam Kikic²; Sally Dawson²; Ranjan Suri³

¹University College London (UCL); ²Ear Institute, UCL;

³Department of Paediatric Respiratory Medicine, Great Ormond Street Hospital and the Portex Unit, Institute of Child Health, UCL

Background

Chemotherapeutic agents such as cisplatin and aminoglycoside antibiotics are two of the most established drugs associated with permanent ototoxicity. Therefore patients repeatedly exposed to these medications, such as oncology and cystic fibrosis (CF) patients, need continuous auditory monitoring for early identification of ototoxicity. This is currently more pertinent as survival rates from both disorders have significantly improved, making maintenance of quality of life essential. The American Speech-Language-Hearing Association (ASHA, 1994) and American Academy of Audiology (AAA, 2009) have produced the most comprehensive guidelines for ototoxicity monitoring to date, but similar guidelines are not available in the UK.

Methods

The aim of this study was to assess the current practice in UK services using online surveys specifically designed for each of the three professions using the UCL Opinion survey tool. Hyperlinks to the surveys were mailed through respective professional bodies such as the British Academy of Audiology, Children's Cancer and Leukaemia Group and CF Trust.

Results from the CF survey were compared with a previous survey by Tan et al (2001) but none existed for oncology or audiology services.

Results

Responses from 56 oncology, 133 audiology and 33 CF clinicians were obtained representing all regions of the UK. Despite 69.6%, 63.9% and 79.3% of the three respective professions indicating that they do perform auditory monitoring, there was significant variation in the reported referral criteria, audiological tests used, criteria for identification of ototoxicity, and indications for change in management. Cisplatin and Carboplatin were considered first line treatments by 94.6% and 78.6% oncologists whereas extended interval Tobramycin was the first line treatment by 97.0% of CF clinicians. 70.6% of the audiologist didn't know whether patients were counselled about ototoxicity prior to treatment or not and 49.4% of them said that baseline testing wasn't routinely performed. More than 90% of testing was performed in audiology departments with limited access to un-well patients and most centres used patients' auditory complaints as the reason for referral, where substantial cochlear damage would have occurred already. There was clear evidence of limited awareness/ agreement of responsibilities of team members so that audiologists' roles were under-utilised for counselling and rehabilitation and clinicians had limited understanding of the criteria for ototoxicity and test battery used to diagnose it.

Conclusion

Recommendations include the development of UK-wide clinical guidelines and professional education programmes, as advocated by the WHO (1994) to increase the profile and standardisation of ototoxicity monitoring in clinical practice.

PS - 038

Ototoxic Effect of Daptomycin Applied to the Guinea Pig Middle Ear

Hidetoshi Oshima¹; Muneharu Yamazaki¹; Tetsuaki Kawase¹; Takeshi Oshima¹; Toshimitsu Kobayashi²; Yukio Katori¹

¹Tohoku University Graduate School of Medicine; ²Senen Riru Hospital

Background

Ototoxic antibiotic eardrops are frequently used to treat external and middle ear infections. Fluoroquinolones are commonly used and provide adequate coverage for *Streptococcus pneumoniae*, *Haemophilus influenzae*, *Staphylococcus aureus*, *Pseudomonas aeruginosa*, and *Moraxella catarrhalis*. However, MRSA does not respond to such antibiotics. Vancomycin, a common anti-MRSA antibiotic, has ototoxic effects in topical use. Daptomycin is a new anti-MRSA drug with unknown ototoxicity. The current study examined the ototoxic effect of daptomycin.

Methods

Fifteen male Hartley guinea pigs (weight, 250-300 g) were divided into 3 groups receiving daptomycin (50 mg/ml), gentamicin (50 mg/ml, positive control), and saline solution (negative control). After insertion of a pressure-equalizing tube, pretreatment auditory brainstem responses (ABRs) were ob-

tained. Topical solutions of 0.1 ml were applied through the tube into the middle ear twice a day for 7 days. Post-treatment ABRs were obtained 7 days after the last treatment. The hair cell loss was investigated by immunohistochemistry.

Results

The saline-treated (negative control) group showed no deterioration of ABR threshold. The daptomycin and gentamicin-treated group showed significant deterioration in ABR threshold. Hair cells were partially damaged in daptomycin group and severely damaged in gentamicin group.

Conclusion

Daptomycin applied topically at a concentration of 50 mg/ml caused statistically significant hearing impairment. Great care must be taken when there is a chance that daptomycin reaches the middle ear.

PS - 039

Auditory Responses in Normal-Hearing, Noise-Exposed Human Ears

Greta Stamper; Tiffany Johnson

University of Kansas Medical Center

Background

Recent investigations in animal ears have described temporary noise-induced hearing loss with permanent deafferentation for up to 50% of auditory nerve fibers in the high-frequency region of the cochlea (Kujawa and Liberman, 2009; Lin et al., 2011, Furman et al., 2013). Although thresholds remained normal, evidence of the deafferentation was apparent in reduced wave I auditory brainstem response (ABR) amplitudes for high-level stimuli. It is unknown if the same phenomenon exists in the human ear. Here, we investigate supra-threshold auditory function in normal-hearing, noise-exposed human ears.

Methods

Data were collected from normal-hearing subjects (n=30; aged 19-28 years) with different voluntary noise-exposure backgrounds. Noise-exposure background was assessed via a detailed case history and a questionnaire (Megerson, 2010) that calculated the number of hours spent annually in specific high-noise environments (occupational, music, power tools, etc). Auditory function was assessed across a wide range of stimulus levels via the ABR and distortion-product otoacoustic emissions (DPOAEs). ABRs were collected in response to 1 and 4 kHz tone bursts and a click stimulus. DPOAEs were assessed at 1, 2 and 4 kHz.

Results

Significantly smaller amplitudes were seen in wave I of the ABR in response to high-level (e.g., 70 to 90 dB nHL) click and 4kHz tone bursts in ears with greater noise-exposure backgrounds. No statistically significant differences were revealed in wave V amplitude to the same stimuli. These findings are consistent with data from previous work completed in animals, in which the reduction in high-level responses was a result of deafferentation of high-threshold/low-spontaneous rate auditory nerve fibers. These data suggest a similar mechanism may be operating in human ears following expo-

sure to high sound levels. There were no statistically significant differences in supra-threshold DPOAEs across ears with different noise-exposure histories. This was expected, given noise-induced auditory damage findings in animal ears did not extend to outer hair cells, the generator for the DPOAE response.

Conclusion

Smaller ABR wave I amplitudes were found in normal-hearing human ears with greater amounts of voluntary noise exposure in response to high-level click and 4 kHz tone bursts. These data provide evidence that noise exposure may damage high-threshold auditory nerve fibers in humans. This damage is only apparent when examining supra-threshold ABR responses.

PS - 040

CD36 is not Needed for Hair Cell Phagocytosis and Plays a Role in Hair Cell Vulnerability to Ototoxic Agents

Song-Zhe Li¹; Hirokazu Suzuki²; Margaret Koeritzer³; Keiko Hirose¹

¹Department of Otolaryngology, Washington University in Saint Louis School of Medicine; ²Department of Otolaryngology, Nagoya University, Nagoya JAPAN;

³Program in Audiology and Communication Sciences, Washington University in Saint Louis School of Medicine

Background

CD36 is a membrane protein expressed on monocytes and macrophages. It functions as a pattern recognition receptor that identifies microorganisms and infected and dying cells, and then initiates an "eat me" signal to neighboring phagocytes. In order to determine whether CD36 is also involved in hair cell phagocytosis after cochlear injury, we characterized the outcome of ototoxic injury in the cochleae of CD36-deficient mice.

Methods

In vivo studies of ototoxicity: CD36 knockout mice were bred with Cx3CR1 GFP mice on a C57Bl6 background, rendering all macrophages fluorescent green. Eight week-old CD36 null mice were treated with kanamycin (1000mg/kg) and furosemide (220mg/kg). At five days after ototoxic injury, ABR thresholds were obtained, and the cochleae were fixed and processed for histologic analysis.

In vitro studies of ototoxicity and phagocytosis: CD36 knockout pups were euthanized, and their cochleas were placed in organotypic culture. Hair cells were loaded with FM4-64, and the cultures then received 1 mM kanamycin. Time-lapse confocal imaging was performed, beginning 18 hr after initiation of kanamycin treatment and continuing for an additional 4 hr. Control animals (CX3CR1 GFP/CD36 WT) were also imaged under identical conditions. Images were compiled using maximum intensity projections, and macrophage activity and movement were evaluated.

Results

In CD36 null mice, kanamycin/furosemide produced little threshold elevation, while in CD36 WT mice, the same treat-

ment produced moderate hearing loss across all frequencies. Also, CD36 null mice demonstrated slightly fewer recruited cochlear macrophages when compared to controls. Notably, only modest loss of hair cells was observed in CD36 KO mice after ototoxic exposure, and there were no defects seen in the reticular lamina, nor was there an excess of hair cell debris observed in the scala media or the scala tympani. In neonatal mouse cochlear cultures, macrophages avidly consumed damaged hair cells in both CD36 null and WT mice; we observed no defects in phagocytosis after CD36 deletion.

Conclusion

Deletion of CD36 does not appear to hinder clearance of damaged hair cells, nor does CD36 deletion impair sensory epithelial repair after hair cell injury. In fact, CD36 null mice produce cochlear macrophages that actively phagocytose hair cell debris *in vitro*. Furthermore, deletion of CD36 appears to protect against hearing loss caused by kanamycin-furosemide. The mechanisms responsible for cochlear protection against ototoxicity in CD36 null mice are unclear, but may relate to reduction in cochlear vascular permeability.

PS - 041

Pulmonary Drug Delivery for Rescue of NIHL in a Chinchilla Model

Ronald Jackson; John Coleman; Heidi Shorter; Jianzhong Liu; Elizabeth Harper; Kejian Chen; Michael Hoffer

Naval Medical Center San Diego

Background

This project was an extension of the earlier successful application of inhaled antioxidants to protect against cochlear injury in a chinchilla animal model when exposed to noise (ARO 2012, Abstr#729).

Methods

In this study animals were administered the same low dose antioxidant combination (AC) as utilized in the earlier investigation of N-acetylcysteine (NAC; 50 mg/Kg), D-Methionine (D-Met; 50 mg/Kg), and acetyl-L-carnitine (ALCAR; 30 mg/Kg). However, in this study AC was delivered via intra-tracheal route for 5 instillations after the noise. The noise exposures (NE) consisted of 75 paired-impulses at 155 dB peak SPL. Antioxidant efficacy was assessed by auditory brainstem response (ABR) measures and histology using vital staining of auditory HCs compared to noise-exposed, saline instilled animals.

Results

Low dose 3-agent AC showed reduced NIHL from impulse noise demonstrating lower threshold shifts from baseline values as early as one week post noise than the saline controls. The improvement in hearing continued for both NE saline controls and 3-agent AC treated animals; however the AC treated animals showed significantly better hearing again in all four ABR test frequencies compared to saline controls at 3 weeks post NE. The range of differences between saline and 3-agent AC was 10.7 to 12.3 dB SPL lower for 2, 4, 6 and 8 kHz test frequencies. The 3-agent AC significantly protected the sensory cells and correlated with the threshold shift data with significantly lower percentage of missing OHCs in

the combination treated animals. NE, saline controls showed from 68 to 82% missing OHCs compared to 8 to 15% missing OHCs for the AC treated group (2-Way ANOVA, $p < 0.01$ for the four ABR threshold shift frequency regions).

Conclusion

The intratracheal delivery of the low dose antioxidant combination was well-tolerated and resulted in reducing hair cell loss and permanent ABR threshold shifts when administered after impulse noise compared to saline treated controls.

PS - 042

Sound Preconditioning Therapy Inhibits Ototoxic Hearing Loss in Mice

Soumen Roy; Matthew M. Ryals; Astrid Botty; Andrew Breglio; Tracy S. Fitzgerald; Lisa L. Cunningham
NIDCD, NIH

Background

Over 20% of patients receiving ototoxic drugs experience significant permanent hearing loss. A critical need exists for therapies that protect the inner ear without inhibiting the therapeutic efficacy of these drugs. We have shown previously that induction of heat shock proteins (HSPs) inhibits both aminoglycoside- and cisplatin-induced hair cell death and hearing loss. We hypothesized that exposure to sound that is titrated to stress the inner ear without causing permanent damage would induce HSPs in the cochlea and inhibit ototoxic drug-induced hearing loss.

Methods

We developed a sound exposure protocol that induces HSPs without causing permanent hearing loss. Mice were exposed to octave-band noise (8-16 kHz) for 2 hrs. We used this protocol in conjunction with a newly-developed mouse model of cisplatin ototoxicity. Pre-test auditory brainstem response (ABR) thresholds were measured 24-48 hours prior to the first drug (cisplatin or kanamycin) administration in CBA/CaJ mice. Post-test ABR thresholds were measured 15 days after the final cisplatin administration or 21 days after the final kanamycin administration. HSP expression in cochlea was tested by RT-qPCR.

Results

Our data indicate that sound preconditioning in the mouse ear induces a temporary threshold shift (TTS) but not a permanent threshold shift. Hearing sensitivity recovered to control levels within 1 week after exposure to preconditioning sound, and no permanent changes in ABR Wave I amplitudes were induced by the preconditioning sound. The data indicate that preconditioning mouse inner ears with sound has a robust protective effect against cisplatin-induced hearing loss and hair cell death. Sound therapy also provided protection against aminoglycoside-induced hearing loss.

Conclusion

Our data indicate that sound preconditioning protects against hearing loss caused by both classes of ototoxic drugs, and they suggest that sound therapy holds promise for preventing hearing loss in patients receiving these drugs. This sound conditioning strategy is noninvasive and inner ear-specific,

suggesting that it is unlikely to inhibit the therapeutic efficacy of cisplatin or the aminoglycosides.

PS - 043

Long-Term Effects of Noise Exposure and Antioxidant Treatment on Chinchilla Cochleae

Xiaoping Du; Ning Hu; Weihua Cheng; Wei Li; Donalt Ewert; Matthew West; Richard Kopke

Hough Ear Institute

Background

Long-term effects of antioxidant treatment on auditory functional damage (ABR, DPOAE, and CAP) induced by noise exposure were previously presented by our group at the 2012 ARO meeting (Abstract #720). In the present study, we performed a complementary histological and immunohistochemical study to examine the long-term effects that this sensorineural insult and subsequent antioxidant treatment regimen had on a subset of cellular components predicted to play key roles in maintaining endocochlear potential (EP) within the cochlea.

Methods

Chinchilla were exposed to 105 dB octave-band noise centered at 14 kHz for 6 hours. One cohort of chinchilla were treated with an antioxidant (300 mg/kg of HPN-07 given intraperitoneally) regimen, beginning four hours after noise exposure and then twice daily for two days. EP was recorded before euthanasia and at different time points (3, 10, 21 days, and 6 months) after noise exposure. The cochleae were harvested, and one cochlea from each chinchilla was used for hair cell counting while another was used for immunohistochemical staining with calretinin, and connexins 26, and 30. The density of calretinin-positive afferent nerve fibers in the spiral lamina and relative immunofluorescence intensities for the GAP junction proteins, connexins 26 and 30, in the organ of Corti were measured and statistically analyzed.

Results

Significantly more hair cells and calretinin-positive afferent nerve fibers were observed in the spiral lamina in the middle turn of the cochleae in the antioxidant treated groups compared to noise exposed only groups. Three days after noise exposure, the mean EP values were significantly lower than those of the normal controls and recovered to normal values after 10 days. Significantly lower connexin 26 expression was observed in the organ of Corti and the spiral ligament in all noise exposed groups while no significant change was observed in connexin 30 expression in the cochlea after noise exposure. No drug treatment effect was observed in EP and connexin protein expression.

Conclusion

Antioxidant treatment provides significant long-term protection to hair cells and their afferent nerve fibers. However, early spontaneous recovery of EP and long-term inhibition of connexin 26 expression following acute acoustic trauma suggests that EP is reestablished via an independent mechanism and that loss of connexin 26 function may be compensated for by other GAP junction proteins (e.g. connexin 30) in the cochlea.

Auditory Brainstem Response: Binaural Difference Potential in the Mongolian Gerbil (*Meriones Unguiculatus*)

Geneviève Laumen¹; Daniel Tollin²; Georg Klump¹

¹*Cluster of Excellence Hearing4all, Animal Physiology and Behavior Group, Department for Neuroscience, School of Medicine and Health Sciences, Oldenburg University;*

²*Department of Physiology and Biophysics, University of Colorado School of Medicine*

Background

The auditory brainstem response (ABR) is a clinical non-invasive tool for investigating hearing loss. When the ABR is measured by stimulating both ears, a binaural difference potential (BDP) can be computed and its properties can be used to evaluate binaural interaction in the brainstem. To establish the BDP as a diagnostic tool BDPs of gerbils, a common model system for studies of binaural hearing, were measured for a wide range of interaural time and level differences (ITD and ILD).

Methods

ABRs and associated BDPs of ketamine-anesthetized young gerbils were measured using flat frequency spectrum (1-14 kHz) clicks presented monaurally and binaurally with ITDs ranging from $\pm 2000 \mu s$ and ILDs ranging from ± 30 dB. Needle electrodes were placed at vertex and neck. The amplitudes and latencies of the most prominent BDP component, DN1, and the corresponding binaurally-evoked ABR wave IV were determined.

Results

As has been observed in humans and other animals, the DN1 component of the BDP correlates in its latency with wave IV of the ABR and it originates from a reduction in the binaural ABR. It was possible to evoke DN1 also for ITDs which exceed the useful physiological range of ITD for gerbils ($>130 \mu s$). The largest amplitude of DN1 and wave IV is obtained with ITDs and ILDs of zero. DN1 amplitude decreases with increasing absolute ITDs and ILDs, whereas the amplitude of wave IV decreases with larger ITDs and increases with larger ILDs. The shortest latency of DN1 and wave IV was observed when the ITD was zero and it increased with larger ITDs.

Conclusion

Since the binaurally-evoked ABR was smaller in amplitude than the sum of the monaurally-evoked ABRs, the BDP is likely to arise from IE-type neurons in the lateral superior olive (LSO) or dorsal nucleus of the lateral lemniscus (DNLL). The decrease in the amplitude of DN1 due to increasing ITD and ILD values could originate from a shift in the relative timing of excitatory and inhibitory input from the two ears to the LSO. The increase in DN1 latency with increasing ITDs may be due to the introduced delays of inhibitory and excitatory input. The BDP is a suitable tool to evaluate binaural hearing in the gerbil and study the decline in binaural hearing abilities with increased age or hearing impairment.

A Electroencephalography Study of Binaural Interactions in Humans Using the Frequency Following Response

Le Wang; Steven Colburn; Barbara Shinn-Cunningham
Boston University

Background

Previous studies found that the auditory brainstem response (ABR), an onset response present in scalp voltages, contains a binaural interaction component (BIC). Here, we investigated whether there is a binaural component in the frequency-following response (FFR), a measure of steady-state synchronous neural activity evoked by a periodic acoustic input.

Methods

All subjects in both experiments had pure-tone thresholds within 20dB of normal hearing level in both ears. FFRs were recorded using a BioSemi Active Two System with a 32-channel electroencephalography (EEG) cap. In Experiment 1, we presented a complex tone with fundamental frequency of 100 Hz either binaurally, monaurally to the left ear, or monaurally to the right ear. For binaural presentations, the complex tone had an interaural time difference (ITD) randomly drawn from the list [0ms, ± 0.1 ms, ± 1 ms, ± 4.3 ms]. In Experiment 2, we presented a 20-Hz binaural beat stimulus consisting of complex tones with different pitches to two ears (253Hz and 273Hz, to left and right, respectively). For each subject, the onset N100 response was fit by a pair of dipoles. We then estimated the evoked FFR by projecting the 32-channel measurements to the fit N100 dipole locations.

Results

In Experiment 1, the phase-locking value (PLV) at 100Hz computed from the FFR in the binaural condition roughly equals the PLV computed from the sum of the monaural responses appropriately phase shifted to account for the ITD. Furthermore, the PLV at F0 is essentially independent of ITD for moderate values, but drops for the largest ITD tested (± 4.3 ms), where the monaural responses are out of phase and cancel each other. In Experiment 2, the PLV of the reconstructed source signal shows a peak at the 20Hz binaural beat frequency; however, the amplitude of this response varies greatly across subjects.

Conclusion

Results in Experiment 1 suggest that, unlike the ABR BIC, the PLV of the 100Hz FFR in the binaural condition is predicted by linearly summing FFRs from the monaural conditions. This casts doubts on the usefulness of the FFR for studying binaural interactions in the brainstem. Results in Experiment 2 suggest that the binaural system phase locks to the 20Hz binaural beat, although the strength of phase locking varies widely among normal hearing subjects. This provides a potential tool to study inter-subject variability in binaural processing.

PS - 046

High School Music Classes Enhance the Neural Processing of Speech in Noise

Jennifer Krizman¹; Adam Tierney¹; Erika Skoe²; Nina Kraus¹

¹Northwestern University; ²Northwestern University;

*Currently at University of Connecticut

Background

Communication often occurs in the presence of noise, which can make speech processing and perception difficult. In life-long musicians, the effects of noise are lessened, including a reduction in noise-induced delays in neural timing. Whether this neural 'resilience' to background noise is a consequence of training or reflects pre-existing differences between musicians and non-musicians is a source of debate. We sought to determine whether training beginning during adolescence is sufficient to engender this neural timing benefit.

Methods

Auditory brainstem responses to a speech syllable presented in quiet and noise were collected from two groups of high school students. These groups were comprised of adolescents attending public high schools in Chicago. Students were enrolled (for credit) in either music or Junior Reserve Officer's Training Corp classes. These classes met 2-3 times per week, averaging about 3 hours of instruction per week; and, participation in one of these two classes is a mandatory part of each school's curriculum. Students were tested prior to beginning the music or ROTC classes, providing a baseline measure of neural function, and again after two years of in-school training.

Results

At pre-test, the noise-induced neural delay was equivalent between the music and JROTC groups. Following two years of training (one year was insufficient), the music group showed a smaller noise-induced neural delay than pre-test. This finding was confirmed through converging evidence from phase shift analyses, quiet-to-noise peak timing shifts, and quiet-to-noise response correlations. On the other hand, the noise-induced neural delay was the same at pre-test and post-test for the ROTC group.

Conclusion

These results suggest that musical training is sufficient to reduce the impact of noise on neural processing. Moreover, this reduced effect of noise on the auditory system was found after only two years of school-based musical training that was not begun until late adolescence, supporting the power of musical training in driving enrichment-based neural plasticity.

PS - 047

Moving to a Beat and Reading Rely on Neural Timing

Adam Tierney; Jessica Slater; Nina Kraus

Northwestern University

Background

To learn to read, children must first develop an awareness of the sounds that make up their native language. The develop-

ment of this phonological awareness in turn depends on the ability to use temporal patterns to detect syllabic boundaries, especially when speech is heard in noise. The acquisition of reading and the development of rhythmic skills such as synchronizing movements to a beat may, therefore, depend on overlapping neural and cognitive resources. Both reading ability and beat synchronization are linked to the consistency of the neural response to sound¹, suggesting that the ability to track patterns in time may rely on neural synchrony in the auditory system. We further tested this hypothesis by examining the relationship between reading ability, the ability to move to a beat, and the latency of the subcortical response to sound.

(1) Tierney A, Kraus N (2013) The ability to move to a beat is linked to the consistency of neural responses to sound. *Journal of Neuroscience* 33, 14981-14988.

Methods

We examined reading ability, beat synchronization, and subcortical auditory function in 2nd graders. Reading ability was assessed with a standardized test. Beat synchronization was measured by asking participants to tap along to a metronome and measuring the variability of the taps. Electrophysiological auditory brainstem responses were recorded to a 40 ms synthesized speech sound.

Results

We find that both better reading ability and better synchronized tapping are linked to earlier auditory brainstem onset responses to sound. Moreover, although reading ability and tapping ability correlate, this relationship is not significant when brainstem latency is controlled for, supporting our hypothesis that the link between reading and synchronization ability is driven in part by a shared reliance on neural timing.

Conclusion

These results indicate that both learning to read and moving to a beat rely upon neural synchrony in the auditory system (as more synchronous firing is linked to earlier responses). This suggests that diminished auditory neural synchrony could cause blurred, imprecise perception of time, resulting in a decreased ability to track temporal patterns, which in turn could compromise both rhythmic and language abilities. The inherently engaging and rewarding nature of rhythm could make music or computer-based rhythm training effective strategies for boosting reading skill in children, supplementing more traditional phonological instruction.

PS - 048

Effects of Frequency Compression on the Neural Encoding of Complex Sounds in the Human Brainstem

Jillian Wendel; Ananthanarayan Krishnan; Joshua Alexander

Purdue University

Background

Nonlinear frequency compression (NFC) has been used to improve speech recognition in individuals with high-frequency hearing loss by compressing essential high-frequency information into an audible lower frequency region. A distin-

guishing feature of this technique is that only the part of the spectrum above a specified start frequency is compressed, while the part of the spectrum below the start frequency is undisturbed. Results from perceptual studies with hearing-impaired individuals are not uniform and improvement is generally seen only for consonant identification, especially for the fricative /s/. However, results from Alexander (2012) indicate that benefits for consonant identification might come at the expense of detriments in vowel identification as start frequency is lowered. Using normal hearing individuals, the focus of this study is to determine whether spectral changes consequent to frequency compression alters neural encoding (as reflected in the human frequency following response, FFR) of the stimulus in general and alters encoding of pitch relevant information in particular.

Methods

FFRs were recorded from 10 normal hearing subjects in response to monaurally presented stimuli differing in parameters of start frequency (SF), compression ratio (CR), and fundamental frequency (F0). Experiment 1 altered the compression ratio (1.75-3.5) while maintaining a fixed SF of 1400 Hz. Experiment 2 manipulated the start frequency (1400, 1000, 600 Hz) with the CR fixed at 1.75. F0s tested in this study were 100 and 200 Hz.

Results

Temporal and spectral analyses of the data indicated both a decreased periodicity strength and F0 magnitude with: (i) increase in compression; and (ii) decrease in start frequency of compression. Consistent with perceptual data (Parsa et al., 2013; Alexander 2012), changing the start frequency of compression had a relatively greater effect on neural periodicity strength than the amount of compression.

Conclusion

The results of this study suggest that compression might have deleterious effects on the neural representation of pitch relevant information. These detrimental effects may have implications for the optimal representation of speech sounds with low second formant frequencies, which are important to distinguish vowels.

PS - 049

Brainstem Correlates of Temporal-Spectral Resolution Tradeoff in the Human Auditory System

Ameenuddin Khaja¹; Gavin Bidelman²

¹University of Memphis; ²School of Communication Sciences & Disorders, Institute for Intelligent Systems, University of Memphis

Background

The peripheral auditory system is often conceived as a bank of overlapping band-pass filters which perform a spectral decomposition on the incoming sound input. Filter theory suggests a physiological tradeoff between frequency and temporal resolution of cochlear signal processing such that “ringing” caused by narrowband filtering limits the system’s temporal precision. Superior temporal processing is achievable but

only at the expense of reduced spectral resolvability. Here, we examine the neurophysiological correlates of this spectrotemporal tradeoff in the human auditory system.

Methods

Temporal resolution was assessed in young, normal-hearing listeners using scalp-recorded auditory brainstem responses (ABRs) elicited by paired click stimuli. The inter-click interval (ICI) between continuous presentations was parameterized between 0.7 and 25 ms to map the recovery of ABR wave V amplitude as a function of stimulus spacing. Behavioral frequency difference limens (DLs) and auditory filter tuning (Q_{10dB} derived from psychophysical tuning curves) were also obtained to assess compromises between listeners’ spectral acuity and electrophysiological estimates of temporal resolvability.

Results

Electrophysiological responses showed a monotonic increase in wave V amplitude with increasing ICI, ranging from total response suppression (0.7 ms) to full recovery (25 ms). Temporal resolution thresholds were estimated from physiological data as the ICI yielding 50% recovery in ABR response magnitude. ABR thresholds revealed temporal resolvability of ~3-4 ms, in close agreement with values obtained from human psychophysical experiments. Initial correlations between electrophysiological estimates of temporal resolution and behavioral measures of frequency resolution (i.e., Q_{10} filter “sharpness”) revealed negative associations such that finer frequency resolution corresponded with poorer temporal resolution (i.e., time-frequency tradeoff).

Conclusion

Our data demonstrate robust neural correlates of the resolution and psychophysical limits to temporal processing in early, pre-attentive responses from the auditory brainstem. Results support the notion that peripheral cochlear filtering plays a key role in limiting auditory temporal processing. The inverse relationship between temporal ABR recovery and perceptual frequency resolution support the notion of a tradeoff between the temporal and spectral resolving power of the auditory system. Given the observed relationship between time-frequency acuity, we infer that temporal properties of the ABR might be used as a rapid, objective estimate of auditory frequency resolution during hearing assessment and the optimization of amplification fittings.

PS - 050

A Human Auditory Brainstem Response Model for Broadband Stimulation

Sarah Verhulst¹; Hari Bharadwaj²; Christopher Shera³; Barbara Shinn-Cunningham²

¹Carl von Ossietzky University Oldenburg; ²Boston University; ³Harvard Medical School

Background

Human auditory brainstem responses (ABRs) are sound-evoked electrical potentials recorded from the scalp, generated from population responses in the human auditory nerve (AN; wave-I), cochlear nucleus (CN; wave-III), and inferior colliculus (IC, wave-V). It is crucial for any model simulating

ABRs and frequency-following responses (FFRs) to account for the phase-locking characteristics at the single-unit level as well as accounting for across-frequency temporal synchronization of broadband cochlear responses. Current functional models of the AN, CN and IC capture the phase-locking, rate-level and adaptation properties observed in single-unit recordings, but they fail to account for the fact that the latency of the ABR wave-V response to a broadband input decreases as stimulus level increases. Here, a human auditory brainstem response model is presented that accounts more precisely for how different contributions interact as a function of level to realistically simulate human brainstem responses to broadband stimuli.

Methods

We use a nonlinear transmission-line model of the cochlea that simulates level-dependent features of click-evoked otoacoustic emissions (CEOAEs; Verhulst et al., 2012). The inner-hair cell and single-unit auditory nerve stages of the model are based on existing models (Heinz et al. 2001; Zilany et al. 2006, 2009), but responses are independent of critical frequency, such that any frequency dependence in the model originates purely from basilar-membrane processing. We included different spontaneous rate fibers, which synapse onto the CN using a coincidence detection mechanism. The CN and IC stages are modeled after the functional computational work of Nelson and Carney (2004). Brainstem responses were obtained by summing up energy across different frequency channels at the level of the IC.

Results

Latencies of simulated ABR wave-Vs showed a ~2 ms decrease as click level increased from 40 to 100 dB peSPL. Level-dependent properties of human ABR and OAEs to transient stimuli are compared, and the models' performance in simulating human frequency-following responses tested

Conclusion

Improving the broadband synchronization properties of auditory brainstem response models can lead to a use of these models for broadband stimuli, such as click-trains or speech. In addition to improving our understanding of the mechanisms generating scalp recorded brainstem responses, this work could also help in understanding how various forms of hearing impairment affect ABR wave-V responses.

PS - 051

Sub-Cortical Phase Locking to Attended and Unattended Streams of Resolved and Unresolved Harmonic Complex Tones

Dorea Ruggles¹; Shihab Shamma²; Andrew J Oxenham¹

¹University of Minnesota; ²University of Maryland

Background

Sub-cortical phase locking (as measured by the scalp-recorded frequency following response, or FFR) has been shown to relate to behavioral auditory tasks associated with timing, localization, and pitch. Important questions remain, however, about how and why such relationships exist. Here we asked whether FFR waveforms can be modulated by atten-

tion within an auditory streaming paradigm. In addition, we asked whether effects of attention might also be observed in cases where the tonotopic differences between the streams are minimized. To answer these questions we used harmonic tone complexes that were bandpass filtered to contain primarily resolved or only unresolved harmonics.

Methods

Filtered harmonic tones with fundamental frequencies (F0s) of 100 and 187 Hz were presented in rapid alternation to create the percept of two streams. The filters were selected to incorporate resolved or unresolved harmonics, and the tones were presented in a background of noise to mask possible distortion products. Subjects were asked to attend to either the high or low stream and ignore the other. Oddball tokens (4 semitones higher) were presented occasionally, and subjects were instructed to report oddballs in the attended stream by button press. FFR responses were recorded with a single (Cz) scalp electrode using a BioSemi Active2 system.

Results

EEG recordings were analyzed by bootstrapping individual trials to calculate phase locking value (PLV), a measure of phase vector strength, in attended and unattended trials of resolved and unresolved presentations. PLV differences will be computed to investigate the possible impact of attention on sub-cortical processing, including differential impact on resolved and unresolved pitch information and build-up over time.

Conclusion

These data will contribute to the ongoing studies regarding the degree to which directed attention modulates the function of sub-cortical pathways and whether such modulation requires some degree of tonotopic separation between streams, or whether attention modulation can be observed based on higher-level features, such as periodicity. The work will form the basis for further explorations of cortical responses to the same stimuli and paradigm.

PS - 052

Simultaneous Measurement of Cortical Responses, Sub-Cortical Responses, and Behavior Performance in an Auditory Attention Task

Lengshi Dai; Barbara Shinn-Cunningham

Boston University

Background

The ability to direct attention to sounds of interest differs across listeners. These behavioral differences depend both on subcortical coding fidelity in the brainstem and modulation of sensory representations in cortex. While both subcortical and cortical responses can be measured using electroencephalography (EEG), the stimuli used to generate robust responses, the number of samples required to obtain good measurements, and the processing schemes used all typically differ for subcortical and cortical measurements. Here, we tested an auditory paradigm that allows simultaneous measurement of frequency following responses (FFR) from

the brainstem, cortical auditory Event Related Responses (AERPs), and behavioral performance.

Methods

EEG was recorded from normal hearing listeners presented with two simultaneous streams. Each stream (75dB SPL) consisted of complex tones of different fundamental frequencies ($F_0 = 97\text{Hz}$ or 159Hz). The two streams had equal magnitude but opposite sign interaural time differences, so that one was on the left and one on the right. Their repetition rates also differed, ensuring that note onsets in each stream were temporally resolvable. Subjects were cued to attend either left or right and count the number of deviant tones in that stream (~ 0.3 semitone offset from the majority of the tones). AERPs were obtained by averaging EEG responses. FFRs were found by averaging negative and positive polarity presentations of each tone and calculating the phase-locking-value (PLV), a measure of the temporal fidelity of brainstem coding. Behavior performance was summarized by the percent correct on the deviant-counting task.

Results

The majority of note-onset AERPs were significantly modulated by attentional focus (larger AERPs to a tone when it was attended compared to when it was ignored). However, brainstem PLVs were not significantly modulated by attention. PLVs for the two different tones (97Hz and 159Hz) were significantly correlated, showing that the brainstem coding fidelity was similar for different pitches. Importantly, PLV strength was positively correlated with behavior performances across subjects.

Conclusion

Top-down selective auditory attention strongly modulates cortical responses, but has little or no effect on subcortical signals. Because detecting pitch deviants required relative fine frequency discrimination, across listeners behavioral ability correlated with brainstem temporal coding fidelity (FFRs), but not on the strength of the attentional modulation of cortical responses. Further experiments are needed to determine if this pattern reverses when performance is not limited by sensory coding ability, but rather on effectiveness of top-down attentional control.

PS - 053

Post-Concussion Brainstem Neural Processing in Quiet and Noise

Kathy Vander Werff¹; Brian Rieger²

¹Syracuse University; ²SUNY Upstate Medical University

Background

Auditory processing problems, including disproportionate difficulty understanding speech in competing noise, appear to be among the common long-term problems a significant number of individuals suffer following concussion/mild traumatic brain injury (mTBI). Because the brainstem is vulnerable in head injury, the goals of the proposed study were to determine 1) whether there is evidence of abnormal neural processing in the at the level of the auditory brainstem using the complex speech-evoked auditory brainstem response (ABR) recorded in quiet and in babble and 2) whether these

ABRs correlate with performance on behavioral measures of auditory processing abilities.

Methods

Participants were individuals who sought rehabilitation in a concussion management program due to on-going symptoms 3-18 months post mTBI ($n=32$) and un-injured age and gender-matched controls ($n=32$). Speech evoked ABRs were recorded in response to a 40 ms synthetic /da/ stimulus in the left and right ears in quiet and in a background of 20-talker babble at a +10 SNR. Measures of transient peaks (amplitude, latency) and sustained components (frequency-following, timing) of the speech ABR were analyzed. In addition, all subjects participated in a battery of behavioral tests of central auditory processing abilities including speech understanding in noise, temporal processing, and dichotic listening measures.

Results

The concussion group showed overall trends for smaller speech ABR peaks with slightly delayed latencies in quiet, and especially in noise, compared to the control group. Few of these group differences reached statistical significance. However, there were significant differences by condition (quiet vs. noise) and significant group by condition interactions for some variables. In addition, some of the speech ABR variables were moderately correlated with performance on behavioral tests of central auditory processing.

Conclusion

In this sample of individuals with on-going post-concussion symptoms 3-18 months following injury, brainstem level processing appears to be generally similar to un-injured controls on the group level. However, there were significant interactions between group and condition, indicating that the addition of noise disrupted brainstem processing to a greater extent in the concussion group. The concussion group showed a wide range of performance on the auditory behavioral tests and the relationship between speech ABR variables and outcomes on such measures will be further discussed in relation to this performance on the group and individual basis.

PS - 054

Cochlear Neuropathy in "Normal Hearing" Humans and the Coding of Supra-Threshold Sound

Hari Bharadwaj¹; Salwa Masud¹; Sarah Verhulst¹; Golbarg Mehraei²; Barbara G Shinn-Cunningham¹

¹Boston University; ²Massachusetts Institute of Technology

Background

Many listeners with clinically normal hearing thresholds (NHT) nonetheless complain of difficulty hearing in everyday challenging environments, and show concomitantly large individual differences in performance under laboratory settings. Converging evidence from human and animal studies points to one potential source of such difficulties: differences in the fidelity with which supra-threshold sound is encoded in the early portions of the auditory pathway. Animal studies show that noise exposure and aging can cause a loss of a large

percentage of auditory nerve fibers (ANFs) without any significant change in measured audiograms. This cochlear neuropathy may be selective to low spontaneous rate (low-SR) fibers. We used a combination of electrophysiological, otoacoustic and behavioral measures, along with computational modeling, to test whether cochlear neuropathy of low-SR fibers explains some of differences in supra-threshold hearing ability.

Methods

High-SR ANFs phase-lock poorly to the temporal envelopes of acoustic high-frequencies at high sound levels and low modulation depths; consequently, low-SR ANFs are particularly important for coding such modulations. Based on simulations using an established ANF model (Zilany et al., 2009) in conjunction with envelope coding models (Nelson and Carney, 2004) of the cochlear nucleus (CN) and the inferior colliculus (IC), we hypothesize that low-SR ANF loss leads to a concomitant deterioration in envelope phase-locking at the level of the IC at high sound intensities and low modulation depths. We measured individual phase-locking to a 100 Hz envelope (4 kHz carrier tone at 75 dB SPL) at various modulation depths for 22 NHT listeners, summarized by the sub-cortical steady state response. For each listener, we also measured (1) modulation detection thresholds (M), (2) thresholds for discrimination of envelope interaural time differences (ITDenv), (3) psychophysical forward-masking tuning curves (PTCfm) at 10 dBSL, and (4) distortion-product OAE growth functions. All behavioral and electrophysiological measurements were made in the presence of off-frequency noise maskers with a notch around 4 kHz to limit off-frequency listening.

Results

Individuals with higher M and ITDenv thresholds showed a more rapid degradation of SSSR phase-locking with decreasing modulation depth. All measures showed strong correlation across listeners. Preliminary analysis indicates that the individual differences are unrelated to cochlear health as measured by DPOAEs and PTCfm.

Conclusion

Our data support the hypothesis that low-SR ANF neuropathy is an underlying cause of suprathreshold deficits in NHT listeners.

PS - 055

Sensitivity of Speech-Evoked Envelope Following Responses (EFR) to Level and Amplification in Normal Hearing and Hearing Impaired Adults

Vijayalakshmi Easwar¹; David Purcell²; Steven Aiken³; Susan Scollie²

¹National Centre for Audiology; Health and Rehabilitation Sciences, Western University; ²National Centre for Audiology; School of Communication Sciences and Disorders, Western University; ³School of Human Communication Disorders & Department of Surgery and Department of Psychology & Neuroscience, Dalhousie University, Halifax

Background

The use of an objective test for validation of hearing aid fittings in young infants has gained interest in recent years. Envelope following responses (EFRs) may be favourable for this purpose as they enable the use of speech stimuli (vowels) in contexts similar to running speech. A naturally spoken speech token /susashi/ was modified so that eight individual EFRs from different spectral regions could be obtained. This was achieved for the vowels by selectively lowering the pitch of the spectrum containing the first formant while maintaining the original pitch in the regions of second formant and higher. This was achieved for fricatives by amplitude modulating the fricatives. This stimulus sequence is likely to represent hearing aid functioning more accurately while maximizing frequency specificity and bandwidth representation. The aim of this study was to investigate the effect of level and amplification on the EFRs elicited by the modified stimulus in normal hearing (NH) and hearing impaired (HI) adults.

Methods

EFRs were recorded from 20 NH and 7 HI adults at stimulus levels of 50 and 65 dB SPL. Stimuli were presented through an ER-2 insert transducer in the unaided condition in both groups and additionally, through individually fit hearing aids in HI adults in the aided condition. Responses were averaged over 300 sweeps and detection was determined statistically using the F-test. Behavioral thresholds were obtained for each carrier using the ER-2 and sensation level of each carrier was determined in unaided and aided conditions.

Results

In both NH and HI adults, the number of EFRs detected (maximum of eight) increased with an increase in stimulus level. In HI adults, the number of EFRs detected increased in aided conditions relative to unaided conditions at the same stimulus level. On average, the response amplitudes of detected EFRs were higher at higher sensation levels in unaided and aided conditions. Although the carriers were at positive sensation levels in aided conditions, the amplitude and the number of EFRs detected in the HI group was lower relative to the NH group at a given stimulus level.

Conclusion

Results support past findings of a positive correlation between stimulus intensity and response amplitude in unaided

and aided conditions. Sensitivity to changes in audibility is an important factor in hearing aid validation and hence this may be a useful tool. Factors influencing the variability of results in HI adults require further investigation.

PS - 056

Effects of Adverse Listening Conditions on Subcortical Neural Representation of Speech Sounds in Normal and Impaired Ears

Saradha Ananthakrishnan¹; Ananthanarayan Krishnan²

¹Towson University; ²Purdue University

Background

Listeners with hearing impairment face significant challenges in adverse listening conditions. Behavioral studies in humans and single-unit experiments in animals have shown increased degradation of TFS processing in adverse listening conditions such as background noise or reverberation, possibly due to reduced phase-locking ability. Additionally, a differential effect of background noise on envelope and TFS encoding speech as indexed by the FFR is observed in normal hearing (NH) subjects. The FFR is a scalp recorded sustained potential, reflecting phase-locked activity from a population of neural elements in the rostral brainstem. Here we evaluate the nature of alterations in the neural representation of envelope and TFS of steady-state and time-variant speech sounds in noise, and reverberant conditions in individuals with normal and impaired hearing.

Methods

FFRs were recorded from NH and HI listeners in response to a steady state synthetic vowel and a time-varying diphthong under conditions of background noise ("clean", +5 dB SNR, -5 dB SNR) and conditions of reverberation ("clean", mild, moderate and severe reverberation). Stimulus-response spectral correlations, autocorrelation functions, spectrograms and correlograms were used to describe the FFRs. In addition, pure tone audiograms, speech-in-noise scores and case-history information were obtained for all subjects.

Results

Spectral correlation results showed an increase in degradation of brainstem neural representation of envelope and TFS as SNR decreased for both groups with more robust representation for the NH group at SNRs greater than 0. NH group showed little or no degradation in neural phase-locking with increased reverberation for envelope but showed a significant degradation of the TFS. Envelope representation was stronger in NH compared to HI, however, the group differences were minimal for TFS encoding.

Conclusion

Degradation of envelope and TFS in NH is likely due to loss of spectral contrast and upward spread of masking in background noise and due to spectro-temporal smearing in reverberation. Degraded brainstem neural encoding of envelope and TFS in HI in background noise is likely due to a combination of lack of audibility, poor frequency resolution, loss of spectral contrasts, impaired neural synchrony, high frequency hearing loss and aging effects. Phase random-

izations at unresolved harmonics and temporal smearing of resolved harmonics superimposed on the effects of hearing loss may explain degraded envelope and TFS encoding in HI subjects in reverberation. Finally, traditionally used autocorrelation and FFT analyses are not sensitive to SNR/reverberation induced changes in subcortical neural encoding in the HI group; hence alternate measurement techniques must be explored and/or developed.

PS - 057

Individual Differences in Auditory Brainstem Response Latency in Noise: A Measure of Auditory Nerve Fiber Deafferentation?

Golbarg Mehraei¹; Hari Bharadwaj²; Sarah Verhulst²;

Barbara Shinn-Cunningham²

¹Massachusetts Institute of Technology, Harvard; ²Boston University

Background

Many listeners with normal hearing thresholds (NHT listeners) report difficulty communicating in situations with multiple sound sources. Such listeners are often diagnosed with "central auditory processing disorder," reflecting the implicit assumption that sound is represented robustly in the auditory nerve. However, recent studies have shown that noise exposure can preferentially reduce the number of low-spontaneous rate auditory nerve fibers (low-SR fibers) responding to sound, leaving normal detection thresholds but degraded encoding of supra-threshold sound. These low-SR fibers (< 20 sp/sec) are critical in sound encoding because they have a higher threshold than high-SR fibers (>20 sp/sec); they are thought responsible for increasing the dynamic range of the auditory periphery and allowing the system to be more resilient to masking by background noise. Motivated by these results, we hypothesize that the number of low-SR fibers conveying information about supra-threshold sound varies among NHT listeners. Models suggest that a low-SR loss will affect how the auditory brainstem response (ABR) wave-V latency changes when measured in different levels of noise. The logic of the current study is that 1) if the wave-V ABR latency is attributable to low-SR fibers, then individual differences should be seen in this latency change as a function of noise level and 2) this difference should correlate well with a measure that reflects the temporal precision of sound encoding of supra-threshold sound, such as interaural timing difference (ITD) sensitivity.

Methods

Here, we measured click-ABRs in quiet at click levels of 50-90 dB pSPL (10 dB steps) and in broadband pink noise with noise levels varying from 42 – 82 dB SPL (10 dB steps, click level=80dB pSPL) in NHT listeners. In the same subjects, we measured envelope ITD just noticeable difference (JND) (re: zero) of a narrowband signal with low-pass and notched-noise maskers.

Results

Results show a significant correlation between the rate of change in the wave-V latency and envelope ITD JND: sub-

jects with the worst ITD sensitivity in notched noise showed the smallest shifts in wave-V with noise level and vice versa.

Conclusion

These results support the hypothesis that NHT listeners differ in the number of low-SR fibers that respond to sound, which affects both perceptual sensitivity to temporal information in supra-threshold sound and ABR wave-V latency.

PS - 058

Persistent Neonatal Exposure to a Moderately-Intense Narrowband Sound Stimulus Alters Tonotopic Maps in Auditory Midbrain

Lisa D'Alessandro; Robert V. Harrison

University of Toronto

Background

Our sensory systems have evolved to provide central representations of the external (and internal) environment. During development, when there are natural patterns of sensory stimulation, ascending pathways develop normally. However, unusual patterns of stimulus-driven neuronal activity can result in the abnormal development of central sensory representations. While cortex is often studied in this regard, we are interested in sound frequency representation in the auditory midbrain following neonatal exposure to a narrowband-sound-enhanced environment.

Methods

Neonatal chinchillas were exposed to a moderately-intense (70 ± 5 dB SPL) narrowband (centered at 2 kHz) sound stimulus for 4 weeks. Frequency-specific auditory brainstem responses (ABRs) and scanning electron microscopy (SEM) were used to verify that such sound exposure did not cause cochlear damage. Standard multi-unit recordings were used to define tonotopic maps in the central nucleus of inferior colliculus (CIC).

Results

Electrode tracks through CIC of sound-exposed subjects were ~30% longer than age-matched controls (c. 4 mm vs. 3 mm). This increase was due primarily to a significant increase in neural representation of low frequencies (below 1 kHz). This over-representation did not occur near the center frequency of the sound-exposure signal, but rather at the low-frequency edge of the band of neural excitation. There were no differences in ABR thresholds across frequency between control and sound-exposed subjects (ANOVA, $p = 0.98$). Hair cells imaged along the length of the cochlea showed no sign of trauma. Taken together, ABR and SEM results suggest no change in hair cell function and structure as a result of sound-exposure.

Conclusion

These data support the hypothesis that persistent exposure to an abnormal sound environment -- during an early post-natal period -- can alter tonotopic organization in auditory midbrain. More broadly, this study contributes to a growing body of literature that suggests that sub-cortical levels of the ascending auditory pathway reorganize following changes in peripheral input during development.

PS - 059

Adaptive Coding of Sound Level in Auditory Midbrain Neurons: An *In Vivo* Intracellular Study

Roberta Donato; Jose' Garcia-Lazaro; Nicholas Lesica;

David McAlpine

UCL - Ear Institute

Background

A fundamental problem facing the auditory system is how to encode accurately the vast range (12 orders of magnitude) of changing stimulus intensities. Recently, we showed that firing rates of neurons in the auditory midbrain (inferior colliculus, IC) adapt to the ongoing distribution of sound intensities, improving coding by the neural population around the most-commonly occurring intensities. Having established the existence of an adaptive code for sound intensity in the auditory midbrain, it remains unclear as to what neuronal mechanisms underlying this rapid form of adaptation. In order to assess how neuronal properties contribute to adaptive coding, we performed *in vivo* intracellular recordings from individual IC neurons in anesthetised gerbils.

Methods

In-vivo intracellular responses to acoustic stimuli were recorded from individual IC neurons of ketamine/xylazine anesthetized, male, adult Mongolian gerbils using sharp glass electrodes. Neurons were characterized by their intrinsic electrical and acoustic responses, respectively, to current steps injected through the recording electrode and to acoustic stimuli consisting of tone pips presented every 150ms. Frequency response areas (FRAs) were obtained for test tones in the range 250 Hz to 8.192 kHz. To investigate the dynamics underlying adaptive coding of sound level statistics, sound levels of white noise (<25kHz) in the range 24-96dB SPL, with levels drawn randomly from a defined distribution, were presented every 40ms. The distribution of sound levels consisted of one or more regions of probable levels (high-probability regions, HPRs), from which sound levels were selected with an overall probability of 0.8; the remaining levels were selected with an overall probability of 0.2.

Results

The technique allowed us to assess the contribution of intrinsic and sub-threshold synaptic neuronal properties to the rapid adaptation to stimulus statistics. Neurons were first characterized on the basis of their frequency-vs.-level response area and their firing pattern in response to depolarizing current steps injected through the recording electrode. Responses were then recorded to dynamic noise stimuli in which the high-probability region of sound levels was systematically altered. Whereas the shape of synaptic responses to noise at different levels showed a remarkable reproducibility, the amplitude of the sub-threshold responses to the most likely intensities was potentiated.

Conclusion

Our preliminary data suggest that potentiation of synaptic responses underpins rapid adaptation to different statistical distributions of sounds

The Role of BK Channels in Shaping Receptive Field Properties in the Mouse Inferior Colliculus

Elliott Brecht; Benjamin Gross; Joseph Walton
University of South Florida

Background

The slow, Ca^{2+} activated, K^+ channels of the BK-type are responsible for controlling action potential duration, firing frequency, and spike frequency adaptation. BK channels can be found in the axon terminal, soma, and dendrites of neurons, and open in response to a rise in intracellular Ca^{2+} . We investigated the effect of applying a specific BK channel blocker, paxilline, on BK channel function, as measured by receptive field (RF) properties of inferior colliculus (IC) neurons in CBA/CaJ mice.

Methods

Young adult CBA/CaJ mice (6-8 months, $N=7$) were mildly tranquilized and placed in a stereotaxic frame using head bolt fixation. The IC was mapped and a location which yielded at least 10 active channels and within the central portion of the topographic map was chosen as the recording location for the experiment. This protocol resulted in 1 animal/dose/experiment. Paxilline was diluted to concentrations of 1 μM and 0.1 μM in 1% DMSO. The diluted doses of paxilline were both applied to the exposed IC via a micro-syringe. Multi-unit activity (MUA) was acquired using a 16-channel vertically oriented NeuroNexus probes. RFs were measured using 25 ms pure tones, presented in the contralateral hemi-field at frequencies between 4 & 64 kHz, from 0 to 80 dB SPL in 5 dB steps and replicated 5 times. For each RF the best frequency (BF), minimum threshold (MT), bandwidth at 10 (Q10) and 40 dB (Q40) above MT, maximum driven rate, and spontaneous rate were recorded.

Results

RFs were obtained from 58 units where 1 μM paxilline was applied and 64 units where 0.1 μM was applied, both resulted in a median decrease in driven rate measured at BF of 97% and 94%, respectively. The median MTs of pre-drug receptive fields were 20 dB and 22.5 dB at BF, following drug application, threshold shifts of 21 dB and 19.5 dB were immediate and were maintained over approximately 7 hours for the 1 μM dose and 5 hours for the 0.1 μM dose. Although there was a wide range of BFs encountered, the majority of BFs shifted towards lower frequencies following blockade of BK channels, with observed median shifts of approximately 1-2 kHz for neurons with BFs > 20 kHz. Both concentrations of drug produced stable BF shifts for over 6 hours.

Conclusion

These results suggest a role of BK channels in the formation and maintenance of receptive field properties of IC neurons. Preliminary data also indicates that blocking BK channels modulation of excitatory drive is intensity dependent. We are currently investigating the expression and functional changes involving BK in the aged IC.

Multiple Combination of Inputs to Inferior Colliculus (IC) Determines Synaptic Domains for Stimulus-Specific Adaptation (SSA) in Rat

Yaneri Ayala¹; Adanna Udeh²; Kelsey Dutta²; Deborah Bishop²; Manuel Malmierca¹; **Douglas Oliver²**

¹*Universidad de Salamanca*; ²*University of Connecticut Health Center*

Background

Survival requires the ability to rapidly identify and respond to unexpected events. Auditory neurons that exhibit SSA may contribute to this process since they respond to rare stimuli but habituate to repetitive ones. Neurons from the cortex of the IC exhibit remarkable SSA levels as opposed to those from the central nucleus, that show very little or no SSA. These physiological findings suggest there may be different neuronal microcircuits related to these distinct SSA properties. Here, we ask whether SSA neurons receive inputs from different pathways than non-SSA neurons.

Methods

Extracellular single-unit responses were recorded from IC neurons in anesthetized rats (Long-Evans) with an oddball acoustic stimulation paradigm (deviant, 10% probability and repetitive, 90% probability). After physiological characterization, tiny microiontophoretic injections (Fluorogold, FG, 2%, 0.5 μA , 1sec) were made at the recording sites. After survival and tissue fixation, and immunohistochemistry, the retrogradely labeled neurons were plotted with a NeuroLucida system, the Nissl cytoarchitecture was drawn, and the density gradients of the injection sites were analyzed with image processing.

Results

We compared the labeling patterns of injection sites with typical SSA neurons with significant (bootstrapped) SSA levels ($\text{CSI}=0.7-0.8$) and broadly tuned, complex frequency response areas (FRA) to those of non-SSA neurons ($\text{CSI}=0$) with sharply tuned FRA. In the SSA cases, FG injections in the IC were localized in the lateral IC cortex ($n=3$) or rostral IC cortex (at level of caudal superior colliculus, $n=3$). The IC in those cases received heavy inputs from auditory neocortex especially the primary and dorsal areas and little or no brainstem input. In the non-SSA cases ($n=3$), FG injections were restricted to the dorsolateral ($n=2$) or ventrolateral ($n=1$) central nucleus. The IC of control cases received projections from cochlear nucleus, superior olivary complex, and lateral lemniscal nuclei with few labeled neurons in more ventral auditory cortex.

Conclusion

Since the sources of input to SSA sites and non-SSA sites were dissimilar, these data suggest that this function may be restricted to synaptic domains in the IC with specific inputs, and it may be absent in other domains. Specifically, it suggests that SSA neurons in IC may receive important corticofugal inputs that may be related to this adaptation process but not available to non-SSA neurons.

Optogenetic Stimulation of the Mouse Primary Auditory Cortex Enhances Concurrent Tone-Evoked Activity in the Lateral – but not Central – Nucleus of the Inferior Colliculus

Keith Darrow¹; Wei Guo²; Maryanna Owoc¹; Daniel Lee³; Daniel Polley³

¹Worcester State University; ²Boston University; ³Harvard Medical School

Background

The auditory corticofugal system has been implicated in a diverse range of cognitive functions ranging from memory consolidation to dynamic sensory filtering. However, a detailed understanding of its role in sound processing has remained elusive due to the technical disadvantages associated with measuring sensory-evoked activity during prolonged electrical stimulation. Here, we have overcome this technical hurdle by optogenetically stimulating the primary auditory cortex (A1) while recording from lemniscal (central nucleus) and non-lemniscal (external cortex) subdivisions of the inferior colliculus (IC).

Methods

Channelrhodopsin-2 (ChR2) was delivered to the auditory cortex through viral-mediated gene transfer in adult CBA/J mice. After 3-5 weeks of incubation, mice were re-anesthetized and the optical fiber placed on a high frequency region of the A1 tonotopic map (26–32 kHz). Laser-evoked spiking thresholds were determined in both IC subdivisions to identify a level of stimulation intensity that might modulate activity without evoking direct excitation. Subsequently, sound evoked unit responses were measured in the IC with and without near-threshold stimulation of A1 with blue laser light. Laser pulses (5 ms pulse width at 30 Hz) began 100 ms prior and co-terminated with sound stimulation.

Results

Histological analysis (n=6) revealed ChR2 infection throughout A1. The fluorescent reporter molecule (mCherry) also illuminated the descending network of axons that primarily innervated the lateral and dorsal cortex, with significantly fewer visible axons in the central nucleus. Unit recordings in the central nucleus revealed a precisely organized dorsal-ventral tonotopic gradient, whereas tonal receptive fields in the external cortex were broadly tuned and non-tonotopically organized. External cortex neurons were entrained to A1 stimulation at intensities as low as 0.5 mW, whereas central nucleus units were rarely directly responsive to A1 stimulation intensities as high as 7 mW. FRAs were recorded with interleaved laser-off and near-threshold laser-on trials. Tone-evoked responses were globally enhanced by A1 stimulation in the external cortex, however modulation in the central nucleus was not observed. Analysis of latency, threshold, and tuning bandwidth did not reveal a significant difference between the laser-on and laser-off conditions in either subdivision. Lesions made in the external and central nuclei of IC confirmed recording location.

Conclusion

These data suggest that corticocollicular projections prime neurons in non-lemniscal regions of the IC to respond more robustly to sound. Efforts to assess cortical influence on several other domains of sound representation in the IC, including rate level functions, amplitude modulation, and tone-in-noise masking, are ongoing.

PS - 063

Neuronal Processing Mechanisms Underlying Masking and Spatial Release from Masking in Gerbils

Astrid Klinge-Strahl; Rainer Beutelmann; Georg Klump
University of Oldenburg

Background

The auditory system of animals and humans developed processing mechanisms to cope with situations in which behaviorally important signals are masked by competing sounds. Experimentally, these can be studied by determining the amount of masking in relation to the sound characteristics of signal and masker. For example, detecting a signal can be facilitated by spatially separating it from a masker. Psychoacoustic studies on spatial (or binaural) release of masking (SRM) were mostly focused on humans. Few of these studies investigated combined effects of several sound characteristics such as harmonicity and spatial location on masking. Lacking altogether are combinations of neurophysiological and behavioral experiments in the same animal species that would allow directly relating changes in neural responses to behaviorally observed masking effects and SRM.

Methods

Here, we determined behavioral masked thresholds and the amount of SRM in gerbils for combinations of five masker types and two spatial configurations (pure tone signal and masker co-located or spatially separated) in a low and a high frequency region (1 and 8 kHz). Results were compared to masked thresholds determined from neural responses in the inferior colliculus (IC) of anesthetized gerbils. As many natural sounds are composed of harmonic complexes and harmonicity is a very important cue in auditory scene analysis we constructed harmonic and inharmonic complex masker stimuli.

Results

Behavioral experiments showed that masked thresholds significantly depended on the masker type. Harmonicity facilitated the detection of the target in the harmonic maskers, while masking by inharmonic maskers resulted in increased masked thresholds. SRM was found only for the 8 kHz region. Responses of neurons in the IC significantly differed for the different masker types and depended on the spatial location of signal and masker for both frequency regions. Mean neuronal masked thresholds were considerably higher than behavioral thresholds. However, the performance of individual neuronal units was comparable to behavioral thresholds, especially in the 1 kHz frequency region. The gerbils' behavioral thresholds are further compared and discussed with those previously reported for humans using the same stimuli.

Conclusion

The behavioral and neurophysiological results suggest that gerbils exploit harmonicity cues to facilitate the detection of a target in a masker. Results further indicate that gerbils exploited interaural level differences as a spatial cue but not interaural time differences. Single neurons or small populations of neurons may be able to account for the behavioral performance.

PS - 064

Asymmetric Temporal Interactions of Excitatory and Inhibitory Inputs in the Auditory Midbrain

Munenori Ono; Douglas Oliver

University of Connecticut Health Center

Background

Inferior colliculus (IC) is a critical auditory center in the midbrain. The synaptic inputs to IC neurons are complex and arrive via ascending and local sources. The IC is unique since inputs ascending from lower centers may be either excitatory or inhibitory. Yet, little is known about the temporal properties of these synaptic inputs in IC, primarily because there are few direct measurements of the excitatory and inhibitory post-synaptic currents (EPSC, IPSC) evoked by sensory stimuli *in vivo*. Especially, it has not been examined in detail how the diverse spike responses in the IC can be generated by synaptic interaction of excitatory and inhibitory inputs.

Methods

Forty three GAD67-GFP knock-in mice of either sex (Postnatal day 26 – 42) were used for this study. We used voltage clamp and whole cell recordings to isolate and investigate EPSCs and IPSCs in IC neurons *in vivo* in response to sustained tones. The EPSCs and IPSCs were isolated by clamping the cell at reversal potentials of IPSCs and EPSCs, respectively. The resting potentials *in vivo* were pharmacologically validated. To simulate the spike responses generated by excitatory and inhibitory inputs, we used an integrate-and-fire model.

Results

We found that most IC neurons have both excitatory and inhibitory synaptic currents evoked by acoustic stimuli in the same ear. The tone-evoked EPSCs and IPSCs had temporal patterns that varied in different ways. The latency of the EPSC peak varied over a wide range from very early to very delayed, while IPSC peak was only early. Both EPSCs and IPSCs had a range of durations, but only IPSCs showed an off response. Within the same neuron, the EPSCs with the shortest latency and shortest duration typically had IPSCs with longer latency and longer duration. We modeled how EPSCs and IPSCs integrate to fire IC neurons. The model showed that the temporal pattern of spikes reflected the time course of the EPSC strongly. It also showed that the balance and temporal relevance of IPSCs to EPSCs profoundly altered the spike responses.

Conclusion

These results suggested that the EPSCs and IPSCs form an asymmetric temporal interaction and contributed to generat-

ing the diverse responses in the IC in different ways; EPSCs provided highly variable driving force, while IPSCs modulated the firing efficiently depending on the balance and temporal relevance to EPSCs.

PS - 066

Rostral Pole of the Inferior Colliculus is a Distinct Entity: Morphological Evidence in Cat, Mole and Rat

Motoi Kudo; Fuduki Inoguchi; Tomoko Kimura; Kousuke Taki

Shiga University of Medical Science

Background

The inferior colliculus (IC) is largely subdivided into the central nucleus (ICC) and the surroundings such as the external nucleus (EN) and the dorsal cortex (DC). While the ICC is referred to as a main/lemniscal center, the EN and the DC are as to shell/extra-lemniscal regions. The nucleus of brachium of IC (NBIC) and the dorsal nucleus of lateral lemniscus (DLL) are also known independent structures closely related to the IC. The present study indicates that the rostral pole of IC (RP) should be classified as a distinct entity.

Methods

In the cat, tract-tracing study was conducted by the tritiated-leucine autoradiography (Kudo and Niimi 1980). In the mole, frontal sections were stained with cresyl violet for cytoarchitecture; parasagittal sections were for myeline stain. In the rat, Alexafluoro®-555 conjugated cholera toxin B subunit are injected into the pretectum and midbrain reticular formation (Pt-MRF). After 3-5 days' survival, rats were fixed and the brain slices were treated with anti-GABA rabbit serum for double fluorescent labeling technique.

Results

In the cat, projection fibers from the ICC terminate in the RP, while those from the EN terminate in the NBIC and the deep layer of the superior colliculus but not in the RP. In the mole, of which auditory system is well developed supplementary to the reduced visual system (Kudo et al., 1997), Nissl and myelin stained specimens of the midbrain were used for cytoarchitecture and myeloarchitecture. We found that the RP of the mole is distinct both in size and shape among the shell regions outside the ICC. In the rat, distribution of GABAergic neurons that project to the Pt-MRF was examined using double fluorescent. The results revealed that GABA immunopositive neurons are distributed exclusively in the RP. Taken these comparative studies together, it is highly possible that the RP is a separate module of auditory brainstem.

Conclusion

Faye-Lund and Osen (1985) have subdivided the IC of the rat using Golgi, Nissl and cell-myelin methods. Based on this demarcation, the EN and the RP have been mixed together as "external cortex of the IC (ECIC)" in Paxinos and Watson's rat atlas (1986-2009). Some authors revisit this matter recently. Loftus et al. (2008) made parcellation in the rat and cat and distinguished the RP from the EN. Cant and Benson (2008)

studied the projection from the cochlear nucleus to the IC in the gerbil and recognized the RP as a separate entity.

PS - 067

***In-Vivo* Whole Cell Recordings Revealed Binaural Mechanism for EI Neurons**

Na Li; George Pollak

The University of Texas at Austin

Background

Cells that receive excitation from one ear and inhibition from the other (EI cells) process interaural intensity disparities (IIDs), the cues for localizing high frequencies. EI cells in the inferior colliculus (IC) fire to contralateral stimulation, while ipsilateral stimulation at progressively higher intensities suppresses the spikes evoked by contralateral stimulation.

Methods

To evaluate the mechanism underlying binaural suppressions, we made whole cell patch-clamp recordings in 28 EI cells in the IC of awake Mexican free-tailed bats. and recorded both spikes and postsynaptic potentials (PSPs) evoked by contralateral, ipsilateral and binaural signals. Excitatory and inhibitory synaptic conductances were also derived from each contralateral, ipsilateral and binaural response in some cells.

Results

Although all EI cells were homogenous in terms of their spike suppression with binaural stimulation, different types of responses were observed in response to ipsilateral stimulation, suggesting that the circuits involved in binaural suppression were more diverse and complicated. Most interestingly, in 7/28 cells, a low ipsilateral intensity evoked an IPSP that was then changed into EPSPs at higher ipsilateral intensities. However, a binaural signal with a higher ipsilateral intensity produced a larger binaural suppression. Based on both PSPs and conductances, we proposed the inputs that innervate this type of EI cells and showed that at a low ipsilateral intensity, the EI suppression was produced mainly by a direct suppression of ipsilateral inhibition in the IC. However, at higher ipsilateral intensities or large IIDs, the inputs driven by the signals are more complicated. An ipsilateral signal drove more excitatory inputs because it evoked a larger excitatory conductance, which in turn evoked an EPSP. At the same time, it also suppressed the binaural lower nuclei which was driven by the contralateral signal. Because this ipsilateral suppression at the lower nuclei has a larger impact than the increase of excitatory inputs. The net outcome is to suppress neuron's response.

Conclusion

These results revealed that both the ipsilateral circuit and the inputs driven by binaural signals are more complicated than what have been shown previously.

PS - 068

Fine-Scale Tonotopic Arrangement in the Dorsal Cortex of the Mouse Inferior Colliculus Studied With Two-Photon Calcium Imaging

Oliver Barnstedt; Peter Keating; Andrew King; Johannes Dahmen

University of Oxford

Background

The inferior colliculus (IC) is the largest auditory structure of the midbrain. It receives ascending input from the brainstem but also descending projections from the auditory cortex. While the central nucleus of the IC has received a lot of attention, very little is still known about the function of the dorsal cortex (ICd) of the IC. In the mouse the ICd is located between the cerebral cortex and the cerebellum and is, therefore, accessible with optical methods. We took advantage of this and set out to investigate the fine-scale tonotopic arrangement of the ICd with two-photon imaging.

Methods

We injected C57BL/6 mice with a viral vector to induce the expression of the genetically encoded calcium indicator GCaMP6m. Injections were targeted either to the dorsal part of the inferior colliculus or layer V of the auditory cortex. Four weeks later we imaged, using a two-photon microscope, populations of ICd neurons or cortico-collicular terminals in anaesthetised mice and characterised their responses to noise bursts and pure tones.

Results

ICd neurons exhibited strong responses to tones and noise bursts and we found robust evidence for a tonotopic arrangement of the cell body populations that we imaged - the difference in characteristic frequency between pairs of neurons increased as a function of distance, and there was evidence for a frequency gradient. Terminals of cortico-collicular neurons showed only weak acoustically driven responses.

Conclusion

Using two-photon calcium imaging in the ICd for the first time, we found robust acoustically driven responses and sharp frequency tuning of cell bodies in the ICd as well as evidence for a tonotopic arrangement. The nature of the responses of the cortico-collicular terminals suggests that they have more of a modulatory rather than a driving influence on the activity of ICd neurons.

PS - 069

Auditory Cortical Axons Contact Both GABAergic and Non-GABAergic Cells in the Auditory Midbrain That Project to the Medial Geniculate Body

Jeffrey Mellott; Brett Schofield

Northeast Ohio Medical University

Background

The projection from the inferior colliculus (IC) to the medial geniculate body (MG) arises from both glutamatergic and GABAergic cells. The GABAergic cells make up 20-40% of the projecting cells, depending on species. Previous studies

have shown that axons from the auditory cortex (AC) contact IC cells that project to the MG, but did not identify the neurotransmitter phenotype of the colliculothalamic cells (Coomes-Peterson and Schofield, 2007). We combined multi-fluorescent tracing with immunohistochemistry to determine whether AC axons contact GABAergic or non-GABAergic (i.e., glutamatergic) colliculothalamic cells.

Methods

We injected FluoroGold into the left MG to label colliculothalamic cells and FluoroRuby into the left AC to label cortical axons in adult guinea pigs. We stained the tissue with anti-glutamic acid decarboxylase (GAD) to identify GABAergic cells. We examined the left IC with fluorescence microscopy to identify putative contacts between the labeled cortical axons and retrogradely-labeled cells.

Results

Labeled cortical boutons form close contacts (apparent synapses) with both GAD-positive (GAD+) and GAD-negative IC-MG cells in all subdivisions of the IC. A minority of the contacted cells are in the central nucleus, whereas the majority are in the surrounding IC subdivisions. In the course of these experiments, we observed several new findings regarding projections from the nucleus of the brachium of the IC (NBIC) to the MG: 1) a subset of the NBIC-MG cells are GAD+ and, 2) AC axons contact both GAD+ and GAD-negative NBIC-MG cells.

Conclusion

Axons from the AC make putative synaptic contacts on both GABAergic and glutamatergic ascending pathways to the thalamus. These include projections from both the IC and the NBIC to the MG. Colliculothalamic projections constitute the major source of ascending auditory input to the MG and are considered to play a role in many auditory functions. The GABAergic projections are assumed to provide feedforward inhibition, but specific functions have yet to be identified. We show here an additional GABAergic projection to the MG from the NBIC. NBIC cells have been associated with sound localization, although additional roles may yet be discovered. Beyond feedforward inhibition and excitation, specific roles of the GABAergic and glutamatergic projections from NBIC to MG are unclear. The results suggest that corticofugal projections are in a position to modulate both excitatory and inhibitory ascending pathways to the auditory thalamus.

PS - 070

Converging Midbrain Afferent Patterns and Auditory Brainstem Responses in Ephrin-B3 Mutant Mice

William Nofzt; Lincoln Gray; Mark Gabriele
James Madison University

Background

Eph-ephrins, a family of receptor tyrosine kinases, provide cell-cell interactions that are necessary for the establishment of topographic mapping and pattern formation in the developing nervous system. Recent studies in our laboratory have shown in mouse the transient expression of certain Eph-eph-

rin members in the developing inferior colliculus (IC) prior to hearing onset. EphA4 and ephrin-B2 expression is graded along the tonotopic axis of the central nucleus (CNIC), while occupying discrete modular domains in layer 2 of its lateral cortex (LCIC). In contrast, ephrin-B3 expression is absent in the CNIC, while highly expressed in extramodular domains of the LCIC.

Methods

Here we utilize multiple-labeling approaches in control and ephrin-B3 mutants to explore the development of converging CNIC and LCIC afferent patterns. Dyes were positioned in the CNIC and either the lateral superior olive (LSO) or the superior paraolivary nucleus (SPON). Additionally, we performed auditory brainstem responses (ABRs) as a physiological assessment of the auditory circuitry for each of our experimental groups.

Results

Tract-tracing studies describe the relative distribution patterns and spatial registry of crossed CNIC and ipsilateral LSO and SPON inputs to the target IC. All three projections exhibit tonotopically-arranged axonal layers within the CNIC. LSO inputs preferentially target more rostral aspects of the CNIC and are largely absent from LCIC modular fields. Crossed CNIC inputs display a frequency-matched dorsal bias in the CNIC, as well as a projection component that targets presumptive extramodular LCIC zones. A projection from the SPON to the LCIC is also described and complementary to that of the CNIC, occupying LCIC modules. Quantitative measures compare CNIC (layering) and LCIC (modular-extramodular) axonal patterns in wild-type and ephrin-B3 mutants. ABR peak V amplitudes reflect midbrain activation and appear reduced and delayed in ephrin-B3 mutants, especially in homozygous mice. Earlier waves also appear altered, again most pronounced in homozygotes.

Conclusion

Taken together, these findings suggest an important role for ephrin-B3 in constructing fully functional auditory circuits prior to experience.

PS - 071

Perisomatic Rings of Glutamatergic Terminals Identify a Subset of GABAergic Cells in Inferior Colliculus That are Surrounded by Perineuronal Nets

Nichole Foster; Brett R Schofield
Northeast Ohio Medical University

Background

Perineuronal nets (PNs) are aggregates of extracellular matrix surrounding certain neurons (preferentially GABAergic) in many brain areas and are known to affect synaptic plasticity, inhibit structural plasticity, and to have neuroprotective effects (Karetko et al. 2009, *Acta Neurobiol Exp* 69:564). PNs surround about 50% of the GABAergic cells in the IC central nucleus (ICc) and ~15-20% of GABAergic cells in other IC subdivisions (Foster et al. 2012, *Soc. Neurosci. Abst.* 365.10). In rats, a subset of GABAergic IC cells can be identified by the

presence of a perisomatic ring of glutamatergic terminals that immunostain for the vesicular glutamate transporter VGLUT2 (Ito et al. 2009, J. Neurosci. 29: 13860). Here, we examined the relationship between VGLUT2+ rings and PNs on IC GABAergic cells.

Methods

In adult guinea pigs, PNs were stained with fluorescent-labeled *Wisteria floribunda* agglutinin, GABAergic cells were stained with an antibody to glutamic acid decarboxylase (GAD), and VGLUT2+ terminals were stained with an antibody to VGLUT2. The labels were distinguished with different fluorescent tags.

Results

VGLUT2 rings were observed in all IC subdivisions, but were most numerous in the ICc. VGLUT2+ rings surrounded about 10% of all GAD+ cells (13% in IC central nucleus). Almost all (88% on average) of these cells were also surrounded by PNs. However, even within the "netted" population, rings were associated with a minority of the GAD+ cells. GAD+ cells without nets make up about 50% of GAD+ cells in the ICc and 80-87% of GAD+ cells in other subdivisions; very few of these cells in any subdivision had VGLUT2 rings (<2% of all GAD+ cells).

Conclusion

VGLUT2+ terminals form perisomatic rings around a small percentage of GABAergic neurons in the IC of guinea pigs. As in rats, these rings are more numerous in the central nucleus than in surrounding regions. Throughout the IC, most GABAergic cells that have VGLUT2+ rings are also surrounded by perineuronal nets. This could have implications for the plasticity of VGLUT2 terminals because PNs have been demonstrated to affect long-term synaptic plasticity. PNs also create a barrier to new synaptic contacts on the surrounded neurons, suggesting that the VGLUT2 rings could become "locked in" by a PN after development. Many other GABAergic IC neurons have nets but not rings, suggesting that the functions of the nets extend beyond those related to the VGLUT2 rings.

PS - 072

Harmonicity Outplays Direction Cues in Grouping Tasks

Lena Eipert; Astrid Klinge-Strahl; Georg M. Klump
Center of Excellence "Hearing4all", Animal Physiology and Behavior Group, Department for Neuroscience, School for Medicine and Health Sciences, Oldenburg University, Germany

Background

Auditory scene analysis refers to the processes that form coherent and functional perceptual representations of distinct sources in the environment (Bregman, 1990, Auditory Scene Analysis, Cambridge, MA). One important mechanism is the simultaneous grouping of frequency components of the sound forming a representation of a single sound source and the segregation of these sounds from other concurrent sounds. Harmonicity is one of the most important cues for the grouping of concurrent sounds. Spatial location of a sound

source can also serve as a grouping cue - even though it appears to be weaker than harmonicity. Furthermore, the ability to employ interaural time differences (ITDs) or its frequency dependent equivalent interaural phase differences (IPDs) in perceptual segregation poses a paradox (Darwin, 1997, Trends Cogn. Sci., 1:327): While ITDs have evident power to define a sound source over time, they are ineffective at producing simultaneous grouping. As it is yet unknown how ITDs/IPDs and harmonicity interact in processing, we evaluate how IPDs are represented in the auditory system if they compete with the harmonicity grouping cue.

Methods

We investigated the representation of IPDs introduced on either the harmonic or mistuned lowest frequency component of a harmonic complex by neurons in the inferior colliculus (IC) of anesthetized gerbils. Furthermore, we tested the perceptual ability of humans to detect IPDs of the lowest frequency component (low frequency condition) or of the 3rd harmonic (high frequency condition) in harmonic and mistuned complexes. Both electrophysiological and psychophysical results were compared and discussed relating thresholds to binaural model predictions (Dietz et al., 2008, Brain Res., 1220:234).

Results

IC neurons could represent IPDs of components of complex sounds. No significant neuronal IPD threshold differences between harmonic and mistuned complexes were observed. Human subjects showed difficulties in detecting IPDs, even though the binaural model by Dietz et al. (2008) predicts small IPD thresholds in low frequency harmonic and mistuned components.

Conclusion

Psychophysically, IPD cues provided by components in a complex stimulus appear to be a weaker grouping cue than harmonicity and IPDs are difficult to detect. However, the gerbil IC neurons demonstrate that the IPD based directional information is available on the level of the IC. Thus, the weighting of the grouping cues leading to the observed psychophysical results must occur at higher levels of the auditory pathway.

PS - 073

The Acoustic Environment Matters: Differential Effects of Different Kinds of Cochlear Damage on Spontaneous Activity in the Central Auditory System of Mice

Warren Bakay¹; L.L. Hesse²; H.C. Ong²; J.F. Ashmore²; D. McAlpine²; J.F. Linden²; R. Schaette²

¹University College London; ²Medical Faculty, University of Luebeck; ²Ear Institute, University College London

Background

A recent study in mice has shown that normal hearing thresholds do not necessarily indicate the absence of cochlear damage. Following temporary threshold shifts induced by noise exposure, a permanent reduction in wave I of the auditory brainstem response (ABR) and deafferentation of auditory nerve fibres (ANFs) have been observed (Kujawa

and Liberman, 2009). In tinnitus subjects with normal audiograms, a similar reduction of ABR wave I has been observed in conjunction with normal amplitudes of the centrally-generated wave V (Schaette and McAlpine, 2011), suggesting that ANF deafferentation together with a compensatory increase in neuronal response gain might underlie the generation of tinnitus. We have now investigated the effects of ANF deafferentation on the central auditory system in a mouse model, and compared them to the consequences of hearing threshold increase.

Methods

A/Ca mice were exposed to octave-band noise (8-16kHz) at 96, 100dB, or 105dB SPL for 2 hours. ABRs were recorded before, 1 day and 4 weeks after trauma. Extracellular multiunit recordings from the inferior colliculus were obtained 4 weeks post-trauma. Cochlear histology was performed on cochleae recovered after the 100dB and 105dB experiments. All experiments were performed under ketamine/medetomidine anaesthesia.

Results

All trauma groups showed significant increases in ABR thresholds and reductions in ABR wave amplitudes 1 day post-trauma. 4 weeks post-trauma, thresholds had recovered fully in the 96dB group, whereas the 105dB group still showed threshold elevations. ABR wave I amplitudes remained decreased in all groups, indicating deafferentation of ANFs, which was confirmed histologically for the 100 dB and 105 dB groups, where immunohistochemistry showed a reduced number of synaptic ribbons with a dose-dependent effect. Amplitudes of ABR wave IV remained below pre-trauma values in the 96dB group, but recovered and reached pre-trauma levels at high sound intensities in the 100 dB and 105 dB groups, suggesting a compensatory increase in neuronal response gain.

Extracellular multiunit recordings were obtained from the inferior colliculus four weeks post trauma. In the 96dB group, there was no significant increase in spontaneous firing rates. In the 105dB group, spontaneous firing rates of neurons with characteristic frequencies in the trauma frequency range were significantly increased, and correlated with increased response thresholds, but not with ANF deafferentation.

Conclusion

Our results suggest that in the mouse, hearing threshold shifts might be a more potent driver for neuronal plasticity than ANF deafferentation.

PS - 074

The Effect of 16p11.2 Chromosomal Deletion on Mouse Hearing

Elena Mahrt¹; Mu Yang²; Jacqueline Crawley²; Thomas Portmann³; Ricardo Dolmetsch³; Christine Portfors¹

¹Washington State University, Vancouver; ²University of California Davis; ³Stanford University, Palo Alto, CA

Background

An increasing number of human autism spectrum disorders are attributable to chromosomal copy number variants.

One such example is a deletion on chromosome 16p11.2. To investigate the role the 16p11.2 deletion plays in autism spectrum disorders, a mouse with the 16p11.2 deletion has been created. This mouse has various neuroanatomical and behavioral abnormalities, but its sensory physiology has not been described. This is a major gap because some humans with the 16p11.2 deletion have sensory deficits, including hearing loss. Thus, it is important to understand what sensory deficits may be present in the 16p11.2 mouse. Moreover, it is important to understand if sensory deficits underlie some of the deficits in social behavior that these mouse models exhibit. The purpose of this study was to test hearing sensitivity of heterozygous 16p11.2 deletion mice.

Methods

Auditory brainstem response (ABR) thresholds of 11 heterozygous 16p11.2 deletion mice were measured and compared to 16 wild-type littermates. Thresholds were determined by presenting pure tone frequencies between 8 and 100 kHz at decreasing intensities in a 5 dB SPL resolution until no response was observed.

Results

None of the 11 heterozygous 16p11.2 deletion mice tested had measurable evoked responses to any frequencies tested when presented at maximum intensity (≥ 79 dB SPL). In contrast, wild-type mice had normal ABR thresholds.

Conclusion

Our results indicate that mice with a 16p11.2 chromosomal deletion are functionally deaf. These results potentially provide insight into a mechanism for hearing loss seen in humans with the 16p11.2 deletion. Additionally, it is unknown if other mouse models of autism exhibiting behavioral deficits suffer from such severe auditory sensory loss. Experiments such as this should be conducted to explore whether social behavior deficits found in mouse models of autism are due to the inability to detect sounds important in social interactions such as vocalizations.

PS - 075

Spatial Distribution of Gap Detection Thresholds and Temporal Modulation Sensitivity in the Mouse Inferior Colliculus

Rüdiger Land; Alice Burghard; Andrej Kral

Hannover Medical School

Background

The ability of the auditory midbrain to follow the temporal structure of sounds at high frequencies is important for the discrimination of complex sounds. The impairment of these temporal properties in the auditory midbrain might be a potential cause underlying the pathology of central auditory processing disorders.

Methods

Here, we studied the spatial distribution of the temporal properties within the inferior colliculus in C57Bl/6 mice. We recorded the depth profile of the inferior colliculus with a multi-electrode array and determined the temporal modulation sensitivity and gap detection thresholds of extracellular

multiunit activity. Gap detection sensitivity is the ability to detect a gap in ongoing sound, whereas temporal modulation sensitivity is the ability to follow the temporal fine structure of an ongoing stimulus. Gap detection was tested for gaps between 0.1 ms to 10 ms within ongoing white noise. Temporal modulation sensitivity was measured for a sinusoidally amplitude modulated (SAM) white noise stimulus at increasing modulation frequencies from 10 Hz up to 1000 Hz and compared to the auditory pulse train resolution at the same temporal rates from 10 Hz up to 1000 Hz.

Results

The gap detection thresholds of multiunit activity ranged between 1-3 ms. Gap detection thresholds were similarly distributed for positions throughout the depth of the inferior colliculus. The modulation frequency sensitivity for SAM stimuli was generally below 200 Hz. The pulse train frequency resolution ranged at similar frequencies below 200 Hz, but generally had a higher signal-to-noise ratio than the multiunit responses for SAM stimuli. Both, modulation frequency sensitivity and pulse train resolution had a characteristic spatial distribution within the inferior colliculus.

Conclusion

The gap detection threshold and the temporal modulation sensitivity are two robust temporal characteristics of the inferior colliculus, and these temporal variables can be exploited for dynamic phenotyping of transgenic mouse models. The comparison of various pathological phenotypes, in which these temporal properties of the auditory midbrain are impaired, might subsequently provide insight into the underlying causes of central auditory processing disorders.

PS - 076

Nonlinear Temporal Envelope Processing in the Inferior Colliculus

Hemant Srivastava¹; Paul Nelson²; Eric Young²; Sharba Bandyopadhyay¹

¹National Brain Research Centre; ²Johns Hopkins University

Background

Temporal envelope of sounds carries information about the sound stimulus and is useful in identification and discrimination of different sound segments. In the periphery the auditory nerve is known to encode temporal information linearly. Further along the auditory pathway responses become nonlinear with context dependence emerging.

Methods

We use a best frequency (BF) tone stimulus that is modulated by an order 12 m-sequence, which takes on 0 or 1 values every 3 ms. By using an m-sequence temporal envelope the neuron is probed with all possible stimulus combinations of 36 ms allowing us to investigate context dependence. Spiking responses from single neurons in the inferior colliculus (IC) of the awake marmoset to such stimuli were collected. We also used model auditory nerve fiber (ANF) responses to same stimuli in order to investigate transformations in temporal processing between the auditory periphery and the IC.

Results

Based on mutual information between responses and different transformations of stimulus we find that almost half of the IC neurons are nonlinear in their temporal processing as opposed to almost none in ANFs. We show that a second order model of temporal envelope processing is sufficient to describe envelope encoding in the IC. Such a model includes interactions between stimuli at different time points preceding the response, which shows dependencies between stimulus segments as large as 20 ms apart. The second order model shows mean prediction fraction of variances of 62% with a 67% improvement on average over the first order model. On the other hand in ANFs there is no improvement in prediction performance with a second order model.

Conclusion

Thus we show that neuronal response to envelope modulations in the IC is strongly context dependent, which can be both excitatory and inhibitory based on the analysis of second order model. ANFs do not show such effects. Such interactions possibly emerge from synaptic depression and also convergence of excitation and delayed inhibition.

PS - 077

Neural Correlates of Behavioral Comodulation Masking Release in the Rabbit

Muhammad Zilany¹; Laurel H. Carney²

¹University of Malaya; ²University of Rochester

Background

Detection of tones in noise improves for maskers with coherent fluctuations across frequency bands, referred to as comodulation masking release (CMR) (Hall et al., 1984, 76:50, JASA). Broadband inhibition in the cochlear nucleus and suppression of envelope locking at higher auditory centers have been hypothesized as neural mechanisms underlying CMR. In this study, neural responses recorded from the inferior colliculus (IC) of the awake rabbit were compared to behavioral CMR in rabbit.

Methods

Detection thresholds for 700 or 1500 Hz tones were estimated in comodulated or random noise maskers using a flanking band (FB) paradigm. The masker consisted of five noise bands (one signal-centered, two upper and two lower FBs); the noise level was 60 dB SPL. Stimulus paradigms for both behavioral and physiological recordings were matched to a study of CMR in human. Rabbits were tested with operant conditioning using a single-interval two-alternative choice task in a tracking procedure. Responses were recorded from neurons in the central nucleus of the IC. Thresholds based on changes in average discharge rate were estimated with a neurometric strategy employing receiver-operating characteristic analysis. Best frequency (BF), modulation transfer function (MTF), and best modulation frequency (BMF) were measured for each cell.

Results

The behavioral CMR in rabbits was ~5-6 dB at 1500 Hz and ~1-3 dB at 700 Hz, in comparison to the ~10 dB CMR reported for humans in the same paradigm at 700 Hz. Preliminary

nary results suggest that the best neural detection thresholds based on changes in average discharge rate explained rabbit behavioral detection thresholds in comodulated or random maskers. Robust changes in rate with tone level were observed for IC neurons that had BF matched to the tone frequency and BMF within the noise envelope bandwidth. Cells with bandpass, and some lowpass, MTFs had rates that *decreased* with increasing tone level (similar to synchrony suppression), because the addition of a tone to the noise flattened the overall envelope. In contrast, the majority of neurons with band-reject or high-pass MTFs had *increasing* rates with tone level.

Conclusion

Results suggested that changes in average discharge rate of some IC neurons could explain behavioral CMR in rabbits. Neural detection thresholds for tones in comodulated or random maskers resulted from either a decrease or an increase in rate depending on the type of MTF. Bandpass responses to comodulated signals were consistent with the same-frequency excitation-inhibition model for bandpass MTFs (Nelson and Carney, JASA, 2004).

PS - 016

Mismatch Negativity-Like Responses in the Rat Auditory System in the Oddball Paradigm

Haruka Nakahara¹; Kazusa Takahashi²; Tomoyo Shiramatsu²; Takahiro Noda⁴; Ryohei Kanzaki³; Hirokazu Takahashi³

¹Teikyo University School of Medicine, Mizonokuchi Hospital; ²Department of Mechano-Informatics, Graduate School of Information Science and Technology, the University of Tokyo; ³Department of Mechano-Informatics, Graduate School of Information Science and Technology, the University of Tokyo, Research Center for Advanced Science and Technology, the University of Tokyo; ⁴Research Center for Advanced Science and Technology, the University of Tokyo

Background

In humans, one of the goals of the auditory pathway may be the cognition of the sounds which we hear. Even if we are unconscious, we are expected to detect a “different” sound stimulus which does not derive from the “common” sounds. The detection of auditory stimuli that deviate from a simple or complex auditory regularity is reflected by the mismatch negativity(MMN) component of the human auditory evoked potential. Simple deviants of an oddball paradigm modulate the preceding middle-latency response of the auditory evoked potential(AEP). In rodents, however, MMN responses have been still controversial. We have developed an experimental system to simultaneously characterize both the auditory cortex and thalamus of rats (see the abstract by Kazusa Takahashi). Using this system, we tried to record the MMM-like responses both in the auditory cortex and the thalamus.

Methods

Rats were anesthetized with isoflurane, and were held with a head holding device. On the exposed right auditory cortex was placed the surface electrode array, through which

the depth array was inserted perpendicularly to the cortical surface to the auditory thalamus. A speaker was positioned 10cm from the left ear. Neural signals were obtained with an amplification gain of 1000, digital filter bandpass of 0.3-500Hz, and sampling frequency of 1 kHz. After recording tuning curves, MMM-like responses in various conditions were tried to record. Test stimuli were tone burst with a 60-dB SPL plateau, 100-ms duration including 5-ms rise/fall times. The inter-stimulus interval was fixed at 600 ms. AEPs were recorded during an oddball paradigm. The test stimulus sequences consisted of 2 tones with differing frequencies serving as either a standard or deviant. Standards were presented with a probability of 90%, and deviants with 10%. In each block, 540 standards and 60 deviants were randomly presented, and the grand average of standard and deviant AEPs were obtained. The sound with characteristic frequency (CF) recorded both in the auditory cortex and the thalamus was chosen as a standard or deviant, and the sound with 1/3 and 2/3 octave below CF were used as a deviant or standard respectively.

Results

The MMN-like responses in the cortex and SSA in both the thalamus and cortex were characterized simultaneously.

Conclusion

To exclude the possibility that MMN-like responses are the mere effect of SSA, further investigation to record the AEPs to the many standard control paradigm is thought to be necessary.

PS - 078

Developmental Conductive Hearing Loss Boosts Inhibitory Synaptic Strength in the Medial Temporal Lobe

Vibhakar Kotak; Dan Sanes

New York University

Background

The medial temporal lobe (MTL) includes the hippocampus and parahippocampal complex that may consolidate short- and long-term memories associated with acoustic context and communication. Since developmental hearing loss has been correlated with cognitive deficits such as working memory, it is possible that auditory experience influences brain regions beyond the central auditory system. We have previously shown that early hearing loss (CHL) leads to a chronic decrease in inhibitory postsynaptic responses throughout the auditory neuraxis (Takesian et al. 2009). Here, we asked whether normal hearing is essential to regulate inhibitory synapse function in the MTL. In particular, the perirhinal cortex (PRh) intercedes between the auditory cortex (ACx) and hippocampus leading us to speculate that there is an exchange of auditory information between these two cortical areas.

Methods

Bilateral CHL was induced in gerbils at postnatal day 10 just prior to hearing onset and inhibitory postsynaptic currents (IPSCs) were recorded from PRh neurons at postnatal days P29-34 in thalamocortical brain slices.

Results

CHL increased the amplitudes of spontaneous IPSCs ($pA \pm SEM$: control = 27.6 ± 2.4 , $n=13$ vs. CHL = 36.6 ± 2.5 , $n=12$, $p=0.01$) and minimum-evoked IPSC ($pA \pm SEM$: control = 8.5 ± 1 , $n=13$ vs. CHL = 12.3 ± 1 , $n=8$, $p=0.01$). There was no change in sIPSC frequency ($p=0.77$) or paired-pulse ratio (PPR) of evoked IPSCs ($p=0.23$) between control and CHL animals suggesting that GABA release was not perturbed.

Conclusion

This finding demonstrates that moderate hearing loss during development causes an increase in the amplitude of inhibitory currents within a key non-auditory brain area. We propose that such augmented postsynaptic inhibitory strength may result in an imbalance of MTL circuit that may hinder synaptic plasticity and contribute to delays in perceptual learning and memory.

PS - 079

Responses to Sinusoidal Amplitude Modulated Stimuli With Variable Presentation Sequences in Auditory Thalamic Neurons of Young and Aged Awake Rats

Rui Cai; Ben Richardson; Donald Caspary
Southern Illinois University School of Medicine

Background

Sinusoidal amplitude modulated (SAM) stimulus has been used as a model to mimic the fast changing temporal features in speech and vocalizations. Previous studies demonstrated neurons at higher levels of the auditory system respond to SAM stimuli with large and complex variations in spike rate. The present study examined unit responses from auditory thalamus (MGB) using two stimulus paradigms to study temporal coding and the impact of aging on temporal processing.

Methods

Individually-advanceable tetrode microdrives were implanted (Richardson et al., 2013) above MGB of young adult (4-6mos) and aged (28-30mos) Fischer Brown Norway rats. SAM stimuli were presented at 30dB SPL above threshold with the modulation frequency (f_m) stepped between 2Hz and 512Hz (broadband or pure tone carriers, 2/sec, 10 trials/ f_m , 100% modulated depth) to evoke unit responses in awake rats. Rate/temporal modulation transfer functions (rMTF/tMTF) were generated by 80 trials of SAM stimuli presented in either a random (RAT) or a sequential (SEQ) manner.

Results

Single units in the MGB of young and aged rats were classified into four categories based on the rMTFs generated by RAT SAM stimuli: bandpass (BP), highpass (HP), mixed (M) and atypical (A). Similar categories and percentages were found in both groups. There was a trend toward higher rate best modulation frequency (rBMF) in the aged group (165.8 ± 38.8 Hz) compared to the young group (90.4 ± 26.5 Hz). Average rBMF values for both groups were higher than our previous data in anesthetized young rats. Most units (47% young and 42% aged) responded better to RAT SAM than to SEQ. Conversely, 18% of young and 26% of aged units

responded better to SEQ SAM. RAT and SEQ SAM stimulus sets resulted in a number of selective changes for different response types, including common response rate decrease at low f_m s and/or increase at high f_m s for BP and M units responding to SEQ SAM when compared to RAT SAM.

Conclusion

Sixty-five percent of young and sixty-eight percent of aged neurons showed response rate differences ($>10\%$) between RAT and SEQ SAM stimulus sets. Similar response types and a trend toward higher rBMF were found in aged units compared to units from young rats. These results suggest that while response types to SAM stimuli remain the same, the observed trend toward higher rBMFs is suggestive of an age-related change in the way temporal signals are processed at the level of thalamus.

PS - 080

Spatial and Frequency Sensitivity in the Subdivisions of the Medial Geniculate Body

Justin Yao; Peter Bremen; John Middlebrooks
University of California, Irvine

Background

The medial geniculate body (MGB) comprises ventral (MGBv), medial (MGBm), dorsal (MGBd), and shell (MGBs) subdivisions, which each possess distinct ascending and descending projections. Although pure-tone-frequency sensitivity has been described in the various subdivisions, less is known about spatial sensitivity. Here, we characterize tuning to sound-source azimuth and pure-tone frequency in these four subdivisions of the MGB and consider implications for thalamo-cortical circuitry involved in spatial coding.

Methods

We recorded extracellularly from the MGB of anesthetized rats. For each unit we measured 1) a frequency-response area (FRA), 2) a repetition-rate transfer function (RRTF) to trains of 5-ms noise bursts, and 3) a rate-azimuth function (RAF) with broad-band noise bursts presented from free-field loudspeakers spanning 360 deg (20 deg increments) in azimuth. We classified units as belonging to the subdivisions of the MGB based on their spiking patterns, FRAs, positions within tonotopic gradients, RRTFs, and histological reconstruction.

Results

We encountered four patterns of responses that we tentatively assigned to distinct MGB subdivisions. Units in MGBv responded with transient onsets to noise or tone bursts, displayed sharp contralateral-hemifield spatial tuning, showed primary-like FRAs, and showed RRTF cutoffs that could reach ~ 100 bursts per second (bps). Units in MGBm resembled those in MGBv but were distinguished by broader frequency tuning and an abrupt change in the tonotopic gradient along a recording track. Units in MGBd exhibited both onset and offset responses with similar or opposing broad spatial tuning, primary-like frequency tuning, and RRTF cutoffs < 20 bps. Units in MGBs showed sustained responses, long latencies, broad spatial and frequency tuning, and RRTF cutoffs < 20 bps.

Conclusion

These differences in spatial sensitivity among MGB subdivisions have implications for thalamo-cortical circuitry. The MGBv is an obligatory synapse in the pathway to layers III/IV of the primary auditory cortex (A1). Here, we see spatial sensitivity similar to that previously reported in rat A1. This suggests that cortical spatial sensitivity is largely inherited from downstream nuclei. Corticofugal projections from A1 layer V reach the MGBd, where neurons showed broad spatial tuning. It is unclear how a pure cortico-thalamic projection could lead to that observed tuning. For that reason, it is likely that other projections to the MGBd (e.g., from dorsal cortex of the inferior colliculus and additional feedback from secondary cortical areas) fill in responses to ipsilateral sounds. Further study is needed to determine how thalamo-cortical circuits shape spatial sensitivity within both structures.

PS - 081

High Gamma Responses to Auditory Stimuli Adapt Over Multiple Time Scales in Human Cortex

Steven Eliades¹; Nathan Crone²; Dana Boatman-Reich²

¹University of Pennsylvania Perelman School of Medicine;

²Johns Hopkins School of Medicine

Background

Cortical auditory evoked responses decrease with stimulus repetition in both humans and animals. This neural response, known as stimulus-specific adaptation (SSA) in animal models, has been used to describe the effects of recent stimulus history on neural activity. Little is known, however, about SSA effects on cortical high-frequency (>60 Hz) oscillations used increasingly to investigate human cortical processing.

Methods

We recorded electrocorticographic (ECoG) activity from seven adult epilepsy patients with implanted subdural electrode arrays. We presented auditory stimuli using a 300-trial passive auditory odd-ball paradigm with tones (frequent: 1000 Hz; infrequent: 1200 Hz) and speech (frequent: /ba/; infrequent: /da/), as well as reversed and equal stimulus probability conditions. Time-frequency analysis was performed to measure event-related changes in high gamma (70-150 Hz) power. High gamma power was compared for different stimulus probabilities and for different positions within the stimulus sequence. Additionally, time-domain averaging was used to derive concurrent auditory evoked responses (N100).

Results

We found strong adaptation in high gamma power of auditory responses, with infrequent stimuli eliciting stronger activity than frequently repeated stimuli, for both tones and speech, consistent with previous descriptions of SSA. Infrequent and equal-probability stimuli yielded similar responses, suggesting that differences between high and low probability stimulus responses reflected adaptation of the high probability response rather than enhancement of the low probability activity. We identified multiple time scales of adaptation, including rapid adaptation at the start of a stimulus block and slower adaptation over stimulus sequence repetitions.

Conclusion

These results suggest a mechanism for coding high probability auditory inputs that adapts to stimulus regularities on multiple time scales.

PS - 082

Attention Modulates the Reset of the Auditory Steady State Response

Brandon Paul; Larry Roberts; Ian Bruce; Daniel Bosnyak; David Thompson

McMaster University

Background

The auditory steady state response (ASSR) is an electrical brain potential evoked by amplitude modulated (AM) sounds which reaches its amplitude maximum at AM rates near 40-Hz. (Galambos et al., 1981). Perturbing the AM stimulus by inserting a brief gap in the AM train desynchronizes the ASSR followed by a recovery period within 200-300 ms after stimulation resumes (Ross & Pantev, 2004). Although this process has been reported to be attention-sensitive (Rohrbaugh, 1990) – revealing how cognitive factors shape sound percepts – the effect of attention on the reset and recovery of the ASSR has not been systematically investigated. We thus conducted a study to examine the effect of attention.

Methods

14 normal-hearing participants were presented with 37-Hz AM tone bursts with a 400 Hz carrier frequency to the left ear. Each tone burst was 2 seconds in length and contained 4 gaps interspersed every ~270 or ~350 ms. Standard gaps embedded in the tone burst spanned 27 ms (1 AM period), but on half of the tone bursts, one of the four gaps was 81 ms in length (3 AM periods, target). In a first condition, 200 tone bursts were presented in the background while participants watched a silent film (passive condition). In a second (active) condition, the video was discontinued and participants pressed a button after each tone burst to indicate the presence of a target gap. A third condition repeated the active trials with the addition of an uninterrupted 41-Hz AM 5125 Hz tone presented simultaneously to the right ear. We recorded the 128-channel electroencephalogram for all trials.

Results

Results indicate that attending to target gaps led to a faster desynchronization of the steady state response in the gap interval, followed by a larger transient gamma band response and a trend toward higher amplitude as the ASSR resynchronized.

Conclusion

These findings suggest that top-down attention modulates temporal properties of the 40-Hz ASSR, revealing endogenous influences on auditory processing. A second question from this study is whether perturbations in the low-frequency carrier in one ear affected the ASSR evoked by the high frequency carrier modulated at a different AM rate in the other ear. We will report these data at the MidWinter Meeting. Overall, we suggest this method may be useful in assessing central processing deficits in disorders related to hearing loss, such as tinnitus.

Simultaneous, 3-Dimensional Mapping of Spatio-Temporal Activity in Auditory Cortex and Thalamus of Rats

Kazusa Takahashi¹; Tomoyo Shiramatsu(Isoguchi)¹; Takahiro Noda¹; Ryohei Kanzaki¹; Haruka Nakahara²; Hirokazu Takahashi¹

¹The University of Tokyo; ²Teikyo University

Background

The interaction between auditory cortex and thalamus plays an important role in the neural computation along the auditory pathway. Here we developed an experimental system to simultaneously characterize both the auditory cortex and thalamus of rats.

Methods

We designed two kinds of microelectrode arrays; a surface and depth electrode array. The surface electrode array had 64 recording points in a 4.5 mm × 3 mm area and through holes in between the recording points, through which the depth array was inserted. The depth array has 3 shanks, each of which was 6 mm long with an inter-electrode distance of 500 µm. Each shank had 15 recording sites for the thalamus and 17 for the auditory cortex. The depth array was designed to measure tone-evoked responses simultaneously at the thalamus and cortex and to characterize layer-specific responses in the cortex. Furthermore, simultaneously with this depth recording, the surface array mapped auditory evoked potentials on the cortical surface. In the isoflurane-anesthetized preparation, we first placed the surface electrode array so that the array could cover the whole area of auditory cortex on the basis of click-evoked potentials. Then, the depth electrode array was inserted perpendicularly to the cortical surface at a location 5.5-mm caudal to the bregma. Tone-evoked multi-unit activities (MUA) and local field potentials (LFPs) were measured simultaneously, and the frequency response areas (FRA) at each recording site were obtained.

Results

Characteristic frequencies (CF) were identified from FRA at approximately 10 sites in medial geniculate body (MGB) and 20 sites in the cortex. The peak latencies in peri-stimulus time response (PSTH) were faster in MGB than in the 4th layer of auditory cortex by a few ms. CFs obtained from MUA in the depth cortical recording were consistent with the tonotopic map in the LFP recording with the surface microelectrode array. Furthermore, the depth recording also exhibited the layer specific waveforms of LFPs.

Conclusion

We have developed a depth microelectrode array to simultaneously characterize the auditory cortex and thalamus. Furthermore, the combined recording with the surface and depth microelectrode array in the auditory cortex allows simultaneous characterization of the planar tonotopic map and laminar cortical structure.

Signal Representation in Anesthetized Auditory Cortex is Impervious to Informational Masking

Peter Bremen; John C Middlebrooks
University of California at Irvine

Background

Psychophysical signal detection in complex listening environments is vulnerable to masking by competing sounds, even if the maskers are remote in frequency from the signal. This phenomenon is called "informational masking" and is thought to reflect a breakdown in the formation of discrete signal and masker auditory objects. Here, we sought evidence of informational masking in primary auditory cortex (A1).

Methods

We recorded from A1 of alpha-chloralose anesthetized cats. All stimuli were presented from calibrated free-field speakers arranged in the horizontal plane. We fixed the signal at contralateral 40 deg and varied masker location between ±80 deg in 20-deg steps. Stimuli consisted of four pure-tone pulses repeated at 2.5, 5 and 10 pulses per second. Each pulse contained 4 masker components and (on half the trials) one signal component. We set signal frequency and level to the unit's characteristic frequency and to various levels above threshold. Masker frequencies were held constant or randomized across pulses. We defined a protected band of ±1/3, ±1/2, or ±1 octave centered at the signal frequency: Within-band maskers had all components within the protected band, whereas out-of-band maskers contained frequencies drawn from a range of 0.2-20 kHz excluding the protected band. We presented individual masker tones at ~40 dB above unit threshold and gated them either synchronously or asynchronously with the signal.

Results

As expected, thresholds for signal detection were lower for 1) out-of-band compared to within-band maskers, and for 2) asynchronously compared to synchronously gated maskers. Furthermore, we found that spatial separation (~80 deg) of the signal and masker sources led to mild improvements in signal detection. These observations could be explained by basic neuronal frequency and spatial tuning properties. There was no indication of differences between signal detection in the presence of constant versus randomized maskers, which in previous human psychophysical studies yielded high and low detection thresholds, respectively.

Conclusion

We found no neuronal signatures of informational masking in A1, nor any indication of across-frequency auditory object formation. That is, all responses could be understood by basic neuronal tuning properties. We deem two explanations possible: 1) informational masking arises outside of A1, and 2) informational masking is a product of cortico-cortical feedback loops, which are effectively silenced under anesthesia. We plan to address these possibilities with future studies in an awake-behaving preparation.

Anesthetic Effect on Tonotopic Organization in Rat Auditory Cortex

Takahiro Noda; Hirokazu Takahashi

The University of Tokyo

Background

Anesthesia has profound effects on cortical response properties. Such effects have been investigated mainly at either an individual neuron level or local population level; however, little has been known about the anesthetic effects on the cortical tonotopic map, which has been considered to be crucial to sensory percepts and learning.

Methods

The present study investigated anesthetic effect on response property over cortical tonotopic map at both a spiking activity level and field potential level. Especially, a microelectrode array was used to record pure-tone-evoked single unit (SU) activities and local field potentials (LFPs) in the auditory cortex of rats at the identical locations both under isoflurane anesthesia and awake head-restrained state. In addition, LFP phase synchrony was examined between recording sites to evaluate how the anesthetic agent modulated temporally coordinated activities between neuronal ensembles.

Results

Anesthesia generally tended to reduce both spontaneous and tone-evoked spiking activities with decrease in the number of detected unit. In terms of frequency responsive area (FRA) of SU, anesthesia elevated the tone response threshold at Characteristic frequency (CF). In addition, receptive field quality deteriorated, whereas the tuning sharpened. Accordingly, the dynamic range of tone frequency in tonotopic map has shrunk, especially in a high CF region (> 40 kHz). At the population level, on the other hand, anesthetic effect led to total increase of gamma-band LFP phase synchrony between neural ensembles across auditory cortical fields; yet, the phase synchrony was not significantly different between recording pairs either among CF sites or among off-CF sites.

Conclusion

Our data suggest that, not only at the individual neuron level but also at the cortical frequency map level, cortical activity becomes more vigorous and asynchronous in awake state, possibly contributing to the fine frequency tuning in auditory cortex as compared to the anesthetic state.

Mismatch Negativity (MMN) in Rat Auditory Cortex

Tomoyo Shiramatsu; Takahiro Noda; Ryohei Kanzaki; Hirokazu Takahashi

The University of Tokyo

Background

Mismatch Negativity (MMN) is an *N*-methyl-d-aspartic acid (NMDA)-mediated, negative deflection in auditory evoked potentials (AEPs) in response to a cognitively discriminable change. MMN cannot be explained by stimulus-specific adaptation (SSA); in human EEG, not only particular changes but

also categorical changes of sound can elicit MMN, indicating the deviance-detecting property of MMN. However, MMN in animal models are still debated, because the mismatch responses in animals were best explained by SSA rather than deviant detection. In this study, we attempted to spatio-temporally characterize mismatch responses in the rat auditory cortex to demonstrate their deviance detecting property.

Methods

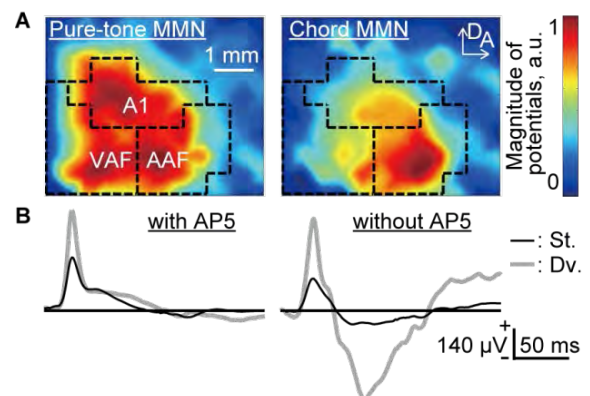
A surface microelectrode array with 64 recording sites within an area of 4.5 × 3.0 mm densely mapped AEPs in the right auditory cortex of anesthetized rats. AEP was investigated in the oddball paradigm, where a train of tone bursts consisting of high-probability standard (90 %) and low-probability deviant pure tones (10 %) was delivered. In the many-standards-control paradigm, tones with 10 different frequencies were presented randomly. Furthermore, three consonant chords as standards (90 %) and one dissonant chord as deviants (10 %) were delivered in the oddball paradigm, and vice versa. The recording was also conducted after putting an agarose gel seat (1 %) with/without AP5 (D-(-)-2-amino-5-phosphopentanoic acid, an antagonist at NMDA receptors, 100 μM) on the surface of auditory cortex for 15 minutes to test whether the mismatch responses were mediated by NMDA.

Results

Like human MMN, only deviant stimuli, but not standard or many-standards-control stimuli elicited negative deflections in AEPs following the positive middle-latency response, termed P1. Furthermore, this MMN-like response was elicited by the categorical difference of chord consonance. These results indicate that the MMN-like response could not be explained by SSA, but can be taken as an evidence of a homolog of human MMN exhibiting deviance-detecting property. Additionally, the spatial distribution was dependent on the test stimulus; pure-tone-elicited MMN occurred broadly in the auditory cortex, including primary, anterior and ventral auditory field (A1, AAF and VAF), while the largest spot of chord-elicited MMN was obtained focally in AAF (Fig. 1A). Lastly, AP5 significantly diminished MMN, but did not affect P1 (Fig.1B).

Conclusion

These results provide compelling evidence of a homolog of human MMN in rats, and our surface microelectrode mapping can probe the spatial distribution of MMN within the auditory cortex.



Awake State and Auditory Cortex Microstimulation Enhance Contralateral-Noise Suppression of Cochlear Responses in Chinchillas

Macarena Bowen¹; Cristian Aedo²; Alex León²; Constantino Dragicevic²; Gonzalo Terreros²; Luis Robles²; Paul H Delano³

¹Universidad de Chile; ²Programa de Fisiología y Biofísica, ICBM, Facultad de Medicina, Universidad de Chile;

³Departamento Otorrinolaringología, Universidad de Chile - Programa de Fisiología y Biofísica, ICBM, Facultad de Medicina, Universidad de Chile

Background

The efferent auditory system comprises descending projections from the auditory cortex to subcortical nuclei, including the inferior colliculus and superior olivary complex (SOC). Olivocochlear (OC) fibers emerge from the SOC and make synapses with outer hair cells and with auditory-nerve fibers. The OC function can be assessed by measuring a brainstem reflex that is activated by contralateral acoustic stimulation (CAS). The influence of cortical descending pathways on the OC reflex is still unknown. We found that the awake state and auditory-cortex electrical microstimulation (MS) enhance the suppressive effects of OC reflex.

Methods

Six anesthetized (protocol 1) and four awake and anesthetized (protocol 2) chinchillas were used to investigate the influence of auditory-cortex descending projections and the awake state in the magnitude of the OC reflex. In protocol 1, in anesthetized chinchillas, cochlear electrical responses to tones (1-8 kHz; 60-90 dB SPL) were recorded before, during and after CAS, and simultaneously to auditory cortex microstimulation (2-50 μ A, 32 Hz rate). In protocol 2, CAS effects on DPOAEs amplitudes were recorded sequentially, first in awake and then in anesthetized condition (ketamine 30 mg/kg and xylazine 4 mg/kg).

Results

In four MS experiments (protocol 1) we found an increase of the suppressive CAS effect in CAP responses to 2-4 kHz tones (from -3.0 to -5.0 dB). In addition, in two cases, cortical MS changed the polarity of the OC reflex (CAP increase to decrease). In awake chinchillas (protocol 2), CAS with noise and tones produced a reduction in DPOAEs amplitudes, reaching up to 10 dB, which were higher for noise than tones. Tone CAS effects were tuned to a frequency between f_1 and $2f_1$ - f_2 for all stimuli. The average CAS-effect magnitude was reduced in about 3 dB (range: -4.2 to -1.1 dB) in the anesthetized condition ($n=4$).

Conclusion

These results demonstrate that awake state and activation of descending projections from the auditory cortex to olivocochlear neurons enhance the CAS suppressive effects on cochlear responses.

Attentional Modulation Strength of Auditory-Evoked Cortical Response Predicts Selective Attention Performance

Inyong Choi; Le Wang; Hari Bharadwaj; Barbara Shinn-Cunningham

Boston University

Background

Past electroencephalographic studies have shown that attention shapes the cortical representation of an auditory mixture by enhancing responses to an attended source and suppressing those to competing sources. However, individual differences in the efficacy of cortical control have received little attention; moreover, few studies have tried to relate individual's performance to cortical control. Here, we ask whether differences in how attention modulates cortical responses reflect differences in normal-hearing listeners' selective auditory attention ability.

Methods

We asked listeners to attend to one of three competing melodies and identify its pitch contour while we measured cortical electroencephalographic responses. We quantified how attention modulated auditory event-related potentials (ERPs) elicited by notes in the target melody and the to-be-ignored melody on an individual subject. The note onsets of the melodies could be temporally resolved, allowing us to associate ERPs with distinct notes in a particular melody. We manipulated the pitch separation of the competing melodies to control how difficult it was to segregate them, which is critical for selective attention. Listeners all performed well on the easy, different-pitch trials, allowing us to quantify how strongly each individual subject modulated his or her ERPs. On same-pitch trials, where it was difficult to segregate the competing melodies, individual differences in behavioral performance were accentuated, differentiating listener ability.

Results

We found large individual difference in behavioral performance, especially when the competing melodies were similar and the task hard. We also found large individual differences in modulation of ERPs, even when the task was easy and all individual performed well. ERPs to an attended melody were amplified compared to passive responses. Importantly, amplification positively correlated with performance: listeners with the strongest attentional amplification of the target melody were the best performers, even when the task was hard.

Conclusion

This study shows that the efficacy of top-down cortical executive processes varies across subjects and that this is correlated with the ability to focus attention on a target sound source in the presence of competing, similar sources. Together with recent results showing that differences in the fidelity of neural coding of supra-threshold sound contribute to differences in selective attention ability, these results begin to shed light on how individual variation in both top-down and bottom-up processing affects the ability to solve the cocktail party problem.

Influence of Acoustic Context on Auditory Responses in the Basolateral Amygdala

Marie Gadziola; Sharad Shanbhag; Jeffrey Wenstrup
Northeast Ohio Medical University

Background

Acoustic communication signals carry information related to the meaning of social interactions by means of their “acoustic context”, defined here as the sequencing and temporal emission pattern of vocalizations. Thus, an accurate interpretation of the meaning of social vocalizations should depend on the acoustic context within which they are presented. To further understand the influence of the acoustic context on amygdalar responses, we characterized both the behavioral and neurophysiological responses to natural, species-specific vocal sequences in adult big brown bats (*Eptesicus fuscus*).

Methods

We first monitored the electrocardiogram during presentation of conspecific vocalizations to understand how vocal sequences modified the internal affective state of a listener. To understand the neurophysiological processing of vocal sequences, we characterized single-neuron responses in the basolateral amygdala of awake, restrained bats to both isolated syllables and vocal sequences. These experiments investigated whether natural sequences improved discrimination of the social context, and quantified the performance of different neural coding strategies at different time scales using the Victor and Purpura spike distance metric.

Results

The heart rate of a listening bat was differentially modulated by vocal sequences associated with different social contexts, showing a significantly greater elevation in response to aggressive sequences than appeasement or neutral sequences. Neurons in the basolateral amygdala were responsive to a variety of acoustic stimuli, including isolated syllables and vocal sequences. Two populations of neurons were distinguished by their background firing rates. High background neurons responded broadly to most of the tested stimuli, whereas neurons with low background rates were highly selective, only responding to one stimulus on average. When vocal sequences were considered at their natural sound levels, population responses of high background neurons effectively discriminated between social contexts, with increased excitatory discharge in response to aggression vocalizations and decreased firing in response to appeasement vocalizations. Further, we find that a temporal coding strategy provided additional information when discriminating vocal sequences.

Conclusion

Taken together, these findings suggest that big brown bat social vocalizations transmit relevant information about the social context that is encoded within the spike discharge pattern of basolateral amygdalar neurons. These data support the notion of valence coding in the amygdala, and highlight the importance of spike timing to the neural code used by amygdalar neurons.

Intensity Tuning in the Pallid Bat Auditory Cortex: Topography and Mechanisms

Kevin Measor; Khaleel Razak
University of California, Riverside

Background

Intensity discrimination is a fundamental function of the auditory system. In echolocating bats, intensity of echoes may provide information relevant to target size and range, and may facilitate reduction of masking by louder sounds. Studies of cat and rat cortex suggest a non-random topography of intensity tuning properties when tested with tones. The topography of intensity tuning for behaviorally relevant sounds is less clear. In this study, we investigate the properties and topography of intensity tuned neurons in the cortical region selective for downward FM sweeps used in echolocation.

Methods

Extracellular recordings were made from 288 neurons in the auditory cortex of pentobarbital anesthetized bats. Neurons were tested for their responses to different intensities to either a FM sweep or a tone burst at the characteristic frequency (CF). Two measures of intensity tuning were quantified: the ‘intensity tuning index’ (ITI), a measure of how sharply tuned neurons are to a range of intensities, and ‘percent turnover’ (%TO), a measure of non-monotonicity of the rate-intensity function.

Results

Minimum thresholds (MT) recorded in the neurons ranged from -5 to 61 dB SPL (mean 23.1 ± 0.73 dB SPL). 98% of neurons exhibited %TO > 0% to FM sweeps. 89% of neurons showed a %TO >25%, indicating that the vast majority of neurons are non-monotonic with a peaked intensity tuning function. The peak intensities ranged from 0 to 60 dB SPL (mean 32.7 ± 1.28 dB SPL). Cortical mapping data indicate that neurons with similar values of ITI and %TO were clustered. Neurons also exhibited more intensity selectivity for FM sweeps than CF tones, indicating mechanisms that enhance intensity selectivity for the echolocation call. Two tone inhibition data suggest that the timing of high-frequency inhibition at higher intensity enhances intensity tuning for FM sweeps compared to tones.

Conclusion

The strong intensity tuning and clustered cortical organization indicate that echoes of different intensities will generate maximal activity across different and predictable areas within the cortical region selective for echolocation calls. This population activity distribution will be further refined by other overlapping feature detectors such as those for spatial cues and sweep rates.

Characterization of Cell-Death Mechanisms Within the Central Auditory Pathway Upon Repeated Noise Exposure

Felix Fröhlich¹; Moritz Gröschel²; Arneborg Ernst²; Dietmar Basta²

¹HNO Klinik, Unfallkrankenhaus Berlin, Charité Medical School; ²HNO Klinik, Unfallkrankenhaus Berlin

Background

Noise exposure leads to pathophysiological and anatomical changes within peripheral and central auditory structures. A single noise trauma induce a cochlear damage as well as a dramatic cell loss within the central auditory pathway. Recent studies showed that apoptosis seems to play a major key role in the underlying cell-death mechanisms. It is of highly interest if a repeated noise trauma elicit additional cell death cascades in a pre-damaged central auditory pathway. Aim of this investigation was therefore to answer the following question: which effects does a second noise trauma have on the cell death mechanisms of the central auditory structures of an animal that suffers from noise-induced hearing loss.

Methods

Mice (NMRI Stain) under anesthesia were sound exposed (5-20 kHz, 115dB SPL for 3h) an investigated two weeks after the first trauma. Some of them were, 7 days after the first trauma, exposed to the same trauma a second time ("Double-Group") while the other animals stayed in there cages ("Single-Group"). The animals' brains were cut in 10µm slices and TUNEL-stained (Terminal deoxynucleotidyl transferase dUTP nick end-labeling) to visualize Cell-Death mechanisms. TUNEL positive cells were counted manually in standardized grids in the ventral and dorsal cochlear nucleus (VCN and DCN), in the central part of the inferior colliculus (ICC), in the dorsal, ventral and medial subdivisions of the medial geniculate body (dMGB, vMGB and mMGB), as well as in the 6 histological layers of the primary auditory Cortex (AI).

Results

There was no significant difference of TUNEL-positive cell density between the single-group and double-group in the basal structures (VCN, DCN and ICC). Significant more TUNEL positive cells were detected in all subdivisions of the MGB (dMGB, vMGB and mMGB), as well as in the layer I and III of the AI of the Double-Group. No significant differences were found in the other layers of the AI.

Conclusion

These results underline the influence of a second noise trauma on the central auditory pathway. We could recently show how a second noise trauma alters the hearing threshold as well as the calcium dependent neuronal activity (Gröschel et al. 2011, *NeuroImage* 57, 190-197). The present findings confirm that noise-exposure induces cell-death mechanisms in peripheral and central auditory structures. A second noise trauma seems to affect mainly the higher auditory structures since the lower auditory pathway is already adapted to the post-traumatic cochlear pathology.

Oscillatory Dynamics of EEG Correlate With Build-Up in an Informational Masking Task

Matthew Wisniewski¹; Eric Thompson²; Nandini Iyer³; Brian Simpson³; Sarah Sullivan⁴

¹Oak Ridge Associated Universities; ²Ball Aerospace; ³711th Human Performance Wing, Air Force Research Laboratory;

⁴The Geneva Foundation

Background

Listeners are more likely to detect a masked target signal when the number of signal presentations are greater, a phenomenon often referred to as build-up. Some neural correlates of build-up have been identified in late auditory-evoked responses, but few have looked at how oscillatory dynamics of EEG may correlate with build-up effects. The current work expands on previous electrophysiological studies by using both traditional evoked-potential analyses and time-frequency analyses of EEG collected during a detection task in which the number of target signal presentations varied.

Methods

Human listeners were assessed on their ability to detect repeating 1000 Hz tone bursts masked by tones with random frequencies at a -20 dB target-to-masker ratio. Masking tones fell outside a 1/3-octave protected region around 1000 Hz in order to limit energetic masking. Each burst was 200 ms in duration, but the number of bursts varied between 2, 4, and 8 bursts across trials. EEG was recorded from 128 electrodes during the entire experiment.

Results

Detection sensitivity (d') increased with increased number of bursts. This build-up effect in behavior was accompanied by an increased negative amplitude auditory evoked potential approximately 100 ms following burst onsets, replicating previous work. Analysis of inter-trial phase coherences (ITC) revealed phase-locking at 5 Hz (rate of bursting) and 10 Hz (harmonic of burst rate), which correlated positively with performance across individuals. Furthermore, the frequency at which maximal coherence was observed varied between trials with different numbers of bursts.

Conclusion

Results suggest that a listener's ability to track the envelope of bursts may influence detection performance. Findings also argue for analyses of spectro-temporal characteristics of the evoked-potential in addition to traditional analyses.

Are There Ear and Sex Differences in Auditory Processing of Signals in Noise Seen in AMLR?

Holden Sanders; Spencer Smith; Barbara Cone

University of Arizona

Background

A neurophysiological systems model of auditory processing disorder takes into account both bottom-up transcription acoustic stimuli into a neural code and the top-down modulation of that code induced by active listening mechanisms. One factor in auditory processing is asymmetry or laterality, present at lower levels of the auditory system, and appreciated in recordings of OAEs and auditory brainstem responses.

In human listeners, sex also appears to play a role in auditory processing, and may interact with laterality. This experiment focused on ear and sex differences at the thalamo-cortical level of auditory processing evident in the auditory middle latency response (AMLR). The aim of the experiment was to measure the ear- and sex-related differences of the AMLR recorded in quiet, and with ipsilateral and contralateral noise masking. The hypotheses were that 1) there would be a right ear advantage for contralateral inhibition of the AMLR; 2) there would be a release from ipsilateral masking of the AMLR with the addition of contralateral noise; and 3) ear differences would be more pronounced in females than males.

Methods

AMLR were obtained in response to consonant-vowel stimuli in quiet, with two ipsilateral and two contralateral noise conditions, and also with combined ipsilateral and contralateral noise. AMLR recordings were made using a 6-channel coronal array. An equal number of normally hearing young adult female and male participants were tested. The order of listening conditions and ear of test were randomized across subjects. AMLR component latencies and amplitudes were measured as a function of listening condition, ear and sex.

Results

Analysis of results to date indicate support for the first hypothesis, and trends in support of the 2nd and 3rd hypothesis. The earlier components of the AMLR, wave V and Na, show differential masking effects from those observed in the later components, Pa, Nb and PB.

Conclusion

Children and adults with auditory processing disorder often exhibit difficulties with understanding speech when noise is present. Additionally, some have weak or aberrant laterality. The results of this experiment, measuring the effect of ipsilateral noise interference and contralateral noise inhibition at the brainstem and thalamo-cortical levels, can be used to refine assessment tools for auditory processing disorder that account for ear and sex differences and their interactions.

PS - 094

Neural Representations of Background Speakers at the Cocktail Party

Krishna Puvvada; Jonathan Z. Simon

University of Maryland, College Park

Background

Selective listening gives a human subject the ability to robustly process speech despite the presence of interfering speakers. In a selective listening scenario with only one interfering speaker, the attended speech is foreground and the other is background, and previous work has demonstrated robust neural representations of each. It is not clear, however, whether the unattended speech has a distinct representation due to the fact that it is a different speech stream or due to the fact that it is background (i.e., everything that the listener is not attending to).

Methods

This critical ambiguity is here investigated using three speech streams, of which only one is attended to. We observe whether the two background speech streams have distinct neural representations or a single unified neural representation. Five human subjects were presented with three spatially co-located speech streams of perceptually equal loudness, but attended to only one of the three (ignoring the others), while their neural activity was recorded with magnetoencephalography (MEG).

Results

Neural MEG signals precisely follow the slow temporal modulations (< 10Hz) of speech. Analysis using the neural responses to reconstruct the stimulus envelopes demonstrates that the envelope of the entire background (as an inseparable mixture of the unattended speakers) can be reconstructed better than either of the envelopes of the individual background speech streams. Further analysis, modeling the neural representation as a temporal response function to be convolved with the stimulus envelope, demonstrates that the amplitude of first positive (M50-like) peak of the temporal response function is not modulated by attention, where as its latency is. In contrast, we find that the first negative (M100-like) peak is modulated in both amplitude and latency.

Conclusion

This indicates that the experimentally measurable neural representation of the background is more consistent with a single unified neural representation than with two distinct neural representations (of the two background streams). Furthermore, the neural origin of the later peak is a strong candidate for representing the perceived (rather than physical) stimulus.

PS - 095

Representation of ITD in the Human Brain: Evidence for the π -Limit?

Nelli Salminen²; Gestur Christianson¹; David McAlpine¹

¹University College London; ²Aalto University

Background

Experimental recordings from small mammals suggest that the representation of interaural time differences (ITDs) is frequency-dependent; the distribution of best ITDs depends upon neural tuning for sound frequency (characteristic frequency, CF), and ITD tuning appears to be almost frequency-invariant when normalised by CF (expressed in terms of cycles-re-CF). From this finding, the existence of a ' π -limit' in ITD processing was proposed; neural tuning for ITD is limited to a maximum of half the period of a neuron's CF. Logically, from this proposition, ITDs separated by a full period of the centre frequency of a sound share a common neural representation. Functional imaging in human subjects supports this view, at least at the level of the midbrain. Here, using an adaptive paradigm in human subjects, and magnetoencephalography, we demonstrate evidence consistent with the π -limit in human cortex.

Methods

Auditory cortical responses were recorded with magnetoencephalography (MEG) in 12 subjects under written informed

consent and the approval of the Ethical Committee of Aalto University. Bursts of bandpass noise centered at 500 Hz were presented in a stimulus-specific adaptation paradigm. A probe sound was presented with ITD -500 μ s (-1/4 cycle) in the context of adaptor ITDs of -1500 (-3/4), +500 (+1/4), and +1500 μ s (+3/4 cycle). The magnitude of adaptation was quantified from the N1 peak amplitude recorded over the auditory cortices.

Results

The data demonstrate that ITDs separated by a full period of the centre frequency, and lateralized to the opposite side, cause stronger adaptation than other ITDs. An Adaptor ITD of +1500 μ s (+3/4 cycle) caused a 46% reduction in the response amplitude to the probe sound with ITD -500 μ s (-1/4 cycle). This is larger than that caused by either the short delay of opposite sign (37%), or the long delay of the same sign (40%).

Conclusion

ITDs beyond the π -limit share a common representation with ITDs within the π -limit, specifically they appear to be encoded by neurons tuned to ITDs a full period away. This supports the notion of a π -limit in ITD coding in the human brain.

PS - 096

Functional Characterisation of Thalamic Input to the Mouse Auditory Cortex

Sebastian Vazquez-Lopez; Peter Keating; Andrew King; Johannes Dahmen

University of Oxford

Background

Tonotopy, the sequential spatial representation of sound frequencies, is a fundamental feature of the auditory system. It has its origin in the organisation of the cochlear receptor surface, is maintained through several subcortical processing stages and can still be observed in the auditory cortex. Most of the subcortical input to the cortex comes from the tonotopically-organised medial geniculate body (MGB) of the thalamus, which sends cortical afferents with distinct laminar distributions. Thus, studying the functional spatial distribution of thalamocortical projections is likely to contribute to our understanding of the basis for the tonotopic organisation of the cortex.

Methods

We injected a viral vector into the MGB of juvenile C57BL/6 mice to drive expression of the genetically encoded calcium indicator GCaMP6m. Four weeks later we imaged populations of thalamo-cortical terminals in the auditory cortex of anaesthetised mice with a two-photon microscope. We characterised the frequency response areas of labelled terminals across dozens of imaging planes and at different cortical depths. This gave us a measure of the local variability in the response properties of inputs as well as their laminar and large-scale functional organisation.

Results

We were able to visualise dense thalamo-cortical input to layers I and III/IV of the auditory cortex with dozens to hun-

dreds of acoustically-responsive boutons per imaging plane (150 μ m * 150 μ m). The fine-scale organisation of the thalamic input was surprisingly heterogeneous with neighbouring terminals often exhibiting differences in characteristic frequency of several octaves. This heterogeneity was seen both in populations of layer I and layer III/IV terminals. As a consequence of this local variability, only a very coarse tonotopic gradient in the functional distribution of thalamocortical inputs was apparent.

Conclusion

Our findings suggest that information about sound frequency, arriving at the primary auditory cortex from the MGB, is highly heterogeneous at the fine spatial scale. Furthermore, our data have so far provided little evidence for functional differences between the thalamic inputs to different layers of the auditory cortex.

PS - 097

Mechanisms of Noise Robust Representation of Speech in Primary Auditory Cortex

Nima Mesgarani¹; Stephen David²; Jonathan Fritz³; Shihab Shamma³

¹Columbia University; ²Oregon Health and Science University; ³University of Maryland

Background

Humans and animals can reliably perceive behaviorally relevant sounds in noisy and reverberant environments, yet the neural mechanisms behind this phenomenon are largely unknown.

Methods

To understand how neural circuits represent degraded auditory stimuli with additive and reverberant distortions, we compared single neuron responses in ferret primary auditory cortex to speech and vocalizations in four conditions: clean, additive white and pink (spectrally matched) noise, and reverberation.

Results

Despite substantial distortion, responses of neurons to the vocalization signal remained stable, maintaining the same statistical distribution in all conditions. Stimulus spectrograms reconstructed from population responses to the distorted stimuli resembled more the original clean than the distorted signals. To explore mechanisms contributing to this robustness, we simulated neural responses using several spectro-temporal receptive field models that incorporated either a static nonlinearity or subtractive synaptic depression and multiplicative gain normalization. The static model failed to suppress the distortions. A dynamic model incorporating feedforward synaptic depression could account for the reduction of additive noise, but only the combined model with feedback gain normalization was able to predict the effects across both additive and reverberant conditions.

Conclusion

Thus both mechanisms can contribute to the abilities of humans and animals to extract relevant sounds in diverse noisy environments.

Neural Correlates of Streaming, Selective Attention, and Expectation in Bilateral Concurrent Sound Segregation

Anahita Mehta¹; Shihab Shamma²; Ifat Yasin¹

¹University College London; ²University of Maryland

Background

This study aims to investigate the neural correlates of an ambiguous percept produced by a constant sequence of alternating high and low frequency tones presented alternately to the two ears, a stimulus roughly similar to one described in Deutsch's "octave illusion" (Deutsch, 1974, 2004). Subjects perceive a constant tone sequence in one ear whose salience only gradually builds up, and whose frequency (high or low) can be controllably altered by a preceding matching tone. Thus, four different perceptual streams can be perceived for exactly the same stimulus, allowing us to study the neural correlates of streaming, and the effects of selective attention (Carlyon et al., 2001; Cusack et al., 2004) and expectation or memory induced by a repeated fixed frequency precursor (Haywood and Roberts, 2013; Thompson et al, 2011; Linke et al, 2011).

Methods

Each ear is presented with opposing, alternating frequency sequences of pure tones simultaneously. For instance, the sequence in the left ear can be a High-Low-High... pattern whereas the sequence in the right ear is its opposite Low-High-Low... pattern. Subjects are then cued to focus on the frequency and side indicated by a priming sequence of three tones that are either all low or all high in frequency and are presented either in the left or right ear. To test the subjects' ability to stream out the targeted sequence, they are asked to detect amplitude deviants that are presented at varying positions in all the tones. Continuous EEG was recorded throughout the task.

Results

Subjects could readily attend to the targeted sequence, and found it significantly harder to detect early deviants in the sequence compared to later ones as would be expected from a build-up of streaming. Preliminary analyses of the EEG recordings indicate a differential pattern of activity that systematically reflected the percept and the task to which the subjects' attention was directed.

Conclusion

Cognitive functions such as attention and expectation modulate stimulus-driven responses in auditory cortex, and their effects can be reliably accessed from continuous EEG recordings. This facilitates exploration of the mechanisms that underlie them as well as potential applications in Brain-Computer Interfaces.

Influence of Double Stimulation on the Representation of Interaural Time Difference in the Barn Owl's ICX: Adaptation in the Auditory Space Map

Roland Feger; Martin Singheiser; Hermann Wagner

RWTH Aachen University

Background

The American barn owl (*Tyto furcata*) is a specialist in sound localization and a common model organism in this field. For localizing sound sources in the horizontal plane it relies primarily on the interaural time difference (ITD). An auditory space map is formed in the external nucleus of the inferior colliculus (ICX) by combining binaural cues for azimuth and elevation and integrating across frequency channels. Adaptation has been observed in many nuclei of the auditory pathway. One aspect of adaptation is that a neuron's response to a first stimulus (masker) is generally higher than to a second, succeeding stimulus (probe). We investigated the impact of response adaptation on the representation of ITD in ICX neurons.

Methods

We used extracellular recordings from neurons in ICX to investigate response adaptation. The stimuli (de novo broadband noise, each 100ms duration, 5ms onset/offset ramps) were presented with earphones. The masker was adjusted to the best combination of binaural cues. The stimulus level was chosen to elicit 50% of the maximal response. The probe followed the masker without a silent interval. Its parameters were chosen identically to the masker but the ITD was varied randomly to span the physiological range. This enabled us to compare the resulting "2nd ITD tuning curve" (response vs. probe ITD) to a reference "ITD tuning curve" recorded by presenting the probe stimuli alone. Additionally we used maskers with ITDs corresponding to the slope or the trough of the reference ITD tuning curve.

Results

By comparing the 2nd ITD tuning curves to reference tuning curves, we found response adaptation throughout the physiological range of ITDs. Adaptation was equal for all ITDs, including the masker ITD. The strength of adaptation depended on the rate a unit responded with to the masker. Therefore, when non-best ITDs were used for maskers, the adaptation was weaker. Under all conditions tested, the shape of the ITD curve remained the same under adaptative conditions as without adaptation.

Conclusion

The representation of ITD in the ICX is very robust against the influences mimicked by our double stimulation paradigm. A preceding sound induces response adaptation. However, adaptation in ICX does neither affect the location nor the acuity of sound localization.

Representation of Spatial and Spectro-Temporal Cues in the Midbrain and Forebrain of Barn Owls.

Philipp Tellers; Kerstin Buelles; Hermann Wagner
Institute of Biology II, RWTH-Aachen

Background

Barn owls identify and catch prey by listening. Thus, they need to know not only the position of a sound source, but also the temporal features of an acoustic stimulus. The interaural time difference (ITD) is the cue used for azimuthal sound localization by this bird. Neurons of the central nucleus of the Inferior colliculus (ICC) are able to represent both the ITD and the temporal structure of the stimulus. The ITD is represented by the firing-rate of the neurons, while the temporal structure of the stimulus is represented by the discharge pattern. After the ICC the representation of ITD is remodeled in two parallel pathways, the midbrain and the forebrain pathway. Since we know that the midbrain pathway is important for sound localization, we hypothesized that the forebrain pathway may be involved in the analysis of temporal features. Therefore, we analyzed and compared both the representation of ITD and temporal fine structure in the auditory arcopallium (AAR) and the external nucleus of the IC (ICX) by recording noise delay function while stimulating with frozen noises.

Methods

Standard extracellular recordings were obtained from ICX and AAR neurons, while the barn owl was repetitively stimulated with broadband frozen noise. The variability in firing-rate, the side-peak suppression and the dynamic range of ICX and AAR neurons were analyzed to assess the ITD representation, while the representation of temporal structure of the stimulus was assessed by analyzing shuffled autocorrelograms.

Results

While both ICX and AAR neurons exhibit significant ITD tuning curves, the quality of spectro-temporal representation differed between the two nuclei. Representation of spatial position was reliable in ICX neurons, while the coding of spectro-temporal features was less prominent in this nucleus. Spike times were variable with exception of the onset spikes. AAR neurons exhibited an even higher variability in spike times, indicating only a weak or no correlation between spectro-temporal structure and the discharge pattern of the neurons.

Conclusion

Coding of spatial features is good in both ICX and AAR, while the representation of temporal features is mediocre in ICX neurons and absent in the AAR. Therefore, we hypothesize that both ITD pathways play only a minor role in representing spectro-temporal features of the stimulus.

Spectral and Temporal Integration in the Auditory System of Barn Owls

Lutz Kettler

Institute for Biology 2, RWTH Aachen

Background

Barn owls localize sound sources in azimuth by detecting the arrival time differences between both ears (ITD). Narrowband noise carries ambiguous information about the position of a sound source. Phantom sources appear at positions differing from the real position by an angle that can be determined from the period at the signal's center frequency and a factor converting ITD into space. Broadband noise helps in disambiguating the sound source position.

We speculated that frequency modulation might also help in disambiguating the sound source. Owl chicks produce narrowband, but highly frequency modulated chirps. Hence, localizing frequency modulated (FM) tones should be of relevance in natural behavior. Since auditory information is processed within brief time intervals, we also shall present an estimation of the duration of the time window underlying across-frequency integration.

Methods

In the experiment 1 the owls had to localize stationary noise signals of different bandwidths. In experiment 2 the owls were stimulated with linear FM tones, called chirps, of different bandwidths and/or chirp rates. We analyzed the latencies, amplitudes, and direction of head turns, especially with respect to the number of phantom source localizations.

Results

The owls made localization errors in experiment 1 as long as the bandwidth of the stationary narrowband noise was below 3 kHz. Experiment 2 revealed that the number of head turns towards phantom sources decreased with increasing bandwidth and chirp rate but was higher than in response to stationary noises covering the same frequency band.

Conclusion

Our findings imply that barn owls are able to localize frequency modulated signals with an adequate chirp rate unambiguously.

Uncertainty Mapped by Frequency-Dependent Spatial Tuning in the Owl's Midbrain

Fanny Cazettes¹; Brian Fischer²; Jose L Pena¹

¹Albert Einstein College of Medicine; ²Seattle University

Background

Our brain must evaluate the reliability of new information. This requires that the brain generates an internal model that matches the statistics of sensory inputs. Theoretical work suggests that neuronal tuning curves encode how certain a cue is. The widths of the tuning curves become broader with less reliable cues. Yet compelling physiological demonstration of this mechanism is still missing. We addressed this question in the sound localization system of the barn owl, which displays a map of space in the external nucleus of the inferior colliculus.

ulus (ICx). ICx neurons are selective to horizontal direction through their tuning to interaural time difference (ITD). This selectivity arises from the convergence of frequency channels that originate in ITD-detector cells narrowly tuned to frequency. It has been shown that the widths of the ITD tuning curves in ICx increase with eccentricity. Because the width of ITD tuning curves is determined by the preferred frequency of the cells, we hypothesized that non-uniform frequency convergence is involved in the broadening of ITD tuning. We hypothesized that these tunings represent the certainty of environmental cues predicted by the filtering properties of the head.

Methods

We examined the tuning properties of ICx neurons using *in vivo* extracellular recordings. ITD and frequency tunings were measured at fine resolution in ICx. We used a computational model to determine whether frequency tuning predicts the broadening of ITD tuning in the periphery. To test if the filtering properties of the head dictate the pattern of frequency convergence, we investigated cue reliability from the head-related transfer functions (HRTFs) of barn owls.

Results

Consistent with our hypothesis, we found that the distribution of preferred frequency depends on ITD tuning and that ITD-tuning width increases as cells become tuned to lower frequencies. We demonstrated that the frequency tuning explains the shape of the ITD tuning. We could predict the frequency tuning and ITD tuning width from the HRTFs.

Conclusion

Neurons favor reliable cues by restricting their frequency tuning to a frequency range where, for a given direction, the reliability of ITD is maximal. As a result, ITD tuning becomes sharper in the front and increases resolution in the frontal space. Yet, localization of frontal and peripheral directions may become more accurate with high and low frequencies, respectively. We are currently testing if this frequency-dependent representation of space carries behavioral biases.

PS - 102

Reversible Inactivation of Primary Auditory Cortex by Cooling in the Awake, Behaving Ferret: Effect on Sound Localisation Ability

Katherine Wood; Stephen Town; Atilgan Huriye; Jennifer Bizley
UCL

Background

Cooling of a brain area can be used to perform reversible inactivation of that brain area (Lomber et al. 1999). Previously, it has been shown that inactivation by cooling of primary auditory cortex in awake, behaving cats causes deficits in localisation contralateral to the side of inactivation and throughout auditory space when cooled bilaterally; the effect is reversed upon warming (Malhotra et al. 2008). Also, lesions of primary auditory cortex in the ferret cause deficits in the localisation of clicks in the azimuthal plane and long term reversible inactivation of primary auditory cortex by GABA_A-subunit inhibitor,

muscimol, causes localisation deficits of brief sounds presented in the horizontal and vertical plane, while performance returns after the removal of the muscimol-releasing Elvax implant (reviewed in King et al. 2007).

Methods

We sought to develop the cooling technique for use in the awake, behaving ferret. Two ferrets were implanted with cooling loops above primary auditory cortex. We cooled this area of ferret auditory cortex while the animal performed an approach-to-target auditory localisation task. Since cooling brain areas may be more sensitive than previous methods of inactivation (ablation and pharmacological) we are testing a range of stimulus durations from 1000-100 ms.

Results

Preliminary results, at stimulus durations 500 and 250 ms, were compared to performance with cooling loop implants but without cooling. Reversible inactivation of A1 causes a significant deficit in the localisation ability of the ferret in the side contralateral to inactivation ($p=0.008$) but not to the ipsilateral side ($p=0.600$).

Conclusion

The technique has been successfully performed in awake, behaving ferrets. Inactivation of primary auditory cortex by cooling causes localisation deficits contralateral to the side of cooling.

PS - 103

The Effect of Task on Auditory Localization Cues in Human Auditory Cortex

Nathan Higgins; G. Christopher Stecker
Vanderbilt University

Background

Human sound localization in the horizontal plane relies on interaural time (ITD) and level differences (ILD); sensitivity to these cues is found in neurons from the superior olivary complex up through and including the auditory cortex. Recent studies have underscored the importance of attentional context in explaining the mechanism for encoding these cues. Here we use functional magnetic resonance imaging to measure the ILD and ITD sensitivity of hemodynamic responses in the human auditory cortex while simultaneously varying participants' attention across spatial, pitch, and visual tasks.

Methods

Image acquisition employed a continuous event-related design (TR=2s, 40 slices, 2.75 x 2.75 x 3mm resolution, 3T) to measure cortical responses to amplitude-modulated noise-burst trains (NBT) varying parametrically in ILD or ITD from trial to trial. Task type (visual, auditory location, or auditory pitch) varied between epochs of 10 trials, each of which potentially carried a target of any type: location (slight change in ILD or ITD), pitch (40% change in burst rate), or visual (brightness change of fixation marker/task indicator). Subjects indicated the direction (left/right, increase/decrease) of each target matching the current task. Following preprocessing, functional data were subjected to a standardized hemodynamic regression analysis, and masked with predefined re-

gions of interest (ROIs) corresponding to Heschl's gyrus (HG) and superior temporal gyrus (STG), as defined by (Desikan et al. 2006). Each ROI was then subdivided into sections to quantify organizational patterns across the axis of interest for that region.

Results

Strong auditory responses were observed in both STG and HG; overall, contralateral ILDs and ITDs produced the strongest responses, but both magnitude and tuning of the response was modulated by task type. Larger overall responses were observed in auditory (location or pitch) compared to visual tasks, and responses in the location task were least strongly dominated by contralateral ILDs and ITDs (in effect, broadening the spatial tuning).

Conclusion

Regional variations in binaural tuning and attentional modulation were also observed, and generally support a regional hierarchy of spatial processing via broadly tuned spatial channels. Consistent with a role in basic but hemisphere-specific auditory processing, HG exhibited contralateral dominance regardless of task. Conversely, ILD and ITD sensitivity in posterior STG was weak during the visual task, but enhanced during the pitch and localization tasks, suggesting a regional hierarchy based on attentional modulation.

PS - 104

Effects of Interaural Decorrelation on Psychophysical and Physiological Sensitivity to Low-Frequency Interaural Level Difference Cues

Andrew Brown; Daniel J. Tollin

University of Colorado School of Medicine

Background

Reflections and reverberation typical of everyday listening environments degrade the interaural correlation of acoustic signals reaching the two ears, leading to reduced psychophysical and physiological detection of source-related interaural time differences (ITDs). Bilateral clinical device (e.g. cochlear implant) processors, which operate independently at each ear, are thought to produce similarly decorrelated signals, thereby also adversely affecting ITD detection by hearing-impaired listeners, even in anechoic environments. Possible effects of interaural decorrelation on psychophysical and physiological detection of low-frequency interaural level differences (ILDs), which are salient localization cues in the absence of reliable ITD cues or for near-field sources, have not been studied in detail.

Methods

Interaurally correlated and uncorrelated narrowband (approximately 1/3-octave bandwidth) noise tokens ranging from low (0.25 kHz) to high (7 kHz) center frequencies were presented to normal-hearing human listeners via headphones in a binaural psychophysical paradigm that simultaneously assessed ILD discrimination and intracranial lateralization. In a separate experiment, correlated and uncorrelated broadband noise tokens were presented to ketamine-anesthetized

chinchillas via earphones, and rate-ILD tuning of low- and high-characteristic frequency neurons of the inferior colliculus was assessed via extracellular recording.

Results

At high frequencies, both psychophysical and physiological ILD sensitivity were robust to interaural decorrelation, consistent with published data. At low frequencies, psychophysical ILD sensitivity, as measured by both discrimination and lateralization, was significantly reduced for uncorrelated stimuli. Physiological ILD sensitivity was drastically reduced in some low-frequency neurons, but was minimally affected in others.

Conclusion

ILD is a salient localization cue in the absence of ITD cues (e.g., in highly reverberant environments or for users of bilateral cochlear implants, who are generally insensitive to ITD cues). Although psychophysical ILD sensitivity was shown to be robust to interaural decorrelation for high-frequency signals consistent with the physiological findings, decorrelation significantly reduced (but did not eliminate) psychophysical ILD sensitivity at low frequencies. The neural substrate of this latter effect may lie in the decorrelation-affected rate-ILD tuning of some low-frequency auditory brainstem neurons.

PS - 105

Searching for the “What” and “Where” Pathways in the Owl’s Auditory Forebrain

Michael Beckert; José Luis Peña

Albert Einstein College of Medicine

Background

We are investigating the existence of segregated “what” and “where” pathways in the primary auditory forebrain structure, Field L. Field L contains three layers, L2 which receives input from the auditory thalamus and is homologous to the mammalian A1, and L1 and L3 which send output to the remainder of the forebrain but whose roles remain unknown. Barn owls are specialized for localizing sounds with high precision. We hypothesize that Field L of the barn owl possesses a pathway for sound localization - ‘where’ pathway - segregated from a pathway for sound identification - ‘what’ pathway.

Methods

We improved upon previous research in this structure by recording from multiple single units using tetrodes. Tetrodes were lowered into Field L using stereotaxic coordinates. Single units were isolated away from background signals. Analysis was performed with custom written MatLab routines. Dichotic sound stimulation was used to measure the tuning to interaural time (ITD) and level (ILD) differences, and frequency. The reliability of each neuron’s response was also tested by presenting frozen broadband noise. These response properties were mapped to the physical location of neurons within Field L.

Results

Field L was found to be tonotopically organized with best frequencies increasing from a postero-lateral to antero-medial direction. In contrast to midbrain structures, Field L did not have a topographic representation of binaural cues. While

this non-topographic organization has been previously reported, the previously termed “clustered” organization, where local populations of neurons are tuned to similar binaural cues, was not found.

All three layers of Field L encoded frontal and contralateral space as well as the entire range of elevations tested. Interestingly, neurons broadly tuned to ipsilateral space were found distributed throughout Field L. Unlike spatial cues, neurons that reliably responded to repetitions of identical sounds - presumably locked to the sounds’ envelope - were limited to the ventral portions of Field L.

Conclusion

Tetrode recordings have allowed for the better characterization of response properties in Field L. Our results are inconsistent with the existence of a “clustered” organization of binaural cues, as previously reported. Similar to mammals, we find a non-topographic organization for spatial cues, a ventral portion that appears to be more involved in the processing of sound identity, and reliable encoding of frontal to contralateral sound space, with some broad tunings to ipsilateral space. These results suggest there is a dorsal “where” and a ventral “what” pathway in Field L.

PS - 106

The Nicotinic Acetylcholine Receptor A7 Subunit and its Modulator Lynx1 Are Highly Expressed in Sound Localization Processing Nuclei of the Gerbil

Sonia Weimann; Elise Esposito; Julie Miwa; R. Michael Burger

Lehigh University

Background

The $\alpha 7$ nicotinic acetylcholine receptor (nAChR) has broad distribution throughout the mammalian brain (Dominguez et al 1942; Marks et al 1996; Morley et al 1977). The functional properties of this receptor can vary based on its cellular location and developmental expression. Recently, $\alpha 7$ nAChR subunit expression was demonstrated in the superior olivary complex (SOC) (Häppel and Morley 2004). However, the expression pattern for $\alpha 7$ nAChRs between or within individual nuclei of the SOC, medial superior olive (MSO), lateral superior olive (LSO), and the medial nucleus of the trapezoid body (MNTB) has yet to be examined. Further, the function of these cholinergic receptors and their modulators is not well understood amongst nuclei involved in the computation of sound location. As a first step toward gaining an understanding of this function, we investigated $\alpha 7$ nAChR expression in the SOC nuclei as well as co-expression of *lynx1* a novel protein modulator of nAChRs (Miwa et al 1999).

Methods

$\alpha 7$ nAChR and *lynx1* expression were characterized using immunohistochemistry (IHC). IHC was performed on paraformaldehyde (PFA) fixed tissue from gerbils aged p19-p60 ($\alpha 7$ nAChR: mouse monoclonal; 1:400; Sigma; cat. # M220; *lynx1*: rabbit polyclonal; 1:1000). The tissue was coun-

terstained with MAP2 (chicken; 1:1000; Neuromics; cat. # CH22103). Tissue was examined using confocal microscopy.

Results

We show that both $\alpha 7$ nAChR and *lynx1* show strong expression in the three major nuclei of the superior olivary complex, MSO, LSO, and MNTB. $\alpha 7$ nAChR protein localization appears to be largely restricted to the soma of all three nuclei mentioned. *lynx1* protein, however, demonstrates somal and dendritic staining patterns in MSO and LSO while maintaining prominent somal localization in MNTB cells.

Conclusion

These results suggest that cholinergic signaling via nicotinic $\alpha 7$ receptors and its modulator, *lynx1*, may play a role in the mammalian sound localization pathway. Further examination will be required to elucidate their role in sound localization.

PS - 107

Coding Frequency-Dependent Interplay Between Low Threshold Voltage-Gated K⁺ Channels and Synaptic Inhibition in Chicken Sound Localizing Neurons

William Hamlet¹; Zheng-Quan Tang²; Yu-Wei Liu¹; Yong Lu¹
¹Northeast Ohio Medical University; ²Oregon Health & Science University

Background

Central auditory neurons that encode the location of sound in horizontal space have highly specialized morphological and physiological properties. These neurons employ a variety of intrinsic and synaptic cellular mechanisms to tightly control the threshold and timing for action potential generation, ensuring the accuracy of sound localization. However, the critical roles of the interplay between intrinsic voltage-gated conductances and extrinsic synaptic inputs in determining neuronal output are not well understood. In chicken, neurons in the nucleus laminaris (NL) behave as coincidence detectors and encode sound location using interaural time difference as a cue. Interestingly, along the tonotopic axis of NL, there exist differences in the expression level of low threshold voltage-gated K⁺ (LTK) channels and the amplitude and kinetics of GABAergic inhibition. Neurons that code low frequency (LF) sound exhibit weaker LTK expression, relatively small and fast phasic inhibition and little to no tonic inhibition, whereas neurons that code middle and high frequencies (MF and HF, respectively) have stronger LTK expression, large and slow phasic inhibition and a tonic inhibition. These properties establish NL as an ideal model to examine the interaction between LTK currents and GABAergic inhibition across the tonotopic axis.

Methods

Brainstem slices (275-300 μ m) were prepared from late chick embryos (E17-E18). Whole-cell voltage clamp experiments were used to measure intrinsic and synaptic currents, and current clamp experiments were used to evaluate the interaction between intrinsic and synaptic currents on membrane potential.

Results

LTK currents were larger in amplitude and density in MF and HF neurons than in LF neurons. Kinetic analysis revealed that HF neurons appeared to have less LTK inactivation than MF and LF neurons. Consequently, blockade of LTK currents using dendrotoxin-I (DTX-I) produced stronger effects (broadening in duration and increase in amplitude) on GABAergic inhibitory postsynaptic potentials (IPSPs) in HF and MF neurons than in LF neurons. Interestingly, DTX-I induced an increase in the frequency of spontaneous synaptic events, suggesting a role of LTK currents on presynaptic GABAergic terminals. Finally, DTX-I transferred subthreshold IPSPs to spikes, suggesting that LTK currents prevent GABA-induced spikes and therefore maintain GABAergic inhibition in the NL.

Conclusion

LTK currents regulate GABAergic inhibition via both presynaptic and postsynaptic actions in NL neurons. Interestingly, both presynaptic and postsynaptic LTK currents influence inhibitory synaptic events, suggesting of a critical role for LTK currents in sound localization at different coding frequencies.

PS - 108

The Effects of Ipsilateral and Contralateral Noise on the “Mid-Level Hump” in Intensity Discrimination

Elin Roverud; Elizabeth Strickland

Purdue University

Background

Psychophysical intensity discrimination limens (IDLs) measured for short, high-frequency pedestals are larger at mid-levels than at lower and higher levels. This increase in IDLs at mid levels, called the mid-level hump, has been theorized to reflect mid-level basilar membrane compression. At higher levels, spread of excitation cues may overcome the limitation posed by compression. Some previous studies have examined the mid-level hump in ipsilateral notched noise (e.g., Plack, 1998). When the pedestal is in the temporal center of a long-duration noise, mid-level IDLs improve relative to quiet. If the mid-level hump is a manifestation of compression, then this result suggests there is a decrease in compression with preceding sound. One possible mechanism for this is the medial olivocochlear reflex (MOCR). The MOCR is a bilateral, slow sound-evoked reflex that reduces gain of the cochlear amplifier, and therefore compression. Because the MOCR is bilateral, a contralateral noise may also lead to improved mid-level IDLs above that produced by ipsilateral noise. Micheyl et al. (1997) reported improved IDLs for a low-frequency pedestal with bilateral broadband noise, but not in the context of the mid-level hump. In the current study, the mid-level hump in ipsilateral and contralateral broadband noise was examined.

Methods

IDLs were measured for a 6-kHz, 30-ms pedestal at low, mid and high levels. IDLs were measured in two ipsilateral noise conditions: the pedestal temporally centered in a 50-ms noise (short) or the pedestal delayed 100 ms from the onset of a 150-ms noise (long). It was thought that the ipsilateral

MOCR could be elicited in the long condition. Then, a 50-ms contralateral noise was added synchronously to the short ipsilateral condition (control condition). A 150-ms contralateral noise was added to the short condition with its onset 100 ms prior to the ipsilateral onset (possibly eliciting the contralateral MOCR). Finally, the 150-ms contralateral noise was added synchronously to the long condition (possibly eliciting the bilateral MOCR).

Results

Preliminary results indicate a decrease in IDLs in long compared to short ipsilateral noise conditions and a further decrease when the long contralateral noise was added.

Conclusion

The mid-level hump may be decreased by ipsilateral and contralateral noise when the noise is long and begins prior to the pedestal. This result is consistent with a sluggish MOCR mechanism of decreasing the compression slope.

PS - 109

Differential Constraints on the Acquisition and Consolidation of Learning on an Interaural Level Difference Discrimination Task

Robert Baudo¹; Nicole Marrone²; Beverly A. Wright¹

¹*Northwestern University*; ²*University of Arizona*

Background

Listeners improve on perceptual tasks with practice, providing a means to enhance normal perceptual abilities and treat perceptual disorders. Development of optimal training strategies requires an understanding of learning mechanisms. Here we investigated the relationship between the two primary learning stages: acquisition, the training stage, and consolidation, the subsequent learning-stabilization stage. We asked whether these stages are functionally distinct for learning on auditory interaural-level-difference (ILD) discrimination by evaluating whether learning on a target ILD condition was blocked by training on a related non-target condition in the same session. The non-target condition was trained either before or after the target condition. Interference of target-condition learning only in the anterograde direction would indicate disruption of acquisition but not consolidation, while interference only in the retrograde direction would indicate disruption of consolidation but not acquisition. Either outcome would indicate that these stages are distinct.

Methods

We examined the influence of four different three-day training regimens on performance on a target ILD-discrimination condition at 4 kHz. On each day, training on the target condition either (1) preceded ($n=10$) or (2) followed ($n=11$) training on a non-target interaural-time-difference (ITD) discrimination condition at 500 Hz, (3) followed training on a non-target ILD condition at 500 Hz ($n=9$), or (4) occurred in isolation on the first day and followed training on the non-target ITD-0.5-kHz condition on the following days ($n=14$). All conditions were performed at midline.

Results

Training ILD-4-kHz before ITD-0.5-kHz yielded improvement on the target ILD-4-kHz condition between days 1 and 3 ($p < 0.01$), showing learning and a lack of retrograde interference. In contrast, training ILD-4-kHz after either ITD-0.5-kHz or ILD-0.5-kHz resulted in no improvement on ILD-4-kHz (both $p \geq 0.3$), revealing anterograde learning interference. Finally, training on ILD-4-kHz alone on day 1, but after ITD-0.5-kHz training on day 2 yielded improvement on ILD-4-kHz between those days ($p = 0.04$), suggesting that the lack of improvement in the ITD-0.5-kHz/ILD-4-kHz case reflected an actual disruption of learning, rather than an interference of performance on the ILD-4-kHz condition.

Conclusion

Training on a non-target ITD- or ILD-discrimination condition caused anterograde learning interference on a target ILD-discrimination condition, implying that these conditions competed for limited resources necessary for learning. Most importantly, ITD-discrimination training prevented learning on ILD discrimination in the anterograde, but not retrograde direction, suggesting that acquisition, but not consolidation, was disrupted. This asymmetry in the vulnerability of these two learning stages suggests that they are functionally distinct.

PS - 110

Slow Oscillations of Number, Level and Frequency of Spontaneous Otoacoustic Emissions After Low-Frequency Sound Exposure in Human Subjects

Kathrin Kugler¹; Eike Krause¹; Robert Guerkov¹; Lutz Wiegbebe²; Markus Drexler¹

¹German Center for Vertigo and Balance Disorders (IFB);

²Department Biology II, LMU Munich

Background

The presentation of intense, low-frequency (LF) sound can cause slow oscillations of cochlear sensitivity after LF stimulus offset, for which the term 'Bounce' phenomenon has been coined. Manifestations are slow oscillations of hearing thresholds, loudness perception, or the level of evoked otoacoustic emissions. There is also anecdotal evidence for changes of spontaneous otoacoustic emissions (SOAEs). Low-frequency sound has been considered to have only marginal effects on cochlear physiology, based on the poor LF hearing capabilities of mammals. We will show that low-frequency sound induces transient changes of cochlear physiology, which cause drastic changes of the number, level and frequency of SOAEs.

Methods

Data has been collected from both ears of 21 normal hearing subjects (13 female, 8 male; aged between 18 and 28 years). The number, level and frequency of SOAEs was followed as a function of time: In the control condition, SOAE level and frequency was recorded for 60 s (14 trials) or 120 s (23 trials) without preceding stimulation. In the LF exposure condition, OAE level and frequency was recorded for 300 s (11 trials) or 420 s (39 trials) following a 90 s LF stimulation (30 Hz, 80 dB A).

Results

We recorded a total of 137 valid SOAEs from 33 ears of 17 subjects. No valid SOAEs were found in both ears of four subjects. In the control condition without LF sound presentation, 80 SOAEs could be recorded from 27 ears of 16 subjects. After the presentation of LF sound, 57 additional, transient SOAEs could be recorded from 26 ears of 17 subjects. The pre-existing SOAEs showed a uniform, slow oscillation of level and frequency with initial enhancement followed by suppression relative to the median level and frequency of the same SOAE in the control condition.

Conclusion

We have shown that LF sound induced changes of SOAE frequency and level that do not resemble alterations induced by postural or middle ear pressure changes. We therefore suggest that the observed level and frequency shifts are not caused by impedance changes at the round window/ middle ear and can be better explained by changes of underlying outer hair cell activity.

PS - 111

The Intracochlear DP-Gram: A Noninvasive Assay of Basilar Membrane Distortion Products in Noise-Exposed Rabbits

Barden B. Stagner¹; Glen K. Martin²; Brenda L. Lonsbury-Martin²

¹Research Service, VA Loma Linda Healthcare System, Loma Linda, CA; ²Research Service, VA Loma Linda Healthcare System, Loma Linda, CA Dept. of Otolaryngology--Head & Neck Surgery, Loma Linda University Health, Loma Linda, CA; ²Research Service, VA Loma Linda Healthcare System, Loma Linda, CA Dept. of Otolaryngology--Head & Neck Surgery, Loma Linda University Health, Loma Linda, CA

Background

The characteristics of distortion product otoacoustic emissions (DPOAEs), i.e., distortion products (DPs) measured in the ear canal, have been thoroughly described. In contrast, less is known concerning the properties of intracochlear DPs (iDPs) propagated toward the DP frequency place (f_{dp}) on the basilar membrane (BM). Recent detailed comparisons of iDPs to DPOAEs have indicated that DPOAEs cannot be assumed to mirror iDPs within the cochlea, because DPOAEs directed toward the ear canal are composed of components that can be widely distributed and sometimes in cancellation, while iDP components directed toward f_{dp} seem to come from more restricted BM regions and add in phase.

Methods

Whitehead et al. (1995) described a technique whereby the behavior of iDPs could be inferred by interacting a probe tone with the DP of interest to produce a 'secondary' DPOAE. The behavior of the secondary DPOAE was then used to deduce the characteristics of the iDP. In the present study, this technique was used in rabbits pre- and post-permanent noise damage from a 4-kHz pure-tone exposure to directly compare DP-grams, level/phase (L/P) maps, and interference response areas (IRAs) to their iDP counterparts. To infer the

iDP, a 50-dB SPL f_3 was placed at a DP/f_3 ratio of 1.25 to evoke a secondary DPOAE at $2f_3-(2f_1-f_2)$. Intracochlear DP-grams (iDP-grams) were performed using the above technique, while presenting the f_1 and f_2 primaries at $f_2/f_1=1.05$, $L_1=L_2=45$ or 55 dB SPL and at $f_2/f_1=1.25$, $L_1=L_2=65$ dB SPL, reflecting stimulus parameters, which have been shown to maximize iDP magnitude in rabbits. Augmented DP-grams (aDP-Grams), which are DP-grams collected in the presence of an interference tone (IT) at 1/3 octave above f_2 to eliminate distributed basal DPOAE components were also collected. In some experiments, an IT was swept in frequency and level to produce an IRA describing the effects of the IT on DPOAEs and iDPs.

Results

It was found that iDP-grams were more sensitive for detecting noise-damage when compared to even the most sensitive low-level primary-tone DP-grams or aDP-grams. Both iDP-grams and aDP-grams were more frequency specific than standard DP-grams for detecting restricted noise-damage lesions. iDP IRAs after noise were relatively unchanged and continued to exhibit sharp tuning, as has been previously shown for DPOAE IRAs elicited by low-level primary tones.

Conclusion

iDP-grams represent a promising new technique for noninvasively measuring BM DPs and may improve our understanding of DPs propagated toward f_{dp} and those measured in the ear canal.

PS - 112

Extraction of Distortion Product Otoacoustic Source Components for Auditory Threshold Estimation

Anthony Gummer; Dennis Zelle; Ernst Dalhoff

University of Tübingen

Background

Distortion product otoacoustic emissions (DPOAEs) evolve as a byproduct of the nonlinear amplification process of two stimulus tones in the cochlea. According to a widely accepted model, DPOAEs comprise a non-linear generation and a coherent reflection component. Wave interference between these components yields variation in DPOAE amplitude with varying frequency, known as fine structure, hampering the objective assessment of the state of the cochlear amplifier. Recently, we showed that extraction of the primary-source component using pulsed DPOAEs (Vetešník *et al.*, 2009) increases the accuracy of auditory threshold estimation derived from semi-logarithmic input-output (I/O) functions (Dalhoff *et al.*, 2013). Here, we present a refined method utilizing short-pulse DPOAE I/O-functions for auditory threshold estimation, which exhibits low standard deviation and at reasonable cost of measurement time.

Methods

DPOAEs were recorded from seven normal-hearing subjects with $f_2 = 1.7-2$ kHz, $f_2/f_1 = 1.2$, $L_2 = 25-55$ dB SPL, and $L_1 = 0.4L_2 + 39$ dB SPL. In this frequency range, the primary-source component attains its steady state 8–10ms after the

onset of the f_2 -tone, while the secondary-source component exhibits an additional delay of 8–10ms. Therefore, presenting a short-pulsed f_2 -tone of 8ms length enables extraction of both components and the computation of I/O-functions without interference from the secondary-source component. Primary-source extraction was achieved by two methods: onset-decomposition (Vetešník *et al.*, 2009) and DPOAE decomposition into pulse basis functions (PBF) (Zelle *et al.*, 2013). The former samples the envelope of the DPOAE signal at a time instant before wave interference occurs, while the latter computes both source contributions by means of least square curve fitting.

Results

I/O-functions utilizing the extracted primary-source component from short-pulse measurements yield reliable auditory threshold estimation with standard deviations of 4.5dB and 5.3dB for the onset-decomposition and the PBF decomposition methods, respectively. Compared with auditory threshold estimation with pulsed DPOAE the measurement time decreased by approximately 80%. Application of objective evaluation criteria (Boege and Janssen, 2002) to the acquired I/O-functions leads to an exclusion rate of 15% when using continuous DPOAE, while none of the I/O-functions acquired with short-pulse DPOAEs need to be discarded.

Conclusion

Short-pulse DPOAEs present a promising approach for accurate auditory-threshold estimation with reasonable measurement time. Furthermore, extraction of both source components might offer additional information, such as latencies of the two source components, to characterize the state of the cochlear amplifier.

PS - 113

Comparison of DPOAE Source Components Measured at High Frequencies in Children and Young Adults

Laura Dreisbach¹; Dawn Konrad-Martin²; Christine Gagner³; Peter Jacobs⁴

¹San Diego State University; ²VA RR&D National Center for Rehabilitative Auditory Research (NCRAR); Department of Otolaryngology, Oregon Health & Science University; ³San Diego State University; University of California San Diego; ⁴VA RR&D National Center for Rehabilitative Auditory Research (NCRAR), Department of Otolaryngology, Oregon Health & Science University; Department of Biomedical Engineering, Oregon Health and Science University

Background

Distortion-product otoacoustic emissions (DPOAEs) provide a non-behavioral assessment of cochlear function that exhibits developmental changes in neonates and is sensitive to senescence in older adults. DPOAE sources are modeled as an intermodulation distortion component generated near the f_2 place and a reflection component arising near the DP place. Several authors have interpreted findings obtained using inverse fast Fourier transforms (IFFTs) of DPOAE frequency sweep measurements as being consistent with this model. A recent study of DPOAE source components suggests that

for frequencies between 1.5-4 kHz, distortion and reflection components are more robust in older infants than neonates, teens, young, middle age, and older adults and that teens and young adults have similar component strengths (Abdala and Dhar, 2012). Children were not included in that study and f_2 frequencies were limited to 4 kHz and below. The current study examines similar measurements for DPOAEs recorded between 10 and 14 kHz among normal-hearing younger children (YC), older children (OC) and young adults (YA). We hypothesized there would be evidence of senescence in young adults for high-frequency DPOAE components.

Methods

Thirty-nine YC between 3-6 years, 41 OC between 10-12 years, and 10 YA between 20-25 years participated in the study. DPOAE ratio sweeps ($f_2/f_1=1.1-1.25$; $L_1/L_2=65/50$ dB SPL) were recorded at fixed f_2 frequencies from 10-14 kHz. Stimuli presentations without a suppressor tone were interleaved with stimuli with a suppressor tone ($21.5 \text{ Hz} < 2f_1-f_2$ at 55 dB SPL) to lend further support for interpretation based on the two source model. A time waveform representation of the data was generated using IFFT techniques to examine the amplitudes and latencies of the distortion and reflection components.

Results

Preliminary analyses indicate that the mean amplitudes of both the distortion and reflection components are largest for YC at all frequencies, followed by the OC. On average, the YA group had distortion component amplitudes that were the smallest at 12 and 14 kHz, yet were similar to the OC at 10 kHz. The YA group also had the smallest mean reflection component amplitudes at all frequencies. For each age group, the mean latency of both components decreased with increasing frequency, as expected based on the tonotopic organization of the basilar membrane, but at a given f_2 , changes were not consistent across age.

Conclusion

Consistent with our hypothesis, YC had the most robust DPOAE components, followed by the OC and then the YA group.

PS - 114

Mapping Cochlear Regions Affected by Acute Acoustic Overstimulation With Distortion Product Otoacoustic Emissions.

Yingyue Xu; Karolina Charaziak; Jonathan Siegel
Northwestern University

Background

Distortion product otoacoustic emissions (DPOAEs) evoked with low-level tones (f_1 and f_2) can accurately reflect changes in neural thresholds following exposure to an intense tone in chinchillas (Siegel and Charaziak, ARO Abstract #122, 2013). However, it has been shown that DPOAEs may be generated over a broad region of the cochlea extending basal to the places of the two evoking tones, particularly at higher stimulation levels (Martin, et al., J Acoust. Soc. Am. 127:2955-72, 2010). These basal contributions to high-level DPOAEs

could be removed by a high-frequency ($1/3$ octave above f_2) interference tone (IT). The resulting "augmented DP-grams" (ADPs), measured in the presence of the IT, are superior to conventional DP-grams in representing notch-like permanent threshold shifts (PTS) in rabbits. We tested whether high-level ADPs could better reflect long-lasting changes in hearing sensitivity following exposure to intense tones than conventional DPOAEs in chinchillas.

Methods

Measurements were obtained in deeply anesthetized chinchillas. Initial exposure to an intense 3-kHz tone created a notch-like shift in compound action potential (CAP) thresholds (~ 40 dB shift). Subsequent exposure to an 8-kHz tone extended the damage to more basal locations. DPOAEs were measured before and after each exposure across a wide frequency range ($f_2 = 0.5-20$ kHz, $f_2/f_1 = 1.2$) for three conditions: (1) low-level DPOAEs ($L_1, L_2 = 50, 35$ dB SPL), (2) high-level DPOAEs ($L_1 = L_2 = 65$ dB SPL), (3) ADPs ($L_1 = L_2 = L_{IT} = 65$ dB SPL).

Results

Levels of DPOAEs were reduced by each exposure for all three stimulus paradigms. The low-level DPOAEs showed the highest correspondence with the CAP threshold shifts. The part of the DPOAE removed by the IT (the residual) was calculated by vector subtraction. The magnitude of the residual dropped dramatically above 10 kHz, indicating that the IT suppressed basal DPOAE generators.

Conclusion

The low-level DPOAEs are more sensitive than high-level DPOAEs and ADPs to threshold changes following acoustic trauma. Contrary to findings in rabbits, we did not observe that ADPs performed better in approximating CAP threshold shifts than high-level DPOAEs. This discrepancy could be due to species differences or may indicate that the acute exposures used in our studies did not abolish the capacity of hair cells to generate OAEs.

PS - 115

Probing the Generation Region of Stimulus-Frequency Otoacoustic Emissions With Exposures to Intense Tones

Jonathan Siegel; Karolina Charaziak; Yingyue Xu
Northwestern University

Background

We have explored the relation between changes in CAP threshold, DPOAE and SFOAE caused by exposing anesthetized chinchillas to intense (100 – 110 dB SPL) 3-kHz pure tones (Siegel and Charaziak, ARO Abstract #122, 2013). The CAP threshold shifts, averaging 30-40 dB, were restricted in frequency, centered approximately at 4 kHz. The average frequency-dependence of shifts in DPOAE levels evoked by low-level tones ($L_1 = 50$ dB; $L_2 = 35$ dB) approximated the shifts in CAP thresholds. However, the average shifts in the level of SFOAE evoked by 30 dB SPL probe tones (65 dB near-probe suppressor) underpredicted the CAP threshold shifts, suggesting that contributions from relatively unaffected

regions basal to the peak of the probe tone contributed to the SFOAE.

Methods

We modified our previous protocol by reducing cochlear sensitivity with a series of exposures to intense high-frequency tones (3 kHz exposure followed by 8 kHz) that broadened the frequency range of threshold elevations of 40 dB or more to approximately 3 – 16 kHz. DPOAE and SFOAE were evoked with the low-level tones described above.

Results

Both DPOAE and SFOAE were reduced to the system's noise floor for stimulus frequencies above 3-4 kHz, corresponding to the boundary between frequencies of normal and elevated CAP thresholds.

Conclusion

Exposure to intense tones similar to those used in these experiments one-half octave below the characteristic frequency (CF) of the basilar membrane recording location has previously been shown to greatly reduce the sensitivity to CF tones (Ruggero, et al., *Aud. Neurosci.* 2:329-345, 1996). Our experiments demonstrate that SFOAE evoked by even low-level tones are not abolished by frequency-restricted elevations in CAP thresholds. Expanding the region affected by the exposures toward the base greatly reduces the emission levels, strongly implying that SFOAE generation is not restricted to the CF place of the evoking tone.

PS - 116

Effects of a Third Tone on Distortion Product Otoacoustic Emissions and Their Intracochlear Sources

Wei Dong

VA Loma Linda Healthcare System

Background

Distortion product otoacoustic emissions (DPOAEs), whose precise origins remain unknown, are sounds generated in active cochlear mechanics that are detected in the ear canal (EC). A third tone suppression technique has been used by others to explore the generation of OAEs and thus cochlear tuning. However, there is little intracochlear observation on the complex effect of a third tone on distortion product (DP) generation. The current study focuses on the third tone effects on the DP generation via simultaneous intracochlear and EC recordings. By comparing two- and three-tone intracochlear and EC responses, we explored the mutual suppression at the primary tones and the suppression caused by the third tone on the DP and DPOAE.

Methods

Experiments were performed in anesthetized young adult gerbils. The left pinna was removed and the bulla was widely opened. The basilar membrane (BM) was accessed through a hand-drilled hole in scala tympani (ST) at a location of best frequency (BF) ~ 20 kHz with introduction of a micro-pressure sensor. The EC and ST pressure responses close to the BM (~ 10 μ m) to single-, two- and three-tone stimulation were simultaneously measured. For two-tone stimuli, two equal-in-

tensity primary tones were delivered at a fixed f_2/f_1 ratio of 1.25 and f_1 & f_2 were swept in frequency. For three-tone stimuli, the third tone was set to a frequency either higher than f_2 , or lower than f_1 .

Results

The current study focused on the $2f_1 - f_2$, the biggest low-frequency side-band, which post-generation, traveled both apically to its own BF place (fdp) and basally to the stapes. In a healthy preparation, the intracochlear DP showed dual-peak across frequency, the higher-frequency peak was in the vicinity of the local BF and the lower-frequency peak was substantially lower. These two peaks seem to be dominated by a locally generated/forward traveling component and an apically generated, reverse traveling component. A higher-frequency third tone ($>f_2$) at certain levels caused dramatic reduction in lower-frequency DP peak that was similar to the variation in the DPOAE, but less reduction in the higher-frequency DP peak. On the other hand, a lower frequency third tone ($<f_1$) caused dramatic reduction in the higher-frequency DP peak, but had little effect on the DPOAE.

Conclusion

Effects of the third tone on the DP and DPOAE were frequency and level dependent. Contribution from fdp place to DPOAE seemed to be minor.

PS - 117

Low-Frequency Sound Exposure Causes Biphasic Changes of the Mechano-Electrical Transducer Operating Point

Markus Drexler¹; Larissa Otto¹; Eike Krause¹; Robert Gürkov¹; Lutz Wiegrebe²

¹German Center for Vertigo and Balance Disorders (IFB);

²Department of Biology II, LM Munich

Background

Presenting intense, non-traumatic low-frequency (LF) sound to the mammalian cochlea induces temporary changes of cochlear sensitivity, for which the term 'Bounce' phenomenon has been coined. Manifestations are for example slow oscillations of hearing thresholds and the level of evoked otoacoustic emissions. It has been hypothesised that the observed changes in humans are caused by slow shifts of the operating point of the mechano-electrical transducer after LF sound offset. Estimates of the operating point can be derived from LF-biased distortion product otoacoustic emissions (DPOAEs).

Methods

Recordings were performed on 27 normal hearing subjects (mean age: 22). Systematic changes of LF-biased modulation patterns of both cubic and quadratic DPOAEs were followed over time before and after LF stimulation. An estimate of the operating point of the mechano-electrical transducer as a function of time was derived by fitting the absolute value of the second and third derivative of a two-exponential Boltzmann function to the modulation patterns followed by a reconstruction of the underlying transfer function.

Results

Most subjects showed biphasic changes of the modulation depth of the LF-biased cubic and quadratic DPOAE modulation patterns after LF sound exposure relative to the control period before LF sound presentation. The modulation depth showed an initial increase followed by a decrease relative to the pre-exposure modulation depth. Estimates of OP changes showed initial shifts away from the inflection point (the point of maximum sensitivity) of the mechano-electrical transducer transfer function followed by shifts towards the inflection point and showed a time course similar to modulation depth changes. Operating point and modulation depth changes lasted about 180 s.

Conclusion

Our results are consistent with the suggestion that LF sound causes slow oscillations of the mechano-electrical transducer operating point after stimulus offset which can lead to the observed manifestations of the Bounce phenomenon in humans.

PS - 118

Basal SFOAE Sources and Fine-Structure of the Reflectivity Function

Renata Sisto¹; Teresa Botti¹; Arturo Moleti²; Christopher Shera³

¹INAIL Research; ²University of Rome Tor Vergata; ³Eaton-Peabody Laboratories

Background

Recent experiments have found evidence for short-latency OAE components at moderate and high stimulus levels. Although the origin of these components is still unknown, they have been hypothesized to arise from sources basal to the peak of the traveling wave. In this work, short-latency SFOAE components are associated with basal peaks in the spatial structure of the reflectivity function due to roughness.

Methods

Approximate SFOAE solutions of a 1-d transmission line cochlear model were studied as a function of the BM tuning factor, Q . The reflectivity function and the solution along the BM were computed using the “double-pole” form of the Zweig model supplemented with random micromechanical irregularities. The SFOAE spectra, numerically computed at the cochlear base, were analyzed in the time-frequency domain and a power-law filtering function was used to separate emission components with different latencies and presumed sites of generation. Peaks in the function representing the local reflectivity were identified and their corresponding phase-gradient delays computed. The spectrogram of the SFOAE and intensity plots representing the local reflectivity as function of frequency and of the spectral latency associated to the BM position were compared.

Results

The SFOAE spectrogram at the base (see Fig.1a) and the intensity plot of the reflectivity in time-frequency domain (see Fig.1b) show good agreement in the energy and time distribution of the signal. The reflectivity function shows peaks whose number, position, and relative intensity depend on the indi-

vidual random roughness function and on the Q of the model response. A relatively low Q yields a multiple-peaked structure of the reflectivity function, which tends to disappear with increasing Q . This is in agreement with OAE observations, which show different-latency sources of comparable size at relatively high stimulus levels but responses dominated by reflections from the BM CF region at lower stimulus levels.

Conclusion

A 1-d cochlear transmission line solved by means of a perturbative approach is able to reproduce different latency components of the SFOAE spectra. The local reflectivity function responsible of the backscattering of the signal shows a multiple peak structure that becomes more evident at low Q values corresponding to saturated dynamical regime. The spatial positions of the peaks of the reflectivity function correspond to the latency of the peaks in the spectrogram of the associated SFOAE spectrum.

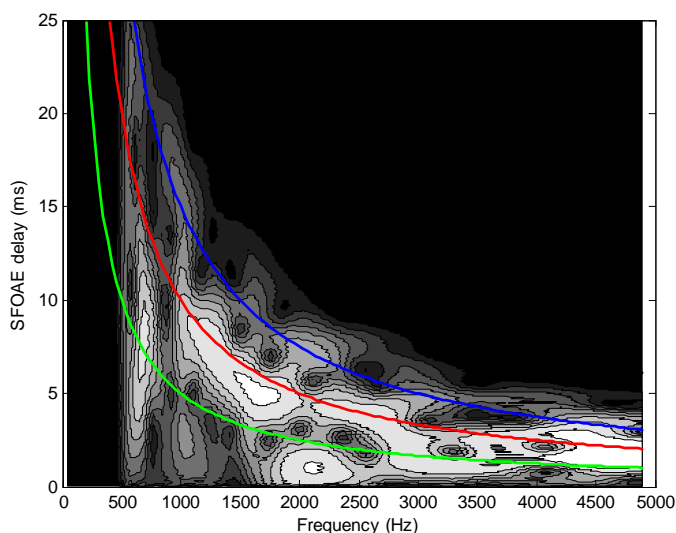


Fig.1a: SFOAE t-f distribution $Q=7$.

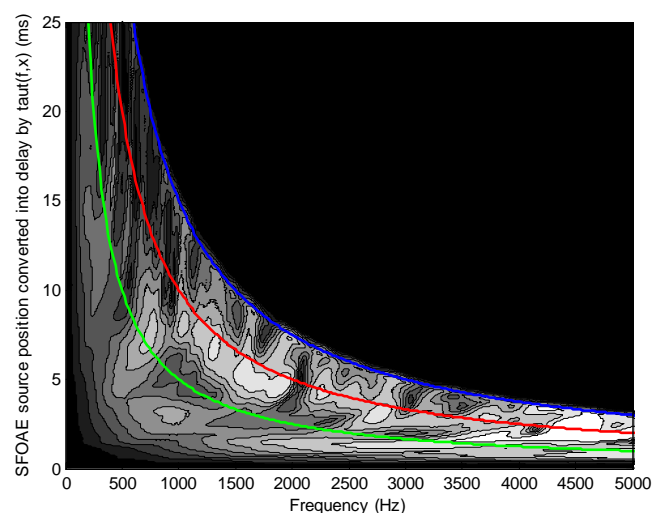


Fig.1b: Time-frequency representation of the sources obtained converting the source position of Fig.3 into time delay by using a theoretical $\tau(f, x)$ function. $Q=7$.

Tuning of SFOAEs Evoked by Low-Frequency Tones is not Compatible With Localized Emission Generation

Karolina Charaziak; Jonathan Siegel
Northwestern University

Background

As a by-product of cochlear processing, otoacoustic emissions (OAEs) could provide a noninvasive window on auditory function, such as frequency selectivity. Single-tone OAEs (SFOAEs) appear to be best suited for assessment of frequency selectivity since, at least on theoretical grounds, they originate over a restricted region of the cochlea near the evoking-tone characteristic place. In support of that view, in previous work in chinchillas we found a good agreement between SFOAE suppression tuning curves and a control measure of frequency selectivity for frequencies above 3 kHz. For lower frequencies, however, SFOAE tuning was unexpectedly broader than the control measure. Here we test the hypothesis that the broad tuning of SFOAEs is due to a broad region of OAE generation extending basal to the characteristic place of the evoking-tone.

Methods

We removed contribution of basally located SFOAE sources by either pre-suppressing them with high-frequency suppressor tones or by reducing hearing sensitivity with intense high-frequency tones. Thus, the 1-kHz SFOAE tuning curves were measured for 7 conditions: baseline, with a high-frequency suppressor present (4.2, 6.2 or 9.2 kHz at 75 dB SPL, random order) and following the exposure to a 110-115 dB SPL tone inducing at least ~40-dB threshold shift (in sequence: 8, 5 and lastly 3 kHz exposure). As a control measure of frequency selectivity we used compound action potential (CAP) suppression tuning curves measured for the same 7 conditions. All data were collected in deeply anesthetized chinchillas.

Results

The baseline SFOAE tuning curves were more than 5 times broader than the corresponding CAP tuning curves. SFOAE tuning was affected by the high-frequency suppressors and the acoustic traumas in an almost indistinguishable way, where little effect was observed due to 8-kHz exposure or 9.2-kHz suppressor and a progressive increase in sharpness of tuning was noted for the subsequent exposures to the intense lower-frequency tones or for lower suppressor frequencies. In contrast, CAP tuning curves were affected relatively little by the either manipulation.

Conclusion

The progressive increase in sharpness of tuning of SFOAE for 1 kHz tones following manipulations affecting progressively more apical regions of the cochlea indicates that SFOAE originate over a broad region of the cochlea. Thus, unlike CAPs (that were not affected by the manipulations), at low frequencies SFOAE cannot be considered as a place-specific measure of cochlear function, at least in chinchillas.

DPOAE Generation Mechanisms and Frequency Ratio Functions

Teresa Botti¹; Renata Sisto²; Arturo Moleti³; Luisa D'Amato³; Filippo Sanjust²

¹University of Insubria; ²INAIL Research; ³University of Rome 'Tor Vergata'

Background

Two different mechanisms are responsible for the DPOAE generation. The nonlinear distortion wave-fixed mechanism generates the DPOAE Short-Latency (SL) component, as a backward traveling wave from the "overlap" region. Linear reflection of the forward DP wave (IDP) generates the DPOAE Long-Latency (LL) component through a place-fixed mechanism. SL and LL components add up vectorially to generate the DPOAE recorded in the ear canal. The 2f₁-f₂ and 2f₂-f₁ DPOAE intensity depends on the stimulus level and on the primary frequency ratio $r=f_2/f_1$. Stagner et al. (ARO Poster 2013) studied the behavior of the DP versus ratio in rabbits, showing an overall bell-shaped SL trend centered at $r=1.25$ and an IDP component decreasing with increasing r . In this study we exploit the different phase behavior of the SL and LL DPOAE components to investigate their separate dependence on r . Numerical simulation from a nonlinear model and analytical computations were also compared to the experimental findings to clarify the generation mechanism details.

Methods

The 2f₁-f₂ and 2f₂-f₁ DPOAEs were measured in a stimulus level range of [35,75] dB, and r range of [1.1, 1.45] in 0.05 steps. An equal primary level (L₁=L₂) paradigm was adopted.

Numerical experiments. A nonlocal nonlinear active cochlear model was solved in Matlab. Simulations were also performed without cochlear roughness, to suppress the linear reflection mechanism. By doing so, one may interpret the model solution at the base as the DPOAE SL component, and the solution at the corresponding DPOAE tonotopic place as the IDP.

Analytical computations. Theoretical phase-gradient delays and latencies were also analytically computed in a linear transmission-line scale-invariant model.

Laboratory experiments. DPOAEs have been measured in six young normal-hearing subjects. A filtering method based on the wavelet transform (Moleti et al. 2012, JASA 132, 2455-2467) was used to separate the DPOAE SL and LL components.

Results

Amplitude/phase vs ratio, ratio-frequency maps and theoretical phase-gradient delays and latencies have been analyzed (see Fig.1, Fig.2, Fig.3). As expected, the generation of 2f₁-f₂ DPOAE is around the f₂ tonotopic place with a maximum around $r=1.2$ for the SL component. The 2f₂-f₁ DPOAE generation occurs in a region close to the 2f₂-f₁ place, for both the SL and LL components.

Conclusion

Both numerical and laboratory experiments on human subjects are suitable tools for noninvasive studies of the DPOAE generation, confirming the expected generation mechanisms and ratio functions.

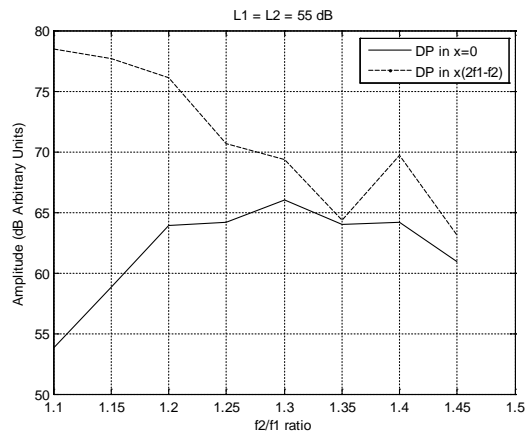


Figure 1. Numerical experiment. SL DP (DP at $x=0$) and IDP (DP at $x(2f_1-f_2)$) amplitudes. A 50 dB-shift has been added to the SL DP component in order to a better compare it with the IDP.

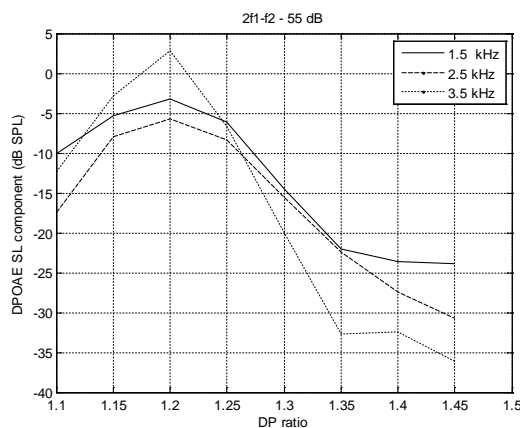


Figure 2. Laboratory experiment. DPOAE ($2f_1-f_2$) SL component amplitude averaged over 12 ears for three 1kHz-wide frequency bands in the [1, 4] kHz range.

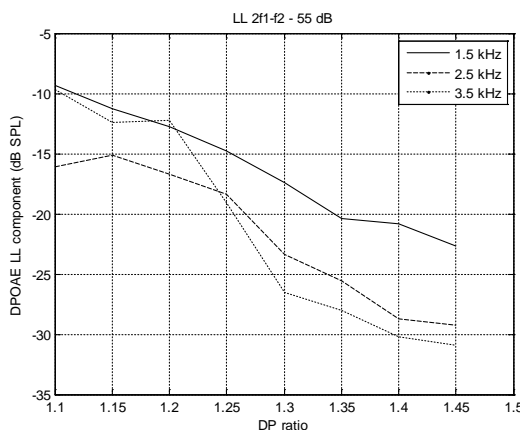


Figure 3. Laboratory experiment. DPOAE ($2f_1-f_2$) LL component amplitude averaged over 12 ears for three 1kHz-wide frequency bands in the [1, 4] kHz range.

PS - 121

Sources of Otoacoustic-Emission Noise-Floor Changes in the Presence of Middle-Ear Liquid

Olubunmi Akinpelu; W Robert J Funnell; Sam J Daniel

McGill University

Background

Noise floors in otoacoustic emission (OAE) tests originate from different sources and are important determinants of the signal-to-noise ratio, which in turn influences test outcomes. Increases in noise floors have been reported in certain middle-ear conditions. It is, however, not clear whether the increase is from environmental or physiological sources or from the measuring equipment. The objective of this study was to identify the source of changes in noise floor in the presence of middle-ear liquid using two different experiments.

Methods

[a] Animal Experiments: 20 adult female chinchillas (with normal hearing) were divided into 2 groups: live animals and euthanized animals; the two groups received equal volumes of normal saline (1.0–2.0 ml) in their middle ears. Noise floors were measured in both groups with a SmartOAE (Intelligent Hearing Systems) machine before and after liquid was introduced into the middle ears. [b] Cavity Experiments: Noise floors were measured in a 5-ml cavity using two different OAE machines in two acoustically different environments (a double-wall acoustically insulated room and an uninsulated room). The probes were inserted snugly in the lumen of the cavity in order to obtain cavity volumes varying between 1 and 5 ml. Comparisons were made between the noise floors in the different conditions and differences were subjected to statistical analysis.

Results

Increases in the noise floor were observed at the low frequencies in both live and dead animals with middle-ear liquid. Similarly, the noise floor increased with decreasing cavity volumes, to a greater extent in the non-sound-treated environment.

Conclusion

The equipment and the environment are likely sources of noise-floor increases in certain middle-ear conditions.

PS - 122

Experimental Evidence for Basal Place-Fixed Generation of Short-Latency TEOAE Components

Arturo Moleti¹; Renata Sisto²; Marco Lucertini³

¹University of Roma Tor Vergata; ²INAIL Research; ³Italian Air Force

Background

Ample experimental evidence is available supporting the place-fixed generation of both the long-latency (LL) and short-latency (SL) TEOAE and SFOAE components (Sisto et al., JASA, 2013, 133, 2240). The shorter latency and faster growth of the SL component indirectly suggest a generation place more basal than the BM resonant place, characterized by lower gain and less compressive response. Numerical

simulations (Moleti et al., JASA, 2013, 133, 4098) have confirmed the basal generation of the SL response, by showing that it vanishes when the roughness is removed from a particular basal BM region, 1-2 mm from the resonant place. This distance corresponds to a relative characteristic frequency shift of about 15-30%. In this study we look for direct experimental evidence supporting this hypothesis, by analyzing the TEOAE response of impaired ears with steep audiograms.

Methods

Pure tone audiograms and TEOAEs have been analyzed in 42 hearing-impaired ears. Firearm noise was the cause of high-frequency hearing loss, with steep audiometric threshold gradients (30-50 dB/kHz), typically localized around 3-4 kHz. Time frequency filtering (Moleti et al., JASA, 2012, 132, 2455) was used to separate the LL and SL components of the TEOAE response.

Results

In ears (see Fig.1) with steep audiometric hearing loss profiles, a clear phenomenology was typically observed: the LL TEOAE level spectra (solid line) dropped abruptly to the noise floor (dashed line), closely following the decreasing audiometric slope, whereas, for the SL spectra (dotted line), the same drop occurred with a shift towards lower frequencies of about 10-20%. The same time-frequency pattern that was obtained in numerical simulations (Moleti et al., JASA, 2013) by removing roughness from the base up to a given place $x(f_0)$ was observed in ears with severe high-frequency hearing loss starting abruptly at f_0 .

Conclusion

The observed phenomenology confirms the hypothesis that the SL component at each frequency f_0 is generated by place-fixed reflection at a cochlear place that is basally displaced from the resonant place $x(f_0)$ by a given longitudinal shift, whereas the LL component is reflected close to the resonant characteristic place.

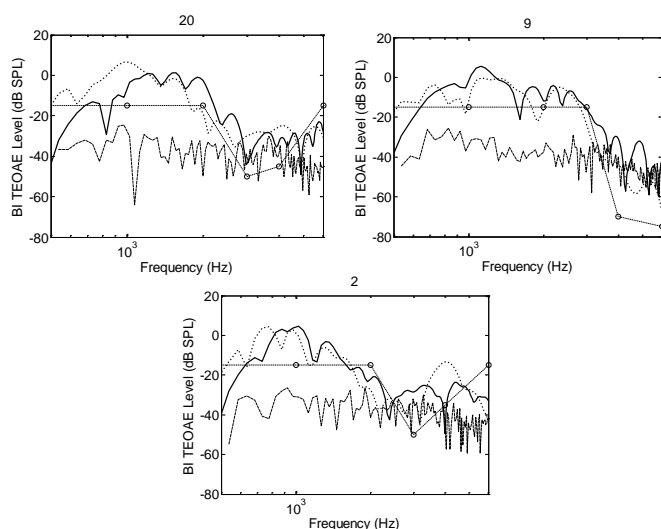


Fig.1: The SL TEOAE component spectrum is shifted towards lower frequencies with respect to both the LL component spectrum and the audiogram, as visible in the three ears above all characterized by steep audiometric gradient.

PS - 123

Multi-Frequency Acquisition of Input-Output Functions Using Short-Pulse Distortion Product Otoacoustic Emissions

Dennis Zelle; Anthony Gummer; Ernst Dalhoff
University of Tübingen

Background

Distortion product otoacoustic emissions (DPOAEs) may be used to assess the functioning of the cochlear amplifier objectively. However, the validity of this method is limited by wave interference of the two DPOAE source components. Using a pulsed f_2 stimulus tone the primary-source component can be extracted without significant interference from the secondary-source component (Vetešník et al., 2009), enhancing the accuracy of auditory-threshold estimates derived from semi-logarithmic input-output (I/O) functions (Dalhoff et al., 2013). Recently, we showed that using a pulsed f_2 tone of 8ms length yields similar standard deviations of the auditory-threshold estimate, while decreasing the measurement time considerably due to shortening of the acquisition blocks used for ensemble averaging (Zelle et al., 2013). However, undersized blocks may yield interference of the DPOAE signal with itself resulting in auditory-threshold estimation errors. Here, we introduce a new method presenting pulse train stimuli for quasi-simultaneous acquisition of multiple I/O-functions to further decrease the measurement time without causing interference.

Methods

DPOAE I/O-functions were acquired from normal-hearing subjects using six primary tone levels with $L_2 = 25-65$ dB SPL, $L_1 = 0.4L_2 + 39$ dB SPL, $f_2 = 1, 2$ and 4 kHz, and $f_2/f_1 = 1.2$. The f_1 tone comprised sequenced pulses each of 40ms length. The f_2 pulses started 10ms after the onset of their corresponding f_1 pulse and had variable half-widths, $T_{HW} = p/f$ with $p = 13.071$ estimated from the results of Vetešník et al. (2009). Band-pass filtering and circular expansion resulted in DPOAE signals without discontinuities even in cases where the signal exceeds the end of the acquisition block. Primary-source extraction was achieved by onset-decomposition (Vetešník et al., 2009) with sampling instants being commensurate to T_{HW} . Individual I/O-functions were recorded to compare the estimated distortion product thresholds (EDPTs) (Boege and Janssen, 2002).

Results

There was no significant difference between EDPTs obtained by the multi-frequency method and EDPTs using individual I/O-functions (< 1 dB). The time to acquire all EDPTs decreased by a factor of 2-3 when using the multi-frequency acquisition method.

Conclusion

Multi-frequency acquisition of short-pulse DPOAE I/O-functions enables quasi-simultaneous auditory-threshold estimation for a set of frequencies with high accuracy and at low cost of measurement time. Therefore, this method represents a promising diagnostic tool for objective auditory threshold assessment.

Repeatability and Stability of Medial Olivocochlear Reflex Effects on Short- and Long-Latency Transient-Evoked Otoacoustic Emissions

Ian Mertes; Shawn Goodman

University of Iowa

Background

Measurement of the medial olivocochlear reflex (MOCR) using otoacoustic emissions (OAEs) may have clinical applications, such as predicting susceptibility to noise-induced hearing loss. A clinically useful test must identify statistically significant effects in individuals and must yield repeatable results in a normal population. Methods for detecting significant MOCR effects in individuals using transient-evoked (TE) OAEs were recently reported (Goodman et al., 2013, JARO). We extended the application of these methods to examine MOCR effects in individual subjects in terms of repeatability (presence/absence of statistical significance across tests) and stability (variation in magnitude and phase across tests). Recent studies have demonstrated that TEOAEs contain short- and long-latency components. Previous work has not examined MOCR effects on short-latency components. Therefore, a secondary purpose was to compare MOCR effects on short- and long-latency components.

Methods

TEOAEs were measured in normal-hearing ears using 30 dB SL clicks presented at a rate of 27.1/s. The MOCR was elicited using 40 dB SL contralateral white noise (CWN) interleaved on and off in 10-s intervals (3.5 min total). Confounds of middle-ear muscle reflex and TEOAE amplitude drifts across time were controlled for. 16 repeated measurements were made (4 visits X 4 measurements per visit). Waveforms were bandpass filtered from 1-4 kHz and analyzed in two time windows that contained either short- or long-latency TEOAEs. Waveforms obtained with and without CWN were subtracted to cancel stimulus artifact, resulting in difference waveforms. Statistical significance of MOCR effects was assessed at each frequency ($\alpha=0.05$). Repeatability and stability of short- and long-latency components were analyzed at all frequencies.

Results

Preliminary results revealed that significant MOCR effects were present for short- and long-latency TEOAEs in 3 out of 4 subjects. Repeatability appeared similar for short- and long-latency components. Stability (standard deviation of the difference waveform magnitudes) in individuals ranged from 0.3-3.4 dB across frequencies and was similar for short- and long-latency components. Results from a larger number of subjects ($N=25$) will be presented at the meeting.

Conclusion

Repeatability and stability of MOCR effects varied across subjects and frequencies. Significant MOCR effects on short-latency components were less prevalent than on long-latency components, possibly due to different signal-to-noise ratios, but each had similar repeatability and stability.

Optimal Transient Stimulation Rate for Recording OAEs in MOC Based Assays

Sriram Boothalingam¹; David Purcell²

¹Western University; ²National Centre for Audiology, Western University

Background

It is well known that the medial olivocochlear system (MOC) influences cochlear activity, and a variety of other auditory processes. An efficient method to investigate the MOC effect on the cochlea is to record changes in otoacoustic emission (OAE) level following activation of the MOC. One of the most commonly available OAEs to clinicians, and researchers alike, is the click-evoked OAE (CEOAE). Click presentation rate, however, has been shown to influence the MOC effect on OAEs. Past studies that investigated this influence have only used click trains in the contralateral ear, as elicitors. However, clicks are also the OAE evoking stimulus, presented in the ipsilateral ear, and hence evoke the ipsilateral MOC pathway.

Methods

To exemplify a real world MOC effect on CEOAEs, a forward masking paradigm was used to investigate the effects of ipsilateral click rate in 10 young normally hearing adults. Clicks were presented at 55 dB ppeSPL, for both eliciting OAEs, and for forward masking. The click rate (in Hz) under test (20.83, 25, 31.25, 41.67 and 62.5) was presented in a 480 ms block that preceded the test clicks (presented at a constant rate of 20.83 Hz). The influence of each click presentation rate on the test clicks was then measured in conditions with and without contralateral broadband noise (BBN). The CEOAE levels in both these conditions were compared against a baseline CEOAE level recorded with no preceding click blocks. A preceding BBN block (480 ms) condition was also incorporated to compare click rates with binaural BBN presentation.

Results

Preliminary results suggest that click rates as low as 20.83 Hz, much lower than the previously reported rate (50 Hz), influences the MOC activity. A linear regression line ($R^2=0.84$) fitted to the current data suggests that the MOC inhibition increases monotonically by 0.06 dB for every one Hz increase in click presentation rate. MOC inhibition produced by binaural BBN is significantly higher than all click presentation rates tested in the present study.

Conclusion

Based on preliminary results, it can be suggested that click rates 20 Hz or lower must be employed for MOC based experiments to avoid contamination from ipsilateral pathways.

The Origin of Short-Latency Transient-Evoked Otoacoustic Emissions

James Lewis¹; Shawn Goodman²

¹Boys Town National Research Hospital; ²University of Iowa

Background

Bandpass filtered transient-evoked otoacoustic emission (TEOAE) waveforms contain short-latency (SL) and long-latency (LL) portions. The latency of the LL portion is consistent with generation through linear coherent reflection at the tonotopic place on the basilar membrane. Low-side, cubic intermodulation distortion ($2f_1-f_2$) has been hypothesized as the generation mechanism of the SL portion of the TEOAE. Two experiments examined the generation mechanism (Experiment 1) and generation location (Experiment 2) of SL TEOAEs in humans.

Methods

Experiment 1: TEOAEs were evoked using 2 kHz tone-bursts with durations of 3-, 6-, 12-, and 24-cycles. With each doubling of tone-burst duration, stimulus energy at f_1 and f_2 decreased by 19 dB. Tone-bursts were presented at 8 levels. TEOAEs were bandpass filtered (2 kHz) and the envelopes, latency-intensity functions, and input-output functions were calculated. These different measures were compared across the different tone-bursts to examine the effect of stimulus duration (and bandwidth) on the SL TEOAE.

Experiment 2: TEOAEs were evoked using a 3-cycle, 2 kHz tone-burst in the presence of different pure tone suppressors (0.5 – 6 kHz) and a high-pass noise-burst (8 – 16 kHz) suppressor. TEOAEs were bandpass filtered (2 kHz). Suppression of the SL and LL portions of the 2 kHz TEOAEs was measured.

Results

Experiment 1: The SL portion of the 2 kHz TEOAE did not depend on stimulus energy at f_1 and f_2 . Across all tone-burst durations, the 2 kHz TEOAE included comparable contributions from LL and SL portions. TEOAE latency decreased at a rate of 0.11 ms per dB increase in stimulus level. TEOAE magnitude increased with stimulus level at a rate of 0.45 dB/dB.

Experiment 2: The LL portion of the 2 kHz TEOAE was most sensitive to suppression by a 2.07 kHz pure tone. The SL portion of the TEOAE was most sensitive to suppression by 2.55 – 3.14 kHz pure tones.

Conclusion

Low-side, cubic intermodulation distortion is not the dominant generation mechanism of the SL portion of the TEOAE. The LL portion of the TEOAE is generated near the tonotopic place, while the SL portion is generated between 1/3 to 3/5-octaves basal to the tonotopic place. Coherent reflection from these more basal regions is a likely candidate for SL TEOAE generation.

Associations Between Threshold Fine Structure and Stimulus-Frequency Otoacoustic Emissions

James Dewey; Sumitrajit Dhar

Northwestern University

Background

Behavioral hearing thresholds often exhibit quasiperiodic fluctuations in level as a function of frequency. This threshold “fine structure” is thought to be associated with, if not a direct consequence of, the generation of otoacoustic emissions (OAEs). More specifically, threshold fine structure has been proposed to arise when stimulus-frequency OAEs (SFOAEs) evoked by the test stimuli undergo multiple reflections between the middle-ear boundary and their site(s) of origin. Cochlear resonances occur at frequencies for which the round-trip SFOAE delay is an integer number of cycles, producing enhancements in thresholds and evoked OAE amplitudes, as well as the potential for self-sustained, spontaneous OAEs. While a common frequency periodicity has been demonstrated between the fine structures of behavioral and OAE measures, no explicit comparisons have yet been made between the strength of the threshold fluctuations and either the overall amplitude or fluctuations in the amplitude of SFOAE responses measured at the same frequencies. Here we present a detailed exploration of these relationships.

Methods

Pure-tone detection thresholds and SFOAEs were obtained from normal-hearing adults. Measurements were made in 1/100th-octave steps across a half-octave span centered near 4 kHz. Stimuli were calibrated in terms of forward-pressure level (FPL), and SFOAEs were evoked at probe levels ranging from 0-18 dB FPL. Slowly-varying trends in thresholds, SFOAE amplitudes, and SFOAE delays were computed with loess fits and subtracted from the raw data to produce detrended curves for subsequent comparison.

Results

Threshold minima (i.e., peaks in sensitivity) were closely associated in frequency with peaks in both SFOAE amplitudes and delays. The frequency spacing of adjacent threshold minima corresponded with accumulation of approximately one cycle of SFOAE phase. In subjects with strong threshold fine structure (i.e., regular fluctuations of 5-10 dB), comparison of the detrended measures revealed a striking correspondence between the frequency and magnitude of fluctuations in thresholds, SFOAE amplitudes, and SFOAE delays. A weaker trend was found in the relationship between the strength of threshold fluctuations and the corresponding raw SFOAE amplitudes, though larger SFOAE amplitudes were typically associated with larger threshold fluctuations.

Conclusion

We provide evidence that the fine structure observed in hearing thresholds is mirrored in the fine structures of SFOAE amplitudes and delays. A common mechanism likely results in the superposition of these fluctuations on the more slowly varying trends for each of these measures.

Investigating the Role of the Medial Olivocochlear Reflex in Perceptual Enhancement

Jordan Beim; Maxwell Elliott; Andrew J. Oxenham;
Magdalena Wojtczak
University of Minnesota

Background

Perceptual enhancement is observed when a component (target) in a multi-tone complex perceptually “pops out” when the complex is preceded by a version of itself (precursor) with the target component removed. Behavioral measurements have shown that threshold for detecting the target tone in a multi-tone complex is lowered by the presence of the precursor. The origin of the enhancement effect is still unknown. Results from animal physiological studies have shown no enhancement of auditory nerve responses in anesthetized animals but an enhancement-like effect in the inferior colliculus of awake marmoset monkeys. In this study, we tested the hypothesis that the enhancement effect results from the activation of medial olivocochlear efferents. The effects of efferent activation can be reduced by anesthesia resulting in their absence in anesthetized animals. It was hypothesized that the precursor would activate the medial olivocochlear reflex (MOCR) rendering the target relatively stronger by turning down cochlear gain for components surrounding the target in a frequency specific manner. The role of the MOCR was investigated using stimulus frequency otoacoustic emissions (SFOAEs). The results were compared with perceptual enhancement observed in a psychophysical task using the same stimuli.

Methods

In a psychophysical experiment, thresholds for detecting the target tone in a multi-component complex were measured with and without the precursor. The amount of enhancement was calculated as the difference between thresholds measured in the two conditions. The effect of MOCR due to the precursor were estimated by measuring SFOAEs for the target tone alone, the target tone embedded in a multi-tone complex, and for the target in the complex preceded by the precursor. Changes in SFOAEs due to the precursor were also measured for the four components of the multi-tone complex that were closest in frequency to the target. Changes in SFOAE due to the presence of precursor were calculated from the heterodyned ear-canal pressure measured in the presence and absence of the precursor.

Results

Psychophysical results showed an average enhancement of 5.7 dB. Changes in SFOAE magnitude between the stimuli with and without the precursor were not systematic in size or direction (decrease versus increase in SFOAE magnitude). There were no consistent changes in SFOAE magnitudes due to the precursor for frequency components surrounding the target tone.

Conclusion

Results from psychophysical and SFOAE measurements do not support the hypothesis that the activation of the MOCR contributes to perceptual enhancement.

PS - 129

Discrete and Swept-Frequency SFOAE With and Without Suppressor Tones

Maryam Naghibolhosseini; Joshua Hajicek; Simon Henin;
Glenis R. Long

Graduate Center, City University of New York

Background

Stimulus frequency otoacoustic emissions (SFOAEs) are traditionally extracted using the difference in ear-canal sound pressure at discrete frequencies with and without a suppressor tone. The suppressor tone is required to separate the evoking stimulus from the SFOAE by suppressing the SFOAE. The use of a suppressor tone takes additional measurement time and the assumption that the SFOAE is always completely suppressed is not always valid. Furthermore, the addition of a suppressor tone may modify cochlear function.

The use of swept tones provides a fast and efficient tool permitting high-resolution estimates of OAE as a function of frequency. The differences in the latencies of the OAE and evoking stimuli allows extraction of SFOAEs from ear-canal recording of swept tones when the expected latency of the SFOAE is known.

Methods

Discrete frequency SFOAEs using a suppressor (35 points/octave, $f_{\text{SFOAE}}=1-3$ kHz, $f_{\text{suppressor}} = f_{\text{SFOAE}} + 50$ Hz), swept SFOAEs with a swept suppressor ($f_{\text{SFOAE}}=1-8$ kHz), and swept SFOAE without a suppressor ($f_{\text{SFOAE}}=1-8$ kHz) were collected from 19 human participants. SFOAE amplitude and phase were extracted using a least squares fit analysis from SFOAE data with and without a suppressor. An a priori estimate of OAE latency was used to separate the SFOAE from the stimulus when no suppressor was used.

Results

Estimates of SFOAE amplitude obtained with all three paradigms are qualitatively similar. Quantitative comparisons will be presented.

Conclusion

Swept SFOAE data collection can replace discrete frequency SFOAEs and provides more efficient and detailed information about OAE over a wide frequency range. In addition, the use of suppressor tones can be eliminated providing faster SFOAE estimates less likely to be contaminated by suppressors.

Differential Patterns of Thalamo-Cortical and Cortico-Cortical Projections to the Primary Auditory Cortex in Early- and Late-Deaf Cats

Blake Butler; Nicole Chabot; Stephen Lomber

University of Western Ontario

Background

When one sensory modality is absent, compensatory advantages are often observed in remaining modalities. This is thought to result from recruitment of cortical areas that typically process stimuli from the missing modality. Early evidence was suggestive of some crossmodal plasticity in primary sensory areas, however recent studies have failed to find evidence of reorganization in primary auditory cortex (A1). There is, however, evidence of a decrease in the size of A1 in deaf animals that is related to the age at the onset of deafness. This study sought to examine how thalamo-cortical and cortico-cortical projections to A1 are altered following deafness.

Methods

A retrograde neuronal tracer (BDA) was deposited in the A1 of hearing cats, and cats ototoxically deafened shortly after birth (early-deaf) or in adulthood (late-deaf). Coronal sections were taken at regular intervals and observed under a light microscope. Neurons showing a positive retrograde labeling were counted. Labelled neurons were assigned to functional cortical and thalamic areas according to published criteria. The proportion of labelled neurons in each area was determined in relation to the total number of labeled neurons in the brain. Additionally, cortico-cortical projections to A1 were isolated to explore cortical changes. ANOVAs and posthoc tests were performed to identify changes in labeling patterns.

Results

Following early deafness, inputs from secondary auditory cortex (A2) were amplified, while the number of neurons originating in the dorsal zone (DZ) decreased. In addition, thalamic inputs from the dorsal medial geniculate nucleus (dMGN) increased, while those from the ventral division (vMGN) were reduced. In late-deaf cats, projections from the anterior auditory field (AAF) were amplified, while those from DZ decreased. All interhemispheric connections arose from auditory areas, with more projections from A1 than any other area. When considering cortico-cortical projections in isolation, those originating in dorsoposterior auditory cortex (dPE) increased and those from anterolateral lateral suprasylvian visual area (ALLS) decreased in late-deaf cats. Although no different at the group level, changes in the labeling in EPp were significantly correlated with the age at the onset of deafness.

Conclusion

Our results show that patterns of projections to A1 are altered following deafness. Moreover, we provide anatomical evidence for crossmodal changes in projections to A1, suggesting that potential crossmodal activation of primary cortex may be dependent upon the age of deafening.

Acute and Chronic Changes in Synaptic Plasticity Gene Expression in Rat Inferior Colliculus Following Unilateral Noise Induced Hearing Loss

Francesca Russo¹; Senthivelan Manohar²; Robert Dingman²; Richard Salvi²

¹Sapienza University of Rome; ²Center for Hearing and Deafness, University at Buffalo

Background

Unilateral, noise induced hearing loss greatly reduces the sensory input to ipsilateral side of the brain thereby altering balance of excitatory and inhibitory synaptic activity in bin-aural processing areas of the brain such as the inferior colliculus, which plays an important role in sound localization and multisensory integration. The imbalances caused by the loss of neural input from the damaged ear and residual input from the intact ear should lead to significant synaptic remodeling within the inferior colliculus, but what synaptic changes occur here and when are largely unknown. To address this question, we unilaterally exposed rats to intense noise and evaluated the acute and chronic changes in the expression of synaptic plasticity genes in the inferior colliculus.

Methods

Using a real time, quantitative RT-PCR array, we screened the expression of 84 synaptic plasticity genes in inferior colliculus of control rats and rats unilaterally exposed to intense noise (2 h, narrow band noise centered at 12 kHz, 126 dB SPL). The unilateral noise exposure resulted in a profound permanent hearing loss over a broad frequency range and significant hair cell loss in the exposed ear. In contrast, there was little or no hearing loss or cochlear damage in the unexposed ear. We evaluated the changes in synaptic plasticity gene expression in the inferior colliculus contralateral to the noise exposure between 2 and 28 days after the exposure.

Results

Significant changes in the expression of synaptic plasticity genes were observed at both the early and late time points compared to the control group. Most of the changes seen in the inferior colliculus contralateral to the exposed ear were seen in the Immediate Early Response Gene family that included Pim1, Arc, Jun, Ngfr, Fos, Egr1, Egr3, Cebpt, and Nr4a1. A significant down regulation was observed at 2 d post-exposure and persisted out to 28 d. Another down regulated gene was Grin2c, involved in NMDA receptor activity.

Conclusion

Following acoustic trauma we identified a subset of synaptic plasticity genes whose altered expression would likely alter the structure and function of the inferior colliculus. Indeed all these genes are involved in long term potentiation processes, a mechanism that enhances synaptic connections and that is known to consolidate memories in other brain areas such as hippocampus.

Development of a Noninvasive Neuromodulation Approach for Treating Tinnitus

Benjamin Smith; Craig Markovitz; Cory Gloeckner; Sarah Offutt; Daniel Kastl; Luke Parker; **Hubert Lim**
University of Minnesota

Background

Tinnitus affects about 250 million people worldwide and has been linked to abnormal activity across the auditory system. We propose a new noninvasive neuromodulation approach for treating tinnitus, which we call Multimodal Stimulation Therapy (MST). An underappreciated organization of the brain for treating neurological disorders is the dense and topographic interconnectivity among sensory, motor, cognitive, and limbic centers. Through coordinated activation of different multimodal pathways, we hypothesize that MST can target and modulate the aberrant neuronal populations to suppress the tinnitus percept. We initially investigated the effects of combined auditory and somatosensory stimulation to induce auditory plasticity that could be relevant for treating tinnitus.

Methods

We positioned 32-site electrode arrays throughout the inferior colliculus (IC) and primary auditory cortex (A1) in ketamine anesthetized guinea pigs and compared spontaneous and acoustic-driven activity in both regions before and after MST. Subcutaneous needle electrodes were used to electrically stimulate different body locations (surface pads will eventually be used in humans), including the left leg, right leg, back, genital area, left shoulder, right shoulder, neck, tongue, mastoid, and pinna. Each body region was paired with an acoustic stimulus (pure tone or broadband noise) with varying delays and levels. We also performed several control conditions, including acoustic stimulation alone, body stimulation alone, and no stimulation.

Results

In IC and A1, MST induced greater changes in spontaneous and acoustic-driven activity compared to the control conditions. Furthermore, the delay between somatosensory and acoustic stimulation elicited differential neural effects. Body stimulation before acoustic stimulation caused more inhibition of IC activity while the reverse order caused more facilitation of IC activity. A more diverse pattern was observed in A1. Encouragingly, MST could alter different neuronal populations by varying the location of body stimulation, which may be achieved through the somatotopy we recently discovered in the IC.

Conclusion

MST can induce differential changes in firing patterns across the auditory system by varying stimulation parameters. We still need to investigate if MST can systematically reverse neural features linked to tinnitus, such as hyperactivity and hypersynchrony, as well as behavior in a tinnitus animal model. Since MST is noninvasive, we will investigate different parameters and pathways (i.e., auditory, somatosensory, visual,

motor, and limbic) directly in tinnitus patients that are guided by the animal findings.

Hearing Experience Changes Neuron-Glia Interaction in the Midbrain of Adult Rats

Nicole Rosskoth-Kuhl; Heika Hildebrandt; Ralf Birkenhaefer; Robert-Benjamin Illing
University of Freiburg

Background

Does neonatal deafness change cellular interactions in the adult midbrain? To answer this question we investigated neuron-glia interactions in the mature midbrain. Immediate-early genes like *fos* are essential players in the learning-associated molecular and cellular processes and the plasticity of neurons. In the auditory system, Fos expression can be induced by acoustical or electrical stimulation and regulates the transcription of late response genes, such as the growth-associated protein 43. Thus, Fos links changes of neuronal activity to structural and functional modifications within the central nervous system. Other important actors to be considered in neuroplastic remodeling are glial cells. These cells may be directly affected by neuronal activity. Specifically, astrocytes modulate neuronal function and synaptic plasticity. Thus, neuron-glia interaction influences the processing of information and enables the remodeling of central networks to changed activity patterns.

Methods

The potential of adult neuroplasticity was studied in normal hearing and neonatally deafened rats. The latter never heard due to hair cell destruction by postnatal kanamycin injections. Upon maturation of the central auditory system, both groups were unilaterally stimulated with a cochlear implant (CI) for 24 hours after inserting an electrode array into the medial turn of the cochlea. Stimulation induced changes on molecular and cellular level were verified in brain slices of the central inferior colliculus (CIC). Using in-situ hybridization, variations in mRNA expression of the neuronal gene *fos* were characterized. By immunohistochemistry we verified changes in protein level of Fos, glial fibrillary acidic protein (GFAP), and calcium-binding protein S100.

Results

As a result of chronic CI stimulation, hearing-experienced rats showed a tonotopically restricted Fos response in contralateral CIC. In contrast, the number of Fos positive neurons was massively increased and widely spread out over the contralateral CIC in hearing-inexperienced rats. However, only in neonatal deaf rats the Fos response was accompanied by a hypertrophy of astrocytes, indicated by a strong increase of GFAP expression (see Fig. 1) Quantification of Fos and GFAP/S100 staining evidenced a strong regional correlation without any direct co-localization.

Conclusion

These data suggest that stimulation-induced remodeling processes in hearing-inexperienced, but not in hearing-experienced, rats involve neuron-astrocyte interaction. To answer our initial question, plastic remodeling of the adult auditory

system requires different cell types to achieve an appropriate plasticity response depending on a given hearing experience.

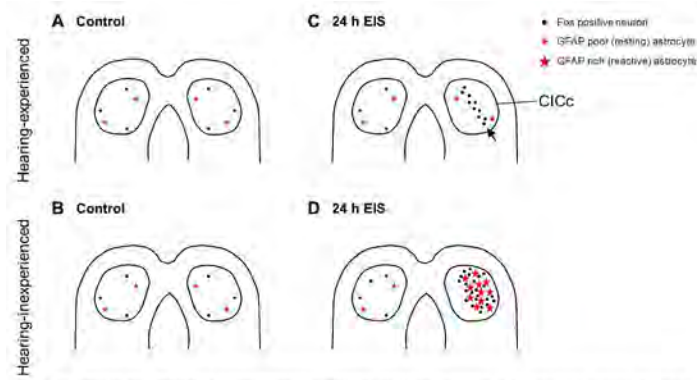


Fig. 1 Neuron-Glia interaction in auditory midbrain as depending on hearing experience. (A, B) Under control condition, the central inferior colliculus (CIC) showed a low level of Fox positive neurons and GFAP poor astrocytes independent of hearing experience. (C) Unilateral electrical intracochlear stimulation (EIS) for 24 h resulted in a forebrain Fox expression (arrow) in contralateral CIC (CICc) of hearing-experienced rats, while the ipsilateral CIC remains on control level. GFAP poor astrocytes were unaffected on both sides of CIC. (D) Activating a hearing-inexperienced system for the first time resulted in a massive Fox expression in CICc, accompanied by a regionally correlated hypertrophy of GFAP rich astrocytes.

PS - 134

Functional Near-Infrared Spectroscopy Reveals Cross-Modal Reorganisation in Auditory Cortex Following Deafness.

Rebecca Dewey; Douglas Hartley

Nottingham University

Background

Imaging studies suggest that deafness induces cross-modal reorganisation in auditory cortex. However, the effects of cochlear implantation on this reorganisation remain largely unknown. Functional near-infrared spectroscopy (fNIRS) is a relatively novel imaging technique that is highly suited to auditory imaging following cochlear implantation, unlike alternative recording techniques that are often plagued by implant-related magnetic and electrical artefacts. We present an fNIRS study of cortical responses to auditory, visual and somatosensory stimuli in 29 profoundly-deaf (mean age 41 ± 11 years) and 30 normally-hearing (mean age 34 ± 13 years) adult participants.

Methods

Auditory stimuli consisting of sinusoidally amplitude-modulated (100% modulation at 10Hz) or unmodulated broadband noises were presented at 80dB SPL in the free-field. Visual stimuli consisting of 1000 randomly or coherently moving white dots on a black background were presented via a computer monitor. Somatosensory stimuli (10 or 20 Hz sinusoidal vibrations) were presented to the palms of both hands by a custom-made stimulator. Stimuli in all modalities were 20s in duration and presented five times each in a pseudorandom order, interleaved with a rest period. The duration of the rest period (25 - 45s) was randomized between stimulus presentations. fNIRS data were acquired using a 24-channel Hitachi ETG4000 system. Behavioural assessments of coherent visual motion sensitivity and somatosensory frequency discrimination were performed in a separate session.

Results

In the region of interest (ROI) that was located over the temporal lobe normal-hearing controls exhibited fNIRS responses

to auditory stimuli, but few responses to visual or somatosensory stimulation. Conversely, responses to visual and somatosensory stimuli in the ROI were frequently observed in profoundly-deaf participants. Unsurprisingly, few responses to auditory stimulation were seen in this group. Together these fNIRS data support previous evidence from alternative imaging modalities to suggest that deafness induces cross-modal reorganisation in the auditory cortex. Preliminary psychophysical results from the current study suggest that profoundly-deaf participants have enhanced coherent visual motion sensitivity, compared with normal hearing controls. Thus far, no effect of hearing loss on somatosensory frequency discrimination has been observed.

Conclusion

We have shown deafness-induced cross-modal reorganisation in auditory cortex using a neuroimaging modality that is compatible with a cochlear implant. Future studies will assess cortical responses to multi-modal stimulation before and after cochlear implantation, along with psychophysical assessments of multisensory perception. We hypothesise that fNIRS may provide a useful prognostic indicator of performance following cochlear implantation.

PS - 135

Withdrawn by author

PS - 137

Tracking Brain Plasticity With Event-Related Optical Signal (EROS) in Cochlear Implant Patients

Chun-Yu Tse¹; Chin-Hong Tan²; Michael Novak³; Jennifer Black³; Brian Gordon⁴; Ed MacIin²; Benjamin Zimmerman²; Gabriele Gratton²; Monica Fabiani²

¹Chinese University of Hong Kong; ²Beckman Institute, University of Illinois; ³Carle Foundation Hospital; ⁴U of Illinois and Washington University

Background

The recovery of hearing ability following cochlear implantation provides a unique window for examining the plasticity of the adult human brain. Evoked potentials provide real time information, but without good localization, while functional magnetic resonance imaging (fMRI) is usually not possible post-implantation. In the current study, we tracked the change in a fronto-temporal network in cochlear implant patients using a new modality, the Event-related Optical Signal (EROS). EROS combines spatial resolution of better than a centimeter with temporal resolution of the order of milliseconds, which makes it ideal to study the time course of neural activity in localized cortical areas. The imaging signal reflects changes in the optical scattering properties of light by neural cells as opposed to vascular changes like fMRI or spectroscopy. Accurate measurements in adults are possible to a depth of about 5 cm from the scalp surface.

Methods

Six adult cochlear implant patients participated in three brain imaging sessions, i.e., pre-operative, 2-weeks post-implantation, and 6-months post-implantation. All had no detection of

the high frequency experimental tones, while most had detection of the low frequency tones. EROS and event-related brain potentials (ERP) were recorded simultaneously in each imaging session. The experiment in each imaging session included three types of blocks: high and low frequency auditory and visual (control). In the auditory blocks, 80% of the tones were 100ms long while the remaining 20% were 50ms long. Visual blocks consisted of vertical (80%) or horizontal (20%) black and white color bars. The task of the participants was to respond to the length of the tones or the orientation of the bars (visual) by button press.

Results

Larger improvement in the behavioral and brain responses was expected in the high-frequency than the low-frequency auditory block in the post-operation sessions compared to the pre-operation session, while the visual block served as the control for training effects across imaging sessions. Behavioral results showed greater improvement in accuracy for the high-frequency than the low-frequency blocks, which corresponded with an increase in the ERP P300 amplitudes across the imaging sessions. EROS results showed an increase in temporal cortex activities in most participants and increase in frontal cortex activities for some participants in the high-frequency blocks.

Conclusion

This is the first study to apply EROS to monitor the reorganization of brain responses associated with recovery of hearing ability. It demonstrated the feasibility of EROS in brain plasticity research in cochlear implant users and in clinical use.

PS - 138

How Musical Expertise Influences Speech Perception in Noise: A Comparison of Drummers, Vocalists and Non-Musicians

Jessica Slater; Britta Swedenborg; Nina Kraus
Northwestern University

Background

A “musician enhancement” for speech-in-noise perception has been demonstrated in instrumental musicians who began playing their instruments early in childhood, and has been associated with more robust neural encoding of sound and strengthened auditory cognitive function. Very little is known regarding which *specific* aspects of musical experience contribute to these effects, and whether different types of musical expertise yield distinct profiles of underlying neural enhancement. The present study compares groups of drummers, vocalists and non-musicians, assessing speech-in-noise perception, rhythm and melody aptitude, neural encoding of speech sounds and cognitive function (auditory working memory).

Methods

Participants were young adult males, aged 18-35 years, and were assessed using a clinical measure of speech-in-noise perception (QuickSIN). Musical competence was measured using the Musical Ear Test (MET), which includes rhythm and melody subtests. Working memory and neural responses to

speech sounds were also assessed. The drummer, vocalist and non-musician groups were matched on age, IQ and hearing thresholds, and the two musician groups were matched on years of musical experience. Musician participants had played consistently for at least the past three years with either drums or vocals as their primary instrument. Non-musician participants had less than three years of musical experience across their lifetime, with no regular musical activities within the seven years prior to the study.

Results

The drummer and vocalist groups both outperformed the age-matched non-musician group at speech-in-noise perception, while the musician groups did not differ from each other. The combined musician group showed enhanced neural encoding of harmonics compared with the nonmusicians, a previously demonstrated musician ‘signature’. Further, the vocalist group demonstrated selective enhancement of the fundamental frequency compared with the drummers. Better speech-in-noise perception related with better working memory and better scores in the rhythm (but not melody) competence subtest of the MET across all participants.

Conclusion

Outcomes demonstrate a musician enhancement for speech-in-noise perception in drummers and vocalists, as well as enhanced neural encoding of harmonics in the musicians compared with age-matched non-musicians. Further, we reveal a relationship between rhythm competence and speech-in-noise perception, and a selective enhancement of the fundamental frequency in the singers only. This represents an advance in the understanding of how different aspects of musical experience influence language-related skills, and may help to inform the use of music in educational and clinical contexts.

PS - 139

Cross-Modal Plasticity of Intracortical Connections in Auditory Cortex

Xiangying Meng; Patrick Kanold
University of Maryland

Background

Sensory systems do not work in isolation and interactions between auditory and visual systems have been shown during sensory loss. For example, cross-modal compensation in blind individuals leads to functional enhancement of the remaining senses, including enhanced frequency discriminations. However, the underlying mechanism for the compensation is not clear. Since our prior studies show that visual deprivation leads to improved frequency selectivity of neurons in primary auditory cortex (A1), we hypothesized that changes in visual experience can cause changes in the synaptic connections within A1

Methods

We investigated this hypothesis by comparing intracortical connections to Layer 2/3 neurons in dark-exposed mice to those from normally reared mice. We study the spatial pattern of excitatory and inhibition connections in acute slices of A1 using laser-scanning photostimulation (LSPS).

Results

We find that excitatory and inhibitory circuits related to layer 2/3 neurons are different in dark exposed mice than those from normally reared mice. The differences are characterized by the amount of input from different layers to L2/3 neurons and averaged maps.

Conclusion

Our results show that visual experience can change circuits within A1 and these change might contribute to enhanced auditory processing after visual deprivations

PS - 140

Stimulus-Timing Dependent Plasticity in Dorsal Cochlear Nucleus is Altered in Tinnitus

Seth Koehler¹; Susan Shore²

¹Johns Hopkins; ²University of Michigan

Background

Tinnitus, the phantom perception of sound, has been linked to somatosensory innervation of the auditory system with tinnitus patients reporting that somatosensory stimuli such as pressure on the face can elicit or modulate tinnitus. In a guinea pig model, tinnitus and cochlear damage are associated with changes in somatosensory-auditory integration and plasticity in the dorsal cochlear nucleus (DCN). Recently, we demonstrated that DCN bimodal plasticity, long-lasting increases or decreases in principal cell firing rates following paired somatosensory and auditory stimuli, is stimulus-timing dependent. The strength and direction of bimodal plasticity depends on the order of bimodal stimulation with Hebbian and anti-Hebbian timing rules reflecting *in vitro* spike-timing dependent plasticity (Koehler and Shore, PLoS One, 2013). In this study, we evaluated the stimulus-timing dependence of bimodal plasticity in a tinnitus model.

Methods

Ten guinea pigs were exposed to a narrowband noise that produced a temporary elevation of auditory brainstem response thresholds. Reduced gap-induced prepulse inhibition of the acoustic startle after noise-exposure provided evidence for tinnitus in 6/10 noise-exposed guinea pigs. Following noise-exposure and tinnitus induction, stimulus-timing dependent plasticity was compared between noise-exposed guinea pigs with (n=6) and without (n=4) evidence for tinnitus and sham-exposed (n=6) guinea pigs. Spiking activity in response to tones was recorded from multi-channel electrodes placed into the DCN. Bimodal plasticity was measured by comparing responses to sound before and after paired somatosensory-auditory stimulation presented with varying intervals and orders.

Results

In comparison with sham and noise-exposed animals without tinnitus, timing rules in tinnitus animals were more likely to be anti-Hebbian and broader for those bimodal intervals in which the neural activity showed enhancement. Furthermore, units from exposed animals with tinnitus were more weakly suppressed than either sham animals or exposed animals without tinnitus. Broadened timing rules in the enhancement phase in animals with tinnitus, and in the suppressive phase

in exposed animals without tinnitus was in contrast to narrow, Hebbian-like timing rules in sham animals.

Conclusion

Our results show that alterations of stimulus-timing dependent plasticity in the DCN are a new neural correlate of tinnitus. Broadened enhancement phase of timing rules and a shift towards enhancement of spontaneous activity in guinea pigs with tinnitus suggests a mechanism for tinnitus-associated hyperactivity after noise-exposure. These findings implicate underlying alterations in DCN bimodal spike-timing dependent plasticity, opening the way for a therapeutic target for tinnitus.

PS - 141

Measurement of Medial Olivocochlear Efferent Activity During Psychophysical Overshoot

Wei Zhao¹; Elizabeth Strickland²; John Guinan¹

¹Massachusetts Eye and Ear Infirmary, Harvard Medical School; ²Department of Speech, Language, and Hearing Sciences, Purdue University

Background

“Overshoot” is a psychophysical phenomenon in which the behavioral threshold of a brief tone in the presence of a gated noise is higher when the tone is presented at the beginning of the noise than when the tone is delayed. It has been hypothesized that overshoot is due to the noise evoking medial olivocochlear (MOC) activity which slowly builds up, thereby reducing cochlear amplification of the low-level noise more than the higher-level tone. If MOC activity produces overshoot, there should be a correlation between overshoot and MOC activity. To test this hypothesis, we measured behavioral overshoot and MOC activity in each trial as subjects did the psychophysical task.

Methods

Human subjects with normal hearing performed a two-interval forced choice task in which they judged which of two bursts of noise also contained a tone burst. In each trial, a 10-ms 1-kHz tone pip was embedded in one of two 30-ms, 60 dB SPL broadband noise bursts (maskers) in the task ear. The tone-pip level was varied following an adaptive procedure (two-up, one-down) that searched for the 71% correct point on the psychometric function. Adaptive sequences were done with and without a broadband noise called the “precursor” which was 70 ms, 170 ms or 400 ms in duration and immediately preceded the masker. Overshoot is the difference in behavioral thresholds with and without the precursor. In each trial, MOC activity was simultaneously monitored by click-evoked otoacoustic emissions (CEOAEs) in the task ear, before, between and immediately after the noise bursts. The change in CEOAE level, relative to the level at the beginning of the task, was taken as an index of the MOC inhibition.

Results

Preliminary results indicate correlations between psychophysical overshoot and MOC activity measured in the same trials, but not in the simple pattern expected from a one-to-one correspondence between MOC activity and psychophysical overshoot.

Conclusion

The paradigm has great potential for exploring the extent to which MOC activity underlies psychophysical overshoot.

PS - 142

Consonant Identification Using Temporal-Fine Structure and Recovered Envelope Cues for Normal-Hearing and Hearing-Impaired Listeners

Agnès Léger; Joseph G. Desloge; Ali Abavisani; Louis D. Braida; Jayaganesh Swaminathan

Research Laboratory of Electronics, Massachusetts Institute of Technology

Background

Hearing-impaired (HI) listeners with sensorineural hearing loss have been shown to have a poorer-than-normal ability to understand speech processed using the Hilbert transform to remove envelope (ENV) cues and preserve temporal-fine structure (TFS) cues. However, this processing may not completely isolate TFS and ENV components. When a broadband signal is filtered through a narrow filter (such as a normal cochlear filter), the TFS component yields an output envelope that is similar to the envelope of the band. TFS-speech intelligibility may partly depend on the use of these recovered envelope (RENV) cues. However, broader cochlear filtering associated with hearing-impairment may lead to less effective recovery of envelopes from TFS. The present study examined the contribution of RENVs to the utilization of TFS cues for normal-hearing (NH) and hearing-impaired (HI) listeners.

Methods

Sixteen-consonant identification was measured using syllables processed to present TFS or RENV cues. For TFS conditions: speech was filtered into N adjacent frequency bands ($N = 1, 2, 4, 8$ or 16) over a range of 80-8020 Hz; TFS components were extracted within each band; the N resulting signals were recombined. For RENV conditions: for each value of N , the TFS stimulus was filtered into 40 adjacent bands; envelope components were extracted to yield RENVs for each band; the resulting RENVs modulated tone carriers equal to the center frequency of each of the 40 bands; the resulting signals were recombined. Stimuli were presented at 70 dB SPL for NH listeners and amplified using a modified half gain rule for HI listeners.

Results

Preliminary results indicate that for both TFS and RENV speech, identification scores were poorer for HI listeners than for NH listeners (for all N). However, for both listening groups, performance with TFS speech could be well accounted for by RENV cues for each N . Scores were smaller for larger N s.

Conclusion

Results suggest that the intelligibility of TFS-speech can be accounted for by the recovery of envelope cues from a sufficiently large number of bands, for both NH and HI listeners. A phenomenological model of the auditory periphery that can account for varying degrees of hearing loss will be used to

better understand the respective contributions of TFS and RENV cues to speech intelligibility. Implications of these results for the design of auditory prostheses will be discussed.

PS - 143

Inter-Individual Variation of Sensitivities to Frequency Modulation, Amplitude Modulation, and Interaural-Phase Difference: Relation With Click-Evoked Otoacoustic Emissions

Sho Otsuka¹; Shigeto Furukawa²; Shimpei Yamagishi³; Koichi Hirota¹; Makio Kashino²

¹The University of Tokyo; ²NTT Communication Science Laboratories; ³Tokyo Institute of Technology

Background

Basic auditory processing, such as sound localization and frequency modulation detection, is assumed to depend on neural phase-locking and firing-rate information. However, factors that determine inter-listener variation of basic auditory abilities have not been identified. This study examined the extent to which cochlear factors can account for inter-listener variation of basic auditory abilities. Otoacoustic emissions (OAEs) were measured to evaluate cochlear functions. Sensitivities to interaural phase differences (IPDs), amplitude modulation (AM), and frequency modulation (FM) were measured to assess listeners' basic auditory abilities.

Methods

Amplitude and frequency modulation detection limen (AMDL and FMDL) were measured for 1-kHz tones of 750-ms duration at a modulation rate of 2 and 16 Hz. IPDs were measured for a 1-kHz tone of 400-ms duration. The tone levels were set at 55 dB SPL. Detection limens were determined by using a 2I-2AFC transformed up-down method. Click-evoked otoacoustic emissions (CEOAEs) were measured for evaluating the cochlear function. To explore features that characterize CEOAE spectra, we applied a principal component analysis (PCA). Then, multiple regression analysis was performed to examine the proportion of the performance variance accounted for by the extracted principal components. Twenty-nine audiometrically normal adults participated in the experiment as listeners.

Results

Low-rate FMDL, low-rate AMDL and IPDs were significantly correlated with the principal component showing a characteristic dip around 2 kHz in CEOAE spectra, while the high-rate AMDL and FMDL were not significantly correlated with any principal components extracted from CEOAE spectra. Given that the CEOAE level is partly determined by the degree of irregularity on the basilar membrane (BM), the specific irregularity profile that generates a characteristic dip around 2 kHz on CEOAE might disturb listeners' ability to use a common cue, presumably phase-locking information, for detecting AM, FM, and IPDs. This hypothesis was tested by simulation on an auditory model where the irregularity was implemented in the BM.

Conclusion

The results showed that an appreciable fraction of inter-listener variability in the performance of basic auditory tasks can be accounted for by cochlear factors revealed as CEO-AE spectra.

PS - 144

A Test of the Assumptions of the Temporal Masking Curve Method of Assessing Cochlear Nonlinearity

Patricia Pérez-González; Peter T. Johannesen; **Enrique A. Lopez-Poveda**

Universidad de Salamanca

Background

The temporal masking curve (TMC) method (Nelson et al. 2001, JASA 110:2045-2064) is a popular technique for behaviorally inferring cochlear nonlinearity. An implicit assumption of this method is that the post-mechanical (or compression-free) rate of recovery from forward masking is identical across all conditions tested. Some authors have suggested, however, that the post-mechanical recovery rate is faster for lower than for higher probe frequencies (Stainsby and Moore, 2006, *Hear. Res.* 218:98-111). Others have suggested that the rate of recovery is slower (half) for masker levels above than below 83 dB SPL (Wojtczak and Oxenham, 2009, JASA 125:270-281). Here, we test the frequency-independence assumption using an improved version of the approach of Stainsby and Moore (2006).

Methods

On-frequency TMCs were measured for subjects with absent DPOAEs (linear cochlear responses) for probe frequencies of 0.5, 1, 2, 4 and 6 kHz. Measured TMCs were then fitted using straight lines, whose slope and intercept were taken as indicative of post-mechanical recovery rate and level, respectively.

Results

TMC slope and level increased and decreased, respectively, with decreasing probe frequency and slope was inversely correlated with level ($R=-0.9$).

Conclusion

The post-mechanical recovery rate could be faster for lower frequencies, consistent with Stainsby and Moore (2006) but the effect is probably due to masker levels being lower at lower frequencies, consistent with Wojtczak and Oxenham (2009). The implications of these results for inferring cochlear gain and compression from TMCs are discussed.

PS - 145

A Fast Method for Psychophysical Estimation of Nonlinear Cochlear Processing Using Schroeder Phase Harmonic Complexes

Sarah Rahmat; Greg A. O'Beirne

University of Canterbury

Background

Schroeder phase harmonic complexes (Schroeder, 1970) have been used in many psychophysical experiments to ex-

amine the phase curvature of cochlear filtering and cochlear nonlinearity. The difference in masked thresholds at different phases of the masker (the "phase effect") is reduced when the cochlea behaves more linearly, e.g. at very high and low stimulus levels and in ears with sensorineural hearing loss (Summers & Leek, 1998). Schroeder phase masking functions have been shown to be more sensitive than pure-tone audiometry in evaluating changes in nonlinear cochlear function as a result of cochlear implant surgery (Gifford et al., 2008). Previous studies have typically used three-alternative forced-choice (3 AFC) techniques to measure Schroeder phase masking functions, taking around 45 minutes per curve. We have developed a fast method of measuring the same function in 8 minutes using a Békésy tracking procedure. We aimed to determine whether our new technique produced results equivalent with the conventional 3AFC technique, to establish its test-retest reliability, and to use it to measure Schroeder phase masking functions in normal hearing and hearing impaired participants.

Methods

44 normal hearing and 15 hearing impaired participants were tested. Schroeder phase masking functions were measured at 500 Hz (75 dB A) using the conventional and fast methods to find the agreement between two tests. For test-retest reliability, the fast method was repeated twice within the same session. The fast method was performed at 250 Hz, 500 Hz, 1 kHz, 2 kHz and 4 kHz at 45 dB and 75 dB masker levels, in normal hearing and hearing impaired participants.

Results

Our fast method showed good agreement with the conventional 3 AFC task, with a mean difference in masked thresholds between the two test methods of less than 1 dB. High repeatability was observed for the fast method, with results for the second trial falling within 1 s.d. of those from the first. Phase effects were significantly reduced at low presentation levels and in participants with SNHL as compared to normal hearing participants ($p<0.05$), consistent with reduction of cochlear nonlinearity in those conditions.

Conclusion

The fast method of measuring Schroeder phase masking functions we describe reduces test time by around 80% compared to the conventional method of measurement, while producing equivalent and reliable results. Our method has the potential to greatly facilitate psychophysical research into cochlear nonlinearity, and may allow the eventual translation of this tool from the lab to the clinic.

PS - 146

Effect of Precursor Duration on Cochlear Gain and Compression Estimates

Vit Drga¹; Ifat Yasin¹; Christopher Plack²

¹*UCL Ear Institute*; ²*School of Psychological Sciences, University of Manchester*

Background

Behavioural and physiological evidence suggests that the amount of gain applied to the basilar membrane may change during the course of acoustic stimulation due to efferent acti-

vation of the cochlea (Liberman, 1996). This efferent effect is sluggish with a delay from sound onset to cochlear response of about 31-43 ms (James et al., 2002). This study used the Fixed Duration Masking Curve (FDMC) method (Yasin et al., 2013) to estimate human cochlear gain and compression, in the presence of a precursor sound of variable duration. Masker level at threshold for a 10-dB SL, 4-kHz signal was obtained in the presence of an on-frequency (4 kHz) and off-frequency (1.8 kHz) forward masker, as a function of signal duration, with total masker-and-signal duration set to 25 ms and masker-signal silent interval set to 0 ms. Presentation of a precursor sound prior to the masker-signal stimulus was used to infer the time- and level-dependence of the efferent effect. The use of the FDMC technique ensured that the effect of the precursor on gain could be measured independently of any masking effects by the precursor. This has been a confound in previous behavioural studies.

Methods

The present study investigated the effect of precursor duration on estimates of gain and compression. FDMCs were obtained from four listeners with and without a precursor noise (1-kHz wide noise band centred at 4 kHz). The precursor was presented at durations of 40, 80, 160, 320 and 640 ms at a level of 60 dB SPL with the silent interval between precursor and masker fixed at 0 ms.

Results

Preliminary analyses with a one-way ANOVA (using an adjusted F statistic) of the effect of precursor duration on estimates of gain, revealed a statistically significant main effect, Welch's $F(5, 7.07) = 9.17$, $p < 0.01$. Post hoc comparisons using the Games-Howell test indicated that the gain reduction achieved with a precursor duration of 40, 80 and 160 ms was significantly greater than in the absence of a precursor [Mean = 22.30, SD = 6.01, p (one-tailed) < 0.05 , Mean = 29.67, SD = 3.78, p (one-tailed) < 0.01 , Mean = 26.49, SD = 5.94, p (one-tailed) < 0.05 , respectively.] A one-way ANOVA of the effect of precursor duration on estimates of maximum compression exponent did not reveal a statistically significant main effect.

Conclusion

The results indicate minimal effect of precursor duration, and the findings are discussed in the context of recent physiological and computational models of the efferent effect.

PS - 147

The Effect of Tone Duration on Detection and its Neuronal Correlates in the Subcortical Auditory System of Nonhuman Primates

Abigail Bernard; Peter Bohlen; Margit Dylla; Ramnarayan Ramachandran

Vanderbilt University

Background

The ability to detect signals, especially in noisy environments, is a fundamental function of the auditory system. Nonhuman primates have U-shaped thresholds as a function of frequency. The addition of noise increases detection thresholds by ~1 dB per dB for frequencies > 1 kHz, and by smaller amounts

at lower frequencies. However, noise level and tone frequency are not the only determinants of detection threshold - the duration of the signal is an important determinant of detection thresholds. This relationship is captured by Bloch's law, which states that the detectability of a signal is related to the product of the tone intensity and duration. It is believed that subjects accumulate information over the duration of a signal to develop a decision variable, which is compared to a criterion to create a decision. How duration affects thresholds, the effect of noise on this function, and how neurons in the subcortical auditory system can support such behavior were investigated as part of a study of the temporal integration properties of the auditory system.

Methods

Two monkeys (*Macaca mulatta*) were trained to detect tones in quiet and in the presence of noise in a reaction time Go/No-Go task using the method of constant stimuli. Tones of different frequencies were presented alone and in noise for durations that ranged between 12.5 and 200 ms. Signal detection theoretic analyses were performed on behavioral data.

Results

Detection thresholds at each frequency decreased gradually as tone duration increased, with an exponential relationship between threshold and duration. Preliminary results also suggest that addition of noise makes the slope of the exponential relationship between threshold and duration shallower. Neuronal responses collected during detection of tones in noise were analyzed over the various durations that matched tone durations used in behavioral experiments. Thresholds for single units in the inferior colliculus (IC) and cochlear nucleus (CN) also decreased exponentially as longer tone durations were analyzed, but the slopes of the relationship for CN neurons were steeper than those computed for IC neurons.

Conclusion

These results indicate temporal integration properties are context dependent, and that they are transformed through the ascending auditory system. These results provide the framework for future studies on the neuronal basis of Bloch's law.

PS - 148

Audiograms, Gap Detection Thresholds, and Frequency Difference Limens in Cannabinoid Receptor 1 Knockout Mice

Katrina Toal; Kelly Radziwon; David Holfoth; Matthew Xu-Friedman; Micheal Dent

University at Buffalo, SUNY

Background

The endocannabinoid signaling pathway plays an important role in regulating neuronal activity. The main receptor, cannabinoid receptor 1 (CB1), is found at several stages in the auditory pathway, but its role in hearing is unknown. To address this problem, we studied the hearing abilities of CB1R knockout mice in order to compare them to normal-hearing mice (CBA/CaJ). Three experiments were performed with these knockouts: audiograms, gap detection thresholds, and frequency difference limens. Audiograms are a measure of

general hearing abilities across different frequencies. Gap detection acuity reflects temporal resolution, and frequency difference limens illustrate the ability to discern different frequencies.

Methods

Nine CB1 KO mice were trained and tested using operant conditioning methods to obtain audiograms (six subjects), and thresholds for gap and frequency difference detection (three subjects). For all three measures, the Method of Constant Stimuli and a threshold d' of 1.5 were used. Audiograms were measured for frequencies ranging from 1 to 42 kHz. Gap detection thresholds were obtained for broadband noise and band-passed noise (high passed at 18 kHz and low passed at 18, 12, and 8 kHz). The gap detection mice were then trained and tested on the frequency difference limen task for 12, 16, 24, and 42 kHz tones.

Results

Overall, training performance for the KOs was similar to that for the wild-types. There were perceptual differences for some tasks, however. Absolute thresholds for pure tones were similar in the two groups at the lowest and highest frequencies. At the middle frequencies, thresholds for the KOs were elevated relative to the wild-type mice. Gap detection thresholds for the KOs were similar to those for the wild-type mice for broadband noise and high passed noise, but when the high frequencies were removed, thresholds increased dramatically for the wild-types but not for the KOs. Frequency difference limens were not statistically different between the two strains.

Conclusion

These results suggest that the CB1 gene impacts the temporal resolution of low-passed noise, improving it in mice that lack the gene. This gene does not, however, appear to affect spectral processing. Although CB1 receptors are found throughout the nervous system, this is the first study to implicate it in auditory processing using behavioral experiments. These behavioral effects may relate to CB1-receptor expression in parts of the auditory pathway devoted to temporal processing.

PS - 149

Better-Ear Glimpsing Efficiency in Hearing-Impaired Listeners

Virginia Best¹; Douglas Brungart²; Nandini Iyer³; Gerald Kidd, Jr.¹; Christine Mason¹

¹Boston University; ²Walter Reed National Military Medical Center; ³Air Force Research Laboratory

Background

It is well known that when competing speech sounds are spatially separated, listeners can make use of the ear with the better signal-to-noise ratio (the better ear). For symmetric listening configurations, this better ear can alternate between left and right at different times in different frequency bands. In a previous study [Brungart and Iyer (2012) JASA 132:2545–2556] it was shown that listeners with normal hearing (NH) are able to efficiently make use of these “better-ear glimpses” and that this can account for performance in spatialized speech mixtures. In the present study we examined

better-ear glimpsing efficiency in young listeners with bilateral sensorineural hearing impairment (HI).

Methods

Targets were MRT sentences, and maskers were samples of continuous discourse. Spatial conditions included: *colocated* (maskers colocated with the frontal target), *binaural* (maskers symmetrically separated to either side), *better-ear* (better-ear glimpses assembled and presented diotically), and *hybrid* (better-ear glimpses assembled and presented to one ear with worse-ear glimpses presented to the other ear). Control conditions included *monaural* and *worse-ear* (worse-ear glimpses assembled and presented diotically). HI listeners received individualized amplification according to the NAL-RP prescription.

Results

Group mean thresholds were 5-6 dB higher in the HI group than in the NH group for all conditions. In contrast to many previous findings, spatial release from masking (difference between *colocated* and *binaural*) was comparable in the two groups. Moreover, within each group, average *binaural* and *better-ear* thresholds were similar although there were substantial individual differences.

Conclusion

Under the conditions tested, HI listeners appeared to be as efficient as NH listeners at better-ear glimpsing. Of interest will be whether this holds true for stimuli that produce a greater amount of informational masking than the stimuli used in this experiment, and for which HI listeners consistently show reduced spatial release from masking.

PS - 150

The Role of Harmonic Spectral Structure in Speech Segregation

Josh McDermott

Massachusetts Institute of Technology

Background

The short-term spectrum of speech and other natural sounds is frequently harmonic, containing Fourier components at multiples of a fundamental frequency. Harmonicity is believed to provide an important acoustic grouping cue underlying sound segregation, though the mechanisms by which this occur, and its importance in real-world conditions, remain unclear. To test the role of harmonicity in the segregation of real-world sound signals, we used a novel speech synthesis method to manipulate the fine-grained spectral structure of otherwise natural-sounding speech tokens. We then measured the ability of human listeners to understand these tokens in isolation and in mixtures with other tokens.

Methods

We utilized a modified version of the STRAIGHT methodology for speech manipulation and synthesis [Kawahara (2006), Acoustical Sci. and Tech.], in which a speech waveform is decomposed into voiced and unvoiced vocal excitation and vocal tract filtering. Unlike the conventional STRAIGHT method, we modeled voiced excitation as a combination of time-varying sinusoids. We could then manipulate individual compo-

nents, altering the frequency of each component by some amount, or omitting some subset of the harmonics entirely [McDermott et al. (2012), Proc. SAPA-SCALE Conference]. We tested the importance of harmonicity by jittering harmonic frequencies up or down by a small amount, rendering the speech inharmonic. We tested the importance of familiar spectral structure by deleting even-numbered harmonics. This latter manipulation left only the odd harmonics, a spectral pattern that, while harmonic, does not normally occur in natural sounds. To assess the effect of these manipulations on speech segregation, we presented listeners with individual words/sentences, and pairs of concurrent words/sentences, and asked them to report what was said.

Results

Performance for isolated words/sentences was comparable across all conditions. For pairs of concurrent words/sentences, there was a small performance decrement for inharmonic speech relative to normal harmonic speech. However, performance for odd-harmonic speech was also poorer, and by a comparable amount.

Conclusion

Harmonic speech excitation aids the comprehension of speech amid concurrent talkers, but the benefit does not generalize to unfamiliar harmonic spectra. This is consistent with the use of familiar spectral templates in sound segregation rather than harmonic structure per se.

PS - 151

Perceptual Calibration to Modest, Predictable Spectral Peaks in Precursor Sounds Influences Vowel Identification

Paul Anderson; Christian Stilp

University of Louisville

Background

When a spectral cue to vowel identity (e.g., spectral tilt, second formant frequency; F_2) is made predictable across precursor sounds and a subsequent vowel target, perception deemphasizes this cue and increasingly relies on more informative, changing properties for vowel recognition (Kieffe & Kluender, 2008 *J Acoust Soc Am*; Alexander & Kluender, 2010 *J Acoust Soc Am*). This process, known as auditory perception calibration, helps perception maintain constancy in the acoustic environment. In these experiments, spectral energy corresponding to target vowel F_2 was made predictable by amplifying that frequency region in precursor sounds by as much as 20 dB. While it is established that perception calibrates to such robust spectral peaks, its sensitivity to more modest but equally reliable spectral peaks is unknown. The present experiments address this question.

Methods

Normal-hearing listeners labeled vowels from a 5 (F_2 : 1000-2200 Hz in 300-Hz steps) by 5 (spectral tilt: -12-0 dB/octave in 3 dB/octave steps) matrix that perceptually varied from [u] to [i]. Listeners responded by clicking the mouse to indicate whether the target vowel sounded more like "oo" or "ee". Reliance upon F_2 and spectral tilt cues for vowel identification

were measured using standardized logistic regression coefficients (i.e., perceptual weights). Listeners first identified vowels in isolation, then following filtered precursors (synthesized rendition of "Please say what vowel this is") with frequencies in the target vowel's F_2 region amplified by 5, 10, or 15 dB. Filtering conditions were blocked and tested in randomized orders. Significant weight changes for vowels tested in isolation versus following filtered precursors indicated perceptual calibration.

Results

Preliminary results support perceptual calibration to modest, predictable spectral peaks. Consistent with previous studies, perceptual weights changed in predicted directions (decrease in F_2 weight, increase in tilt weight) when F_2 information was predictable across precursor and target vowel. All weight changes significantly differed from 0 except tilt weights for 5-dB-filtered precursors. Changes in F_2 weight were reasonably constant across filtering conditions, but changes in tilt weight broadly increased as spectral peaks grew more robust.

Conclusion

Reliable spectral properties need not be particularly robust to elicit perceptual calibration, as amplifying frequency regions in precursors by 5 dB influenced vowel identification. Results shed light on underlying principles supporting auditory perceptual calibration and how perception attunes to predictable properties in the environment most broadly.

PS - 152

Evaluating Single Channel Noise Reduction Algorithms for Hearing Impaired Listeners

Jessica Monaghan¹; Thomas Blumensath¹; Arkadiusz Stasiak²; Ian Winter²; Matthew Wright¹; Stefan Bleeck¹

¹University of Southampton; ²University of Cambridge

Background

Hearing-impaired listeners often have more difficulty listening in noise than listeners with normal hearing. Even when using hearing aids, impaired listeners have lower levels of speech recognition for the same signal-to-noise ratio than do normal-hearing listeners. While single channel noise-reduction strategies can improve speech quality for normal-hearing listeners, in general they do not improve speech intelligibility [Hu, Y. and Loizou, P. (2007). "A comparative intelligibility study of single-microphone noise reduction algorithms", *Journal of Acoustical Society of America*, 122(3), 1777–1786]. Nevertheless, noise-reduction strategies might be more beneficial for hearing-impaired than for normal-hearing listeners since impaired listeners might still obtain improvements in speech intelligibility for those (higher) signal-to-noise ratios at which normal-hearing listeners show 'ceiling' performance. Additionally, impaired listeners may be less sensitive to the distortions that are often generated by noise-reduction algorithms.

Methods

Five single channel noise-reduction algorithms were tested: multi-band spectral subtraction, minimum mean-square error, Karhunen-Loeve transform, wiener filtering and dictio-

nary-based sparse-coding. These algorithms were selected as representative examples of the general classes of strategy currently employed. The algorithms were applied to noisy sentences at different signal-to-noise ratios and to different noise types.

The percentage of keywords correctly identified using the BKB sentence test was measured for ~30 hearing-impaired listeners at SNRs between 0 and 15 dB in stationary (speech shaped) and non-stationary (babble) noise.

Results

Objective measures indicated that multi-band spectral subtraction and sparse coding would provide the greatest benefits in speech quality. Literature review and preliminary data from normal-hearing listeners indicate that noise reduction does not improve overall speech intelligibility. In stationary noise conditions at moderate SNRs, spectral subtraction and wiener filtering appear to provide small improvements in speech intelligibility over the unenhanced conditions.

Conclusion

While noise reduction algorithms do not tend to show any benefit in intelligibility for normal-hearing listeners, they may enhance intelligibility for hearing-impaired listeners.

PS - 153

Effects of Noise Reduction on Temporal Fine Structure and Temporal Envelope Cues

Shayesteh Kiaei; Magdalena Wojtczak; Andrew J. Oxenham

University of Minnesota

Background

Studies implementing single-channel noise reduction algorithms do not provide the improvements in speech intelligibility that would be expected based on the signal-to-noise ratio (SNR). In general SNR is informative for predicting the intelligibility of unprocessed speech in noise, but overestimates performance for stimuli processed by noise reduction algorithms. It has been demonstrated that speech intelligibility in noise is dependent on both temporal envelope (ENV) and temporal fine structure (TFS) information. In this study the effect of selected noise reduction algorithms on performance in basic psychophysical tasks that are thought to involve the use of TFS cues and ENV cues was investigated. The predictive power of SNR was tested by comparing performance in conditions using processed stimuli with that in conditions using unprocessed noise at an appropriately reduced level.

Methods

Listeners' ability to use TFS cues was measured in two tasks, one task involving the measurement of just-detectable interaural time differences (ITDs) at low frequencies, and the other involving detection of a spectral shift of a harmonic complex filtered into the frequency range between 1800 and 2800 Hz. Listeners' ability to use envelope cues was measured in a task involving the detection of interaural envelope phase differences (IPD) for a sinusoidally amplitude modulated 4-kHz carrier. In each task, seven conditions were tested: (1) stimuli were presented in quiet; (2) stimuli were presented in noise

at a fixed SNR; (3)-(5) stimuli in noise were presented after processing using different noise reduction algorithms; (6) and (7) stimuli were mixed with noise whose level was reduced to match that at the output of the noise reduction algorithms used in conditions (3) and (4), respectively.

Results

In all tasks, adding noise impaired listeners' performance. The effects of noise reduction algorithms varied across the tasks and stimulus parameters, but never reached the level observed for the stimuli in quiet. Performance with the reduced-level unprocessed noise estimated for specific algorithms was better than that from the corresponding noise reduction algorithm, indicating that the SNR does not accurately predict performance in these basic psychophysical tasks.

Conclusion

The results confirm that the presence of noise degrades performance in tasks related to both TFS and ENV. The SNR after noise reduction is not a good predictor of performance for either cue. New measures for predicting the availability of TFS and ENV cues after processing will be discussed.

PS - 154

Release from Sequential Informational Masking by Spatial Cues

Lena-Vanessa Dolležal; Sandra Tolnai; Georg M. Klump
Center of Excellence "Hearing4all", Animal Physiology and Behavior Group, Department for Neuroscience, School for Medicine and Health Sciences, Oldenburg University, 26111 Oldenburg, Germany

Background

Binaural cues, like interaural time (ITD) and level differences (ILD) are essential for sound localization in the horizontal plane. Both, ITD and ILD cues help to segregate sound sources. By applying binaural cues to stimuli presented in a simultaneous informational masking (IM) paradigm a release of IM can be observed (e.g., Durlach et al. 2003, JASA 114(1):368-79). The phenomenon of IM describes the masking of a signal by other acoustic events not being due to energetic masking. This non-energetic masking can be measured and defined as an increase in detection threshold caused by stimulus uncertainty (e.g., Durlach et al. 2003, JASA 114(1):368-79).

Methods

We adopted a sequential IM paradigm that was first applied in an EEG study (Winkler et al. 2003, PNAS 100(20):11812-5). In a human psychoacoustic experiment, we presented sequences of constant level standard (500 Hz, 61 dB SPL) and level increment target tones (500 Hz, 62-94 dB SPL) interleaved with distracting tones (455, 477, 522, 546 Hz and 66, 71, 81, 86 dB SPL, randomly selected combination of frequency and level). Different values of ILDs, ITDs or both types of cues were applied to the standard and target tones while distracting tones had ITD=0 and ILD=0. Sensitivity for level increment detection and thresholds were determined using the method of constant stimuli in a Go/NoGo procedure.

Results

Humans' level increment detection thresholds were affected by the size of the ILDs or ITDs applied to standard and target tones. The highest detection thresholds were observed for standard and target tones presented with no or small values of ILDs or ITDs. Low detection thresholds were observed for large values of ILDs or ITDs indicating a release from IM. When a combination of ILD and ITD was applied to standard and target tones we observed detection thresholds smaller than the ones measured for the two cues separately indicating a stronger release from IM for ILD/ITD combinations.

Conclusion

ITD and ILD cues can provide for a release from IM in a sequential IM paradigm suggesting that binaural cues are used to segregate spectrally similar sound sources. This effect is stronger if ITD and ILD cues are combined.

PS - 155

Developmental Auditory Deprivation Reduces Modulation Masking Release

Antje Ihlefeld; Dan Sanes

New York University

Background

For normally-hearing (NH) listeners, it is more difficult to detect a tone in a background of noise when the noise is temporally invariant (unmodulated envelope), than when the noise is temporally gated (modulated envelope). This perceptual benefit is called modulation masking release (MMR). Furthermore, when more masker energy is added outside the critical band of the target, but co-modulated with the original masker, then detection thresholds improve even more. This additional perceptual advantage is referred to as comodulation masking release (CMR). In hearing impaired and cochlear implant listeners, both MMR and CMR are much reduced or absent. Although loss of peripheral spectrotemporal sensitivity is of major importance for this phenomenon, it may not be the only factor involved. Current models suggest the across-channel processing is required for MMR and CMR, raising the possibility that hearing loss-induced changes to the central nervous system could partially explain the perceptual deficits. In fact, even moderate conductive hearing loss (CHL) can disrupt membrane and synaptic properties throughout the auditory CNS. Therefore, the MMR and CMR paradigm could provide insight into the role played by the CNS in subjects with impaired hearing.

Methods

Animals were placed on controlled water access, and a go-nogo appetitive procedure was used to assess performance and obtain psychometric functions. To study the effect of auditory deprivation on MMR and CMR, NH gerbils, and those reared with CHL, were trained to detect tones in different types of background noise.

Results

Relative to the background noise level, the two groups had similar detection thresholds in unmodulated noise (i.e., similar signal-to-noise ratios). However, psychometric functions were shallower for CHL than for NH listeners. Furthermore,

the two groups differed in modulated noise: NH gerbils displayed 15 dB lower tone detection thresholds (i.e., a MMR of 15 dB) and a 5 dB CMR. In contrast, CHL gerbils displayed only a 6 dB MMR and a 0 dB CMR.

Conclusion

These findings indicate that signal detection in CHL animals suffers from higher internal noise than in NH animals. Thus, even when audibility is restored at the periphery auditory system, prolonged auditory deprivation may reduce a listener's ability to listen in the temporary dips of background sound.

PS - 156

The Perception of Reverberation is Constrained by Environmental Statistics

James Traer; Joshua H. McDermott

Massachusetts Institute of Technology

Background

Human sound recognition is remarkably robust to the distortion introduced by reverberation in everyday environments. We explored the hypothesis that this robustness is rooted in the ability to decompose the acoustic input into the contributions of the sound source and the reverberation, the latter of which can be described by a single linear filter. As the separation of source and filter (given only their convolution) is inherently ill-posed, any such capacity should depend on prior assumptions about the nature of filter and/or source. We attempted to measure the distribution of environmental impulse responses (IRs) and to test whether it constrains perception.

Methods

We obtained a large set of locations from surveying volunteers about the spaces they encountered during daily life, and then measured the IR at each location. We then synthesized IRs that were either faithful to the observed distribution of real-world IRs, or that deviated from it in various ways, and tested the effect of such deviations on perception. We assessed a) the sense of reverberation conveyed by different types of IRs, b) comprehension of reverberant speech, c) discrimination of novel sound sources in reverberation, and d) discrimination of IRs given only their convolution with speech.

Results

IR measurements suggested that the diffuse tails of real-world IRs always decay exponentially, with decay rates that are frequency-dependent, being consistently slower at low frequencies than high. Perceptual experiments showed that perception of realistic reverberation is strongly dependent on whether reverberant energy decay maintains this form. The rated realism of synthetic IRs was high when they exhibit frequency-dependent exponential decay that is faithful to the real-world IR distribution, and low otherwise. Speech comprehension was also higher for typical than for atypical IRs of equivalent length. Listeners were able to match novel spectrotemporal patterns convolved with IRs to dry versions thereof, but this ability degraded for atypical IRs. Listeners could also discriminate IRs from convolutions with speech, but again only when the IRs were faithful to the real-world IR distribution.

Conclusion

Naturally occurring IRs have stereotyped properties that have evidently been internalized by the auditory system over the course of development or evolution. Human listeners have some ability to separately estimate the source and filter in reverberant conditions, and are strongly constrained by whether the filter conforms to the naturally occurring distribution.

PS - 157

Severe Selective Inner Hair Cell Loss in Chinchillas; Impaired Listening in Noise With Near Normal Audiograms

Edward Lobarinas¹; Dalian Ding²

¹University of Florida; ²University at Buffalo

Background

The effect of inner hair cell (IHC) loss or synaptic impairment on functional hearing is not well understood but is believed to play a role in disorders such as Auditory Neuropathy/Dysynchrony. In previous experiments, we demonstrated that even profound (>70%) IHC loss had minimal impact on puretone thresholds; results suggesting that clinical threshold measures underestimate underlying IHC/afferent pathology.

Methods

Chinchillas were trained to detect tones (250-11,300 Hz) in quiet, in competing broadband noise (50 dB SPL) and competing narrowband noise (70 dB SPL, centered at 500, 2000, and 4000 Hz). Selective IHC loss was induced with a single dose of 75 mg/kg carboplatin. Testing was performed before and after treatment. Hair cell loss was assessed, post-mortem, by analyzing succinate dehydrogenase (SDH) stained sections of the organ of Corti under light microscopy.

Results

Carboplatin-induced IHC loss, ranging from 30-80%, had minimal effect on quiet thresholds but increased thresholds in broadband noise by 5-10 dB, with no evidence of outer hair cell loss. Thresholds in narrowband noise increased at the center frequency of the noise as well as at both tails of the masked threshold function. These results suggest that both listening in noise and off-frequency hearing were impaired by IHC loss despite normal thresholds in quiet.

Conclusion

Auditory tests using unfavorable listening conditions are likely to reveal deficits consistent with loss of IHC; a form of hearing impairment that is not evident with threshold assessment in quiet. Whereas puretone audiometry has little sensitivity to IHC impairment or loss, suprathreshold hearing tests and background noise testing may further help differentiate peripheral hearing loss from retrocochlear pathology.

PS - 158

Central Unmasking in a Melody Recognition Task

Corey Stoelb; **Brittany N. Jaekel**; Sara M. Misurelli; Ruth Y. Litovsky

University of Wisconsin - Madison

Background

The extent to which we can extract melody and segregate source information in the presence of tonal maskers is not well known. Determining the listening environments in which melody recognition improves or degrades in normal-hearing listeners, and how contralateral unmasking and divided attention affect melody recognition, will provide parameters for comparison with cochlear implant (CI) users. CI users typically receive degraded spectral information via their implants, which may impact their performance for certain conditions of the melody recognition task.

Methods

Stimuli were presented over headphones with target stimuli always in the right ear; participants were instructed to listen for the target in their right ear. Target stimuli were the first seven notes of eight melodies chosen for their familiarity and lack of rhythmic cues, presented as pure tones. Target stimuli were played in silence or with maskers at varying signal-to-noise ratios (SNRs). Maskers were pure tones selected from the same key and octave, but not the same note, as the target, and were presented in one of three configurations: (A) temporally interleaved, (B) temporally overlapping, (C) both interleaved and overlapping with the target melody. Each condition was tested with maskers either in the same or opposite ear as the target. Targets and maskers were transposed to a scale by a random factor to avoid melody recognition based on pitch memorization. The task was one-interval, eight-alternative forced choice.

Results

There is reduced melody recognition with decreasing SNRs in the following same-ear conditions: (1) when the masker overlaps with the target melody, and (2) when the masker interleaves and overlaps with the target melody. Recognition accuracy approaches 100% for most listeners when the target is interleaved with the masker in the same ear, and when the target and masker are presented to opposite ears.

Conclusion

Contralateral separation of masker and target sources improves ability to extract melody in complex listening situations, if the participant is able to attend to the right ear. Conversely, overlapping a masker sequence with the target melody degrades performance, perhaps due to listener uncertainty about which stream to attend to. Loudness does not seem to be a cue for differentiating between masker and target streams, evident by varying SNRs.

Estimating Loudness Growth from Tone-Burst Evoked Responses at Audiometric Frequencies

Michael Epstein; Yonatan Sasson
Northeastern University

Background

Information derived from tone-burst otoacoustic emissions (TBOAEs) and tone-burst auditory brainstem responses (TBABRs) has been used to derive the general slope and form of loudness functions with some success for a limited stimulus frequency range across a wide range of levels. The aim of this work is to investigate this relationship further, expanding the dynamic and frequency ranges to cover what is typically used in detailed audiometric testing.

Methods

The sets of evoked-responses were recorded in normal hearing listeners over a wide range of levels at common audiometric frequencies (250, 500, 1000, 2000, 4000, 6000, and 8000 Hz). Estimates of loudness were made from these recordings and the results were compared with a psychoacoustical cross-modality-matching procedure.

Results

Results show that loudness can be estimated well from TBOAE recordings using this methodology for 500, 1000, and 2000 Hz stimuli. Estimates for 250 and 8000 Hz stimuli were also possible, but less reliable due to reduced robustness of TBOAEs. Recordings of TBOAEs at 4000 and 6000 Hz were too contaminated by ear-canal resonances to produce estimates that matched the psychoacoustical measure. The results from TBABRs indicated that it is possible to reasonably make loudness estimates across the full audiometric range, though such estimates require significantly more trials than TBOAE estimates.

Conclusion

Both TBOAEs and TBABRs have potential as a tool for making objective estimates of loudness functions across a wide range of stimulus frequencies and levels.

PS - 160

Spectral, Temporal and Spatial Filters for Noise Masking of Detection of Tones

Peter Bohlen; Margit Dylla; Courtney Timms; Ramnarayan Ramachandran
Vanderbilt University

Background

Detection of sounds in noisy environments is a critical and fundamental function of the auditory system. Tone detection thresholds for nonhuman primates display a characteristic U-shaped relationship with frequency. Reaction times to detect tones decreased as the tone sound pressure levels increased beyond threshold. Continuous broadband noise causes an increase in detection thresholds at the rate of 1 dB per dB for tone frequencies larger than 1 kHz, and threshold shift rates were lower for lower frequencies. The frequency content of the noise, and the spatial and temporal relationship

between tone and noise can affect the detectability of a tone. The goal of this study was to investigate the spectral, spatial, and temporal determinants of masking of a tone by noise as a precursor to studies of neuronal mechanisms of detection.

Methods

Five monkeys (three *Macaca mulatta* and two *Macaca radiata*) were trained to detect auditory signals presented alone and in continuous broadband noise in reaction time Go/No-Go experiments using the method of constant stimuli, and using appropriate catch trials. Thresholds were measured for tones over the entire audible range for macaques. Experimental data were analyzed using signal detection theoretic methods.

Results

Threshold shifts measured to continuous noise were not different from those caused by simultaneously gated noise. The onset of the tone relative to the noise profoundly affected thresholds. Threshold shifts were largest when the onsets of tone and noise coincided, and decreased as the noise onset either led or lagged the tone. Thresholds were not different from those to tones alone when noise led tone onset by 300 ms or more, or lagged tone onset by 25 ms or more. The spectral content of a simultaneously gated noise was varied by the use of notch filtered noise centered around a target frequency. Tone detection thresholds decreased as the bandwidth of the notch increased logarithmically and symmetrically about the signal until a critical bandwidth was reached when thresholds matched those to tones alone. These critical bands in macaques appear similar to human critical bands. When the tone and noise were separated in space, detection thresholds decreased as the spatial separation increased.

Conclusion

These results suggest that noise was an effective masker when it had specific spectral, temporal and spatial properties relative to the tone being detected. These results form the baseline for future studies of neurophysiological mechanisms of masking.

PS - 161

Making Sound Features Disappear

Neil Rabinowitz¹; Michael Schemitsch¹; Owen Brimijoin²; Eero Simoncelli¹

¹Howard Hughes Medical Institute, New York University;

¹Howard Hughes Medical Institute, New York University;

²MRC Institute of Hearing Research

Background

Perception can be described as a process of inferring the properties of objects in the world from incoming sensory signals [Helmholtz 1867, Kersten et al 2004]. This inverse process is rendered particularly difficult by the entangling of object information with that of contextual "viewing conditions". For example, before emitted sounds reach the ears, they undergo spectro- and spatio-temporal filtering by the room and head. The details of these transformations depend on the complex geometry and physics of a given listening environment, and can change considerably with head position. Thus, in order to make inferences about source objects, the brain

must separate an incoming signal into “source” and “listening condition” components.

Construction of analytic separation models is very difficult [Dokmanić et al, 2013], and we hypothesize instead that the brain accomplishes this feat by factoring out systematic regularities that are learned from experience.

Methods

To test this, we built a novel psychoacoustics chamber, wherein features of sound sources were systematically varied according to human subjects' head positions. We predicted that subjects would passively learn these head-coupled features and, interpreting them as head-angle-related listening conditions, cease to perceive them as source features.

Results

In the first experiment, subjects listened to a regular pulse train in the free field, while performing a visual search task. Subjects had to occasionally report changes in the pulse rate, but were unaware that the (task-irrelevant) pure-tone carrier-frequency of the pulses was systematically coupled to their head angle (yaw). The amplitude of these changes was adjusted to be substantially larger than those that could be produced by real-world room acoustics. After 30-45 minutes of exposure, we found that subjects' pitch judgements were systematically biased according to their head angles, typically by ~15% of their pre-exposure thresholds.

In the second experiment, we reversed the roles of pulse-rate and carrier-frequency, coupling the (task-irrelevant) pulse-rate to the subjects' head angle, while they reported on carrier-frequency. Unlike the first experiment, we found that exposure did not induce systematic head-angle biases in pulse-rate judgements.

Conclusion

These results suggest that the brain can learn to recognize and discount for listening conditions, but only for a limited set of sound features for which it possesses the infrastructure necessary to compensate for head-angle-related changes.

PS - 162

Prevention of Auditory Perceptual Learning Attributed to Distinct Representations of the Same Auditory Stimulus in Quiet and in Noise

David Little¹; Nicole Marrone²; Helen Han¹; Beverly A Wright¹

¹Northwestern University; ²University of Arizona

Background

Perceptual abilities improve with practice. Such learning across days appears to require sufficient training per day, suggesting that the information obtained from practice must accumulate up to a threshold for learning to be stabilized through consolidation. Here we ask at what level of representation stimulus information accumulates during this process. To do so we leverage a recent finding that practice of a frequency-discrimination task alone (for 360 trials/day) does not lead to learning, while complementing this training with additional exposures to relevant stimuli presented without

task practice, or while performing a temporal-interval discrimination task (360 trials/day), does yield learning. We utilize this same paradigm, but present the additional exposures simultaneously with other background stimuli rather than in quiet. If the additional exposures in the background still aid learning, it would indicate that the information accumulates in a representation where the relevant exposures can be separated from the background. If not, the accumulation occurs in a representation where the relevant exposures presented in quiet are processed, and therefore accumulate, separately from those exposures presented with background stimuli.

Methods

All trained listeners practiced (1) frequency discrimination for 360 trials/day using the same standard stimulus (two 15-ms, 1-kHz tones separated by 100 ms) followed by (2) 360 trials/day of additional stimulus exposures delivered through either (a) presentation of an inharmonic ten-tone complex including that standard stimulus while performing a written symbol-to-number matching task (n=7) or (b) practice on a temporal-interval-discrimination task with that standard stimulus in continuous notched noise spanning 0.2-0.6 kHz and 1.4-1.8 kHz (n=10). Controls participated in pre- and post-tests but received no training in between (n=10).

Results

Both trained groups received sufficient stimulus exposures to yield learning when those exposures are presented in quiet, yet neither group improved more than controls when some of those exposures were presented in the presence of background stimuli. The additional stimulus exposures were ineffective when presented passively as part of a tonal complex (ANCOVA $p=0.114$) or in notched noise while practicing the temporal-interval task ($p=0.298$).

Conclusion

The accumulation of information required for learning on this frequency-discrimination task appears to occur in a representation in which relevant exposures presented with background stimuli do not resemble those exposures in quiet and so cannot contribute to the same process of accumulation. Practically speaking these data suggest that additional stimulus exposures can only aid learning when they are presented in quiet.

PS - 163

Ultrasonic Noise in the Animal Facility and Laboratory: The “Silent” Confound

Jeremy Turner

Southern Illinois University School of Medicine, Illinois College, OtoScience Labs

Background

Noise activates a cascade of auditory and non-auditory effects in laboratory animals and humans due to its effects on the ear and on stress pathways. The resulting widespread biological and behavioral effects of noise have the potential to impact virtually every area of biomedical research as an unrecognized source of variability. This potential confound often goes unrecognized because most of our research animals hear in the ultrasonic frequency range above 20 kHz.

Because the human ear is incapable of processing ultrasonic frequencies, the caretakers and animal researchers are generally unaware of the real noise levels experienced by our animal models. This study reports on the prevalence, multiple sources and characteristics of ultrasonic noise present in the laboratory animal facility and the research laboratory.

Methods

Noise measurement were made with a calibrated, mobile noise measurement system consisting of a 1/4" free-field Bruel & Kjaer matching microphone (model #4939) and pre-amplifier (model #2670) set, with a flat frequency response (+/- 2 dB SPL) in the 100-100,000 Hz range. The microphone signal was run through a B&K Nexus Conditioning Amplifier (model #2690-OS2), then digitized with an external National Instruments USB A/D board (model 6251) and sent to a laptop computer for analysis with custom software. Noise measurements were collected from four different research facilities and in multiple locations in those facilities, including vivarium spaces inside and outside of caging, in hallways, and in research laboratories.

Results

Noise and especially ultrasonic noise, with great variability in frequency and intensity characteristics, was measured from fluorescent lighting fixtures in vivarium spaces, cage changing areas, hallways, and in laboratories. Other common sources of ultrasonic noise included ventilated caging motor/control units, gas line microleaks (air, O₂, specialty gas lines), computers, oscilloscopes and a variety of electronic equipment commonly used in hearing research laboratories. One particularly striking finding was the observation of an energy-saving motion detector placed in a research laboratory which used a 40 kHz, 128 dB SPL tone to detect movement and switch lights on. Ultrasonic noise was more common in areas with more equipment, which tended to be research areas close to where manipulations are done or data are collected from animals.

Conclusion

Our research laboratories and vivarium spaces are incorporating more and more technological advancements, and some of these advancements are introducing a "silent" new confounding variable in the form of ultrasonic noise. This study highlights the sources of such noise, its frequency and intensity characteristics, and offers some suggested practices for measuring and mitigating the problem of ultrasonic noise. These results are discussed in the context of the impact on a variety of biomedical research areas but with special focus on the impact in hearing studies.

PS - 164

The Relationship Between Concert Hall Reverberance, Listener Envelopment, Tonal Quality and Overall Listener Preference

Michelle Vigeant¹; Acadia A. Kocher¹; Charles J. Limb²

¹The Pennsylvania State University; ²Johns Hopkins University School of Medicine, Peabody Conservatory of Music

Background

Numerous objective measures have been developed to predict the subjective response to a hall's acoustics. For example, it has been well established that the objective measure of reverberation time correlates well with the subjective perception of reverberance. However, no single measure has been identified thus far that can predict overall listener preference for concert hall acoustics. In addition, the relationships between overall preference ratings for musical stimuli and other subjective attributes of the listening experience, such as listener envelopment (LEV) (the sense of being immersed in the sound field) and tonal quality (spectral balance preferences), remain poorly understood.

Methods

Thirty-two participants with musical training participated in this study. The participants were required to have hearing thresholds of 15 dBHL or lower, in order to obtain more reliable subjective data without the need for extensive training. The listening test was designed in order to investigate the relationship between overall listener preference ratings and ratings of the following subjective attributes: reverberance, tonal quality, and LEV. A total of 18 binaural recordings were made in a 900-seat hall by playing three short anechoic melodies through an omnidirectional loudspeaker. The recordings were taken at three receiver locations and for two variable acoustics settings. The participants were asked to rate the binaural recordings based on the attributes listed above using a five-point Likert scale ranging from 1 (very unpleasant) to 5 (very pleasant). The test was divided into four sets so that the subjects evaluated each attribute separately to minimize bias in the ratings.

Results

The data were analyzed to determine the extent to which the subjects' ratings of LEV, perception of reverberance, and impressions of tonal quality correlated with the overall preference ratings. Linear regression analysis revealed a significant relationship for several of the motifs between LEV, tonal quality and preference. Positive correlations were also found between overall preference and reverberance ratings.

Conclusion

The results of this study indicate that reverberance, LEV, and tonal quality contribute to overall preference ratings. However, no clear metrics for either LEV or tonal quality have yet to be established, and work is currently underway to relate measurable properties of the late sound field to LEV. This work will ultimately contribute to the development of improved metrics to predict room acoustics preferences. Further work is needed to better understand which perceptual characteris-

tics and objective measures of the sound field are key contributors to overall preference. One possible approach is to investigate the neural substrates involved in the evaluation of concert hall acoustics using functional neuroimaging.

PS - 165

Enhanced Amplitude Modulation Sensitivity in Reverberant Soundfields: Effects of Prior Listening Exposure, Soundfield, and Modulation Frequency

Pavel Zahorik; Paul Anderson

University of Louisville

Background

When an amplitude-modulated (AM) sound source is presented in a reverberant soundfield, the modulation depth of the signal at the listener's location can be attenuated relative to that present at the source. The amount of attenuation depends on the modulation frequency and acoustical characteristics of the source and the environment. Recent evidence suggests, however, that AM sensitivity in reverberant soundfields exhibits a degree of resistance to these modulation attenuation effects, and that the resistance requires prior consistent listening exposure to the soundfield. The goal of this study is to further characterize this effective enhancement of AM for multiple soundfields and modulation frequencies.

Methods

AM sensitivity was measured in 4 different listening environments: 2 reverberant room soundfields (T60s of 1 and 1.8 s in the 4 kHz octave band), an anechoic soundfield, and a diotic listening condition (no soundfield). Virtual auditory space techniques were used for all soundfield simulations. The simulated sound source location was directly in front of the listener (0°) at a distance of 1.4 m. The carrier signal was a 1-octave wide band of noise with a center frequency of 4 kHz (400 ms duration). AM detection thresholds were measured using an adaptive 2AFC procedure at AM frequencies of 16 and 64 Hz for two different types of listening contexts: one in which consistent listening exposure to a particular sound field was provided, and a second that intentionally disrupted listening exposure by varying the soundfield from trial-to-trial. Ten normal-hearing participants completed all listening conditions in both contexts (completely within-subjects design).

Results

AM detection thresholds were compared to the acoustical modulation transfer functions (MTFs) for each of the soundfield conditions using a sensitivity gain metric that expresses the degree of AM sensitivity degradation due to a particular soundfield listening condition, referenced relative to non-soundfield (diotic) sensitivity. AM sensitivity was found to be somewhat greater than predicted by acoustical MTF analyses for the reverberant soundfields in most cases. The differences were most-pronounced at 64 Hz, where the reverberant soundfields impart the greatest amount of AM attenuation. For these cases, consistent prior listening exposure was found to enhance the effect

Conclusion

AM sensitivity enhancement is related to the amount of AM attenuation caused by the soundfield at the modulation frequency under test, and consistent prior listening exposure plays a clear role in the enhancement.

PS - 166

Quadrature Model of Binaural Unmasking

Rainer Beutelmann

Center of Excellence "Hearing4all", Animal Physiology and Behavior Group

Background

Binaural unmasking of tones in noise can be modeled quite accurately by several models (e.g., Durlach, 1972, Colburn, 1977, Breebaart et al., 2001). Despite some particular differences, all binaural detection models are fundamentally based on the (cross-)correlation between left and right ear. Evidently, the principle is valid, but the possible physiological delay mechanisms that are needed for the correlation operation are not fully understood. Candidate sources include neural transmission latencies (Jeffress, 1948) and traveling wave delays on the basilar membrane ("stereausis model"; Schroeder, 1977; Shamma, 1989). The stereausis model might be an explanation for the apparent wider binaural critical bandwidth, but the wide range of basilar membrane locations that is necessary in order to display the physiological range of ITDs casts doubt on its validity. We adopted the basic idea of basilar membrane delays in a different way, eliminating the need for long delays at distant basilar membrane locations.

Methods

For each point on the basilar membrane there is another point that is shifted in phase by a quarter period of the corresponding best frequency due to the traveling wave phase delay on the basilar membrane. These points are close enough to be well within one auditory filter (van der Heijden and Joris, 2003) and thus their responses are sufficiently correlated to represent largely overlapping spectral parts of the input signal. The responses from these two points can be considered to be real and imaginary part of a quasi-analytic (quadrature) signal. In combination with their counterparts from the opposite ear they are used to calculate the instantaneous interaural correlation. The time-averaged interaural correlation is then used as a decision variable in a simulated 3-alternative forced choice procedure to model binaural tone-in noise detection thresholds.

Results

The proposed model predicts binaural masking level difference data (van de Par and Kohlrausch, 1999) for different target frequencies and masker bandwidths. The apparent wider critical bandwidth for binaural processes is predicted correctly and results from the binaural processing itself rather than from assuming different properties of the periphery for binaural and monaural processing.

Conclusion

Using the traveling wave delay on the basilar membrane as a phase shift rather than a time delay in order to calculate the

interaural correlation appears to be a promising approach for models of binaural processing.

PS - 167

Development and Validation of a Measure of “Hearing-Related Quality of Life” Sensitive to Binaural Hearing in Adults

Adele Goman; Rhian Bardsley; Sarah-Louise Buggins; Danielle Dickinson; Rachel Williamson; A.Quentin Summerfield

University of York

Background

Generic self-report instruments like the EuroQol Descriptive System and the Health Utilities Index summarise a respondent's health-related quality of life (QoL) on a scale where 1 corresponds to “perfect health” and 0 to “dead”. Policy-makers require researchers to use these instruments in generating the “effectiveness” component of cost-effectiveness ratios. In practice, both instruments are insensitive to the benefits of binaural hearing, thereby complicating policy-making for bilateral cochlear implantation. Accordingly, we have explored the potential for creating an analogous instrument sensitive to binaural hearing.

Methods

We identified three dimensions on which listeners function better with binaural than monaural hearing: localisation, speech perception in noise, and listening effort. We defined three levels of function on each dimension corresponding to “No” “Some”, and “Great” difficulties. Informants considered each of the 27 combinations of the levels. They imagined that they could live n years with that combination or could trade quantity of life for quality of hearing and live fewer years, m , but with perfect hearing. The value of hearing-related QoL for each combination, was calculated as m/n . Valuations were obtained from 95 students and 105 non-students with $n=50$, and 59 students and 52 non-students with $n=10$, yielding four sets of valuations.

We compiled a questionnaire which allowed patients to report their own levels of function on the three dimensions. The questionnaire was completed by 26 implantees (8 unilateral, 10 bimodal, and 8 bilateral). The bimodal and bilateral patients completed the questionnaire twice, once when using their first or only implant and once when using two devices. Each patient was assigned four values of hearing-related QoL; one from each set of valuations. Two years previously, each patient had completed the Speech, Spatial, and Qualities of Hearing Scale (SSQ) and had undertaken performance tests of localisation and speech-in-noise.

Results

Hearing-related QoL correlated with scores from the SSQ (coefficients ranging from 0.6 to 0.7) and with performance measures (0.3 to 0.5). These positive correlations establish the construct validity of the new questionnaire. Increases in hearing-related QoL associated with using two devices rather than one ranged from +0.05 to +0.17 among bilaterals ($p<0.05$ in each case) and from +0.01 to +0.04 among

bimodals ($p<0.05$ in three of four cases). These analyses establish the sensitivity of the new questionnaire to binaural hearing.

Conclusion

This project establishes the potential for a preference-based self-report measure of hearing-related QoL to be sensitive to binaural hearing in adults.

PS - 168

The Haas Effect: Psychophysical Data and Modeling

M. Torben Pastore; Jonas Braasch
Rensselaer Polytechnic Institute

Background

Humans routinely localize sounds to their respective sources while suppressing directional cues contained within reflections. The direct sound emitted by a source dominates the perceived location of the auditory event. As such, this phenomenon is called localization dominance due to the precedence effect. In room acoustic environments the built-up energy of reflections often surpasses that of the direct sound, yet human listeners continue to localize sounds to their sources. This is often referred to as the Haas effect.

In his early experiments, Haas placed two speakers on a rooftop and asked subjects to adjust relative levels such that the auditory event was centered. The lateral extent and degree of image fusion remain unclear.

Methods

This experiment sought to characterize the lateral extent of the Haas effect for a fused auditory object. Noise stimuli were presented over headphones. Gaussian noise bursts with a center frequency at 500-Hz and a bandwidth of 800-Hz were delivered to blindfolded listeners over headphones as a lead/lag pair. The delay between lead and lag was varied from 1-ms to 5-ms. Listeners then used an acoustic pointer to indicate the perceived lateralization of each auditory event. Braasch's precedence effect model was then applied to simulate the resulting data.

The model then uses an autocorrelation mechanism to estimate the delay and amplitude ratio between the lead and lag. An inverse filter eliminates the lag signal for estimation of the stimulus location. This mechanism works with a standard cross-correlation localization algorithm with a basic model of the auditory periphery that includes a gammatone filter bank and hair-cell rectification.

Results

Localization dominance is shown to extend to stimuli whose lag is approximately 8-dB louder than the lead, thus demonstrating the Haas effect. In addition, the model is able to simulate these data.

Conclusion

This experiment shows that localization dominance due to the precedence effect is remarkably robust to the energy levels of reflections, which may imply that some form of inhibition is involved in this human ability. The model explores one

strategy for performing this inhibition and is able to simulate the Haas effect data.

PS - 169

Modeling Based Performance Evaluation of Sound Localization for Binaural CI-Listeners for Different Listening Environments

Christian Wirtz¹; Michele Nicoletti²; Peter Schleich³; Peter Nopp³; Werner Hemmert²

¹MED-EL Deutschland GmbH; ²Technische Universität München; ³MED-EL

Background

Originally intended for monaural use, CIs are nowadays implanted bilaterally in order to benefit from binaural cues and thus enabling sound localization. In the intact hearing system, interaural time differences (ITDs) account for the high spatial acuity especially in the low-frequency region of hearing. Where it is already known that CI users can utilize interaural level differences (ILDs), the focus in this work is to investigate how precise ITDs are coded in left- and right ear auditory-nerve responses.

Methods

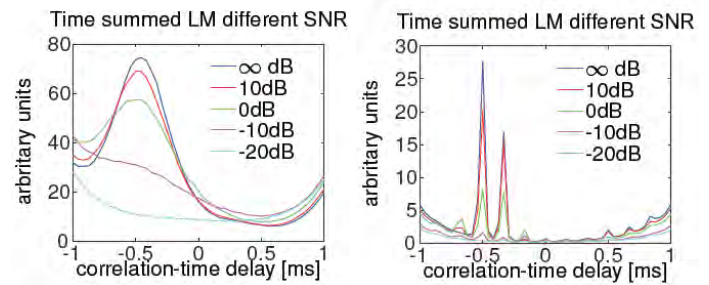
The binaural Lindemann model extends the correlation delay line of the Jeffress model by inhibitory elements, thus adding ILD-sensitivity. We have extended the Lindemann correlation model to process input from auditory nerve spike trains. Together with our large population model of the electrically excited auditory nerve, quantitative comparisons were achieved between different cochlear implant coding strategies and also normal hearing models. A simulated listening setup mimicked a circling loudspeaker by introducing engineered ITDs and ILDs. We emulated a cocktail party setting by studying the degradation of localization cues by adding uncorrelated uniformly exciting noise.

Results

- The CIS coding strategy did not provide useful ITD cues for sound localization, even in quiet.
- The temporal precision of the FS4 is sufficient to provide localization cues, although weaker than in the NH model.
- The robustness of ITD coding in FS4 and NH model were similar.

Conclusion

- We used the Lindemann model to evaluate localization cues of auditory models (normal hearing) and CI coding strategies.
- Whereas the CIS strategy did not provide useful ITD cues, today's latest coding strategies, as FS4 by MED-EL, are already able to convey some viable cues for sound source localization.
- The performance of FS4 under high background noise is remarkably close to the NH-listeners results



PS - 170

A Mechanism for Neural Coding of Sound-Source Distance: Experiment and Model

Duck Kim¹; Laurel Carney²; Brian Bishop¹; Shigeyuki Kuwada¹

¹University of Connecticut Health Center; ²University of Rochester

Background

Studies of neural coding of sound-source location have focused on azimuth and elevation. Consequently, little is known about the neural coding of sound-source distance. The goal here is to fill this knowledge gap.

Methods

Binaural-room impulse responses were measured with rabbits in an anechoic, a moderately- and a highly reverberant chamber. Virtual auditory space (VAS) stimuli were computed using the impulse responses. Distance from the rabbit to the sound source ranged from 10 to 160 cm. Extracellular single-unit discharges were recorded in the inferior colliculus (IC) of unanesthetized rabbits. The sound source was an octave-band noise centered at each neuron's best frequency. The stimulus level was normalized such that the level in the ear was approximately constant across distance.

We extended the neuron model for band-pass (BP) rate modulation transfer function (MTF) (Nelson and Carney, 2004) to obtain a band-reject (BR) model. BP and BR model neurons receive the same excitatory input from a lower brainstem neuron. The BR model neuron also receives inhibition from the BP model neuron. The same VAS stimuli were used for the models and rabbits.

Results

Here we present neural responses to VAS stimuli that were presented monaurally to the ear contralateral to the recording site. One class of IC neurons exhibits BP rate MTF and firing rate that increases monotonically with modulation depth for modulation frequencies around the peak. A mirror-image class of IC neurons exhibits BR rate MTF and decreasing firing rate with modulation depth. Acoustic analysis indicated that, in reverberation, modulation depth of an AM sound was reduced in the ear compared to that at the source. The amount of modulation loss increased with sound distance. We also found that a BP neuron's firing rate to AM sound in reverberation systematically decreased with distance whereas a BR neuron's firing rate increased with distance. In contrast, these neurons' firing rates remained approximately constant across distance when the sound source in reverberation was

unmodulated or in the anechoic environment, regardless of whether or not the sound source was modulated. The BP and BR models reproduced the experimental observations.

Conclusion

The firing rates of BP and BR rate MTF neurons systematically change with distance of AM sounds only in reverberation. This finding can be accounted for by a mechanism where the distance sensitivities are created by a combination of distance dependent acoustic modulation loss in reverberation and modulation-depth dependent firing rates of BP and BR neurons.

PS - 171

Modeling the Role of the Dorsal Cochlear Nucleus in Sagittal-Plane Localization of Human Listeners

Robert Baumgartner; Piotr Majdak; Bernhard Laback
Acoustics Research Institute, Austrian Academy of Sciences
Background

Human sound-source localization in sagittal planes, including front-back discrimination, relies on monaural spectral cues. These cues result from the acoustic filtering of incoming sounds by the torso, head, and pinna. Acoustic spectral features can be well described by head-related transfer functions (HRTFs), but it is still subject of investigations how those features are decoded by the auditory system. Recent physiological studies suggest that the dorsal cochlear nucleus (DCN) plays a crucial role in decoding spectral cues, however, its functionality has not been explicitly considered in existing models for sagittal-plane localization.

Methods

A probabilistic, phenomenological model is proposed, which considers the DCN functionality for sagittal-plane localization of human listeners. This template-based modeling approach aims at predictions beyond the midsagittal plane while accounting for acoustic and non-acoustic listener variability. The model directly outputs commonly used psychoacoustic performance parameters quantifying confusion rates, accuracy, and precision in sound localization. The predictive power of the model was tested under various experimental conditions. The effect of the DCN functionality on localization performance was investigated by comparing model predictions with and without the DCN stage to actual results obtained in previous localization experiments with band-limited (Majdak et al., 2013, JASA 134:2148) and spectrally rippled (Macpherson and Middlebrooks, 2003, JASA 114:430) noise bursts.

Results

The proposed model successfully predicted effects on localization performance of band limitation, spectral warping, non-individualized HRTFs, spectral resolution, spectral ripples, and high-frequency attenuation in speech. Correlation coefficients between listener-specific actual and predicted performances ranged from 0.7 to 0.9. Without the DCN stage, prediction errors for band limitation were at least twice as large compared to the model with the DCN stage. In particular, for the increase of spectral ripple density from 0.25 to 1

ripples/octave, the model without the DCN stage predicted a *decrease* of polar error rates of about 7%, whereas the model with the DCN stage predicted an *increase* of 21%, closer to the *increase* of 16% found in actual experiments.

Conclusion

In the proposed model for sagittal-plane localization, including the functionality of the DCN was shown to improve the predictive power. Improvements were shown particularly in case of macroscopic variations in the spectral shape of the stimulus.

PS - 172

A Novel Paradigm to Investigate Temporal Fine-Structure Processing

Christian Lorenzi¹; Enja Jung²; David Timothy Ives²; Stanley Sheft³

¹*Ecole normale supérieure*; ²*Dept d'Etudes Cognitives, Ecole normale supérieure*; ³*Communication Disorders & Sciences, Rush University Medical Center, Chicago, Illinois, 60612, USA*

Background

A wide range of evidence has been presented to support the idea that ageing and cochlear hearing loss impair the processing of temporal fine-structure (TFS) cues while sparing the processing of temporal envelope (E) cues. However, the reported temporal-processing deficits may partly result from reduced "processing efficiency". To address this issue, we designed a novel psychophysical task aiming to assess TFS-processing capacities indirectly through an interference task.

Methods

All stimuli were presented binaurally. The task was detection of low-rate sinusoidal amplitude modulation (SAM) of a high-frequency pure-tone carrier with the target stimulus always presented diotically. This task was performed in the presence of an "interfering" low-frequency pure tone that was either unmodulated or sinusoidally amplitude modulated at the same modulation rate as the target tone. This low-frequency tone was always presented against a bandpass noise masker centered on the tone (low-)frequency, and its audibility (and thus, the audibility of the superimposed SAM) was altered by changing interaural phase. It was reasoned that a small binaural masking level difference (BMLD) in the low-frequency region would result in reduced modulation detection interference (MDI) and thus, good SAM detection in the high-frequency region, whereas a large BMLD in the low-frequency region would result in strong MDI and thus, poor SAM detection in the high-frequency region.

Results

Pilot data collected on young and elderly normal-hearing listeners will be presented and discussed.

Conclusion

It was expected that elderly listeners should outperform young listeners in their ability to detect SAM in the high-frequency region, if ageing causes a genuine suprathreshold deficit in TFS encoding.

Modeling of Speech Localization in a Multitalker Mixture Using “Glimpsing” Models of Binaural Processing

Peter Toth¹; Angela Josupeit²; Norbert Kopco³; Volker Hohmann²

¹Charles University in Prague, Czech Republic; ²Medical Physics, Carl von Ossietzky Universität Oldenburg, Germany; ³Safarik University, Kosice, Slovakia

Background

A recent study measured the human ability to localize a speech target masked by a mixture of four talkers in a room [Kopco et al., JASA 127, 2010, 1450-7]. The presence of maskers resulted in increases in localization errors that depended on the spatial distribution of maskers, the target-to-masker energy ratio (TMR), and the listener's knowledge of the maskers' locations. The current study investigated the performance of two binaural auditory “glimpsing” models in simulated experimental conditions. The models were tested under the assumption that optimal information about the TMR in individual spectro-temporal glimpses is available, quantifying the ability of the models to encode spatial properties of complex acoustic scenes.

Methods

The framework for the modeling consisted of: 1. auditory preprocessing, 2. extraction of binaural cues, 3. identifying the “glimpses”, i.e., the spectro-temporal bins dominated by energy from only one source, 4. selecting target-related glimpses based on Ideal Binary Masks, and 5. estimating the target position. Two binaural models, one based on short-term running interaural coherence [Faller and Merimaa, JASA 116, 2004, 3075-89] and one on instantaneous interaural phase difference [Dietz et al., Speech Communication 23, 2011, 592-605] were modified and implemented. The stimuli were simulated by convolving speech tokens from the experiment with binaural room impulse responses recorded in a reverberant space similar to the experimental room.

Results

The two models produced similar predictions, both slightly worse than human performance. However, many trends in the data were captured by the models. E.g., the mean responses for lateral target locations were medially biased, the RMS errors were smallest for central target locations, and the overall performance varied with TMR. However, there were also qualitative differences. E.g., the models predicted best performance near the masker locations while humans were better at localizing targets far from the maskers.

Conclusion

The tested binaural models were able to capture several characteristics of human performance. Even though each model extracts binaural information in a different way, the model predictions were comparable, suggesting that the extracted features are equivalent and integrated in similar ways. The differences between the model predictions and human performance might be due to differences in interaural level difference processing, across-channel feature integration, or

the assumed method of combination of target and masker glimpses.

Optimal Prediction of Moving Sound Source Direction in the Owl

Brian Fischer; Weston Cox

Seattle University

Background

Capturing nature's statistical structure in behavioral responses is at the core of the ability to function adaptively in the environment. Sound localization is a critical skill for many species, involving both the localization of stationary sound sources as well as predicting the future location of a moving sound source. An outstanding open question in neural coding for sound localization includes how sensory cues are integrated over time to optimally guide behavior. We address this issue using the system that underlies sound localization in barn owls. The barn owl has been shown to generate localizing behaviors consistent with the prediction of the location of a moving source. Furthermore, it has been shown that the owl's sound localization for brief sounds is consistent with a Bayesian model. Here we address how a neural system can perform Bayesian prediction given sensory information and prior assumptions.

Methods

We first developed a Bayesian model of predictive localization of moving sound sources. The form of the model is determined by a model for the dynamics of the moving target and the statistical relationship between the direction of the target and the ITD observation. Next, we determined conditions on the neural representation of moving sources that allow the population vector to decode the Bayesian prediction.

Results

The work here shows that the population vector decoder will perform Bayesian prediction when the preferred direction of each neuron shifts in response to the target trajectory. Specifically, the model predicts that the amount of shift is proportional to target velocity, with faster speeds requiring greater shifts. The predicted shifts of preferred direction are shown to match the shifts observed in the owl's midbrain.

Conclusion

We find that the owl's localization behavior for moving sounds may be described as Bayesian inference. This work provides a theoretical description of optimal coding of sound localization for moving sources that may be tested in other systems. More generally, we show that neural populations can be specialized to represent the statistics of dynamic stimuli to allow for a vector read-out of Bayes-optimal predictions.

Neural Coding of Acoustic Temporal Fine Structure and Envelope: Psychophysiological Assessment of Peripheral Encoding on Sound Localization

Heath Jones; Tyler Churchill; Alan Kan; Ruth Litovsky
University of Wisconsin

Background

Bilateral cochlear implant (BiCI) users are considerably less accurate at localizing sound sources compared to normal hearing (NH) listeners. Presently, BiCIs only provide access to interaural time and level difference (ITD and ILD) cues retrieved from the acoustic envelope (ENV), but not the temporal fine structure (TFS) of incoming signals. Previous studies have demonstrated the importance of neural ENV encoding for monaural speech-in-noise reception. We extend these studies to sound localization by using non-vocoded and vocoded virtual acoustic space (VAS) stimuli to simulate BiCI listening in NH listeners. We hypothesized that the contributions of acoustic ENV and TFS to BiCI sound localization can be evaluated by correlating performance measures of NH listeners with neural outputs of a computational auditory nerve (AN) model for both stimuli sets.

Methods

NH subjects participated in a sound localization experiment using vocoded and non-vocoded stimuli. Head-related transfer functions were measured for each subject and used to generate VAS stimuli which were then processed using an 8-channel noise vocoder. The vocoded and non-vocoded stimuli were used as inputs to a computational AN model and the neural spike outputs were used to calculate measures of ENV and TFS encoding known as sumcor and difcor functions, respectively [Joris, P., *J. Neurosci.* 23(15):6345–6350(2003)]. ILDs were calculated from the neural spike outputs generated for left and right stimuli; whereas ITDs were calculated from the time delay of the sumcor and difcor maxima peak. The neural data were then correlated with the sound localization results.

Results

Localization errors were $9.5^{\circ} \pm 6.3^{\circ}$ in non-vocoded and $29.8^{\circ} \pm 18.5^{\circ}$ in vocoded conditions. AN modeling outputs of non-vocoded stimuli showed that neural TFS-ITDs change systematically with azimuth, but neural ENV-ITDs did not. No systematic change was observed for any ITDs calculated for the vocoded stimuli. ILDs provided consistent cues for both vocoded and non-vocoded stimuli. Model outputs correlated to listener's psychophysical performance could account for the increases in localization errors between the stimuli sets.

Conclusion

Our analysis showed that neural TFS coding contributed to sound localization performance, as expected; however, neural ENV did not provide an ITD cue that changed systematically as a function of azimuth. These findings suggest that ENV cues alone are not sufficient to produce NH sound localization. This has important implications for cochlear implants, which currently only provide ENV cues and suggest that by

not considering TFS-ITDs, the potential for accurate sound localization in BiCI users will remain limited.

Label-Free Quantitative Mass Spectrometry of Protein Expression in the Developing Cochlear Sensory Epithelium

Lancia Darville; Bernd Sokolowski

University of South Florida, Morsani College of Medicine

Background

The sensory epithelium of the inner ear converts the mechanical energy of sound to electro-chemical energy recognized by the central nervous system (CNS). To obtain insights into proteins involved in hearing, protein expression in the cochlear sensory epithelium was quantitatively compared between young and mature mice. There are commonly used techniques for quantitation such as isotope and fluorescent labeling; however, label free shotgun proteomics in conjunction with mass spectrometry provides a sensitive, rapid and reproducible technique for quantitatively comparing protein expression in biological samples.

Methods

Proteins were extracted and their concentrations measured from cochlear sensory epithelia of 14- and 30-day-old mice (P14 and P30). Three independent replicates were prepared from each age group. Samples were enzymatically digested and the peptide extracts fractionated by strong cation exchange (SCX). LC-MS/MS analysis was performed on an LTQ-Orbitrap mass spectrometer and MS/MS spectra obtained from each fraction were searched by MASCOT. Scaffold was used to validate peptide and protein identification and to calculate normalized spectral counts for relative quantification. A 2-fold change was used to determine biological regulation and the *t* test was used to determine significantly regulated proteins. Gene ontology (GO) classifications of the differentially expressed proteins were obtained using UniProt GO program.

Results

Our results show that 38 and 44 proteins were significantly up-regulated in P14 and P30 proteomes (>2 fold), respectively. Gene ontology classifications of proteins among the two age groups revealed that proteins with catalytic activity exhibited the largest decrease in expression from P14 to P30. A comparison of P14 and P30 proteomes using GO molecular function showed binding, catalytic, signal transducer, structural molecule activity, and transporter activity proteins are over-expressed on P14. More than 60% of the proteins that were up- or down-regulated in these proteomes were expressed in organelles and cytoplasm. Among the proteins up-regulated on P14, four and eight were expressed in the mitochondria and plasma membrane, respectively. In comparison, on P30, ten and ten proteins were expressed in these same regions, respectively.

Conclusion

Utilization of label-free quantitation led to the identification of proteins that are significantly regulated in the mouse cochlea

at different ages. These proteins may have biological significance to the development of hearing. However, the proteome from younger age mice, where hearing is not fully developed, needs further investigation.

PS - 177

FGF and Wnt Signaling Interactions During Otic Placode Induction

Kevin Wright; Amanda Mahoney Rogers; Katherine Shim
Medical College of Wisconsin

Background

In the mouse, Fibroblast Growth Factor (FGF) and Wnt signaling are required during induction of progenitor cells of the inner ear, or otic placode. However, it is not clear how these signaling pathways are coordinated to attain an otic placode that is the correct size. We have previously demonstrated that embryos with compound mutations in *Spry1* and *Spry2* (*Spry1*^{-/-}; *Spry2*^{-/-} mutants) have an enlarged otic placode due to increased response of tissue to FGF signaling. Furthermore, expression of *Wnt8a* in hindbrain adjacent to the otic placode was expanded in *Spry1*^{-/-}; *Spry2*^{-/-} mutant embryos. However, recent work suggests that inactivation of *Wnt8a* or both *Wnt8a* and *Wnt1* (*Wnt8a*^{-/-}; *Wnt1*^{-/-} mutants) result in no defect in otic placode formation (Vendrell et al. 2013 Mechanisms of Development 130,160-8). Thus, the functional significance of FGF/*Spry* regulation of *Wnt8a* expression during otic placode induction is unclear.

Methods

We have used a genetic approach in the mouse to determine whether Wnt signaling components are altered in *Spry1*^{-/-}; *Spry2*^{-/-} mutant embryos. These embryos are analyzed by *in situ* hybridization, immunohistochemistry, and histologically. In addition, we have generated induced pluripotent stem cells that allow for the tamoxifen-inducible inactivation of *Spry1* and *Spry2*.

Results

Expression of three other Wnt genes, *Wnt1*, *Wnt6*, and *Wnt3a*, which are expressed around the time of otic placode formation, was unchanged in *Spry1*^{-/-}; *Spry2*^{-/-} mutants compared to controls. To examine Wnt signaling activity in response to increased FGF signaling, we generated *Spry1*^{-/-}; *Spry2*^{-/-} mutant embryos carrying a TCF/Lef-lacZ reporter allele. We found that Wnt signaling activity was increased in double mutant embryos. To determine whether there is a functional relationship between FGF/*Spry* and Wnt signaling during otic placode induction, we determined whether reduction of gene dosage of the Wnt signaling effector, β -catenin, could rescue expansion of the otic placode observed in *Spry1*^{-/-}; *Spry2*^{-/-} mutants. At the time of otic placode formation, *Foxi2* is expressed in cranial epidermal and epibranchial placode cells, but is excluded from the otic placode. In approximately 50% of *Spry1*^{-/-}; *Spry2*^{-/-}; β -catenin^{+/+} embryos, the *Foxi2*-negative, otic placode was restored to the normal size. This suggests that reduction of β -catenin gene dosage can partially rescue the otic placode expansions observed in *Spry1*^{-/-}; *Spry2*^{-/-} mutant embryos.

Conclusion

These data suggest that FGF and Wnt signaling function cooperatively during induction of the otic placode. Preliminary *in vitro* data describing manipulation of FGF signaling during otic progenitor cell differentiation will also be presented.

PS - 178

Morphological Changes in the Auditory and Vestibular Systems of Transgenic Pax2-Islet1 Mice

Tetyana Chumak¹; Romana Bohuslavova²; Nicole Dodd²; Daniela Buckiova¹; Josef Syka¹; Gabriela Pavlinkova²

¹*Institute of Experimental Medicine AS CR*; ²*Institute of Biotechnology AS CR*

Background

Islet1 is a transcription factor expressed early in the otocyst in the regions that give rise to both sensory and neuronal lineages. To reveal its role we generated transgenic mice overexpressing Islet1 under the Pax2 promoter [Tg(Pax2-Islet1)] on the basis of the FVB strain. As we reported previously, hearing and vestibular functions of the mutant mice were impaired. In the present study, we examined in detail the morphology of the inner ear to identify the structural basis for the functional abnormalities.

Methods

ISL1 and PAX2 expression was examined in frozen sections of E10.5 embryos and postnatal cerebellum. The inner ears were processed as either paraffin sections (for spiral, vestibular ganglion and vestibular epithelium analysis) or surface preparations (for studying the cochlear anatomy). To analyze the morphology of the inner ear in Tg(Pax2-Islet1) and wild type (WT) littermates the following immunocytochemical markers were used: calretinin, phalloidin, anti-myosin 7a, anti-CtBP2, anti-prestin, anti-NF200 and anti-ChAT. The number of spiral ganglion neurons, outer hair cells (OHC) and inner ear ribbon synapses was counted in both groups of animals.

Results

Visible underdevelopment of the cerebellum during postnatal development was found in Tg(Pax2-Islet1) mice compared to littermate controls. While an enlarged otic ganglion was noticed in transgenic E10.5 embryos, the number of neurons in the spiral ganglia in all cochlear turns was lower in Tg(Pax2-Islet1) than in WT animals in the postnatal period. The number of vestibular ganglion cells was not significantly decreased in Tg(Pax2-Islet1) compared to WT mice. A decreased number of calretinin-labeled cells was detected in the vestibular ganglion and in the spiral ganglion in Tg(Pax2-Islet1) compared to WT. Furthermore, decreased calretinin labeling was found in vestibular epithelial cells of Tg(Pax2-Islet1) mice compared to WT. In both groups of animals, a moderate age-related loss of outer hair cells was noticed, predominantly in the high frequency part of the cochlea.

Conclusion

Our data suggest that transgenic *Is1* overexpression under the Pax2 promoter in the inner ear progenitor cells leads to

pronounced morphological and functional impairments of hearing and vestibular organs.

PS - 179

Tracing Sox10-Expressing Cells Elucidates the Dynamic Development of the Mouse Inner Ear

Takanori Wakaoka; Tsutomu Motohashi; Hisamitsu Hayashi; Bunya Kuze; Mitsuhiro Aoki; Keisuke Mizuta; Takahiro Kunisada; Yatsuji Ito
Gifu University

Background

The inner ear is constituted by cochlear and vestibular compartments, which are generated from the otic vesicle, an embryonic structure of ectodermal origin. Although the development of the inner ear has been analyzed using various techniques, the developmental processes have not been fully elucidated because of the intricate nature of the structure. We previously generated a Sox10-IRES-Venus mouse designed to express green fluorescent protein under the control of the *Sox10* promoter. Sox10 is specifically expressed in both neural crest cells and the inner ear epithelium. In the present study, we used the Sox10-IRES-Venus mouse to investigate the Sox10 expression throughout the development of the inner ear.

Methods

Sox10-IRES-Venus mice have a gene encoding a fluorescent protein (Venus, a GFP variant) downstream of the transcription factor Sox10, under the control of the internal ribosomal entry site (IRES) (Motohashi, et al., 2011).

The images of unfixed whole embryos and extirpated inner ears were taken immediately after dissection, and were examined using an Olympus SZX7 fluorescence stereomicroscope. For the histological and immunohistochemical analyses of the inner ear, we made transverse sections of the embryonic inner ear, and examined them using a confocal microscope (Olympus Fluoview FV1000).

Results

The invaginating otic placode clearly expressed Sox10 at embryonic day 9.0 (E9.0). After the invagination, the fused placode and newly-formed otic vesicle expressed Sox10. Sox10 was continuously expressed throughout the inner ear formation. We visualized the morphogenesis of the inner ears until postnatal day 1 in unfixed specimens.

We analyzed the Sox10-expressing cells in the developing inner ear using transverse sections of the embryonic inner ear. Although all mature inner ear epithelia expressed Sox10, the hair cells and mesenchymal cells did not. However, some hair cells which corresponded to immature hair cells in the developing inner ear expressed Sox10. Furthermore, we found that scattered Sox10-expressing cells existed around the otic vesicle at E10.5, some of which had pigmentation in the stria vascularis at E16.5, thus suggesting that they were neural crest cell-derived melanocytes.

Conclusion

We showed that the Sox10-IRES-Venus mouse enabled the non-destructive visualization and understanding of the morphogenesis during the development of the inner ear. Further analyses of the Sox10-expressing cells using the Sox10-IRES-Venus mice may improve the understanding of the development of the inner ear.

PS - 180

Analysis of Transcription Factor Mediated Organ of Corti Cell Fate Changes Help in Understanding the Specific Pattern of Innervation

Isra Jafari, Ning Pan; Jennifer Kersigo; Bernd Fritzsch
University of Iowa

Background

Basic helix loop helix transcription factors are crucial for inner ear neurosensory development: Atoh1 regulates the differentiation of hair cells (HCs) and Neurog1 and Neurod1 regulate specification and differentiation of neurons, respectively. Expression of Delta and Jagged ligands in HCs and Notch receptors in supporting cells (SCs) guides supporting cell differentiation. In addition, diffusible factors from hair cells and other sources consolidate topologically correct differentiation. Hearing defects in human can result in irreversible loss of HCs and SCs. Reconstitution of organ of Corti (OC) requires topologically correct organization of the two types of HCs, inner (IHC) and outer (OHC) hair cells, as well as several types of SCs. How specific cell types differentiate in the right location is unknown.

Methods

We studied several mutant mouse models to investigate how dose and intensity variation of Atoh1 can alter HC type specification.

Results

Deletion of the bHLH gene *Neurod1* results in the premature, aberrant expression of *Atoh1*. Loss of *Neurod1* also results in the conversion of some OHCs into IHCs. Combining *Neurod1* conditional null mouse with haploinsufficiency of Atoh1 or with misexpression of *Neurog1*, we show normalization of OHC development instead of ectopic IHCs, indicating that indeed levels of *Atoh1* expression is important. Even more interesting, IHCs loss in the 'self-terminating' *Atoh1-Cre Atoh1* null mice is rescued if *Neurog1* is expressed in one *Atoh1* allele. This data support the notion that *Neurog1* has some *Atoh1*-like signaling capacity but only if *Atoh1* protein is at least transiently co-expressed. Precise dose and duration of *Atoh1* specifies distinct types of HCs and *Neurog1* misexpression in *Atoh1* locus improves overall HC survival and specifically rescues IHCs type.

Molecular modifications of HCs also affect innervation. Proper sorting of type I and II afferent fibers follow type and topology of specific HCs. In cases of ectopic IHCs in the topology of OHCs, type I fibers outreach to these IHCs in altered position (in *Neurod1* conditional null mutants) whereas in the absence of IHCs all fibers will innervate OHCs if they cannot divert to

nearby IHCs due to increased distances to the nearest IHCs ('self-terminating' *Atoh1-Cre Atoh1* null mice).

Conclusion

Understanding the dosage and cross-regulation of these transcription factors, in regulating specific types of HC development and their specific fiber sorting mechanism will provide useful information for the future attempts to restore hearing through topological correct HC differentiation and proper innervation.

PS - 181

Atoh1 Enhance the Expression of Pou4f3 and Gfi1 During Mouse ES Cell Differentiation

Hyong-Ho Cho¹; Sungsu Lee²; Young-Ho Choi²; Yong-Beom Cho¹

¹Chonnam National University Medical School; ²Chonnam National University Hospital

Background

Atoh1 (also known as Math1) is considered to be essential for differentiation and regeneration of inner ear hair cells. However, its effects on hair cell differentiation of ES cells have not been well known. In this study, we investigated the effects of Atoh1 overexpression on the expression of hair cell related gene (Pou4f3 and Gfi1) during mouse ES cell differentiation.

Methods

ES cells carrying Tet-inducible Atoh1, Atoh1-ES cells, were generated using a flag tagged Atoh1 gene inserted Tet inducible p2Lox plasmid which was co-transfected with pSALK-Cre into the A172LoxP ES cell line using Lipofectamine 2000. For investigating the effects of Atoh1 gene overexpression, we used two different condition. One is monolayer culture the other is embryoid bodies(EB) formation. In monolayer culture, Atoh1-ES cells were cultured for 4 days with or without 2ug/mL of Doxycycline (Dox). In EB condition, EB formed in the absence of Dox for 3 days and they were cultured for an additional 6 days with or without 2ug/mL of Dox. For expression analysis of hair cell related genes (Pou4f3 and Gfi1), we used RT-PCR analysis and immunocytochemistry.

Results

Dox-dependent induction of FLAG-Atoh1 was confirmed by RT-PCR and Western blotting and immunohistochemical analyses using α -FLAG antibodies. In two different conditions, the level of mRNA for Atoh1 after exposure to Dox was highly expressed. Also, expression level of Pou4f3 and Gfi1 was elevated after Dox treatment in the two different conditions. The appearance of EB outgrowths cultured in the presence of Dox was more neural differentiated appearance than the absence of Dox.

Conclusion

Atoh1 may be an important factor for induction of hair cell related gene from differentiating ES cells. Also, using Atoh1-ES cells, we could address the mechanism of the Atoh1 gene on the developing inner ear hair cells.

PS - 182

In Vivo Overactivation of Notch Signaling Pathway in Developing Cochlear Epithelium

Tomoko Tateya¹; Itaru Imayoshi¹; Ichiro Tateya²; Ryoichiro Kageyama¹

¹Institute for Virus Research, Kyoto University; ²Department of Otolaryngology - Head and Neck Surgery, Kyoto University Graduate School of Medicine

Background

A specialized sensory epithelium of the cochlea of the mammalian inner ear, called the organ of Corti, contains sensory hair cells and non-sensory supporting cells. During development, the prosensory domain is formed in the floor of the cochlear duct, and then hair cells and supporting cells differentiate from common prosensory precursor cells. The mechanism of the alternate hair cell and supporting cell formation has been extensively analyzed, and it has been shown that Notch-mediated lateral inhibition plays an important role in this process. It is well established that inhibition of the Notch signaling pathway in prosensory cells results in excessive hair cell formation. It was also demonstrated that activation of the Notch signaling pathway by overexpression of activated Notch1 (NICD) in the cochlear epithelium resulted in ectopic sensory patches where NICD was expressed. However, the effect of Notch activation on the alignment of hair cells and supporting cells in the organ of Corti is not fully understood.

Methods

We used the conditional NICD expressing transgenic mice, and analyzed cochlear hair cells and supporting cells at E17.5 and E18.5.

Results

The conditional NICD cochleae were short. Hair cell number reduced especially in apical turn though hair cells developed where NICD was overexpressed. Ectopic expression of Hes1, Hey1, Hey2 and HeyL was seen where NICD was overexpressed in cochlear epithelium. Ectopic expression of p27Kip1, Hes5 and Prox1 was not observed. Hes5- and Prox1-positive supporting cells were only present around hair cells, and reduced in apical turn.

Conclusion

In summary, our data shows that NICD overexpression *in vivo* delays the differentiation of both hair cells and supporting cells in the cochlea. Our results indicate that factors other than Notch signaling may also regulate the differentiation of hair cells and supporting cells.

Mutation of ELMOD1 Disrupts Stereocilia and Cuticular Plate Development in Vestibular Hair Cells

Jocelyn Krey¹; Rachel Dumont¹; Kenneth Johnson²; Peter Barr-Gillespie¹

¹Oregon Health & Science University; ²The Jackson Laboratory

Background

The ELMO domain-containing protein family (ELMODs) consists of six paralogs in mammals, two of which (ELMOD1 and ELMOD2) have been shown to be novel Arf family GTPase-activating proteins. Mutations in ELMOD1 have recently been linked to deafness and vestibular dysfunction in mice. The roundabout (*rda*) mutation is a deletion in the *Elmod1* gene that results in loss of ELMOD1 protein expression. After postnatal day 7 (P7), *rda/rda* mice develop cochlear hair cell abnormalities, including fusions and elongations of inner hair cell stereocilia and degradation of outer hair cell stereocilia. The effects of the *rda* mutation on vestibular hair cell (VHC) development, however, have not been studied.

Methods

We examined ELMOD1 in mouse VHCs by immunoblotting, confocal immunocytochemistry, and transmission electron microscopy (TEM) in utricles from wild-type and *rda/rda* mice.

Results

ELMOD1 was detected in the utricle as early as embryonic day 18 (E18), and showed peak levels of expression from P7 to P21. By confocal immunocytochemistry, we found that ELMOD1 was expressed in the cell body and hair bundle of VHCs between P5 and P12. In P21 mice, ELMOD1 expression was most intense within the cuticular plate and was difficult to detect within the hair bundle. Phalloidin-labeled utricles from P12 and P21 *rda/rda* mice contained fused and elongated stereocilia, similar to those seen in cochlear hair cells from *rda/rda* mice. At P5 and P7, stereocilia of *rda/rda* VHCs appeared normal, however, apical surfaces were slightly protruded and there were gaps within the cuticular plate actin mesh. These gaps became larger in P12 and P21 VHCs, and were also detected in inner hair cells from P12 *rda/rda* mice. TEM imaging of P12 utricles from *rda/rda* mice confirmed extensive degradation of the cuticular plate and protrusion of microtubules, mitochondria, and vesicles towards the apical surface. Mitochondria and vesicles were also found within the fused stereocilia. At P5, prior to stereocilia fusion, TEM imaging revealed a lifting of the apical membrane as well as an increased amount of vesicles and endosome-like structures within the cuticular plate.

Conclusion

ELMOD1 is expressed in VHCs during postnatal development, and loss of ELMOD1 results in protrusion of the apical surface, degradation of the cuticular plate, and fusion and elongation of vestibular stereocilia. The progression of these defects suggests that ELMOD1 may play a role in regulating membrane trafficking or microtubule dynamics, in addition to its possible function as an actin-regulatory protein.

The Meckel Gruber Syndrome Protein TMEM67/Meckelin Regulates Basal Body Planar Polarization and Ciliogenesis in the Organ of Corti

Dan Jagger¹; Zakia Abdelhamed²; Colin Johnson²

¹UCL Ear Institute, University College London; ²Ciliopathy Research Group, University of Leeds

Background

Meckel Gruber Syndrome (MKS) is the most severe ciliopathy, and is a lethal recessive neurodevelopmental condition with additional cardiovascular, renal and hepatic phenotypes. Mutations in the *TMEM67/MKS3* gene, which codes for the Frizzled-like transmembrane receptor TMEM67/Meckelin, are the most common cause of MKS. As other ciliopathy genes are important regulators of hair cell planar polarity (Ross et al, Nature Genetics 2005; Jagger et al, Human Molecular Genetics 2011), we investigated the localization of TMEM67/Meckelin, and cochlear morphogenesis in the *Tmem67tm1(Dgen/H)* knockout mouse (*Tmem67*^{-/-}, Abdelhamed et al, Human Molecular Genetics 2013).

Methods

Cochleae were dissected from *Tmem67*^{-/-} and wild-type littermate controls, and fixed in 2% paraformaldehyde (PFA) for 20 minutes (immunofluorescence) or 4% PFA for 2 hours (morphogenesis studies). TMEM67/meckelin was localized using a rabbit polyclonal antibody (Adams et al, Human Molecular Genetics 2012; 1:100), ciliary axonemes were detected using a mouse monoclonal anti-acetylated- α -tubulin antibody (Sigma; 1:1000), and ciliary basal bodies were detected using a rabbit anti-ALMS1 polyclonal antibody (Jagger et al, 2011; 1:200). Stereociliary bundles were detected using fluorescent phalloidin (1:1000).

Results

TMEM67/Meckelin was immunolocalized to the ciliary transition zone in postnatal hair cells and supporting cells. At P0, *Tmem67*^{-/-} and wild-type cochleae were comparable in size, sensory epithelial length, and hair cell numbers. However, there were orientation defects of *Tmem67*^{-/-} stereociliary bundles along the whole length of the organ of Corti, and these were most prevalent in outer hair cells (OHC) of the basal turn region. Supporting cells in the basal region were largely devoid of primary cilia. Basal body position was often uncoupled from bundle orientation, suggesting a functional disconnect between kinocilia and stereocilia during bundle formation. Basal body mis-positioning was evident as early as E15.5, as the bundle first appears at the OHC apical surface.

Conclusion

Our results suggest that in common with other ciliopathy proteins, TMEM67/Meckelin plays important roles during cochlear ontogeny. These include regulation of planar cell polarity (PCP) and ciliogenesis. The defects in hair cell morphogenesis appear distinct from those in core PCP gene mutants (eg *Vangl2*; Montcouquiol et al; Nature 2003), but more closely resemble observations in *Kif3a* mutants where bundle orien-

tation uncouples from basal body position (Sipe & Lu, Development 2011). The affected signaling mechanism, which presumably lies downstream of this Frizzled-like receptor, is being further investigated.

PS - 185

Differential Small RNA Expression in Hair Cells of *Dgcr8* and *Dicer1* Conditional Knockout Mice.

Isha Dewan; Marsha Pierce; Colby Bradfield; Sharalyn Steenson; Garrett Soukup
Creighton University

Background

Small RNAs including endogenous small interfering RNAs (siRNAs) and canonical microRNAs (miRNAs) transcriptionally and post-transcriptionally regulate gene expression, respectively. Canonical miRNA processing requires proteins encoded by both *Dgcr8* and *Dicer1*, whereas siRNA processing requires only *Dicer1*. Conditional knockout (CKO) of *Dgcr8* versus *Dicer1* has different effects on hair cell development and maintenance, where *Dgcr8* CKO causes earlier hair cell demise. Therefore, depletion of miRNAs appears to be more detrimental to hair cells than depletion of both siRNAs and miRNAs. One possible explanation is that miRNA depletion brings about an imbalance in siRNAs that exacerbates the hair cell phenotype.

Methods

Hair cell-specific *Dgcr8* CKO and *Dicer1* CKO mice were generated using *Atoh1-Cre* to examine small RNA content in the inner ear by high-throughput sequencing. Total RNA was isolated from inner ear of two biological replicates from each of three groups including *Dgcr8* CKO, *Dicer1* CKO, and control (lacking *Atoh1-Cre*). Illumina small RNA sequencing was performed to identify mappable reads that differ in abundance between groups.

Results

Atoh1-Cre mediated *Dicer1* CKO results in little or no hair cell loss or stereocilia aberrations in mouse cochlea up to two weeks old. However, *Dgcr8* CKO hair cells show disorganized stereocilia and some hair cell loss in the base of the cochlea from one to two weeks old. To address how miRNA depletion effects siRNAs in *Dgcr8* CKO mouse inner ear compared to *Dicer1* CKO inner ear, small RNA sequencing was performed at two weeks of age. Results from the analysis are pending.

Conclusion

Depletion of miRNAs with *Dgcr8* CKO versus depletion of both siRNAs and miRNAs with *Dicer1* CKO leads to earlier hair cell defects and death. This observation suggests that perturbing the balance of small RNA function in hair cells can have adverse effects, and it highlights a possible caveat to the use of small RNAs as therapeutic agents. Examining the small RNA content of these models is expected to lead to a better understanding of small RNAs, target genes, and target processes that are involved in hair cell development and maintenance.

PS - 186

Rho GTPase Cdc42 Regulates Patterning and Polarization of Hair Cells in the Embryonic Organ of Corti

Anna Kirjavainen; Ulla Pirvola

University of Helsinki, Institute of Biotechnology

Background

Embryonic development of epithelial cells of the organ of Corti is characterized by cell polarization, establishment and modulation of actin and microtubule cytoskeletons and formation and rearrangement of intercellular junctions. In addition to apico-basal polarity, cells of the organ of Corti exhibit planar cell polarity (PCP), defined by the orientation of cells within the plane of the sensory epithelium. The most visible readout of PCP is the uniform orientation of the hair cell stereociliary bundles. Cdc42, a Rho GTPase family member, regulates cytoskeletal dynamics, cell polarity and junctional integrity of epithelial cells. Rho GTPases are thought to integrate signals from different signalling pathways to promote morphological and transcriptional changes that affect the behaviour of developing cells. We have found Cdc42 expression in the developing organ of Corti and in our prior study revealed its important role in auditory supporting cells during postnatal maturation (Anttonen, Kirjavainen et al., Sci Rep, 2012). In the present study, we were interested in Cdc42's role during embryonic development of the auditory sensory epithelium.

Methods

In order to study the role of Cdc42 *in vivo*, we used tamoxifen-inducible *Fgfr3-iCre-ER^{T2}* mouse line crossed with *Cdc42^{loxP}* mice to inactivate Cdc42 in outer hair cells and supporting cells during late-embryogenesis. Recombination characteristics were studied by crossing *Fgfr3-iCre-ER^{T2}* mice with the *Ai14(tdTomato)* reporter mouse line. Cdc42 was inactivated between E13 and E14, i.e. after the formation of the progenitor cell population but before the onset of cell type-specific differentiation programmes

Results

We found that Cdc42 inactivation leads to patterning defects of the auditory sensory epithelium, most distinctly to polarity defects in hair cells. The organ of Corti showed a PCP phenotype, based on random orientation of the stereociliary bundles of outer hair cells. In addition, hair cells showed impaired hair bundle morphology and misplacement of the kinocilium. PCP defects were accompanied by defects in outer hair cell shapes. However, global development of the cochlea was unaffected, including unaffected convergent extension of the OC.

Conclusion

Our data suggest that Cdc42 acts downstream or parallel of core PCP components to regulate the establishment of polarity of outer hair cells. In addition, Cdc42 regulates patterning of epithelial cells of the organ of Corti and shape formation of hair cells.

Effects of Growth Hormone (GH) and GH Antagonist on Zebrafish Auditory Hair Cell Regeneration

Amy Ni; **David Monroe**; Michael Smith
Western Kentucky University

Background

A previous microarray study showed that growth hormone (GH) was significantly regulated in the zebrafish inner ear following acoustical trauma. Subsequent research found that GH improves auditory hair cell regeneration when injected intraperitoneally in zebrafish post-sound exposure. The purpose of this study was to use a GH antagonist to examine whether GH is necessary for auditory hair cell regeneration.

Methods

Three groups of six zebrafish were injected intraperitoneally with either GH, phosphate buffer, or GH antagonist. Immediately following the injection, auditory hair cell damage was induced through exposure to acoustic overstimulation (150 Hz tone at 179 dB re 1 μ Pa) for 40 hours. Hearing tests were performed on the fish immediately after the exposure and at 1–5 days post-trauma via auditory evoked potential (AEP) recordings. Following AEP, fish ears were dissected and fixed overnight in 4% paraformaldehyde. Dissected zebrafish sacculi were then subjected to fluorescein-conjugated phalloidin staining, TUNEL-labeling, and BrdU-labeling to quantify hair cell bundle densities, cell death, and cell proliferation, respectively. The sacculi were whole mounted and visualized under fluorescence microscopy.

Results

Hearing thresholds of GH-injected fish were significantly lower than controls at 2 and 3 days post-trauma ($P < 0.05$). In contrast, hearing thresholds of GH antagonist fish were significantly higher than controls at days 3–5 post-trauma ($P < 0.05$). Similarly, GH-injected fish had greater hair cell bundle densities than controls at days 1–3 post-trauma, while GH antagonist-injected fish exhibited reduced hair cell bundle densities compared to controls at day 3 post-trauma ($P < 0.05$). The effects of GH and GH antagonist on temporal patterns in cell death (TUNEL) and cell proliferation (BrdU) will also be presented.

Conclusion

While GH has a positive effect on hearing and hair cell regeneration following acoustic trauma, our results show that GH antagonist has the opposite effect, with higher hearing thresholds and lower hair cell bundle densities than controls. Interestingly, the negative effects of the GH antagonist are delayed 1–2 days relative to the positive effects of GH. While the cause of this delay is currently unclear, it may be related to the binding kinetics of the GH antagonist to GH receptors.

Targeted Mutagenesis for Zebrafish Inner Ear (S100s) Using Transcription Activator-Like Effector Nucleases (TALENs)

In Seok Moon; **Jin Young Seo**; Jae Young Choi
Yonsei University College of Medicine

Background

Transcription Activator-Like Effector Nucleases (TALENs) are artificial restriction enzymes that can be programmed to recognize a pre-determined target locus on genome. Recent advances in genome engineering using TALENs have enabled the creation of targeted gene knockout mutations in zebrafish. We tried to make S100s targeted mutagenesis using TALENs.

Methods

Whole mount in situ hybridization for S100s was performed for verification.

TALEN target sites for S100s were designed using the web-tool TALEN-NT. TALEN expression vectors were constructed using the 'Unit Assembly' method with Sharkey-AS and Sharkey-R forms of FokI cleavage domains. Vectors were linearized by NotI and used as templates for TALEN mRNA synthesis. The dosage showing the highest efficiency and acceptable cytotoxicity was determined by co-injecting two pairs of TALEN mRNAs to one cell stage embryos.

To analyze the deletions induced by TALENs, injected and morphologically normal embryos at 24 hpf (hours post-fertilization) were collected and genomic DNA were prepared for PCR template. Using PCR, the deletions were detected. After several months, tail of founder fishes (>3 months of life) were clipped and same analysis using PCR was performed and rate of transmission to F1 fishes was also investigated.

Results

S100s protein was manifested in the inner ear and lateral line hair cells in whole mount in situ hybridization. Co-injection of the mRNA mixture of the two pairs of TALENs exhibited acceptable toxicity, with more than 50% of injected animals surviving to 3 days of life.

Specific digestion of a S100s gene by TALENs results in the introduction of frame-shift mutations (small insertions and deletions). Deletion events for S100s between the two target sites were detected by PCR in 24 hpf embryos, in which the left half of the first TALEN site (85bp) and the right half of the last TALEN site (350bp). Surviving embryos were grown to adulthood. Of 16 tested founder fish, four showed stable germ line transmission of the distal deletion to F1 fish.

Conclusion

It is the first targeted mutagenesis for zebrafish inner ear and lateral line hair cells, and can be used for study in hair cell regeneration or rescue.

Regulation of Hair Cell Fate: Transcription Factor Combinations and Epigenetics

Ryouchichi Ikeda; Kwang Pak; Eduardo Chavez; Allen F Ryan
UCSD

Background

Expression of Atoh1 in the inner ear is thought to be the earliest determinant of HC fate. Absence of Atoh1 results in a complete loss of both HCs and SCs, and forced over expression of Atoh1 in non sensory cells induces ectopic HCs. However, Atoh1 induces alternative cell fates in tissues outside the inner ear. How Atoh1 determines HC fate is not yet clear. Cell lineages are determined by many factors, including the presence and activity of TFs, cell signaling networks, and epigenetic mechanisms. We investigated TF and epigenetic contributions to Atoh1 induction of HCs.

Methods

We used bioinformatics to identify conserved TF binding sites. Electroporation was employed to transfect neonatal mouse sensory epithelium with TF expression plasmids, with or without epigenetic inhibitors.

Results

We identified TFs that have highly conserved binding sites near sites for Atoh1 on the *pou4f3* gene, an early regulatory 25 target of Atoh1 in HCs. Each of these was co-transfected into the greater epithelial ridge (GER) with Atoh1. Out of the 25 TFs, we identified 5 that enhanced the ability of Atoh1 to induce a HC phenotype, and 3 that reduce the effects of Atoh1. Epigenetic modifications of DNA and/ or histones serve to regulate gene expression by altering access of TFs to DNA. To test the hypothesis that epigenetic changes to target DNA may control the ability of Atoh1 to promote inducing ectopic HCs, we evaluated the effects of DNA methylation inhibitors (5-Aza, zebularine and BIX01294) and histone deacetylation (HDAC) inhibitors (TSA and VPA) on neonatal sensory epithelia transfected with Atoh1. We found that both HDAC inhibitors were ototoxic at the highest dose tested. Non-toxic doses of HDAC's and all tested doses of methylation inhibitors had no influence on Atoh1 HC induction.

Conclusion

The results suggest that TF combinational coding is a more important determinant of HC fate than epigenetic regulation of Atoh1 binding, in the early postnatal mouse sensory epithelium.

Fate-Mapping Supporting Cells in Damaged Organ of Corti

Elizabeth Oesterle¹; Joerg Waldhaus²; Irina Omelchenko¹; Albert Edge³; Edwin Rubel¹; Stefan Heller²

¹University of Washington; ²Stanford University; ³Harvard University

Background

Replacing cells in the cochlea depends on an ability to produce new sensory cells from cells that remain in a deafened

ear. We are characterizing cells that remain in the mouse cochlea after a variety of damage protocols anticipating this will help towards devising ways to use these cells as a starting point for hair cell regeneration. At last year's ARO meeting, we reported that: 1) Differentiated supporting cells can survive despite total hair cell loss and retain some cellular identity in transgenic mice (expressing diphtheria toxin receptor under control of the hair cell-specific promoter *pou4f3*) injected with diphtheria toxin to kill hair cells, and 2) Sulcus cells may migrate into the region formerly occupied by the organ of Corti in mice damaged by aminoglycoside/loop diuretic injection. We extended these studies this past year using fate-mapping technologies to more definitively assess supporting cell survival after aminoglycoside-induced damage.

Methods

To assess the fate of supporting cells after drug damage, adolescent (P19) *Fgfr3-CreERT2*^{+/-}, *Stop-TM*^{+/-} mice were injected with tamoxifen prior to sisomicin/furosemide injection at P21. Mice were killed 6wks later, and whole-mount preparations of the organ of Corti were immunohistochemically processed using supporting cell (acetylated tubulin, Sox2), hair cell (myosin 6), or sulcus cell markers (CD44). Remaining fate-tracked cells were FACS-sorted at various time points after damage and analyzed with a multiplex qRT-PCR system for changes in expression of 96 genes of relevance for inner ear cell identity and signaling pathways.

Results

In controls induced with tamoxifen, but not injected with aminoglycoside, tdTomato expression is seen in the vast majority of pillar and Deiters' cells, with rare expression in Hensen and Claudius cells. Six weeks after sisomicin/furosemide injection, inner hair cells (IHCs) remain throughout the ear, with small patches of IHCs missing in mid, base, and hook regions. Outer hair cells remain in the apex only. Fate-mapped supporting cells (tdTomato⁺) exist throughout the cochlea but are missing entirely in small regions in the mid, base, and hook that miss IHCs. Cells in these regions express CD44, but not Sox2 or acetylated tubulin. Small regions with few remaining fate-mapped (tdTomato⁺) supporting cells, no hair cells, and some CD44 labeling may be progressing towards a flat epithelium state. Initial analysis of the qRT-PCR results will be presented.

Conclusion

After drug-induced damage, pillar and Deiters' cells can die off in regions with complete hair cell loss, and sulcus cells may migrate into the region.

Gene Expression Profiling of Neonatal Mouse Supporting Cells by Next Generation Sequencing

Juan Maass¹; Joanna Asprer²; Martin Basch²; Ying-Wooi Wan²; Zhandong Liu²; Andrew Groves²

¹Hospital Clinico Universidad de Chile, Santiago, Chile
 Clinica Alemana de Santiago, Facultad de Medicina Clinica Alemana-Universidad del Desarrollo, Santiago, Chile;

²Baylor College of Medicine

Background

Hair cell regeneration in non-mammalian vertebrates occurs by the transdifferentiation and division of supporting cells. Mouse supporting cells from neonatal mice also have a transient ability to divide and transdifferentiate into hair cells in culture. However, after early post natal development, there is a progressive decrease in the regenerative response. Therefore, it is important to understand the changes in supporting cell gene expression that occur during this developmental period.

Methods

We have analyzed the mouse supporting cell transcriptome by next generation sequencing of total mRNA obtained at different stages during the early postnatal period. We sorted EGFP+ and EGFP- cells dissociated from micro-dissected neonatal Lfng-EGFP transgenic mouse whole cochlear explants at P1 and P6. We increased the accuracy of the sorting method by selecting the population of cells with the highest Lfng + expression and confirming supporting cell gene enrichment using qPCR. We prepared cDNA libraries using a Truseq kit (Illumina) and sequenced the samples on a HiSeq2000 (Illumina). We mapped the reads to the genome using Tophat. Then we analyzed the differential gene expression between the samples using two distinct software programs: Cufflinks and DESeq.

Results

We obtained two distinct sets of differentially expressed genes (DEG) and, we prepared a list of consensus DEG present in both outputs for every comparison we made. The accuracy of the lists was checked with a list of known supporting cell genes and after confirming by a gene ontology analysis (DAVID and REVIGO), we analyzed the presence of pathways and biological processes also related to supporting cell physiology.

Conclusion

Through this approach we obtained a longer list of potential SC genes, but also and more importantly, lists of genes and pathways that could underlie the differences and changes in supporting cell gene expression and the decrease in regenerative response shown in the postnatal mouse cochlea.

Ablation of Different Quantities of Hair Cells in the Neonatal Mouse Cochlea to Examine Mechanisms of Regeneration

Michelle Randle¹; Jian Zuo²; Brandon Cox¹

¹Southern Illinois University School of Medicine; ²St. Jude Children's Research Hospital

Background

Pancreatic beta cells regenerate via different mechanisms depending on their initial amount of death (Thorel et al., 2010 *Nature*; Nir et al., 2007 *J Clin Invest*). Our lab recently found that neonatal mice are capable of regenerating cochlear hair cells (HCs) after damage. In this model where ~80% of HCs are damaged, we have evidence of two mechanisms of HC regeneration. Supporting cells either underwent direct transdifferentiation or mitotic regeneration to produce new HCs (Cox et al., in revision). We hypothesize that HCs will regenerate using different mechanisms when the HC ablation model is modified to kill 50%, 25%, or 10% of HCs.

Methods

Atoh1-CreERTM is specifically expressed in HCs when tamoxifen is given at neonatal ages. The commonly used ROSA-26^{LacZ} reporter allele was used to measure the number of Cre+ HCs when different dosages of tamoxifen were given. Once we established a tamoxifen induction paradigm that targets 50%, 25%, and 10% of HCs, we used it in a similar mouse model (Atoh1-CreERTM; ROSA26^{DTA}) that kills HCs by forced expression of diphtheria toxin, fragment A (DTA). To fate map supporting cells, we introduced the Hes5-nlsLacZ allele into the Atoh1-CreERTM; ROSA26^{DTA} mouse since Hes5-nlsLacZ has LacZ expression in Deiters' cells, outer pillar cells, and inner phalangeal cells at neonatal ages (Cox et al., in revision) and analyzed samples at postnatal day (P) 2. To detect mitotic regeneration, we used BrdU injections (50mg/kg) given between P3-P6 (2 injections per day, ~6 hours apart) and analyzed samples 24hrs after the final injection. BrdU is incorporated into DNA during S phase and therefore will indicate which HCs were derived by supporting cell division.

Results

Atoh1-CreERTM; ROSA26^{LacZ} mice given 3mg/40g tamoxifen at P0 only had ~50% LacZ+ HCs whereas those given 0.1mg/40g tamoxifen at P0 only had ~10% LacZ+ HCs. Using this new tamoxifen induction paradigm in Atoh1-CreERTM; ROSA26^{DTA} mice, both mechanisms of HC regeneration were detected when ~50% of HCs were ablated and studies for the 10% HC death model are underway. Further research is in progress to obtain a tamoxifen induction paradigm that will target 25% of HCs.

Conclusion

Neonatal mice are capable of regenerating cochlear HCs using either direct transdifferentiation or mitotic regeneration mechanisms *in vivo*. Both mechanisms occur when ~80% or ~50% of HCs are killed.

Characterization of an *In Vivo* Mouse Model of Vestibular Hair Cell Degeneration/Regeneration

Zahra Sayyid¹; Tian Wang¹; Sherri Jones²; Alan Cheng¹

¹Stanford University School of Medicine; ²University of Nebraska- Lincoln

Background

The mammalian vestibular system requires sensory hair cells to detect linear acceleration such as gravity. Within it, the macula utricle exhibits limited capacity to regenerate lost hair cells. Following aminoglycoside insults *in vitro* and *in vivo*, previous studies demonstrated the formation of immature-appearing hair cells. The origin of these regenerated hair cells are likely supporting cells, a phenomenon observed in non-mammalian vertebrates, yet no lineage tracing has been performed to support this notion. These findings suggest that postnatal mouse utricles contain cell types with the innate ability to regenerate new hair cells after pathologic hair cell loss. To establish a hair cell degeneration/regeneration model in mice, we investigated the effects of 3,3'-iminodipropionitrile (IDPN), a synthetic vestibulotoxic nitrile compound.

Methods

Postnatal 30-day-old wild-type mice (CD1 strain) received a single injection of IDPN (0-6 µg/g, intraperitoneal). To assess vestibular function, vestibular evoked potentials (VsEPs) were measured at 1 week, 1 month, and 3 months post-injection. At these ages, animals were recorded to examine behaviors including circling, head bobbing, and gait, which were further assessed by calculating angular velocity. Moreover, animals were challenged with swim tests. Utricles harvested at these ages were immunostained for hair cell and supporting cell markers (Myo7a and Sox2). Densities of hair cells, supporting cells, and traced hair and supporting cells were separately determined in the striolar and extrastriolar regions.

Results

IDPN injection induced a dose-dependent loss of hair cells in the utricular sensory epithelium one week after treatment with IDPN with 64.1% hair cell loss with 4 µg/g. Drug-treated mice showed circling, head-bobbing behaviors, and inability to swim one week post-treatment. They also showed significantly elevated VsEP thresholds (with more than half of treated mice showing undetectable thresholds at > 6 dB re: 1.0g/ms), whereas saline-treated controls had an average threshold of -5.6 dB on average. Three months post-injection, about half of treated mice had reduced circling and angular velocity, detectable but elevated VsEP thresholds, and a significant increase in normalized utricular hair cell number to 30.3% hair cell loss at 3 months.

Conclusion

A single injection of IDPN causes a rapid, dose-dependent loss of hair cells and organ dysfunction in the mature mouse utricle. Three months after injection, a modest recovery of hair cell number and vestibular function is observed. Ongoing studies aim to better characterize the source and functionality of the newly generated hair cells.

An Independent Construct for Conditional Expression of Atonal Homolog-1 (Atoh1)

Mark Parker¹; Yen-fu Cheng²; Rebecca Bieber¹; Albert Edge²

¹Tufts University School of Medicine; ²MEEI

Background

The mammalian homolog of the basic helix-loop-helix transcription factor *atonal-1* (*atoh1* or *math1*) is required for development of cochlear hair cells that function as the mechano-sensory cells required for audition. Forced expression of *atoh1* in cochlear supporting cells may provide a way to regenerate hair cells and provide for a therapy for hearing loss. The goal of these experiments is to improve the method for *atoh1* expression by engineering a genetic construct that may be used in future translational applications. To address the poor control of *atoh1* expression in standard gene expression systems where *atoh1* is expressed constitutively at abnormally elevated levels, our aim was to engineer an inducible system whereby *atoh1* was upregulated by an inducer and could be downregulated once the inducer was removed. A further aim was to engineer a single genetic construct that allows for conditional expression of *atoh1* that was independent of secondary regulatory elements. Here we describe a stand-alone genetic construct that utilizes the tamoxifen sensitivity of a mutated ESTROGEN RECEPTOR (ER) ligand-binding domain for the conditional expression of *atoh1*.

Methods

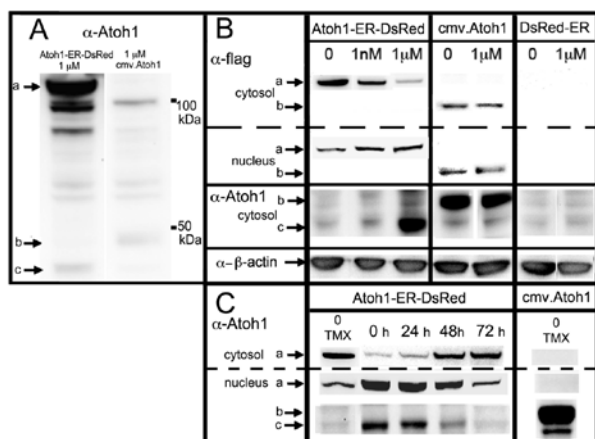
We transfected this inducible *Atoh1-ER-DsRed* construct into HEK cells, isolated cochlear-derived spheres, HEI-OC1 cells, and organ of Corti explants, then incubated the tissue in graded doses of 4-hydroxytamoxifen. We measured cyto-fluorescence of the DSRED moiety of the fusion protein, and the capacity of this construct to potentiate Atoh1 enhancer activity, Atoh1 RNA expression, Atoh1 protein expression, and downstream signaling such as MYOSIN 7A expression.

Results

The *Atoh1-ER-DsRed* construct is translated into an ATOH1-ER-DSRED fusion protein that remains sequestered in the cytoplasm and therefore rendered inactive because it cannot enter the nucleus to activate *atoh1* signaling pathways. However, application of 4-hydroxytamoxifen results in translocation of the fusion protein to the nucleus, where it upregulates transcription and translation of endogenous ATOH1, and activates downstream *atoh1* signaling such as upregulation of the hair cell protein MYOSIN 7A. Removal of tamoxifen reverses the upregulation of endogenous *atoh1* signaling.

Conclusion

This construct serves as an independent genetic construct that allows for the conditional upregulation and downregulation of *atoh1*, and may prove useful in future experiments aimed to upregulate and downregulate *atoh1* *in vivo*.



Reversible tamoxifen-induced ATOH1-ER-DSRED fusion protein expression of the endogenous ATOH1 protein.

HEK cells were transiently transfected with the *Atoh1-ER-DsRed* construct, incubated with different doses of tamoxifen for 72 hr, and cytosolic or nuclear protein was collected and processed for Western blot analysis for ATOH1 expression. Positive control samples were transfected with a *cmv.Atoh1* construct consisting of consecutive flag-tag sequences and negative control samples were transfected with the *DsRed-ER* construct. A) Anti-ATOH1 labeling of the cytosolic fraction isolated from HEK cells transfected with either *Atoh1-ER-DsRed* or *cmv.Atoh1* and incubated with 1 μ M tamoxifen for 72 hrs illustrates the relative expression between the 110 kDa ATOH1-ER-DSRED fusion protein (a), 47 kDa flag-tagged ATOH1 protein (b), and 45 kDa endogenous Atoh1 protein (c). B) The top row shows that increased concentrations of tamoxifen resulted in decreased anti-FLAG immunolabeling of the ~110 kDa ATOH1-ER-DSRED fusion protein in the cytosolic fraction, and increased immunolabeling of this fusion protein in the nuclear fraction. Labeling for the 110 kDa fusion protein is absent in the cytosolic fraction of *cmv.Atoh1* and *DsRed-ER* transfected controls. However immunolabeling for the 47 kDa flag-tagged *atoh1* control vector is present in the cytosolic and nuclear fraction at equivalent levels of cells transfected with the *cmv.Atoh1* construct. (Middle row) Immunolabeling the cytosolic fraction with anti-ATOH1 shows a 47 kDa band corresponding to the transfected flag-tagged *cmv.Atoh1* construct (b), and a 45 kDa signal corresponding to endogenous Atoh1 (c). Since ATOH1 is autoregulatory, *cmv.Atoh1* transfected cells exhibit an increased intensity of endogenous 45 kDa immunolabeling over the low level ATOH1 expression seen in *DsRed-ER* transfected cells. In cells transfected with the *Atoh1-ER-DsRed* construct, increased tamoxifen levels corresponded with increased immunolabeling of the 45 kDa endogenous ATOH1 protein, and no labeling to the 47 kDa flag-tagged ATOH1 signal is observed. The letters a, b, and c correspond to the positions denoted in A. (Bottom row) Immunolabeling to cytosolic β -actin is shown for a control for gel loading. C) The cytosolic and nuclear fractions of HEK transfected with either *Atoh1-ER-DsRed* or *cmv.Atoh1* were isolated 0, 24, 72, or 96 hrs after 72 hr incubation in 1 mM tamoxifen and compared to untreated samples. In the absence of tamoxifen, there was a relatively large concen-

tration of anti-ATOH1 immunolabeling of the 110 kDa fusion protein in the cytosolic fraction compared to the nuclear fraction. Immediately after tamoxifen washout (0h), there was an increase in nuclear anti-ATOH1 immunolabeling for both the 110 kDa fusion protein and the endogenous 45 kDa protein that decreased over time to baseline levels at 72 hrs. The decrease in the nuclear immunolabeling to the 110 kDa fusion protein corresponded to an increase in cytoplasmic immunolabeling of the 110 kDa fusion protein over this same time period. Control cells transfected with *cmv.atoh1* and incubated for 72 hrs in the absence of tamoxifen failed to exhibit labeling to the 110 kDa fusion protein in any condition. The letters a, b, and c correspond to the positions denoted in A.

PS - 195

Activation of HER2 Signaling Causes Supporting Cells to Divide in Mouse Neonatal Cochlea

Jingyuan Zhang; Jonelle Mattiaccio; Patricia White
University of Rochester School of Medicine

Background

Loss of sensory hair cells is the leading cause of deafness in humans. While never observed in mammals, non-mammalian vertebrates such as birds can regenerate lost hair cells from endogenous supporting cells. This regeneration leads to restoration of hearing. However supporting cells in mammalian cochlea lack the ability to proliferate. This project studies possible mechanisms that could stimulate supporting cells to divide *in vitro*. In a previous study, we discovered that signaling from EGFR/ErbB family was required for mouse supporting cell proliferation after supporting cell purification.

Methods

We built an adenovirus construct that expresses an active form of HER2 (HER2-CA), the human version of ErbB2 with a V654E substitution. Neonatal mouse cochlear explants were infected by HER2 virus and control viruses. Edu incorporation in conjunction with immunofluorescence and confocal microscopy were used to analyze cell proliferation. Inhibitors to the phosphoinositol-3 kinase signaling pathway were used to determine if its activation downstream of HER2 is necessary for proliferation *in vitro*.

Results

HER2-CA virus was validated by Western blot that infection with an adenovirus 5 expressing HER2-CA can trigger the phosphoinositol-3 kinase downstream signaling pathway in cell culture. In mouse neonatal cochlear organ cultures, we found significant numbers of supporting cells have incorporate EdU within cochlear explant infected by HER2 virus. Interestingly such proliferation in supporting cell region was non-cell autonomous.

Conclusion

We conclude that activated HER2 signaling is sufficient to cause neonatal mouse supporting cells to proliferate *in vitro*. We discovered that such mitotic effects from HER2 virus on supporting cells were non-cell autonomous. This result suggested the possibility of cross talk between ErbB receptor

mediated signaling and other pathways. The downstream targets of HER2 include phosphoinositol-3 kinase, which may play a role in the regulation of cell cycle re-entry. These findings altogether propose the correlation between epidermal growth factor receptor (ErbB) signal and proliferation of postmitotic supporting cells at neonatal age. Future research will address the effects on cochlear supporting cell division from activated ErbB2 signal *in vivo*.

PS - 196

Temporally Controlled Inactivation of the Retinoblastoma Family of Proteins in the Auditory Supporting Cells

Sonia Rocha-Sanchez¹; Jason Kum¹; Qian Zhang²; Kay-Uwe Wagner²

¹Creighton University School of Dentistry; ²University of Nebraska Medical Center

Background

Hair cell (HC) regeneration through manipulation of the cell cycle machinery of existing supporting cells (SCs) has become an attractive strategy. The retinoblastoma family of pocket proteins (pRBs) composed of *Rb1*, *Rbl1* (p107), and *Rbl2* (p130) are negative regulators of cell cycle progression. Deletion of any individual pRB in the auditory system triggers HC and SC proliferation to different extents. Nevertheless, accessing their combined role in the inner ear cell through conditional or complete knockout technologies is limited by the early mortality of the triple knockout. In most, if not all cells in the body, pRBs are maintained in an inactive hyperphosphorylated state in the presence of increased *Cyclin-D1-cdk4/6* activity. *Cyclin D1* is expressed in the embryonic and neonatal inner ear. In the mature OC, *Cyclin D1* expression is significantly downregulated, paralleling OC permanent mitotic quiescence. Moreover, as shown in the literature, *Cyclin D1* overexpression elicits cell cycle reactivation in inner ear explants.

Methods

Based on these evidences, we hypothesized that spatiotemporally controlled upregulation of CyclinD1 in the auditory SCs is likely to inactivate all three pRBs and lead to cell proliferation. To test our hypothesis we combined two transgenic mouse lines, consisting of the *CAG-bgeo-tTA-GFP* and the novel *TetO-CyclinD1*, generating a *CAG-bgeo-tTA-GFP/TetO-CyclinD1* double transgenic mouse, which, in turn, was bred to the *PLP-GFP-CreERT2* line.

Results

As expected, analyses of the postnatal *tTA-GFP/TetO-CyclinD1/PLP-GFP-CreERT2* mouse cochleae confirmed efficient Tet-controlled activation of the CyclinD1 transgene, promoting generation of supernumerary cells in the expression domain of the *PLP-CreERT2* transgene without any signs of apoptosis.

Conclusion

Regulation of OC cell proliferation and quiescence is a poorly understood process. Recent studies on the retinoblastoma gene family done by our group and elsewhere highlight the

importance of this family in auditory HC regeneration and function. Controlled and temporally regulated pRBs' expression in the OC should provide the much needed foundation for the development of successful therapeutic interventions in future gene therapy and tissue engineering initiatives.

PS - 197

Characterization of a Novel Rb1 Inducible Dominant Negative Mouse Model

Shikha Tarang¹; Channabasavaiah Gurumurthy²; Sonia Rocha-Sanchez¹

¹Creighton University; ²University of Nebraska Medical Center

Background

Genetic mouse models are useful tools for understanding the function of any gene in a physiological context. Retinoblastoma 1 (Rb1) is an essential gene regulating cell proliferation in many tissues and organs, including the auditory system. However, while its potential role in hair cell regeneration has been previously considered, any attempts to manipulate Rb1 function in the inner ear so far has been challenged by Rb1 null's early embryonic lethality or massive cell death after conditional Rb1 deletion.

Methods

To overcome these limitations, we have developed a novel strategy that combines the elegance of the doxycycline (Dox)-dependent transcriptional system to a straightforward strategy employing fusion of *Rb1* with the lysosomal protease cathepsin B (CB). This construct generated a temporarily regulated, Dox-mediated DN-*Rb1* mouse model, to induce dominant negative Rb1 gene knock-down. The resultant *TetO-CB-myc-Rb1* mice were bred with ROSA-CAG-rtTA inducer cell line. Tail biopsies were collected for genotyping and double positive (*TetO-CB-myc-Rb1*+ / ROSA-CAG-rtTA +) mice were treated with Doxycycline (Dox) in drinking water. The expression of Rb protein was investigated by western blotting. The presence of transgene construct was studied by RT-PCR in several tissues (ear, eye, heart, liver, kidney).

Results

The presence of transgene was confirmed in several tissues by RT-PCR with primer sets specific to the CB-Rb1 fusion protein.

The effectiveness of the Dox-induced dominant negative Rb1 inhibition was confirmed with Western blot analyses of Dox-treated double positive mice showing efficient inhibition of the endogenous RB expression in a variety of tissues, including the inner ear.

Conclusion

Our preliminary data support the broad spectrum potential of this novel mouse model and its potential use on studies searching to shed light on the complex biochemical mechanisms underlying the various aspects of *Rb1* activity in the auditory field and elsewhere.

PS - 198

DNA Damage Signalling Plays a Critical Role in Proliferative Capacity of the Inner Ear Supporting Cells

Maarja Laos; Ulla Pirvola
University of Helsinki

Background

Supporting cells (SCs) of the mammalian inner ear show an abrupt decline in proliferative capacity early postnatally. Prior data have shown that a large part of cell cycle reactivated adult utricular SCs are arrested in G2 phase and accumulate DNA damage. A causal relationship between these events was suggested (Loponen et al, PLoS 2011). Only little is known about DNA damage signalling and DNA repair in differentiated cells in general, especially in connection with cell cycle re-entry, an event often included in reprogramming approaches. This understanding is important if the use of SCs as a platform for hair cell regeneration is realized.

Methods

By comparative analysis of juvenile and adult SCs, we studied age-dependency of cell cycle progression and activation of the DNA damage response pathway and DNA repair. We used adenoviral-mediated cyclin D1 overexpression to trigger the cell cycle re-entry of SCs in explant cultures from P6 mouse cochleas and utricles and from adult utricles. We also employed an *in vivo* approach using conditional, inducible *Rb* inactivation (*RbloxP/loxP;Fgfr3-iCre-ERT2* mice) to study the response of auditory SCs.

Results

Juvenile utricular SCs and cochlear Deiters' cells responded to ectopic cyclin D1 by hyperproliferation, resulting in clonal expansion. In contrast, despite S-phase re-entry, most adult SCs failed to progress through the cell cycle. DNA double-strand breaks (DSBs), as detected by nuclear foci of activated H2AX (γ H2AX), accumulated in cell cycle reactivated SCs of both ages. Juvenile SCs showed resolution of γ H2AX foci, suggestive of successful DNA repair, while adult SCs showed delayed γ H2AX resolution and consequent induction of apoptosis. Corresponding results were obtained by studying the dynamics of Rad51 expression, a component of the homologous recombination repair complex. DSBs accumulated specifically in cell cycle reactivated SCs *in vitro* and *in vivo* in *Rb* mutant mice. SC-to-hair cell transdifferentiation did not trigger DNA damage.

Conclusion

Our results suggest that juvenile and adult SCs can respond to DSBs by activating the DNA damage response pathway. DSBs can be repaired early postnatally, whereas adult SCs show delayed DNA repair capacity, consistent with the arrest of these cells upon forced cell cycle re-entry and the induction of apoptosis. Our results underline the importance of DNA damage signalling as an important barrier in the attempts to stimulate cell proliferation as an approach to trigger regeneration in the inner ear.

PS - 199

Alteration of Musashi1 Distribution Following Gentamicin-Induced Hair Cell Loss in the Guinea Pig Crista Ampullaris

Makoto Kinoshita; Chisato Fujimoto; Akinori Kashio; Takashi Sakamoto; Kenji Kondo; Akinobu Kakigi; Tatsuya Yamasoba

Department of Otolaryngology Head and Neck Surgery, University of Tokyo, Japan

Background

Sensory hair cells (HCs) of the inner ear can be easily damaged by excessive stimulation by ototoxic drugs and by the effects of aging. Although recent studies have provided evidence for HC regeneration in mammalian inner ears, the mechanism underlying this regenerative process is still under debate. The RNA-binding protein Musashi-1 (Msi1) has been proposed to maintain stem cell function during development and regenerative processes as a modulator of the Notch-1 signaling pathway. Since Notch lateral inhibition is considered to play an important role in the development of the mammalian inner ear, we investigated Msi1 expression in normal and damaged crista ampullaris (CA) in mature guinea pigs by immunohistochemistry using the anti-Msi1 (14H1) antibody.

Methods

Albino male guinea pigs (200-250 g) were used. Experimental animals received gentamicin (GM) or control saline treatment through the cochleostomy site. The animals (n=5, each) were euthanized 4, 7, 14, 28 and 56 day post-treatment (PT). The paraffin-embedded sections were stained with Hematoxylin and Eosin, and counted HCs of CA under a light microscope. The other paraffin-embedded sections were double-immunostained using the anti-Msi1 and Myosin7a (Myo7a) antibody, and observed under a confocal microscope.

Results

At 7 and 14 days PT, no type I HCs were present, and 44% and 70% of type II HCs were lost. Recovery of the epithelia was evident 28 day PT; 82% were type II HCs, and 27% were type I HCs. The number of Supporting cells (SCs) in all the observation periods did not change. In controls, there was no Msi1-immunoreactivity in the HCs, while it was observed in the nuclei of the SCs. Both 7 and 14 days PT, the Msi1-immunoreactivity was diffusely spread into the cytoplasm of the SCs. 28 day PT, the Msi1 expression in SCs returned to the 'nuclear predominance' pattern, and a few nuclei of the Myo7a-labeled HCs were immunopositive to Msi1. 56 day PT, there was no Msi1-immunoreactivity in the HCs.

Conclusion

We investigated if expression of Msi1 was altered following GM induced HC loss in the mature CA of guinea pigs. Between 14 and 28 days PT, there was an increase of type II HCs, and a few HCs became immunopositive to Msi1 at 28 day PT. At the same time interval the number of SCs remained near normal. These results suggest that new HCs might be the result of SC mitotic division and differentiation.

Hair Cell Death and Clearance in Undamaged Adult Mouse Utricles

Stephanie Furrer¹; Tot Bui Nguyen¹; Brandon Cox²; Remy Pujol³; Jennifer Stone¹

¹University of Washington; ²Southern Illinois University School of Medicine; ³INSERM Unit 1052

Background

In mature birds, vestibular hair cells (HCs) normally undergo programmed death and replacement (turnover), and after ototoxin-induced HC death, vestibular HCs are fully replaced. By contrast, adult mammals replace only small numbers of vestibular HCs after injury. In this study, we assessed HC death and clearance in normal (undamaged) utricles from adult mice as an initial study of whether vestibular HCs undergo turnover in adult mammals.

Methods

We examined HC death and phagocytosis in whole-mounted utricles from normal adult mice (various strains and ages). Utricles were labeled with the following antibodies to detect HCs and phagocytes: anti-myosin VIIa to visualize all HCs, anti-calretinin to label type II HC cytoplasm and calyx nerve endings on type I HCs, anti-Iba1 to label phagocytes in the monocyte/macrophage lineage. We also used phalloidin to visualize F-actin in phagosomes. Dying HCs were identified using TUNEL, cleaved caspase 3, and DAPI labeling. We sought additional evidence of HC death and phagocytosis using TEM.

Results

In normal utricles from adult inbred (CBA/CaJ, C57Bl/6J) and outbred (Swiss Webster) mice, we detected numerous phagocytic pouches, or phagosomes, labeled by phalloidin. Phagosome numbers varied with strain and were highest in Swiss Webster mice (~65/utricle). Phagosomes either appeared empty or contained TUNEL labeling and/or pyknotic nuclei. Up to 6 phagosomes per utricle contained HC markers, suggesting dying HCs are actively cleared under normal conditions. Furthermore, a few normal-appearing HCs per utricle were pierced by F-actin rich "spikes" extending from phagosomes, suggesting they had been targeted for clearance. Phagocytes did not immunolabel for Iba1, suggesting they were SCs rather than professional macrophages. Phagocytic profiles were also seen with TEM. We are currently using mice with SC-specific inducible Cre activity (Plp-CreER^{T2} mice) to drive fluorescent reporter activity in SCs and assess if SCs create these phagosomes.

Conclusion

Death and clearance of utricular HCs, likely by SCs, occurs in normal adult mice, with a higher level of clearance evident in outbred mice. This finding supports the hypothesis that HC turnover occurs in the undamaged adult mouse vestibular epithelia. Future studies will address the factors directing the destruction and clearance of HCs in adult mice. These processes may also limit the number of HCs that can be regenerated following damage.

Characterization of Hair Cell Survival Genes in Regenerated Hair Cells in the Neonatal Mouse Cochlea

Sumedha Karmarkar; Brandon Cox

Southern Illinois University, School of Medicine

Background

Previous studies from our lab show that hair cell (HC) damage in the neonatal mouse cochlea results in spontaneous HC regeneration *in vivo* with new HCs derived from supporting cells (SCs) (Cox et al., in revision). However, most regenerated HCs die by postnatal day (P) 15. Pou4f3 (Erkman et al. 1996, *Nature*), Gfi1 (Wallis et al. 2003, *Development*) and Barhl1 (Xiang et al., 2002, *Development*) have been identified as HC-survival factors, since knockout mice lacking each of these genes show initial HC formation followed by HC loss. Prox1 inhibits Gfi1 expression and ectopic Prox1 expression in cochlear HCs results in HC death (Kirjavainen et al. 2008, *Dev Biol*). Mature HCs express HC-survival factors whereas Prox1 is only detected in SCs during a limited postnatal period. We hypothesized that after HC-damage, regenerated HCs at P4 will lack expression of HC-survival factors but will express Prox1 and this expression pattern will be reversed in the few regenerated HCs that survive until P15.

Methods

HCs are killed in the neonatal mouse cochlea using the Cre-loxP system and forced expression of Diphtheria Toxin fragment A (DTA). Tamoxifen (3mg/40g) injection in Atoh1-CreERTM;ROSA26^{DTA/CAG-tdTomato} mice at P0/P1 produces HC-specific expression of CreER, which results in DTA and tdTomato expression. The CAG promoter in the ROSA-26^{CAG/tdTomato} allele makes its expression much stronger than the ROSA26^{DTA} allele; thus, while ~99% of HCs are labeled by tdTomato, only ~80% are killed by DTA. The surviving HCs (20%) express tdTomato. Regenerated HCs will not express tdTomato since they were not present when tamoxifen was injected. Cochlea samples will be collected at P4, P7, and P15, and expression of Pou4f3, Gfi1, and Prox1 will be assessed by immunostaining and confocal microscopy.

Results

Preliminary experiments demonstrate that 14% of HCs express Pou4f3 in Atoh1-CreERTM;ROSA26^{DTA} mice at P6, while in control samples, all HCs express Pou4f3.

Conclusion

These data suggest that regenerated HCs at P6 do not express the HC-survival factor Pou4f3. However this result is inconclusive as we cannot distinguish between regenerated HCs and original, surviving HCs. We will repeat these experiments using fate-mapping to label original, surviving HCs with tdTomato (regenerated HCs will be tdTomato-negative). Since Barhl1-antibodies are not available, in future experiments, a Barhl1^{lacZ} mouse will be used to recapitulate endogenous Barhl1 expression.

PS - 202

Effects of Unilateral Intratympanic Gentamicin on Vestibulo-Ocular Reflex Function in Rhesus Monkeys

Chenkai Dai; Joong Ho Ahn; Kristin Hageman; Charles Della Santina

Johns Hopkins University

Background

Intratympanic (IT) injection of gentamicin damages vestibular hair cells and has been used to create vestibular-deficient animal models to test the Johns Hopkins Multichannel Vestibular Prosthesis. Whereas the effects of IT gentamicin have been well studied in chinchillas, they have been less well characterized in rhesus monkeys, which have become a preferred animal model of human subjects with vestibular deficiency.

Methods

Multiple injections of gentamicin (26.7 mg/ml) were delivered under general inhalational anesthesia through the left tympanic membrane to the middle ear in five rhesus monkeys. Vestibulo-ocular reflex (VOR) responses to sinusoidal and impulse head rotations in darkness about the horizontal, left anterior/right-posterior (LARP) and right-anterior/left-posterior (RALP) semicircular canal axes were measured 7-10 days post-injection (early) and at multiple time points up to 180–360 days post-injection (late).

Results

Early post-op VOR responses are asymmetric, with significantly larger half-cycle gain during excitation of the right (untreated) labyrinth than for during excitation of the left (treated) labyrinth (ANOVA: $p < 0.01$). In three out of five monkeys, the low VOR gain in the gentamicin treated ear recovered gradually. This recovery was incomplete but significant: 6 months post-injection, VOR gain increased by up to 17% during 2 Hz, 100°/s peak velocity passive whole-body rotations about the mean axis of the horizontal semicircular canals in darkness.

Conclusion

Intratympanic injection of gentamicin causes significant deficits of vestibular sensation in the treated ear, but recovery is possible. This recovery could be due to hair cell restoration or repair, but might also be due in part to central compensation and multimodal integration. Histologic study of treated animals will be required to discern the mechanism.

PS - 203

Comparison of Gentamicin Distribution in the Inner Ear Following Administration Via the Round Window or Stapes Footplate

Ting Zhang; Chunfu DAI

Fudan University

Background

Intratympanic (IT) gentamicin administration to treat patients with intractable vertigo has widespread popularity. It has been widely accepted that drug entry from the middle ear into perilymph occurs primarily via the round window membrane (RWM). More recent studies have demonstrated that

drug may enter the inner ear through both the round and oval windows. In our current study, we used gentamicin-conjugated Texas Red (GTTR) as a tracer to explore the distribution when applied to the RWM compared with the stapes footplate of guinea pigs (GPs)

Methods

Animals

Adult male or female albino GPs weighting 250–300g were used. The animals were anesthetized with intramuscular ketamine (40 mg/kg) and xylazine (10 mg/kg). The right ear was treated in all animals, the left was served as control.

Materials

Purified GTTR solution was diluted to 0.4mg/ml with sterile phosphate buffered saline (PBS, pH 7.4). Three microliters of GTTR was injected into 2-mm disks of absorbable collagen sponge. For the control groups, 3uL of 0.9% normal saline was administered.

Surgical procedures

After local infusion of 1% lidocaine, a post-auricular C-shaped incision was used. The bulla was opened using the drill under the operating microscope to expose the round window (gentamicin=6) and stapes footplate (gentamicin=6, saline=3). The collagen sponge was placed onto the stapes footplate of or RWM respectively. The head was held stationary with the treated ear for 30 min to allow the drug to permeate the structure.

Tissue preparation

At 7 days after treatment, animals were sacrificed then perfused the inner ears with 4% paraformaldehyde. The entire inner ear was immersed in the same fixative solution overnight at 4° C. The vestibular end-organs and basilar membrane of cochlea were harvested in PBS.

Immunohistochemistry

After washing in 0.01 M PBS (3*10 min), tissues were immunoblocked in 10% goat serum, with 0.2% Triton X-100 in 0.01 M PBS for 1 hour at room temperature (20-25° C), subsequently labeled with Phalloidin-FITC (1:500) in PBS for 40 minutes at 37° C. Finally, tissues were transferred to slides and observed under confocal microscopy (TCS SP5, Leica).

Results

There was strong punctate GTTR labeling in cochlear OHCs. The intensity of GTTR fluorescence in OHCs decreased from the basal to apical turn. In vestibular organs, saccular uptake of GTTR is greater than other end-organs which also had GTTR fluorescence. No GTTR fluorescence was found on the control side (left ear). Comparison between the two methods The stapes footplate route yielded less uptake than the RW application.

Conclusion

This study confirms that for local applications of drugs, entry into the ear occurs both through the RWM and a site near the stapes. GTTR more readily enters the inner ear when applied to RWM compared with stapes footplate.

Responses of Non-Eye Movement Central Vestibular Neurons to Sinusoidal Horizontal Translation in Compensated Macaques After Unilateral Labyrinthectomy

Shawn Newlands¹; Min Wei¹; Nan Lin²

¹University of Rochester Medical Branch; ²University of Texas Medical Branch

Background

After vestibular labyrinth injury, behavioral measures of vestibular function partially recover through the process of vestibular compensation. Previous reports have shown severe deficits in the translational vestibuloocular reflex (trVOR) sensitivity after unilateral labyrinthectomy (UL). The current study was performed to improve our understanding of the physiology of macaque vestibular system in the compensated state (>7 weeks) after UL.

Methods

This study included three groups of non- eye movement vestibular nucleus neurons recorded from two rhesus macaques: pre-UL control neurons (n=96), neurons ipsilateral to the UL (n=82), and neurons contralateral to the lesion (n=107). The firing responses of neurons sensitive to linear acceleration in the horizontal plane were recorded during sinusoidal horizontal translation directed along 6 different orientations (spaced 30° apart) at 0.5 Hz and 0.2g (196 cm/s²) peak acceleration for each neuron. This data defined the vector of best response for each neuron in the horizontal plane. Additionally, the responses of the same cells to a series of frequencies (0.25 – 5.0 Hz) at 0.2g peak acceleration either in the intra-aural or fore-aft orientation were obtained to define the frequency response characteristics in each group.

Results

These data revealed a decrease in sensitivity of central neurons overall to translation in the horizontal plane. There is also an alteration in orientation of best responses in the vestibular nucleus contralateral to the UL such that more neurons respond to acceleration towards the intact side, relative to pre-UL controls, causing the proportion of neurons bilaterally responding to ipsilesional translation to be decreased after UL. Additionally, the density of responsive neurons in the ipsilesional nucleus appears reduced. The relationship between responses in the excitatory and inhibitory directions of individual neurons was unchanged by UL. Bilateral central utricular neurons still demonstrated two-dimension tuning after UL, consistent with spatiotemporal convergence from a single vestibular end-organ.

Conclusion

These data represent the most thorough treatment yet of utricular responses recorded in the vestibular nuclei after UL. These neuronal data account for known behavioral deficits after unilateral vestibular compromise. Reduced sensitivity and neuronal number for linear acceleration towards the side of lesion are consistent with the reduction in eye movement responses to ipsilesional acceleration after UL, though not enough is known about the circuitry of the trVOR to know the

role of these neurons in that response. These data also suggest that the spatiotemporal convergence common in central vestibular neurons can be generated by one ipsilateral or one contralateral labyrinth.

Current Density Differences Between Action Potential Firing Patterns in Vestibular Ganglion Neurons

Christopher Ventura; Radha Kalluri

University of Southern California

Background

Regularity of spike timing is a trademark property of the primary afferents of the mammalian vestibular system and may be related to the complement of ion channels intrinsic to the neurons. Various categories of action potential firing patterns have been observed *in vitro*. Sustained-firing neurons fire more than one action potential and transient-firing neurons fire a single action potential. *In Vitro* experiments have shown that a low voltage gated potassium current (I_{KL}) is needed for transient firing. These neurons also contain hyperpolarization-activated inward currents (I_H). In other systems and cell types I_H has the potential to either enhance cell excitability or, when coupled with I_{KL} , inhibit excitability to enhance the precision of spike timing. In the timing pathways of the auditory system, I_H and I_{KL} interact with each other to enhance the fidelity of spike timing.

Methods

To investigate whether I_H and I_{KL} have possible patterns of co-expression or interaction in VGN neurons, we used whole-cell patch clamp techniques to record from VGN neurons dissociated from postnatal day (P) 8-15 rat. Depolarizing current steps were applied to group neurons into sustained and transient firing categories. Hyperpolarizing current steps were applied to indirectly identify the presence of I_H by characterizing the voltage 'sag' characteristic of the influence of I_H . We applied 500 ms voltage steps to compare steady-state inward and outward whole-cell currents as a function of voltage.

Results

The size of the steady-state inward current density at -100 mV (the V1/2 for I_H in VGN) was significantly greater in sustained neurons than transient neurons (4.4 ± 1.3 A/f, n=9; 2.3 ± 1.3 A/f, n = 6, respectively; $P=.007$).

Conclusion

We hypothesize that in the vestibular system those neurons with large I_{KL} (i.e. transient neurons) have small I_H , consistent with previous findings that large diameter VGN have smaller current density for I_H (Soto et. al. 2012). The opposing gradient between I_{KL} and I_H density proposed in vestibular ganglion neurons is in contrast to the co-expression pattern found in the timing pathways of the auditory system. Ongoing studies are exploring the impact of the combined presences of I_{KL} and I_H on spike-timing regularity in vestibular ganglion neurons.

PS - 206**Central Vestibular Neurons of the Vestibulo-Sympathetic Reflex Pathway**

Giorgio Martinelli; Victor L. Friedrich, Jr.; Gay R. Holstein
Icahn School of Medicine at Mount Sinai

Background

Changes in head position and posture, particularly with regard to gravity, are detected by the vestibular system and are normally followed by modifications in blood pressure in order to maintain adequate blood flow to the brain. These compensatory adjustments, which allow humans to stand up without fainting, are mediated by the integration of vestibular pathways with blood pressure control centers in the rostral and caudal ventrolateral medulla (RVLM and CVLM, respectively), the key pre-sympathetic sites for integration of cardiovascular signals. We have previously demonstrated that there are direct projections to RVLM and CVLM from neurons in the caudal vestibular nuclei that are functionally activated by specific vestibular stimulation. The goal of the present study was to examine the neurochemical phenotypes of the activated vestibulo-sympathetic projection neurons.

Methods

Unilateral iontophoretic injections of the retrograde tracer FluoroGold were placed in the RVLM or CVLM of rats. After 10 days, the animals were anesthetized and received sinusoidal galvanic vestibular stimulation (sGVS) while blood pressure changes were detected by photoplethysmography. Animals were perfused 90 min after the stimulation. The brains were harvested and the brainstems were sectioned serially. Sets of sections were used to map the tracer injection sites, and other series of sections were used for multiple label immunofluorescence studies of the caudal vestibular nuclei. Activated neurons were identified using immunodetection of c-Fos protein and additional immunolabels were utilized to identify the FluoroGold tracer, glutamate, GABA, and imidazoleacetic acid-ribotide (IAA-RP), a neuromodulator involved in blood pressure regulation.

Results

FluoroGold was present bilaterally in cell bodies of the inferior and caudal medial vestibular nuclei (IVN and MVNc, respectively) that showed c-Fos protein accumulation in response to sGVS. Of the ~250 activated projection neurons examined, ~42% were intensely glutamate-immunofluorescent (indicative of glutamatergic neurotransmission), whereas ~37% were GABA-immunolabeled. Over 90% of the activated projection neurons contained IAA-RP, including ~75% of the GABAergic and ~78% of the glutamate-immunofluorescent cells.

Conclusion

We conclude that there are multiple chemoanatomic vestibulo-sympathetic projections, and speculate that the vestibular system exerts both excitatory glutamatergic and inhibitory GABAergic control over presympathetic neuronal circuits, both modulated by IAA-RP.

PS - 207
Vasovagal Oscillations from the Vestibulo-Sympathetic Reflex Have a Critical Role in Production of Vasovagal Responses in the Rat
 Sergei Yakushin¹; Giorgio P Martinelli¹; Theodore Raphan²; Yongqing Xiang²; Bernard Cohen¹

¹*Icahn School of Medicine at Mount Sinai*; ²*Brooklyn College of the City University of New York*

Background

Sinusoidal galvanic vestibular stimulation (sGVS) induces oscillations in blood pressure (BP) and heart rate (HR) i.e., vasovagal oscillations (VVO) and vasovagal responses (VVRs) in isoflurane-anesthetized rats.

Methods

We determined the characteristics of the VVOs, whether they played an important role in the generation of VVRs, and whether they could be induced by monaural as well as by binaural stimulation and by oscillation in pitch. We also determined the best frequencies of sGVS that elicited VVRs. Since oscillations in BP and HR have time variant, harmonic distributions, wavelet analyses were used to determine the power distributions of the induced wave forms.

Results

Monaural and binaural sGVS and oscillation in pitch generated VVOs both at the frequency and at twice the frequency of stimulation. VVOs were maximal at low stimulus frequencies (0.025 Hz). Both harmonics were attenuated at higher frequencies and VVRs were rarely induced. Stimulation with sGVS at 0.025 Hz was also the best frequency for induction of VVRs. VVOs could occur without induction of VVRs, but VVRs were always associated with a concurrent VVO.

Conclusion

We posit that the VVOs originated in activity of low frequency otolith neurons that had their orientation vectors close to the spatial vertical. Such neurons would be maximally excited twice during each sinusoidal oscillation as their orientation vectors passed through the spatial vertical. These neurons are likely to provide critical input to the vestibulo-sympathetic reflex to increase BP and HR on changes in head position relative to gravity, and to contribute to production of VVOs and VVRs when the baroreflex is inactivated. The data also imply that VVOs have a critical role in generation of VVRs.

PS - 208
Adult Mice With Vestibular Hair Cell Ablation Show a Decrease in the Vestibulo-Autonomic Reflex and an Increase in Reactivity to Stress
 Jennifer Stone¹; Tot Bui Nguyem¹; James Phillips¹; Edwin Rubel¹; Matti Mintz²

¹*University of Washington*; ²*Tel Aviv University*

Background

In addition to the effects on balance, a common comorbidity of vestibular deficiency is enhanced anxiety. Previous studies demonstrated enhanced anxiety in vestibular mutant mice, validating the model for the study of mechanisms transforming the imbalance to anxiety. We used mice with moderate

or severe ablation of vestibular hair cells (HCs) to test the involvement of the vestibulo-autonomic reflex in the transformation of vestibular deficiency to anxiety.

Methods

Vestibular HCs were ablated by systemic injection of diphtheria toxin (DT) to adult mice engineered to express the DT receptor (DTR) under control of the *Pou4f3* promoter whose inner ear activity is limited to hair cells. *Pou4f3*^{DTR/+} and wild-type mice were injected with a moderate or high dose of DT (25 or 50 ng/g, i.p.), saline or nothing. In one cohort, HCs were counted 2 weeks later. In a second cohort, the vestibulo-autonomic reflex was tested 5-8 weeks after DT treatment by monitoring the response of core body temperature (% change from baseline) under the following conditions: *rotation-only* in a flask; *rotation-with-stress* in a restraining cylinder; *stress-only* in a restraining cylinder w/o rotation; *low-stress* in open-field; and *control* (no manipulation). For rotation, the flask and the cylinder were positioned 23cm off the center of a rotating plate, which was sinusoidally accelerated to 270deg/s within 120s; max centrifugal acceleration =0.52g.

Results

Survival of HCs in the utricle and lateral crista was 31-40% of uninjected mice after low-dose DT and 4-8% after high-dose DT. Wildtype and *Pou4f3*^{DTR/+} mice without DT treatment demonstrated a similar profile of temperature response; a sustained drop in body temperature to rotation-only (1-2% of baseline for 20 min), an acute drop of temperature to rotation-with-stress or stress-only (1.7-5.5% of baseline at 5 min) followed by recovery toward baseline (0-2.5% of baseline at 20 min), and no response to low-stress. In contrast, *Pou4f3*^{DTR/+} mice at either DT dose showed no temperature response to rotation-only. However, after the higher DT dose, they showed a significantly enhanced response to stress (rotation-with-stress, stress-only, and low-stress conditions).

Conclusion

Short vestibular and stress challenges trigger reliable autonomic response. Loss of vestibular hair cells abolishes the autonomic response to vestibular challenge and enhances the autonomic response to stress. Lacking the autonomic response the affected subject may not learn to avoid situations that challenge his compromised vestibular system. Thus, the subject may be prone to develop a chronic anxiety disorder.

PS - 209

Response of Mice to Fluctuating Hyper-G Acceleration is Influenced by Orientation and Repetition

Donald Swiderski; Michelle Kappy; Dwayne Vaillencourt; Chris Ellinger; Yehoash Raphael
University of Michigan

Background

Balance disorders may reflect deficits in neurological or motor function as well as vestibular organ dysfunction. In addition, vestibular organ lesions may be partially compensated by adaptation of other organ systems, which can interfere

with evaluation and treatment, in the clinic and in the lab. Recent studies of vestibular influences on autonomic functions suggest a new avenue of evaluating vestibular organ function: measurement of short-term body temperature changes after controlled fluctuations of centrifugal acceleration. In this study, we demonstrate that the orientation of the acceleration can affect the magnitude of temperature change, and repetition affects its duration.

Methods

All subjects were wild type mice between 21 and 60 days old, without overt hearing or vestibular deficit. Mice were placed in a 50 ml conical tube containing a fixed acrylic bar that constrained their orientation in the tube. The tube was fixed to a rotating arm and oriented to produce a centrifugal acceleration along a specific anatomical axis. An automated controller alternated between arm speeds generating centrifugal accelerations of 2 G and 6 G, maintaining each speed for 10 seconds. Each mouse was spun for two minutes, 6 intervals at each speed. Core body temperature was measured by rectal digital thermometer just prior to acceleration, immediately after, and at specified subsequent times. To control for effects of handling, all mice were subjected to the temperature measurement protocol without additional stimulation.

Results

Repeated temperature measurement with no other stimulation induced an increase in core body temperature within 10 minutes of the first measurement. Spinning that generated an anterior to posterior acceleration vector produced a decrease in core temperature within the same time frame. When the same mice experienced the same acceleration protocol 4 days later, most had the same temperature decrease, but a faster recovery to baseline. When these mice were subjected to dorso-ventral acceleration after another 2-3 days, they exhibited smaller temperature changes than were induced by the antero-posterior acceleration.

Conclusion

A larger temperature decrease was induced by controlled fluctuation of hyper-G acceleration along the antero-posterior axis than by acceleration along the dorso-ventral axis. Both acceleration protocols produced markedly different physiological responses than were induced by repeated temperature measurement. These results suggest that changes in vestibular function due to genetic or ototoxic lesions and protective or reparative treatments will be detected more efficiently by antero-posterior acceleration than by dorso-ventral acceleration.

PS - 210

Effect of an Emetic Gastrointestinal Input on the Processing of Labyrinthine Inputs by Cerebellar Rostral Fastigial Nucleus Neurons

Michael Catanzaro; Milad Arshian; Daniel Miller; Lucy Cotter; Andrew McCall; **Bill Yates**

University of Pittsburgh

Background

Multiple inputs can elicit nausea and vomiting, including ingested toxins and conflicting signals regarding body position in space. Amongst the nervous system regions believed to participate in generating motion sickness is the cerebellar rostral fastigial nucleus (rFN). In addition, there is evidence that gastrointestinal (GI) inputs are transmitted to rFN through a variety of pathways, including projections from the dorsal motor nucleus of the vagus and area postrema. **These observations raise the hypothesis that GI inputs could alter motion sickness susceptibility by altering the processing of labyrinthine inputs by rFN neurons.**

Methods

To test this hypothesis, we recorded activity from rFN neurons in decerebrate cats, and compared responses rFN neurons to whole-body rotations in vertical planes before and after the intragastric infusion of the emetic compound copper sulfate (CuSO₄). Rotations were delivered at 0.1-1 Hz, and at amplitudes up to 7.5°. Since CuSO₄ readily produces nausea and vomiting by irritating the stomach lining, aspirating the compound after each trial eliminated the emetic stimulus.

Results

Infusion of CuSO₄ produced a >30% change in firing rate for ~25% of rFN neurons. A large fraction of rFN neurons had complex responses to vertical vestibular stimulation, including spatial-temporal convergence (STC) behavior. The spatial and temporal characteristics of these responses changed little after injection of CuSO₄. Although infusion of CuSO₄ affected gains of responses to rotations of ~25% rFN neurons, the effects were inconsistent (CuSO₄ augmented responses in some cells and decremented responses in others).

Conclusion

CuSO₄ resulted in much more pronounced changes in responses to vertical tilts of neurons located in brainstem regions that mediate nausea and vomiting, including the "vomiting center" (caudal medullary lateral tegmental field) and the parabrachial nucleus. These data suggest that integration of vestibular and GI inputs by rFN neurons plays little role in affecting motion sickness susceptibility.

PS - 211

Time Constant for Stimulus Transfer from the Scalp to the Macular Vestibular Epithelium in the Mouse

Timothy Jones; **Choongheon Lee**

University of Nebraska-Lincoln

Background

Vestibular macular sensors are activated by a shearing motion between the otoconial membrane and underlying re-

ceptor epithelium. Shearing motion and sensory activation in response to an externally induced head motion does not occur instantaneously. The mechanically reactive elastic and inertial properties of the intervening tissue introduce temporal constraints on the transfer of the stimulus to sensors. Treating the otoconial sensory apparatus as a highly damped second order mechanical system, we measured the short time constant (t_2) for stimulus transfer from the head surface to epithelium. This provided the basis to estimate the upper cutoff for the frequency response curve for mouse otoconial organs. A velocity step excitation was used as the forcing function. Hypothetically, the onset of the mechanical response to a step excitation follows an exponential rise having the form $Vel_{shear} = A(1 - e^{-t/t_2})$, where A is the applied shearing velocity step amplitude. The response time of the otoconial apparatus was estimated based on the activation threshold of macular neural responses to step stimuli having durations between 0.1 and 2.0 ms.

Methods

Twelve adult C57BL/6J mice were evaluated. Animals were anesthetized. The head was secured to a shaker platform using a non-invasive head clip coupled to the platform. The shaker was driven to produce a theoretical forcing step velocity excitation at the otoconial organ. Vestibular sensory evoked potentials (VsEPs) were recorded to measure the threshold for macular neural activation. The duration of the applied step motion was reduced systematically from 2ms to 0.1 ms and response threshold determined for each duration (9 durations). Hypothetically, the threshold of activation will increase according to the decrease in velocity transfer occurring at shorter step durations. The relationship between neural threshold and stimulus step duration was characterized.

Results

Activation threshold increased exponentially as velocity step duration decreased below 1.0ms. The time constant associated with the exponential curve was $t_2 = 0.5ms$ for the head clip coupling. This corresponds to an upper -3dB frequency cutoff point of approximately 318 Hz.

Conclusion

Threshold increases exponentially at step durations below 1.0ms. The findings are consistent with a heavily damped second order mass-spring mechanical system. The shortest time constants of 0.5ms predicts high frequency cutoffs of at least 318 Hz for the otoconial apparatus of the mouse.

PS - 212

Detection of Velocity Storage Mechanism in C57BL6 Mice

Naoki Shimizu¹; Scott Wood²; Adrian Perachio¹; Tomoko Makishima³

¹University of Texas Medical Branch; ²Azusa Pacific University; ³University of Texas Branch

Background

The velocity storage mechanism (VSM) plays an important role in gaze stabilization. This central neural process is activated both by visual and vestibular rotation cues and is modified by gravity. For more than three decades, it has been

thoroughly investigated across a wide range of species from frontal-eyed to lateral-eyed animals. However, it was thought to be absent in mice, partially because the mouse lacks optokinetic after-nystagmus or a dominant time constant of the vestibular ocular reflex, for which the VSM is critical. In this study, we evaluated the eye movements of mouse generated by using a hyper-gravity stimulation. The findings indicate that mice also might have a central neural integrator in the vestibular system.

Methods

C57BL/6J strain mice were tested in this study. Eye movements were induced by a dual yaw axis centrifuge in darkness and recorded using a video-oculography. Two axis rotations at constant velocities were synchronized to generate a similar rotating gravity vector as an off-vertical axis rotation (OVAR) but with a larger resultant gravito-inertial force (pseudo-OVAR).

Results

Similar to those previously described in other animals during OVAR, there were two components in the horizontal slow phase eye velocity: 1) a bias component, which is the mean eye velocity, for which the VSM is thought to contribute to, and 2) a cyclic modulation around the mean velocity, together with the vertical eye movement modulated periodically with head rotation.

Conclusion

We showed the dynamic characteristics of mouse eye movements induced by the pseudo-OVAR paradigm suggesting the existence of the primitive neural integrator working as the VSM in mice. Further application of genetic approaches will help in deciphering the links from genes to the VSM to behavior.

PS - 213

Acetylcholine-Mediated Ionotropic Currents in Vestibular Calyx Afferents and Type II Hair Cells

Zhou Yu¹; Soroush Sadeghi²; Michael McIntosh³; Elisabeth Glowatzki¹

¹The Johns Hopkins University School of Medicine; ²Center for Hearing and Deafness, University at Buffalo; ³The Johns Hopkins University School of Medicine; ³University of Utah

Background

In the mammalian vestibular epithelium, the efferent fibers originating in the brain stem form cholinergic synapses on type II hair cells (HCs), on afferents that form calyx endings and on afferents that form bouton endings. Stimulation of the mammalian efferent vestibular system induces various degrees of excitation of vestibular afferents (Reviewed in Holt et al., 2011). To understand how efferent inputs to these individual cell types together result in the measured excitation, in a first step, we investigated the response of calyx afferents and type II HCs to acetylcholine (ACh) or efferent stimulation.

Methods

Whole-cell patch clamp recordings were performed in excised preparations of rat cristae, on postnatal days 13-17. Caly-

ces and type II HCs were identified by their specific channel conductance, membrane resistance and morphology. Drugs were applied through a local gravity driven system.

Results

Application of 1 mM ACh caused an inward current of 129 ± 80 pA ($n = 28$; holding potential -80 mV) in 60 % of calyces ($n = 131$). The current-voltage relation of the ACh response showed a reversal potential near 0 mV ($n = 5$) suggesting the presence of non-selective cation channels. The inward current was blocked by 10 μ M tubocurarine ($n = 3$; 84%), 10 μ M strychnine ($n = 3$; 90%), and 400 nM α -BTX ($n = 3$; 67%), suggesting the presence of $\alpha 7$ - and/or $\alpha 9$ - containing nAChRs. Type II HCs responded to 1 mM ACh with inward currents of 18 to 184 pA at negative holding potentials (-90 to -74 mV; $n = 4$). The ACh-induced current reversed near -60 mV, suggesting that calcium-dependent potassium channels are involved ($n = 3$). These results suggest that efferents may hyperpolarize or depolarize type II HCs depending on their membrane potential. Efferent synaptic activity triggered by applying a solution containing 40 mM potassium showed events with kinetics similar to cochlear efferent synaptic events ($n = 2$).

Conclusion

These results suggest that vestibular afferents may experience a combined excitatory efferent input via calyces and a more complex excitatory/inhibitory efferent input via type II HCs. Understanding the exact nature of this combined action requires further investigation of the mechanisms for integration.

PS - 214

Physiological Vestibular Dysfunction in Alpha9 and Alpha9/10 Knockout Mice

Barbara Morley¹; Anna Lysakowski²; Sarath Vijayakumar³; Steven D. Price²; Deanna Menapace¹; Timothy Jones³

¹Boys Town National Research Hospital; ²University of Illinois at Chicago; ³University of Nebraska at Lincoln

Background

The alpha9/10 receptor mediates cholinergic efferent activity in both the auditory and vestibular systems. The function of the nicotinic cholinergic efferent synapse on hair cells in the cochlea has been well-characterized. Less is known about the function of cholinergic efferents innervating vestibular hair cells. In the study reported here, we studied vestibular function and light microscopic morphology in alpha9 and alpha9/10 nicotinic knockout mice in comparison to wildtype controls.

Methods

The mouse lines were developed by us and were backcrossed to the C57Bl/6J strain until congenicity was achieved, as determined by Marker-Assisted Accelerated Backcrossing (MAX BAX; Charles River).

Results

Both the alpha9 knockout and the alpha9/10 double-knockout had significantly reduced vestibular sensory evoked potential (VsEP) amplitudes ($p < 0.001$) and elevated thresholds ($p = 0.036$, Mann-Whitney U) compared to wildtype mice,

suggesting significantly reduced sensitivity of the macular sensory epithelium. Neural activation latencies were also significantly shortened in knockout animals ($p < 0.009$). Knockouts were not significantly different from each other. Although the changes in VsEPs were statistically significant, there was substantial variance within the groups. Some knockout animals had normal VsEP amplitudes and thresholds, whereas others had very poor, even absent, VsEP responses. Nonetheless, dysfunction (shortened activation latency) was still evident even in knockout animals having otherwise normal thresholds. These results are consistent with reduced sensitivity and altered timing of neural activation in the macular vestibular neuroepithelium of alpha9, alpha9/10 knockout mice.

Using MAX BAX with 384 SNP markers we found no evidence of a 129 region that distinguished knockouts with normal or abnormal thresholds.

The knockouts have a unique cochlear phenotype, which includes disorganized efferent innervation and aberrant bouton size. Light microscopic evaluation, using otoferlin and calretinin immunohistochemistry, and electron microscopic evaluation of vestibular efferent innervation did not suggest a similar abnormal efferent innervation of vestibular hair cells.

Conclusion

Alpha9 and alpha9/10 knockout mice have elevated VsEP thresholds, but there was significant variation. Variance in inbred mice may be attributable to genetic, epigenetic, or environmental causes. Although our mice are congenic, they retain a small percent of 129 in the alpha9 and alpha10 regions, but that is apparently not the source of variance. Despite the variance in thresholds, neural activation latencies were shortened in all knockouts. Unlike medial olivocochlear efferents terminating on outer hair cells, vestibular efferents have no obvious morphological phenotype.

PS - 215

Characterization of CreER Activity in the Adult Vestibular Sensory Epithelium for Eight CreER Mouse Lines

Brandon Cox¹; Stephanie Furrer²; Tot Bui Nguyen²; Marcia M Mellado Lagarde³; Jennifer S. Stone²

¹Southern Illinois University, School of Medicine; ²University of Washington; ³St. Jude Children's Research Hospital & University of Brighton

Background

The Cre/loxP system in mice allows for cell-type specific control of gene expression. When a modified estrogen receptor is added to the Cre enzyme (CreER), gene expression can be activated at any time via tamoxifen administration. More than 30 Cre or CreER alleles have been described for the cochlea, where gene manipulation or cell fate-mapping was performed, resulting in significant advances for the auditory field. However, few CreER lines have been studied in vestibular sensory epithelia, and none have been described in adult vestibular sensory epithelia (Cox et al., 2012 JARO). Here,

we characterized the Cre activity pattern of eight CreER lines in the adult mouse utricular macula and lateral crista.

Methods

Each of the following CreER alleles was bred with the ROSA26/CAG-loxP-stop-loxP-tdTomato reporter line, given tamoxifen (9mg/40g) at 6 weeks of age (2 injections given ~24 apart) and analyzed one week later: Calretinin-CreER^{T2}, FGFR3-iCreER^{T2}, GFAP-CreERTM (2 different alleles), Otoferlin-CreER^{T2}, Plp-CreER^{T2}, Prox1-CreER^{T2} and Sox2-CreER^{T2}. We also tested for Cre leakiness by examining mice that expressed both CreER and tdTomato but did not receive tamoxifen.

Results

The Otoferlin-CreER^{T2} allele showed expression of tdTomato primarily in Type II hair cells (HCs) and no Cre leakiness was observed. In contrast, the Plp-CreER^{T2} allele had tdTomato expression in ~1,000 supporting cells (SCs) per utricle and in glia near the vestibular nerve, while only rare HCs were labeled. In controls tested for Cre leakiness, we observed ~100 tdTomato+ SCs and some tdTomato+ glia. Very few tdTomato+ cells (<40) were detected in Prox1-CreER^{T2} utricular macula and lateral crista, and no Cre leakiness was observed. The Sox2-CreER^{T2} line expressed tdTomato in the vast majority of SCs, in all Type II HCs, and in rare Type I HCs in utricles and cristae. In samples without tamoxifen, <30 tdTomato+ SCs and Type II HCs were observed. No tdTomato+ cells were detected in vestibular organs of either GFAP-CreERTM alleles. Studies of the Cre activity pattern in other CreER lines are underway.

Conclusion

This work provides new tools for cell-type specific gene deletion and cell fate-mapping in adult vestibular sensory epithelia. Thorough description of Cre activity patterns provides invaluable tools for cell-specific, time-controlled gene manipulation in the vestibular organs. Future studies will examine expression patterns of these alleles at other ages of tamoxifen induction.

PS - 216

Strong Static Magnetic Fields Elicit Swimming Behaviors Consistent With Direct Vestibular Stimulation in Adult Zebrafish

Bryan Ward¹; Grace Tan²; Dale Roberts¹; Charles Della Santina¹; David Zee¹; John Carey¹

¹Johns Hopkins University School of Medicine; ²University of Pennsylvania School of Medicine

Background

Zebrafish (*Danio rerio*) offer many advantages as model animals for studies of inner ear development, genetics and sensitivity to ototoxic agents. However, assessing vestibular function in this species with the vestibulo-ocular reflex requires difficult and labor intensive immobilization in agar. We recently observed that humans have sustained nystagmus in high strength magnetic fields, which apparently engender magnetohydrodynamic forces acting directly on the labyrinths. Here we report that using an MRI machine's magnetic

field to directly stimulate the zebrafish labyrinth results in an efficient, quantitative behavioral assay.

Methods

Fish were individually introduced into the center of an Earth-vertical 11.7 T magnetic field bore for 2-minute intervals and their swimming movements were tracked. To assess for altered heading direction preference relative to a horizontal magnetic field, fish were also placed in a horizontally oriented 4.7 T magnet in IR light. A sub-population was then tested again in the vertical magnet after gentamicin bath to ablate lateral line hair cell function.

Results

Free-swimming adult zebrafish exhibited markedly altered swimming behavior while in strong static magnetic fields, independent of vision or lateral line function. Two-thirds of fish showed increased swimming velocity or consistent looping/rolling behavior throughout exposure to a strong, vertically oriented magnetic field. Adult fish also demonstrated altered swimming behavior in a strong horizontally oriented field, demonstrating in most cases preferred swimming direction with respect to the field. Exposure to magnetic fields did not elicit visible changes in the behavior of a few tested larval or juvenile zebrafish.

Conclusion

Strong static magnetic fields elicit swimming behaviors consistent with direct vestibular stimulation in adult zebrafish. These findings could be adapted for 'high-throughput' investigations of compounds with ototoxic (or otoprotective) potential, genetic manipulations expected to impact inner ear function, and changes in vestibular function during development in zebrafish.

PS - 217

Visualization of Mouse Vestibular Systems Using Optical Coherence Tomography (OCT)

Yosuke Tona; Tatsunori Sakamoto; Akiko Taura; Takayuki Nakagawa; Juichi Ito

Kyoto University

Background

Vestibular systems have intricate internal structures with thin membranous labyrinth and otolithic apparatus surrounded by the bony capsule. Decalcification, dehydration, and staining using organic solvent, which are required for the histological examination, modify morphological and chemical properties of the vestibular system. For example, calcium carbonate, the main component of the otolith, is largely lost during these processes. Optical coherence tomography (OCT) is a non-destructive cross-sectional imaging modality which utilizes near infra-red light. OCT has widely been applied to clinic in the field of ophthalmology, dermatology, and cardiovascular medicine. We previously reported that OCT could visualize normal and pathological morphologies inside mouse cochleae without destruction of outer bony capsules *in vivo* and *in vitro*. In this study, we evaluated potential of OCT for the visualization of the vestibular system including maculae, otolith, and endolymphatic sac and duct of extracted mouse inner ears. Normal and *Slc26a4* knockout mice, which are

known to show severe endolymphatic hydrops, were used in this study.

Methods

OCT images were obtained using OCS-1300SS (Thorlabs Inc., NJ), with a central wavelength of 1300 nm and a theoretical axial resolution of 9 μ m. For visualization of the membranous labyrinth and maculae, adult and P1 mice were administered. For visualization of endolymphatic sac and duct, littermates of adult *Slc26a4* mutants were used. Harvested inner ears were fixed with 4% paraformaldehyde and visualized by OCT, before and after decalcification with 10% ethylenediaminetetraacetic acid for 7 days.

Results

Saccular and utricular maculae were delineated with OCT before and after decalcification. Image quality and imaging depth were better after the decalcification. On the contrary, the signals from both maculae were attenuated after decalcification because of the reduction in the calcium contents. OCT revealed dilation of the endolymphatic sac and duct in *Slc26a4* knockout mice and not in heterozygotes and wild type littermates. All morphological features demonstrated by OCT were consistent with the histopathological findings of the samples.

Conclusion

The membranous labyrinth of the vestibular system and the endolymphatic sac and duct were visualized by OCT. Decalcification resulted in better image quality and imaging depth. However, otolithic apparatus were better visualized before decalcification.

PS - 218

Tomographic Analyses of Afferent Synapses in Mouse Utricular Hair Cells

Ivan Lopez; Kristopher Sheets; Felix Schweizer; Larry Hoffman

David Geffen School of Medicine

Background

The objective of the present study was to investigate whether the ultrastructure of ribbon synapses within utricular hair cells exhibits morphologic heterogeneity based upon hair cell type and utricular topography. This was achieved through conventional transmission electron microscopy (TEM) and EM conical tomography.

Methods

These data were obtained from mice (male C57Bl/6J, aged 4 months) that served as controls for the Russian BION M1 biosatellite mission. Animals were euthanized, and temporal bones were rapidly harvested and infused with mixed aldehyde fixative. Utricular epithelia were processed for TEM and ultrathin sections (95nm) were obtained. We focused upon synaptic ribbons (SRs) in the striola and medial extrastriola using landmarks determined from a separate specimen immunostained with anti-calretinin for striola identification. Conical tomography was conducted using a Gatan 650 single tilt rotating holder in a FEI Tecnai 12 EM (120KV). Projection series were obtained by placing the grid at 55° primary tilt,

then rotating and imaging in 5° increments through 360°. The projections were collected with a CCD camera using a low-dose method, searching at 2700X and focusing 1.5µm from the area of interest.

Results

Our tomographic methods enabled analysis of perisynaptic volumes of approximately 0.4µm³, providing a more comprehensive view of synaptic ultrastructure than conventional TEM. SRs of spherical (90-150 nm diameter) and rod (200-250 nm length) morphologies were seen in type I and type II hair cells. Plate SRs (170-270 nm) were rarely seen in either type I or type II hair cells. Rod SRs were more frequently seen in type I hair cells. Spherical and rod SRs in type II hair cells were also seen opposing the calyx outer face. Though rarely observed, clusters of 2-3 ribbons were found primarily in type I hair cells. No overt differences in ribbon morphology associated with utricular topography have thus far been identified. Vesicles closely associated with SRs exhibited diameters of 25-35 nm. Spherical SRs showed 10-12 vesicles, rod SRs showed 13-20 vesicles, rod 16-20 vesicles. Tomographic reconstructions provided additional information concerning the spatial distribution of synaptic vesicles, inter-vesicle distances, and ribbon-vesicle distances that provide insight into putative distinct vesicle pools.

Conclusion

Tomographic reconstructions provide an enhanced view of synaptic ultrastructure in utricular hair cells, aiding in analyzing ribbon morphology and vesicle distributions. These data provide the foundation for ongoing analyses of spaceflight-induced synaptic plasticity.

PS - 219

Development of Micro-Endoscope for *In Vivo* Ca and FRET Imaging.

Ichiro Nakahara¹; Akihiro Goto²; Kazuo Funabiki³

¹Kyoto University Graduate School of Biostudies; ²Riken BSI; ³Systems Biology, Osaka Bioscience Institute

Background

In vivo imaging is a powerful tool to analyze brain dynamics, especially when it becomes possible with the functional assessment of the circuits. We share our experience in developing a fiber-optic micro-endoscope which enables *in vivo* Ca and FRET imaging at cellular resolution.

Methods

Micro-endoscope was fabricated from a commercially available fiber bundle (diameter 215-350µm, Fujikura, Japan). Endoscopic tip was beveled and polished to have a pencil like shape. We further coated the tip surrounds with Au and insulated with enamel paint to record or stimulate neural circuits in observation electrically. Resonant galvo scanner (CRS GSI Lumonics) was used for video-rate confocal image acquisition. We used DA converter (PCI-6713, National Instruments) to control a galvo motor and lasers, and also used non-standard analog frame grabber to acquire multi-color image. We also developed a micro-drive for micro-endoscope so that we can change the location of probe after implantation. All the

software for galvo motor control, image acquisition and image processing were written in Matlab scripts.

Results

We, first, adopted our system to *in vivo* Ca imaging of the cerebellar granule cells. We used mutants in which only cerebellar granule cells were labeled with GCaMP2 (genetically encoded Ca sensor protein, Díez-García et al, 2007). Endoscope was inserted into the right cerebellar flocculus of head restricted awake mice. The location of probe tip inside the right cerebellar flocculus could be notified by evoking horizontal eye movements toward right ear with electric pulses applied through the endoscope tip surrounds. Slowly activating Ca signals were occasionally observed with optokinetic stimuli. The neural damage by endoscopic (diameter 215µm) insertion was supposed to be minimal because we rarely see paralytic nystagmus (horizontal eye movements toward nose, which indicates the suppression of neural activity in the right cerebellar flocculus).

We, secondly, adopted our system to *in vivo* FRET measurement. We used mutants in which all the cells have PKA or Erk FRET biosensor (Kamioka et al, 2012). We implanted our endoscope with micro-drive into the cerebral cortex covering dorsal striatum. Three days after implantation, we lowered the endoscope into dorsal striatum. When cocaine was injected, PKA and/or Erk showed sustained activity increase in parallel with the locomotion increase.

Conclusion

These results indicate that our fiber bundle based micro-endoscope system will be useful in *in vivo* Ca and FRET imaging.

PS - 818

Transdermal Somatosensory Stimulation Induces Stimulus Timing Dependent Plasticity in Guinea Pig Dorsal Cochlear Nucleus

David Martel¹; Roxana Stefanescu²; Susan Shore²

¹University of Michigan; ²Kresge Hearing Research Institute

Background

In addition to auditory nerve inputs, the dorsal cochlear nucleus (DCN) also processes inputs from other sensory systems. The spinal trigeminal nucleus (Sp5) sends inputs to the DCN that may relay information regarding self-generated sounds. We have shown that the firing patterns of DCN principle cells can be modulated through stimulus timing dependent plasticity (STDP) using bimodal auditory and somatosensory stimuli, with variable intervals and orders of presentation (Koehler and Shore, PLOS ONE, 2013). In that study, normal hearing guinea pigs showed primarily Hebbian-like learning rules, i.e., when auditory nerve inputs preceded trigeminal inputs long-term potentiation resulted. When the bimodal interval order was reversed, long term depression resulted. While our previous studies used deep brain stimulation of the trigeminal system in this study, we use non-invasive transdermal stimulation to activate somatosensory inputs to the DCN to induce STDP in guinea pigs. The ability to regulate neural activity using non-invasive methods is a major step

toward potential treatments for a host of neuropathic ailments including tinnitus.

Methods

Guinea pigs were anesthetized using intramuscular weight-adjusted ketamine/xylazine[s1]. Facial fur was shaved to enable placement of stimulating electrodes on the skin at the center of the cheek, overlying the trigeminal ganglion with the ground on the nasal bridge. Tone-evoked ABRs were recorded prior to surgery to establish hearing thresholds. Anesthetic depth was assessed using hind leg withdrawal areflexia and maintained using ketamine/xylazine. The left DCN was exposed via craniotomy and aspiration of a small amount of overlying cerebellum. In some experiments the recording electrode was placed stereotaxically through the cerebellum. Biphasic current pulses were presented at the highest levels that did not evoke muscle contractions (usually less than 2 miliamps). Spike waveforms were processed using Plexon Offline Sorter and timing rules generated using custom Matlab code.

Results

Preliminary recordings reveal Hebbian-like timing rules for tone-evoked and spontaneous activity, with the strongest changes in firing rate seen at the (+/-) 10- and 20 ms bimodal intervals, 15 minutes after the bimodal stimulation.

Conclusion

The demonstration of Hebbian-like timing rules in response to bimodal stimulation in normal animals similar to Koehler and Shore suggest that transdermal facial stimulation is a useful, non-invasive method for inducing STDP in guinea pig DCN. This will pave the way for the use of non-invasive bimodal stimulation for the treatment of pathologies such as tinnitus.

SY - 014

Mechanisms of Bone Conduction Hearing: Experiments, Models, and Simulations

Stefan Stenfelt

Linköping University

Background

Several theories have been presented to explain the sound perception when stimulation is by bone conduction (BC). It is accepted by most that BC sound cannot be ascribed a single phenomenon but several mechanisms interact and can be important at different frequencies. Also, an anatomical alteration or pathology may change the different mechanisms' relative importance. Two of these mechanisms, and maybe also the overall most important mechanisms, are (1) the inertial forces in the cochlear fluid due to rotational and longitudinal rigid body motion of the bone surrounding the cochlea, and (2) compression and expansion of the cochlear space caused by wave motion in the bone forcing fluid motion between the scalae in the cochlea. Both of these stimulation modes depend on the motion of the bony cochlear shell as well as compliant structures in the cochlear wall enabling a fluid motion.

Methods

Cryosection images of a human head together with corresponding CT images were used to device a 3D finite element model of the human skull. Parameters values were fitted to the different structures and model simulations were validated by experimental BC skull bone vibrations. High-resolution micro-CT images of a cochlea were used to identify and quantify compliant structures of the cochlear shell.

Results

The whole head 3D finite element model was used to quantify the motion of the bony shell of the cochlea. These motions were used to identify inertial effects of the cochlear fluid as well as quantify the cochlear space alteration and a net fluid flow between the scala vestibuli and scala tympani. Compliances of the cochlear shell gives spatially distributed fluid motion within the cochlea important for BC excitation of the two cochlear BC modalities.

Conclusion

Coupled 3D finite element models of a human skull and cochlea using a multi-scale approach gives insight to the relative importance of the two cochlear components of BC excitation and provides understanding of the BC sound physiology.

SY - 015

Intracochlear Pressure Measurements in Human Temporal Bone Evoked With Bone Conduction Stimulation

Hideko Nakajima¹; Christof Stieger²; Defne Abur³; Julie P. Merchant¹; Rosemary B. Farahmand¹; John J. Rosowski¹

¹Massachusetts Eye and Ear Infirmary, Harvard Medical School; ²Dept. of ORL, University Hospital Basel, Basel and University Bern, Inselspital, Switzerland; ³Smith College

Background

Intracochlear Pressure measurements in temporal bones made with fiber-optic micro-sensors (developed by Elizabeth Olson) have allowed us to understand that sound transmission mechanisms leading to the stimulation of the cochlear partition differ during air conduction (AC) compared to round-window stimulation. We have modified our technique of intracochlear pressure measurements for the special requirements in studying bone conduction (BC), as bone vibration produces challenges for viable intracochlear pressure measurements.

Methods

Two methods for sealing and holding the pressure sensors were compared: {1} The sensor tip area at the cochleostomy was sealed with Jeltrate (rubbery dental impression material) and the optical-fiber cable was held firmly with a micromanipulator. {2} Thin layer of dental cement was applied over the Jeltrate to rigidly attach the sensor tip to the bony surface, and the optical-fiber was released from the micromanipulator. Vibrations of the sensor close to the tip and the nearby bony surface of the cochlea were measured. Intracochlear pressures measured by the sensor during both configurations were compared. Various methods of holding the temporal bone were studied.

Results

In method {1}, the vibration of the sensor was generally larger than the bony cochlear surface by 10-30 dB, while in {2}, vibration of sensor and bony surface was similar during BC stimulation. The intracochlear pressure measured with {2} was either similar or larger (up to 10 dB) compared to {1}. The frequency responses of the bone vibration and intracochlear pressure were not smooth when the temporal bone was held rigidly to a metal bowl placed on a rubber ring. Holding the bone more rigidly produced similar results. Specimen set in modeling compound resulted in smoother frequency responses of vibration and pressure. Other compounds with more oil content resulted in unstable vibrational measurements with time.

Conclusion

For measurement of intracochlear pressure in human temporal bones, method {2} is favorable over {1}. Method {2} with cement results in similar sensor and bony surface vibration, which would reduce the possible artifact generated with Jeltrate alone {1}, where difference in pressure can be generated by the difference in vibration of sensor and bone. Also, unlike with {1}, {2} prevents the possibility and variability of compromising the soft Jeltrate seal between sensor tip and cochlear bone that can reduce pressure measurements. Furthermore, setting the preparation in modeling compound allows the cochlear vibration to be smoother across frequency.

SY - 016

Bone-Conduction Pathways of Hearing: Computational Approaches

Namkeun Kim; Charles Steele; Sunil Puria
Stanford University

Background

Many investigators have used experimental techniques to improve our understanding of the bone-conduction (BC) pathways of hearing. For example, von Békésy [1] showed that BC hearing stimulates the basilar membrane (BM) in the same with as the air-conduction (AC) pathway, which is via a traveling wave on the BM. In addition, Tonndorf [2] identified several pathways by which BC stimulation can produce a traveling wave on the BM, including inertial motion of the middle-ear (ME) and cochlear fluid, and occlusion of the ear canal. Computational-modeling approaches can help to codify our measurement-based understanding, leading to new theories that can be further tested in the laboratory.

Methods

We developed 3D finite-element models to simulate the response of the cochlea to the BC and AC hearing pathways. The first model was a simplified box representation of the uncoiled cochlea, and the second was an anatomically accurate 3D model of the middle ear and inner ear based on μ CT imaging (Fig. 1).

Results

The simplified box model indicates that the BM responses are determined by the anti-symmetric pressure component (slow wave) between the scala vestibuli (SV) and scala tympani (ST), regardless of the direction of inertial stimulation to

the box cochlea [3]. The more advanced model, capturing the spiral shape of the cochlea (Fig. 1), revealed the following points: 1) The BM response was shown to be a function of the direction of acceleration, but with the travelling wave instead being initiated by the hook region of the cochlea [4]. 2) With a superior-semicircular-canal dehiscence (SSCD), BC hearing thresholds are clinically observed to improve for frequencies below about 1 kHz, and in the model this was shown to be due to a new fluid path between the RW and SSCD [5]. 3) We showed that the Carhart's Notch phenomenon found in otosclerosis patients can be explained by the combination of two BC mechanisms: compressional input to the cochlea and ME inertia [6]. And, 4) a decrease in ossicular mass was shown to decrease BC hearing, while stiffening the ossicular joints was shown to improve BC hearing.

Conclusion

A number of observations in normal and diseased configurations of finite-element ear models are paving the way towards new theories and improved understanding of the BC pathways of hearing.

References

- [1] von Békésy, G. (1932). Zur theorie des hörens bei der schallaufnahme durch knochenleitung. *Ann. Physik.* 13:111-136.
- [2] Tonndorf, J. (1966). Bone conduction. Studies in experimental animals. *Acta oto-laryng.* Suppl. 213, 1-132.
- [3] Kim, N., K. Homma, and S. Puria. (2011). Inertial bone conduction: Symmetric and anti-symmetric components. *J. ARO.* 12:261-279.
- [4] Kim, N., C.R. Steele, and S. Puria. (2013). The importance of the hook region of the cochlea for bone-conduction hearing. *Biophys. J.* in revision.
- [5] Kim, N., C.R. Steele, and S. Puria. (2013). Superior-semicircular-canal dehiscence: Effects of location, shape, and size on sound conduction. *Hear. Res.* 301:72-84.
- [6] Kim, N., C.R. Steele, and S. Puria. (2013). Carhart's notch: A window into mechanisms of bone-conducted hearing. *Proc of Meeting on Acoust* 19:050133.

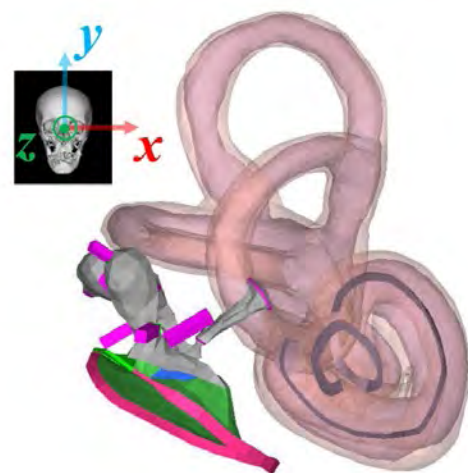


Figure 1: Finite element model including the middle ear, cochlea and semi-circular canals relative to the skull orientation (inset). The spiral shaped BM is highlighted in gray.

SY - 017**Animal Models of Bone Conduction****John Rosowski***Massachusetts Eye and Ear Infirmary, Harvard Medical School***SY - 018****Devices for Bone Conduction Hearing****Gerald Popelka***Stanford*

Bone conduction is used for diagnostic measures (audiometry, eg), in medical hearing devices (BAHA, eg) and in consumer applications (Google Glass, eg). Bone conduction diagnostic devices are held in place with a head band, positioned on the skin and soft tissue overlying the skull, typically on the mastoid process of the temporal bone, and are standardized for how they are coupled and measured. Bone conduction hearing devices can be coupled to the head like a diagnostic device but more typically use quite different coupling methods and locations ranging from surgical implantation of an osseointegrated component to surgical implantation of a subdermal component screwed to the skull to application of a removable dental module held against a tooth surface. Bone conduction hearing devices are not standardized, use a variety of transducer types and have the added requirements of a microphone and portable power supply, all of which affect overall auditory performance. This presentation will describe the devices including transducer type and microphone location, present models of the characteristics of relevant components and show measures of output force, gain and frequency bandwidth with respect to the force needed to drive the skull for auditory perception. The influence of these devices on auditory factors such as binaural hearing, spatial hearing and understanding speech in noise will be described.

SY - 019**Clinical Indications for Bone-Conducting Hearing Devices****Lawrence Lustig***University of California San Francisco*

Beginning with the Bone Anchored Hearing Aid (BAHA) in the 1990's, there are now a number of osseointegrated bone conducting hearing devices available on the market. The availability of these devices has in turn radically transformed the clinician's ability to treat a wide variety of conductive and sensorineural hearing disorders. Whereas middle reconstruction used to be the only option to correct conductive hearing losses, we now have the possibility of bypassing the middle ear auditory transduction mechanism entirely. This is especially important for patients who cannot wear a hearing aid due to chronic draining ears or those who are medically unable or unwilling to undergo surgery. Additionally, treatment for single sided deafness used to be limited solely to the CROS hearing aid; the advent of contemporary osseointegrated bone conducting hearing devices now affords new treatment options for this challenging clinical condition with markedly improved outcomes.

This talk will provide an overview of the clinical conditions that lead to conductive hearing losses that can be rehabilitated with these bone conducting devices. These include chronic infectious disorders of the ear and mastoid, such as chronic otitis media and cholesteatoma. Additionally there are a number of non-infective conditions that lead to loss of the normal sound conducting mechanism, including otosclerosis, congenital ossicular fixation, and congenital aural atresia that are also benefited by these bone conduction devices. Conditions that lead to closure of the external auditory canal, including skull base tumors and cancers of the ear canal are an additional important indication for these devices. Lastly, an overview of single sided deafness from such disorders as idiopathic sudden sensorineural hearing loss and skull base tumors such as acoustic neuroma will also be reviewed.

SY - 020**Anatomical and Neurochemical Basis for Vestibular Control of Blood Pressure****Gay Holstein***Icahn School of Medicine at Mount Sinai*

Changes in head position and posture, particularly with regard to gravity, are detected by the vestibular system and are normally followed by modifications in blood pressure in order to maintain adequate blood flow to the brain. These compensatory adjustments, which allow humans to stand up without fainting, are mediated by integration of central vestibular pathways and blood pressure control centers in the rostral and caudal ventrolateral medulla (RVLM and CVLM, respectively), the key pre-sympathetic sites for baroreflex activity. While the existence of a functional connection between the vestibular system and blood pressure control mechanisms was hypothesized almost a century ago, the anatomical basis for this integration has only recently been addressed directly. This presentation will review the anatomical evidence for vestibulo-sympathetic projections to regions that are critical for blood pressure control, and our current studies of the neurotransmitters, neuromodulators, and receptor systems that participate in these pathways and may serve as therapeutic targets.

SY - 021**Vestibulo-Autonomic Dysfunction: A Clinical Perspective****Gregory Whitman***Harvard Medical School, Massachusetts Eye and Ear Infirmary*

Patients who have a chief complaint of dizziness often report orthostatic intolerance (OI). OI is characteristically described as lightheadedness while standing that improves or resolves, on lying down, and suggests the possibility of an autonomic nervous system disorder. The results of recent investigations are consistent with the conclusion that the vestibular system otolith organs influence autonomic nervous system function, including muscle sympathetic nerve activity, and skin sympathetic nerve activity, both of which tend to prevent excessive lower extremity pooling of blood, and thus counteract OI. Given this modulation of vasoconstriction by the vestibular sys-

tem, it has been proposed that vestibular disorders may play a role, in autonomic syndromes that include OI as a symptom. OI is a feature of an array of syndromes, including orthostatic hypotension (OH), postural orthostatic tachycardia syndrome (POTS), and vasovagal syncope (VVS). All of these latter disorders have in common, the fact that they may be aggravated by insufficient lower extremity sympathetic outflow mediated vasoconstriction. A retrospective study of 641 patients with recurrent syncope and presyncope, referred to subspecialty autonomic disorders services, found that 5% of such patients had vestibular dysfunction.[Mathias CJ, 2001] A retrospective study of 56 dizzy patients, who had undergone both vestibular testing and tilt table testing, found no statistically significant association between tilt table abnormality and caloric weakness.[Heidenreich KD, 2009] However, the authors pointed out that otolith organ function was not directly assessed, and that this should be a subject of future research. Focusing on otolith organ function, a study of 248 dizzy patients found that 20% of those with absent cervical vestibular evoked myogenic potentials (VEMP) met criteria for OH.[Aoki M, 2012] These observations, on the links between the vestibular disorders and autonomic dysfunction suggest the need for further studies, to delineate the interrelationships, between vestibular and autonomic disorders. Because of the need to better define such interrelationships, and because patients with autonomic disorders may present with "dizziness," a best practice approach to dizziness should include a reasonable index of suspicion for OI. For patients with OI, autonomic function should be assessed, by clinical examination, and in some cases, by autonomic laboratory testing.

SY - 022

Multisensory Integration of Vestibular and Other Inputs Influencing Cardiovascular Control

Bill Yates

University of Pittsburgh

Vestibul sympathetic reflexes (VSR) act in parallel with baroreceptor reflexes (BR) in maintaining stable blood pressure during postural changes. VSR elicit regional changes in blood flow at the onset of movements such as head-up tilt that affect blood distribution in the body in both humans and quadrupeds, preventing blood pressure lability. VSR have an advantage over BR, since they are elicited before blood pressure changes, thereby maintaining homeostasis. Together VSR and BR assure that blood pressure remains stable during both unexpected and voluntary changes in body orientation. VSR are exaggerated (nonphysiologic) in decerebrate cats, indicating that higher brain centers regulate VSR gain. There is also evidence that BR gain is adjusted by higher brain centers, implying that cognitive mechanisms adjust the gains of VSR and BR in accordance with the expectation that lability in blood pressure could occur. Elimination of signals from the inner ear through a bilateral labyrinthectomy (BL) results in an increase in BR gain. Furthermore, subsequent to BL, deficits in adjusting blood pressure during head-up tilt resolve over time, indicating that alternate mechanisms sub-

stitute for the loss of VSR. The development of enhanced BR following BL would result in increased vasoconstriction during head-up tilt, and account for recovery of posturally-related blood pressure adjustments after a loss of VSR. These findings imply that regulation of VSR and BR gains is coupled, such that changes in one response alter the other. Uvulectomy (removal of lobule IX of the posterior cerebellar vermis) prevents compensation for loss of VSR, such that blood pressure permanently remains labile during head-up tilt, suggesting that the uvula is critical for adjusting the gain of BR following BL. Furthermore, stimulation or lesions of the uvula elicit changes in sympathetic nerve activity and blood pressure. Purkinje cells in the uvula provide inputs to both the caudal aspect of the vestibular nucleus complex, which mediates VSR, as well as nucleus tractus solitarius, which receives direct inputs from baroreceptor afferents. Thus, the uvula's connections are appropriate for regulating gains of both VSR and BR. The uvula may also participate in adaptive plasticity in these responses following the loss of labyrinthine inputs, analogous to that of the flocculus in modifying the gain of vestibulo-ocular reflexes. These findings suggest that the cerebellar vermis has parallel roles in somatic and autonomic motor control, and imply that cerebellar degeneration during disease or aging could have important but unappreciated impacts on blood pressure control.

SY - 023

Post-Flight Orthostatic Hypotension and Related Vestibulo-Autonomic Challenges Associated With Spaceflight

Joan Vernikos¹; Victor Convertino²

¹Thirdage LLC; ²US Army Institute of Surgical Research

Human Physiology and health have evolved and adapted in the presence of Earth's gravity. The magnitude of the physical stress associated with the development of the force required by muscles to move or lift one's body is dependent on the level of gravity opposing these actions. Thus gravity has traditionally been considered the primary constant stress factor for influencing adaptation and maintaining the human body's health on Earth. Reduction or near absence of gravity presented by spaceflight imposed new physiological adaptations through a reduction in hydrostatic gradients within the cardiovascular system, a decreased mechanical weight load on all muscles and bones, a lower energy requirement and/or output, conflict in directional and relative sensory input and resulting adaptation to the new steady state by rearrangement of central organization to better serve in the new state. A response to everyday standing in Earth's gravity, as well as the immediate post-flight response to standing, are evidenced by a typical stress response sequence. This includes fluid retention with an increase in plasma volume, and a sequence of increased endocrine and autonomic responses designed to support adequate upright circulation. The difference is in the relative magnitude in individual response profiles. A similar response to post-flight occurs on standing up after a period of continuous head down bed rest (HDBR), the ground simulation model of choice for space flight-related research.

Symptoms of OH occur when the changes in the pre-existing condition or steady state adapted to microgravity compromise the normal response on return to gravity. For instance, astronauts who are less prone to OH post-flight respond with a two-fold increase in plasma catecholamines compared to their pre-flight levels. In contrast, pre-syncope astronauts have lower levels of circulating plasma norepinephrine (NE) concentrations, associated with blunted increases of muscle sympathetic nerve activity (MSNA) during post-flight standing, compared to non-pre-syncope astronauts. However, the notion that OH predisposition is due to inadequate sympathetic neural activation alone during orthostatic stress is open to question. Vascular volume, carotid-cardiac baroreflex sensitivity, and elevated parasympathetic nerve input have all been implicated either in concert or independently in the predisposition and/or development of OH. Based on these findings non-medicinal potential lines of treatment have been developed and tested.

SY - 024

Vestibulosympathetic Reflexes in Humans: Contributions to Orthostasis

Chester Ray

Penn State College of Medicine

Evidence indicates that stimulation of the otolith organs in humans activates the sympathetic nervous system. The vestibular-mediated increase in sympathetic activity is commonly referred to as the vestibulosympathetic reflex (VSR) and is believed to assist in maintaining arterial blood pressure during orthostasis. Head-down rotation, which stimulates the otolith organs, selectively increases muscle sympathetic nerve activity (MSNA) but not skin sympathetic nerve activity. Importantly, the increase in MSNA during otolith stimulation is associated with vasoconstriction to various vascular beds. However, a number of factors can alter the VSR. For example prolonged bed rest and exercise training (i.e., running) attenuates increases in MSNA, elicited by head-down rotation. These conditions also experience increased incidence of orthostatic intolerance. Aging, which is also associated with increased prevalence of orthostatic intolerance, attenuates the VSR. Moreover, engagement of the otolith organs during head-down rotation elicits a drop in arterial blood pressure in older but not young subjects. These findings indicate that the VSR contributes importantly to postural regulation of arterial blood pressure. Additionally, we have performed experiments demonstrating that external stimulation of the otolith organs by ultrasonic bone stimulation of the mastoid can increase MSNA, improve blood pressure, and augment orthostatic tolerance during head-up tilt. Future studies will continue to elucidate the important but unappreciated role of the vestibular system in contributing to sympathetic activation and the regulation of postural blood pressure in humans.

SY - 025

Insights Into Vestibulo-Sympathetic Control of the Cardiovascular System from a Rat Model

Bernard Cohen; Sergei Yakushin

Icahn School of Medicine at Mount Sinai

Although fainting due to blood loss and emotional stress has been known for centuries, the underlying mechanisms that produce the faint are still unclear. Several fundamental facts have been uncovered, however. The faint can be caused by activation of the sympathetic nervous system through the vestibulo-sympathetic reflex. In fact, syncope is diagnosed clinically using head-up-tilt, an otolith stimulus. During faints, the baroreflex is inactivated, and cardiovascular stability is lost. Both blood pressure and heart rate fall together in vasovagal oscillations, terminating in vasovagal syncope. However, how the baroreflex is inactivated, a critical step in production of the faint, and the role of the vasovagal oscillations in the production of vasovagal responses (VVR) are still unknown.

We recently discovered that activation of the vestibular nerve with sinusoidal galvanic vestibular stimulation and head-up tilt in isoflurane-anesthetized rats causes typical vasovagal oscillations and VVR. We further showed that the amplitude of the vasovagal oscillations was related to the amount of linear acceleration imposed on the X-Y plane of the head and body. This makes it possible to use the rat as a small animal model of the human VVR. The purpose of this talk is to present new insights into the mechanisms that produce vasovagal oscillations and VVR. In particular, we show that vasovagal oscillations are best generated at very low frequencies of stimulation (0.025 Hz), and that it is obligatory to generate a vasovagal oscillation in order to produce a VVR. Exactly how the vestibulo-sympathetic reflex throws the cardiovascular system into vasovagal syncope, however, is still a subject for further research.

PD - 015

Quantifying Efferent-Induced Inhibition of Cochlear Amplifier Gain from Changes in Human Compound Action Potentials

Jeffery Lichtenhan¹; Uzma Wilson²; John Guinan³

¹Washington University School of Medicine in St Louis;

²Missouri State University; ³Harvard Medical School

Background

The medial olivocochlear bundle (MOC) inhibits the gain of the cochlear amplifier when activated by contralateral acoustic stimulation. In humans, MOC inhibition has been studied almost exclusively using otoacoustic emissions. If a purpose of the efferent system is to assist hearing in the presence of background noise, measuring the MOC inhibition of auditory-nerve responses may be more appropriate. Hence, we quantified the inhibition of click-evoked human compound action potentials (CAPs) produced by efferent-induced attenuation of cochlear amplifier gain.

Methods

CAP measurements were made from young, normal hearing adults using an electrode placed on or near the tympanic membrane. Repeated measurements from multiple visits to

our lab were made from one click level, yielding approximately 10 hours of data collection from each subject. Alternating-polarity clicks at 25-30 dB SL (Sensation Level) were delivered in a free field from a subwoofer placed approximately 12 inches from the antrum of the right ear canal. Contralateral broadband noise was delivered through an insert earphone at 65 dB SPL. CAP measurements with and without contralateral noise were interleaved. Finally, a level-series function was made by varying ipsilateral click level in absence of contralateral noise, to translate the CAP amplitude reductions to equivalent click level shifts, and thereby quantify the extent to which the auditory efferent system turned down the gain of the cochlear amplifier.

Results

CAP amplitude was consistently inhibited by the presence of contralateral noise when enough averaging was done to make the measurement reliable.

Conclusion

We found that when activated by moderate-level contralateral sound, the human auditory efferent system reduced the gain of the cochlear amplifier by up to approximately 3 dB. While CAP-based estimates of efferent inhibition in humans is helpful for basic science purposes, their use for clinical purposes of assessing efferent inhibition in people with reading and learning disabilities is limited by the gargantuan number of averages needed to obtain reliable results.

PD - 017

Comparing Otoacoustic, Auditory-Nerve, and Behavioral Estimates of Cochlear Tuning in the Ferret

Christian Sumner¹; Toby Wells¹; Christopher Bergevin²; Alan Palmer¹; Andrew Oxenham³; Christopher Shera⁴

¹MRC Institute of Hearing Research; ²York University, Department of Physics & Astronomy; ³Department of Psychology, University of Minnesota; ⁴Eaton-Peabody Laboratories, Massachusetts Eye & Ear Infirmary, Boston,

Background

Cochlear tuning provides the initial tonotopic organization that is maintained throughout the auditory pathways at least up to primary auditory cortex. Auditory-nerve (AN) tuning curves provide a direct measure of cochlear tuning that corresponds closely to the mechanical tuning observed on the basilar membrane. Less invasive, but less direct, measures have also been proposed, including ones based on stimulus-frequency otoacoustic emissions (SFOAEs) and behavioral (notched-noise) masking. However, the correspondence between AN tuning and the more non-invasive techniques remains somewhat controversial. Here we present data using all three techniques in the same species to provide a direct test of their correspondence

Methods

Estimates of cochlear tuning were derived from SFOAE measurements, collected in 19 ferret ears at frequencies ranging from 1 to 10 kHz. Some of the ferrets for whom SFOAEs had been collected were then tested behaviorally to derive es-

timates of cochlear tuning using the notched-noise method under forward or simultaneous masking with either a fixed signal level (to mimic AN measures) or fixed masker level (to match more common behavioral estimates in humans). The cochlear tuning estimates from the behavioral and SFOAE methods in ferret were compared with previously published estimates from AN tuning curves in ferrets, and with AN, SFOAE, and behavioral estimates in other species.

Results

Analysis of the SFOAE data produced estimates of cochlear tuning that were in generally good agreement with AN and SFOAE data from other small mammals, including cat, guinea-pig, and chinchilla. A preliminary analysis of the cochlear tuning estimates from the behavioral notched-noise method suggests no large or systematic deviations from the more direct physiological estimates. In all cases, estimates of tuning appear broader, by about a factor of two, than comparable estimates in humans.

Conclusion

Based on preliminary outcomes, no systematic deviations were observed between estimates of cochlear tuning from the AN, SFOAEs, and behavioral methods. If confirmed, the convergent data from all three methods in the same species provide support for the hypothesis that both SFOAEs and behavioral masking techniques can provide reasonable and non-invasive estimates of cochlear tuning. The outcomes are also consistent with the idea that human cochlear tuning (when measured in terms of frequency, as opposed to cochlear extent) is sharper than in most common mammals used for auditory research.

PD - 018

Neural Cell Adhesion Molecule L1 Modulates Type I but not Type II Inner Ear Spiral Ganglion Neurite Outgrowth in an in Vitro Alternate Choice Assay

Yves Brand¹; Michael Sung²; Eduardo Chavez²; Eric Wei²; Kwang Pak³

¹Department of Biomedicine and Clinic of Otolaryngology, Head and Neck Surgery, University Hospital Basel, Hebelstrasse 20, 4031 Basel, Switzerland and Department of Surgery/Otolaryngology, UCSD School of Medicine, 9500 Gilman Drive MC0666, La Jolla, CA 92093, USA;

²Department of Surgery/Otolaryngology, UCSD School of Medicine, 9500 Gilman Drive MC0666, La Jolla, CA 92093, USA; ³San Diego VA Medical Center, 3350 La Jolla Village Drive, San Diego, CA 92161, USA

Background

L1, a neural cell adhesion molecule of the immunoglobulin superfamily, is widely expressed in the nervous system and important in axonal outgrowth, guidance, synapse formation, and signaling. Gene deletion studies emphasize the significance of L1 during development of the central nervous system and L1 is crucial for the topographic targeting of retinal axons. In contrast to the brain and retina, the role of L1 in the inner ear is largely unknown. While previous studies have localized L1 in the developing inner ear of the chicken and

mouse, its function during the innervation of the cochlea still remains largely unclear. We therefore investigated the functional role of L1 in the mammalian inner ear. Our aim was to determine whether or not L1 can modulate type I and/or type II spiral ganglion neuron outgrowth using an *in vitro* alternate choice assay.

Methods

Spiral ganglion explants of neonatal (postnatal day 5) Sprague-Dawley rats (for type I spiral ganglion neuron experiments) or neonatal (postnatal day 2) C57/BL6 mice (for type II spiral ganglion neuron experiments) were cultured on L1 coated culture plates. Uniform coating of the whole surface or 100 μ m alternating stripes of L1 and the neutral substrate poly-L-lysine were evaluated.

Results

We found that L1, presented in stripe micropatterns, provides directional cues to neonatal rodent type I but not type II inner ear spiral ganglion neurites. Because L1 influences rodent type I neurite direction and/or termination preference, we evaluated whether it might also affect neuritogenesis or neurite growth rate. When spiral ganglion explants were cultured on a uniform L1-coated surface (0.1, 1 or 5 μ g/ml, respectively), the number of neurites per explant did not differ from the number on control explants grown on 5 μ g/ml poly-L-lysine. Similarly, the length of neurites did not differ between growth on L1, as above, and control explants grown only on 5 μ g/ml poly-L-lysine.

Conclusion

Immunohistochemistry in the developing mouse cochlea was much stronger in the area near the inner hair cell when compared with the outer hair cell region (Whitlon et al. 1999, *Neurocytol* 28:955–968). This correlates with our results that L1 may play a role in axonal pathfinding of type I spiral ganglion dendrites toward their inner hair cell targets, but not of type II toward the outer hair cells.

PD - 019

Suppression of the Geranylgeranyl Pyrophosphate Pathway Stimulates Neurite Growth From Spiral Ganglion Neurons

Donna Whitlon; Mary Grover

Northwestern University

Background

Very few compounds are known to stimulate the growth of neurites from spiral ganglion neurons. Various authors have commented on the desirability of developing interventions to regrow these neurites after damage to the cochlea for the purpose of improving the function of cochlear implants and to reconnect neurons to disconnected hair cells. Because testing thousands of compounds on animal models of hearing loss is impractical, we developed a novel, *in vitro*, phenotypic screening procedure to pre-evaluate thousands of compounds for their effects on neurite growth from cochlear neurons. The overall aim will be to promote the most promising to in depth evaluation in an animal deafness model.

Methods

Dissociated cultures of newborn mouse spiral ganglia are plated in 384 well plates in the presence of BDNF, NT3 and serum. From 8 mouse pups, 196 cultures can be prepared. Cultures are maintained for 22 hours before compounds are added. Compounds are tested in quadruplicate. After 24 hours, the cultures are fixed, immunolabeled with an antibody against the neuronal specific Beta III tubulin and the nuclei are labeled with Nuclear yellow. Cultures are automatically imaged at 16 images per well (80% of the surface area) and the neurites are measured with the assistance of computer software. Forty five compounds and three controls can be tested with one dissection.

Results

In our phenotypic screen of 480 compounds of the NIH Clinical set, we identified cerivastatin as a compound that increased the lengths of regrowing neurites from mouse spiral ganglion neurons. Dose response studies of cerivastatin and 5 other HMG-CoA inhibitors demonstrated that all but one increased the lengths of neurites in this assay. The lowest effective doses of the active inhibitors differed and their activities ranged from highest to lowest as follows: cerivastatin=fluvastatin>simvastatin=lovastatin> atorvastatin. Pravastatin up to 25 microM had no activity in this assay. Stimulation of neurite length occurred with no effect on the number of neurons in the culture dish. The effect of fluvastatin on neurite length was reversed by supplying geranylgeraniol, a precursor to geranylgeranyl pyrophosphate, which in turn is a substrate for the enzymatic geranylgeranylation of a variety of proteins.

Conclusion

These studies suggest that geranylgeranylated protein(s) are normally involved in slowing the growth of the neurites, and that inhibition of the formation of geranylgeranyl pyrophosphate by inhibiting the formation of its precursors is one way to stimulate growth and elongation of neurites from spiral ganglion neurons.

PD - 020

Glutamate Excitotoxicity and Neuroprotection in the Cochlea

Jean-Luc Puel

Institute for Neurosciences of Montpellier

Background

Intense sound stimulation results in various structural changes leading to functional auditory impairment. Early studies have attempted to correlate the functional impairment with stereocilias of the hair cells. More recently, Liberman's group reported direct evidence showing that massive inner hair cell (IHC) ribbon synapse loss can be a primary result of sound exposure, even when there is no loss of sensory hair cells (Kujawa and Liberman, 2009; Lin et al., 2011).

Methods

One feature of the cochlea's acute response to acoustic overstimulation is a massive swelling below the IHCs, most probably resulting from excess of glutamate release from the inner hair cells.

Results

In cochlea'guinea pigs, swelling of auditory nerve terminals can be prevented by intracochlear perfusion of glutamate antagonists (kynurenate, quinoxalones, GYKI) during the noise exposure, and can be mimicked by perfusion of glutamate agonist (i.e., kainate and AMPA; Puel, 1995). In contrast to noise exposure, intracochlear AMPA disrupted all the IHC-auditory nerve synapses along the tonotopic axis. More intriguing, SGN regenerated their terminals and formed new functional synapses within 5 days after AMPA perfusion. This synaptic repair was also confirmed by the full recovery of CAP thresholds and amplitudes.

Conclusion

The discrepancies between noise-induced loss of afferent fibers and synaptic repair after AMPA perfusion can be reconciled if we consider that noise exposure induces additional injury of the presynaptic element. Finally, our presentation will discuss adapted pharmacological strategies to protect and/or promote the repair of ribbon synapses in excitotoxicity-related hearing loss.

PD - 021

Thyroid Hormone Regulates Pruning of Afferent Type I and Type II During Cochlear Neuronal Development

Qing Fang¹; Srividya Sundaresan²; Diana Mendus²; Dasom Lee²; Felix Wangsawihardja²; Rose Leu²; Sally Camper¹;

Mirna Mustapha²

¹University of Michigan; ²Stanford University

Background

The maturation of the organ of Corti involves axonal growth and co-ordination of a massive rearrangement of afferent and efferent fibers and synapses. These processes take place during the thyroid hormone (TH) critical period of cochlear development, in the perinatal period for mice and in the third trimester in humans. Here, we report the characterization of a mouse model of severe, secondary hypothyroidism (*Pit1dw*) with profound, congenital deafness.

Methods

Using quantitative RT-PCR, we measured expression of afferent pre and postsynaptic genes. Peripherin-GFP crossed to *Pit1dw* mice and immunostaining were used to assess the number of afferent synapses and neurons. Confocal and Velocity 3DImage analysis was applied for synapses and neurons quantification. Inner hair cells (IHCs) function was assessed using electrophysiological tests.

Results

Our data revealed abnormal persistence of temporary afferent type I neurite branching at the base of hypothyroid IHCs. IHCs function, however, is only slightly delayed and eventually matured by P24, independent of the extraneous afferent synapses. In addition to IHCs, afferent synapses of outer hair cells (OHCs) retained their immature innervation pattern into adulthood. Here we report that defects in hypothyroid OHC afferent synapse refinement are related to the lack of large-scale pruning of spiral ganglion SG type II neurons. In

addition to the altered pruning of the SG II, OHCs abnormally retain the expression of afferent presynaptic markers that are involved in neurotransmitter release, such as otoferlin. These proteins normally vanish from OHCs by the end of the first postnatal week in parallel with the regression of temporary afferent neurons (Roux et al., 2006).

Conclusion

Our studies reveal for the first time that the intrinsic requirement for TH in cochlear development is associated with pre- and postsynaptic afferent OHC and IHC refinement. A comparison of the cochlear transcriptome of *Pit1dw* mutant and wild type littermates revealed differential expression of genes that are involved in afferent synapse pruning in the brain and the retina, suggesting that these genes may mediate afferent refinement during cochlear development. Identification of such genes and their functions will enhance our understanding of the mechanism of TH action on synapse refinement in the brain and the peripheral nervous system.

PD - 022

Afferent Neuron Activity in Response to Single Neuromast Deflections in the Posterior Lateral Line System of Larval Zebrafish

James Liao; Otar Akanyeti; Aleksander Ballo; Melanie Haehnel; Rafi Levi

The Whitney Laboratory for Marine Bioscience

Background

At 5 days post fertilization, larval zebrafish (*Danio rerio*) are able to use their lateral line system to detect flow-related information.

Methods

To characterize the system, we performed electrophysiological recordings of posterior lateral line afferent neurons while deflecting individual neuromasts with a piezoelectric stimulator. We applied three distinct stimuli: a single deflection to look at the response to variations in deflection velocity (0.01 - 30 $\mu\text{m ms}^{-1}$), pure sine waves to test which frequencies (1 - 90 Hz) to which cells were most tuned, and a pulse that contained a broad frequency spectrum to quantify the ability of cells to transmit information at various frequencies.

Results

For single deflection stimuli, we found that maximum afferent spike rate increased with stimulation velocity, while the time delay between stimulus onset and maximum spike rate decayed exponentially as a function of velocity. For sine wave stimuli, we used firing rate and vector strength to characterize responses across frequency and found mainly one type of cell with band-pass qualities, although we did record several cells that exhibited high and low-pass qualities. For pulse stimuli, we found that spiking rate did not increase linearly with stimulation frequency. Rather, as stimulation frequency increased, cells transitioned from phase-locking with spontaneous activity to only phase locking, and finally to a decreased ability to phase lock. Cells with higher spontaneous firing rates showed a corresponding sensitivity to higher stimulus frequencies.

Conclusion

Our findings advance our understanding of vertebrate hair cell systems more broadly by revealing *in vivo* patterns of afferent activity in response to controlled, mechanical hair cell deflections.

Introduction to the Symposium

Larry Roberts

McMaster University

Research in the last two decades has suggested that the functional organization of central auditory structures is largely fixed after early development and is modified in the adult brain only by experience with sounds that have signal value. However recent research indicates that passive exposure to complex low level background sounds resembling those of many occupational work spaces can alter neuron response properties in the mature auditory system over wide swaths of cortical territory without threshold shifts, suggesting consequences for perception, hearing, and performance that are not well understood. This symposium, honoring Jos Eggermont for his many contributions to auditory neuroscience, will review evidence for effects of passive sound exposure on central and peripheral auditory function and consider implications for disorders of hearing (tinnitus, hyperacusis, impaired hearing in noise) and for public policy.

SY - 026

Central Changes After Hearing Loss and Their Implications in Tinnitus Mechanisms

Arnaud Noreña

University Aix-Marseille

Tinnitus, the phantom auditory perception, is a very debilitating symptom which can dramatically impair the quality of life. Recent research suggests that tinnitus is produced by central changes which are triggered by some degree of cochlear lesions. We start to have a good idea on the central changes accompanying hearing loss and that may underlie tinnitus (changes in the pattern of firing, time course of the central and peripheral changes, central levels at which the central changes occur, cross-modal plasticity...). In particular, noise trauma is followed by neural hyperactivity at virtually all levels of the central auditory system. A recent hypothesis suggested that this hyperactivity may result from an adaptive mechanism (homeostatic plasticity) adjusting neural sensitivity to the distribution of sensory inputs. From this point of view, tinnitus can be seen as a by-product of this adaptive mechanism. However, while this model postulates that tinnitus is caused by an increase of spontaneous firing in the auditory centers, it does not account for acute tinnitus induced immediately after trauma (as the spontaneous firing in auditory centers is not changed immediately after the trauma). I will present an overview of the central changes induced by hearing loss that are potentially involved in tinnitus mechanisms and I will discuss the merits and limits of a tinnitus model based on central gain adaptation.

SY - 027

Open Questions on the Effects of Persistent Exposure to Non-Traumatic Noise on Hearing Function

Martin Pienkowski

Salus University

see below

Background

Reduced sound input following hearing loss can trigger a compensatory increase in neural activity in primary auditory cortex (A1), which is thought to underlie hyperacusis and tinnitus. Recent studies in the Eggermont lab have shown that similar compensatory changes can be induced in the adult A1, albeit reversibly, by persistent exposure to moderately loud (~70 dB SPL), meaningless noise, in the absence of hearing loss.

Methods

We exposed groups of normal-hearing adult cats to various types of noise backgrounds at non-traumatic levels for several weeks to months.

Results

A main finding was that bandpass noise could lead to a long-lasting suppression of both spontaneous and sound-evoked A1 neural activity in tonotopic regions tuned to the noise band, and to an enhancement of activity in regions less responsive to the noise band. Moreover, bandpass noise could lead to an over-representation in A1 of sound frequencies outside of the noise band at the expense of frequencies within the noise band, a reorganization reminiscent of that resulting from a restricted (e.g., high frequency) hearing loss. There is some indication that persistent exposure to non-traumatic noise could adversely impact auditory perception, but this remains to be substantiated. An important question is whether the observed A1 map changes correlate to frequency-specific changes in loudness: i.e., are sound frequencies within the noise band heard as softer than normal (hypoacusis) while those outside of the noise band heard as louder than normal (hyperacusis)? Could the increases in A1 spontaneous activity and representational area for frequencies outside of the noise band lead to a percept of tinnitus? Could the loudness imbalance across frequency adversely affect speech intelligibility?

Conclusion

Much remains to be learned about this new manifestation of long-term auditory cortical plasticity, including whether or not noisy environments can lead to lasting "auditory processing disorders", including tinnitus, in the absence of damage to the cochlea and auditory nerve.

SY - 028

Environmental and Internal 'Noise' Impacts on Brain Maturation and Aging

Michael Merzenich

SY - 029

Similarities in Cortical Changes Following Traumatic NIHL and Long-Term Exposure With Non-Hearingloss Causing Sounds

Jos Eggermont

University of Calgary

Background

Exposure to a 6 kHz pure tone for 2-4 hrs at 115 dB SPL causes a PTS of ~40 dB above 8 kHz and results after 2-3 weeks recovery in silence in a reorganization of the tonotopic map in cat primary auditory cortex (AI), in such a way that neurons with a CF of 6-40 kHz, now show CFs in the 8-10 kHz range. Letting the cats recover for about 3 weeks in a dynamic enhanced acoustic environment (EAE) consisting of random frequency (4-20 kHz) tone pips at 80 dB p.e. SPL prevents both tonotopic map reorganization and hearing loss above 16 kHz. Adult cats were exposed continuously for weeks to months with band-limited (4-20 kHz) multi-tone sounds presented at 68 or 80 dB SPL. Multi-electrode arrays were used to record multi-unit activity and local field potentials from ketamine anesthetized cat primary auditory cortex.

Methods

Adult cats were exposed continuously for weeks to months with band-limited (4-20 kHz) multi-tone sounds presented at 68 or 80 dB SPL. Multi-electrode arrays were used to record multi-unit activity and local field potentials from ketamine anesthetized cat primary auditory cortex.

Results

Exposing normal hearing adult cats to the same EAE for 4-5 months, did not result in hearing loss (ABR), but resulted in a profound loss of sensitivity for cortical neurons in the 4-20 kHz range. Exposure to the same EAE at 68 dB SPL and for ~6 weeks, qualitatively showed the same loss of sensitivity, which recovered only incompletely after 3 months in quiet. Interestingly the recovery of sensitivity in the 4-20 kHz range was accompanied by tonotopic map changes in AI in that frequency region. A mechanism combining habituation and frequency-dependent changes in lateral inhibition can explain the curative effect after NIHL and the maladaptive effect in normal hearing animals.

Conclusion

A mechanism combining habituation and frequency-dependent changes in lateral inhibition can explain the curative effect after NIHL and the maladaptive effect in normal hearing animals. This maladaptive effect could be present in humans repeatedly exposed to spectrally imbalanced sounds in the workplace and may in the long run cause problems in speech understanding in the absence of audiometric hearing loss.

SY - 030

Primary Degeneration of the Cochlear Nerve in Noise and Aging: Putting the "Neural" Back in Sensorineural Hearing Loss

M. Charles Liberman; Sharon Kujawa

Massachusetts Eye and Ear Infirmary

Work on age-related and noise-induced hearing loss has focused on hair cell damage and permanent threshold shifts, because outer hair cells are among the most vulnerable cells in the inner ear, and their loss results in threshold elevation. The observation that hair cell loss can occur within hours of acoustic overexposure, while spiral ganglion cells do not degenerate for months, has suggested that hair cell damage is "primary" and cochlear neurodegeneration is "secondary" to hair cell death in sensorineural hearing loss. Our work in mice and guinea pigs has shown that primary degeneration of cochlear nerve terminals can be widespread, despite hair cell survival, in both aging and noise-exposed ears. The phenomenon has gone undetected for two reasons: 1) because the neural loss appears first as a synaptopathy revealed only by counting hair cell synapses in the electron microscope or after immunostaining for pre- and post-synaptic markers) and the subsequent degeneration of spiral ganglion cells is extremely slow, and 2) because diffuse neuronal degeneration is not detected by routine measures of cochlear function: a) DPOAEs are unaffected, because only pre-synaptic processes are required for their generation; b) ABR thresholds are unaffected, because the synaptopathy selectively targets cochlear neurons with high thresholds (and low spontaneous rates) and c) behavioral thresholds are unaffected, for the same reason as (b) and because stimulus detection requires less neural information than stimulus discrimination. We hypothesize that this selective low-SR neuropathy is rampant in humans, that it should cause problems in difficult listening situations and that it could initiate the CNS changes that contribute to tinnitus.

SY - 031

Adaptive Manipulation of Loudness by Changes in Low-Level Sound Exposure: Clinical Relevance

Craig Formby

The University of Alabama

Over a half-century period, from the early 1940's to the early 1990's, clinicians focused on therapeutic strategies using moderate- and high-level sound to attack two of the most intractable audiological conditions, namely, limited sound tolerance and tinnitus. In 1991, Hazell & Sheldrake (Proceedings of the Fourth International Tinnitus Seminar, pp. 245-248, 1992) described a novel sound-therapy application of low-level broadband noise to treat tinnitus patients, who also suffered clinically significant hyperacusis. The successful application of low-level sound therapy to treat tinnitus and hyperacusis subsequently became the foundation for Tinnitus Retraining Therapy (TRT). Notwithstanding numerous clinical reports over the past 20 years of successful applications of low-level sound therapy, principally in the TRT literature, randomized trials and controlled investigational studies

have been lacking. In this presentation, we will review our controlled studies of low-level sound therapy, which follow up and support Hazell and Sheldrake's seminal findings. We will show that the application of low-level sound therapy, in combination with specialized counseling (focused on hearing loss and a restricted dynamic range), can be applied successfully to expand the auditory dynamic range of typical hearing-impaired listeners, with or without primary tinnitus or hyperacusis. This promising treatment approach offers audiologists a new clinical tool to treat sensorineural hearing loss and to enhance hearing-aid benefit, with less reliance on wide dynamic range compression. [Research supported by NIDCD R01DC04678]

SY - 032

Cochlear Hearing Loss is a Misnomer; Nothing Happens at the Auditory Periphery Without Central Consequences

Robert Harrison

The Hospital for Sick Children, University of Toronto

Background

This symposium is in honor of Jos Eggermont, who has journeyed through all levels of the auditory system from electro-cochleography to single neuron responses in cortex. He has translated his basic science knowledge to clinical applications, for example in relation to sensorineural hearing loss, auditory neuropathy SD and tinnitus. Jos has proposed and often demonstrated that cochlear insults can have central consequences, and that the auditory system cannot be compartmentalized. In other words events at the auditory periphery can significantly alter the functional organization of the central auditory system. In this presentation this important concept is reinforced. At all times, but most significantly during early postnatal development, patterns of activity at the cochlear level can drive or alter the organization of central auditory areas. Example studies from the authors own work will demonstrate how cochlear lesions or abnormal (experimentally induced) activity patterns can modify central tonotopic maps.

Methods

Cochlear activity patterns are experimentally altered in neonatal animals (chinchillas pups or kittens) by lesioning with ototoxic drugs or by abnormal sound conditioning. Tonotopic (characteristic frequency) maps are derived from single unit recordings. Frequency mapping at the cortical level, and at thalamic and inferior colliculus (IC) levels are described.

Results

In lesion studies, a common finding is that cortical or IC regions that are effectively de-afferented (by peripheral lesions) become connected up to adjacent, normally active input neurons. This results in an expanded region corresponding to the lesion-edge frequency. This occurs at cortical and subcortical levels. In other studies using neonatal cochlear over-stimulation with a tonal signal, tonotopic map alterations also occur at cortical and IC levels. In these cases it appears that frequency map over-representation does not correspond to the

frequency of the conditioning signal, but rather to *the edge* of the activity pattern evoked by the conditioning signal.

Conclusions

The title of this presentation asserts that in cochlear hearing loss there are inevitable central consequences. The experimental lesions of the studies reviewed are equivalent to sensorineural hearing loss, and the effects of such peripheral lesions are seen throughout the auditory pathway. We are now beginning to appreciate that more subtle modifications to cochlear activity patterns can also alter central neural network organization.

Introduction to Neurotrophin *In Vivo* Function Revealed by Targeted Deletion

Bernd Fritzsch; Jennifer Kersigo

University of Iowa

In 1949, the late Nobel laureate R. Levi-Montalcini demonstrated that cochlea nucleus neurons critically depend on innervation from the ear for survival. Mutational analysis has demonstrated an embryonic critical phase of neuronal dependency on neurotrophins comparable to the neuronal dependency of cochlear nucleus neurons on innervation. Instead of the famous nerve growth factor discovered by R. Levi-Montalcini, two different neurotrophins (BDNF, NT3) and their specific receptors (TrkB and TrkC) have been identified in the ear and the combined mutation of either both ligands or both receptors cause complete loss of all neurons before birth. In the cochlea, the ubiquitous expression of the neurotrophin receptors, TrkB and TrkC, in all spiral ganglion neurons is matched with a continuous expression change of the two neurotrophins, BDNF and NT3, that bind to these receptors. As a consequence of these neurotrophin expression changes, loss of one neurotrophin or its receptor cause similar loss of spiral ganglion neurons in areas where at the time of the loss the other neurotrophin is not expressed and thus cannot compensate. Thus, innervation to the base is lost in either NT3 or TrkC null mice whereas innervation density in the apex is reduced in BDNF or TrkB null mice. More recent data have now extended these effects into neonates and adults using ear specific deletion of neurotrophins as either of the simple mutant mice is perinatal lethal. We will report novel observation on combined deletion of both neurotrophins in the ear that show surprising additional effects. Mice that lack neurotrophins only in the ear show a delayed loss of all neurons, maintained apparently by additional neurotrophic factors in the cochlea nucleus. However, when all afferents are lost after 2-3 weeks there is an enhanced premature loss of hair cells which have nearly disappeared by 4 months. Retaining at least on allele of either neurotrophin rescues many neurons and delays hair cell loss in areas with higher innervation retention. These data suggest that cochlear hair cells require some yet uncharacterized support released from neurons, possibly related to the molecularly unknown support for cochlear nucleus neurons. These mice provide therefore an excellent model for a somewhat accelerated, but not catastrophic hair cell loss, closer resembling human age-related hearing loss.

SY - 033

A New Twist to “Trophic Support”: The Roles of Supporting Cell-Derived BDNF and NT3 in the Postnatal Inner Ear

Gabriel Corfas¹; Guoqiang Wan¹; Maria Eugenia Gomez-Casati¹; M. Charles Liberman²

¹*Boston Children's Hospital*; ²*Massachusetts Eye and Ear Infirmary*

It is well established that the neurotrophic factors Brain Derived Neurotrophic Factor (BDNF) and Neurotrophin-3 (NT3) play critical roles in the developing inner ear, promoting the survival of embryonic auditory and vestibular sensory neurons and the establishment of their projections into their respective sensory epithelia. However, even though it is clear these factors and their receptors continue to be expressed in the postnatal and adult inner ear, their roles after birth remain poorly understood. We have used cell-specific inducible gene recombination to test the roles of the endogenous neurotrophins in the postnatal inner ear, and to identify the cells that act as sources of these factors. This talk will review our findings 1) on the distinct roles each neurotrophin plays in inner ear synapse formation and maintenance; and 2) on the identification of supporting cells as a key source of these neurotrophins in the postnatal inner ear.

SY - 034

Long Term Functionally Requirement of BDNF for Sound Processing Revealed by Conditional Gene Deletion

Marlies Knipper

Molecular Physiology of Hearing *Hearing Research Centre Tübingen, THRC*

Marlies Knipper¹, Tetyana Chumak³, Wibke Singer¹, Annalisa Zuccotti¹, Lewis Lee¹, Dario Campanelli¹, Stuart L. Johnson², Walter Marcotti², Josef Syka³, Thomas Schimmang⁴, Lukas Rüttiger¹

¹*Department of Otolaryngology, Head and Neck Surgery, Hearing Research Centre Tübingen, Molecular Physiology of Hearing, University of Tübingen, Elfriede-Aulhorn-Straße 5, 72076 Tübingen, Germany*

²*Department of Biomedical Science, University of Sheffield, S10 2TN, Sheffield, UK.*

³*Institute of Experimental Medicine AS CR, Prague, Czech Republik*

⁴*Instituto de Biología y Genética Molecular, Universidad de Valladolid y Consejo Superior de Investigaciones Científicas, E-47003 Valladolid, Spain*

Background

The precision of sound information transmitted to the brain depends on the transfer characteristics of the inner hair cell (IHC) ribbon synapse and its multiple contacting auditory fibers. Discharge rate and synchronicity of auditory fibers define the amplitude of sound induced brainstem responses.

Methods

We used two mouse lines with either a cell specific deletion of brain-derived nerve growth factor (BDNF) in the cochlea

and parts of the brainstem and midbrain (BDNF Pax2) or with deletion of BDNF within the entire brain (BDNF TrkC). We looked for molecular and functional differences pre and post acoustic trauma.

Results

We found that BDNF is essential for maintaining exocytosis in IHC synapses in high frequency cochlear turns as well as for maintaining proper targeting of associated afferent fibers within this region (Zuccotti et al Knipper 2012 J. Neurosci.). Comparison of this BDNF Pax2 mice with the BDNF TrkC mice revealed that IHC response characteristics pre and post acoustic trauma were triggered by BDNF in the cochlea and not by BDNF in the brain.

Conclusion

Extracellular recording of neurons in the inferior colliculus in BDNF Pax2 mice were performed. A surprising novel role of BDNF dependent steps for sound-processing was unraveled.

SY - 035

Neurotrophic Factor Expression and Function in the Cochlea Post-Trauma

Steven Green

University of Iowa

Neurotrophic factors (NTFs), especially BDNF and NT-3, have been extensively investigated regarding their roles in development of cochlear innervation. Several NTFs are expressed in the mature cochlea, including the neurotrophins BDNF and NT-3, GDNF family members GDNF, neurturin, and artemin, and the cytokine CNTF. Spiral ganglion neurons (SGNs) receive input from cochlear hair cells (HCs) and project from the cochlea to the cochlear nuclei (CN). After destruction of HCs with aminoglycoside, SGNs gradually die. It has been assumed that this is because HCs provide NTFs necessary for SGN survival. Consistent with this assumption is that providing NTFs after HC destruction reduces SGN death. Less consistent is that SGNs can survive for long periods after HC death: months in rodents, years in cats, decades in humans; in some circumstances of HC death, SGNs do not die.

Results from qPCR assay of NTF expression, in hearing and deafened rats, in the organ of Corti (OC) and CN, and from microarray-based gene expression profiling of the spiral ganglion, further imply that SGN death is not due to lack of NTFs. Although expression of NT-3 in the OC declines rapidly after kanamycin treatment, expression of other NTFs, e.g., neurturin and CNTF, is maintained in the OC throughout the period over which SGNs are dying, presumably in supporting cells. CNTF is also expressed in the CN and, with other NTFs, in the spiral ganglion throughout this period. Thus, NTFs known to be capable of supporting SGN survival are available to SGNs, from presynaptic, postsynaptic and autocrine/paracrine sources, even while SGNs are dying after HC loss. This can account for SGN survival after HC loss but raises the question of why SGNs can eventually die. Possibly, inflammatory events in the cochlea triggered by the initial trauma lead to neurodegeneration.

While NT-3 is not unique in ability to support SGN survival, it appears to have a special role, not shared by the closely-related neurotrophin BDNF, in promoting synapse regeneration in the cochlea. Glutamate excitotoxicity destroys synapses between inner hair cells (IHCs) and type I SGNs, some of which regenerate *in vitro*. Genetic substitution of BDNF for NT-3 allows regrowth of SGN neurites but not synapse formation after excitotoxic trauma. Genetic deletion of NT-3 from a random subset of IHCs impairs synapse regeneration on those IHCs. Synapse regeneration is rescued by adding NT-3 to the culture, but not by adding BDNF.

SY - 036

The Dynamic Electrophysiological Phenotype of Spiral Ganglion Neurons is Shaped by Neurotrophins

Robin Davis; Robert A.

Rutgers University

Spiral ganglion neurons possess both trkB and trkC high affinity receptors for brain derived neurotrophic factor (BDNF) and neurotrophin-3 (NT-3), respectively, and are thus capable of responding to both neurotrophins. While serving as an excellent model system to determine how neurotrophins shape firing patterns, experiments on spiral ganglion neurons have also yielded insights into the fundamental nature and complexity of neurotrophin interactions. For example, by evaluating the firing features and related voltage-gated ion channels and synaptic proteins in spiral ganglion neurons exposed separately to BDNF or NT-3, clear evidence has accrued for the idea that trkB and trkC high affinity receptors act through distinct intracellular signaling cascades. Furthermore, by examining the firing properties of neurons exposed to a series of NT-3 concentrations, the potential functional significance of NT-3 promiscuous binding has been revealed. Moreover, by observing the effects of NT-3 on specific electrophysiological characteristics, an argument for multiple signaling pathways for trkC receptor regulation of specific firing features can be made.

Future studies to uncover the full range of neurotrophin actions on spiral ganglion neurons will ultimately reveal much about developmental-dependence and functional impact, and will inform studies examining therapeutic applications of BDNF and NT-3.

SY - 037

Maintenance of Trophic Support to the Deafferented Auditory Nerve: Prospects for Clinical Therapy

Stephen O'Leary

University of Melbourne

Background

Cochlear injury or loss of hair cells is often associated with deafferentation of the auditory nerve. Without continuing trophic support surviving neurons undergo apoptosis, limiting prospects for future regenerative therapies and reducing the potential benefit gained from a cochlear implant. Here we address some of the considerations when entertaining a clinical

application for neurotrophins to maintain the auditory nerve in the pathological cochlea.

Methods

Review

Results

Neurotrophins have a short half-life, and in most models of disease their trophic (survival) effect is lost within weeks of withdrawal. Thus, in chronic disease sustained administration is required which is a major challenge. Slow-release polymers may be engineered to provide more prolonged delivery, but other approaches such as gene therapy or neurotrophin production from implanted cells (that may be encapsulated to minimise immune recognition) are required to achieve sustained release. It is important to consider the time course of the cochlear disease when considering how, and whether, neurotrophins may be a therapeutic option. Deafferentation with degeneration of the peripheral axon occurs when the synapse with the inner hair cell is lost, either through an excitotoxic injury or death of the hair cell. Spontaneous reinnervation of IHCs can occur *in vitro* (and possibly *in vivo*) and this is promoted by the exogenous application of neurotrophins. Therefore, during an acute cochlear injury a short period of neurotrophin treatment may be effective in protecting the auditory nerve by either reducing deafferentation or increasing regeneration and synaptogenesis with hair cells. However, in slowly progressive hearing loss, sustained delivery will be required and this is more difficult to implement. It is worth noting that neurotrophins not only increase the survival of auditory neurons, but may also increase their sensitivity, leading *in vivo* to a reduction in auditory thresholds for electrical stimulation of the auditory nerve and also acoustic stimulation of the cochlea. Consequently, it is possible that neurotrophins could potentially be a medical treatment for sensorineural hearing loss. Neurotrophins hold particular promise in the field of neural engineering of the inner ear. Regeneration of peripheral axons towards cochlear implant electrodes may significantly increase the number and density of implant channels, which it is thought should improve auditory perception, particularly for music and speech discrimination in noise. Axonal growth is promoted by neurotrophins, and may be directed towards a cochlear implant electrode with axonal guidance cues.

Conclusion

The earliest clinical applications for neurotrophins will be to treat acute cochlear injury.

SY - 038

Small Molecular TrkB Agonist Drug Development for Rescuing Neurons in the Absence of Hair Cells or Neurotrophins

Keqiang Ye

Emory University School of Medicine

Background

Brain-derived neurotrophic factor (BDNF) and neurotrophin-3 (NT-3) play essential roles in cochlear development and are required for spiral ganglion neurons (SGN) survival. Most sensorineural hearing loss cases occur as a result of the loss

of hair cells that secrete neurotrophins for promoting the neuronal survival, resulting in secondary degeneration of spiral ganglion neurons (SGNs).

Methods

Through cell-based screening, we have recently identified a flavone family of small molecules that act as TrkB receptor agonists, which bind to TrkB receptor extracellular domain and induce its activation. Systemic administration of 7,8-dihydroxyflavone (7,8-DHF) penetrates brain blood barrier and triggers TrkB receptor activation in central nerve system without demonstrable toxicity, mimicking the physiological functions of BDNF in various neurological disease models. Notably, it exerts the therapeutic efficacy in a TrkB receptor-dependent manner. To improve the oral bioavailability of this compound, we have synthesized a large number of prodrugs of 7,8-DHF and examined the oral bioavailability.

Results

we developed the prodrugs and improved 7,8-DHF's oral bioavailability from 4.6% to more than 50% without formulation manipulation. Application of 7,8-DHF in the bulla of conditional connexin26 (cCx26)-null mice dramatically rescues SGNs in the applied ear compared to untreated control cochlea in the same animal.

Conclusion

Our findings suggest that 7,8-DHF and its derivatives are promising therapeutic agents protecting the SGNs from degeneration both *in vitro* and *in vivo*. Hence, preservation of SGNs by 7,8-DHF prodrugs in the cochlea of patients suffering sensorineural deafness caused by loss of hair cells may be useful for the optimal performance of the cochlear implant.

PD - 024

Effect of Pulse Rate and Polarity on the Sensitivity of Cochlear and Auditory Brainstem Omplant (ABI) Users to Electrical Pulse Trains

Robert Carlyon¹; John Deeks¹; Colette McKay²

¹MRC Cognition & Brain Sciences Unit; ²Univ. Manchester

Background

1) We tested two classes of explanation for the surprising finding that ABI users' thresholds do not drop substantially with increasing pulse rate above 250-500 pulses-per-second (pps): a) greater adaptation at high rates, b) fast-acting processes such as refractoriness or charge interaction between successive pulses. 2) Cochlear implant (CI) users are more sensitive to anodic than to cathodic current, and this finding has been used to provide greater control over the place of excitation. We tested polarity sensitivity in ABI users.

Methods

Experiments 1-3 measured single-electrode thresholds for symmetric biphasic pulses presented in monopolar mode to 7 NF2 users of the Cochlear Corp. ABI and to 5 CI24M CI users. Pulse rates were 71, 500, and 3500 pps. Signal duration was 40 or 400 ms (Experiment 1) or between 2-34 ms (Experiment 2). In Experiment 3 the phase of each pulse was either fixed or alternated from pulse to pulse. Experiment 4

presented ABI users with quadruphasic pulses generated by abutting two symmetric pulses with opposite leading polarity, an 8-microsecond gap between pulses, and a 52-microsecond interphase gap. Threshold and loudness for 99-pps trains were compared for conditions where the two central phases were either anodic ("QP-A") or cathodic ("QP-C").

Results

For 400-ms pulse trains, CI users' thresholds dropped by 3.9 dB from 71 to 500 pps and by 7.7 dB from 500 to 3500 pps. In contrast the corresponding drops for ABI users were 2.2 and 0.6 dB. Similar results were obtained at the 40-ms duration. Threshold differences between 500 and 3500 pps were much smaller for ABI than CI users even at the shortest durations (e.g. 2 ms) tested. ABI users' thresholds were lower for alternating-polarity than for fixed-polarity pulse trains, especially at 3500 pps. This effect was larger than for CI users ($p=0.051$). Both thresholds and balanced loudness levels were lower for QP-A than for QP-C pulse trains.

Conclusion

ABI users' thresholds do not drop substantially between 500 and 3500 pps. This is true even at very short durations, thereby arguing for an explanation involving fast-acting processes such as refractoriness and/or charge interaction, rather than adaptation. The effect of alternating polarity on threshold provides some evidence for greater charge interaction in ABI users. Like CI patients, ABI users are more sensitive to anodic than cathodic current. This raises the possibility of exploiting asymmetric pulses to provide greater control of the place of excitation in ABI users.

PD - 025

Gene Transfer of Chronos to the Cochlear Nucleus: Implications for the Optogenetically-Based Auditory Brainstem Implant

Elliott Kozin¹; Keith Darrow²; Hight Ed²; Ashton Lehmann²; Maryanna Owoc²; Edward Boyden³; Chris Brown²; Daniel Lee²

¹Massachusetts Eye and Ear infirmary / Harvard

Medical School; ²Massachusetts Eye and Ear Infirmary;

³Massachusetts Institute of Technology

Background

Since the inception of the auditory brainstem implant, hearing outcomes have varied widely across users. One possible explanation for this variability may be limited auditory selectivity due to the spread of electrical stimulation. One approach to improving outcomes has been to increase the number of electrode channels, but electrode 'cross-talk' is a limiting factor. An optogenetic-based auditory brainstem implant may be able to increase number of potential channels. Recent work with channelrhodopsin-2 (ChR2) has demonstrated the feasibility of this technique; however, its kinetics appear slow for optimal function in the auditory system. We investigate a newly developed opsin, Chronos, which offers faster kinetics and, thus, may better convey speech signaling.

Methods

CBA/CaJ mice age 6–8 weeks were anesthetized, a left craniotomy was performed, and an adeno-associated viral vector with ChR2 or Chronos fused with a fluorescent protein was injected into the cochlear nucleus (CN). After 4–6 weeks recovery, the left dorsal CN (DCN) and right inferior colliculus (IC) were exposed via craniotomy. Multi-unit recordings from the IC central nucleus (ICc) were conducted in response to acoustic stimulation and optical stimulation via a blue-light laser fiber (473nm wavelength) placed on the surface of the DCN. At the conclusion of the experiment, the brainstems were extracted and the extent of viral infection was studied.

Results

Optical stimulation of the CN in ChR2- and Chronos-infected mice evoked spiking activity throughout the ICc with similar firing rates per pulse. The synchronization index (SI), a measure of synchronization to the stimulus pulse rate, peaked at ~0.4 below 50 Hz and was <0.1 above 50Hz in ChR2-mice. In contrast, in Chronos mice, the peak SI was 0.98 for frequencies <50 Hz and SIs ≥ 0.5 were maintained at stimulation rates up to 400 Hz. An optically driven ABR (oABR) was demonstrated in both ChR2- and Chronos-mice. No light-driven responses were demonstrated in control cases. Histology confirmed infection of CN neurons with both ChR2 and Chronos opsins.

Conclusion

Our results demonstrate the potential of a newly developed light-sensitive ion-channel, Chronos, to be used with an optical neuroprosthetic device in the auditory system. Compared to ChR2, it better maintains synchronization at higher rates of neural firing, important for the relay of speech signals along the central auditory pathway. Efforts are ongoing to analyze the extent of Chronos infection within the CN and compare this to neural recordings.

PD - 026

Identifying Inner Ear Trauma With a Three Dimensional Force Measurement System

Ersin Avci¹; Tim Nauwelaers²; Thomas Lenarz¹; Volkmar Hamacher²; Andrej Kral¹

¹Hannover Medical School; ²Advanced Bionics

Background

Intracochlear trauma caused by the insertion of a cochlear implant electrode array is analyzed after the electrode array has been implanted. Histology and computerized tomography (CT) are the main imaging techniques used for this analysis. To understand the electrode array mechanics, and the dynamic interaction with the human cochlea, we used a combination of a highly sensitive 3-axis force measurement with synchronized microscopic video recordings.

Methods

All experiments were performed on human temporal bones. The inner ear was removed from the temporal bones and dissected. To obtain a clear view of the osseous spiral lamina and the basilar membrane, we removed the bony capsule which covers the scala vestibuli. The temporal bone was then mounted on the 3D force measurement system (Agilent

technologies, Nano UTM, Santa Clara, USA) and a lateral wall electrode array was inserted using a fixed speed by an automated arm. Forces were recorded in 3 dimensions with a sensitivity of 2 μ N. The corresponding angular planes are as follows: Z-forces are recorded in the direction of insertion (horizontal plane), y-forces are recorded in the cochlear vertical plane and x-forces are recorded in the direction orthogonal to "Z" and "Y". The obtained 3D force profiles were correlated with microscopic recordings offline.

Results

Preliminary data show that the z-force is the dominating force present during insertion. Depending on the insertion angle through the round window, trauma to the modiolar wall occurred and was seen as a peak in the z-force profile of approx. 15 mN. Buckling of the proximal part of the electrode array was identified as a rapid rise in forces, mainly in the x-plane. The main force (z-force) started to increase approx. 8 mm from the round window. The amplitude of the z-force is an indication of friction between the electrode carrier and the lateral wall. Penetration of the electrode array through the basilar membrane was identified as an increase of the y-Force of approx. 10 mN. Repeated trials in the same temporal bone showed almost identical force profiles.

Conclusion

3D insertion forces convey detailed information about the electrode mechanics inside the cochlea. We were able to identify the main dynamic effects of a lateral wall electrode array and correlate to possible trauma to the inner ear during the insertion process by using this highly sensitive 3D force measurement system.

PD - 027

High-Resolution Secondary Reconstructions Using Flat-Panel CT in the Clinical Assessment of Patients With Cochlear Implants

Alexis Roy¹; Monica Pearl²; Charles Limb²

¹Harvard Medical School; ²Johns Hopkins University

Background

Cochlear implant (CI) electrode placement contributes to variability in audiologic outcomes. Previous studies suggest that radiologic assessments of the angular insertion depth may provide important prognostic indicators, and information for optimizing speech coding strategies. However, current computed tomography (CT) imaging modalities are limited, mainly due to device-related streak artifacts and the high density of the temporal bones. Post-procedure application of high-resolution secondary reconstructions offers the potential to minimize voxel size and reduce streak artifacts to improve current image quality. In this study, we developed a methodology for applying high-resolution secondary reconstructions to flat panel CT (FPCT) images. We applied this methodology to assess CI course and measure angular insertion depth of the most apical electrode in 18 cochleae with CIs.

Methods

Fourteen CI users (including four bilateral users) implanted with a Med-El standard 31.5-mm electrode array ($n=17$ cochleae) or a Med-El medium 24-mm array ($n=1$ cochlea) underwent FPCTs of the temporal bone. Post-procedure, high-resolution secondary reconstructions were performed under the following parameters: manually generated smaller VOI to include only the electrode array (voxel size of 0.07-0.08 mm), Hounsfield Units (HU) kernel type, and sharp image characteristics. Images were analyzed for their ability to document the insertion site, electrode array course, and individual electrode contacts. To measure angular insertion depths, coronal oblique views were created in which a clear reference line from the insertion point to the center of the apical turn could be delineated. Degrees of rotation of the most apical electrode around the modious were measured for all 18 cochleae.

Results

FPCT with high-resolution secondary reconstruction greatly improved image quality and spatial resolution (smaller voxel size) from standard FPCT procedures. The insertion site, CI course, and all individual electrode contacts could be visualized with minimal artifact. Precise measurement of angular insertion depth (mean = 591.9, SD = 70.9, range 280 degrees for standard arrays) was calculated for all CIs.

Conclusion

FPCT with high-resolution secondary reconstructions provide a useful tool for visualizing the course and individual electrode contacts of CI arrays, and for measuring angular insertion depth. This method provides superior post-operative information about CI placement than current imaging methods and has the potential to provide important prognostic information.

PD - 028

The Effect of Music Therapy and Training on Speech and Music Perception in Cochlear-Implant Users

Rolien Free; Christina Fuller; Bert Maat; Deniz Başkent
University of Groningen, University Medical Center Groningen

Background

Music is reported to be the second most important acoustical stimulus by cochlear-implant (CI) users. Normal-hearing musicians have been shown to have better speech perception in noise, pitch perception in speech and music and voice timbre recognition, as well as a better working memory and enhanced neural encoding of speech. Previous literature has shown that enjoyment and perception of music in CI users is worse than in normal-hearing listeners. Based on these ideas, we explored the hypothesis that music therapy and musical training may have a positive effect on speech and music perception in CI users.

Methods

We aim to recruit three groups of 7 CI users with no professional musical background for six weeks of music therapy, musical training and non-musical training for 2 hours per

week. Music therapy will involve group activities related to rhythm, musical speech, singing, emotion recognition and improvisation. Musical training will involve individual computerized training with melodic contour identification and instrument recognition. Non-musical training will involve group activities of cooking, working with wood and writing. Outcome measures vary. After each music therapy session, CI users will report if they observed improvement on the tasks. Furthermore, before and after the study, all participants will be tested for speech intelligibility, and speech- and music-related tasks, such as gender categorization, emotion recognition and melodic contour identification. Last, quality of life (QoL) will be measured using questionnaires.

Results

The results showed that music therapy in 7 CI users has a positive effect on emotion recognition, both behaviorally and subjectively measured. No other effects were shown in the music therapy group. The data from the other training groups are incomplete. The preliminary data with the musical training group showed an improvement on melodic contour identification for the organ. The preliminary data with the non-musical training group showed no effect on music perception and QoL.

Conclusion

While the full set of results are still to be determined, preliminary data showed indications for positive effects of training. Music therapy has a positive effect on emotion recognition in CI users, and musical training on melody contour identification with organ. These positive effects might point toward the implementation of some form of music therapy or training in the rehabilitation of CI users.

PD - 029

Musician Effect: Does it Matter for Cochlear-Implants?

Christina Fuller¹; John J Galvin²; Rolien Free¹; Deniz Başkent¹

¹*University of Groningen, University Medical Center*; ²*House Research Institute*

Background

Normal hearing (NH) musicians have been shown to have better speech understanding in noise, better musical pitch and timbre perception, better working memory, and enhanced cognitive linguistic processing at cortical, subcortical and brainstem levels, compared to non-musicians. However, the benefits of music training are sometimes quite modest for speech perception. It is unclear whether music training could also improve speech and music perception in cochlear implant (CI) users, who experience significant signal degradation with electric rather than acoustic stimulation. This study investigated the musician effect, the combined effect of past and current musical training and involvement, in NH musicians and non-musicians listening to an acoustic simulation of CI. We hypothesized that the musician effect would persist under conditions of spectral degradation.

Methods

Twenty-five musicians and twenty-five non-musicians participated in the study. The test battery included speech intelligibility tests (CVC-words and sentences presented in quiet and in noise), perception of voice pitch cues in speech (voice gender categorization and vocal emotion recognition) and music perception (melodic contour identification with multiple instruments). Performance in all tasks was measured with unprocessed stimuli and with an 8-channel sine-wave CI simulation.

Results

A small positive musician effect was shown for recognition of CVC-words with the CI simulation, but not with unprocessed speech nor for sentence recognition in quiet or noise (with or without the CI simulation). There was a significant musician advantage for voice gender categorization and vocal emotion recognition, although post-hoc testing did not reveal specific advantages in any of the test conditions, apart from the normal emotion recognition condition. There was a significant advantage for musicians in the melodic contour identification task for both unprocessed signals and the CI simulation.

Conclusion

Literature showed that the musician effect does seem to have an overall positive effect on both speech and music perception and cognitive processing in young and, some situations also older, normal-hearing listeners. Our test battery, however, showed a modest overall musician effect for speech related tasks and a strong positive effect for the melodic contour identification. Taken together this could indicate that musical training might have beneficial effects on the perception of pitch in speech related tasks and on melodies and timbre in CI-patients.

PD - 030

Implications of Rate Pitch on Music Perception and Auditory Object Formation in Cochlear Implants

Bomjun Kwon; Trevor Perry

Gallaudet University

Background

While the pitch of sound in cochlear implants (CIs) is typically controlled by the location of stimulating electrodes, it has been known that pulse stimulation rate, if in the lower range (below approximately 300 Hz), can also influence the pitch—known as “rate pitch.” CI users are able to recognize familiar musical melodies when presented with stimulation delivered on a single electrode using only rate pitch, where pulse rate is adjusted according to the frequencies of the melody (Pijl & Schwarz, *J Acoust Soc Amer* 98, 886-895, 1995). In the present study, we examined auditory grouping and segregation in CI users based on rate pitch, where musical melodies were presented on two electrodes with independent adjustment of stimulation rates.

Methods

Four post-lingually deafened Nucleus CI users with substantial experience in musical activities after implantation partic-

ipated in the study. In experiment 1, one melody was presented on an apical electrode while a more basal electrode delivered the same melody but in one of the following higher keys: major 3rd, perfect 4th, perfect 5th, major 6th, major 11th and perfect 8th (i.e., octave) or unison. Subjects were asked to judge each presentation with regard to perceptual consonance using a scale from 1 to 10, with 10 indicating highest consonance. In experiment 2, two independent sequences of musical notes were simultaneously presented on two electrodes and subjects were asked to recognize the sequences. The sequences of 8 notes consisted of ascending and descending major scales and arpeggio scales of chords, all of which the subjects were able to reliably identify when presented in isolation. Stimulation was controlled with NIC2 (Nucleus Implant Communicator) for precise timing control and timing conflict resolution.

Results

Initial results showed higher consonance ratings for octave and unison presentations than other conditions, demonstrating for the first time that stimulation on two electrodes can be grouped based on rate pitch if the temporal periodicity of stimulation follows a harmonic relation, which is akin to auditory grouping of a tone complex based on harmonic frequencies in acoustic hearing. Second, rate pitch appears to create salient pitch percepts which were sufficient to elicit the perception of polyphonic music, which is extremely challenging to convey in current CIs. These results call for further investigation of rate pitch and its perceptual effects.

Conclusion

Rate pitch has potentially important implications in auditory grouping with CIs.

PD - 031

Signaling Pathways That Control Zebrafish Hair Cell Regeneration by Balancing Differentiation and Amplifying Proliferation

Tatjana Piotrowski; Linjia Jiang; Andres Romero-Carvajal
Stowers Institute for Medical Research

Background

Non-mammalian vertebrates, such as zebrafish regenerate hair cells, whereas mammals do not. We identified the dynamic changes in signaling pathways in zebrafish lateral line support cells during the first few hours of hair cell regeneration. Zebrafish is the only regenerating species that enables such a precise time course as hair cell death occurs within 30min and regeneration happens quickly. To test the function of the identified signaling pathways we performed detailed cell fate analyses of regenerating support cells in control larvae and larvae in which these molecular signals are experimentally abrogated. This assay allows us to test the roles of these pathways in hair cell regeneration in unprecedented detail and informs us which pathways need to be manipulated at what stage to allow hair cell regeneration in mammals.

Methods

We performed whole transcriptome RNA Seq on FACS isolated control and regenerating support cells. Cells were collect-

ed at 1, 3 and 5 hours post hair cell death to determine the earliest changes in signaling pathways during hair cell regeneration. Cell fate analyses of regenerating support cells was performed using 72 hour time lapse movies, as well as BrdU labeling assays.

Results

In contrast to previous reports, the Notch and Wnt pathways are downregulated 1h post hair cell death. Such a drastic downregulation does not occur after injury in mammals, which could be one of the reasons why mammals fail to restore hair cells. Cell fate analyses revealed that during homeostasis support cells either divide to make more support cells (amplifying divisions) or they divide and differentiate into hair cells. Both amplifying and differentiating cell divisions occur in two discrete dorsal and ventral proliferative regions. In contrast, during regeneration differentiating divisions become homogenously distributed. This shift in proliferation patterns is controlled by downregulation of Notch signaling and its interaction with other pathways. Even though in many other organ systems, Wnt/ β -catenin signaling is described as being crucial for regeneration, our studies show that Wnt/ β -catenin signaling is not involved in triggering the regenerative response.

Conclusion

Our studies provide an important framework for identifying the pathways and the appropriate stages after injury to manipulate signaling pathways in the mouse that may allow us to test whether restoration of a functional sensory epithelium is possible in mammals.

PD - 032

In Vitro Hair Cell Regeneration Induced by Ectopic Expression of Atoh1 in Adult Mouse Cochlea

Wenyan Li^{1,2}; Yilai Shu^{1,2}; Zhengmin Wang²; Huawei Li²; Zheng-Yi Chen¹

¹Eaton-Peabody Laboratory, Massachusetts Eye and Ear Infirmary, Harvard Medical School; ²Eye Ear Nose and Throat Hospital of Shanghai medical school, Fudan University

Background

In human, the loss of inner ear hair cells leads to permanent hearing loss and vestibular dysfunction. Hair cell regeneration in mature inner ear is an essential route to achieve restoration of hearing and vestibular function. Atoh1 is necessary and sufficient to induce new hair cells by supporting cell transdifferentiation. However hair cell regeneration has not been achieved in adult mammalian cochlea *in vitro* by Atoh1 expression.

Methods

We used the explant culture system recently established for adult mouse whole cochlea, with the well-preserved overall architecture, to evaluate the effect of adenovirus mediated Atoh1 (Ad-Atoh1) delivery into the supporting cells. Lineage tracing was used to study the origin of new hair cells.

Results

12 days after Ad-Atoh1 infection, cells labeled with differentiated hair cell markers including Myo7a, My6 and Parvalbumin were identified. Further Espin and phalloidin labeling identified stereocilia that were co-labeled with Ptpqr. By dye uptake and showed Esp-positive cells were able to take up FM1-43. Thus in cultured adult cochlea Atoh1 overexpression induced production of new hair cells, which are highly differentiated and possess functional transduction channels. Regenerated hair cells were seen in both the sensory and the non-sensory regions. Using a Sox2-promoter driven Er-tMt (tomato-red) transgenic mouse model, we demonstrated new hair cells were derived from supporting cell transdifferentiation. Multiple supporting cells were able to transdifferentiate. By Tuj-Myo7a labeling, we showed that adult spiral ganglion in the co-culture of cochlea were able to form contact with regenerated hair cells. Finally no proliferation was induced in cultured adult cochlea by Atoh1 overexpression.

Conclusion

Robust hair cell regeneration in cultured adult cochlea contrasts with recent reports that Atoh1 failed to regenerate hair cells in cochlea *in vivo*, strongly indicating a reprogramming process by which cultured adult supporting cells respond to Atoh1, similar to young supporting cells. The use of adult culture system enables us to better control environment and gain insight into the mechanism underlying regenerative potential that will advance hair cell regeneration in adult inner ear *in vivo*. Co-culture with spiral ganglions provides a unique opportunity to study hair cell-neuron interaction *in vitro*. Our system can be adapted for other studies including drug screening, evaluation of degeneration of hair cells due to genetic mutations and analysis of neurofiber regrowth.

PD - 033

In Vivo Synergistic Effects of Wnt/ β -Catenin and Atoh1 Ectopic Expression on Lgr5+ Supporting Cell Proliferation and Hair Cell Transdifferentiation in the Postnatal Mouse Cochlea

Bryan Kuo¹; Emily Baldwin²; Makoto Taketo³; Jian Zuo¹

¹St. Jude Children's Research Hospital; ²University of Bath; ³Kyoto University

Background

Lgr5 is a Wnt signaling target gene that has been proposed to be a stem cell marker and is expressed in the inner ear during the first week of postnatal development. We hypothesize that these Lgr5+ supporting cells (SCs) might represent the progenitor/stem cells of the postnatal mouse inner ear with potential for hair cell regeneration. We previously discovered that overexpression of β -catenin induces proliferation of Lgr5+ SCs at neonatal ages but without transdifferentiation. We recently reported that overexpression of Atoh1, a transcription factor necessary for hair cell (HC) differentiation, converted postnatal mouse cochlear SCs to immature HCs *in vivo*. Here, we examined the effect of ectopic expression of Atoh1 on the transdifferentiation of the β -catenin-overexpressing proliferating Lgr5+ SCs.

Methods

The Lgr5-EGFP-IRES-CreER;Rosa-floxed-stop-beta-catenin knock-in mice were crossed with the CAG-flox-STOP-flox-Atoh1-HA+ transgenic mice. Offspring were induced with tamoxifen at P0-1 and cochlear whole-mounts were analyzed at various postnatal ages for the expression of various HC markers. In addition, we analyzed the proliferative effect of this combination on proliferation by BrdU/EdU incorporation.

Results

The combined ectopic expression of Atoh1 and beta-catenin in Lgr5+ SCs results in the generation of supernumerary HCs. In addition, we observe that this combination resulted in an increased mitotic index (compared to beta-catenin alone), and a greater number of supernumerary HCs (compared to Atoh1 alone), with no apparent endogenous HC death.

Conclusion

The combination of beta-catenin and Atoh1 overexpression has a synergistic effect on the proliferation and differentiation of neonatal cochlear Lgr5+ SCs *in vivo*. We are further characterizing their maturation and viability, and the potential therapeutic application of the overexpression of beta-catenin and ectopic Atoh1.

PD - 034

High-Throughput Screening for Potent P27Kip1 Transcriptional Antagonists for Hair Cell Regeneration in Mammalian Cochleae

Jian Zuo; Brandon Walters; Wenwei Lin; Shiyong Diao; Mark Brimble; Luigi Iconaru; Taosheng Chen
St. Jude Children's Research Hospital

Background

p27^{Kip1} (p27), a known cell cycle inhibitor, plays a key role in maintaining quiescence of supporting cells (SCs) in postnatal mammalian cochleae. *In vitro* and *in vivo* studies have raised the possibility of using p27 antagonists to trigger hair cell (HC) regeneration in mammalian cochleae. p27 is a well-known intrinsically disordered protein that is difficult, if not impossible, to develop inhibitory compounds at the protein level. Here we aimed to identify potent p27 transcriptional antagonists in a robotic high-throughput screen (HTS) of a large chemical compound library. From the candidate hits identified, we aimed to further characterize molecular targets to identify novel pathways for p27 transcriptional regulation.

Methods

We transfected HeLa cells with a p27 promoter (4 kb) driven luciferase reporter construct. We chose cycloheximide as a positive control at 167 μ M that produced optimal repression of luciferase as 100% inhibition. Z' factor was 0.74 \pm 0.06. Cell viability was monitored by measuring Alamar blue activity. A library of 4,359 unique compounds containing the FDA-approved and bioactive compounds was first screened at a final concentration of 10 μ M.

Results

119 compounds demonstrated \geq 50% luciferase inhibition but \leq 30% drop in cell viability. Dose response curves of luciferase and Alamar blue activities of the 119 hits were obtained in a

secondary screen using robots. We further eliminated compounds that repress generalized transcription by transfecting HeLa cells with a SV40 promoter driven lacZ vector and measuring the luminescence signals. Finally, we confirmed their inhibitory effects on endogenous p27 transcription in three independent cell lines (MEF, HeLa, and HEK) and resulting reduction at p27 protein levels. Thus far, we have identified 12 compounds that display potent inhibitory effects of p27 transcription at IC₅₀ (~0.2-50 μ M). For our top compound, we have further demonstrated its inhibitory effects of p27 mRNA in mouse cochlear explants. From this top compound, we also discovered and confirmed a molecular target and pathway that has not been appreciated in regulating p27 transcription.

Conclusion

We have identified >12 potent p27 transcriptional antagonists in cell lines and in cochlear explants. This discovery allowed us to identify a molecular target and pathway for p27 transcription. It is our hope that these p27 transcriptional antagonists will help facilitate HC regeneration in mammalian cochleae either by themselves or in combination with other compounds.

PD - 035

siRNA Therapeutics for Restoration of Hearing and Balance

Swetlana Adamsky¹; Esperanza Bas²; Jennifer Brantley³; Jae Yun Jung⁴; Igor Mett⁵; Sharon Avkin-Nahum⁵; Anat Brafman⁵; Hagar Kalinski⁵; Hagit Ashush⁵; Yehoash Raphael⁴; Hinrich Staecker³; Thomas R Van De Water²; Elena Feinstein⁵

¹Quark Pharmaceuticals, Inc; ²University of Miami Ear Institute, University of Miami, FL, USA; ³Department of Otolaryngology, Head and Neck Surgery, University of Kansas School of Medicine, Kansas City, KS, USA; ⁴KHRI, Otolaryngology, Head and Neck Surgery, The University of Michigan, Ann Arbor, MI, USA; ⁵Quark Pharmaceuticals Inc., Research Division, Nes Ziona, Israel

Background

Hearing and vestibular dysfunctions represent significant public health problems, affecting around 48 million and 69 million Americans, respectively. There are no specific pharmacological treatments currently available. Accumulating evidence suggests that some of the supporting cells in the inner ear can transdifferentiate into sensory hair cells upon ectopic expression of Math1/Atoh1 transcription factor in these cells. Expression of Atoh1 in supporting cells can be achieved by either forced expression or by inhibition of Notch signaling. Our data indicate that siRNA can be efficiently delivered to inner ear structures in both small and large animals. Hence, we investigated whether siRNAs targeting selected genes in the Notch pathway can be effective in initiating the regeneration of damaged inner ear sensory epithelia and promote recovery of lost balance or hearing function in animal models of hearing and balance disorders.

Methods

Three animal models were utilized: two mouse models of toxic vestibular damage (monaural or binaural), and a rat model

of aminoglycoside-induced hair cell loss. In all animal models, target siRNAs or their combinations were introduced after complete hair cell loss, by local administration via the posterior semicircular canal, or the round window membrane. Functional assessments of balance and hearing functions were performed by serial Rotarod balance tests or by measuring ABR thresholds, respectively. Myosin VIIa-positive cells were counted in utricles or cochleae harvested upon termination of the study.

Results

In animal models of toxic vestibular damage, post-insult treatment with Hes5 siRNA alone[1] or in combination with siRNAs targeting additional Notch pathway genes resulted in increased Atoh1 expression, increase in the number of utricular sensory hair cells and partial restoration of otherwise lost balance function, as documented by Rotarod balance testing. Likewise, treatment of animals with a cocktail of siRNAs targeting members of the Notch pathway following induction of toxic damage to auditory hair cells also caused small but significant time-wise decreases in the ABR thresholds compared to permanent ABR threshold increases recorded in control vehicle-treated animals. Morphological examination showed more myosin VIIa-positive cells in the cochlea of siRNA-treated animals as compared with cochleae of control vehicle-treated animals, indicating the presence of newly generated hair cells. Moreover, well-organized rows of these hair cells were observed in some of the siRNA-treated cochlea.

[1] Jung JY et al, *Mol Ther*. 2013 Apr;21(4):834-41

Conclusion

Our data suggest that RNAi provides an effective therapeutic approach to restoration of balance and hearing function by promoting regeneration of inner ear sensory epithelia.

PD - 036

Characterization of Hair Cell-Like Cells From Cochlear and Vestibular Stem Cells

Will McLean¹; Ruth Anne Eatock²; Albert Edge²

¹Harvard-MIT; ²Harvard Medical School

Background

The cochlea and vestibular organs each contain two hair cell subtypes. Inner and outer hair cells in the cochlea differ in patterns of gene expression, which are reflected in their sensitivity to aminoglycosides, bundle morphology and function. Type I and II hair cells in the vestibular organs express unique genes and have different shapes, synaptic contacts, and microvillar bundle characteristics. Patch clamp measurements have shown that these four hair cell subtypes differ in their ion channels and transduction properties. The developmental signals determining if an immature hair cell acquires a vestibular or cochlear fate remain elusive, and even less is known about how the subtypes within each organ emerge. By using a combination of molecular gene expression assays and patch clamping, these studies should help to define signaling pathways that lead to differences in gene expression and help determine whether inner ear stem cells are restricted to differentiate in to their respective organs' hair cell types.

Methods

Cochlear and vestibular tissues were dissected from Atoh1-nGFP mice at P1-P4 and each tissue was processed separately and treated identically for the remainder of the experiments. Stem cells were expanded as spheres and passaged 4 times to remove any native hair cells, and were then differentiated for 7-80 days by removing all added growth factors from the culture medium. Patch clamping, immunostaining, and RT-PCR were used to characterize the differentiated cells from each tissue. Differentiating cells that expressed nGFP were studied further as hair cell candidates.

Results

The Atoh1-positive cells derived from the two organs' stem cells differed in phenotype. Atoh1-positive cells from the vestibular organs exhibited typical vestibular hair cell currents such as outwardly rectifying K_v currents and h-current. Cochlear-derived cells possessed outwardly rectifying K_v currents but lacked h-current, which is similar to preparations of acutely prepared hair cells from the two organs. Furthermore, cochlear-derived cells, but not vestibular-derived cells, expressed the cochlear outer hair cell gene, prestin. Na_v currents were not detected in cochlear or vestibular derived cells.

Conclusion

Differentiated stem cells from both the cochlea and vestibular organs possess typical hair cell proteins and ion channels. However, hair cells from the cochlea and vestibular organs differ in characteristics specific to the cochlear or vestibular phenotype, and the vestibular or cochlear phenotype stays consistent with the source of the stem cells, suggesting restrictions in their capacity to differentiate.

PD - 037

Progenitor/stem Cells from the Human Inner Ear

Pascal Senn¹; Amir Mina¹; Stefan Volkenstein²; Veronika Kranebitter⁴; Kazuo Oshima³; Stefan Heller³

¹Inner Ear Research Laboratory, University Department of Otorhinolaryngology, Head & Neck Surgery, Inselspital, 3010 Bern Switzerland; ¹Inner Ear Research Laboratory, University Department of Otorhinolaryngology, Head & Neck Surgery, Inselspital, 3010 Bern, Switzerland; ²Department of Otorhinolaryngology-Head and Neck Surgery, Ruhr-University of Bochum, St. Elisabeth-Hospital, 44787 Bochum, Germany; ³Departments of Otolaryngology – Head & Neck Surgery and Molecular & Cellular Physiology, Stanford University, Palo Alto, CA 94305-5793 USA;

⁴Department of Otorhinolaryngology AKH, Medical University of Vienna, 1097 Vienna, Austria

Background

The loss of inner ear hair cells leads to incurable balance and hearing disorders because these sensory cells do not effectively regenerate in humans. A potential starting point for therapy would be the stimulation of quiescent progenitor cells within the damaged inner ear. Inner ear progenitor/stem cells, which have been described in rodent inner ears, would be primary candidates for such an approach. Despite the identification of progenitor cell populations in the human fetal co-

chlea and in the adult human spiral ganglion, no proliferative cell populations with the capacity to generate hair cells have been reported in vestibular and cochlear tissues of adult humans. The present study aimed at filling this gap by isolating sphere-forming progenitor cells from surgery-derived and autopsy-derived adult human temporal bones in order to generate inner ear cell types *in vitro*.

Methods

Sphere-forming and mitogen-responding progenitor cells were isolated from vestibular and cochlear tissues. Clonal spheres grown from adult and fetal human utricle and cochlear duct were propagated for a limited number of generations and then differentiated into inner ear cell types.

Results

When differentiated in absence of mitogens fetus derived stem/progenitor cells from vestibular and cochlear tissues robustly gave rise to inner ear cell types such as hair cell-like cells, supporting cell-like cells and neuronal cell types. From adult human tissues, only utricle-derived spheres gave rise to hair cell-like cells, as well as to cells expressing supporting cell-, neuron-, and glial markers, indicating that the adult human utricle harbors multipotent progenitor cells. In contrast to fetal tissues and the adult utricle, spheres derived from the adult human cochlear duct did not give rise to hair cell-like or neuronal cell types, which is an indication that human cochlear cells have limited proliferative potential, but lack the ability to differentiate into major inner ear cell types without additional manipulation.

Conclusion

The generation of human inner ear cell types from fetal or adult surgery-derived or postmortem temporal bones is feasible. The availability of differentiated inner ear cell types in culture provides an interesting platform for further physiological, translational or drug screening studies.

PD - 038

The Ultra-Structural Change of Epidermis Attached to the Bony Wall of Scala Tympani May Be Helpful in the Migration of Mouse Embryonic Stem Cells Transplanted Into the Cochlear of Rats With Aminoglycoside Induced Hearing Loss

Lidong Zhao; Dengke Li; Jianhe Sun; Weiwei Guo; Shiming Yang

Chinese PLA General Hospital

Background

As the hair cells in the mammalian cochlear are not able to spontaneously regenerate when they are injured or under go apoptosis and necrosis, sensory neural hearing loss caused by noise or aminoglycoside antibiotics are not curable at present. Stem cells can be a promising candidate material in treating this kind of hearing loss due to the loss of hair cells or spiral ganglion neurons. In one of our previous research, we noticed that the stem cells transplanted in to the tympanic scala of normal rats didn't migration, while those transplanted into tympanic scala of rats with aminoglycoside induced hear-

ing loss could migrate into the scala media across the bony barrier. We proposed that the epithelia attached to the bony wall of scala might underwent certain ultra-structural change after the administration of aminoglycoside antibiotics, which, together with the numerous small micropores in the bony wall of scala tympani, facilitate the migration of stem cells transplanted into this compartment.

Methods

30 rats randomly divided into experiment group (n=20) and control group (n=10). For the experiment group, amikacin sulfate are injected hypodermically at a dose of 200mg/kg/day for seven days and the control rats were injected physiological saline of the same volume instead. The cochlear were removed 0d, 7d, 14, 21d, 28d when the amikacin administration finished. One random side of cochlea was prepared for SEM observation and the other cochlea for HE examination.

Results

Micatin sulfate administrated to the rat can induce hearing loss and at the same time, the epithelia on the bony wall of scala tympani underwent serial ultra structure change such as inflammatory exudation, enlarge of the intercellular space and recovery in a time dependent manner.

Conclusion

Besides injury and loss of the hair cells in the Organ of Corti, amikacin sulfate treatment could also induce the ultra structure change on the bony wall of scala tympani which might be the structure base for the transplanted stem cell migration from scala tympani in the cochlea.

PD - 039

The Role of Transmembrane Channel-Like Proteins in Hair Cell Mechanotransduction

Robert Fettiplace¹; Kyunghye Kim¹; Maryline Beurg²; Shanthini Mahendrasingam³; Carole Hackney⁴; David Furness³

¹University of Wisconsin - Madison; ²Department of Neuroscience, University of Wisconsin, Madison, USA.;

³Institute of Science and Technology in Medicine, Keele University, Keele, UK.; ⁴Biomedical Science, Sheffield University, Sheffield UK.

Background

Transmembrane channel-like (Tmc) proteins comprise a family of eight isoforms, two of which, Tmc1 and Tmc2, occur in the inner ear and are central to hair cell transduction (Kawashima et al 2011). Mutations in Tmc1 cause deafness in humans, DFNA36 and DFNB7/11, and in mice, *deafness* (dn) and *Beethoven* (Steel & Bock 1980; Kurima et al. 2002; Vreugde et al. 2002) but the functional defect is not well understood. Recently it has been claimed that Tmc1 and Tmc2 are pore forming subunits of the mechanotransducer (MT) channel (Pan et al. 2013).

Methods

We characterized MT currents in response to hair bundle deflections produced by fluid jets in isolated cochleas of neonatal mice with null mutations in Tmc1, Tmc2 or both. Hair

bundle morphology was examined using scanning electron microscopy of isolated cochleas fixed in 2.5 percent glutaraldehyde and processed with the OTOTO technique (Furness & Hackney, 1986).

Results

Mice with the *Tmc1* mutation 'dn' possessed MT currents in the first few neonatal days, but the current in outer hair cells (OHCs) declined after postnatal day (P)6 (Kim & Fettiplace, 2013). The MT channels in 'dn' mutants up to P6 had a larger calcium permeability and reduced single-channel conductance compared to wild-type, these effects being most prominent at the high-frequency base. Recordings from *Tmc1/Tmc2* double nulls in P2 to P6 mice showed OHCs still exhibited MT currents but with anomalous properties. The current responded on the opposite phase of hair bundle displacement and was blocked by FM1-43, dihydrostreptomycin and external calcium at concentrations similar to wild-type. Importantly, the MT current was unaffected by exposure to sub-micromolar calcium buffered with BAPTA which abolishes MT currents in wild-type. OHC hair bundles of P6 double nulls examined with scanning electron microscopy still retained tip links that were destroyed by BAPTA treatment. Prolonged exposure of wild-type OHCs to BAPTA initially abolished the MT current but over 10 minutes it returned, now responding on the opposite phase of bundle motion as in the *Tmc1/Tmc2* double nulls.

Conclusion

The results imply that the *Tmc* isoforms are not themselves pore-forming subunits of the MT channel but are essential for targeting and interaction of the channel with the tip link. Changes in the MT conductance and calcium permeability observed in *Tmc1* mutants may stem from loss of interaction with protein partners in the transduction complex.

PD - 040

Synchronization of Spontaneously Oscillating Hair Bundles

Tracy Zhang; Yuttana Roongthumskul; Dolores Bozovic
University of California, Los Angeles

Background

Under *in vitro* conditions, and decoupled from overlaying structures, hair bundles can spontaneously oscillate. These oscillations have been extensively studied in bullfrog sacculus, and they provide an insight into the active process in hair bundles. *In vivo*, the hair cells are often coupled by overlaying structures. The effect of such coupling on frequency selection and signal amplification has been studied with simulation. Our work studies the coupling of bullfrog hair cells *in vitro*.

Methods

After isolating the sacculus, we remove the otolithic membrane, leaving the hair bundles decoupled. We then couple several hair bundles artificially. One method is to use a glass capillary, which can be manipulated to attach to adjacent hair bundles. The second method is to use micro-sized glass beads, which are suspended in solution and could be deposited onto the hair cells. The first method couples two bundles, while the second method couples three to four. Both the glass

capillary and beads are coated with concanavalin A, to improve adhesion. The hair bundles are then imaged from a top-down view, with a high speed camera.

Results

We found that spontaneously oscillating hair cells can be synchronized by artificial coupling. With the beads method, up to four hair bundles can be synchronized. Oscillation profiles change with coupling. Hair bundles with disparate intrinsic frequencies can be synchronized to a frequency in between. We also observed multi-mode synchronization, where one hair cell can couple to the second harmonic frequency of several others. Applying external stimulus to the coupled hair cells has so far shown no improvement in frequency selectivity.

Conclusion

We were able to mimic the natural coupled state of hair cells, and show that several hair bundles can be synchronized and still spontaneously oscillate. Future work will focus on studying the effect of coupling on signal response.

PD - 041

Spontaneous Bundle Oscillations from Various Sensory Maculae of the Frog Inner Ear

Patricia M. Quiñones¹; Sebastiaan W.F. Meenderink¹;
Rylee J. Shumway²; Dolores Bozovic¹

¹*University of California at Los Angeles*; ²*Marlborough High School*

Background

The hair cell is the functional element of the inner ear which harbors the apparatus, the hair bundles with their mechanically sensitive channels and myosin-motor complex, which transduces mechanical vibrations into electrical responses. The response of hair bundles to incoming signals is highly nonlinear and active, and has been modeled using nonlinear dynamics. One prediction of these models is that, under specific conditions, hair bundles may move spontaneously in a limit-cycle oscillation. Such spontaneous oscillations have indeed been observed in hair cells from both the frog sacculus and the turtle basilar papilla. These observations were consistent with the nonlinear models. However, to our knowledge there are no reports of spontaneous bundle oscillations in other preparations. One possibility is that, while the active process is ubiquitous, spontaneous oscillations only occur in a few and relatively low-frequency organs. In the experiments described here, we searched for spontaneous oscillations in several end organs—which are vestibular and/or auditory in nature—that are found in the frog inner ear.

Methods

The frog ear holds eight end organs, each with its own sensory epithelium holding several to hundreds of hair cells. End organs were freshly dissected from *Rana catesbeiana*. For each of the end organs we studied thus far (i.e. sacculus, utricle, amphibian papilla) we developed a two-compartment recording chamber. This allowed the separation between perilymph and endolymph, a configuration that was shown to greatly enhance the presence of spontaneous bundle oscillations in the sacculus. Hair bundles were visualized with an upright mi-

croscope and their motion recorded with a high-speed CMOS camera.

Results

We hypothesize that spontaneous oscillations should be found in all end organ preparations. Recordings pose a challenge, however, because, unlike the flat sacculus, the other end organs have a 3D structure which makes visualization in a two-compartment configuration difficult. We have observed robust oscillations from utricular hair cells. In the amphibian papilla, we thus far only observed such oscillations for hair cells located in the medial part. These results indicate that the nonlinear dynamics underlying spontaneous oscillations may be generally applicable to hair cells in both vestibular and auditory frog end organs.

Conclusion

With these preliminary results, we have significantly increased the number of sensory end organs in which hair bundles are known to exhibit spontaneous oscillations. This includes an organ, the amphibian papilla, which is sensitive to frequencies in the auditory range.

PD - 042

Force Spectroscopy of Tip Link Proteins: A Study of Inner-Ear Biophysics

Mounir Koussa¹; Marcos Sotomayor²; Wesley Wong¹; David Corey¹

¹Harvard University; ²Ohio State University

Background

Hair cells in the inner ear convert mechanical stimuli, in the vestibular and auditory systems, into electrical signals which can be processed by the brain. Hair cells are highly polarized with a unique elaboration of modified microvilli at their apical surface known as stereo cilia. Sensory stimuli such as sound waves of a particular frequency will result in oscillations of the stereociliary bundle at that frequency. Movements of this bundle couple mechanically to the channel. This force acts to gate the channel in turn resulting in a mechano-electrical transduction. The force is relayed to the channel by filaments known as tip links. Tip links are made of two atypical cadherins, protocadherin-15 and cadherin-23 at the lower and upper ends respectively. The tip link is held together by a non-covalent interaction between two anti-parallel pairs of EC domains. Although much has been discerned about the biophysics of this system the lack of adequate technology has prevented the direct measurement of many of these properties.

Methods

We have developed molecular tools to facilitate the single molecule study of these properties. Self-assembled DNA nanoswitches are functionalized with protocadherin 15 and cadherin 23 fragments using the enzyme sortase. In order to preserve protein function, protein-DNA coupling is performed under physiological conditions. In this two-step process, a small synthetic peptide is first coupled to a DNA oligo. Next, utilizing the enzyme sortase, the protein is coupled to the DNA-peptide chimera under physiological conditions. This strategy frontloads all of the protein-incompatible chemistry so that it is performed on an oligo and a synthetic peptide,

which are far more tolerant of non-physiological conditions. Once assembled, the nanoswitches are then used in an optical tweezer system to measure the rupture forces of the tip link under different conditions.

Results

The data indicate rupture forces of ~36pN for a single tip-link pair at loading rates equivalent to 100-200 Hz stimulation. The zero-force off rate is estimated to be five minutes, and the off rate at resting tensions is estimated to be 1 minute. The distance to the transition state is calculated to be ~1.3nm.

Conclusion

These data suggest that having two interacting pairs in tandem may be crucial for tip-link integrity.

PD - 043

Effects of Cysteine Mutagenesis on Calcium Clearance Rates in PMCA2

Jennifer Thornton; Claire Watson; Bruce Tempel

University of Washington

Background

Calcium ATPase type 2 (PMCA2), encoded by the *Atp2b2* gene, is a transport protein in the plasma membrane that is responsible for rapidly and efficiently removing calcium from the cell. In the auditory system, PMCA2 is critical for removing calcium from hair cell stereocilia, and mutations in PMCA2 can result in various hearing-loss phenotypes, including deafness. While we know that PMCA2 is essential for calcium clearance, it is unclear which residues in the protein are the most essential to effectively remove calcium from the cell. Using cysteine residue replacements, we can determine which substitutions will result in a decrease in calcium pumping. Targeting these specific residues has important implications for identifying residues that alter calcium transport efficiency as well as providing information that may lead to identifying useful drug applications. Here, we use cysteine-scanning mutagenesis to alter residues lining the extracellular vestibule of PMCA2 and measure calcium clearance rates in these mutants via calcium uncaging.

Methods

Site-directed mutagenesis was used to introduce reporter cysteines into two different transmembrane domains, TM4 and TM6, in PMCA2. Each mutagenized fragment was introduced back into the original parent expression vector, a PMCA2 w/a variant with red fluorescent protein (RFP) to aid in live cell imaging. Mutant constructs were transfected into CHO-K1 cells using Lipofectamine 30-48 hours before imaging. Thirty minutes prior to imaging, Fluo4 calcium indicator and UV labile NP-EGTA are applied to the cells. Cysteine modifier 2-aminoethylmethane thiosulfonate hydrochloride (MTSEA) is also applied to the cells prior to imaging. Live cell imaging (Zeiss Axiovert Marianas) is used to measure calcium release from transfected cells following a 500 ms exposure to UV light. Only cells primarily expressing PMCA2 on the membrane are used for analysis, as this is most closely related to PMCA2's function *in vivo*. Mock transfected and vector only (RFP) constructs serve as controls.

Results

Cells with mutations in PMCA2 TM6 (residue Q909C) clear calcium ~90% slower than cells transfected with vector only (PMCA2-RFP) constructs. Additionally, there is no significant difference in calcium clearance rates between Q909C mutants and untransfected CHO-K1 cells.

Conclusion

Slower calcium clearance rates in PMCA2 mutants suggest that Q909C is a critical residue for effectively clearing calcium from the cell. Ongoing testing is currently being performed on other PMCA2 mutations.

PD - 044

Additional Actin-Binding Site in Large Espin Isoforms Affects Actin Bundle Size and Dynamics and Is Regulated by Autoinhibition and a Peptide in the Stereocilia Protein Myosin III

Lili Zheng; Dina Beeler; James Bartles

Northwestern University Feinberg School of Medicine

Background

Hearing and the vestibular sense rely on hair cell stereocilia that contain an actin bundle cytoskeleton with multiple classes of actin-bundling protein, but little is known about what each contributes. The espin actin-bundling proteins, which are the target of mutations that cause deafness and vestibular dysfunction, are required for the growth of stereocilia. Espins are produced in different sized isoforms from a single gene. Here, we characterize an additional actin filament-binding site that is present exclusively in the extended amino termini of the large espin isoforms, espin 1 and espin 2, and show that it can be regulated by autoinhibition and a peptide in myosin III.

Methods

In vitro binding assays and cell transfection assays, including fluorescence recovery after photobleaching, were used to characterize the additional actin filament-binding site in large espin isoforms. In addition, immunocytochemistry with affinity purified polyclonal antibodies was used to localize total espins and large espin isoforms in mouse utricle.

Results

The additional actin filament-binding site was mapped to a novel 13-residue peptide. The site was constitutively active in espin 2 isoforms and had a major effect on biological activity, increasing the size of actin bundles formed *in vitro* and blocking actin treadmilling in the microvilli of epithelial cells. In espin 1, which has an amino-terminal ankyrin repeat domain, the site was autoinhibited by interaction between the ankyrin repeat domain and a peptide near the actin-binding site. This peptide resembled tail homology domain I of myosin III, an espin 1-binding protein concentrated at the tips of stereocilia. Accordingly, a myosin III tail homology domain I peptide, but not scrambled control peptides, inhibited the binding of the ankyrin repeat domain to the internal peptide and released the actin-binding site of espin 1 from autoinhibition. Espin 1 was determined to be the major large espin isoform in mouse

vestibular hair cells, and, like myosin III, large espin isoforms were concentrated at the tip of stereocilia.

Conclusion

The large espin isoforms of hair cell stereocilia contain a regulatable actin filament-binding site in their extended amino termini. This actin-binding site has a major effect on actin bundle structure and dynamics. It could explain the espin requirement to increase stereocilium diameter and the lack of rapid actin treadmilling in stereocilia. The autoinhibition and activation by myosin III peptide could keep the actin-binding site of espin 1 under control until it encounters myosin III in stereocilia.

PD - 045

Deletion of PDZD7 Disrupts the USH2 Protein Complex in Cochlear Hair Cells and Causing Hearing Loss in Mice

Junhuang Zou¹; Tihua Zheng¹; Chongyu Ren¹; Charles Askew²; Xiao-Ping Liu²; Bifeng Pan²; Jeffrey Holt²; Yong Wang¹; Jun Yang¹

¹University of Utah; ²Boston Children's Hospital, Harvard Medical School

Background

Usher syndrome (USH) is the leading genetic cause of combined deafness and blindness. Among its three clinical types, type 1 (USH1) and type 2 (USH2) are the most severe and predominant form, respectively. *PDZD7* was recently reported to be implicated in USH2 and nonsyndromic deafness. It is a paralog of the *USH1C* and *USH2D (WHRN)* genes and encodes a protein with multiple PDZ domains. The biological function of *PDZD7* and the pathogenic mechanism caused by *PDZD7* mutations are currently unknown.

Methods

A *Pdzd7* knockout mouse model was generated and thoroughly characterized. In the *Pdzd7* knockout mice, the auditory function was tested by ABR, DPOAE and CM tests; the mechanotransduction in cochlear and vestibular hair cells was assessed by single cell recording; the morphology of inner ear hair bundles was examined by scanning electron microscopy; the integrity of the ankle link complex in hair cells and the periciliary membrane complex in photoreceptors was studied by immunofluorescence; and the vision function was evaluated by ERG test.

Results

The *Pdzd7* knockout mice exhibit congenital profound deafness, as assessed by ABR, DPOAE and CM tests, and normal vestibular function, as assessed by their behaviors. Lack of *PDZD7* leads to disorganization of stereocilia bundles and reduction in mechanotransduction currents and sensitivity in cochlear outer hair cells. At the molecular level, *PDZD7* determines the localization of the USH2 protein complex, composed of USH2A, GPR98, and WHRN, to ankle links in developing cochlear hair cells, likely through its direct interactions with these three proteins. The localization of *PDZD7* to the ankle links of cochlear hair bundles also relies on the USH2 proteins. In photoreceptors of *Pdzd7* knockout mice,

the USH2 proteins largely remain unchanged at the periciliary membrane complex. The electroretinogram responses of both rod and cone photoreceptors are normal in knockout mice at one month of age.

Conclusion

this study presents novel evidence suggesting the difference between the organization of the USH2 complex in hair cells and photoreceptors. More importantly, this study reveals that PDZD7 is a new component of the USH2 complex and plays an essential role in organizing this complex in cochlear hair cells. Our findings provide valuable insights into the pathogenic mechanism underlying USH and deafness as well as the cell biology of hair cells and photoreceptors.

PD - 046

Generation and Characterization of TRIOBP-5 (T5) Knockout Mouse Generation and Initial Characterization of Its Phenotype

Tatsuya Katsuno¹; Shin-ichiro Kitajiri¹; Kazuya Ono²; Kohei Segawa¹; Juichi Ito¹

¹Kyoto University; ²RIKEN, Center for Developmental Biology

Background

Inner ear hair cells detect sound through deflection of mechanosensory stereocilia. Each stereocilium is supported by a paracrystalline array of parallel actin filaments that are packed more densely at the base, forming a rootlet extending into the cell body. TRIOBP isoforms (abbreviated as T1, T4 and T5) are localized at these stereocilia rootlets. Mutations associated with human hereditary deafness DFNB28 affects T4/T5, and, T4/T5 deficient mice (Triobp Δ ex8/ Δ ex8) show profoundly deaf due to the loss of rootlets. T4 protein showed F-actin bundling activity, but the function of T5 has not been revealed yet. Furthermore, we still do not know which isoform, T4, T5 or both, is indispensable for hearing. To address these issue, we generated the T5 specific knockout mice.

Methods

To investigate the physiological roles of TRIOBP-5, we developed a knockout mouse model system. An overview of the creation of the TRIOBP-5 (T5) isoform specific knockout mice. The murine TRIOBP gene spans 58 kb on chromosome 15. Exons 9 and 10 which coding T5 specific sequences were chosen for deletion. Homologous recombination deletes exon 9 and 10 of Triobp and replaces it with a β -galactosidase reporter cassette. The removal of exon 9 and 10 ablates isoform 5 while bypassing the embryonic lethality resulting from loss of isoform 1. The first 7 base pairs of exon 9 were retained while the remainder was replaced inframe with a cassette containing a β -gal reporter that has a nuclear localization signal (nLacZ). Southern blot analysis shows the correct integration of the 5' and 3' arms of the targeting vector. Deletion of one or both alleles of the BACE gene conveyed no developmental disadvantage, as the genotypes were transmitted in numbers approximating those expected for Mendelian inheritance.

Results

T5 specific deficient mice (Triobp Δ ex9,10/ Δ ex9,10) mice are not profoundly deaf unlike T4/T5 deficient mice (Triobp Δ ex8/ Δ ex8), but likely to show moderate hearing loss. The age related hearing changes and morphological studies will be performed.

Conclusion

TRIOBP shows isoform specific functions in the inner ear. Isoform specific knockout mice will reveal function of each isoform, and shed lights on actin arrangement in the inner ear.

PD - 047

A Spatial Analysis of Hair Cell Development in the Mouse Crista

Amber Slowik; Olivia Bermingham-McDonogh
University of Washington

Background

By understanding how the hair cells of the inner ear sensory epithelia develop, both spatially and temporally, we gain two important tools. First, by understanding how the organs develop, we can recognize any perturbations in their development, for example caused by disease or the loss of genes. Second, we can recognize which areas of the sensory epithelia are the least mature and thus the most likely to still be developing, which is an important caveat to regenerative studies. While in the cochlea and utricle, previous work has characterized both the spatial and temporal development of these organs, very little is known about where and how hair cells are born in the mouse cristae. More specifically, how are hair cells added during development and what are the locations of these hair cells in the mature crista?

Methods

Timed-mated female Swiss Webster mice were given two intraperitoneal injections of 50 mg BrdU/kg of body weight in sterile saline. Injections were given three hours apart on one of the following days: embryonic day 9 (E9) through E17, determined by plug date where the morning of plug is E0.5, Theiler staging, and/or date of birth, which we defined as postnatal day 0 (P0). Cristae were isolated either on the day of injection or from P30 mice. Cristae were immunolabeled for BrdU, Gfi1 (hair cells), and Sox9 (support cells). Cristae were imaged as whole organs using a confocal microscope.

Results

As Ruben described, we found that most hair cells were born between 4-6 days before birth, which we defined as E12.5 to E14.5. These hair cells developed in a gradient on the longitudinal axis cutting through each hemicristae. The hair cells at the apex of each saddle-shaped hemicristae were born first while hair cells at the outer edges of each hemicristae underwent terminal mitoses last.

Conclusion

Here, we describe the spatial development of hair cells in the developing and mature mouse crista. This work, performed using more modern techniques, confirms Ruben's early temporal work using tritiated thymidine and further expands upon

it by adding the spatial dimension. This work not only shows how hair cells are added to the developing cristae over time, but where the hair cells born at different developmental ages are located in the mature organ.

PD - 048

Immunocytochemical Localization of Nebulin in Rat Vestibulo-Cochlear Hair Cells

Robstein Chidavaenzi; Steven D. Price; Anna Lysakowski
University of Illinois at Chicago

Background

The protein composition of vestibulo-cochlear hair cells is elaborate. One protein family at the core of hair cell function has been the actin family. From filamentous assemblages in the stereocilia and rootlets, cortical lattices of cell membranes, and organelles (such as the striated organelle, among others), actin has a storied and active presence in the sensory epithelia.

Methods

We used immunohistochemistry and western blotting, as recently reported (Lysakowski et al., 2011).

Results

We now report the presence of nebulin, a 600-900kDa actin-bundling protein, in vestibular and cochlear hair cells. Nebulin has been ascribed such roles as determination of actin filaments' length, and regulation of actin-myosin interactions in a calcium-calmodulin dependent manner in vertebrate skeletal muscles. With immunohistochemistry and western blotting, we set out to determine its expression and distribution pattern in *Rattus norvegicus* inner ear. Western blots show a single band of high molecular weight (>460 kDa) in vestibular and cochlear tissue. Co-immunoprecipitation experiments suggest associations with α -spectrin, β -spectrin, and g-actin. In the vestibular periphery, confocal microscopy shows nebulin in central calyx afferents and in the cuticular plate and striated organelle in adult type I and type II hair cells. In the early postnatal rat (P0-P6), nebulin is also expressed in the stereocilia (albeit not kinocilia), and cytoplasm of central, but not peripheral, hair cells of both types. In the cochlea, nebulin is more intense in the cuticular plate of inner, compared to outer, hair cells. In outer hair cells, it is also present in the basolateral cell membranes.

Conclusion

We intend to further characterize the observed labeling pattern and discuss the probable role that nebulin might be playing in inner ear sensory epithelia.

PD - 049

Sodium Channel Distribution in Vestibular Afferents – An Update

Anna Lysakowski; Steven D. Price
Univ. of Illinois at Chicago

Background

We have been investigating Na channel distribution with various Pan- Na_v and Na_v isoform-specific antibodies in vestibular afferents to determine the isoforms present at the AIS region of different classes of vestibular afferents. The sodium

channel isoform $\text{Na}_v1.6$ is the canonical sodium channel at the node of Ranvier and the axon initial segment, but we have previously found that this isoform is not present at pure calyx afferents (Lysakowski et al., JNS, 2011; Lysakowski and Price, ARO, 2013).

Methods

Methods used were similar to those used in our recent publication (Lysakowski et al., JNS, 2011), with the exception that most tissue was vibratome-sectioned rather than frozen-sectioned and lower concentrations (0.05%) of Triton X-100 were used.

Results

$\text{Na}_v1.6$ is present at the heminode of dimorphic vestibular afferents, but not at pure calyx afferent heminodes. The afferent class and location of the heminode were determined by co-labeling with calretinin (a calyx afferent marker) and nodal marker antibodies, such as ezrin, Caspr1, and myelin basic protein. We have continued our search for the Na_v isoforms in calyx afferents and now have new results from other isoforms, including $\text{Na}_v1.3$, 1.8, 1.9 and $\text{Na}_v\beta4$, in addition to various Pan- Na_v antibodies. Pan- Na_v and $\text{Na}_v1.9$ label the apical end of the calyx more intensely than expected in most afferents, and the label continues down to the heminode. The majority of calyx afferent heminodes are located above and the majority of dimorphic afferent heminodes below the basement membrane.

Conclusion

We conclude that while $\text{Na}_v1.6$ has a role as the major player at the vestibular dimorphic afferent heminodes, other isoforms, such as $\text{Na}_v1.3$, 1.8 and 1.9, are more prominent in pure calyx afferents and/or have supporting roles in dimorphic afferents.

PD - 050

Do Regional Variations in Calyx K^+ Conductances Contribute to Firing Properties in Crista Afferent Terminals?

Frances Meredith; Katherine Rennie
University of Colorado Denver, Anschutz Medical Campus

Background

Kv1 and KCNQ channels are believed to contribute to firing patterns in vestibular ganglion cells.

Methods

To investigate roles of these K^+ conductances in vestibular calyx afferent terminals, we developed a technique to slice the crista ampullaris transversely. Cristae from gerbils (postnatal days 17 - 29) were embedded in 4% low gelling temperature agarose and sliced to a thickness of 100 μm . Properties of calyx terminals in central and peripheral crista zones were compared using patch clamp techniques.

Results

Spontaneous action potential firing was observed in about 30% of recordings and was either regular or irregular. Firing persisted when mechanotransduction channels were blocked by 500 μM streptomycin sulfate, suggesting that calyceal ion

channels play a role in generating spontaneous action potentials. In voltage clamp, large outward voltage-dependent K⁺ currents were observed at depolarized potentials and varied considerably in their inactivation properties as reported previously in isolated calyces (Dhawan et al. JARO 11:463-476, 2010). Inactivation, expressed as percent reduction of peak current during a standard depolarizing voltage step had a median value of 9.4% in peripheral calyx terminals (n = 66), which was significantly different from the value of 4.2% in central calyces (n = 33; Mann-Whitney Rank Sum Test). CP 339818 (1 μ M), a Kv1.3 and Kv1.4 channel antagonist, reduced a slowly activating, slowly inactivating component of the whole cell current by 46.8% (\pm 7.8%, SEM, n = 4) during a 150 ms voltage step. 4-aminopyridine (1 mM) blocked a rapidly activating, rapidly inactivating K⁺ current, which served to enhance repolarization of spontaneous action potentials. XE991 dihydrochloride (20 μ M) reduced a slowly activating, sustained outward current in both peripheral and central calyx terminals, indicating the presence of KCNQ channels in both locations. However, mean reduction in peripheral calyces was 30.7% (\pm 4.45%, SEM; n = 8) which was significantly greater than the value of 17.6% (\pm 3.3%, SEM, n = 8; paired t-test) seen in central calyces. XE991 also reduced the frequency of spontaneous action potentials by about 50% in central and peripheral calyces.

Conclusion

Taken together, these results suggest that both inactivating and sustained outward K⁺ currents regulate spontaneous firing, but that the relative expression of underlying K⁺ channels may vary across the crista.

PD - 051

Non-Quantal Synaptic Currents in the Vestibular Calyx Terminal

Stephen Highstein¹; Mary Anne Mann¹; Gay R Holstein²; Richard D Rabbitt³

¹Marine Biological Laboratory; ²Mt. Sinai School of Medicine;

³University of Utah, Marine Biological Laboratory

Background

The vestibular calyx terminal is a unique postsynaptic structure that envelopes or cups one or more type I hair cells. In addition to glutamate-based quantal synaptic transmission (EPSC), there is also non-quantal synaptic transmission (nqEPSC) that is responsible for a majority of the excitatory charge entering the postsynaptic cell. Recording from calyces in the turtle lagenar macula suggested that an acid-gated channel might be involved in the genesis of this nqEPSC.

Methods

The lagenar epithelium was dissected, otoconia enzymatically removed and the tissue placed upon the fixed stage of an upright microscope for DIC and fluorescence imaging. We recorded from calyces with patch electrodes in the whole cell voltage clamp configuration. Electrodes were loaded with Lucifer yellow. A fluid jet and/or a piezo pusher were employed to deflect type I hair cell hair bundles.

Results

Calyceal recordings were confirmed by visualization of the Lucifer-filled terminal with its axon leaving the tissue. Type I bundles were identified by bundle size and the presence of a calyx surrounding the hair cell below the epithelial surface. Recorded terminals were voltage clamped at -60mV. In 70% of responsive cells, deflection of the hair bundle produced an amplitude graded nq inward post-synaptic current that persisted for as long as the bundle was held deflected, i.e., nqEPSC did not adapt. nqEPSC varied from 0 to 200pA depending upon the cell and the intensity of bundle deflection. While CNQX had no effect upon nqEPSCs, it reversibly blocked the quantal EPSC. Imaging pH sensitive dyes indicated that the synaptic cleft between the type I hair cell and calyx terminal became acidified following bundle deflection. Ionic substitution and current - voltage studies indicated that nqEPSC is carried by sodium and potassium in normal Ringers' but can be carried by potassium when NMDG is substituted for sodium. Varying the pKa of the pH buffer changed the nqEPSC onset and decay time constants; i.e., high pKa buffer slowed and low pKa buffer sped up the nqEPSC kinetics. Psalmotoxin, a specific ASIC1 blocker partially blocked the nqEPSC. Antibody staining demonstrated ASIC positive processes within the lagenar and semicircular canal epithelia.

Conclusion

Results suggest that nqEPSC results from proton gating of an acid-sensitive post synaptic channel. That the nqEPSC did not adapt to maintained bundle deflection suggests it reflects the tonic component of the transduction current. NqEPSC could convey low frequency and tonic signals, e.g. gravity.

PD - 052

Spontaneous and Evoked Quantal Synaptic Currents in the Vestibular Calyx Terminal

Mary Mann¹; Richard D Rabbitt²; Stephen Highstein¹

¹Marine Biological Laboratory; ²University of Utah

Background

We recorded spontaneous and evoked excitatory post synaptic currents (EPSCs) in vestibular calyx nerve terminals from the lagena of adult red-eared slider turtles, *trachemys scripta elegans*.

Methods

The lagenar epithelium was dissected, otoconia enzymatically removed and the tissue placed upon the fixed stage of an upright microscope for DIC and fluorescence imaging. We recorded from calyces with patch electrodes in the whole cell voltage clamp configuration. A fluid jet was employed to deflect hair cell hair bundles. DIC imaging was used to identify and patch calyx nerve terminals in the striola. The patch pipette contained Lucifer yellow which allowed the visualization of the terminal field using confocal microscopy and to subsequently image the full structure using two photon microscopy.

Results

Two-photon imaging revealed most calyces were dimorphic and complex, enveloping multiple type I hair cells and extending collaterals forming bouton synapses with one or more type II hair cells. Spontaneous EPSCs occurred at an

average rate of 52 s⁻¹ and, after correcting for series resistance and capacitance, had a mean size of 22 pA and a mean decay time constant of 584 μ s (from log-normal distributions). During maintained hair bundle deflection, EPSCs occurred at an average rate of 87 s⁻¹ and had distinct fast or slow kinetics depending on the particular hair cell stimulated. Fast EPSCs had a mean size of 26 pA and a mean decay time constant of 410 μ s, while slow eEPSCs had a mean size of 24 pA and a mean decay time constant of 650 μ s. On average, EPSCs carried ~20 fC event⁻¹. Deconvolution in the time domain suggests EPSCs might consist of a summation of unitary quantal events of size 16 pA and quantal charge ~14 fC event⁻¹. In most cells, increases in EPSC rate evoked by maintained hair bundle deflection adapted over time while in other cells increases in rate were tonic, i.e., non-adapting. Quantal EPSCs were often accompanied by a non-quantal EPSC that did not adapt over time.

Conclusion

These diverse inputs provide the calyx with very broad dynamic range with ability to encode tonic signals such as gravity and phasic signals such as vibration of low frequency sound.

PD - 053

Latent Herpes Simplex Type I Infection Reactivates Due to Nutrient Withdrawal

Pamela Roehm¹; Shruti Nayak²; Lifan He¹

¹Temple University School of Medicine; ²New York University School of Medicine

Background

Vestibular neuritis is the second most common peripheral cause of spinning vertigo. Many studies have found that vestibular neuritis results from herpes simplex type I (HSV1) reactivation in the vestibular ganglia. Using an *in vitro* cell culture system of HSV1 latency and reactivation our lab and others have previously implicated the PI3-kinase/ Akt/ mTOR signaling pathway in the maintenance of HSV1 latency. Involvement of mTOR signaling implies that HSV1 reactivation might be triggered by absence of key nutrients, because following cues from nutrient availability, mTOR signaling changes gene expression. In this study we use this *in vitro* system to determine whether nutrient withdrawal can induce HSV1 reactivation, and which nutrients can be reintroduced into the system to prevent reactivation.

Methods

Primary rat neuronal cultures were latently infected with HSV1 modified with a US11-green fluorescent protein (GFP) chimera. Percent baseline reactivation rates were assessed by fluorescent microscopy for GFP fluorescence and by viral titers of infectious virus. Trichostatin A was application was used to induce HSV1 reactivation as a positive control. Nutrient deprivation was performed by change of normal culture media to media lacking key nutrients: the amino acid leucine, all amino acids, insulin, glucose, intracellular calcium, and all divalent cations. During these experiments neurons continued to be maintained in the presence of neurotrophins. Cultures were monitored daily for GFP fluorescence. Media was

harvested 5 days following change in media for infectious viral particles. Total RNA was harvested from cells and assess for viral RNA production by reverse-transcription polymerase chain reaction.

Results

Reactivation of latent HSV1 occurred following deprivation of certain nutrients at substantially higher rates than baseline (3%). Following withdrawal of all amino acids, leucine alone, or all divalent cations, HSV1 reactivation occurred in 100% of wells. Following deprivation of glucose or insulin, HSV1 reactivation occurred at higher levels than baseline (45% and 22%) but with high variability between experiments. Supplementation of completely deprived media (Hank's balanced salt solution plus neurotrophins) with zinc sulfate prevented viral reactivation.

Conclusion

Withdrawal of certain nutrients causes HSV1 reactivation in cultured neurons. These findings further support the key role of mTOR signaling in HSV1 reactivation.

PD - 054

Mechanisms Underlying the Effects of Estrogen Deficiency on Otoconia

Yunxia Lundberg; Liping Yang; Yinfang Xu; Yan Zhang

Boys Town National Research Hospital

Background

Otoconia-related balance deficits and vertigo/dizziness (such as BPPV) are common. Our recent studies in humans show that, while BPPV prevalence greatly increases with age in both genders, peri-menopausal women are especially susceptible.

Methods

We used an ovariectomized mouse model to examine the effects of estrogen deficiency on otoconia maintenance and the underlying mechanisms, and devised an effective remediation strategy.

Results

We show that estrogen deficiency compromises otoconia maintenance and anchoring by reducing the expression of otoconial component and anchoring proteins, and that phytoestrogen is effective in rescuing the otoconia abnormalities. In addition, there is ectopic debris formation in the ampulla under estrogen deficiency due to aberrant matrix protein expression. By comparing the expression patterns of known estrogen receptor (Esr) subtypes and related proteins (Esrr), and by examining the otoconia phenotypes of null mice for selected receptors, we postulate that Esr2 may be the main receptor mediating the effects of estrogen on otoconia.

Conclusion

Estrogen deficiency compromises otoconia maintenance and anchoring, which can be effectively rescued by phytoestrogen. Esr2 may be the main receptor mediating the effects of estrogen on otoconia. Combined with future studies, the findings can help solve a profound clinical problem.

Functional Characterization of Stem Cell-Derived Hair Cells in the Inner Ear Organoid

Karl Koehler¹; Xiao-Ping Liu²; Andrew M Mikosz¹; Jeffrey R Holt²; Eri Hashino¹

¹Indiana University School of Medicine; ²Harvard Medical School

Background

Sensory epithelia in the inner ear contain mechanosensitive hair cells that detect auditory and vestibular stimuli. The controlled derivation of sensory epithelia from pluripotent stem cells will be essential for generating *in vitro* models of inner ear disorders or developing cell-based therapies. We recently established a novel 3D culture system capable of generating otic vesicles from an aggregate of pluripotent stem cells. Remarkably, the stem cell-derived otic vesicles developed into large cysts with a vestibular-like sensory epithelium containing supporting cells and hair cells, the latter of which were innervated by neurons. We have designated these stem cell-derived structures inner ear organoids. The goal of this study was to address two outstanding questions: 1) Are derived hair cells innervated by authentic inner ear neurons? 2) Are derived hair cells functional?

Methods

We used small molecule inhibitors and recombinant proteins to precisely control BMP, TGF β and FGF signaling during the first 8 days of 3D culture with aggregates of mouse embryonic stem cells. Cell aggregates were transferred to a long-term floating culture on day 8 to allow the self-organized development of inner ear organoids. From day 12 to 24, aggregates were examined for the expression of markers for inner ear neurogenesis. From day 22 to 26, organoids were dissected and individual hair cells were interrogated for functionality by single-cell patch-clamp recording and FM1-43 uptake assays.

Results

We found that the pattern of Myo7a staining in the E9.5 otic vesicle and delaminating neuroblasts provides a unique signature with which to identify otic neurogenesis *in vitro*. Between days 14-16, stem cell-derived otic vesicles produce Myo7a⁺ Brn3a⁺ Islet1⁺ TuJ1⁺ neuroblasts mimicking neurogenesis in the E9.5 otic vesicle. We stimulated stem cell-derived hair cells that had prominent hair bundles visible with DIC microscopy using voltage steps and hair bundle deflections. Preliminary measurements revealed evidence of large voltage-dependent delayed rectifier potassium currents and small fast inward currents characteristic sodium currents in immature vestibular hair cells. Furthermore, assays for selective uptake of FM1-43 and direct measurement of mechanotransduction currents suggested that some derived hair cells acquired mechanosensitivity.

Conclusion

These results strongly suggest that stem cell-derived hair cells in the inner ear organoid are mechanosensitive and innervated by authentic inner ear sensory neurons. This novel *in vitro* model properly recapitulates inner ear organogenesis

and thus can be used to gain deeper insight into inner ear development and disorder.

Heterogeneity of the Pluripotent HESCs Compartment and its Impact on the Generation of Otic Progenitors

Marcelo Rivolta; Sarah Jacob Eshtan; Darrell Barrott
University of Sheffield

Background

Otic progenitors can be derived from pluripotent, human embryonic stem (hES) cells using the ligands FGF3 and FGF10 in a serum-free, monolayer culture system. Two populations of progenitors are in this way obtained, namely otic epithelial progenitors (OEPs) and otic neural progenitors (ONPs). They differ in their phenotypic appearance, lineage potential and the distinct labelling pattern of the tight junction marker ZO-1. Despite their morphological differences, OEPs and ONPs share the same cohort of otic markers. In addition, significant improvement of auditory evoked response thresholds were observed when ONPs were transplanted to a model of auditory neuropathy.

A variable degree of heterogeneity has been described within the pluripotent hESC compartment. Cell fate decisions in stem cell populations can be substantially affected by these variations, generating lineage bias and becoming an important factor to consider when fine tuning protocols of potential clinical application. In this study we have aimed to address if fluctuations within the pluripotent state affects the differentiation outcome. More specifically, if these fluctuations generate subsets of cells that are primed to favourably differentiate into otic lineages.

Methods

To address these questions we sorted hES cells for stage specific embryonic antigen 3 (SSEA3) and subjected the positive and negative fractions to our differentiation protocol. SSEA3 is a sensitive marker of the ground, pluripotent state. Furthermore, we combined the SSEA3 selection together an otic-specific reporter. Differentiating cells were analysed for derivatives of the different germ layers, as well as using otic markers such as *PAX8*, *PAX2*, *FOXP1* and *NESTIN*.

Results

Our data showed that the SSEA3⁺ and SSEA3⁻ populations had a differential response to the same differentiation cues, with the SSEA3⁺ fraction being more efficient at producing otic phenotypes. On the other hand, cells expressing early otic-reporter activity did not yield enhanced otic differentiation.

Conclusion

Ours results suggest that, at least in this system, otic differentiation is better achieved by the most pristine, pluripotent population and a 'primed' state of pluripotency is not necessarily conducive to otic differentiation.

Histone Deacetylase Inhibitor Induces the Expression of Epithelial Features in Mouse Utricle-Derived Prosensory-Like Progenitors

Jue Wang; Zhengqing Hu
Wayne State University

Background

Adult mammalian inner ear hair cells cannot be regenerated naturally after they are damaged in acoustic overstimulation, aging, and ototoxic insults. Mouse utricle-derived progenitor cells (MUCs), which obtained hair cell progenitor and mesenchymal features via epithelial-to-mesenchymal transition (EMT) as previously described, provide a potential approach for hair cell regeneration. Histone acetylation is involved in the regulation of gene expressions through the balance between the activities of histone acetyltransferase (HAT) and histone deacetylase (HDAC). Recent studies showed that the HDAC inhibitor trichostatin A (TSA) could stimulate the expression of epithelial marker E-cadherin via the inhibition of induced EMT. In this study, we treated MUCs with TSA to determine whether HDAC inhibitor is able to stimulate the expression of epithelial genes, which is an essential step for guiding prosensory-like MUCs to become sensory epithelial cells.

Methods

MUCs were treated with TSA or control medium for 24-72 hr. Cells were examined every day for observing cell morphology changes using phase contrast microscopy. Total RNA was extracted from MUCs treated with TSA or control medium. The gene expression was examined using reverse-transcription PCR and real time quantitative PCR. Immunofluorescence and western blotting were used to detect the protein expression. A two-tailed Student's *t*-test was used to analyze statistical significance.

Results

MUCs acquired epithelial cell-like features in response to TSA treatment, which was indicated by increased expression of epithelial markers such as *Cdh1*, *Krt8*, *Krt18*, *Tjp1* and *Dsp*. The up-regulation of epithelial marker E-cadherin (encoded by *Cdh1*) was further detected in TSA-treated MUCs using western blotting. Additionally, TSA treatment decreased the expression of mesenchymal markers including *Zeb1*, *Zeb2*, *Snai1* and *Snai2*, and prosensory genes *Lfng*, *Hes1*, *Six1* and *Dlx5*. Moreover, the expression of hair cell markers *Myo6* was increased in TSA-treated MUCs. We observed a significantly decreased expression of *Hdac2* and *Hdac3* in TSA-treated MUCs, indicating that TSA-induced HDAC inhibition may contribute to this mesenchymal to epithelial phenotype change.

Conclusion

Our studies showed that a non-selective HDAC inhibitor TSA plays an essential role in inducing the expression of epithelial marker in MUCs. These data provide evidence that prosensory-like MUCs are able to obtain an epithelial phenotype, which indicates that MUCs may serve as potential candidates for the generation of new hair cells.

Applicability of Choroid Plexus Cells for the Repopulation of Hair Cell Depleted Cochlear Sensory Epithelium in the Primate Model

Dongguang Wei¹; Brent Wilkerson²; Sona Santos³; LiPing Nie²; Rodney Diaz²

¹University of California Davis Medical Center; ²Department of Otolaryngology - Head and Neck Surgery, University of California Davis Medical Center; ³California National Primate Research Center

Background

Irreversible loss of cochlear hair cells (HCs) leads to hearing loss and affects the quality of life of millions of patients worldwide. The increasing incidence of patients with profound hearing loss who are awaiting novel therapies for cure inspires the translational study of cochlear regeneration. Current attempts to repopulate the hair cell depleted inner ear with mechanosensitive cells that can replicate HC function has thus far focused on the non-primate mammalian and non-mammalian vertebrate animal models. Some of these investigations are encouraging, however solutions to the challenges of restoring damaged HCs in the inner ear remain elusive. Currently, no identifiable biological implants have been identified or generated which extensively parallel the molecular and morphological characteristics of inner ear HCs. Given the inefficient or incomplete phenotypic conversion of stem cells into HCs demonstrated thus far, identification of a pre-existing, surgically accessible, readily available population of autologous cells that can be implanted into the cochlea and can serve to replicate HC form and function is an avenue of advantageous investigation.

Methods

Rhesus monkeys (*Macaca mulatta*) used for this study are housed at the California National Primate Research Center. Tissues are obtained from wild type rhesus monkeys that have undergone scheduled necropsy for unrelated purposes and that have no demonstrated neurological deficits. Choroid plexus (CP) tissue from necropsy animals are harvested and prepared under surgical microscope. CP epithelial sheets are processed for immunofluorescent staining, reverse transcriptase polymerase chain reaction, and scanning electron microscopy.

Results

Primate CP cells demonstrate strikingly similar molecular and morphological characteristics with cochlear HCs. CP cells express myosin VIIa, myosin VI, prestin, whirlin, ATOH1, Brn-3c, calretinin, CtBP2. Additionally, CP cells express HC-associated ionic channel proteins such as the pore forming subunits of L-type Ca²⁺ channel (Cav1.3), large conductance Ca²⁺-activated K⁺ channels, voltage-gated K⁺ (BK) channels (KCNQ4, Kv7.4), and small conductance Ca²⁺-activated K⁺ (SK2) channels. CP cells demonstrate polarized columnar epithelial cell polarity with enriched stereocilia-like microvilli localized to apical membrane. CP cells express neurotrophic factors which may locally support spiral ganglion neurons.

Conclusion

Primate CP cells demonstrate strikingly similar molecular and morphological characteristics with cochlear HCs and may serve as potential autologous biological implants for the repopulation of hair cell depleted cochlear sensory epithelium.

PD - 059

Generation of Hair Cells in Neonatal Mice by b-Catenin Overexpression in Lgr5-Positive Cochlear Progenitors

Fuxin Shi; Lingxiang Hu; Albert Edge

Massachusetts Eye and Ear Infirmary, Harvard Medical School

Background

Wnt signaling is required for the maintenance of progenitor cells in tissues, such as intestine, skin, the hematopoietic system and the central nervous system. β -catenin, the intracellular mediator of canonical Wnt signaling, enters the nucleus to activate transcription of target genes that control key decision points in proliferation and differentiation of stem cells. Lgr5, a G-protein coupled membrane receptor, augments Wnt signaling by binding to the soluble R-spondins. We recently identified Lgr5-expressing cochlear supporting cells with the capacity for self-renewal and hair cell differentiation *in vitro*. We found that these cells, a subset of cochlear supporting cells, were responsive to Wnt-signaling. Here, we asked whether these Lgr5-positive cells, despite their lack of contribution to hair cell replacement after degenerative loss, could be driven by forced expression of b-catenin to act as hair cell progenitors *in vivo*.

Methods

We used *Sox2-Cre-ER* mice to activate b-catenin constitutively in all supporting cells by crossing to a *b-catenin^{flox(exon3)}* mouse, in which conditional deletion of exon3 (*b-catenin Δ exon3*) blocks b-catenin degradation and induces accumulation of b-catenin. BrdU or EdU was given to label proliferating cells, and the source of the new hair cells was assessed by lineage tracing by crossing the *Sox2-Cre-ER* mouse to a floxed *tdTomato* reporter mouse and to the *b-catenin^{flox(exon3)}* mouse. We administered tamoxifen to activate Cre at P1 and dissected the cochlea at P5.

Results

We showed that forced stabilization of b-catenin in supporting cells in neonatal animals resulted in proliferation of supporting cells and generation of hair cells. Although b-catenin expression was increased by genetic means in all supporting cells, entry to the cell cycle and differentiation to hair cells of the normally post-mitotic cells was restricted to the Lgr5-positive population.

Conclusion

Our finding suggests that Wnt/b-catenin can drive Lgr5-positive cells to act as hair cell progenitors, even after their exit from the cell cycle and apparent establishment of cell fate.

PD - 060

The Role of FGF Pathway in the Planar Cell Polarity of the Vestibular Hair Cell Regeneration Induced by Gene Atoh1/Math1

Dong-Dong Ren¹; Rui Ma²; Xiao-Yu Yang¹; Wen-Wei Luo¹; Juan-Mei Yang¹; Fang-Lu Chi¹

¹Eye, Ear, Nose and Throat Hospital (EENT Hospital), Fudan University; ²Dept. of Otolaryngology, Eye, Ear, Nose and Throat Hospital (EENT Hospital), Fudan University

Background

Planar cell polarity (PCP) signaling regulates cochlear extension and coordinated orientation of sensory hair cells in the inner ear. Fibroblast growth factor (FGF) signaling is important for a host of developmental processes such as proliferation, differentiation, tissue patterning, and morphogenesis, including the development of the inner ear. We and other researches have demonstrated that over-expression of Atoh1/Math1 in the mouse utricle could induce the ectopic hair cell-like cells (HCLCs), but arranged randomly without coordinated polarity. In our study, we explore that the role of FGF pathway in the vestibular hair cell regeneration and cell polarity formation induced by gene Atoh1/Math1 through inhibition of FGF signaling.

Methods

Ad5-EGFP-math1 and/or FGF inhibitor (SU5402) were used to over-express math1 and/or inhibit the FGF signaling in the utricle of neonatal mice *in vitro*. We compared the number, position and proliferation of new HCLCs between in sensory regions and the ectopic non-sensory regions, investigated the establishment of hair cell-like cells polarity through the Spectrin/ γ -tubulin staining.

Results

It showed that there are more new HCLCs in the sensory region and non-sensory regions co-transfected with Ad5-EGFP-math1 and FGF inhibitor together than those transfected with Ad5-EGFP-math1 alone, but the number of EDU(+) cells had no difference in two groups. After regenerated Myo7a(+) cells induced by Ad5-EGFP-math1 and/or FGF inhibitor developed actin-rich stereocilia, their basal body moved from center to the distal side, suggesting the underlying PCP establishment in single regenerated new HCLCs. The coordinated polarity of the new HCLCs demonstrated the same polarity as the neighbouring hair cells all oriented toward the reversal line in the sensory region. Interesting, in the non-sensory regions the polarity of the new HCLCs arranged randomly.

Conclusion

Math1 gene transfer could induce the production of original and ectopic HCLCs *in vitro*. Inhibition FGF signaling could promote more new HCLCs in the Ad5-EGFP-math1 transfected utricle through trans-differentiation of supporting cells. The planar cell polarity of new generated HCLCs in the sensory region is consistent with the original hair cells. There maybe the PCP proteins or other pathways in the sensory region play roles in formation of the coordinated polarity of the new HCLCs.

Mechanisms for Hearing Recovery by Topical IGF-1 Treatment: Regeneration of Synapse Between Inner Hair Cells and Auditory Neurons

Takayuki Nakagawa; Nakarin Asaka; Norio Yamamoto; Tomoko Kita; Akiko Taura; Masa-aki Ishikawa; Juichi Ito
Kyoto University

Background

IGF-1 plays crucial roles in the development and the maintenance of the cochlea. Our previous studies have demonstrated the efficacy of topical IGF-1 treatment for attenuation of noise- or ischemia-induced hearing loss. In addition, a clinical trial to investigate the safety and efficacy of topical IGF-1 therapy in patients with sudden deafness indicated the efficacy of topical IGF-1 therapy for sudden deafness. Interestingly, significant hearing recovery appeared at 4 weeks after treatment, which suggests that regenerative processes rather than protection could be involved in mechanisms for hearing recovery in patients with sudden deafness. To test this hypothesis, we examined effects of IGF-1 on regeneration of synapses between inner hair cells and spiral ganglion neurons *ex vivo* and *in vivo*.

Methods

For *ex vivo* experiments, slice cultures of cochlear mid turns of postnatal day-2 mice were used. Degeneration of synapses between inner hair cells and spiral ganglion neurons was induced by supplementation of NMDA and kainite into culture media, afterwards IGF-1 was applied to culture media. At 48 h after IGF1 application, cochlear specimens were provided histological analyses. *In vivo* effects of IGF-1 on synapses between inner hair cells and spiral ganglion neurons were assessed using a noise trauma model of guinea pigs. Topical application of IGF-1 was performed 7 days after noise exposure. Auditory function was assessed by ABR measurements, and cochlear specimens were harvested 2 weeks after IGF-1 application.

Results

IGF-1 induced regeneration of afferent dendrites of spiral ganglion neurons, pre- and post-synaptic vesicles in cochlear explants in a dose-dependent manner. An antagonist of IGF-1 receptor eliminated IGF-1 effects. In addition, the expression of phosphorylated Akt was found in spiral ganglion neurons, and an inhibitor for PI3K/Akt pathway deteriorated IGF-1 effects. ABR assessments revealed better hearing recovery in IGF-1-treated animals than that in controls. Better preservation of afferent dendrites of spiral ganglion neurons, pre- and post-synaptic vesicles in IGF-1-treated specimens was also found *in vivo*.

Conclusion

These findings indicate that IGF-1 promotes regeneration synapses between inner hair cells and spiral ganglion neurons after damage, which could be involved in mechanisms for hearing recovery that was observed in patients with sudden deafness following topical IGF-1 treatment.

Effects of BDNF and NT-3 on Promoting Spiral Ganglion Neuronal Survival and Peripheral Fiber Re-Growth in the Deafened Adult Guinea Pig Cochlea

Cameron Budenz¹; Hui Tui Wong²; Donald S. Swiderski¹; Bryan E. Pfingst¹; Yehoash Raphael¹

¹Kresge Hearing Research Institute, University of Michigan;

²Graduate Program in Biology, Johns Hopkins University

Background

Cochlear hair cell loss often results in secondary regression of peripheral auditory fibers (PAFs) and loss of spiral ganglion neurons (SGNs). Cochlear implants (CI) rehabilitate hearing by directly stimulating the remnant auditory neural structures, suggesting their enhanced survival may lead to improved CI outcomes. Prior work has demonstrated that BDNF and NT-3 improve SGN survival and induce PAF regrowth following deafening. We have previously shown that there are significantly more PAFs in the basilar membrane area (BMA) of neomycin deafened inner ears treated with either BDNF or NT-3 than in controls. Here we compare the effects of BDNF and NT-3 on guinea pig ears deafened systemically or locally.

Methods

Adult guinea pigs were deafened by either local administration of neomycin into the cochlea or systemic administration of kanamycin and furosemide (KF). *BDNF* and *NTF-3* were delivered to the guinea pig inner ear via adeno-associated viral vectors one week following deafening, and all animals were sacrificed three months following treatment. PAF regrowth was assessed on whole-mounts of the BMA, and SGN survival on midmodiolar plastic sections through Rosenthal's canal from a second subset.

Results

Systemic KF deafening produced a less severe lesion of the auditory epithelium than locally administered neomycin, with greater hair cell survival in apical turns and supporting cell survival in basal turns. There was no significant difference in the number of re-grown PAFs in the BMA of animals based on the method of deafening or neurotrophin treatment delivered. In KF deafened ears, PAFs were restricted to areas flat epithelium devoid of differentiated supporting cells. Either neurotrophin produced more substantial SGN survival after neomycin deafening than after KF deafening, likely related to the less severe SGN loss associated with KF. Furthermore, in neomycin deafened ears, NT-3 had a slightly greater effect than BDNF on PAF regrowth, whereas BDNF had a significantly greater effect on SGN survival.

Conclusion

Gene therapy with either BDNF or NT-3 leads to PAF regrowth, and treatment with BDNF leads to enhanced SGN survival. Through these effects on PAF and SGN survival, neurotrophins may lead to improved CI outcomes. The presence of supporting cells may inhibit PAF regeneration into the BMA. Further study is needed to characterize the effects of severity of lesion and etiology of deafening on SGN survival

and PAF regrowth, as these could influence clinical translation of neurotrophin therapy.

PD - 063

TMC Function in Hair Cell

Mechanotransduction

Bifeng Pan¹; Gwenaëlle Geleoc¹; Kiyoto Kurima²; Andrew J. Griffith²; **Jeffrey R. Holt**¹

¹*Boston Children's Hospital, Harvard Medical School*; ²*NIH/NIDCD*

Background

Sensory hair cells of the mammalian inner ear convert sound stimuli and head movements into electrical signals that are transmitted to the brain. The molecules and mechanisms of sensory transduction in inner ear hair cells have been the focus of considerable interest and investigation. Recently, we suggested that Transmembrane channel-like proteins 1 and 2 (TMC1 and TMC2) may be components of the mechanosensitive ion channels in hair cells. *Tmc1* and *Tmc2* are expressed in hair cells and both dominant and recessive mutations in *Tmc1* cause deafness in mice and humans.

Methods

To investigate this hypothesis we used the whole-cell, tight-seal technique to record mechanotransduction currents from cochlear inner hair cells that expressed wild-type *Tmc1*, *Tmc2*, both or neither. To further narrow in on the function of *Tmc1* we recorded from hair cells of mice that expressed the dominant *Tmc1 Beethoven* (*Bth*) mutation. The *Bth* mutation was isolated by crossing *Bth* mice onto a *Tmc1/Tmc2*-null background. We also investigated the contribution of *Tmc1*, *Tmc2* and mutant *Tmc1* to the function of single transduction channels. For these experiments we developed a novel stimulation paradigm in which stimulus pipettes were designed to deflect single stereocilia of inner hair cells.

Results

The data show that TMC1 or TMC2 are required for hair cell transduction and that expression of either one is sufficient to retain mechanosensitivity. Although the molecules are somewhat redundant in their function, there were significant differences in the biophysical properties of mechanotransduction in hair cells that expressed only TMC1 or TMC2. The biophysical differences included the rate and extent of adaptation, calcium permeability and single-channel conductance. Wild-type hair cells that expressed both TMC1 and TMC2 had a broad range of single-channel conductances, raising the possibility that the proteins may interact to form channels with a range of biophysical properties.

To investigate the consequences of the *Tmc1 Bth* mutation - a methionine to lysine substitution at amino acid position 412 - we examined mechanotransduction in hair cells of *Bth* mice. We found that the *Bth* point mutation is not a dominant-negative, or loss-of-function mutation, but caused a change of function, as it altered several biophysical properties of hair cell transduction. Relative to cells that expressed wild-type *Tmc1*, cells that expressed the *Bth* mutation had smaller single-channel conductance, larger calcium block, reduced calcium permeability and slower adaptation.

ARO Abstracts

Conclusion

The data implicate TMC1 and TMC2 as components of hair cell mechanotransduction channels.

PD - 064

Positional Gradients and Voltage Dependence of Permeant Block of the Hair Cell's Mechano-Electrical Transducer Channel by the D-HIV-TAT and D-JNKi1 Peptides

Terri Desmonds¹; Nerissa Kirkwood¹; Richard Goodyear¹; Marco Derudas¹; Jonathan Gale²; Sietse van Netten³; Simon Ward¹; Guy Richardson¹; Corne Kros¹

¹*University of Sussex*; ²*UCL*; ³*University of Groningen*

Background

We have identified a novel class of high-affinity mechano-electrical transducer (MET) channel blockers based on the HIV-TAT peptide. Here we report marked differences in the interaction with outer hair cell (OHC) MET channels of two of these polycationic peptides, D-HIV-TAT (12 amino acids, 8 basic residues) and D-JNKi1 (31 amino acids, 12 basic residues).

Methods

MET currents were elicited in outer hair cells (OHCs) in cochlear cultures with a fluid jet and recorded under whole-cell voltage clamp. Currents in the absence and presence of the peptides were compared to study their actions on the MET channels at two locations along the cochlear coil: mid-apical and mid-basal. Dissociation constants (K_D) were fitted to currents at 104 mV. Uptake of Texas Red (TR) conjugated derivatives of the peptides was imaged using confocal microscopy.

Results

Block of OHC MET currents by D-HIV-TAT is relieved at positive membrane potentials by electrostatic repulsion. At extreme negative membrane potentials the block is also substantially reduced: strong evidence for permeant block (Gale et al, J Neurosci 2001; Marcotti et al, J Physiol 2005). The K_D was 29 nM in the mid-basal and 25 nM in the mid-apical coil. D-JNKi1 had an even lower K_D of 12 nM in mid-basal OHCs and is also a permeant blocker.

TRconjugated D-HIV-TAT accumulates in basal and apical OHCs. The larger compound, TRconjugated D-JNKi1, accumulates mostly in basal OHCs but shows little labelling of OHCs from the middle of the apical coil onwards. Consistent with these findings, D-JNKi1 is considerably less effective at blocking MET currents in mid-apical OHCs, with a K_D of 74 nM, although it can still permeate. The voltage dependence of block by D-HIV-TAT was considerably steeper than that by D-JNKi1. The block was strongest around 104 mV for both, but the latter compound showed much more block at positive membrane potentials.

Conclusion

The dependence of the block by D-JNKi1 on cochlear position is consistent with the longitudinal gradient in the pore properties of the OHC MET channels (Beurg et al, J Neurosci 2006; Kim and Fettiplace, J Gen Physiol 2013; Pan et al, Neuron

2013). The difference in voltage dependence suggests substantial differences in the interaction of both compounds with the MET channel, which we estimate to have a minimum pore diameter of some 2 nm from preliminary molecular modeling of the peptides.

PD - 065

A Novel Mode of Off-Frequency Hearing as a Result of Defective Outer Hair Cells' Hair Bundles Unveiled by *Nherf1*^{-/-} Mice

Aziz El-Amraoui¹; Kazusaku Kamiya¹; Vincent Michel¹; Fabrice Giraudet²; Maria-Magdalena Georgescu³; Paul Avan²; Christine Petit¹

¹Institut Pasteur; ²Université d'Auvergne; ³Université d'Auvergne; ³Anderson Cancer Center, Houston

Background

Structural defects of hair bundles, the sensory antennas of auditory hair cells, are expected not only to compromise mechanoelectrical auditory transduction, but also to affect the frequency selectivity of the cochlea.

Methods

Mutant mice, subtracted inner ear library, yeast-two hybrid screen, confocal and scanning electron microscopy, ABR, DPOAEs and masking tuning curves measurements.

Results

Nherf1, a PDZ-domain-containing protein, was identified in the hair bundle, the sensory antenna of auditory hair cells, in differentiating outer hair cells (OHCs). *Nherf1*^{-/-} mice showed apparently mild hearing-threshold elevations at mid/high sound frequencies, associated to OHC hair-bundle shape anomalies, prominent in the basal cochlea. This mild impact on hearing sensitivity clashed with the finding of almost non-responding OHCs in the basal cochlea as assessed by distortion-product otoacoustic emissions and cochlear microphonic potentials. Responses of *Nherf1*^{-/-} mice to high-frequency (20, 32 and 40 kHz) test tones were not masked by tones of neighboring frequencies as in normal mice. Actually, masker tones at levels up to 25 dB below test-tone level acted in a broad interval of low frequencies, up to two octaves lower than the test tone. Together with the relative growth of the masker and test tones, and the abnormally long latencies and distorted waveforms of neuronal responses to high frequencies, these unusual characteristics suggest that high-frequency tones of moderate intensity are detected off-frequency, within the whole functionally unaffected apical cochlear region.

Conclusion

Our results establish the critical role of *Nherf1* in the hair-bundle morphogenesis. As high frequencies cannot reach the apical region via the basilar membrane, a novel, leaking mode of off-frequency detection is revealed, that allows the spreading of high-frequency vibrations over most of the cochlear apical region, possibly in relation to the persistent anchoring of OHCs to the tectorial membrane in *Nherf1*^{-/-} mice. These findings suggest how to circumvent major pitfalls in

hearing assessment of some patients, by avoiding misleading interpretations of hearing thresholds.

PD - 066

Reverse Transduction in Saccular Hair Cells

Sebastiaan W.F. Meenderink; Patricia M. Quiñones; Dolores Bozovic

University of California, Los Angeles

Background

The apical surface of hair cells contains specialized organelles —hair bundles—that contain mechanically gated ion channels. These channels are involved in the *forward transduction* of mechanical perturbations into electrical signals that are ultimately relayed to the brain. The opposite, however, also occurs: there is a mechanical response at the level of the hair bundle following potential changes within the cell. One of the most prominent manifestations of such *reverse transduction* is the occurrence of spontaneous otoacoustic emissions. Here, we present measurements of this reverse transduction process for hair cells from the frog sacculus.

Methods

Saccular epithelia were freshly dissected from American bullfrogs (*R. catesbeiana*), and mounted into a two-compartment recording chamber. This configuration mimics the *in vivo* situation in that it keeps the separation between the apical, endolymphatic and the basal, perilymphatic space. The preparation was viewed with an upright microscope that was equipped with a high-speed CMOS video camera (operated at 1000–10,000 fps). Individual hair cells were whole-cell voltage-clamped to different potentials, while the position of their hair bundles was simultaneously recorded.

Results

In response to both de- and hyperpolarizing voltage steps, the position of the associated hair bundle changes. We could identify several components in these bundle motions. Immediately following a depolarizing voltage step (to potentials ≥ -30 mV), there is a fast and transient motion of the bundle towards the kinocilium. This is then followed by a more sustained shift in the bundle position. For hyperpolarizing steps, the initial fast component is usually absent. Adaptation in the bundle position is observed in a fraction of the cells. In ongoing experiments we are studying the effects of external calcium concentration, membrane potential, and blockers that interfere with mechano-transduction on these induced motions.

Conclusion

We have successfully patch-clamped saccular hair cells while maintaining the separation between peri- and endolymph. Using this approach, we observe that voltage steps sent to a hair cell elicit mechanical movements of the bundle. This reverse transduction is biphasic with a fast and a slow component.

PD - 067

Actin Dynamics and Regulation in Stereocilia Maintenance

Benjamin Perrin¹; Praveena Narayanan¹; Paul Chatterton¹; David Corey²; James Ervasti¹

¹University of Minnesota; ²Harvard Medical School

Background

Our recent study using multi-isotope imaging mass spectrometry and conditional ablation of actin isoforms demonstrated that the actin in stereocilia is stable, except at tips, where turnover is more rapid. Several proteins that modify actin dynamics have been detected in stereocilia suggesting that actin turnover is regulated. Of these proteins, Wdr1 is an interesting candidate because it catalyzes disassembly of polymerized actin into monomeric actin, which may contribute to actin dynamics at stereocilia tips.

Methods

We performed two types of experiments to further define actin dynamics in stereocilia. We photobleached stereocilia on cultured hair cells that constitutively expressed GFP-actin and monitored fluorescent recovery over a 24 hour timecourse. To study actin dynamics in adult mice, we developed a transgenic line where GFP-actin expression can be initiated by drug treatment. Finally, we used the GFP-actin photobleaching assay together with auditory brainstem recordings and scanning electron microscopy to characterize mice expressing a mutant Wdr1 that has reduced activity.

Results

Only the tips of photobleached stereocilia recovered GFP-actin fluorescence. In addition, blocking actin polymerization with the drug cytochalasin prevented fluorescence recovery, supporting the idea that stereocilia actin is stable except at tips where filaments disassemble and repolymerize. Results from our inducible GFP-actin mice are also consistent with this model of stereocilia actin dynamics. When GFP-actin was switched on early in development it was incorporated along the entire length of stereocilia. In contrast, when GFP-actin expression was not induced until adulthood, incorporation was limited to the stereocilia tips of both auditory and vestibular hair cells. Finally, using our GFP-actin photobleaching assay, we found that mutant Wdr1 slowed actin turnover at stereocilia tips. Furthermore, while Wdr1 mutant mice had normal stereocilia morphology at young ages, by 6 months of age they developed high frequency hearing loss and shortening of outer hair cell stereocilia.

Conclusion

Data from two additional experimental approaches are consistent with a model where the actin filaments that form stereocilia are very stable, except at stereocilia tips. We found that the actin disassembly factor Wdr1 stimulates actin turnover at stereocilia tips and contributes to the maintenance of stereocilia morphology and auditory function. Together, this data indicate that although actin turnover is very slow, misregulation can contribute to age-related hearing loss.

PD - 068

Xirp2 : A Stereociliary Actin-Binding Protein Involved In Hair Bundle Maintenance

Déborah Scheffer¹; Jun Shen²; Duan-Sun Zhang¹; Zheng-Yi Chen³; David Corey¹

¹Harvard Medical School and Howard Hughes Medical Institute; ²Pathology Department, Brigham and Women's Hospital and Harvard Medical School; ³Massachusetts Eye & Ear and Harvard Medical School

Background

To identify genes important for the development and function of hair cells, it is useful to know the complete transcriptome of hair cells at various times during their differentiation and maturation. We have previously used mutant animals lacking hair cells (*Atoh1*), or mutants with hair cells but no bundles (*Pou4f3*) to approach a hair-cell transcriptome (Scheffer *et al.*, 2007a; 2007b), but these are not perfect models and cannot be used for later developmental stages.

Methods

We used a mouse strain that expresses eGFP only in hair cells, and fluorescence-activated cell sorting (FACS) to purify dissociated hair cells and non-hair cells. Cells were purified from cochlear and utricular epithelia at E16, P0, P4, P7 and P16 and mRNA was purified for deep sequencing.

Results

These data sets allowed us to identify new hair-cell-specific genes. Their expression was confirmed by *in situ* hybridization and immunostaining. One in particular was enriched 26-fold in hair cells compared to the surrounding cells. *Xirp2*, an actin-binding protein, was localized at the cuticular plate and stereocilia of hair cells. We studied the consequence of *Xirp2* disruption in a mouse knock-out strain and found that these animals exhibit a unique phenotype in hair cells. The paracrystallin organization of the stereocilia actin core was disrupted, leading to stereocilia degeneration. These mice also exhibited multiple long membrane protrusions at the foniculus of hair cells. To our knowledge, such structures have not been described in any other mutants. Based on its chromosomal location, this gene is a good candidate for human deafness. We have started sequencing *Xirp2* in a large consanguineous candidate family.

Conclusion

The discovery of *Xirp2* as an important actin crosslinker in the hair cells illustrates the power of deep sequencing on FACS-sorted cell populations. Similar FACS-based approaches might be used for identifying genes expressed in subsets of hair cells, for instance outer-hair-cell-specific genes that might participate in electromotility.

PD - 069

Hair-Cell-Specific Translatome Profiling Reveals Dynamic Gene Regulation During Acquisition of Mechanoelectrical Transduction in Mice

Xudong Wu¹; Jun Shen²; David Corey¹

¹Harvard Medical School and HHMI; ²Department of Pathology, Brigham & Women's Hospital and Harvard Medical School

Background

One approach to understanding the mechanotransduction apparatus in hair cells is to understand the regulation of gene expression during the developmental acquisition of mechanosensitivity. This has been challenging, due to the intermixed cell types in the inner ear, the small number of hair cells, and the degradation of mRNA during sample preparation. Recently, we carried out expression profiling at pre- and postnatal stages using mouse lines with hair-cell-specific GFP expression and isolation of hair cells with fluorescence-activated cell sorting, followed by RNA-Seq (shield.hms.harvard.edu). A concern with this approach is that the dissection, dissociation and cell sorting might have induced short-term changes in gene transcription. Additionally, protein abundance is not directly linked to mRNA level: in general only ~40% of the variation in protein concentration can be explained by mRNA abundance (transcription and mRNA degradation), and most of the remaining 60% is determined at a posttranscriptional level, by translation and protein turnover. A new approach to assess protein translation is to use RiboTag immunoprecipitation RNA profiling (Sanz et al., 2009).

Methods

We have used the RiboTag mouse. Excision by Cre recombinase of one exon of the gene encoding the RPL22 ribosome large subunit appends a hemagglutinin (HA) tag to the protein. Harvesting of tissue and subsequent immunoprecipitation by anti-HA pulls down tagged RPL22, and with it mRNAs that are being actively translated, the so-called "translatome." We made the HA tag hair-cell-specific by crossing the RiboTag mouse to a mouse line in which Cre is specifically expressed in hair-cells under the Gfi-1 promoter. RNA-seq was performed to profile the translatomes.

Results

We determined the hair-cell translatomes from P0, P2, and P4 mouse cochleas. To understand tonotopic differences along the cochlea, we also determined the hair-cell translatomes from apical, middle, and basal turns of cochlea at P2. Ranking genes by fold enrichment in hair cells over total cochlea, we found that 56% of the top 50 encode deafness genes or other genes important in hair-cell function. Some, such as Myh14 and Myh9, did not stand out in our FACS-sorting transcriptome profiling.

Conclusion

Our results have demonstrated that the RiboTag approach can effectively enrich cell-type-specific translatomes. In addition, the results have shown that the hair-cell-specific trans-

latome differs from the transcriptome, and may be a rich source of new proteins important for hair-cell function.

PD - 070

CRISPR/Cas-Mediated Generation of Transgenic Mice With Mutations in Novel Hair Bundle Proteins

Shimon Francis; Wenhao Xu; Jung-Bum Shin

University of Virginia

Background

Approximately 40% of identified deafness genes code for proteins located in the sensory hair bundle. We have previously used mass spectrometry to identify and quantify more than 1,100 bundle proteins, many of which were previously uncharacterized. We are especially interested in proteins involved in formation and maintenance of the stereociliar actin cytoskeleton, such as a novel actin crosslinker protein, XIRP2. The rate-limiting step for functional analysis of candidate deafness genes has been the generation of transgenic animal models. Therefore, we have applied the novel Clustered Regularly Interspaced Palindromic Repeat (CRISPR)/Cas9-mediated genome editing technology, to generate transgenic mice with mutations in genes coding for novel hair bundle proteins.

Methods

Any 20 base pair sequence followed by a so-called PAM sequence (NGG) can be targeted by the *S. pyogenes* CRISPR/Cas system. We identified such sites on our genes of interest and generated target-guiding RNAs (sgRNAs) using in-vitro transcription. sgRNAs were injected together with mRNA coding for the Cas9 endonuclease into mouse zygotes. Embryos were implanted into foster moms and resulting offspring were genotyped and characterized.

Results

We successfully generated transgenic mice with presumably deleterious mutations in two genes thus far. One of these proteins, XIRP2, was previously unknown to have any expression or function in hair cells, but is a known actin-crosslinker in cardiac myocytes. Because mutations in other actin-crosslinkers (espin, plastins, and fascins) result in hearing loss, and its chromosomal location overlaps with the human deafness loci DFNB27 and DFNA38, XIRP2 is a logical candidate for investigation of involvement in hearing function. CRISPR-mediated simultaneous targeting of two sites on the *Xirp2* gene resulted in a wide variety of mutations on the *Xirp2* locus. Mutation rates were as high as 59% in injected mouse embryos. The mice of the F0 generation were mostly mosaic for the mutation, and consequently, immunolabeling experiments in vestibular and auditory organs revealed a loss of XIRP2 protein expression in a subset of hair cells. In addition, we found that CRISPR/Cas-mediated mutations are germ-line transmissible, with expected rates of Mendelian heritability.

Conclusion

We are now in the process of characterizing these mice. In addition to presumably KO deletion mutants, the CRISPR method yielded a variety of mutation types, many of which

are in-frame deletions of various length (3 bp to 33 bp). It is expected that such transgenic mice will be valuable for discerning the function of certain domains on the proteins of interest.

PD - 071

How to Model OAEs ?

Hendrikus Duifhuis¹; Karolina Charaziak²; Jonathan Siegel²

¹University of Groningen, the Netherlands; ²Northwestern University

Background

Over the last 2 decades or so, theory and data about Oto-Acoustic Emissions (OAE) have been analyzed quantitatively primarily using Coherent Linear Reflection cochlea models (CLR). In these models specific reflections are predicted that depend on specific BM-impedance irregularities. This 'roughness' is tied to irregularities in the hair cell row (in particular OHC) structure.

Although irregularities in OHC-structure have been observed in several primate cochleae, in which the number of OHC-rows can exceed 3, irregularities have not been documented extensively for other mammals. Nevertheless, mammals like cat, guinea pig, and chinchilla just appear to have spontaneous (S)OAEs even though there is no irregularity found in the cochlea.

However, it also has been ascertained experimentally that the healthy cochlea in all mammals (and more) behaves nonlinearly. Cochlear nonlinearity generates –as a by-product– OAEs. Therefore, nonlinear (NL) models seem to provide an interesting alternative for CLR-models.

Methods

The focus of a series of model studies is on a number of phenomena of which experimental data have been obtained. We are particularly interested in similarities and differences of the matches between data and the two model classes: CLR-models and NL-cochlea models.

Results

Using time-domain model studies, several OAEs predictions of CLR- and NL(A=active)-class models have been compared. Some examples are given below:

Single tone behavior:

1. In 1991 Brass and Kemp introduced a time domain analysis using a novel paradigm based on increment –and decrement– responses. So far only a comparison with a rather simple Van der Pol-type NL model have been presented. This is now extended to predictions by additional CLR- and NL-models.
2. Studies of chinchilla OAEs, in particular stimulus-frequency (SF)OAE based estimates of tuning, were compared to CAP tuning. Different results have been found between basal and apical ends. Probe frequencies that maximally excite the apical end seem to originate over a broad region of the basilar membrane as indicated by

broad OAE tuning curves. At these frequencies SFOAE cannot be considered a space-specific measure of cochlear function as predicted by CLR.

Conclusion

Several open issues about OAE modeling are addressed in greater detail. In particular predictions from CLR and general NL(A) models are compared quantitatively. Evoked emissions can be generated by a normal healthy (nonlinear) cochlea and do not require specific coherent reflections.

PD - 072

Stimulus Ratio and Level Dependence of Low- and Mid-Frequency Distortion-Product Otoacoustic Emissions

Anders Christensen; Rodrigo Ordoñez; Dorte Hammershøj Aalborg University

Background

Active amplifiers within the cochlea generate, as a by-product of their function, distortion-product otoacoustic emissions (DPOAEs) in response to carefully chosen two-tone stimuli. Focus has been on invoking emissions in a mid-frequency range from 500 to 4000 Hz. Below 500 Hz, physiological noise from heartbeating, breathing and swallowing contaminates the measurement. Above 4000 Hz, calibration of the equipment involved is challenging, if not impossible, to do reliably. Here, we investigate alternative measurement parameters to see if the DPOAE is limited to frequencies above 500 Hz. Few examples of low-frequency DPOAEs exist in the literature. Overcoming the decreasing response level and increasing noise level with decreasing frequency may provide a non-invasive window into the inner-ear mechanics of low-frequency hearing.

Methods

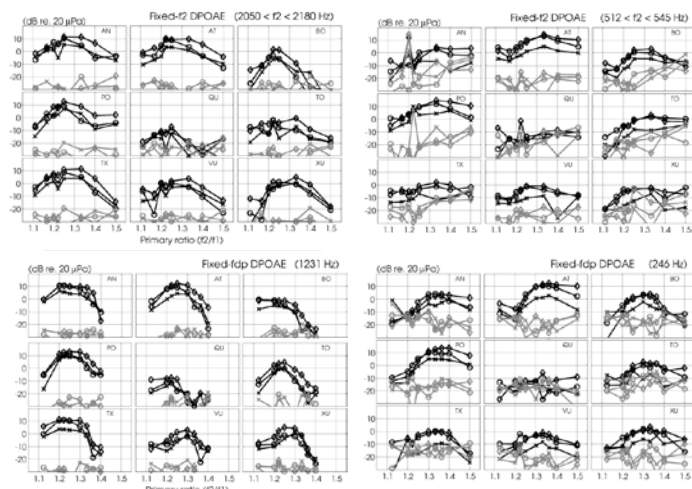
Eighteen out of 21 young human adults screened (19-30 years) had audiometrically normal hearing for inclusion in our experiment. DPOAEs were measured with pure-tone stimuli in four configurations: f₂ fixed around a mid-frequency (2050-2180 Hz), f₂ fixed around a low frequency (512-545 Hz), fdp fixed at a mid-frequency (1231 Hz) and a low frequency (246 Hz). Eight stimulus ratios f₂/f₁ (1.05-1.50) and three stimulus sound pressure levels L₁/L₂ (65/45, 65/55, 70/60) were measured in each configuration. The DPOAE response was isolated with the discrete Fourier transformation (DFT). The DFT measures the DPOAE response accurately only when the DPOAE frequency and both stimulus frequencies are exactly at a DFT bin. This makes for slightly odd parameter choices.

Results

Trends in ratio-magnitude responses for the mid-frequency DPOAE agree well with those reported in previous literature. Not reported previously is the change when going from mid- to low-frequency DPOAEs. In the mid-frequency range, ratio-magnitude responses typically have maxima at ratios <1.30. In the low-frequency range, maxima are typically at ratios >1.30.

Conclusion

DPOAEs are not limited to frequencies above 500 Hz, but the stimulus ratio invoking the largest DPOAE in the mid-frequency range does not do so in the low-frequency range. The stimulus level has similar effects in both frequency ranges, that is, the ratio-magnitude response increases and broadens with increasing level. The combined observations could indicate a difference between apical and basal cochlear physiology.



PD - 073

Low-Frequency Otoacoustic Emissions in Children and Adults

Wiktor Jedrzejczak; Krzysztof Kochanek; Anna Piotrowska; Łukasz Olszewski; Henryk Skarzynski
World Hearing Center, Institute of Physiology and Pathology of Hearing, Warsaw/Kajetany, Poland

Background

Click evoked otoacoustic emissions (CEOAEs) are known to be good indicators of hearing function when used in the frequency range 1–4 kHz. The present study investigates the usefulness of responses in the lower frequency range of 0.5–1 kHz evoked by 0.5 kHz tone bursts.

Methods

Otoacoustic emissions (OAEs) were recorded from the ears of school age children and adults. The following measurements were performed: first with a standard click stimulus at 80 dB pSPL (CEOAEs), a second using a 0.5 kHz tone burst at 80 dB pSPL (TBOAEs), and a third of synchronized spontaneous OAE (SSOAE). Pure tone audiometry and tympanometry were also conducted. Half-octave-band values of OAE signal to noise ratios (SNRs) and response levels were evaluated. Additionally, time-frequency (TF) analysis of the recorded signals was done by decomposing them into their basic waveforms. For this, a method of high-resolution adaptive approximation was used, a technique based on the matching pursuit (MP) algorithm.

Results

As expected, the CEOAE magnitudes were greatest over the range 1–4 kHz, with a substantial decrease below 1 kHz. Responses from the 0.5 kHz TBOAEs were complementary in that the main components occurred between 0.5 and 1.4

kHz. Additionally, it was investigated how 0.5 kHz TBOAEs are affected by the presence of SSOAEs.

Conclusion

0.5 kHz TBOAEs could be measured in children as effectively as CEOAEs. They can provide additional information about the frequencies up to 1 kHz, a range over which CEOAEs do not usually contain responses above the noise floor.

PD - 074

Otoacoustic Emission and Behavioral Estimates of the Contribution of Inner and Outer Cell Dysfunction to Audiometric Loss

Peter Johannesen; Patricia Pérez-González; Enrique A. Lopez-Poveda

Universidad de Salamanca

Background

Based on behavioral estimates of cochlear gain loss, we have previously suggested that the relative contribution of inner and outer hair cell dysfunction (HL_{IHC} and HL_{OHC} , respectively, in decibels) to the audiometric loss (HL_{TOTAL}) can vary largely across listeners with similar losses (Lopez-Poveda and Johannesen, 2012, JARO 13:485-504). The aim of the present study was twofold: first, to extend our earlier analysis to a wider frequency range (0.5, 1, 2, 4 and 6 kHz) and for a larger sample of subjects ($n=64$) with mild-to-moderate cochlear hearing loss; and second, to explore more convenient approaches for estimating HL_{OHC} and HL_{IHC} using distortion product otoacoustic emissions (DPOAE) methods (Lopez-Poveda et al., 2009, Audiol. Med. 7:22-28).

Methods

We assumed that HL_{IHC} can be estimated as the difference between HL_{TOTAL} and HL_{OHC} and that HL_{OHC} can be estimated from cochlear input/output (I/O) curves as a reduction in cochlear gain with respect to normal hearing. Cochlear I/O curves were inferred using the behavioral temporal masking curve (TMC) method and DPOAEs I/O curves measured with optimal primary levels. DPOAEs were obtained for a baseline condition without suppressor, and using two suppressor conditions to minimize the influence of the DPOAE reflection source: the suppressor rule of Johnson *et al.* (2006, JASA 119:3896-3907), and an individualized optimal suppressor. Correlations were then sought between several characteristics of the DPOAE I/O curves and behavioral HL_{OHC} estimates.

Results

TMC-based results suggest that HL_{IHC} and HL_{OHC} vary considerably across subjects with similar hearing loss at any given frequency. DPOAE I/O curves could be measured only for listeners with mild hearing loss (~50% of the subjects). Mild correlation was observed between DPOAE- and TMC-based HL_{OHC} estimates. Suppression of the DPOAE reflection source improved the correlation only slightly.

Conclusion

The present behavioral data confirm our earlier conclusion that HL_{IHC} and HL_{OHC} can vary considerably across subjects with similar hearing loss at any given frequency. TMC and

DPOAE methods cannot be used interchangeably to estimate HL_{IHC} and HL_{OHC} for hearing impaired listeners.

PD - 075

DPOAE Mapping for Detecting Noise-Induced Cochlear Damage

Abigail Fellows¹; Odile Clavier²; Jesse Norris²; Deanna Meinke³; Robert Kline-Schoder²; **Jay Buckey**¹

¹Geisel School of Medicine at Dartmouth; ²Creare, Inc.;

³University of Northern Colorado

Background

DPOAE level/phase mapping provides a comprehensive picture of cochlear responses over a range of frequencies and $f2/f1$ ratios. But, whether these data provide improved detection of noise-induced damage is not known.

Methods

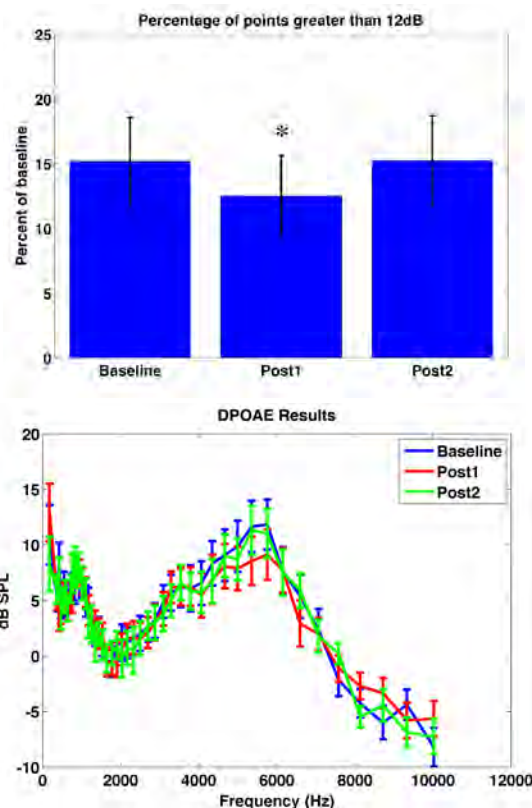
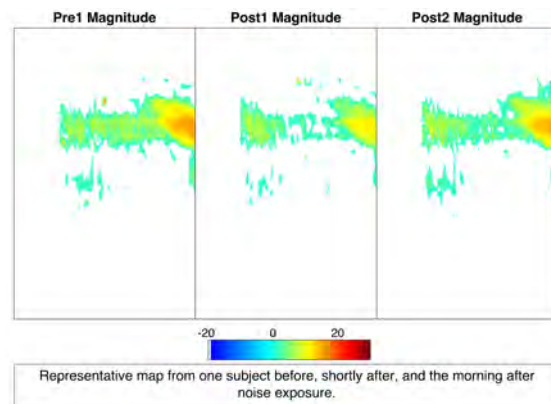
11 normal hearing subjects were studied before and after attending music concerts. Noise exposures varied among subjects. Threshold audiometry, DP-grams (0.3-10kHz), SOAES, and DPOAE maps were collected prior to, as soon as possible after, and the morning after the concerts. DPOAE maps were analyzed as images. Areas where the DPOAE was less than 3 dB above the noise floor (3dB SNR) were omitted, and then points corresponding to emissions greater than 0 dB were counted. The points were sorted into bins corresponding to 0-3dB, 3-6dB, 6-9dB, 9-12dB, and >12dB above the 0 dB threshold. Mapping data and DP-gram magnitudes were analyzed across time periods using a repeated measures analysis of variance.

Results

Figure 1 shows a set of maps from one subject. Mapping data showed a significant reduction in the percentage of points >12dB ($p<0.05$) immediately after the concert, which recovered by the next morning (Figure 2). The percentage of points <3dB showed a tendency to increase after the concert. The total area of the map with a 3dB SNR or greater also showed a tendency to decrease after the concert and recover the next morning. Analysis of DPOAE magnitudes over time did not show significant changes at any frequency, although there was a tendency for the DPOAEs to be lower after the concert (Figure 3).

Conclusion

The maps showed significant changes that were not detected using the standard DP-gram. The mapping data showed a loss of higher level DPOAEs, and suggest both a decrease in the total number of DPOAEs detected, a loss of higher level DPOAEs, and a shift to lower level DPOAEs. The DPOAE mapping provides comprehensive information on cochlear responses, which can be analyzed using image processing techniques. Changes in DPOAE amplitudes after noise exposure can be complex, and mapping offers detailed data amenable to multiple analysis techniques.



PD - 076

Evaluation of Techniques for Measuring Distortion Products of Bone Conduction Vibrators and Bone Conduction Stimulated Otoacoustic Emissions

Teru Kamogashira; Shotaro Karino; Tatsuya Yamasoba
University of Tokyo

Background

Conventional bone conduction transducers, which are used in clinical hearing evaluations, suffer from poor distortion performance particularly at low frequencies and a resonant frequency. In general, such transducers are shipped under a specified distortion quality rating, which is approximately 5% at maximum; however, the absolute distortion of any given transducer is not accurately known. Bone-anchored hearing aids are now available in many countries, and therefore, the proper evaluation of bone conduction hearing thresholds and bone conduction stimulated otoacoustic emissions has be-

come increasingly important. In this study, we evaluated various signal processing techniques for measuring the distortion products of bone conduction vibrators and bone conduction stimulated otoacoustic emissions.

Methods

Conventional impulses, which comprise a certain type of pseudorandom noise sequence called the maximum length sequence, linear and log sine sweeps, dual sine sweeps, and log and linear silence noise sweeps of maximum length sequences were used as signals to stimulate the bone conduction vibrator RION BR-41. Measurements were performed using a RION AG-04 OAE amplifier and a B&K artificial mastoid. The recorded signals were processed using the fast Fourier transform, fast Walsh–Hadamard transform, inverse maximum length sequence convolution, or inverse sine sweep convolution depending on the type of stimuli. The distortion products of the response obtained for each method were analyzed.

Results

The use of the sine sweep and silence sweep techniques resulted in harmonic distortion products in the vibrator output and the otoacoustic emissions. The dominant component in the total harmonic distortion was second-order harmonic distortion at all frequencies for both stimuli. The impulse responses of the sweep techniques exhibited two components, which could be clearly separated.

Conclusion

The harmonic distortions of the bone conduction vibrators were not sufficiently small due to the presence of second-harmonic distortion. This should be noted when evaluating the distortion products of bone conduction stimulated otoacoustic emissions. The sine sweep techniques realized high signal-to-noise ratios, and they could retrieve the impulse responses that were separated according to each distortion product. Analyses of the fundamental frequency by other techniques were influenced by noise in the recording environments.

PD - 077

Interrelations Between Otoacoustic Emission Delays and Neural Tuning in the Barn Owl

Christine Köppl¹; Geoffrey Manley¹; Christopher Bergevin²

¹Carl von Ossietzky University; ²York University

Background

While numerous studies have used otoacoustic emissions (OAEs) to estimate cochlear frequency selectivity, controversy remains. Clarification is hampered by outstanding questions regarding the biophysics of OAE generation. Here, we examined stimulus-frequency emission (SFOAE) properties for the barn owl, a bird species with a known “auditory fovea” (i.e. expanded high frequency representation; Köppl et al., 1993, *J Comp Physiol A* 171:695-704). The auditory fovea does not correlate with enhanced frequency resolution at the neural or behavioral level (Köppl, 1997, *J Neurophysiol* 77:364-377; Dyson et al., 1998, *J Comp Physiol* 182:695-702). This provides a unique case for investigating the interrelationship between SFOAE delays, neural frequency selectivity, and cochlear space constants.

Methods

Nine adult barn owls (*Tyto alba*) were lightly anesthetized with ketamine/xylazine. The middle ear was vented on one side, and an Etymotic ER-10C probe sealed to the ear canal. SFOAEs were evoked by swept tones, generally between 1 and 11 kHz, and extracted using a suppression paradigm (Kalluri and Shera, 2013, *JASA* 134: 356-68). Probe levels varied from 0-50 dB SPL.

Results

Owls exhibited robust SFOAE activity, most prominently over the range of 3-11 kHz, which correlates well with the frequency region of their auditory fovea. SFOAEs were detectable down to probe levels of 0 dB SPL. Their behavior was clearly level-dependent, with both linear and nonlinear features. Delays typically decreased above moderate levels (>30 dB SPL). SFOAE phase-gradient delays for a 40 dB SPL stimulus were slightly larger than in other birds (chicken and parakeet), typically decreasing from 2 to 1 ms with increasing frequency. A ‘tuning ratio’ (Shera et al. 2010, *JARO* 11:343-365) was computed and found to vary between 1 and 2 across frequencies, similar to mammals but lower than in chickens.

Conclusion

The present study confirmed a basic relationship between SFOAE delays and neural frequency selectivity for the barn owl, consistent with their unremarkable frequency tuning in the auditory nerve. As a visual fovea is associated with improved acuity, a larger cochlear space constant is often assumed to correlate with enhanced frequency resolution. This is clearly not the case in the barn owl, whose tonotopic map deviates significantly from exponential. These data provide further insight into what role cochlear spatial representation plays in hearing and how this compares across broad classes of morphologies, including the mammalian cochlea.

PS - 220

Spike Time Based Intensity Encoding During Dynamic Range Adaptation in Model Auditory Nerve Fibers

Kamini Sehrawat; Ritu Jain; Sharba Bandyopadhyay

National Brain Research Centre

Background

Rate responses of auditory nerve fibers (ANF) adapt to continuous or repeated stimuli. Adaptation of dynamic range to the distribution of intensities in a continuous dynamic stimulus through dynamic range shift towards the most probable stimulus is observed in the inferior colliculus (IC) and primary auditory cortex (A1) along with ANFs. In the process ANFs show rate suppression and threshold shifts of 10-20 dB depending on the intensity of the most probable stimulus. However non-monotonic, intensity tuned, neurons in A1 adapt to such dynamic stimuli (with a high most probable sound level) and maintain sensitivity to lower sound levels that are below the new shifted rate threshold for ANFs.

Methods

We use responses of model ANFs (developed by Carney and colleagues) to continuous best frequency (BF) tones with rap-

idly varying intensity. The above model incorporate power law adaptation which explains dynamic range shifts in response to such continuous stimuli. The intensity of the stimulus, a BF tone, is chosen randomly from 17 sound levels from 0 to 80 dB SPL in 5 dB steps and is changed every 50 ms. Certain sound levels (3 successive sound levels) has very high probability of occurrence and is the sound level to which ANF responses adapt.

Results

We show that in spite of lack of rate information in the periphery for low intensity sounds, with dynamic range adaptation, high and medium spontaneous rate ANF spike times carry information about soft intensities. Such spike time based information allows the central nervous system to encode those sounds during dynamic range adaptation. We quantify temporal information in ANF spike times through phase projected vector strength and Fisher information in period histograms to show robust encoding of soft intensity sounds during dynamic range shift. We further show that such dynamic range adaptation gets stronger in cases of mild to moderate hearing loss. Stronger adaptation causes larger dynamic range and hence threshold shifts in mild to moderate impaired ANFs than in normal ANFs. We also compare spike timing information of low intensities under mild to moderate hearing loss to that of normal ANFs.

Conclusion

Thus our results show the importance of spike timing in ANFs for normal as well as hearing-impaired listeners. The gain in dynamic range of intensity encoding observed in ANFs due to spike timing information under normal conditions is conserved during adaptation in spite of large suppression of ANF response rates. Further, stronger dynamic range adaptation effects in the mild and moderate hearing-impaired lead to steeper rate versus intensity functions, which may amount to faster growth of loudness in such cases.

PS - 221

Computational Model Predictions of Age and Hearing Loss Effects on Concurrent Vowel Identification

Ananthakrishna Chintanpalli; Jayne B. Ahlstrom; Judy R. Dubno

Medical University of South Carolina

Background

Differences in formant and fundamental frequencies (F0) are important cues for segregating and identifying two simultaneously presented (concurrent) vowels. For older adults with normal and impaired hearing, concurrent vowel identification is substantially reduced, even when identification of single vowels is unaffected. To reveal mechanisms that may underlie these deficits, this behavioral and computational modeling study was designed to estimate age- and hearing-loss-related changes to the cochlea and auditory nerve (AN) that may alter phase locking to formants and F0s of concurrent vowels.

Methods

Younger and older adults with normal hearing, and older adults with hearing loss listened to concurrent vowels with a range of F0 differences. Individual vowels were presented at 65 dB SPL for subjects with normal hearing and at 85 dB SPL for subjects with hearing loss, to minimize confounding effects of reduced audibility. Predictions from a computational AN model were used to estimate formant and F0 difference cues available for vowel identification by each of the three subject groups. Three versions of the model were developed based on known anatomical and physiological changes to the cochlea and AN due to increased age and hearing loss. All model simulations included age-related declines in AN fibers. To predict AN responses by older adults with normal hearing, the model simulated a reduced proportion of low-medium spontaneous-rate fibers; functional changes in outer and inner hair cells were also simulated to predict AN responses by older adults with hearing loss. For each group, average localized synchronized rate and template contrast were computed from AN responses to quantify phase locking to formants and F0s, respectively.

Results

Compared to scores for younger adults, identification of both vowels was reduced for older adults with normal hearing and further reduced for older adults with hearing loss. Preliminary model predictions revealed that phase locking to formants of both vowels declined with increased age and hearing loss, which differed based on vowel-pair formant characteristics. These predictions will be discussed in relation to age- and hearing-loss-related declines in concurrent vowel identification.

Conclusion

Identification of concurrent vowels is substantially poorer than normal for older adults with normal and impaired hearing, while identification of single vowels is relatively unaffected. Assessment of these results in the context of model predictions may provide physiologically appropriate explanations of age- and hearing-loss-related peripheral-processing deficits for segregating and understanding target speech in complex listening environments.

PS - 222

A Parsimonious Model of Phase Locking by Mammalian Auditory-Nerve Fibers

Adam Peterson¹; Dexter Irvine²; Peter Heil¹

¹*Leibniz Institute for Neurobiology*; ²*Bionics Institute and Monash University, Melbourne, Australia*

Background

Phase locking of the spikes of auditory-nerve fibers (ANFs) to low-frequency acoustic stimuli is one hallmark of the temporal precision of the auditory system. Common analyses of phase locking include the calculation of the mean phase angle, which provides an estimate of the preferred response phase, and of the vector strength, which provides a measure of the strength of the preference. However, these measures do not capture all salient features of phase-locked ANF responses. We developed a parsimonious model to account for

more details of such responses and their changes with tone frequency and level.

Methods

The model uses spike times obtained from extracellular recordings of ANFs in barbiturate-anesthetized cats. Stimuli were 100-ms tones of relatively low frequency (<5 kHz). Tones were presented at different sound pressure levels at each frequency (mainly characteristic frequency) and repeated at least 50 times at a rate of 4 Hz. The model was fitted to the cumulative spike count per stimulus period, rather than to the traditional period histogram. Cumulative spike count functions maintain maximal temporal precision and thus retain more information than most PSTHs, yet are smooth and allow precise fits.

Results

The phase-locking model we propose contains few free parameters and is able to describe, with small residual errors, ANF responses to tones across the entire phase-locking range. The model reproduces the saturation in maximum spike rate, while at the same time preserving the sinusoid-like shapes observed in period histograms. Remarkably, this is achieved with a dynamic nonlinearity in the form of a Boltzmann function that changes in a highly systematic way with sound pressure level. Furthermore, the driving forces for ANF spike generation estimated with the model are consistent with multiple features of in-vivo recordings of inner hair cell (IHC) membrane potentials. We find evidence for a power-of-3 relationship between the instantaneous stimulus amplitude and ANF spike probability.

Conclusion

Because a single ANF is driven by a single IHC, the precise characterization of the instantaneous responses of ANFs, as achieved by our parsimonious model of ANF phase-locking behavior, may also yield important insights into the operation of individual IHCs in the fully intact cochlea. We attribute the model's dynamic nonlinearity to fast adaptation of the IHC transduction machinery, ensuring its operation in a nearly linear range across multiple orders of magnitude of sound pressure.

PS - 223

Pulse Infrared Laser Evoked Auditory Brainstem Responses Recorded in Normal Hearing Guinea Pigs

Bingbin Xie; Chunfu Dai

Eye and ENT Hospital, Fudan University

Background

Pulsed infrared lasers have been applied to evoke neurophysiological responses by stimulating motor and sensory neurons directly, as an alternative to electrical stimulation, because of its advantaged features compared to electrical stimulation: better spatial resolution and no stimulation of artifacts. It could be beneficial to improve cochlear implants if infrared stimulation was taken advantage in the auditory system. When optical evoked auditory brainstem response

(oABR) could be recorded in animals had been proved, it is important to know the energy required to evoke oABR.

Methods

Experiments were performed on 18 guinea pigs, 250g to 300g weight. Acoustic ABR (aABR) records were performed to all animals to make sure the normal hearing prior to a flat polished 200 μ m-diameter optical fiber (NA=0.22) was inserted into the scala tympani, that the distal of the fiber pointed to the spiral ganglion with a distance of 500 μ m approximately. The diode laser output with 1850nm wavelength was coupled to the other distal of the fiber. The pulse duration were: 150 μ s, 100 μ s, 90 μ s, 80 μ s, 70 μ s, 60 μ s, and 50 μ s respectively, the pulse repetition rate was 10Hz. The oABR were recorded by Tucker Davis Technologies (TDT) neurophysiological systems, the overall noise of the recordings was reduced by bandpass filtering, with the highpass filter cutoff frequency set to 300 Hz and the lowpass filter cutoff frequency set to 3000 Hz, the amplifier gain was set to 20.

Results

Steadily oABR evoked by the pulsed infrared laser at different pulse durations were recorded in all 18 guinea pigs. For the different pulse durations, the stimulation thresholds were: 150 μ s, 17.9 \pm 4.36 μ J; 100 μ s, 9.22 \pm 1.82 μ J ; 90 μ s, 8.83 \pm 2.44 μ J ; 80 μ s, 8.30 \pm 1.52 μ J ; 70 μ s, 7.67 \pm 1.93 μ J ; 60 μ s, 7.30 \pm 2.05 μ J ; 50 μ s, 6.73 \pm 1.52 μ J. The aABR thresholds of animals obtained before and after infrared stimulation were similar and normal.

Conclusion

Pulse infrared laser could stimulate spiral ganglion cells to evoke steadily oABR. The energy required to evoke oABR by stimulating the spiral ganglion cells increases as the pulse duration gets longer.

PS - 224

Simultaneous Recordings of Pairs of Auditory Nerve Fibers Contacting the Same Inner Hair Cell

Jingjing Wu; Eric Young; Elisabeth Glowatzki

The Johns Hopkins University School of Medicine

Background

Each inner hair cell (IHC) is contacted by 10 – 30 auditory nerve fibers (ANFs). Anatomical studies in cat have shown that individual IHCs can be contacted by ANFs with different response properties (Liberman, *Hear. Res.* 1980; Merchant-Perez and Liberman, *J. Comp. Neurol.* 1996). Simultaneous recordings from pairs of ANFs have been performed on fibers with similar characteristic frequencies, but not yet from fibers that contact the same IHC (Johnson and Kiang, *Biophys. J.* 1976). Thus, the relationship between the firing patterns of ANFs contacting the same IHC remains elusive.

Methods

We recorded pairs of ANFs (n = 11) contacting the same IHC from acutely dissected cochlear preparations of hearing rats (3 – 4 week old). Extracellular loose patch recordings were obtained directly at the dendritic endings of ANFs, close to where they contact the IHCs. The spontaneous firing patterns

of ANFs (in extracellular solution with 5.8 mM potassium and 1.3 mM calcium) were monitored and analyzed.

Results

Our recordings demonstrate directly that ANFs contacting the same IHCs can have different spontaneous firing rates, ranging from 0 – 50 spikes per second. Individual firing patterns were analyzed by inter-event interval (IEI) histograms, joint IEI plots and hazard functions. The firing patterns of our recordings resembled those of ANFs recorded *in vivo* (Li and Young, *Hear. Res.* 1993). Correlations between the firing activities of ANFs contacting the same IHC were assessed using cross-correlograms on selected stationary phases of the recordings. So far, we did not observe any correlations between the spontaneous firing patterns of ANFs contacting the same IHC.

Conclusion

Our results suggest that the spontaneous firing patterns of ANFs contacting the same IHC arise independently and are set by local pre- and postsynaptic conditions at individual ribbon synapses.

PS - 225

Preservation of Auditory Nerve Synapses in Ventral Cochlear Nucleus of Mice With Early-Onset Progressive Hearing Loss

Amanda Lauer¹; Brian McGuire¹; Benjamin Fiorillo²; David Ryugo³

¹Johns Hopkins University School of Medicine; ²Johns Hopkins University Summer Internship Program and Bowdoin College; ³Garvan Institute of Medical Research and School of Medical Sciences, University of New South Wales

Background

Loss of auditory nerve synapses in ventral cochlear nucleus (VCN) has been reported after noise trauma, ablation of the organ of Corti, and kanamycin ototoxicity. The effects of other forms of acquired deafness on these synapses are unclear. We investigated changes in VCN gross morphology and auditory nerve synapse integrity in DBA/2J mice with progressively increasing auditory brainstem response thresholds beginning with high frequencies at ~4 weeks of age. These mice display profound hearing loss by ~4 months of age.

Methods

We used design-based stereology to investigate the volume, number of principal neurons, and number of VGLUT1-positive auditory nerve terminals in the VCN of DBA/2J mice with hereditary early-onset progressive hearing loss. Transmission electron microscopy was used to verify the stereology results and reveal ultrastructural features of auditory nerve synapses in VCN.

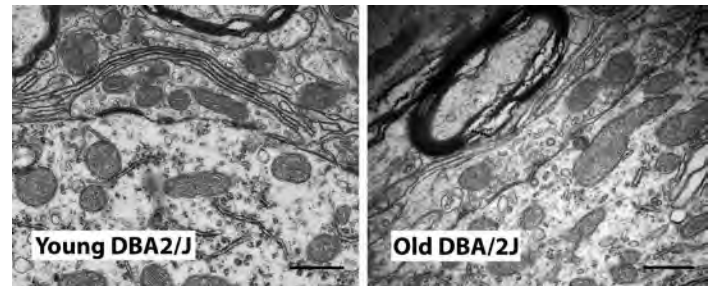
Results

Adult DBA/2J mice had smaller VCN volumes with fewer principal neurons than normal-hearing CBA/CaJ mice, despite reports of a longer basilar membrane and an increased number of hair cells in DBA/2J mice. We found no difference between young adult and older DBA/2J mice on any of the parameters

measured using stereological techniques. Transmission electron microscopy confirmed the presence of numerous auditory nerve synapses in VCN, but hearing-impaired mice could exhibit abnormally large and flattened postsynaptic densities. No signs of degenerating synapses were detected.

Conclusion

Survival of central auditory nerve synapses likely affects the outcomes of deaf patients receiving cochlear implants, and the present results suggest that synapses can be preserved in some forms of acquired deafness. Elucidating the mechanisms promoting survival of central auditory nerve synapses in models of acquired deafness may provide new opportunities for therapeutic intervention.



PS - 226

Modulation of BDNF Mediated Outgrowth in a Mouse Spiral Ganglion Cell Model

Marcus Müller; Anke Tropitzsch; Benedikt Kramer; Claudia Frick; Hubert Löwenheim

University of Tübingen Medical Center

Background

Cochlea implant (CI) technology is state of the art in the cure of deafness. However, electrical stimulation by a CI does not result in the performance of normal hearing. One reason is the limited number of electrode contacts that stimulate the auditory nerve. A way to improve the nerve-electrode interface is to stimulate the outgrowth of neurites towards and onto the electrode. This may be achieved by neurotrophins such as brain derived neurotrophic factor (BDNF). Via TrkB receptors neurite outgrowth is stimulated, however as a paradox, this effect is inhibited by simultaneous BDNF binding to the low-affinity p75NTR receptor. We thus set out to investigate the TrkB and p75NTR mediated pathways in more detail.

Methods

An organotypic culture model of the postnatal (P4-6) mouse spiral ganglion was used. Neurite outgrowth was analyzed and quantified by customized Sholl analysis using ImageJ.

Results

At the top of the BDNF pathway the Tyrosine kinase-inhibitor, K252a inhibited BDNF induced neurite outgrowth at a EC 50 concentration of 0.1 μ M. Further down the pathway supplement of H-89 and KT5720, both Protein kinase A inhibitors, and resulted also in dose dependent inhibition of BDNF induced neurite outgrowth, as did the PI3K (phosphoinositide 3-kinase) inhibitors LY294002 and wortmannin. In the p75NTR receptor pathway application of MAG-Fc (my-

elin-associated glycoprotein) created a p75NTR associated inhibitory environment which suppressed BDNF activated outgrowth. The effect of the inhibitory environment was abolished by the application of a selective TrkB ligand and the interruption of p75NTR signaling by a Rho-associated kinase inhibitor (Y27632).

Conclusion

The organotypic culture model of the spiral ganglion is suitable for the evaluation of compounds stimulating or inhibiting neurite outgrowth. To overcome inhibitory environment, more potent TrkB-agonists are required. Selective inhibition of the p75NTR pathway improves neurite outgrowth in an inhibitory environment.

PS - 227

CGRP Potentiates Kainate-Induced Ca^{2+} Entry Into Spiral Ganglion Neurons Via a CAMP-Dependent-Protein Kinase (PKA)-Dependent Mechanism

Ning Hu; Catherine Kane; Zarin Rehman; Steven Green
University of Iowa

Background

Kainate causes excitotoxic trauma to synapses ("synaptopathy") between inner hair cells (IHCs) and type I spiral ganglion neurons (SGNs) (Wang & Green, J Neurosci, 2011), associated with Ca^{2+} entry via Ca^{2+} -permeable AMPA receptors (Hu et al, ARO Abstract, 2013). Kainate synaptopathy is exacerbated by calcitonin gene-related peptide (CGRP), a neurotransmitter in the olivocochlear efferent system but the mechanism is not understood. cAMP is an important second messenger for CGRP signaling and this is also the case for kainate-induced synaptopathy. Because excitotoxic trauma is due, at least in part, to Ca^{2+} entry, we asked whether CGRP potentiates the increase in cytosolic Ca^{2+} caused by kainate and whether cAMP-dependent-protein kinase (PKA) is involved.

Methods

Dissociated SGN cultures (Hegarty et al, J Neurosci, 1997) were prepared from P4 to P5 rat pups. Intracellular Ca^{2+} concentration ($[\text{Ca}^{2+}]_i$) was determined using Oregon Green-BAPTA-1 (Molecular Probes) as the Ca^{2+} reporter with the cells maintained in HEPES-buffered saline, pH 7.4, 1 mM Ca^{2+} , 1 mM Mg^{2+} , at room temperature. Excitotoxic trauma was accomplished by addition of kainate at indicated concentrations. CGRP (10 nM), PKA activator 8-cpt-cAMP (1 mM) or PKA inhibitor H89 (0.01 mM) were present 30 min before kainate. Viability of SGNs was verified by observation of an increase in $[\text{Ca}^{2+}]_i$ upon depolarization with 30 mM K^+ .

Results

Increased $[\text{Ca}^{2+}]_i$ in SGNs was just detectable at 0.01 mM kainate and approaching the maximum above 0.1 mM kainate ($\text{ED}_{50} \approx 28 \mu\text{M}$). 8-cpt-cAMP did not cause increased $[\text{Ca}^{2+}]_i$ but pretreatment with 8-cpt-cAMP potentiated the kainate-induced increase in $[\text{Ca}^{2+}]_i$ so that 0.02-0.05 mM kainate produced maximal $[\text{Ca}^{2+}]_i$ increase. Similarly, CGRP did not cause increased $[\text{Ca}^{2+}]_i$ but pretreatment with CGRP po-

tentiated the kainate-induced increase in $[\text{Ca}^{2+}]_i$, so that 0.05 mM kainate produced maximal $[\text{Ca}^{2+}]_i$ increase. The ability of CGRP to potentiate the Ca^{2+} response of SGNs to kainate was abrogated by co-treatment with H89, implying that CGRP achieves this effect by recruiting the cAMP-PKA signaling pathway.

Conclusion

The results show that CGRP potentiates kainate-induced Ca^{2+} influx to SGNs. This is consistent with a hypothesis that Ca^{2+} entry is necessary, at least in part, for kainate-induced synaptopathy. It is also consistent with our finding that CGRP exacerbates kainate-induced synaptopathy. The results implicate cAMP-PKA signaling as an important regulator of Ca^{2+} influx during excitotoxic trauma to synapses between IHCs and type I SGNs.

PS - 228

Functional Effects of Semaphorin3A on Membrane Excitability in Spiral Ganglion Neurons

Victor Wong; Marc Meadows; Ebenezer Yamoah
University of California Davis

Background

The development and survival of spiral ganglion neurons (SGNs) are dependent on multiple trophic factors as well as membrane electrical activity. Semaphorins (Sema) constitute a family of membrane-associated and secreted proteins that have recently garnered significant attention as a potential SGN "navigator" during cochlea development. Specifically, previous studies using mutant mice demonstrated that Sema3A plays a role in the SGN pathfinding, and this signaling likely occurs through a receptor and co-receptor complex involving neuropilin1 and plexinA1/plexinA3 respectively. The mechanisms, however, by which Sema3A shapes SGNs firing behaviour continue to elude our comprehension. In these studies, we have found that in addition to neuronal guidance, Sema3A plays a novel role in regulating SGN resting membrane potential and its excitability.

Methods

Our approach uses a well-characterized primary culture system of dissociated SGN from pre-hearing (P3-P5) and post-hearing mice (P12-P15; C57Bl/6J). From these cultured SGNs *ex vivo*, we further separate apical and basal SGN populations, and we recorded membrane potentials using whole-cell patch clamp recording techniques. Recombinant Sema3A were applied to examine their effects on intrinsic membrane properties and action potentials evoked by current injections.

Results

Apical and basal SGNs from newborn mice treated with recombinant Sema3A (100ng/ml) displayed a higher resting membrane potential (apical = $-55.9 \pm 0.9 \text{ mV}$ vs. $-58.2 \pm 1.4 \text{ mV}$; basal = $-54.6 \pm 1.6 \text{ mV}$ vs. $-57.2 \pm 0.7 \text{ mV}$), higher threshold (apical = $-25.3 \pm 2.1 \text{ mV}$ vs. $-32.3 \pm 1.2 \text{ mV}$; basal = $-26.33 \pm 2.0 \text{ mV}$ vs. $-34.0 \pm 1.1 \text{ mV}$), decreased amplitude (apical = $40.1 \pm 3.8 \text{ mV}$ vs. $61.6 \pm 2.7 \text{ mV}$; basal = $43.9 \pm 4.8 \text{ mV}$ vs. $72.5 \pm 3.0 \text{ mV}$), and

prolonged latency (apical = 3.6 ± 0.2 ms vs. 3.1 ± 0.2 ms; basal = 3.25 ± 0.3 ms vs. 2.9 ± 0.2 ms) and duration of spikes (apical = 3.3 ± 0.4 ms vs. 2.5 ± 0.2 ms; basal = 3.7 ± 0.5 ms vs. 2.2 ± 0.1 ms). Although similar phenomenon was observed in SGNs from post-hearing mice, the resting membrane potential was essentially indistinguishable before and after *Sema3A* exposure (apical = -57.0 ± 0.9 mV vs. -55.6 ± 1.6 mV; basal = -57.2 ± 1.0 mV vs. -59.2 ± 4.0 mV). Interestingly, preliminary studies revealed that *Sema3A* increased interspike intervals and decreased spike frequencies in SGNs from newborns and adult mice. Further studies are underway to delve into the mechanisms of *Sema3A*-mediated changes in SGN electrical properties.

Conclusion

SGNs undergo rapid and considerable changes in their intrinsic excitability during the first 2 weeks of postnatal development. *Sema3A* may not only serve as an axon guidance factor but also play a central role in modulating SGN excitability during development.

PS - 229

Auditory Nerve Coding of Concurrent Fundamental Frequencies Following Noise Exposure

Ann Hickox; Michael G. Heinz

Purdue University

Background

Distinguishing competing speech signals relies in part on separating talkers by differences in voice pitch, or fundamental frequency (F0). Individuals with sensorineural hearing loss (SNHL) often have increased difficulty differentiating between talkers, potentially from loss of pitch cues. Degraded coding of resolved and unresolved harmonics, e.g. reduced temporal fine structure (TFS) and envelope (ENV) cues, may contribute to this deficit. Auditory nerve (AN) responses normally contain sufficient temporal information to distinguish F0s of two concurrent harmonic tone complexes (HTCs) (e.g. Larsen et al., 2008). Here, we compare accuracy and strength of AN F0 coding in noise-exposed vs. unexposed chinchillas for F0 estimates based on TFS vs. ENV coding.

Methods

AN responses to concurrent HTCs were recorded in anesthetized chinchillas (some exposed to octave-band noise at 500 Hz, 116 dB SPL, 2 hrs). Each HTC included harmonics 2-20, where F0 of the lower complex (F01) was chosen to place the third harmonic at the fiber's characteristic frequency (CF), and F0 of the higher complex (F02) was scaled to produce 1- or 4-semitone separation between F01 and F02. Responses to alternating polarity stimuli from a population of fibers with similar CFs (± 0.6 octaves) were predicted from responses of a single fiber using spectro-temporal manipulation procedures assuming cochlear scaling invariance. Pooled responses derived from individual-CF shuffled auto-correlograms (SACs), difcors (TFS information) and sumcors (ENV information) were passed through a "pitch sieve", or periodic template, to quantify accuracy and strength of F0 coding for each sub-population of virtual fibers.

Results

Accuracy and strength of F0 coding in temporal responses were greatest for lower CFs (< 2 kHz), as in previous studies, and SACs, difcors and sumcors produced similarly accurate F0 estimates. For some exposed fibers with elevated thresholds and spared tuning (suggestive of IHC damage), F0 estimates and coding strength were within normal bounds. For some exposed fibers with elevated thresholds and slightly poorer tuning (suggestive of OHC damage), strength of F0 coding was normal, or even enhanced, especially for sumcor-based analyses, and accuracy was not severely diminished.

Conclusion

For mild SNHL, AN representation of competing F0s (minimum 1-semitone separation) does not show diminished accuracy, but rather shows enhanced coding strength or "pitch salience" potentially related to previous reports of enhanced ENV coding. Degraded pitch discrimination ability may arise in more severe cases of SNHL from mechanisms like loss of tonotopicity or reduced "relative" TFS salience from an increased reliance on ENV cues.

PS - 230

Temporal Resolution in the Periphery Fails to Explain Species Differences in Dip Listening

Katrina Schrode; Mark A. Bee

University of Minnesota

Background

Humans and some other animals achieve a release from masking by exploiting dips in the amplitude of background noise. In behavioral experiments, females of Cope's gray treefrogs (*Hyla chrysoscelis*), but not the green treefrog (*Hyla cinerea*), experienced a release from masking when maskers fluctuated at slow rates typical of natural acoustic scenes. Abilities to listen in the dips are dependent on temporal processing. Therefore, we should expect gray treefrogs (dip-listeners) to exhibit better temporal processing than green treefrogs (non-dip-listeners). In a previous study, however, we found that green treefrogs showed slightly better phase locking of the auditory nerve to some frequencies. Here, we used a paired-click, evoked potential paradigm to test the hypothesis that differences in dip listening could be accounted for by better temporal resolution in the gray treefrog auditory system.

Methods

We recorded auditory evoked potentials in males and females of gray and green treefrogs in response to paired click stimuli. Two clicks were presented with short inter-click intervals that ranged from 0.25 to 10.0 ms. We measured the amplitudes of the auditory brainstem responses (ABRs) evoked by the clicks. From these amplitudes, we calculated ABR recovery and evaluated its dependence on inter-click interval in the two species.

Results

ABR recovery increased with increased inter-click interval for both species. The responses of both species had fully recovered (100% recovery) at an inter-click interval of 8 ms. Over-

all, the recovery functions were very similar between the two species. Green treefrogs had slightly greater recovery than gray treefrogs at short (1- 2 ms) intervals, but there were no statistical differences between the species.

Conclusion

The results of the current study indicate that there are no differences in temporal resolution at the level of the auditory nerve which could account for the apparent differences in release from masking seen in these two species. However, these results do not preclude differences in temporal resolution between the species at ascending levels of the auditory system.

PS - 231

Infrared- and Nanoparticle-Enhanced Stimulation of Auditory Neurons *In Vitro*

Karina Needham¹; William Brown²; Jiawey Yong²; Bryony Nayagam¹; Paul Stoddart²

¹University of Melbourne; ²Swinburne University of Technology

Background

Infrared neural stimulation (INS) is an emerging technique that has been demonstrated in a wide range of peripheral and central neural tissue, predominantly in the context of bionic devices. INS uses pulsed infrared laser light to generate stimuli in neural tissue, and shares many of the advantages of other optical techniques such as a high degree of spatial selectivity and non-contact stimulation. Previous work has shown that INS is mediated by rapid heating due to absorption of incident light by water molecules in the tissue. This rapid heating causes transient changes in membrane capacitance, and can also directly activate temperature sensitive ion channels in cells that express them. Here we examine which mechanisms are activated in primary auditory neurons during INS. Further, we investigate the use of nanoparticles and near-infrared light for enhancing the process of infrared neural stimulation.

Methods

Patch clamp recordings were made from cultured rat primary auditory neurons ($n \geq 100$) exposed to pulsed infrared light (1535 nm and 1870 nm), or incubated with gold nanorods that are specifically tailored to absorb 780 nm light and illuminated by light of this wavelength.

Results

Neurons exposed to pulsed infrared light responded with membrane depolarization and small inward currents during stimulation, but did not activate action potentials. Neural responses *in vitro* occurred at substantially higher stimulation levels than reported by *in vivo* studies. Neither capsazepine nor ruthenium red blocked the response. Neurons incubated with gold nanorods and exposed to 780 nm light displayed similar membrane depolarization and inward currents, yet action potentials were also observed in a subset of cells. Neurons cultured either in the absence of gold nanorods, or the presence of gold nanospheres (nanoparticles that do not strongly absorb 780 nm light) did not respond to 780 nm pulsed light.

Conclusion

Both infrared light and near-infrared light in the presence of gold nanorods induce depolarization in primary auditory neurons *in vitro*, with the latter also able to activate neural firing. The combination of nanoparticles and near-infrared light might allow the stimulation of deeper tissues *in vivo*.

PS - 849

Characterization of the Neonatal Mouse Spiral Ganglion - Establishing a Method for Ca²⁺ Current Recordings in Spiral Ganglion Neurons

Tobias Eckrich; Veronika Scheuer; Friederike Stephani; Kerstin Blum; Stefan Münkner; Jutta Engel
Saarland University

Background

Spiral ganglion neurons (SGNs) transmit sensory stimuli to the brain and are the bottleneck for the entire auditory information transduced by hair cells (HCs). Myelinated type I SGNs contact inner HCs, establish a precise 1 to 1 connection and comprise 95% of all SGNs. The contribution of Ca²⁺ channel subtypes has been revealed in hearing wildtype mice (Lv et al., J Neurosci 2012), but very little is known about neonatal SGNs. Hence we set out to record Ca²⁺ currents in SGNs aged P5-P6 for future phenotyping of mutant mice deficient for various Ca²⁺ channel subunits.

Methods

Whole cell patch-clamp recordings and live-imaging experiments using Ca²⁺ sensitive indicators in cultured SGNs were complemented using immune fluorescence labelling.

Results

We found that mouse SGNs type I are myelinated as early as P2. Patch-clamp recordings using acute spiral ganglion (SG) whole-mounts were unsuccessful, and enzymatically dissociated SG cultures yielded only few viable neurons. Culturing SG for ≥ 7 days led to growth of neurites and loss of myelin from SGNs. Patch-clamp recordings revealed large K⁺ currents that were blocked by extracellular TEA (30 mM), 4-AP (15 mM), intracellular Cs⁺ (110 mM). Large voltage-dependent Na⁺ currents were fully blocked by TTX (2 μ M) unmasking Ca²⁺ currents of about 1 nA. Ca currents could be blocked by 100 μ M Cd²⁺ or by removing Ca²⁺ from the extracellular solution. To test whether 7 days *in vitro* severely affected the composition of Ca²⁺ currents, we performed Ca²⁺ imaging with SGNs cultured overnight using FluoForte-AM and a ZEISS LSM700. Somatic Ca²⁺ transients (increases in $\Delta F/F_0$) could be elicited by multiple applications of a depolarising high K⁺ solution and were abolished when the high K⁺ solution contained either 0 mM Ca²⁺ or 1.3 mM Ca²⁺ in conjunction with 100 μ M Cd²⁺. Furthermore, the application of 10 mM nimodipine and 1 μ M mibefradil largely reduced depolarization-induced increases in $\Delta F/F_0$, indicating that somatic Ca²⁺ channels were mostly L- and T-type.

Conclusion

Taken together, we have established a culture method that is suitable for patch-clamp recordings in neonatal mouse

SGNs. Using additional Ca imaging we are able to estimate if culturing SG tissues changes the contribution of Ca channel subtypes.

PS - 232

Lack of Immune System Genes Causes Loss in High Frequency Hearing but Does not Disrupt Cochlear Synapse Maturation in Mice

Dasom Lee; Melissa Calton; Diana Mendus; Felix Wangsawihardja; Rose Leu; Srividya Sundaresan; **Mirna Mustapha**
Stanford

Background

Early cochlear development is marked by exuberant outgrowth of axons that innervate multiple targets. Important for the establishment of mature cochlear neural circuits is the pruning of inappropriate axons and synapse connections. Such synaptic refinement also occurs in the central nervous system and recently, genes ordinarily associated with immune and inflammatory processes have been shown to play non-immune roles in synaptic pruning in the brain. These molecules include the complement cascade (C1q) and the major histocompatibility complex class 1 (MHC1) genes, H2-K^b and H2-D^b. We investigated whether MHC1 and C1q genes may be involved in synaptic refinement in the cochlea. These immune genes are upregulated during the period of cochlear functional development making them attractive candidates for our study. We characterized mice lacking both MHC1 genes (termed K^bD^b-/-) and C1q for auditory function and synaptic patterning.

Methods

Our data were collected from postnatal day 15 (P15) and P29. Using quantitative RT-PCR, we measured MHC1 and C1q expression at different developmental ages. Immunostaining were used to assess the number and pattern of afferent and efferent synapses. Confocal and Volocity 3DImage analysis was applied for synapses and neurons quantification. Auditory function was assessed by electrophysiological tests.

Results

Our results suggest that afferent synapse pruning occurs normally beneath both IHCs and OHCs of C1q -/- and K^bD^b-/- mice as compared to wild type controls. Patterning of afferent fibers type I and type II that innervate IHCs and OHCs respectively, are normal as well. We analyzed efferent synapse and fiber patterns and these appeared unaltered in both C1q-/- and K^bD^b-/- as compared to control mice. Hearing tests show that C1qa expression is not necessary for hearing development or maintenance but lack of MHC1 expression causes hearing impairment. K^bD^b-/- mice exhibit elevated thresholds at high frequency (32 kHz) at P29 of age compared to their wild type controls.

Conclusion

Taken together, these results indicate that while C1q and MHC1 genes are not primary players in cochlear synaptic pruning, lack of MHC1 genes results in high frequency hearing loss. Further studies will be necessary to explain the in-

creased threshold at high frequencies in K^bD^b-/- mice and to identify the other candidate factors that may be involved in the critical process of synaptic refinement in the cochlea.

PS - 233

Voltage-Gated Sodium Currents in Pre- and Post-Hearing Spiral Ganglion Neurons

Marc Meadows; Ebenezer Yamoah
University of California Davis

Background

Afferent type-I spiral ganglion neurons (SGNs) innervate inner hair cells (IHCs) of the cochlea, which receive synaptic output encoding acoustic stimuli. Rapid inward currents from voltage-gated sodium channels (VGSCs) located at node, internode junctions, and cell body are responsible for generating the initial phase of action potentials encoding auditory signals. Previous studies on mouse SGNs have reported the expression of VGSC subtypes Na_v1.2 and Na_v1.6. However, functional properties of VGSCs are unknown. We propose that VGSCs are expressed in the soma of cultured mouse SGNs, and there are differences in sodium currents from SGNs located in apical and basal regions of the organ of Corti.

Methods

SGNs were isolated from C57BL/6J mice grouped by ages (postnatal days, P) P0-5 and P12-15. Whole cell voltage-clamp recordings were performed to study inward sodium activation currents in type-I SGNs. We have also performed cell attached voltage-clamp to measure unitary current properties. Finally, we used immunohistochemistry to identify VGSC subtypes in SGNs.

Results

Our findings confirmed expression of VGSC subtypes Na_v1.2 and Na_v1.6 in mouse SGNs. These channels were localized in the soma of isolated neurons. Moreover, Na_v1.7 expression was also detected in the soma. Whole cell patch-clamp revealed spatial differences in the half activation voltage ($V_{1/2}$) of sodium currents in SGNs. Specifically, $V_{1/2}$ of whole cell sodium current in apical was -40.5 ± 0.39 mV ($n = 4$) and basal SGNs was -47.3 ± 0.23 mV ($n=3$). Single channel recording from SGNs at the basal turn of the cochlea revealed VGSCs with brief early openings followed by late openings. The mean amplitude of single-channel current at -40 mV was -1.1 ± 0.14 pA ($n=4$) and the slope conductance was 23.8 ± 0.8 ps ($n=2$).

Conclusion

Our findings suggest *ex vivo* mouse SGNs express VGSCs in the soma, which contribute to whole cell and single channel currents. The spatial differences in whole cell sodium current properties may underlie some of the fundamental differences in the electrical properties of apical versus basal SGNs. Furthermore, late openings in VGSCs in SGNs may contribute towards persistent firing of SGNs.

Time Course of Degeneration of Peripheral and Central Processes of Spiral Ganglion Cells in Deafened Guinea Pigs

Huib Versnel; Dyan Ramekers; Emma Smeets; Ferry Hendriksen; Wilko Grolman; Sjaak Klis
University Medical Center Utrecht

Background

Severe trauma to the organ of Corti, including loss of inner hair cells and supporting cells, leads to progressive loss of spiral ganglion cells (SGCs). There have been several studies of SGC degeneration, pointing to the peripheral processes as site where degeneration starts. In contrast, the central processes (axons) have scarcely been studied, although their role is relevant in understanding for example auditory nerve function to electrical stimulation through a cochlear implant. Here we compare time courses of degeneration of the SGC somata, and both their central and peripheral processes.

Methods

One group of guinea pigs was normal-hearing (n=6), two groups were deafened by co-administration of kanamycin (400 mg/kg) and furosemide (100 mg/kg) two (n=6) or six weeks (n=6) before histological preparation. In each animal the right cochlea was sectioned along different planes of interest including (1) myelinated portion of peripheral processes in the osseous spiral lamina, (2) the cell bodies in Rosenthal's canal, and (3) central processes near the internal auditory meatus. Packing densities and cross-sectional areas of cell or process were determined using light microscopical analyses of basal, central and apical cochlear regions.

Results

The packing densities of peripheral processes and cell bodies, which decrease with duration of deafness, were linearly related with an intercept near zero indicating a parallel degeneration process. In contrast, the relation between the packing densities of the axons and cell bodies showed a significant intercept indicating a lag in the degeneration process of the axons. The cross-sectional areas of peripheral processes, which shrink after deafness, were significantly correlated to the SGC areas, while the central process areas were weakly correlated to the SGC areas.

Conclusion

The myelinated portions of the peripheral processes degenerate along with the cell bodies, and not, as often assumed, prior to. Shrinkage of the peripheral processes also parallels the shrinkage of the cell bodies. The axons seem to degenerate slower than the cell bodies, which supports current views.

Level Dependence of Neural Phase-Locking Assessed With Mass Potentials Recorded at the Round Window

Eric Verschooten; Philip Joris
University of Leuven

Background

Phase-locking is a fundamental property of the peripheral auditory system. In single auditory nerve (AN) fibers, phase locking declines with frequency and becomes undetectable at an upper frequency limit which differs between species. We assess the level dependence of phase-locking and its frequency limit using a method previously developed to quantify neural phase-locking from mass-potentials (neurophonic, NP) at the round window (RW).

Methods

We measured potentials at the RW of anesthetized cats, sometimes combined with recording of the mass-potential on the AN. With a forward masking paradigm, we disambiguated contributions of receptor (CM) and neural (NP) origin: probe tones with alternating polarity were preceded by a forward masker of the same frequency to temporally mask the neural contribution in the response. The fundamental component of the NP was extracted from the difference between the unmasked and the masked responses; other components such as the compound action potential, noise and higher harmonic components were removed by subtracting the results to stimuli of opposite polarity and by filtering. Stimuli were repeated and responses averaged.

Results

The NP and CM show increasing amplitude with probe level, but with distinctly different behavior and timing. First, the amplitude of the CM increases linearly with intensity whereas the amplitude of the NP shows a saturating trend. Second, while the phase of the NP advances with increasing level, phase of the CM is nearly invariant. The NP shows a band-pass characteristic which is similar for different probe levels (40-70dB), with a steep decline in phase-locking above 3-4kHz. However, at high probe levels (60dB and higher) there can be a small remaining adaptive component at frequencies above this pass band, i.e. >5kHz. This component attenuates with a shallow slope of 6dB/oct and is similar to that previously observed by Snyder and Schreiner (1984) at the AN. We surmise that the origin of this high-frequency adaptive component is not in the AN but in the CM, perhaps induced by efferent activation.

Conclusion

We conclude that the contributions of AN and hair cells to the mass potential measured at the RW differ in their behavior with level in both amplitude and phase. The upper limit of phase-locking is reflected in a steep decline of the NP at a stable frequency which is consistent with single-fiber recordings of the auditory nerve, but at higher levels an additional adaptive component can appear above this upper limit.

Specifying the Integrity of Neurons in the Auditory Periphery: Influence of Acoustic Overexposure

Brian Earl¹; Mark Chertoff²; Maggie Schad¹

¹University of Cincinnati; ²University of Kansas Medical Center

Background

Difficulty with understanding speech, especially in noisy listening situations may be attributed to auditory nerve degeneration that may not necessarily involve threshold elevation. Recent research has indicated that degeneration of the peripheral auditory nerve can be detected by measuring the amplitude of auditory evoked potentials, including the compound action potential (CAP). The location-specificity of amplitude measures may be improved by tracking CAP amplitude growth while systematically limiting the region of neural firing with a high-pass masking paradigm. Our previous experiments have indicated that the pattern of CAP amplitude growth for high-level stimuli is independent of outer hair cell pathology and is sensitive to neural lesions in the basal region of the cochlea. The objective of this study was to determine if the CAP growth pattern is also sensitive to lesions in the middle to apical regions of the cochlea.

Methods

Gerbils with hearing loss (induced with mid to low-frequency tonal stimuli at 120-124 dB SPL; N=14) were compared to normal-hearing gerbils (N=12). CAPs were evoked with broadband chirps at 90 dB SPL during simultaneous white noise that was high-passed in 1/3 octave intervals between 0.4 and 50 kHz. Cumulative amplitude functions were constructed by plotting the normalized amplitudes of the masked CAPs as a function of distance from cochlear apex (inferred from masker cutoff frequencies). Cochlear hair cell and peripheral auditory nerve anatomy were analyzed under confocal and light microscopy.

Results

Cumulative amplitude functions in normal-hearing gerbils were sigmoidal in shape and approached saturation at the basal end of the cochlea. In the majority of noise-exposed gerbils, the cumulative amplitude functions plateaued in regions that corresponded with the anatomical location of missing/damaged outer and inner hair cells evident in confocal microscope images of phalloidin-stained cochleae. Light micrographs of the same cochleae stained with osmium, however, did not reveal neural damage at the level of the myelinated processes of peripheral auditory nerve fibers (with one exception).

Conclusion

These data indicate that the location and extent of the plateaus observed in CAP-derived cumulative amplitude functions may predict the location of anatomical damage secondary to acoustic overexposure. Future experiments will include additional anatomical analyses to differentiate the effects on the cumulative amplitude function related to hair cell pathol-

ogy from those related to neural degeneration at the level of the afferent dendrites.

Effects of Furosemide-Induced Metabolic Hearing Loss on Temporal Coding of Fine Structure and Envelope in Auditory-Nerve Fibers

Kenneth Henry; Ann E Hickox; Mark Sayles; Michael G Heinz

Purdue University

Background

Previous studies show that noise-induced hearing loss (NIHL) causes substantial changes in temporal coding of complex signals. One of our previous NIHL studies used Wiener-kernel analyses to quantify the frequency tuning of auditory-nerve fiber responses to the temporal fine structure (TFS) and slower-varying envelope (ENV) of broadband Gaussian noise. Whereas TFS and ENV coding are normally tuned near a fiber's characteristic frequency (CF), NIHL caused a dissociation in which ENV coding remained tuned to CF while TFS coding shifted to lower frequencies (0.5-1 kHz). In cases of greater NIHL, temporal coding near CF was lost as both TFS and ENV coding shifted to lower frequencies.

Metabolic hearing loss (MHL) involving reduction of the endocochlear potential is another common form of hearing loss in older individuals that has attracted less study than NIHL. Here, we quantify the extent to which TFS and ENV coding of Gaussian noise responses in the auditory nerve differ between MHL and NIHL.

Methods

MHL was induced in anesthetized chinchillas using intravenous furosemide injections that allowed data collection from the same fiber before, after, and during recovery from hearing loss. The degree of MHL was monitored using tuning curves and the compound action potential. Gaussian noise was presented at 10-15 dB sensation level.

Results

In response to furosemide, tuning curves showed threshold elevation, increased tuning bandwidth, and small shifts in best frequency as in previous work. For Gaussian noise responses, furosemide usually increased the tuning bandwidths of TFS and ENV coding to the same extent as the tuning curve. In contrast to NIHL, the best frequencies of TFS and ENV coding generally remained near CF; dissociation of TFS and ENV coding occurred in a few cases of profound MHL (e.g., 70-80 dB) and substantial downward shifts in both TFS and ENV coding were not observed.

Conclusion

Compared to NIHL, MHL caused relatively minor changes to the tonotopic representation of TFS and ENV in the auditory nerve. The difference may reflect that, for a given degree of threshold elevation, tuning curve shape (i.e., the ratio of tip to tail sensitivity) is more affected by NIHL than by MHL. The results suggest that current hearing aids may provide greater benefit in individuals with MHL. Furthermore, fundamentally

different signal processing strategies might be required to effectively compensate for MHL and NIHL.

PS - 238

Post-Natal Development of Type I Spiral Ganglion Neurons in Rats

Radha Kalluri

University of Southern California

Background

Mature mammalian auditory neurons form functionally distinct subgroups that differ in their spontaneous discharge rate, sensitivity, and dynamic range. These response properties are correlated with where they make contact with the inner hair cell, the size of the presynaptic ribbon that provides input to the neuron and the size and type of glutamate receptor on the post-synaptic membrane of the neuron. *In vitro* studies suggest that diversity in ion channel properties intrinsic to the neuron may also play a role in shaping the functional characteristics of auditory neurons.

Methods

To characterize the anatomical and biophysical development of spiral ganglion neurons, we recorded using whole-cell patch clamp techniques from a semi-intact *in vitro* preparation of spiral ganglion neurons from the middle turn of neonatal rat cochleae (post-natal day 2-9). The semi-intact preparation contained spiral ganglion cell bodies, the peripheral dendrite and hair cells. Biocytin was included in the recording pipette to label the neuron post-recording. Streptavidin conjugated to biocytin was used to fluorescently visualize the labeled neuron. A confocal scanning microscope to generate a z-stack of images. A 3-D representation of the terminal was reconstructed using the Amira imaging software.

Results

We recorded from 45 neurons ranging in age from P2- 9. As previously characterized from dissociated neurons, we noted both rapidly and slowly accommodating spike trains. Whole cell currents progressively increased with age, suggesting that the biophysical properties of SGN continue to mature during the first two post-natal weeks. In 25 of 45 recordings, the biocytin successfully labeled the neuron from the cell body to the synaptic terminals formed on the haircells. All 25 labeled neurons terminated on inner hair cells and did not further branch to outer hair cells. Although at P2 the spiral ganglion neuron branched to form as many as 18-25 branches, by P9 the neuron no longer branched but formed a single terminal on the inner hair cell.

Conclusion

These results suggest that the biophysical and anatomical features of auditory neurons undergo significant developmental changes during the two weeks preceding the onset of hearing.

PS - 239

Properties of Auditory Nerve Driven Feed-Forward Inhibitory Synaptic Circuit Associated With Fusiform Cells in the Mouse Dorsal Cochlear Nucleus

Miloslav Sedlacek; Stephan Brenowitz

NIDCD/NIH

Background

In sensory systems, the relative balance of excitation and inhibition determines how timing and temporal fidelity of action potentials are achieved. The temporal resolution of neuronal integration depends on the time window within which excitatory inputs can be summated and reach the threshold for firing an action potential in the postsynaptic neuron. In the cochlear nucleus, auditory nerve provides excitation to both principal neurons and inhibitory interneurons. Here, we investigated a complex synaptic circuit associated with fusiform cells (FCs), principal neurons of the dorsal cochlear nucleus (DCN) that receive direct excitation from the auditory nerve and disynaptic, auditory nerve driven inhibition from tuberculoventral cells (TVCs) in the deep layer of the DCN and/or from D-stellate cells in the ventral cochlear nucleus (VCN). Mechanisms determining the balance between excitation and inhibition in this local synaptic circuit are not well understood.

Methods

Therefore, by using patch-clamp recordings from FCs and TVCs in parasagittal slices of posthearing (postnatal day 17-22) mouse DCN, we examined basic properties, timing and plasticity of feed-forward inhibition onto FCs.

Results

We show that the feed-forward EPSC-IPSC sequence can be activated even at very low stimulation intensities. In some FCs the excitatory and inhibitory components of the feed-forward inhibitory circuit had the same thresholds indicating they were triggered by activation of the same auditory nerve fibers, whereas in others the thresholds were different, suggesting activation of FCs and TVCs by different auditory nerve fibers. Our results further show that during repetitive stimulation the feed-forward inhibition exhibits activity dependent short-term synaptic plasticity. During trains of ten synaptic stimuli delivered to the auditory nerve, the disynaptic inhibition shows significant amount of synaptic depression when stimulated at 10, 20, 50 and 100 Hz. Multiple mechanisms can be responsible for this activity dependent reduction in auditory nerve driven inhibition onto FCs, such as depression of glutamatergic synapses onto TVCs, or depression of inhibitory synapse between TVCs and FCs. Our results show that when directly stimulated, inhibitory inputs depress only moderately at 10 and 20 Hz and even facilitate at 50 and 100 Hz, whereas the AN-TVC synapse exhibits prominent depression at all frequencies.

Conclusion

We demonstrate that a dynamic and activity dependent regulation of synaptic circuits associated with transmission of acoustic information onto FCs takes place in the DCN which

can have significant consequences for the output from the nucleus and further auditory processing.

PS - 240

Spectral-Temporal Heat Maps of Auditory Nerve Fiber Activation by Speech in Background Noise

Christopher Boven; Robert Wickesberg
University of Illinois at Urbana-Champaign

Background

Humans are remarkably good at recognizing speech in noise. While humans still perform well at -12 dB signal-to-noise (SNR) ratios and lower, even the best automatic speech recognition systems have significant performance decrements at 0 dB SNR. How humans achieve this robust performance remains unclear. There is evidence that auditory nerve fibers with low spontaneous rates, which have been traditionally thought to be most important for encoding a large dynamic range, may play a significant role (e.g. Silkes and Geisler, 1992). This proposal has been explored for frequency features (Reiss et al., 2011) and temporal cues (Boven and Wickesberg, 2013), but not for the speech cues that have been recently described (e.g. Li and Allen, 2009).

Methods

In this study, we presented speech consonants in quiet and with background noise to ketamine-anesthetized chinchillas while recording from individual auditory nerve fibers. A peristimulus time histogram (PSTH) was computed from the responses of each auditory nerve fiber to each consonant. These PSTHs were sorted into 20 frequency regions, derived from critical bands, according to each fiber's characteristic frequency. PSTHs were then averaged within critical band regions and graphed to create a spectral-temporal heat map of auditory nerve fiber activation.

Results

This method produced heat maps that had a unique spectro-temporal structure for each consonant in quiet and that displayed the speech cues identified using AI-grams by Allen and colleagues. For consonants presented in noise, the spectro-temporal structure was highly degraded. Using only the PSTHs from low spontaneous rate fibers to compute the heat maps, however, allowed for a reasonable recovery of the speech cues.

Conclusion

It appears that low spontaneous rate fibers may act as noise gates and are critical for carrying speech information when consonants are heard in background noise.

PS - 241

Loss of Spiral Ganglion Neuron Synaptic Contact is Associated With Hearing Loss After Acute High Intensity Intracochlear Electrical Stimulation in Hearing Mice

Lichun Zhang; Jonathan C. Kopelovich; Barbara Robinson; Hakan Soken; Marlan R. Hansen
University of Iowa Hospitals and Clinics

Background

Acoustic hearing loss after cochlear implantation is a well-described phenomenon, resulting in an average threshold increase of 10-12 dB. In most instances, this process subsequently plateaus. However, a minority of patients (20%) experience acceleration of hearing loss after activation of the stimulating electrodes and go on to develop limited acoustic hearing, thus negating some of the benefit of the implant for those patients. Using a murine model, we have begun to explore the possibility that high intensity electrical stimulation causes excitotoxic damage in susceptible cochleae, exacerbating their predisposition to hearing loss.

Methods

Thirty-three C57Bl6J mice and 11 CBA/CaJ mice underwent unilateral round window implantation under general anesthesia at 3 months of age. Of these subjects, 20 C57Bl6J and 5 CBA/CaJ mice were stimulated with 2 hours of monopolar stimulation at eABR saturation, while the remainder served as operative controls. Serial acoustic click ABR and OAE measurements were obtained. Subsets of these cochleae were sectioned and immunostained for CTBP-2, PSD95, Myosin VII, DAPI and/or neurofilament. They were examined with confocal microscopy to provide density measurements of hair cells and synaptic markers.

Results

In C57Bl6J mice, both implantation alone and implantation with electrical stimulation caused significant hearing loss compared to the unoperated contralateral ears. While there was a trend towards greater hearing loss in the stimulated group, the two experimental conditions did not significantly differ in terms of extent of hearing loss, inner hair cell density, or pre-synaptic puncta density (CTBP2). In contrast, CBA/CaJ mice experienced significantly greater hearing loss after electrical stimulation compared to operative controls. While hair cell counts did not differ, preliminary data indicate that the number of PSD95 puncta/inner hair cell was significantly decreased after acute electrical stimulation.

Conclusion

These preliminary data support a role for excitotoxicity due to high-level electrical stimulation in loss of acoustic hearing after hearing preservation cochlear implantation and point to post-synaptic terminals as the most vulnerable elements. These findings mirror features of noise-induced excitotoxicity and point to possible therapeutic strategies. In that operative trauma causes less hearing loss in CBA/CaJ mice compared with C57Bl6 mice, CBA/CaJ may be a more appropriate strain to model this phenomenon.

PS - 242

Adeno-Associated Virus Vector Delivery of Channelrhodopsin-2 Into Spiral Ganglion Neurons.

Xiankai Meng; Elliott Kozin; Gang Q. Li; Ruth Anne Eatock; Daniel J. Lee; Albert Edge

Eaton Peabody Laboratory, Massachusetts Eye and Ear Infirmary; Department of Otolaryngology, Harvard Medical School

Background

Expression of opsins in spiral ganglion neurons (SGNs) is the first hurdle in efforts to use light for activation of the peripheral auditory pathway. Adeno-associated virus (AAV) has been used extensively in gene therapy research due to its non-pathogenic properties and broad host tissue range. Previous studies have shown that AAV can efficiently deliver opsins, such as channelrhodopsin-2 (ChR2), into both central and peripheral neurons. In this study, we examine the potential use of optogenetics in the peripheral auditory system, and examine viral vector-mediated gene delivery of channelrhodopsin-2 into SGNs *in vitro* and *in vivo*.

Methods

For the *in vitro* study, dissociated SGNs were exposed to adeno-associated virus (AAV2/1)-ChR2 conjugated with mCherry for 48 hours. For the *in vivo* study, AAV2/1-ChR2 was injected directly into the cochlea of neonatal CD-1 mice. After 48 hours of co-culture *in vitro* or 4 weeks following *in vivo* injection. SGNs were examined by confocal microscopy for expression of mCherry.

Results

Confocal microscopy demonstrated transfection of SGNs *in vitro* and *in vivo*. Efficiency of *in vitro* transduction was <10%. In mice injected with AAV2/1-ChR2, we identified expression of ChR2-mCherry in the soma and neurites of mature SGNs. ChR2-mCherry was predominately expressed in neurons (~90% of neurons in the injected area) as opposed to Schwann cells based on immunohistochemistry for TuJ and MBP.

Conclusion

We demonstrate successful *in vivo* and *in vitro* transfer of ChR2 into SGNs using AAV2/1. These findings are consistent with previous work in the central nervous system, which showed that AAV2/1 preferentially infected neurons rather than glial cells. To assess innervation of the auditory system by optogenetically activated neurons we are now recording evoked brainstem responses after application of blue light to the photosensitized cochlea. These experiments may lay the groundwork for a cochlear implant based on optogenetics.

PS - 243

A Multiscale Computational Model of Guinea Pig Cochlea to Probe Neuropathy Mechanisms

Jérôme Bourien; Antoine Huet; Gilles Desmadryl; Régis Nouvian; Jean-Luc Puel

Inserm U1051

Background

Sound-evoked compound action potential (CAP) of the auditory nerve is a common proxy to probe deafness in experimental and clinical framework. It is generally accepted that this electrophysiological index reflects the progressive activation of different pools of fibers that populate the auditory nerve: the high-spontaneous rate (SR) auditory nerve fibers, which detect lowest-sound level, and the medium- and low-SR fibers, which translate higher-sound level stimulation.

Methods

To examine the weight of each auditory fibers fraction on CAP threshold and amplitude, we designed a multiscale computational model of guinea pig cochlea.

Results

This model includes all the components involved in the cochlear sound-transduction and enables to analyze the ANF firing assembly (up to 800 ANFs) as well as the CAP in response to basilar membrane velocity evoked by increasing sound level

Conclusion

Using such model, we found that the low-SR fibers have a small contribution into the CAP.

PS - 244

Probing Auditory Nerve Fiber Loss Using Round-Window Neural Noise

Charlène Batrel; Jing Wang; Marc Lenoir; Jean-Luc Puel;

Jérôme Bourien

Inserm U1050

Background

Recent studies have shown that a selective degeneration (up to 50%) of auditory nerve fibers (ANFs) may coexist with normal auditory brainstem thresholds, making the detection of auditory neuropathies difficult.

Methods

Here, we described a robust and minimally invasive method to probe the degree of ANF loss in gerbil. Spontaneous and sound-evoked neural noise of the cochlea were recorded through an electrode placed onto the round window niche. The difference between the power spectral density of spontaneous and sound-evoked neural noise enable to probe the sound-driven activity of the ANFs.

Results

From 1.6 to 20 kHz, the amplitude of the ANFs sound-driven activity matches the bimodal histogram of the ribbon synapse distribution (indicated by the double immunostaining of synaptic ribbons and glutamate receptor clusters with anti-CtBP2 and anti-GluR2 antibodies, respectively). In animals treated with ouabain, known to induce selective ANFs loss, the ANFs

sound-driven activity became uni-modal (i.e., reduction of the response above 8 kHz), and thus predicting a partial depletion of basal ANFs. Accordingly, confocal microscopy revealed ribbon-synapse deletion in the basal region above 8 kHz.

Conclusion

These results suggest that the cochlear neural noise can be a faithful proxy to quantify the degree of ribbon-synapse loss and can be translated into clinic to phenotype human neuropathies.

PS - 245

Long-Term Protective Effects of Neurotrophic Treatment of the Auditory Nerve in Deafened Guinea Pigs

Dyan Ramekers¹; Huib Versnel¹; Stefan Strahl²; Wilko Grolman¹; Sjaak Klis¹

¹University Medical Center Utrecht; ²MED-EL

Background

After severe damage to the organ of Corti spiral ganglion cells (SGCs) degenerate as a result of lost neurotrophic support. Local treatment with exogenous brain-derived neurotrophic factor (BDNF) prevents SGC degeneration up to two weeks after cessation of the treatment. The goal of this study was to investigate the extent of this preservative effect on both structure and function of the auditory nerve on the long term.

Methods

Guinea pigs were deafened by co-administration of kanamycin (400 mg/kg) and furosemide (100 mg/kg). Two weeks after deafening the animals were implanted with an intracochlear electrode array with cannula connected to an osmotic pump filled with either BDNF or phosphate-buffered saline (PBS). Normal-hearing controls were implanted with an electrode array and a PBS-filled pump. Immediately upon implantation electrically evoked compound action potentials (eCAPs) were recorded using the intracochlear electrode array and a MED-EL PULSAR cochlear implant. Four weeks later the treatment was stopped by surgically removing the osmotic pump. Eight weeks later another series of eCAPs was recorded after which the animals were sacrificed for histological analysis of the SGCs.

Results

Either directly or eight weeks after the four-week treatment with BDNF, SGC packing density was similar to that in two-weeks deaf animals (at which time the treatment started), although some degeneration had occurred in the cochlear apex. Packing density in all three groups was 20-30% lower than in normal-hearing controls. In contrast, the 14-weeks deaf PBS-treated controls suffered severe SGC degeneration (up to 75%). In accordance with SGC degeneration, the eCAP amplitude became smaller after deafening, roughly stabilized in response to BDNF treatment, and was much smaller in PBS-treated controls. The slope of the input-output curve followed the same pattern as the amplitude, but there were no significant differences in the eCAP threshold. The

eCAP latency became shorter after deafening, and was also shorter for BDNF-treated animals.

Conclusion

The preservative effect of BDNF extended significantly beyond the four-week treatment period. This implies that brief neurotrophic treatment, possibly by activating an autocrine survival mechanism, can permanently put progressive neuronal degeneration to an end. These findings make clinical application of neurotrophic treatment more appealing, since it may be sufficient to administer BDNF for a short time in order to ensure long-lasting auditory nerve preservation.

PS - 246

Chronic Microelectrode System for Penetrating Auditory Implants

Vanessa Tolosa; Angela Tooker; Sarah Felix; Kedar Shah; Heeral Sheth; Satinderpall Pannu

Lawrence Livermore National Laboratory

Background

Studies show that there are significant benefits to implanting auditory prosthetics in younger and younger patients. Additionally, more recent studies show that auditory nerve implants can restore additional function due to their ability to provide focal stimulation and selective activation of nerve fibers. Unfortunately, most cochlear implants cause too much damage to use intraneurally. Thus, there is a need for a chronically implantable minimally invasive prosthetic to study both short-term and long-term effects of intraneural auditory stimulation.

Methods

To this end, LLNL has developed a complete implant incorporating a polymer electrode array that is suitable for chronic use as a neural prosthesis. The electrode array is integrated with a chronic percutaneous connector and a removable stiffener. The flexible arrays could minimize adverse tissue response, compared to traditional silicon arrays.

Results

LLNL's fabrication process produces thin-film electrode arrays with integrated cables. The array design is customizable, utilizing multiple layers of polymer and trace metal to fabricate up to 64 electrodes based on current connector design. The electrodes (material, size/shape, arrangement, dual-sided) can be optimized for stimulation or recording. Similar arrays have passed FDA mandated ISO 10993 biocompatibility testing for fully implanted devices.

A stiffener is required for surgical implantation of the electrode arrays due to their flexibility. This is accomplished using a temporary stiffener attached with biodissolvable polyethylene glycol (PEG). The stiffener can be extracted from tissue within 5 – 15 minutes of insertion with an average probe displacement of 28 +/- 9 mm. *In vivo* tests show arrays inserted with the removable stiffener are able to detect single-unit neural signals.

The percutaneous connector provides a chronic interface between the microelectrode array and external electronics. It is

designed to be user-friendly with low connect and disconnect force, passive alignment, and a magnetic clamp. The chronic connector has been tested with up to 64 channels in its current form factor of 18 mm x 11 mm, but can be re-configured with any number of fewer channels. If combined with electronics, the adapter can be modified into a fully-implantable, hermetic device.

Conclusion

The versatility of LLNL's system allows for use in a variety of neural applications, including stimulation of auditory nerves to restore function to patients whose cochlea is damaged by illness or injury.

PS - 247

Cochlear Responses to Amplitude Modulation in Normal Hearing Gerbils

William Merwin III; Eric Formeister; Joseph H McClellan; Ken Hutson; Craig A. Buchman; Oliver F Adunka; Douglas C. Fitzpatrick

The University of North Carolina at Chapel Hill

Background

The signal obtained from Electrocochleography (ECoG) is a mixture of components from different sources. Hair cell-related potentials include the cochlear microphonic (CM) and the summing potential (SP) while nerve related potentials include the compound action potential (CAP) and auditory nerve neurophonic (ANN). Use of the ANN to measure neural activity is restricted to low frequencies within the range of phase-locking to the fine structure. However, auditory nerve fibers of all CFs phase-lock to low frequency amplitude modulations. Consequently, responses to envelope modulations could be used to separate neural and hair cell sources to the ECoG. We investigated the effect of kainic acid (KA) neurotoxin on amplitude modulated (AM) signals as a method to separate the nerve and hair cell responses. We hypothesized that if all the signal energy at the modulation frequency were due to phase locking in auditory nerve fibers, KA should reduce this energy to zero. However, if hair cell transduction also produced energy at the modulation frequency, KA should have less than total effect. These results could be useful for helping to predict outcomes in cochlear implant patients based on ECoG responses prior to implantation.

Methods

Normal Hearing gerbils were anesthetized with urethane and Nembutal. Round window ECoG recordings were taken from gerbils in response to a sinusoidally amplitude modulated tone with a carrier frequency of 3000 Hz and modulation frequencies of 50, 100, 200, 300, 400, and 500 Hz, or a carrier frequency of 500 Hz and modulation frequencies of 25, 50, and 100 Hz. Responses were tested before and after KA was applied to the round window (60 mM in lactated Ringer's solution for 1 hr.)

Results

The KA administration abolished the CAP, indicating loss of nerve activity. The KA caused a decrease in the response to the modulating frequency to both the low and high frequency carrier and across all modulation frequencies, indicating that

neural phase locking to the envelope was lost. However, with most modulation frequencies and most intensities, including low intensities, energy at the modulation frequency remained, indicating that hair cell transduction also produces energy at the modulation frequency.

Conclusion

Hair cell transduction and neural phase-locking produce energy at the modulation frequency when recorded at the round window. Whether both sources also contribute in animals with noise induced hearing loss or CI patients will be addressed in future studies.

PS - 248

A Polymer Based Multi-Channel Cochlear Electrode Array

Kyou Sik Min¹; Seung Ha Oh²; **Min-Hyun Park**³; Joonsoo Jeong¹; Ho Sun Lee²; Sung June Kim¹

¹*School of Electrical Engineering and Computer Science, Seoul National University, Seoul, Republic of Korea;*

²*Department of Otorhinolaryngology-Head and Neck Surgery, Seoul National University College of Medicine;*

³*Department of otorhinolaryngology, Boramae Medical Center, SMG-SNU, Seoul Korea*

Background

Compared to conventional cochlear electrode arrays which are hand-assembled and wire-based, polymer-based implants have several advantages. They are very precise, and their fabrication is inexpensive due to the use of thin-film processes. In the present study, a cochlear electrode array based on a high-performance liquid crystal polymer material is devised. Further, the device is encapsulated in silicone elastomer.

Methods

The fabrication steps introduced here include thin-film processes with liquid crystal polymer (LCP) films and customized self-aligning molding processes for the electrode array. To assess the feasibility of the proposed electrode array, the charge storage capacitance and impedance were measured using a potentiostat. Vertical and horizontal deflection forces were measured using a customized fixture and a force sensor. Insertion and extraction forces were also measured using a transparent human cochlear plastic model, and five cases involving human temporal insertion trials were undertaken to assess the level of safety during the insertion process.

Results

The charge storage capacity and impedance at 1 kHz were 33.26 mC/cm² and 1.02 k Ω , respectively. Likewise, the vertical force and horizontal force of the electrode array were 3.15 g and 1.07 g. The insertion force into a transparent plastic cochlear model with displacement of 8 mm from a round window was 8.2 mN, and the maximum extraction force was 110.4 mN. Two cases of human temporal bone insertion showed no observable trauma while three cases showed a rupture of the basilar membrane.

Conclusion

An LCP-based intracochlear electrode array was fabricated and its electrical and mechanical properties were found to be suitable for clinical use.

PS - 249

Influence of Surface Nanopatterns on the Impedance Development After Cochlear Implantation

Ines Linke¹; Elena Fadeeva²; Verena Scheper¹; Boris Chichkov²; Thomas Lenarz¹; **Gerrit Paasche¹**

¹Hannover Medical School; ²Laser Zentrum Hannover e.V.

Background

During the first weeks after cochlear implantation the electrical impedances at the electrode contacts increase. This increase is associated with the formation of fibrous tissue around the electrode carrier. By introducing nanopatterns on the surface of platinum the water contact angle can be increased and finally the growth of cell on these samples was reduced with an increasing water contact angle. In the current study we transfer these patterns on animal electrodes and test them *in vivo*.

Methods

For patterning the electrode surface, a positioning system was developed allowing the controlled and selective patterning of either the stimulating contact or the silicone surface between the contacts by a femtosecond laser. Dunkin Hartely guinea pigs were implanted for 28 days with standard or surface patterned multichannel cochlear implant electrodes. Impedances were measured daily until day 14 after implantation and later weekly using the standard fitting software Custom-Sound (Cochlear Ltd). Additionally, weekly frequency-specific impedance measurements were done in the range from 1 Hz to 100 kHz. Acoustic hearing thresholds were determined before implantation and after 28 days and electrically evoked auditory brainstem responses were measured weekly from implantation until day 28.

Results

It was possible to pattern stimulating contacts of silicone surfaces of CI electrode selectively by a femtosecond laser. The risk of damage to the electrode array could be reduced over time for Pt contacts but is lowest for patterning of the silicone surface. All animals showed an implantation related shift in hearing thresholds. Additionally, all groups showed an elevated eABR threshold on day 7, but only with standard or silicone-patterned electrodes a consistent recovery was found. Impedances increased over time in all groups even though this increase seemed to be smaller in animals with nanopatterns on the silicone surface.

Conclusion

Technically it is possible to reliably generate nanopatterns on the surface of cochlear implant electrodes. Nevertheless, a promising reduction in impedances compared to control electrodes was not found.

PS - 250

Electrical Stimulation of the Cochlear Nucleus With a Thin Flexible Polymer Microelectrode Array: Designing the Next Generation Auditory Brainstem Implant

Amelie Guex¹; Rohit Verma²; Ariel Hight³; Elliott Kozin³; Keith Darrow³; Christian Brown³; Philippe Renaud¹; Daniel Lee³; Stephanie Lacour¹

¹Ecole Polytechnique Federale de Lausanne; ²University of Manchester; ³Massachusetts Eye and Ear Infirmary

Background

The auditory brainstem implant (ABI) provides meaningful hearing sensations to patients who are not candidates for cochlear implants (CI). Clinical outcomes among ABI users, however, vary among similar cohorts. This variable performance may be due to the rigid electrode design of current ABIs that only access a limited range of the tonotopical arrangement of the dorsal cochlear nucleus (DCN) and may induce extra-auditory sensations due to the spread of electrical current to neighboring non-auditory structures. In this study, we examine thin (<100µm width) and small (<200µm diameter) electrodes integrated on flexible polyimide (PI) substrates. Our novel ABI design may offer a better physical interface with the curvilinear surface of the cochlear nucleus. Further, our design may allow for a reduction of the spread of electrical currents, access a greater tonotopic range of the CN, and limit the recruitment of neighboring non-auditory neurons.

Methods

5-channel microelectrode arrays (MEAs) are fabricated on polyimide substrate using standard microfabrication processes. The electrode sites are coated with PEDOT, a conducting polymer, electropolymerized at the sites to decrease electrode impedance and increase charge injection capacity. *In vivo* experiments are performed on anesthetized Sprague Dawley rats (350-500g). The MEA is placed on the exposed surface of the DCN and a bipolar stimulation is induced, consisting of symmetric biphasic waveforms with 0.2ms phase duration, at a frequency of 23Hz. Responses of the auditory system are assessed by auditory brainstem responses (ABR) and recordings from the central nucleus of the inferior colliculus (CNIC) using a 16-channel electrode array (Neuronexus Technologies, Inc.)

Results

ABRs were successfully generated using our newly designed implant and activation of the central auditory pathways was identified at the level of the inferior colliculus using both monopolar and bipolar conditions. Stimulation at different electrode locations on the DCN surface of the same animal exhibited a relatively broad activation of the neuronal population.

Conclusion

Our results demonstrate that ABI electrodes can be manufactured with well-established MEMS technology. Electrode geometry and density may be optimized to produce implants with higher selectivity and better conform to DCN compared to current designs. Future work includes the optimization of

implant geometry and mechanical compliance. We believe this technology may be readily scaled up for use in larger animal models and ultimately employed for clinical use in the next generation of auditory brainstem implants.

PS - 251

Comparison of Electrical Parameters Between Perimodiolar and Lateral Type Electrode Arrays in the Same Individuals

Junhui Jeong; Ji Hye Heo; Mi-Young Bang; Mi Ran Bae; Bo Gyung Kim; Jae Young Choi
Yonsei University College of Medicine

Background

Cochlear implantation(CI) gave many patients with hearing impairment opportunity to improve their hearing. Perimodiolar electrode arrays were developed to improve stimulation of specific neuronal populations and to decrease power consumption. There had been studies in comparison of benefit between perimodiolar and lateral type electrodes but it had been comparison in different individuals. We compared electrical parameters between perimodiolar and lateral type electrodes in the same individuals who received bilateral cochlear implant with different devices.

Methods

Eight patients(three males, five females) who received cochlear implant in both ears with perimodiolar type electrode and lateral type electrode respectively were enrolled. The patients received cochlear implant sequentially or simultaneously in both ears. Threshold level(T level), comfortable level(C level), dynamic range which means difference between T level and C level, distance from spiral center to electrode in transocular radiographic findings and the amount of battery consumed were compared between two types of electrodes in the same individuals.

Results

Distance from spiral center to electrode was farther at apical portion and nearer at basal portion in lateral type electrode than in perimodiolar type electrode. T level and C level was significantly higher in lateral type electrode than in perimodiolar type electrode at all channels. However, dynamic range was significantly wider in lateral type electrode than in perimodiolar type electrode. The amount of battery consumed was not significantly different between two types of electrodes.

Conclusion

The wider dynamic range in lateral type electrode is advantageous audilogically with similar amount of battery consumption. Considering that residual hearing is more preserved and anatomic structure is more saved so electric acoustic stimulation is available in lateral type electrode, lateral type electrode is a good choice.

PS - 252

First Steps Towards a Gapless Interface Between Auditory Neurons and Multi-Electrode Arrays

Stefan Hahnewald¹; Marta Roccio¹; Anne Tscherter¹; Jürg Streit¹; Julien Brossard²; Herbert Keppner²; Hans Rudolf Widmer³; Pascal Senn³

¹University of Bern; ²Haute Ecole Arc Ingénierie; ³Inselspital Bern

Background

Cochlear implants (CIs) have become the gold standard treatment for deafness. Despite all the success, some limitations remain. Our project: "NANO CI" (www.nanoci.org) aims at developing a new generation of CIs where the peripheral processes of the auditory neurons grow towards the electrode array to form a gapless interface in the cochlea. In theory, this strategy should result in i) a better auditory resolution and ii) lower energy consumption, two of the main limitations of current CI systems.

As a first step towards this ambitious goal, we aim at testing auditory neurons activity in the context of a gapless interface on multi electrode arrays (MEAs) *in vitro* to analyze parameters influencing response profiles, including neuron density, neuron morphology and surface structure.

Methods

First, different cell preparations of rodent auditory neurons were comparatively assessed *in vitro* with respect to morphology and physiological response profiles. Four different types of preparations were studied: a) primary dissociated, b) primary partially dissociated explant cultures (micro explants), c) undissociated spiral ganglion explant cultures and d) stem cell generated spiral ganglion-derived neuronal cells. Response profiles of auditory neurons were evaluated using MEAs. Second, we tried to guide primary neurons along structured surfaces patterned with specific adhesion proteins.

Results

All primary spiral ganglion cultures, dissociated, partially dissociated and undissociated were superior in terms of plating density, cell morphology and response profiles compared to stem cell-derived neuronal cell types. On our MEAs, auditory neurons were not spontaneously active, but upon electrical stimulation, they gave rise to action potentials of about 100 mV. On glass slides, neurons could efficiently and selectively be guided along poly-L-lysine and laminin coated micro channels.

Conclusion

We have established functionally mature spiral ganglion neuron cultures on multi electrode arrays. In addition, the nano-structurization of glass surfaces allowed selective and precise growth of neurons along micro channels. Although still preliminary, these results will lay the foundation to stimulate and record from auditory neurons via a gapless interface *in vitro*, and ultimately for future *in vivo* applications.

Neurotrophin Gene Therapy in Deafened Ears With Cochlear Implants: Long-Term Effects on Nerve Survival and Functional Measures

Bryan Pfingst; Deborah J. Colesa; Melissa M. Watts; Gina L. Su; Cameron L. Budenz; Yehoash Raphael
University of Michigan

Background

The condition of the auditory nerve is believed to affect the quality of information transferred by cochlear implants. A number of studies are attempting to reduce the degeneration of the nerve in deaf ears using neurotrophins. The objectives of the current study were: (1) use adeno-associated viral vectors (AAV) for delivery of neurotrophins, taking advantage of their safety and prolonged expression; (2) use mature guinea pigs to test procedures known to be effective in younger animals; (3) test the effectiveness of the gene-therapy procedure in the presence of a cochlear implant; and (4) compare histological and functional effects of the procedures.

Methods

Mature male guinea pigs were trained to perform psychophysical stimulus-detection tasks. Neomycin was infused bilaterally into the scala tympani, intended to destroy hair cells and supporting cells leaving a flat epithelium in the organ of Corti. The experimental group was then inoculated in one ear with AAV.*NTF-3* (n=15) or AAV.*BDNF* (n=2). The cochlea was then implanted with a Nucleus animal cochlear implant. The control group (n=5) was treated in a similar fashion except that the inoculation was with an empty AAV. Psychophysical detection thresholds and ECAP and EABR thresholds and amplitude growth functions were monitored over time after implantation until sacrifice 5 to 14 months after inoculation. Animals were then euthanized and the cochleae were processed histologically.

Results

Spiral ganglion neuron (SGN) survival in the 17 neomycin injected, AAV.*NTF-3* and AAV.*BDNF* inoculated, implanted ears ranged from near normal to poor across animals and across cochlear turns. In contrast, SGN survival in the 5 animals in the neomycin injected, AAV.empty inoculated, implanted animals was poor in all cases. Some animals showed much better SGN survival apical to the implant than in the implanted region, suggesting that the implant or associated fibrous tissue growth might have interfered with the diffusion of neurotrophins from the AAV infected mesothelium to the SGN cells. The degree of nerve survival was correlated with slopes of EABR and ECAP amplitude growth functions.

Conclusion

Neurotrophin gene therapy can be very effective in long-term preservation of SGN neurons in implanted mature deaf ears, but additional work is needed to reduce variability in outcomes. Electrophysiological measures provide a useful tool for noninvasively assessing the effectiveness of these procedures.

Cochlear Implantation for Chronic Electrical Stimulation in the Mouse

Sam Irving; Mathew Trotter; James Fallon; Rodney Millard; Andrew Wise; Robert Shepherd
Bionics Institute

Background

The use of mice in cochlear implant research has not been possible due to the lack of a stimulator small enough for murine use, coupled with the difficulty of the surgery in this species. We describe a fully-implantable cochlear implant designed for chronic application in the mouse.

Methods

The cochlear implant consists of an electromagnetic coil, a current regulator, capacitor and electrode array. Following encapsulation in silicone the stimulator unit is 3x10 mm and weighs <1 g. A leadwire connects the stimulator to a 0.2 mm diameter bipolar platinum electrodes. The stimulator is driven by an external magnetic field produced by three orthogonal coils placed around the animal enclosure, allowing the animal to move freely during stimulation. The stimulator produces charge-balanced biphasic current pulses and shorts the electrodes between stimuli. We developed a surgical technique suitable for implantation that involved the insertion of the electrode array into the scala tympani via the round window. Recording electrically-evoked auditory brainstem responses (EABRs) demonstrated functional efficacy. Chronic electrical stimulation was carried out in three mice. They were stimulated 6 dB above their EABR threshold for 4 hours/day for one month and on completion their cochleae were examined histologically.

Results

Insertion of the electrode array into the mouse cochlea was performed without damaging the inner ear. EABRs were successfully recorded in implanted animals. Chronic stimulation did not significantly alter the density of spiral ganglion neurones (SGNs) compared to unstimulated control animals ($p > 0.05$). Chronically implanted cochleae showed evidence of a fibrous tissue response in the basal turn. The extent of the tissue response was not related electrical stimulation.

Conclusion

We describe a fully implantable cochlear implant suitable for chronic use in mice. While the surgery requires considerable experience, the results demonstrate that it is feasible to perform chronic electrical stimulation studies in this species. The 0.2 mm diameter electrode array can be safely inserted into the mouse cochlea, EABRs were readily recorded and chronic electrical stimulation did not adversely affect the SGN population.

Improving Surgical Implantation Techniques to Access the Superior Temporal Gyrus in Macaca Mulatta.

Deborah Ross¹; Yoshinao Kajikawa Kajikawa¹; Arnaud Falchier²; Troy Hackett³; Charles Schroeder⁴

¹The Nathan S. Kline Institute for Psychiatric Research;

²Nathan Kline Institute for Psychiatric Research; ³Vanderbilt University; ⁴Columbia University

Background

There is increasing interest in exploring, and conducting electrophysiological recordings from, higher-order regions along the auditory pathway in awake behaving non-human primates. Several such regions lie on the superior temporal gyrus (STG). Results from human studies suggest that the STG processes various aspects of communication signals. However due to the difficult location of the STG corresponding sites have not previously been accessed in an awake behaving macaque. One of the main concerns in regard to surgical implantation in this region is the possibility of tissue disruption which may distort the animals hearing. In order to minimize tissue disruption we devised, and are assessing a new surgical implantation technique.

Methods

Two animals were implanted using different surgical techniques. Both animals underwent an initial MRI to determine the underlying brain anatomy and define the stereotaxic co-ordinates for accessing the STG. We used a standard surgical approach for the first animal i.e. placing a Cilux Crist chamber embedded in surgical cement to access and maintain a craniotomy for laminar multielectrode recordings. This animal was naïve and was simply required to listen passively to the stimuli. The second animal was trained to discriminate and respond to auditory stimuli in a behavioral task. Once trained this second animal was implanted using a customized titanium chamber manufactured by Rogue Research. The data from the MRI were used to create a titanium chamber that matched the contours of the skull overlying the target region in this particular animal. The chamber was attached using standard titanium screws. We used Mi-mix as a gasket to ensure a water tight seal necessary for electrophysiological recordings. No additional cement was used to secure the chamber. 6 weeks was allowed for healing and oseointegration of the chamber.

Results

We were able to carry out laminar recordings from both animals successfully. The behavioral performance of the second animal indicates that they are able to perform the auditory discrimination task. The level of post-surgical performance was comparable to that of pre-surgical performance.

Conclusion

The new surgical technique allows for the systematic study of previously inaccessible regions on the Superior Temporal Gyrus in awake-behaving macaques. In particular this will facilitate the study of higher order auditory areas that may correspond to areas that have been studied in humans.

Progress Report on Developing Intra-Cochlear Pressure Sensor for Implantable Microphone and a Novel Fluid-Assisted Electrode Insertion Method

Andy Zhang; Sushrut Kale; Ioannis (John) Kymissis;

Elizabeth Olson

Columbia University

Background

Cochlear implants (CI) could be improved by replacing the external microphone by an intracochlear microphone, and with a more robust technique for performing deep insertions without cochlear trauma. We report on research projects aimed at these two improvements. One project is the development of a piezoelectric polymer pressure sensor, capable of picking up the sound pressure in the cochlear fluid. A potential application of such a pressure sensor is the microphone for a totally implantable CI. One significant advantage of such a microphone placement is that the microphone input utilizes the natural functions of the outer and middle ears. The second project focuses on developing a fluid-assisted CI-electrode insertion method. The motivation to develop such a method is to standardize the CI electrode insertion technique to achieve consistently deeper and atraumatic electrode insertion and to preserve residual hearing.

Methods

For the intra-cochlear pressure sensor project, we developed prototypes that are based on micro-fabrication of PVDF polymer films (which is piezoelectric) on PDMS (silicone). Thin film gold layers were deposited and patterned to form the sensor electrodes. Each of the sensors was designed to have a broad frequency range to pick up intra-cochlear sound pressure. To perform fluid-assisted CI-electrode insertion, flow of sodium hyaluronate (diluted with artificial perilymph) was setup from round window to a small opening made in scala vestibuli in anesthetized Mongolian gerbils. Mock-up, silicone electrodes were introduced in the ongoing flow and were flowed into the cochlea.

Results

For the pressure sensor project, the performance of various prototypes was tested both in air and water in the frequency range up to 10 kHz. We will present an evaluation of the pressure sensor performance and the feasibility of this design concept. Fluid-assisted insertion resulted in deeper and relatively atraumatic insertion in all the subjects. We will present the report on effectiveness of the technique to preserve residual hearing.

Conclusion

These novel approaches to improve cochlear implantation technique are progressing. Our goal is to improve outcomes and make cochlear implants accessible to a larger population of hearing impaired individuals.

Hearing the Light: A Behavioral and Neurophysiological Comparison of Two Optogenetic Strategies for Direct Excitation of Central Auditory Pathways

Jenny Chen¹; Wei Guo²; Ariel Hight¹; Nathan Klapoetke³; Barbara G. Shinn-Cunningham⁴; Edward Boyden³; Daniel B. Polley⁵; Daniel J. Lee⁵

¹Harvard Medical School; ²Mass. Eye and Ear Infirmary; Boston University; ³MIT; ⁴Boston University; ⁵Mass. Eye and Ear Infirmary

Background

Optogenetics uses light to control the activity of genetically modified neurons expressing light-gated ion channels, providing a means to manipulate specific neural circuits with temporal and spatial precision. This technology has been used to examine the behavior of various animal models, including models of deep brain stimulation in Parkinson's disease and, more recently, the generation of false memories. Here, we apply optogenetics to develop an animal model of the auditory implant in the inferior colliculus (ICc).

One obstacle to the application of optogenetics to auditory prostheses is that most known channelrhodopsins are unable to reconstruct the submillisecond precision and speed of central auditory representations. Thus, it is necessary to explore novel opsins that could support a behavior model of auditory pathways. In this study, we compare optogenetically driven responses in the ICc using channelrhodopsin-2 (ChR2) with those from Chronos, a new generation opsin that can be driven at much higher rates of stimulation.

Methods

We used viral-mediated gene transfer to express ChR2 or Chronos in neurons of the murine ICc. Three weeks after infection, multiunit responses in the ICc to optical stimulation (7mW, 0-300Hz) and acoustic stimulation (narrow-band noise bursts, 80 dB SPL, 0-300 Hz) were measured via an optrode.

Results

We observed non-adapting responses with ChR2 as high as 80 Hz, but rapidly adapting onset-like responses at higher rates. By contrast, neurons infected with Chronos accurately exhibited sustained responses for stimulation frequencies as high as 200 Hz, approximating the entrainment limit for natural acoustic stimulation in the same neurons. Optical stimulation of Chronos at higher rates evoked non-adapting responses as high as 300 Hz, although spikes were no longer synchronized to pulse trains. We also implemented neural decoders to classify laser pulse rates based on spike responses. Responses from Chronos-infected cells show significantly better discriminability than responses from ChR2-infected cells, especially at higher rates. These results demonstrate that an objectively defined neural code for pulse rate is superior with Chronos when compared with ChR2.

Conclusion

Our preliminary results suggest that light-driven responses in the ICc using Chronos can reconstruct the rapid responses

needed for meaningful central auditory stimulation. Ongoing experiments seek to implant the murine ICc with chronic optical fibers to determine whether the enhanced temporal coding range of Chronos translates into better behavioral discrimination of optogenetic excitation at high rates.

Modeling Auditory Nerve Fiber Responses Using a Hidden Markov Model

Petrina LaFaire¹; Brian Dougherty²; Alan Micco³; Pamela Fiebig²; Claus-Peter Richter²

¹Northwestern University; ²Northwestern University Feinberg School of Medicine; ³Northwestern Memorial Hospital

Background

A novel method using pulsed infrared radiation has been proposed for neural stimulation, termed Infrared Neural Stimulation (INS). INS works by local heating of the neuronal tissue. Delivery of each pulse deposits heat into the tissue with the risk of heat accumulation and thermal damage. It would be advantageous to the development of INS to encode speech information in the form of low rate pulse trains to minimize the heat delivered to the auditory tissue. A Hidden Markov model (HMM) can be used to regenerate sequences of action potentials (spike trains) that maintain high frequency fine structure encoded in spike trains of less than 250 pulses per second. The HMM models the states of a neuron through probability matrices of emission of an action potential or transition between one states to the next.

Methods

The HMM models recorded spike trains via MATLAB. The built in MATLAB code `hmmtrain` takes the inputs of the recorded spike train data and transition and emission probability matrices to better estimate the probability matrices. The estimated matrices are then inputted to the built in MATLAB code `hmmgenerate` to produce the regenerated spike train data. The model has been tested using spontaneous and evoked activity from pigeon auditory neurons. Accuracy and model robustness are determined by comparing autocorrelation functions of the original and regenerated spike trains.

Results

While the regenerated spike train does not appear to match the original auditory neuron spike train in the temporal domain, the frequency information is still maintained as can be seen from the autocorrelation function. Neighboring contacts have little to no overlap in stimulation.

Conclusion

The stochastic nature of the regenerated spike trains from the HMM can allow for more areas of the cochlea being stimulated simultaneously without the interference. The low rate stimuli will allow for less energy usage than higher rate coding strategies while still preserving the high frequency information of the acoustic signal. When applied to INS, the benefits of more spatially selective stimulation coupled with the stochastic nature of the signal would allow for an increase in independent channel stimulation, benefiting the speech perception of the CI user.

PS - 259**Quantification of Infrared Stimulation-Evoked Damage in Organ of Corti Explants**

Ravin Sajnani; Chhavi Gupta; Vicente Lumbreras; Adrien Eshraghi; **Suhруд Rajguru**

University of Miami

Background

Infrared stimulus provides a non-contact, artifact free method that acts through endogenous mechanisms to stimulate neurons and provides an alternative tool to excite cells with advantages over conventional stimuli. Previous studies have suggested a role of mitochondrial calcium cycling in the IR response. It is likely that IR generates ROS in the mitochondria and affects mitochondrial respiration. In addition, at high rates of stimulation required in cochlear implants, application of IR may lead to accumulation of thermal energy. This study characterized pulsed IR damage thresholds *in vitro*.

Methods

Organs of Corti were explanted from p2-p4 rat pups in culture dishes coated with Cell-Tak, an adhesive compound and placed in serum-free media. The middle turn of the organs were irradiated for 15 minutes under aseptic conditions with 100 μ s pulses at 100 pps and various energy levels (60-330 μ J/pulse), using a 400 μ m optical fiber coupled to Capella laser (λ =1863 nm, Lockheed Martin Aculight). Control explants were maintained for the same duration without IR stimulation. After irradiation, the explants were incubated for 48 hours. Following incubation, the organs were fixed in 4% Paraformaldehyde and stored in 4°C for 24 hours. All explants were stained for HCs after 96hrs *in vitro*. Levels of total reactive oxygen species (ROS) with CellROX® and 4-Hydroxy-2-nonenal (HNE) were studied. Phalloidin-FITC stain was used for hair cell counts.

Results

There was no evidence of either reactive oxygen species (ROS) (CellROX®) or HNE immunolabeling in hair cells of both the control and IR (up to 330 μ J/pulse) stimulated groups. Moderate CellROX staining was observed in the supporting cells of the irradiated organs. Reactive nitrogen species were not present in the irradiated organs. In addition, the hair cell counts in irradiated organs were similar to those of control explants. Additionally, there was no immunolabeling of either CellROX or HNE at apical or basal turns (away from the site of IR stimulation).

Conclusion

The results suggest that acute IR stimulation did not adversely affect mitochondrial respiration even at a high rate of stimulation. ROS are involved in oxidative stress pathway but were found only in moderate doses at support cell level localized near the site of exposure. HNE a marker of membrane lipid peroxidation and hair cell loss were not observed in the irradiated organs.

PS - 260**Vestibular Function - a Parameter for Structural Preservation in Cochlear Implantation?**

Anvarbek Ishchanov; Hayo Breinbauer; **Mark Praetorius**
University of Heidelberg Medical Center

Background

Cochlear Implantation is currently the most promising option to restore lost hearing. As the electrodes are placed in the cochlea, its delicate structures separating the scalae are at risk. Besides the audiological testing to define the results, the vestibular function may impact the patient as well, however, it may be not in the focus as much.

Methods

Ongoing study, 23 patients who received Cochlear implants, 17 unilateral, 6 bilateral were evaluated using vestibular evoked myogenic potentials VEMP), audiological testing and structured interviewed. The postoperative position of the electrode was checked with flat panel computed tomography in the early postoperative days. The time between implantation and audiological and vestibular testing was more than 6 months in all cases.

Results

While all the patients did achieve good results in the audiological tests and were satisfied with their hearing abilities, 4 unilaterally implanted and 1 bilaterally implanted patient complained about ongoing dizziness. In the VEMP measurements, however, 14 unilaterally implanted (82%) and all 6 bilaterally implantees showed reduced response amplitudes. VEMP responses on implanted ears were significantly lower in absolute and relative amplitudes (in comparison to non-implanted ear in the same patient), $p < 0,01$ Fisher exact test.

Conclusion

While we keep being enthusiastic about the hearing outcome, the vestibular function is easily neglected. Our results show a decline in VEMP amplitudes in implanted ears in the majority of patients, while most of them do not complain about this. The vestibular testing may be a surrogate marker for the structural preservation of the inner ear structures.

PS - 261**Safe Direct Current Stimulator Microfluidic Design for Vestibular Prosthesis**

Gene Fridman; **Evan Kararo**; Bryan Kuo; Charles Della Santina

Johns Hopkins University

Background

Previously we demonstrated that the range of head velocities encoded by the vestibular prosthesis can be nearly doubled if the spontaneous activity of the vestibular nerve afferents is suppressed by low amplitude anodic direct current. We developed a safe direct current stimulator (SDCS) to deliver direct current to the nerve and to overcome the safety concerns of electrolysis and corrosion at the metal electrode-tissue interfaces. The electrodes inside the device always experience

alternating current for safety, but the device synchronously switches valves arranged in a fluidic bridge circuit inside the system to deliver direct ionic current at the output. In the present study, we sought to develop a next generation microfluidic SDCS system.

Methods

The miniaturized SDCS design consists of three subsystems: A microfluidic circuit of electrolyte-filled channels embedded in a silicone substrate, valves actuated by Nitinol muscle wires that open and close these channels to ionic current flow, and a combination analog/digital circuit to control the overall system. We used a standard MEMS process to design a microfluidic circuit consisting of hollow channels embedded in a 20x20x2mm two-layer Polydimethylsiloxane (PDMS) silicone substrate. To implement an ionic current flow valve, the Nitinol wire squeezes a channel within the PDMS to turn off the ionic current flow or releases the channel to allow it to conduct ions. The electronics controlling the miniaturized SDCS state machine contain a separate current source to power each of the muscle wires, a current driver circuit to deliver the pulses to the metal electrodes embedded in the microfluidic circuit, and a feedback amplifier to monitor the ionic current output of the system.

Results

We successfully implemented a prototype of each of the three SDCS subsystems and tested them separately on the bench. We ensured that the microfluidic circuit could be created free of leaks. The Nitinol wire could be actuated to modulate the microfluidic channel impedance with approximately 5x impedance difference between the on and the off states. All parts of the control circuit functioned according to the design criteria.

Conclusion

We demonstrated that we could build each of the individual components of the SDCS to function as intended. Further integration of the overall system will be necessary to ensure that it can deliver safe direct ionic current for an extended duration to enable chronic animal studies with the vestibular prosthesis.

PS - 498

Optically-Evoked Auditory Brainstem Responses (oABR) Mediated by Optogenetic Manipulation of the Cochlear Nucleus

Ariel Hight¹; Keith Darrow²; Elliott Kozin³; Ashton Lehmann¹; Maryanna Owoc²; Edward Boyden⁴; Chris Brown¹; Dan Lee³

¹Harvard Medical School; ²Worcester State University;

²Worcester State University; ³Eaton Peabody Laboratories, Massachusetts Eye and Ear Infirmary; ⁴Massachusetts Institute of Technology

Background

Recent findings indicate that optogenetic tools can enable light sensitivity in the central auditory system. Stimulation of neurons by light may provide substantial benefits over stimulation by electrical current. For example, in the auditory

brainstem implant (ABI), a neuroprosthetic device that stimulates the cochlear nucleus, electrode cross-talk and spread of current may limit audiologic outcomes and result in side effects. A light-based approach may better focus the stimulation and lead to better performance. One way to assay stimulus-evoked (e.g. ABI) responses is to record the auditory brainstem response (ABR), which is multi-peaked far-field potential. Here, we characterize the optically-evoked ABR (oABR) in CBA/CaJ mice, with the eventual goal of understanding the extent of light sensitivity in the cochlear nucleus.

Methods

To induce light sensitivity, viral mediated channelrhodopsin-2-mcherry (ChR2, n=7 mice) or Chronos-GFP (n=5 mice) was injected into the CN of 4-6 week old CBA/CaJ mice. After 3-5 weeks of incubation, the CN was re-exposed and an optical fiber connected to a blue-light laser was placed on the surface of the DCN. The ABR was recorded using conventional electrode configurations. In most cases with oABR recordings, multi-unit activity was also recorded in central nucleus of the inferior colliculus (ICc). At the conclusion of the experiment, the brainstems were prepared for histological examination.

Results

Recorded oABRs were significantly variable across animals. There was variation in the number of peaks (from 1 to 7), peak amplitudes (up to 70 μ V baseline to peak), and peak latencies (0.2-9 ms). For example, in one case the oABR was two positive-peak waves with 0.2 ms and 4 ms latencies and 4 μ V and 3 μ V amplitudes, respectively. In this animal, histological examination revealed strong chronos-GFP expression throughout the CN and limited expression in surrounding brainstem areas. In all ICc recordings of injected mice, there were clear responses evoked by both acoustic and optical stimuli. However, no optically-evoked potentials were recorded in two non-injected/control mice. In contrast to the oABRs, acoustically-evoked ABRs showed a stereotyped response with less interanimal variability.

Conclusion

In contrast to the ABR evoked by sound, there is significant variability of the oABR response. Ongoing efforts to understand this variability includes analysis of injection site, infection efficiency, and/or laser placement. The oABR may eventually be a quick and non-invasive assay for assessing the extent of light sensitivity in the cochlear nucleus.

Comparison of Bilateral Brain Cortex Signal from Normal Hearing and Single Side Deaf Rat With Multi-Channel Neural Recording System

Min Young Lee¹; Su Kyoung Park²; Sang Beom Jun³; Doo Hee Kim¹; Seung-Ha Oh¹

¹Department of Otolaryngology Head & Neck Surgery, Seoul National University Hospital; ²Department of Otolaryngology Head & Neck Surgery; ³Department of Electronics Engineering, College of Engineering, Ewha Womans University

Background

Recently, rehabilitation for single side deafness patients has been emphasized. Also various kinds of management modality have been introduced for this single side deafness. In dealing with single side deafness, brain plasticity is expected to play a important role deciding proper management period, as bilateral deaf cases. Many studies about single side deafness is in progress with imaging techniques, but very little study is done with direct recording from brain cortex. The aim of this study is to find out changes of brain cortex signal responses after single side deafness with a multi-channel acquisition process system.

Methods

12 Sprague-Dawley rats were used as experimental animals. They are anesthetized with zoletil, and deaf model was made by cochlear ablation (opening the promotory and round window after bulotomy) surgery with kanamycin irrigation. The auditory cortex was exposed by surgical procedure and sited by vascular landmarks. After positioning the animal in the sound proof booth, it was fixed by stereotaxic frame. Using micromanipulator, 4 x 4 channel tungsten multichannel electrode array was inserted at depth of 500~900 um depth from cortical surface. Acoustic stimulation was generated by Digital Signal Generator (AP2; Tucker-Davis Technology, FL). Brain cortical response to this stimulus was recorded by spike-sorting software and neural explorer. At 4 weeks, 6 weeks, 8 weeks, with 2 rats each poststimulus timehistogram was recorded. We analyzed response area, summation of action potential and mean latency of PSTH (poststimulus timehistogram) of each brain hemisphere in normal hearing and single side deaf animals.

Results

6 animals which were deafened by cochlear ablation surgery, has tested with click ABR and they found to have no residual hearing. 6 animals whose hearing was within normal range revealed typical brain cortex recording; contralateral cortex had more responsible area to acoustic stimuli and the summation of action potential spikes. In contrary ipsilateral cortex revealed less responsible area and less action potential spikes. However in single side deaf animals, lateralization of excitatory signals revealed more variation and ipsilateral brain cortex revealed more excitation area and more summation of spikes than normal hearing animals. There was no difference in latency between two groups, and no correlation with deaf duration.

Conclusion

According to result of this study, inter-hemispheric reorganization of auditory cortex occurred. After unilateral profound hearing loss, brain cortex responses revealed variable results, and mostly ipsilateral brain cortex revealed more active response than normal hearing. With further study, certain rule of interhemispheric plasticity after single deafness might be discovered.

PS - 263

Cortical Voice Processing in Cochlear-Implanted Children: An Electrophysiological Study

David Bakhos; Emmanuel Lescanne; Frédérique Bonnet-Brilhault; Sylvie Roux; Nicole Bruneau

Université François-Rabelais de Tours, CHRU de Tours, UMR-S930, Tours, France

Background

In children with prelingual deafness, the use of cochlear implants can restore both auditory input to the auditory cortex and the ability to acquire spoken language. Language development is strongly intertwined with voice perception. The aim of this electrophysiological study was to investigate human voice processing with cortical auditory evoked potentials (AEPs) in cochlear-implanted (CI) children.

Methods

Eight CI children (2 males, 6 females) aged 4-12 years (mean age: 8 years), fitted with a unilateral cochlear implant (CI group) for congenital sensorineural hearing loss were included in this study. All of them had good auditory and language performance. They were investigated with cortical AEPs and compared with 8 normal-hearing age-matched controls (mean: 8.5 year-old). The electroencephalogram were recording from 28 Ag-AgCl cup electrodes. The auditory stimuli were vocal and non-vocal sounds delivered in free field. The vocal non-speech sounds were produced by a large number of speakers of both genders and different ages. Non-vocal sounds consisted of sounds from a wide variety of sources, including human environments, musical instruments, and nature. Independent component analysis was used to minimize the cochlear implant artifact in cortical AEPs. Differences between the Voc and NVoc responses were evaluated by performing permutation tests with a correction for multiple comparisons.

Results

Fronto-temporal positivity to voice was found in normal-hearing children with a significant effect in the 140-240 ms latency range. In the CI children group, we found a positive response to voice in the 170-250 ms latency range with a more diffuse and anterior distribution than in the normal-hearing children. Fronto-central responses (P1-N2-N4 waves) did not differ between the 2 groups.

Conclusion

Response to voice was recorded in normal-hearing and CI children. The topography and latency of response to voice differed from that recorded in normal-hearing children. This

finding argued for cortical voice processing reorganization in congenitally deaf children fitted with a cochlear implant.

PS - 264

Modulation of the Auditory-Evoked Potential by Continuous Laser Irradiation: Effects of Wavelength and Induced Temperature Change

Shigeto Furukawa¹; So Ikeda²; Ryota Numata²; Shunji Sugimoto²; Junsei Horikawa²

¹NTT Communication Science Laboratories; ²Toyohashi University of Technology

Background

Laser irradiation has been known to affect neural activity. Specifically, an earlier report [Maki et al., ARO Midwinter Meeting, 2010] showed that a continuous irradiation by a near-infrared (NIR) laser on the rat auditory cortex (AC) reversibly reduces the amplitude of auditory-evoked potential (AEP) recorded from the AC. The present study, using the guinea pig as an animal model, explored the factors underlying this phenomenon by examining the effects of laser intensity, wavelength, and temperature change induced by the irradiation.

Methods

AEPs were recorded with a tungsten electrode placed on the primary or dorsocaudal auditory cortex of guinea pigs under anesthesia (ketamine + xylazine). The stimulus was a wide-band noise (0.5-20 kHz, 100 ms long, 5 ms on-off cosine ramps, 75 dB SPL), presented every 2 s. The AEP responses were measured before, during, and after the continuous irradiation by a NIR (wavelength 830 nm) or red laser (RED, 650 nm) for 5 minutes (total of 15 min). The temperature of the cortical surface was also monitored simultaneously with thermocouple electrodes and a thermocamera.

Results

Both the NIR and RED laser reversibly reduced the AEP amplitude. The transition period for the amplitude to reduce after the beginning of irradiation was 1 – 2 min, and that to recover after the cessation was 1 – 2.5 min. These results are consistent with those reported in the earlier study on the rat auditory cortex using NIR. The size of laser-induced amplitude reduction was linear to the laser intensity, but the slope of the regression line was steeper for RED than for NIR, showing a wider dynamic range for NIR than for RED. When the AEP reduction size was re-plotted against the irradiation-induced temperature change of the cortical surface, the regression lines showed no statistical difference between NIR and RED.

Conclusion

The present results showed that the sensitivity to laser intensity of the AEP amplitude is wavelength dependent. It was shown also that AEP reduction could be well accounted for by the irradiation-induced temperature change regardless of the wavelength. This suggests that the cortical temperature increase is a crucial factor of the reduction of AEP, rather than the laser intensity or the wavelength *per se*.

PS - 265

Responses of Primary Auditory Neurons to Vocoded Vocalizations.

Jean-Marc Edeline¹; Yonane Aushana²; Chloe Huetz²; Christian Lorenzi³

¹CNRS and Université Paris-Sud; ²CNPS, UMR 8195, CNRS and Université Paris-Sud; ³Audition Team, CNRS, Ecole normale supérieure

Background

Over the last decade, a vast literature has suggested that the acoustic temporal envelope (E) and the temporal fine structure (TFS) of speech sounds play an important role in speech intelligibility for human subjects (eg, see Gilbert and Lorenzi 2010). Whereas many psychoacoustic studies have been carried out, only a few electrophysiological studies have been performed in animals to understand the responsiveness of auditory cortex (ACx) neurons to E and TFS cues. Here, we aim at determining how responses of primary ACx neurons are modified when the acoustic TFS is degraded in natural communication sounds.

Methods

Neuronal activity was collected in the ACx of urethane anesthetized guinea pigs using arrays of 16 electrodes placed in the tonotopic field A1. Tuning curves were quantified by presenting gamma tones from 0.1-36kHz at 75-45dB; then the responses to conspecific and heterospecific vocalizations were measured. Each vocalization (played at 75dB) was presented in its normal version then without TFS cues. The removal of TFS cues was performed by processing each vocalization with a tone vocoder: a gammatone filterbank decomposed the signal, then the original TFS was replaced by a sine tone at the central frequency of each band. We used tone vocoders implementing 38 (lowest degradation), 20 and 10 (highest degradation) frequency bands. Normal and vocoded vocalizations were also presented against a steady noise masker set at 65dB.

Results

Compared with the responses to normal vocalizations, the responses of ACx neurons to vocoded vocalizations were altered in terms of firing rate and temporal organization. The lower the number of frequency bands, the largest the decrease in firing rate and in spike timing precision; the strongest effects were obtained with the 10 frequency bands vocoder. The addition of noise impacts more the response to vocoded-vocalization than the responses to normal vocalizations.

Conclusion

We show that in anesthetized conditions, the responses of primary auditory cortex neurons are severely altered by the vocoding process, both in terms of response strength and in terms spike-timing precision.

Expression of c-Fos in the Rat Auditory and Limbic Systems Following 22-KHz Vocalization

Ladislav Ouda; Josef Syka

Institute of Experimental Medicine, Academy of Sciences of the Czech Republic

Background

The 22-kHz rat ultrasonic vocalization is known to be produced during various aversive or dangerous situations and can induce anxiety and an avoidance reaction in the conspecific animals listening to the vocalization. In the present study, we aimed to evaluate differences in the pattern of neuronal activity in response to the 22-kHz vocalization under different conditions and in response to a complex artificial sound simulating the 22-kHz natural vocalization.

Methods

Adult Long-Evans rats were exposed either to natural 22-kHz vocalizations or to an artificially generated call with comparable spectro-temporal features. The natural 22-kHz vocalization was either played from a recording or produced by an irritated animal located nearby (live calling). The expression of c-Fos, an immediate-early gene, was investigated in the structures of the auditory system (inferior colliculus, medial geniculate body and auditory cortex) and limbic system (hippocampus and basolateral amygdala).

Results

In comparison with controls (non-exposed), c-Fos immunoreactivity was significantly increased in the inferior colliculus, auditory cortex, hippocampus and basolateral amygdala of rats exposed to either live or recorded 22-kHz natural callings. Exposure to the direct calling of an irritated animal resulted in a similar pattern of c-Fos activity as did exposure to the playback of the 22-kHz vocalization. The expression of c-Fos was also increased in the inferior colliculus and auditory cortex in animals exposed to the artificial calling, when compared to controls; however, the increase was much less pronounced. In this case, c-Fos expression was not increased in the hippocampus or basolateral amygdala. Interestingly, almost no c-Fos expression was found in the medial nucleus of the geniculate body in any of the experimental groups.

Conclusion

These findings suggest that differences exist between the processing of important natural conspecific vocalizations and artificially produced calls with comparable spectro-temporal features, and moreover it suggests a different role of individual brain structures in the processing of such calls.

Stimulus Specific Adaptation and Sensory Memory

Leila Khouri; Bshara Awwad; Israel Nelken

Hebrew University of Jerusalem

Background

Stimulus Specific Adaptation (SSA) describes neuronal adaptation to a common (standard) stimulus that does not

generalize to a rare stimulus (deviant). In the Auditory System, SSA is mostly studied using pure tone stimuli. In this case, emphasis of the deviant tone results from decreased responses to the standard tone. This emphasis has been interpreted as an error signal, indicating violation of the regularity created by the standard, independent of the deviant. However, recent evidence suggests that in Auditory Cortex (AC) both responses to deviant and standard are sensitive to the temporal structure of the tone sequence (Yaron et al. 2012). We hypothesize that a memory for standard and deviant sounds is created over the sequence and that SSA can be employed to study formation of sensory memory in the Auditory System.

Methods

To investigate sensory memory in the Auditory System, we employed SSA sequences composed of sets of broadband stimuli. These stimuli (tone clouds) consist of 36 tones spanning 6 octaves and 6*16 ms time bins. A tone is played within each time bin and octave. Tone frequency is chosen from 1/6 of an octave bins, and tone onset is random in 16 ms bins for each one of the tone clouds. The tone cloud sequences employed consist either of (1) repeated presentations of different clouds with equal probability, (2) pairs of clouds one common and the other one rare (oddball sequences) or (3) a set of several different tone clouds among which one is repeated (diverse sequence). Neural responses to tone clouds were recorded from AC and IC of anesthetized rats.

Results

We observed SSA to tone clouds in the majority of neurons recorded from Auditory Cortex when presented with oddball sequences. In contrast, we rarely observed SSA in IC neurons. Interestingly, in AC, SSA to tone clouds did not only result from a decrease in response to standard, but also from an increase in response to deviant clouds. The increased response to the deviant was not present in IC. Moreover, when the standard cloud was played against a set of different deviant clouds (diverse sequence), we did not observe an increased response to the deviant cloud, suggesting that the increase in response to the deviant cloud was stimulus specific.

Conclusion

This finding is the first indication of sensory memory for complex non-sense sounds occurring as early as the Auditory Cortex.

Timbre Discrimination in Ferrets: Exploring the Neural Basis of Perceptual Constancy

Stephen Town; Katherine Wood; Jennifer Bizley

UCL Ear Institute

Background

Perceptual constancy (or invariance) is the ability to recognize an object as the same despite variation in sensory input. For example when hearing a vowel (e.g. /u/), we can recognize a constant sound identity despite variation in pitch or voicing within or between speakers. Furthermore, we can maintain vowel identity in a variety of background noise conditions despite degradation in sensory input. We are interested in the

neural mechanisms underlying perceptual constancy in hearing and specifically in vowel perception.

Methods

Using the ferret as an experimental model, we have trained animals in a two-alternative forced choice task to discriminate between two artificial vowels (e.g. /u/ and /e/). Vowels were presented at a range of pitches ($n = 8$), using a voiced or voiceless sound source ($n = 6$ ferrets) and also in varying noise conditions ($n = 3$ ferrets). In three ferrets trained in this task, we have implanted electrodes for chronic recording of neural activity in auditory cortex during vowel discrimination.

Results

We find that ferrets are able to accurately discriminate vowels despite task-irrelevant variation in sensory input due to vowel pitch, voicing or low level background noise (10 dB signal to noise ratio).

Conclusion

We will discuss current work examining the responsiveness of auditory cortical neurons to vowels when discriminating across task-irrelevant parameters and the extent to which neuronal invariance exists within auditory cortex. To determine a causal role for auditory cortex in maintaining perceptual invariance during vowel discrimination we are also performing reversible inactivation of auditory cortex via cooling.

PS - 269

The Mushroom Spine Density of Auditory Cortical Pyramidal Neurons

Richard Hallworth

Creighton University

Background

Dendritic mushroom-type spines are the principal loci of excitatory input to cortical pyramidal neurons. In the large layer 5 (L5) pyramidal neurons in the auditory cortex (AUD), inputs are segregated, such that local circuit inputs predominate at the level of layer 4 (L4), while more remote inputs predominate at the more distal layers 2 and 3 (L2/3). The density of mushroom spines varies to an unknown extent between neurons and within neurons. In this study, I examine to what extent the density of mushroom spines at L4 correlates with the density in L2/3 in a single AUD neuron, and in neurons of other sensory cortices.

Methods

The brains of *Thy-1 YFP-H* mice (Jackson Labs), 30-45 days old, were examined in 200 μm coronal sections using two-photon confocal microscopy. *Thy-1 YFP-H* mice express yellow fluorescent protein a sub-set of L5 pyramidal neurons, which enables quantification of mushroom spines in L4 and L2/3 spines in the same neuron. L5 pyramidal neurons were studied in AUD, as well somatosensory regions S2, S1 barrel field (S1BF), and S1.

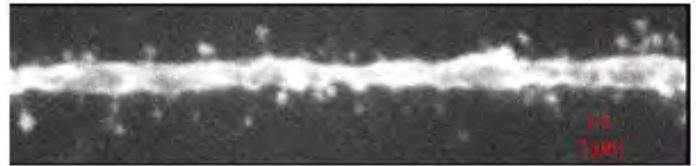
Results

The density of spines at either the L4 or the L2/3 level did not differ significantly between cortical regions AUD, S2, S1BF, and S1. In all regions, the density of spines was on average

significantly lower in L2/3 than in L4. However, the density of spines in L2/3 dendrites did not correlate with the density in L4 in a single neuron in any region, including AUD.

Conclusion

These results have implications for models of cortical circuitry in sensory cortices.



PS - 270

Antioxidants Attenuate Axonal Injury and the Accumulation of Neurotoxic Tau Variants in a Rat Model of Blast-Induced Traumatic Brain Injury

Matthew West¹; Xiaoping Du¹; Weihua Cheng¹; Wei Li¹; Donald Ewert¹; Robert Floyd²; Richard Kopke¹

¹Hough Ear Institute; ²Oklahoma Medical Research Foundation

Background

Traumatic brain injury (TBI) is a serious clinical challenge that negatively impacts millions of people worldwide. Repetitious low-impact concussive events or a single severe TBI can lead to early onset dementia and other related neurodegenerative diseases. Paradoxically, there are currently no effective treatment strategies for ameliorating the cognitive dysfunction and adverse physiological responses associated with TBI. Our laboratory previously demonstrated that damage to the central auditory pathway resulting from blast-induced TBI (bTBI), a common form of TBI encountered in battlefield conditions, could be significantly attenuated by a combinatorial antioxidant treatment regimen. In the present study, we have begun to assess whether this treatment strategy can also reduce bTBI-related damage to the non-auditory central nervous system, more specifically the hippocampus, a primary center for blast-induced pathophysiological changes.

Methods

We used antibodies to examine biomarker expression levels, including neurotoxic variants of Tau, in the brain, following three successive blast overpressure exposures in non-transgenic rats. These analyses were extended to evaluate the therapeutic effects of post-traumatic intraperitoneal injection of the antioxidants 2,4-disulfonyl α -phenyl tertiary butyl nitron (HPN-07) and *N*-acetylcysteine (NAC) in this rodent model of bTBI.

Results

Our model of bTBI induced significant oxidative stress and axonal injury in the hippocampus, as evidenced by pervasive *de novo* production of the oxidized lipid, 4-hydroxynonenal (4-HNE), and acute increases in neurofilament 68 (NF-68) levels, respectively. We also observed a marked increase in the levels of both hyperphosphorylated and oligomeric Tau, structural variants of this microtubule-associated protein that

are believed to potentiate the neurodegenerative effects associated with synaptic dysfunction in this region of the brain. Remarkably, a combinatorial regimen of HPN-07 and NAC resulted in striking reductions in both manifestations of oxidative stress and the corresponding pathophysiological changes observed in hippocampal neurons in response to bTBI.

Conclusion

Combinatorial treatment with the antioxidants HPN-07 and NAC resulted in a significant attenuation of pathophysiological response features in the hippocampus associated with acute blast-induced trauma in rats. Thus, this treatment strategy represents a promising therapeutic approach for simultaneously reducing both primary auditory injury as well as non-auditory changes associated with bTBI-induced neurodegeneration and maladaptive neuroplasticity in the hippocampus, potential underlying contributors to afflictions such as dementia and tinnitus.

PS - 271

Laminar Profile of Spiking Activity in Auditory Cortex in Response to Thalamic Stimulation

Matthew Banks¹; Bryan Krause²

¹University of Wisconsin School of Medicine and Public Health; ²University of Wisconsin

Background

Recent evidence suggests that the state of the cortical network prior to sensation can have a profound impact on neural responses and perception. Thus, in rodent auditory cortex, sensory responses are reported to occur in the context of network events, similar to brief UP states, that produce 'packets' of spikes and are associated with synchronized synaptic input and stereotyped responses to diverse sensory stimuli. Current models of sensory neocortical microcircuits, such as the canonical microcircuit model, fail to capture this state-dependence. These models, based primarily on data from somatosensory and visual cortex, posit specific spatio-temporal activation patterns in response to core thalamocortical (TC) excitation. Here, we tested these predictions in brain slices using electrophysiological and imaging techniques.

Methods

We investigated the laminar profile of synaptic and spiking responses to TC afferent stimulation in murine auditory TC slices (B6CBAF1/J, 3 - 10 weeks). Ca imaging (OGB-1 AM) was used to identify spiking cells as a function of laminar depth. Synaptic and spiking responses on finer time scale were measured using patch clamp and multichannel current source density (CSD) recordings from layers 2 - 6.

Results

CSD recordings indicated TC stimulation evoked large current sinks in layers 3 and 4. The laminar and temporal pattern of subthreshold and superthreshold responses to TC stimulation did not match the L4>L2/3>L5 activation sequence predicted by the canonical microcircuit model. Monosynaptic subthreshold responses with similar latencies were observed throughout layers 2 - 6, presumably via synapses onto dendritic processes located in thalamo-recipient layers. TC afferents often triggered brief UP states, during which the

vast majority of spikes occurred, primarily in pyramidal cells. These network events always involved infragranular layers, and less frequently spread to supragranular layers. In many cells, spike timing during these events was phase-locked to ongoing afferent stimulation, but in some cells spike timing did not appear to be influenced by these stimuli. Latencies were shortest in layers 4 and 5 and longer in layer 2/3. In the absence of evoked UP states, spiking responses were dominated by L5 cells, especially putative GABAergic interneurons, suggesting that early activation of these cells regulates the occurrence of evoked UP states.

Conclusion

Our data indicate that in auditory cortex, TC-evoked spiking activity does not conform to predictions of the canonical microcircuit model. Instead, spiking occurs primarily in the context of UP states and is dominated by presumed descending projection cells in L5.

PS - 272

Long-Term Cortical Inhibitory Deficits Result from Transient Hearing Loss Prior to Critical Period Closure

Todd Mowery; Vibhakar Kotak; Dan Sanes
NYU

Background

During development, primary sensory cortices go through brief epochs of increased plasticity known as critical periods (CP). Sensory deprivation during these sensitive periods can lead to functional and perceptual deficits in adulthood. In gerbil auditory cortex, the CP for hearing loss-induced reduction of inhibitory synaptic strength is postnatal day (P) 18 (Mowery, Kotak and Sanes, in revision). That is, when hearing loss is induced with bilateral earplugs after P18, the manipulation does not produce any significant change in inhibitory synapse function. Here, we report that a transient period of earplugging before the CP closes (i.e., before P18) leads to disparate short-term and long-term effects.

Methods

Transient hearing loss was induced via bilateral insertion of earplugs (EP) in gerbils (*Meriones unguiculatus*) at P11 and EP removal at P17 (prior to closure of the inhibitory critical period). A second group received EPs from P11-86. Whole-cell voltage-clamp recordings were obtained from L2/3 pyramidal neurons in a thalamocortical brain slice preparation. Spontaneous inhibitory synaptic currents (sIPSCs) were recorded following blockade of ionotropic glutamate receptors. Recordings were performed either at P35 (short-term survival) or P86 (long-term survival).

Results

Transient hearing loss (EP from P11-17) led to increased sIPSC amplitude when assessed at P35 after two weeks of normal hearing (mean pA \pm SEM; Control P35: -32.4 ± 3.0 vs. EP11-17: -46.7 ± 4.1 , $p = .019$; $n = 15$ control, $n = 26$ EP). Furthermore, the IPSC time constant was faster (mean ms \pm SEM, Control P35: 13.7 ± 1.3 vs. EP11-17: 8.5 ± 0.6 , $p = 0.0001$; $n = 15$ control, $n = 26$ EP). In contrast, when

assessed at P86, after 2 months of normal hearing, sIPSC amplitude was significantly smaller (mean pA \pm SEM; Control P86: -39.4 ± 2.1 vs. EP11-17/record P86: -31.7 ± 2.6 , $p = 0.027$; $n = 26$ control, $n = 17$ EP) and slower (mean ms \pm SEM: Control P86: 9.5 ± 0.6 vs. EP11-17/record P86: 12.5 ± 1.1 , $p = 0.018$; $n = 26$ control, $n = 17$ EP), as compared to age-matched controls.

Conclusion

These results imply that transient hearing loss prior to the closure of the CP leads to two different pathologies, depending on the latency from restored hearing: at short intervals inhibition is stronger and faster than normal, while at long intervals inhibition is weaker and slower than normal.

PS - 273

Activity in Human Auditory Cortex is Contralateral to Monaural Sound but Bilateral for Slow Amplitude Modulation

Alexander Gutschalk; Iris Steinmann

University of Heidelberg

Background

Spiking activity in response to monaural sound is observed almost exclusively in the contralateral inferior colliculus (IC) and auditory cortex (AC) in cat. In contrast, auditory EEG and MEG responses evoked by monaural sound in human AC are typically bilateral and only 10 – 50% stronger in contralateral AC. Lateralization for monaural sound in AC found with fMRI is stronger than in MEG, but the degree of lateralization varies between reports. Here we explore the source of this variability with MEG and fMRI. Our hypothesis was that lateralization of monaural sound in AC derives from a blending of at least two components: One is the continuous activity evoked by the carrier, which we expected to be strongly lateralized in fMRI but without clear-cut correlate in MEG. The other is the activity evoked by slow, periodic amplitude modulation, which we expected to be bilateral in MEG and fMRI.

Methods

12 listeners participated in the fMRI and 11 listeners in the MEG part of the experiment. Stimuli were 32-s-long segments of monaural white noise, which was either unmodulated (UM) or amplitude modulated (AM) with a rate of 8 Hz. The stimuli were presented in alternation with 32-s long silent intervals in fMRI and 8-s long silent intervals in MEG.

Results

In fMRI, activity evoked by monaural sound was strongly lateralized to contralateral IC and AC. For UM noise, BOLD reduction in comparison to baseline was observed in ipsilateral Heschl's gyrus. The AM versus UM contrast, which separates the specific activity evoked by AM, revealed bilateral enhancement of BOLD activity in AC, but not in IC. This enhancement in AC by AM was similar in contra- and ipsilateral AC. In MEG, the 8-Hz AM evoked an ongoing steady-state response, which showed a trend for stronger activity in right AC, but no change of lateralization depending on the stimulus ear.

Conclusion

These results reveal a striking dissociation of hemispheric lateralization in AC. Unmodulated noise activates only contralateral AC, whereas the additional activity imposed by 8-Hz AM is bilateral in fMRI and MEG and not significantly contralateral to the stimulus ear. The reduced activity in ipsilateral AC in comparison to baseline might be a direct correlate of ipsilateral inhibition observed in binaural compared to monaural conditions.

PS - 274

Contextual Effect of Streaming on Perception

Sahar Akram¹; Bernhard Englitz²; Claire Chambers²; Daniel Pressnitzer²; Shihab Shamma³

¹University of Maryland; ²Département D'études Cognitives, Ecole Normale Supérieure; ³University of Maryland & Département D'études Cognitives, Ecole Normale Supérieure

Background

Perception of an auditory scene can be strongly dependent on the surrounding context. Priming and modifying perceptual structures via context can best be studied using ambiguous stimulus, while the stimulus is held fixed and context is changing or in an streaming scenario, listener's attention is manipulated toward different acoustical features of the context.

Methods

Here we have gathered psychoacoustic results along with neural recordings from human's auditory cortex, using Magnetoencephalography to investigate neural correlates of contextual effect in an streaming paradigm. According to a number of previous studies, perceived pitch direction of an ambiguous Shepard pair consisted of half-octave shifted Shepard tones, can be precisely modified to an upward/downward direction depending on the spectral location of the tones in a biasing sequence, presented prior to the test pair. We have used this paradigm to examine the streamability of the biasing sequence and its role in the strength of biasing effect.

Results

To this end we focused on temporal coherence as a known key factor in streaming process and compared completely synchronous versus desynchronized Shepard tones in their ability to bias directional percept of the Shepard pair. While both stimuli individually lead to a biased percept, the synchronous Shepard tone leads to a stronger bias, both when presented alone and coincident with the asynchronous tone.

We recorded MEG responses in human subjects listening to similar sequences of Shepard tones. In order to measure the effect of the biasing sequence, we interspersed a periodic sequence of Shepard tones between the bias and the test pair, centered in frequency at spectral locations following synchronous or asynchronous biasing sequences. Neural suppression obtained in regions following synchronous biasing sequences is shown to be stronger than asynchronous regions correlated with stronger behavioral biasing effect in the direction of synchronous sequences.

Conclusion

While additional experiments need to be performed to safely conclude that streaming is a main contributor to the strength of the biasing effect, present experiment suggests that one of the main enablers of streaming (coherence), modulates the strength of the biasing effect.

PS - 275

Direct Human Recordings of Dynamic Tinnitus Correlates

William Sedley¹; Phillip Gander²; Hiroyuki Oya²; Hiroto Kawasaki²; Matthew Howard²; Timothy Griffiths¹

¹Newcastle University; ²University of Iowa

Background

Recent research has used experimental manipulations to investigate dynamic correlates of tinnitus; i.e. correlating real-time neural activity with the perceptual intensity of the phantom sound. Research using residual inhibition (RI), a reduction in tinnitus loudness following presentation of a 'masker' sound, and residual excitation (RE), the opposite phenomenon, has identified dynamic oscillatory tinnitus correlates in auditory cortex. These data were recorded with magnetoencephalography, and therefore provided relatively poor estimates of precise anatomical locations and spatial extent. Direct recordings, using invasive electrodes, taken during tinnitus modulation provide excellent temporal and spatial precision, but such opportunities are limited.

Methods

A 50 year-old male patient with moderate bilateral hearing loss and bilateral tonal tinnitus underwent one week of diagnostic electrocorticographic epilepsy monitoring. He had tinnitus unrelated to his seizure phenomenology. Coverage included high-impedance depth electrode contact in left primary auditory cortex and grid contacts over large parts of left auditory cortex.

To investigate dynamic tinnitus correlates, RI and RE were achieved following 30 s masking stimuli (pure tone or white noise), and the subject provided feedback on tinnitus loudness at regular intervals (minimum 10 s) for 3 blocks following each masker. For each trial spectral power was calculated in 10 s epochs, following masker offset. Pearson product moment correlation coefficient was calculated between subjective tinnitus intensity for each frequency band for each electrode.

Results

Of three repetitions of the experiment, the most successful psychophysically achieved a modest degree of RI lasting less than 10 seconds for 15 out of 30 trials using a white noise masker. A common profile of oscillatory power change occurred that was statistically significant in 30 separate electrodes, including almost all of the auditory cortex sites sampled, the whole of the superior temporal gyrus, angular and supramarginal gyri, temporal pole, amygdala, and posterior hippocampus. The pattern was of a correlation with tinnitus loudness that was positive for all frequencies below 20 Hz, and negative for gamma power above 30 Hz. The other experiments showed a similar pattern of power changes. In

contrast, the RE experiment showed the opposite pattern of correlation between tinnitus loudness and oscillatory power.

Conclusion

In the context of hearing loss, intensity of tinnitus perception in real-time was coupled to neural activity in a large number of brain locations within and outside auditory cortex. The directions of oscillatory power change depended on the type of tinnitus modification, against the existence of any single unvarying 'oscillatory code' of tinnitus.

PS - 276

Electrophysiological Recordings from the Parabelt Region in Behaving Macaque Monkeys

Yoshinao Kajikawa¹; Deborah Ross¹; Troy Hackett²; Charles Schroeder³

¹Nathan Kline Institute; ²Vanderbilt University; ³Columbia University

Background

Human studies suggest that the superior temporal gyrus (STG) processes various aspects of communication signals. A corresponding STG region in non-human primates is the parabelt region of auditory cortex. Given the likely involvement of the parabelt in cognitive functions related to communication, it is of great interest to determine how the basic physiological properties of parabelt neurons underpin such cognitive functions. However, systematic electrophysiological studies of parabelt neurons in behaving macaques have not yet been conducted. Recently we devised methods that enable direct approach to the STG in awake-behaving monkeys. We describe results from STG recordings in one monkey performing auditory and audiovisual tasks.

Methods

A macaque monkey was trained to perform auditory and audio-visual oddball tasks. The monkey initiated each trial by pulling a lever using its right hand. Then, a series of identical sounds/movies, intermixed with occasional random oddballs was presented. Upon detection of an oddball, monkey released the lever to obtain a reward. Non-target and oddball sounds were chosen randomly from a list of one category (tones, bandpass noises, vocal sounds, click trains) within each block. A monkey was then implanted with a custom-made titanium recording chamber on the left hemisphere. Field potentials and multiunit activity were recorded using linear array multi-contact electrodes (23 contacts, 100 micron spacing). At every penetration site, spectral tuning was characterized by pseudo-randomly presented 100 ms tones and 1/3-octave band-pass noises (0.5 octave intervals) at 40 dB SPL during and before or after tasks.

Results

Implanting a recording chamber anterior to one ear did not interfere with the monkey's task performance. Responses to tones and BPN had similar response magnitudes and spectral tuning between conditions of passive listening and active monitoring during the oddball tasks in the parabelt. Some anterior sites responded only to complex sounds used in the

tasks. Caudal sites responded to tones with spectral tuning. The auditory responsive zone elongated in the anterior-posterior orientation was flanked superiorly by an area of mouth movement-related activity (M1/S1) and inferiorly by visual responses to faces presumably of the inferior temporal gyrus. We will examine any cognitive effects in those data.

Conclusion

Our results indicate that laminar recordings from the parabelt in behaving macaques is feasible. Though parabelt neurons were believed to respond preferentially to spectrotemporally complex sounds, as observed in the rostral parabelt, the caudal parabelt area responded well to simple sounds with topographically organized distribution of spectral tuning.

PS - 277

State-Dependent Behavioral Changes in Ferret Higher Order Auditory Cortex

Diego Elgueda¹; Stephen David²; Susanne Radtke-Schuller³; Shihab Shamma¹; Jonathan Fritz¹

¹University of Maryland; ²Oregon Health & Science University; ³Ludwig-Maximilians-Universität München

Background

Primary auditory cortex (A1) neurons in the ferret enhance their ability to encode task-relevant stimuli through rapid spectrotemporal receptive field (STRF) plasticity during auditory tasks requiring the discrimination between classes of reference and target sounds (Fritz *et al.* 2003, 2005, 2007; Atiani *et al.*, 2009; David *et al.*, 2012). Overall, such task-induced STRF plasticity in A1 leads to enhanced contrast between reference and target stimuli. In order to better understand attentional modulation in higher order auditory cortical processing, we investigated responses in secondary auditory areas that lie ventral to A1, including areas PSF/PPF in the dorsal Posterior Ectosylvian Gyrus (dPEG) and areas in the anterior-ventral PEG (Pro-PPF/VPr) and on the adjacent posterior bank in the PSS (pseudo-sylvian sulcus).

Methods

Four ferrets were trained in a go/no-go conditioned avoidance tone-detection (spectral) and click-rate discrimination (temporal) tasks, in which they had to refrain from licking water when presented with a target stimulus. We recorded single-unit responses in awake, head-fixed ferrets during passive listening and performance of behavioral tasks. We also characterized frequency tuning of all recorded neurons.

Results

We report results from >180 single units. Compared to A1 and dPEG, neurons in vPEG were more broadly tuned, and displayed longer response latencies. Ventral PEG neurons had weaker phase locking to the envelope of rippled noise stimuli, making it difficult in most cases to obtain STRFs. They displayed, however, robust responses to ferret vocalizations, which were not predicted from their frequency tuning to tones.

During performance of auditory tasks, we observed several modulatory effects, with a general tendency to selectively enhance the response to the target sound, or enhance the

difference between responses to target and reference stimuli. We also observed suppression of responses to distractor sounds. Although most behavioral effects were transient and rapidly recovered to pre-behavior firing rates, there were also cases of post-behavioral persistent effects. This is consistent with our previous observations in ferret A1 and dorsal frontal cortex (dFC) in which similar patterns of transient and persistent effects were observed.

Conclusion

Our results show striking behavioral effects in vPEG neurons that suggest that auditory processing in this area lies in the processing hierarchy between sensory encoding in A1 and abstract sound meaning encoding in dFC, consistent with preliminary neuroanatomical studies showing connectivity between vPEG and PSSC and the dFC, and earlier work (Fritz *et al.*, 2010) suggesting top-down signals from dFC can trigger changes in STRFs in auditory cortex.

PS - 278

Streaming of Repeated Embedded Noise in Ferret Primary Auditory Cortex

Daniela Thorson¹; Josh McDermott²; Stephen David¹

¹Oregon Health and Science University; ²Massachusetts Institute of Technology

Background

In order to function in natural auditory environments, the brain must segregate different components of sound mixtures, a process known as auditory streaming. Many natural sounds contain repetitive patterns that provide a cue for auditory grouping (McDermott *et al.* 2011). The present study sought first to test if ferrets can use temporal regularities to stream auditory stimuli and second to explore if a streaming effect can be measured at the level of the primary auditory cortex (A1) in passive and/or active listening conditions.

Methods

Stimuli consisted of the superposition of two broadband, spectrally overlapping noise signals, each composed of a continuous sequence of 300-ms noise samples with spectro-temporal correlations matched to natural stimuli. The stimuli were perceived as a single stream until a target sample started to repeat in one of source signals, thereby generating a perceptually distinct foreground.

Experiment 1: Auditory responses were recorded extracellularly from single A1 neurons of an awake, task-naïve ferret during presentation of single and two simultaneous noise sequences. Single-unit activity was recorded from four independently movable high-impedance electrodes in a sound-attenuating chamber.

Experiment 2: We trained two animals to detect the repeated noise target using a go/no-go behavioral paradigm, in which they were rewarded for correct responses to the target. Target samples were varied between behavioral blocks.

Results

Experiment 1: The noise stimuli evoked robust neuronal responses in A1. A simple test for streaming revealed pref-

erential encoding of the repeated target relative to the random background stream. Specifically, for some neurons, the PSTH response to the repeated target in noise was more similar to the response to the target in isolation (measured by correlation coefficient) than the response to the non-repeated target in noise. The opposite pattern, greater similarity between non-repeated target and isolated target responses, was never observed.

Experiment 2: Ferrets, like humans, can hear and report the occurrence of the repeated noise when embedded in the non-repeated mixture of sounds.

Conclusion

Preliminary data from experiment 1 suggest that segregated sounds might be represented at the level of A1. Data from experiment 2 demonstrate that ferrets are able to reliably perform the repeated noise detection task, therefore providing an animal model for studying the neurophysiological basis of repetition-based streaming. Ongoing studies are exploring whether training on the repetition detection task leads to enhanced streaming effects in the neural data during passive listening and/or during task behavior.

PS - 279

Nonlinear Spectro-Temporal Integration of Natural Stimuli in Primary Auditory Cortex

Ivar Thorson; Stephen David

Oregon Health and Science University

Background

Hearing requires integration of spectral information from different locations on the cochlea and spatial information between the two ears. Classical receptive field models for auditory neurons treat this integration as a linear weighted sum of inputs across spectral and spatial bands. Previous studies have identified nonlinear interactions between these inputs, but data limitations have often prevented the validation of general receptive field models that reliably account for these nonlinearities. We have developed a vocalization-modulated noise stimulus that can be described in a low-dimensional space, permitting characterization by a wide range of nonlinear receptive field models while evoking activity with natural temporal dynamics.

Methods

Vocalization-modulated noise was composed of bandpass noise modulated by the temporal envelope taken from a natural vocalization, producing a stimulus similar to noise-vocoded speech. Multiple noise bands, modulated by independent vocalization envelopes, were combined to produce the stimuli presented in experiments. A spectral "center-surround" stimulus combined narrowband noise (0.5-1 octave) centered over the excitatory tuning band of the neuron and broadband noise spanning five octaves at the same spatial location. A spatial stimulus consisted of two independent narrowband noise streams presented 15-degrees left and right of the midline. We presented these stimuli in free field to awake, passively listening ferrets while recording single-neuron activity from primary auditory cortex (A1).

Results

The vocalization-modulated noise stimulus was effective at driving activity in most A1 units. We fit two different receptive field models with distinct temporal and spectral nonlinearities to characterize the functional relationship between stimulus and response. The first model mimicked nonlinear synaptic depression of the inputs to a linear filter. The second, a second-order Volterra model, accounted for multiplicative interactions between stimulus channels prior to linear filtering. Both nonlinear models produced consistently more accurate predictions of the time-varying neural response than a simple linear filter model for a reserved validation dataset. Furthermore, a joint model that combined nonlinear synaptic depression and multiplicative interactions performed better than either model with a single nonlinear component. Improvements in performance by the nonlinear models were similar for both the center-surround and spatial datasets.

Conclusion

Our results demonstrate that predictive filter models of A1 neurons can be improved by accounting both for nonlinear temporal processing (synaptic depression) and for nonlinear spectral and spatial integration (multiplicative interactions). These findings establish new directions toward complete functional models that fully describe the representation of natural vocalizations and other stimuli in auditory cortex.

PS - 280

Noise-Induced Hearing Loss Alters Hypothalamic-Pituitary-Adrenal Axis Activity in Rats

Sarah Hayes¹; Senthilvelan Manohar¹; Brian Allman²; Richard Salvi¹

¹*University at Buffalo, Center for Hearing and Deafness;*

¹*University at Buffalo, Center for Hearing and Deafness;*

²*University of Western Ontario*

Background

The deleterious effects of intense noise exposure on the inner ear and central auditory pathway structures have long been documented, however, the effects of acoustic trauma on non-classical auditory brain regions are less understood. Previously, we demonstrated that a single high intensity unilateral noise exposure resulted in reduced hippocampus neurogenesis measured 10 weeks post noise exposure. Given the known ability of stress hormones to reduce hippocampal neurogenesis, we hypothesized that the reduction in hippocampal neurogenesis following unilateral noise exposure might be mediated by changes in basal or reactive stress hormone levels.

Methods

To test our hypothesis, adult male Sprague Dawley rats underwent unilateral intense noise exposure (12kHz narrowband noise, 126 dB SPL, 2 hrs, isoflurane anesthesia) or sham exposure (2 hrs isoflurane anesthesia). Half of the rats were used to quantify changes in basal stress hormone levels, and the other half were used to quantify changes in reactive stress hormone levels over a period of 10 weeks. For both groups, blood samples were collected before and after

noise or sham exposure. For basal stress hormone quantification, blood samples were collected in the morning once per week for 10 consecutive weeks. For reactive stress hormone level quantification, blood samples were collected before, immediately after, and one hour after exposure to 30 minutes of acute restraint stress which occurred once biweekly for 10 consecutive weeks. Plasma corticosterone levels were measured using an enzyme immunoassay kit. Auditory function was assessed by measuring DPOAEs 24 hours post exposure and ABRs 10 weeks post exposure.

Results

Unilateral noise exposure resulted in suppression of DPOAEs and a significant elevation of ABR thresholds in the exposed ear. Acoustic trauma, known to cause a short-term increase in corticosterone levels, did not result in a long-term elevation in basal corticosterone levels in the weeks following noise exposure. However, unilateral acoustic trauma did result in a blunting of reactive stress hormone levels over 10 weeks.

Conclusion

The reduction in neurogenesis observed following unilateral noise exposure is not likely mediated by an elevation in basal or reactive stress hormone levels. Interestingly, our observation of a blunted stress response suggests that unilateral noise exposure results in a malfunction of the HPA axis, similar to what is seen in human tinnitus patients. Future studies are planned to investigate the mechanisms underlying and the consequences of HPA axis malfunction in rodents with unilateral noise-induced hearing loss.

PS - 281

Genes Associated With Hereditary Hearing Loss May be also Affect Susceptibility of Noise Induced Hearing Loss

Xukun Yan¹; Xijun Xue²; Qinglei Dai²; Yongyi Yuan¹; Chongfeng Xu³; Jing Dong²; Jingqiao Lu⁴; Xi Lin⁴; Pu Dai¹
¹Chinese PLA General Hospital; ¹Chinese PLA General Hospital; ²Kunming General Hospital of Chengdu Military Command; ³Chinese Academy of Sciences; ⁴Emory University School of Medicine

Background

Noise induced hearing loss (NIHL) is a common disease affecting life quality in modern society. NIHL influenced by both environmental and genetic factors. People, which have hereditary susceptibility, suffer from noise will induce hearing loss easily. But there are still many gene changes associated with NIHL have not been known clearly so far. In this study, we want to see if there is overlap of hereditary hearing loss genes and NIHL genes and find some predisposing mutations of NIHL in Chinese people. If the susceptible populations of NIHL can be found, and take protective measures in advance, we can largely avoid the occurrence of NIHL.

Methods

We preliminarily investigated 375 persons suffered from noise exposure in China, concluding basic personal information, noise exposure history, clinical symptoms, ENT examination, hearing test by pure-tone audiometry (PTA), and other nec-

essary examinations. And then selected 23 noise susceptible persons and 12 noise tolerated persons for further studies. Peripheral blood was collected from all the 35 respondents. Genomic DNA was isolated from peripheral blood for next generation sequencing screened 67 deafness genes and 64 genes associated with deafness in human. When we found the gene mutations by NGS, would verify the accuracy of results by Sanger sequencing again. If the identified gene mutations cause amino acid changes, evolutionary conservation analysis of amino acids in deafness gene protein was made among different species. SIFT or Polyphen2 software was used to predict the hazard of amino acid changes. Analyzing the differences in the distribution of mutations in the two groups. Checking the mutations in databases and literatures and analyzing the functional changes of the protein after gene mutation.

Results

All the subjects didn't have obvious abnormalities in otology examination or other diseases except for hearing loss in susceptible group. We found that 30 genes have mutations/SNPs, and noise susceptible persons carrying many mutations associated with hereditary hearing loss, especially in potassium recycling pathway genes and monogenic deafness genes. Three mutations, *WFS1* c.1726 G>A (het) (7/23), *GJB2* c.109 G>A (het) (7/23) and *COL11A2* chr6: 33136310 g>t (het) (6/23), are the most common mutations discovered in noise susceptible persons. Some other mutations, *MYO7A* c.4805G>A (het) (2/12), *GJB2* c.368C>A (het) (3/12), only exist in noise tolerated persons.

Conclusion

This result strongly indicates that gene mutations associated with hereditary hearing loss may be also affect susceptibility of NIHL. Which could guide how to prevent NIHL.

PS - 282

Genetic Variants of CDH23 Associated With Noise-Induced Hearing Loss

Mariola Sliwinska-Kowalska¹; Tomasz Kowalski²; Malgorzata Pawelczyk³; Elzbieta Rajkowska⁴
¹Nofer Institute of Occupational Medicine; ²UCLA, Department of Orthopedics; ³Medical University of Lodz, Poland; ⁴Nofer Institute of Occupational Medicine, Lodz, Poland

Background

Noise-induced hearing loss (NIHL) is a complex disease resulting from the interaction between external and intrinsic/genetic factors. One of the most interesting candidate gene for NIHL susceptibility is *CDH23* encoding Cadherin 23, a component of the stereocilia tip links, which are thought to gate mechanotransduction channel in hair cells. The aim of this study was to analyze selected *CDH23* polymorphisms and to evaluate their interaction with other environmental and individual factors known to determine NIHL development.

Methods

A study group consisted of 314 susceptible and 313 resistant to noise subjects. Five SNPs in *CDH23* were genotyped using Real-Time PCR. Subsequently, the main effect of gen-

otype and its interaction with selected environmental and individual factors were evaluated.

Results

The most prominent results (i.e. significant within the main effect of genotype) were obtained for 2 SNPs localized in exon 21 – rs3752751 and rs3752752. The effect of the latter one was observed in particular in the subgroup of young subjects, and in these exposed to impulse noise; CC genotype was more frequent among susceptible subjects while genotype CT appeared more often among resistant to noise subjects. Moreover, the effect of rs3752752 polymorphism was not modified by none of environmental/individual factors except for blood pressure; the latter one however should be further investigated.

Conclusion

The results of this study show that *CDH23* genetic variant may modify the susceptibility to NIHL development in humans, what is in agreement with earlier observations in mice.

PS - 283

Sequencing-Association Study on Calcium Signaling Genes Contributing to Age-Related Hearing Loss

Ruqiang Liang¹; Hui Li¹; Dina Newman²; Robert Frisina³; Jianxin Bao¹

¹Washington University in St. Louis; ²Rochester Institute of Technology; ³University of South Florida

Background

Age-related hearing loss (ARHL) is a complex trait that has been the subject of many genetic studies. However, known common genetic variants cannot presently account for the full range of hearing ability with age seen in patients. Next generation sequencing (NGS) is a powerful tool for detecting not only common variants, but also rare variants and new variants in a high throughput manner. Although costs associated with NGS are rapidly decreasing, the cost of high throughput whole genome sequencing (WGS) or whole exome sequencing (WES) can still be prohibitive. Target-enriched exome sequencing offers a promising economical approach for sequencing-association studies. Patients taking calcium channel blockers have shown better hearing with age, suggesting cellular calcium dysregulation contributes to ARHL. We hypothesize that variants of calcium signaling genes associate with hearing ability in aged people.

Methods

The study cohort consisted of 636 individuals from the Rochester, NY greater metropolitan area. Their genomic DNA was used to make sequencing libraries with 96 barcodes. Target enriched bait (2.1 Mb) was synthesized by Agilent technology for 264 genes, including all known voltage-gated calcium channels, genes involved in calcium signaling and drug metabolism pathways, and known deafness genes. Ninety-six libraries were pooled at equal amount for target enrichment, followed by pair-end sequencing for 2x 100 bp on Illumina HiSeq 2500. Sequencing-association with continuous phenotype Z scores of hearing capability was performed using the

SNP-set (Sequence) Kernel Association Test (SKAT) method, taking into consideration both common and rare genetic variants, with post hoc Bonferroni correction.

Results

The average Z scores for subjects' better ears at 2, 4, and 8 kHz were used as a continuous phenotype, with a range from -1.460 to +4.017 (mean \pm SD, 0.2885 \pm 0.795). There were 242 individuals with better hearing than average, and 394 worse than average. Genomic DNA was amplified using a whole-genome amplification method with phi29 DNA polymerase. We are constructing sequencing libraries of these genomic DNA samples using Roland and Reich's method. SKAT software will be used to associate hearing Z scores with common and rare variants of the 264 genes selected.

Conclusion

If this method is successful, we will have 636 sequencing libraries ready for WGS, WES, and/or target-enriched sequencing. We hope to demonstrate that the combination of SKAT and high throughput sequencing libraries can be used to find genetic variants that contribute to ARHL.

PS - 284

Genome-Wide Association Study, Whole Genome Sequencing and Animal Models to Study Normal Hearing Function and Age-Related Hearing Loss

Giorgia Giotto¹; Dragana Vuckovic¹; Maria Pina Concas²; Teresa Nutile³; Marina Ciullo³; Mario Pirastu²; Paolo Gasparini¹

¹Institute for Maternal and Child Health-IRCCS "Burlo Garofolo", University of Trieste, Italy; ²Institute for Maternal and Child Health-IRCCS "Burlo Garofolo", University of Trieste, Italy; ³Institution of Population Genetics, CNR, Sassari, Italy; ³Institute of Genetics and Biophysics, CNR, Naples, Italy

Background

Little is known about the molecular bases of Normal Hearing Function (NHF) and Age-Related Hearing Loss (ARHL). Quite recently a Genome-wide association study (GWAS) meta-analysis identified a series of candidate genes for both NHF and ARHL in 3417 individuals coming from several countries (Giotto G. et al. JMG 2011). 19 selected candidate genes from GWAS were then tested by immunohistochemistry in the mouse cochlea. 12 of them were expressed in specific cell types in the mouse cochlea and 9 replicated in an independent cohort from Silk Road countries (Giotto G. et al. manuscript under revision). Despite these results, research still needs additional efforts, thus a new powerful strategy for gene identification has been designed (Fig.1).

Methods

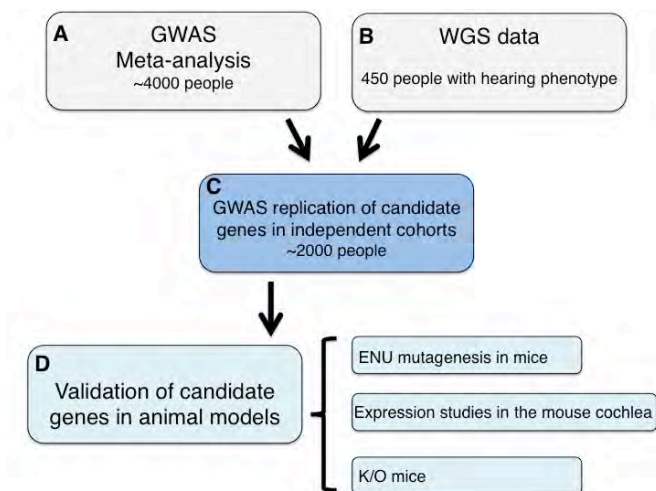
This strategy is based on the following approaches: A) GWAS meta-analysis on increased sample size both on NHF as well as on ARHL using 1000g imputed data, B) Whole genome sequencing (WGS) of 450 subjects with hearing phenotype including ARHL cases, C) replication of the results in independent cohorts and D) validation in animal models.

Results

In the first step, several new SNPs/genes were detected including 2 highly statistically significant associations: top SNPs were rs78043697 ($p=4.71 \times 10^{-10}$) and rs7032430 ($p=2.39 \times 10^{-9}$). These SNPs are located respectively close to *PCDH20* and *SLC28A3*, both belonging to families of genes whose members have been already described as involved in hearing loss. Sanger sequencing to detect functional variants in these genes is now in progress. Other 9 statistically significant candidate genes with a $p \sim 10^{-8}$ (*GPR17*, *PDE1A*, *DNAH11*, *CTSD*, *PSD3*, *WWOX*, *BEND5*, *PDCD1LG2*, *PVT1*) and many others with suggestive p-values (including *ESRRG* gene) are now under evaluation. These data together with those from WGS are defining a final list of candidates that will be replicated in an independent cohort (1958 UK cohort, S. Dawson). The final validation step includes *in vitro* and *in vivo* analyses in mouse models (in collaboration with our UK colleagues). Up-to-date data will be presented and discussed.

Conclusion

The combined approach of GWAS analysis and WGS led either to 1) the identification of new suggestive loci/genes for both NHF and ARHL, and 2) the detection of common and rare variants including those located in regulatory regions. Moreover, functional studies validated some of these genes/variants providing new insights into the molecular basis of NHF and ARHL.



PS - 285

Screening of 250.000 DNA Functional Variants in Large Cohorts of Age-Related Hearing Loss Patients and Normal Hearing Subjects

Dragana Vuckovic; Giorgia Giroto; Paolo Gasparini
Institute for Maternal and Child Health-IRCCS "Burlo Garofolo", University of Trieste, Italy

Background

The vast majority of genetic and environmental/lifestyle factors contributing to normal hearing function (NHF) and age-related hearing loss (ARHL) still needs to be identified. Many different molecules have a role in modulating NHF and causing ARHL. To better investigate the genetic factors in-

involved in these traits, we analyzed 250.000 DNA functional variants in a large cohort of 2319 samples from isolated populations in Italy, Caucasus and Central Asia.

Methods

HumanExome BeadChips (Illumina) deliver unparalleled coverage of putative 250,000 functional exonic variants. They were used to test 719 ARHL cases and controls and 1600 normal individuals (NHF). Common variants were analyzed by regression mixed model, and rare ones by burden and SKAT test.

Results

Preliminary results in a subset of subjects (910 for NHF and 425 for ARHL) led to the identification of two strong hits for these traits. For NHF, the top associated variant (rs150266212, $p=3.67 \times 10^{-11}$) is a missense mutation (p.Arg248His) located within *ITFG2* gene, and predicted to be damaging. Itfg2-deficient mice present autoimmune phenotype. For ARHL the top associated variant (rs201029011, $p=2.83 \times 10^{-5}$) is a missense mutation (Ala642Thr), again predicted to be damaging and located within *FLYWCH1* gene, whose function needs to be elucidated. Interestingly, the minor allele frequency for both these SNPs is much bigger in our isolated population compared to that reported in dbSNP database (0.04 vs. 0.0001 and 0.01 vs. 0.0008 respectively), underlining the importance of inbred populations in detecting rare variants. Nine additional functional variants were associated to either NHF or ARHL. In particular, 4 SNPs are located within HL loci (DFNA59, DFNA33, DFNA30, DFNB13) for which the causative genes are yet unknown. As regards DFNA59 locus the variant (rs8192466, $p=2.18 \times 10^{-6}$) is a missense mutation (p.Thr2Ile) in a gene (*BDNF*) already described as involved in auditory system. The remaining 5 SNPs are missense variants found in the following genes: *PKP2*, *ABCA3*, *OR2C1*, *FOXP2* and *OR1F1*. Whole exome sequencing studies are in progress to search for additional rare variants specific of our population. Finally, all these results will be replicated and further investigated in additional cohorts.

Conclusion

The screening of a large amount of functional variants led to the identification of a series of interesting mutations in different genes most likely underlying either NHF or ARHL. Future steps are needed to further elucidate the role of these genes/variants.

Diagnostic Massively Parallel Sequencing Using OtoSCOPE® for Hereditary Hearing Loss in Japan

Hideaki Moteki¹; Hela Azaiez¹; Kevin Booth¹; A. Eliot Shearer¹; Shin-ichi Usami²; Richard JH Smith¹

¹Molecular Otolaryngology and Renal Research Laboratories, Department of Otolaryngology, University of Iowa; ²Department of Otorhinolaryngology, School of Medicine, Shinshu University

Background

Non-syndromic hearing loss (NSHL) affects at least 1 in 500 newborns, with genetic causes accounting for 50-70% of all childhood hearing loss. Recent advances in massively parallel sequencing (MPS) with targeted genomic enrichment (TGE) have made comprehensive genetic testing for NSHL possible. In this study, we used OtoSCOPE® to determine the cause of hearing loss and evaluate the spectrum of genetic causes of hereditary hearing loss in Japan. The OtoSCOPE® platform analyzes all coding exons of all genes implicated in NSHL simultaneously.

Methods

We examined DNA from 202 probands with NSHL collected through 33 otolaryngology clinics and hospitals nationwide in Japan. Hearing loss segregated as autosomal dominant in 53 families and autosomal recessive in 37 families; it was sporadic in 112 families. In all probands, mutations in *GJB2* were excluded by Sanger sequencing. We performed TGE on probands using post-capture multiplexing followed by OtoSCOPE® screening of pooled libraries on the Illumina HiSeq. For genetic diagnoses, data analysis was performed on a local installation of Galaxy using the Burrows-Wheeler Alignment (BWA) for read mapping, Picard for removal of duplicate reads, GATK for local re-alignment and variant calling, and ANNOVAR and a custom workflow for variant annotation. All causative mutations were verified by Sanger sequencing.

Results

The average per sample total reads was 8,766,764, with 10X target coverage of 99.3%. Causative mutations were identified in 33% of probands with solve rates of ~45%, ~50% and ~10% for dominant, recessive and sporadic NSHL, respectively. Copy number variant analysis identified homozygosity for deletion of *STRC* as a cause of mild-moderate HL.

Conclusion

Comprehensive genetic screening using OtoSCOPE® identifies a genetic cause of hearing loss in about one-third of Japanese patients with NSHL. To facilitate variant calling, ethnic-specific filtering by allele frequency is essential. OtoSCOPE® should be used to identify genetic causes of hearing loss in the clinical care of all Japanese patients with NSHL.

Mutation of Foxo3 Causes Adult Onset Auditory Neuropathy and Alters Cochlear Synapse Architecture in Mice

Felicia Gilels; Stephen Paquette; Jingyuan Zhang; Irfan Rahman; Patricia White

University of Rochester Medical Center

Background

Foxo3 is a member of the Foxo winged-helix transcription factor family. Foxo3 mediates oxidative stress responses, apoptosis, and cell cycle withdrawal in many systems. Foxo3 can be activated by excitotoxicity or mechanical stress.

Previously we had shown that loss of Foxo3 causes adult onset auditory neuropathy. Here we have characterized the synaptic phenotype of the Foxo3-KO mouse.

Methods

All experiments were conducted on Foxo3 wild-type and knock-out littermates, on the FVB/n strain, at two and four months of age. Immunohistochemistry was used to analyze Foxo3 expression in the sensory region of the ear. Auditory function was assessed with Auditory Brainstem Responses (ABR) and Distortion Product Otoacoustic Emissions (DPOAE). Synaptic analyses were performed using Amira 3-D reconstructions and algorithmically assessed with custom scripts written in Mathematica.

Results

Foxo3-KO mice have adult onset hearing loss with the hallmark characteristics of auditory neuropathy, namely, reduced peak I amplitudes and elevated auditory thresholds concomitant with normal outer hair cell function. We found that acoustic stimulation promotes Foxo3 nuclear translocation in spiral ganglion neurons. Previously, we have shown that there are no cellular losses observed in the affected turn of the Foxo3-KO. In addition, there is no depletion in the number of synaptic pairs in the Foxo3-KO mice, compared to wild-type littermates. However, we find that in the hearing affected 32kHz cochlear turn, there is both abnormal inner hair cell morphology and altered distribution of paired synapses from the basolateral surface.

Conclusion

We conclude that Foxo3 activity contributes to the maintenance of synaptic function in the adult cochlea. We speculate that the altered inner hair cell morphology and synaptic distribution exhibited in the four month-old Foxo3-KO mouse is a consequence of increased oxidative stress. We have discovered, acoustic stimulation promotes Foxo3 nuclear localization *in vivo*, implying a possible connection between cochlear activity and the maintenance of synaptic function. These findings support a new role for the canonical damage response factor, Foxo3, in auditory synaptic transmission and early adult onset auditory neuropathy. Future research will address the mechanism of Foxo3's role in hearing preservation.

A New Mutation of the *Atoh1* Gene in Mice With Normal Life Span Allows Analysis of Inner Ear and Cerebellar Phenotype in Aging

Qing Zheng; Juan Hu; Kianoush Sheykhoslamy; Vikrum Thimmappa; Casey Nava; Xiaohui Bai; Heping Yu; Tihua Zheng

Case Western Reserve University

Background

Atoh1 is a transcription factor that regulates neural development in multiple tissues and is conserved among species. Prior mouse models of *Atoh1*, though effective and important in the evolution of our understanding of the gene, have been limited by perinatal lethality.

Methods

Atoh1^{trhl/trhl} mutation was obtained from an ethylmethane-sulfonate (EMS) program. Genetic mapping and sequencing analysis was performed to identify the *trhl* hypomorphic mutation. ABR, DPOAE, *Histology and SEM*, Cytocochleograms were used to characterize function and morphology of auditory hair cells and cerebellum, *Q-RT-PCR* was used to compare gene expression differences in target genes of the *ATOH1* between mutants and controls.

Results

Gross phenotype, genetic mapping and sequence comparison of the *Atoh1*^{trhl} mutation define the first viable normal-life-span mutant without conditional gene targeting. mRNA expression of several genes specific to *Atoh1* targets was down-regulated in the inner ear tissue from *Atoh1*^{trhl} mice. The study revealed that in homozygous *Atoh1*^{trhl} mice, outer hair cells (OHC) and inner hair cells (IHC) exhibited losses throughout the cochlea that were already present at the initial 3 weeks time point, and exhibited similar, but progressive, losses at 7 weeks of age as compared to heterozygote controls. There are more cells missing in the *trhl* mutant than in controls and the hair cells present are oriented haphazardly. SEM views show the classic disorientation of hair bundles and missing cells in homozygous mutants as compared to the wild-type controls, confirming the inner ear morphological dysfunction of the model. Progressive hearing loss indicated by ABR and DPOAE.

Conclusion

Since the *trhl* mutant mice have a normal life span, unlike previous *Atoh1*-null mutations, which are perinatally lethal, we can take advantage of this new model to investigate many aspects of downstream hearing and balance pathophysiology, molecular biology, proteomics and cancer biology. In addition to the normal life span, the *Atoh1* mutant mice display unique features as a model for progressive age related hearing loss. These characteristics may reflect a crucial requirement for *Atoh1* in the lifelong maintenance of cochlear hair cells. Conceivably, an understanding of this requirement at the molecular level will provide significant insights into the pathology of aging-related deafness, creating further demand for this model as a significant tool to explore human diseases

including lung cancers, intestinal tumorigenesis, and neuroblastoma formation.

Deafness Models With Amino Acid Substitution in Plasma Membrane Calcium Pump Suggest Pathways That Differentiate the Phenotype

Osamu Minowa¹; Hiromi Motegi¹; Hideaki Toki¹; Maki Inoue¹; Hideki Kaneda¹; Tomohiro Suzuki¹; Hiroshi Masuya¹; Shigeharu Wakana¹; Yoichi Gondo¹; Tetsuo Noda²

¹RIKEN Bioresource center; ²RIKEN BioResource Center / Cancer Institute, JFCR

Background

Developing new mouse deafness models will greatly increase our understanding of the mechanisms underlying hearing impairments, as well as improving the diagnosis and treatment of these disorders [1]. Here, we used an ENU-mutagenesis screening platform to identify mice with hearing impairments, with the aim of developing a novel mouse model of human deafness. [1] Brown SD, Hardisty-Hughes RE, Mburu P. "Quiet as a mouse: dissecting the molecular and genetic basis of hearing." Nat Rev Genet, 9, 277-90, 2008.

Methods

We screened mice by observing the startle responses evoked by a click box and then measuring the auditory brainstem responses (ABR) [2-3]. The isolated mutants showed a phenotype that was not accompanied by other traits, which is a characteristic typical of human diagnostic-type nonsyndromic deafness. [2] Bull KR et al., "Unlocking the bottleneck in forward genetics using whole-genome sequencing and identity by descent to isolate causative mutations." PLoS Genet. 9, Epub 2013 Jan 31. [3] Gondo Y, "Trends in large-scale mouse mutagenesis: from genetics to functional genomics." Nat. Rev. Genet., 10, 803 - 10, 2008.

Results

The mutations in four of the lines were mapped to the distal region of chromosome 6. Direct sequencing showed that these lines harbored missense mutations in different domains of *pmca2*, indicating a possible defect in hair cell calcium-ion mobilization [4]. Mutations in the other 10 lines were mapped to chromosome 10. Five of these lines harbored missense mutations in the extracellular domains of *Cdh23* gene products. We observed clear phenotypic variations in the four lines harboring mutations in *pmca2*, including differential increases in the ABR threshold at the early stage of deafness, followed by the eventual loss of hair cells and spiral ganglion cells at different time points. [4] Spiden SL, Bortolozzi M, Leva FD, Angelis MH, Fuchs H, Lim D, Ortolano S, Ingham NJ, Brini

M, Carafoli E, Mammano F, Steel KP. "The Novel Mouse Mutation Oblivion Inactivates the

PMCA2 Pump and Causes Progressive Hearing Loss"

PLOS Genetics, 4, e1000238, 2008

Conclusion

This phenotypic variation seems to result from the enzymatic activity differences of the mutated gene products. The pathway through which these phenotypes evolve is thought to branch into two parts: one to functionally impair hair cells and the other to threaten their survival. Clarifying these pathways may help to understand the pathogenesis of human age-related hearing disorders.

PS - 290

Transcriptional Regulation of PMCA2 in Inbred Mouse Strains

Rebecca Minich; Claire Watson; Bruce Tempel
University of Washington

Background

The plasma membrane Ca^{2+} ATPase 2 (PMCA2) protein regulates intracellular Ca^{2+} levels and is encoded by the *Atp2b2* gene. *Atp2b2* mutations have given rise to an allelic series of *deafwaddler* mouse mutants. Studies in heterozygous *deafwaddler* mutants derived from different strain backgrounds (*dfw2J* and *dfwi5*) suggest that *Atp2b2* expression levels are regulated by ancestral *Atp2b2* haplotypes (Watson and Tempel, submitted). We have shown that transcription of the *Atp2b2* C57BL/6J (B6) allele is under-expressed relative to CBA/CaJ (CB) in heterozygous mice (CB/B6). A study of the parental strains reveals that both neuronal transcripts of *Atp2b2* (α and β) are down regulated in B6 mice. α -*Atp2b2* is the main transcript of the auditory hair cells and is the focus of this study (Silverstein and Tempel 2006).

Methods

To detect sequence nucleotide changes that are polymorphic between CB and B6, the 5kb region upstream of the transcriptional start site of α -*Atp2b2* was sequenced. From this analysis, 9 single nucleotide polymorphisms (SNPs) were identified and analyzed using MatInspector, a software engine that predicts transcription factor (TF) binding sites. To empirically confirm the proximal promoter, we generated a series of CB like luciferase promoter constructs and transiently transfected them into OC-1 organ of corti immortalized cells (from Matthew Holley). To study SNPs predicted to be involved in altering α -*Atp2b2* transcript expression in B6, luciferase constructs containing B6 SNPs were compared to constructs containing CB SNPs.

Results

MatInspector software predicts that 7 of the 9 identified SNPs in the B6 promoter of α -*Atp2b2* will alter the binding of TFs necessary for normal auditory development and maintenance (i.e. *Pou4F3* and *Dlx*). This suggests that B6 may have a 'weaker' α -*Atp2b2* promoter than CB, leading to decreased expression of α -*Atp2b2*. Luciferase constructs have promoter activity when they include the CpG island and 5'UTR exons of α -*Atp2b2*. Promoter constructs comparing strain specific SNPs identify possible contributors to the decreased transcript expression seen in B6.

Conclusion

There is less α -*Atp2b2* and β -*Atp2b2* mRNA transcript expressed in B6 mice when compared to CB mice. There is

strong α -*Atp2b2* promoter activity when the predicted CpG island is expressed in front of the 5'UTR exons. Several SNPs have been identified that may contribute to differences in transcript expression between CB and B6 mice.

PS - 291

Inhibiting Histone Modifications in the Adult Organ of Corti

Wanda Layman; Jian Zuo
St. Jude Children's Research Hospital

Background

Mammalian cochlear supporting cells remain quiescent at later postnatal ages, and age-dependent changes in supporting cell proliferative capacity are evident. Our data indicate that cofactors of repressive complexes such as NuRD and PRC2 are expressed and present in the postnatal organ of Corti. The NuRD and PRC2 cofactors are present throughout most of the organ of Corti from P8 through adulthood.

Methods

Our data suggests that the continued expression and presence of histone deacetylases, histone methyltransferases, and histone demethylases within the organ of Corti may provide therapeutic targets for drug inhibition to increase the capacity, speed, and efficiency of cellular reprogramming. Our goal is to use a combination of genetic manipulation (via *Atoh1* induction) and inhibitors of repressive histone modifications to determine whether the potential for cellular reprogramming can be altered and improved within the adult organ of Corti.

Results

Cellular reprogramming studies in other adult tissues have shown that inhibition of repressive histone marks significantly improves reprogramming efficiency.

Conclusion

Reducing repressive histone marks within the organ of Corti will create a more open chromatin state allowing transcription factors such as *Atoh1* better access to target genes.

PS - 292

Auditory Discrimination Learning - a Tool for Phenotyping Mice

Simone Kurt
Hannover Medical School

Background

Understanding neural mechanisms of brain plasticity due to motor, auditory and perceptual learning in mammals requires a reliable training and test apparatus, controlled procedures for measuring learning progress as well as success in an easily accessible animal model.

Methods

Here we present examples for studying auditory discrimination learning in mice using a shuttle-box apparatus to test (i) discrimination of auditory stimuli, (ii) auditory perception, (iii) development of sensory-motor learning and (iv) auditory processing disorders.

Results

Genetically modified mice, serving as model organisms for various diseases, were used to test specific effects of malfunction of a particular gene on the parameters mentioned (behavioural phenotyping).

Conclusion

The results indicate that mice are a promising animal model of general relevance for research on the genetics of auditory perception and learning. In conclusion, the shuttle-box auditory discrimination learning paradigm opens up a new window to study brain functions in mice via a behavioural approach.

PS - 293

Functional Analysis of the DIAPH1 Formin Protein Associated With DFNA1 Hearing Loss

David Kohrman¹; Alex Figacz²; Jessica Winkels²; Jing Zheng³

¹University of Michigan; ²University of Michigan Medical School; ³Northwestern University

Background

Formin proteins function in a wide variety of cellular processes, including cell division, organelle trafficking, and the formation of specialized cytoskeletal structures (Chesarone et al., Nat. Rev. Mol. Cell Biol. 11: 62-74, 2010). A splicing mutation in the formin gene *DIAPH1* has been associated with progressive, low frequency hearing loss (*DFNA1*) (Lynch et al., Science 278:1315-1318, 1997). This mutation results in a translational frameshift in the coding region and a predicted truncation of *DIAPH1* protein. To investigate the cellular and molecular mechanisms that underlie *DFNA1* hearing loss, we have begun to evaluate the effects of mutant *DIAPH1* in cultured cells.

Methods

Using RT-PCR, we evaluated *DIAPH1* splice isoforms in RNA prepared from human inner ear and generated a wild type *DIAPH1* construct expressing the predominant isoform. *In vitro* mutagenesis of the wild type clone was used to produce a mutant *DIAPH1* cDNA corresponding to the transcript identified in humans with *DFNA1* hearing loss. The expression constructs were transfected into cultured fibroblast (human 293T) and epithelial (pig LLC-PK1-CL4) cells, and *DIAPH1* protein was evaluated by Western and immunocytochemical approaches.

Results

Exons 2 and 18, which are alternatively spliced in some tissues, are included in the predominant *DIAPH1* transcript present in adult human inner ear. Exon 2 encodes an N-terminal region near the GTPase-binding domain involved in formin regulation, while exon 18 encodes a portion of the FH2 domain required for catalyzing actin filament growth. Transfection of wild type and mutant clones into fibroblast cells indicated similar steady state levels of wild type and mutant *DIAPH1* protein. Similarly, transfection of the clones into epithelial cells indicated a similar, broad cytoplasmic distribution of the wild type and mutant proteins.

Conclusion

Hearing loss has not been reported in mice carrying null mutations of mouse *DIAPH1* (Peng et al., Cancer Res. 67:7565-7571, 2007; Sakata et al., J. Exp. Med. 204:2031-2038, 2007), suggesting that the dominant human mutation results in a gain rather than loss of function. The comparable stability and subcellular distribution of the mutant *DIAPH1* protein in the current study is also consistent with a gain of function mutational mechanism. Further investigation of the impact of mutant *DIAPH1* on known formin activities such as cytoskeletal organization and vesicle trafficking should provide greater insight into potential dominant negative or neomorphic functions of the protein.

PS - 294

Identification of Novel Functional Null Allele of SLC26A4 Associated With Enlarged Vestibular Aqueduct

Jeong Hun Jang¹; Ah Reum Kim²; Min Young Kim³; Young Mi Cho³; Byung Yoon Choi³

¹Kyungpook National University College of Medicine;

²Department of Otorhinolaryngology Seoul National

University College of Medicine; ³Department of Otorhinolaryngology-Head and Neck Surgery, Seoul National University Bundang Hospital, Seoul National University College of Medicine

Background

Mutations in the *SLC26A4* gene encoding pendrin, a transmembrane exchanger, are a common cause of congenital hearing loss and is associated with enlargement of the vestibular aqueduct (EVA). In cases of the bi-allelic *SLC26A4* mutations with one known pathogenic mutant allele, evaluating the pathogenic potential of the newly detected *SLC26A4* mutant allele could be important for clinical assessment and diagnostic and therapeutic approaches. This evaluation includes the genotypic, phenotypic context, and functional characterization of the intracellular trafficking and anion exchange properties. In this study, we sought to define the pathogenic potential of the novel missense variant.

Methods

A 3 year-old girl with progressive sensorineural hearing loss and the parents were included in this study. Patient and parents underwent clinical, audiological, radiological and genetic evaluations. DNA sequencing of *SLC26A4* gene was performed to identify genetic mutations. The protein processing and anion exchange activities were examined to evaluate the effects of mutations. DNA sequence analyses of *SLC26A4* were performed by polymerase chain reaction (PCR) amplification of 21 exons and splice sites. We characterized the ability of mutant pendrin products to traffic to the plasma membrane in COS-7 cells and to transport Cl⁻ and HCO₃⁻ in HEK 293 cells.

Results

The pure tone average was 66dB HL in the right ear and 75 dB HL in the left ear, respectively. Temporal bone computed tomography showed enlarged vestibular aqueduct and Mondini's malformation bilaterally. By sequencing analysis,

bi-allelic mutations were identified; one pathogenic variant (p.H723R), and one novel missense variant (p.V510D). The Cl/HCO₃⁻ exchange activity of the p.V510D mutant pendrin was evaluated to address the pathogenic potential as compared with those of wild type, a known polymorphism, p.P542R, and a known null function control p.H723R. The Cl/HCO₃⁻ exchange activity for the novel p.V510D and p.H723R variant was measured to be 10.96±4.79% and 12.57±3.72% of the corresponding wild type, respectively. On the other hand, the exchange activity for a polymorphism control, p.P542R was 82.40±10.11% of the corresponding wildtype. The p.V510D pendrin product showed a reticular pattern in the cytoplasm, not trafficking to the plasma membrane in COS-7 cells.

Conclusion

The newly detected p.V510D is a novel missense variant, not described in literature. A *trans* configuration with pathogenic p.H723R, and impaired cellular trafficking and anion exchange property suggested that the p.V510D would be a functional null allele.

PS - 295

Identification of Recessive Hearing Impairment-Causing Genes in Consanguineous Tunisian Families

Saber Masmoudi¹; M'hamed Grati²; Imen Chakchouk¹; Mariem Bensaid¹; Mohamed Ali Mosrati¹; Mounira Hmani-Aifa¹; Abdelaziz Tilili¹; Denise Yan²; Rahul Mittal³; Xue Zhong Liu²

¹Microorganisms & Biomolecules Laboratory, Centre of Biotechnology of Sfax, Sfax University, Sfax, Tunisia;

²University of Miami Miller School of Medicine, Department of Otolaryngology, Miami, FL 33136, USA; ³University of Miami School of Medicine, Department of Otolaryngology

Background

Hearing impairment (HI) is the most common sensorineural disorder in humans, and congenital HI affects about 0.16% of the newborns. Approximately half of these cases are estimated to be genetically determined, and the remaining cases are likely due to environmental causes. Up to 80% of the hereditary nonsyndromic HI is autosomal-recessive. So far, over 95 chromosomal loci (known as DFNB) have been localized, and the responsible genes have been identified in about 50% of DFNB loci, mainly using linkage analysis/candidate gene approach (<http://hereditaryhearingloss.org/>). However, this strategy was very challenging to apply in the identification of HI genes localized in large genetic intervals. Whole-exome sequencing (WES) has proven to be a highly efficient method for identifying HI-causing mutations, and for discovery of new genes within consanguineous families. We have collected several multi-generational consanguineous Tunisian families (North Africa) with hearing-impaired probands and sibs with normal hearing for few of which preliminary linkage analysis have been performed and provided a relatively precise chromosomal localization of the causative genes. For other families, no linkage data was available.

Methods

We performed genome-wide linkage studies and used next generation whole-exome sequencing for genome wide mutation identification in patients from 4 distinct families. After alignment of sequences against reference genomes, we used Genome Management Application (GEM-app) and applied selection criteria to identify relevant homozygous nucleic variants. Several pathogenicity prediction softwares are used to evaluate the impact of detected genomic variations. Sanger sequencing is performed to study the segregation of candidate variations within the family members.

Results

Linkage studies allowed us to highlight candidate intervals for HI causing genes, and led us to exclude with relatively high confidence, previously known recessive deafness loci. Next generation whole exome sequencing on patients within the 4 families detected homozygous variations in novel genes within the candidate chromosomal intervals, and few of these variations were predicted to be highly pathogenic. Segregation analyses of all candidate variations are underway to determine the causative genes.

Conclusion

Our study of the genetics of HI on consanguineous Tunisian families shows promises to identify novel causative genes.

PS - 296

A Novel Missense Variant in WFS1 Segregates With Autosomal Dominant Low Frequency Hearing Loss in a Multigenerational Indian Family

Jun Shen¹; Tomi L. Toler²; Sami S. Amr⁴; Renu Saxena³; Ishwar Verma³; Heidi L. Rehm⁵; Angela E. Lin²

¹Brigham and Women's Hospital and Harvard Medical School; ²Massachusetts General Hospital; ³Sir Ganga Ram Hospital, New Delhi 110600, India; ⁴Laboratory for Molecular Medicine, Partners HealthCare Center for Personalized Genetic Medicine; ⁵Laboratory for Molecular Medicine, Partners HealthCare Center for Personalized Molecular Medicine

Background

Autosomal dominant low frequency sensorineural hearing loss (LFSNHL) is associated mostly with missense mutations in *WFS1* (wolframin) at the *DFNA6/14/38* locus. Many pathogenic mutations clustered in the C-terminal domain of the wolframin protein have been reported in patients with LFSNHL. However, numerous missense single nucleotide polymorphisms in *WFS1* have also been identified in large population studies. Therefore, the clinical significance of missense variants in *WFS1* cannot be easily determined.

Methods

We studied a 34 year-old woman from India with LFSNHL and autosomal dominant family history. The entire coding region and splice sites of exons 1-8 of *WFS1* (NM_006005.3) in the proband were amplified using primer sets flanking each exon. DNA samples from available family members were amplified using primer sets flanking the region containing the variant.

PCR products were sequenced using an ABI fluorescence automatic DNA sequencer. Public databases (dbSNP, EVS, HGMD, DVD, and *WFS1* Mutation Database) were searched to assess the frequency of the variant. Computational analyses (biochemical amino acid properties, conservation, AlignGVGD, PolyPhen2, and SIFT) were performed to predict the impact.

Results

Audiological evaluation of the proband at the Massachusetts Eye and Ear Infirmary showed LFSNHL. Genetic evaluation at the Massachusetts General Hospital indicated a five-generation family history consistent with an autosomal dominant inheritance pattern. DNA sequencing of coding regions and splice sites of *WFS1* in the proband identified a novel missense mutation c.2141A>C (p.Asn714Thr) in the C-terminal domain of the wolframin protein where most LFSNHL-causing mutations cluster. This variant was absent from public databases. Computational analyses suggested that the variant may impact the protein. Testing of the proband's family members revealed that the variant segregated with hearing loss in five affected relatives and absent from four unaffected ones.

Conclusion

The novel Asn714Thr variant in *WFS1* likely causes the LFSNHL in this family based on significant segregation, absence from the general population, computational prediction, location within the mutation cluster, consistent audioprofiles and family history. Additional functional studies are needed to establish the pathophysiological mechanism of this variant. Single gene tests can economically and efficiently identify the causative variant when there is a strong genotype-phenotype correlation. Family history and segregation studies greatly enhance clinical interpretation of the variant.

PS - 297

Genetic and Phenotypic Heterogeneity in Chinese Patients With Waardenburg Syndrome Type II

Shuzhi Yang¹; Pu Dai²; Dongyang Kang²; Xin Zhang²; Chengyong Zhou³; Huijun Yuan²; Bo Hua Hu⁴

¹The First Affiliated Hospital of Chinese PLA General Hospital; ²Inst. of Otolaryngology, Chinese PLA General Hospital; ³Dept. of Otolaryngology, The First Affiliated Hospital of Chinese PLA General Hospital; ⁴Center for Hearing and Deafness, Department of Communicative Disorders and Sciences University at Buffalo

Background

Waardenburg Syndrome (WS) is an autosomal-dominant disorder characterized by sensorineural hearing loss and pigmentary abnormalities in the eyes, hair, and skin. Mutations in Microphthalmia-associated transcription factor gene (*MITF*) are responsible for approximately 15% of WS type II (WS2) cases. While 40 mutations in *MITF* have been identified in patients with WS2, most are identified in non-Chinese descents. The current investigation was performed to investigate the clinical and genetic heterogeneity in Chinese WS2 patients.

Methods

Twenty WS2 patients from 14 families were identified using the criteria proposed by the WS consortium. Their blood samples were collected. *MITF* gene mutation was analyzed with the ABI Prism 3100 DNA sequencer. Bioinformatics analysis was also conducted to predict the putative functional effects of the missense mutations. In addition, a comprehensive clinical history was collected, physical and audiological evaluation were performed as well.

Results

Among the 20 WS2 patients, 17 (85.0%) displayed sensorineural hearing loss with large individual variation within the family and among families, ranging from moderate to profound hearing loss. Bilateral hearing loss was more prevalent than unilateral hearing loss (80% vs. 5%). The age of the onset of the hearing loss varied from congenital to 40 years. Younger patients (age from 2 to 18 years old) frequently had prelingual, profound, bilateral hearing loss (14/20, 70.0%). Screening of *MITF* Mutation identified five variations: c.20A>G, c.332C>T, c.649A>G, c.648_650delAAG, and c.763C>T. Bioinformatics analysis suggested that the missense mutations, c.20A>G and c.332C>T, are likely have neutral effects, while the remaining three mutations, c.649A>G, c.648_650delAAG and c.763C>T are likely to have disease-causing effects. The total mutational frequency of the *MITF* gene in our study was 21.4% (3/14), higher than the reported rate of 15% for patients of Western descent.

Conclusion

Sensorineural hearing loss is the most common feature of WS2 in Chinese patients; consistent with the previous findings obtained from other patient populations. However, *MITF* mutations are relatively more frequent among Chinese WS2 patients and the mutation features a high heterogeneity.

PS - 298

Wbp2-Deficient Mice Show Progressive High-Frequency Hearing Loss and Abnormal Cochlear Innervation

Annalisa Buniello¹; Andreea Huma²; Raquel Martinez-Vega²; Neil Ingham¹; Karen Steel¹

¹King's College London; ²Wellcome Trust Sanger Institute

Background

The Wellcome Trust Sanger Institute Mouse Genetics Programme generates targeted mouse mutants and screens them for a wide range of disease features, including using Auditory Brainstem Responses (ABR) at 14 weeks to detect new hearing-impaired lines. The *Wbp2* homozygous mutant showed raised thresholds at high frequencies only in this screen. *Wbp2* encodes the WW domain-binding protein 2 that acts as a transcriptional coactivator, binding to the estrogen receptor α (*Esr1*) in the nucleus (Dhananjayan et al. 2006, Mol. Endocrinol. 20:2343).

Methods

ABRs were recorded from ketamine/kylazine anaesthetised mice, aged 4, 14, 28 and 44 weeks, using custom software and TDT hardware, in response to clicks (10us duration) and

tone pips (5ms duration, 6-30 kHz or 3-42 kHz). Immunocytochemistry was performed on paraffin sections from wt mice at postnatal day five. The gross structure of the ear was analysed by middle ear dissection, inner ear clearings and hematoxylin and eosin staining on paraffin sections, at 5 and 30 weeks of age. Scanning Electron Microscopy was performed to assess any sign of hair cell degeneration in the *Wbp2* mutants compared to littermate controls at 5 and 30 weeks of age. We examined the innervation of the cochlea using antibodies to neurofilament to label unmyelinated nerve fibres, to CtBP2 to label pre-synaptic ribbons, and to GluR2/3 to label post-synaptic densities, viewed using confocal imaging of mutant and control littermates at 4 weeks old.

Results

We found that ABR thresholds were raised as early as 4 weeks of age in the mutants and progressively increased and extended to lower frequencies by 28 and 44 weeks old, indicating progressive hearing loss. Immunocytochemistry revealed widespread expression of *Wbp2* in nuclei of multiple cell types in the cochlea. The gross structure of the mutant middle and inner ears appeared normal, and scanning electron microscopy of the organ of Corti showed no obvious damage or degeneration at 4 and 30 weeks old. Our innervation studies showed that in the mutants, nerve endings below inner hair cells appeared swollen, synapses were more widely-spread around the basolateral hair cell membranes, synapses appeared smaller, and double labeling suggested that pre- and post-synaptic markers were not as well-aligned as in control inner hair cells. We are looking into the possibility that these features result from glutamate excitotoxicity, and also investigating the link between *Wbp2*, *Esr1* and synaptic defects. In details, we built a pathway showing that *Esr1* controls the expression of a number of post-synaptic proteins involved in synaptogenesis.

Conclusion

The loss of high frequencies is often a first sign of age-related hearing loss; therefore, this study will help us in understanding the role of *Wbp2* in ear function and gaining more insights on progressive age-related hearing loss in mice as well as in humans and to develop new therapeutic strategies. Moreover, this study could provide new knowledge on the mechanisms behind cochlear synaptogenesis.

PS - 299

The *Ildr1* Knockout Mouse: A Model of Autosomal-Recessive Hearing Impairment DFNB42

Neil Ingham¹; Guntram Borck²; Tobias Moser³; Karen P. Steel¹

¹King's College London; ¹King's College London; ²University of Ulm; ³University of Göttingen

Background

Autosomal-recessive hearing impairment DFNB42 has been described in several families as a nonsyndromic moderate-profound bilateral hearing impairment, which is prelingual and sensorineural in nature and can be caused by a variety of loss-of-function mutations in the *ILDR1* (immunoglobulin-like

domain containing receptor 1) gene (Aslam et al., 2005; Borck et al., 2011). No balance problems were noted in these patients. *ILDR1* is required to establish a normal epithelial barrier and is expressed in many epithelia, including the organ of Corti, stria vascularis and the utricle (Higashi et al., 2013).

Methods

Mice carrying a targeted mutation of the *Ildr1* gene (*Ildr1tm1(-KOMP)Wtsi*) and littermate controls aged 2, 4 and 8 weeks were anaesthetised with ketamine/xylazine and recordings of Auditory Brainstem Responses (ABR) were used to estimate thresholds for click stimuli and tone pips ranging from 3–42kHz. Some mice were anaesthetized with urethane at 10 weeks old and prepared for retroauricular insertion of a glass micropipette into the scala media of the basal turn of the left cochlea and measurement of endocochlear potential.

Results

Mice that were homozygous for the targeted mutation of *Ildr1* showed a profound hearing impairment, having no ABRs for stimuli up to 95dB SPL at 2, 4 or 8 weeks old. However, mice heterozygous for the mutation showed ABR sensitivity that was comparable to wildtypes. Endocochlear potential was found to be normal in homozygous mutant mice, having a mean of 114.2 ± 8.1 mV (n=7) compared to 116.8 ± 6.3 mV (n=4) in wildtypes and 114.2 ± 2.4 mV (n=4) in heterozygotes. These mice did not show balance problems.

Conclusion

ABR recordings showed that *Ildr1* knockout mice were profoundly hearing impaired from as young as P14, only 2 days after the onset of hearing in wildtype mice. Heterozygous mice had normal hearing sensitivity. These observations suggest that this knockout mouse is a good model for DFNB42, having both severe ABR threshold elevations and recessive inheritance characteristics. The lack of a balance phenotype and a normal endocochlear potential in homozygous mutants suggest that the underlying cause of the deafness in these mice may lie within the organ of Corti and that vestibular hair cells and the stria vascularis appear to function normally.

PS - 300

Contributions of Somatic Mutations to Schwannoma Tumorigenesis

Nathan Schularick; Rick Nelson; Benjamin Darbro; Thomas Bair; Kevin Knudtson; Marlan Hansen
University of Iowa Hospitals and Clinics

Background

Neurofibromatosis type II (NF2)-associated and sporadic vestibular schwannomas (VSs) are associated with mutations in the *NF2* tumor suppressor gene (*merlin/Schwannomin*). Despite this association, only 66% of schwannomas have *NF2* mutations and there is a widely variable clinical presentation among NF2 patients and variable growth rates among tumors arising in the same patient. In addition, cancerous and other benign neoplasms such as meningiomas display multiple disease-driving genetic mutations. We hypothesize that somatic mutations, in addition to those found in the *NF2* gene, contribute to tumorigenesis of NF2-associated and sporadic

VSs and account, at least in part, for the heterogeneity of the disease and associated tumors.

Methods

We harvested schwannoma tissue and paired peripheral blood leukocytes from 6 patients (1 with NF2). DNA was extracted and massively parallel exome sequencing was performed. This was performed with exonic enrichment with NimbleGen's Exome Library kit, sequenced via 100 bp paired-end exome sequencing via the Illumina HiSeq 2000 following Illumina's standard protocols. Next, we subtracted mutations present in the blood leukocytes from the list of mutations present in the VSs, resulting in a "somatic mutation list" of variants unique to VS tissue. QD, or Phred-like Quality/Depth at a variant position, is used to classify variant quality (set at QD = 5). Microarray analysis was also performed using Illumina Infinium HumanCoreExome BeadChip microarrays (>240,000 exonic probes) to evaluate Copy Number Variants (CNV), large chromosomal rearrangements, and as a quality control measure for the HiSeq exome results.

Results

Exome coverage was excellent, with 85x median read depth, and 95% capture of target reads at a depth of >30x. Tumors averaged ~125 somatic mutations (non-synonymous, insertion/deletion, splice site). We detected *deleterious somatic NF2* mutations in 5 of 6 schwannoma samples (2 of the 5 had only one altered copy of *NF2*). Interestingly, 1 schwannoma had no *NF2* mutations, but had the highest number of somatic non-synonymous mutations (475). We discovered recurring somatic mutations, unique to VS tissues, that are: 1) in genes actively transcribed in schwannoma tissues; 2) predicted to be deleterious to protein function; and 3) have been previously been linked to cancer and cell growth in other tissues.

Conclusion

These data suggest that somatic mutations in genes in addition to *NF2* contribute to schwannoma tumorigenesis and the heterogeneity of the disease. Ultimately, they have a high likelihood of helping identify effective targeted medical therapies for VSs.

PS - 301

Defective Light-Dependent Translocation of Phototransduction Proteins in Usher Mouse Models Renders Photoreceptors Susceptible to Light-Induced Degeneration

Dominic Cosgrove; Marisa Zallocchi; Linda Cheung; Mei Tian; Duane Delimont; Wei-min Wang; You-Wei Peng
Boys Town National Research Hospital

Background

Usher syndrome, the leading cause of deaf-blindness, results in congenital deafness associated with delayed onset progressive retinitis pigmentosa. There are 10 known genes associated with the syndrome which has three clinical subtypes. The genes encode an array of transmembrane and scaffold proteins and protein variants that interact in a variety of ways to form functional complexes localizing to stereocilia

and ribbon synapses. In the mature cochlear hair cells, specific proteins form structural and anchoring elements of the tip links of stereocilia, which are components of the mechanoelectrical transduction apparatus. Studies of Usher mouse models show a common phenotype of dysmorphic hair cell stereocilia indicating a critical role in stereocilia development that is still relatively uncharacterized. In the photoreceptor, Usher proteins localize to the periciliary region near the connecting cilia and the ribbon synapses. Usher protein function in photoreceptors and the mechanism of photoreceptor degeneration are unknown.

Methods

Light induced protein translocation, retinal degeneration assays, subretinal gene delivery

Results

The phototransduction protein α -transducin shows elevated light thresholds for activating translocation from the outer to the inner segments of photoreceptors in models for both USH1B and USH2D and show sensitivity to light-induced photoreceptor degeneration in both models under conditions that don't affect strain/age matched wild type mice. We rescued both the translocation and degeneration phenotypes by sub-retinal delivery to photoreceptors of a gene therapy vector harboring wild type myosin VIIa in the shaker-1 model for USH1B. We further demonstrate elevated light thresholds to activate translocation of RGS9/G β 5L complex from the inner to the outer segments in USH1B mice, which happens at light intensities much lower than that required to activate α -transducin translocation. The R9AP/RGS9 G β 5L GTPase activating complex functions in the inactivation of α -transducin in rod outer segments as a means of converting the phototransduction process from the high sensitivity to the low sensitivity modes.

Conclusion

We predict these threshold shifts account for light sensitivity to photoreceptor degeneration in these models. We suggest that the Usher protein complex(es) at the connecting cilia of healthy photoreceptors function to regulate light-dependent protein transport, which is critical to prevent light damage to these cells under normal environmental conditions.

PS - 302

Hearing Impairment and Human Inner Ear Degeneration Caused by Missense Mutation in WFS1 Gene

Rudolf Glueckert¹; Mario Bitsche²; Michael Blumer²; Helge Rask-Andersen³; Wei Liu³; Irina Alafuzoff⁴; Lisbeth Tranebjærg⁵; Anneliese Schrott-Fischer⁶

¹Medical University Innsbruck, Austria; ²Medical University of Innsbruck; Department of Anatomy, Histology and Embryology, Division of Clinical and Functional Anatomy; ³Medical University of Innsbruck, Department of Anatomy, Histology and Embryology, Division of Clinical and Functional Anatomy; ⁴Department of Surgical Sciences, Section of Otolaryngology, Uppsala University Hospital, SE-75185, Uppsala, Sweden; ⁵Department of Immunology,

Genetics and Pathology, Uppsala University, 75185 Uppsala, Sweden and Department of Pathology and Cytology, Uppsala University Hospital, Dag Hammarskjöld väg 20 751 85 Uppsala, Sweden; ⁵*Wilhelm Johannsen Centre for Functional Genome Research, Department of Cellular and Molecular Medicine (ICMM), The Panum Institute, University of Copenhagen, Copenhagen, Denmark and Department of Audiology, Bispebjerg Hospital, Copenhagen, Denmark;* ⁶*Department of Otolaryngology, Inner Ear Research Laboratory; Medical University Innsbruck, Austria*

Background

The WFS1 gene codes for a protein called wolframin located in the endoplasmic reticulum of many cell types and is thought to regulate protein folding the amount of calcium in cells. Missense mutations result in progressive, neurologic and endocrinologic degenerative disorders. Diabetes mellitus and insipidus, optic atrophy, hearing impairment and olfactory disorders are common phenotypic manifestations.

A Swedish family that was clinically described with symptoms of optic atrophy, hearing impairment as well as psychiatric problems was originally described in 1940 [1] and was reinvestigated with genetic analysis for mutations in the WFS1 gene causing Wolfram syndrome in 2010 [2].

Here, we present histology of the inner ear from a patient with molecular diagnosed mutation in the WFS1 gene caused by a de-novo mutation in this family. The patient had cochlear implantation at age 57 in one ear, experienced considerable improvement of hearing and died at age 81 in 2012.

Methods

Sequencing of the WFS1 gene was performed as described in [2]. The unimplanted inner ear was processed according to standard epon embedding procedures and sectioned at 1 and 10µm.

Results

Sequencing of the WFS1 gene identified a heterozygote sequence change c2051C>T in exon 8 leading to a substitution of alanine for valine at position 684 of Wolframin (p.A684V). Plastic embedding and sectioning of the un-implanted inner ear for light- and electron microscopy revealed absence of hair cells and great loss of peripheral processes. Spiral ganglion neurons were found in Rosenthal's canal mainly as mono-polar neurons surviving even with severe hearing impairment. Lipofuscin-like granules were accumulated in neurons of the cochlea and vestibular organ.

Conclusion

Heterozygote missense mutation in the WFS1 gene causes hair cells loss but not severe loss of neurons. The good outcome of cochlear implantation in the contra-lateral ear emphasizes our previous results of robust survival of spiral ganglion neurons in humans suggesting a much slower degeneration of neurons following de-afferentiation [3].

References
[1] Samuelson A. 1940. Familjärt uppträdande synnervsatrofi och dövhet. Nordisk Medicine (Hygiea) 6:769–772.

[2] Rendtorff, N.D., Lodahl, M., Boulahbel, H., Johansen, I.R., Pandya, A., Welch, K.O., Norris, V.W., Arnos, K.S., Bitner-Glindzicz, M., Emery, S.B., Mets, M.B., Fagerheim, T., Eriksson, K., Hansen, L., Bruhn, H., Moller, C., Lindholm, S., Ensgaard, S., Lesperance, M.M., and Tranebjaerg, L., 2011, Identification of p.A684V missense mutation in the WFS1 gene as a frequent cause of autosomal dominant optic atrophy and hearing impairment: Am.J.Med.Genet.A, v. 155A, p. 1298-1313. [3] Glueckert, R., Pfaller, K., Kinnefors, A., Rask-Andersen, H., and Schrott-Fischer, A., 2005, The human spiral ganglion: new insights into ultrastructure, survival rate and implications for cochlear implants: Audiol.Neurotol., v. 10, p. 258-273.

PS - 303

Taperin is also in the Nucleus and Interacts With Chromodomain-Containing Proteins

Spencer Goodman; Jonathan Bird; Stacey Cole; Erich Boger; Thomas Friedman; Meghan Drummond
NIDCD, NIH

Background

Mutations of *TPRN*, encoding taperin, are the cause non-syndromic deafness DFNB79 (Rehman *et al*, 2010; Li *et al*, 2010). In auditory and vestibular hair cells, taperin is concentrated at the taper region of stereocilia. However, over-expression of EGFP-tagged *TPRN* in cultured cells revealed nuclear targeting (Rehman *et al*, 2010; Ferrar *et al*, 2012). We sought to determine if taperin is present endogenously in the nucleus and to understand the possible functional relevance of this localization based on characterization of interactions with nuclear protein partners.

Methods

Endogenous taperin expression was assayed in primary mouse tissue and cultured COS-7 and mIMCD-3 cells using immunohistochemistry as well as subcellular fractionation followed by western blot analyses. Candidate interacting proteins were identified by yeast two-hybrid (Y2H) screens of mouse vestibular and kidney cDNA libraries. Putative partners were validated with a myosin-based protein-protein interaction assay that relies on quantitative detection and evaluation of bait and prey proteins colocalized in filopodia.

Results

Immunohistochemistry and subcellular fractionation confirmed localization of endogenous taperin to the nucleus in primary kidney tissue and cultured cells. Two Y2H screens identified several nuclear proteins, including the chromodomain-containing proteins CHD3 and CHD4. Interactions were validated and the domains mediating these interactions were identified using peptide fragments of taperin, CHD3 and CHD4. Our data indicate that taperin binds CHD3 and CHD4 through their DEXDc helicase domain.

Conclusion

Endogenous taperin is found in the nucleus and its function is under investigation. The association of taperin with CHD3 and CHD4, which form the catalytic core of the NuRD complex, suggests a role in chromatin remodeling and histone deacetylation. In addition to a role at the base of stereocilia

lia, we speculate that taperin also regulates gene expression through CHD3 and CHD4. While mutations of *CHD3* and *CHD4* are not reported to affect hearing, a variety of mutations of *CHD7* are one of the causes of CHARGE (Vissers *et al*, 2004), a syndrome characterized by specific neurological anomalies and deafness (MIM #214800). The DEXDc helicase is conserved in many chromodomain proteins, including CHD7. Several missense mutations of *CHD7* occur in its DEXDc domain and cause CHARGE syndrome (Lalani *et al*, 2006; Jannssen *et al*, 2011), and these substitutions occur in residues that are conserved in CHD3 and CHD4. We are exploring the intriguing possibility that taperin also binds CHD7 in the nucleus, and this interaction is disrupted by CHARGE mutations, perhaps contributing to the deafness feature of this syndrome.

PS - 304

Microglial Activation in Auditory Nerve of the Postnatal Mouse Ear

LaShardai Conaway; Yazhi Xing; Jeremy Barth; Hainan Lang

Medical University of South Carolina

Background

A fine wiring pattern between the auditory nerve and cochlear hair cells is needed for proper auditory function. In the mouse, auditory nerve refinement is initiated during the first postnatal week, just before the onset of hearing, by unknown mechanisms. Microglia are specialized immune cells in the nervous system that respond to inflammation. Although microglia-neuron interactions are critical in nervous system development, the role of microglia in the developing auditory nerve has not been established. We hypothesized that microglia present in the postnatal auditory nerve play an important role in the refinement of auditory nerve during inner ear development.

Methods

Immunohistochemical and gene microarray analyses were performed on auditory nerves isolated from CBA/CaJ mice at postnatal days 0, 3, 7 and 14. Cochlear glial cells and microglia were identified by immunostaining for IBA-1 and CD11b (microglia), ED1 (phagocytosis), and Sox10 (glial cells). Quantitative analysis of IBA-1⁺ cells was completed in two locations of the peripheral auditory nerve: Rosenthal's canal (RC) and the osseous spiral lamina (OSL). Candidates associated with microglial activation and nerve projection refinement were identified by analysis of existing published microarray datasets; review of temporal expression profiles of candidate genes in auditory nerve microarray data was conducted using dChip software. Profiles of selected candidates were validated using quantitative PCR.

Results

Immunohistochemistry revealed that at P7, microglia are mostly phagocytic and directly interact with cochlear glial cells. IBA-1⁺ cell counts indicated that the peak microglia density occurred around P7, concurrent with initiation of auditory nerve refinement. A decrease in IBA-1⁺ cells was seen after P14, when refinement of the auditory nerve is nearly complete. Gene array analysis detected putative microglial

activation and nerve projection refinement genes exhibiting peak expression coincident with maximal IBA1⁺ cell density.

Conclusion

Active microglial cells are present in mouse inner ears during initiation of auditory nerve refinement. Engulfment of Sox10⁺ glial cells by IBA-1⁺ cells in RC and OSL indicate that microglia may play a role in removing extraneous glial cells during postnatal development. Gene array analysis demonstrates that peak microglia density corresponds with the time of maximal expression of many genes with presumptive links to nerve projection refinement, suggesting that microglia may play a critical role in auditory nerve refinement and the onset of auditory function in the mouse ear.

PS - 305

Selective Deletion of Cochlear Hair Cells Causes Age-Dependent Neuronal and Glial Changes in the Mammalian Cochlear Nucleus

Melissa Strong¹; Tejbeer Kaur²; Samantha Motley¹; Mark Warchol²; Edwin Rubel¹

¹*University of Washington*; ²*Washington University*

Background

Neurons in the ventral cochlear nucleus (VCN) are dependent on excitatory afferent input for survival during a critical period of development. Cochlear removal in young mammals and birds results in rapid death of target neurons on the cochlear nucleus. The same manipulation in older animals has little or no effect on neuronal survival. While previous studies suggest that afferent action potentials are a requirement in the neonatal brain, and that glial cells may be involved in the protection of the mature neurons, several questions remain unanswered. They include: i) To what extent is the neuronal death seen in neonatal brain dependent on the elimination of afferent activity emanating from the hair cells, per se? ii) What cellular interactions and intracellular pathways are responsible for the protection of cellular viability in the mature brain? We begin to answer these questions by using a new mouse in which the inner ear hair cells can be selectively ablated at any postnatal age and by comparing the responses of neurons and non-neuronal cells in the VCN at various times after hair cell ablation in neonatal and mature animals.

Methods

The studies reported here utilize a mouse model that allows temporal control of cochlear hair cell deletion. The human diphtheria toxin receptor is expressed in hair cells using the Pou4f3 promoter. Mice are given injections of diphtheria toxin (DT): 25ng/g in Postnatal day (P)21 and older mice, and 5ng/g in P5 mice. These injections of DT result in nearly complete loss of organ of Corti hair cells within 5-7 days, without directly affecting the surrounding cells in the sensory epithelium. Cellular and molecular changes in the VCN are examined at multiples time points (days to weeks) following DT, using a combination of transgenic reporter mice (CX3CR1-GFP) and antibodies detecting glia and neurons.

Results

Results confirm that neonatal hair cell death affects neuronal survival in the VCN as a function of age. Neonatal mice injected with DT have a similar magnitude of neuronal loss in the VCN as age-matched mice that have undergone a cochlear removal. Furthermore, complete neuronal survival persists in animals injected with DT as adults (P21 or older). On the other hand, changes in glial cells do not appear to differ as a function of the age at which hair cells are ablated by DT injection. At both ages, there is an increase in the number of microglia, and an increase in GFAP by 14 days post DT. There is also an increase in the marker for activated microglia.

Conclusion

This work demonstrated a partial dissociation between microglial and astrocyte responses and neuronal degeneration after selective elimination of hair cells. Further assessment of neuron-glia interactions after early postnatal hair cell ablation will be necessary to fully understand the role of glia in the establishing this critical period.

PS - 306

Stepwise Mechanisms for Hearing Loss in NOD/LtJ Mice

Jeong Han Lee; Hyo Jeong Kim; Wenying Wang; Ebenezer Yamoah

Center for Neuroscience, University of California, Davis

Background

NOD/LtJ inbred mice undergo early and rapid progressive hearing loss, partly due to the presence of at least two alleles, *Cdh23^{ahl}* and *Ahl2*. The *Ahl* locus is a major contributor to age-related hearing loss (AHL) in several inbred strains. We used the NOD/LtJ mouse as a model for AHL, and to study the relationship between spiral ganglion neurons (SGNs) and hair cell innervation.

Methods

To investigate the function of hair cells and SGNs in NOD/LtJ mice, we used auditory-evoked brainstem response (ABR), distortion product otoacoustic emissions (DPOAE), as well as electrophysiological and immunostaining techniques. Specific auditory stimuli (broadband click and pure-tone pips of 4, 8, 16, and 32 kHz) from high frequency transducers were delivered binaurally through plastic tubes to the ear canals. Evoked brainstem responses were amplified and averaged. DPOAEs were measured by a probe tip microphone in the external auditory canal. Two tones (f1 and f2) were of equal intensities and stepped from 10 to 90 dB SPL in 2 dB increments. The cochleae were collected for immunofluorescence analyses. Electrophysiological analyses of the properties of SGNs were performed as well.

Results

The onset of hearing loss began at ~3 weeks of age. The average ABR threshold of NOD/LtJ mice was greater than 90 dB SPL by 12 weeks of age. Basal turn inner hair cells (IHCs) and outer hair cells (OHCs) showed the greatest degree of damage, followed by hair cells in the middle and apical turns at all ages. Basal SGNs showed the greatest cell damage, whereas SGNs at apical turns showed moderate cell loss.

Interestingly, type 2 SGNs were more susceptible to damage than type 1 SGNs. OHC and IHC stereocilia damage occurred at 4 weeks of age. Expression of synaptic protein was reduced in an age-dependent manner. Synapses between OHCs and axons of SGNs were damaged at 4 weeks of age. However, synapses between IHCs and SGNs degenerated at ~12 weeks of age. We will outline the physiological changes that accompany SGN loss.

Conclusion

The report is first to provide mechanistic insight on the stepwise degeneration of hair cells and SGN synapses. We have confirmed that NOD/LtJ mice have progressive hearing loss. We have also provided detailed functional analyses on the relationship between hair cells and SGN innervations, and how they are critical for the mechanisms of hearing loss in NOD/LtJ mouse model.

PS - 307

Re-Distribution of Inhibitory Synapses Onto Proximal Sites of LSO Principal Cells Occurs Before Hearing Onset

Alan Cooper; Javier Alamilla; Deda Gillespie

McMaster University

Background

The ascending projection neurons (principal cells) of the lateral superior olive (LSO) exhibit a bipolar morphology and integrate ipsilaterally-derived excitatory and contralaterally-derived inhibitory inputs. Although the subcellular location of these inputs necessarily influences signal integration, little has been known about precisely how these inputs are distributed, how their distribution affects circuit-level processing, and how their specific distribution pattern is achieved during development.

In the neighboring medial superior olive, inhibitory synapses onto principal neurons are diffusely distributed throughout the dendritic tree shortly before hearing onset, and in the next two weeks are re-distributed to occupy more proximal sites through an experience-dependent process (Kapfer et al, 2002). As the major inhibitory input to the LSO undergoes significant refinement before hearing onset in the rat (Kim & Kandler, 2004), we asked whether inhibitory synapses onto LSO principal cells are redistributed before hearing onset.

Methods

In tissue from postnatal days 4 and 11 (P4 and P11) rats, we labeled cells in the medial and middle limbs of the LSO. Principal cells were identified under IR-DIC optics based on their shape, size, and orientation within the LSO, and whole-cell patched. Slices were fixed, resectioned at 50 μ m, labeled for immunoreactivity to gephyrin, and imaged at the confocal microscope. The resulting Z-stacks were analyzed in Imaris (Bitplane): the dendritic arbor was reconstructed in 3-D, gephyrin-positive puncta were identified, and puncta associated with the labeled neuron were selected as markers of inhibitory synapses.

Results

In the week before hearing onset, number and surface density of gephyrin puncta at the soma increased (by 190% and 140%). We calculated the linear densities of gephyrin-positive puncta within 25- μ m segments of dendrites at three distances from the soma (0-25, 50-75, and 100-125 μ m). Between P4 and P11, the linear density of gephyrin-positive puncta increased by 90% within 0-25 μ m of the soma, increased by 40% within 50-75 μ m of the soma, and decreased by 20% within 100-125 μ m of the soma.

We also assessed dendritic complexity using the number of Sholl intersections at 5 μ m intervals. The greater complexity of younger neurons was most apparent near the soma: P4 neurons had 130% more intersections than P11 neurons within 0-20 μ m and 35% more intersections within 25-40 μ m. Beyond 40 μ m from the soma, P4 and P11 had similar numbers of intersections.

Conclusion

Inhibitory synapses in the LSO undergo significant redistribution in the absence of acoustically driven activity.

PS - 308

Characterization of Novel Glycinergic Innervation of the Superior Olivary Complex

Stefanie Altieri¹; Stephen Maricich¹; Walid Jalabi²

¹University of Pittsburgh; ²Case Western Reserve University

Background

The lateral superior olive (LSO) processes interaural level differences (ILDs) by comparing ipsilateral excitatory and contralateral inhibitory inputs. The majority of these inhibitory inputs are thought to originate in the medial nucleus of the trapezoid body (MNTB). Recently, we showed that mice lacking the MNTB retain functional inhibitory, glycinergic inputs to the LSO and superior paraolivary nucleus (SPN), suggesting that other brainstem centers supply a portion of this innervation.

Methods

We used immunohistochemistry and axon tracing techniques to compare the developmental timing and source of glycinergic innervation in mice lacking the MNTB with control mice. We also investigated whether changes in glycine receptor subunit composition explain different decay constants observed in mice that lack MNTB neurons.

Results

We report the first characterization of developing glycinergic neurons in the superior olivary complex in mice. We found that in addition to control mice, glycinergic neurons in mice lacking the MNTB are first detected during the first postnatal week. Ongoing work is being done to identify origins of this innervation.

Conclusion

Results from this mouse model challenge perspectives on the traditional role of the MNTB in sound localization pathways.

PS - 309

Timelapse Imaging of Live Intact Cochlea Reveal SGNs Undergo Region-Specific Growth Patterns and Dynamic Branching Near Synaptic Targets During Development.

Noah Druckenbrod; Lisa Goodrich

Harvard Medical School

Background

To form the precise connectivity necessary to capture complex sound information, SGNs extend peripheral processes that grow through the ganglion and then form radial bundles in the mesenchyme. Upon reaching the organ of Corti, the radial bundles defasciculate and individual neurites target their synaptic partners. Type-I SGNs contact inner hair cells, whereas Type-II SGNs instead spiral along the cochlea and contact outer hair cells. Analysis in fixed tissue demonstrated that these circuits emerge in a stereotyped fashion, with radial bundles appearing first and followed shortly by the appearance of neurites with either Type I or Type II like morphologies. However, axon guidance choices occur quickly and involve transient cell-cell contacts that are difficult to capture in fixed tissue. Thus, it is still unknown how SGN growth cones behave in real time as they contact diverse cell types along their trajectory.

Methods

Here, we used a new live imaging method to study SGN neurite behavior. Because simple 2D explants of cochlea fundamentally disrupt the growth and spatial relationships under study, we suspend cochleae in the imaging chamber. This method allows us to image SGN dynamics within intact cochleae for over 24 hours, with SGNs labeled either globally or sparsely with fluorescent reporters. Importantly, imaged cochleae grow normally and match the morphology and neurodevelopment of stage-fixed tissue.

Results

We have characterized live SGN development and organization at the cohort and single axon level. We find that SGNs exhibit complex changes in branching, fasciculation, and velocity as they pass through different regions of the cochlea. Wild-type neurite extension tracking reveals that SGNs have a rapid and then less-rapid phase of growth that appear to be region dependent. In addition, wild-type SGNs rapidly bundle along apparent 'pioneer neurites' that are first to emerge from the ganglionic border. After a period of directed and rapid outgrowth through the mesenchyme, SGN growth cones slow down and exhibit highly exploratory and branched morphology behavior within the organ of Corti, rapidly contacting both inner and outer hair cells. Imaging at this later stage show diverse and transient dynamic branching of SGN neurites in both IHC and OHC regions.

Conclusion

These studies suggest that SGN growth cones are intrinsically programmed to respond to a variety of cues as they encounter multiple cell types along their path. In addition these studies provide a template to study the effects of mutations or signaling molecules on normal SGN behavior.

Bone Morphogenic Protein (BMP4) Signaling in the Development of the Medial Nucleus of the Trapezoid Body.

Zafar Sayed; Augusta Fernando; Tammy McGuire; John Kessler; Lixin Kan; Akihiro Matsuoka
Northwestern University

Background

The calyx of Held represents a unique neuronal synapse in the auditory pathway in that it processes action potentials at high frequencies while maintaining a high degree of fidelity. To do so, the calyx, which functions between the large pre-synaptic axons of the anteroventral cochlear nucleus and the inhibitory principal cells of the medial nucleus of the trapezoid body (MNTB), employs a large number of action sites with varying degrees of release probability. Both bone morphogenic protein (BMP4) and its inhibitor Noggin have recently been implicated in determining nerve terminal size during the development of these distinct synapses. The effect of these morphogens on post synaptic MNTB neuronal numbers, however, remains largely unknown. Using transgenic mice overexpressing either BMP4 or Noggin, we hope to elucidate key differences in murine MNTB neuronal numbers to better understand signaling pathways leading to their differentiation.

Methods

Groups of age matched neuron-specific enolase BMP4, Noggin, and wild type mice were euthanized with CO₂ gas prior to intracardiac perfusion with 4% paraformaldehyde. Whole brains were immediately harvested and placed in a buffer solution with 10% sucrose for cryoprotection. Using a cryostat at -25° C, 30 µm coronal sections of the pons were mounted on glass slides. These specimens underwent immunofluorescent staining for the presynaptic calcium sensor synaptotagmin-2 (found with high specificity in the MNTB), as well as counterstaining with DAPI. Unbiased cell counting was performed on section intervals using photomicrographic images of the MNTB. Following correction by a calibration factor, the total number of cell nuclei were then used to estimate the total number of neurons in the area of interest.

Results

Our results indicate a significant difference in the average number of MNTB principal cells between BMP4 and Noggin animal groups ($p < 0.05$). Specifically, mice overexpressing BMP4 were noted to have a greater total number of neurons at a higher density when compared to both wild type and Noggin mice. In contrast, Noggin mice had a smaller population of neurons in the MNTB with a relatively sparser arrangement of calyceal synapses.

Conclusion

Our investigation reveals significant differences in the number and morphology of MNTB neurons in murine models overexpressing either BMP4 or its inhibitor Noggin. This data has implications for recreating high frequency neural connections, such as those at the calyx of Held, following *in vivo* stem cell delivery to the inner ear.

Mapping Subplate Microcircuits in Developing Prefrontal Cortex With Relevance to Auditory Dysfunction in Autism

Daniel Nagode¹; Patrick Kanold²

¹University of Maryland College Park; ²University of Maryland

Background

Autism is neurodevelopmental disorder characterized by deficits in social interaction and communication, which are caused in part by abnormal cortical processing of sound. Neuroanatomical studies have revealed increased cell numbers in the prefrontal cortex (PFC) of autistic individuals, suggesting that improper wiring of prefrontal circuits during development might contribute specifically to problems in speech perception or interpretation.

The first functional microcircuits in the developing cortex are formed by the transient population of subplate neurons (SPNs), which are present in all cortical areas. SPNs in primary sensory cortices are critical for establishing mature thalamocortical and intracortical connections. While SPNs and their associated circuits in primary sensory areas have been studied previously, they are largely unexplored in prefrontal areas. Here we characterize functional microcircuits associated with SPNs in the PFC during development in mice.

Methods

Using transgenic mouse lines expressing fluorescent markers under the control of subplate-specific gene promoters, we are characterizing the cellular diversity of SPNs in the PFC. To investigate the functional excitatory and inhibitory circuits within the prefrontal subplate, we are performing laser-scanning photostimulation (LSPS), combined with whole-cell patch clamp electrophysiology, in an *in vitro* slice preparation.

Results

The subplate in PFC occupies a broader, less distinctive layer than in primary sensory areas. PFC SPNs receive strong within-layer excitation and inhibition, however; unlike primary sensory areas, they appear to project more prominently to L5 and L6 than to the thalamorecipient layer in PFC, L2/3. PFC SPNs also receive feedback excitation from the same layers to which they project.

Conclusion

Subplate circuits in developing PFC exhibit several distinct differences from those in primary sensory areas. We continue to use high-resolution techniques to map PFC circuitry during different stages of brain development, and explore a potential role of abnormal PFC connectivity in the autistic auditory phenotype.

Inhibiting Sonic Hedgehog-Dependent Medulloblastoma by Modulating Expression Levels of Atoh1 and Neurod1

Ning Pan¹; Joyce Li²; Andrew Leiter²; Israt Jahan¹; Bernd Fritzsche¹

¹University of Iowa; ²University of Massachusetts Medical School

Background

The proneural basic helix-loop-helix (bHLH) transcription factor Atoh1 is among several genes that are needed for normal cochlear hair cell formation, and thus has been extensively used in hair cell regeneration studies. As many other transcription factors, Atoh1 is expressed and plays essential roles in other parts of the body. It is needed for the proliferation of cerebellar and cochlear nucleus granule neuron precursors (GNPs), the most frequent neurons of the brain. Atoh1 also plays a role in medulloblastoma (MB), the most common malignant child brain tumor. Atoh1 regulates sonic hedgehog (Shh) signaling and is required for formation of Shh-induced MB. We previously showed that another bHLH transcription factor, Neurod1, acts downstream of Atoh1 but also downregulates Atoh1 via a negative feedback loop in both cerebellum and inner ear. In the current study, we want to further understand the cross-regulation between these two transcription factors and explore the therapeutic use to counteract tumorigenesis in MB patients and investigate the role of Neurod1 to regulate specific hair cell types.

Methods

We generated genetically engineered mice with Atoh1- or Neurod1-Cre-induced constitutive activation of Smoothed homolog (Smo) to induce MB formation and combine with altered expression of either Atoh1, or Neurod1, or both. We characterized their effect on both cerebellum development and inner ear neurosensory development using immunohistochemistry and *in situ* hybridization.

Results

Constitutively active Smo triggered by an Atoh1-cre transgene induces MB and this transformation is reduced by deleting one copy of Atoh1. MB formation can also be induced using Neurod1-cre to drive constitutively active Smo expression in GNPs. This MB can be suppressed by simultaneous overexpression of Neurod1 in GNPs.

Conclusion

Our preliminary data suggest that the expression levels of Atoh1 and Neurod1 affect the balance between cell proliferation and differentiation of GNPs and play crucial roles in both normal cerebellar development and MB tumorigenesis. Therefore our studies of these novel mouse models imply potential new therapeutic approaches for human Shh-dependent MB by quantitatively controlling levels of these two key bHLH transcription factors, such as through siRNA treatment. Our data also caution to use Atoh1 for hair cell differentiation when expressed in proliferative precursors that could possibly be transformed into a MB like tumor.

Elucidating Pathological Mechanisms of Hearing Loss Induced by Hypothyroidism Using Duox2 Mutant Mice

Sera Park; Jae Young Choi; Jinwoong Bok
Yonsei University College of Medicine

Background

Developmental thyroid disorders can lead to hearing loss. Previous studies showed that the tectorial membrane, middle ears, and otic capsule were defective in various mouse models of hypothyroidism. However, it is still unclear how the lack of thyroid hormones leads to such defects in the inner and middle ear structures, which may be responsible for the hypothyroidism-induced hearing loss.

Methods

To investigate the pathological mechanisms of the hypothyroidism-induced hearing loss, we analyzed the inner ears of a spontaneous mutant from the Jackson Lab, which carries a mutation in *dual oxidase 2* (*Duox2*). *Duox2* is an essential enzyme in thyroid hormone synthesis, and mutations in the *DUOX2* gene in humans have been shown to cause typical phenotypes of congenital hypothyroidism. We evaluated serum levels of T4, hearing function by ABR analysis, histological phenotypes by H&E staining, and gene expression patterns by *in situ* hybridization.

Results

In *Duox2* mutants, serum levels of T4 were about 10-fold lower compared to controls and the growth was severely retarded. ABR analyses demonstrated profound hearing loss in the *Duox2* mutants. Histological analyses showed that the tectorial membrane was severely thickened in the *Duox2* mutant cochlea. To understand the molecular mechanisms of thickening of the tectorial membrane, we examined expression levels of transcripts encoding alpha-tectorin (*Tecta*) and beta-tectorin (*Tectb*), which are major components of the tectorial membrane. Expression patterns of *Tecta* in the *Duox2* mutant cochlea were comparable to controls until P0, yet significantly upregulated and prolonged at P8. In contrast, *Tectb* expression appeared to be slightly reduced in the *Duox2* mutant cochlea. We also examined expression patterns of receptors for thyroid hormones. Since thyroid hormone receptor alpha (*Thra*) has been shown to be irrelevant to the hypothyroidism-induced hearing loss, we focused on the receptor beta (*Thrb*), which showed abnormal upregulation and prolonged expression during neonatal development in the *Duox2* mutant cochlea.

Conclusion

Our results suggest that abnormal upregulation and prolonged expressions of *Tecta* and *Thrb* are a major cause of the thickened tectorial membrane in the *Duox2* mutant cochlea. We are currently analyzing possible anomalies of the middle ears and otic capsule in the *Duox2* mutants. In addition, we are trying to rescue the hypothyroidism-induced hearing loss by supplying thyroid hormones to the *Duox2* mutant pups.

Does Spectral Ripple Resolution Mature During Infancy?

David Horn¹; Jay Rubinstein²; Lynne Werner³

¹University of Washington School of Medicine, Seattle Children's Hospital; ²University of Washington School of Medicine, Virginia Merrill Bloedel Hearing Research Center, Department of Otolaryngology - Head and Neck Surgery;

³University of Washington, Department of Speech and Hearing Sciences

Background

Spectral ripple discrimination (SRD) has been used to measure sensitivity to spectral change across a broad frequency range in adults with hearing impairment. SRD has been shown to be strongly related to spectral factors in speech understanding for adults who use cochlear implants (CIs). SRD might similarly be used to assess spectral resolution in infants with CIs but it is not known whether SRD is a good measure of spectral resolution in infants. An important consideration for testing infants is that SRD thresholds are affected both by spectral resolution as well as non-spectral efficiency factors such as attention and intensity resolution. In order to tease spectral factors apart from non-spectral factors, we examined SRD at low and high modulation depths across ages in normal hearing (NH) infants. Subjects with immature spectral resolution should demonstrate a smaller effect of modulation depth (less improvement in SRD with increasing depth) than those with more mature spectral resolution.

Methods

NH 3, 7, and 9 month old infants were tested. Stimuli were broad-band noise bursts filtered by a sinusoidal spectral envelope with logarithmically-spaced peaks. We used the Observer-based Psychoacoustical Procedure to determine the highest ripple density at which a participant could detect a 90 degree phase shift in the spectral envelope. Ripple depth (either 10 or 20 dB) was varied within-subjects and SRD threshold in ripple density was assessed.

Results

Preliminary results demonstrate a significant main effect of ripple depth on SRD threshold (better SRD at 20dB than 10dB). Main effect of age was not significant. Results currently do not show a statistically significant interaction between age and ripple depth: visually, the effect of ripple depth on SRD threshold appears similar in younger and older infants.

Conclusion

Further data collection, particularly from older infants, is needed to determine whether the effect of ripple depth increases across ages in NH infants. If demonstrated, this finding would suggest that spectral ripple resolution matures during infancy – similarly to frequency resolution.

Evaluating Speech in Noise Perception in Preschoolers: Effects of Age and At-Risk Development

Elaine Thompson¹; Travis White-Schwoch¹; Dana Strait²; Nina Kraus¹

¹Northwestern University; ²University of Maryland

Background

For young children, the ability to perceive speech-in-noise is especially important, as learning environments tend to be noisy. For example, ambient noise exceeds 60dB SPL in typical classrooms (Bradley and Sato, 2008). Individuals with learning impairments may face even greater communication challenges if they have difficulty hearing in noise, as speech-in-noise perception relies in part upon cognitive mechanisms, such as attention and working memory. Relatively little is known about the development of speech-in-noise perception in pre-school children, however, either those who are typically-developing or at risk for a learning disability.

Methods

65 children, ages 3.0 to 4.9 years, participated in this study. To measure speech perception in noise, we used the CRISP test (Litovsky, 2005, JASA) to obtain perceptual thresholds in two-talker babble. The CRISP, an adaptive speech intelligibility measure, utilizes a familiarization phase to establish a known set of words for each child that will be used in the test phase; this process eliminates the confound of vocabulary in that only the words known by the child are used. In the test phase, the children hear a single word spoken by a male in two-talker female babble. A four-alternative force choice paradigm is used to obtain the child's response, and a threshold (dB SPL) is generated after 4 reversals.

Results

Older children heard better in noise (i.e., had lower speech reception thresholds). This suggests a rapid developmental trajectory for speech in noise perception even within a few months of development. Across the two-year age-span, we also found that children who are at risk for a language impairment (family history of dyslexia) performed worse on this speech in noise test than individuals not at risk.

Conclusion

The ability to hear speech in noise improves rapidly with age in young children. However, children at risk for speech and learning impairments have difficulty hearing in noise. This suggests that early evaluations of speech-in-noise perception may play an important role in identifying children who have difficulty with everyday communication, especially in noisy listening environments.

Assessment of Task Learning and Performance Following Developmental Hearing Loss

Ishita Aloni; **Gardiner von Trapp**; Stephen Young; Dan H. Sanes

New York University

Background

Degraded auditory input during development induces long lasting structural and functional changes to the central nervous system. In humans the consequences of early hearing loss have been reported to include both sensory (discrimination thresholds) and cognitive deficits (e.g. attention, short-term memory and learning). To investigate these deficits in an animal model of hearing loss, auditory associative learning abilities were compared between normal hearing animals and those reared with conductive hearing loss using two auditory tasks that differed in listening strategy.

Methods

At postnatal day 10, before ear canal opening, gerbil pups underwent bilateral malleus removal to induce a permanent conductive hearing loss (CHL). Both CHL and control animals were trained to approach a water spout upon presentation of a 'GO' stimulus, and withhold for 'NOGO' stimuli. Two tasks were used to assess gerbils' task acquisition rate and asymptotic performance: a discrimination task and a detection task. For the discrimination task, animals learned to discriminate between amplitude modulation rates, while for the detection task animals learned to detect the presence of any amplitude modulation rate. Behavioral performance was calculated using a signal detection theory framework.

Results

When compared to controls, animals with developmental CHL displayed a slower rate of acquisition on the discrimination task, but not on the detection task. For the discrimination task, control animals were better able to generalize to newly introduced stimuli when compared to CHL animals. Measurement of discrimination thresholds across consecutive testing blocks revealed that NH animals reached asymptotic threshold values faster than CHL animals. However with sufficient training, CHL animals were able to approach control-like performance.

Conclusion

When animal performance was monitored continuously during training and testing, CHL animals were found to lag behind controls in acquiring and reaching asymptotic performance on a demanding discrimination task. These results suggest that both sensory and cognitive processes are disrupted by developmental hearing loss.

A Brief Period of Developmental Hearing Loss Transiently Disrupts Amplitude Modulation Detection

Melissa Caras; Dan Sanes

New York University

Background

Transient hearing loss in children has been correlated with developmental delays in speech and language processing that can persist for years after normal auditory input is restored. Although recent findings indicate that mild bilateral hearing loss can impair membrane and synaptic properties in gerbil auditory cortex, the impact of such deprivation on the perception of complex, time-varying sound sources remains unknown. Here, we asked whether a brief period of developmental hearing loss subsequently impairs performance on an auditory task: amplitude modulation (AM) detection. Both animal and human vocalizations are composed of low frequency AM fluctuations, and such cues are necessary and sufficient for speech comprehension. Furthermore, AM detection capabilities display a prolonged maturational time course in both gerbils and humans, leading us to hypothesize that they are particularly vulnerable to developmental deprivation.

Methods

Mild hearing loss was induced in Mongolian gerbil pups by inserting bilateral earplugs at the day of ear canal opening, postnatal day (P) 11. Normal hearing was restored at P23 by removing the earplugs. After weaning at P30, animals were trained to report the presence of AM (noise carrier; 5 Hz rate), using a go-nogo procedure. After learning the task, animals were tested with a range of modulation depths. Behavioral sensitivity (d') was calculated from hit and false alarm rates, and the values were fit with psychometric functions. Threshold was defined as the modulation depth at which animals displayed a sensitivity of $d'=1$. Performance was tracked over the course of 10 consecutive testing days.

Results

Task acquisition was similar for control and earplug-raised animals. Animals in both groups took the same number of trials to reach criterion performance (i.e., d' maintained at or above 1 for 100% AM depth). In contrast, earplug-raised animals demonstrated significantly poorer AM detection thresholds when tested on a range of depths. The deficit gradually resolved over repeated testing sessions, such that performance in both groups was identical by testing day 10.

Conclusion

These findings demonstrate that mild transient, developmental auditory deprivation disrupts the maturation of auditory perception, and may help to explain speech and language delays associated with temporary hearing loss in children.

Sustained Firing of the Auditory Nerve Contributes to the Envelope of the Response to Tones Recorded at the Round Window

Joseph McClellan; Eric Formeister; William Merwin III; Matthieu Forgues; Ken Hutson; Claire Iseli; Craig Buchman; Oliver Adunka; Douglas Fitzpatrick
UNC Chapel Hill School of Medicine

Background

Since its discovery in the 1950s, the summing potential (SP) has been the subject of numerous studies, especially regarding its origin. Currently, the most widely accepted view is that the SP arises from dc potentials produced by both inner and outer hair cells and is represented in electrocochleography (ECoG) as the envelope of the response. The magnitude of the envelope can be modified by changes in the position of the basilar membrane. A contribution of the auditory nerve to the envelope of the response has been seen in birds (*Sun et al., JASA 107: 2136-42, 2000*) but not in mammals. In the present study we revisit the idea of neural contribution to the envelope using kainic acid (KA), a glutamate analog, to cause acute auditory nerve deafference in the gerbil.

Methods

ECoG was performed in gerbils using an electrode at the round window (RW). The compound action potential (CAP), cochlear microphonic (CM), auditory nerve neurophonic (ANN) and envelope were recorded in response to tone bursts at a variety of frequencies and intensities. Recordings were repeated after application of KA (60 mM in Lactated Ringer's solution) to the RW for 1 hour.

Results

The KA administration abolished both the CAP and ANN, indicating that near complete deafference was achieved. In addition, post-KA ECoG responses exhibited a significant shift in the envelope. Whether the initial envelope and the shift in the envelope were positive or negative varied across different animals and was also dependent on stimulus frequency and intensity. The magnitude of the shift was greatest for high intensities and high frequencies. In general the contribution of the nerve opposed that of the envelope remaining after KA.

Conclusion

Previous studies have suggested that KA-induced deafference has no effect on the envelope of the ECoG response in the mammalian cochlea. Here we show that in gerbil cochleae exposed to KA, there is an acute shift in the magnitude of the envelope, indicating that the envelope derives not only from receptor potentials in hair cells but is also influenced by the sustained firing of the auditory nerve.

Predicting Outer Hair Cell Loss: Influence of a Neural Contribution to the Cochlear Microphonic

Aryn Kamerer¹; Mark Chertoff¹; Marcello Peppi¹; Brian Earl²
¹*University of Kansas Medical Center*; ²*University of Cincinnati*

Background

Current procedures used to diagnose hearing loss are limited in locating and describing the underlying pathophysiology. Further advancements in the treatment of hearing loss will require identification of the anatomical structures that are damaged or dysfunctional. The cochlear microphonic (CM) is a physiologic signal from hair cells in the cochlea, however, new research suggests an additional neural contribution. The purpose of this study was twofold: to test the ability of the CM to locate missing outer hair cells (OHCs) along the length of cochlea, and separate the CM into its hair cell and neural components in order to discern its sensitivity to hair cell damage.

Methods

For the first study, Mongolian gerbils were assigned to a control group, or one of two cochlear damage groups: overexposure to tonal stimuli or laser light. For the second study, gerbils were assigned to a control group, or one of two groups treated with 5 or 10 mM of a selective Na⁺/K⁺-ATPase inhibitor (ouabain) placed in the round window niche. CM was recorded in all subjects to a low-frequency tone burst embedded in 25 high-pass filtered noise conditions. A cumulative amplitude function (CAF) was created by plotting the CM amplitudes as a function of position along the cochlear partition (converted from the high-pass filter cutoff frequency). Histology was performed on animals in the first study to locate anatomical onset of missing OHCs. For the second study, the CM, compound action potentials (CAPs) and distortion-product otoacoustic emissions (DPOAEs) were obtained before and after application of ouabain.

Results

In the first study, the plateau of the sigmoidal CAF corresponded with the onset of OHC damage and showed a significant correlation ($r=.73$) with the anatomical location where OHC loss first occurred along the cochlear partition. In the second study, ouabain-treated animals showed a reduction in amplitude of, or absent CAP, but no significant effects on DPOAEs (with the exception of 24 kHz). CM amplitudes were reduced, especially at low stimulus levels.

Conclusion

The first study suggests the efficacy of the CAF as a measure to approximate the location of the onset of missing OHCs. The ouabain study confirms a neural contribution to the low-frequency CM for low-level stimuli, an indication that application of the CAF to predict hair cell loss may be best at high stimulus levels.

Mechanical Contributions of Cochlear Infrared Neural Stimulation (INS)

Hunter Young; Xiaodong Tan; Claus-Peter Richter
Northwestern University

Background

Pulsed mid-infrared lasers have been used as a method for neural stimulation, including cochlear stimulation. The use of lasers is appealing for many reasons, namely the spatial selectivity and non-contact method of stimulation. The mechanism of INS is believed to be involved with local heating of discrete neuron populations. In cochlear INS, some of the heat is absorbed in the cochlear fluid proximal to the stimulation site, resulting in measurable stress relaxation waves. These waves may vibrate the basilar membrane or directly stimulate hair cells, causing a stimulation by-product. Hair cell stimulation due to INS-created stress relaxation waves has been observed in vestibular system optical stimulation. The goal of the present study was to determine the mechanical contributions of cochlear INS response.

Methods

In this study, guinea pigs were chronically deafened with a trans-tympanic injection of neomycin. Cochlear damage from the neomycin occurred over at least 4 weeks. After hearing thresholds were confirmed by testing for auditory-evoked CAPs recorded from a silver ball electrode at the round window, an optical fiber was inserted through a cochleostomy created in the basal turn. A laser input output curve was generated and the effect of continuous noise masking on INS was measured with CAPs. The experiment was repeated in normal hearing guinea pigs. The cochleae were harvested and processed using classic histology to determine the presence of hair cells.

Results

Current data shows a masking effect present in normal hearing animals, but not in chronic deaf animals. Interestingly, the level at which masking occurs is correlated to the hearing threshold. Therefore, in good hearing animals masking occurred at a lower SPL level than it did for poor hearing animals. Preliminary histology shows approximately 84% fewer inner hair cells in the deafened cochlea, compared to the non-deafened cochlea of the same animal.

Conclusion

The effects of mechanical stimulation caused by INS can be observed through continuous noise masking over optical stimulation. When hair cells are damaged or no longer present, INS still generates a neural response that is not masked by continuous noise. These findings lead to the conclusion that although INS-induced stress relaxation waves may have some interaction with hair cells, INS occurs through the direct interaction of the radiation and the neuron.

Inhibitory Responses to Infrared Neural Stimulation (INS) in the Deaf White Cat

Claus-Peter Richter; Hunter Young; Alan Robinson; Xiaodong Tan
Northwestern University

Background

Infrared neural stimulation (INS) is the method by which neurons, their axons, or their dendrites are stimulated by an infrared laser. Inhibition of neural responses by INS has recently been demonstrated in *Aplysia californica* and in the rat sciatic nerve. Observation of excitatory or inhibitory effects appears to be determined by the level of radiant energy exposure. We used a congenitally deaf animal model to test whether INS stimulation and inhibition could be achieved in the auditory system.

Methods

Deaf white cats were used for the study. These animals have a genetic defect, which results in the loss of hair cell and subsequent loss in spiral ganglion neurons. For the measurements the animals were anesthetized and their cochleae were surgically accessed. A cochleostomy was created, an electrical monopolar ball electrode was placed through the opening in the basal turn for electrical stimulation, and a 200 μm optical fiber was inserted through the cochleostomy for INS. For electrical stimulation biphasic electrical pulses (250 μs /phase, 0-2mA) in amplitude were delivered. A diode laser (Aculight, Capella) was used to deliver optical pulses (0.12-1ms, J/pulse). Responses to optical, electrical, and both optoelectrical stimulation were recorded. The time of stimulus presentation of the optical and electrical stimulus were varied during the experiment. Cochleae were harvested at the end of the experiments and were processed for histology. Spiral ganglion density and the status of the organ of Corti were examined.

Results

Cochleae could be stimulated electrically at high current amplitudes (> 1.5mA). No compound action potentials could be seen for optical stimulation. However, optical stimuli could be used to modulate responses to electrical stimulation. The effects of co-stimulation depended on the timing of the optical and electrical stimulus presentation. INS could be used to reduce responses to electrical stimulation. Histology showed no hair cells and a largely reduced density of spiral ganglion neurons.

Conclusion

INS allows modulating neural responses. Exposure of neural tissue to optical radiation can result in inhibition or excitation.

Temporal Properties of Inferior Colliculus Neurons to Cochlear Infrared Neural Stimulation

Xiaodong Tan; Hunter Young; Claus-Peter Richter
Northwestern University

Background

Cochlear infrared neural stimulation (INS) exhibits an improved spatial selectivity of activated spiral ganglion neurons, indicating its potential to be an alternative to electrical stimulation in cochlear implants. However, the temporal properties of single auditory neurons to cochlear INS have yet to be studied. Although it has been shown that INS elicits neuron depolarization by changing membrane capacitance, the involvement of hair cell input via opto-acoustic effects of INS is also possible. Nevertheless, to what extent the temporal properties of auditory neurons are shaped by photo-acoustic effects of INS is unclear.

Methods

In this study we characterized the temporal properties of auditory neurons in the central nucleus of inferior colliculus (ICC) to pulsed cochlear INS. Single units were recorded from Normal hearing, acute and chronic deaf guinea pigs using single tungsten or 16-channel electrodes. Pulsed infrared light was delivered through a cochleostomy in the basal turn of the guinea pig cochlea at different repetition rates ranging from 5 to 500 Hz. Pulsed trains of acoustic clicks were also delivered with a speaker as a control measurement. Deafening was achieved through trans-tympanic (chronic) or trans-cochleostomy (acute) neomycin delivery and was verified by acoustic CAP measurements and histological examination. The temporal properties of ICC single units were characterized through the analysis of phase-locking, latency and firing efficiency.

Results

The experiments demonstrated that cochlear INS elicited single unit responses in ICC in both normal hearing and deaf animals. In each animal, only a subpopulation of neurons in certain depth or frequency range responded to INS. Furthermore, the temporal properties of cochlear INS showed limited change between hearing and deaf animals. It was also observed that the responses of ICC neurons to cochlear INS showed lower limiting rates, longer latencies and lower firing efficiencies compared to those of acoustic stimulations. In addition, various neuron types and profound inhibitions responding to cochlear INS were also observed.

Conclusion

The results indicate that the temporal properties of ICC neurons to cochlear INS are different from those to acoustic or electrical stimulation. Recordings of single units in the ICC of deaf animals also show that cochlear INS is able to stimulate spiral ganglion neurons directly. The location and restrained activation of cochlear INS might both contribute to shaping the temporal properties of ICC neurons.

Spatially Differentiated Infrared Neural Stimulation of the Guinea Pig Cochlea

Daniel O'Brien; Hunter K Young; Xiaodong Tan; Claus-Peter Richter

Northwestern University Feinberg School of Medicine

Background

Optical stimulation with pulsed near-infrared radiation has been shown to generate neural excitation in a variety of tissues, including the mammalian cochlea. Auditory prostheses utilizing optical stimulation may improve the operating characteristics of traditional cochlear implants by enabling greater special selectivity and providing a non-contact stimulation source. Though early animal models have shown that *in vivo* infrared neural stimulation of the cochlea is able to generate an auditory signal at upstream points along the auditory pathway, it is not yet clear whether this is due to an "optoacoustic" effect created by pressure changes within surrounding fluids or whether the response represents the direct effect of optical stimulation of spiral ganglion cells. The aim of the present study is to record action potential responses in the guinea pig cochlea to laser stimulation of adjacent cell populations within the basal turn at discrete points along two perpendicular axes in order to assess the extent to which such responses are concordant; high degrees of concordance would favor the optoacoustic hypothesis as the light source and its subsequent auditory artifact are not changed, whereas a lack of concordance would suggest that a direct optical effect is responsible for the induced auditory signal.

Methods

A 2x1 array of 200-micrometer fiber-optic wires was surgically implanted into the basal turns of 5 guinea pig cochleae. Compound action potentials (CAP) elicited by illumination of one fiber at a time over a series of radiant energy outputs were recorded by an electrode placed at the round window. When possible, the fiber-optic bundle was turned 90 degrees and responses to optical stimulation along the perpendicular axis were assessed. Differences in CAP amplitudes generated by discrete fibers along like axes were calculated. An analysis of variance (ANOVA) was then used to compare differences in CAP amplitude along the horizontal and vertical axes.

Results

ANOVA results show greater variability along the vertical compared to the horizontal axis (variances of 602.9 vs. 335.9, respectively), with an F-ratio of 12.1 ($P=0.0007$). These data suggest that, over a series of radiant energy exposures, response-levels to illumination of adjacent fibers are more variable along the vertical than the horizontal axis.

Conclusion

Auditory response to infrared neural stimulation may be due to the direct effect on nervous tissue of optical stimulation. Furthermore, stimulation along the vertical axis may produce more response-selectivity than stimulation along the horizontal.

Increased Uptake of Fluorescently-Tagged Gentamicin in the Stria Vascularis After Diphtheria Toxin Ablation of Macrophages

Jianping Liu^{1,2}; Zachary Urdang¹; Hongzhe Li¹; Peter Steyger¹

¹Oregon Health & Science University, Portland, Oregon, USA; ²Eye & Ear Nose and Throat Hospital, Fudan University, Shanghai, China.

Background

Transgenic mice expressing the *Diphtheria* toxin receptor (DTR) on macrophages (and presumptively, cochlear perivascular resident macrophages) are reported to lose blood-labyrinth barrier (BLB) integrity and auditory sensitivity following treatment with *Diphtheria* toxin (DT). We hypothesized that DT treatment will increase fluorescently-tagged gentamicin (GTTR) entry into the stria vascularis and spiral ligament, via a structurally-disrupted BLB in these transgenic mice.

Methods

Three groups of mice were used: (A) an experimental group of transgenic mice expressing DTR on macrophages treated with DT, and two control groups including (B) DTR mice treated with saline, and (C) wildtype C57BL/6 mice treated with DT. Five days after the initial DT injection, auditory brainstem response (ABR) thresholds were obtained, and mice received GTTR (or Texas Red) one hour prior to transcardiac perfusion and fixation. The cochlear lateral wall tissues were excised and examined by confocal microscopy, using identical setting for all specimens. The fluorescence intensity of GTTR in different cell layers of the stria vascularis and spiral ligament region were obtained and statistically analyzed.

Results

ABR threshold shifts were not observed following DT treatment. DT significantly enhanced GTTR (but not Texas Red) fluorescence in marginal cells, intermediate cells and basal cells of the stria vascularis and in the fibrocytes of spiral ligament in DTR mice, compared to PBS-treated DTR mice and DT-treated wildtype mice. DT did not significantly enhance GTTR fluorescence in marginal, intermediate or basal cells of the stria vascularis, nor in the fibrocytes of spiral ligament in DT-treated wildtype mice compared to those in PBS-treated DTR mice.

Conclusion

This regimen of DT treatment did not alter the auditory thresholds of any mouse strain. In wildtype mice, DT at low doses did not enhance stria uptake of GTTR. In transgenic mice expressing DTR on macrophages, DT treatment enhanced GTTR (but not Texas Red) entry into the stria vascularis and spiral ligament across the BLB. *In toto*, this suggests that DT-induced lysis of macrophages triggered an inflammatory response that enhanced cochlear uptake of GTTR, likely without compromising BLB structural integrity.

Bioenergetics of Cochlear Oxidative Stress in Basement Membrane Pathology

Collin Chen¹; Brendan Smyth²; Michael Anne Gratton¹

¹Saint Louis University; ²Baxter HealthCare Corporation

Background

Alport Syndrome is an inherited disorder of type IV collagen. The cochlea of the mouse model of autosomal recessive Alport Syndrome is characterized by progressively thickening stria capillary basement membranes (SCBM) and a related hearing loss. Our lab has shown that the cochlear lateral wall (LW) of the Alport mouse is inherently hypoxic with increased ROS levels linked to an increased glutathione (GSSG/GSH) ratio. Furthermore there is upregulation of the Na⁺/K⁺-ATPase protein availability, yet decreased functional Na⁺/K⁺-ATPase activity with subsequent reduced endocochlear potential and vulnerability to noise-induced hearing loss (NIHL). These data suggest the mitochondrial dysfunction in the LW of the Alport mouse. In the current study, mitochondrial dysfunction was further assessed by the supply/demand cellular energy index (extramitochondrial ATP/ADP ratio).

Methods

Cochlear LW tissue was microdissected from 7-9 week old Alport mice and their wildtype (WT) littermates. A subset of each genotype was noise-exposed (10 kHz OBN, 120 dB SPL, 10h). The samples were stored (-20°C) in 1% TCA in Krebs-Ringer Bicarbonate Buffer. Samples from 3 mice were pooled, homogenized and pelleted (10G, 10 min). Levels of ATP and ADP in the supernatant were assayed with a bioluminescence assay (Promega) and referenced to protein (BCA, Pierce).

Results

No difference was found between quiet or immediately post-noise WT mice in the levels of ATP, ADP or the ATP/ADP ratio. By contrast, in quiet KO mice an elevated ATP level, but decreased ADP level was noted. However, the resultant overall ATP/ADP ratio was comparable to that of the WT mice. Conversely, in immediately post-noise KO mice the ATP level decreased to a level comparable to the WT mice yet the ADP level was substantially elevated. The resultant ATP/ADP ratio was significantly lower than observed in quiet and noise-exposed WT mice as well as the quiet KO mice.

Conclusion

- These results suggest mitochondrial respiratory dysfunction, with loss of redox potential and formation of excessive free radicals plays an important role in the pathogenesis of the hearing loss associated with Alport syndrome.
- The loss of control of cellular energy homeostasis in the LW of the Alport mouse warrants further study.

PS - 325

Aquaporin 4 Expression in Perivascular Resident Macrophages is Essential for Sustaining the Endocochlear Potential

Lingling Neng; Jinhui Zhang; Ju Yang; Fei Zhang; Xiaorui Shi

Oregon Health & Science University

Background

Normal blood-labyrinth barrier (BLB) integrity in the stria vascularis requires a high degree of structural and functional integration between barrier component cells (endothelial cells, pericytes, and perivascular resident macrophages (PVMs)). In particular, the tight ensheathment of perivascular resident macrophage (PVM) end-feet around vessel walls is a critical component of BLB integrity, essential for sustaining a normal endocochlear potential (EP) and establishing hearing function.

Methods

In this study, using, RT-PCR, western blotting and confocal microscopy combined with fluorescence immunohistochemistry label and EP measurement.

Results

We report that aquaporin 4 (AQP4, M23 isoform), the AQP family member with the highest osmotic water permeability, is critical for hearing and richly expressed in the PVMs that surround vascular endothelia. Suppression of AQP4 with siRNA dramatically changes PVM morphology. Normally elongated PVMs become star-shaped (or stellate) by day 3 with siRNA silencing in primary cultured PVMs. AQP4 suppression also significantly reduces capillary coverage and gap junction protein Cx43 expression by day 3 in siRNA/AQP4 treated animals compared with controls. Furthermore, we found that suppression of AQP4 reduces EP to approximately 50 mV.

Conclusion

Taken together, the study suggests that AQP4 in PVMs is important for controlling PVM structure, facilitating communication with ECs, and sustaining the EP.

PS - 326

Isolation and Culture of Endothelial Cells, Pericytes, and Perivascular Resident Macrophage-Like Melanocytes from the Young Mouse Vestibular System

Jinhui Zhang; Lingling Neng; Fei Zhang; Xiaorui Shi

Oregon Health & Science University

Background

The cochlear blood-labyrinth barrier (BLB) tightly regulates the inner ear micro-environment for auditory function and balance. In particular, the blood barrier in the vestibular system is critical for maintaining the ionic, fluid, and energy balance necessary for functional balance. Like the BLB structural organization in the stria vascularis, BLB in the vestibular system also includes a large number of perivascular-resident macrophage-like melanocytes (PVM/Ms) and pericytes (PCs) in addition to endothelial cells (ECs) and basement membrane. Over the past few decades, *in vitro* cell-based models wide-

ly used in studies of the blood-brain barrier and blood-retina barrier have been powerful tools for studying cell-cell interactions.

Methods

To better understand how barrier component cells interact in the vestibular system to control BLB function, we developed a novel growth medium-based method for obtaining ECs, PCs, and PVM/Ms primary cultures from tiny explants (mini-chips) of sacculus, utricle, and ampullae of semicircular canal tissue from young mouse ears at age postnatal 8 to 12 days.

Results

The mixed population of vestibular cell types is grown in specific culture medium to selectively support the growth of each phenotype. The unwanted phenotypes do not survive passaging. The harvesting process takes less than 2 h and does not require additional equipment or special enzyme treatment. Primary cell types are generated within 10-12 d. Purities of >90% are obtained of the primary culture ECs, PCs, and PVM/Ms with two passages (~3 weeks).

Conclusion

The protocol is simple and provides consistent results. The highly purified primary cell lines enable cell culture-based *in vitro* modeling of cell-cell interactions, barrier control function, and drug action.

PS - 327

Ceacam16 is Required for the Formation of Striated-Sheet Matrix in the Mammalian Tectorial Membrane

Richard Goodyear¹; Kevin Legan²; Julia Korchagina²; Souvik Naskar²; Kazuaki Homma³; Claus-Peter Richter³; Jing Zheng³; Mary Ann Cheatham³; Peter Dallos³; Guy Richardson¹

¹Sussex Neuroscience, University of Sussex; ²University of Sussex; ³Northwestern University, Chicago and Evanston, IL USA; ³Northwestern University, Chicago and Evanston, IL USA.

Background

Carcinoembryonic antigen-related cell adhesion molecule 16 (Ceacam16) is a novel, non-collagenous component of the mammalian tectorial membrane (TM), and a missense mutation in *Ceacam16* was identified as a cause of late-onset deafness in an American family (Zheng et al., 2011). *Ceacam16* interacts with Tecta (Zheng et al., 2011) and it has been suggested (Kammerer et al. 2012) that it is a component of the striated-sheet matrix, the laminated matrix within which the collagen fibrils of the TM are imbedded (Hasko and Richardson, 1987). To investigate the structural and functional role of *Ceacam16* we created a *Ceacam16* null mutant mouse.

Methods

A targeted ES cell line in which the first coding exon of *Ceacam16* is replaced with the bacterial lacZ open reading frame encoding beta-galactosidase (b-gal) was obtained from the Knock Out Mouse Project at UC Davis, CA. Chimeras were produced by injecting C57Bl6/N blastocysts with the ES cells

and germ-line transmitting chimeras were bred to C57Bl6J mice (Harlan UK) to establish a colony producing *Ceacam16*^{+/+}, *Ceacam16*^{+/bgal} and *Ceacam16*^{bgal/bgal} mice. Beta-gal staining was used to indicate sites of Ceacam16 expression; immunofluorescence microscopy and western blotting were used to determine distributions and levels of TM proteins, and transmission electron microscopy (TEM) was used to study the ultrastructure of the TM matrix.

Results

Beta-gal staining is first detected in the basal region of the cochlea at P12, and along its entire length by P14. Staining is observed in interdental cells, inner sulcus cells, border cells, pillar cells and Deiters' cells, and persists until at least 6 months of age. TEM reveals clearly defined striated-sheet matrix first appears at P14 in the basal end of the TM in *Ceacam16*^{+/+} mice, and is present throughout the TM by P16. Striated-sheet matrix and Hensen's stripe fail to form in *Ceacam16*^{bgal/bgal} knockout mice, and there is a subsequent age-related decline in Tectb protein levels and a loss of matrix surrounding the collagen fibrils of the TM, with the latter effect being especially prominent in the apical low-frequency end of the cochlea.

Conclusion

The onset of *Ceacam16* expression and the appearance of striated-sheet matrix occur close to the onset of hearing, and Ceacam16 is required for striated-sheet matrix formation. The continual expression of Ceacam16 may stabilise the non-collagenous TM matrix, the principal proteins of which are only produced during a short window of time early in development (Rau et al., 1999).

PS - 328

Young Ceacam16 Knockout Mice Display Enhanced SOAEs, SFOAEs and TEOAEs, as Well as Reduced Tectorial Membrane Stiffness

Mary Ann Cheatham¹; Guy Richardson²; Kazuaki Homma¹; Claus Peter Richter¹; Richard Goodyear²; Kevin Legan²; Julia Korchagina²; Souvik Naskar²; Ted Kim¹; Peter Dallos¹; Jing Zheng¹

¹Northwestern University; ²University of Sussex

Background

The carcinoembryonic antigen-related cell adhesion molecule (Ceacam) family contains 22 members and the secreted glycoprotein, Ceacam16, is expressed in the tectorial membrane. Recent evidence indicates that this gene is mutated in American Family 1070, which is known to have hearing loss beginning in adolescence and progressing to an ~50 dB threshold shift across frequency consistent with loss of cochlear amplification (Chen et al., 1995; Zheng et al., 2011). Of the noncollagenous tectorial membrane (TM) proteins, alpha and beta tectorin dominate the proteinaceous content but their mRNAs are not expressed after ~3 weeks of age (Rau et al., 1999), which makes it difficult to imagine how the TM is maintained throughout life. In contrast, Ceacam16 mRNA is observed in older animals (Zheng et al., 2011; Kammerer et al., 2012). Because alpha tectorin and Ceacam16 are known

to interact, it is possible that Ceacam16 is important for maintaining TM structure.

Methods

In order to learn more about the functional significance of Ceacam16, we created Ceacam16 null mutant mice using a targeted ES cell line obtained from the Knock Out Mouse Project at UC Davis. Because we discovered that the striated-sheet matrix, in which the collagen fibers are imbedded, as well as Hensen's stripe are both missing in mice lacking Ceacam16, we measured otoacoustic emissions (OAE) and auditory brainstem responses (ABR), along with TM measurements of point stiffness and Young's modulus using the hemicochlea preparation.

Results

Although a low frequency ABR threshold shift is observed similar to that measured in another Ceacam16 knockout mouse produced by Kammerer et al., our data demonstrate that distortion product OAEs are near normal in very young mice. However, both stimulus frequency (SF) and transiently evoked (TE) OAEs are much larger in KOs. We also observed spontaneous emissions (SOAE) in 2/3 of the mice lacking Ceacam16. This incidence is remarkable since less than 2.5% of controls were found to have SOAEs. Stiffness of the TM was also significantly reduced in Ceacam16 KOs.

Conclusion

Changes in the physical properties of the TM may limit the dissipation of energy longitudinally along the cochlear partition, thereby increasing the incidence of spontaneous activity and improving thresholds for both SF and TEOAEs. These results from the Ceacam16 KO mouse imply that the mammalian organ of Corti in normal animals has evolved for stability to prevent self-sustaining oscillations and prolonged after-responses within the high-gain feedback loop.

PS - 329

Characterization of the Primary Auditory Synapse in the Turtle Using Paired Recordings and Real Time Cell Capacitance Measurements.

michael Schnee; Anthony Ricci

Stanford University

Background

Inner hair cell afferent fibers transfer sound information at high rates for long periods of time with extraordinary fidelity. Postsynaptic EPSC recordings from the turtle auditory periphery are fast AMPA type receptors with rapid rise and decay kinetics and a wide range of amplitudes (15X)¹. We have extended the characterization of the turtle auditory synapse with simultaneous voltage clamp recordings of the hair cell and afferent fiber.

Methods

Recordings were performed in hair cells and afferent fibers in the turtle auditory papilla using standard voltage clamp techniques. The two sine technique for tracking membrane capacitance (CM) was used to monitor real time Cm changes independently of membrane conductance².

Results

Paired recordings demonstrate that capacitance measurements and evoked EPSC charge are tightly coupled (R^2 of 0.84 and slope of 0.93 pC/fF $N=15$). This data suggests that desensitization or receptor saturation are not occurring for sub maximal stimulations. Stimulation to less than the peak Ca current release consisted of linear release of EPSCs with a wide range of amplitudes. The interpulse interval for such stimulations could be fit with a single exponential suggesting that release is stochastic and each release site is independent. In 6/12 cells large steps of 1-3s to the peak Ca current produced a postsynaptic response that peaked and then rapidly decayed to a baseline of slower release similar to responses in bipolar and mammalian inner hair cells (IHCs)^{3,4}. In contrast to IHCs, the peak represented $12.4 \pm 11\%$ of the total response. The decay in postsynaptic current was best fit with 2 exponentials 18.7 ± 18 ms (range 1.9-53 ms) and 237 ± 215 ms (range 27-519 ms). The sustained release following the peak is much more substantial ($83 \pm 13\%$ of the total) in turtle than at IHC synapses possibly due to the 20-50 synapses per hair cell in the turtle.

References

- ¹*J Neurophysiol* (2013) 110:204-220,
²*Neuron* (2011) 70: 326–338.
³*PNAS* (2007) 104:16341-16346
⁴*Nature* (1999) 397: 157-160

Conclusion

Cm measurements closely follow the EPSC charge and show that Cm is a reliable measure for synaptic release at the turtle auditory synapse .

PS - 330

Short Pulse-Induced Synaptic Vesicle Releases Display Cooperativity at a Hair Cell Ribbon Synapse

Geng-Lin Li

University of Massachusetts Amherst

Background

The classic quantal theory of synaptic transmission states that in response to one presynaptic action potential a single release site can release maximally one synaptic vesicle and that the releases are independent among different release sites. In the retinal bipolar cell ribbon synapse, however, it has been established that in response to a transient Ca^{2+} tail current a single release site could release more than one synaptic vesicle, i.e., multivesicular release. It was also demonstrated that at this synapse the releases are still independent. In a hair cell ribbon synapse where multivesicular release has also been established, we have shown that the releases in response to sinusoidal cycle stimulations are cooperative. Although the use of sinusoidal cycles for stimulation makes our study more physiologically relevant, it is quite distinct from the transient stimulations that have been applied to other synapses in the form of either action potentials or Ca^{2+} tail currents, which makes it questionable to interpret the data under the same theoretical framework.

Methods

Split-open amphibian papillae were prepared from bullfrogs as previously described. The hair cells and afferent fibers were visualized under an upright Olympus microscope with a 60X water-immersion objective. Paired patch-clamp recording was performed through a Heka EPC10/2 amplifier. The evoked EPSCs were recorded and their quantal contents were estimated as previous described.

Results

Hair cells were depolarized from -90 mV to -30 mV briefly (0.5 ~ 1 ms) and repetitively (1 trial per second) to evoke single discrete EPSCs on afferent fibers. For shorter pulses (e.g. 0.5 ms), the failure rate can be as high as 90%. As the pulse duration increases, the failure rate decreases. Pulse duration was varied systematically so that a pulse duration can be found to induce EPSCs at a failure rate of about 50%. Then the same pulse was applied as many times as possible. The quantal contents of evoked EPSCs were estimated and a distribution was plotted together with the failure rate. The data cannot be fitted to a binomial distribution, but instead can be fitted very well to a cooperative model where the release of one synaptic vesicle increases the release probability of other vesicles being released.

Conclusion

Hair cells can release synaptic vesicles in a cooperative manner.

PS - 331

Probing Frequency Tuning of Bullfrog Hair Cells With a ZAP Current Protocol

Daniil Frolov¹; Geng-Lin Li²

¹*University of Massachusetts Amherst*; ²*Biology Department, University of Massachusetts Amherst*

Background

In the vertebrate auditory system, acoustic signals are firstly decomposed into different frequency components and then processed in parallel. It is widely accepted that for low vertebrates the decomposition happens mainly in auditory hair cells. That is, the hair cells selectively amplify signals at their characteristic frequencies while suppressing signals at other frequencies. In response to step current injections these hair cells show a damped oscillation, from which a resonance frequency can be determined to approximate the characteristic frequency and a quality factor can be calculated to predict the tuning curve of these hair cells. However, neither the peak frequency nor the tuning curve has been determined directly through experiments.

Methods

Amphibian papillae or sacculi were carefully dissected out from the bullfrog inner ear, and the hair cell-containing epithelium was isolated and placed in a recording chamber continuously perfused with an oxygenated external solution. Without further mechanical or enzymatic treatment, we made whole-cell patch-clamp recording on these minimally perturbed hair cells. Zap currents were generated by the formula $I_{zap}(t) = I_{holding} + I_{zap,peak} \sin(2\pi f_i t^2)$, in which $I_{holding}$ is the holding current amplitude, $I_{zap,peak}$ is the Zap current peak amplitude,

and V_f is the speed of frequency change (e.g. 300 Hz/s). The Zap current protocols were applied to the hair cells under current-clamp and the voltage responses were recorded.

Results

Firstly, the Zap current protocols allowed us to sweep from 0 to 1.5 kHz within 5 s, and the tuning curves can be determined conveniently by performing Fast Fourier Transformation on the voltage responses. Secondly, by varying I_{holding} while fixing $I_{\text{Zap,peak}}$, we were able to study how the change in the resting membrane potential affects the hair cell's tuning capability; by varying $I_{\text{Zap,peak}}$ while fixing I_{holding} , we were able to study the linearity and non-linearity of coding across different frequencies. Lastly, we applied both the step and Zap current protocols to the same cells and compared the tuning curves obtained through the two protocols. Our results suggested the traditional approach with step current protocols leads to overestimations of both the peak amplitude frequency and the tuning capability of individual hair cells.

Conclusion

The Zap current protocol provides a promising new approach to study cellular mechanisms of frequency tuning in auditory hair cells of low vertebrates.

PS - 332

Clearing of the Mouse Temporal Bone Using a Modified CLARITY Protocol

Rebecca Cook; Adrian Perachio; Tomoko Makishima
University of Texas Medical Branch

Background

Histological and anatomical studies of the mouse inner ear are technically difficult due to its small size and its location embedded in the temporal bone. A recently published protocol, CLARITY, allows the clearing and the visualization of a whole brain in mice in a 3D fashion. Our goal was to modify the CLARITY protocol to achieve 3D visualization of inner ear organs encased in the temporal bone. We sought to establish the optimal protocol for clearing bone and cartilage in the mouse temporal bone to be suitable for immunofluorescent labeling.

Methods

Temporal bones were dissected from mice at either postnatal day 1 – 2 (P1-2) or at P30. The CLARITY protocol was modified for the mouse temporal bone. Briefly, the adult temporal bones were decalcified before starting the process. The cartilaginous temporal bone of younger mice was processed directly without calcification. After fixation with 4% paraformaldehyde in PBS, the samples were incubated in a hydrogel solution (4% acrylamide, 0.05% bis, 0.25% VA-044 initiator, 4% paraformaldehyde, 0.05% saponin) for one week, and then allowed to polymerize. Then the samples were extracted from the gel and incubated in clearing solution (200mM boric acid, 4% sodium dodecyl sulfate, pH 8.5) for one week, and were treated under electrophoresis for 96 hours. Then the samples were incubated in a series of fructose solutions with increasing concentrations. The cleared samples were labeled with fluorescent markers including Neurotrace Fluorescent

Nissl Stain, Phalloidin, and Hoechst. Samples were mounted and viewed using fluorescent microscopy.

Results

Successful clearing of cartilaginous temporal bone and partial clearing of decalcified temporal bone was achieved.

Conclusion

Our modified version of the CLARITY protocol was low-cost using readily available materials. Using this protocol, we were able to clear and visualize immature and mature mouse temporal bones. We hope to optimize the protocol for immunofluorescent labeling that is specific to the mouse inner ear.

PS - 333

Imaging Cochlear Synaptic Connectomes

Dan Liu; Ruqiang Liang; Christy He; Jianxin Bao
Washington University in St. Louis

Background

Understanding vertebrate auditory perception depends on knowing, in part, the complete synaptic network of at least one representative cochlea. Acquiring such synaptic connectomics in an intact cochlea lodged within the bony labyrinth is very challenging. To map out fine structures of ribbon synapse between hair cells and spiral ganglion neurons (SGNs), as well as trajectories of SGN dendrites were near impossible until now. To image these intact fine structures at high resolution, synaptic proteins need to be kept in intact while the whole cochlea needs to be transparent and permeable for large biomacromolecules such as antibodies against specific synaptic proteins. Based on recent developments of imaging methods, we employed polyacrylamide mesh to keep the fine structure of a formaldehyde-fixed cochlea while light-absorbing lipids are removed by electrophoresis, allowing the intact cochlea to be imaged. Therefore, we have developed an imaging system to study synaptic connectomes in the intact cochlea.

Methods

Y12 mice were perfused with a hydrogel solution, which the hydrogel essentially replaces the lipids in the membrane to maintain cellular structures. In Y12 mice, synaptic terminals of spiral ganglion neurons (SGNs) and efferent fibers are genetically labeled by yellow fluorescent protein (YFP). Intact cochleae were removed from these mice after the perfusion, followed by incubating in a decalcification buffer to remove the minerals in bone. After removing lipids in an active electrophoresis approach, we placed cochleae in FocusClear for several days to match the refractive index and then imaged synaptic connectomes by a Zeiss microscope.

Results

The intact cochlea from Y12 mouse has been made optically transparent and imaged by Zeiss microscope. SGNs and its projections labeled by YFP were observed in the intact cochlea. Hair cells immunostained with myosin VIIa could also be directly observed in the same intact cochlea. We are currently working on imaging ribbon synapses in the whole cochlea.

Conclusion

Based on recent developments in imaging of intact brains, we are developing a method to image hair cells, SGNs and their synaptic connections in the intact bony mouse cochlea. If this method is successful, we will have a powerful method to study detail neuronal connections in the intact cochlea to understand the first step of auditory processing. Furthermore, this method will greatly facilitate our understanding of hearing loss.

PS - 334

Swept Source Optical Coherence Tomography for Imaging and Vibrometry Inside the Mouse Cochlea in Vivo

Hee Yoon Lee¹; Patrick Raphael¹; Audrey Ellerbee¹; Brian Applegate²; John Oghalai¹

¹Stanford University; ²Texas A&M University

Background

Optical coherence tomography (OCT) can be used to make *in vivo* measurements of cochlear mechanics. Its potential benefits over conventional laser Doppler vibrometry include the ability to make measurements in the unopened cochlea and to measure from multiple depth positions within the organ of Corti. However, one downside to using OCT in the cochlea has been its relatively low SNR, such that the lowest intensity sound stimulus that can be measured is on the order of 40-50 dB SPL.

Methods

We built a novel swept-source OCT (SS-OCT) system with particular attention paid to addressing potential sources of noise that can affect the noise floor during these types of *in vivo* studies. We characterized the SNR of our system, the noise floor of the basilar membrane in the mouse cochlea *in vivo*, and its sensitivity for measuring sound-induced basilar membrane vibrations.

Results

First, we measured the SNR of our system against a perfect reflector and found it to be ~112dB. The displacement accuracy of our SS-OCT system was assessed by measuring the displacement of a piezo. We compared the magnitude and the phase of the piezo vibration using both our system and a commercial laser Doppler vibrometer. At low stimulation frequencies, the SS-OCT system accurately tracked the vibration of the piezo. However, because the sweep rate of the light source used in our SS-OCT system was 50kHz, there was a high-pass roll off associated with its frequency response. The magnitude was attenuated by 10% and the phase was delayed by ~1.2 rad at the maximum frequency of 25kHz. These fringe washout effects were close to predicted values. Next, we used the OCT system to image the living mouse cochlea through the otic capsule bone. Cross-sectional images and 3D reconstructions were performed. The system could reliably image the entire apical turn and visualize the basilar membrane, Reissner's membrane, tectorial membrane, sub-tectorial space, and tunnel of Corti. Lastly, we measured vibrations of the apical turn basilar membrane in living mice through the otic capsule bone. We applied sound stimuli

ranging in frequency from 2.5-11kHz and in intensity from 10-80dB SPL. We could reliably measure tuning curves in the mouse cochlea with characteristic frequencies of 8-10kHz. The displacement noise floor of the basilar membrane using 10k sample points was 60±30pm (mean±SD). Thus, at the characteristic frequency, we could measure vibrations using sound stimulus intensities as low as 10dB SPL.

Conclusion

SS-OCT permits vibratory measurements within the apex of the unopened mouse cochlea with a displacement sensitivity noise floor similar to that achievable *in vivo* with laser Doppler vibrometry and the use of a reflective glass bead.

PS - 335

Cellular Mechanisms of Genetic Mutations in Kv7.1 Gene

Atefeh Mousavi Nik; Ebenezer Yamoah

University of California Davis

Background

Mutation in Kv_{7.1} gene cause Jervell and Lange-Nielsen (JLN) syndrome which is associated with bilateral deafness. There is a positive endocochlear potential (EP) in the inner ear which is a main driving force to maintain ionic flow in the hair cells which leads to hearing. There are various types of channels and transporters in lateral wall that help ionic flow specially potassium flow in the inner ear, any mutation or disruption in them will lead to drop in EP and hearing loss or deafness.

Methods

To have better understanding about the cellular mechanism of Kv_{7.1} mutant gene, 7 known mutants including; R518G, T322M, T311I, A336fs, G589D, E543f and Q530X has been generated by using site-directed mutagenesis and used for electrophysiology and immunofluorescence with confocal microscope.

Results

Using HA-tag and Myc-tag demonstrate trafficking defect of these channels to the plasma membrane and also illustrate their Endoplasmic Reticulum maintenance. Additionally, expression of these mutants in CHO cells result in nonfunctional channel, but co-expression of them with wild type result in functional channel with reduced current in compare to wild type alone.

Conclusion

In conclusion, these mutations in Kv_{7.1} gene produce non-functional channels mainly because of trafficking defect which eventually reduce EP and lead to hearing loss as seen in JLNS patients.

Functional Contributions of Calcium-Activated Chloride Channels to the Excitability of Primary Auditory Neurons

Xiao-Dong Zhang¹; Ping Lv²; Wei Chun Chen¹; Tsung-Yu Chen¹; Hyo Jeong Kim¹; Jeong-Han Lee¹; Wenying Wang¹; Karen Doyle¹; Nipavan Chiamvimonvat¹; **Ebenezer Yamoah¹**

¹University of California Davis; ²Hebei Medical University

Background

Spiral ganglion neurons (SGNs) are responsible for transmitting sound evoked activity from the hair cells to the cochlear nucleus. The action potential (AP) firing by SGNs is the key signal for the acoustic activation of the central auditory pathways. To understand the electrical properties of SGNs, we examined the contribution of chloride channels in SGNs.

Methods

We used patch-clamp, caged-calcium photolysis and confocal fluorescence microscopy to examine the function and expression of chloride channels in SGNs.

Results

We found that the inhibition of chloride channels by niflumic acid (NFA) and 5-nitro-2-(3-phenylpropylamino)-benzoate (NPPB) hyperpolarized the resting membrane potential and significantly reduced the SGN AP firing. To reveal the molecular identity of the chloride channel, we used gene knockout mice to test the inhibitory effects. We found that there was no significant inhibition of the AP firing of SGNs from the calcium-activated chloride channel (ANO1) knockout mice, suggesting the participation of ANO1 in the regulation of SGN excitability. We further tested the effects of ANO1 activation in SGNs by using caged-calcium photolysis. The activation of ANO1 generated significant chloride currents, depolarized the resting membrane potential and increased the AP firing. Knockout of ANO1 reduced the calcium-activated chloride currents and AP firing in SGNs. Further immunostaining of the cochlea preparation demonstrated the expression of ANO1 in SGNs. To identify the role of chloride ions and ANO1 in the SGN function, we measured the $[Cl^-]_i$ in SGNs. Surprisingly, $[Cl^-]_i$ in SGNs from P2-P3 mice was significantly higher than that from the adults, suggesting the altered roles of chloride channels in the developing cochlea. The chloride currents could be either outward or inward depending on the $[Cl^-]_i$, the ECl and membrane potential. The reduction of $[Cl^-]_i$ in adult SGNs would shift ECl to a more hyperpolarization potential, which will regulate the contribution of chloride channels to AP firing. The higher $[Cl^-]_i$ in SGNs of neonatal mice may increase the AP firing by increasing the outward driving force for chloride ions and enhancing the inward current.

Conclusion

ANO1 chloride channels are expressed in SGNs and contribute to the regulation of the SGN excitability. The changes in $[Cl^-]_i$ between pre- and post-hearing neurons may partly explain alterations in SGN AP firing before and after hearing onset.

Acid Sensing Ionic Channels Mediate an Excitatory Synaptic Input to the Cochlear and Vestibular Afferent Neurons

Enrique Soto; Rosario Vega; Antonia González; Aída Ortega

Universidad Autónoma de Puebla, México

Background

Extracellular pH (pHo) falls sharply during episodes of intense neuronal activity or with ischemia. It is generally thought that pHo has transitory nonspecific effects because of the existence of extensive buffering mechanisms. However, it has been found that H⁺ (protons) would constitute signaling molecules for specific cellular processes. In fact, the discovery of the acid sensing ionic channels (ASIC), provide a basis to study signaling mechanism mediated by pHo. At the synapse, the possibility of physiological extracellular acidification is derived from evidence showing that glutamate vesicles are acidified (with pH 5.7) by an ATP-dependent proton pump, which in turn provides a significant source of protons in the synaptic cleft when the vesicular release occurs. The inner-ear hair cells establish glutamatergic ribbon synapses with an afferent neuron, tonically releasing the neurotransmitter. In vestibular type-I hair cell calyceal endings and in the inner cochlear hair cells the synaptic complex covers a significant part of the basolateral pole of the cell. This geometry produce a diffusionally restricted synaptic cleft that may lead to a significant pHo changes under sustained synaptic activity.

Methods

Experiments performed in cultured vestibular ganglion afferent neurons (P7-10 rats) and in cochlear spiral ganglion afferent neurons (P3-6 mouse) using the whole cell voltage clamp technique. Immunohistochemical studies of the expression of ASIC1..4 subunits were performed in the vestibule and the cochlea. Extracellular recording of afferent neuron activity in the isolated vestibule of the rat (P7-10).

Results

Voltage clamp recordings shown that both types of neurons expressed robust inward currents evoked within milliseconds of extracellular acidification. These currents were blocked by ASIC blockers amiloride and gadolinium, indicating that they are due to ASIC activation. Also immunohistochemical studies showed that both the vestibular and the cochlear afferent neurons express ASIC subunits including ASIC 1a, 2a, 2b 3 and 4. The functional expression of acid sensing ionic channels (ASICs) in the vestibular and cochlear afferents of rodents indicate that pHo acidification and subsequent ASICs activation may form part of the normal function of the afferent synapse in hair cells. In fact evidence obtained from afferent neuron activity recorded in the isolated vestibule preparation in the rat, shows that afferent activity is positively modulated by FMRFamide peptides which have been shown to increase ASIC currents and negatively modulated by amiloride, that among other actions has been shown to block ASIC currents.

Conclusion

These data lead to the conclusion that afferent neurons from both the cochlea and the vestibule may be modulated by extracellular proton concentration changes through the activation of ASIC currents which would significantly contribute to shape the postsynaptic response of the afferent neurons. It is worth to mention that previous data also shown that extracellular pH changes modulate other ionic currents apart from the ASICs in both the hair cells and the afferent neurons.

PS - 338

Phosphoinositide Signaling Provides a Brake on Spiral Ganglion Neuron Excitability

Lorcan Browne¹; Katie Smith²; David McAlpine²; David Selwood³; Daniel Jagger²

¹University College London; ²UCL Ear Institute; ³Wolfson Institute for Biomedical Research - UCL

Background

The activity of numerous ion channel types is regulated by membrane-localized metabolites of phosphatidylinositol (PI). Certain voltage-gated K⁺ (Kv) channels are particularly sensitive to binding of PI 4,5-bisphosphate, known as "PIP2" (Kruse et al., J Gen Physiol, 2012). Consequently, PIP2 levels can be an important determinant of neuronal excitability. Here we have assessed the contribution of PIP2 binding to the function of Spiral Ganglion Neurons (SGNs).

Methods

SGNs from juvenile C57BL/6 mice (P10-P21) were cultured for 2-3 days for whole-cell patch clamp recordings.

Results

Under control conditions ~70% of SGNs under current clamp fired rapidly-adapting ("phasic") action potentials, and the remaining cells were non-adapting ("tonic" firing). ~20% exhibited spontaneous action potentials at their resting membrane potential. Pre-incubation with 100 μ M Wortmannin, a non-specific enzyme inhibitor of PIP2 production (Suh & Hille, Curr Opin Neurobiol, 2005), resulted in an increase of the tonic firing population to ~50%, and spontaneous action potential firing to ~40%. The effects of Wortmannin treatment could be partially rescued by the inclusion of 100 μ M diC8-PIP2, a non-metabolized analogue of PIP2, in the patch electrode. Voltage clamp experiments suggested that Wortmannin treated cells displayed comparably smaller low voltage-activated (LVA) K⁺ current. In separate experiments, SGN were depleted of membrane-bound PIP2, by transient exposure to a membrane-targeting palmitoylated peptide ("pal-peptide") based on the putative PIP2 binding domain of the Kv7.2 channel (Robbins et al., J Neurosci 2006). Bath application of 1-3 μ M pal-peptide induced tonic firing in 33% of previously rapidly-adapting cells, and slowed adaptation in all the others. Under voltage clamp, the pal-peptide caused specific inhibition of the LVA K⁺ current. This current was also sensitive to dendrotoxin-K, suggesting it was carried by the Kv1 sub-family of channels (Mo & Davis, J Physiol, 2002). In some cells the pal-peptide activated transient inward currents, reminiscent of spontaneous Na⁺ currents.

Conclusion

PIP2 acts as an endogenous regulator of SGN excitability via activation of Kv1-type channels. Our observations suggest PIP2 binding may provide a physiological brake on the output of the auditory nerve, and identify phosphoinositide signaling as a novel putative therapeutic target in the cochlea.

PS - 339

Kv1.2 is a Key Regulator of Intrinsic Excitability in Post-Hearing Spiral Ganglion Neurons

Katie Smith; Lorcan Browne; David McAlpine; Daniel Jagger

University College London

Background

Type I Spiral Ganglion Neurons (SGNs) innervate cochlear inner hair cells and transmit action potentials to the auditory brainstem. In pre-hearing mice, the intrinsic excitability of the SGN population shows heterogeneity, with a contribution from rapidly-adapting and more slowly-adapting neurons (Mo & Davis, J. Neurophysiol., 1997). Rapid adaptation is associated with a Dendrotoxin-sensitive low voltage-activated (LVA) K⁺ current, implicating the involvement of voltage-gated K⁺ (Kv) channel subunits of the Kv1 subfamily (Mo et al., J. Physiol., 2002). Here we examined the potential involvement of Kv1.2 subunits in generating the LVA K⁺ current in post-hearing SGNs.

Methods

Whole-cell patch clamp recordings were performed on P12-P21 C57BL/6 mouse SGNs, cultured for 2-3 days *in vitro*. Immunofluorescence was performed on mouse cochlear sections and cultured SGNs to examine the spatio-temporal expression of Kv1 subunits.

Results

Current-clamp recordings performed on SGNs from animals both around the onset of hearing (P12-P14), and one week post-hearing (P20-P21), revealed the presence of rapidly-adapting and slowly-adapting neurons. Rapidly-adapting neurons were associated with prominent LVA K⁺ currents which had similar mean amplitudes between the two age groups. The subunit composition of the LVA K⁺ current was investigated using the Kv1.2 specific blocker, Tityustoxin-K α (TsTx; Werkman et al., Mol. Pharmacol., 1993). In P12-P14 SGNs, block of the LVA current by 100 nM TsTx was variable, ranging from ~30-80% (8/11 cells) with a subset of neurons that were insensitive. In all P20-P21 SGNs, 100 nM TsTx blocked the LVA current (by 45-80%; n = 6). The TsTx-insensitive current was examined further by the co-application of Dendrotoxin-K (DTX-K), which blocks Kv1.1 and Kv1.2. The extent of the additional block by DTX-K was variable in both age groups, suggesting further heterogeneity in the underlying TsTx-insensitive channels. In SGNs of both age groups under current-clamp, TsTx application could increase SGN excitability, characterized by lowered action potential threshold and increased action potential number. Consistent with the electrophysiological recordings, immunofluorescence localised Kv1.1 and Kv1.2 subunits to SGNs both *in situ* and

in vitro. By P20 the Kv1.2 subunits were expressed within the somatic plasma membrane, but more prominently in the proximal region of both peripheral and central neurites.

Conclusion

Kv1.2 subunits contribute to the LVA K⁺ current in post-hearing SGNs and so are key regulators of excitability of the auditory nerve.

PS - 340

Structural (Corrosion Cast) Analysis of Cochlear Blood Vessels in a Mouse Model of Age Related Hearing Loss.

Mattia Carraro¹; Robert V. Harrison²

¹The Hospital for Sick Children; ²Auditory Science Laboratory, Department of Otolaryngology, and Program in Neuroscience and Mental Health, The Hospital for Sick Children, Toronto, ON, Canada M5G 1X8; Institute of Biomaterials and Biomedical Engineering, University of Toronto, Toronto, ON, Canada M5S 1A1; Department of Otolaryngology-Head and Neck Surgery, University of Toronto, Toronto, ON, Canada M5S 1A1

Background

Many causes of age related hearing loss have been proposed including degenerative changes to cochlear vasculature. This is the basis for the concept of stria presbycusis. However a close relationship between auditory threshold changes and local vascular degeneration has not been clearly demonstrated. Here we quantify structural properties of stria vascularis and its supply vessels along the cochlear length in a mouse model of presbycusis using corrosion cast methods. Cochleotopic patterns of vasculature are compared with local cochlear function based on frequency specific ABR thresholds.

Methods

We used 2 age groups of C57BL/6 mice (<2 weeks and 32-36 weeks old). This strain has previously been employed as an animal model for presbycusis. Frequency specific cochlear function was monitored using ABR threshold measures to tone pip stimuli. Cochlear vasculature was visualized using a corrosion cast technique. Briefly, after aortic cannulation, heparinization and blood wash-out, Mercor polymer was infused at normal physiological pressures through arterial and venous vessels. After polymerization, tissue was digested with KOH 16% and EDTA 10%. Novel manipulations of specimens (partial corrosion methods to maintain specimen integrity and removal of vessels feeding spiral ligament) were employed to allow accurate quantification of stria vascularis and supply vessels from scanning EM images.

Results

In preliminary data we generally observe that basal stria vascularis has a more sparse capillary blood system. Specifically, in the basal regions of old (32-36 week) mice we find a significant reduction in the stria capillary vessel diameter and a less dense capillary network compared with more apical cochlear regions.

Conclusion

Stria capillary vessel diameters and the capillary network density appears to be reduced at the cochlear base compared with upper turns in old (32-36 week C57BL/6) mice compared with young animals. The relationship between such morphological features and functional hearing loss will be further evaluated.

PS - 341

Progressive Hearing Loss, Supernumerary Outer Hair Cells and Degeneration of Multiple Cochlear Cells in NOD/SCID-Il2Rg^{null} Mice

Yazhi Xing; Nancy Smythe; Juhong Zhu; Bradley Schulte; Hainan Lang

Medical University of South Carolina

Background

NOD/SCID-Il2Rg^{null} (NSG) mice, which do not express the X-linked *Il2rg* gene, have been widely used as a xenotransplantation model for *in vivo* studies of adult human stem cells. In this study, we examined auditory function and cochlear morphology in early postnatal, young adult and aged NSG mice.

Methods

Auditory function in NSG mice was evaluated via auditory brainstem response (ABR) measurements at postnatal days 14 and 21 and in 3 month and 1 year old mice. Cochleas were processed for flat surface preparations or frozen sectioning. Similarly aged CBA/CaJ mice were used as normal controls. Hair cells were counted by labeling with myosin VIIa antibody or phalloidin. Neurofilament 200 (NF200) antibody was used to identify spiral ganglion neurons (SGNs) and their processes. The efferent components of the auditory nerve were labeled with choline acetyltransferase (ChAT) antibody. Ultrastructural features of the NSG mouse cochlea were examined by transmission electron microscopy (TEM).

Results

Hearing loss was seen in NSG mice beginning at postnatal day 21. ABR wave I input/output function analysis indicated a progressive decline of function until the auditory nerve response totally disappeared at 2 month of age. Supernumerary outer hair cells (OHCs) were scattered sporadically along the apical and middle turns (76 spots in 13 ears). Among all of the extra OHCs, 43.4% (33/76) had 2-4 extra hair cells together, 34.2% (26/76) had 5-7 extra hair cells in a row and 22.4% (17/76) had more than 8 extra hair cells. OHC losses were seen in the basal turns of mice aged 2 months and older. A significant loss of type I SGNs and afferent nerve fibers in young adult and aged mice was documented by both immunohistochemistry and TEM. Ultrastructural changes in the lateral wall of young adult and aged NSG mice included a loss of integrity of marginal cells and enlarged spaces separating intermediate cells from marginal and basal cells.

Conclusion

Sensory hair cell and SGN losses along with pathological changes in the lateral wall contribute to a severe hearing

loss in NSG mice, suggesting that the innate immune system may be involved in the maintenance of multiple cell types in the mouse inner ear. In addition, NSG mice may be a useful model for studies of the determination of hair cell number and arrangement in the cochlea.

PS - 342

High Dose, Local Application of Gentamicin Induces a Total Hair Cell Loss in Cochlear and Vestibular System

Jintao Yu^{1,2}; Dalian Ding¹; Haiyan Jiang¹; Hong Sun²; Richard Salvi¹

¹University at Buffalo; ²Xiangya Hospital of Central South University

Background

Contemporary studies of hair cell regeneration and programmed cell death often seek to induce complete destruction of the sensory hair cells in the cochlear and/or vestibular system while preserving the neurons that innervate the sensory epithelium. Aminoglycoside antibiotics (AG) can be used to selectively destroy the sensory hair cells, while preserving the neurons in the inner ear. Hair cell lesions can be induced with systemic AG treatment, but the lesions develop slowly and are often incomplete or unpredictable. Combination treatments with AG and diuretics, which disrupt the blood-labyrinth barrier, can lead to a complete loss of cochlear hair cells, but spares the vestibular hair cells.

Methods

Local application of AG to the round window membrane is an effective alternative and eliminates systemic toxicity problems; however, moderate AG doses often lead to incomplete inner ear damage. In an effort to produce near total loss of hair cells in both cochlear and vestibular system, a large volume and high concentration (40 mg/ml) of gentamicin was unilaterally injected through the tympanic membrane to fill the middle ear cavity in guinea pigs.

Results

AG treatment abolished the vestibular nystagmus response (VNR) and compound action potentials (CAP) in the treated ear, but the VNR and CAP were normal in the untreated ear. Two days after treatment, animal exhibited obvious head tilt in the direction of the treated ear. Head position gradually was nearly normal 7-10 days post-treatment, but animals showed obvious balance disorder while swimming. Anatomical analysis revealed complete hair cell loss in both cochlear and vestibular end organs in AG-treated ears

Conclusion

Transtympanic administration of a high concentration of AG could be a useful method for completely destroying cochlear and vestibular hair cells in studies aimed at investigating hair cell regeneration, hair cell death and delayed degeneration of cochlear and vestibular neurons

PS - 343

Metabolome Analysis of Inner Ear Fluid in Guinea Pigs Cochlea After Intense Noise

Daisuke Yamashita; Yuriko Fukuda; Takeshi Fujita; Hitomi Shinomiya; Go Inokuchi; Shingo Hasegawa; Naoki Otsuki; Ken-ichi Nibu

Kobe University

Background

The metabolome analysis is to analyze metabolites resulting from all cellular activity to have of the organism cyclopedically. The intracellular dynamics which are not understood by expression of mRNA and proteome analysis are found by the profile of the metabolome analysis. Various clinical conditions such as cancer and immune disease have been recently apparent by metabolome analysis with many organs and tissues. This time we examined metabolome analysis of inner ear fluid in guinea pigs cochlea after intense noise using gas-chromatography/mass-spectrometry (GC/MS).

Methods

Eighteen pigmented guinea pigs (250-300g; Hartley male) with normal Preyer's reflex were used in this study. The experimental protocol was approved by the Animal Care and Use Committee at the University of Kobe. Animals were exposed to one octave band noise (OBN) centered at 4 kHz, at 120-dB SPL for 5 h. Assessments were performed prior to and on immediately, Days 1, 3, 7 after intense noise. After animals were deeply anesthetized decapitated, the temporal bones were immediately removed. Under a dissecting microscope, the round and oval windows were opened and the lymphatic fluids were taken. At the same time decapitating, plasma fluid were also taken. We extracted water-soluble metabolite from the inner ear lymphatic and plasma fluids. After freeze dry and a process of derivatizing, metabolites were measured with GC/MS-QP2010. The obtained data examined the metabolite by principal component analysis.

Results

As control, twenty-nine kinds of metabolites that were specific for the inner ear fluid of guinea pig cochlea were detected. Amino acids, carbohydrates and hydroxy-acids accounted for approximately two-thirds of the metabolites. We identified seven metabolites that were more abundant in inner ear fluid than in plasma; these metabolites included ascorbic acid, inositol, galactosamine, fructose, glutamine, pyruvate+oxalacetic acid ($p < 0.01$), and lactic acid ($p < 0.05$). Results of metabolite after intense noise will be shown at poster.

Conclusion

The present study reports for the first time that metabolome analysis of the inner ear. As results, it was detected 29 kinds in total, for the metabolite which was specific for inner ear fluid of cochlea. Also, the metabolite, which was significantly frequent in inner ear fluid compared to plasma, was detected totally seven kinds. It seems that these results lead to clinical condition elucidation of the sensorineural hearing loss including noise-induced hearing loss for a diagnostic tool and treatment therapy.

Human Spiral Ganglion Neuron Survival is Independent of Supporting Cells in the Organ of Corti

Joni Doherty¹; Fred H. Linthicum, Jr.¹; Michael Hoa²

¹House Research Institute; ²NIDCD

Background

In animal models, spiral ganglion neurons (SGN) degenerate up to 95% within a few weeks after the loss of organ of Corti (OC) elements, including hair cells (HC) and supporting cells (SC), but human SGN are much less affected by such losses, and many survive eighty or more years after deafness. Recently, research using a mouse model has suggested that SC are responsible for SGN survival through the maintenance of peripheral neurites. We sought to determine whether evidence supports such a relationship in humans.

Methods

Histopathology of 30 routinely processed human temporal bones (hTB) were studied under light microscopy: HC, SC, and SGN counts as well as OC and SC volume measurements were correlated.

Results

Twenty-five hTB demonstrated surviving SGN despite absent OC elements. Average age at death was 74.1 years (range: 51-93). Average duration of hearing loss prior to death was 16.7 years (range: 2-32). The volume of remaining SC in the bones with no surviving neuritis ranged from 0 to 3.4, with a mean of 0.99, while the mean normal SC volume was 5.07 (range 3.7 to 7.0; $p \leq .001$). SC volume was not related to age at death, years of deafness or percent remaining spiral ligament. SC volume correlated with percent remaining stria vascularis ($r=.54$, $p \leq .006$). SGN counts had no correlation to remaining SC volume ($r=.04$, $p > .85$, NS). Complete eradication of the OC by fibrosis or ossification was observed in four hTB that had a population of up to 17,415 SGN.

Conclusion

The tenacity of human spiral ganglion cells to survive the loss of input from any of the elements of the organ of Corti helps to explain why the cochlear implant remains functional for the lifetime of the recipients.

Immunocytochemical Localization of Cubilin and Megalin in the Human Inner Ear

Seiji Hosokawa¹; Kumiko Hosokawa¹; Ivan Lopez²; Gail Ishiyama³; Akira Ishiyama²

¹(1) David Geffen School of Medicine, University of California, Los Angeles (2) Hamamatsu University School of Medicine; ²(1) David Geffen School of Medicine, University of California, Los Angeles; ³(3) Department of Neurology, David Geffen School of Medicine, University of California, Los Angeles

Background

Cubilin and megalin are multiligands with endocytotic receptors expressed in many absorptive epithelia. These receptors are structurally very different, and each binds distinct ligands

with different affinities, and may act in concert. In recent years, much information about the physiological role of these receptors has come from targeted gene-knockout animal models of receptor dysfunction. Cubilin and megalin distribution is well documented in the inner ear of several animal models but not in the human inner ear. In this study we determined the immunolocalization of megalin and cubilin in the human inner ear.

Methods

We used microdissected human cochlea frozen sections obtained from temporal bones from subjects with a documented history of normal auditory and vestibular function ($n=5$ ages 75-95 years old, male and female). Formalin-fixed celloidin-embedded (FFCE) human temporal bone sections ($n=6$, ages 65-83 years old, male and female) were also used in this study. For immunocytochemistry we used a goat polyclonal antibody against cubilin and rabbit polyclonal antibody against Megalin. Temporal bone removal, inner ear tissue processing and immunocytochemistry methods have been described in detail (Balaker AE, Anat Rec, 296:326-332, 2013).

Results

In the cochlea, cubilin Immunoreactivity (IR) was seen at the apical surface of the stria marginal cells, epithelial cells at the spiral prominence and epithelial cells of Reissner's membrane. Megalin-R was also detected in epithelial cells of the endolymphatic sac. In vestibular endorgans, cubilin-IR was found in dark cells of the utricle and those flanking the crista ampullaris of the semicircular canals. Megalin-IR, followed a similar IR patterns as observed for cubilin was observed in the same epithelial cells. Frozen and celloidin sections showed a similar pattern of Megalin and cubilin immunoreactivity.

Conclusion

Cubilin and megalin colocalize in epithelial cells on the human inner in a similar pattern as reported in the inner ear of animal models, and suggest that both proteins may play important roles in inner ear homeostasis.

Immunocytochemical Expression of Nuclear Factor Erythroid 2-Related Factor 2 (Nrf2) in the Human Inner Ear and the Changes With Aging

Kumiko Hosokawa¹; Seiji Hosokawa¹; Ivan Lopez²; Gail Ishiyama³; Akira Ishiyama²

¹(1) David Geffen School of Medicine, University of California, Los Angeles (2) Hamamatsu University School of Medicine; ²(1) David Geffen School of Medicine, University of California, Los Angeles; ³(3) Department of Neurology, David Geffen School of Medicine, University of California, Los Angeles

Background

Nuclear (erythroid-derived 2)-like 2, or Nrf2, is a transcription factor encoded by the NFE2L2 gene. The expression of several antioxidant enzymes is regulated by this transcription factor. Nrf2 is induced by oxidative stress. Oxidative stress in a physiological setting occurs when there is an excessive bio-

availability of reactive oxygen species (ROS), which is the net result of an imbalance between production and destruction of ROS. We investigate the expression of Nrf-2 in the normal and pathological human inner ear. A component hypothesis is that changes in the expression of Nrf-2 could confer cellular protection and prevent deterioration of the inner ear during age related diseases or chronic conditions like Meniere's disease.

Methods

Formalin-fixed celloidin-embedded (FFCE) human temporal bone sections were immunoreacted with rabbit primary antibodies against Nrf2. Temporal bone removal, inner ear tissue processing and immunocytochemistry methods have been described in detail (Balaker AE, Anat Rec, 296:326-332, 2013). In this study we used 32 temporal bones of 24 male and female patients, average age 65 years old (11 normal auditory function, 5 Meniere's disease, and 16 other otological diseases). Image acquisition and quantitative immunohistochemical analyses were made using micrographs acquired at 200x. The immunoreacted area was quantified using the computer image analysis software ImageJ. Univariate analysis of variance analysis (ANOVA) was performed to test an association between the variables "Age <70 years-old Group" and "Age 70< years-old Group". Post-hoc individual univariate group comparisons were made for any significant results. A p value of 0.05 was used in all statistical tests for establishing significance.

Results

Nrf2 immunoreactivity (IR) was detected in the organ of Corti at the basal, middle, and apical turn of the cochlea. Nrf2-IR was present in sensory hair cells and supporting cells. Cells in the spiral prominence were also Nrf2-IR. Nrf2-IR was not present in the stria vascularis and spiral ganglia neurons. Nrf2-IR was present in sensory hair cells and supporting cells of the macula utricle, saccule and cristae ampullaris. Nrf2-IR was not seen in vestibular ganglia neurons. Nrf2-IR decreased in the organ of Corti of older age individuals. There was a statistically significant difference between the "Age <70 years-old Group" and "Age 70< years-old Group" ($p=0.037$).

Conclusion

Nrf2 expression in sensory hair cells and supporting cells of the inner ear suggest that Nrf2 may protect the inner ear in different pathological conditions and that a decrease in its expression with age maybe detrimental.

PS - 347

The Expression of Glutamate Aspartate Transporter (GLAST) Within the Human Cochlea and its Distribution in Various Patient Populations

Sameer Ahmed¹; Nopawan Vorasubin²; Ivan Lopez²; Seiji Hosokawa²; Gail Ishiyama³; Akira Ishiyama²

¹David Geffen School of Medicine, University of California—Los Angeles; ²Department of Head and Neck Surgery, David Geffen School of Medicine, University of California—Los Angeles; ³Department of Neurology, David Geffen School of Medicine, University of California—Los Angeles, Los Angeles

Background

Glutamate plays an important role in the central nervous system as an excitatory neurotransmitter. However, its abundance can lead to excitotoxicity which necessitates the proper function of active glutamate transporters. The glutamate-aspartate transporter (GLAST) has been shown to exist and function within non-human cochlear specimens regulating the inner ear glutamate concentration. However, no studies have been done examining GLAST in the human cochlea. And since mice and rats are not perfect analogues to humans, it was conceivable that differences in GLAST expression could be found between humans and non-human species.

Methods

In this study, we examined micro-dissected human cochleas from formalin-fixed celloidin-embedded temporal bone specimens of three different types of patients (Meniere's disease, normal controls, and other otopathologic conditions) and examined the differential expression of GLAST in the spiral ligament of the basal, middle, and apical turns of the cochlea. Immunohistochemical staining was performed with polyclonal antibodies against GLAST and image analysis was carried out with the Image J analysis software.

Results

In contrast to other studies with non-human specimens, GLAST was expressed in the spiral ligament fibrocytes but was not detected in the satellite cells of the spiral ganglia or supporting cells of the organ of Corti in the human cochlea. Our data also showed that GLAST expression significantly differs in the basal and apical turns of the cochlea. Lastly, post-hoc analysis showed a difference in the GLAST immunoreactive area of patients with Meniere's disease when compared to that of patients with other otopathologic conditions—such as presbycusis or ototoxicity.

Conclusion

Glutamate clearance is vital in maintaining cochlear homeostasis. Our study is the first to demonstrate GLAST in fibrocytes of the spiral ligament of the human cochlea. In contrast to previous studies done on non-human specimens, GLAST was not found in the satellite cells of the spiral ganglia or in the supporting cells of the Organ of Corti. We have shown that intra-cochlear location correlates with the total immunoreactive area of GLAST. These results may potentially lead

to further understanding of different disease states that affect hearing.

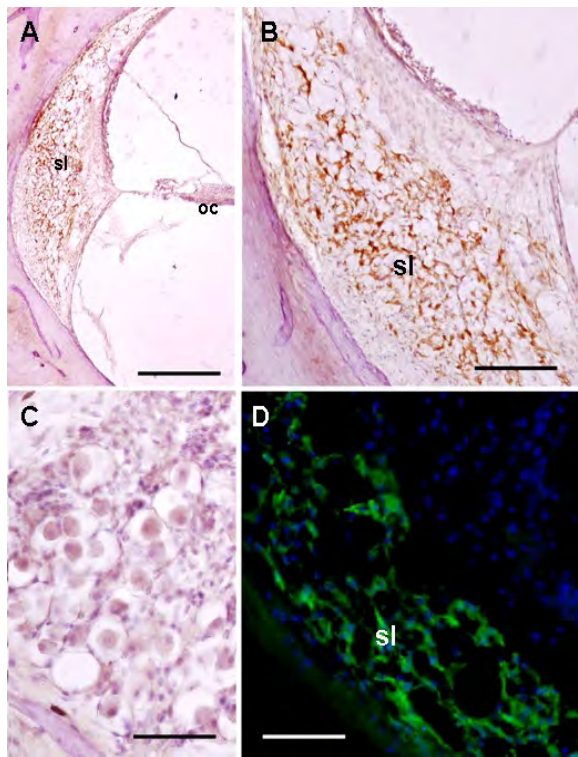


Figure 1: GLAST Expression in the human cochlea. **A.** Low magnification of the human cochlea showing GLAST in the spiral ligament (sl) but not in the Organ of Corti (oc). **B.** Higher magnification view showing GLAST in the spiral ligament fibrocytes (amber color). **C.** The spiral ganglia showed no immunostaining for GLAST. Nuclei were counterstained with hematoxylin in Figs A, B, and C. **D.** GLAST immunofluorescence (green) in the human spiral ligament. The cell nuclei were stained with DAPI (blue). The rabbit secondary antibody was tagged with Alexa 488 in a protocol described by Balaker et al (2013). Magnification bar in Fig. A: 500 μm ; Fig. B: 200 μm ; Figs. C and D: 100 μm . sl: spiral ligament; oc: Organ of Corti.

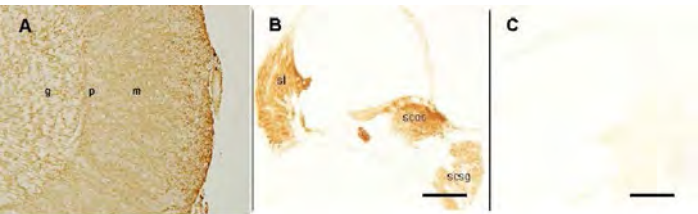


Figure 2: Control specimens for GLAST-IR. **A.** A section of human cerebellum stained for GLAST serves as a human positive control. The immunoreactive staining is strongest in the molecular layer (m) of the cerebellum. **B.** A section of mouse cochlea stained for GLAST serves as a mouse positive control. The spiral ligament (sl), satellite cells of the spiral ganglia (scsg), and supporting cells of the Organ of Corti (scoc) all stained positive. **C.** Mouse negative control. The primary GLAST antibody was omitted and no immunoreactivity was seen in the mouse cochlear tissue. g: granular cell layer; p: Purkinje cell layer; m: molecular cell layer; sl: spiral ligament; scsg: satellite cells of the spiral ganglia; scoc: supporting cells of the Organ of Corti. Magnification bar is 150 μm for all figures.

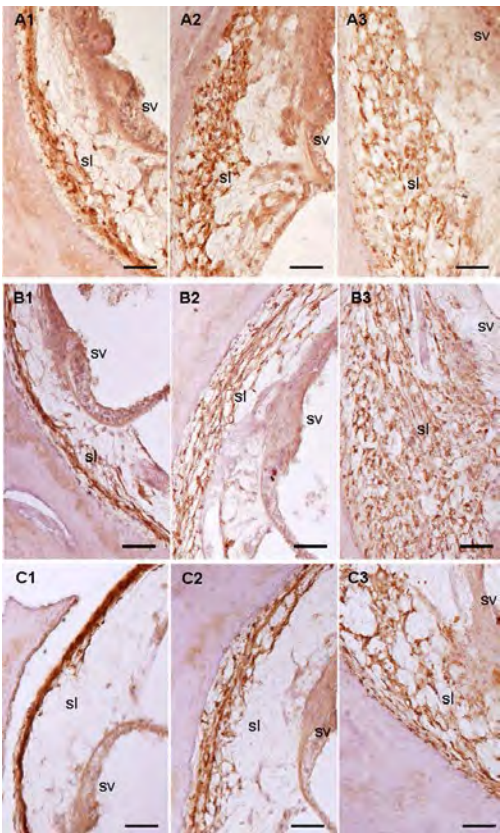


Figure 3: Distribution of GLAST in formalin-fixed celloidin-embedded temporal bone sections of different patients. **A1-A3:** GLAST-IR in the cochlea of a patient in the "Normal" group (75 year-old female without any hearing problems). GLAST-IR was localized to the spiral ligament in the apical (**A1**), middle (**A2**), and basal (**A3**) turns of the cochlea. **B1-B3:** GLAST-IR in the spiral ligament of the apical (**B1**), middle (**B2**), and basal (**B3**) turns of the cochlea of a patient in the "Meniere's disease" group (83 year-old female with a 20 year history of Meniere's disease). **C1-C3:** GLAST-IR in the spiral ligament of the apical (**C1**), middle (**C2**), and basal (**C3**) turns of the cochlea of a patient in the "Other" group (80 year-old male with a 15 year history of presbycusis). Magnification bar is 80 μm for all figures.

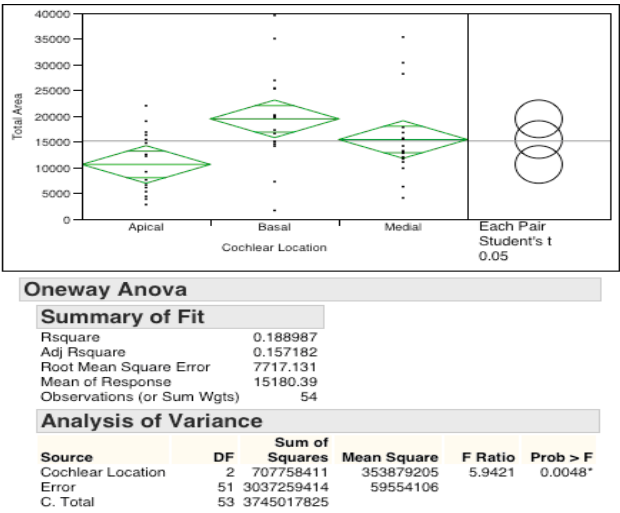


Figure 4: ANOVA One Way Analysis of Total GLAST-IR Area by Cochlear Location.

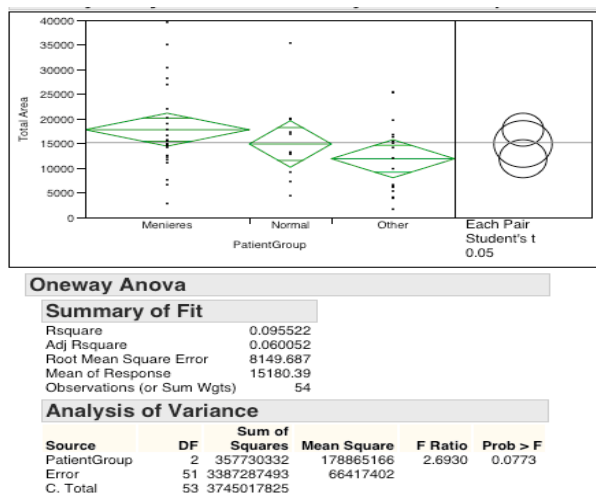


Figure 5: ANOVA One Way Analysis of Total GLAST-IR Area by Patient Grouping.

PS - 348

Localization of Fatty Acid-Binding Protein 7 (Fabp7) in the Vestibular Organ in Mice.

Hiromitsu Miyazaki¹; Jun Suzuki²; Izumi Yahata²; Iori Takata²; Yusuke Takata²; Noriko Osumi³; Tetsuaki Kawase⁴; Yukio Katori²

¹*Tohoku University Graduate School of Medicine;*

²*Department of Otolaryngology, Head and Neck Surgery, Tohoku University Graduate School of Medicine;* ³*Division of Developmental Neuroscience, Tohoku University Graduate School of Medicine;* ⁴*Laboratory of Rehabilitative Auditory Science, Tohoku University Graduate School of Medicine*

Background

Fatty acid-binding proteins (Fabps) are known as intracellular carriers of unsaturated fatty acid, such as docosahexaenoic acid (DHA). Fabps function as a metabolic regulator, a controller of phospholipid membrane constitution, a regulator of transcription and so on. A recent study showed that Fabp7 is expressed in the mouse cochlea and revealed that Fabp7 deficiency slows the progression of age-related hearing impairment (poster presentation on this ARO meeting, Jun Suzuki). However, localization of Fabp7 in the vestibular organ has not been studied yet. In the present study, we show Fabp7 expression in the mouse vestibular organ by using immunohistochemistry.

Methods

We used adult C57BL/6 mice at 2 months of age. Anesthetized mice were transcardially perfused with cold PBS and 4% PFA. Their cochleae were removed and were post-fixed in 4% PFA. The fixed cochleae were decalcified in 10% EDTA. After sequential treatment in a graded series of 10% and 30% sucrose, the tissues were embedded in O.C.T. compound and were frozen. Sections 10 µm in thickness were cut on a cryostat. Using these tissue sections, we investigated the ampulla of semicircular canal, the otolith organ, and the vestibular ganglion by immunohistochemistry with antibodies to Fabp7, Tuj-1, s-100 beta, Sox2, and Myosin 7a.

Results

The results of immunohistochemistry showed that Fabp7 was expressed in the Tuj-1-negative Schwann cells and s-100 beta-positive stromal cells at the ampulla and the otolith organ, and was localized in the Tuj-1-negative satellite cells of the vestibular ganglion.

Conclusion

The current study revealed that Fabp7 is expressed in non-hair cells or non-neuronal cells in the vestibular organ as well as in the cochlea. Considering the protective effects of Fabp7 deficiency against the cochlear degeneration, the lack of Fabp7 could also relieve the age-related vestibular dysfunction.

PS - 349

Molecular and Developmental Analysis of a Cochlear HPA-Equivalent Signaling System

Douglas Vetter; Kathleen Yee

Univ. Mississippi Medical Center

Background

We previously described expression of hypothalamic-pituitary-adrenal (HPA) axis-related proteins in the mouse cochlea. This included pro-opiomelanocortin (POMC), adrenocorticotrophic hormone (ACTH), melanocortin 2 receptor (MC2R), corticotropin releasing factor (CRF), and the CRF receptors (CRFR1 and CRFR2). Ablation of CRFR1 results in structural and functional deficits, including smaller inner hair cells, abnormal afferent innervation to those cells, and a significant increase in ABR thresholds. Conversely, a significant decrease in ABR thresholds, accompanied by a greater susceptibility to noise-induced hearing loss, occurred in CRFR2 nulls. Despite local expression of HPA-like signaling molecules in the cochlea, it remained unknown whether the cochlea is capable of local synthesis and release of its own glucocorticoids, or whether glucocorticoids affecting cochlear processing were derived only from adrenal release. The significance of this issue lies in our hypothesis of cochlear HPA-like signaling, that it is a mechanism for local response to cellular stress, and thus not tied to systemic HPA activity. A major test of this hypothesis is a determination of whether the cochlear HPA-equivalent system functions locally to release bioactive steroids.

Methods

In our studies, we used standard ELISA analysis of culture media conditioned by cochlear ex vivo cultures to study release of corticosterone. To follow development and expression of the corticosterone biosynthetic pathway in the cochlea, standard immunostaining techniques and CRFR1 null mutant and CRFR1-GFP- BAC transgenic mouse lines were used.

Results

ELISA analysis revealed spontaneous and CRF-inducible ACTH and corticosterone release from the cochlea as early as P7 that continues throughout adulthood. Release is fully dependent on cochlear expression of CRFR1. CRFR1 null mice do not spontaneously release ACTH or corticosterone from cochlear tissue or in response to application of CRF. We

also investigated expression of steroid signaling-related molecules in the cochlea. 11-beta HSD2, which degrades corticosterone, and corticosterone-binding globulin, which binds free corticosterone, are expressed in the cochlea. Using a BAC transgenic mouse expressing GFP under the control of the CRFR1 promoter, we determined the time course of cochlear CRFR1 expression. At P0.5, only the extreme apex of the cochlea expresses CRFR1, but by P7, all turns express CRFR1. However, unlike adult (2-3 month) stages, early CRFR1 expression is limited to support cells around the outer hair cell field. Kölliker's organ, postulated to control spontaneous activity prior to hearing onset, seems to not express CRFR1.

Conclusion

Thus, the mammalian cochlea expresses a functional local HPA-like signaling system and is able to synthesize and release corticosteroids.

PS - 350

Low-Periodicity, Low-Amplitude Micropatterns Exert Greater Influence on Spiral Ganglion and Trigeminal Ganglion Neurite Guidance Than a Repulsive Biochemical Interface

Daniel Lee¹; Linjing Xu²; Bradley Tuft³; Allan Guymon³; Marlan Hansen²

¹University of Iowa Carver College of Medicine;

²University of Iowa Hospitals and Clinics - Department of Otolaryngology - Head and Neck Surgery; ³University of Iowa - Department of Chemical Engineering

Background

Directing nerve fiber regrowth towards a neural prosthesis may help overcome the limitations imposed by poor integration of the prosthesis with the target neurons. In particular, regrowth of spiral ganglion neuron (SGN) afferent fibers towards stimulating electrodes would likely reduce current spread and improve spatial resolution provided by current cochlear implant electrode designs. We recently demonstrated that micropatterns consisting of parallel ridges and grooves direct SGN neurite growth, thus raising the possibility that topographic features, which are inherently stable and amenable to facile fabrication, could be used to precisely guide SGN neurite growth. Here, we used a competition assay to assess the relative contribution of topographical and chemorepulsive cues on SGN and TGN neurites.

Methods

Photopolymerization of methacrylate polymers was used to generate micropatterned polymer substrates that have parallel ridge-groove features of 1.5 μm amplitude and periodicities of 10-50 μm . Micropatterned substrates were formed in a single-step reaction by selectively blocking light with photomasks which have parallel line-space gratings. Feature amplitude is controlled by light exposure time and photoinitiator concentration, while periodicity is controlled by varying photomask periodicity. A perpendicular chemorepulsive border consisting of an interface of laminin and tenascin-c was applied to the polymer surface. Rat SGNs and TGNs were cultured on these polymers and neurite behavior was cate-

gorically described at the chemical border. When neurites cross this repulsive border, it implies dominance of the physical features of the polymer substrate over the biochemical border.

Results

On unpatterned surfaces, the majority of SGN and TGN neurites either stalled or were repelled, failing to cross the laminin/tenascin-C border, confirming that it functions as a chemorepulsive cue. Neurites cultured on micropatterned surfaces lacking the laminin/tenascin-C border aligned to the micropatterned surface with neurite growth that parallels the pattern. In cultures plated on micropatterned surfaces with the laminin/tenascin C border, the proportion of neurites that crossed the chemorepulsive border increased significantly with decreasing feature periodicity at constant amplitude. Conversely, significantly fewer neurites crossed the border on pattern with higher periodicities. These results indicate that physical topographic features on polymer substrates dictate neuronal guidance at low periodicities while biochemical cues prevail at higher periodicities.

Conclusion

On low-periodicity, low-amplitude micropatterns, physical topographic cues direct neurite guidance. These features may be used to direct neurite growth with increased specificity for cochlear implants and other neural prostheses.

PS - 351

Using Cre-LoxP Mouse Genetics to Target Specific Cochlear Supporting Cell Subtypes

Joseph Brancheck; Brandon Cox

Southern Illinois University School of Medicine

Background

When compared to our knowledge of hair cell (HC) physiology, relatively little is known about the differences among supporting cell (SC) subtypes and the roles each subtype plays in normal and pathological conditions. The known SC subtypes in the cochlea include Claudius' cells, Hensen's cells, Deiters' cells (DC), pillar cells (PC), inner phalangeal cells (IPhC), and cells of the greater epithelial ridge. Development of SC subtype-specific CreER alleles would provide important tools for the field, allowing gene deletion, ectopic gene expression, and fate mapping of individual subtypes. Previously published CreER lines that target SCs have Cre expression in multiple subtypes and some even show Cre expression in HCs (Cox et al., 2012); however, these findings are based on tamoxifen induction paradigms (TIPs) that are quite robust. Altering the tamoxifen concentration and number of injections can decrease the Cre expression pattern and increase cell-type specificity. There are also several reporter alleles which have different expression patterns even when the same CreER line and TIP are used. I hypothesize that altering both the TIP and reporter allele will modify the Cre expression pattern in existing CreER mouse lines to become specific to certain SC subtypes.

Methods

We will use the following CreER alleles known to have expression in SCs at neonatal ages (FGFR3-iCreER, Prox1-CreER,

Sox2-CreER, and Plp-CreER) in combination with one of three different reporter alleles (CAG-eGFP, ROSA26^{CAG/tTomato}, or ROSA26^{LacZ}). We will alter previously published TIPs to decrease both the tamoxifen concentration and/or number of injections to increase specificity.

Results

When Plp-CreER; ROSA26^{CAG/tTomato} mice were injected with tamoxifen (3mg/40g) at postnatal day (P)0 and P1, tdTomato expression was present in 5-10% of DC and PC and 50% of IPhC (Cox et al., 2012). By instead using a Plp-CreER; CAG-eGFP mouse and giving tamoxifen (3mg/40g) at P0 only, we found GFP expression in approximately 2.5% of DC and 1.5% of PC while still labeling 32% of IPhC. Similar experiments using other reporter alleles and modified TIPs with FGFR3-iCreER, Prox1-CreER, and Sox2-CreER lines are underway.

Conclusion

Development of SC subtype-specific CreER mouse models would allow for fate mapping of individual subtypes, as well as targeting specific subtypes for gene deletion or ectopic gene expression. This would provide powerful tools to the hearing field to increase our knowledge of SC subtype roles and plasticity. More importantly, it would provide a means to exploit these differences through targeted gene modification.

PS - 352

KCNE4 Auxiliary Beta Subunit Modulates Kv7.4 Channel to Generate IK,n in Cochlear Outer Hair Cells

Choong-Ryoul Sihh¹; Hyo Jeong Kim¹; Jeong-Han Lee¹; Karen Jo Doyle Doyle²; Ebenezer Yamoah¹

¹University of California, Davis, School of Medicine, Center for Neuroscience; ²UC Davis Health system

Background

Kv7.4, a voltage gated potassium channel, is highly expressed in outer hair cells (OHCs) and spiral ganglion neurons of the inner ear. Mutations in Kv7.4 are associated with DFNA2, an autosomal dominant nonsyndromic hearing loss (ADNHL). In cochlear OHCs, Kv7.4 channels (which generate IK,n) are located on the basal membrane to mediate the outflow of potassium ions. IK,n tends to be highly activated, even in the hyperpolarized potentials where the half activation voltage is around -85 to -95 mV. In contrast, when Kv7.4 is expressed in heterologous systems, its half activation voltage is ~-15 mV. It is assumed that Kv7.4 requires other auxiliary subunits to confer the native OHCs current phenotype. The goal of this study was to identify potential binding partners of Kv7.4.

Methods

We used electrophysiological and biochemical strategies in this study.

Results

Among the potential candidates, we identified KCNE4 to have a strong interaction with Kv7.4 channels in CHO cells. Additionally KCNE4, when expressed with Kv7.4, mediates a large negative shift in voltage dependence of the current. Moreover, we have observed apparent co-expression of

Kv7.4 and KCNE4 from whole mount preparations and cryosections of cochleae. We will demonstrate that gene knock-down of KCNE4 in OHCs produces a rightward shift in the voltage-dependence activation of IK,n in OHCs, raising the possibility that the interaction between KCNE4 with Kv7.4 contribute towards the properties of IK,n in OHCs.

Conclusion

We suggest that functional association between Kv7.4 and KCNE4 suffices to produce IK,n in cochlear OHCs.

PS - 353

Biochemical, Biophysical and Cellular Characterization of P2X2 Function *In Vitro* and in Zebrafish Model.

Rahul Mittal¹; M'hamed Grati¹; Denise Yan¹; Zhongmin Lu²; Xi Lin²; Yanbin Zhang³; Xue Zhong Liu¹

¹University of Miami Miller School of Medicine, Department of Otolaryngology, Miami, FL 33136, USA; ²Department of Biology, University of Miami, Miami, FL 33146, USA;

³University of Miami Miller School of Medicine, Department of Biochemistry, Miami, FL 33136, USA

Background

Hearing loss is one of the most common disorders affecting humans. Our previous studies have demonstrated that mutation p.V60L occurring at the end of the first transmembrane domain of the ATP-gated P2X2 receptor (ligand-gated ion channel, purinergic receptor 2) cause hearing loss and increased susceptibility to noise. Moreover, p.G353R mutation of the "gate" residue of P2X2 has been found to cause dominant hearing loss in an Italian family. The aim of the present study was to examine the effects of these two mutations on the ATP-binding properties and the cationic permeability of the trimeric P2X2 receptor *in vitro*, as well as their respective effects on the development and operation of the hair cell mechanotransduction in zebrafish model.

Methods

The ability of wild-type (WT) and mutant P2X2 to bind ATP was characterized by biochemical assays. The targeting properties of WT and mutant P2X2 was analyzed in biolistically transfected organotypic rat hair cells. Cationic permeability was determined by FM1-43X fluorescence labeling on polarized MDCKII cells expressing WT and mutated constructs of P2X2. Electrophysiological recordings of HEK293 cells expressing WT and mutated forms of P2X2 in the presence and absence of ATP were performed using patch-clamp technique. The expression of P2X2 was examined in 1 and 3 day post-fertilization (dpf) zebrafish embryos by whole mount *in situ* hybridization. Mutant constructs of P2X2 were generated and *in vitro* synthesized mRNA was injected into the zebrafish to observe the development of inner ear morphology using whole mount confocal microscopy, and to record the cochlear microphonics.

Results

Mutant P2X2 targets the stereocilia hair bundle as does WT form. ATP-induced FM1-43 fluorescence dye uptake was reduced in cells expressing mutated P2X2 forms compared to

WT form expressing cells. We observed that P2X2 is highly expressed in the otic vesicle of both 1 and 3 dpf zebrafish embryos. Expression and characterization of the effects of several P2X2 isoforms on zebrafish hearing is being investigated.

Conclusion

Both p.V60L and p.G353R P2X2 mutant forms target the hair cell stereocilia bundle, and found to cause a reduction in ATP-induced cationic permeability in MDCKII. Microinjection of synthetic mRNA encoding for both mutant isoforms in zebrafish would better decipher the morphological and physiological effects of these dominant mutations.

PS - 354

Spatio-Temporal Pattern of Action Potential Firing in Developing Inner Hair Cells of the Mouse Cochlea

Régis Nouvian¹; Gaston Sendin¹; Jérôme Bourien¹; François Rassendren²; Jean-Luc Puel¹

¹Institute for Neurosciences of Montpellier; ²IGF, CNRS UMR 5203 - INSERM U661

Background

Inner hair cells (IHCs) are the primary transducer for sound encoding in the cochlea. In contrast to the graded receptor potential of adult IHCs, immature hair cells fire spontaneous calcium action potentials during the first postnatal week. This spiking activity has been proposed to shape the tonotopic map along the ascending auditory pathway.

Methods

Here, we used the perforated patch-clamp recordings in a current-clamp mode ($I_{inj}=0$ pA) to probe the spontaneous activity of the developing IHCs (between P1 to P7) at room and body temperature.

Results

Immature IHCs fire spontaneous bursts of action potentials and the spiking behavior is similar between the basal and apical coils of the cochlea. In addition, the spiking activity in both apical and basal cells undergoes a developmental change, i.e., the bursts of action potential tend to occur at regular time interval. While the disruption of the purinergic signaling did not interfere with the AP firing pattern, pharmacological ablation of the alpha9-alpha10 nicotinic receptors elicited an increase of the discharge rate.

Conclusion

We therefore suggest that in addition to carrying place information to the ascending auditory nuclei, the IHCs firing pattern conveys a temporal signature of the cochlear development and we propose that this pattern is controlled by the alpha9-alpha10 receptor activity.

PS - 355

Maturation of Inner Hair Cell Calcium Signaling

Kuni Iwasa; JeeHyun Kong; Anthony Ricci
Stanford University

Background

Hair cells use ribbon synapses to transmit information at high rates for prolonged periods of time to the central nervous system. Previous data demonstrate that calcium channels cluster at presynaptic sites to rapidly regulate vesicle release properties. High speed calcium imaging suggests that calcium is released from internal stores upon depolarization and that this release may regulate rapid vesicle turnover. The present work investigated calcium signaling and release at different developmental stages in an attempt to isolate the steps in synaptic maturation.

Methods

Whole cell patch clamp recordings were made from rat inner hair cells during P3-P22. Fluo4ff was used to image calcium signals using two photon microscopy and simultaneously monitoring capacitance changes with the two sine wave technique. A mathematical model was formulated to reproduce the calcium signals at different developmental stages. A two chamber model was created where the first compartment is a region near the plasma membrane containing calcium channels and calcium pumps. The second chamber is more cytoplasmic and has a calcium activated calcium release mechanism. We assume that a fixed calcium buffer in the second compartment and that calcium diffusion depends on free calcium concentration as described by Wagner and Keizer (1994).

Results

Electrophysiological recordings demonstrate capacitance changes are weak at P3, presenting a single component while at P8 a more robust release was obtained including a second superlinear component. Release became stronger at P14 and by P22 appears mature with strong linear and superlinear components. Calcium imaging similarly showed rather diffuse changes at P3 that became more localized at P8 and older. A second stronger calcium signal appeared at P8 and 14. At P14 the two components of calcium signaling were tightly coupled. The two compartment model reproduced the experimental time course of calcium signals and their changes during development for a given level of stimulation. The model indicates that calcium induced calcium release appears around P8 and becomes more tightly coupled to calcium entry with maturation. Calcium influx is based on experimental values and unadjustable. A small initial step-like rise in the calcium signal near the plasma membrane is reproduced as an interplay between the calcium concentration dependence of calcium diffusion and calcium pumps.

Conclusion

Our study indicates that structural reorganization underlies the functional maturation of inner hair cells.

Intrinsic Disorder in the BK Channel and Its Protein Partners

Zhenling Peng¹; Yoshihisa Sakai²; Lukasz Kurgan¹; Vladimir Uversky²; Bernd Sokolowski²

¹University of Alberta; ²University of South Florida, Morsani College of Medicine

Background

The large-conductance Ca^{2+} -activated K^+ (BK) channel is broadly expressed in various mammalian cells and tissues and can be found in neurons, skeletal and smooth muscles, exocrine cells, and the inner ear. Due to its ability to encode negative feedback regulation of membrane voltage and Ca^{2+} signaling, it plays a central role in numerous physiological processes, including the regulation of action potential firing, neurotransmission, muscle contraction, secretion, and hearing sensitivity. Topologically, BK has seven membrane-spanning segments that form a pore and voltage sensor similar to the corresponding regions of K_v channels. In addition, it contains a long intracellular C-terminal domain that is important for Ca^{2+} -induced gating and an N-terminus that is located extracellularly. Previous studies suggest that BK channels are promiscuous binders that are involved in a multitude of protein-protein interactions.

Methods

To gain a better understanding of the potential mechanisms underlying BK interactions, we analyzed the abundance, distribution, and potential mechanisms of intrinsic disorder in 27 BK channel variants from the mouse cochlea and in 104, previously reported, BK-Associated Partners (BKAPS) from cytoplasmic and membrane/cytoskeletal regions. Disorder was evaluated using the MFDp algorithm, which is a consensus-based predictor that provides a strong and competitive predictive quality. Disorder-based binding sites or molecular recognition features (MoRFs) were found using the MoRFpred method. BKAP functions were categorized based on Gene Ontology (GO) terms.

Results

The analyses revealed that the BK variants contain a number of intrinsically disordered regions (IDRs). These are frequently affected by alternative splicing and posttranslational modifications, and contain multiple potential ligand binding and protein-protein interaction sites. Intrinsic disorder is also common in BKAPs, of which ~5% are completely disordered. Curiously, intrinsic disorder is very differently distributed within BK and its partners. Approximately 65% of the disordered segments in BK channels are long intrinsically disordered regions (IDRs) (>50 residues), whereas >60% of the disordered segments in BKAPs are short IDRs that range in length from 4 to 30 residues.

Conclusion

Intrinsic disorder is important for the function of BK and its protein partners. Long IDRs of this channel are engaged in protein-protein and protein-ligand interactions, contain multiple post-translational modification sites, and are subjected to alternative splicing. The disordered structure of BK and its

BKAPs provides one of the underlying mechanisms of their interaction.

PS - 357

Maintenance of Stereocilia and Apical Junctional Complex by Rho GTPase

Hirofumi Sakaguchi¹; Shigefumi Morioka¹; Takashi Nakamura¹; Takehiko Ueyama²; Naohisa Saito²; Yasuo Hisa¹

¹Kyoto Prefectural University of Medicine; ²Kobe University

Background

The sound-evoked mechano-electrical transduction takes place in cochlear hair cells via coordinated movement of stereocilia, specialized stable actin protrusions on their apical surface. The architecture of stereocilia is thus precisely determined by tightly regulated actin-turnover, although its mechanism is not fully understood. Here we focused on the role of a specific Rho GTPase in inner ear hair cells.

Methods

We employed inner ear hair cell (HC)-specific conditional knockout to analyze the role of a specific Rho GTPase in HCs. Hearing function was assessed by ABR and DPOAE measurement, and the ultrastructural morphology of HCs was analyzed by SEM and TEM. We also confirmed the localization and activation of the Rho GTPase in HCs using adenoviral expression of GFP-tagged protein and transgenic mice expressing fluorescence resonance energy transfer (FRET) biosensor. Using MDCK cells induced stable knockdown of the Rho GTPase as an in-vitro model of HCs, formation of microvilli and actin regulatory signaling were studied.

Results

HCs of the Rho GTPase-KO mice developed normally but progressively degenerated after maturation, resulting in progressive hearing loss particularly for high frequencies. Cochlear HC degeneration began as stereocilia fusion and depletion, accompanied with thinning and waving circumferential actin belt at apical junctional complexes (AJCs). Imaging of the GFP-tagged protein and the FRET biosensor indicated that this Rho GTPase was present and active at the stereocilia membranes and AJCs in cochlear HCs. MDCK cells displayed phenotypes similar to those of KO-HCs, including abnormal microvilli and disrupted AJCs, and downregulated actin turnover that was represented by the enhanced levels of phospho-Cofilin.

Conclusion

Our data provide evidence that the Rho GTPase plays important roles in maintenance but not development of stable actin structures including stereocilia, microvilli and apical junctional complex through elaborate tuning of actin-turnover, and maintains function and viability of cochlear hair cells.

Cessation of Neurotrophin Gene Therapy Does Not Accelerate Auditory Nerve Degeneration

Benjamin Case; Lisa Beyer; Donald Swiderski; Yehoash Raphael

University of Michigan

Background

Loss of auditory hair cells may lead to a secondary death of spiral ganglion neurons (SGNs), thereby compromising efficacy of cochlear implant therapies and future hair cell replacement procedures. Viral-mediated neurotrophin gene therapy in deaf ears promotes SGN health and survival. However, levels of the neurotrophins may potentially decrease over time due to latency of the viral vector or death of the cells that are transduced with the virus. For this treatment to be clinically feasible, it is necessary to determine the fate of SGNs in cases where neurotrophin levels drop.

Methods

To assess the effect of decrease in neurotrophin level on SGN survival, we used 2 groups of guinea pigs that were bilaterally deafened by neomycin. Adenovirus with the *BDNF* gene insert (*Ad.BDNF*) was injected to the left ear 7 days after deafening, when hair cell degeneration is complete. Adenovirus-mediated transgene expression is expected to last 4-6 weeks. One group was sacrificed 3 weeks after the inoculation (short term), when BDNF levels are expected to be high, and the other group at 3 months (long term), after the *Ad.BDNF* is presumed to be inactive. Perilymph was collected just before animals were sacrificed, to analyze BDNF concentrations by ELISA. Cochleae were sectioned to assess SGN density.

Results

ELISA assays of the perilymph from treated ears show BDNF levels above the detection threshold in the 3-week group, and below the threshold in the 3-month group. In both short and long term groups, the left (*Ad.BDNF*-treated) ears exhibited robust survival of SGNs, with densities markedly higher than in the contralateral untreated deafened ear.

Conclusion

The results show that the beneficial effects of neurotrophin treatment continue after cessation of the treatment, and that withdrawal of neurotrophin support weeks after the loss of hair cells does not lead to the demise of SGNs. Similar results were found by Agterberg et al. (2009) using osmotic pumps to deliver neurotrophins. Together, these studies reduce the safety concern for long term neurotrophin treatment in the cochlea.

Interaction of Caspases and RIP Kinases Modulates Noise-Induced Apoptotic and Necrotic Outer Hair Cell Death Pathways

Hong-Wei Zheng; Jun Chen; Su-Hua Sha

Medical University of South Carolina

Background

Inhibition of caspase activation prevents noise-induced hearing loss (NIHL) and hair cell death. However, inhibition of caspase-8 promotes the activation of receptor-interacting protein (RIP) kinases. Our recent studies have revealed that RIP kinases promote noise-induced necrotic outer hair cell (OHC) death pathways. Here, we investigated the interaction of activated caspases and RIP kinases in noise-induced apoptotic and necrotic OHC death pathways using adult CBA/J mice.

Methods

Broadband noise from 2–20 kHz at 106 dB SPL for 2 hours was used to induce permanent threshold shifts (PTS). Propidium iodide labeling of OHC nuclei to identified apoptosis and necrosis via morphological criteria. Auditory brainstem responses were used to measure auditory function. Western blot assays were used to evaluate the levels of RIP1 and RIP3 in whole cochlear homogenates. Anti-cleaved caspase-8, caspase-9, and endonuclease G (EndoG) immunolabeling of cochlear surface preparations detected corresponding protein levels in OHCs. A caspase inhibitor or RIP3 siRNA was delivered to the round window via intra-tympanic injection to observe for inhibition of apoptotic and necrotic OHC death. Combination treatment of a caspase inhibitor via intra-peritoneal (IP) injection with RIP3 siRNA was performed to assess for a synergic effect on NIHL.

Results

Both apoptotic and necrotic OHC nuclei were observed in the basal region of the cochlea 1 hour after noise exposure. Treatment with pan-caspase inhibitor ZVAD blocked noise-induced activation of caspase-8 and reduced the number of apoptotic nuclei, while increasing levels of RIP1 and RIP3 and necrotic OHCs. Conversely, blocking noise-induced over-expression of RIP1 and RIP3 by treatment with necrosis inhibitor necrostatin-1 (Nec-1) or RIP3 siRNA (siRIP3) decreased the number of necrotic OHC nuclei, but increased the number of apoptotic nuclei without increasing activation of caspase-8. In addition, ZVAD treatment caused elevation of noise-induced p-AMPK α levels. Furthermore, pretreatment with siRIP3 did not alter the activation of caspase-8, but instead increased activation of caspase-9 and promoted EndoG translocation into OHC nuclei. Finally, ABR functional measurements and morphological assessment of OHCs showed that ZVAD treatment reduced noise-induced deficits. This protective function is potentiated when combined with siRIP3 treatment.

Conclusion

Noise-induced OHC apoptosis and necrosis are modulated by caspase-8 and RIP kinases, respectively. Inhibition of either pathway shifts the prevalence of OHC death to the alternative pathway.

Interplay Between Oxidative Stress and Autophagy in Noise-Induced Hearing Loss

Hu Yuan¹; Jun Chen¹; Hill Kayla¹; Shi-Min Yang²; Su-Hua Sha¹

¹Medical University of South Carolina; ²PLA General Hospital, Beijing

Background

Reactive oxygen species (ROS), well-known to induce outer hair cell (OHC) death, have been shown to play a dual role as signaling molecules that induce both cell stress responses and defense pathways, such as the induction of autophagy. Autophagy has also been suggested to play a role in regulating the elimination of ROS and ROS-related cellular damage. Recent results from our laboratory have shown autophagy to be a defense against noise-induced hearing loss. Here, we investigated the relationship between autophagy, ROS, and noise-induced temporary and permanent auditory threshold shifts (TTS and PTS, respectively).

Methods

Broadband noise from 2–20 kHz at 98 dB SPL for 2 hours was used to induce permanent threshold shifts (PTS), 106 dB to induce severe PTS (sPTS), or 96 dB SPL to induce temporary thresholds shifts (TTS). Auditory brainstem responses were used to measure auditory function. Myosin VIIa and diaminobenzidine (DAB) staining of cochlear epithelia was used for quantification of OHC loss. Western blot assays evaluated the levels of autophagosomes with anti-LC3B and oxidative stress with anti-3-nitrotyrosine (3-NT) in whole cochlear homogenates. Anti-LC3B and anti-3-NT immunolabeling of cochlear surface preparations determined the expression of autophagosomes and the formation of oxidative stress in OHCs. Delivery of LC3B siRNA to the round window via intra-tympanic application was used to detect oxidative stress. Treatment with 3-methyladenine (3MA) and rapamycin via intra-peritoneal injection was employed to detect oxidative stress.

Results

The levels of 3-NT significantly increased in OHCs 1 hour after TTS-, PTS-, and sPTS-noise exposures. The levels of 3-NT positively correlated with the noise intensity. Treatment with the autophagy stimulator rapamycin significantly diminished noise-induced 3-NT levels, increased expression of LC3B, and prevented noise-induced PTS. In contrast, treatment with autophagy inhibitor 3MA resulted in an increase in 3-NT levels and down-regulation of noise-induced LC3B expression, exacerbating deficits from TTS to PTS. Finally, pretreatment of LC3B siRNA increased noise-induced expression of 3-NT, in agreement with the effects of 3MA treatment.

Conclusion

Our results suggest that the generation of small amounts of ROS under TTS-noise conditions causes a stronger induction of autophagy that maintains hair cell survival by reducing oxidative damage. However, excessive ROS formation under sPTS-noise conditions induces extreme oxidative damage in sensory hair cells leading to hearing loss.

Paraquat Induces a Novel, Apex-to-Base Hair Cell Lesion in Neonatal Mouse Cochlear Cultures

Haiyan Jiang¹; Dalian Ding¹; Senthilvelan Manohar¹; Tomas Prolla²; Richard Salvi¹

¹University at Buffalo; ²University of Wisconsin

Background

We have previously shown that mitochondrial oxidative stress plays a causal role in AHL through induction of the pro-apoptotic protein BAK. We have also shown that AHL is retarded by caloric restriction, and that this effect requires the mitochondrial sirtuin SIRT3. The superoxide radical is believed to participate in many different forms of cochlear damage. Paraquat, a widely used herbicide, is potent superoxide generator. Intracellularly, paraquat accepts an electron from NADPH oxidase and transfers it to molecular oxygen to form the highly toxic superoxide radical. In an earlier study (Nicotera et al., 2004, Audiol Neurotol), we showed that paraquat produced high levels of superoxide in neonatal cochlear organ cultures and damaged hair cells in a dose-dependent manner; however, we did not investigate the base-to-apex damage gradient.

Methods

We used WT and Sirt3^{-/-} and Sirt3^{+/-} mice to test the hypothesis that paraquat (10 or 50 mM) would produce the classic damage gradient in the cochlea in which inner and outer hair cell loss would be greater in the high-frequency base than the low-frequency apex of the cochlea.

Results

Cochlear cultures treated for 24 h with 10 μ M paraquat showed only minor hair cell loss in the apical half of the cochlea, but none in the basal half. When the dose was increased to 50 μ M for 24 h, there was massive hair cell loss in the apical low-frequency region and minimal hair cell loss in the basal high-frequency region. Outer hair cell loss was greater than inner hair cell loss. Nearly the same pattern of hair cell loss was seen in WT and Sirt3 strains.

Conclusion

Paraquat produced greater hair cell loss in the apex of the cochlea than the base. This lesion pattern conflicts with the prevailing view that the base of the cochlea is always more vulnerable to oxidative stress than the apex. The mechanisms underlying this unusual lesion gradient are unclear, but could be due to the gradient of superoxide dismutase expression in P3-4 mice.

Acute Ototoxic Effects of Trimethyltin in Chinchilla

Vijaya Prakash Krishnan Muthaiah; Jintao Yu; Dalian Ding; Haiyan Jiang; Senthilvelan Manohar; Richard Salvi
University at Buffalo

Background

Trimethyltin (TMT), a biocide and heat stabilizer used in PVC, is highly neurotoxic to granule and pyramidal cells in the limbic system, cerebral cortex, and brainstem. TMT has also

been shown to be ototoxic in guinea pigs and rats. Because the chinchilla exhibits an unusual ototoxic response to some drugs, we speculated that its ototoxic effects might be different from other species.

Methods

To evaluate this hypothesis, we treated chinchillas with 2 mg/kg TMT and measured the compound action potential (CAP), auditory brainstem response (ABR) and distortion product otoacoustic emissions (DPOAE) before and during the first 24 h post-treatment.

Results

DPOAE from outer hair cells were totally abolished at the high frequencies and greatly reduced at 2 kHz at 12 h post-TMT and showed little or no recovery. CAP thresholds at 4, 8 and 12 kHz increased rapidly during the first 12 h reaching a maximum loss of ~50 dB and then recovering to a loss of around 30 dB at 24 h post-treatment. In contrast, CAP thresholds increased approximately 30 dB during the first 12 h and remained stable out to 24 h post-treatment. ABR thresholds exhibited a different frequency-time dependent pattern of loss. ABR thresholds at 2 and 4 kHz reached a maximum loss of approximately 50 dB at 12 h post-treatment and declined to a 30 dB loss at 24 h. In contrast, ABR thresholds at 8 and 12 kHz increased approximately 40 dB and remained at this level out to 24 post-treatment.

Conclusion

These results suggest that TMT causes significant damage to the hair cells and neurons in the cochlea and possibly additional histological changes in the central auditory pathway; results which will be confirmed by histological analysis. Preliminary results suggest that the damage patterns in the chinchilla are similar to other rodents.

PS - 363

Nicotinamide Adenine Dinucleotide Prevents Neuroaxonal Degeneration Induced by Manganese in Cochlear Organotypic Cultures

Lu Wang¹; Dalian Ding²; Richard Salvi²; Jerome Roth²

¹University at Buffalo; Third Xiangya Hospital of Central South University; ²University at Buffalo

Background

Manganese (Mn), a divalent trace metal, is required for normal growth and development. However, workers exposed to high levels of manganese often develop severe neurotoxic symptoms known as manganism characterized by extrapyramidal symptoms resembling Parkinson's disease. In previous studies (Ding et al., 2011), we demonstrated that mM concentrations of Mn caused severe damage to hair cells, spiral ganglion neurons (SGN) and auditory nerve fibers (ANF) in postnatal day 3 rat cochlear organotypic cultures. However, the biological mechanisms underlying these degenerative changes are unclear. Nicotinamide adenine dinucleotide (NAD), a coenzyme involved in electron transfer system within mitochondria, has been reported to protect against axonal degenerations caused by various neurodegenerative injuries. Therefore, we hypothesized that NAD might protect auditory

nerve fibers (ANF) and spiral ganglion neurons (SGN) from manganese injury.

Methods

To test this hypothesis, cochlear organotypic cultures were treated with different doses of Mn (0.5-3.0 mM) alone or combined with 20 mM NAD to determine if it would prevent the neural or hair cell regeneration.

Results

The percentage of hair cells, ANF and SGN decreased with increasing doses of Mn between 0.5 and 3.0 mM. Mn treatment caused significant blebbing of ANF, considerable shrinkage of SGN soma and increased TUNEL, caspase-3, caspase-8 and caspase-9 labeling, morphological features of programmed cell death. The addition of 20 mM NAD to Mn treated cultures failed to significantly reduce hair cells loss. However, the density of ANF and SGN was significantly greater in cochlear cultures treated with Mn plus 20 mM NAD versus Mn alone. NAD also reduced the TUNEL and caspase-3, caspase-8 and caspase-9 staining of SGN.

Conclusion

In vitro, excess Mn is highly toxic to hair cells, ANF and SGN. Mn-induced damage appears to arise from apoptotic cell death. NAD suppressed prevented Mn-induced programmed cell death of ANF and SGN, but failed to prevent hair cell degeneration.

PS - 364

In Vitro Evaluation of the Effects of Clinical Sepsis Parameters on the Murine Cochlea.

Joachim Schmutzhard; Christian Pritz; Simon Zaar; Rudolf Glueckert; Leyla Pinggera; Nathalie Fischer; Annelies Schrott-Fischer

Medical University Innsbruck

Background

Lately sepsis has been identified as ototoxic in a murine sepsis model. In these animals sepsis was induced with the cecal ligation puncture technique showing significant threshold shifts. These changes could be related to apoptosis in the supporting cells, glutamate excitotoxicity on the base of the inner hair cells and an anti-apoptotic activity in the spiral ligament. The following clinical parameters were evaluated the preliminary study: Hypothermia, positive blood cultures for *E. coli* and serum lactate evaluation. So far the observed changes in the ear could not be related to one specific stimulus. The aim of this study is to evaluate the effect of the above listed parameters on the murine cochlea in an *in vitro* setting.

Methods

The cochleae were taken from 21 to 24 day old C57 BL/6J and cultured with a minimal-gravity whole organ culturing system. The cultured cochleae were then incubated with hypothermia, *E. Coli* lysate or lactate at pH level of 7.0 for 24 hours. Cochleae with no intervention served as control. Afterwards the inner ears were evaluated morphological including DAPI counterstaining, with immunohistochemical for BAX, Cleaved Caspase 3 and with Immunofluorescence for Class

III beta tubulin (TuJ-1) as neuronal marker and with Phalloidin as cytoskeletal marker.

All slides were evaluated manually. Furthermore a HistoFAXS tissue analyzing system was used to compute acquired data.

Results

Controls; Hypothermia and E.Coli showed well preserved cochlea. The nuclei were of round and regular size. Some activity for BAX and Cleaved Caspase 3 could be detected. Furthermore Phalloidin and TuJ-1 staining was strong.

The lactate group showed a strong degeneration of the cochlea structures. The Organ of Corti was strongly disintegrated. The nuclei were polymorphic and small in size with chromatin condensation. A strong BAX and Cleaved Caspase 3 staining was found in the spiral ligament. Phalloidin and TuJ-1 were reduced.

Conclusion

The well preserved controls with low levels of apoptotic activity, strong neuronal and cytoskeletal markers prove the quality of the experiment. The similar results in the hypothermia and E.Coli group show, that these parameters do not affect the cochlea. The severe changes in the lactate group suggest strong pathologic activities of lactate elevation and pH reduction in the cochlea. To finally prove the pathologic effect of blood lactate elevation and pH reduction further studies *in vivo* will be necessary.

PS - 365

Screening for Protective Effect in Herbal Medicine Using the Zebrafish Lateral Line

Yoshinobu Hirose; Kazuma Sugahara; Hiroshi Yamashita
Yamaguchi University Graduate School of Medicine

Background

The zebrafish lateral line is a powerful system for studying hair cells and hair cell death. Hair cells can be easily labeled and imaged *in vivo* with fluorescence microscopy. We have previously described a screening system to rapidly assess drugs for possible ototoxic effects in anti-cancer drugs (Hirose et al., 2011). Also it is possible to screen protective effect against some ototoxicity drugs.

Methods

Now we have screened the herbal medicine for protective effects against aminoglycoside. 5-7 dpf Zebrafish (*Danio rerio*) embryos of the AB wild type strain were used in this study. Zebrafish larvae were exposed to herbal medicine (1mM) for 1 hour before 200 μ M Neomycin for 1 hour. After that, they were fixed in 4% paraformaldehyde, incubated with anti-parvalbumin, Alexa 488, and hair cell damage was assessed by fluorescent microscope.

Results

We will show herbal medicine dose-response curves to evaluate protective effect.

Conclusion

In conclusion, if some of herbal medicine show protective effect against zebrafish hair cell, this study shown that trophic

factors can be a powerful protective drug against inner ear damage.

PS - 366

Effect of Redox-Sensitive GFP Expression in the Murine Inner Ear

Kazuaki Homma; Roxanne Edge; Ted Kim; Chongwen Duan; Mary Ann Cheatham; Paul Schumacker; Jing Zheng
Northwestern University

Background

Outer hair cells (OHCs) are extremely sensitive to acoustic trauma, antibiotics (i.e., aminoglycosides), and chemotherapeutic drugs (i.e., cisplatin) (for a review see Rybak and Ramkumar 2007). Increasing evidence suggests that OHC death induced by these various physical and chemical insults is associated with overproduction of reactive oxygen species (ROS). Therefore, an animal model that allows monitoring of redox status in OHCs and other inner ear cells would be valuable for studying the process of ROS overproduction and, thus, for understanding the pathology of ROS-related cell death. Because reduction-oxidation-sensitive GFP (roGFP, Dooley et al., 2004) is capable of illustrating the redox status of living cells, we created a mouse model expressing roGFP in the mitochondrial matrix using a CMV promoter. The CMV-mito-roGFP mice appear to be normal and have been used to monitor the redox status of dopaminergic neurons in the substantia nigra pars compacta (Guzman et al., 2010). The purpose of our study is to explore the possibility of using the roGFP mouse model for inner ear research.

Methods

The hearing phenotypes of roGFP-expressing mice (CMV-mito-roGFP mice) were determined by measuring distortion product otoacoustic emissions (DPOAEs) and auditory brainstem responses (ABRs). The expression of roGFP was determined using a fluorescence microscope equipped with 408 and 480 nm excitation band-pass filters that allow roGFP ratiometry to determine the redox status of roGFP-expressing cells. Fluorescence ratios indicating maximum oxidation and maximum reduction were determined using 0.1 mM aldrethiol and 5 mM dithiothreitol, respectively.

Results

RoGFP expression was confirmed especially in inner hair cells, OHCs, and the stria vascularis in CMV-mito-roGFP mice. Fluorescence ratios changed when oxidizing or reducing reagents were applied. Examination of cochlear whole mounts indicated significant hair cell loss (also some Deiters' cells) as early as P10. Consistent with this observation, neither DPOAEs nor ABRs were detected in roGFP positive mice at P47, irrespective of copy number. This result did not change at an earlier postnatal stage (P22) although one of five animals showed an ABR above ~90 dB. No mouse exhibited a pinna reflex.

Conclusion

Although CMV-mito-roGFP mice show significant hearing impairment and premature cell death, it is currently unknown why roGFP mitochondrial expression damages cells in the inner ear without affecting other tissues. This mouse model

may be useful when investigating cell death by monitoring redox status in mitochondria.

PS - 367

Capsaicin Protects Against Cisplatin Ototoxicity by Activating Cannabinoid Receptors

Puspanjali Bhatta¹; Debashree Mukherjee²; Kelly Sheehan²; Leonard P Rybak²; Vickram Ramkumar³

¹SIU School of Medicine; ²SIU Department of Surgery; ³SIU Department of Pharmacology

Background

Cisplatin is a widely used chemotherapeutic drug for the treatment of solid tumors. However, the drug accumulates in cochlea, and damages the inner ear structures, resulting in bilateral and permanent hearing loss. Previous data from our laboratory indicate that activation of the transient receptor potential vanilloid 1 (TRPV1) receptors (by capsaicin) increases the NOX3 isoform of NADPH oxidase, leading to the generation of reactive oxygen species (ROS) in the cochlea, transient cochlear inflammation and transient hearing loss. We also demonstrated that the transient inflammation was produced by ROS-mediated activation of signal transducer and activator of transcription 1 (STAT1). Surprisingly, capsaicin was able to protect against cisplatin ototoxicity. The goal of the present study was to determine the mechanism underlying protection of cisplatin ototoxicity by capsaicin.

Methods

Baseline auditory brainstem responses (ABRs) of male Wistar rats were recorded. Functional assessments include ABRs and scanning electron microscopy. Gene expression studies were conducted using real time PCR, and by immunohistochemistry of the mid-modiolar sections of the rat cochleae. Cell viability was determined by MTS assay in UB/OC-1 cells. Annexin V- FITC assays were used to assess cell apoptosis. Phosphorylation of STAT1 and STAT3 and the levels of cannabinoid receptors (CB1 and CB2) were determined by Western blotting and immunocytochemistry.

Results

Capsaicin (2.5 μ M) increased Ser⁷²⁷ but not Tyr⁷⁰¹ p-STAT1. Capsaicin also increased Tyr⁷⁰⁵ but not Ser⁷²⁷ p-STAT3. Inhibition of TRPV1 by ruthenium red reduced the Ser⁷²⁷ p-STAT1 but not Tyr⁷⁰⁵ p-STAT3. However, inhibition of CB1 (by AM251) and of CB2 receptors (by AM630) reduced capsaicin-mediated Tyr⁷⁰⁵ p-STAT3, but had little effect on Ser⁷²⁷ STAT1. Expression of cannabinoid receptors were observed in UB/OC1 cells as well as rat outer hair cells (OHCs). Capsaicin protected UB/OC-1 cells against cisplatin-induced apoptosis. This protection was reversed by CB2 antagonist but potentiated by TRPV1 inhibition. Significant cell death was observed following treatment of UB/OC1 cells with AM630 alone, underscoring the importance of CB2 receptors in survival of these cells. Furthermore, capsaicin-mediated protection was reversed by inhibition of STAT3, implicating STAT3 in otoprotection.

Conclusion

We conclude that otoprotection mediated by capsaicin is produced by activation of CB receptors which activate STAT3. Activation of STAT1 by capsaicin could contribute to the transient inflammatory response previously observed *in vivo*. The net protective action of capsaicin could result from an increase in the STAT3/STAT1 ratio of cells in the cochlea, abrogating the negative impact of cisplatin on this ratio.

PS - 368

The Efficiency of Bofutsushosan and Daisaikoto, an Oriental Herbal Medicine to Prevent the Presbycusis of TSOD Mouse

Takeshi Hori; Kazuma Sugahara; Junko Tsuda; Yoshinobu Hirose; Hiroaki Shimogori; Makoto Hashimoto; Hiroshi Yamashita

Department of Otolaryngology, Yamaguchi University Graduate School of Medicine

Background

A frequent thing that hearing loss in diabetes is shown in past epidemiologic studies. However, the cause is still unknown. Recently, it was reported that TSOD (Tsumura-Suzuki-Obese-Diabetes) male mouse presented metabolic abnormality such as obesity and hyperlipidemia, high blood pressure, diabetes with aging. We reported that hearing loss progressing with aging and the narrowing of the blood vessel in the inner ear were accepted in TSOD mice in the last meeting. For metabolic syndrome, there are some reports that Chinese medicine is effective recently. In the present study, we evaluated the effect of Kampo medicine (Bofutsushosan and Daisaikoto) on the age-related hearing loss in TSOD mice.

Methods

TSOD male mice used in study were derived from the Tsumura Research Institute. Animals were divided into three groups (Normal food group; NF group, Bofutsushosan group; BF group and Daisaikoto group; DS group). The Chinese medicine mixed 3% into the normal foods in BF group and DS group each other. We measured the weight and blood glucose level and auditory brainstem response thresholds in 7, 8, 9, 10 month of age. In addition 10 months aged TSOD mice were dissected for histological examination.

Results

There were no difference in the body weight and the blood glucose level among the 3 groups. The ABR thresholds elevated in each group with age. However, the threshold tended to rise more gently in the BF group and the DS group than in NF group. Furthermore, the diameter of blood vessel in the stria vascularis was significantly larger in DS group compared with those on the other groups.

Conclusion

The result suggested that Chinese medicine prevented the hearing loss of the diabetic by preventing the narrowing of the blood.

Increased Presence of Cells of the Immune System in the Spiral Ganglion During Spiral Ganglion Neuron (SGN) Death Post-Deafening

Erin Bailey; Zarin Rehman; Nicole Pulliam; Steven H Green
University of Iowa

Background

Hair cells (HCs) are the sole afferent input to SGNs. Following HC death due to aminoglycoside exposure from postnatal day 8 (P8) to P16, rat SGNs degenerate and die over a period of ~3 months (Alam et al. JCN 503: 832-52, 2007). The reason for SGN death is not clear. In some cases, HC death does not result in SGN death and neurotrophic factors remain expressed in the cochlea and cochlear nuclei after HC loss. Possibly, SGN death is an indirect outcome of HC loss, due to inflammatory or degenerative changes in the cochlea initiated by HC loss. We used microarray-based gene expression profiling to identify changes in the spiral ganglion during the SGN death period and gain insight into why SGNs die.

Methods

Rats were deafened by daily kanamycin injection P8-P16 and euthanized at P32, when SGN loss is just becoming significant, or at P60, when ~50% of the SGNs have died. RNA was isolated from microdissected apical and basal portions of spiral ganglia. cDNA was hybridized in triplicate to Nimblegen HD2 rat gene expression arrays with three separate biological repetitions. Expression of selected representative genes was verified by qPCR. Immunofluorescence was as in Alam et al., *ibid*.

Results

Of the genes expressed in the spiral ganglion, expression of ~0.8% decreases by >2X and of ~2.0% increases by >2X in deafened P60 rats, relative to hearing littermates. Many of these are indicative of infiltration of inflammatory or innate immune-related changes. For example, interferon-inducible genes, e.g., Mx1, Mx2, and C-C and C-X-C chemokines are upregulated (CCL3 verified by qPCR). Previously, we have shown evidence for activation of the resident macrophage population in the deafened ganglion while SGNs are dying. Here, we show evidence for infiltration of natural killer (NK) cells into the spiral ganglion during this same time period. Transcript levels for genes characteristic of NK cells (e.g., Ly49i9 and Ly49si, verified by qPCR) increases >2X by P60. This was verified by detection, by immunofluorescence, of a greatly increased number of HNK1-positive cells in the deafened spiral ganglion at P60.

Conclusion

Gene expression profiling provides evidence for increased presence of cells of the innate immune system, including macrophages and NK cells, in the spiral ganglion at the time when SGNs are dying. While their presence may be related only to clearance of debris, the observations raise the possibility that they are involved in SGN death.

Effects of Vitamin A Deficiency on Age-Related and Noise-Induced Hearing Loss in Mice

Dae Bo Shim¹; Mia Ki²; Jin Woong Bok²; Jae Young Choi²

¹Myongji Hospital; ²Yonsei University College of Medicine

Background

Vitamin A deficiency (VAD) causes a variety of pathologic phenotypes in human and animal subjects, which are pathologic problems in skin differentiation, spermatogenesis, and immune system function. Although numerous authors reported that the vitamin A deficiency (VAD) in human and animals induces a reduction in hearing ability, its effects on the inner ear have been unclear. In the present study, we evaluated the effect of VAD on changes of hearing level and histopathology of inner ear in a mouse model of VAD.

Methods

We have analyzed the auditory brainstem responses (ABR) of two mouse strains: ICR, albino type and C57BL/6, pigmented mice. For each strain, mice were divided into two groups as follows: group 1 (VAD group) was fed a purified vitamin A-free diet from 7 days after pregnancy, and group 2 (control group) was fed a normal diet. Hearing threshold was measured by ABR until 20 weeks after birth. And we have recorded the changes of hearing threshold after noise exposure in C57BL/6 strain.

Results

After the level of retinoic acid was reached less than a half of control mice, the hearing threshold of only ICR VAD group was increased compared to those of the other groups ($p < .05$). We observed that pigmented VAD mice present poorer recovery of auditory thresholds, especially in low frequency (4 kHz), after noise exposure than pigmented wild-type mice.

Conclusion

In conclusion, the hearing threshold of VAD mice was impaired by aging and noise insult when compared to the other groups, although cochlear melanocytes might have some protective role in pigmented VAD mice. These results demonstrate that VAD may cause age-related hearing loss and the recovery of noise-induced hearing loss in mice.

Suppression of the Expression of Pro-Inflammatory Cytokines by Esculentoside A Attenuates Noise-Induced Cochlear Damage

Guiliang Zheng¹; Yide Zhou¹; Hongliang Zheng¹; Bo Hua Hu²

¹Department of Otolaryngology-Head and Neck Surgery, Changhai Hospital, Second Military Medical University;

²Center for Hearing and Deafness, State University of New York at Buffalo, 137 Cary Hall, 3435 Main Street, Buffalo, NY 14214, USA.

Background

The cochlea has an active immune capacity. In response to stresses, cochlear cells activates immune response genes and recruits immune defense cells. This stress response initiates cochlear inflammation. While the inflammatory re-

sponse can be beneficial for tissue recovery, over-reaction is detrimental and can cause secondary damage to the cells. In the current study, we investigated the protective effects of suppression of cochlear inflammatory responses to acoustic trauma using esculentoside A (EsA), a saponin isolated from the roots of *Phytolacca esculenta* that has anti-inflammatory properties.

Methods

Forty mice were randomly divided into four groups: naive control, noise only (white noise, 115 dB SPL for 8 hrs), noise + EsA (10mg/kg/d for 7 d), and noise + saline. Auditory brainstem response (ABR) and distortion product otoacoustic emission (DPOAE) were measured before and after the treatments. The cochleae were collected at 7 d after the noise exposure. Using Milliplex Map ELISAs, the expression levels of eight inflammatory cytokines (IL-1 α , IL-2, IL-3, IL-10, IL-6, IL-1 β , VEGF and TNF α), were examined for one cochlea collected from each animal (n=5 cochleae for each group). The other cochlea from each animal was used for assessment of sensory cell damage using nuclear staining (n=5 cochleae for each group).

Results

The acoustic overstimulation induced a significant threshold shifts of ABRs and DPOAEs. Among the eight examined cytokines, four (IL-6, IL-1 β , VEGF and TNF α) exhibit a significant expression increase after the acoustic overstimulation, suggesting that the acoustic injury provoked an inflammatory response in the cochlea. These expression increases were reduced after the EsA treatment. Moreover, the EsA treatment reduced the threshold shifts of both ABRs and DPOAEs compared to the noise only and the noise + saline groups. By contrast, neither the ABR nor DPOAE values differed between the noise only group and the noise + saline group. The morphological assessment of sensory cell damage showed a decrease in the number of sensory cell death after the EsA treatment, consistent with the finding of the functional assessment.

Conclusion

The EsA treatment reduces noise-induced sensory cell damage by suppressing the expression of proinflammatory cytokines in the cochlea.

PS - 372

Autophagy May Play a Critical Role in the Process of Aminoglycoside-Induced Delayed Ototoxicity

Yeon Ju Kim; Young Sun Kim; Chunjie Tian; Hye Jin Lim; Juyong Chung; Hun Yi Park; **Yun-Hoon Choung**
Ajou University School of Medicine

Background

Autophagy is a process of bulk degradation of damaged organelles, protein aggregates, and other macromolecules in the cytoplasm. Autophagy regulates cell survival and death in both physiological as well as pathophysiological conditions. While under normal conditions, autophagy is a mechanism to maintain cell homeostasis, autophagy induction under patho-

logical conditions is generally considered to provide a pro-survival role; however, extensive or inappropriate activation of autophagy results in cell death by bulk elimination of cells. The purpose of the study is to evaluate the role of autophagy in the process of auditory cell death and survival, especially in the gentamicin-induced ototoxicity.

Methods

HEI-OC1 auditory cells were used in this study. The expression of autophagic proteins was evaluated by Western blot and immunocytochemistry (ICC) in gentamicin-induced cell toxicity. For *in vivo* animal study, total 12 SD rats were distributed into the group I and II. Gentamicin (GM) was administered intraperitoneally (160 mg/kg) for 5 days in both groups. Autophagy inducer (mTOR inhibitor), rapamycin (RPM; 50 pM for group I; 100 pM for groups II) was done by intratympanic injection (ITI) in the left ears 4 times, and the opposite ears were given with saline as a control. Assessment of hearing was evaluated at 16 and 32kHz by auditory brainstem response (ABR) test. Morphologic change of organ of Cortis was analyzed by SEM imaging.

Results

The accumulation of LC3 (the mammalian ortholog of Atg8) was observed as autophagic vesicles in the GM-treated cells. In contrast, the diffused form of LC3 was detected in the control. Western blot showed that the levels of LC3 and Beclin 1 were up-regulated by GM treatment. Also, the blockade of autophagy (chloroquine) sensitized to GM. In animal studies, the hearing thresholds of ABR in RPM + GM-treated ears (18.3 \pm 2.8 dB at 16 kHz /21.7 \pm 2.9 dB at 32 kHz) were significantly better than those in the GM - only treated ears (31.7 \pm 2.9 dB at 16 kHz /33.3 \pm 2.9 dB at 32 kHz) (P < 0.05). The SEM findings of organ of Cortis showed that the loss of stereocilia in outer hair cells was much more in the GM-treated ears than in the RPM + GM-treated ears.

Conclusion

Autophagy activates cell survival of auditory cells at the early stage of gentamicin-induced ototoxicity. Autophagy may be used as a protection strategy against ototoxicity.

PS - 373

Low-Level Laser Therapy for Prevention of Noise-Induced Hearing Loss

Atsushi Tamura; Takeshi Matsunobu; Katsuki Niwa; Takaomi Kurioka; Satoko Kawauchi; Shun-ichi Satoh; Akihiro Shiotani

National Defense Medical College

Background

Laser-induced phototherapy, such as low-level laser therapy (LLLT), is widely applied as a noninvasive treatment promoting cell regeneration and repair process. LLLT has been approved by the US Food and Drug Administration (FDA) for the treatment of several diseases. In this study we investigated the effect of LLLT on preventing hair cell damage of the cochlea after acute acoustic trauma.

Methods

Eleven SD rats were exposed to noise (octave band noise centered at 4 kHz). After the noise exposure, the right ears of the rats were irradiated at an energy output of 110 or 165 mW/cm² for 30 min with 808 nm diode laser for 5 days in a row. The right ears of the five normal rats were assigned as the control group. Auditory brainstem responses (ABR) were measured before and immediately after the noise exposure, and then 2, 4, 7, 14 and 28 days after the noise exposure.

Results

ABR measurements revealed that LLLT attenuates noise-induced threshold shift at 12, 16 and 20 kHz. Outer hair cells (OHCs) loss was examined using surface preparation technique and significant higher survival rate of OHCs was observed in the LLLT group as compared to the non-LLLT group. Immunohistochemical analyses for inducible nitric oxide synthase (iNOS) and cleaved caspase-3 were performed to examine the control of oxidative stress and apoptosis, and weaker immunoreactivities against iNOS and cleaved caspase-3 were observed in the LLLT group as compared to the non-LLLT group.

Conclusion

Our findings suggest that LLLT is therapeutically effective in helping to prevent oxidative damage that can occur as a result of noise-induced hearing loss.

PS - 374

Designer Aminoglycosides That Selectively Inhibit Cytoplasmic Rather Than Mitochondrial Ribosomes Show Decreased Ototoxicity

Jochen Schacht¹; Eli Shulman²; Valery Belakhov²; Ann Kendall³; Gao Wei³; Esther G. Meyron-Holtz⁴; Dorit Ben-Shachar⁵; Timor Baasov²

¹University of Michigan; ²The Edith and Joseph Fischer Enzyme Inhibitors Laboratory, Schulich Faculty of Chemistry, Technion IIT, Haifa 32000, Israel; ³Kresge Hearing Research Institute, University of Michigan;

⁴Laboratory for Molecular Nutrition, Faculty of Biotechnology and Food Engineering, Technion IIT, Haifa 32000, Israel.; ⁵Laboratory of Psychobiology, The Department of Psychiatry, Rambam Medical Center and B. Rappaport Faculty of Medicine, Technion IIT, Haifa 31096, Israel.

Background

There is compelling evidence that aminoglycoside antibiotics can bind to the mammalian ribosome and suppress disease-causing nonsense mutations thereby partially restoring the expression of functional proteins. However, prolonged aminoglycoside treatment can cause detrimental side effects in patients, including most prominently, ototoxicity. This toxicity was recently suggested to be connected to a more effective inhibition of mitochondrial rather than cytoplasmic protein synthesis by aminoglycosides, causing mitochondrial dysfunction. We are testing this hypothesis using designer aminoglycosides with different affinities to mitochondrial and cytoplasmic ribosomes.

Methods

The following analyses were applied: mitochondrial protein synthesis; cell respiration; superoxide production; mitochondrial aconitase activity; free mitochondrial iron; toxicity to hair cells in murine cochlear explants; ototoxicity in guinea pig *in vivo*, assessed by auditory brain stem evoked responses and hair cell count.

Results

Aminoglycosides inhibit mitochondrial protein synthesis in mammalian cells and perturb cell respiration. This results in a time- and dose-dependent increase in superoxide overproduction and accumulation of free ferrous iron in mitochondria due to oxidative damage to mitochondrial aconitase, ultimately leading to cell apoptosis via the Fenton reaction. These deleterious effects increase with the increased potency of aminoglycosides to inhibit mitochondrial rather than cytoplasmic protein synthesis. Inhibition of mitochondrial protein synthesis, in turn, correlates with the ototoxic potential of the drugs both in murine cochlear explants and the guinea pig *in vivo*. The adverse effects of aminoglycosides were alleviated in synthetic derivatives possessing low affinity towards mitochondrial ribosomes and designed for the treatment of genetic diseases caused by nonsense mutations.

Conclusion

Our results support inhibition of mitochondrial rather than cytoplasmic protein synthesis as a major determinant of aminoglycoside ototoxicity. Furthermore, this work highlights the benefit of a mechanism-based drug-redesign strategy that can maximize the translational value of "read-through therapy" while mitigating drug-induced side effects. This approach holds promise for patients suffering from genetic diseases caused by nonsense mutations.

PS - 375

ROCK-Dependent Ezrin-Radixin-Moesin Phosphorylation Modulates the Actin Cytoskeleton in Noise-Induced Hair Cell Death

Yu Han; Jun Chen; Su-Hua Sha
Medical University of South Carolina

Background

Small GTPases are the major modulators of the actin cytoskeleton. Our previous work has suggested that traumatic noise activates Rho GTPase pathways, leading to cochlear outer hair cell (OHC) death. Activated Rho GTPases bind to a spectrum of effectors to stimulate downstream signaling pathways. Rho-associated kinases (ROCKs) are the major targets of Rho for reorganization of actin-based cytoskeletons. The ezrin-radixin-moesin (ERM) proteins are the targets of ROCKs and act as cross-linkers between the plasma membrane and the actin cytoskeleton. Here, we investigated the Rho pathway in the regulation of the cochlear actin cytoskeleton using adult CBA/J mice under noise exposure conditions.

Methods

Broadband noise from 2–20 kHz at 98 dB SPL or 06 dB SPL for 2 hours was used to induce permanent threshold shifts

(PTS), and 92 dB SPL or 96 dB SPL to induce temporary thresholds shifts (TTS). Auditory brainstem responses were used to measure auditory function. Myosin VIIa and diaminobenzidine (DAB)-stained cochlear epithelia were used to quantify OHC loss. Western blot assays assessed ROCKs and p-ERM protein in whole cochlear homogenates. Anti-ROCK2 and anti-p-ERM immunolabeling of cochlear surface preparations were used to examine levels of ROCK2 and p-ERM in OHCs. Delivery of ROCK2 siRNA to the round window via intra-tympanic injection was performed to inhibit the expression of ROCK2 and reduce p-ERM. An in-vivo actin assay kit was used to determine the ratio of F-actin/G-actin. Treatment with Rho pathway activator 1-oleoyl lysophosphatidic acid (LPA) via intra-peritoneal injection was done to assess for protection against noise-induced hearing loss (NIHL).

Results

ROCK2 and p-ERM protein significantly decreased in the mouse whole cochlear homogenates 1 hour after PTS- or TTS-noise exposure. The levels of ROCK2- and p-ERM-associated immunofluorescence in OHCs decreased significantly after PTS-noise, but not after TTS-noise exposure. Treatment with LPA significantly attenuated the reduction of ROCK2 and p-ERM caused by noise exposure in OHCs, and also prevented NIHL and OHC death. In contrast, the genetic down-regulation of ROCK2 by pretreatment with ROCK2 siRNA reduced the expression of ROCK2 and p-ERM in the OHCs and worsened the TTS, resulting in permanent hearing deficits. Finally, noise exposure resulted in changes in the F-actin/G-actin ratio.

Conclusion

Our results suggest that noise-induced activation of Rho pathways result in modulation of the actin cytoskeleton in sensory hair cells through molecular targets of the ROCK2/ERM pathway.

PS - 376

XBP1 Mitigates Mistranslation-Induced ER Stress and Protects Against Spiral Ganglion Cell Death

Naoki Oishi¹; Stefan Duscha²; Heithem Boukari²; Martin Meyer²; Jing Xie³; Gao Wei³; Erik C. Böttger²; Jochen Schacht³

¹Keio University School of Medicine; ²Institut für Medizinische Mikrobiologie, Universität Zürich, 8006 Zürich, Schweiz; ³Kresge Hearing Research Institute, Department of Otolaryngology, University of Michigan, Ann Arbor, MI 48109-0506

Background

Translational fidelity is maintained throughout all three domains of life, suggesting a high selective pressure during evolution to minimize errors of protein synthesis. Various layers of control mechanisms contribute to the accuracy of protein synthesis: correct charging of tRNA with the cognate amino acid, accurate tRNA selection by the ribosome by induced-fit, and proofreading mechanisms. Protein misfolding has been connected to various diseases, in particular neuropathologi-

cal disorders. Here we study potential links between translation fidelity, protein misfolding and neuropathy in a model of aminoglycoside-induced mistranslation.

Methods

Misreading in human HEK cells was assessed by a dual luciferase reporter assay. ER stress and unfolded protein response (UPR) pathways were assessed by transcriptomic and proteomic approaches. As pathological consequences of aminoglycoside-induced mistranslation, we examined ER stress, integrity of hair cells and spiral ganglion cells in both in-vitro and in-vivo models of ototoxicity.

Results

Aminoglycosides induced pronounced misreading in human HEK cells. The drugs also induced ER stress and unfolded protein response (UPR) pathways as documented by transcriptomic and proteomic analyses, by quantitative changes in mRNA expression of key UPR components, and by phosphorylation of eukaryotic initiation factor 2 alpha (eIF2α). In cochlear cultures of postnatal day 2-3 CBA/J mice gentamicin induced CHOP expression in spiral ganglion neurons but not in hair cells. A potential *in-vivo* neurotoxicity was then explored by intratympanic injection of gentamicin in haploinsufficient XBP1 mice. In contrast to wild-type littermates, XBP1^{+/-} mice showed high-frequency hearing loss upon aminoglycoside treatment. This hearing loss was attenuated by systemic co-injection of tauroursodeoxycholic acid, a chemical chaperone preventing protein misfolding. Despite auditory threshold shifts, sensory hair cells were preserved in the cochleae of gentamicin-treated XBP1^{+/-} mice. However, densities of spiral ganglion cells and synaptic ribbons were significantly decreased.

Conclusion

Our results have uncovered neurotoxic properties of aminoglycoside antibiotics that are independent of their toxicity to renal and auditory sensory cells. These neurotoxic properties are linked to the ability of the drugs to cause mistranslation and protein misfolding and can be unmasked in cells with a compromised UPR. A compromised UPR system may also be a reason why primary auditory neuronal cell death has occasionally been observed in patients undergoing aminoglycoside therapy. Furthermore, XBP1^{+/-} mice may provide a new experimental model to study neuropathy associated with protein misfolding.

PS - 377

Melanin as a Possible Oto-Protective Pigment in the Ears of *Poecilia Latipinna* and *Cyprinus Carpio*

Bethany Coffey; Michael Smith
Western Kentucky University

Background

Melanin is a ubiquitous natural pigment found in most organisms, and is a determinant for the coloration of hair, eyes, and skin. Melanin allows the critically important tanning response, which protects the body from DNA mutations caused by ultraviolet radiation. It has been hypothesized that melanin plays

a protective role in the inner ear as well. Lack of melanin (i.e. albinism) is often associated with deafness in mammals. This may be because melanin-producing cells (melanocytes) form the intermediate layer of the stria vascularis in the cochlea. All classes of vertebrates can exhibit albinism, but fishes do not possess a cochlea. Therefore, although melanophores surrounding the brain and the inner ears of fishes have been observed, the importance of melanin in the fish ear is still uncertain. The purpose of this project was to examine the potentially protective role of melanin in the ear of teleost fishes.

Methods

Specifically, we performed hearing tests and inner ear dissection on three groups of sailfin mollies (*Poecilia latipinna*) and two groups of koi (*Cyprinus carpio*) that differed in pigmentation. The molly groups consisted of black, silver, and albino, and the koi groups consisted of black and white (not albino) color morphs. Hearing tests were performed by recording auditory evoked potentials (AEP) at six frequencies (100, 250, 400, 600, 800, 1000, 1500, 2000 Hz) in a repeated measures design. Control AEP hearing tests were first performed for each group of fish. Then fish were exposed to a 150 Hz tone stimulus at 167 dB re 1 μ Pa for 48 h, followed by an additional post-exposure hearing test. Threshold shifts were calculated by subtracting control thresholds from post-exposure thresholds. Then the inner ears of each fish were dissected, photographed, and melanin levels were quantified via absorption spectrophotometry.

Results

If melanin plays a protective role in the inner ear of fishes, then one would predict that black fish would experience less sound-induced hearing loss compared to white or albino fish. Preliminary results show that black mollies had significantly greater numbers of melanophores and much higher levels of melanin in their ears compared to those of white mollies. Black mollies also had significantly lower AEP hearing thresholds than white mollies following sound exposure.

Conclusion

This suggests that there may be a link between the amount of melanin in the teleost ear and hearing abilities following acoustic trauma. Future research is needed to elucidate the mechanisms of this protection.

PS - 378

High-Throughput Drug Screen for Protection Against Cisplatin Ototoxicity Using the HEI-OC1 Immortomouse Inner Ear Cell Line

Tal Teitz; Asli Goktug; Taosheng Chen; Jian Zuo
St. Jude Children's Research Hospital

Background

Cisplatin is a common chemotherapeutic drug used to treat various childhood malignancies including neuroblastoma, retinoblastoma, bone tumors, medulloblastoma and sarcoma. Ototoxicity is a major side effect of cisplatin treatment for young children and more than 50% of pediatric cancer patients suffer from mild to severe hearing loss due to cisplatin regimens. At the concentrations given to patients, cisplatin

has been shown to cause cell death by apoptosis mainly in the cochlear hair cells, spiral ganglion neurons and the lateral wall cells in the spiral ligament and stria vascularis. There are no FDA approved drugs that antagonize cisplatin-induced ototoxicity and the mechanisms by which currently available cisplatin-antagonists work in the inner ear are not completely understood.

Methods

A high-throughput drug screen employing the immortomouse inner ear cell line HEI-OC1 was used to screen libraries of 4,359 unique FDA approved and biologically-active compounds to identify compounds that could confer protection from cisplatin-induced cell death. Protection was measured by the ability to inhibit caspase-3/7 cleavage activity triggered by cisplatin treatment. The screening assay, done in 384-well plates by robots, was optimized for cell number, cisplatin concentration, assay time and the reference compound Pifithrin- α to give statistically significant results. The screen average z' value was 0.75, signal window was 12 and signal fold was 4.9. Pifithrin- α was chosen as reference compound as it has been shown in previous reports to confer good protection against cisplatin in inner ear cells and in mouse cochleae.

Results

Our primary screen gave >100 compounds (1-2% hit rate) that, at 8 μ M, the concentration the screen was done, had more than 50% inhibition of the caspase-3/7 activity in the cells induced by cisplatin and thus were effective at lower concentrations than Pifithrin- α . We are now validating these results by performing dose response curves in the HEI-OC1 cell line and by a viability assay to exclude compounds that may be toxic to the cells.

Conclusion

Our unbiased cell-based screen identified potential drugs for protection against cisplatin-induced ototoxicity. Our next steps will focus on testing the promising compounds in cochlear explants and *in vivo* in mice. These compounds will also be evaluated in tumor cell lines and in other species. Promising compounds will be further tested in clinical trials, given that we have previously studied >303 pediatric cancer patients with cisplatin treatment at St. Jude.

PS - 379

Ups and Downs of Viagra: Revisiting Ototoxicity in the Mouse Model

Adrian Au; John Gerka-Stuyt; Daniel Chen; Kumar Alagramam

Case Western Reserve University

Background

Sildenafil citrate (Viagra), a phosphodiesterase 5 inhibitor (PDE5i), is a commonly prescribed drug for erectile dysfunction. Since the introduction of Viagra in 1997, several case reports have linked Viagra to sudden sensorineural hearing loss. However, these studies are not well controlled for confounding factors, such as age and noise-induced hearing loss and none of these reports are based on prospective double-blind studies. Further, animal studies report contradictory data. For example, one study (2008) reported hearing loss

in rats after long-term and high-dose exposure to sildenafil citrate. The other study (2012) showed vardenafil, another formulation of PDE5i, to be protective against noise-induced hearing loss in mice and rats. Whether or not clinically relevant doses of sildenafil citrate cause hearing loss in normal subjects (animals or humans) is controversial. One possibility is that PDE5i exacerbates age-related susceptibility to hearing loss in adults.

Methods

We tested sildenafil citrate in C57BL/6J, a strain of mice that displays increased susceptibility to age-related hearing loss, and compared the results to those obtained from the FVB/N, a strain of mice with no predisposition to hearing loss. Six-week-old mice were injected with the maximum tolerated dose of sildenafil citrate (10 mg/kg/day) or saline for 30 days. Auditory brainstem responses (ABRs) were recorded pre- and post injection time points to assess hearing loss. Entry of sildenafil citrate in the mouse cochlea was confirmed by qRT-PCR analysis of a downstream target of the cGMP-PKG cascade.

Results

ABR data indicated no statistically significant difference in hearing between treated and untreated mice in both backgrounds. Results show that the maximum tolerated dose of sildenafil citrate administered daily for 4 weeks does not affect hearing in the mouse.

Conclusion

Our study gives no indication that Viagra will negatively impact hearing and it emphasizes the need to revisit the issue of Viagra related ototoxicity in humans.

PS - 380

Temporary Threshold Shift Breaks Tip Links in Hair Cells and Enhances Uptake of Gentamicin

David Furness¹; Peter Steyger²; Hongzhe Li²

¹*Institute for Science and Technology in Medicine, School of Life Sciences, Keele University;* ²*Oregon Hearing Research Center, Oregon Health & Science University*

Background

Ototoxicity is synergistically enhanced by dual exposure to both acoustic overstimulation and aminoglycoside antibiotics. Sound exposures that induce temporary threshold shifts (TTS) have been found to enhance uptake of gentamicin in cochlear outer hair cells (OHCs). We hypothesized that sound-enhanced aminoglycoside uptake occurs via the mechanoelectrical transducer (MET) channels in OHCs as a candidate mechanism for this ototoxic synergy. To test this hypothesis, we systematically varied the sound level to induce TTS, exposed animals to gentamicin and examined the effect of TTS on tip link survival.

Methods

To induce TTS, adult C57Bl/6 mice were exposed to wide-band noise (WBN; 86-96 dB SPL) for 6 hours/day for 3 days. The degree of TTS was assessed by tonal ABR measurements (4, 8, 12, 16, 24 and 32 kHz) before and after sound

exposure. Mice were then intraperitoneally injected with fluorescently-conjugated gentamicin (GTTR) to track gentamicin uptake. Thirty minutes later, fixed cochlear tissues were excised and processed for confocal microscopy. The intensity of GTTR fluorescence was measured in OHCs under identical confocal settings. An independent batch of mice, exposed to 91 dB SPL WBN, were cardiac perfused, cochlear tissues fixed and processed for scanning electron microscopy. The number of identifiable stereociliary tips and visible tip links per hair bundle (10 per OHC row) were counted at a mid-cochlear location corresponding to a frequency range of 12-16 kHz.

Results

Higher sound levels (91 and 96 dB SPL) produced demonstrable TTS at higher frequencies (16, 24 and 32 kHz). Sound levels that induced TTS also enhanced hair cell uptake of GTTR at higher frequency locations examined along the organ of Corti. Identifiable stereociliary tip links were present at ~50% of potential positions between shorter and taller stereocilia. Tip link survival rate was substantially less in the majority of animals that received WBN.

Conclusion

Sound exposure that caused TTS enhanced GTTR uptake but reduced the number of tip links. This suggests that sound-enhanced GTTR uptake is unlikely to occur through tip link-gated MET channels, and shows that further research into the mechanisms of sound-potentiated aminoglycoside uptake is warranted.

PS - 381

Bisphenol-A Kills Hair Cells in the Zebrafish Lateral Line

Allison Coffin; Lauren Hayashi; Meghal Sheth

Washington State University

Background

Environmental toxins are prevalent in the water supply, soil, and many food products, yet the effects of these contaminants on the auditory system are generally unknown. The present study asks if one ubiquitous contaminant, bisphenol-A (BPA), is toxic to hair cells. BPA is used in plastic and resin production and is a component of many common products, including plastic bottles, aluminum can linings, and some dental sealants. Prior research suggests that BPA functions as an endocrine disrupter, but it can have additional toxic effects. Here, we use the larval zebrafish lateral line as a model to study BPA ototoxicity.

Methods

We exposed 5 day-old larvae to varying concentrations of BPA over a period of 1-24 hours. Hair cell survival was assessed by relative fluorescent intensity of the vital dye DAS-PEI and with counts of anti-parvalbumin-labeled hair cells. Larvae were then co-treated with BPA and one of several cell death pathway inhibitors in order to understand the mechanism(s) by which BPA damages hair cells.

Results

BPA-induced hair cell loss is both dose- and time-dependent. BPA concentrations of 1 μ M or higher kill lateral line hair cells

during a 24-hour exposure period. 40% hair cell loss is evident with 40 μ M BPA, while concentrations higher than 60 μ M have negative effects on overall fish health. Higher BPA concentrations induce significant hair cell loss within 3 hours, while 1 μ M BPA is only ototoxic after 24 hours of exposure. Preliminary experiments with cell death inhibitors suggest that BPA may activate EGF signaling in hair cells, although this result remains to be verified.

Conclusion

We demonstrate that the environmental toxin BPA is toxic to lateral line hair cells. Future experiments will determine the cell death pathways activated in BPA-damaged hair cells and ask if similar ototoxicity is observed in the mammalian cochlea.

PS - 382

Noise Induced Oxidation Impairs Membrane Fluidity.

Anna Fetoni; Sara L.M. Eramo; Giuseppe Maulucci; Fabiola Paciello; Marco De Spirito; Diana Troiani; Gaetano Paludetti

Catholic University of Rome

Background

The common basis for OHC loss by acoustic over-stimulation is triggered by the unbalance of cellular redox status due to reactive oxygen species (ROS) overload. It is suggested that increased metabolic activity can strongly affect the membrane structural organization. To address this issue, we investigated first, in OHC different functional zones the mechanisms linking metabolic functional state (NAD(P)H intracellular distribution) to the generation of lipid peroxides and to the physical state of membranes following noise exposure. Secondly, we studied the protective effects of an antioxidant molecule, rosmarinic acid, in prevention the lipid peroxidation in the OHCs.

Methods

Hartley albino guinea-pigs (age 3 months) were used as model of acoustic trauma and they were exposed to a 6 kHz pure tone noise for 1 h at 120 dB. Hearing function was evaluated in all animals by measuring ABR. To assess the oxidative damage induced by noise exposure we used 4-hydroxy-2-nonenal (4HNE) immunostaining at 1, 6, 9, 18, 24h after acoustic trauma and RA protection (10 mg/kg 1 day and 2 hour before noise exposure). The middle/basal turn of control and noise exposed cochleae were rapidly dissected and the specimens were analyzed for NAD(P)H microscopy (the right cochlear specimens) and prepared for Laurdan microscopy (the left cochlear parts). All Images were obtained with an inverted confocal microscope (DMIRE2, Leica Microsystems, Germany) using a 63X oil immersion objective

Results

In the OHCs of control animals, a more oxidized NAD(P)H redox state is correlated with a less fluid membrane structure. In noise exposed animals, excessive noise induces a topologically differentiated NAD(P)H oxidation in OHC rows, which is damped between 1 and 6 h. Peroxidation occurs after ~ 4h from the noise insult, while ROS are produced in the first 0.2h and damages cells for a period of time after the noise expo-

sure has ended (~ 7.5h) when a decrease of fluidity of OHC plasma membrane occurs. Lipid peroxidation is prevented by antioxidant supplementation. Lipid peroxidation and hearing loss were reduced in the animals treated with RA

Conclusion

The time course of NAD(P)H oxidation, lipid peroxidation and membrane fluidity indicates that a perturbation of OHC metabolism triggers lipid peroxidation, which impairs membrane fluidity characterized by a lower metabolic activity with respect to other rows. On the whole, membrane fluidity is regulated by NAD(P)H redox state and lipid peroxidation which represent therefore key targets for a therapeutic rescuing plan from noise insults

PS - 383

Hepatocyte Growth Factor Mimetic Protects Lateral Line Hair Cells From Aminoglycoside Exposure

Phillip Uribe¹; Leen Kawas²; Joseph Harding²; Allison Coffin¹

¹*Washington State University, Vancouver*; ²*Washington State University*

Background

Application of exogenous hepatocyte growth factor (HGF), a neurotrophic factor, prevents kanamycin ototoxicity in rats. HGF itself is not an ideal therapeutic due to a short half-life and limited ability to cross the blood brain barrier. Dihexa is a chemically stable, blood brain barrier permeable, synthetic HGF mimetic that can form a functional ligand to activate the HGF receptor and consequently its downstream signaling cascade. The purpose of this project is to explore whether allosteric activation of the HGF cascade via dihexa can protect hair cells from aminoglycoside damage.

Methods

We use the larval zebrafish lateral line model to evaluate dihexa as a potential hair cell protectant. The lateral line possesses hair cells that are functionally and structurally similar to mammalian inner ear hair cells, and cells in both systems respond similarly to toxins. Optimal dose-response and time-response relationships for dihexa protection were established using two ototoxins, neomycin and gentamicin. These aminoglycosides activate distinct cell death cascades, therefore, it was necessary to assess each separately. Fish were treated with fluorescently tagged gentamicin (GTTR) following dihexa treatment to test if dihexa affects uptake of aminoglycosides vs. inhibiting intracellular death pathway(s).

Results

We found that dihexa concentrations as low as 1 pM protect hair cells from neomycin- or gentamicin-induced toxicity. We observed no difference in intracellular fluorescence of GTTR, suggesting that dihexa does not inhibit cellular uptake of aminoglycosides. This experiment further suggests that dihexa does not inhibit mechanotransduction, since aminoglycoside uptake requires functioning mechanotransduction channels.

Conclusion

Our data suggest that dihexa confers protection through inhibition of cell death pathways and not aminoglycoside uptake. The overall effectiveness of dihexa as a hair cell protectant at very low concentrations supports its potential clinical utility and predicts minimal off target effects. Future studies will elucidate downstream signaling pathways activated by dihexa and examine the protective potential of dihexa in aminoglycoside-treated mammalian hair cells.

PS - 384

Virally-Mediated Overexpression of Neurotrophin Protected Spiral Ganglion Neurons from Degeneration in the Cochlea of Conditional Connexin26 Knock out Mice

Qi Li; Qing Chang; Jianjun Wang; Xi Lin

Emory University School of Medicine

Background

Brain-derived neurotrophic factor (BDNF) and Neurotrophin3 (NT-3) play important roles in the development and maintenance of normal innervation of hair cells by the spiral ganglion (SG) neurons. Hereditary hearing loss is one of the most common forms of congenital deafness in the otology practice. For decades, among many therapies that are developed to treat hearing loss, cochlear implant is still the most effective treatment for patients suffering severe sensorineural hearing loss. Survival of SG neurons is necessary for successful performance of the cochlear implant. In our previous work we have shown that activation of TrkB receptors by small molecule analog of BDNF significantly improved survival of SG neurons in the cochlea of conditional connexin26 (cCx26) knockout mice, which suffer from secondary degeneration of SG neurons due the death of large amount of hair cells.

Methods

Here we used adeno-associated virus (AAV) to express the BDNF or NT-3 gene in the scala media of the cochlea in order to test whether such a strategy of over-expression is able to offer neuroprotective effects for SG neurons against degeneration in the cochlea of cCx26 knockout mice.

Results

We injected the AAV in early postnatal mice (P0 to P2) into the scala media. Cochlear morphology was checked two months after injections. Results obtained from resin cochlear sections showed that the density SGNs was significantly higher in the injected ear comparing to the contralateral un-injected ear. In the basal turn, the average number of SGNs in untreated side was $128 \pm 16/100\mu\text{m}^2$, comparing to the treated side of $468 \pm 53/100\mu\text{m}^2$. In the middle turn, the average number of SGNs in untreated and treated side was $214 \pm 14/100\mu\text{m}^2$ and $562 \pm 61/100\mu\text{m}^2$ respectively. The differences in both the basal and middle turns were statistically significant. The neuroprotective effect could not be tested in the apical turn of cCx26 knockout mice because SG neurons didn't show significant degeneration there. We also found that the threshold of the auditory brainstem responses didn't show improvement after the treatment.

Conclusion

Result suggested that BDNF over-expression by a virally-mediated approach enhanced the survival of the SG neurons. Our experiments to test the effect of over-expressing NT-3 are still ongoing.

PS - 385

In Situ Observation and Image Analysis of the Cochlear Sensory Epithelium in Mouse Cochleae

Daniel Cartwright; Qunfeng Cai; Bo Hua Hu

University at Buffalo

Background

The mouse is an excellent model for investigating molecular mechanisms of hearing loss. However, due to its small size and structural complexity, dissection of mouse cochleae for surface preparation is a technical challenge for many molecular biologists. This challenge has been addressed using a tissue-clearing technique. However, this technique requires time-consuming tissue preparation. Moreover, clearing solutions can affect the immunoreactivity of proteins in the tissue. Here, we developed a method of partial cochlear dissection to remove the step of chemical preparation of the cochlea. In combination with improved image analysis, this method provides a valuable alternative for surface preparation in quantitative analysis of cochlear pathologies.

Methods

The method involves three basic steps. First, the cochlea was partially dissected to expose the cochlear sensory epithelium. Second, the cochlea was observed *in situ* using one of three methods of microscopy: fluorescence, confocal, and two-photon. Third, the collected images were digitally analyzed for quantitative assessments. For a routine cochleogram, the cochlear sensory epithelium was photographed at multiple focal depths. Each image from this process was loaded as a layer into an Adobe PhotoShop® image and aligned using the Auto-Align function to ensure that all images overlapped correctly. The clearest sections of each layer were then merged into a single continuous image. To compare the current partial dissection method with a tissue-clearing technique, additional cochleae were processed using Scaleview-A2, an optical clearing agent.

Results

The *in situ* observation has three significant advantages. First, the structural integrity of the sensory epithelium is well preserved. Second, the dissection procedure is substantially simplified. The most challenging step of dissection, separating the sensory epithelium from the lateral wall and the modiolus, is no longer needed. Third, chemical tissue preparation for tissue clearance is avoided. Although the image resolution is limited due to the use of a low magnification lens, the quantity of the images is sufficient for routine quantification of sensory cell damage. In combination with confocal microscopy or two-photon microscopy, this method provides a valuable tool for observing the intact sensory epithelium.

Conclusion

In situ observation provides an alternative for surface preparation with excellent protection of tissue structures. It is particularly valuable for researchers who have limited skill in cochlear dissection.

PS - 386

***In Vitro* Model of Inner Ear Trauma and Otoprotection Using a Combination of JNK Inhibitor, Steroid and Antioxidant**

Chhavi Gupta¹; Brenda Puwoll²; Amir Tarsha²; Jeenu Mittal²; Esperanza Bas²; Thomas R. Van De Water²; Fred Telisch²; Adrien Eshraghi²; Helio Rodrigues²

¹Hearing Research laboratory, Department of Otolaryngology, University of Miami Miller School of Medicine; ²University of Miami

Background

Inner ear trauma such as cochlear implant electrode trauma initiates multiple molecular mechanisms such as oxidative stress, JNK activation and caspase-3 activation in hair cells or support cells resulting in initiation of programmed cell death within the damaged tissues of the cochlea which leads to loss of the residual hearing. In earlier studies L-N-acetylcysteine (L-NAC) (an excellent antioxidant), dexamethasone (DXM) (a steroid) and Mannitol (with osmotic and diuretic effects) has been shown independently to protect the HCs loss against tumor necrosis factor α (TNF α). These 3 molecules have different otoprotective effects; goal of this preliminary study is to test the efficacy of a combination of these molecules to enhance the otoprotection of HCs against electrode induced trauma (EIT).

Methods

OC explants were dissected from P-3 rats and placed in serum-free media. Explants were divided into three groups: 1) untreated controls; 2) EIT; 3) Tri-therapy cochlea EIT+L-NAC (5mM)+ DXM (20 μ g/mL) + Mannitol (100mM). In Groups 2 and 3, a 0.28-mm diameter monofilament fishing line was introduced through the small cochleostomy located next to the round window area, allowing for an insertion of between 110° and 150°. Oxidative stress, inflammatory and cleaved caspase-3 markers were studied in all explants at different time intervals post EIT.

Results

There was an increase of total hair cell (THC) loss in the EIT OC explants when compared with control group HC counts or the tri-therapy cochlea. The insertion of the monofilament line through the cochleostomy resulted in an increased production of the total reactive oxygen species (ROS) in both the HCs and the supporting cells (SCs). Cleaved caspase-3 activation was observed in EIT group as compared to control group cochlea.

Conclusion

Various molecular mechanisms are involved in post EIT trauma, the tri-therapy proposed may be a promising treatment for protection of the auditory HCs undergoing electrode induced trauma.

PS - 387

Audiometric Analysis of Cystic Fibrosis Patients Receiving Obligate Aminoglycoside Treatment

Angie Garinis¹; Patrick M. Feeney²; David Cohen¹; Jeff Gold¹; Daniel Putterman²; Troy Lubianski¹; Peter Steyger¹

¹Oregon Health and Science University; ²Oregon Health and Science University; ²Portland VA- NCRAR

Background

Ototoxicity is defined as dysfunction and/or damage to cochlear or vestibular sensory mechanisms by exposure to a chemical source. Aminoglycosides are one group of ototoxic medications that are clinically essential to treat life-threatening infections in chronic diseases such as cystic fibrosis (CF). Around 30% of patients with CF develop permanent hearing loss due to obligate aminoglycoside therapy, impacting speech discrimination, cognition and quality of life. The severity of hearing loss in CF patients is not entirely dose-dependent, and most CF patients receive large cumulative exposure to aminoglycosides over their lifespan, yet many do not exhibit signs of hearing loss.

Methods

This investigation used a systematic approach to evaluate the cochleotoxicity of aminoglycoside exposure in 90 patients with CF, ages 15-63, treated at Oregon Health and Science University CF adult and pediatric centers. Hearing was assessed across the standard clinical frequency range of hearing (250-8,000Hz) and an extended high frequency range (9,000-16,000 Hz) that often exhibits the initial effects of cochleotoxicity.

Results

Preliminary data analysis revealed a subgroup of subjects with excellent hearing thresholds from 250 to 16,000 Hz (40%), and a second group exhibited sensory hearing loss in the standard range (4%), extended range (31%), or both ranges (25%). This bi-modal distribution, despite aminoglycoside exposure across all participants, is suggestive of inter-individual variability in susceptibility to ototoxicity.

Conclusion

The dichotomous distribution of hearing thresholds in CF patients treated with aminoglycosides is suggestive of a genetic basis. Extended high frequency threshold testing is necessary in most cases to detect the cochleotoxic changes in puretone thresholds. Genomic analysis for correlation with audiometric profiles is underway.

Early Molecular Mechanisms Involved in Electrode Insertion Trauma and Oto-Protection Provided by a JNK Inhibitor or Dexamethasone

Adrien Eshraghi¹; Chhavi Gupta²; Carolyn Garnham³; John Saman²; Thomas Van De Water²; Ileana Rivera²; Dustin Lang²; Helio Rodrigues²

¹Hearing Research laboratory, Department of Otolaryngology, University of Miami Miller School of Medicine; ²University of Miami; ³MED-EL Corporation

Background

We described previously, the pattern of hearing loss post cochlear implantation (CI) and electrode insertion trauma (EIT) in animal models. Cochlear implant induced EIT, not only causes direct tissue trauma and cell losses, but also generates molecular events that may initiate programmed cell death (PCD) via various mechanisms such as oxidative stresses, release of pro-inflammatory cytokines; activation of the caspase pathway which can result in apoptosis; generation of pro-apoptotic signal cascades via, for example, mitogen-activated protein kinases/c-Jun-N-terminal kinases (MAPK/JNK) within the damaged tissues of the cochlea which can lead to a loss of residual hearing. Objectives of this study is: a) to dissect the molecular mechanisms involved in PCD of hair cells and support cells, b) to analyse otoprotection provided by AM-111 or DXM against EIT.

Methods

Guinea pigs were categorized in four groups: EIT; pre-treated with AM-111 or DXM at round window ½ hr before EIT, and unoperated contralateral ears as controls. Immunostaining for phospho-c-Jun, activated Caspase-3, CellROX and HNE were performed at 6hrs, 12hrs and 24hrs post-EIT

Results

6 hrs Post-EIT immunostaining of both HCs and SCs demonstrated that phosphorylation of c-Jun and activation of caspase-3 starts in SCs. Caspase-3 activation was not observed in HCs of any turn at 12 and 24hrs, but p-c-Jun labeling was observed at 12 hrs in both HCs and SCs of middle and basal turn and in HCs of all turns at 24hrs. Lipid peroxidation starts 12hrs post EIT in both HCs and SCs of basal turn, and reaches up to apex turn at 24hrs post EIT. EIT+ AM-111 and DXM groups showed no phosphorylation of HCs and SCs at 6hr, 12hr and 24hrs post-EIT.

Conclusion

It appears that PCD starts in SCs initially followed by PCD in HCs. Molecular mechanisms involved in PCD of hair cells are different than the one involved in PCD of support cells. PCD initially starts in the basal turn of cochlea and then propagates to middle and apical turn between 12 and 24 hrs after EIT. There is a window of opportunity to treat the cochlea before onset of cell death in HCs.

Susceptibility to Cytomegalovirus Induced Hearing Loss Is Mediated by Ly-49H Natural Killer Cell Activation in a Murine Model

Albert Park; Matt Firpo; Elaine Hillas

University of Utah

Background

We have previously successfully demonstrated Cytomegalovirus (CMV) induced labyrinthitis in BALB/c murine newborn pups that recapitulates human viral mediated hearing loss in infants. We then evaluated the role of Ly49H natural killer (NK) cell activation in a mouse model for Cytomegalovirus (CMV) induced sensorineural hearing loss (SNHL) in this animal model.

Methods

C57BL/6 and BALB/c mice underwent intracranial injection at postnatal day 3 with 200 pfu of green fluorescent protein (GFP) expressing murine (m) CMV; controls received either saline or no injection. C57BL/6 mice were also administered anti-Ly49H antibody prior to inoculation to determine the role of this receptor in CMV susceptibility to hearing loss. Hearing thresholds were assessed using auditory brain stem response testing (ABR). Temporal bones were harvested and sectioned for histologic analysis. A subset of BALB/c and C57BL/6 temporal bones were harvested for histologic analysis at variable days after inoculation.

Results

- All BALB/c mice had profound hearing loss by 8 weeks.
- mCMV-GFP expression was seen in the BALB/c spiral ganglion and adjacent scala tympani at 7 days post-injection and absent by 4 weeks.
- C57BL/6 mice showed no hearing loss.
- C57BL/6 did not show any evidence of mCMV infiltration of the cochlea at 3 or 7 days post inoculation.
- All C57BL/6 mice pretreated with anti-Ly49h antibody demonstrated hearing loss.

Conclusion

These results suggest that resistance to CMV mediated hearing loss is mediated by Ly49H NK receptor activation

Release of Secretory Exosomes as a Mechanism of Protection Against Hair Cell Death

Lindsey May; Lisa Cunningham

NIH/NIDCD

Background

We showed previously that supporting cells act as mediators of hair cell survival by secreting HSP70 (May et al. 2013, *JCI*). Here we have examined the mechanism of HSP70 secretion from supporting cells. HSP70 is released from a variety of cell types via secretory exosomes, which are endosome-derived microvesicles that are 50-200 nm in size. Recent research

has shown that exosomes are released from many cell types, and they play important roles in intercellular signaling.

Methods

We utilized both nanoparticle tracking analysis and TEM to examine exosome release from control and heat-shocked utricles as well as from two cell lines. For exosome isolation, utricles were heat shocked, cultured overnight, and the surrounding media was collected 24 hours later. An exosome-producing tumor cell line (CT26, ATCC) was grown to confluence, and the surrounding media was collected 48 hours later. Exosomes were isolated from both the utricle and cell culture media by ultracentrifugation and further purified using a sucrose cushion. Purified exosomes were added to utricle cultures to determine if exosomes inhibit neomycin-induced hair cell death.

Results

Our nanoparticle tracking analysis data indicate that heat shocked utricles release secretory exosomes. Isolated exosomes inhibit neomycin-induced hair cell death in whole-organ cultures of utricles from adult mice.

Conclusion

Our data indicate that heat-shocked utricles release secretory exosomes, and that isolated exosomes are protective against hair cell death. Further studies are designed to examine 1) the protein and mRNA cargo contained in exosomes, and 2) the roles of exosomes in supporting cell-mediated signaling and protection.

PS - 391

Distinct Patterns of Cochlear Hair Cell Loss Following Exposure to Different Intensity and Duration of Acoustic Trauma

Christopher Neal; Stefanie Kennon-McGill; Hinrich Staecker; Thomas Imig; Dianne Durham
University of Kansas Medical Center

Background

One potential mechanism for tinnitus is that insult to the peripheral auditory system changes the nature of excitatory and inhibitory inputs to central auditory neurons. The initial insult that begins this cascade of central auditory changes may be the loss of hair cells (HC) or changes in afferent input from the cochlea. Prior electrophysiological recordings from awake, behaving rats in our laboratory (Kennon-McGill, et al. ARO 2013) have shown that exposure to a 16 kHz, 114 dB pure tone for 1 hour increases average spontaneous activity in inferior colliculus (IC) units. However, exposure to a 16 kHz, 118 dB pure tone for 4 hours resulted in more subtle changes only seen in untuned units >8 kHz.

Here we quantify changes in HC number that may elucidate changes occurring in the IC. We hypothesize the 4 hour 118 dB exposure causes more inner and outer HC loss in a more diffuse area relative to 1 hour 114 dB exposure.

Methods

We unilaterally exposed anesthetized, male Long-Evans rats to either a 114 dB SPL, 16 kHz pure tone for 1 hour or a 118

dB SPL, 16 kHz pure tone for 4 hours. Following a three to four week recovery period, the animals were sacrificed and cochleae harvested. Cochleae were fixed, stained, embedded in Araldite and sectioned parallel to the modiolar axis at 40 μ m. Hair cell counts were accomplished without knowledge of the noise exposure. Cytocochleograms plotting hair cell number as a function of frequency were constructed using Greenwood's equation transforming percent distance to frequency (Hearing Res. 94, 157–162; 1996).

Results

Compared to unexposed control animals, prominent HC loss was seen in the 8-16 kHz region as well as above 32 kHz for both sound damage groups. Animals exposed to a 16 kHz, 118 dB pure tone for 4 hours had loss of both inner and outer hair cells in affected regions of the cochlea, while the animals exposed to a 16 kHz, 114 dB pure tone for 1 hour had greater outer HC loss relative to inner HC in affected areas.

Conclusion

The two sound damage paradigms cause unique patterns of HC loss when compared to unexposed, control animals. It is intriguing that less severe hair cell death, particularly for inner hair cells, is observed following sound exposure that results in an increase in spontaneous activity in the IC.

PS - 392

Low Level Laser Irradiation Affects Adenosine Triphosphate and Reactive Oxygen Species Productions in Auditory Cell Line.

Jae Yun Jung¹; So-Young Chang²; Jae Wook Lee³; Il Yong Park⁴; Myung-Whan Suh⁵; Chung-Ku Rhee³; Phil-Sang Chung³

¹Dankook University; ²Beckman Laser Institute Korea, Dankook University; ³Department of ORL-HNS, Dankook University; ³Department of ORL-HNS, Dankook University; ⁴Department of Biomedical Engineering, Dankook University; ⁵Department of Otorhinolaryngology, Seoul National University

Background

Low-level laser (LLL) irradiation in the field of peripheral and central nervous system disorders have been investigated. Recently low level laser irradiation has been showing its possible role in inner ear using animal models. But, how laser irradiation is acting on inner ear hair cells and auditory nerves after various insults is yet to be elucidated, urging further mechanism study. We investigated how LLL irradiation affects hair cells (HEI-OC1 cell line) survival and adenosine triphosphate (ATP) production and reactive oxygen species (ROS) production after aminoglycoside administration.

Methods

The HEI-OC1 cells used in this study were maintained in DMEM with 10 % FBS at 33°C under 5 % CO₂ in air. The cells (2.5X10³ cells/well) were incubated with two fold diluted gentamicin (GM, Sigma, US) for 24 h, and the dose -dependent effects of GM were measured using a MTT assay. Based on MTT assay results as a function of GM concentration, two different concentrations (6.6 and 13.1 mM) were chosen for

further analysis to see the effects of LLL irradiation on ototoxicity with given concentration. The ATP assay and the Reactive oxygen species (ROS) production in HEI-OC1 cells were measured immediately, 1 hour and 2 hours after laser irradiation. The ATP concentration was measured using an ATP assay kit (Colorimetric assay, Abcam, UK) with the OD at 540 nm. The ROS was stained using fluorescent dye, H2DCFDA (Invetrogen, US) and observed under confocal microscope (Carl Zeiss, Germany).

Results

Reduced ATP production was not observed with 6.6 mM-GM, but with 13.1 mM compared to control. LLL irradiation (without GM) increased ATP production compared to control. With GM concentration of 13.1mM, LLL augmented ATP production measured immediately, 1hour and 2hours after 15 minutes irradiation.

ROS generation was increased with both GM concentration (6.6, 13.1 mM) showing decrease from 5 hours after GM application. Like ATP production, with 13.1mM-GM, LLL reduced ROS production measured immediately, 1hour and 2hours after 15 minutes irradiation. But, with 6.6 mM-GM, LLL didn't show obvious effects on ROS production.

Conclusion

LLL irradiation facilitates auditory cell line survival increasing ATP productions and reducing ROS generations.

PS - 393

Acetylcholine Enhances Aminoglycoside Uptake in Neonatal Hair Cells, Via Putative Activation of Nicotinic Acetylcholine Receptors.

Lauren Luk¹; Douglas E. Vetter²; Peter S. Steyger³; Hongzhe Li³

¹Oregon Health & Science University; ²Department of Neurobiology and Anatomical Sciences, University of Mississippi Medical Center; ³Oregon Hearing Research Center, Oregon Health & Science University

Background

Efferent activation of hair cells via cholinergic synapses provides fundamental regulation of auditory perception, and otoprotection against noise exposure. Stimulation of efferent terminals releases the neurotransmitter acetylcholine, which activates nicotinic acetylcholine receptors (nAChRs) at the post-synaptic membrane of hair cells, and induces a Ca²⁺ influx that activates nearby SK2 channels to hyperpolarize the cell. In the neonatal rodent (P8-11 in rats and mice), morphogenesis of the cochlea is ongoing, and postsynaptic nAChRs are thought to modulate spontaneous activity in hair cells that is critical for the maturation of central tonotopicity. Concomitant with this transient postnatal window, we recently observed enhanced aminoglycoside uptake by individual murine hair cells *in vivo*. Because hair cell nAChRs are blocked by aminoglycosides, we hypothesized that they may also be aminoglycoside-permeant and facilitate uptake of aminoglycosides into hair cells.

Methods

Neonatal mice of various postnatal ages were intraperitoneally injected with fluorescently-conjugated gentamicin (GTTR). Fixation was performed up to 30 minutes following injections. Cochlear tissues were excised and processed for confocal microscopy and fluorescence quantification. Explants of cochlear coils were also treated with GTTR, with or without acetylcholine, fixed, and analyzed.

Results

In vivo, between P7-P11, many basally located outer and inner hair cells take up more GTTR compared to adjacent cells showing baseline levels of uptake. This may occur via the MET channel. This heterogeneity was also observed in *Myo7a8J/8J* and *Pcdh153J/3J* mouse strains with decreased or absent MET activity respectively. This suggests that the observed heterogeneous uptake pattern is MET channel-independent. Heterogeneity was largely absent in mice lacking the $\alpha 9$ nAChR subunit. Wildtype explants at P4 or P7 treated with both GTTR and acetylcholine had increased GTTR fluorescence in mid and basal cochlear coils compared to explants treated with GTTR alone. These results were also replicated with P4 explants from *Myo7a8J/8J* mice.

Conclusion

These data suggest that GTTR entry into hair cells can be facilitated by basolaterally located ligand-gated cation channels, independent of the mechanoelectrical transduction (MET) channel. It remains to be determined whether aminoglycoside uptake that is independent of the MET channel contributes to an increased (synergistic) risk of ototoxicity, for example, during sound exposure.

PS - 394

The Morphological Change of Reticular Lamina by Three Myosin II Inhibitors.

Tomoki Fujita¹; Hirofumi Sakaguchi¹; Sigenobu Yonemura²; Yasuo Hisa¹

¹Kyoto Prefectural University of Medicine; ²RIKEN Center for Developmental Biology, Kobe

Background

We previously presented morphological changes and plasticity of Reticular Lamina by blebbistatin which is direct non-muscle myosin II inhibitor and Y27632 which is ROCK inhibitor. In this presentation, by using ML-7 which is myosin light chain inhibitor, we tried to verify more detail mechanism about non-muscle myosin II relation to morphology by comparing the morphological differences by the three inhibitors.

Methods

By using murine organ of corti primary culture, we tried to visualize the morphological changes after blebbistatin, Y27632 and ML-7 treatment and their plasticity by confocal microscope and analyse that images by using ImageJ (NIH).

Results

By using ML-7, we visualized some murine organ of corti morphological changes. Deiter's cell 1-3 didn't grow wider about their perimeter and area after inhibition by ML-7 when com-

pared with Blebbistatin and Y27632. Except Inner hair cell (IHC), OHC1-3 also doesn't change so much by the inhibition.

Conclusion

By using three non-muscle myosin II inhibitors, we ascertained morphological change differences of murine organ of Corti. There are some novel morphological change differences among inhibition by blebbistatin, Y27632 and ML-7.

PS - 395

Feasibility of AAV-Mediated Neurotrophin Expression in the Deafened Cochlea

Patricia Leake; Stephen Rebscher; Omar Akil
University of California San Francisco

Background

Postnatal development and survival of cochlear spiral ganglion (SG) neurons depend upon both neurotrophic support and neural activity. Our prior studies in cats deafened prior to hearing onset have shown that electrical stimulation from a cochlear implant (CI) can help prevent SG degeneration, and intracochlear infusion of the neurotrophin (NT) BDNF can further improve SG survival and promote survival and ectopic sprouting of radial nerve fibers. Improved neural survival should be beneficial for CI outcomes, but disorganized, ectopic radial nerve fiber sprouting could be deleterious. Further, in these studies NT was delivered by an osmotic pump, which is not practical for clinical application. Thus, current studies are exploring the use of adeno-associated viral vectors (AAV) to force NT expression by cells in the cochlea.

Methods

AAV2-GFP (green fluorescent protein) or AAV2-GDNF (glial-derived neurotrophic factor) was injected into the scala tympani of the cochlea in FVB mice one to 2 days after birth, directly through the round window. Mice were studied 7-14 days later. Preliminary studies also assessed AAV2 efficacy in transfecting the cat cochlea: Kittens were deafened as neonates by systemic injections of neomycin prior to hearing onset. ABRs demonstrated profound hearing loss by 16-18 days postnatal. Animals were injected with AAV2 vectors (10 ml) at one month of age and studied 5-6 weeks later.

Results

After AAV2-GFP injections in mice, immunohistochemistry revealed strong expression of the GFP reporter gene in inner and outer hair cells, inner pillar cells, and also in SG neurons. After injections of AAV2-GDNF, RT-PCR using cDNA from the mouse cochlea showed expression of both human GDNF and endogenous mouse GDNF, and qPCR demonstrated that human GDNF (elicited by AAV2) was expressed at a level about 1500 times higher than the endogenous mouse GDNF.

After AAV2-GFP injections in deafened cats, immunohistochemistry showed robust GFP expression in supporting cells and SG neurons throughout the cochlea. Preliminary *in situ* hybridization data showed a similar pattern of expression, with robust transfection of SG neurons.

Conclusion

Robust GFP expression was elicited in SG neurons in both mice and cats. If AAV2-NT similarly elicits SG expression of NTs, this should directly promote their survival. Moreover, NT expression in hair cells and supporting cells could attract re-sprouting radial nerve fibers, thereby helping to restore more normal neuroanatomy and possibly allowing reinnervation of hair cells in ears with hearing loss due to loss of SG neurons.

PS - 396

Predicting Perceived Lateral Position for Large Interaural Time Delays and Straightness Sensitivity: A Comparison of Three Models

Clayton Rothwell; Robert Gilkey
Wright State University

Background

The binaural system is sensitive to interaural time differences (ITDs) beyond the physiological range (i.e., roughly ± 600 ms). This sensitivity varies as a function of bandwidth and interaural phase differences (IPD), becoming more sensitive as bandwidth increases and less sensitive as IPD increases and *straightness* thereby decreases (*straightness* refers to the shape of cross-correlation trajectories across frequency; Stern, Zeiberg, & Trahiotis, 1988). Three models, all using Jeffress/Colburn type coincidence detection, have been proposed to explain this sensitivity: the second-level coincidence model (SLC; Stern & Trahiotis, 1992), the across-frequency averaging model (AFA; Trahiotis, Bernstein, & Akeroyd, 2001), and the wideband correlation model (WBC; Zurek, 2012). The models are shown in Figure 1.

Methods

Some comparisons have been made between models (Bernstein et al., 2001; Zurek, 2012), but to the authors' knowledge, no single paper has considered all three. This work compares the three models using the Stern et al. (1988) stimuli and data, which first suggested the importance of *straightness*. Stimuli were 200-ms noise bursts centered at 500 Hz. Depending on condition, one of four bandwidths (50, 100, 200, and 400 Hz) and one of four combinations of ITD & IPD (1500 ms & 0°, 1000 ms & 90°, 500 ms & 180°, and 0 ms & 270°) were used. These combinations of ITD and IPD were chosen to systematically vary the straightness of the cross-correlation trajectory while keeping the interaural delay of the 500-Hz component the noise fixed at 1500 ms (Figure 2).

Results

The Stern et al. data and the predictions for the models are shown in Figure 3. Position predictions (in μ s) were multiplied by a "best fitting" scale factor (db/ μ s) for each model and compared to the data. The models from poorest to best fitting were: the AFA model ($R^2 = 0.02$), the WBC model ($R^2 = 0.31$), and the SLC model ($R^2 = 0.73$). Further analyses showed that across-frequency averaging is unable to overcome the weighting of the central cross-correlation peaks (i.e., centrality weighting) and the predictions of the WBC model are limited by its restriction of the cross correlation surface to ± 700 μ s.

Conclusion

This comparison found support for the SLC model, yet further investigation is merited to replicate the Stern et al. (1988) seminal data and model other stimuli that manipulate straightness in order to determine if second-level coincidence detection is the only mechanism that can account for human sensitivity to *straightness*.

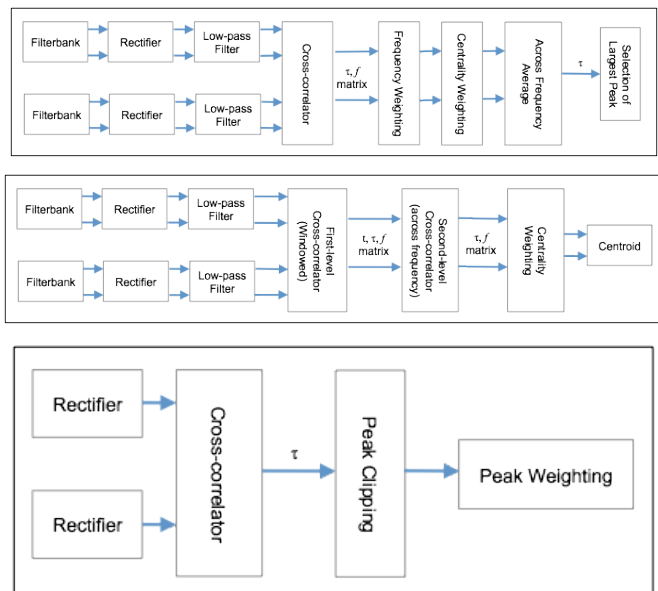


Figure 1. The second-level coincidence model (top), the across-frequency averaging model (middle), and the wideband correlation model (bottom).

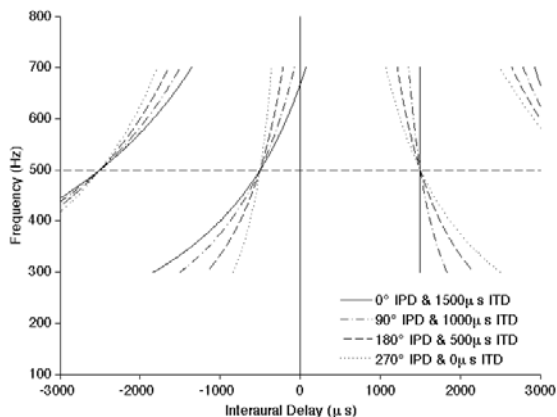


Figure 2. First-level cross-correlation trajectories of 4 combinations of ITD and IPD shown for the 400 Hz bandwidth.

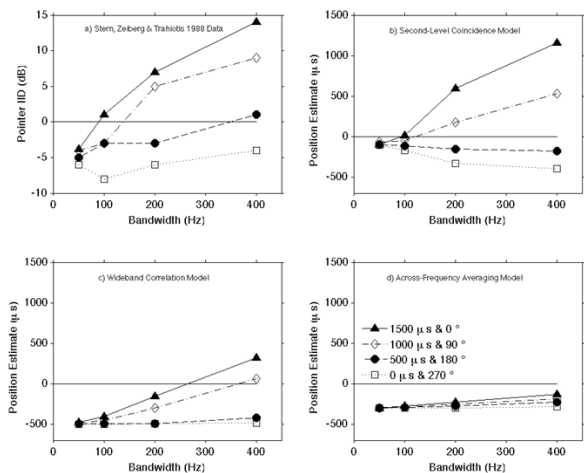


Figure 3. Panel a) Data from Stern et al. (1988), Panels b-d) predictions for the three models.

PS - 397

Binaural Speech Perception in Noise for Users of Bilateral and Bimodal Hearing Devices

Kostas Kokkinakis; Natalie Pak

University of Kansas

Background

Three binaural advantage effects have been found to benefit normal-hearing listeners on measures of speech perception in noise. The effects of head-shadow and squelch occur when the speech and noise sources are spatially separated. The effect of summation occurs when speech and noise coincide in space. We assess to what extent users of bilateral and bimodal fittings should expect to benefit from each of these binaural advantages. Prior work indicates that bilateral listeners benefit from a robust head-shadow effect, but the contributions of squelch and summation remain unclear. For bimodal listeners, the relative contributions of head-shadow, squelch, and summation to speech understanding in noise are inconclusive.

Methods

Speech perception abilities of bilateral and bimodal listeners were tested using BKB-SIN sentences corrupted with four-talker babble. Speech reception thresholds were measured in sound-field under various speech and noise spatial configurations, as well as different listening conditions (e.g., monaural, binaural).

Results

Statistical analysis revealed significant advantages of head-shadow and summation (average improvements across participants of 8.1 dB and 2.5 dB, respectively) but no significant squelch effect for bilateral listeners. Bimodal listeners benefited significantly from all three effects, although the effect of squelch was only weakly significant (average improvement = 2.9 dB; $p = 0.048$). Bimodal listeners experienced the greatest benefit from summation, which lowered speech reception thresholds an average of 7.6 dB across participants. Head-shadow was also significant, resulting in an average improvement of 6.7 dB across participants. The

independent contributions of head-shadow and squelch were not significantly different for bilateral as opposed to bimodal listeners, but the effect of summation was significantly greater for bimodal than for bilateral listeners.

Conclusion

The current findings are consistent with those of previous studies involving bilateral listeners, which indicate that head-shadow yields the most pronounced and consistent binaural advantage, while summation contributes to a somewhat smaller degree. The finding that the squelch effect produces little to no benefit in bilateral listeners is also consistent with the majority of cochlear implant literature, and it may be partially attributed to a poor sensitivity to interaural time difference cues. Bimodal listeners received the most benefit from summation, which was also significantly greater than the effect of summation for bilateral listeners. The magnitude of this effect may be attributed to the complementary spectral information supplied by the hearing aid. Whether bimodal listeners may expect to benefit from binaural squelch remains unclear.

PS - 398

Sound Localization Model for Reverberant and Noisy Environments

Tom Goeckel; Gerhard Lakemeyer; Hermann Wagner
RWTH Aachen University

Background

Sound localization capabilities are valuable for various applications and it is a hard task to achieve a high accuracy in noisy and echoic environments. We have developed a biologically inspired binaural sound localization model based on interaural time differences with the aim of a high efficiency in terms of computational complexity and a good accuracy concerning the localization performance.

Methods

We use interaural coherence as a measure of reliability to highlight segments of the signal that resemble free-field cues and suppress noisy parts, similar to the precedence effect. In addition, a histogram is used to improve robustness of the system against noise and provide a basic method to highlight persistent sources across time. The algorithm has been tested under several conditions both in simulated environments using an auralization software, and in an office environment with a microphone mount. To test the performance the system had to detect white noise, narrow band noise and speech signals. Additionally, we added uncorrelated noise at different signal-to-noise ratios to test the performance in noisy conditions.

Results

We quantified the accuracy of the model by measuring the mean error in azimuth direction, the standard deviation and the number of exact hits. All of the signals could be successfully localized in anechoic and slightly echoic conditions with mean errors below 1 degree azimuth. Only for signal-to-noise ratios below -10 dB did the algorithm lose the signal position. While white noise delivered good results even in highly reflective rooms, narrowband noise and speech was slightly

more difficult to localize and the system had a tendency to underestimate the source position in echoic conditions, especially for laterally situated signals. This was to be expected because the localization information of the source across frequencies decreases with decreasing bandwidth of the signal.

Conclusion

We were able to prove the robustness and efficiency of our localization system in various situations. However, it is only intended as a starting point for more complex localization systems that also make use of interaural level differences and other cues as binaural interaural time difference solutions are unable to resolve the front-back confusion.

PS - 399

Effect of Stimulus Duration on Transient and Ongoing Contributions to the Precedence Effect

Richard Freyman¹; Amanda Griffin¹; Charlotte Morse-Fortier¹; Patrick Zurek²

¹University of Massachusetts; ²Sensimetrics Corporation

Background

Much previous research has shown that lateralization is dominated by interaural cues within a leading binaural transient in comparison to a trailing binaural transient. However, it has become increasingly clear that the control of lateralization by leading sounds also occurs within longer steady state signals that do not contain abrupt onsets. This "ongoing precedence effect" operates for signals with durations of several hundred milliseconds, but less is known about intermediate durations lasting tens of milliseconds. This study investigated the importance of onset transients in the precedence effect as signal duration was increased from 4 ms to 250 ms.

Methods

Normal-hearing subjects listened to trains of 1-ms binaural noise bursts which alternated in interaural time delay (ITD) between τ and $-\tau$, where values of τ ranged from -500 to +500 microseconds in 100-microsecond steps. The onset-to-onset delay between bursts was 2 ms. The sample of noise was identical for every two binaural bursts (a "quad"), and changed to a fresh sample after each quad. Thus, each quad contained a leading burst with an ITD of τ and a lagging burst with an ITD of $-\tau$. A single binaural noise burst made from a fresh sample of noise with an ITD of $-\tau$ (matching the lagging sound) was inserted at signal onset. The number of quads in the stimulus train ranged from 1 to 62. Lateralization of these stimuli was determined through an acoustic pointing technique.

Results

The importance of a transient onset to the lateralization of noise-burst trains decreased gradually as stimulus duration and the number of quads increased. The data obtained thus far are somewhat subject dependent and are left-right asymmetric in some instances, but overall, the transition between dominance by the onset ITD and dominance by the ongoing lead ITD occurred at durations of approximately 16 to 32 ms

for small values of tau and was somewhat longer for larger values of tau.

Conclusion

For noise-burst trains lasting tens of milliseconds, both the onset transient and the ongoing lead contribute substantially to lateralization. The relative contribution of the onset transient and the ongoing lead depended critically on stimulus duration for durations less than 50-100 ms. For many realistic sounds, the precedence effect probably depends on a combination of transient and ongoing interaural cues.

PS - 400

Sensitivity to Envelope ITDs at High Modulation Rates

David McAlpine¹; Jessica Monaghan²; Stefan Bleeck²

¹University College London; ²Southampton University

Background

Sensitivity to interaural time differences (ITDs) conveyed in the temporal fine structure of low-frequency tones and the modulated envelopes of high-frequency modulated tones are considered comparable, especially when envelopes are shaped to transmit the same fidelity of temporal information normally present for low-frequency sounds (using 'transposed' envelopes). Notwithstanding this similarity, discrimination performance for envelope modulation rates above a few hundred Hz is reported to be poor or absent, compared with the much higher (>1000 Hz) limit for low-frequency ITD sensitivity, suggesting the presence of a low-pass filter in the envelope domain.

Methods

We assessed the sensitivity of human listeners to ITDs conveyed in pure tones and in the envelopes of transposed tones. Low pass noise was added to exclude the contribution of distortion products - generated by the non-linear mechanics of the cochlea - to listeners' performance. ITD discrimination was determined for transposed tones with a fixed envelope ITD. ITD discrimination thresholds were measured as a function of both modulation frequency and center frequency.

Results

The data indicate that well-trained listeners are able to discriminate ITDs extremely well, even at modulation rates in excess of 500 Hz for 4-kHz carriers and high levels of low pass masking noise (50dB spectrum level). The data indicate that some listeners appear able to access temporal information that can only be conveyed as relatively shallow modulations in the skirts of auditory filters in order to extract interaural temporal information.

Conclusion

The upper limit of sensitivity to ITDs conveyed in the envelope of high-frequency modulated sounds appears to be higher than previously considered.

PS - 401

Nonuniform Temporal Weighting of Interaural Time Differences in Low Frequency Tones Presented at Low Signal-to-Noise Ratio

Anna Diedesch; G. Christopher Stecker

Vanderbilt University

Background

Listeners' access to binaural spatial cues is temporally non-uniform, favoring cues appearing early (near sound onset) and—in some cases—late in a sound's duration. As a consequence, the effects of sound duration on interaural time difference (ITD) perception appear reduced relative to statistical expectations (Houtgast & Plomp, 1968 JASA 44:807-812). The results of several recent investigations of ITD discrimination in pure tones and high-frequency click trains further demonstrate a dominance of early cues over late cues present in the envelope or fine structure of brief sounds.

Houtgast & Plomp (1968) tested 500Hz octave band noise in the presence of a 500 Hz noise masker. When the signal-to-noise ratio (SNR) was high, results revealed modest duration effects consistent with testing in quiet. When SNR was low (5 dB), lateralization thresholds were higher overall, but improved optimally with duration, suggesting that masking might enable (or force) listeners to utilize spatial information in a temporally uniform manner.

Methods

In this study, we measured fine-structure ITD thresholds for 500 Hz pure tones in the presence of a continuous 500 Hz octave-band masker, at a 5dB signal-to-noise ratio (SNR) similar to conditions tested by Houtgast & Plomp (1968). The temporal profile of the sounds was measured using three test conditions. In the "RR" condition, sounds were presented with a fixed ITD over the sound duration, while in the "OR" and "R0" conditions, the ITD progressed linearly to eliminate the ITD cue from either the beginning or end of the sound, respectively. In condition RR, thresholds were measured across durations of 40-640ms; R0 & OR conditions were tested at 80 & 320ms. Statistical threshold predictions, confirmed by binaural cross-correlation modeling, indicate that thresholds improve with duration T at a rate of $1/\sqrt{T}$. Since conditions OR and R0 carry, on average, half the ITD cue of the RR condition, ideal integration predicts equivalent thresholds approximately double those obtained in condition RR. Importantly, none of these predictions are sensitive to SNR.

Results

In contrast to model expectations but consistent with past results, the data show only suboptimal threshold improvements with duration despite higher overall thresholds than obtained in quiet. Yet thresholds in conditions R0 & OR were approximately twice those of condition RR, consistent with a mutual influence of both early and late cues.

Conclusion

Results support nonuniform (in some cases, onset-dominated) temporal weighting of ITD for tones presented in noise or in quiet.

PS - 402**Self-Motion Facilitates Human Echo-Acoustic Orientation**

Ludwig Wallmeier; Sebastian Erath; Lutz Wiegrebe
Ludwig-Maximilians-Universität München

Background

Many blind humans successfully use echolocation, i.e., the auditory analysis of echoes from self-generated sounds, for orientation and navigation purposes. More than other sensory systems, echolocation is subject to voluntary motor-control: both bats and toothed whales control the directionality of their acoustic emitters and receivers through dedicated accessory elements to optimise their sonar system for a given task.

Methods

This study investigates the influence of self-motion on echo-acoustic orientation in humans. To that end, two blind and five sighted human subjects were asked to adjust their orientation in a virtual corridor to match its longitudinal axis, starting out from a random orientation.

Results

When the task was implemented as a formal 2AFC paradigm where subjects had to discriminate a leftward deviation from a rightward deviation from the required orientation, subjects performed quite well when they were positioned with equal distances to the lateral walls, but thresholds were significantly worse when subjects were closer to one wall than to the other.

In the second experiment, the relative contributions of auditory, vestibular, and proprioceptive cues to echo-acoustic orientation were investigated. Here subjects could voluntarily control their orientation in the virtual corridor, whereas their position was fixed. Rotations were conducted (i) via rotation of the corridor around the subject's (fixed) body and head, (ii) via rotation of the subject's whole body in a rotating chair relative to the virtual corridor (fixed in world coordinates), or (iii) via independent rotation of both the subject's head and body relative to the fixed virtual corridor.

Results from the first version of the experiment confirmed the detrimental effect of the asymmetric placement of the subject and showed that the subjects made systematic errors, biased away from the closer lateral wall. This systematic error was absent when we allowed for whole-body rotation of the subject in the fixed corridor, indicating that the subjects benefitted from the vestibular stimulation induced by the rotating chair. However, the subjects still made systematic front-back confusion errors. These, however, could well be resolved by the subjects in the third version, where head rotations were additionally allowed. These voluntary head rotations added both proprioceptive and (strong) vestibular input.

Conclusion

Thus, the current study shows that this sensory information facilitates echo-acoustically guided orientation not only in echolocation specialists like bats and toothed whales, but also in humans trained on echo-acoustic orientation tasks.

PS - 403**Spatial Stream Segregation in Cat Psychophysics**

Lauren Javier; Elizabeth McGuire; John Middlebrooks
University of California, Irvine

Background

Stream segregation permits listeners to disentangle multiple interleaved sequences of sounds, such as streams of syllables from multiple talkers. That process is facilitated by spatial separation between the target and competing sound sources. The current study investigated the spatial acuity with which cats can segregate sequences of sounds from two sources and identified the spatial cues that provide maximum acuity in that species.

Methods

Cats were trained to perform a spatial rhythmic-masking-release task. The cat pressed a pedal to initiate a rhythmic train of sounds from a target source that was interleaved with a complementary train from a masker source. When the target rhythm changed, the cat could release the pedal to receive a food reward. Stimuli were sequences of 20 ms broadband (0.4-16 kHz), high-band (4-16 kHz), or low-band (0.4- 1.6 kHz) pulses presented at a base rate of 10 pulses per second. The target source was fixed at 0° azimuth, and the masker source varied in azimuth from trial to trial. Detection of the rhythm change was possible only when target and masker were separated sufficiently that they were heard as segregated streams. We tested the hypotheses that: 1) cats exhibit sequential stream segregation with spatial acuity similar to that of humans and 2) cats achieve higher-acuity stream segregation based on high-frequency interaural level differences rather than on low-frequency interaural time differences.

Results

Two animals are able to segregate between two broadband sound sources with threshold acuity approaching 10°, which is comparable to average human thresholds of 8°. High-band stimuli gave finer acuity than did low-band stimuli. That conflicts with psychophysical results from human but agrees with cortical recordings in cats.

Conclusion

The results indicate that cats will be a good animal model for planned physiological studies of spatial stream segregation in behaving animals. The observation that the use of high- and low- frequency spatial cues differs between cats and humans likely is due to differences in the head sizes of those species.

PS - 404**Azimuthal Distance Judgements Produce a "Dipper" Sensitivity Function.**

Simon Carlile; Alex Fox; Johahn Leung; Emily Orchard-Mills; Alais David

University of Sydney

Background

Auditory localisation is dependent on the analysis of acoustic cues at each ear. Some neurophysiological findings show spatially circumscribed neural response patterns while other

findings are more consistent with an opponent channel code of azimuth. In this psychophysical study the just noticeable differences (JNDs) for auditory distance judgements for different regions of space were compared with JNDs for interaural time (ITD) and level (ILD) differences over comparable cue ranges.

Methods

The distance between two concurrent speech tokens presented under anechoic conditions was varied in a 2AFC task for 6 subjects to obtain the JNDs for sources with different base separations ranging from 0° to 45° (Fig 1). Regions tested were 0° (directly ahead) and 30° and 45° to the right. The end points were jittered between each stimulus pair to avoid lateral displacement judgements. ILD and ITD JNDs were also measured using headphones for standing differences corresponding to the different base intervals.

Results

Regardless of the spatial region over which the distance JNDs were measured, JNDs were relatively high with small base intervals, fell to a minimum at medium base intervals and then increased with increasing base interval (Fig 1 D & E). The pattern of distance JNDs was reminiscent of the 'dipper' sensitivity function seen in the visual system and a similar spatial coding model was successfully applied to the auditory data. ITD JNDs did not vary with the magnitude of the standing difference however, the JNDs for ILD increased with increased standing difference. The minimum JNDs for each spatial region corresponded well with the ILD JNDs.

Conclusion

These data are consistent with a channel processing model of auditory spatial localisation that accords with recent auditory cortical recordings demonstrating restricted spatial receptive fields for two concurrent sound stimuli(1). The patterns in the binaural JNDs are consistent with a quantised sensitivity to ITD and an absolute level dependent sensitivity to ILDs.

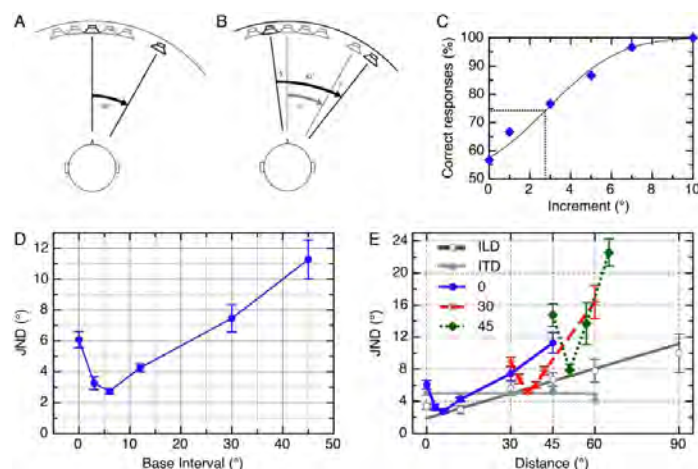


Figure 1: (A-C) The jittered distance judgements are shown for one base interval (30°) for locations around 0° azimuth. (D) The change in the JND (threshold) for different base intervals shows a characteristic dipper function. (E) The dipper functions for 0°, 30° and 45° eccentricity are plotted with the variations in the ITD (light grey) and ILD (heavy grey) JNDs for match standing differences.

PS - 405

Auditory Motion Perception and Tracking in Schizophrenia

Martin Burgess; Johahn Leung; Simon Carlile

University of Sydney

Background

We examined auditory motion perception and head tracking performance for schizophrenic sufferers. Eye tracking dysfunctions (ETD) affects over 80% of these patients and have been associated with deficits in the frontal eye field (FEF) (Levy et al., 2010), part of a network involved in spatial attention and saccadic eye movements. Recent evidence suggests this network is supramodal, being activated during visual and auditory spatial attention tasks (Lee et al., 2013). We hypothesized that dysfunction in this region and its connections could also impair performance in spatially mediated and audio-motor related tasks.

Levy, D. L., Sereno, A. B., Gooding, D. C., & O'Driscoll, G. A. (2010). Eye Tracking Dysfunction in Schizophrenia: Characterization and Pathophysiology. *Current Topics in Behavioral Neurosciences* (Vol. 4, pp. 311–347).

Lee, A. K. C., Rajaram, S., Xia, J., Bharadwaj, H., Larson, E., Hämäläinen, M. S., & Shinn-Cunningham, B. G. (2013). Auditory selective attention reveals preparatory activity in different cortical regions for selection based on source location and source pitch. *Frontiers in neuroscience* (Vol. 6, pp. 1–9).

Methods

Schizophrenic and control subjects participated in two psychophysical experiments, using individualized Virtual Auditory Space (VAS) rendered stimuli over headphones.

The first experiment assessed participants' velocity discrimination of three reference velocities (15, 30 and 60 °/s) in the frontal hemisphere around ±90°. Using a 2AFC constant stimulus paradigm, subjects were asked to determine the interval with the faster target.

In the second experiment, participants were asked to track by pointing their nose to an auditory target as it moved along the audiovisual horizon of ±90° at velocities 15°/s, 30°/s and 60°/s.

Results

Results showed no difference between the two groups in velocity discrimination, as confirmed using a Wilcoxon U-test.

In the tracking task, results showed significant differences between the two groups using open and closed loop metrics. Onset error, an open-loop measure of tracking ability, was significantly increased by a factor of around three in the schizophrenic group. Two closed-loop measures of tracking, RMS error and gain error, were also significantly increased in schizophrenic patients by a factor at least two. Significance was determined using a Wilcoxon U-test comparing the two groups at each stimulus velocity, with $p < 0.05$.

Conclusion

When asked to track a moving auditory stimulus, patients with schizophrenia have significantly decreased performance in both open and closed-loop phases. These results suggest that patients with schizophrenia have intact velocity information, as indicated by the threshold for velocity discrimination as well as the peak velocity of the head when tracking. However, these patients are unable to access or use feedback information to correct any error in head velocity and “catch-up” to the stimulus. These preliminary results are consistent with the decreased activity in the FEF observed in schizophrenia in previous studies and linked to ETD.

PS - 406

Sound-Localization in Noise Performance is Determined by Sensitivity to Spectral Shape

Guillaume Andeol¹; Ewan Macpherson²; Andrew Sabin³

¹*Institut de Recherche Biomédicale des Armées*; ²*Western University, London, CA*; ³*Northwestern University*

Background

Analysis of the spectral shape imposed on an incoming signal by a listener's head-related transfer functions (HRTFs) is required to localize its source in the up/down and front/back dimensions. Noisy environments both impair sound localization in those dimensions and increase differences in performance across participants. Because noise smoothes the spectral shape of the stimulus, the effects of noise on sound localization might be related to the original prominence of the HRTFs' spectral shape (spectral strength, an acoustical factor), or to the listener's sensitivity to spectral shape (a perceptual factor). In the current study we compared those two hypotheses.

Methods

Listeners sat on an elevated chair inside an anechoic room with their head placed at the center of an 8-loudspeaker cubic array. The wideband noise target was presented in quiet or in wideband noise at six different signal-to-noise ratios (from -7.5 to +5 dB in 2.5 dB steps). Listeners had to identify which loudspeaker had emitted the signal. Sensitivity to spectral shape was quantified by spectral-modulation detection thresholds measured with a broadband (0.2–12.8 kHz) or high-frequency (4–16 kHz) carrier and for different spectral modulation frequencies (below 1 cycle/octave, between 1 and 2 cycles/octave, above 2 cycles/octave). Spectral strength was computed as the spectral distance between the magnitude spectrum of the listener's HRTFs and a flat spectrum.

Results

Data obtained from 19 normal-hearing listeners showed no correlation between HRTF spectral strength and localization performance. A significant correlation was found, however, between sensitivity to spectral shape for high-frequency carrier/low spectral-modulation frequency and localization performance.

Conclusion

These results suggest that the perceptual ability of the listener rather than the acoustical properties of the HRTFs determine sound localization performance in noise.

PS - 407

Perception of Spatial Sound Statistics by Gerbils

Andrea Lingner; Daniel Neusius; Benedikt Grothe; Michael Pecka; Lutz Wiegrebe

Ludwig-Maximilians-Universitaet Munich

Background

In natural habitats, sound sources are typically distributed in space. A sudden change in this distribution may indicate a vitally important change in the environment. Electrophysiological recordings indicate that binaural processing is indeed sensitive to the statistical distribution of sound source locations. However, the extent to which this neural sensitivity is reflected in the behaviour of an animal is unclear.

Methods

Experiment I

In the first experiment we probe the perceptual sensitivity of Gerbils to a 180° switch in sound azimuth. The Gerbils' sensitivity is quantified in terms of prepulse inhibition (PPI), i.e., a decrease in the startle amplitude elicited by the detection of the switch. Stimuli consisted of a train of 50 ms noise bursts with 10 ms gaps. This noise train was presented from one azimuthal position for a variable duration and was then switched by 180° for the last 2, 5, 10, or 20 bursts preceding the startle pulse.

Experiment II

Here we probe the perceptual sensitivity of Gerbils to a 180° switch as a function of the salience of the switch. We produced a train of 10 ms noise bursts with 10 ms gaps. Each noise burst is presented from a discrete azimuth. The azimuthal position is stochastically distributed between 12 equidistant locations with a defined overrepresentation of 33, 50, 67, 83, and 100% towards one particular sound azimuth. Similar to the first experiment, the overrepresented sound azimuth is then switched by 180° for the last 20 bursts preceding the startle pulse.

Results

Experiment I

Overall, PPI decreases with increasing number of bursts. A short switch (2 to 5 bursts) elicits the strongest PPI.

Experiment II

Surprisingly, the animals showed a significantly stronger PPI if the 180° switch is embedded in a stochastic distribution of sound azimuths. In contrary, if the azimuthal position before and after the switch was not distributed, the gerbils did not show significant PPI.

Conclusion

Our data show that PPI is suitable to assess sound localization in gerbils. A relatively low number of noise bursts after the azimuth switch elicits the strongest PPI in gerbils. Surprisingly, the animals show a significantly stronger PPI when the 180° switch is embedded in a stochastic variation of sound azimuth. Recent reports of binaural adaptation have shown how the binaural system can focus on a small range of azimuths. As the current stochastic stimulation works against

binaural adaptation, our data indicate that stochastic distribution of sound locations increase the perceptual sensitivity of sudden changes in sound azimuth.

PS - 408

Comparison of Intensity Difference Limen Thresholds Obtained by Operant Conditioning and Pre-Pulse Inhibition in the Mouse.

Georg Klump¹; Derik Behrens²

¹Center of Excellence "Hearing4all", Oldenburg University;

²Center of Excellence "Hearing4all", Animal Physiology and Behavior Group, Department for Neuroscience, School for Medicine and Health Sciences, Oldenburg University, 26111 Oldenburg, Germany

Background

The reflex-based pre-pulse inhibition (PPI) method has become an important tool to obtain behavioral thresholds in conditions in which operant training of subjects is difficult or a high number of subjects need to be tested. To evaluate the sensitivity measures obtained with PPI in comparison to those measures obtained with the widely used operant conditioning procedures we determined the intensity difference limen (IDL) using both methods in the same animal subjects.

Methods

We presented repeated 100 ms 10-kHz tone pulses as an acoustic background to C57Bl/6 mice (n=12). The same tone pulses with a level increment of +1, +2, +4, +6, +10 or +15 dB were presented as test signals instead of a background signal (reference) at random times. IDLs for four different background levels (30, 50, 75 dB SPL and 35 dB HL) were tested in separate sessions. In the operant conditioning measurements a Go/NoGo-procedure with food rewards was used and hit and false-alarm rates served to calculate the sensitivity measure d' . In the PPI experiments the movement of the mouse elicited by a 105 dB startle sound (35 ms, 2-50 kHz) was measured using a piezo-sensor. To allow for a comparison between both methods we applied ROC analysis to the startle amplitudes and calculated d_a values as the sensitivity measure that corresponds to d' .

Results

For both methods, the mean sensitivity measures increase from low to high level increments. The sensitivity in the operant conditioning procedure reaches d' -values > 2.8 for the highest level increments. The results obtained by the PPI procedure show a much lower sensitivity, for the highest level increments sensitivity increased up to a d_a -value of 1.1. The psychometric functions varied more between background level conditions in the PPI experiments than in the operant conditioning experiments.

Conclusion

In situations where operant condition procedures are not applicable, PPI methods appears to be an appropriate tool to measure behavioral thresholds. However, the lower level of sensitivity of the PPI method will result in higher thresholds than for the operant methods. Furthermore, the higher variability in the results of PPI experiments at different back-

ground level makes it necessary that more data are obtained. Thus, operant conditioning procedures should be a preferred method for studying IDLs.

PS - 409

Perception of the Instantaneous Changes in Velocity of a Moving Auditory Target

Johahn Leung¹; Shannon Locke¹; Simon Carlile²

¹School of Medical Sciences, University of Sydney; ²School of Medical Sciences and The Bosch Institute, University of Sydney

Background

Accurate perception of motion requires sensitivity to velocity and to ongoing changes in velocity. While there are a few studies of sensitivity to constant velocity we focussed here on the perception of velocity changes. A previous study by Perrott (1993) showed participants were able to distinguish between acceleration and deceleration, but the paradigm was unable to identify the variables which characterise this detection. We measured the minimum spatial arc/duration required to detect the change in velocity after an instantaneous acceleration or deceleration.

Methods

The angular-moving sounds (30 or 60°/s) were presented within $\pm 90^\circ$ in the horizontal plane using individualised Virtual Auditory Space. Participants were presented 1 second of stimulus at the initial velocity (V1) before the sound instantaneously transitioned to its final velocity (V2). V2 was determined by a multiplicative (or divisive) factor of 2, 3 and 4. The spatial extent of the stimulus at V2 varied between 5 and 90°. Subjects were required to determine whether the velocity increased (or decreased) in a yes/no task. Each condition was assessed in a single session, with the condition order randomised. Catch trials with no change in velocity were interspersed with target trials.

Results

All but one of the participants failed to reach 75% correct response rate for factors 2 and 3, indicating these changes in velocity were insufficient for robust detection. This was unexpected as all velocities changes were clearly suprathreshold according to previously measured velocity discrimination thresholds (Carlile and Best, 2002). False alarm rates, however, were near zero for all conditions for most subjects. At factor 4, where a reference velocity of 60°/s will increase to 240°/s and decrease to 15°/s, all subjects were able to do the task. Here, we found that the mean spatial arc threshold was $32.7^\circ \pm 3.1$ and $14.8^\circ \pm 1.7$ for increase and decrease in velocities respectively. There was also a substantial interaction between velocity factor and spatial threshold.

Conclusion

There were two outstanding findings from this experiment. Firstly, detection of instantaneous changes in velocity appear to be harder than comparisons between the velocity of two different sounds. Secondly, the detection of the velocity change is not solely dependent on V2. Instead, the relative difference in velocity, as well as the initial velocity of the stimulus are significant factors for this task.

Infants' Sound Localization Accuracy Measured by Corneal Reflection Eye-Tracking: A Pilot Study

Filip Asp; Erik Berninger; Åke Olofsson

Department of Clinical Science, Intervention and Technology

Background

The ability to locate the source of a sound has a survival value and thus exists in many species. Assessment of the immature human sound localization (SL) ability during infancy includes subjective observation of infants' behavior (e.g. head turns, eye movements). We have developed an objective method for SL measurements in infants from 6 months of age, based on the assumption that gaze direction may be a good estimate of the perceived sound-source location.

Methods

Eleven full-term and healthy subjects with a mean age of 14 months (7–36 months) who passed the neonatal newborn hearing screening participated in this pilot study. SL was measured in sound field by presenting a cartoon movie at 63 dB SPL_{Ceq} from 1 of 12 equidistantly placed loudspeaker/display-pairs spanning a 110 degree arc in the frontal horizontal plane. The continuous sound was shifted to a random loudspeaker and the visual stimulus was simultaneously stopped and reintroduced after 1.6 seconds beneath the next sounding loudspeaker. During the period without visual stimulus, infant pupil positions relative to the visual displays (1 to 12) were sampled at 20 Hz using an objective corneal reflection eye-tracking technique. The median pupil position of the final 500 ms of the sampling period was defined as the infant's perceived sound-source location. Loudspeaker shifts continued until the sound was presented twice per loudspeaker, or until infants lost interest. SL accuracy was expressed as an Error Index (EI), reflecting the variability in SL ability. The aim was to study if gaze may be used for the study of SL accuracy during infancy and early childhood.

Results

The mean (SD) EI was 0.43 (0.21), ranging from 0.15 to 0.74. Linear regression analysis revealed a decreasing EI with increasing age ($EI = 0.64 - 0.015 \times \text{months}$, $r = -0.61$, $p < 0.05$, $n = 11$). All the infants were cooperative and data collection possible for 10 to 24 loudspeaker shifts (median = 16.5). During the shifts, 8 – 24 perceived sound-source locations were recorded (median = 12).

Conclusion

Infants' gaze may be used as an objective measure of perceived sound-source location from 6 months of age. The preliminary results suggest an age-related improvement of sound localization accuracy.

Detection of Modulated Tones in Modulated Noise by Nonhuman Primates

Courtney Timms; Peter Bohlen; Margit Dylla; Ramnarayan Ramachandran

Vanderbilt University

Background

Detection of sounds, especially in noisy environments, is a critical and fundamental function of the auditory system. In natural environments, sounds can show temporal fluctuations; both distractors and signals can be dynamic, influencing the detectability of the signal. Our previous studies found that detection of tones in dynamic noise (amplitude modulated noise) and dynamic signals (amplitude modulated tones) in noise resulted in lower thresholds to the detection of signal relative to detection of tones in static noise. These results suggest that detection thresholds of dynamic signals in dynamic noise could be enhanced. This study describes the results of experiments investigating how detection is modified when both signal and noise were time varying. The experiments investigated how parameters of temporal modulations of signals and noise, namely modulation frequency, modulation depth, and the phase relationship between signal and noise modulation influence detection performance.

Methods

Two monkeys (*Macaca mulatta*) were trained to report detection of dynamic signals (amplitude-modulated tones) in continuous, dynamic (amplitude-modulated) broadband noise in a Go/No-Go detection task, with appropriate catch trials. Experimental data were analyzed using signal detection theoretic methods.

Results

Behavioral detection thresholds varied sinusoidally with phase difference, and were highest when the modulations of tone and noise were in phase and lowest when the modulations of tone and noise were in anti-phase. Increasing the modulation frequency caused an exponential reduction in behavioral detection thresholds, with larger reductions observed when modulation frequency of the tone was changed relative to when the modulation frequency of the noise was changed. There was an interaction between the modulation phase difference and the effect of varying the modulation frequency of signals and noise. When the depth of amplitude modulation of the noise was changed, behavioral detection thresholds of steady state tones decreased, as expected. The behavioral detection thresholds of modulated tones decreased if the tone and noise modulations were anti-phase, but the detection thresholds remained unchanged if the tone and noise modulations were in phase.

Conclusion

These results suggest that the parameters of the modulation of signals and maskers heavily influence detection in very predictable ways. Reaction time data was also gathered and investigated for all modulation experiments, but were not significantly influenced by the parameters modified. The results of the modulation experiments are similar to the results

reported for humans and avians, and form the baseline for future studies of neurophysiological mechanisms of detection and auditory scene analysis.

PS - 412

Auditory Motion Elicits Ocular Smooth Pursuit to Real (Free-Field) but not Simulated (Dichotic) Auditory Targets

Christina Cloninger; Paul Allen; Justin Fleming; William O'Neill; Gary Paige
University of Rochester

Background

The perception of moving sounds remains poorly understood. Previous theories have posited motion-specific versus 'snapshot' (sequential position) mechanisms, although these are not mutually exclusive. One way to access auditory motion processing is with smooth pursuit (SP) eye movements. SP is a visually-dominant velocity feedback system that serves to maintain ocular gaze on moving targets. Here, we exploit the SP system to quantify responses to moving auditory, as well as visual, targets. We previously demonstrated that SP of moving sounds occurs in a manner similar to SP of visual targets, but with lower gain and wider variance. These experiments address how SP of real (free-field) and simulated (dichotic) auditory targets is affected by bandwidth-limited central channels underlying sound localization.

Methods

We presented auditory or combined audio-visual moving targets as ramps of constant velocity (10 and 30°/s). Free field auditory targets were broadband (0.2-20 kHz), low-pass (0.2-1 kHz), or high-pass (3-20 kHz) noise. Targets were presented in the free-field using a loudspeaker/LED target at 2m distance moving on a concealed robotic arm (Experiment 1), or dichotically (broadband only) under headphones by varying inter-aural time (ITD-Experiment 2) or intensity (ILD-Experiment 3) cues. Eye movements of head-fixed subjects were recorded using EOG.

Results

SP did not differ significantly for real auditory targets of different bandwidths moving at 10°/s (SP gain ~0.7, or 7°/s) or 30°/s (SP gain ~.35, or 10°/s). SP for visual targets held at a gain ~1.0 for both these target velocities. In all subjects, attempts to follow continuously varying ITDs or ILDs simulating similar 'spatial' parameters failed to produce SP greater than that for purely imagined targets (<5°/s in all subjects).

Conclusion

Smooth pursuit of auditory targets in the *free-field* is robust but with approximately half the gain of visual SP. Broadband, high- or low pass noise proved equally effective. However, SP of simulated motion (ITD or ILD cues alone under headphones) proved ineffective and no different than SP of imagined targets. This suggests a true spatial reliance for auditory SP, consistent with visual SP, which always occurs in the external environment. This externalization likely underlies the more robust SP derived from real environmental sounds.

PS - 413

The Role of External Ear Acoustics of the Adult Guinea Pig in a Spatial Hearing Behavioral Task

Kelsey Anbuhl¹; Nathaniel Greene²; Alexander Ferber³; Daniel J. Tollin⁴

¹*University of Colorado - Anschutz Medical Campus, Aurora, CO 80045 USA*; ²*Department of Physiology and Biophysics, University of Colorado- Anschutz Medical Campus, Aurora, CO 80045 USA*; ³*Neuroscience Training Program, University of Colorado- Anschutz Medical Campus, Aurora, CO 80045 USA*; ⁴*Neuroscience Training Program, Department of Physiology and Biophysics, Department of Otolaryngology, University of Colorado- Anschutz Medical Campus, Aurora, CO 80045 USA*

Background

The guinea pig has been a common model for investigating the neural mechanisms of binaural and spatial hearing. However, neither their cues to sound location nor their behavioral sensitivity to these cues have been thoroughly examined.

Methods

We computed the cues to location in adult animals (n = 9) from measurements of the directional components of the head-related transfer functions (DTFs). DTFs were measured at both ears from 325 locations, with steps of 7.5° in both azimuth and elevation. To test behavioral spatial hearing, we used the 'speaker swap' paradigm, based on the pre-pulse inhibition (PPI) of the acoustic startle reflex. We determined the smallest angle that adults (n = 13) could discriminate between two speaker locations across the horizontal midline by presenting continuous broadband, high-pass (4 kHz cutoff) or low-pass (2 kHz cutoff) noise from one speaker and then swapped to a second speaker for a short interval (ISI; 5-300 μs) preceding a loud (~110 dB SPL) startle-eliciting stimulus presentation. The startle response was captured via a cage-mounted accelerometer and quantified as the PPI of the startle, defined as 1 minus the ratio of RMS amplitude of response to control; a positive PPI indicates stimulus discrimination.

Results

DTFs reveal that maximum ITDs averaged 215 ± 5.8 μs (mean ± std), and that maximum ILDs were generally < 12.2 dB for frequencies < 4 kHz, and ranged from 12.2 - 40 dB for the frequencies from 4-16 kHz. Behaviorally the animals showed substantial PPI (i.e., they could discriminate the change in source angle) in response to source locations separated by at least 7.5° for broadband, 15° for high-pass, and 30° for low-pass noise. These results correspond to interaural time and level differences of ~100 μs and 3.5 dB for low-pass, 37 μs and 3.8 dB for high pass and 26 μs and 1.9 dB for broadband noise conditions.

Conclusion

The DTF recordings reveal the range of cues that animals experience, yet the ability of the central auditory system to encode and utilize these cues is not well established. Here, we report evidence that guinea pigs can discriminate sound source locations of both low- and high-pass sounds, suggest-

ing that they can effectively utilize both low-frequency ITDs and high-frequency ILDs. The behavioral results suggest that guinea pigs can discriminate ~26 μ s of low-frequency ITD and ~2 dB of ILD consistent with values reported for other mammals.

PS - 414

Behavioral Assessment of Binaural Spatial Hearing Ability in a Population of Adult Guinea Pigs (*Cavia Porcellus*)

Alexander Ferber¹; Nathaniel Greene²; Kelsey Anbuhl³; Paul Allen⁴; Daniel J Tollin⁵

¹University of Colorado - Anschutz Medical Campus, Aurora, CO 80045 USA; ²Department of Physiology and Biophysics, Department of Otolaryngology, University of Colorado - Anschutz Medical Campus, Aurora, CO 80045 USA; ³Neuroscience Training Program, University of Colorado - Anschutz Medical Campus, Aurora, CO 80045 USA; ⁴Department of Neurobiology and Anatomy, University of Rochester Medical Center, Rochester, NY 14642 USA; ⁵Neuroscience Training Program, Department of Physiology and Biophysics, Department of Otolaryngology, University of Colorado - Anschutz Medical Campus, Aurora, CO 80045 USA

Background

Guinea pigs are commonly used for investigations of the neural mechanisms of spatial hearing, yet their behavioral capabilities have not been thoroughly investigated. To better characterize their abilities, we assessed spatial acuity in a population of adult guinea pigs using a task employing the pre-pulse inhibition (PPI) of the acoustic startle response.

Methods

Experiments were conducted inside a double walled sound-attenuating chamber lined with acoustic foam. Animals (n = 13) were placed in an acoustically transparent wire cage, with their head facing either towards, or 45° away from, the midline of a 1-m radius hemispheric ring of loudspeakers mounted every 7.5°. Continuous broadband, high-pass (4 kHz cutoff) or low-pass (2 kHz cutoff) noise was presented from one speaker for a variable period of time, then immediately swapped to another speaker a short time interval (5-300ms) before a loud (~110 dB SPL) startle-eliciting stimulus was presented overhead. A cage-mounted accelerometer captured the startle response, which was then quantified as the PPI of the startle (1 minus the ratio of RMS response amplitude to control), such that a positive PPI indicates stimulus discrimination. A unilateral conductive hearing loss was induced in a subset of these animals through injection of silicone ear impression material into the ear canal.

Results

For all stimulus conditions, PPI was directly proportional to angular separation, such that large angles produced greatest inhibition. The data provide an estimate of localization acuity and suggest that guinea pigs can discriminate changes in source location across the midline of at least 7.5° for broadband noise, 15° for high-pass noise (4 kHz cutoff), 30° for low-pass noise (2 kHz cutoff), and 30° for broadband noise

sources placed within a hemisphere. Unilateral ear plugging produced profoundly reduced sound localization acuity.

Conclusion

These results yield estimates of guinea pig spatial acuity and confirm that guinea pigs can discriminate changes in source location both across and within a lateral frontal hemifield. Furthermore, guinea pigs can discriminate sources of low- and high-pass sounds, demonstrating that they effectively utilize low-frequency interaural time (ITD) and high-frequency level difference (ILD) sound localization cues. Disruption of this ability with a unilateral silicone earplug indicates that guinea pigs discriminate changes in sound source location using binaural cues. Together these data support the use of guinea pigs as model systems for studying anatomical and physiological mechanisms of sound localization.

PS - 415

Echolocating Bats Adapt Their Sonar Calls to Separate Echoes from Obstacles and Prey

Beatrice Mao; Murat Aytekin; Cynthia Moss
University of Maryland, College Park

Background

The echolocating bat uses acoustic information reflected from objects in its environment to localize obstacles and track prey, and its adaptive sonar behavior provides a window into its spatial perception. We previously showed that big brown bats, *Eptesicus fuscus*, trained to rest on a platform and track a moving target, adjust the features of their echolocation calls in response to the distance of moving prey and a stationary 'distracter' object. When the distracter was present, the bats adapted their call duration to the distance of the prey when it was in front of the distracter. When the prey was at distances beyond the distracter, the bat's adaptive vocal behavior was influenced by the distance and angular offset of the distracter. In the present experiment, we expanded on the previous study by using two distracter objects at the same distance and angular offset, and a tethered moving target was positioned to pass between them and approach the bat.

Methods

Big brown bats used echolocation to track and intercept the moving tethered prey item from a stationary platform. We recorded the animal's echolocation calls with ultrasonic microphones and used an optical sensor to measure target distance.

Results

We found that the duration and pulse interval patterns were similar in the one and two distracter experiments, but surprisingly, call duration was longer in the two distracter condition when the target was close to the distracter position.

Conclusion

We hypothesize that the bats adapted call duration in the two distracter task to detect and track the prey item when it was close to and just behind the obstacles. These findings demonstrate the bat's active control of vocalizations to obtain acoustic information used to separate closely spaced objects.

Assistive and Rehabilitative Effects of a Head-Mounted Vibrotactile Prosthesis (BALCAP) for Chronic Postural Instability

Joel Goebel¹; Neal Richardson²; Brian Clark²; B. Eugene Parker²; Belinda Sinks¹

¹Washington University School of Medicine; ²Barron Associates, Inc.

Background

Maintenance of postural control requires a combination of sensory input from the visual, vestibular, and somatosensory end organs, central integration of available sensory inputs, and appropriate motor output to the antigravity musculature. In cases of chronic postural instability from a variety of sensory deficits, the addition of ancillary orientationally-correct somatosensory and haptic cues have been shown to be of benefit for fall prevention and ambulation. Previous work from our group has demonstrated increased stability on computerized dynamic posturography (CDP) SOT Conditions 5 and 6 in patients with bilateral vestibular loss while using a head-mounted accelerometer and vibrotactile stimulators [Goebel2009].

Methods

In the present study, five patients with chronic postural instability from a variety of etiologies were fitted with the latest version of the BALCAP vibrotactile prosthesis and enrolled in a six-week home exercise program using the prosthesis on a daily basis. Outcome measures included two objective measures: (1) CDP SOT conditions 5 and 6; and (2) the Dynamic Gait Index (DGI), and two validated subjective instruments: (1) the Dizziness Handicap Inventory (DHI); and (2) the Activities-specific Balance Confidence (ABC) questionnaire, in addition to a customized usability questionnaire. All patient data were analyzed for assistive (i.e., BALCAP active during testing) and rehabilitative (i.e., testing following 6-week BALCAP-enabled rehabilitation therapy sessions) benefits.

Results

Given the small sample size, a considerable improvement in empirical results was required to demonstrate statistical significance. Despite this limitation, our results demonstrated that use of the BALCAP prosthesis yielded significant assistive and rehabilitative benefits for multiple objective and subjective measures, along with excellent user-acceptance of the device.

Conclusion

The addition of orientationally-correct vibrotactile cues had a significant positive assistive and rehabilitative effect on patients with chronic postural instability unresponsive to physical therapy rehabilitation alone.

Vestibular Physical Therapy of Persons With Traumatic Brain Injury Using a Computer Assisted Rehabilitation Environment(CAREN) in the Department of Defense

Kim Gottshall¹; Pinata Sessoms²; Seth Reini²

¹Naval Medical Center San Diego; ²Naval Health Research Center

Background

Traumatic brain injury secondary to blast exposure is a significant operational issue and a rising international concern. We have had experience evaluating and treating a large group of patients with this injury pattern. In this abstract we describe the cognitive/visual patterns seen in these patients before and after clinical vestibular physical therapy treatment and computer assisted rehabilitation environment (CAREN).

Methods

A set of visual/cognitive and visual/vestibular tests were performed on individuals with mTBI. Their baseline (income) results were compared to outcomes taken at 3 weeks and again at 6 weeks after beginning therapy. Self reports of the Dizziness Handicap Inventory (DHI) and Activities Balance Confidence Scale (ABC) were administered. Computerized posturography sensory organization test (SOT), functional gait test (FGA), and visual cognitive tests including a static visual acuity, perception time, target acquisition, target tracking, dynamic visual acuity (DVAT), and gaze stabilization (GST) were readministered.

Results

The self-reports of DHI and ABC were improved in both groups and were not significantly different. The mean post-treatment SOT scores were significantly better for the TVPT group, but improved in both groups. The FGA reached optimal scores at 3 weeks in the CVPT group, but were not significantly different from the TVPT group by week 6. Target tracking, DVA, and GST significantly better in the TVPT group, but did improve in the CVPT group. TVPT exercise programs included vestibuloocular reflex (VOR) exercises, cervicocolic reflex (COR) exercises, depth perception training, somatosensory exercises, dynamic gait tasks, ball skills, positional exercises, aerobic exercises, proprioceptive neuromuscular facilitation exercises (PNF), and plyometrics CVPT at the Naval Health Research Center Warfighter Performance Lab. employed four interactive applications designed to integrate visual and tactile inputs for processing by the patient. Patients were trained by the vestibular physical therapist twice weekly for both groups.

Conclusion

Both TVPT and CVPT groups improved after six weeks of training. Rapid improvement of the FGA in the CVPT group may have been a reflection of the treadmill training in three of the four exercise scenarios. Somatosensory exercises with the eyes closed in the TVPT group may have contributed to improved SOT scores. Specific VOR tasking in the TVPT group may have specifically improved target tracking, DVA, and GST.

Involvement of Vestibular Organs in Idiopathic Sudden Hearing Loss With Vertigo: An Analysis Using OVEMP and CVEMP Testing.

Chisato Fujimoto; Naoya Egami; Makoto Kinoshita; Tatsuya Yamasoba; Shinichi Iwasaki

The University of Tokyo

Background

Our group has previously demonstrated that, in patients with idiopathic sudden hearing loss (ISHL) with vertigo, the sacculle is more frequently involved than the semicircular canals by virtue of the study of cervical and ocular vestibular evoked myogenic potential (cVEMP) and caloric tests. In the present study, we investigated the extent of vestibular lesions in ISHL with vertigo using cVEMP and ocular vestibular evoked myogenic potential (oVEMP) testing and caloric testing.

Methods

We reviewed the clinical records of 25 consecutive new patients with ISHL with vertigo. For vestibular function tests, cVEMP, oVEMP and caloric tests were employed. All the patients underwent audiometry, cVEMP and caloric tests. Twenty-three patients underwent oVEMP testing as well. We classified patients based on their pattern of vestibular dysfunction. All the patients showed cochlear damage and we labeled them C (cochlear) type. If a patient showed abnormal cVEMP, oVEMP or caloric responses, we added an S (sacculle), U (utricle) or L (lateral semicircular canal) respectively to their label.

Results

Among the 25 patients who underwent cVEMPs and caloric tests, 18 (72%) showed abnormal cVEMP responses on the affected side and 13 (52%) had abnormal caloric responses on the affected side. Among the 23 patients who underwent oVEMP testing, 12 (52%) showed abnormal oVEMP responses on the affected side. Of the 23 patients who underwent cVEMP, oVEMP and caloric testing, 5 (22%) were classified as C type; 4 (17%) as CS type; 2 (8%) as CSU type; 2 (8%) as CSL type; 10 (43%) as CSUL type.

Conclusion

In ISHL with vertigo, the vestibular end organs close to the cochlea tended to be preferentially affected.

Reducing Between Subject Variability of Cervical Vestibular Evoked Myogenic Potentials (cVEMPs) Using Normalization

Mark van Tilburg; Barbara Herrmann; John Guinan; Steven Rauch

Massachusetts Eye and Ear Infirmary, Harvard Medical School

Background

Many studies have shown that the variability of cervical vestibular evoked myogenic potentials limits their clinical use. Several attempts have been made to reduce the variability, with limited success. Normalization by the electromyogram amplitude is a method to reduce variability by correcting for

amplitude differences in muscle contraction. Previous studies of cVEMP *intrasubject* variability have shown no significant effect of normalization. We hypothesize that *intersubject* variability will be influenced by normalization and show significantly reduced variability.

Methods

20 healthy subjects were tested. Peak-to-peak (PP) amplitude (P1 to N1) of the ipsilateral cVEMP was measured at 4 frequencies (250, 500, 750, 1000Hz) for each ear. Each subject underwent 2 sessions to evaluate test-retest variability. Main outcome variables were means and standard deviations of the PP and normalized amplitudes. Test-retest variability was assessed by the intraclass correlation coefficient (ICC). Coefficients of variation were calculated for both methods (PP and normalized) and were analyzed using the non-parametrical Levene's test.

Results

Mean PP and normalized amplitude were highest for 750Hz and lowest for 250Hz stimulus frequencies. Test-retest variability was excellent (i.e. >0.70) for all conditions (PP and normalized) at all frequencies. The coefficient of variation was high (~0.90) for PP amplitudes but was significantly lower (~0.50) in the best normalized results (p=0.000) at all frequencies.

Conclusion

The cVEMP is a robust test with low test-retest variability. Intersubject variability can be significantly reduced by normalization.

Problems in Epidemiologic Screening of the Vestibular System

Helen Cohen¹; Haleh Sangi-Haghpeykar¹; Ajitkumar Mulavara²; Brian Peters³; Jacob Bloomberg⁴; Natalia Ricci⁵; June Kampangkaew¹; Sharon Congdon¹; Melody Fregia¹; Anedra Williams¹; Valory Pavlik¹; Jeffrey Vrabec¹; Robert Williamson¹

¹Baylor College of Medicine; ²Universities Space Research Association; ³Wyle Science, Technology and Research Group; ⁴NASA/Johnson Space Center; ⁵Federal University of Sao Paulo

Background

The literature has few epidemiologic studies of the vestibular system. As part of an on-going series of experiments to improve the available screening tests and to evaluate some of the currently used tests we performed two experiments.

Methods

Experiment 1 screened 300 people for vestibular disorders, using Dix-Hallpike maneuvers, head impulse tests and standing balance tests (CTSIB). We subsequently tested 69 of them in the ENG lab with objective diagnostic tests. In Experiment 2 we tested the usefulness of the Fukuda stepping test, the head impulse test and tandem walking to detect patients with known vestibular impairments compared to asymptomatic controls.

Results

In Experiment 1 we found the expected 1% of people with responses consistent with benign paroxysmal positional vertigo. The scores on the screening were related to the total ENG but odds ratios were not significant for some variables probably due to the small sample size. In Experiment 2 on Fukuda tests, both walking and marching in place, and on tandem walking patients differed from controls on some measures but the ROC values were all < 0.80 , so those tests are not useful for screening. The head impulse test was unable to detect subjects with bi-thermal caloric weakness $< 60\%$ (ROC = 0.64) although it was better able to distinguish patients with caloric weakness $\geq 60\%$. ROC values were > 0.80 only for those subjects, with the highest values observed for subjects with severe caloric weakness and age ≥ 60 (ROC = 0.88).

Conclusion

Experiment 1 suggests that Dix-Hallpike and head impulse tests are useful for screening. Experiment 2 suggests that the head impulse is useful for screening people for more severe disease, especially older people, but a negative response might not indicate the presence of less severe disease. The Fukuda stepping test is of no value for screening and should not be used.

PS - 421

Epidemiology of Dizziness and Balance Problems in U.S. Children: Results from the 2012 National Health Interview Survey (NHIS)

Chuan-Ming Li¹; May S. Chiu¹; Helen Cohen²; RoseMarie Rine³; Bryan K. Ward⁴; **Howard J. Hoffman¹**

¹National Institute on Deafness and Other Communication Disorders (NIDCD), NIH; ²Baylor College of Medicine;

³Specialty Therapy Source, LLC and Marshall University;

⁴Johns Hopkins University and Hospital

Background

The 2012 NHIS Child Balance Supplement (CBS), the first U.S. large-scale, nationally-representative health survey on dizziness and balance problems of children, ages 3-17 years, ascertained: age at first steps; general problems with standing, walking, or using limbs; occurrence of vertigo, light-headedness or fainting, poor balance or unsteadiness, problems with body or motor coordination or clumsiness, frequent falls, or related symptoms; diagnosis by health professionals and participation in recommended treatments during the past year; limitations on participation in home, school, or recreational activities; and parent's perception of the severity of the dizziness/imbalance symptoms.

Methods

Statistical analyses of this population-based survey (N=10,954) were adjusted for the complex sampling design to ensure estimates accurately represent national percentages of children and, also, to derive variance estimates for significance testing and 95% confidence intervals (CI). Multi-variable logistic regression was used to calculate odds ratios (OR).

Results

5.3% of U.S. children (3.3 million) were reported to have had problems with dizziness or balance during the past year. This increased with age: 3.7% for ages 3-7 years, 5.0% for 8-12 years, and 7.2% for 13-17 years. Symptomatic children had at least one problem: "poor body/motor coordination" (46%), "light-headedness/fainting" (35.1%), "poor balance/unsteadiness" (30.9%), "vertigo/spinning feeling" (29.0%), "frequent falls" (25.0%), and "other dizziness/balance problems" (8.5%). Covariates associated with dizziness/imbalance were: female sex (OR=1.4; CI: 1.04-1.8); age 12-17 years (OR=1.7; CI: 1.1-2.6); hay fever (OR=1.9; CI: 1.3-2.6); reported hearing trouble (OR=2.7; CI: 1.5-5.1); stuttering (OR=2.8; CI: 1.6-4.9); learning disability (OR=2.6; CI: 1.9-3.6); other developmental delays (OR=2.8; CI: 1.8-4.2); regular excessive daytime sleepiness (OR=3.4; CI: 2.4-5.0); frequent headaches/migraines (OR=3.6; CI: 2.6-5.0); and seizures past year (OR=4.3; CI: 1.8-10.3). Although for most, the child's dizziness/imbalance symptoms were perceived either as small or not a problem (81.7%), 18.3% reported that the problem was moderate or worse. In the past year, 37.4% of the children saw a health professional, 30.6% had tried treatments, and 22.3% had limited participation in home, school (work/jobs), or recreational activities. The most common diagnoses were neurologic disorders (14.1%), ear infections (11.3%), head/neck injuries or concussions (9.3%), and "some other cause--not specified" (46.3%).

Conclusion

Symptoms of balance/vestibular dysfunction have a relatively high prevalence - 5.3% of U.S. children. The findings described should be useful to clinicians and for assessing Healthy People 2020 objectives to promote diagnosis and treatment of children with these problems.

PS - 422

Evaluation of a Direct Posturographic Method in Daily-Life Tasks

Dietmar Basta; Arne Ernst

Dept. of ENT at ukb, Charité Medical School, University of Berlin

Background

Mobility is crucial to maintain a sufficient quality of life. Posturography should be therefore focused on the investigation of daily-life activities. This would help to determine the mobility of an individual patient. Nowadays, postural control is often estimated by stance tasks on a force plate under different sensorimotor conditions. This technique applies an indirect approximation of the centre-of-body-mass and is not related to tasks required for mobility. An alternative approach would be the direct measurement of body sway during daily-life conditions close to the centre-of-body-mass (Mobile Posturography). The present study was aimed at investigating age-dependent postural control strategies by analyzing the body sway of males and females in daily-life tasks.

Methods

Trunk sway measures were performed in 246 healthy volunteers (20-85 years) using the Vertiguard®-D device. With

the device fixed by a belt at the hip (centre-of-body-mass), the subjects had to undergo fourteen daily-life tasks under different sensorimotor conditions. The median values were compared with those of 76 age and gender matched patients which suffered from peripheral vestibular disorders. The sensitivity to distinguish between normal and pathological sway was determined.

Results

A non-linear relationship between age and body sway was observed in the majority of all the conditions. This holds especially true for most walking tasks. In contrast to this findings the body sway increased nearly linearly with increasing age in most standing tasks. However the opposite holds true for some walking tasks in the female group. Furthermore, large gender-related differences in body sway were observed.

The data also shows the age dependent influence of different sensory inputs on postural control.

Conclusion

The analysis of postural control in mobile conditions seems to be more complex compared with those of simple standing tasks. Therefore a high number of age groups within the investigated age range is crucial. Even if the analyzed movements have additional degrees of freedom in most tasks of the Mobile Posturography, the sensitivity of this method was higher than reported in literature before for any posturographic method. The present results indicate that this method can quantify the follow up of any treatment for a vestibular disorder on an individual daily-life related basis.

PS - 423

Quantitative Analysis of Smooth Pursuit Eye Movement by Video-Oculography

Hironori Fujii; Makoto Hashimoto; Kazuma Sugahara; Hiroaki Shimogori; Takuo Ikeda; Hiroshi Yamashita
Department of Otolaryngology, Yamaguchi University Graduate School of Medicine

Background

It is essential to use an infrared CCD camera in clinical examination of the vestibular system. Devices are currently available that can quite accurately record human eye movement, based on principle of video-oculography (VOG). Smooth pursuit eye movement (SPEM) abnormalities are an essential clinical feature of the central disorders. The examination of SPEM needs an electronystamography (ENG) or a device dedicated. We devised an original VOG system using a commercialized infrared CCD camera, a personal computer and public domain software program (ImageJ) for SPEM analysis. The present study aims to quantitatively evaluating the SPEM examination by VOG without using a special device.

Methods

We evaluated six subjects. Three cases were diagnosed normal pattern using ENG and three cases were saccadic pattern. Subjects were seated with their heads stabilised by chin rest. We focus here on the pursuit tracking movements which were elicited by sinusoidally movement. We used the infrared CCD camera with half mirror (ET-60LW, NEWOPT Inc) to re-

cord patients' eye movement. The horizontal eye movements was recorded with VOG system (ImageJ and Mac Book Pro) at a sampling rate of 30 Hz. The target moved in the horizontal direction (amplitude ± 30 deg) at frequencies of 0.25Hz. Raw eye position data were processed using spreadsheet software. Parameters to evaluate SPEM were the number of saccadic eye movement, the mean and variance of eye movement velocity, the mean and variance of the difference between the eye movement velocity and the target velocity and the phase difference.

Results

The number of saccadic eye movement was a large number in the saccadic pattern. The mean and variance of eye movement velocity were small in saccadic pattern. The mean and variance of the difference between the eye movement velocity and the target velocity were small in saccadic pattern. The phase difference was no difference.

Conclusion

Using this method we may be able to evaluate SPEM quantitatively without a special device.

PS - 424

Canal Conversion Between Anterior and Posterior Semicircular Canals in Benign Paroxysmal Positional Vertigo

Minbum Kim; Kyu-Sung Kim
Inha University College of Medicine

Background

There have been several reports regarding canal switch between posterior canal (PC) and horizontal canal (HC) in BPPV. However, canal conversion between anterior canal (AC) and PC has not been described. Because the AC and PC are connected with each other via the common crus, conversion can occur between two canals during canalith repositioning procedures (CRPs). In this study, we investigated the characteristics of AC and PC conversion cases in BPPV.

Methods

A retrospective chart review at a secondary referral center.

A total of 709 patients who were treated with the Epley maneuver for BPPV of the anterior or posterior semicircular canal were included. Vestibular examinations with videonystagmography and the canalith repositioning procedure (CRP) to treat BPPV were done.

Results

Canal conversion between the anterior and posterior semicircular canals was observed in 18 (2.9%) patients who underwent CRP. In 13 (2.3%) out of 564 patients initially diagnosed with posterior canal BPPV (PC-BPPV), switch to anterior canal BPPV (AC-BPPV) was observed at a follow-up visit. In 5 (12.1%) out of 41 patients who presented with AC-BPPV, canal switch to PC-BPPV occurred more frequently ($p=0.005$). The average number of CRPs before nystagmus resolution was 3.6 in conversion cases versus 1.6 in the non-conversion group ($p<0.001$).

Conclusion

Canal conversion between the anterior and posterior semicircular canals can occur during treatment. The possibility of canal conversions should be considered for appropriate management of BPPV of the vertical semicircular canals.

PS - 425

Impact of Near-Spectacle Correction on Angular Vestibulo-Ocular Reflex Gain in Older Individuals

Carol Li; Robert Geary; David Solomon; David Zee; Howard Ying; Yuri Agrawal

Johns Hopkins University School of Medicine

Background

Quantitative angular vestibular-ocular reflex (AVOR) testing is an important diagnostic tool for the evaluation of individuals with vestibular disorders. In recent studies of video head-impulse testing (vHIT) in healthy older individuals, we observed super-unity horizontal AVOR gains in a moderate proportion of subjects. This study aims to explore whether super-unity gains could be explained by AVOR gain adaptation due to habitual use of magnifying lenses for near spectacle correction by older individuals. Additionally, we investigated whether subjects can “de-adapt” their AVOR gain over a 1-hour period following spectacle removal such that their “true” AVOR gain can be ascertained.

Methods

Five individuals (age ≥ 55) who habitually wore magnifying lenses were enrolled in the study. Four subjects had no history of vestibular disease; one had a history of benign positional vertigo. The effective lens diopter correction in the horizontal meridian (D_{horiz}) and the resultant rotational magnification of the visual scene (M_{pred}) were calculated for each eye using a manual lensometer. A standardized vHIT protocol was administered to each subject: patients removed their spectacles at the start of testing, and testing was performed at 0, 5, 15, 30, and 60 minutes. Between intervals, subjects watched a video on a screen located 124 cm away. In a follow-up phase of testing, subjects performed x1 viewing exercises (involving both eye and head movements) between intervals. AVOR gain was calculated for each time point by dividing median horizontal eye velocity by horizontal head velocity at 60 ms. We evaluated changes in AVOR gain over time and as a function of mean D_{horiz} and M_{pred} across both eyes.

Results

Three out of five subjects had super-unity AVOR gains at the start of testing (1.06 – 1.30). We observed a trend towards higher AVOR gains with increasing diopter correction. For the study paradigm where subjects viewed a video between intervals, we did not observe any change in AVOR gain over time after spectacle removal. Data collection is currently in progress for the study paradigm involving x1 viewing exercises between intervals.

Conclusion

Super-unity AVOR gains were observed in the majority of older individuals recruited to this study. There was a trend

towards an association between increased lens diopter correction and higher AVOR gains. Evidence of AVOR gain de-adaptation, manifest as a decrease in AVOR gain over time, was not observed in this study, although experimental protocols designed to elicit de-adaptation are ongoing.

PS - 426

Measurement of OVEMP in the Inverted Position

Toru Seo; Takamitsu Kobayashi; Mitsuo Sato; Mle Miyashita; Kazuya Saito; Katsumi Doi
Kinki University Faculty of Medicine

Background

Otolith dysfunction is now able to be detected by vestibular evoked myogenic potential (VEMP) testing. Reduced or absent response on VEMP suggest being otolith dysfunction. Disturbed sensory cells may cause reduced or absent response on oVEMP. Is there any other pathogenesis which causes reduced response? When the subject is in an inverted (upside-down) position, the direction of the gravitational force inverts in the utricle. Measurement of VEMP in an inverted position may provide some insights into otolith pathophysiology.

Methods

Subjects in this study comprised 4 healthy adults (age range, 28 to 36 years) who had not suffered from any otological or neurotological symptoms. Subjects underwent ocular VEMP (oVEMP) for air-conducted sound (ACS) and bone-conducted vibration (BCV) in both upright and inverted (handstand) positions. Peak-to-peak amplitude of the n1-p1 wave and peak latencies of the p1 and n1 waves were measured in each subject. Amplitudes were normalized by dividing the obtained value by the integrated value during the 20 ms before stimulation.

Results

In all subjects, oVEMP to ACS and BCV in upright positions were recorded. In the inverted position, 2 subjects did not show any response and the other 2 subjects showed reduced amplitudes of the n1-p1 on oVEMP to ACS. For oVEMP to BCV, amplitudes of the n1-p1 waves were reduced in all subjects. Peak latencies of n1 and p1 waves were within normal limits in all detected waves.

Conclusion

Our results indicate that oVEMP is reduced when patients are in an inverted position. Under this condition, the otoconia may detach from the otolith membrane due to the force of gravity. This suggests that not only disturbance of otolith sensory cells, but also detached otoconia, may induce reduced responses on oVEMP.

PS - 427

Three-Dimensional Head Movement Video Image Analysis Technique Using Personal Computer and Public Domain Software.

Makoto Hashimoto; Takuo Ikeda; Hironori Fuji; Kazuma Sugahara; Hiroaki Shimogori; Hiroshi Yamashita
Yamaguchi University Graduate School of Medicine

Background

Usually motion analysis is performed using several cameras or sensors. On the other hand, we previously have developed a three-dimensional eye movement image analysis technique using commercialized infrared CCD camera, personal computer and public domain software. In this study, we devised a new three-dimensional head movement video image analysis technique using one camera, personal computer and public domain software.

Methods

Head movement video image from the top of the head was captured directly to the personal computer at 30 frames per second. Image analysis was performed automatically using public domain software ImageJ. For analysis of forward-backward and right-left direction, the XY center of the head was calculated. For analysis of rotation of the head, the shape and hair pattern of the head, which was rotated each 0.1 degrees, was overlaid with the same area of the next head image and the angle that both area matches most was calculated.

Results

Using this technique, it is possible to perform inexpensively the three-dimensional head movement analysis from video image recorded by one camera. In addition, this technique does not require any equipment attached to the subject and is easy to prepare.

Conclusion

We conclude that this new head movement image analysis technique is useful for clinical examinations and research into vestibular function.

PS - 428

Abnormalities in Vestibulo-Spinal Pathways Are Indicators of Poor Prognosis for Migrainous Vertigo

Jong Woo Chung; Jae Hoon Jung; **Chan Il Song**; Hong Ju Park

Asan Medical Center

Background

We evaluated abnormal vestibular function test results in migrainous vertigo patients including caloric, vestibular-evoked myogenic potential and dynamic posturography measurements and assessed their association with treatment responses.

Methods

We investigated a cohort of 116 patients who had suffered recurrent vertigo attacks for more than 6 months. A combination of life style modifications and medications were used to treat these subjects. The patients were asked to score the treat-

ment success by ranking from 0 to 100% the improvement in overall severity of headache and vertigo. Patients were then classified as complete remission, symptomatic improvement $\geq 50\%$, or $< 50\%$ improvement after 6 months of treatment. The periods needed for symptomatic improvement in the $\geq 50\%$ patient group were recorded and the responsiveness to medications and the vestibular test result metrics were analyzed to identify clinical outcome predictors.

Results

A symptomatic improvement of $\geq 50\%$ in vertigo and headache was observed in 72 % and 78% of the study subjects, over mean periods of 2.4 and 2.3 months, respectively. Improvements in vertigo and headache did not coincide. Abnormal caloric, VEMP, and vestibular ratio measurements were found in 27%, 30%, and 55%, of cases, respectively. Although abnormal caloric results showed no significant difference among our three groups, an abnormal vestibular ratio on posturography showed significant correlation with a poor treatment response of vertigo and a normal VEMP was significantly related to complete remission from headache. A poor response of vertigo symptoms to treatment was observed in 7% of patients with a normal vestibular ratio and 35% of patients with abnormal vestibular ratio. Complete remission from headache was observed in 62% of patients with a normal VEMP and 30% in patients with an abnormal VEMP.

Conclusion

Most patients with migrainous vertigo experienced improvements in both headache and vertigo through a combination of life style changes and medication. Abnormal vestibular ratios on posturography and abnormal VEMP responses were frequent findings in our cohort and were indicators of a poor prognosis. The pathophysiology of migrainous vertigo appears to be closely related to vestibular abnormalities, especially in vestibule-spinal pathways.

PS - 429

Clinical and Physiologic Predictors of Near Dehiscence Syndrome

Michael Baxter¹; Bryan Ward¹; Carolina Trevino²; Alexander Carter³; Geraldine Zuniga²; Charley Della Santina¹; John Carey¹

¹Johns Hopkins School of Medicine; ²Johns Hopkins;

³University of Pittsburgh

Background

Recent work identified patients with symptoms and diagnostics suggestive of superior semicircular canal dehiscence syndrome (SCDS) but who were found to have thin rather than dehiscent bone overlying the superior semicircular canal during surgery. The purpose of this case-control study is to identify predictors of near dehiscence.

Methods

The records of 184 patients who underwent middle cranial fossa approach for repair of SCDS at Johns Hopkins Hospital between 1998 and December 2012 were reviewed to identify cases of near dehiscence as well as controls with frank dehiscence. Twelve cases of near dehiscence (11 patients, 12 ears) and 23 controls with frank dehiscence were identified.

Results

Lower peak-to-peak amplitude ocular vestibular-evoked myogenic potential (oVEMP), OR=0.95 (95%CI 0.91-0.98), higher cervical vestibular-evoked myogenic potential (cVEMP) thresholds, OR=1.09 (95%CI 1.02-1.17), and smaller average low-frequency air-bone gap (ABG), OR=0.85 (95%CI 0.76-0.96) predicted near dehiscence rather than frank dehiscence, as did the presence of pulsatile tinnitus (OR=13.91, $p=0.032$). Age, sex, and the presence of conductive hyperacusis or Tullio phenomenon were not predictive of near dehiscence ($p>0.05$).

Conclusion

In the setting of symptoms and diagnostic testing consistent with SCDS, the presence of pulsatile tinnitus, higher cVEMP thresholds, and smaller oVEMP amplitudes and ABG suggest temporal bone thinning rather than true dehiscence. These findings may aid clinicians in counseling patients prior to surgical repair.

PS - 430

Relationship Between Posttraumatic Stress Disorder and Vestibular Function

Yaa Haber¹; Helena Chandler²; Jorge Serrador³

¹Rutgers Biomedical Health Sciences; ²WRIISC, Dept of Veteran Affairs; ³Rutgers Biomedical Health Sciences & WRIISC, Dept of Veteran Affairs

Background

Posttraumatic stress disorder (PTSD) is common in veterans and associated with a number of symptoms including dizziness, a symptom of PTSD that impairs function [1]. Furthermore, clinical data from our center demonstrates increased reports of symptoms of dizziness among PTSD patients. Dizziness symptoms are also highly associated with vestibular dysfunction [2-4]. Despite this, current PTSD assessments do not include an assessment of vestibular function. Therefore, our aim is to determine whether there is an increased incidence of vestibular impairment among PTSD patients.

Methods

A group of 27 veterans (Age 27 to 58) were evaluated at the War Related Illness and Injury Study Center (WRIISC), East Orange VA for vestibular function. Vestibular function was assessed by posturography and rotational chair testing. PTSD was classified based on scoring 44 or higher on the post-traumatic checklist civilian (PCL-C). Head injury status was determined from a level two polytrauma interview.

Results

Ten veterans were classified as having PTSD. Examination of posturography demonstrated that in Veterans with PTSD they had significantly poorer equilibrium scores on SOT2 (eyes closed), Controls – 91.7 ± 3.5 vs PTSD – 85.9 ± 6.5 , $P<0.05$. In contrast there was no difference in the SOT5 condition (eyes closed, unstable platform). Consistent with no differences in SOT5, the vestibular ratio was also not different between groups (Controls – 0.54 ± 0.30 vs PTSD – 0.52 ± 0.22). Consistent with this, ocular counter-roll (OCR), an otolith mediated vestibular ocular reflex was also not different between groups (Controls – 0.13 ± 0.06 vs PTSD – 0.18 ± 0.07).

Conclusion

Our preliminary data indicate that veterans with PTSD appear to have normal posturography and normal balance. This was in contrast to our original hypothesis that vestibular dysfunction may be more prevalent in veterans with PTSD. One possible confounder is the effect of mild TBI on vestibular function. However, controlling for mTBI did not affect our results. Another possible explanation is that veterans with PTSD may have canal rather than otolith dysfunction. Thus, future work is necessary to examine both otolith and canal function in this population.

PS - 065

Influence of Inhibition on Encoding

Vocalizations in the Mouse Auditory Midbrain

Alexander Dimitrov; Graham Cummins; Zachary Mayko;

Christine Portfors

Washington State University Vancouver

Background

Many animals use a diverse repertoire of complex acoustic signals to convey different types of information to another animal. One way in which the auditory system may discriminate among different vocalizations is by having highly selective neurons. Another strategy is to have versatile neurons with specific spike timing patterns for particular vocalizations. Both of these strategies occur in the auditory midbrain of mice. However, the neural mechanisms underlying these selectivities are unclear. Here, we examined whether inhibition plays a role in creating neural selectivity to vocalizations in the mouse inferior colliculus (IC).

Methods

We examined extracellular single unit responses to vocalizations before and after iontophoretically blocking GABA A and glycine receptors in the IC of awake mice. We used two different distance measures between neural event sequence, one based on vector space embedding, and one derived from the Victor/Purpura metric, to direct hierarchical clustering of responses. We estimated the rate of loss of mutual information with increasing amounts of noise in the timing of response rates. A major challenge in this analysis was debiasing, due to large response space size, relatively small numbers of measurements, and a large number of null responses (containing no spikes). We used a shuffle-based debiasing procedure in the mutual information measurements, and both a modification of the distance function, and a resampling procedure in the clustering analysis to address these issues.

Results

We observed two main effects: 1) Highly selective neurons maintained this selectivity and information about the stimuli, while increasing response rate. 2) Cells with conserved response structure, with similar timing and pattern, but with a greater number of spikes. The information rate generally increases, but the information per spike decreased. In many of these cells, stimuli that generated no responses in the control condition generated some response in the test condition. Interestingly, in some neurons, blocking inhibition had no effect on vocalization-evoked responses.

Conclusion

The activity of the neurons affected by blocking inhibition is consistent with a model of a single response pattern, more of which exceeds threshold in the absence of inhibition. On the other hand, it could also indicate a change in the code, particularly in the degree of selectivity. We hypothesize that these neurons in IC use inhibition to improve the energy efficiency of the information they represent.

Introduction/Overview

Anthony Cacace

Wayne State University

SY - 039

Effect of Blast Exposure on Peripheral Vestibular Function in Humans

Faith Akin

SY - 040

The Role of Vascular Damage in Blast Induced TBI

Ewart Haacke; Tilak Gattu; Tony Cacace

Wayne State University

In this work, we will present new imaging results related to traumatic brain injury and tinnitus.

Background

Our goal is to better understand the neurobiology of tinnitus and evaluate its relationship to white matter changes in the brain using advanced magnetic resonance imaging (MRI) methods.

Methods

To address these issues, we focused on two advanced neuroimaging methods: diffusion tensor imaging (DTI) and susceptibility weighted imaging (SWI), collected on a Philips 1.5T scanner. These were used in a group of subjects who were exposed to: a) blast induced trauma (TB) (n=20), b) trauma only (T) (n=4) and c) blast only (B)(n=7). To quantify differences in white matter structures, tract-based spatial-statistical analysis (TBSS) and 50 regions in white matter including the global white matter (WM) analysis was used. In this presentation, we will report on 13 trauma subjects, 1 blast subject and 7 healthy controls (HC) studied so far. SWI and QSM (quantitative susceptibility mapping) were used to detect changes in oxygen saturation and to quantify the amount of iron present in micro bleeds. Together, these strategic and methodological factors were used to enhance the specificity of the findings and to help distinguish neuroplasticity associated with hearing loss from putative structural changes in white matter anatomy associated with tinnitus. All images were processed using our internally developed MR software SPIN (Signal Processing in NMR).

Results

SWI showed vascular damage, i.e., abnormal veins, in two cases. DTI revealed no significant major changes with global WM FA analysis in the 13 blast subjects. However, the majority of findings from TBSS and the regional analysis for each of these individual blast subjects suggested the presence of

decreased FA for major white matter structures such as the superior longitudinal fasciculus (SLF), superior corona radiata (SCR), posterior thalamic radiation (PTR) as well as the genu and splenium of the corpus callosum.

Conclusion

The presence of vascular damage in two of the cases suggests that the range of forces during impact can have a variable effect in mTBI. No direct correlation has been found between the SWI and DTI results at that this time. On the other hand, the neuroanatomical abnormalities revealed by DTI may have implications in the study of the connective patterns of white matter tracts to the frontal lobe and primary auditory cortex. It would seem that the information provided by DTI and SWI is quite distinct and each likely represents a different type of damage.

SY - 041

Window's to the Brain: The Neuropsychiatry of TBI for Otolaryngology

Robin Hurley

SY - 042

Visualizing Vestibular Injury in the Invisible Wounds of War

Carey Balaban

SY - 043

Expression Profiling of Auditory Functional Genes in the Brain After Repeated Blast Exposures

Manoj Valiyaveetil

Clinical Research Management

The mechanisms of central auditory processing involved in auditory/vestibular injuries and subsequent tinnitus and hearing loss in active duty service members exposed to blast are currently unknown. Recently, we established a tightly-coupled repetitive blast-induced traumatic brain injury model in mice with significant neuropathology and neurobehavioral changes (Wang et al., 2011). We further demonstrated significant changes in various biomolecules involved in cholinergic and inflammatory pathways, mitochondrial dysfunction, neuronal injury biomarkers, and fragmentation of DNA after the blast exposure using the same model (Valiyaveetil et al., 2011, 2013a, 2013b; Arun et al., 2013a, 2013b; Wang et al., 2013). To extrapolate the effects of repeated blast exposure on the central auditory processing in mice, we analyzed the expression of hearing related genes in different regions of the brain at 6 h after the blast exposure using microarray (Valiyaveetil et al., 2012). Results showed that the expression of the deafness-related genes otoferlin and otoancorin was significantly changed in the hippocampus after blast exposures. Differential expression of cadherin and protocadherin genes, which are involved in hearing impairment, was observed in the hippocampus, cerebellum, frontal cortex, and midbrain after repeated blasts. A series of calcium-signaling genes that are known to be involved in auditory signal processing were also found to be significantly altered after repeated blast exposures. The hippocampus and midbrain showed signifi-

cant increase in the gene expression of hearing loss-related antioxidant enzymes. Histopathology of the auditory cortex showed more significant injury in the inner layer compared to the outer layer. In another set of experiments, we evaluated the modulation of hearing related proteins in the brain and inner ear of repeated blast exposed mice (Arun et al., 2012). Proteomic and Western blot analysis showed up-regulation of two major calcium buffering proteins, calretinin and parvalbumin in the cerebellum and inner ear of blast exposed mice indicating altered calcium homeostasis after the blast exposure. In summary, mice exposed to repeated blasts showed injury to the auditory cortex and significant alterations in multiple genes in the brain known to be involved in age- or noise-induced hearing impairment. Also, repeated blast exposure resulted in modulation of hearing related proteins in the central and peripheral auditory processing which are known to be involved in calcium homeostasis.

SY - 044

Stimulus Timing Dependent Plasticity in the Auditory Cortex

Johannes Dahmen

University of Oxford

Adult cortical circuits possess considerable plasticity, which can be induced by modifying their inputs and which is likely to underlie perceptual learning. One mechanism proposed to underlie changes in neuronal responses is spike-timing-dependent plasticity (STDP), an up- or down-regulation of synaptic efficacy contingent upon the order and timing of pre- and postsynaptic activity. The repetitive and asynchronous pairing of a sensory stimulus with either another sensory stimulus or current injection can alter the response properties of visual and somatosensory neurons in a manner consistent with STDP. By recording from neurons in the primary auditory cortex of both anesthetized and awake adult ferrets, we have shown that such plasticity also exists in the auditory system (Dahmen et al., 2008). The repetitive pairing of pure tones of different frequencies induced shifts in neuronal frequency selectivity, which exhibited a temporal specificity akin to STDP. Only pairs with stimulus onset asynchronies of 8 or 12 ms were effective and the direction of the shifts depended upon the order in which the tones within a pair were presented. Six hundred stimulus pairs (lasting ~70 s) were enough to produce a significant shift in frequency tuning and the changes persisted for several minutes. The magnitude of the observed shifts was largest when the frequency separation of the conditioning stimuli was < ~1 octave. Moreover, significant shifts were found only in the upper cortical layers.

Our findings highlight the importance of millisecond-scale timing of sensory input in shaping neural function and strongly suggest STDP as a relevant mechanism for representational plasticity in the mature auditory system. STDP has also been implicated in the cortical plasticity that follows partial deafferentation of sensory cortex by whisker trimming (Celikel et al., 2004) or focal retinal lesions (Young et al., 2007). Similarly, our results provide support for the possibility that STDP is involved in the reorganization of cortical tonotopicity produced by partial cochlear lesions, potentially implicat-

ing STDP in the changes that may underlie tinnitus. All the same, it is essential to show that this plasticity is behaviorally relevant. Unlike studies on the visual system (Yao and Dan, 2001; Fu et al., 2002), however, we were unable to find a perceptual correlate of the frequency plasticity demonstrated in cortical neurons. Nevertheless, we were able to show that plasticity of auditory spatial perception can follow STDP-like timing rules, although, in this case, it is unlikely that STDP is the underlying mechanism.

SY - 045

Spike-Timing Dependent Plasticity in Auditory Cortex: Modulation by Cholinergic Receptors, and Potential Roles in Circuit Reorganization and Neural Synchrony

Paul Manis

The University of North Carolina at Chapel Hill

The ability to selectively change the strength of transmission at individual synapses is thought to be a fundamental mechanism that supports learning and memory, including learning that shapes sensory perception. Spike-timing dependent plasticity (STDP) is an operational measure of changes in synaptic strength, where the strength is regulated by the temporal order of presynaptic transmitter release and signals initiated by synaptic receptors and postsynaptic action potentials. However, STDP itself is subject to modulation in ways that can alter the timing rules. In this presentation, I will discuss two issues. The first is an experimental exploration of the STDP timing rules in layer 2/3 of mouse primary auditory cortex (A1) and the mechanisms of cholinergic modulation of this STDP. Recurrent synapses in layer 2/3 of A1 exhibit STDP with an interesting rule. Presynaptic stimulation after postsynaptic stimulation produced a long-term depression (tLTD) that is maximal for intervals near -20 msec. Presynaptic stimulation that precedes postsynaptic action potentials produced long-term potentiation (tLTP) at short intervals (~10 msec). However, at longer intervals, (~50 msec) the pre-post pairing order produced tLTD. Thus, STDP in A1 exhibits a temporal-surround structure, with tLTP at short pre-post pairing intervals, bounded by tLTD. Pharmacological activation of muscarinic receptors (mAChR) depressed tLTP induction at +10 msec. This depression occurred as a result of a decreased postsynaptic NMDA receptor conductance following mAChR activation, which in turn reduced the postsynaptic increase in dendritic calcium. The mechanism appeared to be entirely postsynaptic, as there was no evidence for a change in presynaptic transmitter release. The second issue to be discussed will be the theoretical considerations of how STDP (and other mechanisms) can drive the functional connectivity of the cortical circuits, and how it may contribute to remodeling circuits after partial loss of peripheral function. STDP can be engaged by cortical rhythms, and can also contribute to the formation of dynamic circuits that support synchronized firing in response to both temporal structures in the sensory input, and to intrinsic activity. STDP may thus contribute to the adaptation of central sensory processing following changes in peripheral function or the sensory environment.

SY - 046

Bimodal STDP in Dorsal Cochlear Nucleus and Auditory Cortex in Normal and Noise-Damaged Tinnitus Models

Susan Shore

University of Michigan

Robust functional connections from peripheral and brain-stem somatosensory neurons to the cochlear nucleus (CN) provide a substrate for auditory-somatosensory integration. Our studies have shown that combining auditory with somatosensory stimulation can result in long term suppression or enhancement ("bimodal plasticity") in principal neurons of the dorsal CN (DCN) and auditory cortex. Recently, we demonstrated that this bimodal plasticity is stimulus-timing dependent, with Hebbian and anti-Hebbian timing rules that reflect *in vitro* spike-timing dependent plasticity (Koehler and Shore, PLOS ONE, 2013; Basura et al., Brain Research, 2013). Subsequently, we assessed the stimulus-timing dependence of bimodal plasticity in a noise-damage tinnitus model. Guinea pigs were exposed to narrowband noise that produced a temporary threshold shifts and tinnitus. Following noise-exposure and tinnitus induction, stimulus-timing dependent plasticity was measured after pairing somatosensory and auditory stimulation with varying intervals and orders. In comparison with sham and noise-exposed animals that did not develop tinnitus, timing rules from DCN units in animals with tinnitus were more likely to be anti-Hebbian and broader for those bimodal intervals in which the neural activity showed enhancement, but narrower for bimodal intervals causing suppression. The broadening of the timing rules in the enhancement phase in animals with tinnitus, and in the suppressive phase in exposed animals without tinnitus was in contrast to narrow, Hebbian-like timing rules in sham animals. Furthermore, these timing rules are altered by neuromodulators that target NMDA (Stefanescu and Shore, ARO) 2014) and cholinergic receptors. These findings implicate underlying alterations in bimodal spike-timing dependent plasticity in tinnitus, opening the way for a novel therapeutic target (Martel et al., ARO 2014).

SY - 047

Waves of Synchrony: Abnormally Increased Synchrony is Potentially Linked to Reduced Alpha Oscillations

Thomas Hartmann

Center for Mind / Brain Sciences

Traditionally alpha oscillations have been regarded as a functionally irrelevant, thus "idling", background activity of the brain. However recent evidence has implicated modulations of alpha to be critically involved in several cognitive functions such as attention, working memory and perception. In general the functional relevance of alpha oscillations are now interpreted in a regulatory direction: high alpha power (e.g. over task-irrelevant regions) indicates states of inhibition and low alpha power states of high excitability. Furthermore ideas have been advanced, proposing locally expressed alpha modulations to shape long-range synchronization in functional networks. While these views are becoming more ac-

cepted in the cognitive neuroscience community, the strong clinical implications have been hardly explored. In a first part of my talk I will describe how these insights from cognitive neuroscience have helped in shaping our ideas on an earlier finding, showing reduced alpha power in temporal regions of tinnitus sufferers. Since direct evidence for the involvement of abnormal alpha oscillations cannot be shown by comparing a clinical with a healthy control group, my work group has devised studies inducing auditory illusory percepts in normal hearing participants. These works support the view of an auditory phantom percept being mediated by reduced alpha power in auditory cortex. Furthermore, (relatively) successful treatment of tinnitus via rTMS or neurofeedback is characterized by increasing alpha power in auditory cortical regions. I will attempt to summarize these findings in order to address a final important part: how local alpha modulations mediate the integration or decoupling of respective regions into a distributed functional network. In several studies and modalities we have been now able to show in absence of sensory stimulation, low alpha power to be associated with increased and high alpha power with reduced network integration. Crucially the level of network integration predicts upcoming conscious percepts of near-threshold or ambiguous stimuli. Transferring these results into the clinical domain we assume abnormally reduced alpha e.g. in auditory cortex not only to underlie "hyper-synchrony" at a local level but importantly enable "hyper-synchrony" on a large-scale.

SY - 048

Directing Cortical Plasticity to Understand and Treat Tinnitus

Michael Kilgard¹; Sven Vanneste¹; Michael Borland¹; Elizabeth Buell¹; Dirk De Ridder²

¹University of Texas at Dallas; ²University of Otago

Background

Pathological neural plasticity plays a major role in the genesis and maintenance of chronic tinnitus. Reversal of aberrant plasticity is therefore a promising approach to the treatment of tinnitus.

Methods

We have developed a novel method to direct highly specific and long lasting neural plasticity. Brief bursts of vagus nerve stimulation (VNS) trigger release of neuromodulators that direct brain changes specific to associated neural activity patterns.

Results

Pairing VNS with tones is sufficient to powerfully shape responses in the central auditory system. We have demonstrated that this therapy can be therapeutic in an animal model of tinnitus and in human patients. We are now optimizing the clinical parameters through parallel studies in humans and preclinical studies in animals.

Conclusion

We will present evidence suggesting that with further study VNS-directed plasticity may be optimized to become a reliable, safe, and long-lasting therapy for chronic tinnitus.

Unlearning Pathological Neuronal Synchrony by Coordinated Reset Neuromodulation

Peter Tass

Juelich Research Center

Subjective chronic tinnitus is related to abnormal neuronal synchrony in a network comprising auditory and non-auditory brain areas. Acoustic Coordinated Reset (CR) neuromodulation is a non-invasive stimulation technique which specifically counteracts abnormal synchrony by desynchronization, in this way ultimately inducing an unlearning of both abnormal synaptic connectivity and synchrony. In a proof of concept study acoustic CR neuromodulation caused a significant decrease of tinnitus symptoms along with a significant decrease of abnormal EEG power as well as a normalization of interactions within a tinnitus-related network of brain areas.

Background

A number of brain diseases, e.g. Parkinson's disease (PD) and tinnitus, are characterized by abnormal neuronal synchronization. To specifically counteract neuronal synchronization we have developed Coordinated Reset (CR) stimulation, a spatio-temporally patterned desynchronizing stimulation technique. According to computational studies, CR stimulation induces a reduction of the rate of coincidences and, mediated by synaptic plasticity, an unlearning of abnormal synaptic connectivity, so that a sustained desynchronization is achieved. Computationally it was shown that CR effectively works no matter whether it is delivered directly to the neurons' somata or indirectly via excitatory or inhibitory synapses.

Methods

In a randomized single blind placebo-controlled proof of concept trial non-invasive acoustic CR neuromodulation was applied to patients suffering from tinnitus. Apart from clinical standard scores EEG recordings and inverse calculations were performed in order to assess therapy-induced changes of spectral power in different brain areas as well as changes of effective connectivity.

Results

Acoustic CR neuromodulation delivered during 4-6 hours/day during 12 weeks led to a significant decrease of tinnitus loudness and annoyance (as assessed by visual analogue scale scores) and a significant decrease of the tinnitus questionnaire. Furthermore, power and functional connectivity analysis of EEG recordings demonstrated that acoustic CR therapy caused a significant decrease of pathological neuronal synchrony in a tinnitus-related network of auditory and non-auditory brain areas along with a normalization of tinnitus characteristic abnormal interactions between different brain areas, especially between the posterior cingulate cortex and the primary auditory cortex as well as between the dorsolateral prefrontal cortex and the primary auditory cortex.

Conclusion

According to our acoustic CR neuromodulation causes a long-lasting desynchronization of pathologically synchronized neuronal populations, as predicted theoretically, along with a significant decrease of tinnitus symptoms. The CR ap-

proach appears to be a promising novel therapeutic option for the therapy of tinnitus.

Neurites from Spiral Ganglion Neurons Align More Closely to Unidirectional Micropatterned Topographical Surfaces Compared to Surfaces With Multidirectional Patterns.

Alison Seline¹; Bradley Tuft²; Linjing Xu³; Andrew M.

Erwood¹; Marlan R. Hansen³; C. Allan Guymon²

¹University of Iowa Carver College of Medicine; ²University of Iowa Department of Chemical and Biochemical Engineering; ³University of Iowa Department of Otolaryngology-Head and Neck Surgery

Background

Directing spiral ganglion neuron (SGN) neurite growth towards cochlear implant electrodes using topographical guidance may allow for greater spatial and temporal resolution. Our previous work has shown that unidirectional linearly-patterned polymer surfaces effectively guide SGN neurite growth. These topographical patterns are readily produced on nano- and micrometer-scales using photomasks that control polymerization speeds across the polymer surface. This work compares the neural path-finding behavior of SGN neurites on uni-directional and multi-directional micropatterned surfaces and on unpatterned controls.

Methods

Micropatterned surfaces, consisting of ridges and grooves in parallel lines or repeating 90-degree angles, were created by using photomasks to spatially control photo-induced polymerization of methacrylate monomers. Interferometry and scanning electron microscopy were used to measure micropattern morphology and create 3D images.

Dissociated SGN cultures were grown on unpatterned or patterned substrates. The relationship of SGN neurites and Schwann cell (SCs) to the micropatterns was characterized. Preference of neurites for the depressed or raised features of the polymer surface was determined by comparing the portion neurite segments on the depressed and raised features. Neurite alignment to the horizontal was defined as a ratio of unaligned length of the neurite to total neurite length. A customized algorithm that compared the angle of alignment for neurite segments with the more proximal segment was used to assess neurite turning. SC alignment was determined by measuring the angle made between the major axis of an ellipse drawn around the cell and the horizontal plane.

Results

SGN neurites preferentially grow in depressed features of the polymer surface on both parallel patterns and patterns with repeating 90-degree angles. Neurites and SCs align more closely to parallel patterned surfaces as compared to surfaces with 90-degree angles. Indeed, neurites on surfaces with 90-degree angles, but not parallel lines, frequently cross multiple ridge and groove features. Furthermore, neurites on surfaces with 90-degree angles turn more frequently than neurites on parallel patterned surfaces, but less often

than neurites on unpatterned surfaces. Also, SGN neurites are significantly shorter on patterns with repeating turns compared to substrate surfaces with linear features, suggesting stalling of neurite growth associated with turning.

Conclusion

These results demonstrate that SGN neurites and SCs align more faithfully to uni-directional parallel line micropatterns compared with multi-directional micropatterns composed of 90-degree angles. The findings may inform future design of neural prostheses, such as cochlear implants, to address spatial resolution limitations.

PD - 079

Abnormal Binaural Spectral Integration in Hearing Aid and Cochlear Implant Users

Lina Reiss¹; Emily Walker²; Rindy Ito³; Jessica Eggleston¹; David Wozny⁴

¹Oregon Health & Science University; ²Whitworth University;

³VA Pacific Islands Health Care System; ⁴Carnegie Mellon University

Background

There is significant variability in the speech perception benefit that hearing-impaired individuals receive from combining two hearing devices bilaterally, whether the devices are bilateral hearing aids (HAs), bilateral cochlear implants (CIs), or a CI worn with a HA in the contralateral ear (bimodal CI+HA). Some individuals even experience interference with two hearing devices compared to one alone. One contributing factor may be an experience-induced change in the central processing of binaural inputs. Hearing-impaired listeners have large interaural pitch mismatches due to either hearing loss (diplacusis) or CI programming (frequencies allocated to the electrodes differ from the electrically stimulated cochlear frequencies). Previously we showed that pitch perception adapts to reduce this mismatch in some, but not all, CI+HA users (Reiss et al., 2007, 2011). Here we tested whether some individuals might also adapt binaural fusion to reduce the perception of mismatch. We also tested whether, as in other sensory modalities, this fusion leads to averaging of spectral information between ears.

Methods

Subjects were tested on three tasks: 1) *Interaural pitch matching*, in which a reference stimulus (pure tone or electrode, depending on that ear's device) was pitch-matched to sequentially presented comparison stimuli (again depending on device) in the contralateral ear; 2) *Dichotic fusion range measurement*, in which a reference stimulus was presented simultaneously with a stimulus in the contralateral ear, and the contralateral stimulus varied to find the frequency or electrode range that fused with the reference; 3) *Fusion pitch matching*, in which a fused reference-contralateral stimulus pair was pitch-matched to sequentially presented stimuli in the contralateral ear. A subset of subjects was also tested on *synthetic vowel discrimination* under both monaural and binaural conditions.

Results

9 bilateral HA and 21 bimodal CI+HA users had abnormally wide dichotic fusion frequency ranges of up to 2-3 octaves. Similarly, a bilateral CI user fused one electrode with over half of the contralateral electrodes. These fused stimuli elicited a new binaural pitch that was an average of the monaural pitches, suggesting integration of mismatched rather than matched information. Synthetic vowel discrimination curves were also averaged between ears, such that binaural averaging sometimes worsened discrimination performance compared to the best monaural condition.

Conclusion

The increased fusion and associated spectral averaging between ears indicates abnormal binaural spectral integration in the hearing-impaired population, and may account for speech perception interference observed with binaural compared to monaural hearing device use.

PD - 080

The Role of Extended Preoperative Steroids in Hearing Preservation Cochlear Implantation

Jafri Kuthubutheen¹; Vincent Lin¹; Joseph Chen¹; Harvey Coates²

¹Sunnybrook Health Science Centre; ²University of Western Australia

Background

Steroids have been shown to reduce the hearing threshold shifts associated with cochlear implantation. However at present, previous studies have only examined the administration of steroids just prior to surgery. It is well known that steroid effects are dependent upon the duration of exposure, both before and after surgery. The aim of this study is to examine the role of extended preoperative systemic steroids in hearing preservation cochlear implantation.

Methods

An animal model of cochlear implantation was used. 24 Hartley strain guinea pigs with normal hearing were randomised into a control group, a group receiving systemic dexamethasone one day prior to surgery and a group receiving systemic steroids daily for 5 days prior to surgery. A specially designed cochlear implant electrode by Med-EL (Innsbruck) was inserted through a dorsolateral approach to an insertion depth of 5mm and left in-situ. Auditory brain stem responses at 8kHz, 16kHz and 24 kHz were measured preoperatively, and 1 week and 1 month postoperatively. Cochlear histopathology was examined at the conclusion of the study.

Results

The animals receiving systemic dexamethasone had lower threshold shifts at 1 week and 1 month following surgery compared to control. These threshold shifts were significantly lower at 32kHz indicating a frequency selectivity and maximal effect around the basal turn of the cochlea. This effect was larger in the group receiving steroids for 5 days. The animals receiving steroids also had reduced variability in hearing thresholds compared to controls. We will present the histological findings, specifically spiral ganglion counts and cochlear fibrosis

Conclusion

This is the first study to demonstrate the benefits of extended preoperative steroids on hearing outcomes in cochlear implantation as well as a preference for the basal turn of the cochlea. The benefits appear to be larger for longer periods of preoperative steroid administration compared to a single preoperative dose. This has implications for considering the concept of “complete steroid coverage” where steroids are used before, during and after implantation.

PD - 081

Dexamethasone Modulates the Inflammatory and Fibrogenic Responses in Cochlear Tissue Explants Initiated by Electrode Insertion Trauma

Esperanza Bas Infante; Bradley Goldstein; Michelle Adams; Thomas R Van De Water

University of Miami

Background

Profound sensorineural hearing loss has been successfully treated with cochlear implantation (CI). However, insertion of a CI electrode array can initiate an inflammatory response that is known to induce loss of auditory hair cells and growth of fibrotic tissue. This fibrotic process can have a negative impact on the function of a patient's implant.

The objective of this study is to gain insight into the cellular and molecular mechanisms of fibrous tissue and bone formation that can occur following electrode insertion trauma (EIT).

Methods

We studied monocyte recruitment in the EIT-cochlear explants from 3 days old rat pups and compare these observations with control un-lesioned explant and with EIT explants that were treated for 24 hours with dexamethasone (DXM, 50 μ M). From previous studies we know that trauma to the cochlea induces the expression of Transforming Growth Factor Beta-1 (TGF β -1) which can cooperate with the Wnt/beta catenin pathway to elicit fibrogenesis. By immunostaining we identified in which cells of the organ of Corti (OC) and lateral wall (LW) explant tissues beta-catenin was activated after the mechanical trauma and the effect of DXM treatment on this activity. We also studied the implication of Phospho-Inositol-3-Kinase (PI3K) in the fibrotic response initiated by EIT in the explant tissues.

Results

EIT explants treated with DXM experienced less recruitment of monocytes compared to EIT explants ($p < 0.01$) and was comparable to control explant tissue results. This supports our previous observations, where DXM downregulates levels of pro-inflammatory cytokines (TNF α and IL1 β) and inducible enzymes (iNOS and COX2). PI3K was activated in OC upon mechanical trauma and by TGF β 1 treatment. DXM treatment dropped the activity of this enzyme to the control levels. Similar pattern was observed in the LW tissues. When we looked at the active form of beta-catenin we saw that in the EIT and in TGF β 1 treated explants the enzyme was present in the tight junctions and in the cytosol of the inner sulcus

cells. However in control, EIT+DXM, and EIT+PI3K inhibitor groups, the non-phospho beta catenin was only present in the tight junctions, but with high rate of hair cell loss in the last group. Gap junction disruption was observed in the EIT-LW tissues, while EIT+DXM group was similar to the control group of explants.

Conclusion

DXM treatment abolished the inflammatory response and the TGF β 1-catenin initiated fibrogenesis, making this drug a first choice in CI eluting electrodes.

PD - 082

Acoustic Change Complex to Amplitude Modulation in Cochlear Implant Subjects

Yang-soo Yoon¹; JiHye Han¹; Michael Scott¹; Lisa Houston²; John Grienwald¹; Ravi Samy²; Fan-Gang Zeng³; Andrew Dimitrijevic¹

¹*Cincinnati Children's Hospital Medical Center*; ²*University of Cincinnati, Dept. Otolaryngology*; ³*University of California, Irvine, Dept. Otolaryngology*

Background

The current study examined the use of auditory cortical potentials to assess the brain's ability to process sound through a cochlear implant (CI). Having an objective, brain-based measurement of auditory and speech perception would be beneficial for assessing CI performance in young children who cannot reliably perform speech perception tasks as part of a standard clinical test battery. In the present study, we used an amplitude modulation stimulus known to have strong a psychoacoustic relationship to speech and speech in noise performance measures in CI users.

Methods

Auditory cortical indices of temporal processing were examined in adults with cochlear implants (CI). Three outcome measures were performed: speech perception, AM depth detection threshold, and cortical evoked responses. Speech perception was unilaterally measured in consonant, vowel, and sentence as a function of signal-to-noise ratio when speech and noise were presented in front of the subject in sound field. AM depth detection threshold was measured in a 3-alternative forced choice paradigm for each of four AM rates (4, 40, 100, & 300 Hz). Auditory cortical responses (N1/P2; or Acoustic Change Complex, ACC) to a change in AM in an ongoing Gaussian noise were examined during a passive listening task using 64-channels of EEG. The ACC was measured to stimuli with 4 AM rates (4, 40, 100, & 300 Hz) and with 3 AM depths (100%, 50%, & 25%). Independent Component Analysis was used to minimize CI artifacts, and brain electrical source analysis was used to confirm auditory cortical activations.

Results

Preliminary data suggests that subjects with poor sentence perception have different N1 amplitude vs. AM rate functions compared to those with good sentence perception. Brain source analysis also demonstrated greater N1 frontal activation in good performers compared to poor performers.

Conclusion

The results of the preliminary data suggest that cortical evoked potentials to AM can show differences between good and poor performers.

PD - 083

Deficits in Pitch Sensitivity by Cochlear-Implanted Children Speaking English or Mandarin

Mickael Deroche¹; Hui-Ping Lu²; Julie Christensen³; Charles Limb¹; Yung-Song Lin⁴; Monita Chatterjee³

¹Johns Hopkins University School of Medicine; ²Chimei Medical Center, Tainan, Taiwan; ³Boys Town National Research Hospital; ⁴Taipei Medical University, Chimei Medical Center, Tainan, Taiwan

Background

Children's sensitivity to pitch is important as they acquire their native language, especially when this language is tonal such as Mandarin. We examined i) whether children with cochlear implants (CI) exhibited deficits in simple pitch discrimination tasks compared with children with normal hearing (NH), ii) whether this sensitivity depended on age at implantation or time in sound, and iii) whether having a tonal native language might affect pitch sensitivity.

Methods

Psychometric functions were measured for the discrimination of fundamental frequency (F0) of broadband sine-phase harmonic complexes, and for the discrimination of sinusoidal amplitude modulation rate (AMR) of broadband noise, in a 3-interval 3-alternative forced choice task. A total of 70 school-aged (at least 6 years old) CI children and a number of NH children were tested in the US and Taiwan. To mimic common voice pitch, the reference F0 was 100 and 200 Hz, as was the reference AMR. Stimuli were presented via loudspeakers and CI children listened through their speech processors. Data were fitted using a maximum-likelihood technique that extracted lapse, threshold and slope.

Results

In the F0 discrimination task, CI children displayed higher thresholds (and shallower slopes) than NH children. The magnitude of the deficits was substantial, on the order of 3-4 semitones versus 20-30 cents. Differences between NH and CI children were expectedly smaller in the AMR discrimination task. Interestingly, neither age at implantation nor time in sound were relevant factors for pitch sensitivity in CI children. Taiwanese children performed a little better than American children in the F0 discrimination task, but not in the AMR discrimination task.

Conclusion

The tonal language related benefit suggests that there is room for enhancement in pitch sensitivity by some forms of auditory training to pitch. However, the magnitude of the observed benefit is small and likely to be limited in CI children due to constraints inherent to the devices. While pitch discrimination is likely to play an important role in everyday tasks such as voice emotion recognition, lexical tone recog-

nition, and speech intonation recognition, it is likely that sensitivity to pitch contours will be more predictive of listeners' performance in such tasks. Therefore, we have also initiated a study of F0 contour discrimination by CI and NH children, preliminary results of which will be presented at the meeting. This research has important implications for the development of future generations of CI speech processors.

PD - 084

Stimulation and Excitation Patterns of Standard and Spanned Partial Tripolar Modes in Cochlear Implants

Ching-Chih Wu; Xin Luo

Purdue University

Background

Electrode spanning in partial tripolar (pTP) mode has been proposed to create additional spectral channels and fully explore the benefits of current focusing in cochlear implant (CI) users. Previous pitch-ranking results showed that in general, moving the apical return electrode away from the main electrode (i.e., apically spanned pTP mode) elicited a higher pitch, while basally spanned pTP mode elicited a lower pitch, which were consistent with the shifts of centroid of neural excitation pattern in a computational model. Spanning both apical and basal return electrodes (i.e., symmetrically spanned pTP mode) consistently elicited a higher pitch, although the simulated excitation centroid was not shifted. This study aims to understand the pitch changes perceived by individual CI users by examining the stimulation and excitation patterns of standard and spanned pTP modes.

Methods

Five post-lingually deafened adult CI users were tested. To examine the physical-level stimulation pattern, the electric field imaging (EFI) technique was used to measure the voltage distribution across all electrodes for a biphasic pulse (66 μ s/phase) on EL8 at a sub-threshold level (32 μ A) in the experimental pTP modes. To examine the neural-level excitation pattern, electrically evoked compound action potential (ECAP) was measured using a forward masking subtraction method for a probe on EL8 in the experimental pTP modes as a function of masker electrode from EL1 to EL16 (in monopolar mode). Both the probe and masker were comfortably loud biphasic pulses (32 μ s/phase). The perceptual-level excitation pattern was measured using a psychophysical forward masking paradigm for a comfortably loud masker on EL8 in the experimental pTP modes. The masker's spread of excitation was calculated as the differences between unmasked and masked thresholds of standard pTP-mode probes on EL3 to EL13.

Results

The centroid of psychophysical forward masking pattern shifted with the apically or basally spanned pTP mode in directions consistent with the perceived pitch changes. Although the symmetrically spanned pTP mode elicited higher pitches than the standard pTP mode, both modes had similar centroids and bandwidths of psychophysical forward masking pattern. Different from the psychophysical results, the ECAP

forward masking patterns and the EFI potential distributions had no consistent shifts with the experimental pTP modes, possibly due to the different measuring parameters.

Conclusion

Psychophysical forward masking patterns may better predict the perceptual effects of electrode spanning in pTP mode for CI users than the EFI and ECAP measures.

PD - 085

Cochlear Implant on 1681 Patients in Chinese PLA General Hospital

Shi-Ming Yang²; Jia-Nan Li¹; Pu Dai¹; Wei-Ju Han¹; Jun Liu¹; Hui Zhao¹; Yi-Hui Zou¹; Zhao-Hui Hou¹; Qing-Shan Jiao¹; Li Sun¹; Ai-Ting Chen¹; Meng-Di Hong¹; Qian Wang¹; Xin Xi¹; De-Liang Huang¹; Wei-Yan Yang¹; Dong-Yi Han¹

¹Dept of Otolaryngology Head and Neck Surgery, Chinese PLA General Hospital; Chinese PLA Institute of Otolaryngology; ²Chinese PLA General Hospital

Background

To analyze the general information in a China Cochlear Implantation Center and the outcome of postoperative speech rehabilitation of cochlear implantation in Chinese patients.

Methods

There were 1681 cases accepting cochlear implantation between March, 1997 and May, 2013 in our department, 992 male and 689 female. Among them, 992 cases accepted Australian Nucleus implant, with 471 accepting Austria MED-EL implant, 122 accepting American Advanced Bionics implant and 55 accepting Nuo Erkang implant (China). Among those patients, there were 55 cases with postlingual deafness and 1626 patients with prelingual deafness. The age ranged from 8 months to 79 years, 8.6 on average. Cases aged 1 to 3 were most common, and those aged 3 to 6 and 6 to 18 were secondary. Inner ear developmental deformity was seen in 421 cases (278 cases with large vestibular aqueduct syndrome, 59 with Mondini deformity, 22 with Waardenburg syndrome, 21 with stenosis of internal acoustic meatus and acoustic nerve maldevelopment, 7 with severe inner ear deformity, and 8 accompanied by other deformities). Acoustic nerve disease was present in 19 cases, and ossification and fibrosis were shown in 14. Stability and safety of cochlear implantation was studied by statistically analyzing intraoperative conditions, postoperative imaging and complication, and outcomes of cochlear implantation was explored into by statistically analyzing categories of auditory performance (CAP) and speech intelligibility rating (SIR) of 276 cases who had a history of more 2 years since the implantation.

Results

Since the first cochlear implantation in our department, the yearly surgery amounts rised from 1-3 during 1996-1997 to 362 during 2011, showing linear rising trend. Among the 1681 cases, abnormal events occurred in 87 cases, among which 15 accepted a second implant, 7 received incomplete implantation (4 cases with severe cochlear ossification), 11 showed cerebral dura damage (all were repaired successfully), 3 exhibited tympanic perforation, intraoperative CSF Gusher occurred in 10, aural skin split appeared in 1, tardative facial

palsy affected 5, subcutaneous hematoma of head occurred in 10, severe post-operative vertigo affected 30, implant rejection occurred in 1, with the general complication rate of 3.3%. All the abnormal events were solved successfully. CAP scores and SIR scores of the 276 cases who had a history of more than 2 years since the implantation were 4.5 (total scores, 5) and 7.8 (total scores, 8), respectively.

Conclusion

Cochlear implantation was safe and stable, and outcomes of postoperative speech rehabilitation were satisfactory in Chinese patients. Cochlear implantation was effective for severe deafness, and the long-term outcomes required further study.

SY - 050

Listening Effort in Cochlear Implant Users

Carina Pals¹; Anastasios Sarampalis²; Deniz Baskent¹

¹University Medical Center Groningen; ²University of Groningen

Background

Front-end processing and the limited number of electrodes of cochlear implants (CIs), as well as individual differences in, for instance, auditory nerve survival, can affect the quality of the transmitted speech signal. Even if intelligibility appears unaffected, such differences in signal quality can influence listening effort, i.e. the cognitive processing demand required to understand the speech. Previous research has shown, in normal hearing listeners presented with noise-band vocoded speech, that changes in spectral resolution can result in changes in listening effort, even when they may not affect intelligibility or subjective self-report. Our current study aims to investigate how spectral resolution, manipulated by changing the number of active electrodes, affects speech intelligibility and listening effort in CI users.

Methods

CI users were tested with four experimental maps using 15, 11, 9, and 7 active electrodes, based on their most used clinical map. A dual-task paradigm and a sentence-verification task were used to measure intelligibility and listening effort. The dual-task paradigm combined a sentence intelligibility task and a visual response-time task providing measures of intelligibility and effort, respectively. In the sentence-verification task participants listened to sentences and were instructed to press a button to indicate whether the sentence was true or false. This task yielded accuracy scores and response times, which were interpreted to reflect intelligibility and listening effort.

Results

In our previous study, in normal hearing subjects, the dual-task results showed reductions in listening effort for increased spectral resolution, even when intelligibility did not change. The preliminary results with CI users show much larger variability between and within subjects than the results with normal hearing listeners. So far, no clear effect of spectral resolution on listening effort, nor on speech understanding has been observed.

Conclusion

Although participants reported experiencing more interference of background noise in everyday listening with the maps with fewer electrodes, when tested without background noise in the quiet lab environment, both intelligibility and listening effort appeared to be unaffected by the number of active electrodes. Perhaps effects of reduced number of active electrodes, on intelligibility or listening effort, are revealed only in the presence of noise or other demanding listening conditions.

SY - 051

Speech Enhancement in Bilateral CI Users

Stefano Cosentino

University College London

Cochlear Implants (CI) are hearing prostheses that have proven successful for many subjects with severe to profound hearing loss. While speech intelligibility scores with cochlear implants are generally high in quiet, understanding speech in noisy and reverberant environments is a challenging task for most CI users. To improve the speech intelligibility in these conditions, several speech enhancement algorithms from the hearing aid technology and the engineering fields have been tested for CI users, and found to offer different degrees of success. More recently, much research effort has been directed towards bilateral implantations. The bilateral hardware allows more information to be coded (e.g., spatial information) and a wider range of speech enhancement algorithms to be implemented. The extent to which bilateral implantation has led to improvement in speech intelligibility scores is still under investigation. The present talk describes recent developments in speech enhancement algorithms for unilateral and bilateral CI users.

SY - 052

Recent Developments in the Research on Speech Perception and Production in Children With CIs

Daan van de Velde

SY - 053

The Perception of Voice Pitch and Prosody by CI Recipients

David Morris

University of Copenhagen

While Cochlear Implants (CI) can offer severe and profoundly hearing impaired recipients an alternative or supplement to amplification, they are unable to transmit all the nuance of speech in all types of listening environments to a recipient. Results of functional measures of speech perception by CI recipients are often encouraging, yet prosody is an aspect of speech that is generally not well perceived by this group of listeners. Consideration will be given to reports that examine the abilities that underlie prosody perception including pitch, intensity and modulation sensitivity. In comparison to normal hearing listeners CI listeners show reduced sensitivity to these cues, but also seem to integrate and use them differently in prosodic speech perceptual tasks. The availability

of software that performs re-synthesis of speech has allowed researchers to control the variation of acoustic cues that signal prosody for use as experimental stimuli. This paper will examine a handful of studies that have taken this approach and will also present results from studies carried out in Swedish and Danish language environments. This presentation will be of interest to CI rehabilitation initiatives and the development of speech processing strategies that promote the cues that are necessary for prosody perception.

SY - 054

Temporal Representation of Pitch

Richard Penninger¹; Charles Limb²; Marc Leman¹;

Ingeborg Dhooge³; Andreas Büchner⁴

¹University Ghent; ²Johns Hopkins University School of Medicine; ³University Hospital Ghent; ⁴Medical University Hannover

Background

Music perception is a very challenging task for CI users. In music, multiple tones often occur simultaneously, an essential feature of harmony. Proper encoding of simultaneous tones is crucial to musical perception and appreciation. With current implant processing strategies CI users are severely impaired in the perception of pitch and polyphony.

Methods

The ability of CI users to identify the number of simultaneous tones was assessed. First seven CI subjects were asked to identify the number of one single or two simultaneous tones. Stimuli were applied with direct electrical stimulation. Stimuli with one modulation frequency were applied on a basal, a middle and an apical electrode to determine if there was an effect of cochlear region. Stimuli with two modulation frequencies were applied on combinations of an apical electrode together with a basal or a middle electrode. Additionally, two modulations frequencies were presented at the same time on an apical electrode only. Ten further CI subjects were asked to identify one, two and three simultaneous pitches applied on different electrodes using sinusoidal amplitude modulation. All stimuli were loudness balanced before the actual identification task.

Results

Results demonstrate that subjects were generally able to identify the number of modulation frequencies in the presented stimuli. Performance for one modulation frequency-stimuli was significantly above chance level on all three electrodes tested. Subjects were also able to identify two modulation frequencies significantly above chance level on all three combinations tested. Performance was best on combination apical-basal followed by apical-middle. Performance was worst when two modulation frequencies were applied on an apical electrode only but it was still significantly above chance level. Subjects were also able to identify one, two and three simultaneous pitches. The further the distance between the two electrodes, the better was the performance in the two modulation frequency condition.

Conclusion

If sound processing strategies were to use concurrent modulation frequencies on multiple or single electrodes, then possibly polyphonic tones would be better perceived by CI users yielding better music and language perception. Subjects are able to identify complex polyphonic stimuli based on the number of active electrodes. The additional polyphonic rate pitch cue improves performance in some conditions.

SY - 055

Primary vs Secondary Cochlear Neurodegeneration: Prevalence, Mechanisms and Functional Consequences

M. Charles Liberman

Massachusetts Eye and Ear Infirmary

After acoustic trauma or ototoxic drugs, hair cell loss appears within hours, whereas spiral ganglion cell death is not seen for months. This delay has suggested that hair cells are the "primary" target of cochlear insults, and that neuronal death is a "secondary" event. Recent work in mice and guinea pigs shows that cochlear neurons die after noise exposure, even if hair cells survive and recover normal function, likely from a type of glutamate excitotoxicity. Although noise-induced loss of hair cell synapses is immediate, the synaptopathy is invisible in routine histological material, and death of spiral ganglion cells can take years. This neuronal dysfunction has no impact on thresholds of functional measures like the ABR, because only cochlear neurons with high thresholds and low spontaneous rates (SRs) are affected. Thus the neuropathy has remained hidden. However, since low-SR fibers are more resistant to noise masking, their loss is likely critical when listening in a noisy environment. Cochlear synaptopathy also precedes hair cell death in aging mice, and work in gerbil suggests that age-related neuropathy is also selective for low-SR fibers. In humans, there is a steady age-related decline in spiral ganglion counts, even with a full complement of hair cells. Hair cell synapses can be counted in immunostained cochlear whole mounts from human specimens, and preliminary data suggest a dramatic reduction in aged cases without explicit ear disease. Thus, primary neuronal degeneration may be widespread in humans and may be a major factor in the age-related decline in auditory performance.

SY - 056

Primary Cochlear Neurodegeneration in Noise and Aging

Sharon Kujawa

Harvard Medical School

Age-related and noise-induced hearing loss comprise two common forms of acquired sensorineural hearing loss in humans. Loss of threshold sensitivity in each case is primarily peripheral in origin, and often sensory (i.e. related to hair cell receptor damage or loss) in nature. Our recent work in a mouse model of normal auditory aging, however, has documented a cochlear synaptic loss that progresses gradually throughout the lifespan and is seen throughout the cochlea long before age-related changes in thresholds or hair cell counts. Losses ultimately reach ~50%, paralleled, after a de-

lay, by proportional cochlear nerve loss. Such declines can be accelerated dramatically after noise, with up to 50% of synapses lost within hours of exposure, including those producing only temporary changes in thresholds and no hair cell loss. Since this synaptic complex is the primary conduit for information flow from the cochlea to the brain, such age-related and noise-induced synaptic and neural losses would be expected to have significant perceptual consequences. Although threshold measures fail to capture such subtotal losses, key functional clues to the underlying degeneration are available in the neural response; these can be accessed non-invasively, enhancing the possibilities for translation to human clinical characterization. Research supported by R01 DC 008577 and P30 DC 05029.

SY - 057

Glutamate Excitotoxicity and Neuroprotection in the Cochlea

Jean-Luc Puel

Inserm U1051 and University of Montpellier, France

SY - 058

Developing Models of Nervous System Disease with Patient-derived Induced Pluripotent Stem Cells: Challenges, Opportunities and Applications

Steven Finkbeiner

University of California - San Francisco

Developing models of nervous system diseases with patient-derived induced pluripotent stem cells: challenges, opportunities and applications.

The failure to translate discoveries made in many preclinical models into success in clinical trials has raised concerns about the heavy dependence placed on murine models for elucidating disease mechanisms and for serving as gatekeepers for the advancement of therapies into the clinic. Perhaps mice and humans are more different than previously imagined? In addition, some sporadic neurological diseases are difficult to model in the laboratory because the underlying cause is often unknown. Patient-derived induced pluripotent stem (iPSCs) cells offer the opportunity to create complementary cell and organoid models of genetic or sporadic disease from people with established diagnoses that are fully human and can be used to investigate mechanisms of disease, identify and validate therapeutic targets and to optimize putative therapies before clinical trials begin. In this talk, development of iPSC models of Parkinson's disease, Huntington's disease, and amyotrophic lateral sclerosis will be presented to illustrate how models are made and how they can be used for basic and translational research. Some of the challenges associated with developing iPSC models, particularly heterogeneity, will be discussed along with new technologies to overcome these obstacles, such as high throughput longitudinal single cell analysis.

SY - 059

Cochlear Nerve Degeneration in Humans: The Temporal Bone Perspective

Joseph Nadol

Massachusetts Eye and Ear Infirmary

PD - 086

More Pain More Gain: Longer Training on Time-Compressed Speech Widens the Scope of Generalization to Untrained Tokens

Karen Banai¹; Yizhar Lavner²

¹University of Haifa; ²Tel-Hai College

Background

Brief experience with distorted (e.g., time-compressed) speech, which is often incomprehensible to naïve listeners, yields both learning and generalization. Whether such learning continues beyond the learning induced by experience with a few dozen sentences is not clear, because the outcomes of intensive training and brief exposure were rarely compared for the same type of distortion. Although a prolonged learning-phase was documented in some studies, the difficulties experienced by even highly experienced non-native speakers in their second language suggest that this learning might generalize to a lesser extent than initial learning. The goals of the current study were therefore to determine whether protracted training on time-compressed speech yields additional learning to that induced by brief exposure, and whether this protracted training affects the generalization of learning to untrained conditions.

Methods

Naïve normal-hearing native Hebrew speakers practiced the semantic verification of time-compressed simple Hebrew sentences for either one ($n = 10$) or three ($n = 10$) sessions of 300 trials each. During training, the degree of compression varied adaptively. Post-training identification of tokens compressed to 0.3 of their original duration was compared between the trained listeners and a group who was previously exposed to 20 time-compressed sentences ($n = 10$) on three conditions: tokens from the trained condition; new tokens (presented by the trained speaker); and tokens from the training set presented by a new speaker). A WSOLA algorithm was used for time compression.

Results

Significant training-phase learning was observed in both trained groups throughout training. Both trained groups learned significantly more than the brief-exposure group on the trained condition. Likewise, significant generalization to an untrained talker was observed in both trained groups. On the other hand, only listeners who practiced for three sessions significantly generalized their learning to new tokens not encountered during the training phase.

Conclusion

In young, normal-hearing native speakers, learning on a time-compressed speech task continues beyond an initial exposure phase for at least three sessions of 300 trials each. Furthermore, longer training was associated with more learn-

ing and wider generalization than shorter training, consistent with previous findings from non-speech auditory learning also showing that generalization might lag behind learning. These findings suggest that although learning of distorted speech can occur rapidly, more stable learning and generalization might be achieved with longer, multi-session practice.

PD - 087

Auditory and Visual Short-Term Memories Are Forgotten Differently

Samuel Mathias¹; Christophe Michey²; Barbara Shinn-Cunningham¹

¹Boston University; ²Starkey Hearing Research Center

Background

Recently, vision scientists have measured the probability and precision with which representations of visual objects are committed to, and stored in, short-term memory. Surprisingly, this work suggests that the precision of visual representations does not change over time; visual representations are instead maintained with fixed precision until they simply vanish without trace from memory—a phenomenon called “sudden death.” We investigated whether auditory representations experience sudden death.

Methods

In three experiments, listeners discriminated pairs of sequential pure tones in terms of their frequency or intensity. The tones were separated by silent intervals (ISIs) of 0.5, 2, 5, or 10 s. The magnitude of the stimulus difference on each trial (Δ) could take on many values, including those well above each listener's discrimination threshold. This design allowed us to fit psychometric functions to the data per listener and ISI with very high accuracy. We investigated how two key parameters changed with the ISI: σ , characterizing the precision of listeners' pitch/loudness representations; and λ , the probability of sudden death. We also performed formal model comparisons (using Akaike information criterion, AIC, and Bayesian information criterion, BIC) to investigate how well the psychometric functions explained the data when both σ and λ were allowed to change with the ISI compared to when only one of them was allowed to change with the ISI.

Results

In all three experiments, σ estimates increased monotonically with increasing ISI, whereas λ estimates were roughly the same at all ISIs. Accordingly, the model comparisons revealed that in all three experiments, allowing σ but not λ to change with the ISI provided the best explanation for the observed data (i.e., lowest AIC and BIC). Allowing both parameters to change provided an intermediate explanation for the data, and allowing λ but not σ to change provided the poorest explanation (highest AIC and BIC).

Conclusion

Contrary to recent findings from vision, we found that auditory representations are no more likely to die after 10 s than 0.5 s; instead, they decline in precision gradually over time. The results point to a qualitative difference between how auditory and visual representations are forgotten from short-term memory.

Effects of Attention on Change Deafness Depend on the Task Relevance of the Attended Object

Vanessa Irsik¹; Christina Vanden Bosch

derNederlanden¹; Melissa Gregg²; Joel Snyder¹

¹University of Nevada, Las Vegas; ²University of Wisconsin, Parkside

Background

Multiple processes are likely to be involved in the detection of changes within complex auditory scenes and in failures to detect such changes, known as *change deafness*. Previous research concerning the role of attention has suggested that attending to the to-be-changed object largely eliminates change deafness. It remains to be shown, however, whether attention toward an object that is irrelevant to the change increases change deafness. The current experiment compared change deafness when attention was cued toward an auditory object with a valid cue (i.e., when the cued object is changed), an invalid cue (i.e., when the cued object is not changed), or no cue.

Methods

Participants heard two auditory scenes, each composed of four 1,000 ms environmental sounds, separated by a 350 ms silent interval. The effect of directed or undirected attention was assessed separately in two blocks of 200 trials, with the blocks presented in counterbalanced order. In both blocks, participants made same/different judgments assessing whether a new object replaced an object from the first scene or remained the same (half of the trials were same and half were different). In the directed attention block, participants saw a verbal label that corresponded to one of 15 environmental sounds before the two scenes were presented. Participants were instructed to pay attention to the cued sound, which correctly identified the changed sound 75% of time and was an invalid cue 25% of the time.

Results

Error rates were higher for different trials compared to same trials for both directed and undirected attention blocks, indicating change deafness. Significantly less change deafness occurred for valid cue trials compared to undirected trials, although change deafness still occurred on around 20% of trials with valid cues. Furthermore, significantly more change deafness occurred for invalid cue trials (62%) compared to valid cue (20%) and undirected trials (29%).

Conclusion

Directing attention to the to-be-changed object reduces change deafness, but does not eliminate it. Also, directing attention toward an object that does not change significantly increases change detection for unattended objects. These results suggest that attending to relevant objects is helpful for reducing change deafness, but additional factors may play a role in instances of change deafness that occur even when attention is focused on to-be-changed objects.

Attentive Tracking of Sound Sources

Kevin Woods¹; Josh McDermott²

¹Harvard University; ²MIT

Background

Auditory scenes often contain concurrent sound sources, but listeners are typically interested in just one of these, and must somehow select it for further processing. Part of the challenge of doing so is that real-world sound sources such as speech vary over time, such that attending to particular values of particular features may be insufficient to maintain selection of a source of interest. We investigated the ability of human listeners to attentively track sound sources in such conditions.

Methods

Simulated voices were synthesized that varied in several feature dimensions (e.g. f0, f1, and f2) according to independent, randomly generated trajectories. Listeners were presented with mixtures of two such time-varying sources, and were cued beforehand (with the starting portion of one voice) to attend to one of them. We measured listeners' ability to attentively track this cued voice by subsequently presenting them with the tail end of one voice. Their task was to judge whether this repeated segment belonged to the cued voice. Trajectories were selected for which the cue was on average equidistant in feature space from the endpoints of each voice, such that the task could not be performed without encoding the full voice trajectory. Trajectories for the voices in a mixture were also required to cross each other at least once in each of the varied feature dimensions, such that listeners could not perform the task simply by attend to a high or low value of one of the features. Success at this task is thus intended to reflect accurate tracking of the cued voice as it varied throughout the mixture.

Results

Pilot results to date suggest that (1) multiple dynamic features can be used in concert to selectively track a target sound in a mixture, (2) tracking cannot be explained with individual features, as these alone are insufficient to support performance, (3) performance deteriorates when the source trajectories approach each other in feature space, consistent with an attentional index of relatively coarse resolution, and (4) performance deteriorates as the source trajectory speed increases.

Conclusion

Attentive tracking of sound sources can be assessed with a novel paradigm in which mixtures of synthetic voices vary over time along several feature dimensions. Combinations of features can be used to attentively track sound sources, consistent with object-based theories of attention.

Which Linguistic Skills And Components Of Intelligence Are Involved In The Top-Down Restoration Of Interrupted Speech?

Michel Benard¹; Jorien Mensink; Deniz Baskent¹

¹University Medical Center Groningen

Background

Speech intelligibility in difficult listening environments can be enhanced using top-down processes. Linguistic and cognitive factors play an important role in understanding speech in general, but which of these are specifically involved in perceptual restoration of temporally interrupted speech is not clearly shown. In this study, we systematically explore the association between linguistic and cognitive skills, quantified using standardized clinical tests, and the top-down speech restoration, quantified with measuring intelligibility of periodically interrupted sentences.

Methods

Normal hearing participants of varying ages, all native speakers of Dutch, were assessed with the Peabody Picture Vocabulary Test (PPVT-III-NL), a measure of the receptive vocabulary and verbal intelligence, and with the Wechsler Adult Intelligence Scale (WAIS-IV-NL), a measure of verbal comprehension, working memory, perceptual reasoning and processing speed. Besides these tests, the participants were both trained and tested with 104 unique meaningful Dutch sentences, played at original and slow speeds, interrupted at two different rates with silent gaps or with gaps filled with noise bursts (8 conditions in total).

Results

In correspondence with literature, the addition of filler noise (phonemic restoration) and slowing down the play-rate of the sentences increased the intelligibility of interrupted speech. To explore the involvement of linguistic and cognitive elements, linear regression analyses were performed between the individual scores on the PPVT and on the four index scores of the WAIS, and the individual speech intelligibility scores. Preliminary results showed that the PPVT highly and significantly correlated with the intelligibility scores in 5 out of the 8 conditions tested. The WAIS showed only significant correlations between verbal comprehension and the speech scores in 3 out of 8 conditions. The other index scores of the WAIS, working memory, perceptual reasoning and processing speed, did not correlate with the speech scores, but these also did not reach sufficient statistical power as yet.

Conclusion

The intelligibility scores are characteristic for top-down restoration of interrupted speech, as was previously reported in literature. Preliminary data suggest that linguistic factors like receptive vocabulary and verbal intelligence (PPVT) and verbal comprehension (WAIS) are more important for top-down restoration than the cognitive factors working memory, perceptual reasoning and processing speed (WAIS). Future research with more statistical power will be conducted to determine which linguistic skills and components of intelligence are involved in the comprehension of interrupted speech.

The Influence of Nearby Maskers on Informational Masking in Complex Real-World Environments

Adam Westermann; Jörg Buchholz

National Acoustic Laboratories

Background

Attending a target talker in the presence of multiple spatially distributed masking talkers and reverberation is one of the main challenges for the auditory system. Literature divides masking occurring in such environments into energetic and informational masking. Whereas energetic masking (EM) relates to peripheral auditory processing, Informational masking (IM) is caused by confusions between target and masker in either the auditory stream formation or selection process. Listening tests with simplified spatial configurations and speech corpora with exaggerated confusions have found IM effects of more than 10 dB. However, Westermann et al. (WASPAA, 2013) considered a realistic cafeteria environment and only found significant involvement of IM when the target and maskers were both co-located and the same talker. The present study further investigates IM in such cafeteria environment, but focusing on the effect of nearby talkers.

Methods

Speech reception thresholds (SRTs) were measured with normal hearing listeners by presenting Bamford-Kowal-Bench (BKB) sentences in a simulated cafeteria environment. The environment was reproduced by a 41 channel spherical loudspeaker array (radius 1.85 m) with two additional speakers suspended inside the array at 1 m distance and $\pm 11^\circ$ in reference to the listener. The target was simulated at 2 m and 6 m distance directly in front of the listener. The masker had two components, two nearby maskers at a distance of 1 m and seven dialogues spread throughout the cafeteria. The suspended loudspeakers recreated only the direct sound of the nearby maskers and the array the reverberation and the rest of the signals. The nearby maskers were either monologues with the same talker as the target (maximum IM) or an unintelligible vocoded version of the monologues (minimum IM). All conditions were measured with and without the seven dialogues.

Results

The SRTs significantly improved in all conditions between the nearby talker dialogues and their vocoded masker versions, illustrating a significant involvement of IM. However, this improvement was considerably smaller than found in literature. Removing the seven dialogues improved overall SRTs, because of increased gap listening, and increased the effect of IM.

Conclusion

The present study confirms that IM is less prevalent in real-life listening as compared to what is observed in listening tests. However, where Westermann et al. could only observe IM in a realistic cafeteria environment when target and distractors were co-located, here significant IM was also found

for nearby distractors. This suggests a dominance of nearby sound sources in auditory processing of speech.

PD - 092

Dynamic Versus Static Spectral Cues to Identification of IRN-Vocoded Concurrent Sentences

Marjorie Leek¹; Frederick G. Gallun²; Michelle R. Molis²; Heather Belding²

¹VA Loma Linda Healthcare System; ²National Center for Rehabilitative Auditory Research

Background

Pitch of a selected voice is a strong cue to attending to a target speech stream in the presence of other sounds. We reported previously that both hearing loss and moderately advanced age reduce the ability to use pitch to separate multiple concurrent speech talkers. In this follow-up study, we investigated two forms of vocoding to reduce fine temporal cues to identification of concurrent speech sounds: one preserves dynamic spectral cues, while the other only preserves more static spectral cues. Neither of these processing forms affects the envelope, but both eliminate temporal fine structure cues to speech.

Methods

Speech from the Coordinate Response Measure corpus with one male talker and two female talkers was used. Stimuli were created by vocoding the stimuli, using iterated rippled noise (IRN) as the carrier. The pitch strength of the IRN carrier was modified by varying the gain of the iterated waveforms during their addition to the IRN, and by using either 2 or 8 iterations. Two different vocoding processes were evaluated. In the “band-vocoded” condition, the stimuli were filtered into 6 frequency bands, and a Hilbert transform was applied to extract the envelope that was used to modulate the IRN carrier noise. A second form of vocoding used the FFTs of sixteen-ms overlapping time slices extracted from sentences. The amplitude spectrum of each slice was combined with the phase spectrum of similar slices of the IRN carrier, and the combination was reconverted into the time domain. A range of gain factors of the IRNs was used to evaluate the effect of different degrees of pitch strength.

Results

Identification performance was worse for hearing-impaired subjects than for normal-hearing subjects. Younger normal hearing listeners were more sensitive to the effects of increasing pitch strength than were either hearing-impaired or older subjects. The loss of dynamic spectral cues (6-band vocoded condition) resulted in reductions in identification for all, suggesting that concurrent identification is dependent on those cues particularly when temporal cues are disrupted.

Conclusion

Increases in pitch strength of target speech sounds overlapping in time with other talkers results in a consistent and beneficial effect on speech identification for both NH and HI listeners. Vocoded speech that preserves dynamic spectral

cues produces better identification performance than when only static frequency cues are present.

PD - 093

A Modeling Study of Dynamic Response Patterns of Cortical Neurons During Fast Head Turns of Marmoset Monkeys

Yi Zhou; Sravanthi Simhadri

Arizona State University

Background

Head fixation is a necessary procedure for obtaining reliable neural activity in most neurophysiological research. In studying spatial selectivity of cortical neurons, sound source location is moved from trial to trial, while the animal's head remains fixed in place. Using this preparation, we observed that many neurons in the auditory cortex of awake marmoset respond selectively to restricted regions in space (Zhou and Wang, 2012). However, head-fixed preparation offers an unnatural listening experience for animals. Free-moving marmoset monkeys make frequent, fast head turns after the onset of a sound. Using a modeling approach, this study investigates the dynamic response patterns of cortical neurons during simulated head movement.

Methods

We simulated the responses of cortical neurons to noise and vocalization stimuli delivered from a fixed loudspeaker when the animal turns its head from straight ahead to back. Ear-canal signals during head movement are simulated by convolving the source stimuli with the conspecific head-related transfer functions (HRTFs) obtained in head-fixed preparations. The time duration of convolution with each HRTF is determined by the estimated speed of the marmoset's head movement. The left and right ear-canal signals serve as the input to the cortical neuronal models, whose spatial-spectral selectivity is based on averaged excitatory and inhibitory tunings of neurons observed in marmoset auditory cortex.

Results

The simulation results show that the monaural spectral profiles of input signals remain relatively steady during fast head movement and the binaural spectral profiles show large variations in interaural level differences over a range of frequencies. The monaural and binaural input weights alter the on and off response patterns of model neurons – stimuli with similar spectral contents may not evoke similar model responses as the head turns.

Conclusion

These results suggest that during fast head movement the network activity of neurons in marmoset auditory cortex has the potential to track both spectral and spatial information of stimuli delivered from a stationary source. This mechanism may help improve signal detection in escape situations for marmoset monkeys.

PD - 094

Intravascular and Trans-Round Window Membrane Approach for Recombinant AAV Mediated Cochlear Gene Transfer in Neonatal Mouse

Seiji Shibata; Moteki Hideaki; Richard Smith
University of Iowa, Molecular Otolaryngology and Renal Research Laboratories

Background

Hearing loss is the most common sensory impairment in humans, 1 in every 500 newborns has hearing loss and genetic etiology accounts for 70% of these cases. Inner ear gene therapy offers a gene-specific treatment strategy to restore or prevent hereditary hearing loss thereby preserving biological hearing. Previous studies have demonstrated the cochlea as a viable target for gene transfer utilizing adeno-associated virus (AAV). Transduction pattern and efficiency of various recombinant AAV serotypes (1-9) in the cochlea have been characterized. Delivery methods of transgenes into the inner ear have historically resorted to direct or indirect surgical interventions, which has the potential of iatrogenic side-effects. Recent finding of rAAV2/9 and other serotypes traversing the BBB and transducing cells in the CNS following systemic injection may provide an alternative inner ear delivery method that is devoid of surgical manipulation. Our goal was to assess transgene expression of rAAV2/1 or 2/9 in the inner ear of neonatal mice following intravascular injection (IV) or trans-round window membrane (RWM) inoculation.

Methods

We used two different routes: IV or trans-RWM, to inoculate neonatal mice at P1-2 with either rAAV2/1 or 2/9. For IV inoculation, 100µl of rAAV was injected systemically via the temporal vein. For trans-RWM inoculation, 0.5µl of rAAV was delivered into the perilymph via the RWM. The cochleae were assessed histologically, one or two weeks after the inoculation. Auditory thresholds were assessed with ABR for trans-RWM inoculated mice after P30, contralateral non-injected ear served as control.

Results

Robust transgene expression in the cochlea and vestibular organs with rAAV2/9 following both IV and trans-RWM injections was confirmed. Overall transgene expression in the cochlea hair cells following IV approach was superior to that of trans-RWM approach. Similarly, the transduction of hair cells in the vestibular organs was highest with IV injections of rAAV2/9. Auditory thresholds of trans-RWM inoculated mice were comparable to contralateral non-injected ears following either rAAV2/1 or rAAV2/9. Global transduction in brain astrocytes following systemic rAAV2/9 delivery was also noted.

Conclusion

Our data demonstrates the feasibility of rAAV2/1 or 2/9 as a vector for cochlear gene transfer with either intravascular or trans-RWM inoculation methods. rAAV2/9 may be especially useful for atraumatic systemic delivery of transgenes to ears of neonatal mice.

PD - 095

Correction of Hearing in the Mouse Model of Hereditary Deafness by Gjb2 Gene Transfer Using Adeno-Associated Viral Vectors

Takashi Iizuka¹; Kazusaku Kamiya²; Osamu Minowa³; Tetsuo Noda⁴; **Katsuhisa Ikeda²**

¹*Juntendo University Faculty of Medicine*; ²*Juntendo University*; ³*Riken Institute*; ⁴*Cancer Institute*

Background

Hearing loss is the most widespread sensory disorder, with the incidence of congenital genetic deafness present in one in 1,600 children. The most prevalent form of genetic deafness in many ethnic populations is due to recessive mutations on the gene encoding Cx26 (*GJB2*). However, pre-existing treatment strategies cannot completely acquire intelligible speech perception.

Methods

Here we show that hearing can be rescued by gene delivery to a new mouse model of *Gjb2* deletion.

Results

Mice lacking Cx26 are characterized by profound deafness from birth and improper development of the cochlear cells. Cochlear delivery of *Gjb2* using adeno-associated virus (AAV) significantly recovered auditory response and correct the development of cochlear structure.

Conclusion

A successful restoration of hearing mediated by gene replacement in the genetically created deaf mouse model of *Gjb2* contributes a tremendous and universal benefit on clinical application to fundamental therapy of human hereditary deafness.

PD - 096

Connexin Deletion Associated Hearing Loss is Treatable

Ryosei Minoda; Toru Miwa; Takao Yamada; Momoko Ise; Eiji Yumoto

Kumamoto University, Graduate School of Medicine

Background

Although numerous causative genes for hereditary hearing loss have been identified, there are no fundamental treatments for this condition. Mutations or deletions in the connexin (Cx) genes are common causes of profound congenital hearing loss in both humans and mice. We set out to examine whether embryonic gene therapy could cure hearing loss caused by deletion of one of the Cx genes. We utilized Cx30-deficient mice and targeted the otocysts for gene transfer.

Methods

We performed gene transfer of wild-type Cx30 genes into the otocysts of homozygous Cx30-deficient mice (C57BL/6 Cx30^{-/-} mice; courtesy of Prof Klaus Willecke, Germany). Gene transfer was achieved via Electroporation-Mediated Transuterine Gene Transfer into Otocysts (EUGO) (Miwa; Neuroreport 2011, Mol Ther. 2013) as follows. At 11.5 days

post-coitum, pregnant mice were deeply anesthetized. The uterus was exposed by a low-midline laparotomy, placed on a transparent surgical stage and illuminated from below with a fiber-optic beam to illuminate the rostral and caudal branches of the primary head vein, between which each otocyst is located. Plasmid vectors were microinjected by oral pressure into the lumens of the left-side otocysts of one or two embryos per dam using glass micropipettes (Minoda, 2003 ARO meeting). The plasmid-filled otocysts were electroporated using CUY21EDIT®. Cesarean sections were performed on the dams at E18.5. The pups that were to receive an injection of vehicle were removed and used for histological and auditory assessments at E18.5. The other treated pups were allowed to survive until auditory function assessments at P30.

Results

EUGO induced gene transfection in the spiral limbus, the organ of Corti, the stria vascularis, the spiral ligament, and the spiral ganglion at P30. EUGO of the wild-type Cx30 gene into Cx30^{-/-} mice restored the lack of Cx30 expression in the cochleae. The auditory thresholds of the treated sides of Cx30^{-/-} mice were significantly better than those of the untreated sides. There were no significant differences between the auditory thresholds of the treated sides and those of the wild-type mice. The endocochlear potential results of the Cx30^{-/-} mice that underwent Cx30 transfection are maintained at normal level.

Conclusion

These results demonstrate that supplementation therapy with wild-type genes can restore postnatal auditory functioning in mice with Cx30 deletion-associated hearing loss. We believe that this concept will also be applicable to other causative genes for hearing loss, potentially in humans.

PD - 097

Dominant Deafness Mutations of P2X2 ATP Receptors Have no Dominant Negative Effect on Wildtype Isoform Function

Yan Zhu; Hong-Bo Zhao

University of Kentucky Medical Center

Background

Recently, it has been found that purinergic ATP receptor P2X2 mutations (V60L and G353R) can induce nonsyndromic hearing loss (DFNA41) (Yan et al., PNAS, 110: 2228-2233, 2013; Giroto et al., 2013 ARO Meeting abstract). Our previous study showed that P2X2 V60L mutant has no function to response to ATP stimulation (Yan et al., PNAS, 110: 2228-2233, 2013). However, P2X2-null mice show normal hearing under normal environment. This leads to that the deafness mechanism underlying P2X2 mutations induced autosomal dominant hearing loss still remains unclear. The P2X2 receptor mutations induced deafness (DFNA41) is an autosomal dominant hearing loss, that is, the deafness is caused by heterozygous mutations. This means that mutants have dominant negative effect on either function of wildtype (WT) isoforms or other partner(s). In this study, the effect of dominant deafness P2X2 mutants on WT P2X2 receptor isoforms was studied.

Methods

P2X2 WT, V60L and G353R mutants were cloned and transfected into HEK 293 cells. ATP-evoked responses were recorded by patch clamp. P2X2-null mice were also used to re-assess hearing function using ABR recording with WT littermate controls.

Results

Both P2X2 V60L and G353R mutants targeted to plasma membrane but had no response to ATP stimulation. The ATP-evoked inward current is not visible. However, at co-transfection with WT P2X2 receptors, the WT response retained and the ATP-evoked inward current was visible. The response had slight reduction in comparison with sole-transfection with P2X2 WT isoforms but had no statistical significance. The reduction was also smaller than the prediction of dominant negative effect by theoretical analysis. Re-examination of P2X2-null mouse hearing function also shows that adult P2X2-null mice had no hearing loss in comparison with littermate WT controls. There was no difference in ABR threshold between littermate WT and P2X2 knockout mice (mouse age < 2 months).

Conclusion

These data demonstrate that P2X2 V60L and G353R dominant deafness mutants have no dominant negative effect on WT isoform function. Other mechanisms, such as compromising function of other partner(s), may play a role in this autosomal dominant DFNA41 nonsyndromic hearing loss.

PD - 098

MicroRNA-Target Regulation in Inner Ear Inflammation

Karen Avraham¹; Anya Rudnicki¹; Shaked Shivatzki¹; Lisa A. Beyer²; Yohei Takada²; Yehoash Raphael²

¹Department of Human Molecular Genetics and Biochemistry, Sackler Faculty of Medicine and Sagol School of Neuroscience, Tel Aviv University, Tel Aviv, Israel; ²Kresge Hearing Research Institute, Department of Otolaryngology - Head and Neck Surgery, University of Michigan

Background

Among inner ear pathologies, inflammation may lead to structural, neuronal and vestibular defects and is associated with hearing and balance impairment. While major genetic factors are not yet known to play a role in these forms of dysfunction, we suggest that regulatory factors, such as those inherent in microRNA (miRNA) regulation, are involved. Hundreds of miRNAs are expressed in the inner ear and play a critical role in the development and regulation of auditory and vestibular function. Mutations in miRNAs have been discovered to lead to deafness in both humans and mice. Here we screened for auditory-related miRNAs and targets that might be involved in inflammation.

Methods

Quantitative real-time (qRT)-PCR and in situ hybridization were used to identify the spatial expression of the miRNAs in the mouse inner ear. Bioinformatics software was used to predict the targets of these miRNAs. The miRNA-target interaction was verified by over-expression in cell lines and lucif-

erase assays. Lipopolysaccharide (LPS) was injected in the scala tympani of mouse inner ears to induce inflammation and miRNA and protein levels were measured. Immunohistochemistry was used to evaluate the presence of immune cells and activation of the innate immune system, detected by levels of complement component C3.

Results

miRNA-224 was detected in a microarray screen and predicted to target Ptx3, a regulator of the innate immune response. miR-224 and Ptx3 are both expressed in mouse inner ear sensory epithelia. Luciferase and over-expression assays demonstrate that miR-224 targets Ptx3. miR-224 and Ptx3 expression was increased in LPS-induced inflammation. An increase in infiltration of immune cells into the scala tympani, as well as C3 staining indicative of activation of the complement system, was present in the LPS-treated samples.

Conclusion

We found that miR-224 directly targets Ptx3 in the NF- κ B inflammatory pathway in inner ear LPS-induced inflammation. We predict that Ptx3, as a powerful protein in the immune cascade, is subject to tight regulation and plays an essential role in the inner ear. This finding defines a role for miRNAs in the regulation of inflammation and suggests an involvement in inflammatory diseases of the inner ear.

PD - 099

Alterations of Sensory Hair Cells Following AAV-MiR96 Application to Postnatal Mouse Cochleae

Yazhi Xing¹; Michelle L. Stoller²; Vidhya Munnamalai²; LaShardai N. Conaway¹; Karen P. Steel³; Hainan Lang¹; Donna M. Fekete²

¹Medical University of South Carolina; ²Purdue University;

³King's College, London

Background

Mutations in the non-coding microRNA, miR-96, have been linked to dominant nonsyndromic progressive hearing loss in human families at the DFNA50 locus. A mouse model of this disorder, *Diminuendo* (*Dmdo*), offers an opportunity to ask whether gene therapy may rescue the progressive loss of hearing and the deterioration of sensory hair cells (HCs) caused by point mutations in miR-96. Two possible therapeutic options are to supplement cochlear HCs with additional miR-96 or to remove the miR-96 *Dmdo* variant using antisense technology.

Methods

To approach this, we designed AAV2/8 adeno-associated viral vectors to encode marker genes together with either an intron carrying Mir96 genomic sequence (AAV-GFP-Mir96) or a sponge consisting of 6 tandem binding sites for miR-96 *Dmdo* (AAV-mCherry-anti-miR96 *Dmdo*). Concentrated virus preps ($8-30 \times 10^{12}$ genomes/ml) are delivered into the scala media of either CBA mice or to the offspring of *Dmdo*/+ matings on postnatal day 3. Auditory function is evaluated by auditory brainstem response measurements at 2-4 weeks. Cochleae are collected at 5, 7, 11 and 25 days after virus inoculation

and HCs are observed with confocal microscopy for detection of GFP, mCherry and phalloidin.

Results

In vitro luciferase assays and Northern blots of plasmid-transfected cells indicate that mature bioactive miR-96 is generated from the Mir96 intron. Similarly, luciferase assays confirm that the sponge binds with enhanced specificity to the *Dmdo* variant compared to wildtype miR-96. All viruses, including a GFP control, show marker expression in HCs, supporting cells, auditory nerve/ganglion and other cochlear locations. Over 60% of the AAV-GFP-Mir96-treated animals show moderate to robust GFP expression in many HCs. A few of the infected inner HCs display unusual stereocilia bundles that resemble outer HCs. Furthermore, some abnormally small GFP⁺ IHCs are seen after inoculations of AAV-GFP-Mir96 with or without the sponge virus. To date, hearing loss is not improved in animals inoculated with AAV-GFP-Mir96. Preliminary experiments with the sponge virus confirm sensory cell expression of mCherry at 7-18 days post-injection.

Conclusion

Results suggest that sensory cells may be sensitive to the relative levels of miR-96 either for their maturation or for the differential morphology of stereocilia bundles between inner and outer HCs. Experiments are ongoing to determine whether any combination of vectors is able to improve hearing, HC morphology or the long-term survival of HCs in *Dmdo* mice.

PD - 100

Interferon-Gamma Signaling May Play a Protective Role in Autoimmune Induced Hearing Loss and Balance Disorder

Brent Wilkerson¹; Dongguang Wei²; Hong Qiu³; Athena Soulika³; Rodney Diaz²

¹University of California Davis Medical Center; ²Department of Otolaryngology - Head and Neck Surgery, University of California Davis Medical Center; ³Institute for Pediatric Regenerative Medicine, Shriners Hospital for Children - Northern California & University of California Davis Medical Center

Background

Murine experimental autoimmune encephalomyelitis (EAE), a model for multiple sclerosis, presents typically as ascending paralysis. However, in mice in which interferon-gamma (IFN γ) signalling is disrupted by genetic deletion, limb paralysis is accompanied by atypical deficits, including head tilt, postural imbalance, and circling, consistent with cerebellar and/or vestibular dysfunction. This balance disorder was previously attributed to intense cerebellar and brainstem infiltration by peripheral immune cells and formation of neutrophil-rich foci within the central nervous system. However, the exact mechanism underlying atypical EAE remains elusive.

Methods

EAE is induced in wild type (WT) mice and in interferon-gamma receptor knockout (IFN γ R^{-/-}) mice. Auditory brainstem responses (ABR) are recorded prior to EAE induction and at D15-D19 after EAE induction, the timeframe in which atyp-

ical symptoms are manifest, in both cohorts. Cochlear and vestibular sensory epithelial tissues are collected from WT and IFN γ R $^{-/-}$ mice and analyzed for changes in neuronal and sensory cell populations.

Results

After EAE induction, hearing thresholds of WT mice are elevated 20 ± 7.07 dB at 32000Hz, 27.5 ± 17.7 dB at 16000Hz, 30 ± 7.07 dB at 8000Hz, and 32.5 ± 31.8 dB at 4000Hz. In IFN γ R $^{-/-}$ mice, hearing thresholds are elevated 38.9 ± 17.3 dB at 32000Hz, 38.5 ± 17.9 dB at 16000Hz, 48 ± 15.6 dB at 8000Hz, and 41.5 ± 12.2 dB at 4000Hz. Immunohistochemistry of IFN γ R $^{-/-}$ mice vestibular tissue demonstrates overall reduction in both hair cell population as well as neuronal fiber counts as compared to that in WT mice.

Conclusion

EAE induction causes more severe hearing loss in IFN γ R $^{-/-}$ mice than in WT mice. Vestibular hair cell loss and corresponding neuronal deafferentation are detected in IFN γ R $^{-/-}$ mice but not in WT mice. Our data suggest that interferon-gamma signaling plays a protective role in autoimmune induced hearing loss and vestibular dysfunction in the murine EAE model.

PD - 101

SMAD4 Defect Causes Auditory Neuropathy Via Dysfunctional of Cochlear Ribbon Synapse

Ke Liu¹; **Fei Ji**³; Guan Yang²; Zhao-hui Hou³; Jia-na Li³; Xu-kun Yan³; Yu-hua Zhu³; Qing-qing Hao³; Hui Zhao³; Jian-he Sun³; Xiao-yu Wang³; Wei-wei Guo³; **Ning Yu**³; **Wei Sun**⁴; wei-yan Yang³; Xiao Yang²; **Shi-ming Yang**³

¹Chinese PLA General Hospital; ²The State Key Laboratory of Proteomics, Genetics Laboratory of Development and Disease, Institute of Biotechnology, AMMS; ³Department of Otolaryngology, Head and Neck Surgery, The Institute of Otolaryngology, Chinese PLA General Hospital;

⁴Department of Communicative Disorders & Sciences, the State University of New York at Buffalo, Buffalo, New York

Background

More than one hundred genes have been demonstrated to associate with deafness. However, SMAD4 was rarely proposed to contribute to deafness of human except its well-defined role in cell differentiation and regeneration.

Methods

Here, we reported a novel heterozygous SMAD4 mutation (c.457C>G) affecting the codon for Pro153Ala in an individual with auditory neuropathy, a mysterious hearing disorder which the genetic background remain unclear. Moreover, auditory restoration has been obtained after the cochlear implant in this individual.

Results

Correspondingly, these results have been fully mimicked in the mice with SMAD4 defect. Animal study showed that SMAD4 deficit can cause a failed development of cochlear ribbon synapse, however, the SMAD4 defect does not affect

the function of outer hair cells (OHCs) and postsynaptic auditory nerves.

Conclusion

Thus, our findings suggested that SMAD4 defect causes auditory neuropathy via specialized destruction of cochlear ribbon synapse.

PD - 102

Sustained Vesicle Release at the IHC Ribbon Synapse Depends on the Intravesicular Domain of Otoferlin

Jacques Boutet de Monvel¹; **Saaïd Safieddine**²; Didier Dulon³; Christine Petit²; Sylvie Nouaille²; Yohan Bouleau³; Philippe Vincent⁴; Adeline Mallet²; anna Sartori Rupp²

¹Pasteur Institute; ²Institut Pasteur; ³University of Bordeaux II; ⁴University of Bordeaux

Background

Otoferlin, a six C2-domain synaptic vesicle (SV) transmembrane protein defective in a genetic deafness form, is present at the ribbon synapses of auditory inner hair cells (IHCs) where it may function as the major calcium sensor to trigger exocytosis. Deaf mutant mice defective for otoferlin lack both the fast and sustained components of synaptic exocytosis of IHCs, despite normal synaptic structure.

Methods

In order to progress in our understanding of Otoferlin function, and shed new light on the IHC synaptic vesicle dynamics we have engineered knock-in mice expressing an otoferlin-GFP fusion gene (Otof-GFP) from the endogenous locus, by homologous recombination.

Results

We found that the expression of Otof-GFP in IHCs occurs at appropriate developmental stages with a subcellular distribution similar to that of the native protein. In addition, ribbon synapse maturation proceeds normally in these mice, and 3D reconstructions by electron tomography show similar number and distribution of SVs surrounding ribbons as in wild-type IHCs. Electrophysiological investigation of IHCs from homozygote Otof-GFP knock-in mice showed normal Ca²⁺-currents and normal Ca²⁺-dependent exocytosis up to postnatal day 6. However, at P8, IHC exocytosis was significantly impaired. Mobilization of the readily releasable pool (RRP) appeared normal, but the sustained component (SRP) was nearly abolished, and recovery of the RRP was strongly reduced during a paired-pulse protocol. Next we analyzed the mobility of the pool of Otof-GFP-containing SVs at adult stages by two-photon FRAP experiments. We found that in heterozygote mice the mobile fraction of the basolateral area increases upon cell depolarization. In addition, the mobile fraction of GFP-otoferlin associated vesicles in IHCs from homozygote mutants was higher and less sensitive to depolarization than in the heterozygote, consistent with an impaired balance between exocytosis and endocytosis in the homozygote mutants.

Conclusion

Our results indicate that the behavior of otoferlin-associated SVs depends on their location within the IHC, and that a nor-

mal intravesicular otoferlin domain is essential for the maintenance of sustained exocytosis at the IHC synapse.

PD - 103

Robust Ribbon Synaptic Transmission Is Limited by Peripheral Membrane Insertion of Synaptic Tail-Anchored (TA) Proteins

Shuh-Yow Lin; Elena Cardenas; Sara Mangosing
UCSD

Background

The hair cell ribbon synapse works rapidly and continuously to transmit sensory signal to the brain. With the insertional zebrafish mutant line *pinball wizard* (*pwi*), we identified WRB, a putative TA receptor for post-translational membrane insertion that is required for consecutive trigger of sound-evoked startle reflex and sound evoked Ca^{2+} response in primary auditory neurons. These phenotypes are linked to down-regulation of synaptic TA proteins including Otoferlin (Otof). We also found that the ERG b-wave and the SNARE TA protein Synaptobrevin are diminished at the photoreceptor synapse. To further understand WRB's role, we investigated where WRB is located, and TA protein are inserted into the membrane, by re-introducing WRB-fluorescent protein chimeras into *pwi* mutant hair cells.

Methods

WRB-EGFP and WRB-mCherry were inserted downstream to 5xUAS-E1b elements in a hair cell-expressing Tol2 vector with PPV3b-GAL4. The WRB-EGFP coding sequence was further mutated to create WRB(E72A,R73A)-EGFP by site-directed mutagenesis. Plasmids were injected with Tol2 transposase mRNA into one-cell-stage *pwi* embryos for somatic transgenesis. 5-day old wildtype and mutant larva with fluorescent hair cells were subsequently fixed, cryoprotected, embedded and cryosectioned. These sections were later permeabilized, blocked and incubated with HCS-1 antibodies specific to Otof, before observed under a confocal microscope.

Results

We found WRB-EGFP was able to rescue the diminished expression of Otof in the mutant hair cells. However, WRB-mCherry failed to rescue Otof. Surprisingly, we found that WRB-EGFP was localized in peripheral puncta-like structures, whereas WRB-mCherry was distributed homogeneously on the ER membrane, as indicated by a fluorescent ER marker with a KDEL motif. Because mCherry possesses more positive charges, it may interfere the function of WRB. To test this hypothesis, we constructed a WRB-EGFP chimera with point-mutations (E72A, R73A) disrupting the formation of TA protein processing machinery. As expected, WRB(E72A,R73A)-EGFP failed to rescue Otof in the WRB-deficient hair cells. Instead of in peripheral puncta, WRB(E72A,R73A)-EGFP was localized diffusely on the ER membrane identical to WRB-mCherry.

Conclusion

These results strongly suggest that the location of WRB is tightly coupled to successful membrane insertion of TA proteins

in hair cells. Since the hair cell and photoreceptor ribbon synapse require numerous synaptic vesicles for fast and continuous transmitter release, recruitment of a large supply of membrane-bound synaptic TA proteins is crucial to their function. WRB appears to mediate this process in hair cells through a distinct, puncta-like peripheral organelle.

PD - 104

The Ca^{2+} Channel Subunit $\alpha_{2\delta 2}$ Regulates Ca^{2+} Channel Abundance and Function in Mouse Inner Hair Cells and is Required for Normal Hearing

Barbara Fell¹; Gerald J. Obermair²; Dietmar Hecker¹; Martin Jung¹; Stefan Münkner¹; Bernhard Schick¹; Jutta Engel¹

¹Saarland University; ²Medical University Innsbruck

Background

Voltage-gated calcium channels (VGCCs) are protein complexes composed of an α_1 pore-forming subunit and auxiliary subunits β and $\alpha_2\delta$. VGCCs of cochlear inner hair cells (IHCs) are mainly composed of the subunits $\text{Ca}_v1.3$ (contributing to ~90% of I_{Ca} ; Platzter et al., *Cell* 2000) and $\beta 2$ (contributing to ~70% of I_{Ca} ; Neef et al., *J. Neurosci.* 2009). Lack of either $\text{Ca}_v1.3$ or $\beta 2$ causes deafness. So far, expression and contribution of the four $\alpha_2\delta$ subunits $\alpha_{2\delta 1-4}$, which assist in channel trafficking and can modulate I_{Ca} gating properties, are unknown.

Methods

To identify transcripts of $\alpha_{2\delta 1-4}$, real time quantitative RT-PCR was employed using cDNA reverse-transcribed from inner and outer hair cell mRNA. To elucidate the role of the $\alpha_{2\delta 2}$ subunit for hair cell function, we measured IHC Ca^{2+} channel currents and hearing function of an $\alpha_{2\delta 2}$ null mouse mutant, the ducky mouse ($\alpha_{2\delta 2}^{\text{du/du}}$).

Results

In mature IHCs ($\geq \text{P20}$, after the onset of hearing), only $\alpha_{2\delta 2}$ mRNA could be detected at low levels around the detection threshold. In $\alpha_{2\delta 2}^{\text{du/du}}$ mice, the mean auditory brainstem response threshold for click stimuli was significantly increased by 18 dB SPL compared with wildtype indicating a moderate hearing loss. Distortion products of the otoacoustic emissions of $\alpha_{2\delta 2}^{\text{du/du}}$ mice were larger than in controls, excluding impaired OHC mechanics. Immunolabeling showed normal expression of IHC presynaptic $\text{Ca}_v1.3$ and $\text{Ca}_v\beta 2$ in close apposition with synaptic ribbons in $\alpha_{2\delta 2}^{\text{du/du}}$ mice. However, peak Ca^{2+} and Ba^{2+} current densities of IHCs were reduced by 29 % and voltages for half-maximum activation of I_{Ca} and I_{Ba} were shifted by 5 mV and 7 mV. Surprisingly, $\alpha_{2\delta 2}$ -immunopositive spots could still be detected at synaptic ribbons of $\alpha_{2\delta 2}^{\text{du/du}}$ mice IHCs. Because a truncated $\alpha_{2\delta 2}$ protein is produced in cerebellar Purkinje cells, the existence of such a truncated protein in IHCs cannot be ruled out completely.

Conclusion

The $\text{Ca}^{2+}/\text{Ba}^{2+}$ current reduction and shift of the I-V curves are in accordance with the classical role of $\alpha_2\delta$ subunits in surface expression and gating modulation of VGCCs. They can explain the hearing deficit of $\alpha_{2\delta 2}^{\text{du/du}}$ mice. Despite the indis-

pensable co-assembly of $\text{Ca}_v2.1$ with $\beta 4$ and $\alpha_2\delta 2$ in wildtype cerebellar Purkinje cells for normal neuronal function, $\alpha_2\delta 2$ combines with $\text{Ca}_v1.3$ and $\beta 2$ to form functional Ca^{2+} channels in IHCs. In conclusion, the ducky mouse is a model for an IHC synaptopathy.

PD - 105

In Vivo Tagging of Cav1.3 Calcium Channels Reveals C-Terminal Modulation of Gating Properties and Expression of the Full-Length Channel at All Ribbon Synapses in Inner Hair Cells

Stephanie Eckrich¹; Anja Scharinger²; Kai Schöning³; Stefan Münkner¹; Dietmar Hecker¹; Anupam Sah²; Nicolas Singewald²; Amy Lee⁴; Mathias Gebhart²; Dusan Bartsch³; Alexandra Koschak⁵; Martina Sinnegger-Brauns²; Bernhard Schick¹; Jutta Engel¹; Joerg Striessnig²

¹Saarland University; ²University of Innsbruck; ³Central Institute of Mental Health and Heidelberg University;

⁴University of Iowa; ⁵Medical University of Vienna

Background

Ca^{2+} currents through voltage-gated calcium channels (VGCCs) formed by the $\alpha 1$ subunit $\text{Ca}_v1.3$ are crucial for synaptic transmission of inner hair cells (IHCs). Generally, VGCCs exhibit calcium dependent inactivation (CDI), which is mediated by calmodulin (CaM) binding to the channel's C-terminus. In IHCs, $\text{Ca}_v1.3$ exhibits unusually weak CDI, probably caused by calcium binding proteins (CaBP) competing with CaM. It has been shown that gating properties of $\text{Ca}_v1.3$ channels are modified by (tissue-specific) C-terminal alternative splicing within the $\alpha 1$ subunit. IHCs express long and short splice variants identified by RT-PCR. The spliced channel either includes (long variant, $\text{Ca}_v1.3_L$) or excludes (short variants) a C-terminal modulatory domain. In expression systems – lacking CaBPs – the C-terminal modulatory mechanism (CTM) functions via intramolecular interaction of a proximal (PCRD) and a distal C-terminal regulatory domain (DCRD) and fine-tunes channel activity by inhibiting CaM binding near the PCRD, thereby inhibiting CaM-mediated CDI (Bock et al., JBC 2011). Here, the role of the CTM for IHC VGCCs was investigated in $\text{Ca}_v1.3_L$ -DCRD^{HA/HA} mice in which CTM was disrupted by partial replacement of the DCRD with an HA tag.

Methods

Localization of HA-tagged $\text{Ca}_v1.3$ channels in IHCs was determined by immunohistochemistry. Channel properties were investigated by whole-cell patch-clamp recordings of IHCs. Hearing was assessed by recording auditory brainstem responses (ABR) and distortion products of otoacoustic emissions (DPOAE).

Results

Specific anti-HA immunolabeling was present at all presynaptic ribbon synapses of $\text{Ca}_v1.3_L$ -DCRD^{HA/HA} IHCs. Patch-clamp recordings of mature IHCs revealed that CDI was significantly reduced in $\text{Ca}_v1.3_L$ -DCRD^{HA/HA} IHCs following 300 ms depolarizations to V_{max} . The amplitude of Ca^{2+} and Ba^{2+} currents (I_{Ca} , I_{Ba}) was increased by 33% and 40%, respectively. Non-stationary fluctuation analysis of I_{Ba} revealed that the

number of $\text{Ca}_v1.3$ channels and the single channel current were unaffected in $\text{Ca}_v1.3_L$ -DCRD^{HA/HA} IHCs. Voltage dependence and activation kinetics of I_{Ca} and I_{Ba} , as well as ABR thresholds and DPOAEs were unaffected.

Conclusion

Our data demonstrate that the long $\text{Ca}_v1.3$ isoform is an intrinsic component of $\text{Ca}_v1.3$ clusters at all IHC ribbon synapses and that its DCRD is required for normal CDI and I_{Ca} amplitude. Disruption of the DCRD of $\text{Ca}_v1.3_L$ in IHCs may enable increased binding of CaBPs to the unmasked PCRD, thereby further reducing CDI.

PD - 106

Optical Stimuli Reveal Competing Mechanisms of Synaptic Vesicle Release

Richard Rabbitt¹; Qiang Liu²; Erik Jorgensen³

¹University of Utah and Marine Biological Laboratory; ²The Rockefeller University; ³University of Utah and HHMI

Background

Excitable cells respond to pulsed laser light through photochemical, photothermal and photomechanical mechanisms. The dominant mode of excitation depends upon the stimulus parameters and the cell type. Inner ear sensory hair cells, for example, are exquisitely sensitive to photomechanical stimulation of mechano-electrical transduction channels using nanosecond pulsed lasers¹, and to photothermal stimulation of synaptic vesicle release using microsecond to millisecond infrared (IR) laser diodes². In the present study we examined photothermal excitation of synaptic transmission in more detail using a model synapse. Results demonstrate IR modulation of a Ca^{2+} insensitive synaptic release mechanism that is blocked when release is driven by channelrhodopsin (ChR) activation. This novel temperature sensitive mechanism is the primary origin of IR evoked vesicular release.

Methods

Thermal transients (IR) were delivered to *C. elegans* neuromuscular junction using a 400 μm diameter optical fiber while recording end plate post synaptic currents (PSCs) in whole cell voltage clamp. A single 500 μs IR pulse rapidly increased the temperature by 0.25 $^{\circ}\text{C}$ followed by thermal relaxation. To explore potential targets of IR, we presented single IR pulses alone, or IR pulses paired with blue light pulses to activate presynaptic ChR. Experiments were done in normal extracellular media and in zero Ca^{2+} . ChR evoked synaptic vesicle release was quantified by the canonical model of Ca^{2+} dependent release by Schneggenburger and Neher³. A second Ca^{2+} independent mechanism was added to the model in order reproduce IR and IR+ChR vesicular release.

Results

Results show dramatic IR evoked increases in synaptic vesicle release that are completely independent of extracellular Ca^{2+} and independent of major intracellular Ca^{2+} release mechanisms. IR evoked release was a function of the temperature rise (T) and was completely independent of the rate of temperature rise (dT/dt). Results show that thermal modulation of the capacitive membrane double layer⁴ does not contribute to IR evoked vesicular release in this system.

A model including Arrhenius modulation of the reaction rate constants, and a mechanism for ChR activation to block thermal activation of the Ca^{2+} independent pathway, reproduced the data.

Conclusion

Present results are consistent with the hypothesis that pulsed IR evoked vesicular release occurs through direct thermal modulation of Ca^{2+} binding and release rate constants in the classical release pathway, and through thermal modulation of a Ca^{2+} independent pathway. ¹*Biomed Opt Express* **3**, 3332-3345 (2012). ²*J. Physiol* **589**, 1295-1306 (2011). ³*Nature* **406**, 889-893 (2000). ⁴*Nat Commun* **3**, 736, (2012).

PD - 107

Dopaminergic Modulation of Hair Cell Synaptic Complex Protein Pathways

Dakshnamurthy Selvakumar; **Marian Drescher**; Dennis Drescher

Wayne State University School of Medicine

Background

cAMP molecular pathways delineated in teleost saccular hair cells predicted D1A and D2L dopamine receptor expression, confirmed in both teleost and mammal (Drescher et al., 2009). In mammalian saccular hair cells, D1A and D2L proteins were immunolocalized to basolateral membrane sites apposed to dopaminergic efferents and heavily concentrated at subcuticular Golgi-enriched sites, the latter suggesting a role in dopamine-activated hair cell trafficking. Two overlapping molecular pathways for dopamine D1A and D2L have now been identified in hair cells, consistent with molecular mechanisms for modulation by dopamine of receptoneural secretion and stereociliary protein function.

Methods

We sought evidence that transcripts were actually expressed by hair cells, and that the corresponding proteins interacted strongly with specific synaptic complex proteins for both teleost purified hair cells and their mammalian counterparts. For methods, we used RT-PCR for hair-cell transcript analysis, yeast two-hybrid protocols, pull-down assays, and surface plasmon resonance to determine kinetic constants and calcium-dependency of the protein-protein interactions (PPIs) (Selvakumar et al., 2012; 2013).

Results

Dopamine D2L in trout saccular hair cells was found to interact with calmodulin-binding Purkinje-cell protein 4 (PCP4), itself a binding partner of hair-cell CNGA3. Rat cochlear outer hair cells also express transcript for D2L and PCP4 (and CNGA3), and the mammalian proteins interact similarly. Competitive pull-downs indicate that PCP4 either interacts with CNGA3 or D2L but not both. CNGA3 interacts with AP2M1, a subunit of the clathrin AP2 complex localized to the subcuticular plate, believed to orchestrate a role for otoferlin in synaptic vesicle recycling (Duncker et al., 2013). CNGA3 also interacts with intraflagellar transport protein 20 (IFT20), now identified in vestibular hair cells, which directs cilia protein trafficking from Golgi sites. D1A forms a second pathway in interacting with

snaphin, an otoferlin-binding partner, with all three interactions cooperative. NSF, also identified in the saccular hair cells, binds to both D1A and D2L, potentially integrating these signaling pathways. The interactions between each pair of proteins in the two dopamine receptor pathways have different kinetics and dependence on Ca^{2+} .

Conclusion

Due to known localizations of proteins in these two hair-cell dopamine receptor pathways, the PPIs implicate control of trafficking initiated by dopamine agonist activation of respective dopamine receptors basolaterally. PKC moves to Golgi as a consequence of D2L activation, described *in vitro*, where PKC-phosphorylation of targeted proteins at Golgi-rich subcuticular plate sites would control protein trafficking to the stereocilia and to the synaptic complex.

PD - 108

Postsynaptic Calcium Regulation in Hair Cells

Howard Moskowitz¹; Gi-Jung Im²; **Paul Fuchs**³

¹Montefiore Medical Center; ²Korea University College of Medicine; ³Johns Hopkins University School of Medicine

Background

Calcium is the linchpin for transmitter release as well as mediating pre- and postsynaptic plasticity. Postsynaptic calcium fluxes can modulate transmission as during long-term depression or via nitric oxide (NO) as the retrograde messenger for presynaptic facilitation. Calcium-triggered, NO-dependent retrograde facilitation of efferent release onto inner hair cells occurs in the immature cochlea (Kong et al. JARO 14:17). Calcium entry through acetylcholine receptors (AChRs) or through voltage-gated calcium channels (VGCCs) can drive this process, perhaps through the intercession of the postsynaptic cistern that aligns with the efferent terminal.

Methods

This question was explored by giga-ohm seal whole-cell recording from short hair cells of the embryonic (E17-20) chicken's basilar papilla (auditory end-organ). Like outer hair cells in the mammalian cochlea, short hair cells are the principal targets of cholinergic efferent neurons, and respond to exogenous acetylcholine (ACh) with combined inward cation, and outward potassium current at the resting potential (~-50 mV). The lifetime of the cholinergic calcium signal was examined by stepping the membrane potential to a positive value (+40 mV) where calcium driving force and so influx is greatly reduced, terminating the ACh-evoked SK current..

Results

The SK tail current at +40 mV decayed exponentially (time constant ~ 100 ms), consistent with the steady dissipation of calcium when influx halted. However, at -20 to 0 mV, the ACh-evoked SK tail current had a prolonged, complex time course, as though responding to a second, slower calcium signal. The prolonged SK tail current at -20 mV was abbreviated by application of the L-type calcium channel blocker, nimodipine, and extended by exposure to the channel activator BAY-K 8644, suggesting that VGCCs might be this secondary source of calcium. In separate experiments exposure to 1 μM

ryanodine elongated the SK tail current at -20 mV while the sarco-endoplasmic calcium pump antagonist, benzo-hydroquinone greatly abbreviated the ACh-evoked SK tail current.

Conclusion

These effects are consistent with voltage-gated calcium influx loading an endoplasmic store that can modulate the ACh-evoked SK current. The most likely candidate is the postsynaptic cistern that aligns with the efferent terminal. Transmission electron micrographs show that synaptic ribbons (the presumed locus of VGCCs) can occur in near proximity to the cisterns.

PD - 109

Intravital Confocal Microscopy Assay for the Evaluation of Antioxidant Capacity

Yu Matsumoto; Kazuko Toh; Kazunori Kataoka; Tatsuya Yamasoba

The University of Tokyo

Background

It has increasingly been recognized that reactive oxygen species (ROS) plays an important role in aging, neurodegenerative disorders, cardiovascular diseases, cancer and diabetes mellitus. There is a continuous search for new compounds and unidentified food ingredients with antioxidant potential. A number of chemical techniques have been developed in an attempt to measure the antioxidant capacity *in vitro*. However, the data for antioxidant capacity of any compounds measured by *in vitro* cannot be extrapolated to *in vivo* effects because most of the compounds are prone to chemical metabolism and excretion, thus poorly conserved in the living body. Besides the antioxidant (pro-) vitamins, such as vitamin E, C and β -carotene, no food compounds have been proved to have antioxidant efficacy *in vivo*. In this regard, we established an intravital confocal microscopy assay for the evaluation of antioxidant capacity.

Methods

Mice were anesthetized and placed onto a temperature-controlled pad integrated into the microscope stage and maintained in a sedated state throughout the measurement. Ear lobe dermis tissue was accessible without surgery and easily fixed beneath the cover slip with a single drop of immersion oil. Different antioxidant compounds were administered intraperitoneally solely or in combination prior to image acquisition. Saline was used as a control. All picture / movie acquisitions were performed using a Nikon A1R confocal laser scanning microscope system attached to an upright ECLIPSE FN1 (Nikon Corp., Tokyo, Japan) equipped with a 20 \times objective, 488 nm diode laser, and a band-pass emission filter of 525/50 nm. Fluorescein was intravenously administered, and the fluorescent intensity of extravascular skin tissue was assessed over time.

Results

Arterial entrance, venous migration, and extravasation of the fluorescein were directly observed in the ear lobe dermis. Time-lapse imaging was conducted to quantify the degree of fluorescence photobleaching induced by the excitation light. Photobleaching is the photochemical destruction of a fluoro-

phore due to the generation of ROS, particularly singlet oxygen (1O_2) in the specimen as a byproduct of fluorescence excitation. Mice administered with antioxidant compounds such as vitamin C (ascorbic acid) and E (trolox) demonstrated sustained antifade effect. Mice administered with saline showed rapid decrease of fluorescent intensity in extravascular skin tissue.

Conclusion

We developed an intravital confocal microscopy assay for the evaluation of antioxidant capacity. This technique is useful for screening antioxidant compounds *in vivo*. It is also noteworthy that ascorbic acid and trolox can be used as intravital antifade reagents.

PD - 110

Discovery of a Biological Mechanisms of Active Transport Through the Tympanic Membrane

Allen Ryan¹; Andrew Baird⁴; Marlen Bernhardt²; Kwang Pak³; Arwa Kurrabi⁴

¹University of California, San Diego and the VA Medical Center; ²University of California, San Diego - Surgery / Otolaryngology; ³University of California, San Diego - Surgery / Otolaryngology and the VAMC; ⁴University of California, San Diego - Surgery / Trauma and the VAMC

Background

Otitis media (OM) is a serious disease, especially in developing countries where the WHO estimates that it causes >50,000 deaths/year and half the world's burden of severe hearing loss. It is often treated by systemic antibiotics, leading to side effects including induction of antibiotic resistance in bacteria throughout the body and potentially serious gastrointestinal disorders in infants. While local treatment would avoid these issues, the tympanic membrane (TM) is an impermeable barrier that prevents drug penetration unless surgically breached. We hypothesized that the TM might harbor innate biological mechanisms that could mediate trans-TM drug transport.

Methods

We used M13 bacteriophage display of peptides and sequential biopanning to search for mediators of trans-TM transport. OM was induced in rats by intrabullar inoculation of non-typeable *Haemophilus influenzae*, while leaving the TM intact. 48 hrs later, aliquots of a phage library displaying 10¹² random 12-mer peptides were applied to the TM for 2 hrs. The ME contents were then harvested and applied to *E. Coli* to amplify any phage that might be present. This process was repeated twice with the resulting amplified ME phage. Samples of phage recovered from the ME were sequenced after rounds 2 and round 3.

Results

In 22 phage isolate sequences, four unique peptides with similar amino acid structure were represented. Each phage isolate was applied to the TM for varying periods of time and ME recovery was compared to that for wild-type (WT) phage as a control. All four peptide-bearing phage exhibited ME re-

covery significantly greater than that of WT phage, with one exhibiting recovery enhanced 10^5 - 10^6 times. TM transit was dependent upon temperature and ceased after death, indicating an active mechanism. Phage transit was inhibited by free peptide, demonstrating that the peptide was the determinant of trans-TM transport.

Conclusion

The ability of peptides to mediate the transport of 2 nm bacteriophage particles across the TM identifies a novel biological process with considerable cargo-carrying capability that can be harnessed for drug delivery.

PD - 111

Withdrawn by author

PD - 112

Sustained Release of Triamcinolone-Acetonide from an Intratympanically Applied Hydrogel Designed for the Delivery of High Glucocorticoid Doses

Clemens Honeder¹; Elisabeth Engleder²; Hanna Schöpper³; Franz Gabor²; Gottfried Reznicek⁴; Wolfgang Gstöttner⁵; Christoph Arnoldner⁵

¹Medical University of Vienna; ²Department of Pharmaceutical Technology and Biopharmaceutics, University of Vienna, Austria; ³Department of Pathobiology, Institute of Anatomy, Histology and Embryology, University of Veterinary Medicine Vienna, Austria; ⁴Department of Pharmacognosy, University of Vienna, Austria; ⁵Department of Otorhinolaryngology, Medical University of Vienna, Austria

Background

Topical glucocorticoid therapy of the inner ear leads to significantly higher perilymph drug-levels than systemic therapy, but is hampered by the rapid loss of fluids through the Eustachian tube. In recent years, different application procedures including repeated injections, the implantation of wicks or catheters and the use of hydrogels have been evaluated, trying to overcome this problem. Thereby, the use of poloxamer 407, which is fluid at low temperatures and forms a gel at body-temperature, emerged as a promising drug delivery system for glucocorticoids. Dexamethasone, the glucocorticoid most extensively tested so far, has a short elimination half-time in perilymph. This is undesirable if the apical region of the cochlea should be exposed to significant levels of the drug. Therefore, we evaluated an alternative glucocorticoid, Triamcinolone-acetonide (TAAc), for the use in such a hydrogel.

Methods

The poloxamer 407 hydrogel was loaded with 30% TAAc and intratympanically applied in a guinea pig model. 1, 3 and 10 days after the application, perilymph was sampled from the apex of the cochlea and CSF as well as plasma samples were taken. TAAc levels in these biological fluids were quantified by HPLC/MS. Hearing thresholds were determined by ABR on days 1, 3 and 10. Bullae were removed and histologically evaluated after perilymph sampling. Histological meth-

ods included classic histology and the preparation of organ of Corti wholemounts.

Results

Clinically relevant perilymph levels of TAAc were found in the perilymph at every sampling time-point ($107.5 \pm 51.7 \mu\text{g/ml}$ at day 1; $3.8 \pm 2.9 \mu\text{g/ml}$ at day 10). CSF and plasma levels of TAAc were significantly lower than the levels measured in perilymph. The application of the hydrogel caused a small hearing loss on day 3, which resolved by day 10. No significant histological alterations were found after TAAc treatment and hair-cell counts did not show any statistically significant differences between TAAc treated animals and untreated controls.

Conclusion

The TAAc loaded poloxamer 407 hydrogel appears to be a safe and effective drug delivery system, which should be tested in trauma models and could be quickly translated into clinical practice.

PD - 113

Magnetic Injection of Steroids Into the Inner Ear Mitigates Acute Hearing Loss in Rats

Didier Depireux; Azeem Sarwar; Alek Nacev; Ben Shapiro
University of Maryland, College Park

Background

It is difficult to deliver drugs into the inner ear because it is located deep in the skull and protected/isolated by the blood-labyrinth barrier. The standard-of-care for treating sudden hearing loss and other hearing problems has been to either inject steroids trans-tympanically into the middle ear and to rely on free diffusion of drugs from the middle into the inner ear, a procedure that creates undesirable drug gradients along the cochlea, or to administer steroids orally, procedures which result in widely varying patient outcomes.

Methods

We have developed a method to direct drugs into the inner ear using a magnetic system. Biocompatible nanoparticles, with a magnetic core and a chitosan coating are loaded with prednisolone, which will elute from the particles over an extended period of time.

Results

We validated this method in Long-Evans rats, showing transport of drugs from the middle to the inner ear. This magnetic injection achieved about 1 microgram/mL prednisolone average cochlea concentration, within an hour of intervention. Magnetic delivery was also found to yield a more uniform drug concentration in the cochlea, and provides a strategy to bypass the rapid clearance of drug from the middle and inner ear by using magnetic particles in the cochlea as a slow-release drug reservoir. Behavioral studies showed that magnetic delivery had a therapeutic effect for acute hearing loss following noise trauma, compared to trans-tympanic injection followed by passive diffusion in control animals.

Conclusion

Our new drug delivery method promises a non-invasive, effective way to deliver drug to the cochlea, with an extended spatial and temporal profile.

PD - 114

Diverse Pattern of Perilymphatic Space Enhancement After Intratympanic Injection of Two Different Types of Gadolinium: A 9.4 Tesla MR Study

Myung-Whan Suh; Mi Na Park; Ho-Sun Lee; Jun Ho Lee; Seung Ha Oh

Seoul National University Hospital

Background

Intratympanic gadolinium has been reported as a method to evaluate the inner ear in patients with endolymphatic hydrops and Meniere's disease. But most of the previous studies were performed with a single gadolinium contrast agent. To the best of our knowledge there is no study in the literature that has reported the difference in inner ear enhancement between two or more different gadolinium contrast agents. In this study we aimed to compare the pattern of perilymphatic enhancement after intratympanic injection of two different types of gadolinium (gadoterate meglumine and gadobutrol) with a 9.4 Tesla micro MRI.

Methods

Gadolinium was injected into the middle ear in 5 Sprague-Dawley rats, via transtympanic method. The right ear was injected with gadolinium A while the left ear was injected with gadolinium B. MRI images of the inner ear were acquired 1, 1.5, 2, 2.5, 3, 3.5, and 4 hours after the intratympanic injection with an Agilent MRI System 9.4T/160/AS. In order to evaluate the delayed enhancement effect, 8 and 12 hour delayed images were also acquired in some animals. The normalized signal intensity was quantitatively analyzed at the scala vestibuli (SV), scala media (SM), scala tympani (ST) with Marosis M-view system. The temporal changes of signal intensity were compared between the two different gadolinium contrast agents.

Results

As for gadolinium A, the post injection 1 hour signal intensity in the basal turn was 2.6 ± 0.7 at SV, 1.6 ± 3.2 at ST and 1.1 ± 2.1 at SM. The signal intensity did not change for the following 8 hours, but started to decline after 12 hours. In the apical turn, the maximal signal intensity was reached after 2.5-4.0 hours. The maximal signal intensity in the apical turn was 1.7 ± 0.8 at SV (2.5 hr) and 1.7 ± 0.3 at ST (4 hr) and 1.2 ± 0.1 (4 hr). As for gadolinium B, the signal intensity was low as 1.0-1.3 throughout 1-4 hours at SV and ST of the basal turn. The highest signal intensity was reached at 8-12 hours, but still under 2.0 in every case. Delayed enhancement was also found in the apical turn. The maximal signal intensity was 1.9 ± 0.8 at SV (8 hr) and 1.4 ± 0.3 at ST (8hr).

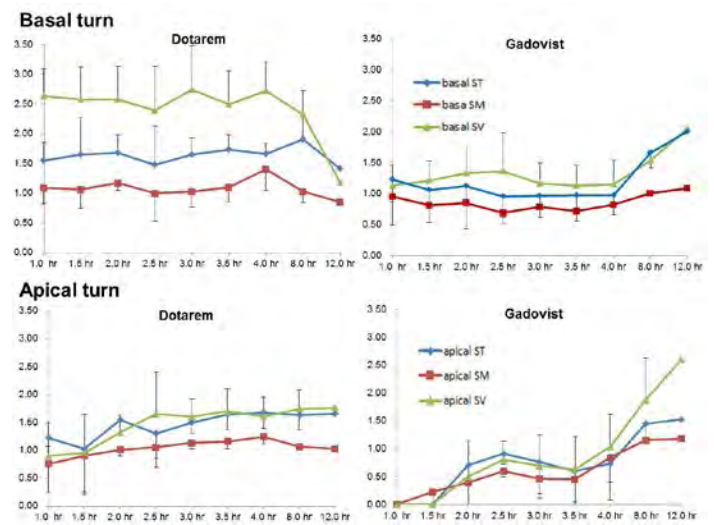
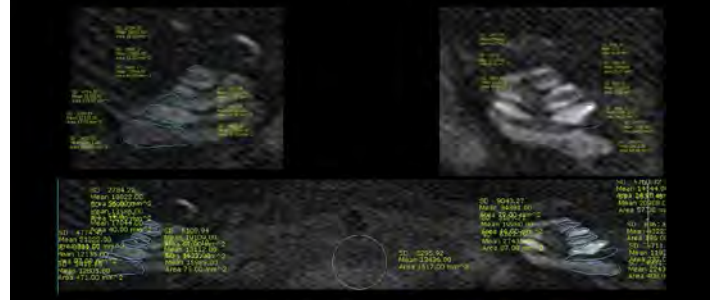
Conclusion

The signal intensity of the perilymphatic enhancement with gadolinium A was always stronger than gadolinium B. While

maximal enhancement was reached after 1 hour with gadolinium A, 8-12 hour delayed enhancement was found with gadolinium B. Signal intensity of the SV was stronger than that of the ST, especially in the basal turn.

Quantification of Signal Intensity

- Translating 3D T1-weighted images to DICOM file
- Measurements using computer-based ROI in the PACS system



PD - 115

Direct Visualization of Cochlear Drug Delivery Using a Novel Fluorescent Bisphosphonate Compound

Woo Seok Kang¹; David Jung¹; Alicia Quesnel¹; Shuting Sun²; Adam Hacking³; Charles McKenna²; William Sewell¹; Michael McKenna¹

¹Massachusetts Eye and Ear Infirmary; ²University of Southern California; ³Massachusetts General Hospital

Background

Otosclerosis is a disease of abnormal bone metabolism that affects the otic capsule, which can result in a fixed stapes footplate and present as a conductive hearing loss. Cochlear otosclerosis describes a typically extensive otosclerotic lesion that involves the cochlear endosteum, resulting in a sensorineural hearing loss (SNHL). Otosclerosis has similarities to other metabolic bone diseases, and we have recently described positive findings following treatment of cochlear otosclerosis with systemic bisphosphonates. However, given the

potential toxicities of systemic bisphosphonate treatment, a local, non-ototoxic delivery method would be advantageous.

Methods

We used a novel, fluorescently labeled compound of zoledronate (FAMZOL) to directly visualize patterns of bisphosphonate delivery. Male albino guinea pigs were treated with FAMZOL either systemically or locally, via placement on the round window or by direct intracochlear injection. Hearing was monitored both before and after FAMZOL treatment. We analyzed the animals by embedding the temporal bones within resin, grinding them down to a mid-modiolar cochlear section, and quantifying the amount of drug delivered using fluorescent microscopy.

Results

Systemic administration of FAMZOL resulted in deposition of FAMZOL in otic capsule bone, albeit at a lower level than cortical bone. Local administration, either across the round window membrane or via intracochlear injection, also resulted in measurable deposition of FAMZOL in the wall of the cochlea. Critically, as measured by DPOAE and ABR, neither systemic nor local delivery of FAMZOL resulted in ototoxicity at doses similar to those given systemically to humans.

Conclusion

Local delivery of bisphosphonates can be achieved without incurring ototoxicity. Our system, which exploits a tagged bisphosphonate that can be directly visualized in bone, may be efficacious in the rapid evaluation of other drug delivery systems for the ear. Further work is required to determine the optimal effective dose for local delivery of bisphosphonate in the treatment of otosclerosis.

PD - 116

N-Acetylcysteine Lacks Protective Effect on the Human Inner Ear

Anders Fridberger¹; Dan Bagger-Sjöback²; Karin Strömbäck³; Pierre Hakizimana¹; Christina Larsson²; Jan Plue⁴; Malou Hultcrantz²; Henrik Smeds²; Sten Hellström²; Ann Johansson⁵; Bo Tideholm⁵

¹Linköping University; ²Karolinska Institutet; ³Uppsala University Hospital; ⁴Stockholm University; ⁵Karolinska University Hospital

Background

Animal studies show that hearing loss induced by noise, surgical trauma, and ototoxic drugs can be prevented by N-Acetylcysteine and other antioxidants. It is unclear if antioxidants have a protective effect on the human inner ear.

Methods

The inner ear is exposed to loud sounds and surgical trauma during stapedotomy, an operation performed to treat otosclerosis. Surgery improves speech perception, but high-frequency hearing often suffers. We performed a randomized, double-blind, and placebo-controlled multicenter trial to determine if perioperative N-acetylcysteine protects from decline in high-frequency hearing. Using block-stratified randomization, 152 patients were assigned to intravenous N-Acetylcysteine (150 mg/kg body weight) or matching placebo. Hearing

thresholds were measured 6 – 8 weeks and one year after surgery, and patients also rated the severity of tinnitus and vertigo at these time points.

Results

Six weeks after surgery, high-frequency hearing (> 4 kHz) had improved 0.8 ± 3.8 dB in the placebo group and 2.4 ± 3.7 dB in the N-acetylcysteine group (means \pm 95% confidence intervals [CI], $p = 0.82$); at one year the change in hearing as compared to baseline was 2.7 ± 3.8 dB in the placebo group and 2.2 ± 3.8 dB in the treated group (means \pm 95% CI, $p = 0.54$). Surgery led to immediate improvement of tinnitus, but there was no significant difference between groups. Balance disturbance was common after the operation, remained present at 6 weeks, but improved during the first year, without significant intergroup differences.

Conclusion

In patients undergoing stapedotomy, N-acetylcysteine has no significant hearing-protective effect and alters neither tinnitus nor vertigo.

PD - 117

Mouse Organ of Corti Cytoarchitecture from Base to Apex, Imaged In Situ With Two-Photon Microscopy

Joris Soons¹; Anthony J. Ricci²; Charles R. Steele³; Sunil Puria⁴

¹Department of Mechanical Engineering, Stanford University and Laboratory of Biomedical Physics, University of Antwerp; ²Department of Otolaryngology – Head and Neck Surgery, Stanford University; ³Department of Mechanical Engineering, Stanford University; ⁴Department of Mechanical Engineering, Stanford University and Department of Otolaryngology – Head and Neck Surgery, Stanford University

Background

The cells in the Organ of Corti (OoC) are highly organized, with their precise 3D microstructure hypothesized to be important for the high sensitivity and frequency selectivity of the cochlea. Here we extend our knowledge base by providing quantitative data obtained *in situ* on mTmG mouse by using two-photon microscopy.

Methods

Cochleae from 13 mTmG mice, whose cell membranes fluoresce in red, were opened at 5 different locations along the cochlear duct: at the apex (~5 kHz), middle (~10 kHz), middle basal view (~20 kHz), base (~40 kHz), and hook region (~70 kHz). For each location, 4 to 5 *in situ* measurements were performed on different specimens (totaling 24 measurements). Each resulting three-dimensional image stack of the OoC spans approximately 112 μm . Amira (ver. 3.2) was used to measure inter-cell distances and diameters. Points were placed in the image stacks and analyzed in MATLAB to acquire lengths and relative angles for each inner and outer hair cell (IHC and OHC), Deiters cell (DC), phalangeal process (PhP), and inner and outer pillar (IP and OP).

Results

Figure 1 shows a representative OoC reconstruction from the apical region. New features of this study include quantitative data for the longitudinal tilt of the OHCs and the PhPs. Relative to the basilar membrane, these angles are (mean \pm std. error of the mean): OHC1 = $104.9 \pm 0.5^\circ$, OHC2 = $99.6 \pm 0.5^\circ$, and OHC3 = $96.6 \pm 0.7^\circ$ (significant different, $p < 0.01$). The PhPs are tilted in the opposite direction and link the base of one OHC with the apex of a more apical OHC, over a distance of 3 hair cells for the first and second rows. In the third row, the PhPs span distances of 1 hair cell at the base and apex of the cochlea, and 2 hair cells in the middle of the cochlea.

Conclusion

The lengths and angles between the OHCs, DCs, and PhPs are not fixed within the OoC, as had been previously thought, but instead vary from base to apex and between OHC rows. This has implications for cochlear amplifier theories, which can be tested using computational models.

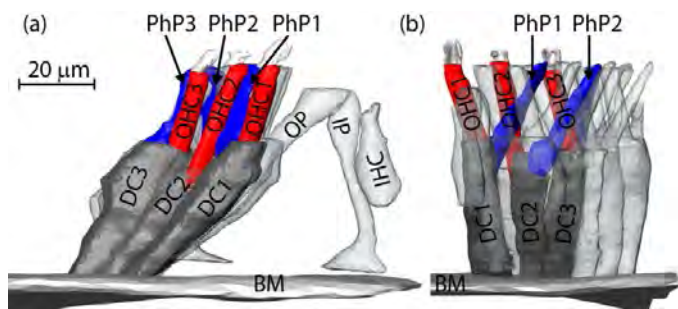


Figure 1: Radial (a) and longitudinal (b) views of the geometrical OoC model, in the apical region, with the basilar membrane (BM), Deiters cells (DC1–3), outer hair cells (OHC1–3), phalangeal processes (PhP1–3), inner hair cell (IHC), and inner and outer pillars (IP and OP) indicated.

PD - 118

Quantitative Polarized Light Microscopy of Human Cochlear Sections

Jacob Low¹; Thomas Ober²; Gareth McKinley³; Konstantina Stankovic⁴

¹The University of Manchester, Manchester UK;

²Massachusetts Eye and Ear Infirmary; ³Massachusetts Institute of Technology; ⁴Massachusetts Eye and Ear Infirmary, Harvard Medical School

Background

Dysfunction of the inner ear is the most common cause of sensorineural hearing loss, which is the most common sensory deficit worldwide. To develop a greater understanding of inner ear pathology, it is vital to explore imaging modalities that are capable of revealing the microanatomy of the ear. We have previously shown that quantitative polarized light microscopy (qPLM) has important advantages over immunohistochemistry when analysing mouse cochlear sections. We now focus on accessing the utility of qPLM in characterizing the optical properties of human cochlear sections, with an eye toward the ultimate application *in vivo*.

Methods

Eight cadaveric human cochleas from children aged 0 (term) to 24 months were selected from the US National Temporal Bone Registry based on excellent tissue preservation on serial sections, and no documented cochlear histopathology. Midmodiolar sections that had been stained with hematoxylin and eosin were imaged using qPLM. Pseudocolour magnitude retardance and orientation images were captured with the Abrio Birefringence Imaging System. Retardance values of the following structures were measured using image J: the otic capsule, basilar membrane, organ of Corti, stria vascularis and the spiral ligament. The retardance values were compared across cochlear half turns.

Results

Retardance values of the otic capsule (ranging from 3.89 \pm 1.52 nm in the lower basal to 2.78 \pm 1.41 nm in the upper middle turn) and basilar membrane (ranging from 2.25 \pm 0.62 nm in the lower basal to 1.36 \pm 0.57 nm in the upper middle turn) were substantially higher than the retardance of the other microstructures. These results are in general agreement with those in mice, with the exception of the spiral ligament, which has substantially lower retardance in humans (0.52 \pm 0.23 nm in the lower basal to 0.40 \pm 0.13 nm in the upper middle turn) than in mice.

Conclusion

This is the first study to characterise the optical properties of human cochlear sections using quantitative polarized light microscopy. This non-invasive imaging modality has the potential to provide quantitative and qualitative information about the inner ear, and awaits future exploration *in vivo*.

PD - 119

Age Related Hearing Loss is Accompanied by Efferent Innervation of Inner Hair Cells

Stephen Zachary; Paul Fuchs

Johns Hopkins School of Medicine

Background

Before postnatal day 14 (P14), inner hair cells (IHCs) receive cholinergic synaptic input from olivocochlear efferents. IHCs express $\alpha 9/\alpha 10$ containing nicotinic acetylcholine receptors (nAChRs), which are Ca^{2+} permeable. Ca^{2+} influx through these nAChRs gates functionally coupled SK channels, leading to potassium efflux and membrane hyperpolarization. Efferent activity is thought to pattern the intrinsic spiking behavior of immature IHCs. After P14, IHCs lose their efferent contacts, SK channels, and are no longer responsive to exogenously applied ACh. A 2012 study by Lauer et al. (Neurobiology of Aging 33:2892) presented ultrastructural evidence that efferent contacts return to IHCs in aged mice with severe hearing impairments. This innervation correlated with the age of the animals, the extent of outer hair cell loss, and the level of hearing impairment.

Methods

Whole cell recordings were performed on apical turn IHCs from C57BL6j mice at 3 ages: 1 month, 7-8 months, and 11-12 months. Efferent transmitter release was evoked by application of elevated potassium solution from a nearby mul-

tichannel application pipet, which also delivered drugs for pharmacological experiments. Hearing thresholds were assessed via auditory brainstem response (ABR).

Results

We found efferent synaptic activity in ~60% of apical turn IHCs recorded from 11-12 month old animals. Consistent with published reports, ABR measurements at this age revealed a severe hearing impairment across all frequencies tested. Inward synaptic currents recorded in elevated potassium solution were completely and reversibly blocked by curare (1 μ M), strychnine (1 μ M), and ACV1 (500 nM). When apamin (400 nM) was applied, the waveform of the inward synaptic currents was altered and a reduction in the time constant of decay was observed. In normal external solution, ACh (500 μ M) induced inward currents at -80mV (E_K) and the ACh induced current reversed to outward current between -60 and -70mV.

Conclusion

Efferent innervation returns to IHCs during age related hearing loss. Efferents contacting aged IHCs are cholinergic and aged IHCs use $\alpha 9$ -containing nAChRs. Additionally, SK channels are coupled to these nAChRs, rendering these synapses functionally inhibitory. Efferent-IHC synapses found in aged animals are functionally similar to the efferent synapses found during development. It remains to be determined whether efferent innervation of IHCs exacerbates, ameliorates, or is merely coincidental with age-related hearing loss.

PD - 120

Pannex1 is Required for Endocochlear Potential (EP) Generation

Jin Chen; Jing Chen; Yan Zhu; Chun Liang; **Hong-Bo Zhao**
University of Kentucky Medical Center

Background

Endocochlear potential (EP) is a driving force for hair cells to generate receptor current and potential. EP is generated in the cochlear lateral wall. However, the mechanisms underlying EP generation are still largely undetermined. It has been reported that gap junctions play a critical role in the EP generation. Pannexin is a new-found gene family to encode gap junctional proteins in mammals. Panx1 extensively expresses in the inner ear, including the spiral ligament (SPL) in the cochlear lateral wall. In this study we found that Panx1 expression in the cochlear lateral wall is required for EP generation.

Methods

Panx1 expression in the cochlear lateral wall was targeted-deleted by loxP-Cre technique. EP was directly recorded. Cochlear morphology and Panx1 expression were verified by immunofluorescent staining with confocal microscopy. Mouse hearing function was also assessed by ABR and DPOAE recordings.

Results

Panx1 in the cochlear lateral wall is mainly expressed at the type II fibrocytes in the SPL. After targeted deletion of Panx1 in the SPL, EP was reduced to 40-50 mV. Cochlear microphonics (CM) was also reduced by 70%. ABR recording

shows that Panx1 conditional knockout (cKO) mice had hearing loss. The thresholds of ABR were elevated about 40-50 dB SPL. The hearing loss was severe at the high frequency. DPOAE was also reduced and the reduction was severe at high frequency. However, no significant hair cell degeneration was visible. The cochlea also had normal development.

Conclusion

These data indicate that Panx1 expression in the cochlear lateral wall is required for EP generation. The data also provide the first direct evidence that not only stria vascularis but also the SPL in the cochlear lateral wall have a critical role in EP generation and that Panx1 deficiency can induce hearing loss.

PD - 121

Mechanosensitivity Beyond Hair Cells and its Functional Roles in Precision and Acuity of Auditory Information Coding

Ebenezer Yamoah; Maria Cristina Perez-Flores; Jeong Han Lee

University of California Davis

Background

Action potentials (AP) can be accompanied by propagating membrane deformations. Mechanical impulses have also been recorded at axon terminals during AP firing and vesicle fusion. Indeed, dendritic spines experience rapid actin-mediated contractions in response to synaptic activity. How these cellular-mechanical dynamics influence the neuronal function remains a mystery. In the cochlea, spiral ganglion neurons (SGNs) are continuously subject to mechanical stimulation mediated by basilar membrane motion. For the first time, we have determined that SGNs express mechanically sensitive ionic channels that confer mechanosensitivity of these neurons. We will show that mechanosensitivity of SGNs is a bona fide component of their phasic firing properties.

Methods

To perform these experiments, SGNs were isolated from C57 mice; the apical and basal aspects were dissociated using a combination of enzymatic and mechanical procedures. The neurons were maintained in culture for 3-4 days. The cells were stimulated through a series of mechanical displacements.

Results

Mechanical stimulation of the soma clearly elicited adapting, bursting and non-adapting firing response in the SGNs. Similar responses were elicited by stimulating neurites through their substrates. Simultaneous stimulation with current injection and mechanical stimuli evoked adapting and bursting spikes of smaller amplitude, but the firing pattern of non-adapting neurons remained unchanged. In voltage clamp experiments, mechanical stimulation elicited an inward current (100-500 pA) at a holding potential of -70 mV, with a reversal potential of ~0 mV. The current and the mechanically evoked changes in the firing of SGNs were sensitive to known blockers of mechanosensitive channels.

Conclusion

We propose for the first time that the unrelenting firing of SGNs may rely partially on the activity of mechanosensitive channels in response to mechanical forces induced by basilar membrane motion.

PD - 122

Cl/HCO₃⁻ Anion Exchanger AE1 May Serve as a Catalyst for Prestin-Mediated Electromotility

Wei Chun Chen¹; Hyo Jeong Kim¹; Choong-Ryoul Sihm¹; Jeong Han Lee¹; Gary Shull²; Ebenezer Yamoah¹

¹University of California, Davis; ²University of Cincinnati

Background

Mammalian prestin (SLC26A5) is a voltage-dependent membrane motor protein that controls outer hair cell contraction and elongation, a process essential for sound amplification. It has been demonstrated that conformational changes of prestin requires allosteric binding of intracellular Cl⁻ ions. Here, we proposed that Cl/HCO₃⁻ anion exchanger AE1 (SLC4A1) functions in accordance with prestin to modulate its voltage sensitivity.

Methods

Using a whole-cell voltage-clamped electrophysiological technique, we measured nonlinear capacitance (NLC) of transfected CHO cells expressing either prestin alone or both prestin and AE1 together. Biochemical techniques were used to identify the expression of AE1 and prestin in outer hair cells (OHCs).

Results

We showed that prestin-transfected CHO cells exhibited NLC characteristics (voltage at peak capacitance (V_h) at pH 7.4 = -90.1 ± 3.3 mV, ionic valance (z) = -0.78 ± 0.05 , operating voltage (V_{op}) = $\{-165.1, -15.2\}$ mV, $n = 13$), which were significantly different from those of CHO cells transfected with both prestin and AE1 (V_h at pH 7.4 = -34.1 ± 3.8 mV, $p < 0.01$; $z = -0.57 \pm 0.03$, $p < 0.01$; $V_{op} = \{-134.4, +66.2\}$ mV, $n = 14$). Furthermore, under different intracellular pH conditions (pH 6.2, 7.4, and 8.0), there were apparent shifts in V_h of prestin-transfected CHO cells (V_h at pH 6.2 = -105.1 ± 4.8 mV, $n = 9$; V_h at pH 7.4 = -90.1 ± 3.3 mV, $n = 13$; V_h at pH 8.0 = -69.3 ± 6.3 mV, $n = 6$; one-way ANOVA Bonferroni post hoc test: $p < 0.01$). When high intracellular [Cl⁻] was replaced with low intracellular [Cl⁻] (10 mM) to mimic *in vivo* conditions in OHCs, similar patterns were observed: a positive V_h shift and a wider operating voltage range in CHO cells expressing both prestin and AE1 (V_h at pH 7.4 = -27.2 ± 7.6 mV, $p < 0.01$; $z = -0.69 \pm 0.03$, $p < 0.05$; $V_{op} = \{-110.8, +56.3\}$ mV, $n = 12$) compared to those of prestin-transfected CHO cells (V_h at pH 7.4 = -63.8 ± 5.4 mV, $z = -0.84 \pm 0.06$, $V_{op} = \{-133.2, +5.5\}$ mV, $n = 9$).

Conclusion

We report that the activity of AE1 may provide Cl⁻ ions in the immediate vicinity of prestin to confer OHC electromotility.

PD - 123

Kv1.1 and Kv1.2 Channels Differentially Modulate Action Potential Firing in Spiral Ganglion Neurons

Wenying Wang¹; Hyo Jeong Kim¹; Ping Lv¹; Bruce Tempel²; Ebenezer Yamoah¹

¹UCDAVIS; ²University of Washington School of Medicine

Background

Temporal precision and fidelity in the auditory system is critical to coding stimulus parameters, such as intensity and frequency. The Kv1 family has been localized to soma, axons, synaptic terminals, and proximal dendrites of spiral ganglion neurons (SGNs). With their low-threshold activation and rapid activation kinetics, Kv1 channels effectively regulate the shape and the rate of action potentials. Here, we examined differential roles of Kv1.1 and Kv1.2 using Kcna1 and Kcna2 null mutant mice.

Methods

SGNs were isolated from postnatal (P) mice 10-12 and 19-22 day-old mice. Whole-cell voltage and current clamp recordings were performed on cultured SGNs from wild-type, as well as Kcna1 and Kcna2 null mutants.

Results

Using Kcna2 null mutant mice, we demonstrate a surprising paradox in changes in the membrane properties of SGNs. The resting membrane potential of Kcna2^{-/-} SGNs was significantly hyperpolarized compared to age-matched wild-type SGNs. Analyses of outward currents in the mutant SGNs suggest an apparent ~2-fold increase in outward K⁺ currents. We show that *in vivo* and *in vitro* heteromultimerization of Kv1.2 and 1.4 α -subunits underlies the striking and unexpected alterations in the properties of SGNs. The results suggest that heteromeric interactions of Kv1.2 and 1.4 dominate the defining features of Kv1 channels in SGNs. Similar analyses on Kcna1 null mutant mice SGNs will be presented.

Conclusion

We have demonstrated that *in vivo* and *in vitro* association of Kv1.2 and Kv1.4 α -subunits is the mechanism underlying the unexpected results, providing insights into the complex interaction of K⁺ channel subunits in SGNs.

PD - 124

Genetic, Cellular and Functional Evidence for Ca²⁺ Inflow Through Cav1.2 and Cav1.3 Channels in Murine Spiral Ganglion Neurons

Hyo Jeong Kim¹; Ping Lv²; Jeong-Han Lee¹; Choong-Ryoul Sihm¹; Somayeh Fathabad¹; Wenying Wang¹; Karen Doyle¹; Ebenezer Yamoah¹

¹University of California Davis; ²Hebei Medical University

Background

Spiral ganglion neurons (SGNs) of the eighth nerve serve as the bridge between auditory hair cells and the cochlear nucleus. In mammals, SGNs are equipped with multiple Ca²⁺ channels (Ca_v) to mediate Ca²⁺-dependent functions. Ca²⁺ inflow through Ca_v in auditory neurons in spiral ganglion triggers neurotransmitter release to induce short-term synaptic plas-

ticity and thereby orchestrates peripheral auditory information coding. For long-term structural changes and growth, membrane depolarization and Ca^{2+} inflow through L-type Ca_v promote SGN survival *in vitro*. Here, we examined L-type channels in SGN using $\text{Ca}_v1.3^{+/+}$ and $\text{Ca}_v1.3^{-/-}$ mice to determine the differential roles of $\text{Ca}_v1.2$ and $\text{Ca}_v1.3$.

Methods

SGN tissue was dissected and split into three equal segments apical, middle and basal across the modiolar axis. Apical and basal segments were used to ensure adequate viable neuronal yield for the experiments

Whole-cell and cell-attached single channel voltage-clamp recordings of $\text{Ca}^{2+}/\text{Ba}^{2+}$ currents were performed on cultured SGNs. Existence of $\text{Ca}_v1.2$ and $\text{Ca}_v1.3$ expression in SGNs were examined using immunostaining in cryosections of the cochlea as well as cultured SGNs.

Results

Significant membrane hyperpolarization, prolongation of action potential duration, latency, and spike numbers ($P < 0.01$) were observed in isolated $\text{Ca}_v1.3^{-/-}$ neurons.

Application of two different DHP antagonist, nifedipine (10 μM) and nimodipine (5 μM), resulted in a significant reduction of whole-cell Ca^{2+} currents from $\text{Ca}_v1.3^{-/-}$ SGNs. A remnant L-type current persisted after null deletion of *Cav1.3*. Additionally two-distinct DHP-sensitive single-channel Ba^{2+} currents were recorded from wild-type SGNs from single-channel patches in the cell-attached configuration.

Positive labeling against $\text{Ca}_v1.2$ and $\text{Ca}_v1.3$ were observed in the membrane and cytoplasm of apical and basal SGNs in both isolated neurons as well as cryosections of the cochlea.

Conclusion

The DHP-sensitive current in $\text{Ca}_v1.3^{-/-}$ SGN is derived from $\text{Ca}_v1.2$ channel activity. SGNs functionally express the cardiac-specific $\text{Ca}_v1.2$ as well as neuronal $\text{Ca}_v1.3$ channels. We will discuss the functions of the L-type channel subtypes in SGNs.

PD - 125

The Effects of Aging on Dynamic and Static Encoding of Speech Processing

Alessandro Presacco; Rachel Lieberman; Kimberly Jenkins; Samira Anderson
University of Maryland

Background

Older adults often report that during a conversation they can hear what is said, but cannot understand the meaning, particularly in a noisy environment. Recently, Anderson et al. (2012) showed that the loss of temporal precision may be one of the key factors causing subcortical timing delays and decreases in response consistency and magnitude in older adults. In that study, Anderson and colleagues used the speech syllable /da/, which is characterized by transient (/d/) and steady-state (/a/) regions, because stop consonants are particularly challenging to younger and older populations. A key finding of the study was that the timing delays were present in response

to the transition region only, not the steady state. Here, we compared subcortical responses in younger and older adults with normal hearing to the stop consonant (/da/) and the vowel (/a/), hypothesizing that aging mainly affects dynamic rather than static encoding of speech components.

Methods

Participants comprised 10 young adults (21 – 30 years old) and 10 older adults (59 - 69 years old) with normal hearing and normal IQ scores who had no history of neurological or middle ear disorders and were native English speakers. Frequency following responses were recorded at a sampling rate of 13.3 kHz to 170-ms speech syllables, /da/ and /a/, presented binaurally with alternating polarities at 80 dB SPL at a rate of 4.3 Hz through electromagnetically shielded insert earphones. Six thousands sweeps for each syllable were recorded, averaged and band-pass filtered (70 – 2000 Hz).

Results

Older adults show a significant shift in neural response timing for the onset in both /da/ and /a/. However, this shift does not extend past the onset in the /a/ response because of the steady-state nature of the stimulus. Conversely, in the /da/ response, significant differences are observed in the transition before the steady state, presumably because of the dynamic nature of that region. For both syllables, a significant reduction in the amplitude of the fundamental frequency (100 Hz) over the entire response was observed.

Conclusion

Our results showing that timing delays are specific to the onset and the transition regions of speech stimuli reinforce the hypothesis of a selective timing deficit for dynamic speech encoding rather than a pervasive delay in older adults. This timing deficit could contribute to the difficulty experienced by older adults in extracting the correct meaning of speech.

PD - 126

Reduced Expression of Critical Inner Ear Genes With Aging

Dennis Trune; Fran Hausman; Beth Kempton; Barbara Larrain; Carol MacArthur
Oregon Health & Science University

Background

While it is known that aging has a significant effect on the cochlear hair cells, it is not clear if other ear functions are compromised with age. This could lead to direct tissue degeneration, as well as reduce the ability of the ear to protect itself from insults such as inflammation, noise trauma, vascular compromise, ototoxic drugs, etc.

Methods

To begin evaluating gene expression in the aging ear, we measured the expression of multiple inner ear genes as aging progressed in 3, 6, and 11 month old (N=8 each age) Balb/C mice. Inner ears were collected, RNA harvested, and evaluated by qRT-PCR of genes related to tissue remodeling, ion homeostasis, and innate immune response cytokines.

Results

Compared to the 3 month old mice, older mice showed altered expression for a significant number of genes as aging progressed. A panel of 8 cytokine genes showed only IL-10 and TNF α were slightly upregulated at 11 months, 2.7 and 1.5 fold, respectively. Thus, cytokine expression was largely unaffected. Of the 24 ion homeostasis genes assessed, half were significantly suppressed. These involved mainly the ATPases, aquaporins, gap junctions, K⁺ channels, and Na⁺ channels. Only Gjb3, aquaporin 3, and one Na⁺ channel were expressed at higher levels than at 3 months. A significant number of tissue remodeling genes also were affected by 11 months, also mostly downregulated. These included matrix metalloproteinases, bone morphogenetic proteins, and FGF receptors. Only the FGFs as a group were routinely expressed at higher levels than in the younger mice.

Conclusion

These results show a significant impact of aging on the inner ear, with most genes expressed at lower levels compared to 3 month old mice. This reduction in normal ion homeostatic and tissue metabolic functions could reduce the ability of the ear to respond to insults and make it more susceptible to hearing loss as aging proceeds.

PD - 127

Calcium-Related Neuronal Activity in Auditory Brain Structures After Age-Related or Noise-Induced Hearing Loss – a Manganese-Enhanced MRI Study

Moritz Gröschel¹; Nikolai Hubert¹; Susanne Müller²; Arne Ernst¹; Dietmar Basta¹

¹Department of Otolaryngology, Unfallkrankenhaus Berlin, Charité Medical School, Germany; ²Neuroscience Research Center, Charité University Medicine Berlin, Germany

Background

Beside functional and structural changes in the periphery, hearing loss has profound impact on the central auditory system as well. Recent studies demonstrated several pathologies in different structures, e.g. neuronal hyperactivity, changes in synaptic transmission or neurodegeneration. However, it remains unclear how far the observed effects differ in relation to the cause of hearing loss. Using manganese-enhanced MRI, we were able to show that a noise trauma induces alterations in calcium-related neuronal activity in central auditory structures, whereby the observed effects vary depending on the time of investigation. Therefore, it was the aim of this study to compare the time-dependent changes in calcium-dependent neuronal activity in mice with age-related or noise-induced hearing loss.

Methods

One group of mice (NMRI strain) was exposed to traumatizing broadband noise (5-20 kHz at 115 dB SPL for 3 hours). Another group consisted of old animals showing age-related hearing loss. Auditory threshold shifts were determined by ABR recordings. Calcium-dependent neuronal activity was measured by 7T-MRI scanning 24 hours after injection of a manganese chloride solution. Hearing loss and MRI signal

strengths in several central auditory structures were measured in both groups at different points in time and compared to normal hearing controls.

Results

The ABR recordings demonstrate a significant threshold shift in the experimental groups compared to normal hearing animals. The level of hearing loss is independent of the time of investigation within the groups. Further, animals with age-related and noise-induced hearing loss show an increase in manganese accumulation in several structures compared to controls in the earlier measurements, which is followed by a subsequent decline at the later points in time.

Conclusion

The data indicate that hearing loss has large effects on calcium-dependent activity in central auditory structures. Although auditory threshold shift seems to be persistent over the investigated period, calcium-dependent neuronal activity is increased over a specific period in both noise-induced and age-related hearing loss and decreases afterwards. These effects could be explained by the appearance of hyperactivity and especially neuroplasticity early after the onset of threshold shift, whereby these processes are partly reduced in case of a permanent, long-lasting hearing loss. Future studies should investigate further correlations of pathophysiological changes in central auditory structures between age-related and noise-induced hearing loss to give a more detailed insight into similarities in the underlying mechanisms.

PD - 128

Relationship Between Frequency Following Responses and Other Measures of Auditory Function in an Animal Model of Aging

Aravindakshan Parthasarathy; Jyotishka Dutta; Edward Bartlett

Purdue University

Background

Hearing thresholds determined using auditory brainstem responses (ABRs) to brief stimuli are the predominantly used clinical measure to objectively assess auditory function. However frequency-following responses (FFRs) to longer-duration stimuli are rapidly gaining prominence as a measure of complex sound processing in the brainstem and midbrain. In spite of numerous studies reporting changes in hearing thresholds, ABR wave amplitudes and the FFRs under pathological conditions, including aging, the relationships between the FFRs and the ABRs are not clearly understood. In this study the relationships between ABR thresholds, ABR wave amplitudes and FFRs are explored in a rodent model of aging.

Methods

ABRs to broadband click stimuli and FFRs to sinusoidally amplitude modulated noise carriers were measured in young (3-6 months) and aged (22-25 months) Fischer-344 rats. ABR thresholds and amplitudes of the different waves as well as phase locking amplitudes of FFRs were calculated. Responses from neurons of the inferior colliculus (IC), a known

generator of the evoked potentials, were measured to similar stimuli.

Results

Age-related differences were observed in all these measures, primarily as increases in ABR thresholds and decreases in ABR wave amplitudes and FFR phase-locking capacity. There were no observed correlations between the thresholds and ABR or FFR amplitudes. Significant correlations between the FFR amplitudes and most ABR wave amplitudes were observed in the young. However, these were not present in the aged. The neuronal measures of synchrony in the IC were correlated to a greater degree with the FFRs, especially in the aged.

Conclusion

These results suggest that ABR thresholds, ABR wave amplitudes and FFRs measure different neurophysiological processes, and these measurements change asymmetrically with age. How this relates to the underlying changes in neural processing remains unclear.

PD - 129

Studies on Tinnitus and Hyperacusis After Loss of Auditory Function in the Aging Rat

Lukas Rüttiger; Dorit Möhrle; Sze Chim Lee; Dan Bing; Mahdih Alinaghikhan; Ksenia Varakina; Marlies Knipper
University of Tübingen

Background

Progressing loss of sensory function is a major problem of aging populations. In humans and animals, loss of auditory function becomes perceptible by increased hearing thresholds, altered sound processing of temporally and spatially modulated auditory stimuli, but also through abnormal perception of above-threshold sounds or phantom perceptions, like hyperacusis and tinnitus (Knipper et al. *Prog Neurobiol* 2013; Singer et al. *Mol Neurobiol* 2013).

Methods

The age related loss of synaptic structures, afferent synaptic contacts, and auditory fibers was studied in an animal model on young (3-9 month old) and aged (20-24 month old) rats. The impact on the hearing sensation was monitored by auditory evoked brainstem responses (ABR) and otoacoustic emissions (DPOAE). Hyperacusis and tinnitus sensation were tested using a behavioral approach (Rüttiger et al. *Hearing Res* 2003). To gain insight into the function of the ascending auditory pathways above-threshold responses to click and frequency specific stimuli were analysed in detail for recruitment and latencies of ABR wave deflections (wave amplitudes and latencies).

Results

Auditory thresholds are increased and auditory response range is reduced over age. Loss of auditory function was related to a loss of IHC synaptic structures similar to what was reported recently for the aging mouse (Sergeyenko et al. *J Neurosci* 2013). Characteristic changes over age are similar to changes observed after exposure to traumatizing sound. However, preliminary results from behavior studies on young

and aged rats show that the brain may compensate for the peripheral loss (Rüttiger et al. *PLoS1* 2013), preventing tinnitus or hyperacusis

Conclusion

Age related and noise induced decline of hearing function are correlated with auditory responses and morphological specifications of hair cell molecular phenotype. Behavior studies will clarify the individual impact of the observed functional and structural changes on tinnitus and hyperacusis in the rat.

PD - 130

An Evaluation of the Effect of Cognitive Impairment on Auditory Cortical Brain Volumes

Richard Gurgel; Priscilla Auduong; Jeffrey Anderson; Brandon Zielinski; Angela Wang; Cindy Weng; Norman Foster

University of Utah

Background

Epidemiologic studies have suggested that hearing loss is an independent risk factor for cognitive impairment. It is not known, however, whether this association is due to neurobiological susceptibility, psychosocial complications, or an artifact of cognitive test scoring when there is hearing loss. We hypothesize that as evidence of neurobiological susceptibility, the auditory cortex is affected by cognitive status. The objective of this study was to evaluate the degree to which cognitive impairment affects structural integrity of the auditory cortex.

Methods

High-resolution brain MRIs from 633 patients evaluated in a cognitive neurology specialty clinic were parsed to calculate grey-matter density in pre-specified brain regions. To normalize for individual variation in brain volume, we calculated ratios of grey matter volume between primary A1 auditory cortex and whole brain (A1-C ratio) as well as the planum temporale including A1, Heschl's gyrus, belt/parabelt regions and early auditory association cortex to whole brain grey matter density (AC ratio). Patients were compared by their mini-mental state exam (MMSE) performance. Patients were also compared based on their clinical diagnosis of probable Alzheimer's disease (AD) versus mild cognitive impairment (MCI). Multivariable general linear regression controlling for age and sex was performed.

Results

The adjusted average difference of the left and right AC ratios for patients with a MMSE ≤ 25 ($n=325$) compared to patients with MMSE >25 ($n=269$) was -0.03 (95% CI -0.04 to -0.02, $p<0.0001$) and -0.04 (95% CI -0.06 to -0.03, $p<0.0001$), respectively. There was no statistically significant difference in the A1-C ratios between the MMSE groups. The adjusted averaged difference of left and right AC ratios between AD patients ($n=218$) compared to MCI patients ($n=121$) was -0.03 (95% CI -0.05 to -0.01, $p=0.004$) and -0.05 (95% CI -0.07 to -0.03, $p<0.0001$), respectively. There was no statistically sig-

nificant difference in the A1-C ratios between the AD and MCI groups.

Conclusion

The auditory association cortex for patients with MMSE ≤ 25 and for those with AD shows greater relative atrophy when compared to patients with better cognitive function. Interestingly, there was no difference between subjects when evaluating only the primary A1 auditory cortex. This finding raises the possibility that while patients with impaired cognition may have intact neural hearing, their ability to make meaningful cortical connections and interpret sounds could be impaired.

PD - 131

The Harwell Aging Mutant Screen Identifies Novel Models of Age-Related Hearing Loss

Michael Bowl¹; Carlos Aguilar¹; Sue Morse¹; Joanne Dorning¹; Prashanthini Shanthakumar¹; Ruairidh King¹; Lauren Chessum¹; Laura Wisby¹; Michelle Simon¹; Andrew Parker¹; Giorgia Giotto²; Sally Dawson³; Paolo Gasparini²; Sara Wells¹; Paul Potter¹; Steve Brown¹

¹MRC Harwell; ²University of Trieste; ³UCL Ear Institute

Background

Age-related hearing loss (ARHL), also called presbycusis, is the most common sensory deficit experienced by the elderly. The prevalence of the condition increases significantly with age, and contributes to social isolation, depression, and loss of self-esteem. ARHL is a complex disorder that is not fully understood, but the onset and progression of this condition is known to be influenced by environmental factors and genetic susceptibility. Elaborating the genetics of ARHL will allow the development of therapeutic strategies to ameliorate hearing deterioration. However, the study of ARHL in humans is very limited, due to the genetic heterogeneity within the population and the age of onset, therefore we are utilizing age-challenged mice to investigate the genetics of ARHL.

Methods

At MRC Harwell we are undertaking a large-scale *N*-ethyl-*N*-nitrosourea (ENU) mutagenesis screen to generate mouse models of age-related disease. G3 pedigrees, of ~100 mice, are bred and enter a phenotyping pipeline comprising recurrent assessment across a wide range of disease areas, up to 18 months of age. The Deafness Models and Mechanisms team is taking advantage of this screen to identify models of ARHL, employing recurrent Clickbox and Auditory-Evoked Brainstem Response phenotyping.

Results

As of September 2013, 126 pedigrees have entered the pipeline, of which 103 have completed auditory screening. To date 18 pedigrees (~14%) have confirmed auditory phenotypes. Of these, 12 pedigrees display early-onset hearing loss, as evidenced by elevated hearing thresholds by 3 months of age, and 6 pedigrees exhibit ARHL with elevated hearing thresholds evident from 6 months of age. To date, 5 of the ARHL pedigrees have been mapped and whole genome sequenced, identifying lesions in 3 novel, and 2 known, deafness-associated genes. Interestingly, we have shown that 2 of the novel genes show association with age-related

auditory function in humans. Studies to relate mutant gene to phenotype are ongoing. Genome mapping and sequencing of the remaining ARHL pedigree is underway.

Conclusion

The Harwell Aging Mutant Screen is producing pedigrees with interesting age-related auditory phenotypes resulting from lesions within novel and known hearing loss-associated genes. Investigation of these, and as yet unidentified pedigrees, promises to increase our understanding of the genetics and pathobiology of ARHL.

PS - 431

Rapid Task-Dependent Plasticity in Local Field Potentials from Primary Auditory Cortex

Nikolas Francis; Diego Elgueda; Jonathan Fritz; Shihab Shamma

University of Maryland

Background

Auditory task-dependent spiking activity in primary auditory cortex (A1) is characterized by increased differential responses to behaviorally meaningful sounds (Fritz et al, 2003; David et al, 2012). Because local field potentials (LFPs) are largely generated by synaptic currents that drive spiking activity, we hypothesized that auditory task-dependent plasticity could also be observed in A1 LFPs.

Methods

Two ferrets were trained on a conditioned avoidance pure-tone detection task. In each trial, a series of rippled noise stimuli was followed by a pure-tone. Ferrets were trained to refrain from licking a water spout upon detection of the target tone. We recorded LFPs in A1 using a 24-channel laminar probe (Plextrode) in behaving, head-fixed ferrets to study auditory task-dependent LFP plasticity across the depths of A1. Penetrations were made orthogonal to the cortical surface. Laminar electrode sites were spaced 75 μ m apart, covering 1.8 mm of a cortical column.

Results

We found a pattern of auditory task-dependent LFP plasticity that was dynamic, frequency specific, and decayed quickly after the end of the behavioral session. During the task, low frequency power (<30 Hz) was suppressed for both noise and tones (ie., reference and target sounds, respectively). The suppression was greater for references than targets, and was greatest near stimulus onsets, where suppression was also observed at frequencies above 30 Hz. The latency and magnitude of task-dependent changes in LFP waveforms varied across cortical layers.

Conclusion

Our results confirm the existence of task-dependent LFP plasticity in sensory cortex, and extend this phenomenon to auditory cortex. The LFP plasticity resembled single-unit plasticity in that there were two distinct task-related changes: (1) in general, LFPs tended to be suppressed as a result of performing an auditory task and (2) the suppression differed according to a sound's behavioral meaning. The laminar structure of LFP plasticity suggests that task-related informa-

tion is processed differently across layers to produce task-dependent spiking activity. Further analyses on these data will include comparisons of LFP-based spectro-temporal receptive fields, and correlating changes in LFP features with task performance.

PS - 432

Thalamocortical Organization in the Mustached Bat (*Pteronotus Parnellii*): Distribution of Calcium-Binding Proteins

Julia Heyd¹; Emanuel C. Mora²; Manfred Kössl³; Marianne Vater⁴

¹University of Potsdam; ²Research Group in Bioacoustics and Neuroethology, University of Havana, Havana, Cuba;

³Institute for Cell Biology and Neuroscience, University of Frankfurt, Frankfurt 60438, Germany; ⁴Institute for Biochemistry and Biology, University of Potsdam, Potsdam 14476, Germany

Background

The calcium-binding proteins (CaBPs) calbindin D-28K (CB) and parvalbumin (PV) differentiate the core- and belt-regions of the auditory forebrain in several mammalian species (e.g. Jones, EG 2003; Ann N Y Acad Sci 97:218-33). The labeling with PV is heaviest in the tonotopically organized core-regions (ventral division of the auditory thalamus and primary auditory cortex) whereas the labeling-pattern with CB shows a complementary distribution, with intense labeling of non-tonotopically organized belt regions of the auditory thalamus (dorsal and medial division), that project more diffusely to primary and nonprimary auditory cortex.

Methods

In order to further investigate the thalamocortical organization in the mustached bat, we analyzed the CaBP distribution in the auditory cortex (AC) and in the medial geniculate body (MGB). We employed immunoperoxidase- and double-immunofluorescence-techniques using antibodies directed against PV, CB and a third CaBP, calretinin (CR).

Results

Most MGB-subdivisions contained double-labeled neuronal somata (CR/PV and CB/PV) and could not be differentiated by their CaBP profiles. Significantly, the distribution of CaBP in nontotopically organized dorsal and rostral subdivisions devoted to specialized processing of the echolocation signal was similar to that of the adjacent tonotopically organized ventral division of the MGB. There were no conspicuous differences in the distribution of CaBP-ir somata and neuropil between the tonotopically organized primary AC and the dorsally located nontotopically organized "FM/FM"-area that is sensitive to echo delay.

Conclusion

These findings support a redefinition of the affiliation of functional areas of the AC and MGB of the mustached bat to core and belt regions (Pearson JM et al. 2007; J Comp Neurol 500:401-18). It is suggested that the FM/FM area as well as other nontotopic fields of the AC involved in processing of

sonar signals as well as their MGB input belong to the lemniscal system and represent core regions.

PS - 433

The Effect of Audiovisual Synchrony on Cortical Responses and Target-Detection Performance: A Functional Near-Infrared Spectroscopy (fNIRS) Study

Ian Wiggins; Douglas Hartley

NIHR Nottingham Hearing Biomedical Research Unit

Background

Deafness is associated with changes in multisensory processing that may have a bearing on cochlear implant (CI) outcome. Functional near-infrared spectroscopy (fNIRS) is an optical neuroimaging technique that is well suited to studying these issues because of its non-invasiveness and compatibility with CI use. This initial study with normal-hearing listeners aimed to evaluate the feasibility of using fNIRS to measure a modulatory influence of sounds on brain activity in visual cortex, as the temporal synchrony between auditory and visual events was varied.

Methods

Participants were asked to respond as quickly as possible to occasional "target" flashes (checkerboards with moderate contrast ratio) presented within a stream of "standard" flashes (checkerboards with low contrast ratio). The mean flash rate was ~1.6 Hz and "targets" occurred every 2–5 s. The flashes were presented alone or alongside streams of synchronous or asynchronous 1-kHz tone pips. In the asynchronous case, flashes and tone pips were separated by at least 200 ms. Though the sounds did not provide any task-relevant information, based on past fMRI studies that used related paradigms, we hypothesized that, compared to visual-only stimulation, detection of visual targets would be enhanced (made quicker and more accurate) by synchronous sounds, and degraded by asynchronous sounds. Simultaneously with the psychophysical task, visual-cortex haemodynamic responses were measured using a Hitachi ETG-4000 fNIRS system, with a 3x5 optode array placed over the occipital lobe. A block-design paradigm was used with 20 s stimulation periods, 20–40 s rest periods, and 5 repetitions of each condition.

Results

Preliminary data from 16 participants suggest that, contrary to our experimental hypothesis, participants made significantly more errors (misses and false alarms) when synchronous sounds were presented. The sounds did not have any clear effect on response times. Preliminary analysis of the fNIRS data suggests that the degraded behavioural performance with synchronous sounds was associated with a weaker haemodynamic response in visual cortex, possibly reflecting a distraction of attention away from the visual domain.

Conclusion

Preliminary results suggest that the presence of synchronous task-irrelevant sounds degraded visual target-detection accuracy and led to a weaker haemodynamic response in visual cortex, seemingly at odds with past studies. Ongoing work

aims to confirm these preliminary findings and to identify the stimulus-related and procedural factors determining the nature of this audiovisual interaction.

PS - 434

Discrimination of Vcoded Speech in the Ascending Auditory System

Mark Steadman; Chris Sumner

MRC Institute of Hearing Research

Background

The auditory system has a remarkable ability to extract salient information from spectrally and temporally degraded inputs. This has been shown in many studies involving cochlear implant users and vocoded speech. The perceptual effects of this type of degradation on speech recognition are well established, but the neural bases of these are not yet clear.

Methods

A set of 16 vowel-consonant-vowel phoneme sequences with varying medial consonants each produced by 3 male talkers were processed using a noise vocoder and presented to anaesthetised guinea pigs. The number of vocoder channels was varied between 1 and 8, and envelope bandwidth between 16 and 500 Hz. Extracellular responses were recorded in the inferior colliculus (IC) and primary auditory cortex (A1). Auditory nerve (AN) responses were generated using a model of the guinea pig cochlea. Response pattern discriminability was quantified using a classifier. The classifier was trained on average response patterns for each consonant and novel responses were classed as the consonant whose average pattern was closest in Euclidean space. Response patterns were allowed to temporally shift such that all distances were minimised. Responses were also parametrically smoothed to examine the effect of spike timing precision on neural discriminability.

Results

AN and IC performance was as good as or better than human performance in all conditions. For unprocessed speech, 1 channel 500 Hz and 8 channel 16 Hz speech, performance was near perfect. However the temporal resolution of this information differed. In the AN model, response discriminability was a low pass function of the smoothing window duration and best for the shortest (1 ms) window. In the IC, discriminability was a bandpass function of the smoothing window; it fell off rapidly at < 2ms, and only gradually at long analysis windows (>> 10ms), even for unprocessed speech. Preliminary recordings in A1 suggest that the discriminability of neural representations of medial consonants is, under anaesthesia, much poorer than at subcortical sites. Additionally, unlike previously reported results for onset responses to consonants, discrimination was poor for the shortest analysis windows, peaking at around 100ms.

Conclusion

These results show a systematic change in the representation of degraded speech up the auditory pathway. Subcortically, fine timing information carries information useful for discriminating speech tokens even when high rate envelope cues have been removed from the stimulus.

PS - 435

Facilitated Inhibition Biases Tritone Comparison in a Network Model

Chengcheng Huang¹; Bernhard Englitz²; Shihab Shamma³; John Rinzel⁴

¹New York University; ²Auditory Behavior & Computational Neuroscience Group, Equipe Audition, Ecole Normale Supérieure, Paris; ³Auditory Behavior & Computational Neuroscience Group, Equipe Audition, Ecole Normale Supérieure, Paris. The Institute for Systems Research, University of Maryland, College Park, United States; ⁴Center for Neural Science and Courant Institute of Mathematical Sciences, New York University

Background

Perception can be strongly influenced by preceding context. Ambiguous stimuli are well suited to study the contextual effect. Shepard tones are comprised of octave-spaced pure tones, represented by their base pitches within one octave. A sequentially played pair of Shepard tones can be perceived as ascending or descending if the second tone is less than one-half octave above or below, respectively, the first tone [Shepard 1964]. The comparison task is ambiguous when two Shepard tones are separated by a half octave (tritone). However, using a preceding sequence of Shepard tones with base pitches between the tritone pair biases the shift perception - toward ascending/descending for biasing tones above/below the first tone [Chambers 2011]. Paradoxically, a pitch-based decoding algorithm of neurophysiological recordings indicates a repulsive shift of the neural tone representations [Englitz 2012], raising questions about mechanisms.

Methods

Our network model consists of 3 subpopulations (linear arrays, with tonotopy): two excitatory arrays (UP and DOWN) that drive a common inhibitory array that provides recurrent feedback but with oppositely directed asymmetric footprints (Fig1). Inhibitory synapses slowly facilitate, strengthening inhibition in the biasing direction. From the particular spectral property of Shepard tones, our model inherits a ring structure with periodic boundary conditions. Decisions are made by comparing response levels of UP and DOWN units to the test pair.

Results

The UP and DOWN units are direction selective (for successive tone pair presentations) due to the asymmetric inhibition [Kuo&Wu 2011]. Comparisons of Shepard tone pairs using the model agree with those in psychophysical studies. When preceded by biasing tones with frequencies above the first tone, the tritone pair, ambiguous without biasing, leads to a dominant UP response, i.e. Ascending (Fig2). The facilitation level of inhibitory synapses accumulates in the biasing region (between the tritone pair). The biasing effects gradually build up with the number of bias tones, reaching above 90% after 5 tones. Non-uniform inhibitory synaptic strengths can account for variation among subjects in the tritone paradox. We compare alternative mechanisms for adaptation, such as feedforward synaptic depression and intrinsic spike-frequency adaptation with our model within this idealized framework.

Conclusion

Our model can detect the direction of change in pitch by comparing the responses of UP and DOWN units. Previous tones facilitate inhibitory synaptic strengths, resulting in activity reduction (adaptation) inside the biasing region and enlargement of the detection range for UP and DOWN units at the upper and lower boundaries of the biasing region, respectively.

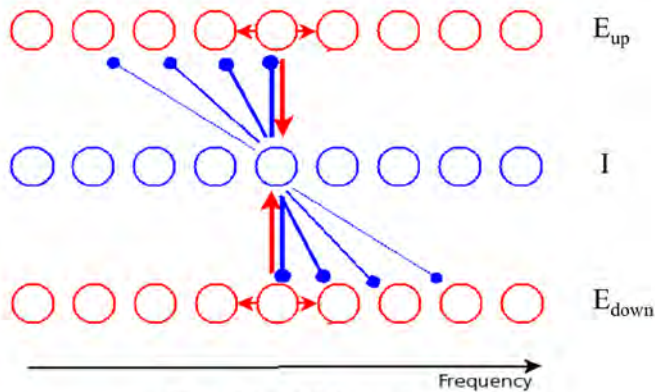


Fig 1: Model Schematic.

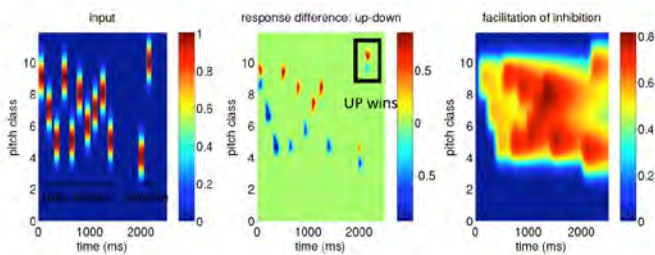


Fig 2: Response to tritone pair preceded by 10 biasing tones. Left: input; middle: response difference $E_{up} - E_{down}$; right: facilitation level of inhibition.

PS - 436

Cortical Representation of Spectrally Degraded Speech: An Intracranial Electrophysiology Study

Kirill Nourski¹; Ariane Rhone¹; Mitchell Steinschneider²; Hiroto Kawasaki¹; Hiroyuki Oya¹; Matthew Howard¹

¹The University of Iowa; ²Albert Einstein College of Medicine

Background

Accurate speech perception can occur despite considerable amounts of signal degradation. This phenomenon is exemplified by cochlear implant users who demonstrate remarkable speech comprehension despite severely limited spectral information provided by the implant. Understanding the cortical processing of speech spectrally degraded by noise vocoding can help define the specific roles of different auditory cortical fields in speech perception and potentially contribute to improvements in cochlear implant design and stimulation paradigms. This study investigated cortical responses to natural and spectrally degraded speech in normal hearing individuals.

Methods

Experimental subjects were neurosurgical patients undergoing chronic invasive monitoring for medically refractory epilepsy. Stimuli were nonsense utterances /aba/ and /ada/, spoken by a male talker. The stimuli were spectrally degraded using a noise vocoder (1-8 bands) and were presented in target detection and stimulus identification tasks. Electrophysiological data were recorded simultaneously from Heschl's gyrus (HG) and lateral superior temporal gyrus using multicontact depth electrodes and subdural grid arrays, respectively. Responses were characterized as averaged auditory evoked potentials (AEPs) and event-related band power (ERBP).

Results

Natural and noise-vocoded stimuli elicited short latency AEPs and high gamma (70-150 Hz) responses that were similar in magnitude across the electrodes located in posteromedial HG (core auditory cortex). AEPs featured additional peaks that reflected changes in the stimulus envelope and, in responses to natural (unprocessed) stimuli, frequency-following responses to the voice fundamental. Responses to natural and vocoded stimuli from non-core cortex on anterolateral HG were also similar in magnitude and had longer latencies than those in auditory core. In posterolateral superior temporal gyrus (PLST), natural stimuli elicited substantially larger and broader patterns of activation compared to spectrally degraded stimuli regardless of the number of vocoder bands. While early response components were typically similar across vocoded stimuli, later components of high gamma response were found to parallel stimulus intelligibility in some sites. The differences between natural and spectrally degraded speech were observed in data obtained from PLST of both left and right hemispheres.

Conclusion

The present findings indicate a marked difference in processing of noise-vocoded and natural speech within non-core auditory cortex (PLST). Activity in this area is influenced by stimulus acoustics and intelligibility. The results are consistent with the proposed role of PLST in transforming acoustic input into phonetic representations. Responses to vocoded speech in naïve normal hearing listeners are hypothesized to approximate cortical speech processing in cochlear implant users following device activation.

PS - 437

Differential Attentional Modulation of Auditory Responses to Speech in Different Listening Conditions

Ying-Yee Kong¹; Ala Mullangi¹; Nai Ding²

¹Northeastern University; ²New York University

Background

Recent work on the neural mechanisms for auditory attention has shown enhanced phase-locked responses to the temporal envelope of the attended speech stream in a competing background. This study further investigates how selective attention differentially modulates auditory cortical responses in different listening conditions: in quiet, with weak speech interference, and with strong speech interference.

Methods

Continuous speech was presented via insert earphones to the subjects. Each subject was tested under two quiet listening conditions (active and passive listening) and two noise conditions at 6dB and 0dB signal-to-noise ratios (SNRs). For noise conditions, subjects attended to one of two speech streams presented diotically. Ongoing EEG responses were measured in each condition. Cross-correlation between the speech envelope and the EEG responses was calculated at different lags.

Results

In quiet, similar neural phase-locked response to the speech envelope was found for the active and passive listening conditions. The cross-correlation function showed a positive peak with latency near 150ms. When two speech streams were presented simultaneously, cortical activity was more correlated with the attended speech than the unattended speech at both 6dB and 0dB SNRs. The cross-correlation function showed one negative and one positive peak with latencies near 90 and 180ms, respectively. The positive peak of the cross-correlation function for the attended speaker was delayed compared to the positive peak for speech in quiet. The cross-correlation function for the unattended speaker, however, only showed a positive peak at 50ms.

Conclusion

Cortical activity was phase locked to the temporal envelope of speech. In quiet, these responses remained robust in a passive listening condition where listeners were distracted by visual interferers. The longer peak latency for the attended speech in a competing background compared to the quiet conditions may indicate the differences in the level of difficulty of the tasks. The opposite signs of correlations between the attended and unattended speech supports the neural mechanism of suppression of the competing speech stream.

PS - 438

A Minimal Neuromechanistic Model for Stimulus Specific Adaptation (SSA).

Li Shen¹; Zitian Yu¹; Bo Hong¹; John Rinzel²

¹Tsinghua University; ²New York University

Background

Neuronal responses to a frequently presented tone (the 'standard') decrease but not for rare or deviant tone stimuli. This phenomenon is called stimulus specific adaptation (SSA) and relates to novelty detection. Distributed network models test various hypotheses for neuronal adaptation mechanisms of SSA: synaptic depression (SD) either feedforward (Mill et al, 2012) or recurrent within the network (Yarden et al, 2011) or intrinsic cellular (spike frequency) adaptation, SFA (Yu et al, 2012).

Methods

Our minimal, firing-rate, network model consists of frequency-specific excitatory (e) and inhibitory (i) subpopulations with a reduced tonotopic architecture having three e-i pairs: pair "1" driven mostly by tone f1 and least by tone f2, pair "2" driven mostly by f2 and pair "0" (the recording location) driven some by f1 and f2 (Fig1). We allow adaptation as: "internal"

with recurrent SD and SFA (SFA occurs only in e-units) or "external" with feedforward SD.

Results

Each local e-i pair shows, for step "sound" input, a sizable onset response and sustained response. Recurrent self-excitation leads to local amplification. The driven response, say of pair "1" to f1, may be large and spreads to "0" with attenuation, not full amplitude propagation. Each mechanism for adaptation can support SSA. With SFA, adaptation develops primarily in the e-unit being most driven directly; the affect transfers with attenuation to "0" (Fig1). For feedforward SD, adaptation is independent of the network's responses. The model's behavior (with internal adaptation) shows SSA trends as observed in experiments and with some models: stronger for decreased oddball probability, stronger for increased tone frequency difference (f2-f1), non-monotonic dependence on sound intensity. These dependencies are under study now for the external mechanism of feedforward SD. The sustained component appears to adapt more for external adaptation than for internal.

Conclusion

Our minimal firing rate model with lumped tonotopy exhibits observed dynamic features of SSA in the oddball paradigm. The model's framework enables comparison of the different adaptation mechanisms – "internal" (recurrent SD, intrinsic cellular SFA) or "external" (SD of feedforward afferents). SFA, when present, leads to strongest adaptation at the input site, affecting the observations at the recording location indirectly. Non-monotonic dependence on sound intensity arises from amplification by recurrent excitation at the deviant site.

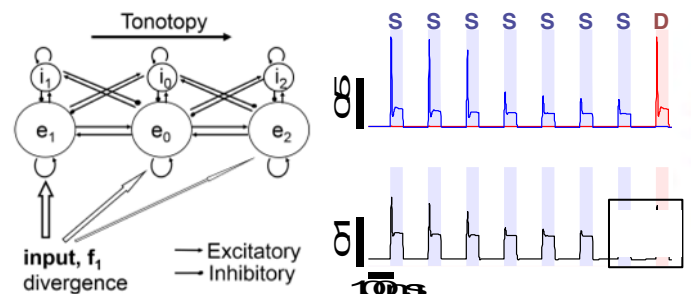


Fig1. Left, schematic of minimal network model. Right, illustrative time courses of firing rates in response to 7 successive STDs (f1) and 1 DEV (f2) at the primary input sites e_1 and e_2 (upper) and at the "recording site" e_0 (lower). Adaptation is "internal" due to intrinsic spike frequency adaptation (SFA) and synaptic depression of recurrent synapses that are driven by the excitatory subpopulations, e_i . The black box highlights substantial SSA in onset response and little in sustained response.

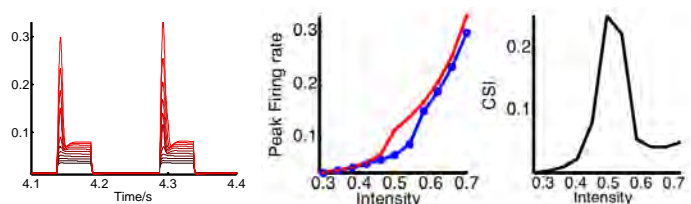


Fig2. Intensity dependence of SSA for the internal mechanism,

SFA. Left, firing rate time courses at e_0 for 7th STD and DEV (as in Fig1, right, black box) for range of input levels. Middle, peak firing rate for DEV (red) and STD (blue) and, right, CSI, (difference of peaks)/(sum of peaks), vs input intensity (right).

PS - 439

Deviant Responses to Harmonic Complexes in Auditory Cortex

Simon Jones; David McAlpine
UCL

Background

Human Electro-EncephaloGraphy (EEG) studies have shown that oddball stimulus blocks containing harmonic complexes with mistuned harmonics elicit responses with both a Mismatch Negativity (MMN) component and an Object Related Negativity (ORN) component. The underlying physiology and the brain regions involved remain obscure but animal models are routinely used for studying responses to oddball stimuli with pure tones. Human studies have employed oddball stimulus blocks of harmonic complexes with or without a mistuned component. Here, we examine responses to deviants from such blocks in a region of guinea pig primary auditory cortex (A1).

Methods

Tricolour guinea pigs were anaesthetised with urethane, A1 was exposed and a single-shank, 16-channel Neuronexus multi-electrode array was implanted through a 4x4 16 channel surface array. Stimuli, delivered to each ear through ear phones, consisted of 3 blocks of 500 stimuli; one a control condition with equal numbers of 400ms duration tuned and mistuned harmonics and two with a 10% deviant probability in which tuned or mistuned harmonic complexes were the standard and the other the deviant. For all harmonic complexes the fundamental frequency was 200Hz, the first 12 harmonics were used (up to 2400Hz), mistuning was always applied to the 400Hz component which was mistuned to 464Hz (16% mistuning) and the presentation period was 1300ms.

Results

Most A1 neurons generated greater firing rates in response to tuned harmonic complexes when these were presented as deviant stimuli than when they were presented as standard stimuli in sequence. This response pattern was reversed when mistuned stimuli were examined.

Conclusion

Many A1 cortical neurons respond to deviants with mistuned harmonics differently to deviants with tuned harmonics reflecting processing differences for the two stimuli that have also been observed in human EEG studies. Preliminary analysis suggests that typically both harmonic and mistuned deviants evoke changes in firing rates of A1 neurons, the former higher rates when presented in a stream of sounds with a mistuned harmonic, and the latter lower rates when presented in a stream of fully harmonic sounds.

PS - 440

ASSRs to Varying Depths of Amplitude Modulation in Young and Elderly Subjects

Andrew Dimitrijevic¹; Jamal Alsamri²; Sasha John³; David Purcell⁴; Sahara George²; Fan-Gang Zeng²

¹Cincinnati Children's Hospital Medical Center, University of Cincinnati; ²University of California, Irvine, Dept. Otolaryngology; ³University of Toronto, Dept. Biomedical Engineering; ⁴University Western Ontario, School of Communications Sciences and Disorders

Background

This study examines the use of Auditory Steady-State Responses (ASSRs) to objectively assess temporal processing ability. Auditory steady state responses are normally collected using 100% modulation depth. Although modulation-rate transfer functions have been explored by increasing the rate of the amplitude modulation (AM-rate), this has not been examined for amplitude modulation depth (AM-depth). Both measures should be examined since AM-rate and AM-depth may serve as objective measures related to the temporal modulation transfer function (TMTF) and temporal processing ability related to the perception of complex sounds such as speech.

Methods

Young and elderly subjects (aged 20 to 91) participated in the study. We explored the use of a stimulus sweep technique, in which the depth of AM of broadband noise stimuli continuously varied from 2% to 100%. We also quantified behavioral thresholds of AM detection using a 3-interval forced choice task.

Results

Significant ASSRs were elicited using the sweep AM depth technique. Young and elderly subjects differed in their AM depth vs. ASSR functions. Young subjects showed a steady increase in ASSR amplitude up to 100% while elderly subjects were characterized by an ASSR amplitude saturation near 40% AM depth. Significant correlations were seen between behavioural thresholds of AM depth detection and AM depth ASSR thresholds.

Conclusion

ASSR- AM depth functions differ with different age-related temporal processing abilities and may provide an objective measure of the TMTF.

PS - 441

Identification of Attended Speech Stream from Ongoing Cortical Response in Diotic Listening

Ala Mullangi¹; Nai Ding²; Shalini Purwar¹; Deniz Erdogmus¹; Ying-Yee Kong¹

¹Northeastern University; ²New York University

Background

Recent studies have shown that neural responses phase lock to the attended speech envelope in a cocktail party listening situation. This study investigates methods that could identify which speech stream the listener was attending to in a diotic listening condition based on EEG responses.

Methods

Eight participants attended to one of two speech streams presented diotically at equal intensities. Each participant was tested with four blocks of one-minute speech stimuli with each block consisting of 10 trials. Ongoing EEG responses were measured using a 16-channel g.USBamp system with a sampling rate of 256 Hz.

The EEG data was preprocessed by high-pass filtering with a cutoff frequency at 1Hz. Further filtering parameters were chosen based on individual subject data. Feature extraction for classification of the EEG signals was performed by cross correlating the neural responses with the known temporal envelope of each speech stream at different lags ranging from 0 to 400ms. The length of the data used for cross correlation varied from 5 to 40s. The dimensionality of the feature vector was then reduced using Principal Component Analysis (PCA). Regularized Discriminant Analysis (RDA) was used to classify the EEG signals. Area under the curve (AUC) was calculated to evaluate the classifier performance using 5-fold cross validation. Higher AUCs represent greater accuracy.

Results

Overall, AUC decreased as the trial length decreased. AUC was 0.70 or above for trial length of 40 and/or 20s for all participants and approached chance level performance at 5s. AUC values of 0.80-0.95 were found for three participants at the longest trial length of 40s.

Conclusion

Prior EEG classification studies were conducted when the two separate streams were presented dichotically (Lalor et al., 2013; Rajaram et al., 2013). Using our classification method, we demonstrated that high levels of classification accuracy could be achieved for diotic listening.

PS - 442

Characterization of the Direct Amygdalo-Cortical Connection

Gregory Mlynarczyk; Diana Peterson
Iowa State University

Background

Stimulus significance can alter the attention of an animal to auditory cues in its environment. The amygdala receives inputs from sensory, memory, and association cortices. It is thought that the combination of these inputs contribute to an animal's interpretation of sensory relevance. Projections from the amygdala back to sensory systems may alter the animal's attention to sensory cues. Amygdalar projections to auditory cortex occur through both direct and indirect pathways. The indirect pathway through the nucleus basalis of Meynert has been reported to have long-term (minutes, hours) plastic effects on cortical firing patterns. These changes are thought to be associated with auditory conditioning. Little is known about the direct amygdalo-auditory cortex pathway. The current experiments describe the anatomy and physiology of this direct pathway.

Methods

Anterograde and retrograde tracing techniques were utilized to label the direct amygdalo-auditory cortex projection. To identify a potential functional significance for the pathway, frontal cortex was removed and single-unit electrophysiological recordings were obtained in primary auditory cortex before, during, and after amygdalar stimulation.

Results

Neurons were labeled throughout the basal and lateral nuclei of the amygdala. A high percentage of these neurons were pyramidal, indicating glutamatergic projections. However, many non-pyramidal neurons were also labeled. The neurons terminate throughout both primary and secondary regions of auditory cortex with en passant and terminal boutons. Boutons were predominantly observed in layers V and VI, however less dense projections were observed throughout all cortical layers. Electrical stimulation of the amygdala (with the nucleus basalis pathway removed) had transient effects on the firing rate of neurons in auditory cortex.

Conclusion

The focus of amygdalo-auditory cortex terminals within layers V and VI indicate that the projection may target descending auditory pathways. Therefore it may also function to alter activity of lower-order auditory nuclei toward relevant sensory cues. Because the changes in cortical firing are transient, we hypothesize that the direct amygdalar projection may prime the cortical circuit and thereby influence the long-term plastic changes induced by the nucleus basalis of Meynert circuit.

PS - 443

Neural Representation of Concurrent Vowels in Monkey Primary Auditory Cortex: Implications for Models of Auditory Scene Analysis

Yonatan Fishman¹; Christophe Micheyl²; Mitchell Steinschneider¹

¹*Albert Einstein College of Medicine;* ²*Starkey Hearing Research Center*

Background

The ability to perceptually separate spectrally and temporally overlapping voices is critical for successful hearing in complex acoustic environments (e.g., a noisy cafeteria). Vowels contain a broad range of frequencies (harmonics) that are integer multiples of a common fundamental frequency (F0). When two spectrally-overlapping vowels differing in F0 are presented concurrently, they can be readily perceived as two separate 'auditory objects' with pitches at their respective F0s. Thus, a difference in pitch between two simultaneous voices provides a powerful cue for their segregation. Perceptual segregation of concurrent vowels is facilitated when their harmonics are individually resolved by the auditory system (Micheyl and Oxenham, 2010). We have shown (Fishman et al., 2013) that neuronal populations in monkey primary auditory cortex (A1) can resolve the lower harmonics of single harmonic complexes (HCs) via a 'rate-place' code. In principle, the pitches of the HCs can be extracted from these 'rate-place' representations via 'harmonic templates' implemented

by neurons in downstream cortical areas (e.g., Bendor and Wang, 2005). However, it is unknown whether A1 can represent the harmonics (spectral fine structure) and formants (spectral envelopes) of single and concurrent vowels differing in F0 with sufficient resolution to enable their identification and perceptual segregation.

Methods

Here, we examined neural representation of single and double concurrent vowels (/a/ and /i/) in A1 of alert monkeys using a stimulus design employed in auditory-nerve studies of pitch encoding (Larsen et al., 2008). F0s of the double vowels differed by 4 semitones, an amount sufficient for them to be heard as two separate 'auditory objects' with distinct pitches (Assmann and Paschall, 1998). Vowel F0s were varied in increments of 1/8 harmonic number relative to the best frequency of the recorded neural populations to generate 'rate-place' representations of the single and double vowels.

Results

We found that neural population responses could resolve lower harmonics of both single and double vowels and discriminate the vowels based on their spectral envelopes. Furthermore, rate-place representations of single vowels could be reliably recovered from rate-place representations of the concurrent vowels.

Conclusion

We conclude that A1 represents the lower harmonics and formants of concurrent vowels with sufficient resolution to enable their identification and perceptual segregation via template-matching mechanisms. Improved understanding of central mechanisms contributing to concurrent sound segregation may facilitate the development of approaches toward alleviating speech perception deficits in hearing-impaired listeners.

PS - 444

Cortical Pitch Response Components Indexes Multiple Attributes of Pitch Contours

Ananthanarayan Krishnan; Jackson Gandour; Saradha Ananthakrishnan; Venkat Vijayaraghavan
Purdue University

Background

Voice pitch is an important information-bearing component of language and music that is subject to experience dependent plasticity at both cortical and subcortical stages of processing. We recently demonstrated that the EEG derived Na component of the Cortical Pitch Response (CPR) is sensitive to both pitch and its salience (similar to the MEG derived pitch onset response (POR), presumably from the pitch processing center in the lateral Heschl's gyrus). In addition Na, the CPR is characterized by several transient components that may also carry pitch relevant information and may provide a new, complementary window to examine the influence of language/music experience on pitch encoding as well as shed more light on the hierarchical nature of pitch processing along the auditory pathways. To this end, we characterize here the multiple transient components of the CPR, and label them in relation to specific aspects of our dynamic, curvilinear pitch

stimuli (e.g., pitch onset, pitch acceleration, pitch duration, and pitch offset).

Methods

CPRs were recorded from 10 Chinese listeners in response to IRN stimuli, representing three variants of Mandarin Tone 2: short (T2_150), intermediate (T2_200), and long duration (T2_250). The average velocity rates (in st/s), for T2_250 (25.6), T2_200 (32.1), and T2_150 (42.7) fall within the physiological limits of speed of rising pitch changes. Each IRN stimulus contained a 500 ms noise precursor. Stimuli were presented binaurally at 80 dB SPL at a repetition rate of 0.93/sec.

Results

Absolute latency (Pb, Nb, and Pc) and the inter-peak latencies (Na-Pb, Pb-Nb) increased with decreasing acceleration rate, with smaller changes for Na and Pa. Peak-to-peak amplitude for components Na-Pb and Pb-Nb also increased systematically with decrease in pitch acceleration. Pa-Nc interval increased with duration. Pc/Nc latency was consistent with an offset response.

Conclusion

These results suggest that components of the CPR may be indexing different aspects of the pitch-eliciting stimulus. For example, components Na-Pb and Pb-Nb may index the more rapidly-changing portions of the stimuli, i.e. pitch acceleration; the time-invariant Na may reflect an initial estimate of pitch onset. Thus, the CPR provides a physiologic window to evaluate early, sensory level cortical processing of dynamic, curvilinear pitch stimuli that are ecologically representative of those that occur in natural speech. Thus, we are now able to investigate experience-dependent enhancements (language, music) in *pitch-specific* encoding at the cortical and brainstem levels concurrently that offers promise of illuminating the hierarchical nature of pitch processing along the auditory pathways.

PS - 445

Predicting Cortical Response Variability in Awake-Behaving Mice: The Role of Arousal, Behavioral Performance, and Auditory Stimuli

Matthew McGinley¹; Stephen David²; David McCormick¹

¹Yale University; ²Oregon Health and Science University

Background

Action-potential firing in cortical neurons is highly variable, even in response to repeated presentation of the same stimulus (Vogels, Spileers and Orban, 1989). Similarly, cortical membrane potentials (Vm) fluctuate irregularly at a wide range of frequencies in awake animals, likely shaping spiking variability. It has been widely hypothesized that behavioral state contributes substantially to the variability in sensory responses. However, a close relationship between quantitative behavioral state measures and cortical Vm has not been demonstrated.

Methods

To address this issue, we conducted whole-cell patch-clamp recordings of excitatory neurons in auditory cortex of head-

fixed mice on a cylindrical treadmill engaged in a psychometric auditory discrimination task. Mice were trained to detect a tone embedded in broadband rippled noise (temporally-orthogonal ripple combinations) in which the tone sound level varied trial-to-trial. Hit rates and reaction times varied systematically with tone level, allowing trial-by-trial assessment of behavioral performance. To independently measure arousal, a 16-channel laminar electrode was placed in CA1 of dorsal hippocampus to measure theta (6-10 Hz) power and detect fast ripples (~150 Hz) associated with sharp-waves in the local field potential. Simultaneous high-speed and high-definition video of the mouse's head allowed monitoring of whisking, ear movements, and pupillometry. Ambient sounds (including those generated by the mouse) were monitored using a sensitive omni-directional ultrasonic recording system (Avisoft Bioacoustics) and walking patterns were recorded from treadmill rotation.

Results

The membrane potential of auditory cortical neurons was responsive to sounds, and response magnitude changed during task-engagement. Furthermore, locomotion consistently depolarized cortical neurons and caused a reduction in sound response magnitudes. Recording epochs sorted by ripple and theta power in the hippocampus were associated with changes in the slow components of sound responses and spontaneous fluctuations. Strikingly, pupil dilation (which is correlated with activity of the locus coeruleus) was tightly coupled to slow (< 1 Hz) fluctuations in Vm, reaching coherence levels of 0.8-0.9.

Conclusion

These results demonstrate that precise accounting of behavioral state and task performance can help explain a significant portion of the variability in cortical Vms in awake, behaving animals. In particular, the close relationship between pupil diameter and cortical Vm provides a simple mechanism for the proposed gain-modulation function of central norepinephrine and demonstrates a close relationship between the autonomic and central arousal systems. These results indicate that the waking state is not captured by a discrete set of modes, but rather varies along a continuum that strongly influences neural and behavioral responses.

PS - 446

Rapid Spectrotemporal Plasticity in Primary Auditory Cortex (A1) During Contour Direction Discrimination Task

Pingbo Yin; Jonathan Fritz; Shihab Shamma

Institute for Systems Research, University of Maryland, College Park

Background

Task-related rapid receptive field plasticity in A1 has been demonstrated in the spectral domain by using pure tones or tone complexes in tone detection and discrimination tasks. Plasticity in these spectral tasks can be described by the "matched-contrast-filter" hypothesis in which receptive fields systematically change during behavior to enhance responses to behaviorally-relevant sounds and suppress responses

to sounds that are behaviorally-irrelevant. However, most acoustic stimuli such as speech, music, animal vocalizations, and environmental sounds convey information along *both* spectral *and* temporal dimensions. To test the matched contrast-filter hypothesis in the combined spectrotemporal domain, this study explored whether an auditory task involving complex spectrotemporal stimuli would induce a matching spectrotemporal pattern of rapid plasticity. In the spectrotemporal discrimination task used, ferrets learned to discriminate the direction (upward vs downward) of two-tone contours in a variable frequency tone-sequence.

Methods

Two ferrets were trained on a two-tone frequency-contour discrimination positive-reinforcement task using liquid reward. One ferret was trained to respond to upward shifting vs. downward shifting tone-sequences and the other ferret learned the opposite task version. Two independent data sets of single unit activity from A1 were collected while the animals performed the task with/without embedded background noise and also while they passively listened to the same stimuli. STRFs (spectrotemporal receptive fields) for each neuron were computed from task-evoked responses to noise, and also from pre- and post-task responses. Neuronal directionality functions were computed directly from activity evoked by the task tone-sequences, and during both pre- and post-task passive listening. Changes in the STRF and directionality function were compared between the trained ferrets, as well as between the trained ferrets and two naïve control ferrets.

Results

Cortical processing in A1 rapidly adapted to enhance the contrast between the two discriminated contour stimulus categories, by changing STRF properties to encode both spectral and temporal structure of the tone-sequences. These changes were closely linked to task reward structure: stimuli associated with negative reward became enhanced relative to those associated with positive reward. These task-and-stimulus-related STRF and directionality changes occurred only in trained animals during, and immediately following, behavior.

Conclusion

Our findings confirm the matched contrast filter hypothesis by demonstrating rapid neuronal spectrotemporal plasticity in A1 during performance of a spectrotemporal discrimination task. These results open the doors to the study of rapid task-related plasticity in perception and learning of complex spectrotemporal natural sounds such as speech, music and animal vocalizations.

PS - 447

Adaptation to ITDs in Auditory Cortex

Bjorn Christianson; **Simon Jones**; David McAlpine
UCL

Background

Single neuron studies in central auditory nuclei support the existence of a π -limit for the processing of Interaural Time Differences (ITDs): the distribution of best ITDs varies with neural Characteristic Frequency (CF) and is consistent across

frequencies when expressed in cycles of CF limiting neural coding of ITD to \pm half the period of a neuron's CF (π when phase is expressed in radians). This led to the prediction that ITDs separated by a full period of the centre frequency of a sound should result in similar neural activity and thus be subject to similar adaptation. We used stimuli similar to those used in human experiments presented elsewhere to probe the physiology underlying cortical responses consistent with the π -limit.

Methods

Tricolour guinea pigs were anaesthetised with urethane, primary auditory cortex (including A1) was exposed and a single-shank, 16-channel 'Neuronexus' multi-electrode arrays was implanted through a 4x4 16-channel surface electrocorticogram array (ECoG). Stimuli, delivered through earphones, consisted of paired 'adaptor-probe' bursts of pink noise, of 200ms duration (1000ms repetition period), where the probe ITD was fixed and the adaptor ITD varied. Responses to the probe were compared across adaptor ITDs and normalised to when the adaptor and probe had equal ITD.

Results

While a variety of response profiles was found both at cortical surface sites (ECoG) and at depth in cortical penetrations, most recordings showed less adaptation when adaptor and probe had different ITDs, except at the most extreme adaptor ITDs where the probe response was again suppressed. Less frequently, neurons showed a facilitation effect which increased with adaptor-probe ITD difference or an adaptation that did not reverse at extreme adaptor ITDs. Such adaptation profiles were rarer among ECoG traces.

Conclusion

Many cortical neurons appear to be π -limited in their responses to ITDs, responding to stimuli a full period of centre frequency and lateralized to the opposite side as if they were similar to the probe ITD. This is reflected in simultaneously recorded ECoG traces which we attribute to their reflecting gross summed neural activity.

PS - 448

Excitation by GABA Spillover in a Sound Localization Circuit

Catherine Weisz; Karl Kandler

University of Pittsburgh

Background

The lateral superior olive (LSO), an auditory nucleus involved in horizontal sound localization, receives tonotopically organized inhibitory glycinergic inputs from the medial nucleus of the trapezoid body (MNTB). The MNTB-LSO pathway undergoes refinement before hearing onset through synaptic strengthening and silencing. In addition to glycine, developing MNTB neurons also release glutamate and GABA, but their function is poorly understood. Here, we investigate a possible role for GABA.

Methods

Whole-cell voltage-clamp recordings were performed from LSO neurons in brain slices from P3-P14 C57BL/6J mice.

Electrical stimulation of MNTB axons elicited post-synaptic currents (PSC) in LSO neurons.

Results

In about half of recordings an unusual PSC occurred characterized by two distinct components following a single stimulus. We term these responses "doublets". In doublets, the second component did not occur without the first, but the first could occur without the second. Both components of a doublet reversed at -20 mV (60 mM Cl⁻ internal, n=4), suggesting that both components are chloride currents most likely due to inhibitory neurotransmitter release from MNTB neurons. The short latency from the first to the second component (~3 ms) is faster than MNTB neurons can release neurotransmitter at these ages (300 Hz stimulation), suggesting that the two components are elicited by different populations of axons. Our results suggest that doublets are the result of GABA spillover between nearby MNTB axons: 1) The probability of recording a doublet increased with stimulus strength (increased neurotransmitter release). 2) The second component in a doublet was blocked by the GABA_A antagonist gabazine (30 μ M), without loss of the first PSC (n = 9 of 17 cells). 3) Doublet occurrence was enhanced by the GABA reuptake blocker guvacine (30 μ M, 3 of 9 cells). 4) Higher frequency stimulation increased the occurrence of doublets in ~20% of cells. To test the presynaptic excitatory action of GABA on MNTB axons, current-clamp recordings were performed from MNTB somata and axons were filled with dye to visualize terminals in the LSO with 2-photon imaging. Focal pHp-GABA (200-500 μ M) uncaging at the MNTB axon terminals in the LSO depolarized the soma ~5 mV (>500 microns distant) indicating direct axonal excitation by GABA (n=11). In some cells an action potential was elicited (n=4).

Conclusion

We suggest that GABA spillover excitation of neighboring MNTB axons may play a role in the refinement of tonotopic projections from the MNTB to the LSO.

PS - 449

Nitric Oxide Signaling Removes Inhibitory Constraint in Superior Paraolivary Nucleus Neurons

Lina Yassin¹; Susanne Radtke-Schuller¹; Benedikt Grothe¹; Ian Forsythe²; Conny Kopp-Scheinplug¹

¹Ludwig-Maximilians-University Munich; ²University of Leicester

Background

Glycinergic inhibition plays a central role in auditory brainstem circuitries involved in sound localization and encoding of temporal patterns, so whichever signaling mechanism regulates that inhibition will be able to fine-tune information processing in these networks. We have recently described that inhibition in neurons of the superior paraolivary nucleus (SPN) is very powerful due to the strong chloride driving force generated by the neuronal potassium chloride co-transporter (KCC2) (Kopp-Scheinplug et al., *NEURON*, 2011).

Methods

Mice (p13-p20) were scarified by decapitation; brainstem slices (200µm) containing the superior olivary complex were cut and whole-cell patch-clamp recordings were made at $36\pm 1^\circ\text{C}$ from individually visualized cells using an EPC10/2 HEKA amplifier. Patch pipettes (3-4MΩ) were pulled from filamented borosilicate glass and were filled with internal recording solution. Whole-cell access resistance was $<10\text{ M}\Omega$ and series resistance was routinely compensated by 50-70%. Synaptic currents were evoked by afferent fiber stimulation with a concentric bipolar electrode driven by voltage pulses generated by the HEKA amplifier and post amplified by a linear stimulus isolator (ISO-Flex). Glutamatergic currents were blocked (50µM D-AP5, 10µM DNQX) and inhibitory currents were analyzed in IGOR Pro, results are presented as mean \pm SEM and statistical significance was determined using Student's *t* test with a significance threshold of $p < 0.05$.

Results

The medial nucleus of the trapezoid body (MNTB) provides glycinergic inhibition to the SPN and has previously been shown to generate nitric oxide (NO) following synaptic activity (Steinert et al., NEURON, 2008; Steinert et al., NEURON, 2011). Here we apply an NO donor (100µM SNP) to demonstrate that NO signaling modulates the synaptic strength of inhibition by altering the ion flow through open synaptic receptors via a change of the chloride driving force. Our data show that NO caused a depolarizing shift of the IPSC reversal potential from $-76.9 \pm 5.3\text{mV}$ to $-50.3 \pm 3.6\text{mV}$ ($n=8$); reducing the strength of inhibition without changing the presynaptic firing rate. A similar shift in IPSC reversal potential from $-84.9 \pm 3.6\text{mV}$ to $-55.4 \pm 5.7\text{mV}$ ($n=7$) was found following bath application of 0.5mM furosemide, a potent blocker of KCC2.

Conclusion

This NO-mediated suppression of KCC2 function provides a new mechanism for target-specific modulation of inhibition which is especially important wherever a major inhibitory hub supplies multiple targets each serving different functions.

PS - 450

Intermittent High Frequency Stimulation and the Role of Glycine Transporter 2 in MNTB-LSO Synapses

Martin Fuhr; Eckhard Friauf

Animal Physiology Group, Department of Biology, University of Kaiserslautern, D-67653 Kaiserslautern, Germany

Background

During ongoing neurotransmission, synaptic strength can undergo short-term depression (STD). STD has been extensively investigated for excitatory synapses, but much less is known about STD in inhibitory synapses. The glycinergic projection from the medial nucleus of the trapezoid body (MNTB) to the lateral superior olive (LSO) is ideally suited to study short term plasticity at inhibitory synapses. The aim of this study was to analyze the performance of the inhibitory MNTB-LSO synapses during ongoing and prolonged stimulation. The contribution of the glycine transporter GlyT2, a presynaptic replenishing machinery, was also addressed.

Methods

MNTB-LSO synapses were characterized in brainstem slices of P10-12 wild-type and GlyT2^{-/-} mice. Electrical activation of MNTB axons was combined with patch-clamp recordings of LSO principal neurons at 37°C . Prolonged stimulation comprised continuous electrical activation over a period of 60 s at various frequencies (50 to 333 Hz). Since such stimulation patterns are unlikely to mimic natural inputs, we also introduced gaps of silence with various durations, up to 200 ms. Peak amplitudes of evoked inhibitory postsynaptic currents (eIPSC) were determined.

Results

eIPSC amplitudes of wild-type mice showed frequency-dependent STD upon continuous stimulation (45-55% at 50 Hz within the first 10 s). A steady state level was obtained at 30%. Upon introduction of gaps, the steady state level increased to 40-60%. Higher stimulation frequencies resulted in higher STD, but the steady state level never fell below 20% when gaps of silence were applied. eIPSCs occurred still at high fidelity, i.e., failures were rare. In contrast, continuous stimulation ($> 50\text{ Hz}$) resulted in STD levels of $< 10\%$. An interesting rebound effect occurred in eIPSC amplitudes between 30-40 s at some gap durations. In analog recordings in GlyT2^{-/-} mice, STD of eIPSC peak amplitudes was drastically stronger than in wild-types. This was accompanied by an intense reduction of fidelity, i.e., many failures occurred. In summary, our results demonstrate a remarkably high performance of the inhibitory MNTB-LSO synapses upon prolonged stimulation. The performance is increased when short gaps of silence are introduced. When glycine reuptake via GlyT2 is abolished, the performance is poor.

Conclusion

We conclude that neurotransmission in the MNTB-LSO synapses is tuned to faithfully act in the sound localization process via computing interaural level differences. By doing so, in adds to the unique specializations seen in the neuronal pathway from the contralateral ear to the LSO, namely endbulbs in the cochlear nucleus, thick axons, and calyces in the MNTB.

PS - 451

Role of Ih in the Axon Initial Segment of MSO Neurons Revealed With Light-Dependent Channel Blockers

Kwang Woo Ko¹; Richard H. Kramer²; Nace L. Golding¹

¹University of Texas at Austin; ²University of California at Berkeley

Background

The principal neurons of medial superior olive (MSO) compute microsecond temporal differences in arrival time of sounds to the two ears to localize sounds. Despite the crucial role of the axon initial segment (AIS) as the site of action potential initiation in MSO neurons, the technical difficulty in isolating the effects of voltage-gated ion channels in the AIS from those of the soma and dendrites has precluded a clear understanding of how AIS properties influence the coding of

auditory information. Here we show the first evidence that the AIS is influenced by hyperpolarization-activated currents (Ih).

Methods

To focally block voltage-gated ion channels in the axon of MSO neurons, we combined whole-cell recordings, confocal microscopy, and the use of light-sensitive channel blockers (photoswitches) in gerbil brainstem slices. Slices were pre-incubated extracellularly with photoswitches (300 μ M; DENAQ for voltage clamp experiments, and AAQ for current clamp experiments) for 20–30 mins, and kept in the dark thereafter. Alexa 568 (50 μ M) was included in patch pipette solutions for axon visualization. Photoswitch-induced ion channel block was induced by scanning spatially restricted regions of MSO neurons.

Results

We found that both DENAQ and AAQ block significant fraction of Ih in MSO neurons. In voltage-clamp experiments using DENAQ, Ih in the AIS (50–100 pA, $n=5$) exhibited similar properties as Ih in the soma and dendrites: the voltage dependence and slope of Ih activation in the AIS was similar to values in the soma and dendrites (Soma/dendrite $V_{1/2} = -68.6$ mV, $k=9.4$; AIS $V_{1/2} = -68.4$ mV, $k=9.8$; $n=5$). The kinetics of Ih activation were also similar. In current-clamp experiments using AAQ as the photoswitch, blockade of Ih in the AIS hyperpolarized the somatic resting potential by 1–2 mV, but in response to trains of synaptic stimuli (10 trains of 100 Hz synaptic stimulation, 10 trials), blockade of Ih in the AIS significantly increased spike probability (0.42 in control, 0.52 in axonal block; $p=0.015$). In addition, spike threshold significantly decreased during AIS Ih blockade (-56.1 ± 0.2 mV to -58.6 ± 0.3 mV, $p<0.01$), while the maximum dV/dt of the action potential increased (109 ± 14 mV/ms to 146 ± 6 mV/ms; $p<0.01$). These results are consistent with membrane hyperpolarization in the AIS driving an enhanced recovery of voltage-gated sodium channels from inactivation.

Conclusion

We find that HCN channels in the AIS improve the resolution of binaural coincidence detection indirectly, primarily through an increase in Na channel inactivation and the resulting decrease in spike probability.

PS - 452

Effects of NBQX, Kainate, and Ibotenic Acid on the Neurophonic Potential in the Nucleus Laminaris of the Barn Owl

Paula Kuokkanen¹; Thomas McColgan¹; Go Ashida²; Christine Koeppel³; Hermann Wagner⁴; Richard Kempter¹; Catherine Carr⁵

¹Humboldt-Universität zu Berlin; ²Carl von Ossietzky University Oldenburg; ³Carl von Ossietzky University; ⁴RWTH Aachen; ⁵Univ Maryland

Background

Barn owls are able to locate sound sources based on interaural time difference (ITD) with microsecond precision. The first binaural processing stage is nucleus laminaris (NL), where a strong ITD sensitive, frequency-following evoked potential

called the neurophonic is observed. The sources of this potential are the subject of current investigation. Sources may include currents due to spikes in the afferent axons originating from nucleus magnocellularis (NM), synapses of these axons on NL cell bodies, and spiking activity of NL neurons. Previous experiments with pressure injections of kainate and ibotenic acid reduced the neurophonic, but damaged the myelinated axons entering NL, thus confounding interpretation of these results.

Methods

In order to separate the possible sources of the neurophonic, we iontophoretically applied an AMPA receptor blocker (10 mM NBQX) to inhibit synaptic transmission in NL, while recording the neurophonic in urethane anesthetized owls. We then analyzed the recordings before, during and after NBQX iontophoresis and compared the effects of synaptic blockage on different spectral components. For iontophoresis we used glass-pipette barrels of Carbostar-3 microiontophoresis electrodes (Kation Scientific, Minneapolis, MN). One barrel was filled with NBQX in saline and the other with saline for current balancing. A carbon fiber served as the recording electrode. NBQX was retained in the pipette barrels with a negative holding current of 10 nA, and ejected by the application of a positive current (typically 70 nA). Controls were performed by recording in the adjacent NM.

Results

The neurophonic remained largely unaffected by the administration of NBQX. These data therefore suggest that NM axons are the origin of the best-frequency component of the neurophonic. Action potentials in NL neurons may contribute to the power spectral density below 1 kHz. These data also confirm previous analyses and numerical simulations of the neurophonic that estimated the number of independent sources contributing to the neurophonic to be at least 250 (Kuokkanen et al., 2010 and 2013). That NM axons are the main source of the neurophonic potential in NL is supported by further control experiments in NM where NBQX iontophoresis, using the same electrode and parameters, significantly diminished auditory evoked responses.

Conclusion

The neurophonic in the barn owl is largely presynaptic in origin, originating from the densely packed interdigitating NM axons in NL.

PS - 453

Simulating the Neurophonic Potential in the Barn Owl Nucleus Laminaris: Contribution of Nucleus Magnocellularis Axons

Thomas McColgan¹; Paula Kuokkanen¹; Hermann Wagner²; Catherine Carr³; Richard Kempter¹

¹Humboldt-Universität zu Berlin; ²RWTH Aachen; ³Univ Maryland

Background

The barn owl uses interaural time differences to determine the direction of sound sources in the azimuthal plane with extraordinary precision. Nucleus laminaris is the first process-

ing stage where binaural interaction takes place. The field potential in nucleus laminaris is closely related to auditory stimuli received by the owl and is thus called neurophonic. The impulse response of the neurophonic, measured by presenting monaural clicks to the owl, contains distinct low- and high-frequency components. The high-frequency component has been previously studied, and phase delay was shown to have microsecond precision (Wagner et al., 2005 and 2009). The low-frequency component gradually changes polarity between ventral and dorsal recording sites. The origin of this polarity reversal is unknown.

Methods

We studied the click-evoked neurophonic using a computational model. We hypothesized that the polarity reversal of the low-frequency component is related to the spatial organization of the axons projecting from nucleus magnocellularis into nucleus laminaris. To test this hypothesis, we constructed a model of the input to nucleus laminaris. The activity of nucleus magnocellularis was simulated, taking into account both the high spontaneous discharge rate and the neurons' refractory periods. This activity was then fed into a multi-compartment model of magnocellular axons from which we simulated the extracellular potential caused by membrane currents. We then compared the resulting compound potential for different activation patterns and axonal geometries to the observed field potentials.

Results

The computational model qualitatively reproduced the structure of the neurophonic in nucleus laminaris. Both low- and high-frequency components showed a similar temporal and spatial behavior as observed in the data, demonstrating that axonal sources are able to explain the observed effects.

Conclusion

This finding is consistent with the hypothesis that the neurophonic in the barn owl nucleus laminaris is mainly due to the activity of magnocellular axons. The simulation approach we present here can provide methods of analyzing and predicting magnitudes and dynamics of the spectral components in absolute terms and in relationship to each other.

PS - 454

Ephaptic Effects in the Medial Superior Olive – A Simulation Study

Joshua Goldwyn; John Rinzel

New York University

Background

Sustained and stimulus-evoked extracellular potentials, *Vext*, known as the *auditory neurophonic* surround the medial superior olive (MSO) (Mc Laughlin et al., 2010). We ask: *does the auditory neurophonic influence the activity of MSO neurons?* MSO neurons have no direct synaptic connections, but *Vext* effects have been observed and termed *ephaptic effects* (Arvanitaki, 1942). Weak *Vext* can alter spike timing in cortex (Anastassiou et al., 2011) and MSO neurons require exceptional temporal precision to encode interaural time differences. Ephaptic coupling is instantaneous so it may impact binaural processing in the MSO.

Methods

Our computational model dynamically couples membrane potential, *V_m*, of MSO neurons to the surrounding *Vext* field. We simulate MSO neuron activity using a biophysically-based model developed for gerbil MSO (Mathews et al., 2010). Post-synaptic currents generate *Vext*, the simulated neurophonic. We replicate important features of *Vext* for pure tone stimuli: its dipole-like spatial profile, ~100 μ V to 1mV amplitude scale, and ~1mm spatial spread (Goldwyn et al., ARO 2013). We embed a “test neuron” in this endogenously generated *Vext* to investigate ephaptic effects. We first test how the neurophonic response alters dendritic EPSPs. We then add Na⁺ currents in an axon initial segment (AIS) and measure field effects on action potential generation and coincidence detection.

Results

In our simulations, the neurophonic perturbs *V_m* of the test MSO neuron. The neurophonic response to monolateral inputs is dipole-like and depolarizes/hyperpolarizes the ipsilateral/contralateral dendrite. For coincident bilateral input both dendrites of the test neuron depolarize while the soma hyperpolarizes. The effects are relatively modest: maximum *V_m* perturbations are smaller than the maximum amplitude of *Vext*, ~1mV or less. When we include spike-generation, spike thresholds change depending on the location of the AIS. When near the soma, the AIS hyperpolarizes and increases the spike threshold. This can enhance coincidence detection by suppressing spikes evoked by synaptic inputs with large time differences.

Conclusion

The neurophonic is a possible source of ephaptic coupling in the auditory brain stem. Our results suggest that field effects may subtly influence dendritic integration and spike initiation. Our simulation study is a first step toward characterizing ephaptic coupling in the MSO. Future theoretical and experimental work can further elucidate the role of influence of ephaptic coupling on coincidence detection and sound localization.

PS - 455

Nonlinear Interplay Between Monaural Inputs and Intrinsic Conductances Shapes ITD Tuning in MSO Neurons

Tom Franken¹; Michael T. Roberts²; Nace L. Golding²; Philip X. Joris¹

¹KU Leuven, Leuven (Belgium); ²University of Texas at Austin

Background

Neurons in the medial superior olive (MSO) are sensitive to interaural time difference (ITD). This property is thought to arise from coincidence detection of monaural inputs but this process is ill-characterized. Intracellular *in vitro* recordings have revealed unusual intrinsic properties in MSO neurons but it is unknown how these affect responses to sound. Recent *in vivo* juxtacellular recordings suggest that monaural inputs sum linearly and that spikes are predictable simply from the maximum of this sum.

Methods

We performed an extensive set of *in vivo* intracellular recordings of MSO neurons in Mongolian gerbils under general anesthesia, during monaural and binaural presentation of tones and noise. Additional *in vitro* experiments allowed us to manipulate the membrane potential and study the effect on spike generation.

Results

To characterize the coincidence process, we compared monaural and binaural *in vivo* responses. We found that monaural responses extracted from binaural responses by averaging to the stimulus frequency from one side ("pseudomonaural") often differed from the real monaural response to that side. This included differences in phase, gain, and DC level. Comparison of the sum of monaural responses with the actual binaural response showed differences in ITD tuning in many, but not all, cases. This included shifts in the range of ITDs triggering maximal output (Best Delay), and these shifts could be large when compared to the range of ITDs available to the animal. Examination of average membrane potential before events that successfully triggered output spikes, compared to large unsuccessful EPSPs, revealed that surprisingly small differences in membrane potential could have large effects on probability of spiking. This was further tested in *in vitro* dual somatic recordings in which membrane potential was manipulated in small steps preceding injection of an EPSP. Indeed, changes of surprisingly small magnitude affected spike probability. Our interpretation is that the number and pattern of input events in binaural conditions influence intrinsic conductances differently than in monaural conditions, and that this difference can affect ITD tuning.

Conclusion

We conclude that knowledge of monaural responses is insufficient to predict ITD tuning. Intrinsic properties of the post-synaptic neuron can significantly affect the range of ITDs to which the MSO neuron is maximally responsive.

PS - 456

Number of Synaptic Inputs Affects Coincidence Detection in the Auditory Brainstem

Go Ashida¹; Kazuo Funabiki²; Jutta Kretzberg¹; Catherine Carr³

¹Carl von Ossietzky University Oldenburg; ²Osaka Bioscience Institute; ³University of Maryland

Background

A wide variety of sensory neurons encode temporal information via phase-locked spikes. In the auditory brainstem, coincidence detector neurons that are involved in sound localization receive phase-locked synaptic inputs and change their output spike rates according to the interaural time difference (ITD). Previous modeling studies suggested that converging phase-locked synaptic inputs give rise to a periodic oscillation in the membrane potential of their target neuron. *In vivo* intracellular recordings revealed that the oscillation amplitude changes periodically with ITD. In this study, we examine how

the number of phase-locked synaptic inputs affects the oscillating membrane potential and coincidence detection.

Methods

Based on previous studies, we constructed an auditory coincidence detector neuron model with leak and low-threshold potassium conductances. Phase-locked inputs were modeled as an inhomogeneous Poisson process. In our numerical simulations, we changed the number of input fibers and examined how signal and noise components of the membrane potential are affected. We also applied our signal-to-noise ratio (SNR) analysis to neurophysiological data recorded from the nucleus laminaris (NL) of the barn owl *in vivo* and examined frequency-dependence of the input properties.

Results

Simulated waveforms of the model membrane potential were greatly affected by the number of phase-locked synaptic inputs. When the number of synaptic inputs was between a few to ten, individual synaptic inputs were visible in the simulated membrane potential. When the input number was on the order of 100 or more, however, synaptic inputs showed smooth sinusoidal oscillations similar to what was observed in the owl's NL *in vivo*. This observation was confirmed by theoretical calculations of ITD-dependent signal and ITD-independent noise amplitudes of the model synaptic input. SNR analysis of the membrane potential data showed a good agreement with theoretical calculations for mid-to-high-frequency NL neurons (>2 kHz). For low-frequency neurons (<2 kHz), however, measured SNRs were lower than theoretical predictions.

Conclusion

Our simulation results indicate that the number of phase-locked synaptic input converging on auditory coincidence detector neurons needs to be tuned to achieve efficient ITD coding. The results of our SNR analyses predict there should be a significant difference in synaptic inputs between low and mid-to-high frequency NL neurons. Further investigation is needed to accurately count the actual number of synaptic inputs in the auditory brainstem.

PS - 457

Sensitivity of Inferior Colliculus Neurons to Interaural Timing Differences Within the Envelopes of Acoustic Waveforms

David Greenberg¹; Mathias Dietz²; David McAlpine¹

¹Ear Institute, University College London, London, UK;

²Medizinische Physik, Universität Oldenburg, Oldenburg, Germany

Background

Studies that explore the influence of envelope shape on ITD JNDs often have co-varying elements. This led Klein-Hennig et al. (2011, J. Acoust. Soc. Am. 129 p. 3856-3872) to conduct psychophysical experiments that aimed to clarify the role of individual envelope components. This was achieved by manipulating independently the duration of the four envelopes components; Attack, Sustain, Decay and Pause. The results demonstrated that with a short Attack duration and a

long Decay duration, the mean ITD JND was 114 μ s. Reversing the signal in the time domain resulted in a mean ITD JND of just under 400 μ s.

Methods

Using tungsten microelectrodes, we recorded the responses of single neurons in the inferior colliculus of anaesthetised guinea pigs. For each neuron, carrier frequencies corresponded to the neuron's characteristic frequency. Responses for 18 envelope shapes were analysed that explored the influence of temporally asymmetric envelope shapes, modulation frequency and duty cycle as well as the individual influence of the four envelope components. The current study assesses how each envelope waveform segment influences the ITD JNDs and rate-ITD-functions of inferior colliculus neurons for each envelope shape.

Results

Rate-ITD-functions were highly modulated - indicating improved ITD discriminability - for envelope shapes that had a short attack component. ITD JNDs were best at low modulation frequencies. Phase-locking was greatest for envelope shapes that included a short attack component. The neural ITD JND was defined using the measure of Standard Separation (D). The responses of 71 neurons that were sensitive to ITDs in at least one envelope shape were analysed. 30/71 neurons have a significant ($D \geq 2$) ITD discrimination threshold for a short attack, long decay envelope shape with best ITD JNDs at 141 μ s compared to 9/71 and 452 μ s for the temporally reversed envelope shape.

Conclusion

The data indicate the importance of envelopes with fast-attack, low modulation frequency and optimal pause durations in providing the best ITD sensitivity in high characteristic frequency neurons.

PS - 458

Resonant and Integration Properties of Principal MSO and LSO Neurons.

Jimena Ballester¹; Roberta Donato¹; Michiel Remme²; John Rinzel²; David McAlpine¹

¹UCL Ear Institute, University College London; ²Center for Neural Science, New York University

Background

Neurons in the medial superior olive (MSO) are specialised to extract information concerning the temporal fine structure of sounds underpinning sensitivity to interaural time differences (ITDs). Conversely, neurons in the lateral superior olive (LSO) neurons extract interaural level differences (ILDs) and ITDs conveyed in the envelope of high frequency sounds (envelope-ITDs). This implies that neurons in the auditory pathway should have the flexibility of extracting these different features either by circuit computation or by filtering inputs at the single cell level. We recently described an intrinsic resonance in the electrical response of principal cells in the MSO/LSO, for which the peak resonance frequency (fres) decreases as a neuron's (presumed) characteristic frequency increases. Through a modelling approach we showed that this resonant gradient would underlie the transition from coding of temporal

fine structure to coding of temporal envelope (Remme et. al. 2013 under revision).

Methods

Here, we further explore the gradient in resonance across the LSO and its consequence for the integration properties of principal neurons. Patch-clamp, whole-cell recordings were made in LSO neurons from P14 rat and MSO neurons of P6-10 guinea pig brainstem slices.

Results

Resonant properties of principal LSO and MSO neurons were evaluated by applying subthreshold current ZAP stimulus. As previously reported MSO neurons showed high fres (~400Hz) while LSO neurons showed either lower fres (~80Hz) or low pass profiles. By applying suprathreshold ZAP stimulus we showed that resonant neurons fire action potentials when the inputs frequency matches fres. Blocking either Kv1.1 channels or HCN channels abolished resonant responses, demonstrating a role for both of these currents in resonant behaviour. As previously reported all resonant neurons presented phasic firing. We tested whether spike initiation was triggered by a fix change in voltage (voltage threshold) or if depended the rate at which the voltage changed (slope threshold) by applying a family of depolarization ramps of decreasing slope. Tonically-firing neurons responded as voltage detectors while phasically-firing neurons were sensitive only to fast, rising inputs. Blocking Kv1.1 channels in phasic neurons abolished their slope sensitivity.

Conclusion

Our data supports the MSO/LSO resonant gradient as a mechanism for filtering auditory inputs. Furthermore, we provide details on the molecular mechanism involved in the resonant response.

PS - 459

Inhibitory Inputs to MNTB Principal Cells – an Anatomical and Electrophysiological Study in Rodents

Otto Albrecht; Anna Dondzillo; Florian Mayer; Achim Klug
University of Colorado School of Medicine

Background

The medial nucleus of the trapezoid body (MNTB) is a prominent structure in the ascending auditory pathway. Located in the auditory brain stem, it receives excitatory inputs from the contralateral cochlear nucleus via the calyx of Held, a giant type of synapse. Its main function is thought to be turning this fast and well-timed excitation into inhibition which is then projected to a number of auditory nuclei, including those of the sound localization pathway. Recent studies have found that MNTB neurons also receive substantial inhibitory inputs, mediated by both glycine and GABA. The functional role, as well as the source(s) of these inhibitory inputs are not well understood.

Methods

We performed a series of anatomical (immunohistochemistry against GAD-67 and retrograde as well as anterograde tracing) and physiological (in-vitro patch-clamp recordings) tests

to elucidate these source(s) in both the Mongolian gerbil and the mouse.

Results

Our results suggest that the ventral nucleus of the trapezoid body (VNTB) is at least one source nucleus providing inhibition to MNTB. Our retrograde and anterograde tracing experiments confirmed fiber connections between the VNTB and the MNTB. We also found that electrical stimulation of the VNTB elicits glycinergic currents in MNTB principal cells. Moreover, the same inhibitory currents can be elicited via glutamate-un-caging in both VNTB and MNTB, suggesting that the MNTB itself could be another source of inhibition. Since many auditory brain stem centers undergo a switch from GABA to glycine during early postnatal development, we also looked at the proportions of mixed (GABA/glycine) and purely GABAergic synaptic inputs to MNTB neurons and compared that to the presence of GABAergic markers (GAD-67) in glycinergic VNTB neurons. The GABAergic component decreased with age, and there was a strong correlation between the changes seen in our anatomical studies of the VNTB and the physiological switch in MNTB, further supporting the VNTB as a source nucleus of inhibitory inputs to MNTB.

Conclusion

The VNTB is an inhibitory source of the MNTB. In addition, the MNTB itself is possibly providing recurrent inhibition to its principal cells. The timeline of the GAD-67 expression in glycinergic VNTB neurons follows that of the physiological switch from glycine and GABA to mainly glycine in MNTB neurons.

PS - 460

Binaural Spectral Processing in Mouse Inferior Colliculus

Xi Bie; Douglas Oliver

University of Connecticut Health Center

Background

Frequency coding is one of the basic properties maintained throughout the auditory system. The inferior colliculus (IC) in the midbrain integrates virtually all of the information ascending from the lower auditory brainstem nuclei then sends it to the thalamus and cortex. Binaural and monaural pathways are integrated in the IC to form one tonotopic map. However, it is unknown how the frequency tuning is affected by interaction between binaural and monaural inputs in the IC.

Methods

We studied the spectral processing in the mouse IC with a closed acoustic stimulation system that presented pure tones at different frequencies and intensities. Sounds were binaural stimuli or monaural stimuli presented to either the ear contralateral or ipsilateral to the extracellular recording site. Spectral sensitivity was examined with stimuli from 2 kHz to 76 kHz in 0.25 octave steps and sound pressure levels from threshold to 80 dB.

Results

The results showed the frequency response areas (FRA) shapes are changed for many neurons under binaural stim-

ulation compared with contralateral condition. Binaural stimuli have different effects on spectral tuning of neurons. Most cells have inhibitory inputs from ipsilateral stimulation but 35 out of 108 cells had excitatory ipsilateral inputs. The best frequency (BF), the characteristic frequency (CF), the maximum firing rate, BF to CF ratio, Q10 and Q30 were extracted from the response to binaural, contralateral and ipsilateral stimuli for each neuron. Together 18 parameters were used in cluster analysis to compare how binaural stimulation change the spectral tuning of neurons. The cells were grouped into three different clusters based on the similarities of those parameters. Cells in the first group have a higher or equal firing rate under contralateral stimuli ($n=28/39$) and the BF is lower with binaural stimuli ($n=29/39$). Cells in the second group have excitatory inputs from ipsilateral ear ($n=11/14$), and binaural stimulation increases firing rates. Cells in the third group have a narrow bandwidth through all intensities ($n=3/3$).

Conclusion

These data suggest that binaural stimuli can change the spectral processing of neurons in different ways. Binaural frequency tuning is not a simple summation of information from the two ears. The integration of monaural and binaural inputs may alter the frequency tuning of an IC neuron.

PS - 461

Coding of Frequency Information in Neurons of the Inferior Colliculus of the Unanesthetized Rabbit That is Conveyed by Pathways That Carry Information About Interaural Temporal Disparities

Ranjan Batra; John Shapiro

University of Mississippi Medical Center

Background

Frequency is arguably the most important facet of hearing, yet it remains enigmatic how information about frequency ascending the lower brainstem via multiple pathways is re-integrated in the inferior colliculus. Previous studies of frequency coding by collicular neurons employed chiefly contralateral stimulation. Such stimulation curtails the influence of pathways through the superior olive that are maximally activated by binaural stimulation. Furthermore, most previous studies used anesthetized preparations, in which collicular responses are altered. Here we examined tuning in the inferior colliculus using stimuli that strongly activate the binaural nuclei of the superior olivary complex.

Methods

Stimuli were of two types: low-frequency (≤ 2 kHz), which consisted of tones to each ear that differed slightly in frequency resulting in a continuous variation in interaural temporal disparity (ITD), and high-frequency (≥ 1 kHz), in which each ear received sinusoidally-modulated tones with identical carrier frequencies but slightly different modulation frequencies. Individual collicular neurons of unanesthetized rabbits were tested using both kinds of stimuli over a range of frequencies and intensities. The amplitude of the first harmonic at the difference frequency was used to gauge sensitivity to ITDs.

Tuning obtained with these stimuli was compared with that of a group of neurons tested monaurally with tones.

Results

Response areas of less than half the neurons were "V-shaped," and were nominally similar to those of auditory nerve fibers in that these areas had a steep high-frequency limb and a shallower low-frequency limb. This proportion is similar to that among the monaurally tested neurons. The majority of neurons had irregularly shaped binaural response areas. Sharpness of tuning 10 dB above threshold was similar to that among monaurally-tested neurons but tuning in both groups of neurons was broader than that published for auditory nerve fibers of the rabbit. Despite the similarity in the proportions of neurons with V-shaped tuning measured using the two approaches, shapes of the response areas differed in about half the neurons that were tested both ways, although the characteristic frequencies were similar.

Conclusion

Our results indicate that information about frequency arriving from binaural nuclei of the superior olivary complex has been shaped in a variety of ways, presumably by circuitry within the inferior colliculus. Some neurons appear to adapt their processing of frequency depending on which inputs are activated.

PS - 462

Optogenetic and Electrophysiological Analyses of Neurons in the Low Frequency Region of the Gerbil Inferior Colliculus in Vitro.

Michael Roberts; Lauren Kreeger; Nace Golding
The University of Texas at Austin

Background

The central nucleus of the inferior colliculus (ICC) contains a diverse array of neurons which differ in their intrinsic excitability, morphology, and local and ascending circuit connectivity. Using patch clamp electrophysiology and optogenetics in acute midbrain slices, we are investigating how these properties combine to enable the processing of low frequency auditory information in the Mongolian gerbil.

Methods

Whole cell current clamp recordings were made from neurons in the ICC in acute midbrain slices from P21-59 gerbils. Slices were prepared in the laminar plane to preserve ICC neuron dendrites, with special attention paid to the most dorsal, low frequency laminae. The intracellular solution contained biocytin to allow for post hoc reconstructions of neuron morphology. In some experiments, channelrhodopsin-2 was expressed in IC neurons via injection of an adeno-associated virus vector and was activated by illuminating the slice with blue light.

Results

We used whole cell current clamp recordings to assess the intrinsic properties of neurons in the low frequency region of the ICC. Consistent with previous findings in rat and mouse, we observed neurons with sustained, build-up, adapting, re-

bound, and onset firing patterns. Surprisingly, we identified a subset of neurons that appear adapted for speed. These neurons have input resistances less than 30 M Ω , membrane time constants ≤ 1 ms, strong hyperpolarization activated currents (I_h), and fire rebound spikes. In response to large depolarizing current steps, they exhibit instantaneous firing frequencies > 1 kHz, sustained firing at frequencies > 600 Hz, and weak adaptation. With smaller current steps, firing becomes strongly adapting. To investigate how these and other ICC neurons form functional circuits, we are using optogenetics to examine local and long range inputs. We have confirmed channelrhodopsin-2 expression in neurons intrinsic to the ICC and in commissural projections from the contralateral ICC.

Conclusion

Our results show that a subset of neurons in the low frequency region of the ICC possess intrinsic properties adapted for speed. Such adaptations have not previously been reported in slices from animal species that lack low frequency hearing. This suggests that the processing of low frequency sound information in the ICC may employ neurons that use temporal coding. Using optogenetics, we will investigate how these and other neurons in the low frequency region of the ICC are impacted by local and long range inputs.

PS - 463

Spatial Separation Between Standard and Deviant Sounds in an Oddball Paradigm Changes the Sensitivity of a Neuron to the Deviant Sound in the Rat's Inferior Colliculus

Chirag Patel; Huiming Zhang
University of Windsor

Background

Studies using monaural stimuli have revealed that neurons in the rat's inferior colliculus (IC) are sensitive to novel sounds. These neurons display stronger firing in response to a tone burst presented as a deviant stimulus than as a standard stimulus in an oddball paradigm. The IC is an auditory integration center receiving monaural and binaural inputs from multiple structures on both sides of the brain. Sources of inputs include forebrain structures with neurons sensitive to novel sounds. Integration among inputs to the IC renders neurons in the structure abilities for processing directional acoustic cues. We hypothesize that under free-field stimulation the sensitivity of an IC neuron to a novel sound depends on the spatial relationship between this novel sound and a standard sound.

Methods

We tested the hypothesis using an oddball paradigm. Single unit activities were recorded in the rat's IC. Responses were elicited by two speakers located in the horizontal plane with equal distance to a rat's interaural midpoint. One speaker was located at the frontal midline (0°) while the other one was at an off-0° azimuth. The tone bursts for creating an oddball paradigm had frequencies at 0.951BF and 1.051BF (BF: best frequency at 0°). Standard and deviant stimuli (90% and 10%

presentation probabilities) were delivered using either one speaker at 0° or two separate speakers.

Results

When both standard and deviant sounds were at 0°, IC neurons displayed various degrees of sensitivity to the deviant sound, with those showing high sensitivities typically located in the dorsal and external cortices of the structure. For many neurons, spatial separation between deviant and standard sounds changed neural sensitivity to the deviant sound. The sensitivity to a deviant sound located at 0° was typically enhanced by moving a standard sound from 0° to an ipsilateral azimuth. When a standard sound was at 0°, the sensitive to a deviant sound was typically enhanced when the deviant was moved from 0° to an ipsilateral azimuth. For many individual neurons, moving a high frequency sound and a low frequency sound from 0° to the same off-0° azimuth caused different changes in the neural sensitivity to a deviant sound. For the entire neuron population, however, no difference was observed between changes in sensitivity caused by the two acoustic manipulations.

Conclusion

Spatial separation between standard and novel sounds changes the sensitivity of an IC neuron to the novel sound.

PS - 464

Estimation of Characteristic Phase and Delay from Broadband Interaural Time Difference Tuning Curves

Jessica Lehmann; Philipp Tellers; Hermann Wagner; Hartmut Führl
RWTH Aachen University

Background

Interaural time difference (ITD), the time shift between the signals reaching the two ears, is a perceptual cue to localize sounds used by many animals. The variation of responses with ITD may be quantified in a so-called ITD (tuning) curve. ITD curves may be described in terms of frequency-dependent (CP=characteristic phase) and frequency-independent (CD=characteristic delay) components. After the stage of detection remodeling of the neural response occurs. Remodeling involves across-frequency integration which Yin and Kuwada (J Neurophysiol 50:1020 (1983)) initially quantitatively analyzed by estimating CD and CP from phase-frequency plots. While this analysis is mathematically sound, the data collection is time consuming. Following initial observations by Vonderschen and Wagner (J Neurosci 32:5911 (2012)), we here formally outline a simpler method to estimate CD and CP by taking into account the relation between broadband ITD tuning and frequency tuning.

Methods

We assume that the ITD and frequency tuning of a broadly tuned neuron arise by integrating input from narrowly tuned coincidence detector neurons. Each input neuron has a preferred ITD and narrowband frequency tuning, and it is the systematic dependence of best ITD on best frequency that is responsible for the CP and the CD in the response behavior

of the broadly tuned neuron. The tuning behavior of the neuron and/or the signals used in the determination of the broadband tuning curve are restricted to a certain frequency band. We determine the minimal mean square error for fixed values of the CD and the CP between the given and the estimated ITD tuning curve. The best values for the CD and the CP minimize the approximation error.

Results

Application of the algorithm to modeled noisy broadband ITD tuning curves with predetermined CD and CP values revealed that its estimation performance was bandwidth dependent, and, to a smaller degree, dependent on the position of the frequency band. An increase in the signal-to-noise ratio also increased the estimation accuracy. Further applications to electrophysiological data are in agreement with already published results.

Conclusion

The novel method presented here allows to calculate CD and CP values of already recorded data when tonal ITD tuning curves might not be available. However one should be aware that the spacing and number of data points in the ITD tuning curve influence the significance of the estimates.

PS - 465

Is the Neural Coding of Dynamic Interaural Time Differences Related to the Coding of Amplitude Modulation?

Nathaniel Zuk; Bertrand Delgutte
Massachusetts Eye and Ear Infirmary

Background

Neurons in the inferior colliculus (IC) are sensitive to temporal variations in interaural time differences (ITD) such that their firing patterns deviate from those expected based on tuning to static ITDs (Spitzer & Semple, J. Neurophysiol 69:1245). Such dynamic sensitivity is not observed in the superior olivary complex, where ITD is initially encoded. We hypothesized that dynamic ITD sensitivity in the IC may be created by the same neural mechanisms that also give rise to sensitivity to amplitude modulation. To test this hypothesis, we measured responses of IC neurons to both broadband noise with dynamic ITDs and sinusoidally amplitude modulated (SAM) noise in an awake preparation.

Methods

We recorded from single units in the IC of unanesthetized Dutch-Belted rabbits in response to broadband noise stimuli with ITDs varying in a sawtooth motion over a 600 μ s range at rates of 2-64 Hz. Responses were modeled using the cascade of a binaural cross-correlation model (Hancock & Delgutte, J. Neurosci 24:7110) and a filter model of IC responses to SAM (Nelson & Carney, J Acoust Soc Am. 116:2173). For each neuron, the parameters of the cross-correlation model were fit to static ITD tuning curves, and then the parameters of the SAM filter model were fit to period histograms of responses to dynamic ITD stimuli. Best fitting model filters were compared to temporal modulation transfer functions (tMTFs) measured from the same neuron with SAM noise.

Results

Deviations from predictions based on the static ITD tuning curve previously reported in anesthetized animals were also observed with dynamic ITD stimuli at high modulation rates in awake rabbit. These included sharper ITD tuning, systematic shifts in best ITD, and hysteresis when the direction of ITD motion was reversed. The quality of the cascade model fits to the dynamic ITD data was variable across the small number of neurons tested (coefficients of determination R^2 ranged from 0.19 to 0.73), but the fit was always statistically better than predictions from the static ITD tuning curve. Best-fitting filter frequency responses for the model resembled measured tMTFs for SAM noise.

Conclusion

Because the tMTFs estimated from responses to dynamic ITD resemble tMTFs measured with SAM, similar neural mechanisms may be responsible for the dynamic sensitivity of IC neurons across different stimulus conditions, suggesting there may be no specialization for motion sensitivity at the level of the IC.

PS - 466

Visual and Auditory Responses in the Mongolian Gerbil Midbrain

Todd Jennings; Benedikt Grothe

Ludwig Maximilians University of Munich

Background

The central nucleus of the inferior colliculus (ICC) and the superior colliculus (SC) are two of the primary sites of convergence for sensory information in the midbrain. The SC is the primary multimodal integration area in the midbrain, with neurons sensitive to a variety of sensory modalities such as visual, auditory, and somatosensory, as well as cells sensitive to multiple sensory modalities. The ICC, on the other hand, is the primary auditory integration area, with neurons sensitive to a variety of auditory cues as well as combinations of auditory cues.

However, the ICC also receives indirect projections from multimodal structures, particularly the SC and the primary auditory cortex. Further, both sound and vision are inherently directional senses in many vertebrates. This means both that it is likely that information about visual cues is reaching the ICC, and that ICC processing could benefit from such cues. However, such effects have not yet been demonstrated in ICC.

Methods

The purpose of this study is two-fold. First, to combine visual inputs with auditory inputs in order to look for any visual influences on ICC single-neuron responses in-vivo. Second, to compare responses to identical multimodal stimuli in the SC and ICC. Responses were recorded extracellularly in anesthetized Mongolian gerbils. Visual stimuli were provided by a pair of tube headphones. Visual stimuli were provided by means of an LCD screen.

Results

Directional visual stimuli were applied alongside binaural sound stimuli in both the ICC and SC, with the goal of detect-

ing both direct and modulatory effects of multimodal stimuli. For auditory neurons, auditory stimuli that drive the neurons near the middle of their dynamic range were applied alongside a broad range of visual stimuli. For visual neurons, visual stimuli that drive the neurons near the middle of their dynamic range were applied alongside a broad range of auditory stimuli.

Conclusion

As two of the primary sites of convergence for sensory processing, understanding if and how multimodal stimuli influence the ICC and SC is critical to understanding how the brain integrates the broad range of sensory stimuli it receives.

PS - 467

Disruption of Binaural Hearing in a Family Harboring a Mutation in the Kv3.3 Voltage-Gated Potassium Channel

John Middlebrooks¹; Michael F Waters²

¹*University of California at Irvine*; ²*University of Florida*

Background

We studied a human family that carries an autosomal dominant mutation causing the adult-onset allelic form of spinocerebellar ataxia 13. The affected gene codes for the Kv3.3 voltage-gated potassium channel, which is expressed at high levels in binaural auditory brainstem pathways. We tested the hypothesis that individuals carrying the mutant allele would show disorders in binaural hearing.

Methods

Genotype status of affected and unaffected family members was confirmed by complete forward and reverse strand sequencing of the Kv3.3 gene. Clinical status of cerebellar ataxia was rated by the Scale for the Assessment and Rating of Ataxia (SARA), which can range from 0 (asymptomatic) to 40 (severe disability). We conducted hearing tests with 13 family members who were heterozygous for the mutation ("affected listeners"), 6 family members who lacked the mutation ("familial controls"), and an age-matched control group of 16 non-related normal-hearing individuals ("non-familial controls"). All listeners showed essentially normal age-appropriate pure-tone audiograms in both ears. We used an adaptive psychophysical procedure to measure thresholds for detection of interaural time differences (ITD) in low-passed sounds (<1600 Hz) and, in separate procedures, to measure thresholds for detection of interaural level differences (ILDs) in high-passed sounds (>3000 Hz).

Results

Most, but not all, of the affected listeners showed striking disruption of binaural hearing, with ITD and ILD thresholds around the highest values that we tested. In contrast, all familial and non-familial control listeners showed ITD and ILD thresholds within normal ranges. Across affected listeners, thresholds for ITD correlated significantly with those for ILD. Surprisingly, there was no significant correlation between binaural hearing status and cerebellar ataxia. That is, the 3 affected listeners having the best ITD thresholds had moderate ataxia (SARA scores 8.5 to 11), and 4 affected listeners

having little or no ataxia (SARA scores 0-1.5) had moderate or high ITD thresholds. That lack of correlation suggests that expression of the mutant allele is regulated differently in auditory and cerebellar pathways.

Conclusion

Affected listeners had essentially normal monaural hearing in either ear. The disruption of their sensitivity to interaural differences demonstrates the importance of the Kv3.3 channel subtype for the specific task of high-acuity comparison of signals from the two ears. Individuals with ITD and ILD thresholds as high as those observed presumably suffer deficits in sound localization and in spatial release from masking.

PS - 468

Pupil Dilation and Hearing Level

Determination

Soo Kim; Nadia Aguilon-Hernandez; Joëlle Martineau; Emmanuel Lescanne; David Bakhos
Université François-Rabelais de Tours, CHRU de Tours, UMR-S930, Tours, France

Background

There is currently no objective measure of hearing level we could use during cochlear implant fittings in young children at pre lingual stage, which makes difficult the assessment of comfort level in this population. According to the literature, the variation of pupil size is related to the complexity of mental processing and can be considered as the reflection of cognitive load. The aim of this preliminary study is to develop a new objective measure of auditory comfort threshold in adult patients with cochlear implant by measuring their pupil size during a listening task.

Methods

Thirteen post lingual cochlear-implanted adults (mean age 48 y.o. +/-17,7) were included. The experience with cochlear implant was 6 years +/- 5,7. The sex ratio was 1,5F/1M. The main etiology of deafness was progressive hearing loss. Patients were exposed to 4 lists of 10 spoken french words available in 4 different intensities (30, 50, 70, 90 dB SPL). A silence period of 5 seconds was placed between each list. No order was given to the participants. Pupillometry data were recorded every 17 ms using an eye-tracking system in a quiet room. Data were compared to a control group of 32 normal hearing adults (25 y.o. +/- 4,1) who passed an audiometry test. We investigated the latency and amplitude of dilation and constriction, the pupil mean size variation, and the relative peak of dilation which corresponds to the ratio between maximum peak dilation divided by the pupil-size dynamic range between dilation and constriction. All the data were compared to the baseline, which is the mean value of pupil size within the last second before stimulation.

Results

Mean pupil size was larger at high intensity (90 dB SPL) compared to low intensity (30 dB SPL) in both groups. The relative peak of dilation was higher when exposed to high intensity (90 dB SPL) than low intensity (30 dB) in both groups. The amplitude of dilation was significantly larger at 90 dB than 30 dB in the control group. No significant difference was

observed concerning the dilation latency and the constriction latency in both groups.

Conclusion

Pupil dilates with cognitive load and high intensity. The measure of pupil size during a listening task such as exposure to different intensities could be a new method to assess the patient's discomfort threshold, especially in young children in order to identify pupil's largest value during the implant fittings.

PS - 469

Evaluation of Cochlear Implant Performance Using a Biophysical Model

Sujin Kang¹; Hyejin Yang¹; Jong Ho Won²; Sung Hwa Hong³; Jihwan Woo¹

¹University of Ulsan; ²University of Tennessee; ³Samsung Medical Center

Background

Advances in signal processing for cochlear implants (CIs) have resulted in improved speech perception outcomes over the past two decades. The evaluation of a speech processing strategy generally utilizes human behavioral testing in the clinic or in laboratory settings. However, clinical trials may not be feasible to obtain extending data for various types of signal processing strategies, mapping parameters, and stimulus conditions. We have developed a three-dimensional imaging technique, the neurogram, that captures the simulated neural responses of the auditory nerve fiber (ANF).

Methods

Vowels were processed with an 8-channel CIS strategy to produce electric pulse trains. Using an ANF model (Woo et al., 2010, JARO), neural responses were simulated in response to the pulse trains over 8 channels. Using the neural firing activity information, a neurogram was constructed for each vowel, representing a neural response in the time-frequency domains. To quantify the similarity between neurograms, a neurogram similarity index (NSIM, Hines and Harte, 2012, Speech Commun.) was used to estimate the discrimination distance among eight vowels. As a showcase, we illustrate the effects of stimulation rate (900, 1200, and 1800 pulse/sec) and the presence of background noise (-5 to +10 dB SNR) on discrimination distance.

Results

As more background noise was added to vowels, the temporal precision of neural responses and the representation of vowel spectrum were smeared out; and as a result, the discrimination distance was significantly decreased. As the stimulation rate increased, the temporal precision of neural response increased, but the increase in the discrimination distance was not prominent.

Conclusion

The use of a biophysical model along with the NSIM provides an opportunity to examine the interaction between the processed electric signals and physiological conditions in the implanted ears. The method presented herein illustrates an efficient way of evaluating CI performance using the biophysical computational model. The proposed method, both objec-

tive and automated, can be used for a wide range of stimulus conditions, signal processing, and different biological conditions in the implanted ears. This technique is positioned to be an invaluable tool for customizing signal processing for individual CI users.

PS - 470

The Effect of Front-end Processing on Comodulation Masking Release Obtained in Cochlear Implant Users

Stefan Zirn¹; John-Martin Hempel²; Maria Schuster¹; Werner Hemmert³

¹Medical Center of the University of Munich; ²Medical Center of the University of Munich, ENT clinic; ³Technische Universität München, Bio-Inspired Information Processing

Background

Numerous experiments demonstrate the ability of listeners to compare the outputs of different auditory filters to enhance masked signal detection. This highly adaptable spectro-temporal pattern analysis has its optimum for maskers with envelopes fluctuating correlated across different frequency bands. Comodulation masking release (CMR) illustrates this effect. An earlier study (Zirn et al. 2013) already indicated that some listeners provided with multi-channel Cochlear Implants (CI) have remaining CMR capabilities. Aim of the present study was to reveal the integrity of current CI signal processing in terms of preserving cues necessary for CMR. Therefore, we compared results of two similar CMR experiments in the same group of subjects either using their CI processor running ACE or using a research interface running a modified ACE strategy.

Methods

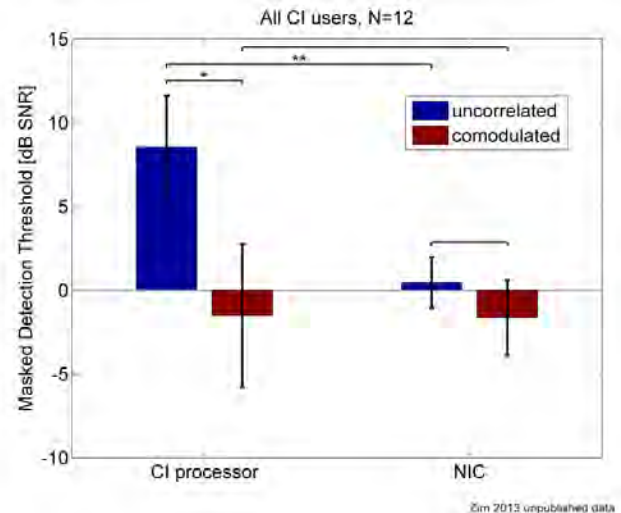
The stimuli consisted of five narrow-bands of noise with different center frequencies (masker components) and a target pure tone signal at the center frequency of the medial masker component. Masker envelope fluctuation was either correlated or uncorrelated across components. The difference of masked thresholds of the target between the correlated and the uncorrelated condition determined CMR. Thresholds were measured using an adaptive 3-AFC paradigm. Stimuli were either processed by the standard CI processor via audio cable (Cochlear type CP810) or via a modified ACE strategy using the Nucleus Implant Communicator (NIC). The modified ACE strategy bypasses front end signal processing and the filter bank of ACE. Stimuli were directly inserted into the frequency-time matrix and processed with further steps of ACE.

Results

Average CMR of 9 dB was measured in 12 participants using their CI processor, whereas CMR was only 3 dB using NIC (based on identical maps). Interestingly, underlying masked thresholds in the uncorrelated test condition were significantly higher using the CI processor than using NIC (about 8 dB). However, masked thresholds in the comodulated test condition were similar across test systems.

Conclusion

The relatively large amount of CMR obtained by stimulation using the CI speech processor running ACE was mainly based on extraordinary high masked thresholds in the uncorrelated test condition. Voltage measurements of CI channel outputs indicate potential reasons for this poor performance. Optimizing front-end processing in this regard may be beneficial for CI users in fluctuating interference.



PS - 471

Functional Changes Over Time After Deafening, Post-Deafening Treatments, and Cochlear Implantation

Melissa Watts; Bryan E. Pflingst; Deborah J. Colesa; Yehoash Raphael; Lisa L. Kabara; Cameron L. Budenz
University of Michigan

Background

Large variability has been seen in cochlear implant function for the first month or more after surgery. In this study we monitored these changes over time using various non-invasive measures. We sought to determine (1) the time required to achieve stability in implant function after various treatments and (2) to determine if all tested measures of implant function reflected the same time course of underlying events.

Methods

Behaviorally trained adult male guinea pigs underwent electrophysiological and psychophysical testing. Electrically-evoked compound action potentials (ECAPs) and psychophysical detection thresholds were recorded at frequent intervals after implantation until animal sacrifice. Three different treatment groups were used to create a variety of conditions in the implanted cochlea. 1. Hearing group: implanted in a hearing ear. 2. AAV.neurotrophin (*NTF-3* or *BDNF*) treated group: deafened with neomycin, inoculated with an adeno-associated viral vector (AAV) containing an active neurotrophin gene. Implantation occurred 30 min after inoculation in about half of the cases and after 2 weeks in the other half. 3. AAV. Empty group: deafened with neomycin, inoculated with an empty AAV.

Results

ECAP thresholds exhibited two distinct patterns in the data. Approximately half the animals exhibited an initial rise in thresholds that then decreased to a stable point. In the other half, thresholds started high and decreased to a stable point. Animals that were implanted two weeks after inoculation always exhibited the pattern of initial decrease suggesting that the initial rise seen in ECAP thresholds was a result of the first surgery. Most animals reached relative stability 30 to 90 days post implantation. Psychophysical thresholds exhibited similar variability across animal treatment groups with 17 out of 22 animals reaching stability by 30 days. ECAP growth function slopes, which reflect auditory nerve density, showed an initial decrease followed by an increase and then relative stability after 30 to 90 days. Both the ECAP and psychophysical results showed that once the data reached stability, the pattern typically remained relatively stable. However, some animals, regardless of treatment group, exhibited small but steady improvements in thresholds and slopes up to the time of sacrifice.

Conclusion

Results for the three measures showed similar timecourses, which suggests that the underlying mechanisms were similar. Studies of implant function should take this initial variability into account.

PS - 472

Temporally Coordinated Activity in the Brain is Promoted by Long-Term Cochlear Implant Use in Children

Salima Jiwani¹; Sam M. Doesburg²; Blake C. Papsin¹; Karen A. Gordon¹

¹Archie's Cochlear Implant Laboratory, The Hospital for Sick Children; ²Department of Diagnostic Imaging, The Hospital for Sick Children

Background

Cochlear implants (CI) are most effective at restoring the developmental trajectory of the auditory system in children when the duration of bilateral deafness is limited and both ears are implanted. Unfortunately, CIs were traditionally provided to children in only one ear, leaving the opposite and deprived pathways susceptible to reorganization. More than a decade later, many such children in our program have received a second implant in their opposite ear, allowing us to ask whether the neural network that supports hearing in these children is compromised by long-term unilateral auditory stimulation. Synchronized activity across brain areas is understood to mediate communication within the cortical hearing network that is activated by sound in normal hearing individuals, but these cortical networks have not been defined in children using CIs. We hypothesize that long durations of unilateral CI use will promote coordinated cortical activity between brain areas that are normally activated by sound, but that the deprived pathways are segregated from this network.

Methods

Electrically-evoked auditory cortical responses were recorded within the first week of bilateral cochlear implant activa-

tion in 33 children who used a unilateral CI to hear for 12.4 ± 1.7 years and received a second implant on the opposite and deprived side. Responses were collected from each ear separately using 64 scalp electrodes. Neural synchrony was calculated between electrodes in the theta, alpha, beta and gamma bands to assess temporally coordinated responses to sound across brain regions. Inter-electrode time series of phase locking values were calculated for each 1Hz intervals between 4 and 60Hz among electrode pairs.

Results

Preliminary findings indicate that stimulation of an experienced right cochlear implant evoked increased inter-electrode phase synchronization activity across the latency range in the theta frequency band with bursts of activity in the gamma frequencies. Alpha synchronization was decreased in the latencies underlying the evoked response. On the naïve side, theta activity was desynchronized across the latency range, and synchronization in the alpha frequencies increased with bursts of gamma activity.

Conclusion

The findings of decreased alpha and increased gamma synchronization evoked by the experienced ear are consistent with reports of increased demands of attention and alertness, despite the seemingly passive auditory task. The very different coordinated activity evoked by stimulation of the naïve ear indicates a distinct neural network at work on that newly implanted side.

PS - 473

A Fast Method for Measuring Psychophysical Thresholds Across the Cochlear Implant Array

Julie Bierer¹; Steven Bierer¹; Heather Kreft²; Andrew Oxenham²

¹University of Washington; ²University of Minnesota

Background

Detection threshold for individual channels in cochlear-implant listeners can be used clinically for device fitting, but is time-intensive. In the acoustic domain, thresholds can be estimated quickly with a technique similar to Bekesy audiometry using frequency sweeps. Here we evaluated a similar technique for cochlear implants, and compared estimates with traditional single-channel threshold estimates.

Methods

Postlingually deafened adult cochlear-implant users participated. Quadrupolar stimulation was used with four adjacent electrodes. The active current was delivered to the two center electrodes, with a fraction, alpha, directed to the more basal site and the remainder to the apical site. A fraction, sigma, of the return current was delivered evenly to the outer two (flanking) electrodes with the remainder flowing through a distant ground electrode. Analogous to an upward acoustic frequency sweep, the alpha value was increased from 0 to 1 in small steps for the most apical set of active electrodes; this process was repeated for the next, more basal, set of electrodes until all available electrode sets were tested (2 to 15) in a single sweep. Listeners were also tested with downward sweeps. Listeners pressed a button when the signal was audible and

released it when it became inaudible, and the current level was decreased while the button was pushed and increased while the button was released. Stimuli were 200-ms trains of biphasic pulses, 97 μ s per phase, at a rate of ~1000 pulses per second, repeated at 300-500 ms intervals. Sigma was fixed at 0.9 or 1.0, and the size of the alpha steps, the level steps, and the number of stimulus repetitions were varied to assess their effect on the measured thresholds. For comparison, thresholds were also measured using a standard, adaptive two-interval, two-alternative forced choice procedure for a subset of electrodes using the same stimulus parameters.

Results

Preliminary results show similar averages for sweep and adaptive thresholds when alpha was the same. The sweep method took approximately 12 minutes (with a 500-ms stimulus interval) to complete two runs of forward and backward sweeps. In comparison, the two-interval forced choice procedure took approximately 8 minutes to complete four runs for one channel, or nearly 2 hours for all 14 channels.

Conclusion

Preliminary findings demonstrate the potential of a new method for measuring psychophysical thresholds for individual cochlear-implant channels that, if successful, could be implemented clinically.

PS - 474

Single- and Multi-Channel Modulation

Detection by Cochlear Implant Users

John Galvin¹; Qian-Jie Fu¹; Sandy Oba¹; Deniz Baskent²

¹House Research Institute; ²University of Groningen

Background

Modulation detection has been used to characterize cochlear implant (CI) users' temporal processing. While single-channel modulation detection has been extensively studied, little is known about multi-channel temporal processing. How does modulation sensitivity on single channels contribute to the multi-channel percept? Do CI users integrate stimulation on all channels or attend to only the best (or worst) channel? How does the loudness summation associated with multi-channel stimulation affect modulation detection? For a fixed number of pulses, is modulation sensitivity similar for single- and multi-channel stimulation?

Methods

In this study, single- and multi-channel modulation detection was measured in 9 CI users. Experimental electrodes were evenly distributed from the base to apex. The stimulation rate for each electrode was 500 pulses per second. Modulation detection thresholds (MDTs) were measured at relatively low and high presentation levels and modulation frequencies. Single- and multi-channel channel MDTs were measured at equally loud presentation levels; multi-channel MDTs were also measured without compensation for loudness summation. To test whether multi-channel envelope coding improved modulation sensitivity, multi-channel MDTs were also measured with coherent modulation applied to one of four channels or to all four channels

Results

MDTs were generally better at the higher presentation level and at the lower modulation frequency. Differences in single-channel MDTs across stimulation sites ranged from 1.78 to 15.56 dB. However, multi-channel stimulation largely mediated single-channel deficits. Without the loudness compensation, multi-channel MDTs were most comparable to the best single-channel MDT. Coherent modulation applied multiple channels produced better MDTs than when applied to only of the four component channels. There was a small but significant advantage to distributing the pulses used to code modulation to multiple channels, rather than to a single channel.

Conclusion

The present data suggest that for some CI users, multi-channel modulation sensitivity may be largely driven by the best component channel. For CI users with less across-site variability in MDTs, multi-channel stimulation may enhance modulation sensitivity. Because component channel stimulation levels must be reduced to compensate for multi-channel loudness summation (as in clinical fitting), modulation sensitivity is reduced for individual channels. As such, selecting only channels with good modulation sensitivity may reduce summation and allow for higher stimulation levels on component channels, which may improve overall modulation sensitivity.

PS - 475

The Study of Molecule Pathogenesis in 1123 Cochlear Implantation Recipients

Jun Liu; Shasha Huang; Fei Yu; Guojian Wang; Yongyi Yuan; Mingyu Han; Dongyang Kang; Mengdi Hong; Aiting Chen; Pu Dai

Department of Otolaryngology and Head & Neck Surgery, Otorhinolaryngological Institute, Genetic Testing Center for Deafness, Chinese People's Liberation Army General Hospital

Background

Cochlear implantation(CI)is one of the effective methods for severe and profound sensory deafness. It has been used successfully to restore hearing in more than 20,000 patients with severe and/or profound sensory deafness in China. However, up to date, the molecule pathogenesis about these patients were remaining unclear in China. There is no systematical study in a large sample size has been carried out in China. The influence of various hereditary etiological factors on the curative effect of CI has not been studied. In this study, we studied the genetic molecule pathogenesis of cochlear implantation recipients with severe and profound sensory deafness, and its effect on curative effect.

Methods

1123 patients, aging from 9 months to 75 years old, who received CI from February 2009 to February 2013 in the Department of Otolaryngology in Chinese PLA General Hospital, were recruited in this study. The patients had received Cochlear implantation, made from Australia Cochlear straight electrode(73) and curved electrode(350), cases

Australian Cochlear FREEDOM(116), American Advanced Bionics 90K(87), Austria MED-EL C40+(173), MED-EL SONATA(135), MED-EL PULSAR(83), and Chinese CI(106). The molecule pathogenesis of 1123 CI recipients has been analyzed. Mutation screening of mtDNA A1555G, *SLC26A4* gene, *GJB2* gene, and *GJB3* gene were carried out. The evaluations of curative effect was estimated by auditory threshold, speech recognition and questionnaire survey with meaningful auditory integration scale (MAIS), categories of auditory performance (CAP), and speech intelligibility rating (SIR). The postoperative outcomes were also analyzed between the patients with positive and negative results of screening of gene mutations.

Results

GJB2 gene mutations had been identified in 292 cases(26%). *GJB2* gene mutations at 235delC, 176del 16, 299delAT, and 35delG, are the hot mutational spots. 192 cases had been found *SLC26A4* gene mutations(17.1%). The major *SLC26A4* gene mutations distributed from Exon 7, 10, 19, 17, and Exon 5. IVS7-2 A>G is the most common *SLC26A4* gene mutation. Five patients were found carrying mtDNA A1555G mutation. Three *GJB3* gene polymorphism, 357C>T, 474G>A, and 94C>T were also had been identified. Both of the auditory thresholds with CI of patients with positive *GJB2* gene and *SLC26A4* gene mutation are 30 dB HL. The evaluations of curative effect, including auditory threshold, speech recognition and questionnaire survey, in patients with positive *GJB2* gene and *SLC26A4* gene mutation had no significant difference compared to the control group ($P>0.05$).

Conclusion

The genetic background of 43.6% CI recipients is autosomal recessive inheritance hearing loss. *GJB2* gene mutations is the major cause for the autosomal recessive non-syndromic hearing impairment with the gene mutational frequency of 26%. *SLC26A4* related gene, *SLC26A4*, accounts for about 17.1% cases. Mitochondrium DNA A1555G mutation accounts for 0.5% cases. *GJB3* gene mutations is rare in Chinese population. We speculated that the incidence of hereditary hearing loss is 60% in general deafness population. The genetic backgrounds of 16.4% cases remain unclear, future genetic molecular analysis should be carried out. Postoperative outcomes of hearing and speech in the patients with *GJB2* (Cx26) gene mutation and *SLC26A4* were satisfied.

PS - 476

Changes in Hearing Thresholds and Hair Cell Synapses After Chronic Electro-Acoustic Stimulation in Guinea Pigs With High-Frequency Hearing Loss

Gemaine Stark¹; Hongzhe Li¹; Kayce Spear¹; Hongzheng Zhang²; Chiemi Tanaka³; Anh Nguyen-Huynh¹; Lina Reiss¹
¹Oregon Health & Science University; ²Zhujiang Hospital, Southern Medical University; ³University of Hawaii at Manoa

Background

The goal of Hybrid or electro-acoustic stimulation (EAS) cochlear implants (CIs) is to provide high-frequency electric hearing while preserving residual low-frequency acoustic

hearing for combined electric and acoustic stimulation in the same ear. However, a third of EAS CI patients lose 30 dB or more of low-frequency hearing months after implantation (Gantz et al., 2010; Gstöttner et al., 2009). We recently showed that EAS may increase hearing loss beyond that induced by surgery in normal-hearing guinea pigs, but these threshold shifts are not explained by hair cell or spiral ganglion cell loss (Tanaka et al., ARO 2012). Hearing loss may be caused by more subtle synaptic changes rather than cell death. In addition, pre-existing hearing loss may influence the effects of EAS on residual hearing. Here we extend the investigation of EAS effects on hearing to guinea pigs with high-frequency hearing loss similar to that in EAS CI patients, and use immunolabeling to determine whether changes at the hair cell synapse explain the threshold changes.

Methods

Sixteen guinea pigs were exposed to 24 hours of octave-band noise (12-24 kHz) at 116 dB to induce a high-frequency hearing loss. After 5 weeks of recovery, twelve animals were implanted with an 8-electrode array and divided into two groups: chronic acoustic and electric stimulation (CAES; n=6) and no stimulation (NS; n=6) controls. Four non-implanted animals served as chronic acoustic stimulation controls (CAS; 6 ears). CAES and CAS animals were stimulated 3 hours/day, 5 days/week for 9.5 weeks with modulated white noise. Auditory brainstem responses were recorded biweekly to monitor changes in hearing. At the conclusion of the study, cochleae were immunostained for confocal imaging with phalloidin, anti-CtBP2, and anti-GluR2. Hair cells, ribbons and post-synaptic receptors were quantified.

Results

After chronic stimulation, animals in the CAES group had a statistically significant 9 dB greater threshold shift at 1 kHz compared to the NS group, but not at 2 or 4 kHz. Immunolabeling results will be presented and correlated with the ABR results.

Conclusion

The increased hearing loss at 1 kHz with EAS compared to surgery alone is consistent with the previous study in normal-hearing animals, indicating suitability of this model for EAS CI patients. EAS-induced hearing loss may arise from an excitotoxic mechanism from combined electric and acoustic stimulation similar to that seen for noise-induced hearing loss.

PS - 477

Electrophysiological Monitoring of Residual Hearing During and After Cochlear Implantation

Adrian Dalbert; Jae Hoon Sim; Alexander M Huber
 University Hospital of Zurich

Background

Improvement of surgical techniques and electrode design increased hearing preservation rates after cochlear implantation in recent years. However, in a considerable amount of patients partial or complete loss of residual hearing still oc-

curs. The underlying mechanisms are poorly understood so far. Among many others acute direct trauma from electrode insertion and hydraulic forces as well as delayed events such as foreign body reaction and molecular activation leading to delayed neural injury are discussed. Our goal was to further assess time and mechanisms of loss of residual hearing after cochlear implantation and see if changes in electrocochleographic hair cell and neural responses correlate with postsurgical psychoacoustic test findings.

Methods

Patient with some degree of residual hearing undergoing cochlear implantation were included. Electrocochleographic measurements were conducted by a monopolar measurement electrode placed next to the round window before opening the cochlea and immediately after cochlear implantation. In some patients further measurements with different electrodes of the cochlear implant itself as measurement electrode followed in growing intervals in the first few days and weeks after surgery. At each session cochlear microphonic (CM), summating potential (SP), compound action potential (CAP), and auditory nerve neurophonic (ANN) responses to tone bursts of different intensities at frequencies of 250 to 2000Hz were recorded. Additionally, pre- and postsurgical psychoacoustic tests including pure tone audiometry and speech perception tests were performed.

Results

Even in patients with very limited residual hearing in presurgical pure tone audiometry hair cell and neural responses were measurable by electrocochleography. Immediately after surgery hair cell and neural responses were still detectable in most patients. These findings correlated not with partial or complete loss of residual hearing in pure tone audiometry after 4 weeks.

Conclusion

Electrocochleography allows the assessment of cochlear and neural status during and after cochlear implantation. Immediately after surgery loss of electrocochleographic responses occurs rarely. This suggests that with current surgical techniques and electrode designs in most cases loss of residual hearing is not due to acute trauma during surgery. More likely changes within the first weeks are causing hair cell or neural injury. Further assessment of these mechanisms is possible by repeated electrocochleographic measurements with the electrodes of the cochlea implant itself.

PS - 478

Cortical Surface Current Source Density Analysis of Acoustic and Electric Stimulation

James Fallon¹; Sam Irving¹; Satinderpall Pannu²; Angela Tooker²; Andrew Wise¹; Robert Shepherd¹; Dexter Irvine¹
¹Bionics Institute; ²Lawrence Livermore National Laboratory

Background

Current source density (CSD) analysis from arrays of penetrating electrodes has been used to examine the layer-specific activation of the auditory cortex and highlight the plastic changes associated with long-term deafness and chronic intracochlear electrical stimulation. Here, we used CSD anal-

ysis of surface array recordings to highlight the different activation patterns seen with acoustic and electric stimulation.

Methods

Two groups of cats were used: 2 normal hearing controls (NHC) and four neonatally partially deafened cats that received approximately 6 months of intra-cochlear electrical stimulation from a clinical cochlear implant and speech processor (NDS). Thin-film polyimide substrate arrays (4 x 8 electrodes, 0.4 mm pitch) were used to record surface evoked potentials from the auditory cortex in the cats as adults. Stimuli were either tone-pips (100-ms duration, 5-ms rise/fall) at a range of stimulus intensities and frequencies (NHC & NDS) or single biphasic current pulses (25 us/phase, 8-us interphase gap) at a range of current levels on a range of intracochlear electrodes (NDS only).

Results

Robust evoked potentials could be elicited to stimuli in all animals, from which it was possible to determine the distribution of 'characteristic frequencies' or 'best electrodes' across the cortical region under the recording array. CSD analysis (along caudal-rostral cortical strips) of the responses to tone-pips presented at frequencies represented in the cortex under the recording array demonstrated a stereotypical single current source flanked by current sinks on both the caudal and rostral sides. In contrast, tone-pips at frequencies not represented in the region under the array, but known (on the basis of normal tonotopic organization) to be represented caudal to the recording array, had a more complex pattern of many sources and sinks. In the NDS group, although the morphology of the evoked potentials were similar to that of responses to tone-pips, CSD analysis of the responses to electrical stimulation of cochlear locations represented in the cortical region under the recording array had a complex pattern of multiple sources and sinks.

Conclusion

The CSD analysis revealed a simple pattern of a single current source and flanking sinks for tone-pips that is consistent with side-band inhibition. The more complex pattern of current sources and lack of surrounding current sinks in response to electrical stimulation is likely due to the broad peripheral activation produced by such stimulation.

PS - 479

Effects of Therapeutic Hypothermia on Cochlear Implantation Trauma

Efrem Roberson; Suhrud Rajguru

University of Miami

Background

Over the last few decades, mild hypothermia has been shown to have neuroprotective qualities following ischemic and traumatic injuries. More recent studies have shown potential therapeutic application of mild to moderate hypothermia in the auditory pathway to prevent functional loss post cochlear implant surgery. This may be particularly important for protecting residual hearing in patients given the recent trend to implant hybrid electro-acoustic stimulation devices. In the present study we have designed a device to fit proximal

to the middle turn of the cochlea that provides localized mild hypothermia. Here we evaluate the efficacy of our device in preventing functional loss correlated with surgical trauma.

Methods

Auditory Brainstem Responses (ABRs) were performed on sedated guinea pigs to assess their hearing function before and after cochlear implant surgeries. Surgeries were performed on one ear while providing localized mild hypothermia to the middle turn of the cochlea for 30 minutes before and after induction of trauma. The hearing thresholds were compared to controls that did not receive hypothermia during surgery. In all cases the contralateral ear was used as an internal control. In acute experiments, ABRs were performed before surgery and at 30-minute intervals after surgery for 150 minutes. In the chronic experiments, ABRs were performed before surgery and at various time points up to 30 days after surgery. At the conclusion of the trials, inner ears were harvested for histology. All procedures were approved by the IACUC of University of Miami.

Results

In control ears that did not receive hypothermia during cochlear implantation we saw initial hearing threshold loss of 40 dB on average. With the hypothermia device we observed near three degrees Celsius cooling from measurements taken at the round window. Hearing thresholds from the cochlea that received local hypothermia during cochlear implantation were similar to contralateral naive cochlea after initial insult. In chronic experiments, we saw functional improvement in implanted cochlea that received hypothermia a few days after implantation surgery.

Conclusion

Histology showed hair cell loss in the basal turn of the cochlea from implantation surgery that corresponded to hearing loss caused by surgical trauma. Initial results show that hypothermia prevented significant functional loss due to the cochlear implant surgery. Further experiments are underway to characterize the therapeutic benefits of localized hypothermia.

PS - 480

Auditory Evoked Responses to Pitch Matched Electroacoustic Stimuli in Unilateral Cochlear Implant Users With Residual Hearing in the Contralateral Ear

Chin-Tuan Tan¹; Brett Martin²; Keena Seward¹; Ksenia Prosolovich¹; Ben Guo¹; Elizabeth Glassman¹; Mario Svirsky¹

¹New York University, School of Medicine; ²CUNY, Speech and Hearing

Background

Some unilateral cochlear implant (CI) patients who have residual hearing in their unimplanted ears are able to compare the pitch percepts elicited by electrical stimulation with those elicited by acoustic hearing. The goal of this study is to use the changes in the pitch percepts elicited by a given electrode over time as a metric to examine the perceptual process in adapting to their devices, after implantation.

Methods

Experiments were conducted using a real-time pitch matching platform which presents interleaving short intervals (500ms) of acoustic and electrical stimulation to CI patients. CI patients were instructed to adjust the frequency of the acoustic tone to match the percept elicited by electrical stimulation; six repetitions for several electrodes in the array. Same stimuli of longer interval (1000ms) were used for recording their Auditory Evoked Potentials. Cochlear CI patients received electrical stimulation in electrode 20 which is associated with a frequency band centered at 500Hz in their clinical map and the other ear was stimulated with six different acoustic frequencies between 250Hz and 1000Hz including the pitch matched frequency to electrode 20. For Advanced Bionics CI patients, electrode 3 (which is associated with a frequency band centered at 540Hz in the clinical map) was used instead. Each pair of electric and acoustic stimuli was repeated 500 times and the recording trigger was inserted at the onset of the acoustic stimulus. We also tested 10 normal hearing (NH) control subjects, where a fixed 500Hz tone was presented to one ear (instead of the electrical stimulation) and tones of 250Hz, 375Hz, 500Hz, 625Hz and 1000Hz were presented to the other ear.

Results

All 11 CI patients tended to show tonotopic pitch percepts, but not for every electrode. As for AEP recordings with CI patients, N1 latency was minimized when the acoustic and the electrical stimulus were pitch-matched. In the case of NH listeners, N1 latency was minimized when both ears were stimulated with the same frequency. These results suggest that the latency of N1 can potentially be used as an objective measure of pitch matching across two ears for the CI patients.

Conclusion

Our data appears to support N1 latency as a potential marker of frequency mismatch in both normal hearing subjects and CI users who have acoustic hearing in the contralateral ear and who can perform the pitch matching task successfully.

PS - 481

Use of the Phantom Electrode Strategy to Improve Bass Frequency Perception For Music Listening in Cochlear Implant Users

Tina Munjal¹; Alexis Roy¹; Courtney Carver¹; Patpong Jiradejvong¹; Charles Limb²

¹Johns Hopkins University School of Medicine; ²Johns Hopkins University School of Medicine, Peabody Conservatory of Music

Background

Low-frequency hearing in cochlear implant (CI) users has previously been limited by the electrode length and insertion depth of the implant, factors which determine the extent to which apical cochlear stimulation can be achieved. It has been shown that partial bipolar stimulation—involving the application of current to the most apical electrode along with a compensating current to the more basally located adjacent electrode—allows for a pitch percept that is lower in frequen-

cy than the most apical physical electrode. This approach is referred to as the “phantom” electrode (PE) strategy. The objective of this study is to determine the effect of PE stimulation on CI users’ perception of bass frequency information in music.

Methods

We used the previously developed CI-MUSHRA tool (Multiple Stimulus with Hidden Reference and Anchor) to assess changes in bass frequency perception when PE stimulation was applied to the most apical electrode. Six Advanced Bionics CI users (4 unilateral and 2 bilateral) implanted with either the CII or HiRes 90K implant using the HiRes Fidelity 120 processing strategy and ten normal hearing controls offered musical sound quality ratings from 0 (poor) to 100 (excellent) for 7 versions of the same musical segment. Five versions were high pass filtered to remove all frequencies below 200, 400, 600, 800, or 1000 Hz; one version was band pass filtered to remove all frequencies between 1000 and 1200 Hz (“anchor”); and one was unaltered (“hidden reference”). This test was performed for each of 25 five-second musical segments. The CI users performed this test both with and without PE stimulation, with randomization of the starting condition. Performance on the task was captured as a one-number score, which reflected mean deviation (across all versions) from the performance by normal hearing listeners on the task. Thus, a score closer to zero indicated improved performance.

Results

Partial bipolar stimulation of the most apical electrode reduced CI users’ CI-MUSHRA score by an average of 7.895 points (Paired $t(5) = 2.65$, $p = 0.045$ (two-tailed), 95% confidence interval [0.02368, 15.5532]). This suggests that PE stimulation of the most apical electrode improves CI users’ perception of bass frequency information in musical stimuli.

Conclusion

Creation of a phantom electrode percept through partial bipolar stimulation of the most apical electrode appears to improve CI users’ perception of bass frequency information in music, contributing to greater accuracy in the ability to detect alterations in musical sound quality. The phantom electrode processing strategy may enhance the experience of listening to music without the need for a longer electrode or deeper insertion. Further studies are needed to examine the optimal parameters for the phantom processing strategy.

PS - 482

Musical Sound Quality in Cochlear Implant (CI) Users: A Comparison in Bass Frequency Perception Between Med-El’s Fine Structure Processing (FSP) and HDCIS Strategy

Alexis Roy¹; Courtney Carver²; Patpong Jiradejvong²; Charles Limb²

¹Harvard Medical School; ²Johns Hopkins University

Background

Med-El’s newest generation fine structure processing (FSP) strategy offers the potential to improve musical sound quality for cochlear implant (CI) users by increasing bass frequency

representation. Current assessments of musical quality differences between FSP and Med-El’s older generation HDCIS strategy have been limited to subjective rating scale appraisals. The aim of this study was to compare performance between Med-El’s FSP and HDCIS strategies using the CI-MUSHRA method, which can provide a more objective assessment of musical sound quality perception.

Methods

8 CI users implanted with a standard Med-El array and utilizing an OPUS II speech processor and FSP strategy for at least 9 months were enrolled in this study. In the first session, participants completed the CI-MUSHRA evaluation utilizing their current FSP strategy. Patients were then programed with the default HDCIS strategy and acclimatized for two months. In the second session, participants were retested with HDCIS and then switched back to their FSP strategy and tested acutely. For each CI-MUSHRA evaluation, participants were required to detect sound quality differences between versions of musical pieces with various amounts of bass frequency removal. The ability to detect differences among musical sound quality versions served as a quantitative indicator of sound quality perception.

Results

CI users performance significantly declined when utilizing HDCIS, as compared to FSP at baseline ($p < 0.05$). Baseline performance with FSP was significantly better than acute testing with FSP after two months practice with HDCIS, suggesting that participants had (at least partially) acclimatized to HDCIS ($p < 0.05$). Furthermore, performance more closely resembled that of NH controls with FSP than with HDCIS, and CI users were able to make more fine-grained sound quality discrimination with FSP as well.

Conclusion

CI users had improved musical sound quality discrimination (as quantified by CI-MUSHRA) when utilizing the clinical default FSP strategy than with HDCIS. This is the first study (to our knowledge) that has demonstrated objective improvements in musical sound quality perception with the newer generation FSP strategy

PS - 483

Perception of Musical Noise in Cochlear Implant and Normal Hearing Listeners

Stefano Cosentino; Torsten Marquardt; David McAlpine

Ear Institute - UCL

Background

Cochlear implants (CI) are hearing restoration instruments that have proven successful for many listeners with severe to profound hearing loss. Speech perception in adverse listening conditions, such as in noisy or reverberant environments, however, is still a major challenge for CI users. To maintain high speech intelligibility in these conditions, several speech enhancement algorithms from hearing aid research and the engineering field have been tested for CI users, and some are already commercially available in commercial devices. In this study, we focus on the effect on speech intelligibility of a

specific sound artifact - known as musical noise - that is produced by certain enhancement algorithms.

Methods

Here, musical noise was artificially generated such that three parameters could be independently controlled, namely the peak height (PH), the peak width (PW) and the peak density (PD). With respect to a speech enhancement algorithm, PH, PW and PD relate to the working signal-to-noise ratio (SNR) of the algorithm, its analysis time window, and the accuracy of the speech enhancement algorithm, respectively. The effect of these parameters on the speech intelligibility was tested in three listening modes: normal hearing, cochlear implant simulated via vocoder, and cochlear implant via acoustic input.

Results

Experimental results show that by increasing the PD from zero (clean condition) to one (continuous white noise condition), the speech intelligibility scores decrease for all listening modes, although with different rates. The measurements were repeated by keeping the PH constant (i.e., constant SNR). Finally, in all three listening conditions, an optimal analysis time window was derived with respect to speech intelligibility.

Conclusion

These findings have direct practical implications for the parameterisation of speech enhancement algorithms for CI users.

PS - 484

A Psychophysical Measure of Neural Health Predicts Speech Recognition in Humans With Cochlear Implants

Ning Zhou^{1,2}; Bryan Pfingst¹

¹University of Michigan; ²East Carolina University

Background

Comparisons of performance with cochlear implants and postmortem conditions in the cochlea in humans have shown mixed results. These results however can be confounded by many factors including cognitive variables, the cause of death, and the time intervals between the functional measurements and the temporal bone analysis. Animal models, where some of these factors are better controlled, have revealed non-invasive functional measures that can be used to assess cochlear health in living organisms. One such measure is multipulse integration. Animals with better neural health near the implant are able to better integrate multiple pulses in a given time window yielding steeper threshold-versus-pulse-rate (multipulse-integration) functions.

Methods

The present study examined the relationship between the slopes of multipulse-integration functions in humans with cochlear implants and their speech recognition performance. To avoid confounding effects of across-subject cognitive differences, a within-subject design was used, where the ear differences in neural health as predicted by the multipulse-integration function slopes were compared to the ear differences in speech recognition. Eight bilaterally implanted subjects were tested. For measuring multipulse integration, psycho-

physical detection thresholds were measured using method of adjustment for two pulse rates (80 pps and 640 pps) for all functioning stimulation sites in both ears. Slopes of threshold versus pulse rate functions were derived. Speech reception thresholds and phoneme recognition in noise were measured for both ears.

Results

Subjects who had steeper slopes of the multipulse integration functions in one ear also had better speech reception thresholds for sentences in noise and better consonant and vowel recognition in the same ear. Furthermore, magnitude of ear differences in the multipulse-integration slopes predicted the magnitude of ear difference in consonant recognition in noise and in the transmission of place of articulation of consonants.

Conclusion

These results support the idea that neural health in the inner ear is important for speech recognition with cochlear implants, particularly for tasks that rely on spectral information.

PS - 485

Binaural Unmasking With Temporal Envelope and Fine Structure in Cochlear Implant Listeners

Ann Todd¹; Matthew Goupell²; Ruth Litovsky¹

¹University of Wisconsin-Madison; ²University of Maryland, College Park

Background

In noisy environments, binaural hearing provides a benefit to speech reception and signal detection. This benefit, known as binaural unmasking, is partially due to the reduction in interaural correlation that occurs in temporal envelope and fine structure when there is spatial separation between sources. Listeners with bilateral cochlear implants (BiCIs) have shown binaural unmasking for signal detection. However, the extent of unmasking is limited, which may be a result of speech processing strategies that present information in the temporal envelope but not in the pulse timing. This study aimed to determine whether presentation of acoustic temporal fine structure information in the pulse timing would improve binaural unmasking for BiCI users.

Methods

Diotic (N0S0) and dichotic (N0Spi) signal detection thresholds were measured in 4 adults with BiCIs and 8 adults with normal hearing (NH) who listened to a BiCI simulation. Noise bands had center frequencies at 500 and 750 Hz for the BiCI users, and 125, 250, and 500 Hz for the NH listeners. The envelope of the noise was presented with either (1) a pulse train presented at a constant rate equal to the noise center frequency or (2) a pulse train presented at a non-constant rate that was timed to the positive peaks in the noise fine structure.

Results

BiCI users' N0Spi thresholds were approximately 13 dB lower than N0S0 thresholds in both the constant and non-constant rate conditions. For NH listeners, the N0Spi thresholds improved with the non-constant rate compared to the constant

rate, but only at rates less than 500 Hz. This improvement was due to poorer N0Spi thresholds at lower rates with the constant rate stimuli rather than an improvement in N0Spi thresholds at lower rates with the non-constant rate stimuli.

Conclusion

The results suggest that presentation of acoustic temporal fine structure in pulse timing does not improve binaural unmasking at rates 500 Hz or greater. This result is contrary to findings in previous studies that non-constant pulse timing can improve sensitivity to interaural time differences at high rates [Laback and Majdak, 2008, Proc Natl Acad Sci USA, 105, 814-817; Goupell, Laback, and Majdak, 2009, J Acoust Soc Am, 126, 2511-2521]. The discrepancy between findings may be due to the modulation in the pulse trains used in the present experiment, which appears to decrease the importance of pulse timing at high pulse rates.

PS - 486

Influence of Pulse Shape and Electrode Position in Cochlear Implants: Experimental and Modeling Studies

Marek Rudnicki; Karg Sonja; Christina Lackner; Werner Hemmert

Technische Universität München

Background

Cochlear implants (CIs) stimulate the auditory nerve with charge-balanced biphasic pulses. However, in animal experiments, monophasic or asymmetric pulses result in higher efficiency (Wiler et al. 1989). Additionally, spiral ganglion cells in the modiolus of the cochlea do not reach up to the very end of the cochlea. It is therefore likely that the electrical stimulation at far apical locations differs from medial and basal positions. We therefore investigated responses to triphasic and biphasic pulses elicited by apical and medial electrodes.

Methods

We tested 7 CI patients (MED-EL-PulsarCI100) using standard biphasic pulses and compared their loudness perception with triphasic pulses. All leading-phase polarity combinations were investigated on the 1st (most apical) and the 6th (middle) electrode. The task was to adjust the loudness (2-AFC, 2-down/1-up) of the triphasic pulses to the biphasic reference at a near-threshold level (threshold+25µA).

We complemented our experiments with a multi-compartment Hodgkin-Huxley type neuron model. It consisted of alternating nodes of Ranvier with active ion channels (Negm and Bruce 2008) and myelinated inter-nodes. Electrical stimulation was simulated with a point electrode assuming a homogeneous medium.

Results

We found a significant threshold difference when we switched pulse polarity for triphasic pulses, but only at the most apical (1st) electrode. At the middle (6th) electrode, changes were smaller and not statistically significant. Additionally, our results showed that triphasic pulses were less efficient than biphasic pulses which is in agreement with Coste and Pfingst (1996).

We could replicate our findings with a multi-compartment neuron model. The model predicted two stimulation regions along the neuron. For the electrode positions beside the neuron, the compartment closest to the neuron received the highest stimulation, sidelobes were much smaller. In contrast, when the electrode moved close to the end of the neuron and beyond, the stimulation by the sidelobe started to dominate. This change inverted the efficiency between both polarities.

Conclusion

Polarity affects the efficiency of triphasic pulses significantly at the most apical electrode position. Model calculations suggest that this is probably caused by an edge effect, when the stimulation electrode is located close to the end of the neuron.

PS - 487

Efficient Environment Detection for Adaptive Speech Enhancement in Cochlear Implants

Oldooz Hazrati; John Hansen; Emily Tobey

The University of Texas at Dallas

Background

Although cochlear implant (CI) users are able to identify speech in anechoic quiet environments well, their speech recognition performance drops significantly in noisy and/or reverberant environments. Therefore, speech enhancement algorithms that can suppress the impact of noise and/or reverberation in CIs are of great interest. Several strategies have been proposed in order to alleviate adverse effects of noise and reverberation on speech, resulting in substantial speech intelligibility/quality gains for CI users.

Despite effectiveness of speech enhancement strategies in improving the quality and/or intelligibility of noisy, reverberant, and noisy reverberant speech for CI users, tackling the negative effects of each type of maskers requires environment-specific strategies which are often dependent on the nature of distortion (e.g., convolutive vs. additive interferences). Hence, environment detection and classification becomes an essential element to adaptively provide proper speech enhancement strategies for different listening environments.

Methods

In this study, we propose three features for the environment classification task in CIs. These features (extracted from the output of the maxima-selection stage in the advanced combination encoder-ACE) are based on the average inter-stimuli intervals (ISI), stimulation length (SL), and stimulation energy (SE) of frequency channels in the CI device. Gaussian mixture model (GMM), and support vector machine (SVM) classifiers are trained based on these features computed in different acoustic environments.

Results

Performance of the proposed feature set is evaluated in the context of environment classification tasks under anechoic quiet, noisy, reverberant, and noisy reverberant conditions. Speech material from the IEEE database are used to simulate different acoustic environments with 1) three measured room impulse responses (RIR) with distinct reverberation

times (T_{60} = 0.3, 0.6, and 0.8 s) for generating reverberant environments, and 2) car, train, white Gaussian, multi-talker babble, and speech-shaped noise samples for creating noisy conditions at -5, 0, 5, and 10 dB signal-to-noise ratios. Experimental results indicate effectiveness of the proposed features for environment classification (over 97% correct environment classification was achieved using SVM and GMM classifiers). This is due to the efficacy of the proposed feature vector in pertaining environment specification and consequently training robust classifiers.

Conclusion

The environment classification is of great importance for CIs where there exist speech enhancement algorithms that function well in a specific environment but degrade speech quality/intelligibility in other environments. Incorporating speech enhancement strategies in environments for which they are optimized will avoid unnecessary battery usage and extra signal processing in the CIs.

Condition	SVM				GMM			
Clean	96.11	1.19	2.70	0.00	94.70	1.66	3.64	0.00
Reverberant	1.30	97.86	0.64	0.20	1.67	97.37	0.85	0.12
Noisy	2.17	0.29	97.33	0.21	2.43	0.41	97.16	0.00
Noisy reverberant	0.00	0.16	0.00	99.84	0.03	0.27	0.40	99.31

Table 1. Environment classification confusion matrices for SVM and GMM classifiers.

PS - 488

Temporal Processing and Speech Perception in Cochlear Implant Users and Normal Hearing Controls

Chelsea Blankenship; Fawen Zhang; Robert Keith
University of Cincinnati

Background

Despite improvements in cochlear implant (CI) speech recognition abilities, substantial variability across individual outcomes remains. Temporal processing capabilities contribute strongly to the variability in speech recognition (Fu, 2002). Across-frequency gap detection may better reflect speech recognition performance since speech sounds consist of components in various frequency ranges (Lister et al., 2007). The purpose of this study was to determine if Cortical Auditory Evoked Potentials (CAEPs) to gaps in pure tones are related to behavioral temporal processing abilities assessed with gap detection thresholds (GDTs) and speech perception performance. Results can help increase our understanding of the large variability in speech perception performance.

Methods

Ten post-lingual CI recipients and age- and gender-matched NH controls were recruited. Speech perception materials

consisted of the following measures; CNC words, AzBio sentences, Bamford-Kowel-Bench Speech in Noise Test (BKB-SIN).

GDTs were measured using an adaptive two-alternative forced-choice paradigm for two "frequency" conditions: (1) within-frequency:2000 Hz pre- and 2000 Hz post-gap tone; (2)across-frequency:2000 Hz pre-gap and 1000Hz post-gap tone.

CAEPs were recorded using a 40-channel Neuroscan system. A total of 8 conditions (two "frequency" x four "gap duration") were used to evoke the CAEP. The two "frequency" conditions are outlined above and the four "gap duration" conditions are: (1) subjects' behavioral GDT; (2)3xGDT; (3)3/ GDT; (4)0xGDT.

Results

Data from 10 CI and 6 NH listeners showed that across-frequency GDTs are significantly higher in CI users than NH listeners (CI users: M=26.67ms; NH listeners: M=7.11ms; $p<0.01$) but not for within-frequency GDTs (CI users: M=8.19ms; NH: M=2.0ms; $p>0.05$).

CI users' speech perception performance (CNC:M=68.42%; AzBio:M=82.75%; BKB: M=8.69dB) was significantly poorer than NH listeners (CNC:M=99.5%; AzBio:M=99.48%; BKB:M=-0.71dB, $p<0.01$)).

NH listener CAEP amplitude increases and latency decreases as the gap size increases for the within-frequency conditions. This trend is not evident for across-frequency data. CAEP data for CI users has been collected and is in the process of being analyzed.

Conclusion

The study is ongoing. The data collected indicates that CI users have temporal processing limitations in the behavioral GDT across-frequency condition. Further data will show if this is true for the within-frequency condition. Full results will show the correlation between CAEP to gaps in pure tones, behavioral across and within-frequency GDTs, and speech perception in NH and CI recipients.

PS - 489

Voice Emotion Recognition By Cochlear-Implanted and Normally-Hearing Children

Monita Chatterjee¹; Danielle Zion²; Mickael Deroche³; Brooke Burianek¹; Alison Goren²; Charles Limb³

¹Boys Town National Research Hospital; ¹Boys Town National Research Hospital and Doane College; ²University of Maryland; ³Johns Hopkins University School of Medicine

Background

Relatively little is understood about how children process voice emotion cues, particularly under conditions of spectral degradation such as that experienced by cochlear-implanted (CI) children. Recent research suggests that CI children have deficits in voice emotion recognition and production. The focus of the present study is on voice emotion recognition by CI children, compared with normally hearing (NH) children listening to original speech as well as to noise-vocoded speech.

Methods

Stimuli were a corpus of 12 semantically neutral sentences, each read with five emotions (HAPPY, ANGRY, NEUTRAL, SAD and SCARED) by one male and one female speaker in a child-directed manner. After initial training, participants (NH adults and children, and CI adults and children; the children were least 6 years old) listened to each sentence and indicated which of the five emotions they heard by clicking on the appropriate button on a computer screen. Results were obtained in the form of confusion matrices, although this presentation will focus on percent correct scores.

Results

To date, results obtained with 8 NH adults indicates excellent performance with full-spectrum speech (98.6% correct), and expected declines with noise vocoding (e.g., 75% correct with 8 channel noise-vocoded speech). Results obtained with 31 NH children also show excellent performance with full-spectrum speech (95.6% correct), but much poorer performance with 8 channel noise-vocoded speech (43.3% correct) than adults. Five post-lingually deaf CI adults (76.5% correct) and 36 CI children (73.43% correct) achieved good performance with full-spectrum stimuli. Note that the CI children's performance far exceeded that of their NH peers' with 8-channel noise vocoded speech. A strong developmental effect was found in the NH children's performance with 8-channel vocoded speech ($p < 0.001$). There was no effect of age or age at implantation in the CI children's data, but a significant effect of time in sound was observed ($p = 0.025$).

Conclusion

Results confirm a deficit in the CI population in this task, but also show considerable deficits in NH children's performance with noise-vocoded speech. It is apparent that experience with the CI contributes to CI children's success in the task. It is known that younger NH children have greater difficulty with spectrally degraded speech than older children and adults. It is possible that the cognitive load of decoding the degraded speech signal limits younger children's access to resources for the voice emotion recognition task.

PS - 490

Perception of Noise-Vocoded Reflexives and Pronouns by Children

Deniz Başkent¹; Jacolien van Rijn²; Zheng Yen Ng³; Rolien Free¹; Petra Hendriks³

¹University of Groningen, University Medical Center Groningen; ²Eberhard Karls Universität Tübingen;

³University of Groningen

Background

Speech perception skills in cochlear-implant users are often measured with simple speech materials. In children, it is crucial to fully characterize linguistic development, and this requires more linguistically meaningful materials. Comprehension of reflexives and pronouns may be used for this purpose, as these specific skills are acquired at different ages. According to the literature, normal-hearing children show adult-like comprehension of reflexives at the age of 5 years, while their comprehension of pronouns only reaches adult-

like levels around the age of 10 years. To provide normative data, in the present study, younger and older normal-hearing children, as well as a control group of normal-hearing adults, were tested for perception of reflexives and pronouns, that were presented with or without an acoustic simulation of cochlear implants.

Methods

Perception of reflexives (Example: "The elephant hit herself.") and pronouns (Example: "The elephant hit her.") was tested with a group of younger children (5 to 8 years old), older children (10 and 11 years old), and adults, all normal hearing and native speakers of Dutch. The test materials were spectrally degraded using a noiseband vocoder that simulated cochlear-implant speech transmission with 4 and 8 channels.

Results

The results with no degradation confirmed the ages of acquisition of reflexives and pronouns as known from literature. Adding spectral degradation reduced overall performance, a severer reduction with 4 channels than 8 channels, as would be expected. However, it did not change the general pattern of the acquisition ages observed with non-degraded stimuli.

Conclusion

This finding confirms that these linguistic milestones can also be measured in cochlear-implanted children, despite the potentially reduced quality of sound transmission. Thus, the results of the study have implications for clinical practice, as they could contribute to setting realistic expectations and therapeutic goals for children who receive a cochlear implant.

PS - 491

Top-Down Repair of Speech: Adding Pitch to Spectrally Degraded Speech

Jeanne Clarke; Etienne Gaudrain; Deniz Baskent

University Medical Center Groningen

Background

The top-down repair mechanisms of speech can be measured with phonemic restoration, by the improvement of intelligibility observed when silent interruptions of periodically interrupted speech are filled with loud noise bursts. Cochlear implant (CI) users seem to benefit from the top-down repair of speech differently from normal-hearing (NH) listeners [Bhargava et al., 2013, ARO]. This difference could be due to poor spectral resolution and/or to the lack of pitch cues that results from this poor spectral resolution in CIs. As pitch cues are important for perceptual organization, here we varied the spectral resolution and the presence or absence of pitch cues independently. We expect perceptual restoration of speech to improve when the pitch cues are added to the spectrally degraded speech signal.

Methods

To separate the effects of pitch presence and spectral resolution on restoration, we created unvoiced speech (no pitch cues but full spectral resolution), noise-band vocoded speech (no pitch cues) at different spectral resolutions (4, 6, 8, and 16-bands) and the same vocoded speech with additional pitch cues. We measured speech intelligibility of NH partici-

pants with the resynthesized voices in a phonemic restoration paradigm.

Results

Data show, as expected, an overall decrease of intelligibility as the spectral resolution is reduced. However the effect of pitch presence or absence does not follow exactly our expectations. The addition of pitch showed improvement of restoration only at 8- and 6-bands spectral resolution, which is fully due to improvement of intelligibility when the interruptions are filled with noise.

Conclusion

With the addition of pitch, NH listeners may be better able to discriminate the speech from the noise, and may therefore avoid interpreting the latter as (spurious) speech cues, thus yielding fewer errors. Moreover, the addition of pitch to the spectrally degraded speech also provides more bottom-up cues that seem to trigger the top-down repair of the missing segments (especially at 8- and 6-bands). When the speech is intelligible enough, adding new speech features does not enhance restoration any further. When the speech is too degraded, adding pitch is not sufficient to improve intelligibility. The present results suggest that phonemic restoration also depends on the amount of speech features available in the speech segments. Adding pitch information to CIs could lead to the improvement of top-down repairs in noisy listening situation.

PS - 492

Interaural Place-Mismatch Estimation With Two-Formant Vowels in Unilateral Cochlear-Implant Users

François Guérin¹; Sébastien Santurette¹; Josef Chalupper²; Iris Arweiler²; Torsten Dau¹

¹Technical University of Denmark; ²Advanced Bionics European Research Center GmbH

Background

For patients with one cochlear implant (CI) and residual hearing in the opposite ear, a default frequency-to-electrode map is typically used despite large individual differences in electrode-array insertion depth. This non-individualized fitting rationale might partly explain the variability in long-term speech-reception benefit among CI users. Knowledge about the electrode-array location is thus crucial for adequate fitting. Although electrode location can theoretically be determined from CT scans, these are often unavailable in audiological practice. Moreover, existing behavioral procedures such as interaural pitch-matching are rather tedious and time-consuming. Here, an alternative method using two-formant vowels was developed and tested.

Methods

Eight normal-hearing (NH) listeners were presented synthesized two-formant vowels embedded between consonants /t/ and /k/, with first-formant frequencies (F1) at 250 and 400 Hz and second-formant frequencies (F2) between 600 and 2200 Hz. F1 was presented unaltered to the left ear, while F2 was presented to the right ear via a vocoder system simulating 3

different CI insertion depths. In each condition, the listeners indicated in a forced-choice task which of 6 vowels they perceived for different [F1, F2] combinations. Ten CI users (5 bimodal and 5 single-sided deaf) performed the same task for F1 presented acoustically to the non-CI ear and F2 presented either acoustically to the same ear or electrically to the CI ear.

Results

After some training, all NH listeners were able to fuse the unaltered F1 and vocoded F2 into a single vowel percept, and vowel distributions could be reliably derived in 7 listeners. Vocoder simulations of reduced CI insertion depth led to clear vowel-distribution shifts in these listeners. However, these shifts were overall smaller than their theoretical value, with high across-subject variability. Vowel distributions could be derived for all CI users in the monaural acoustic condition, indicating an ability to perform the task reliably. Despite this, large individual differences were observed for dichotic bimodal stimulation, with listeners showing either basal or apical shifts, or generally-poor vowel discrimination.

Conclusion

The two-formant-vowel method is a fast and clinic-friendly candidate to derive interaural place mismatches from a simple vowel-recognition task. However, it remains unclear whether the measured "vowel spaces" in CI users are directly related to insertion depth, and whether they are influenced by the ability to fuse acoustic and electric stimuli or habituation to the CI. The comparison of the present results to CT-scan and speech-intelligibility data in the same listeners will shed light on the validity of the proposed method.

PS - 493

The Effect of Spectral Resolution on Temporal Processing Abilities in Simulated Electric Hearing

Fawen Zhang¹; Chelsea Blankenship¹; Jing Xiang²; Qiangjie Fu³

¹University of Cincinnati; ²Cincinnati Childrens Hospital Medical Center; ³University of California

Background

Gap detection threshold (GDT, the shortest intervals a person can perceive) is a commonly used measure of temporal processing resolution. Normal GDT is critical for speech encoding. It has been reported that the large variability in cochlear implant users' speech perception may be related to the temporal processing deficits in some cochlear implant (CI) users (Muchnik et al., 1994; Fu et al., 2002). Unlike the GDT measured using direct electric stimulation through the electrode, the GDT measured via clinical processors may also reflect additional limitations imposed by limited spectral resolution due to CI processing. The purpose of this study is to determine how spectral resolution may affect GDTs in normal hearing (NH) subjects listening to acoustic simulation of CI processing. Additionally, the neural correlates of gap detection were examined using the late auditory evoked potential (LAEP). If a correlation between behavioral and LAEP measures exists, a clinically useful outcome would be to use the

LAEP to objectively assess temporal processing abilities in difficult-to-test patients.

Methods

Thirteen NH young subjects participated. The stimulus was a 600-ms pure tone, with gaps of varies durations in the middle. The GDTs were measured using original stimuli and 3 different CI simulations (4-, 20-, and 30-channel). For the LAEP measure, the original stimulus with 4 different gaps (0, 2, 6, and 16 ms) and the stimulus with 16-ms gap under the CI simulation conditions.

Results

ANOVA shows that there is a significant effect of spectral resolution on the GDT ($p < 0.05$). The GDT was significantly higher for 4- and 20-channel stimuli (4-ch: $M = 3.26$ ms; 20-ch: $M = 3.32$ ms, $p < 0.05$) than for the original stimuli ($M = 2$ ms). The GDT was not different between the original and the 32-channel stimuli ($M = 2.20$ ms, $p > 0.05$).

The LAEP exist for 2-, 6-, and 16-ms gaps, but not for 0-ms. The LAEP becomes larger when the gap increases. The LAEP evoked by 16-ms gaps did not show any difference between original and simulated stimuli.

Conclusion

The number of spectral channels in CI processing may have a significant effect on the GDTs in simulated electric hearing. The LAEP can be used to objectively assess the temporal processing ability as it well reflects behavioral GDTs. The LAEP does not show the effects of spectral resolution on the brain process of encoding superthreshold gaps, though, because these gaps can be well perceived by the subjects.

PS - 494

Factors Limiting Perception of Vocal Characteristics in Cochlear-Implants

Etienne Gaudrain; Deniz Başkent

University of Groningen / University Medical Center Groningen

Background

Voices are principally characterized by two anatomically-related properties: the fundamental frequency (F0) and the vocal-tract length (VTL). The perception of vocal characteristics is the basis of gender categorization, but is also crucial for the segregation and comprehension of competing talkers. Recent studies showed that gender categorization is abnormal in CI users. Although F0 representation is notoriously poor in cochlear-implant (CI) users, these studies have highlighted that this gender categorization impairment was due to a deficit in the perception of differences in VTL rather than F0. In turn, this deficit could also contribute to CI users' poor speech segregation performance in cocktail party situations. The origin of this VTL perception deficit is, nevertheless, as yet unknown. In the present study we aim to identify which aspects of CI stimulation are responsible for poor VTL discrimination performances.

Methods

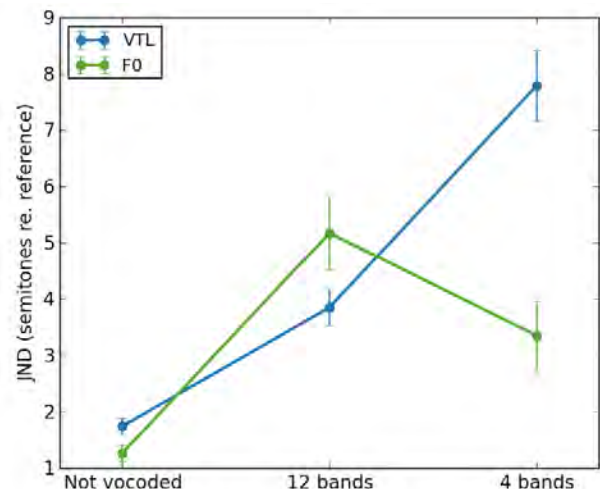
We measured just-noticeable-differences (JNDs) for VTL and F0 using an adaptive procedure, in normal-hearing participants listening to various CI simulations. The CI simulations differed in terms of number of channels, types of carriers and the amount of spread of excitation. These measures are also to be compared to similar measures in actual CI users.

Results

The JND for F0 increases, i.e. worsens, when the spectral resolution is degraded, but quickly reaches a plateau when a sine-wave is used as carrier. In contrast, the JND for VTL steadily increases when spectral resolution decreases. The nature of the carrier seems to mostly affect F0 JNDs, but also has a minor influence on VTL JNDs. Finally it is expected that spread of excitation would directly increase the JND for VTL.

Conclusion

Spectral resolution, and in particular the spread of excitation, seems to be the strongest factor limiting VTL perception in CIs. Current focusing thus appears as a potential solution to improve VTL perception.



PS - 495

Investigating the Effects of Interaural Place-of-Stimulation Mismatch and Channel Interaction in Multi-Electrode Stimulation in Bilateral Cochlear Implant Users

Alan Kan¹; Matthew Goupell²; Ruth Litovsky¹

¹University of Wisconsin-Madison; ²University of Maryland-College Park

Background

In bilateral cochlear implants (CIs), the insertion depths of electrode arrays in the two ears can be different. Therefore, a bilateral pair of electrodes assigned to present the same frequencies in a speech processing strategy can have a place-of-stimulation mismatch which may degrade binaural fusion, as well as the effectiveness of binaural cues. In multi-electrode stimulation, channel interactions between adjacent electrodes can also occur due to current spread along the cochlea. The combination of these effects on binaural fusion and binaural sensitivity in CI users is largely unknown.

We hypothesize that when there is mismatch, activating two adjacent electrodes might aid in binaural fusion since current spread will increase the amount of interaural overlap in the spatial excitation area. However, channel interactions may adversely affect the salience of binaural cues, thus sound localization would benefit from activating electrodes that are farther apart.

Methods

Bilateral CI users participated in two experiments, where two interaural electrode pairs were stimulated simultaneously with a 300 ms, 100 Hz pulse train. The pairs were either pitch-matched or mismatched by 2, 4 or 6 interaural electrodes. The effect of electrode spacing was investigated by using pairs that were spaced 2 or 6 electrodes apart within the same ear. In experiment one, binaural fusion was measured by having subjects describe the number, location and compactness of auditory images heard when stimuli were presented to both ears at perceptually equal loudness. In experiment two, binaural sensitivity was measured by separately applying non-zero interaural time and level differences (ITD and ILD, respectively) to the stimuli. Subjects responded by indicating the number and location(s) of auditory images inside the head.

Results

In experiment one, increasing mismatch decreased binaural fusion and non-centered auditory images were perceived. Electrode spacing appears to have little effect on binaural fusion. In experiment two, mismatch decreased the lateral range of auditory image locations, more so for ITDs than ILDs. In addition, activating closely spaced electrodes appeared to reduce ITD sensitivity in some subjects.

Conclusion

With interaural mismatch, single- and multi-electrode stimulation appear to yield similar results (decreased fusion and lateralization when interaural differences were zero; ILDs more robust to mismatch than ITDs). Activating adjacent electrodes does not appear to improve binaural fusion or binaural sensitivity. These results suggest that clinical mapping could benefit by considering interaural place-of-stimulation matching in order to maximize sensitivity to binaural cues for CI users.

PS - 496

Ginsenoside (Rg1) Has Anti-Inflammatory Properties in the Inflamed Murine Middle Ear

Carol MacArthur; J Beth Kempton; Fran Hausman; Dennis R Trune

OHSU

Background

While glucocorticoids have excellent anti-inflammatory properties, their side effect profile dampens enthusiasm for use in otitis media, especially in children. Ginseng, the root of *Panax ginseng* (*P. ginseng*) has been used in Chinese medicine for over 1000 years. The molecular compounds responsible for ginseng's activity are ginsenosides (triterpene saponins). Among the ginsenosides, Rg1 is the most abundant and is the active component of *P. ginseng*. Rg1 has been shown to be a functional ligand of glucocorticoid receptors (GR) and inhibits

LPS-stimulated cytokine production *in vitro*, indicating that Rg1 may exert anti-inflammatory effects via the GR. Rg1 has been shown to inhibit inflammation via GR but with minimal side effects on osteoblast proliferation and differentiation *in vitro*. This study was designed to measure the impact of Rg1 on cytokine and ion homeostasis gene expression in the acute otitis media mouse model.

Methods

Balb/c mice were screened for absence of ear disease. Five mice in each treatment arm were treated with subcutaneous (SQ) injections of Rg1 or vehicle only (10% EtOH) daily for three days. On day 3, they were sedated per protocol and treated trans-tympanically with 0.5 μ l heat-killed *Hemophilus influenza*. Middle ear tissues were collected at 6 and 24 hours, mRNA extracted for quantitative RT-PCR of 8 cytokine and 24 ion homeostasis genes. Gene expression in the inflamed middle ears was compared to controls.

Results

Expression of Il-6, Il-10 and Cxcl1 genes was significantly downregulated in the treatment group compared to controls at 6 and 24 hour time points. Expression of Cldn3, Gjb6, Apq5, Kcnq1 and Scnn1g genes was significantly downregulated at 6 and/or 24 hours.

Conclusion

The ginsenoside Rg1 has effect on cytokine and ion homeostasis gene expression in murine middle ear tissues. The downregulation of cytokines observed, although less robust than that seen with glucocorticoids, supports an anti-inflammatory effect in the acute otitis media mouse model. Interestingly, ion homeostasis genes were also downregulated in tight junction, gap junction, aquaporin, K⁺ and Na⁺ channel genes. Lack of ion homeostasis gene upregulation suggests that Rg1 does not have as much activity as the glucocorticoids on the mineralocorticoid receptor, and therefore may not have as much impact on middle ear fluid clearance compared to Prednisolone. Rg1 may prove worthy of further investigation for therapeutic use in acute otitis media, especially as an anti-inflammatory agent.

PS - 497

Analysis of Publication Concerning Otitis Media 1940 -2012

Robert Ruben

Albert Einstein College of Medicine

Background

There have been numerous conferences since the first international otitis media conference in 1975. What outcomes in terms of number and type of scientific communication and changes in the epidemiology occurred during these four decades?

Methods

A PubMed search was conducted for articles which were classified as otitis media(OM), acute otitis media (AOM) serous otitis media(SOM), otitis media with effusion(OME), middle ear effusion(MEE) or chronic otitis media(COM) from January 1 1940 through December 31 2012. These data were

then analyzed for a number of sub classifications which included randomized clinical trials, clinical trials phases I –IV, guidelines, conferences, meta analysis and incidence and/or prevalence.

Results

19,962 articles were identified for OM from 1975 through 2012 and 4,992 from 1940 through 1974. In the 1975 – 2012 cohort the percentage of increase in publication from the previous year for OM was in all years less than that for all indexed article for the same time period. From 1975 -2012 there were 5,398 articles indexed as AOM, 5,826 as SOM, OME and/or MEE and 5,488 COM. Each form of OM was analyzed for type of publication. There were 1,705 articles which noted incidence and/or prevalence of OM.

Conclusion

Otitis media articles had increased at a lesser rate than all indexed articles for the period 1975 -2012. The data showed that there appeared to be only 2 phase IV clinical trials but a total of 840 OM randomized clinical trials. The analysis of the OM incidence and/or prevalence data found little or no diminution in incidence or burden of disease since 1975 with great discrepancies in geography and socio – economic status. These data mandate that prevention is the area with which resources must be applied to reduce the burden of OM worldwide.

PS - 499

Imaging Mass Spectrometry Revealed the Specific Phosphatidylcholines in Thyroid Papillary Cancer

Seiji Ishikawa¹; Ichiro Tateya²; Takahiro Hayasaka³; Noritaka Masaki³; Morimasa Kitamura²; Shigeru Hirano²; Mitsutoshi Setou³; Juichi Ito²

¹Kyoto University; ²Department of Otolaryngology-Head & Neck Surgery, Graduate School of Medicine, Kyoto University; ³Department of Cell Biology and Anatomy, Hamamatsu University School of Medicine, Hamamatsu

Background

Numerous molecular studies have demonstrated beneficial treatment and prognostic factors in various molecular markers. Whereas most of previous reports have focused on genomics and proteomics, few have focused on lipidomics. Lipids, especially phosphatidylcholines (PCs), play important roles in the composition of the cell membrane and are associated with cell membrane structure, proliferation, differentiation, metabolic regulation, inflammation, and immunity.

Imaging mass spectrometry (IMS) is an emerging application for lipid research that provides a comprehensive and detailed spatial distribution of ionized molecules. In IMS, the tissue sections are directly raster-scanned by laser performing matrix-assisted laser desorption/ionization (MALDI) and the ionized molecules are separated by time-of-flight (TOF) mass spectrometer. The distribution of a biomolecule is two-dimensionally visualized as the relative signal intensities among the measurement points of the tissue section. Although IMS is spreading explosively in many fields including biology and

pathology, there has been no report in otolaryngology. The purpose of this study was to elucidate the distribution of PCs in thyroid papillary cancer by comparing with the normal thyroid tissue.

Methods

Tissue samples were obtained from seven patients with thyroid papillary carcinoma who underwent surgery in Kyoto University Hospital. The study was performed in accordance with the guidelines for pathological specimen handling, which was approved by the ethical committee of Kyoto University. We conducted an IMS analysis focusing on the distribution of PCs.

Results

HE staining was performed to determine the cancerous and normal thyroid region. After picking up the specific molecules by statistical analysis, tandem mass (MS/MS) analysis was performed for the m/z value with a significant difference to identify the molecular species. The expression levels of PC (16:0/18:1) and PC (16:0/18:2) in the cancerous region was significantly higher than those in the normal tissue.

Conclusion

IMS identified the detailed spatial distribution of PCs with different fatty acid compositions in thyroid papillary cancer. These distributional differences might be associated with the biological behavior of thyroid papillary cancer. Our study demonstrated a useful model for lipid research in thyroid papillary cancer tissues using a new modality.

PS - 500

Optimizing Structural Segmentation for Surgical Simulation Through Iterative (User-Mediated and Automatic) Image Processing

Gregory Wiet¹; Kimerly Powell²; Bradley Hittle³; Don Stredney³

¹Nationwide Children's Hospital/The Ohio State University;

²The Ohio State University; ³Ohio Supercomputer Center

Background

Learning surgical technique requires safe and effective methods for deliberate practice. Unfortunately, recent pressures on surgical education limit opportunities for technical skills training. These include time restrictions on trainee hours, risk to trainee health and cost of the use of cadaveric specimens as well as safety risks when novice operators are directly involved in a patient's surgical care.

Consequently, many surgical residencies are exploring use of simulation-based training to augment traditional methods. To simulate otologic microsurgical techniques, the precision of the data is critical for providing the intricate structural and spatial representation required. As more increasingly virtual representations are pursued, the data becomes the critical basis for multi-sensory, (i.e., visual, aural, and haptic) representation. In addition to technical skills training, scientists exploring structural relationships in high-resolution imaging require methods for image processing and visualization.

We present methods to process the high-resolution image data of the regional microanatomy of the temporal bone. We provide our workflow to optimize these acquisitions depending on the type of structure or region (e.g., surface or recess).

Methods

Automated segmentation of temporal bone structures such as the tegmen and sigmoid sinus in high-resolution microCT images require anatomical landmarks in the bony structure that are not always readily available in the image. Manual segmentation of these structures based on 2D slice views is difficult and time-consuming. Therefore, we have developed an interactive manual segmentation method based on a 3D volume-rendered image of the entire temporal bone. This technique allows the user to visualize and manipulate a volume-rendered version of the original bone image and 'paint' the structures of interest in the 3D volume image directly. The 'painted' structures are based on a set of pre-processed images that have been designed to highlight the structures of interest. For example, one pre-processed image is used for segmenting bony surface structures such as the sigmoid and tegmen while another is used for segmenting signal-void structures such as the canals for nerves and sensory organs. Additional pre-processed images can be included in the volume editing program as needed and multi-scale segmentation is possible in defined regions-of-interest. This method allows the use of variable spatial resolutions to perform 3D segmenting processes while maintaining real time performance with the ability to retrieve the original spatial resolution for selected areas.

Results

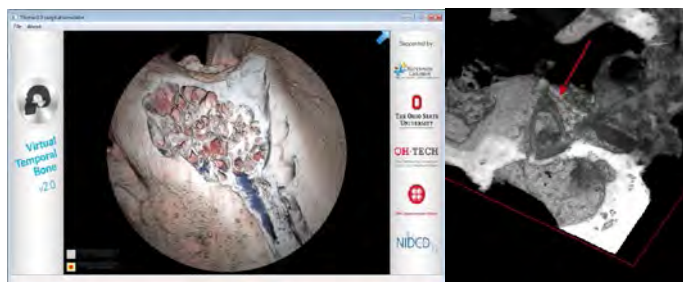
See Supporting files for figures:

Figure 1 High-resolution 3D view of the stapes (red arrow) obtained from μ CT image at spatial resolution of 45 microns.

Figure 2 Three dimensional reconstruction of processed data visualized in the surgical context within the 3D simulation environment at spatial resolution of 100 microns.

Conclusion

We have presented a flexible, iterative approach that allows various automatic and user-mediated methods to process the data. This approach will provide for the optimum quality for a useful and engaging interactive, 3D simulation environment.



PS - 501

Increased Expression of Phosphatidylcholine With Arachidonic Acid in Superficial-Type Pharyngeal Cancer Revealed by Imaging Mass Spectrometry

Ichiro Tateya¹; Seiji Ishikawa¹; Takahiro Hayasaka²; Shigeru Hirano¹; Morimasa Kitamura¹; Mitsutoshi Setou²; Juichi Ito¹

¹Kyoto University; ²Hamamatsu University School of Medicine

Background

The number of cases with superficial-type pharyngeal squamous cell carcinoma (STPSCC) has increased since narrow band imaging (NBI) with magnifying endoscopy was developed. STPSCC is in situ and early invasive squamous cell carcinoma. Exploring of biological character in STPSCC may lead to reveal the mechanism of pharyngeal cancer invasion.

Imaging mass spectrometry (IMS) based on matrix-assisted laser desorption/ionization (MALDI)-time-of-flight (TOF) is a technique to visualize the spatial distribution of molecules two-dimensionally as the relative signal intensities among the measurement points of interests on a tissue section. The analytes are nucleic acids, phospholipids (PLs), peptides, proteins and drugs. It is a useful tool for lipids because it can identify fatty acids binding to PLs on a tissue section. It is generally known that cell membrane characteristics are determined by the components of PL species, and are related to the cell mobility in cancer invasion and metastasis. The composition of PL species is determined by the containing fatty acid species, however it had been impossible to identify containing fatty acids in PLs on a tissue section until IMS was developed.

In the present study, we applied IMS technique to elucidate the distribution of PLs-bound fatty acids for STPSCC section. This study is the first to successfully identify PLs that are expressed higher in submucosal invasive region of STPSCC using IMS analysis.

Methods

Sample collection and archiving of patient data was performed under informed consent and approval by the ethical committee of Kyoto University. 5 patients who underwent endoscopic laryngo-pharyngeal surgery at Kyoto University were assessed in this study. The tissue sections of STPSCC were analyzed using a MALDI-TOF/TOF-type instrument, Ultraflex II TOF/TOF (Bruker Daltonics). Each fifty peaks with high intensities excluding isotopic ones were picked up from superficial and submucosal invasive regions of STPSCC defined by HE staining, and significant difference was statistically analyzed by Welch t-test. Iterating these peak picking and statistical analysis 5 cases, we picked up reproducibly observed m/z values those had significantly higher intensities in submucosal invasive region. The m/z values were employed for tandem MS analysis to identify the molecular species. MS/MS was performed on the submucosal invasive region of STPSCC using QSTAR Elite (Applied Biosystems/MDS Sciex, USA), a MALDI hybrid quadrupole/TOF MS.

Results

Phosphatidylcholine (16:0/20:4), (18:0/20:4) and (18:1/20:4) were significantly expressed in submucosal invasive region higher than in the superficial region of STPSCC.

Conclusion

The results of our study clearly show that phosphatidylcholine containing arachidonic acid is related to submucosal invasion of STPSCC.

PS - 503

Dysplastic Vestibule and Semicircular Canal Predict Increased Sensorineural Hearing Loss in Children With Enlarged Vestibular Aqueducts.

Farhan Huq¹; Cedric Pritchett²; Amanda Philips¹; Glenn Green³; Marc Thorne³; Hemant Parmar³; Mohannad Ibrahim³; Teresa Zwolan³; Steven Telian³

¹University of Michigan Medical School; ²University of Michigan; ³University of Michigan Health System

Background

An Enlarged Vestibular Aqueduct (EVA) is a congenital anomaly associated with sensorineural hearing loss (SNHL). Diagnostic radiographic criteria using computed tomography of the temporal bone has been defined as a measurement of > 0.9 mm at vestibular aqueduct midpoint (VA) or > 1.9 mm at the operculum. Patients may present with any level of hearing loss that classically is progressive, but may fluctuate. Most commonly both ears are affected. The effect of age and VA size on SNHL is not fully understood.

Methods

Retrospective review of institutional records from 2003 to 2013 was conducted identifying children with an EVA. Excluded individuals were those: greater than 18 years at time of diagnosis; > 90dB hearing loss at presentation; < 1 year of follow up; or < 3 audiograms separated by at least two months. General demographics (age, gender, uni- or bilateral involvement) were collected. Audiometric performance over time was followed. Temporal bone CT scans were reviewed, and measurement of vestibular aqueduct midpoint (VAM) and operculum (VO), and concomitant dysplasia of the vestibule (VD) or semicircular canal (SCD) was noted. Statistical analysis using SAS (SAS institute Inc., Cary, NC) was conducted with chi-square analysis to compare categorical variables and a linear mixed model to investigate the effect of radiologic measurements on hearing loss.

Results

Forty-seven children met inclusion criteria; 36 (76%) had bilateral EVA. Sixty-five percent were female. Mean age of presentation and length of follow up were 5.36 and 5.58 years, respectively. Mean PTA at presentation was 52.0 dB (S.D. 30.4). Each additional month of age increased PTA by 0.1 dB (95% CI: 0.064 – 0.110, $p < 0.01$). Size of VAM or VO did not correlate with severity of PTA (VAM: 5.43dB (95% CI: -3.29 – 14.15, $p = 0.23$), VO: 2.76 dB (95% CI: -4.43 – 9.95, $p = 0.45$)) Labyrinthine dysplasias (VD or SCD) were predictive of increased SNHL. Across all times, a 24.1 dB higher PTA

(95% CI: 8.2 – 40.1; $p < 0.01$) and 19.9 dB higher PTA (95% CI: 3.9 – 35.9, $p = 0.02$) was seen with VD and SCD respectively. VD and SCD were significantly correlated ($R = 0.44$); and combined in the model did not both remain significant: VD 18.7 dB higher PTA, $p = 0.06$; SCD 9.7 dB higher PTA, $p = 0.32$.

Conclusion

Progressive hearing loss is commonly seen in children with an EVA. In these children concomitant dysplastic labyrinthine anatomy is more predictive of PTA than size of the VA.

PS - 504

Hyposmia as an Early Effect Biomarker for the Occupational Exposure to Organic Solvents Mixtures

Giovanna Tranfo; Rossana Claudia Bonanni; Maria Pia Gatto; Monica Gherardi

INAIL Research

Background

The primary sensory neurons of the olfactory system are chronically exposed to the environment and therefore they are susceptible to damage from occupational exposure to volatile chemicals. Sniffin'Sticks are currently used to perform smell tests for the objective diagnosis of hyposmia and other smell disorders: we used this method on workers occupationally exposed to organic solvents, coupled to air and urine analysis, in order to test its capability to reveal early adverse effects as biomarkers of exposure.

Methods

Olfactory capacity was evaluated in workers exposed to styrene and other organic solvents in a fiberglass-reinforced plastic plant, and in a group of matched controls, using the Sniffin'Sticks (Burghart, Germany), a smell test based on a penlike odor-dispensing. The test is divided in Threshold (T), Discrimination (D) and Identification tests (I): the total score is TDI and normal value is > 30. The personal monitoring of airborne styrene and benzene, toluene and xylene (BTX) was performed using Radiello diffusive samplers, followed by quantitative analysis by Gaschromatography/Mass Spectrometry Detection (GC/MS). Styrene concentrations were determined in urines collected at end of work-shift by means of headspace sampling and GC/MS analysis.

Results

The median scores of the smell tests for the eleven workers (34 ± 4.8) are lower than those of the controls (38 ± 2.9) for the complete test (TDI) and singularly. Only one subject (painter) resulted hyposmic (TDI = 27). Air monitoring results show an average styrene concentration of 107.8 ± 41.1 mg/m³ for molding workers, higher than the ACGIH TLV-TWA of 85 mg/m³, and an average concentration of styrene of 63.7 ± 7.2 ng/ml in end-of-shift urine. The airborne styrene exposure level for the painter was lower (4.2 ± 1.0 mg/m³) but he resulted exposed to ten times higher airborne BTEX than other workers (5.6 ± 1.0 mg/m³ vs 0.5 ± 0.1 mg/m³).

Conclusion

Results suggest a synergic effect of solvent mixtures on the olfactory capacity of exposed workers. Despite the small number of workers studied, the Sniffin' Sticks seem to be an effective tool for the detection of olfactory damage as an effect biomarker of exposure to organic solvents. These indications encourage further investigations on more groups of workers exposed to inhalation of neurotoxic chemicals like metals, pesticides, organic solvents and their mixtures.



1. Casjens S, Eckert A, et al.. Diagnostic value of the impairment of olfaction in Parkinson's disease. PLoS One. 2013 May 16;8(5), <http://dx.doi.org/10.1371/journal.pone.0064735>
2. Wolfensberger M, Schnieper I. et al. Sniffin' Sticks: a new olfactory test battery. Acta Otolaryngol 2000; 120:303-306.
3. Mascagni P, Consonni D. et al. Olfactory function in workers exposed to moderate airborne cadmium levels. Neurotoxicology 2003; 24 (4-5):717-724
4. Gobba F. Olfactory toxicity: long-term effects of occupational exposures. Int Arch Occup Environ Health 2006; 79: 322-331.
5. Cheng SF, Chen ML. et al. Olfactory loss in poly (acrylonitrile-butadiene-styrene) plastic injection-moulding workers. Occup Med 2004; 54 (7): 469 - 474
6. Polo L, Calcinoni O. et al. La valutazione strumentale oggettiva e soggettiva nelle disosmie. Atti VII Convegno Nazionale di Medicina Legale Previdenziale. http://www.inail.it/internet_web/wcm/idc/groups/internet/documents/document/ucm_portstg_114636.pdf
7. Dalton P, Lees PSJ et al. Evaluation of Long-Term Occupational Exposure to Styrene Vapor on Olfactory Function. Chem Senses 2007; 32: 739-747.
8. Tranfo G, Gherardi M. et al. Occupational exposure to styrene in the fiberglass reinforced plastic industry: comparison between two different manufacturing process. Med Lav 2012; 103(5) :402-412

PS - 505

The Value of Magnetic Resonance Imaging in Patients With Audiovestibular Disorders.

Hisaki Fukushima; tamotsu harada

Kawasaki medical school

Background

Magnetic Resonance Imaging (MRI) is routinely used for retrolabyrinthine pathology such as acoustic schwannoma. However, its value in the diagnosis of cochlear pathology associated with sensorineural hearing loss (SNHL), tinnitus and vertigo has been less clear. This article addresses the value of MRI in analysis of the complete audiovestibular pathway.

Methods

This study is retrospective evaluation of case histories and gadolinium-enhanced MRIs of 304 patients (mean age 55 years, range 9 to 82 years) with audiovestibular disorders.

Results

MRI detected one intralabyrinthine schwannoma, 2 acoustic schwannomas in the internal auditory canal, 1 intracochlear hemorrhage, 1 intraendolymphatic duct hemorrhage, 1 inflammatory lesion of acoustic neuron in the internal auditory canal, 2 inner ear anomaly and 1 temporal bone metastasis.

Conclusion

This study indicates that MRI can be used to assess a significant number of pathologic conditions in patients with audiovestibular disorders.

PS - 506

Metrics for Evaluating Surgical Microscope Usage During Tympanostomy Tube Placement

Brandon Wickens¹; Arefin Shamsil¹; Philip Doyle¹; Sumit Agrawal²; Hanif Ladak¹

¹Western University; ²London Health Science Centre

Background

Although teaching and learning surgical microscope maneuvering is a fundamental step in Otolaryngology surgical training, currently there is no objective method to teach or assess this skill. A basic skill taught to Otolaryngology residents that requires surgical microscope use is the placement of a drainage tympanostomy tube within the tympanic membrane to treat middle ear dysfunction. This study was designed to implement and test sets of metrics capable of quantitatively and qualitatively evaluating microscope use and surgical expertise of subjects during tympanostomy tube placement.

Methods

8 Otolaryngology trainees and 3 Otolaryngology experts were asked to use a microscope to insert a tympanostomy tube into a cadaveric myringotomy in a standardized setting. Microscope movements were tracked in 3 dimensional space and tracking metrics were applied to the data. The procedure was video-recorded and then analyzed by blinded experts using operational metrics. Results from both groups were compared, and discriminatory metrics were determined.

Results

The following tracking metrics were identified as discriminatory between the trainee and expert groups: total completion time, operation time, still time, jitter, and number of microscope repositions. A variety of operational metrics were found to be discriminatory between the two groups, including several positioning metrics, optical metrics and procedural metrics.

Conclusion

These discriminatory metrics could form the basis of an automated system for providing feedback to residents during training using a myringotomy surgical simulator. Additionally, these metrics may be useful in guiding a standardized teaching and evaluation methodology for training in the use of surgical microscopes.

PS - 507

Improved ECAP Detection Algorithm Based on Latency Constained Peak-Picking.

Jonathan Laudanski¹; Boris Gourévitch²; Yann Nguyen³; Olivier Sterkers³; Jean-Marc Edeline²

¹Neurelec-Oticon Medical; ²Centre Neuroscience Paris Sud, CNRS UMR 8195, Université de Paris Sud, Orsay, France; ²Centre Neuroscience Paris Sud, CNRS UMR 8195, Université de Paris Sud, Orsay, France; ³UMR-S 867 / Inserm / Université Paris 7, France Service d'Oto-rhino-laryngologie, Hôpital Pitié-Salpêtrière, AP-HP, Paris, France

Background

Electrically evoked compound action potentials (ECAPs) are routinely used in clinical audiology to set the patient's threshold level but the estimation of ECAPs threshold is often left to the judgment of experts. Although automated algorithms have been developed, they usually face two issues: 1) errors on the estimated ECAP amplitude and 2) errors when interpolating threshold from the ECAP growth function. Estimating the ECAP amplitude is often done by peak-picking, an estimator which is not accurate since at threshold the SNR is typically low. Furthermore, setting the threshold by interpolating the ECAP growth function can prove a difficult task since interpolations of different types produce different thresholds. To circumvent these problems, we developed an ECAP detection algorithm with refined estimates of ECAP amplitude and statistical threshold criterion.

Methods

Four guinea-pigs were implanted with chronical miniaturized electrode arrays. Using a custom-made stimulation platform, bi-phasic pulses of different shapes were delivered to the apical electrode. The ECAPs were recorded from adjacent electrodes with a 24bit $\pm 10V$ -ADC (TDT RP2.1) using a 97656Hz sampling rate. Amplitude growth functions were obtained by either increasing the stimulation pulse amplitude or its duration.

Two estimators of the ECAP amplitude were used: 1) peak-picking (PP) and 2) latency constrained peak-picking (LCPP). The probability distributions of PP vs. LCPP are then used in a signal detection task. The receiver-operating characteristic of both estimators are compared by measuring hit rate at fixed false alarm rate.

Results

First, using simulations from an ECAP model, the LCPP is shown to improve hit-rate at all SNR. Similarly, analyses of most ECAPs recordings obtained in guinea-pigs show an improved hit rate independently of the SNR. However, in contrast with simulations, data recorded on guinea-pigs are sensitive to artifact cancellation. The blanking of the first few samples used to remove residual artifacts has a strong impact on the hit-rate increase when comparing PP and LCPP. The thresholds obtained using interpolation of amplitude growth functions are compared to those obtained at fixed false-alarm rate.

Conclusion

An increased hit-rate at all SNR has been demonstrated using LCPP compared to PP, implying that LCPP has better detection performance. This improved performance can be used at high SNR to reduce the number of averages necessary to obtain an ECAP. Similarly at low SNR, LCPP performance implies detecting lower ECAP threshold or detecting similar threshold level at a reduced averaging cost.

PS - 508

Pattern of Concha Recorded Cochlear Microphonics Across Acoustic Frequencies

Ming Zhang

University of Alberta & Glenrose Rehabilitation Hospital

Background

Both cochlear microphonics (CMs) and otoacoustic emissions (OAEs) may be measured to assess the cochlear and outer hair cell functions. Combining concha electrode, tone burst evoked CM waveforms (CMWs), and pattern of CMWs across acoustic frequencies may be useful for hearing clinics. This combination differs from a conventional ear canal or tympanic membrane electrode, click evoked CMs in a conventional electrocochleogram (ECoChG), and CM tests with one frequency and without analysis across acoustic frequencies. Therefore, such a combination may be also interesting to hearing research in cochlear studies.

Methods

Normal hearing subjects were recruited. A 14-msec tone burst across acoustic frequency range was delivered to the ear canal. A concha electrode was used to try to record the CMW responses. When the CMW were recorded through the concha electrode, the recorded CMW amplitudes among different frequencies were to be analyzed and compared. Finally, the response patterns based on the amplitude of CMWs across acoustic frequencies were to be estimated and modeled.

Results

The CMW responses were recordable using the concha electrode. Amplitudes of CMW evoked with different frequencies could be analyzed. A special pattern based on the amplitude of the CMWs across acoustic frequencies could be derived. In the derived pattern, two features could be observed: (1) the CMW amplitude decreased upon an increase in frequency of a stimulus tone-burst; and (2) such a decrease in amplitude

occurred more quickly at lower frequencies than at higher frequencies.

Conclusion

The concha electrode can be used to record the CMWs and to measure the pattern of the CMW responses. After further improvement, the concha electrode and the approach for such recording may be used to measure CMW response pattern in the clinic and for the cochlear research. The concha-recorded response pattern may be further studied so as to be used in interpreting the CMW measurement. CMWs may be used for the same purpose as OAEs are, or may be used as a complement to the OAE measurement.

PS - 509

Comparison of Peripheral Compression Estimates Using Auditory Steady-State Responses and Distortion Product Otoacoustic Emissions

Gerard Encina Llamas¹; Torsten Dau²; Bastian Epp²

¹Technical University of Denmark; ²Oticon Centre of Excellence for Hearing and Speech Sciences, Department of Electrical Engineering

Background

The healthy auditory system shows a compressive input/output function, commonly assumed to be a result of healthy outer-hair cell function. Hearing impairment often leads to a decrease in sensitivity and a reduction of compression. Compression estimates in human listeners are commonly based on psychoacoustical procedures, or on measurements of otoacoustic emissions (OAEs). Psychoacoustical procedures are time consuming and rely on assumptions regarding the ability to selectively investigate cochlear processing. OAEs allow to selectively study cochlear processing, but the interpretation of results based on individual data is challenging. Auditory steady-state responses (ASSR) represent a method allowing fast, reliable and frequency-specific objective measurements of hearing function. In the present study it was investigated if ASSR can be used to estimate compression along the peripheral auditory pathway. The hypothesis was to observe compressive behaviour in normal-hearing (NH) listeners and reduced compression and sensitivity in hearing-impaired (HI) listeners. ASSR data were compared to compression estimates based on distortion-product otoacoustic emissions (DPOAEs).

Methods

ASSR were measured using 64-channel EEG with active electrodes. Input-output functions were obtained for NH and HI listeners using multi-frequency stimulation with four sinusoidally amplitude modulated tones (SAM) at carrier frequencies from 500-4000 Hz and modulation frequencies between 80 and 100 Hz. The input level was varied between 20 and 80 dB SPL in steps of 5 dB. Results were compared to compression estimates from DPOAEs within the same listeners.

Results

The data showed that ASSR growth functions can be measured in NH listeners for input levels between 20 and 80 dB

SPL. Strong compression was found for input levels of 20-30 dB SPL and above. For HI listeners, the results showed a larger variability compared to NH listeners. Reliable responses could only be obtained for levels corresponding to about 30 dB SL and above. The compression estimates obtained with ASSR were larger than those obtained using DPOAE.

Conclusion

ASSR could be used to estimate peripheral compression simultaneously over a large frequency range. In the HI listeners, compression estimates could be derived for levels at and above 30 dB SL. ASSR might represent a useful method for fast and reliable estimates of peripheral input-output functions and hence the state of the active processes in the inner ear.

PS - 510

Sinusoidal ASSR is Better Than Tone-Burst Evoked ABR for Estimating Low-Frequency Hearing Thresholds

Uzma Wilson¹; Wafaa Kaf¹; Jeffery Lichtenhan²; Ali Danesh³

¹Missouri State University; ²Washington University School of Medicine in Saint Louis; ³Florida Atlantic University

Background

Threshold estimation of low-frequency hearing is a challenge with tone-burst auditory brainstem responses (TB-ABR) and auditory steady state responses (ASSR), as a large correction factor is needed. While conventional ASSR only rely on statistical algorithms for response detection that can be influenced by noisy test situations, sinusoidal ASSR (sASSR) also provide an interpreter-based response analysis for more sensitive response detection. However, little is known about the performance of sASSR for estimating low-frequency hearing thresholds. We determined the accuracy of 40-Hz sASSR thresholds by comparing to TB-ABR and behavioral thresholds, each measured from the same subjects.

Methods

TB-ABR and chirp-evoked 40-Hz sASSR thresholds (dBnHL) were obtained using the Kalman weighted filtering technique in 14 awake, normal, young-adult male humans, and compared to their behavioral threshold (dBHL) counterparts at 500, 2000 and 4000 Hz. Responses from the right ear were measured ipsilaterally with electrodes on *Fz* (non-inverting), *M2* (inverting) and *Fpz* (common). TB-ABR and sASSR responses were judged by 3 different raters. A within-subject repeated measures ANOVA for test type (TB-ABR, 40-Hz sASSR, and behavioral threshold) was conducted for each frequency. Post-hoc paired-samples *t*-tests were performed on the main effect of test type.

Results

The mean sASSR and TB-ABR thresholds were significantly worse (i.e., higher) than the behavioral thresholds at all frequencies. However, the mean sASSR threshold for 500Hz (21.4±5.3 dBnHL) was significantly better (i.e., lower) than the 500Hz TB-ABR threshold (36.1±5.9 dBnHL). There were no significant differences between sASSR and TB-ABR thresholds for 2000Hz and 4000Hz.

Conclusion

We have demonstrated that 500Hz sASSR thresholds were closer to behavioral thresholds than 500Hz TB-ABR thresholds were to behavioral. This validates the superior use of sASSR for low-frequency hearing threshold estimation.

PS - 511

40-Hz Multiple Auditory Steady-State Responses to Narrow-Band Chirps in Sedated and Anaesthetized Infants

Jesko L. Verhey¹; Torsten Rahne³; Roland Mühler²

¹University of Magdeburg; ²Department of Experimental Audiology, University of Magdeburg, Germany; ³Department of Otorhinolaryngology, Martin-Luther-University Halle-Wittenberg, Halle (Saale), Germany

Background

One of the key factors influencing the amplitude of auditory steady-state responses (ASSR) is the stimulus repetition rate. Since the amplitude is particularly high at 40 Hz, this repetition rate is commonly used in the clinical routine as an objective measure of the hearing abilities of the patients. Several early studies from the 90th on 40-Hz ASSR showed, however, a remarkable detrimental influence of maturation, sleep, and anaesthesia on the amplitude of the 40-Hz ASSR in infants. This finding was used as an argument against the usage of 40 Hz in those patients. Recently, Tlumak et al. (2012, IJA 51, 418-423) showed that the amplitudes of 40-Hz-ASSR in infants are still larger than those at higher stimulus rates. Hence it is hypothesized in the present study that the amplitude of 40-Hz ASSR in infants is large enough to record these potentials in the clinic even under sedation and anaesthesia and to use it as an estimate of their hearing ability.

Methods

Chirp evoked auditory brainstem responses (ABR) and ASSR from 34 infants below the age of 48 months were analysed. ABR to a broadband chirp stimulus and 40-Hz ASSR for a multiple stimulus consisting of four one-octave wide chirps centred at 500, 1000, 2000 and 4000 Hz were recorded under chloral hydrate sedation or general anaesthesia.

Results

40-Hz ASSR were consistently detected at the hearing threshold in all infants. Since reliable behavioral hearing thresholds of the infants were not available, the ASSR thresholds were compared with the corresponding broadband ABR thresholds. The mean differences between ABR and ASSR thresholds were found at 6.8 dB.

Conclusion

In contrast to the common assumption (consensus in all textbooks on evoked potentials) that 40-Hz ASSR are not appropriate for threshold estimation in sedated and anaesthetised infants it is shown in the present study that 40-Hz-ASSR could be consistently recorded in infants below the age of 48 months, even under sedation or general anaesthesia. The large chirp ABR amplitudes recorded in sedated and anaesthetised infants indicate a large robust brainstem contribution to the ASSR at this frequency.

PS - 512

Results of a 6-Year Government-Funded Newborn Hearing Screening in Korea

Su-Kyoung Park¹; Hak-Young Kim²; Chanhee Yang³; Seung-Ha Oh⁴

¹Hallym University College of Medicine; ²Department of Nursing, Korea National Open University; ³Division of population policy of Ministry of Health and Welfare;

⁴Department of Otorhinolaryngology, Seoul National University College of Medicine

Background

South Korea has about 450 thousand neonates every year. We have very low birth rate and our fertility rate is the lowest in the world. Korean Ministry of Health and Welfare (KMHW) has been supported early newborn hearing loss detection for low-income families from 2007 year nationwide. The aim of this study is to investigate the results of national newborn hearing screening through 2007 to 2012 (6 years).

Methods

For launching a nationwide program, a step wise approach was performed. First, we investigate the incidence of newborn hearing loss (HL) via a nationwide sample survey in 2006 year. In 2007 to 2008, the 1st and 2nd national exhibition NHS project was implemented. The 3rd national NHS project for low income babies have been conducted in all area from 2009 through 2012 year. From 2009, we adopted a coupon system to improve the quality of NHS data and tracking. A free coupon is issued to pregnant women at the public health centers. The coupon consists of two parts, screening test and confirming test with same ID number. Collected coupons from each institute were sent to the KMHW to get reimbursement. By analyzing coupons, a tracking of baby will be possible. The criterion of hearing loss is 40dBnHL and over in diagnostic auditory brainstem response (ABR) with click stimulus sound.

Results

For NHS authorized screening centers, woman's clinics were 76%, ENT departments of general hospitals 13% and other local clinics 19%. The 77% of all institute used AABR and 23% used AOA. The annual average referral rate was 1.3% in 2009, 1.2% in 2010 and 2011 and 1.5% in 2012. The incidence of hearing loss (HL) including unilateral HL was 0.27% in 2009, 0.40% in 2010, 0.42% in 2011 and 0.50% in 2012. The NICU admission babies more than 5 days were about 2% of the all babies and their referral rate was 10.1% in 2012 and HL rate was 4.11% in 2012.

Conclusion

According to Korean CDC data, Korean actual NHS coverage was about 75% but KMHW support only around 9% of the total newborns. Average hearing loss rate of total babies in this study was 3~6.5 per 1,000 babies (> 40dBnHL). We have been tried for KMHW to support all newborn NHS and organized expert group for NHS, produced clinical guideline of NHS in 2010 and opened on-line education site for screening in 2013.

Crossed and Un-Crossed Acoustic Reflex Latencies in Normal Hearing Adults, Typically Developing Children and Children With Suspected Auditory Processing Disorders (APD)

Udit Saxena; Chris Allan; Prudence Allen

National Centre for Audiology, Western University, Ontario, Canada

Background

Many children presenting with listening difficulties are evaluated for auditory processing disorders (APD). Assessment for APD often includes behavioral tests of complex listening and objective tests of auditory neural integrity. One measure of neural integrity is the Acoustic Reflex. Elevated or absent acoustic reflex thresholds have been reported in some children with APD (Allen & Allan, 2007; Meneguello et al., 2001; Thomas, et al., 1985; Downs & Crum, 1980). More recently (Saxena, Allan & Allen, 2013) examination of the growth of acoustic reflex magnitude with changes in stimulus level showed that children presenting with listening problems suspected to arise from an APD often showed shallower acoustic reflex growth functions (ARGF) than did typically developing children and adults. These differences were largest when measured in the crossed condition. These results suggested possible deficits in the lower auditory pathways of the children with APD.

Acoustic reflex latencies, in addition to acoustic reflex thresholds and growth functions, may provide additional insight into the mechanisms underlying the integrity of the acoustic reflex pathways. Latencies may provide important information about the time course of the acoustic reflex. This paper presents data examining reflex latencies in children with listening disorders, typically developing children and adults.

Methods

Crossed and uncrossed reflex latencies were measured in 17 adults, 19 normal hearing, typically developing children and 19 children with suspected APD. Activators were pure tones at 500, 1000 and 2000 Hz. Latencies were measured for each frequency in both crossed and uncrossed conditions. Measures of 10 and 90% on latency, 10 and 90% off latency were taken at 10 dB SL re: ART.

Results

For all groups latencies tended to be longer at higher frequencies and longer when measured in crossed than uncrossed conditions. The effect of group was only significant for 90% on latencies for which children with suspected APD showed longer latencies. No significant ear effects were observed.

Conclusion

Acoustic reflex thresholds and growth functions have been shown to differ in children with suspected APD. These data suggest there may also be some differences in acoustic reflex latencies in children with suspected APD, measurable only at the 90% on latency. The use of acoustic reflex measures may provide useful information regarding the integrity

of lower brainstem pathways in children presenting with listening difficulties.

Binaural Signal Processing. Effects of Induced Lateral Asymmetry on Speech Recognition and Sound Localization Accuracy — a Pilot Study

Anne-Marie Jakobsson¹; Filip Asp²; Erik Berninger³

¹Karolinska University Hospital, Karolinska Institutet, Stockholm, Sweden; ²Department of Clinical Science, Intervention and Technology, Karolinska Institutet, Stockholm, Sweden; ³Dept of Clinical Science, Intervention and Technology, div. of ENT Diseases, Karolinska University Hospital, S-141 86 Stockholm, Sweden

Background

This study was done to analyse perceptual consequences of unilateral hearing loss including two aspects of binaural signal processing – noise suppression and sound localization ability. Unilateral hearing loss often leads to barriers in communication and deterioration in sound localization ability, even at moderate unilateral hearing loss. For example, some children with unilateral hearing exhibit learning difficulties and do not perform as well as normal hearing pupils. Nevertheless, many avoid hearing aids. The aim was to study effects on speech recognition in competing speech and sound localization accuracy following two levels of induced lateral asymmetry in normal-hearing adults, in a human model resembling slight, or, moderate unilateral hearing loss.

Methods

Eight otologically normal subjects aged 18-40 years participated. They all had pure-tone thresholds ≤ 20 dB HL (125-8000 Hz). Speech recognition in (non-correlated) competing speech (SCS, 4 loudspeakers, 63 dB SPL_{Ceq}) and sound localization accuracy (SLA, 63 dB SPL_{Ceq}) were recorded in sound field (audiometric test room). The speech threshold corresponding to 40% speech recognition was expressed as a signal-to-noise ratio (S/N). The setup for SLA comprised 12 loudspeakers separated by 10 degrees, spanning a 110 degree arc in the frontal horizontal plane. SLA was quantified as an Error Index (EI) using objective eye tracking technique. EI=0 corresponds to perfect match between perceived and presented azimuths, while EI=1 corresponds to pure guess. Two levels of right ear sound attenuation were achieved by hearing protectors (earplug; earplug + circum-aural hearing protector). Testing order was randomized.

Results

The mean (SD) shift in S/N was 2.0(1.5; $p<0.02$) dB, and 3.0(2.0; $p<0.01$) dB, while the corresponding shift in EI was 0.16(0.05; $p<0.01$), and 0.49(0.25; $p<0.01$), at the two attenuation levels (e.g., 40 and 50 dB at 3000 Hz), respectively ($n=8$). At base line, mean(SD) S/N, and mean(SD) EI, was -15.1(1.6) dB, and 0.05(0.02), respectively ($n=8$).

Conclusion

Distinct and highly significant deterioration of SCS and SLA occurred following an induced slight lateral asymmetry. Clini-

cal implications include noise suppression testing and sound localization accuracy tests even in patients with minor unilateral hearing loss, and the need for further research on the potential benefit of hearing aid usage.

PS - 515

Relationship Between Frequency Selectivity and Perceived Quality Of Nonlinearly Distorted Speech and Music by Hearing Impaired Patients

Stefania Goncalves¹; Tan Chin Tuan¹; Mario Svirsky¹; Brian Moore²

¹Laboratory for Translational Auditory Research;

²Department of Experimental Psychology, University of Cambridge

Background

Most current assistive hearing devices nonlinearly distort speech or music while trying to improve audibility and compensate for loudness recruitment in hearing impaired listeners. In addition, the output sound quality of these devices can also be affected by each patient's individual hearing deficits. In particular, this study examined how assistive hearing device sound quality may be affected by the listeners' frequency selectivity.

This study aimed to establish the relationship between frequency selectivity measured using Psychophysical Tuning Curves (PTC) and perceived quality of speech and music subjected to different nonlinear distortions by hearing impaired patients. This will provide insights into the effect of suprathreshold deficits on sound perception by hearing impaired listeners.

Methods

11 hearing impaired patients participated in the study. PTCs were measured using the "fast" method (Moore et al., 2005) with a 10 dB SL pure tone signal at 500 Hz, 1000 Hz and 2000 Hz, and with a narrowband noise masker. Patients were also asked to rate the perceived quality of speech and music subjected to various forms of artificial and real nonlinear distortions in two separate sessions. The artificial distortions, including clipping, compression, and full-range nonlinear distortion, are inherent to most assistive hearing devices. For real nonlinear distortions, nonlinearly distorted speech and music were recorded at the output of 3 different compression hearing aids with different compression settings. The recordings were digitally filtered so that the long-term spectrum of the output closely matched that of the input to retain only the nonlinear distortion. All stimuli were bandpass-filtered between 300 and 5000 Hz and amplified by the "Cambridge formula" (Moore et al., 1998) before presentation via Sennheiser HD600 earphones.

Results

Patients with broader PTCs, were less able to rate consistently the perceived quality of distorted speech or music between test sessions. The 10dB Q of PTCs at 500 - 1000 Hz obtained from the patients have higher correlations with their perceived quality ratings for most forms of distorted speech ,

while 10dB Q of PTCs at 2000 Hz yield higher correlations for most forms of distorted music instead.

Conclusion

These results seem to suggest that frequency selectivity should be considered as one of the parameters in fitting process of different hearing devices. Fast PTC technique would be a quick and easy tool for assessing frequency selectivity.

PS - 516

Auditory Games as a Novel Tool for Aural Rehabilitation

Xinyu Song¹; Noah Ledbetter¹; Mitchell Sommers¹; Nancy Tye-Murray²; Dennis Barbour¹

¹Washington University in St. Louis; ²Washington University School of Medicine

Background

Auditory training (AT) is a promising aural rehabilitation technique for millions of Americans with hearing loss. Despite the therapeutic potential of AT, however, its utility is still limited by the tedious nature of many existing AT regimens, often leading to poor subject compliance. Improving the potential of AT as a useful therapeutic tool requires reevaluating its presentation techniques.

Methods

To combat the current limitations of AT, we have developed a suite of video games designed to deliver effective AT in an intrinsically engaging format. These games are intended to be distributed on mobile electronic devices to maximize the accessibility of training. The first game is a fast-paced "action game" where players must complete short AT tasks in quick succession; this game is optimized for training on analytic tasks. The second game is a slower, narrative-driven game where players must converse with a number of in-game characters; this game is optimized for delivery of synthetic tasks. These two example games are built upon established AT protocols but have been modified to enhance engagement and encourage subjects to participate for longer periods of time, thus ultimately increasing training efficacy. Training tasks employed in the gaming suite have been designed with special consideration to ecological validity and semantic context, requiring players to process not only the sound but also the meaning of the acoustic stimuli delivered in behaviorally relevant contexts.

Results

Compared to traditional AT programs, our mobile game-based format is able to achieve or exceed rates of trial delivery while maintaining engagement with the subjects playing them. Ongoing studies are quantifying the extent of this engagement and efficacy of training in laboratory as well as portable settings.

Conclusion

Novel auditory training games designed from inception to represent compelling experiences can achieve high subject compliance for extended training while still maintaining relatively high presentation rates. This suggests that mobile game-based training may represent a successful method of

increasing participation with effective AT, empowering subjects to engage in substantial amounts of training outside of the audiology clinic and thereby maximize training gains from AT. Continual refinement of the game formats will enable further improvements of this intervention and ultimate application as a standard audiological therapy.

PS - 517

Evaluating Functional Hearing Deficits in Blast-Exposed Personnel With Normal Audiometric Thresholds

Douglas Brungart¹; Lina Kubli²; Benjamin Sheffield²; Sandeep Phatak²; Matthew Makashay²; Ken Grant¹

¹*Walter Reed Bethesda*; ¹*Walter Reed Bethesda*; ²*Army Public Health Command*

Background

The recent conflicts in Iraq and Afghanistan have resulted in a large number of US service members and veterans with combat-related exposure to explosive blast. This has led to anecdotal reports by military and VA audiologists that they are encountering blast-exposed patients who have normal audiometric thresholds but have difficulty understanding speech in complex auditory environments. Speech-in-noise difficulty in listeners with normal audiograms is often attributed to central auditory processing disorder (CAPD), which in these cases may have been caused by brain trauma during blast-exposure. Although there is some evidence that these blast-exposed individuals perform worse than non-blast-exposed listeners on traditional CAPD tests, their performance on these tests does not always provide clear insight into the problems these patients are likely to encounter in real-world listening. The purpose of this study was to conduct a detailed evaluation of the functional hearing abilities of blast-exposed listeners in complex listening tasks designed to mimic the acoustic cues that are likely to be encountered in real-world environments.

Methods

Participants with normal or near normal audiometric pure-tone thresholds (no more than 30 dB HL) were recruited into two groups: 1) a blast-exposed group of active-duty service members or veterans who reported being close enough to an explosive blast to experience heat or the effects of a pressure wave; and 2) a control group of service members or military dependents with no history of blast exposure. These groups were asked to participate in a test battery designed to examine a variety of aspects of functional hearing ability, including speech perception in the presence of noise, speech and babble maskers, audiovisual speech perception, perception of fast speech in reverberant environments, spatial release from masking, and sound localization.

Results

Traditional descriptive statistics revealed relatively small differences between the two groups, presumably because the blast-exposed group contained many listeners with normal auditory function. However, when the distributions of the individual scores in each group were analyzed, several tests indicated that a significantly larger number of blast-exposed

individuals were performing in the bottom range of normal performance than could be predicted by chance.

Conclusion

The results of the study suggest that a significant portion of blast-exposed individuals may be suffering from impaired spatial perception and difficulty understanding fast speech in reverberant environments. It is believed that a relatively fast screening tool based on these two tasks could serve as a robust method of identifying blast exposed individuals who may be experiencing central auditory processing difficulties.

PS - 518

Central Auditory Processing Following Blast Exposure

Frederick Gallun; Robert Folmer; Melissa Papesh; Michele Hutter; Leslie Grush; M. Samantha Lewis; Marjorie Leek
Portland VA Medical Center

Background

Military personnel tested within six months of being exposed to high-intensity blasts on the battlefield are significantly more likely than controls to perform abnormally on one or more behavioral and/or electrophysiological tests of central auditory processing (Gallun et al., *J Rehabil Res Dev.* 2012;49(7):1005-24). The current presentation describes initial findings from an ongoing four-year study of Veterans exposed to blasts during their military service over the past 10 years. The results will reveal the extent to which the acute injuries revealed in the previous work either resolve or become chronic issues.

Methods

Veterans and age and hearing-matched control subjects completed a battery of behavioral and electrophysiological tests of central auditory function. Areas of processing examined included binaural sensitivity, comprehension of competing speech with and without spatial cues, temporal processing using gap detection, and spectrotemporal pattern identification.

Results

Early data suggest that Veterans who have been blast exposed are susceptible to the same auditory processing difficulties observed immediately after exposure. Abnormal performance was not limited to particular areas of central processing ability, although most participants with abnormal results displayed a particular pattern of deficits suggestive of deficits in particular areas of function. Age and abnormal peripheral hearing were more likely to result in increased abnormal central ability for both groups, but the combined effects for those who had experienced blast exposure led to substantial rates of abnormal performance.

Conclusion

This study of Veterans whose blast exposures occurred up to ten years ago replicate the results of the previous study on subjects with more recent exposures, suggesting that the central auditory system recovers incompletely from blast exposure, if at all. Additionally, auditory processing difficulties appear to be more pronounced for individuals who are old-

er or who have more peripheral hearing loss. This implies that central auditory system dysfunction is likely to be found among Veterans with blast exposure for years after the initial incident(s). Furthermore, the aging and increasing peripheral hearing loss expected in this population over the next twenty to forty years are likely to combine with blast exposure to result in substantially greater difficulties communicating in complex and noisy environments than will be common for their age and hearing-matched peers.

PS - 519

Untangling Tinnitus and Hyperacusis Through Models and Measurements

Fan-Gang Zeng; Matthew Richardson; Thomas Lu
University of California Irvine

Background

Tinnitus is a sensation of sound in the absence of external stimuli. Hyperacusis is an increased sensation to external stimuli, and usually characterized by intolerance or even pain for ordinary sound levels. Although tinnitus and hyperacusis are often concomitant, it remains to be determined whether or not they have the same underlying mechanisms. An active loudness model suggests that tinnitus is due to increased central noise and hyperacusis is due to increased nonlinear gain (Zeng, 2013, *Hearing Research*, 295:172-179). This active model explicitly predicts that the slope of loudness growth function is normal or shallower than normal in tinnitus subjects but steeper than normal in hyperacusis subjects.

Methods

Pure tones were used to measure the slope of loudness and N100 cortical potential growth functions in normal-hearing, cochlear-impaired, tinnitus and hyperacusis subjects. Frequencies of the pure tones were in both normal hearing and hearing impairment regions as well as in both tinnitus and non-tinnitus regions.

Results

Comparing with the normal hearing control, tinnitus subjects produced a similar slope of the loudness growth function while hyperacusis subjects produced a steeper than normal slope, similar to loudness recruitment observed in the cochlear-impaired subjects. In subjects with concomitant tinnitus and hyperacusis, the increased slope was observed in both tinnitus and non-tinnitus regions. Preliminary data showed that these slope differences can be seen in the N100 growth functions, suggesting that the increased central noise and nonlinear gain mechanisms are located at the primary auditory cortical level or below.

Conclusion

The present results support the notion that tinnitus and hyperacusis have different primary mechanisms despite their concomitance. Theoretical and practical implications for these results will be discussed.

PS - 520

Hearing Loss Patterns Associated With Independent Risk Factors: Results from the Nord-Trøndelag Hearing Loss Study (NTHLS)

Howard Hoffman¹; Seonjoo Lee²; Chuan-Ming Li¹; May S. Chiu¹; George W. Reed³; Bo Engdahl⁴; Kristian Tambs⁴

¹National Institute on Deafness and Other Communication Disorders (NIDCD), NIH; ²Division of Biostatistics, Department of Psychiatry, Columbia University; ³University of Massachusetts Medical School and CORRONA, Inc.;

⁴Norwegian Institute of Public Health (NIPU), Oslo, Norway;

⁴Norwegian Institute of Public Health (NIPH), Oslo, Norway

Background

The adult population (≥ 20 years) of Nord-Trøndelag County, Norway participated during the past three decades from 1984-2008 in the Nord-Trøndelag Health Study, HUNT 1, 2, and 3. An integrated hearing examination, the NTHLS (n=51,975), was included in HUNT 2, 1995-1997.

Methods

We examined sex-specific multivariate multiple regression models - the array of thresholds in left and right ears constituted multivariate dependent variables - on a random subsample (n=13,000) of NTHLS participants to distinguish the effects of independent risk factors on hearing loss across eight pure-tone frequencies 250-8000 Hz, each ear. Bootstrap resampling was used to derive 95% confidence intervals for regression estimates.

Results

Age was a significant, major hearing loss risk factor in this Norwegian adult population cohort, aged 20-101 years (mean=50.2; standard deviation=17.0). The hearing loss pattern with age was a sloping trend that increased as frequency increased, identical in left and right ears for each sex separately. More gradual sloping trends were found for females than males. In both sexes, the average hearing loss decline per year increased from 0.25 decibels (dB) hearing level (HL) to 0.50 dB HL over the range 250-1000 Hz. Above 2000 Hz for males, and above 6000 Hz for females, the average hearing decrement exceeded 1 dB HL per year. After adjusting for age, specific risk factor conditions, e.g., ear-related disorders/diseases, draining ears, ear operations, damaged ear drums, tinnitus, and dizziness were significantly associated with hearing loss in both sexes across all frequencies. Loud music exposure was associated with hearing loss at low frequencies in both sexes. Among males participating in hunting and sports shooting, both ears showed significantly more hearing loss in a high-frequency "notch" pattern at 3000, 4000, and 6000 Hz and the left ear had significantly larger notches at these frequencies compared to the right ear. Some noise exposures, e.g., use of a hair dryer, were associated with modest hearing protection. Bilateral high-frequency noise "notch" patterns were found for males with history of loud noise exposure; however, among females with history of noise exposure, only a dip at 4000 Hz was significant.

Conclusion

These multivariate multiple regression results provide insight into the frequency-specific impact of different independent risk factors. This information can be used to predict potential benefit of interventions to preserve hearing based on reduction or elimination of risk factors in the population.

PS - 521

Pure Tone Audiometric and Subjective Hearing; a Cross-Sectional Register-Based Study on a Swedish Population Aged 18 Through 50 Years

Pernilla Videhult Pierre¹; Ann-Christin Johnson¹; Anders Fridberger²

¹Karolinska Institutet; ²Linköping University

Background

Subjective hearing impairment is increasingly common in young Swedish adults, but it is unknown whether it is related to elevated hearing thresholds measured with pure tone audiometry. The aims of the present study were to determine the prevalence of pure tone audiometric (PTA) and subjective hearing impairment and the associations between these measures in a young to middle-aged adult Swedish population.

Methods

A cross-sectional study was carried out using questionnaire and PTA data (500, 1000, 2000, 3000, 4000, and 6000 Hz) from 15322 subjects (62% women) aged 18 through 50 years participating in the Swedish LifeGene project. Statistics were performed with chi-square, least square, binary logistic regression, and generalized estimating equations (GEE) analysis.

Results

The population comprised mainly well educated and urban subjects. The prevalence of PTA hearing impairment, here defined as a hearing threshold above 20 dB in both ears at one or more frequencies, was 6.0% in men and 2.9% in women ($p < 0.001$) and could be expressed according to Equation 1 in men and Equation 2 in women. Prevalence = $17.1 - 1.45 \times \text{Age} + 3.23 \times 10^{-2} \times \text{Age}^2$ (Equation 1) Prevalence = $6.31 - 5.06 \times 10^{-1} \times \text{Age} + 1.18 \times 10^{-2} \times \text{Age}^2$ (Equation 2) Slightly impaired subjective hearing was reported by 18.5% of the men and 14.8% of the women ($p < 0.001$), whereas 0.5% of the men and women reported very impaired subjective hearing. GEE modelling showed that there were significant associations between PTA and subjective hearing ($p < 0.001$), which were dependent on frequency ($p = 0.001$). The area under the receiver operating characteristic (ROC) curve of the GEE model was 0.904 (95% CI: 0.892-0.915) in men and 0.886 (0.872-0.900) in women, and a cutoff value of 0.01058 in men yielded an approximate sensitivity of 0.90 and specificity of 0.74, whereas in women, an approximate sensitivity of 0.90 was obtained with a cut-off value of 0.00459; the specificity was then 0.68.

Conclusion

Even though subjective hearing impairment was much more common, it predicted PTA hearing impairment well when including frequency, age, and tinnitus as independent variables in a model adjusting for the clustered nature of the PTA assessment.

PS - 522

Acceptable Noise Levels Using Korean and Non-Semantic Speech Signals in Normal Hearing Subjects

Eun Jin Son¹; Ah Young Park¹; Seong Ah Hong¹; Sun Keum Kim¹; Jae Hee Lee²

¹Yonsei University College of Medicine Gangnam Severance Hospital; ¹Yonsei University College of Medicine Gangnam Severance Hospital; ²Hallym University of Graduate Studies

Background

The acceptable noise level (ANL) test measures the maximum noise level that a subject can tolerate while listening to the running speech. ANL has been shown to correlate with hearing aid use pattern. This study aims to compare ANL performance using the Korean language speech signal and non-semantic speech signals (reverse Korean speech, and ISTS) in normal hearing subjects.

Methods

Twenty subjects with normal hearing thresholds were recruited. ANL measurements were obtained using standardized protocols. Three different materials (Korean speech, reversed Korean speech, and ISTS) were used as the speech signal and 8-talker babble as the competing noise.

Results

Among the subjects with bilateral normal hearing, ANL measurements were widely varied. However, ANL measurements were similar for three different speech materials.

Conclusion

The results suggest that ANL tests could be performed using Korean and non-semantic signals, such as reverse Korean and ISTS, as the signals, and the ANL measurements were similar in each condition.

PS - 523

How We Apply Individual Auditory Features to Mobile Phones: In Samsung Galaxy S3 and S4

Sung Hwa Hong; Hayoung Byun; Il Joon Moon; Nam Gyu Ryu; Heesung Park; Hyun-Yong Shim; Sun Hwa Jin; Won-Ho Chung; Yang-Sun Cho

Sungkyunkwan University School of Medicine, Samsung Medical Center

Background

The number of mobile phones in use is beyond the population (>100%) in many developed country in 2013. It is approaching 50% even in developing country. People who use mobile phones have diverse individual auditory features, even within normal hearing thresholds. The serial studies were aimed

to see effectiveness and usefulness of individualized sound quality adjustment in mobile phones.

Methods

Four separate PC-based studies (P1-P4) were conducted for adult mobile phone users from 2012 to 2013. The modified and simplified version of audiometry for mobile phones by the Samsung Electronics was adapted to adjust the sound quality. Two of 4 studies (P1, P2) were conducted in normal hearing subjects (n=25), and the others (P3, P4) were performed in both normal hearing (n=30) and mild hearing loss subjects (n=30). To test the sound quality for voice and music, 4 (P1) or 6 (P2) kinds of voices and 5 music sources from different genre were used. Under blind conditions, subjective quality scoring was performed using VAS scale and/or MUSHRA tool, followed by open questions about sound qualities of two (adjusted vs. default) sound sources.

Results

For the questions about daily life, normal hearing subjects answered that they sometimes experience discomforts about voice quality of mobile phones in approximately 50%, while patients with mild hearing loss sometimes feel it in 75%. Test results showed that adjusted voice was significantly preferred by normal hearing subjects (for 2/3 of voice sources) and mildly impaired patients (for all voice sources). As the preferences for music sounds were more diverse, detailed descriptive analysis was mainly performed. Based on these results, sound adjustment functions for voice and music were added on Galaxy S3 (P1, P2) and S4 (P3, P4).

Conclusion

Sound quality adjustments depending on individual auditory features are useful in mobile phones, in subjects with both normal hearing and mild hearing loss. Further studies may help improving subjective satisfaction in using mobile devices.

PS - 525

The Difference Between Bone-Conducted Ultrasound and Audible Sound in Japanese Monosyllable Recognition.

Akinori Yamashita¹; Tadashi Nishimura¹; Tadao Okayasu¹; Yoshiki Nagatani²; Hiroshi Hosoi¹

¹Nara Medical University; ²Kobe city College of Technology

Background

The auditory perception of bone-conducted ultrasound(BCU) is not well known in general. However, since Gavreau first reported, many interesting characteristics have been reported about bone-conducted ultrasonic perception. Especially, It's interesting to note that some profoundly deaf subjects as well as normal-hearing subjects can discriminate BCU whose amplitude is modulated by different speech sounds. These findings suggest the usefulness of developing a bone-conducted ultrasonic hearing aid (BCUHA). In this study, to assess a possibility of development of a BCUHA, we compared BCU and air-conducted audible sound(ACAS) in terms of their associated speech perception tendency and investigated the different perceptual characteristics of BCU and ACAS.

Methods

Thirteen adults (seven males and six females) took part in the experiment. All were native Japanese speakers. All subjects had hearing within 20 dB HL at all frequencies from 125 to 8000 Hz as measured by conventional pure tone audiometry. Speech discrimination tests using both BCU and ACAS were performed with normal hearing subjects using List 67-S, which comprises 20 Japanese monosyllables used frequently in daily conversation. BCU and ACAS were compared for intelligibility and hearing confusion.

Results

With BCU, the maximum percentage correct totaled about 75%. Our comparison of the hearing confusion with ACAS and BCU according to the individual syllabic nuclear group showed a clear difference in the incorrect rates. In addition, the stimulus nuclear groups were often perceived in other nuclear groups in BCU.

Conclusion

Our results suggest that it is possible to transmit language information with BCU stimulation to normal-hearing subjects. Although the highest average score from speech discrimination testing with BCU was about 75%, it may be possible to improve intelligibility through training or by improving signal processing. However, the possibility that BCU and ACAS differ in terms of the mechanism of speech recognition has also been suggested. Therefore, further investigation is important. This result cannot be applied directly to profoundly deaf subjects. The present findings provide important clues for the development of BCUHA. Improved sound processing and further study with hearing impaired subjects are needed to develop the BCUHA for elderly hearing-impaired and profoundly deaf subjects.

PS - 526

Effect of Cisplatin Induced Hearing Loss on Human Ultrasonic Perception.

Tadao Okayasu¹; Tadashi Nishimura¹; Akinori Yamashita¹; Osamu Saito¹; Fumi Fukuda¹; Shuichi Yanai²; Hiroshi Hosoi¹

¹Nara Medical University; ²Tokyo Metropolitan Institute

Background

Ultrasound can be heard by bone-conduction. It is hypothesized that this bone-conducted ultrasonic perception is a result of direct ultrasonic stimulation of inner hair cells in the basal turn of the cochlea. In contrast, it has also been suggested that a lower frequency sound is generated in non-linear process during the transmission pathway to the cochlea to induce an auditory sensations. In order to verify this hypothesis, the present study evaluated changes in hearing sensitivity for both bone-conducted ultrasound and air-conducted audible sound following cisplatin administration. If ultrasonic perception is induced by not ultrasound itself but a low-frequency sound generated in non-linear process, hearing sensitivity for bone-conducted ultrasound would decrease in accordance with hearing loss of air-conducted sound by cochlear disorder.

Methods

Twenty hospitalized participants (40 ears) who suffered from head and neck cancer and were scheduled to undergo cisplatin chemoradiation therapy participated in this study. The hearing sensitivity for air-conducted sound in the conventional audiometric range at frequencies of 0.125, 0.25, 0.5, 1, 2, 4, and 8 kHz, high-frequency air-conducted sound at frequencies of 9, 10, 11, 12, 14, 16, 18, and 20 kHz and bone-conducted ultrasound at frequencies of 27, 30 and 33 kHz were measured before and after the treatment using cisplatin.

Results

Hearing loss was diagnosed according to the criteria of the American Speech-Language-Hearing Association. In total, hearing loss was observed in 25 ears (62.5%). The decrease of sensitivity to air-conducted sound occurred in the high-frequency range from 8 to 14 kHz. In contrast, bone-conducted ultrasound sensitivity at 27, 30 and 33 kHz was significantly improved after the treatment.

Conclusion

If ultrasonic perception is induced by not ultrasound itself but a distortion products generated in the signal path before the cochlea, hearing sensitivity for bone-conducted ultrasound would decrease in accordance with hearing loss of high-frequency air-conducted sound by cisplatin administration. Our result found that cisplatin induced hearing loss didn't decrease the hearing sensitivity for bone-conducted ultrasound. Considering that both air-conducted high-frequency sound and BCU are perceived in the cochlear basal turn, these findings indicate that ultrasonic perception is independent of hearing a lower frequency sound generated in the signal path before the cochlea. In addition, our findings support the hypothesis that ultrasound itself induces ultrasonic perception in the cochlea.

PS - 527

Towards a Stem Cell-Based “Otoxic Hearing Loss-in-a-Dish” Model – Enrichment of Otic Differentiated Cells

Aur lie Dos Santos¹; Andreas Eckhard¹; Ngoc-Nhi Luu¹; J rg Waldhaus²; Marcus M ller¹; Hubert L wenheim¹

¹University of T bingen Medical Center; ²Stanford University, School of Medicine

Background

Otoxic insults may cause irreversible hearing loss because cell regeneration in the mammalian organ of Corti is prohibited. Towards a rational therapy for the cure of sensorineural hearing loss, an *in vitro* culture model of ototoxic hair cell loss that can be utilized to screen for otoprotective or otoregenerative drugs is needed. To establish an “ototoxic hearing loss-in-a-dish” model, we aimed to increase in the number of *in vitro* differentiated otic hair- and supporting cell-like cells.

Methods

Using FACS and MACS, inner hair cell supporting cells that express the glutamate aspartate transporter (GLAST) and outer hair cell supporting cells expressing p75-neurotrophine receptor (p75-NTR) were purified from the murine neonatal

(P4) organ of Corti. The proliferative capacity and the potential to re-differentiate into otic hair and supporting cell-like cells were investigated by immunohistochemical and qPCR. Furthermore, the potential of the gamma-secretase inhibitor L-685,458 (24 h, 1.5 μ M) to induce otic cell differentiation was analyzed in *in vitro* cultures of the murine P0 organ of Corti. As a “hearing loss in a dish model”, Neomycin (1 mM) was added for 24 h, and the number of supporting and hair cell like cells were analyzed after 48, 72, 96 and 120 hours.

Results

FACS and MACS purified GLAST+, p75-NTR+ and GLAST-/p75-NTR- cells proliferated *in vitro* as determined by EdU-incorporation and expression of stem cell markers. MACS purified GLAST+ and p75-NTR+ cells showed a higher differentiation potential for hair and supporting cell like cells *in vitro* than GLAST-/p75-NTR- cells; however, compared to unsorted cells, the sorting process reduced the absolute number of MACS-derived *in vitro* cultured cells by a factor of 100. Treatment of *in vitro* cultured cells from the P0 organ of Corti for 24 h with the gamma secretase inhibitor L-685,458 increased the absolute number of hair cells and supporting cells *in vitro* by a factor of 6.4 and 19.6, respectively. Addition of neomycin *in vitro* 120 h before the end of the culture period resulted in an almost complete loss of hair cell like cells, while the number of supporting cell like cells remained constant.

Conclusion

Treatment of *in vitro* cultured cells from the murine P0 organ of Corti with L-685,458 increases the number of hair and supporting cell-like cells. Neomycin selectively kills hair cell-like cells *in vitro* in a time-dependent fashion, and therefore can be used for an “ototoxic hearing loss-in-a-dish” model.

PS - 528

Beat Synchronization and Speech Encoding in Preschoolers: A Neural Synchrony Framework for Language Development

Kali Woodruff Carr¹; Travis White-Schwoch¹; Adam Tierney¹; Dana Strait²; Nina Kraus¹

¹Northwestern University; ²University of Maryland

Background

Rhythmic sensitivity is an important skill for language development. Infants use rhythmic cues to discern word boundaries and syllable segments in speech, facilitating phonological awareness. Temporal encoding of speech is impaired in individuals with developmental dyslexia, and dyslexics struggle to synchronize motor movements to a beat at syllable rates of speech. Poor neural synchrony throughout the auditory pathway may contribute both to rhythmic and phonological deficits observed in poor readers, as both beat synchronization and reading skills relate to subcortical and cortical phase locking to speech. However, the development of these skills remains poorly understood. Here we provide evidence for an auditory neural synchrony framework for reading, demonstrating links between motor synchronization, subcortical envelope encoding of speech, and phonological awareness in pre-readers.

Methods

We analyzed preschoolers' ability to entrain to a beat by asking them to drum along with an experimenter, who was drumming at speeds consistent with speech syllable rates. Auditory brainstem responses to the speech syllable [da], presented in quiet and in noise, were collected. We also measured participants' phonological awareness.

Results

Children who were able to entrain to the experimenter's beat had more faithful encoding of the speech envelope, as evinced by a higher correlation between the envelope component of the brainstem response and the stimulus. In addition, children who were able to synchronize to a beat scored higher on tests of phonological awareness.

Conclusion

The ability to move to a beat is linked to the precision of neural encoding of the speech envelope and phonological awareness in pre-readers. Auditory neural synchrony, therefore, may be at the core of rhythmic performance, sound processing, and language learning. Children who struggle to move synchronously to a beat may have poorer neural representation of sounds, which could predict future struggles learning to read or put them at risk for developing auditory processing disorders.

PS - 529

Do the Organ of Corti and Stria Vascularis Depend on Each Other for Development and Survival?

Huizhan Liu¹; Yi Li¹; Qian Zhang¹; David Nichols¹; Ning Pan²; Bernd Fritsch²; **David He¹**

¹Creighton University; ²University of Iowa

Background

Hearing depends on normal operation of the organ of Corti and stria vascularis. The organ of Corti contains hair cells which transduce mechanical stimuli into electrical signals while the stria vascularis is responsible for generating endocochlear potential (EP), which is the driving force for mechanotransduction. EP with a magnitude of 5-10 mV is first observed at P9 (postnatal day 9), and increased significantly till P20, by which time it reaches the adult value (~95 mV) in mice. Hair cells also undergo significant development after birth and by P18, hair cells are functionally mature. The goal of our study is to determine whether the hair cells and stria vascularis depend on each other for development, function and survival. Two mouse models with hair cell loss at different time points after birth were used for our study. The *Atoh1* conditional knockout mouse self-terminates expression of *Atoh1* in hair cells around birth. Development of hair cells before birth is normal but there is a progressive loss of all hair cells within three weeks after birth due to the self-termination of *Atoh1* expression. We used this model to determine whether absence of the hair cells would affect the function and organization of the stria. The other mouse model has a mutation of the microphthalmia-associated transcription factor (*MITF*) gene expressed in melanocytes, one of three types of cells in the stria vascularis. Loss of melanocytes due to *MITF* mu-

tation causes abnormality of the stria morphology and function, leading to hearing loss. We used this model to determine whether hair cells were able to develop and survive without a normal ionic environment in the endolymph maintained by the stria.

Methods

Confocal microscopy was used to examine hair cell and stria morphology. Hearing threshold, cochlear microphonic and EP were measured to examine the operation of the organ of Corti and stria. Development of outer hair cell motility and membrane conductances was examined using whole cell voltage-clamp techniques.

Results

We showed that stria defect (reflected by lack of EP) led to outer hair cell (OHC) apoptosis after P18 when OHCs are functionally mature. However, stria defect did not affect the survival of inner hair cells (IHCs) and development of IHCs and OHCs. Interestingly, stria morphology and EP magnitude remained normal after hair cells and supporting cells in the organ of Corti were completely degenerated.

Conclusion

Our studies suggest that while hair cell differentiation and development do not require the ionic environment in the endolymph, normal function of the stria are necessary for survival of adult OHCs. However, the survival and normal operation of stria do not depend on a functional organ of Corti.

PS - 530

Hair Cell-Like Cells Induced from IPS Cells Using Mouse Utricle Tissues.

Shohei Ochi; Akiko Taura; Shin-ichiro Kitajiri; Takayuki Nakagawa; Juichi Ito

Kyoto University

Background

Millions of people worldwide suffer from hearing and balance disorders caused by loss of hair cells in inner ear. In mammalian, hair cells hold limited potential for regeneration once they were damaged. Up to now, several approaches have been done to induce hair cells. Oshima et al reported the induction of hair cell-like cells from mouse ESC/ iPSC (Oshima et al., 2010). However the efficiency for induction of hair cells was not so high and it is still unclear that what kinds of factors are critical for induce hair cells. In order to apply to clinical research, we should develop more efficient method and reveal key factors for the induction of hair cells. This study examined the potential of iPS cells for differentiation into hair cells and is aimed to produce enormous hair cells.

Methods

We used the same method as Oshima's method for differentiation of iPS into ectodermal lineage. At first, we cultured iPS under D/S/I (Dkk-1, SIS3 and IGF-1) for 5 days and under bFGF (basic Fibroblast Growth Factor) for following 3 days. We confirmed whether differentiated iPS cells were Pax2 positive or not. After differentiation into ectodermal lineage, we co-cultured iPS with mouse utricle tissues of various conditions instead of chicken utricle stromal cells.

Results

When we cultured iPS cells with mouse utricle stromal tissue, there are some round clusters containing myosin7A positive cells and Ds Red positive cell between iPS cells colony and stromal tissue, These cells have phalloidin positive hair bundle like structures in the center of cluster.

Conclusion

Our findings revealed that mouse stromal tissues have important factors to induce hair cells from iPS cells, although the efficiency of induction was not so high. However, our results can lead to reveal what key factor to induce hair cells is, by analyzing the difference between each condition. Furthermore, we investigated the several factors increasing the efficiency of hair cell induction.

PS - 531

Bioinformatic Reconstruction of the Mouse Otocyst (and Neuroblasts) Using Single Cell QRT-PCR Data

Robert Durruthy-Durruthy; Assaf Gottlieb; Byron Hartman; Jörg Waldhaus; Russ Altman; Stefan Heller
Stanford University

Background

The otocyst comprises committed progenitor cells required for the development of most cell types of the mature inner ear including sensory hair cells, non-sensory supporting cells and neurons. Individual marker genes are expressed in defined regions of the otocyst suggesting that it harbors precursors with distinct cellular identities. Our objective is to delineate the transcriptional heterogeneity of the otocyst, to model its cellular organization on a genetic level, and to outline potential functional relationships that are involved in patterning regionally discrete domains.

Methods

To address this aim, we selected 96 different marker genes including known otic markers as well as putative novel otic genes identified from microarray data, and a selection of signaling pathway-associated transcripts. These genes are the basis of a multiplex quantitative RT-PCR assay that we conducted with otocyst cells at single cell resolution.

Here, we utilized Pax2(Cre)/Rosa26(mT/mG) mice and fluorescence-activated cell sorting to isolate individual cells from the otocyst and delaminating neuroblasts of E10.5 (embryonic day) embryos.

Results

Single cell gene expression profiling of 382 cells, encompassing 36,672 individual qRT-PCR reactions, and subsequent multivariate cluster methods revealed the presence of distinct sub-populations and describes the global heterogeneity of otocyst and neuroblast cells. Comprehensive bioinformatics approaches further identified specific cellular gene expression profiles within lineages such as neuroblasts, consistent with different temporal stages of differentiation.

Finally, we developed a technique that integrates previously reported expression knowledge from individual genes with

recorded single cell data and accurately mapped various gene-group specific domains onto a three-dimensional representation (reconstruction) of the otocyst.

Conclusion

This enabled us to validate existing expression data, to recognize and allocate previously uncharacterized and transcriptionally divergent subgroups of cells to precise axis-associated octants in the otocyst. Ultimately, we envision that single cell qRT-PCR technology will revolutionize developmental biology because it allows the analysis of spatial organization but also dynamic processes such as neuroblast delamination with unprecedented depth and highly parallel fashion.

PS - 532

The BK Channel Affects Extrinsic and Intrinsic Mechanisms of Apoptosis

Yoshihisa Sakai; Bernd Sokolowski

University of South Florida, Morsani School of Medicine

Background

Numerous proteins that intricately interact with one another regulate different aspects of the cell cycle such as survival and apoptosis. Among these are p53 and FADD, which play important roles in intrinsic and extrinsic apoptotic pathways, respectively. The large conductance Ca^{2+} -activated potassium channel (BK) is ubiquitously expressed and contains a highly conserved amino acid sequence that underlies numerous physiological functions. Recent reports suggest that BK has a role in preventing brain ischemia. Our previous work, in the cochlea, detected novel BK interacting proteins that participate in cell survival. Here, we tested whether BK could affect intrinsic and extrinsic apoptotic pathways by interacting with p53 and FADD

Methods

Reciprocal coimmunoprecipitation (coIP) studies, using whole brain, were performed initially to determine BK interactions with p53 or the Fas-Associated Protein with Death Domain (FADD). To further understand these interactions, a BK-DEC variant was cloned from mouse cochlea, and four variants constructed with a tandem HA tag. Two were full-length with a C- or N-terminus tag, while two were truncated, lacking either the N- or C-terminus. Each of these was separately co-transfected into HEK cells with either V5-tagged p53 or FADD. Interactions and colocalizations were examined using reciprocal coIPs and immunocytochemistry, respectively. Apoptotic assays were performed using a BK/HEK stable cell line treated with TNF-related apoptosis-inducing ligand (TRAIL) to stimulate FADD or Mitomycin C (MMC) to activate p53. Apoptosis assays included counting apoptotic cells, using a photometric enzyme-immunoassay that detects cytoplasmic histone-associated DNA fragments, and determining the expression of cleaved caspase 8.

Results

Reciprocal coIPs showed that BK interacts with p53 and FADD in mouse brain and in cotransfected HEK cells. Moreover, p53 interacts with both the N- and C-terminus of BK, whereas FADD only interacts with the C-terminus. Immunocytochemistry revealed colocalization of BK with p53 and FADD

in the mitochondrion and at the plasmalemma, respectively. Apoptosis assays showed that BK increases cell survival rate by ~40%, during the activation of p53 or FADD in a BK/HEK stable cell line. Furthermore, cleaved caspase 8 expression decreased by ~20% in this BK/HEK cell line.

Conclusion

We demonstrate that BK interacts with p53 and FADD and protects cells from apoptotic events. Thus, BK affects both intrinsic and extrinsic pathways of apoptosis. In addition, p53 and FADD both bind to the C-terminus, whereas p53 also binds to the N-terminus.

PS - 533

Atoh1 Expression Levels Define the Fate of Nonsensory Epithelial Cells of Cochlea in Neonatal Mammals in Vitro

Juanmei Yang¹; Wenwei Luo²; Zhao Han²; Fanglu Chi²

¹Eye & ENT Hospital of Fudan University; ²Eye & ENT hospital of Fudan University, Department of otolaryngology-head and neck surgery

Background

Atonal homolog1 (Atoh1) is a bHLH transcription factor that is essential for inner ear hair cell differentiation. Previous studies have reported that Atoh1 gene transfer can induce the production of ectopic hair-cell-like cells, but the relationship of Atoh1 expression level and the formation of new ectopic hair cell-like cells is unclear.

Methods

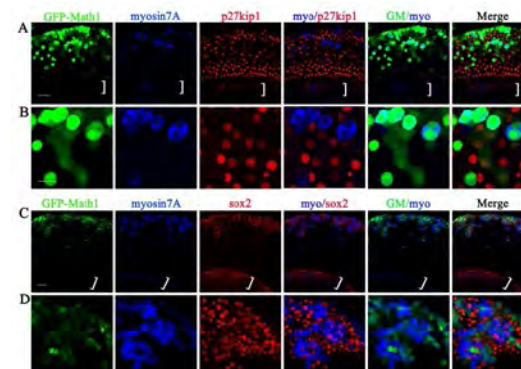
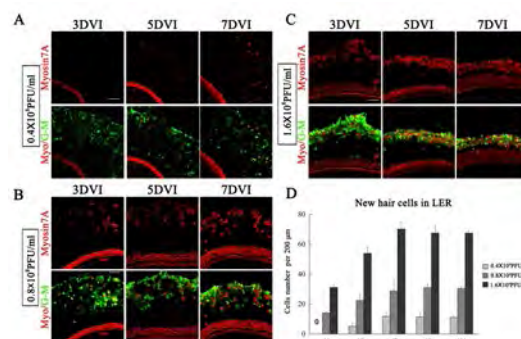
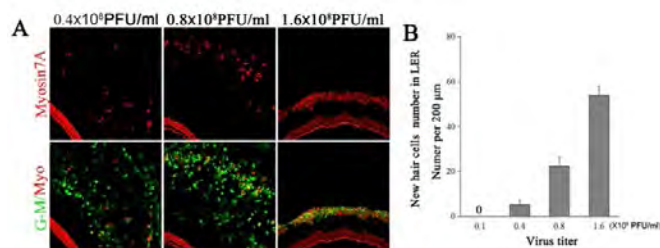
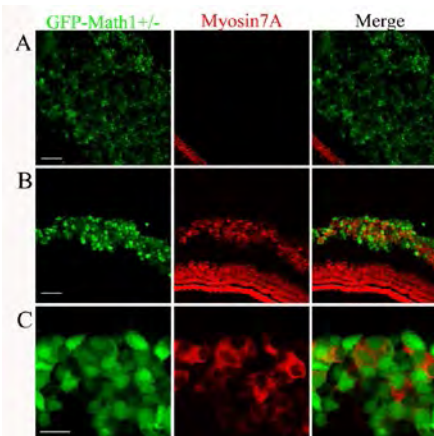
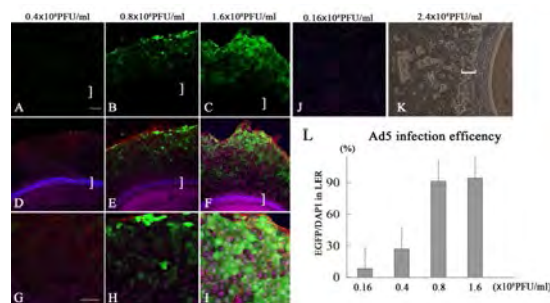
We examined the effect of different Atoh1 expression levels and the duration of new ectopic hair cell-like cells formation on the lesser epithelial ridge (LER) of cochleae using a human adenovirus serotype 5 (Ad5) vector encoding *atoh1* and the reporter gene *EGFP*. Different virus titers were added to cultured cochlear explants, and we detected new ectopic hair cell-like cells in the LER at different time points.

Results

GFP alone did not induce new ectopic hair cell-like cells. However, Atoh1 expression induced new ectopic hair cell-like cells as early as 2.5-5 days after *EGFP-atoh1* infection in the LER, depending upon the viral titer; the number of new ectopic hair cell-like cells increased with time. Higher *Ad5-EGFP-atoh1* titers induced greater Atoh1 expression, resulting in an increase in new ectopic hair cell-like cells. Lower *Ad5-EGFP-atoh1* titers required more time for new ectopic hair cell-like cells formation, whereas very low titers of *Ad5-EGFP-atoh1* induced only weak Atoh1 expression without inducing new ectopic hair cell-like cells formation.

Conclusion

In conclusion, we used an appropriate *Ad5-EGFP-atoh1* titer range for Atoh1 expression to induce new ectopic hair cell-like cells. The Atoh1 expression level defined the fate of LER cells as either new ectopic hair cell-like cells or nonsensory epithelial cells.



Prestin Expression is Modulated After the Onset of Threshold Shifts in Oncomodulin Knockout Mice

Dwayne Simmons¹; Mike Jau Jiing Dai¹; Aubrey Hornak¹; Kevin Ohlemiller²

¹UCLA; ²Washington University School of Medicine

Background

The tight regulation of Ca²⁺ is essential for cochlear function, and yet the role of Ca²⁺ binding proteins (CaBPs) remains elusive. While most CaBPs are found extensively throughout the nervous system, oncomodulin (Ocm), a member of the parvalbumin family, has a restricted expression pattern limited in the cochlea to outer hair cells (OHCs). Recent studies find Ocm immunoreactivity (Ocm-ir) overlaps with prestin localization. We investigated prestin expression in Ocm null mutants. We compared prestin immunoreactivity (-ir) with alpha-parvalbumin (α PV) and changes in OHC efferent innervation.

Methods

We generated a conditional Cre-lox knockout line with Cre-recombinase driven by the β -actin promoter (*Ocm^{tm1.1}Ddsi*). The absence of Ocm expression was confirmed by RT-PCR and immunocytochemistry. Hearing function was assessed by auditory brainstem responses (ABRs) and distortion product otoacoustic emissions (DPOAEs). For immunocytochemistry, we used the following primary antibodies: anti-prestin (rabbit, a kind gift from R. Fettiplace), anti- α PV (goat), and anti-choline acetyltransferase (anti-ChAT, goat). Staining with phalloidin (for actin) and DAPI (for nuclei) was also done.

Results

Targeted deletion of Ocm results in progressive hearing loss beginning at 2 months with significantly elevated threshold shifts. We found that prestin-ir developed normally through the postnatal period. Beginning at 2 months, Ocm null mutants have increasing amounts of hair cell loss in basal high frequency regions. However, the most dramatic changes in prestin-ir occurred at 3 months. In general, prestin-ir in surviving hair cells was much more intense than in wild type controls consistent with either an increase in prestin expression or a decrease in OHC volume. Mutant animals exhibited a basal to apical prestin-ir intensity gradient, a greater number of prestin-labeled plaques, and regions of prestin-labeled OHC fragments. Additionally, prestin-labeled OHCs were shorter especially in apical regions. We did not observe any changes in α PV-ir in mutants compared to wild type controls. In mutants, efferent terminals were found on intact prestin-labeled OHCs but not on any prestin-labeled OHC fragments. In general, the OHC efferent terminals in mutants were smaller in size than wild-type controls.

Conclusion

In Ocm null mutants, the elevation of hearing thresholds occurs prior to any significant changes in prestin expression. However, the loss of efferent terminals coincides with changes in prestin expression.

An *Ildr1* Knockout Mouse is a Model of Human Deafness DFNB42

Eva Morozko¹; Ayako Nishio¹; Tracy Fitzgerald¹; Elizabeth Wilson¹; Rashmi Chandra²; Philine Wangemann³; Rodger A. Liddle²; Thomas B. Friedman¹; Inna A. Belyantseva¹

¹National Institute on Deafness and Other Communication Disorders; ²Duke University Medical Center; ³Kansas State University

Background

In the cochlea, tricellular and bicellular tight junctions contribute to paracellular barriers that are crucial for separation of endolymph from perilymph, which have distinct ionic compositions. Immunoglobulin-like domain containing receptor 1 (ILDR1) has been shown to localize to tricellular contacts between cells within the organ of Corti and vestibular sensory epithelia (Higashi et al., 2013). Mutations of *ILDR1* have been reported to be associated with nonsyndromic deafness DFNB42 (Borck et al., 2011). Another tricellular tight junction (tTJ) protein, tricellulin, encoded by *TRIC*, has a similar localization to ILDR1. Mutations of *TRIC* cause human deafness DFNB49 (Riazuddin et al., 2006). In Eph4 cells, ILDR1 recruits tricellulin to tTJs, suggesting that ILDR1 has a critical role in the formation of tTJs in the inner ear (Higashi et al., 2013). Here we characterize the auditory phenotype of an *Ildr1* knockout (*Ildr1*^{-/-}) mouse (Chandra et al., 2013).

Methods

Mice were genotyped (Chandra et al., 2013). The hearing phenotype of *Ildr1*^{-/-} mice and normal hearing controls were assessed by measuring ABRs, DPOAEs and EPs. Immunocytochemistry was used to localize tricellulin and ILDR1 and investigate changes in the morphology of the organ of Corti.

Results

Ildr1^{-/-} mice have elevated ABR thresholds of 70-90 dB SPL at P15-16 and are profoundly deaf by 1 month of age, while *Ildr1*^{+/-} and *Ildr1*^{+/+} mice maintain normal hearing. *Ildr1*^{-/-} mice do not exhibit an obvious vestibular dysfunction such as head bobbing or circling behavior. DPOAEs are absent indicating a loss of OHC function in *Ildr1*^{-/-} mice at P15-16, which corresponds with the time we observe a rapid degeneration of OHCs from base to apex. IHCs remain grossly unaffected. No differences in EPs are observed between *Ildr1*^{+/+} adult littermates and *Ildr1*^{-/-} mice. In *Ildr1*^{+/+} organ of Corti, both ILDR1 and tricellulin span the entire depth of tight junctions between hair and supporting cells. However, in *Ildr1*^{-/-} mice, tricellulin does not span the entire depth of tTJs.

Conclusion

Ildr1^{-/-} mice are severely deaf at P15-16 and become profoundly deaf by P30. Partial mislocalization of tricellulin at tTJs in *Ildr1*^{-/-} mice indicates that ILDR1 is not the sole recruiter of tricellulin to tTJs. Absence of ILDR1 in conjunction with mislocalized tricellulin at tTJs and a normal EP likely lead to defective ion and small molecule permeability through the paracellular pathway and may cause the observed hair cell degeneration.

PS - 536

Stress Dependent Inner Hair Cell Vulnerability

Mirko Jaumann; Kamyar Kasini; Carina Meiser; Lukas Rüttiger; Marlies Knipper
University of Tübingen

Background

Emerging evidence suggests that the inner hair cell synapse plays a crucial role in the development of hearing problems. Understanding the process of inner hair cell synapse damage after a noxious stimulus is of great importance for the development of specific therapies aiming to protect hearing function. We recently described a negative influence of stress (Singer, 2013, Mol Neurobiol) and positive impact of cyclic guanosine monophosphate (cGMP)-signaling on acoustic trauma induced damage of the inner hair cell synapse (Jaumann, 2012, Nat Med) and here question a related influence on both.

Methods

Wistar rats were exposed to an acoustic overstimulation. Hearing function was determined using measurements of the auditory brainstem response before and after the acoustic overexposure. Urinary corticosterone concentration was measured to determine the individual stress level using ELISA. The number of ribbon synapses was analyzed by Immunohistochemistry as a metric of deafferentation. The influence of cGMP-signaling was investigated by treating the animals with a PDE5-inhibitor or 7-Nitroindazole.

Results

Here we describe an influence of stress and cGMP-signaling on the inner hair cell synapse integrity before and after acoustic overstimulation.

Conclusion

We discuss the finding in the context of the development of hearing problems.

PS - 537

Profound Deafness and Hair Cell Loss in MiR-183 Family Knockout Models

Marsha Pierce; Heather Jensen-Smith; Garrett Soukup
Creighton University

Background

MicroRNAs (miRNAs) are small-noncoding RNAs that function to post-transcriptionally regulate target genes affecting crucial cellular processes including development, differentiation and maintenance. Each member of the miR-183 family (miR-183, miR-96, and miR-182) is strictly conserved among vertebrates and coordinately expressed in neurosensory cells responsible for mechanosensation, photoreception, electroreception and chemosensation. Mutations in *miR-96* lead to hair cell (HC) loss and profound deafness in both humans and mice. However, in the *Diminuendo* mouse, one such mutation in *miR-96* can contribute to both loss of function (LOF) and gain of function (GOF). To investigate miR-183 family member LOF exclusively, we are examining two miR-183 family knockout (KO) models.

Methods

To assess miR-183 family member LOF, we acquired *miR-183/96* KO and *miR-182* KO mouse lines generated for the Knock Out Mouse Project (KOMP) by the Sanger Institute. To confirm each model and assess effects on remaining miR-183 family members, we performed in situ hybridization (ISH) using locked nucleic acid (LNA) probes labeled with digoxigenin (DIG). To grossly assess HC function, behavioral observations and evaluation of Preyer's reflex were used. To assess HC loss, we performed immunohistochemistry (IHC) using anti-MyoVIIa antibody on mice ranging in age from postnatal day 0 (P0) to P180.

Results

ISH for miR-183 family members demonstrated that both models function as expected. In *miR-183/96* nullizygous mice, miR-183 and miR-96 were not detected, and there was no apparent perturbation of miR-182. Likewise, in *miR-182* nullizygous mice, miR-182 was not detected, and there was no apparent perturbation of miR-183 or miR-96. *miR-183/96* nullizygous mice exhibit head-bobbing and circling beyond ~P70, while *miR-182* nullizygous mice do not. Moreover, *miR-183/96* nullizygous mice fail to exhibit Preyer's reflex at any age, whereas *miR-183/96* hemizygous mice and *miR-182* nullizygous mice show an age-dependent loss of Preyer's reflex. IHC for MyoVIIa demonstrates HC loss consistent with loss of Preyer's reflex and behavioral observations.

Conclusion

Results demonstrate that miR-183 family LOF leads to HC loss and hearing loss. Additionally, HC loss in *miR-183/96* hemizygous mice suggests that miRNA concentration or "dose" is crucial for hair cell function and survival. Moreover, profound vestibular defects are only observed in *miR-183/96* nullizygous mice, suggesting that vestibular HCs are less sensitive to miR-183 family expression levels. However, the underlying mechanism(s) remain to be elucidated. Understanding miR-183 family effects on target genes and pathways is expected to provide insight to approaches for preventing HC loss or stimulating regeneration of neurosensory cells.

PS - 538

Effect of Neomycin Administration to the Cochlea in Neonatal Mice

Lingxiang Hu^{1,2}; Hao Wu¹; Albert Edge²; Fuxin Shi²

¹Shanghai Jiaotong University School of Medicine, Xinhua Hospital; ²Harvard Medical School, Massachusetts Eye and Ear Infirmary

Background

Aminoglycoside antibiotics are a major cause of hearing loss. They enter hair cells specifically through mechanotransduction channels, and initiate apoptosis of hair cells. Our aim was to assess the affect of neomycin on neonatal hair cells *in vivo*. We attempted to develop a procedure for antibiotic delivery that would leave the cochlea intact in the absence of drug. We followed the mice after the acquisition of hearing to assess both cochlear morphology and function after hair cells degenerate early in postnatal life.

Methods

A single dose of neomycin (200 nl) was administered into the scala media of the neonatal cochlea at postnatal day 2 (P2) in the following groups: neomycin injection at 1 mM (n=4), 10 mM (n=5), 50 mM (n=8) and 100 mM (n=8) at 60 nl/min, injection of water at 20 nl/min (n=3) and 60 nl/min (n=3), and surgical procedure without injection (n=6). The injections were done with a nanoliter micro-injection system. Hair cells were examined at 1, 3 and 42 days after surgery. DPOAEs and ABRs were recorded at 42 days.

Results

After the injection, all mice (n=42) survived and the external wounds healed. Mechanical damage to hair cells was seen at the high injection speed, showing the loss of a small number of hair cells at the injection site (water). Injection of neomycin resulted in a dose-dependent loss of hair cells. Compared to the surgery and carrier controls, 1 mM neomycin induced a significant loss of outer hair cells, and 10 mM, 50 mM and 100 mM neomycin caused significant loss of both inner and outer hair cells 3 days after injection ($P < 0.05$). Neomycin at 50 mM induced hair cell loss within one day, with no significant further loss after 3 days. Moreover, 50 mM neomycin resulted in a complete loss of hair cells in the basal and middle turns without damage to supporting cells. Whereas DPOAEs and ABRs were normal in carrier controls, DPOAE and ABR thresholds were elevated (above 80 and 100 dB) at all frequencies (4 to 45 kHz) by treatment with 50 mM neomycin.

Conclusion

Direct application of neomycin into the cochlea in neonates resulted in specific hair cell loss. Preservation of hearing in the control animals allowed us to see specific effects of neomycin, which was delivered without adverse systemic effects. The rate of hair cell loss was high and resulted in increased DPOAE and ABR thresholds.

PS - 539

From Optical Coherence Tomography (OCT) Data to Cochlear Mechanics

Egbert de Boer¹; Fangyi Chen¹; Dingjun Zha²; Anders Fridberger³; Alfred L. Nuttall²

¹Academic Medical Centre; ¹Oregon Hearing Research Center, NRC04, Oregon Health & Science University, 3181 SW Sam Jackson Park Road, Portland, Oregon 97239-3098, USA; ²Oregon Health & Science University;

³Karolinska Institutet, Stockholm, Sweden

Background

A new technique for the study of cochlear mechanics is Optical Coherence Tomography (OCT). With a variation of this technique it is possible to measure simultaneously movements of the Reticular Lamina (RL) and the Basilar Membrane (BM) in the cochlea.

Methods

Because of the difficulty of the experiments the data are sparse, have missing values across the domain of parameters, and are subject to high noise levels at low sound or vibration levels. These problems require the introduction of creative data interpolation and extrapolation approaches.

Results

In a viable guinea-pig cochlea, the RL moves in the region of maximum response with an amplitude of up to three times that of the BM. There are also consistent differences in phase between RL and BM.

Conclusion

In view of the principle of constant fluid volume within the organ of Corti, we must assume that the RL velocity averaged over the width is the same as for the BM.

The findings on amplitude and phase of BM and RL responses, both at low and at high levels of stimulation, pose questions on details of cochlear mechanics. A solution in line with the physics of the system will be presented. We ascribe the amplitude differences partly and the phase differences entirely to the process of cochlear amplification effected by the Outer Hair Cells (OHCs).

PS - 540

Simultaneous In Vivo Measurement of Mouse Organ of Corti Vibrations in Two Cochlear Turns Using Phase-Sensitive Fourier Domain Optical Coherence Tomography

Sripriya Ramamoorthy¹; Yuan Zhang¹; Tracy Petrie¹; Ruikang Wang²; Steven S. Jacques¹; Alfred L. Nuttall¹

¹Oregon Health & Science University; ²University of Washington-Seattle

Background

Being a mammal and amenable to genetic manipulations, the mouse is an excellent animal model to study human hearing and its pathology. However, it has been very challenging to measure the vibration response of the mouse cochlea as the available technology is limited. Furthermore, most measurements of vibrations in the mammalian ear, in general, have been limited to the apical turn or the basal turn.

Methods

We have developed a custom phase-sensitive Fourier domain optical coherence tomography (PSFDOCT) and interferometry system with center optical wavelength at 840 nm. In this study, we used this system to measure the organ of Corti vibrations in mice. Surgical operation was performed in anaesthetized mice to expose the left bulla, which was then incised to open for access to the cochlea. During the experiment, the core temperature of the animal was maintained at 37 °C - 38 °C by a heating blanket. A dorsal approach exposed the round window membrane through which the organ of Corti was optically accessed in the live animal.

Results

Using the PSFDOCT system we developed, we have measured compressive non-linearity in the organ of Corti vibrations in sensitive mice *in vivo* in the round-window region where the CF is above 50 kHz. Furthermore, we were able to simultaneously measure the loud sound induced organ of Corti vibrations from two cochlear turns with best frequencies around 53 kHz and 32 kHz respectively.

Conclusion

Simultaneous measurement of organ of Corti vibrations in two cochlear turns in live mice is possible using PSFDOCT. This development will generate new insights on distortion product otoacoustic emissions as it enables simultaneous measurement of the distortion products (DP) near the DP generation site (53 kHz place) and the DP reflection site (32 kHz place).

PS - 541

Imaging Micromechanical Motion in the Organ of Corti With Direct Stimulation of the Basilar Membrane

Aleks Zosuls; Laura Rupprecht; David Mountain
Boston University

Background

A number of recent experimental results suggest that the micromechanics of the organ of Corti are quite complex and some investigators have even suggested that forward and reverse traveling waves may involve different propagation mechanisms. In this study we stimulated the basilar membrane directly and used modern imaging techniques to estimate the motion of different cochlear structures both apical and basal to the stimulation site.

Methods

A vibrating probe was used to stimulate the basilar membrane (BM) of gerbil in fresh excised cochlear preparations. The basilar membrane (BM) was accessed and imaged through windows cut in the scala vestibuli and scala tympani. The vibrating probe consisted of a blunted micropipette attached to a piezoelectric actuator. The probe tip was placed under the outer pillar cell foot. The in plane displacement of a number of different structures was captured over a wide range of frequencies (10 Hz – 42 kHz) with an inverted microscope using stroboscopic imaging. The displacement magnitude and phase was estimated using a cross correlation edge-tracking algorithm and then referenced to the transverse motion of the probe. We report here displacement measurements for the second cochlear turn.

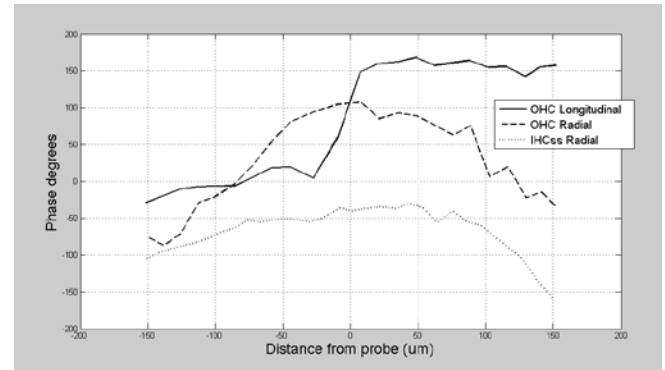
Results

At frequencies much lower than the stimulus site characteristic frequency (CF), the OHCs motion was similar to that of the IHCs. The displacement was almost entirely in the radial dimension and was consistent with internal mechanical longitudinal coupling on both the basal and apical sides of the probe. The displacement in the OHCs was typically smaller in overall magnitude than the IHCs. The phase as a function of location was almost constant indicating little reactive behavior.

Conclusion

At higher frequencies in the CF region (1.5 to 4 kHz) both forward and reverse travelling waves of radial displacement were seen in the IHCs. The traveling wave motion is characterized by a phase delay that increases with distance from the probe. At these frequencies, there was no significant longitudinal motion of the IHCs or pillar cells (PC). Figure 1 shows a typical result for the displacement phase as a function of

distance from the probe for a stimulus frequency of 4 kHz. The OHCs exhibited radial dimension displacement patterns that were similar to the IHCs and PC. In contrast, the OHCs exhibited a significant longitudinal displacement not seen in the IHCs or PCs and which differed significantly from the radial OHC displacement pattern.



PS - 542

Volume Compliance Measurement of the Cochlear Partition Excised from the Gerbil Cochlea

Talat Jabeen; Daniel Marnell; Jong-Hoon Nam
University of Rochester

Background

Defining the mechanical attributes of cochlear structures is fundamental to understanding mechano-transduction in the cochlea. Wide range in the stiffness values of the cochlear partition (CP) reflects the difficulty of measurement. In most measurements, calibrated microprobes were used to estimate the stiffness of the CPs. However, the microprobe method has some complications. For example, the force-displacement relations are highly nonlinear, and the point force is different from natural stimulus (pressure). As von Békésy noted (1960) the volume compliance might better represent the mechanics of CP than the point stiffness. We developed a method to measure the volume compliance of the CP.

Methods

Cochlear partitions are harvested from young gerbil cochlea (8-11 days old) and attached to a micro-chamber system. The micro-chamber system has two ports for fluid circulation and two ports for pressure application and release (analogous to oval and round windows in the cochlea). It also has a 200 μm-wide and 600 μm-long arc-shaped slit on which the tissue is attached. Gold-coated beads (10 μm in diameter) are spread on top surface of the cochlear partition. As the pressure is delivered through different ways (speaker, flexible probe and hydrostatic pressure), the displacements of the beads are measured 3-dimensionally using a laser velocity meter and a dual-photodiode sensor.

Results

Mechanical stimulation was delivered using three different methods and the tissue displacements were measured in nanometer scale. Three-dimensional deforming patterns agreed to plate deformation theory when the tissue boundaries were stably attached to the micro-chamber. The volume

compliance at the apical turn (about 9.5 mm from the basal end) was 100-400 mm⁴/Pa. In most preparations, the tectorial membrane was detached from the outer hair cell hair bundles. As a result, the beads on the tectorial membrane surface have higher in-plane to transverse displacement ratio than the beads on the organ of Corti.

Conclusion

An alternative method to the microprobe technique has been developed to measure the volume compliance of excised cochlear partition. This new method can be extended to measure the mechano-transduction at a section of the organ of Corti under controlled mechanical, electrical and chemical conditions.

PS - 543

Electrically Evoked Organ of Corti Vibration in Mice With Alpha Tectorin C1509G Mutation

Wenxuan He; Tianying Ren

Oregon Health & Science University

Background

The shortened tectorial membrane deactivated forward transduction causing hearing loss in mice with the alpha tectorin C1509G mutation, but enhanced electrically evoked otoacoustic emission (Xia, et al. 2010). However, acoustically induced basilar membrane and reticular lamina vibrations decreased simultaneously in this animal model (He, et al. 2013). To determine how the outer hair cell-generated energy exists the cochlea, the electrically induced reticular lamina vibration was measured in mice with the shortened tectorial membrane in this experiment.

Methods

Using a custom-built low coherence heterodyne interferometer, reticular lamina and basilar membrane responses to acoustical and electrical stimulation were measured through the intact round window membrane in wild-type and alpha tectorin C1509G mutation mice. Sinusoidal currents were delivered into the basal turn of the cochlea at the same longitudinal location as for the vibration measurement. The reticular lamina location in the transverse direction was determined by the carrier signal obtained by the vertical scanning. When the object beam was focused on the reticular lamina or basilar membrane, vibration magnitude and phase were measured as a function of frequency at different stimulus levels.

Results

In comparison with responses in wild-type mice, the magnitude of acoustically evoked reticular lamina and basilar membrane vibrations decreased significantly and the low-level (<40 dB SPL) responses were not detectable. In addition, the response peak became broader and shifted toward low frequencies while the growth function became linear. In contrast to the acoustical responses, the electrically evoked basilar membrane vibration decreased significantly more than the reticular lamina vibration. The group delay of electrically evoked stapes vibrations was only a few microseconds.

Conclusion

Robust reticular lamina vibration and small stapes group delay show that electrically evoked otoacoustic emissions result from outer hair cell somatic motility, and that the outer hair cell-generated energy exits the cochlea almost instantaneously. The data also indicate that the cochlear partition vibrations play an insignificant role in the backward propagation of otoacoustic emissions.

PS - 544

Elastic Propagating Waves in the Cochlear Partition Modulated by the Outer Hair Cells

Jong-Hoon Nam¹; C. Daniel Geisler²

¹University of Rochester; ²University of Wisconsin-Madison

Background

According to current theory of the cochlear traveling waves, differential hydrodynamic pressures between the cochlear scalae deflect the elastic cochlear partition to create displacement waves propagating along the length of the partition from base toward apex. There has been the hypothesis that the outer hair cells (OHCs) interact with the cochlear traveling waves, forming the so-called cochlear amplifier. The force transmission from the OHCs to the cochlear fluid through organ of Corti (OC) may help test the hypothesis (Dong & Olson, 2013). Recent model studies incorporate more realistic interactions between the OHCs and their supporting structures in the OC (Yoon & Steele, 2011; Meaud & Grosh, 2011; Nam & Fettiplace, 2012). Through model simulations, we present evidence that the OHCs can modulate the cochlear traveling waves.

Methods

A highly detailed electro-mechanical model of the cochlear partition using the finite element method was developed. The model incorporates three-dimensional characteristics of the OC, such as the Y-shaped structure formed by the OHC, Deiters cell and Deiters cell phalangeal process (DCpp) and the longitudinal coupling across the basilar membrane, tectorial membrane and the OC. Mechanical properties were validated by comparing simulated point stiffnesses and longitudinal space constants with experimental measurements. The amplification by OHC motility was incorporated and verified by reproducing stimulus level-dependent phase relations between OC structures using realistic OHC electrical properties (Nam & Fettiplace, 2012).

Results

When the basilar membrane is stimulated with sinusoidal force uniformly distributed along the length, elastic propagating waves (EPWs) are observed. The EPWs are distinguished from the traveling waves of classical theory in that they are not the result of fluid-structure interaction. The characteristics of the EPW, such as the wavelength, speed and phase lag, are remarkably similar to those of observed in the living cochlea. Three conditions are required for the existence of our observed EPWs: 1) the stiffness gradient of the cochlear partition, 2) the elastic longitudinal coupling and 3) the Y-shaped structure in the OC formed by the OHC, the Deiters cell and the DCpp. The EPWs become more prominent (have

more wave cycles) when the active force of OHCs are significant compared to the applied force.

Conclusion

Our results suggest that the micro-mechanical push-pull action of OHCs, facilitated by the Y-shaped structure (formed by OHC, Deiters cell and DCpp), can control the tuning and amplification by modulating the cochlear traveling wave.

PS - 545

Spontaneous Otoacoustic Emissions Are Generated by Active Oscillators Clustered in Frequency Plateaus

Bastian Epp¹; Hero P. Wit²; Pim van Dijk²

¹*Technical University of Denmark*; ²*Department of Otorhinolaryngology/Head and Neck Surgery, University Medical Center Groningen, University of Groningen*

Background

Spontaneous otoacoustic emissions (SOAEs) are sounds emitted from the inner ear in the absence of external stimulation. While the exact mechanism underlying SOAEs is still matter of discussion, it is commonly assumed that the active process linked to hair-cell motility is an important factor contributing to SOAEs. A chain of coupled, active and nonlinear oscillators with tonotopic organization can be used to account for key aspects of cochlear processing, including SOAEs and related phenomena when random irregularities of the mechanical parameters (roughness) are introduced. It was hypothesized that this roughness causes sudden impedance mismatches leading standing waves evoked by multiple reflections at places of SOAE frequencies and the oval window. The energy of these reflections could be partially transmitted into the ear canal and manifest as SOAE. Recently it was shown [Wit&vanDijk,2012; J.Acoust.Soc.Am. 132,918--926] that a linear array of active oscillators with nearest neighbor coupling produces clusters of oscillators with a common frequency (frequency plateaus) and a preferred frequency separation. The frequency plateaus can also be entrained to the frequency of an external tone. Both of these aspects are properties found in SOAEs. It is investigated if frequency plateaus are also found in a TM which is able to generate realistic SOAEs and if these frequency plateaus can be used to explain the formation of SOAEs.

Methods

Self-sustained oscillations found in two different numerical models were investigated. The first model was a linear array (LAM) of active oscillators with nearest neighbour coupling. The second model was a nonlinear and active transmission line model (TM) previously used to account for SOAEs.

Results

The TM showed a clustering of oscillators at frequencies corresponding to simulated SOAEs. Both, the LAM and the TM show travelling-wave like behaviour along the oscillators coupled into one frequency plateau. While in the TM roughness is required in order to produce SOAEs, no roughness is required to trigger frequency plateaus in the LAM.

Conclusion

Frequency plateaus can be found in a TM that is able to simulate realistic SOAEs. Travelling-wave like behaviour can be found in a linear array of coupled, active oscillators. The formation of frequency plateaus as a consequence of coupling between neighbored active oscillators might be the mechanism underlying SOAEs. The travelling wave behaviour seems to be at odds with standing waves as predicted by the theory of multiple reflections.

PS - 546

Active Contribution to Ear-Canal Reflectance in a Model of Cochlear Mechanics

Daniel Rasetshwane¹; Yi-Wen Liu²; Stephen Neely²

¹*Boys Town National Research Hospital*; ²*National Tsing Hua University*; ²*Boys Town National Research Hospital*

Background

Cochlear reflectance (CR), which we define as the cochlear contribution to total ear-canal reflectance, can provide important information about cochlear status. Comparisons between measurements and models provide a basis for (1) interpretation of the measurements and (2) for making improvements in the models. This study compares measurements of cochlear reflectance to simulations by cochlear model.

Methods

CR data were collected in humans using procedures described by Rasetshwane and Neely (2012). In this procedure, measurements of ear-canal reflectance (ECR) are made in the ear canal, and then CR is extracted from ECR. Simulation of ECR was performed using a combination of a middle-ear model and a one-dimensional cochlear model. Simulated CR then was the ECR difference between active and passive conditions of the model. The same time-frequency analysis was applied to both measured and simulated CR.

Results

The model simulation results in both the time-domain and frequency-domain were in substantial agreement with measured data for both ECR and CR. In a log-delay versus log-time analysis both measured and modeled CR were mostly confined to a rectangular region spanning 4 to 40 cycles and 0.5 to 30 ms. Some aspects of the stimulus-level dependence of measured CR could be simulated by varying cochlear-amplifier gain in the model, but complete agreement will require other changes to the model. Minor disparities between measurements and model will provide a basis for improvements in the model.

Conclusion

The observed agreement between measured and simulated CR validates the representation of coherent reflection in an existing cochlear model. In other words, CR observed in the ear-canal is consistent with linear coherent reflection due to random impedance perturbations along the cochlear partition.

PS - 547

Prestin Induced Currents in HEK Cells

Jun-Ping Bai¹; Shumin Bian¹; Joseph Santos-Sacchi²; Dhasakumar Navaratnam¹

¹*Yale Dept. of Neurology*; ²*Yale Dept. of Surgery*

Background

We have previously reported that prestin expressing cells exhibit a current under voltage clamp. We further examine this phenomenon in light of work from Faklers group that demonstrated a significant current in prestin expressing cells in the presence of extracellular thiocyanate. The implications of the presence of this current is significant as a single OHC has been estimated to have up to a million molecules of prestin on its surface.

Methods

We used a tetracycline inducible prestin expressing HEK cell line for these experiments. The characteristics of these cells have been previously published. Currents were measured using a two-sine voltage ramp under voltage clamp, which enabled simultaneous measurements of current and NLC.

Results

We confirm our prior observation that there is a linear relationship between the size of the prestin current and NLC in inducible prestin expressing HEK cells. We also demonstrate an increase in the size of the current co-incident with NLC when inducible HEK cells were released from temperature dependent Golgi block with rapid increase in surface expression of the protein. With substitution of extracellular chloride with thiocyanate we find a significant increase in the amplitude of the current. Substitution with extracellular NMDG demonstrated a significant reduction in current compared to extracellular Na or K. In contrast, substitution of Cl⁻ with extracellular malate, oxalate and methanesulfonate showed no demonstrable change in current. We also noted that deforming the extracellular surface of the cell with a fluid jet altered the size of the current to a significant degree. Lastly, we recorded resting membrane potentials under current clamp and, separately, using a voltage sensitive dye, and note that prestin expressing cells demonstrate a significant depolarizing tendency.

Conclusion

Our data confirm that prestin expression leads to a current that is carried by both anions and cations. The cation selectivity is poor with Na/K and Tris showing little difference and yet were separable from NMDG. A marked increase in current was noted in the presence of extracellular thiocyanate, as has been previously described. The reduction in resting membrane voltage in prestin expressing cells is discussed in the context of these currents.

PS - 548

Prestin is Trafficked to the Basolateral Surface of the Cell Using the AP1B Pathway

Yifan Zhang¹; Jun-Ping Bai²; Ying Wu²; Iman Naghani²; Joseph Santos-Sacchi³; Dhasakumar Navaratnam²

¹*Choate Rosemary Hall School*; ²*Yale Dept. of Neurology*;

³*Yale Dept. of Surgery*

Background

Prestin is expressed along the lateral wall of OHCs, where its localization is critical for OHC function and cochlear amplification. OHCs are modified polarized epithelial cells. In previous experiments we have demonstrated that prestin is targeted to the basolateral surface of the cell using specific tyrosine motifs. The clathrin-adaptor protein (AP) complexes constitute a family of heterotetrameric protein complexes that are important in the sorting of proteins from the *trans*-Golgi network (TGN) to endosomes and the plasma membrane. Of the seven distinct AP complexes, AP1B is a specific isoform expressed in polarized epithelial cells that is important for the basolateral sorting of a number of basolateral proteins including transferrin receptor and the low-density lipoprotein receptor.

Methods

We used MDCK cells expressing prestin YFP and LLC-PK cells which lack the μ 1B subunit to determine prestin trafficking to the basolateral surface of the cell. YFP fluorescence was quantified along the basolateral surface of the cell and expressed as a percentage of the total YFP fluorescence in a cell.

Results

We determine that basolateral expression of prestin is significantly reduced in LLC-PK cells, which lack the μ 1B subunit. Expression of the subunit restores basolateral expression of prestin. We show that MDCK cells expressing prestin show marked reduction of prestin at the basolateral surface of the cell after siRNA mediated knockdown of the μ 1B subunit. Finally, using temperature mediated Golgi block we demonstrate that prestin exits the Golgi and enters early endosomes en route to the basolateral plasma membrane.

Conclusion

We conclude that prestin is targeted to the basolateral surface of MDCK cells using the AP1B pathway. We also confirm that prestin exits the Golgi and uses early recycling endosomes to reach the surface of the cell.

PS - 549

Development of a YFP Chloride Sensor to Measure Chloride Flux in Prestin-Expressing Cells

Sheng Zhong; Dhasakumar Navaratnam; Joseph Santos-Sacchi

Yale University

Background

Chloride is the major anion in cells, and related to many diseases with disordered Cl⁻ regulation. In prestin-expressing cells, intracellular Cl⁻ ([Cl⁻]_i) flux plays a preeminent role

in promoting prestin activity since the resulting V_h shift in prestin's state-probability function along the V_m axis is expected to effect a motile response. Nevertheless, the mechanism underlying Cl^- flux in prestin-expressing cells is not clear. For the non-invasive investigation on Cl^- flux across the cell membrane, YFP-H148Q and its derivatives have been introduced as genetically encoded chloride indicators. Unfortunately, neither the Cl^- sensitivity nor the pH-sensitivity is satisfactory enough for accurate Cl^- measurements under physiological conditions. Additionally, the relatively poor photostability of YFP derivatives hinders their application for dynamic and quantitative Cl^- measurements. In this study, we developed a series of YFP derivatives to remove the pH sensitivity, increase photostability and chloride sensitivity thereby increasing the usefulness of the sensor.

Methods

To better define Cl^- flux, new versions of YFP-based Cl^- indicators were developed through targeted mutation to increase photostability, remove pH interference by shifting pK_a , and enhance chloride sensitivity. Sensitivities were assessed with an Andor camera and Nikon fluorescence microscope.

Results

With perforated patch clamp and local perfusion, changing extracellular Cl^- concentration from 1 mM to 140 mM using prestin's NLC as a measure of intracellular Cl^- indicates a several mM increase in intracellular Cl^- concentration. Using CFP-YFP ratiometric imaging of fluorescence, there are significant difference of $[\text{Cl}^-]$ flux between induced- and non-induced prestin-expressing HEK cell-lines. These results will be confirmed with our best designed Cl^- sensor to date, termed mCIY, which has a Cl^- K_d near 10 mM, pK_a below 5.9 and a photostability near 200 seconds. A fusion construct of prestin and mCIY has been made, as well as with two other membrane proteins, BTLA and CD80, which serve as controls. Perforated patch will be performed in HEK-293 cells transfected with these constructs to investigate the chloride flux during prestin activation.

Conclusion

We have developed a sensitive chloride sensor that will enable measures of physiological fluxes, and allow us to gage prestin's ability to move chloride across the plasma membrane.

PS - 550

Functional Prestin Expression Varies With Tectorial Membrane Malformations

Yohan Song; Rosalie Wang; Anthony Ricci; John Oghalai
Stanford University School of Medicine

Background

Humans with the C1509G mutation in alpha tectorin experience partial hearing loss at birth that progressively worsens. The same mutation in the mouse displays a shortened TM that does not contact any of the outer hair cells (OHCs) in the *Tecta*^{C1509G/C1509G} and only contacts the first row of OHCs in the *Tecta*^{C1509G/+}. Previously, our laboratory showed that both mutant strains have increased expression of prestin, a unique OHC protein necessary for electromotility. We aimed to con-

firm whether this increased prestin was functional by measuring OHC nonlinear capacitance (NLC).

Methods

The apical organ of Corti epithelium was dissected from P10, P15, P20 and P30 mice and OHCs were whole-cell voltage clamped in the epithelium. Cell capacitance was measured using a continuous two-sine wave stimulus protocol superimposed onto a voltage ramp from -150 to +120 mV. Prestin mRNA levels were also quantified using qPCR at the different developmental ages.

Results

At P30, the average NLC of OHCs from *Tecta*^{+/+} mice was 6.1 ± 0.2 pF, and there was no difference between the three rows of OHCs (ANOVA, $p = 0.6$). However, OHCs from *Tecta*^{C1509G/C1509G} mice had a significantly higher NLC (8.2 ± 0.3 pF; t -test, $p < 0.001$) with no NLC difference between the rows (ANOVA, $p = 0.8$). Interestingly, OHCs from the first (most medial) row of *Tecta*^{C1509G/+} had a NLC of 6.0 ± 0.3 pF, which was similar to that of *Tecta*^{+/+} OHCs (t -test, $p = 0.8$) but lower than that of *Tecta*^{C1509G/C1509G} OHCs (t -test, $p < 0.001$). In contrast, OHCs from the second and third rows of *Tecta*^{C1509G/+} mice had NLCs that were neither significantly different from each other (row 2: 8.0 ± 0.2 pF; row 3: 7.7 ± 0.1 pF; t -test, $p = 0.3$) nor different from that of *Tecta*^{C1509G/C1509G} OHCs (t -test, $p = 0.3$), but which was significantly higher than that of first-row *Tecta*^{C1509G/+} OHCs (t -test, $p < 0.001$) and that of *Tecta*^{+/+} OHCs (t -test, $p < 0.001$). This pattern whereby OHCs not attached to the tectorial membrane had higher NLC was not present at P10 but was established by P15. Consistent with the patch clamp data, prestin mRNA levels were significantly higher at P15 and P30 in *Tecta*^{C1509G/C1509G} OHCs compared to *Tecta*^{+/+} OHCs.

Conclusion

These findings confirm that *Tecta*^{C1509G} mutants have increased functional prestin expression within OHCs that are not attached to the tectorial membrane. This pattern is established after the onset of hearing.

PS - 551

Prestin Lateral Mobility and Self-Association in Outer Hair Cells.

Jing Guo¹; Guillaume Duret¹; Frederick Pereira²; Robert Raphael¹

¹Rice University; ²Baylor College of Medicine

Background

The diffusion of prestin in the membrane has been previously studied through fluorescent recovery after photobleaching (FRAP) experiments, in HEK293 cells. We were able to determine that up to 50% of the prestin population was immotile. This suggests that intermolecular interactions between prestin, the membrane and the cytoskeleton were essential for prestin organization and function. We have created transgenic mouse lines co-expressing prestin-TFP and prestin-YFP. OHCs isolated from these mice have non-linear capacitance (NLC) and electromotility comparable to wild-type mice.

Methods

We used FRAP to measure the diffusion of prestin-YFP by irreversibly photo bleaching a 2.9 μm -diameter area of the membrane. Fluorescent resonance energy transfer (FRET) was used to measure changes in prestin-prestin interactions, by monitoring the energy transferred from the excited donor fluorophore YFP to the acceptor TFP, through dipole-dipole interactions. Lastly, we used FLIM (fluorescence lifetime imaging microscopy)-FRET to detect interactions at the nanometer scale.

Results

The presence of a labeled prestin in the membrane of functional OHCs allows us to explore the lateral motility of prestin in its native environment through FRAP, as well as the prestin-prestin interactions through FRET. FLIM-FRET experiments revealed a FRET efficiency of 25-35%. FRAP analysis indicated that, unlike what has been observed in HEK, the entire prestin population is immotile in OHCs. This motility was partially recovered by inhibition of the actin filament polymerization.

Conclusion

Prestin is highly anchored and prevented to diffuse freely in the native outer hair cells. This suggests a strong interaction of prestin with other membrane proteins or the cytoskeleton, as previously indicated by studies in HEKs. The high FRET signal measured on functional OHCs is promising and will allow studying prestin-prestin interactions in different conditions, including alterations in membrane composition and potential.

PS - 552

Acute Ischemia Activates Chloride Channels in Capillary Cells of Guinea Pig Cochlear Lateral Wall

Yu-Qin Yang; Alfred Nuttall; Zhi-Gen Jiang
Oregon Health & Science University

Background

Cochlear function is highly vulnerable to ischemia/hypoxia due to high energy-demand of the auditory transduction; particularly, the positive endocochlear potential, critical for the transduction, is extremely sensitive to the altered microcirculation in spiral ligament (SL) and stria vascularis (SV) of the cochlear lateral wall. The ischemic pathology of the local capillary cells remains poorly understood.

Methods

Using acutely isolated capillary segments, dispersed endothelial cells (EC) and pericytes (PC) from the SL and SV and whole-cell recording techniques, we investigated the membrane responses to acute ischemic treatment (AIT, hypercapnic pH 6.5, $\text{pO}_2=0$ mmHg) and the pharmacology of the responsive ion currents.

Results

We found: (1) In addition to morphological features, the capillary EC and PC could be distinguished by their distinct whole-cell currents in physiological solutions: PCs showed a Ba^{2+} -sensitive inward rectifier current whereas ECs have

a prominent outward rectifier current. (2) AIT (5 – 25 min) caused a partially reversible and repeatable outward current at holding potential -20 mV in a major portion of isolated ECs and PCs, resulting in a transient 2 – 15 mV hyperpolarization and a swell in some cells. (3) The AIT-activated current I-V curves showed a robust outward rectification with a reversal potential between -30 to -62 mV initially but may shift positively during repeated and lasting AIT applications. (4) This AIT-induced current was suppressed by Cl^- -channel blockers 10-30 μM niflumic acid or flufenamic acid and but weakly by 300 μM DIDS or DPC in all cells tested. The elicited current had time-dependent increasing and decreasing activation during the strong depolarizing and hyperpolarizing 0.5 s steps, respectively. (5) In a few cases, the AIT-activated current showed a time-independent outward rectification which was inhibited by BK_{Ca} channel blocker 1 mM TEA. (6) AIT also reduced the slope conductance in deep negative domain of whole-cell I/V curves, which was obscured by pre-application of 100 μM La^{3+} . (7) Hypotonic (2/3 normotonic) solution activated an outward rectifier current with a biophysical feature different from the AIT-activated Cl^- current.

Conclusion

We conclude that acute ischemia activates the Ca^{2+} -activated rather than volume-gated chloride channels, less significantly the BK_{Ca} channels, and inactivates a non-selective cation channel thus to hyperpolarize the capillary cells and dilate the microvessels, resulting in counteracting the inadequate cochlear blood flow.

PS - 553

DNA Damage Repair in the Mammalian Organ of Corti

Sum-yan Ng; Robert Rainey; Neil Segil
University of Southern California and House Research Institute

Background

Mutations in some genes involved in the nucleotide excision repair (NER) pathway(s) lead to progressive hearing loss in humans. NER can be divided into at least 2 sub-pathways: transcription-coupled (TC-NER) and global genome (GG-NER), which are responsible for repairing actively-transcribed regions, and non-transcribed regions of the genome, respectively. Some terminally differentiated cells have been reported to exhibit lower GG-NER repair capacity than their proliferating precursors – a phenomenon that is hypothesized to conserve energy by only focusing repair efforts on actively transcribed regions of the genome.

Hearing loss is observed in Cockayne syndrome patients with mutations in the CSB and CSA genes that affect TC-NER, as well as in patients with some forms of xeroderma pigmentosum (XP). Interestingly, hearing loss is rare in XP-complementary group C (XPC) patients, whose mutation only appears to affect the GG-NER pathway, but leave TC-NER intact. The differential susceptibility to hearing loss in TC-NER vs GG-NER mutations suggests that hair cells depend on TC-NER for survival. In spite of the human mutation

data, the relationship between DNA damage repair and hearing loss remains largely uncharacterized.

Methods

For the *in vitro* experiment, organotypic cultures of the organ of Corti from mouse models with TC-NER or GG-NER mutations are treated with cisplatin, a common chemotherapy agent that causes hearing loss. The number of surviving hair cells and amount of cisplatin-DNA adducts are quantified 48h after treatment by immunohistochemistry. For the *in vivo* study, mice defective with TC-NER or GG-NER are given a single dose of cisplatin i.p. injection. Hearing thresholds are measured by auditory brainstem recording pre- and 2-week post-cisplatin injection. Cochleae from injected animals are harvested after the last ABR recording for further immunohistochemical analysis.

Results

In organ cultures, hair cells from TC-NER mutants are differentially hypersensitive to cisplatin treatment, and remove cisplatin-DNA adducts at a slower rate. In contrast, mutation in XPC affecting the GG-NER is significantly less sensitive to cisplatin. Our *in vivo* data shows that TC-NER deficient animals experience significant ABR threshold shifts after cisplatin treatment when compared to wildtype animals.

Conclusion

The overall results suggest that sensory hair cells in the mammalian inner ear depend differentially on TC-NER for survival following DNA damage caused by cisplatin.

PS - 554

Vulnerability of Hearing Loss Over Age Subsequent to the Deletion of BDNF or CaV1.2 in the Cochlea

Sze Chim Lee¹; Dario Campanelli²; Ksenya Varakina²; Dan Bing²; Annalisa Zuccotti³; Wibke Singer²; Lukas Rüttiger²; Thomas Schimmang⁴; Marlies Knipper²

¹Hearing Research Centre Tübingen, Molecular Physiology of Hearing, University of Tübingen; ²Department of Otolaryngology, Hearing Research Centre Tübingen, Molecular Physiology of Hearing, University of Tübingen; ³Department of Clinical Neurobiology of University Hospital and DKFZ Heidelberg; ⁴Instituto de Biología y Genética Molecular, Universidad de Valladolid y Consejo Superior de Investigaciones Científica

Background

We recently showed that tissue-specific deletion of brain-derived neurotrophic factor (BDNF) in the cochlea prevents loss of thresholds and auditory brainstem response (ABR), and loss of inner hair cell (IHC) synaptic ribbons after exposure to traumatizing sound (Zuccotti et al., 2012; *Journal of Neuroscience*, 32, 25, 8545-53). These effects could be partly mimicked by the deletion of L-type voltage-gated calcium channel Ca_v1.2 in the cochlea (Zuccotti et al., 2013; *Frontiers in molecular neuroscience*, 6). The present study aimed to assess if deletion of BDNF or Ca_v1.2 in the cochlea alters the vulnerability of hearing over age.

Methods

We compared the hearing function by auditory brainstem response (ABR) and distortion product otoacoustic emission (DPOAE) measurements on young and aged (1) conditional BDNF^{Pax2} KO mice (Zuccotti et al., 2012) with the deletion of BDNF in the whole cochlea, the dorsal cochlear nucleus, and inferior colliculus, and (2) conditional Ca_v1.2^{Pax2} KO mice (Zuccotti et al., 2013) with deletion Ca_v1.2 in the same tissues as in the BDNF^{Pax2} KO mice. We furthermore analyzed the influence of acoustic noise exposure on hearing loss.

Results

Hearing function of both young and aged BDNF^{Pax2}KO and Ca_v1.2^{Pax2} KO mice were compared and related to outer hair cell (OHC) function and IHC synaptic structures. Suprathreshold ABR was analyzed in relation to young and aged mice. An interesting differential role of BDNF and Ca_v1.2 in the cochlea related to hair cell synaptic formation for sound processing became evident.

Conclusion

We discuss the results in the context of a differential role of BDNF and Ca_v1.2 for hair cell and neuronal vulnerability during aging.

PS - 555

Protective Effect of Metformin on Gentamicin-Induced Vestibulotoxicity in Rat Primary Cell Culture

Ji Young Lee¹; Se Hee Lee¹; Jiwon Chang¹; Jae June Song²; Hak Hyun Jung¹; **Gi Jung Im¹**

¹Korea University College of Medicine; ²Dongguk University Ilsan Hospital

Background

One of the antidiabetic drugs, metformin, have shown that it prevented oxidative stress-induced death in several cell types through a mechanism involving the opening of the permeability transition pore and cytochrome c release. Thus, it is possible that the antioxidative effect of metformin can also serve as protection against gentamicin-induced cytotoxicity related to ROS. Therefore, the aim of this study was to examine the potential protective effect of metformin on gentamicin-induced vestibulotoxicity in primary cell culture derived from rat utricle.

Methods

For vestibular primary cell culture, rat utricles were dissected and incubated. Gentamicin-induced cytotoxicity was measured in both the auditory and vestibular cells. To examine the effects of metformin on gentamicin-induced cytotoxicity in the primary cell culture, the cells were pretreated with metformin at a concentration of 1 mM for 24 h, and then exposed to 2.5 mM gentamicin for 48 h. The intracellular ROS level was measured using a fluorescent dye, and also measured using a FACScan flow cytometer. Intracellular calcium levels in the vestibular cells were measured with Fura-2 AM and calcium imaging.

Results

Vestibular cells were more sensitive to gentamicin-induced cytotoxicity than auditory hair cells. Metformin protects against gentamicin-induced cytotoxicity in vestibular cells. Metformin significantly reduced a gentamicin-induced increase in reactive oxygen species, and also reduced an increase in intracellular calcium concentrations in gentamicin-induced cytotoxicity.

Conclusion

Metformin significantly reduced a gentamicin-induced increase in ROS, stabilized the intracellular calcium concentration, and inhibited gentamicin-induced apoptosis. Thus, Metformin showed protective effect on gentamicin-induced cytotoxicity in vestibular primary cell culture.

PS - 556

Dexamethasone-Eluting Electrode Arrays Protect Against Increases in Impedance in a Guinea Pig Model of Electrode Insertion Trauma-Induced Hearing Loss

Thomas Van De Water¹; Esperanza Bas¹; Jorge Bohorquez²; Chhavi Gupta¹; Carolyn Garnham³; Teresa Melchionna³; Adrien Eshraghi¹

¹University of Miami Miller School of Medicine; ²Biomedical Engineering, University of Miami; ³MED-EL

Background

Several clinical studies support intracochlear application of a steroid during the process of cochlear implantation to limit increases in electrode impedances that can be associated with the insertion of an electrode array into a patient's scala tympani (De Ceulaer, et al., 2003; Paasche et al., 2009). Steroid application in animal models of cochlear implantation have been more equivocal with some benefit on preventing increases in impedance but with no long term benefit (Huang et al., 2007). The present study examines the ability of 3 different concentrations of dexamethasone (DXMb), i.e. 10%, 1% and 0.1%, in silicone electrode arrays to protect the cochlea against electrode insertion trauma-induced increases in impedance in a guinea pig model of cochlear implantation.

Methods

Adult (350 gm) pigmented guinea pigs were the experimental animal with all procedures approved by the University of Miami IACUC (#11-308). A post-auricular approach exposed the bulla and a cochleostomy was made in the basal turn of the cochlea near the round window. Either a control silicone electrode or a silicone with 10, 1.0, or 0.1 % DXMb was inserted 5mm into the scala tympani. The impedance was measured by delivering trains of 50 μ sec biphasic square wave current pulses (25 μ sec/pulse) and current intensity of 100 μ A at a rate of 100 pulses/sec. The intracochlear electrode is the active electrode while the epidural screw electrode is the current return. Impedance thresholds were recorded pre-surgery and post-insertion days 1, 3, 7, 14, 30, 60 and 90 days. Statistical analysis performed with 2-way ANOVA with Bonferroni post-hoc testing, a p value of <0.05 was considered significant.

Results

Impedance of control electrodes started to increase after 2 weeks and continued to increase over time post-insertion reaching a maximum at 90 days, i.e. >3-fold increase. The impedance for electrodes containing 10% DXMb decreased from starting values over time reaching a minimum at 90 days post-insertion, i.e. a 2-fold decrease (p <0.001 when compared to the control electrode impedance). The impedance for the electrodes containing 1.0% and 0.1% DXMb rose slightly over the 90 days post-insertion period but were significantly lower than control silicone electrode values that did not contain any DXMb (0.0%), i.e. p <0.01 and p <0.05, respectively.

Conclusion

All three concentrations of DXMb in the electrodes protected against insertion trauma-induced increases in impedance, with the highest concentration (10%) being the most effective.

PS - 557

Cochlear Explants Treated With Kainic Acid Provide Molecular Insights Into Excitotoxicity and Neuronal Regeneration in the Inner Ear

Chen-Chi Wu^{1,2}; Aurore Brégeaud^{1,2}; Giovanni Coppola⁴; Albert S. B. Edge^{1,2,3}; Konstantina M. Stankovic^{1,2,3}

¹Department of Otolaryngology, Massachusetts Eye and Ear Infirmary, Boston, Massachusetts; ²Department of Otolaryngology and Laryngology, Harvard Medical School, Boston, Massachusetts; ³Program in Speech and Hearing Bioscience and Technology, Harvard Medical School and Massachusetts Institute of Technology, Cambridge, Massachusetts; ⁴Program in Neurogenetics, Department of Neurology, University of California Los Angeles, Los Angeles, California

Background

Glutamate-mediated excitotoxicity is implicated in many hearing disorders. To explore the molecular mechanisms of this excitotoxicity and the subsequent neuronal regeneration in the inner ear, we established an *in vitro* model by applying kainic acid (KA) to neonatal cochlear explants, and studied differentially expressed genes with microarrays and network analyses.

Methods

Neonatal cochlear explants were cultured for 5 h, 24 h, or 72 h after KA treatment. The explants were then microdissected into a spiral ganglion neuron (SGN) fraction and a micro-isolate fraction, containing the organ of Corti with hair cells, for RNA extraction. Genome-wide transcriptional analysis was performed using microarrays (Illumina). Differentially expressed genes were analyzed using Ingenuity Pathway Analysis to identify key molecular networks and their hubs. Select genes were validated using the on-line SHIELD database and immunofluorescent staining of cochlear sections.

Results

Microarray analyses revealed a total of 2.4% transcripts (583 out of 24,000) to be differentially regulated after KA treatment based on a threshold of p <0.005. Genes with significant

changes in SGNs were completely different from those with significant changes in the micro-isolates, indicating the tissue specific effects of KA in the inner ear. KA treatment resulted in a two-phase response in SGNs: an acute immunological response within hours of KA treatment, followed by neuronal regeneration at ~24 h after KA treatment. We identified four genes with significant changes at both 5 h and 24 h after KA treatment as compared to the untreated controls: *Elavl4*, *Ppp1r1c*, *Psd2*, and *Syn1*. Fluorescent immunohistochemistry confirmed the expression of these genes in the inner ear, with specific localization of *Elavl4*, *Psd2* and *Syn1* in SGNs.

Conclusion

Our findings are in line with the tissue-specific and reversible morphological and electrophysiological changes in the inner ear after KA treatment described previously, and indicate that neuroinflammation may contribute to excitotoxicity and neurogenesis in SGNs. Immunohistochemical validation of *Elavl4*, *Ppp1r1c*, *Psd2*, and *Syn1*, suggests that these four genes might play an important role in neuronal regeneration after KA treatment.

PS - 558

In Vitro Uptake of Rhodamine-Conjugated Platinum Into Mouse Utricle Hair Cells

Henry Ou¹; Patricia Wu²; Andrew Thomas²

¹University of Washington, VM Bloedel Hearing Research Center, Seattle Children's Hospital; ²University of Washington, VM Bloedel Hearing Research Center

Background

Rho-Pt is a rhodamine-conjugated platinum reagent that we have used previously to study cisplatin uptake. In the zebrafish lateral line, uptake of Rho-Pt into hair cells is dependent on functional mechanotransduction and is blocked by chemical or genetic inhibition of mechanotransduction. Similarly, inhibition of functional mechanotransduction protects against cisplatin-induced hair cell death in the zebrafish lateral line. Uptake of Rho-Pt into mammalian hair cells has not previously been described.

Methods

We have examined uptake of Rho-Pt into both free floating and "in-bone" (cultured in situ within the temporal bone) CBA/J mouse utricles. Using spinning disk confocal microscopy, Rho-Pt uptake into utricular hair cells was quantified at 15 minute intervals for 1 hour.

Results

Rho-Pt was taken up rapidly into hair cells of the mouse utricle. Uptake into free floating utricles was found to be more diffuse and nonspecific compared with uptake into mouse utricles cultured using the in-bone preparation.

Conclusion

Rho-Pt enters mouse utricle hair cells *in vitro* and can be used to study cisplatin uptake.

PS - 559

The Effects of Nerve Deafferentation on Round Window Electrocochleography in a Gerbil Model of High Frequency Sensorineural Hearing Loss

Eric Formeister; Christopher McLaughlin; Malika Rakhmankulova; William Merwin; Joseph McClellan; Mathieu Forgues; Craig Buchman; Oliver Adunka; Douglas Fitzpatrick

University of North Carolina School of Medicine

Background

The signal obtained through round-window electrocochleography (ECoG) represents a composite of signals from hair cells, including the cochlear microphonic (CM) and the summing potential (SP), and neurally-derived signals, including the compound action potential (CAP) and the auditory nerve neurophonic (ANN). Recently, the ECoG has been used to monitor cochlear damage during cochlear implantation (CI) and to assess surviving hair cell and neuronal populations to predict auditory outcomes post-CI (e.g., Fitzpatrick et al. Otol Neurotol 2013 (in press); Radeloff et al. Otol Neurotol 2012;33:348-54.). In this study, we sought to characterize the ECoG signals obtained from a gerbil model of high frequency sensorineural hearing loss in order to simulate the common deficit in patients with presbycusis or occupational noise damage leading to CI. By evaluating the responses to acoustic stimulation before and after application of the neurotoxin kainic acid, we aimed to further identify the contributions of responses from hair cells versus nerve fibers in the ECoG signal from noise-damaged cochleae.

Methods

Male gerbils were exposed to high pass noise with a 4 kHz cutoff at 121 to 122 dB SPL for four hours to model a reproducible pattern of high-pass noise-induced hearing loss (HP-NIHL). Four weeks post-exposure, ECoG signals to low frequency tones (<2000 Hz) and varying intensities were recorded at the round window under urethane anesthesia before and after application of kainic acid to the round window (60 mM in lactated Ringer's for 1 hour). Normal hearing gerbils served as controls.

Results

ECoG recordings from the round windows of gerbils with HP-NIHL were smaller and demonstrated saturation of the response growth function at relatively low intensities compared to normal hearing gerbils. The amount of harmonic distortion was greatly increased in the HP-NIHL animals. After KA, the harmonic distortion was greatly reduced, implicating a neural source (the ANN) for much of the distortion to the low frequency stimuli. Overall, the proportion of total ECoG distortion due to the presence of the ANN was greater in the HP-NIHL animals compared to those with normal hearing.

Conclusion

These results in an animal model indicate that if a high degree of distortion to low frequency tones is seen in round-window or intracochlear recordings from human CI patients a large contribution from the ANN is indicated. In contrast, a low level

of distortion would indicate that the signal is dominated by the CM.

PS - 560

Acceleration of Sensory and Neural Cochlear Aging After TTS

Katharine Fernandez¹; Kumud Lall¹; Penelope WC Jeffers²; M. Charles Liberman¹; Sharon G. Kujawa¹

¹Harvard Medical School; ²Massachusetts Eye and Ear Infirmary

Background

Once an ear has been compromised by noise, the question of whether this insult influences future changes in the ear and hearing has remained unresolved, but is of significant clinical and public health importance. In prior work, we studied the long-term effects of an exposure producing permanent threshold shift (~40 dB) and showed exacerbation of subsequent age-related changes (Kujawa and Liberman, 2006: J. Neurosci 26:2115). However, because the exposure acutely and permanently damaged the cochlear amplifier, our metrics of ongoing functional decline captured only progressive neural compromise. Here, we assess the interactions between noise exposure and aging, when the initial exposure produces only a temporary threshold shift (TTS).

Methods

Mice (CBA/CaJ) were exposed (8-16 kHz, 100 dB SPL, 2 h) at 16 wks and held, with age-only controls, for up to 2 yrs post exposure. We characterized cochlear function via DPOAEs and ABRs, and studied immunostained cochlear whole mounts and plastic-embedded sections to quantify hair cells, cochlear neurons and the synapses that connect them.

Results

Noise-exposed animals showed a TTS of 35 – 45 dB, followed by complete threshold recovery by 2 wks. Subsequent age-related threshold elevation in noise-exposed animals outpaced that in controls: this was a late divergence, beginning more than 1 yr post-exposure, and yielding DPOAE and ABR thresholds averaging ~10 and 20 dB greater, respectively, in the TTS group. This threshold difference was accompanied, with a similar time course, by greater OHC losses. As expected, IHC synaptic loss of ~40% was seen immediately post-exposure in the region of maximum TTS, i.e. near the 32 kHz place (Kujawa and Liberman, 2009: J. Neurosci 29: 14077). With increasing age, synaptic losses in all cochlear regions were significantly greater in TTS animals than in age-matched controls.

Conclusion

Here, we show that a single exposure episode producing robust, but reversible TTS accelerates both structural and functional losses as animals age. Beyond the audibility problems that result from increased OHC loss, and the threshold elevation this produces, the increased synaptic loss likely contributes to problems hearing in noise and to central changes associated with persistent tinnitus, both common in the aging population.

PS - 561

Therapeutic Effect of Dexamethasone for Noise Induced Hearing Loss

Shi-Nae Park¹; Sang A Back²; Myung Joo Shim²; Dong Kee Kim²; Min A Han²; So Young Park²; Hong Lim Kim³; Sang Won Yeo²

¹The Catholic University of Korea, College of Medicine;

²Department of Otolaryngology-Head & Neck Surgery, The Catholic University of Korea, College of Medicine, Seoul, Korea; ³Laboratory of Electron Microscopy, Integrative Research Support Center, The Catholic University of Korea, College of Medicine, Seoul, Korea

Background

Dexamethasone is a well-known anti-inflammatory agent, which is usually prescribed for acute hearing loss. To evaluate the effect of dexamethasone on rescuing noise-induced hearing loss, we compared hearing and cochlear morphologies among different routes of dexamethasone-administered mice groups and control groups after noise exposure.

Methods

Mice were exposed to white noise at 110-dB sound-pressure level for 60 minutes at the age of 1 month. Dexamethasone were administered intraperitoneally (IP-DEX) for five consecutive days and intratympanically (IT-DEX) twice per week after noise exposure. Auditory brainstem responses, distortion product otoacoustic emissions and cochlear pathology were evaluated and compared among dexamethasone groups and control groups (noise and normal controls). Western blotting was performed to observe several protein expressions in the cochlea.

Results

Compared with mice of noise control, IP- and IT-DEX groups showed less severe hearing loss from low to high frequencies at 7 days after noise exposure. Cochlear morphologic studies showed the less severe outer hair cell damages in DEX-groups compared to noise control group and IP-DEX group demonstrated better cochlear morphology than IT-DEX group. Expressions of several proteins in the cochlea among different groups were also different in western blotting and immunohistochemical staining.

Conclusion

Immediate administration of dexamethasone, both IP and IT routes, were therapeutically effective in hearing loss and cochlear damage after noise exposure in mice.

PS - 562

Cisplatin Ototoxicity is Mediated in Part by Protein Synthesis Inhibition

Brian Nicholas¹; Shimon Francis²; Jung-Bum Shin²

¹Upstate Medical University, State University of New York;

²University of Virginia

Background

The clinical application of cisplatin, a widely used chemotherapeutic drug, is limited due to its ototoxic side effects. We have previously shown that aminoglycoside (AG) ototoxicity is in part mediated by protein synthesis inhibition. Despite the

lack of structural analogy between AGs and cisplatin, the cellular stress pathways elicited by both drugs share certain similarities. We thus reasoned that protein synthesis inhibition might also play a role in cisplatin ototoxicity. In this project, we tested this hypothesis by studying the effect of cisplatin on inner ear cell protein synthesis, and dissected concurrent activation of various stress pathways in cochlear explants exposed to cisplatin and AGs.

Methods

We measured protein synthesis inhibition in cisplatin-exposed P4 mouse organ of Corti explant cultures using the previously described BONCAT (bioorthogonal noncanonical amino acid tagging) method. At the same time, we measured activation of various cellular signaling pathways, including the JNK and mTOR pathway, and assessed cell death.

Results

We discovered that cisplatin, similar to AGs, inhibits protein synthesis in sensory hair cells, and activates the mTOR and JNK pathway. In contrast to AGs, cisplatin also inhibits protein synthesis in all other cell types. Cisplatin-induced hair cell death in explant cultures is partially prevented by pre-emptive activation of the mTOR pathway. As reported previously by an independent study, we found that very high, supraclinical concentrations of cisplatin (>500 micromolar) paradoxically prevents hair cell death. Activation of the JNK and mTOR pathways remains despite these high cisplatin concentrations, which may suggest that the mechanism of cellular protection is not via an inhibition of cisplatin uptake. We hypothesize that the supposedly “rescued” hair cells are in fact fully committed to cell death, but cannot execute the active apoptosis program, possibly due to complete inhibition of cellular protein synthesis. Consistent with this notion, very high concentration of cisplatin also cross-inhibits aminoglycoside-induced hair cell loss.

Conclusion

The presented study suggests that protein synthesis inhibition might represent an unifying feature of various ototoxicity pathways. While we cannot exclude the possibility that AG- and cisplatin-induced protein synthesis inhibition is an epiphenomenon, we favor the hypothesis that protein synthesis inhibition is a causative factor for ototoxicity. We thus suggest that prevention or restoration of protein synthesis activity can be developed as an intervention strategy to prevent ototoxicity.

PS - 563

Epigallocatechin Gallate (EGCG) Protects Against Cisplatin-Induced Hearing Loss by Altering the Balance Between STAT1 and STAT3 Proteins

Vikrant Borse¹; Tejbeer Kaur²; Kelly Sheehan¹; Puspanjali Bhatta¹; Sandeep Sheth¹; Sumana Ghosh¹; Sarvesh Jajoo¹; Debashree Mukherjee¹; Leonard Rybak¹; Vickram Ramkumar¹

¹SIU School of Medicine; ²Washington University

Background

Cisplatin is widely used as an effective anticancer drug to treat various types of cancer. However, cisplatin produces permanent hearing loss and nephrotoxicity in a high percentage of cancer patients. Various drugs have been screened or are in clinical trials to treat cisplatin-induced hearing loss and nephrotoxicity. We have previously shown that cisplatin increases cochlear inflammation by increasing reactive oxygen species (ROS) and signal transducer and activator of transcription 1 (STAT1). This inflammatory response precedes apoptosis of outer hair cells (OHCs) and hearing loss. The goal of this study was to determine the efficacy of inhibition of STAT1 by epigallocatechin gallate (EGCG), a green tea extract, on cisplatin-induced hearing loss in male Wistar rats.

Methods

Organ of Corti-derived cells (UB/OC-1) were cultured and treated with cisplatin in the absence and presence of EGCG to determine effects on STAT1 activity and cell apoptosis. Male Wistar rats (200-250g) were treated with oral EGCG (100mg/kg), followed by cisplatin (11mg/kg, i.p.). Auditory brainstem responses (ABRs), scanning electron microscopy (SEM) and cochlear whole mount studies were performed to assess hearing loss and OHC morphology. Western blots were performed to assess the levels of STAT1, STAT3 and apoptotic proteins. University of Michigan squamous cell carcinoma (UMSCC) 10B cells were used to test for potential antitumor interference by EGCG.

Results

Exposure of UB/OC-1 cells to EGCG led to inhibition of cisplatin-induced Ser727 STAT1 phosphorylation and activation, decreased the levels of pro-apoptotic proteins (p53, caspase-3, Bax) and increased the levels of anti-apoptotic proteins (Bcl-2, Bcl-xl). EGCG also protected against cisplatin-induced apoptosis in UB/OC1 cells, as measured by Annexin V immunolabeling. Interestingly, EGCG significantly increased Tyr705 STAT3 phosphorylation in UB/OC-1 cultures. *In vivo* studies indicated that EGCG protected against cisplatin-induced loss of OHCs. Manual hair cells count demonstrated significant decrease in cisplatin-induced damage/loss of OHCs and reduced hearing threshold shifts. Studies for potential interference of EGCG against cisplatin-induced tumor killing were performed in human head and neck cancer cells (UMSCC 10B). EGCG potentiated cisplatin-induced cell killing in both the cisplatin-sensitive and -resistant cell lines (UMSCC 10B/15S), indicating a potential benefit of EGCG against these cancer cell lines.

Conclusion

Our study suggests that EGCG could serve as a model agent for treating cisplatin-induced hearing loss, since it inhibits STAT1-dependent apoptotic pathway while promoting the STAT3-mediated pro-survival pathway. Furthermore, EGCG potentiated cisplatin-induced killing of head and neck cancer cells.

PS - 564

Characterisation of SH-SY5Y-Cells as an Alternative for Freshly Isolated Auditory Neurons

Verena Scheper¹; Jana Schwieger¹; Karl-Heinz Esser²; Peter Paul Müller³; Thomas Lenarz¹

¹Hannover Medical School; ²University of Veterinary Medicine Hannover, Foundation; ³Helmholzzentrum für Infektionsforschung Braunschweig

Background

Auditory implants are electrically stimulating neuronal cells of the auditory pathway. One research focus to optimize these implants is drug delivery. The goal of implant based drug delivery is the preservation, regeneration and outgrowth of the stimulated neurons and their neurites. The necessary tissue for basic research on drug effects on cell cultures from the auditory system are harvested from experimental animals. Worldwide every year thousands of mice, rats and guinea pigs are euthanized for harvesting the relevant tissue. Up to now no adequate alternative is established to avoid the use of this tremendous number of animals. An additional advantage is a better test planning by getting independent of animal reproduction and cell preparation. Though one tries to reduce the number of experiments on primary cells from animals by performing experiments with cell lines such as PC-12 cells, the characteristics of these cell lines do not correlate with those of neuronal cells from the auditory pathway. Previous research shows that the cell line SH-SY5Y may potentially be an appropriate alternative to auditory primary cells. The aim of this work is to establish an alternative cell culture method for freshly isolated auditory neurons to reduce the need of animals for *in vitro* research.

Methods

We characterize the genetic potential and receptor expression and function of SH-SY5Y-cells and compare those to spiral ganglion cells (SGC) related parameters. Using Immunopanning SGC are purified and their gene expression profile is compared to those of SH-SY5Y cells. Receptor expression is evaluated using immunocytochemistry and the biological function of the receptors is determined by addition of growth factors (BDNF, GDNF, CNTF, NT-3, VEGF) to the culture system and analysis of cell survival and neurite length.

Results

Preliminary results on receptor expression and biological function of SH-SY5Y-cells suggest that this cell line may be an adequate alternative for primary auditory neurons such as spiral ganglion cells. The comparison of the gene expression profiles of SGC and SH-SY5Y-cells is under investigation and future research has to determine if the electrophysiology

responsiveness and the adhesion behaviour of both cell types is comparable.

Conclusion

SH-SY5Y-cells may be an alternative for SGC used in *in vitro* screening tests for inner ear research. Further research has to be performed to investigate if this cell line is suitable as an alternative for other auditory neuronal tissue such as colliculus inferioris as well.

PS - 565

In Vitro Assessment of Ototoxicity Associated With Antiretroviral Drugs

Pru Thein; Gilda Kalinec; Federico Kalinec

House Research Institute and David Geffen School of Medicine, UCLA

Background

Several studies have reported an increased incidence of auditory dysfunction among HIV/AIDS patients.

Methods

We performed dose-dependence, cell viability and caspases 3/7-activation studies with auditory HEI-OC1 cells to investigate the potential ototoxicity of fourteen HIV antiretroviral agents: Abacavir, AZT, Delavirdine, Didenosine, Efavirenz, Emtricitabine, Indinavir, Lamivudine, Nefinavir, Nevirapine, Tenofovir, Ritonavir, Stavudine and Zalcitabine. In addition, we investigated the effects from combinations of these agents as used in the common anti-HIV cocktails AtriplaTM, CombivirTM, EpzicomTM, TrizivirTM, and TruvadaTM.

Results

Most of the assayed anti-HIV drugs resulted in dose-dependent cytotoxicity. The cocktails, on the other hand, decreased auditory cells' viability with high significance, with the following severity gradient: Epzicom ~ Trizivir > Atripla ~ Combivir > Truvada. Interestingly, our results suggest that cell death induced by Truvada, Combivir and Atripla was associated, at least in part, to activation of caspase-dependent apoptotic pathways, but Trizivir- and Epzicom-induced cell death was mediated by different, caspase-independent mechanisms. L-Carnitine, a natural micronutrient known to protect HEI-OC1 cells against some ototoxic drugs as well as to decrease neuropathies associated with anti-HIV treatments, increased viability of cells treated with Lamivudine and Tenofovir as well as with the cocktail Atripla, but had only minor effects on cells treated with other drugs and drug combinations.

Conclusion

Altogether, these results suggest that some frequently used anti-HIV agents could have deleterious effects on patients hearing, and provide arguments in favor of additional studies aimed at elucidating the potential ototoxicity of current as well as future anti-HIV drugs.

Adult Human Nasal Mesenchymal-Like Stem Cells Restore Spiral Ganglion Neurons in Gentamicin-Lesioned Neonatal Cochlear Explants

Bradley Goldstein; Esperanza Bas; Thomas R Van De Water; Vicente Lumberras; Suhrod Rajguru; Goss Garret; Joshua M. Hare
University of Miami

Background

Cochlear implantation is an important option for patients with profound sensorineural hearing loss. However, an intact population of spiral ganglion neurons is required for cochlear implantation to be useful.

We hypothesize that adult human nasal mesenchymal-like stem cells (hnMSCs) can be used to repair a damaged population of spiral ganglion neurons, by either directly replacing these neurons or via activation of endogenous cell replacement and/or repair.

Methods

To test our hypothesis, hnMSCs were obtained, expanded *in vitro*, and used to treat gentamicin-lesioned postnatal rat organotypic cochlear explants. Explants were analyzed by immunostaining and confocal microscopy, as well as by voltage sensitive calcium dye imaging utilizing infrared laser stimulation. The hnMSCs used in this study were analyzed by flow cytometry and shown to be CD90 (+); nestin (+), STRO-1 (+) and CD105 (+); all markers common to hnMSCs. In addition, these cells did not express markers characteristic of olfactory epithelium, such as cytokeratins, or markers typical of a hematopoietic lineage (e.g. CD34 and CD45).

Results

Our results show that: 1) hnMSCs engraft in lesioned rat cochleae; 2) the engrafted hnMSCs are located mainly in the region of the spiral ganglion and that these cells promote an increase in spiral ganglion neurons; and 3) the treatment of explants with hnMSCs restores the explants' spiral ganglion cell populations by differentiating into neurons. The engrafted hnMSCs form clusters of TuJ-1 (+) neurons with large, round cell bodies, with synapsin expression overlapping their cell bodies and neurites resembling the spiral ganglia neurons of unlesioned control explants. These hnMSCs-derived neurons are excitable by infra red laser stimulation and may be functionally similar to spiral ganglion neurons. We observed that activation of the Wnt/beta-catenin pathway increased the density, branching and complexity of the spiral ganglion neurons dendritic processes.

Conclusion

Stem cell, i.e. hnMSCs, harvested from adult humans is efficacious in the repair of spiral ganglion neurons lost in experimentally-lesioned cochlear explants. Our demonstration of the ability of an easily obtained and autologous adult human stem cells to repair auditory neuron loss should enhance progress towards establishment of cell-based therapies for certain forms of deafness.

Influences of Acute Alcohol Intake on Hearing Recovery of CBA Mice from Noise-Exposure

Myung Hoon Yoo¹; Ji Won Lee²; Hyo Kyoung Kwon²; Jong Woo Chung¹; **Joong Ho Ahn¹**

¹Asan Medical Center; ²Asan Institute of Life Science

Background

Aldosterone is known to control endolymphatic homeostasis of cochlea via mineralo-corticoid receptor existing in stria vascularis and alcohol is known as an inhibitor of the synthesis of aldosterone with lowering concentration of aldosterone in other organs. Therefore, alcohol might play some role in formation of endocochlear potential even though it doesn't have direct toxicity to the inner ear.

Methods

We divided CBA mice with normal hearing into 4 groups; control, 1, 2, 4 g/kg alcohol group, 7 mice for each group. In alcohol group, ethanol was administrated intragastrically via feeding tube while same amount of normal saline was administered in control group. One-hour after alcohol ingestion, mice were exposed for 1 hour to 100-dB PE SPL white noise (300 - 10,000 Hz). Hearing thresholds were checked with tone-burst ABR and DPOAE before and after noise exposure, following 1th, 3rd, 5th, 7th, and 14th days.

Results

In control group, hearing thresholds were elevated immediately after noise exposure with gradual improvement within 2 weeks, while mice in 4 g/kg alcohol group showed elevated hearing thresholds which were significantly higher than control group without recovery. Mice in 1 g/kg and 2 g/kg groups showed no significant differences compared with control group.

Conclusion

Although alcohol itself doesn't affect hearing, high dose alcohol might inhibit hearing recovery after noise exposure via impairment of inner ear homeostasis.

Functional Characterization of STAT3 in the Inner Ear

Teresa Wilson; Irina Omelchenko; Sarah Foster; Alfred L Nuttall

Oregon Health & Science University

Background

Signal transducers and activators of transcription 3 (STAT3) is a stress responsive transcription factor that relays signals from ligand-bound cytokine and growth factor receptors in the plasma membrane to the nucleus. The primary mechanism of STAT3 activation is through phosphorylation leading to dimer formation, nuclear translocation and transcriptional activation. Many of its target genes, such as VEGF, MnSOD, and HIF-1a are involved in the regulation of pro-survival and cellular proliferation functions. Additionally, STAT3 possesses transcription-independent activities of including direct regulation mitochondrial respiration and complex I activity as well as inhibition of autophagy under normal physiological con-

ditions. In this study, we examined the role of STAT3 in the inner ear.

Methods

For general STAT3 activity inhibition, male CBA/CaJ (8 weeks old) mice (n=5/group) were injected with JSI-124 at 24 and 1 hr prior to exposure to a moderately damaging level of sound (110 dB SPL, 4-48 kHz, 3 hrs). At 1 day, 1 week and 2 weeks post-noise exposure, Auditory Brain Stem Response (ABR) and Distortion Product Otoacoustic Emission (DPOAE) levels were measured. To generate outer hair cell specific STAT3 knock-out mice (*STAT3OHC*^{-/-}), *STAT3^{fllox/flox}* mutant mice were crossed with prestin-CreER mice. STAT3 localization and transcriptional activity was analyzed by immunolabeling and quantitative RT-PCR.

Results

Noise exposure-induced phosphorylation and nuclear translocation of STAT3 occurred in many cell types in the inner ear including the marginal cells of the stria vascularis, type II fibrocytes, inner hair cells, and in the supporting cells in the organ of Corti. Treatment with JSI-124 attenuated noise-induced VEGF transcript upregulation in the cochlea and improved recovery of OHC function (based on DPOAE measurement) following noise exposure. In *STAT3OHC*^{-/-} mice, the OHCs appeared morphologically normal and alterations in markers of autophagy were observed. Additionally, ABR and DPOAE threshold levels were comparable to wild-type littermates.

Conclusion

Exposure to moderately damaging levels of loud sound induces phosphorylation and nuclear translocation STAT3 in many different cell types in the cochlea. Chemical inhibition of STAT3 phosphorylation proved protective of OHC function following noise exposure. Further, the comparable hearing thresholds of *STAT3OHC*^{-/-} and wild-type littermates indicate that STAT3 activity is not required for OHC function under normal physiological conditions

PS - 569

Selected Cytokines Activate Chloride Channels in Capillary Endothelial Cells from Guinea Pig Cochlear Lateral Wall

Zhi-Gen Jiang; Peter Steyger; Yuqin Yang
Oregon Health & Science University

Background

Endotoxemia elevates systemic and cochlear proinflammatory cytokine levels, enhances cochlear uptake of aminoglycosides, and subsequent ototoxicity in mice, a model of aminoglycoside ototoxicity in patients with bacterial sepsis. The underlying mechanisms are poorly understood. We hypothesized that cytokines alter the electrophysiology of endothelial cells to facilitate the aminoglycoside ototoxicity.

Methods

We tested whether an endotoxin (LPS) or selected interleukins (ILs) alter whole-cell membrane potential and currents in endothelial cells (ECs) and pericytes (PCs) of dissociated cochlear lateral wall capillaries.

Results

We found that (1) isolated ECs normally showed a resting potential ~-20 mV and high input resistance (1 – 4 GΩ) with mild outward rectification but no inward rectification in I/V curves. PCs typically displayed a Ba²⁺-sensitive inward rectification. (2) In ECs, but not PCs, 5 -10 min application of IL-6 (0.1 nM) or IL-10 (1 nM) slowly activated a robust long-lasting (>1 h) and partially reversible outward rectifier current with a reversal potential between -30 and -40 mV, causing a transient (~10 min) 3–18 mV hyperpolarization. Boltzmann function fit to the activated current I/V revealed a $G_{max} = 3-10$ nS, $V_{1/2} = -40$ to -60 mV and $k = 30-40$ mV/e-fold. In contrast, IL-1α (10-100 nM) and LPS (20-100 μg/ml) had no such effect. (3) This IL-activated current was suppressed by the Cl⁻ channel blocker niflumic acid (30 μM) and slightly by the classic Cl⁻-channel blockers DIDS (300 μM) and DPC (300 μM), but not sensitive to K⁺-channel blockers TEA, 4-AP or Ba²⁺ (all 1 mM) or cation channel blockers La³⁺ (100 μM) and Gd³⁺ (30 μM). (4) Hypotonic solution (200 mOsm/l) activated a current with a voltage- and time-dependency, dynamics and pharmacology profile similar to those of the IL-activated current. (5) The actions of hypotonicity and the ILs had inter-masking rather than additive or facilitating effect with each other when applied one after another with ~30 min interval. (6) Application of either the effective ILs or the hypotonic solution often caused visible swelling of the recorded and adjacent cells.

Conclusion

At least two interleukins activate a chloride current with biophysical and pharmacological profiles similar to those of volume-gated Cl⁻ channels, resulting in hyperpolarization and swelling of lateral wall capillary endothelial cells. These changes will increase the electrophoretic driving force for aminoglycosides entering the endothelial cells and promote the circulating drug passing into intrastrial space. These data suggest that proinflammatory cytokines contribute to enhanced aminoglycoside ototoxicity in endotoxemia.

PS - 570

Increased Survival of Spiral Ganglion Neurons in Auditory Neuropathy by Treatment With Small Molecule Trk Receptor Agonists

Mingjie Tong; Katharine A. Fernandez; Kumud Lall; Sharon G. Kujawa; Albert Edge
Massachusetts Eye and Ear Infirmary, Harvard Medical School

Background

Neurotrophins, such as BDNF, are necessary for the survival of spiral ganglion neurons (SGNs) both *in vitro* and *in vivo*. Small molecule tricyclic antidepressants, amitriptyline and imipramine, displayed Trk receptor agonist activity and exerted neurotrophic effects on CNS neurons. In the present study, we assessed protection of SGN as well as preservation of cochlear function after treatment with these small molecule Trk receptor agonists in both *in vitro* organotypic explants of the mouse organ of Corti and an *in vivo* adult noise-damage model (Kujawa et al).

Methods

In *in vitro* experiments, SGN explants of P4 or P5 CBA mice were treated with various concentrations of amitriptyline or imipramine with or without concurrent kainate treatment to induce degeneration of SGN by glutamate toxicity. Thirty minutes after culture, the explants were collected and Western blotting was performed with antibodies against phospho-TrkB or phospho-TrkC. Two to six days after culture, immunostaining by antibody against beta-tubulin III was used to assess SGN survival. In the *in vivo* experiments, animals (16 wk CBA/CaJ) were treated with amitriptyline (25 or 50 mg/kg i.p., 5-9 d) or saline, noise exposed (8-16 kHz, 100 dB SPL, 2 h) and then held for various post-exposure times to 1 yr. Response thresholds and amplitudes were quantified by DPOAE and ABR. Hair cell, cochlear ganglion cell and synaptic counts were made in immunostained cochlear whole mounts and plastic-embedded sections.

Results

Imipramine induced significant phosphorylation of TrkB receptors and protected neurons from cell death in neonatal organ of Corti in the *in vitro* organotypic culture. Protection from glutamate toxicity was also assessed. *In vivo*, acute and chronic noise-induced threshold shifts were not altered by treatments. However, 1 year post exposure, suprathreshold neural, but not hair cell response amplitudes showed dose-responsive preservation relative to saline-treated controls. Consistent with this result, synaptic and ganglion cell counts also were better preserved in drug-treated animals.

Conclusion

Small molecule tricyclic antidepressants act as TrkB agonists. Results from our glutamate and noise toxicity models indicate that the tricyclic antidepressants can protect cochlear ganglion cells and preserve suprathreshold amplitudes in the ABR.

PS - 571

Effect of Different Delivery Methods of Antioxidant Drugs on Acute Acoustic Trauma Chul-Hee Choi¹; Xiaoping Du²; Richard Kopke²

¹Catholic University of Daegu; ²Hough Ear Institute and Oklahoma Medical Research Foundation

Background

Pharmacological interventions or approaches have been developed for the prevention or treatment of noise induced hearing loss using antioxidant drugs to restore the balance between antioxidant defense and the formation of free radicals in the cochlea. Antioxidant drugs such as N-acetyl-L-cysteine (NAC), acetyl-L-carnitine (ALCAR), and phenyl-N-*tert*-butyl-nitron (PBN), disufenton sodium (NXY-059), and 4-hydroxy PBN (4-OHPBN) have been used to reduce the excessive formation of free radicals. Although the most-commonly used administration of drugs in human is oral dosing, our previous studies on the treatment of noise induced hearing loss used intraperitoneal (IP) injection. Therefore, the objective of this study was to investigate the effect of different delivery systems (oral administration and IP injection) of the combination of 4-OHPBN and NAC on treating acute noise induced

hearing loss. We tested if there are significant differences between IP injection and oral administration.

Methods

Chinchilla were used as subjects and exposed to a 105 dB octave band noise centered at 4 kHz for 6 and randomly assigned to a control group (saline only) and four experimental groups [4-OHPBN (10 mg/kg) plus NAC (20 mg/kg), 4-OHPBN (20 mg/kg) plus NAC (50 mg/kg), and 4-OHPBN (50 mg/kg) plus NAC (100 mg/kg)]. The drugs were either orally administered or intraperitoneally injected beginning 4 hour after noise exposure and then administered twice daily for the next two days. Permanent auditory brainstem response threshold shifts and the percentage of missing outer hair cell were determined.

Results

Oral administration of the combined antioxidant drugs (4-OHPBN plus NAC) produced a significant reduction in permanent ABR threshold shifts and percentage of missing OHCs. This suggests that the orally administered antioxidant drugs are effective in treating acute noise induced hearing loss. The ABR threshold shifts and the percentage of missing OHCs of the oral administration were greater than those of the intraperitoneally administered 4-OHPBN alone.

Conclusion

These differences may result from the intrinsic bioavailability limitations of the oral administration. In addition, the differences in pharmacokinetics, bioavailability, and metabolism between the different routes of drug administration can be other factors affecting the inconsistency.

PS - 572

Auditory Damage Criterion: Reassessing Acceptable Exposure Limits for Steady State and Impulse Noise

Christopher Smalt¹; Thomas F. Quatieri¹; Karl E. Friedl²

¹Massachusetts Institute of Technology Lincoln Laboratory, Lexington MA, USA; ²Knowledge Preservation Program Fellow, Oak Ridge Institute of Science and Education, Oak Ridge, TN, USA

Background

Noise-induced hearing loss (NIHL) among military service members is a large and growing concern that can affect performance, safety, and quality of life. Furthermore, hearing loss and tinnitus are the number one and two medical claims among veterans, according to the Department of Veteran's Affairs. Protective hearing devices provided to servicepeople are not commonly worn during operations, as they can limit situational awareness and may suffer from a lack of comfort, usability, and acceptability. Current and proposed military standards have set exposure limits based on the assumption that temporary threshold shifts less than 25 dB are occasionally acceptable. Further complicating the validation of these standards is a lack of standard noise databases in military environments and sufficient "ground truth" linking exposure to damage.

Methods

Auditory damage auditory models and standards (MIL-STD-1474D, A-weighted equivalent 8-hour level (L_{Aeq8hr}), and the Auditory Hazard Assessment Algorithm for the Humans) were used to analyze acoustic waveforms impulsive sound and acoustic operational simulations. This process included measurement of high intensity sound pressure waveforms, including impulsive sounds and wind noise to characterize the effect of incidence angle and body location. Damage models were then compared with recent research documenting primary afferent degeneration in animal models.

Results

Initial analysis of current damage models indicates that current standards may not be restrictive enough to prevent long-term afferent nerve fiber damage. Kujawa and Liberman (2009) have previously demonstrated in animal models that this damage can occur over weeks to month, not just what is measured immediately following exposure. This may partially explain the contrasting effort to lessen military noise-exposure criterion while hearing related medical problems in veterans continue to rise. Other weaknesses of current standards include accounting for both impulsive noise and continuous background noise and their interaction. Inter-impulse timing information has been shown to affect damage in animal models, and is not included in current damage criterion.

Conclusion

Our aim is to advance auditory damage models increasing their accuracy to better predict consequences of noise exposure for military personnel – including shifting the mindset of “better deaf than dead”. In order to validate damage criterion, clinical pure tone thresholds are not sufficient to capture true auditory damage. New data sets that more accurately characterize exposure coupled with enhanced physiological biomarkers can be used to test new and existing damage models while informing next generation hearing protection and enhancement.

PS - 573

Recovery from Noise-Induced Hearing Loss is Enhanced by the Immunomodulator Glatiramer Acetate

JoAnn McGee¹; Edward Cohn¹; Kristen Drescher²; Kelly Roark²; Katyarina Brunette¹; Alexander Anton¹; Edward Walsh¹

¹Boys Town National Research Hospital; ²Creighton University School of Medicine

Background

Although efforts to identify effective treatment protocols for noise-induced hearing loss (NIHL) have shown some promise in recent years, the identification of treatment strategies that either prevent significant permanent hearing loss or rescue pre-existing hearing loss has been challenging. In this study, a novel hearing loss (HL) treatment strategy involving a drug known to protect the central nervous system and the retina from injury by blocking the neurodegenerative consequences of inflammation is considered. The compound in

question is glatiramer acetate (GA), an immunomodulator otherwise known as Copaxone.

Methods

To achieve the goals of this study, GA was administered (100 mg/kg, IP) 1 month and 7 days prior to noise exposure (an octave band of white noise centered on 11.3 kHz and presented at 109 dB SPL for 30 min) and daily during the early post-exposure period to CBA mice. Following determination of pre-noise exposure thresholds, hearing sensitivity was tracked during the post-noise exposure period using auditory evoked brainstem responses (ABRs) and distortion product otoacoustic emissions (DPOAEs). One group of animals was euthanized approximately one week following noise exposure to assess cytokine expression. GA treatment was continued beyond week one in a second group of animals and recovery of function was tracked for as long as 2 months following noise exposure. The effect of GA on pro- and anti-inflammatory cytokine expression was assessed using qRT-PCR.

Results

Immediately following exposure to traumatizing noise, ABR thresholds were elevated 60-70 dB relative to pre-exposure, baseline values in both GA-treated and saline-treated mice. The magnitude of threshold recovery following noise exposure, computed as the average recovery across all stimulus frequencies tested, ranged from approximately 40 dB to approximately 10 dB in the cases of GA-treated mice and <30 dB to approximately 5 dB in saline-treated controls. The total extent of recovery approximately one week following exposure was nearly 25 dB in the GA cohort and approximately 17 dB in control animals. Similar DPOAE findings suggest GA influences both sensory and neuronal systems. Pro-inflammatory and anti-inflammatory cytokine expression profiles were consistent with a positive GA influence.

Conclusion

Findings reported here suggest that recovery from NIHL is enhanced by treatment with the immunomodulator, glatiramer acetate. Molecular studies suggest that the up-regulation of anti-inflammatory and down-regulation of pro-inflammatory cytokines may contribute to the efficacy of glatiramer acetate-induced protection from NIHL.

PS - 574

Protection of Vestibular Neuroepithelia from Gentamicin Toxicity

Larry Hoffman; Peihan Orestes; Kristel Choy; Ivan Lopez
Geffen School of Medicine at UCLA

Background

We have previously shown that defined lesions in the vestibular neuroepithelia result from intraperilymphatic administration of 1µg gentamicin, characterized by complete afferent calyx loss and modest hair cell loss in the central crista. These lesions were associated with paralysis in stimulus-evoked afferent discharge while spontaneous discharge was preserved. In the present study we used this vestibulotoxicity model to investigate whether metformin, an agent previously shown to be protective against gentamicin nephrotoxicity, could protect the vestibular epithelia from gentamicin-induced lesions.

Methods

A 2.5µl solution of gentamicin (1µg, approx. 130µM) and metformin (400µM) were administered directly into the perilymph over a one-hour period in isoflurane-anesthetized chinchillas, using previously described procedures (Sultemeier & Hoffman, submitted). After postadministration periods of approx. 2 months, the pentobarbital-anesthetized animals were prepared for single-afferent electrophysiology. Immediately prior to these surgical procedures distortion product otoacoustic emissions were recorded to verify cochlear functional integrity in labyrinths administered the gentamicin•metformin treatment. Following the electrophysiology recording sessions and euthanasia, fixative was infused bilaterally into the vestibule and vestibular epithelia were harvested. Anti-calretinin and anti-β3-tubulin immunohistochemistry was conducted on intact epithelia for quantification of calyces within the central cristae; phalloidin histochemistry enabled quantification of hair cell densities. Electrophysiologic and histologic findings from treated labyrinths were compared to epithelia from untreated specimens to determine whether and to what extent the treated epithelia were protected.

Results

In contrast to the effects associated with intraperilymphatic administration of 1µg gentamicin alone, we found that labyrinths treated with metformin and gentamicin remained responsive to natural stimuli and were absent of histopathologic alterations. Sine-evoked sensitivity and phase measures of individual afferents projecting from horizontal and superior cristae were similar to measures from untreated afferents. Stimulus-response coherence measures of perstimulus afferent discharge during 1.6Hz sine and complex (band-limited Gaussian) stimuli, which we previously found to be compromised in partially lesioned labyrinths resulting from gentamicin doses <1µg, were also similar to untreated afferents. Histologic analyses revealed that the densities of hair cells and calretinin-positive calyces in treated cristae were also similar to untreated epithelia.

Conclusion

These data demonstrate that metformin profoundly protected vestibular epithelia from gentamicin ototoxicity. Because metformin was previously shown in other systems to protect the mitochondrial permeability transition pore, our findings infer that the cellular compromises associated with gentamicin-induced focal lesions result from its effect on this functional entity of hair cell and afferent mitochondria.

PS - 575

Changes in Cochlear Transcriptional Activity Associated With Noise-Induced Primary Neuronal Degeneration

Andrew Lysaght¹; Christine Seidman²; Jonathan Seidman²; Konstantina Stankovic³

¹Harvard - MIT; ²Harvard Medical School; ³Massachusetts Eye and Ear Infirmary

Background

Acoustic exposures previously believed to cause only temporary reductions in hearing sensitivity have recently been

shown, in mouse models, to cause delayed death within the spiral ganglion nerve. This noise-induced death of cochlear neurons without previous loss of sensory or supporting tissues is termed noise-induced primary auditory neuropathy (NI-PAN), and has important clinical implications. While pure-tone audiograms appear normal, the reduction in effective information channels hinders a listener's ability to attend and comprehend complex acoustic stimuli.

Methods

To gain insight into the genetic mechanisms underlying the progressive degeneration of spiral ganglion neurons, we have performed high-throughput RNA sequencing to characterize the transcriptional activity within microdissected murine spiral ganglia and sensory epithelia at 24 hours, 2 weeks, 2 months and 16 months post exposure to neuropathic and non-neuropathic noise. The *R* statistical environment and *DESeq* were used to analyze and filter the data set to identify transcripts differentially expressed as a result of neuropathic exposure. To uncover the biological significance of differential expression and identify target transcripts for future studies, annotation, network and transcription factor enrichment studies were performed using *DAVID* and *IPA*.

Results

One hundred and sixty genes were differentially expressed in response to NI-PAN exposure; estimation-maximization clustering grouped these transcripts into 7 distinct expression profiles. The functional consequences of differential expression were significantly enriched for immune cell motility and function. Several transcription factors were found, and enriched for, within the differentially expressed genes and may have core regulatory roles in the progression of neural damage. Only 6 of our 160 genes were identified in previous studies investigating differential expression in response to noise-induced permanent or temporary threshold shifts, suggesting that different mechanisms may dominate the response to NI-PAN.

Conclusion

Noise-induced primary auditory neuropathy is a subtle, but significant, pathology that likely contributes to the widespread prevalence of hearing impairment within elderly populations. The genes identified in this study of NI-PAN inducing exposures have little overlap with previously documented genes found to respond to TTS and PTS exposures. However, the functional consequences of these expression patterns (dominated by recruitment, movement and activity of immune cells) bear significant similarity to previous work demonstrating immune cell invasion of the ear post PTS trauma.

Protective Effects of Dexamethasone Against Noise-Induced Hearing Loss in the Retrocochlear Auditory Centers

Ana Kim; Leon Chen; Clare Dean; Michele Gandolfi; Edmund Nahm; Linda Mattiace
New York Eye and Ear Infirmary

Background

Noise-induced hearing loss (NIHL) has been a growing public health issue over the last half century. Dexamethasone (Dex) has been demonstrated to attenuate NIHL by reducing outer hair cell death and other glucocorticoid receptor mediated effects in the cochlea. These studies, however, have not investigated the effects of NIHL and Dex in the central auditory system. The purpose of our study was to examine the effects of Dex on the retrocochlear auditory centers when used prophylactically against NIHL.

Methods

CBA male mice were exposed to 110-120dB noise over 6 hours. Auditory function was assessed using auditory brainstem response (ABR) and distortion product otoacoustic emission (DPOAE) at 1-day, 1-week, 1-month, and 2-months after the acoustic trauma. Dexamethasone (Dex) was applied intratympanically (IT) prior to the acoustic trauma for otoprotection. Retrocochlear neuronal cells were labeled with FluoroGold.

Results

Average click ABR thresholds for the five traumatized groups consisting of untreated, 2 and 10ul IT saline, 2 and 10ul IT Dex were 21.7 ± 2.9 dB, 20 ± 0 dB, 20 ± 5 dB, 18.3 ± 2.9 dB, and 18.3 ± 2.9 dB, respectively. At 1-day post NIHL, all five groups demonstrated profound hearing loss. By 1-week, only the 2 and 10ul Dex groups demonstrated threshold decrease to 63.3 ± 14.4 dB and 48.3 ± 17.6 dB, respectively, while thresholds for the untreated, 2ul and 10ul saline groups remained profound. At 2-weeks, the 2 and 10ul Dex thresholds returned toward baseline at 47.5 ± 3.5 dB and 53.3 ± 17.6 , respectively. Mean cell counts in the cochlear nucleus (CN), superior olivary complex (SOC), and lateral lemniscus (LL) of control mice were 1483 ± 190 , 2807 ± 67 , and 112 ± 20 , respectively. In contrast, untreated, 2 and 10ul saline groups yielded respectively, 1390 ± 404 , 1293 ± 327 , and 1357 ± 204 in the CN; 2083 ± 190 , 2061 ± 146 , and 2034 ± 164 in the SOC; and 104 ± 21 , 147 ± 19 , and 143 ± 32 in the LL. The 10ul Dex group was the only group similar to the control group with counts of 1883 ± 186 (CN), 2774 ± 182 (SOC), and 166 ± 18 (LL).

Conclusion

Our NIHL mouse model demonstrated a dose dependent Dex pre-treatment option against NIHL. While the exact mechanism requires further exploration, administration of Dex prior to NIHL preserved neurons and hearing recovery.

Rescue From Progressive Bone Remodeling and Hearing Loss by Systemic Bisphosphonate

Penelope Jeffers¹; Arthur G. Kristiansen¹; Michael J. McKenna²; Sharon G. Kujawa²

¹Massachusetts Eye and Ear Infirmary; ²Harvard Medical School

Background

The otic capsule normally exhibits little or no bone remodeling; however, under pathologic conditions, e.g. otosclerosis, it may undergo substantial remodeling. Osteoprotegerin (OPG) is one of several cytokines that regulate such processes. OPG is highly expressed within the inner ear and otic capsule, where it inhibits bone remodeling. Our previous work has described progressive, mixed hearing loss and otic capsule remodeling in OPG $-/-$ mice (Zehnder et al 2006) and has shown that both are responsive to treatment with systemic bisphosphonates, potent inhibitors of bone resorption and remodeling (Adachi et al 2008). We transferred the existing mouse model from C57BL/6 to CBA/CaJ background to better characterize the otopathologic consequences of OPG deficiency (Kujawa et al 2013) and to investigate the long-term efficacy of drug treatment without the complication of the accelerated age-related hearing loss of C57BL/6. Here, we describe effects of systemic bisphosphonate against the hearing loss and bone remodeling of OPG $-/-$ in the new background.

Methods

OPG-deficient mice and wildtype littermates receive a single i.p. injection of bisphosphonate (zoledronate, 0.56 mg/kg i.p.) as young pups (p5 – p10) and are then held, along with untreated controls, for various post-drug times before undergoing auditory function testing using DPOAEs and ABRs. We process paraffin-embedded, H&E-stained middle and inner ear tissues for examination by light microscopy.

Results

Untreated OPG $-/-$ in CBA demonstrate rapidly progressive hearing loss: mild/moderate high frequency loss at 8 weeks progresses to severe loss across frequency by 32 weeks. DPOAE losses exceed those by ABR, suggesting conductive involvement affecting both forward and backward transmission through the middle ear. Remodeling and thinning of bone of the otic capsule and ossicles are prominent features in untreated OPG $-/-$. Changes are dramatic in young animals and progress with age. Spiral ligament pathology occurs in regions adjacent to active remodeling. Heterozygotes are wildtype-like in structure and function at all ages. In zoledronate-treated animals, threshold protection is nearly complete for both response metrics at all post-drug monitoring times. Histologic evaluation of middle ear and cochlear tissues is ongoing, and shows dramatically reduced otic capsule remodeling.

Conclusion

Results suggest that systemic bisphosphonate therapy has good, long-term efficacy in the treatment of hearing loss and

otopathology associated with inner ear bone remodeling disorders.

PS - 578

Transplatin: An Effective Treatment for Noise-Induced Hearing Loss

Sumana Ghosh¹; Debashree Mukherjee²; Kelly Sheehan²; Puspanjali Bhatta²; Vikrant Borse²; Leonard P Rybak²; Vickram Ramkumar²

¹SIU School of Medicine; ²SIU

Background

Noise induced hearing loss (NIHL) is a significant problem in the United States. Chronic noise exposure leads to irreversible damage to inner ear structures and hearing loss. There are no known treatments available for NIHL. Recent data from our laboratory indicates that increase in cochlear ROS generation and inflammation is seen within 2h of noise exposure. This acute increase in pro-inflammatory gene expression evolves into a chronic inflammatory response which can be detected at 21d post noise exposure. Mediators of this inflammatory response include the cochlear specific NADPH oxidase, NOX3, TNF- α , COX2, iNOS and the transient receptor potential V1 (TRPV1), a nonspecific cation channel. Our laboratory has shown that transplatin inhibits cisplatin-mediated hearing loss. The purpose of this study was to determine whether a single dose of transplatin could prevent and/or rescue NIHL.

Methods

Auditory brainstem responses (ABRs) of naïve male Wistar rats were recorded. Noise exposure (NE) parameters were: 122dB, 60 minutes, OBN centered at 16kHz. Functional assays performed include post noise exposure ABRs, scanning electron microscopy (SEM) and cochlear whole mount performed at 21days. Gene expression studies were conducted using real time PCR, and by immunohistochemistry of the mid-modiolar sections of the rat cochleae or surface preparations.

Results

Our data indicate that a single oral, intraperitoneal or transtympanic administration of transplatin ameliorates NIHL, assessed at 21days. Intraperitoneal administration of transplatin (3 and 5 mg/kg) immediately prior to or 48h prior to (transtympanic route, 50ul of 0.5mg/ml) noise trauma inhibits the early up regulation (48h post noise trauma) of stress response and inflammatory genes as well as chronic increases (21days post noise trauma) in both the stress response and inflammatory markers in the rat cochlea. Most importantly, oral transplatin (3 and 5.5mg/kg) administered up to 6 h post noise exposure protect against NIHL. Noise exposure causes an average threshold shift of 35, 42 and 45dB at 8,16 and 32kHz. However, single oral transplatin treatment (3 and 5.5mg/kg) up to 6 h post NE shows a threshold shift of 3,10 and 10 dB at the 3 frequencies tested at 21 days.

Conclusion

These data demonstrate the efficacy of a single pretreatment dose of transplatin, administered by diverse routes to protect against NIHL. Oral transplatin is also able to **rescue** the

cochlea from NIHL. We propose that transplatin could serve as an effective treatment for NIHL, particularly for those who work in a noisy environment and military personnel in combat situations.

PS - 579

Cobalt Chloride Does not Protect Against Progressive Hearing Impairment in Mice With the GJB2 p.V37I Mutation

Ting-Hua Yang; Ying-Chang Lu; Chen-Chi Wu; Yin-Hung Lin; Hsiao-Chun Lin; Chuan-Jen Hsu

National Taiwan University Hospital

Background

The *GJB2* p.V37I is a common recessive mutation identified in Asians with progressive mild-to-moderate sensorineural hearing impairment (SNHI). To elucidate its pathogenicity, we generated a knock-in mouse strain homozygous for the *Gjb2* p.V37I mutation (i.e. *Gjb2tm1Dontuh/tm1Dontuh* mice). Similar to the human counterpart, *Gjb2tm1Dontuh/tm1Dontuh* mice also revealed progressive hearing impairment with age. Moreover, *Gjb2tm1Dontuh/tm1Dontuh* mice appeared more vulnerable to noise exposure, indicating that reactive oxygen species (ROS) might play a role in hearing loss associated with *GJB2* p.V37I. By applying cobalt chloride (CoCl₂), an antioxidant mineral against oxidative injury, to the animals, this study was designed to investigate whether antioxidants could be used to halt the progression of *GJB2* p.V37I-related hearing loss.

Methods

Thirty wild-type and thirty *Gjb2tm1Dontuh/tm1Dontuh* mice were randomly assigned to 3 groups, respectively, including: no-treatment group (n=10 each), low-dose group treated with 0.5 mM CoCl₂ (n=10 each), and high-dose group treated with 5 mM CoCl₂ (n=10 each). CoCl₂ were given in the drinking water for 9 months since three weeks old. All animals were subjected to audiological evaluations at 1, 3, 6, and 9 months.

Results

In both the wild-type or *Gjb2tm1Dontuh/tm1Dontuh* mice, significant difference was not observed between the no-treatment group and low-dose group treated with 0.5 mM CoCl₂. However, severe degeneration of hair cells and increased apoptotic cells were detected in the high-dose group treated with 5 mM CoCl₂ in both strains mice.

Conclusion

Application of low dose CoCl₂ does not protect progressive hearing impairment in *Gjb2tm1Dontuh/tm1Dontuh* mice. Application of high dose CoCl₂, however, exerts ototoxic effects on both the wild-type and *Gjb2tm1Dontuh/tm1Dontuh* mice.

Effect of Gentamicin on WDR1 Localization and Peroxisomes in COS7 Cells

Henry Adler¹; Allan Kachelmeier²; Meiyang Jiang²; Peter Steyger²

¹Rochester Institute of Technology, National Technical Institute for the Deaf; ²Oregon Health & Science University, Oregon Hearing Research Center

Background

WD40 repeat 1 protein (WDR1) is upregulated as part of the stress response to acoustic overstimulation in mammals and birds, but its role following ototoxic drug treatment remains to be determined. Ototoxic drugs, like gentamicin, promote the genesis of intracellular free radicals. We examined the relationship between peroxisomes (as major producers of free radicals) and WDR1 after ototoxic drug exposure.

Methods

COS7 cells were transfected with green fluorescent protein (GFP) specific for peroxisomes for 18 hours at 37°C, followed by treatment with gentamicin (5 mg/mL or 100 mg/mL) at 22°C for one hour to preclude endocytosis. Controls received culture medium without gentamicin, and were incubated at 22°C for one hour. Cells were allowed to recover at 37°C for 0, 1, 3, or 6 hours, prior to fixation, processing for WDR1 immunocytochemistry, and examination by confocal microscopy. For comparison with WDR1 localization, GFP-transfected COS7 cells (specific for peroxisomes) were treated with GTTR (5 mg/mL) and processed for confocal microscopy without WDR1 immunocytochemistry.

Results

WDR1 was immunolocalized to a compact region adjacent to one side of the nucleus of COS7 cells, regardless of gentamicin dose or recovery duration. The number of WDR1-labeled regions increased during 6 hours of recovery after gentamicin treatment. Also, the compact region of WDR1 labeling was often surrounded by GFP-conjugated peroxisomes, but little co-localization was observed between WDR1 and peroxisomal labeling.

Conclusion

The increase in number of WDR1-labeled regions near the nucleus following gentamicin treatment suggests that gentamicin may induce upregulation of WDR1 expression. The close proximity of peroxisomes and WDR1-labeling and the increase in WDR1/peroxisome number following gentamicin treatment suggest that WDR1 function may be associated with peroxisomes. However, their interaction and contribution towards auditory and/or balance (dys)function or protection against cytotoxicity remain to be elucidated. Further studies will ascertain why WDR1 is largely circumscribed to a region adjacent to the nucleus, as well as determine the effects of cytoplasmic gentamicin on WDR1 activity in that region.

Attenuation of Cochlear Oxidative Stress and Synaptic Conservation: Effects of Methylene Blue on Noise-Induced Cochlear Injury

Jung-sub Park; Ilo Jou; Sang Myun Park

Ajou University School of Medicine

Background

Overproduction of reactive oxygen species (ROS) contributes significantly to the pathogenesis of noise-induced hearing loss. Interestingly, based on the redox property of methylene blue (MB), it can prevent electron leakage, increase mitochondrial oxidative phosphorylation, and reduce ROS overproduction under pathological conditions. Therefore, we targeted the mitochondrial electron transport chain to utilize the redox cycling properties of MB.

Methods

Young male BALB/c mice were exposed to 112dB sound pressure level of broad-band white noise for 3 h. ABRs for the 16 and 32 kHz stimuli were recorded before noise exposure as well as at 1 and 14 days after noise exposure. To detect generation of oxidative stresses, sections were incubated with primary antibody against 4-hydroxynonenal (4-HNE) and 3-nitrotyrosine (3-NT). Phalloidin staining was performed to detect the changes in hair cells. Cytochrome c oxidase (COX) staining was assessed by measuring at the basal turn area. Anti-synapsin-1, and anti-postsynaptic density protein 95 was used to label nerve endings in organ of Corti. For Western blot, membranes were incubated with primary antibodies against 4-HNE, brain-derived neurotrophic factor and neurotrophin-3 (NT-3). UB-OC1 cells were treated with vehicles, rotenone (0.2µM), antimycin A (1 µM) and oligomycin (5µM) in the presence or absence of 2µM of MB. Cell viability was assessed by water soluble tetrazolium assay. The level of ATP and mitochondrial complex IV activity was also determined.

Results

We found that MB pretreatment for 4 consecutive days significantly decreased both compound threshold shift (CTS) and permanent threshold shift (PTS) after noise exposure (Fig. 1A). MB reduced outer hair cell (OHC) death in the cochlea that was identified by surface preparation (Fig. 1B) and scanning electron microscopy, and it also reduced ROS and RNS formation after noise exposure (Fig. 2A-C). MB significantly protected against rotenone- and antimycin A-induced cell death (Fig. 2D, E), and also reversed ATP generation *in vitro* (Fig. 2F). Furthermore, MB effectively attenuated noise-induced impairment of complex IV activity *in vivo* (Fig. 2G). MB increased the neurotrophin-3 (NT-3) level (Fig. 3A) and promoted the conservation of both efferent and afferent nerve terminals on the OHC and inner hair cells (Fig. 3B).

Conclusion

These findings suggest that amelioration of impaired mitochondrial electron transport and potentiation of NT-3 expression by treatment with MB have a significant therapeutic value in preventing ROS-mediated sensorineural hearing loss.

Figure 1. Park et al.

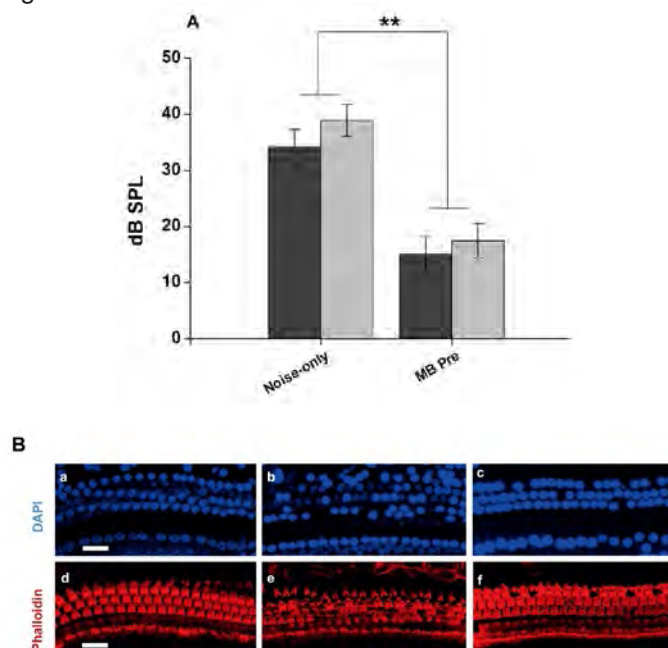


Figure 2. Park et al.

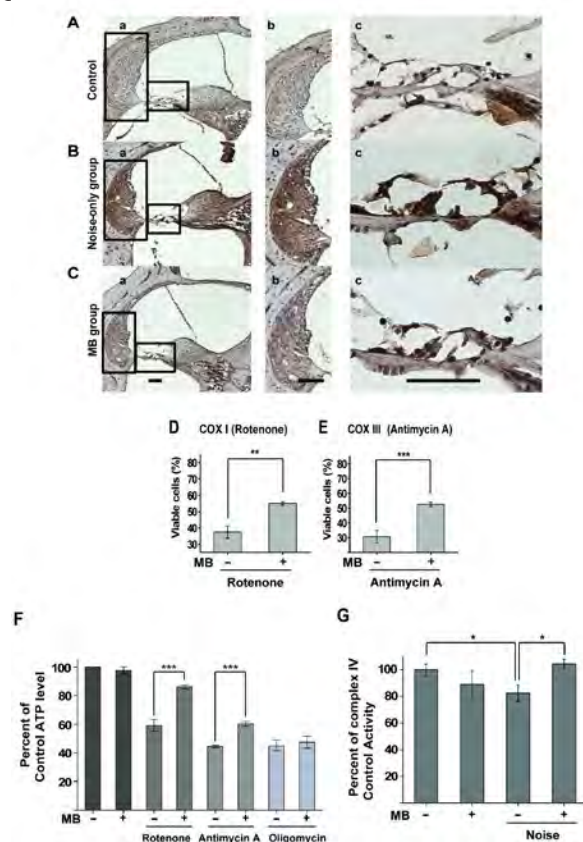
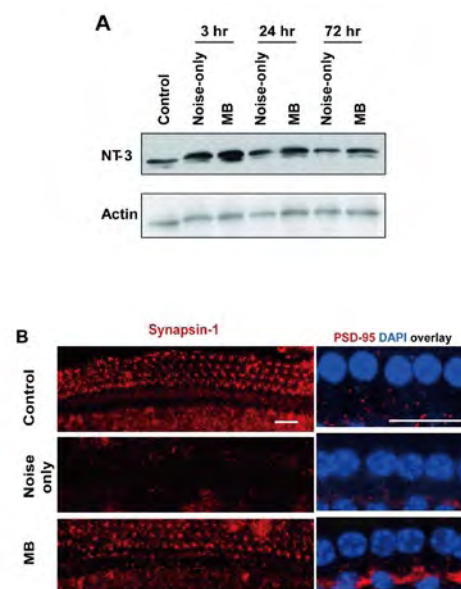


Figure 3. Park et al.



PS - 582

Conditional Knockout of *Cdh1* in OHCs Reveals Supporting Cell Contribution to *Cdh1* Response to OHC Damage Induced by Acoustic Overstimulation

Bo Wang^{1,2}; Donald Coling¹; Krystal Vera¹; Dalian Ding¹; Qunfeng Cai¹; Jie Fang³; Jian Zuo³; Shiming Yang²; Bo Hua Hu¹

¹University at Buffalo; ²Chinese PLA General Hospital; ³St. Jude Children's Research Hospital

Background

We have documented an increase in *Cdh1* expression in the cochlear sensory epithelium following acoustic trauma. Immunohistology reveals that the increased immunoreactivity of *Cdh1* protein is located in the membrane junctions between the damaged outer hair cells (OHCs) and their surrounding supporting cells at the level of the reticular lamina. The current study was designed to investigate the contribution of *Cdh1* in OHCs to hair cell apoptosis induced by acoustic overstimulation using a mouse model of conditional *Cdh1* knockout.

Methods

A Cre-loxP mouse model for conditional knockout of *Cdh1* in OHCs was generated using B6.129-*Cdh1*^{tm2Kem/J} and Prestin-CreER^{T2} mouse lines. Mating of these animals produced a mouse line: the *Cdh1*-floxed/floxed (+/+) Prestin-CreER^{T2} (+/-). These mice received an injection of tamoxifen to activate Cre recombinase in OHCs. Then, the animals were exposed to a broadband noise at 121 dB SPL for 1 hour. At 2 hours or 1 day post-noise exposure, the animals were sacrificed. Enriched hair cell tissues containing sensory cells, Deiters cells, pillar cells, and inner sulcus cells were collected for transcriptional analysis of *Cdh1* and its related genes (*Cdh1*, *Cdh2*, *Vinculin*, α -catenin and β -catenin). In addition, cochlear sensory epithelia were collected for assessment of *Cdh1* protein distribution using immunohistology, and the staining pattern was examined using laser scanning confocal microscopy and transmission electron microscopy.

Results

Wild-type mice (C57BL/6J) showed a time-dependent increase in *Cdh1* expression following the noise exposure (13.2 fold increase at 2 h post-exposure). The knockout mice (*Cdh1*-floxed/floxed (+/+) *Prestin-CreER*^{T2} (+/-)) also showed the expression increase (12.0 fold). In both knockout and WT mice, the noise-induced increase in immunoreactivity of *Cdh1* in the junction between damage OHCs and their surrounding supporting cells persisted. In addition, apoptotic activity in these *Cdh1* positive cells continued. Further 3-D reconstruction of confocal images and transmission electron microscopy revealed that *Cdh1* protein was distributed primarily in the head plates of outer pillar cells, the phalangeal apical plates, and the phalangeal processes of Deiters cells.

Conclusion

OHC *Cdh1* is not required for activation of noise-induced apoptosis. The increase in *Cdh1* expression in the membrane junctions between damaged OHCs and their neighboring supporting cells is contributed by *Cdh1* in supporting cells. This *Cdh1* expression change is likely involved in the recovery process of the organ of Corti.

PS - 583

Growing Cochlear Fibrocytes on Collagen I Gels

David Furness¹; Rachel Gater²; Shanthini Mahendrasingam

¹Keele University; ²Institute for Science and Technology in Medicine

Background

Fibrocytes are located in the lateral wall of the cochlear duct and function in homeostatic processes, such as potassium recycling. Fibrocyte degeneration is one potential cause of homeostatic failure, likely leading to reduced endocochlear potential, degeneration of other cochlear structures and hearing impairment (Mahendrasingam et al, 2011). A strategy for preventing this is to replace dying fibrocytes, e.g. from fibrocyte cultures that could be used for transplantation. Cultures are typically grown flat on culture dishes, requiring the cells to be harvested in solution and injected for transplantation. We here evaluate an alternative approach, which is growing cells on the surface of collagen gels which may make cultures easier to manipulate.

Methods

Collagen gels were made from 3 mg/ml collagen I solution, polymerised by addition of NaOH. 400 ml volumes were placed into wells incubated at 37°C. Fibrocyte culture cells obtained from frozen stocks were seeded on top of the collagen gels at a density of X5 - 10000 per cm², allowed to settle and grown for up to 13 days. The density and morphology of the cells was evaluated over time and compared with controls consisting of cells seeded at the same density and grown onto uncoated wells. Finally, gels were fixed and immunolabelled for fibrocyte markers or prepared for scanning electron microscopy (SEM).

Results

From 5 hours after seeding to 8 days, cell density started high but reduced on the gels, whilst the non-gel culture showed an increase initially and then remained at higher density. Morphologically, cells on the gels tended to be smaller and rounder, with small processes extending from many. Cells grown on the well alone were flatter and larger overall. Immunofluorescence showed that cells expressed caldesmon (a marker for type III fibrocytes) and to a lesser extent, NaKATPase (a marker for other fibrocytes). SEM showed incorporation of cells into the gels rather than simple growth on the surface. The gels could be picked up and transferred relatively easily and thus were easier to handle than cells in solution.

Conclusion

The data suggest that the cells proliferate better on flat surfaces than gels, but their morphology resembles cochlear fibrocytes more in the latter. Physically manipulating the gels was relatively easy and would be a clear advantage to harvesting cells in solution.

PS - 584

Acute Characterization of Gentamicin Induced Inner Hair Cell Ribbon Synapse Degeneration and Formation of New Auditory Neuron Connections

Matthew Abernathy¹; Theodore Baird¹; John Spitsbergen²; Robert Eversole²; Josef Miller³; Richard Altschuler³

¹MPI Research; ¹MPI Research; ²Western Michigan University; ³Kresge Hearing Research Institute, University of Michigan

Background

Recent evidence indicates that aminoglycoside antibiotics induce degeneration of the inner hair cell ribbon synapse in the mouse, suggesting there may be an excitotoxic component to aminoglycoside induced hair cell cytotoxicity and subsequent neurotoxicity. The objective of this experiment was to evaluate the acute effects of intra-aurally administered gentamicin on inner hair cell ribbon synapse plasticity.

Methods

Five female albino guinea pigs were instrumented with bilateral middle ear catheters. 200 mg/ml gentamicin sulfate was administered into the right ear and a volume equivalent of saline was administered into the left ear. Bilateral auditory brainstem response (ABR) evaluations were conducted pre-test, and at 3 and 24 hours following treatment. All cochleae were harvested and the organs of Corti were immunostained to identify auditory hair cells, CtBP2 ribbon proteins, and GluR2/3 glutamate receptor subunits. Hair cell counts were conducted over the entire length of the organ of Corti to create cytochleograms. The regions 15.68 through 19.60 mm from the apex (20 - 60 kHz) were then imaged using confocal microscopy, and z-stacks were created to evaluate the CtBP2:GluR2/3 co-localization density per inner hair cell. Additionally, the prehabenular areas located directly beneath the inner hair cells were evaluated for CtBP2:GluR2/3 co-localization.

Results

The results of the experiment revealed a significant increase in ABR threshold at 3 hours post dose, which increased through 24 hours post dose. The hair cell counts revealed a pattern of severe outer hair cell loss in the base of the cochlea, which decreased to mild loss in the medial turns. When compared to the saline controls, the gentamicin treated ears displayed a significant reduction in ribbon synapse densities throughout all of the basal regions examined, in spite of minimal inner hair cell loss.

Conclusion

These results indicate that gentamicin produces significant inner hair cell ribbon synapse degradation in the basal turn of the cochlea without an associated inner hair cell loss. The prehabenular area co-localization assessment displayed a distinctive increase in co-localized CtBP2:GluR2/3 puncta expression in the basal regions of the organ of Corti as compared to saline controls. This suggests that the induced cochlear pathology results in the formation of new connections, perhaps between unmyelinated neural membranes which could be similar to the en passant synapses between unmyelinated auditory nerves reported in old world monkeys by Hozawa and Kimura.

PS - 585

Disruption of OHC Amplification Function Reduces Cochlear Response to Acoustic Overstimulation

Qunfeng Cai¹; Bo Wang²; Krystal Vera¹; Jie Fang³; Jian Zuo³; Shiming Yang²; Bo Hua Hu¹

¹Center for Hearing and Deafness, University at Buffalo, the State University of New York; ²Department of Otolaryngology and Head & Neck Surgery, Institute of Otolaryngology, Chinese PLA General Hospital; ³Developmental Neurobiology, St. Jude Children's Research Hospital

Background

Outer hair cells (OHCs) play an essential role in cochlear amplification, and are responsible for the extraordinary hearing sensitivity of the ear. Ample empirical evidence has shown that this function is essential for threshold hearing. However, it is not clear whether this function also plays an important role for cochlear stress responses when the contribution of cochlear amplification function to basilar membrane vibration decreases with the increase in the level of acoustic stimuli. The current investigation was designed to investigate how dysfunction of cochlear amplification affects cochlear responses to acoustic overstimulation.

Methods

Two experimental models of disruption of cochlear amplification function were used. The first was a genetic model of OHC dysfunction in mice; created by insertion of an internal ribosome entry site (IRES)-CreER^{T2}-FRT-Neo-FRT cassette into the prestin locus after the stop codon. The second model was a rat model of mechanical suppression of basilar membrane vibration, generated by surgically blocking the round window membrane. The animals were exposed to a broad-

band noise at 120 dB SPL for 1 hour. The auditory function, cochlear pathology, and expression of stress-related genes were examined to define the impact of the suppression of cochlear amplification function on cochlear responses to acoustic overstimulation. Moreover, the prestin mRNA and protein expression were examined using qRT-PCR and immunohistochemistry assays.

Results

The prestin-CreER^{T2} homozygous mice exhibited a relative flat threshold elevation (16-21 dB) with large individual variation. However, the prestin expression remained consistent at both transcriptional and protein levels. The ears having round window closure showed 5- 20 dB threshold shifts after the surgery of round window closure. Both the genetic and mechanical models of the animals showed a threshold elevation and an I/O function shifts of the DPOAEs, suggesting the reduction of cochlear amplification function. After the acoustic trauma, there was an overall reduction in the threshold shifts of the cochleae having the OHC dysfunction or basilar membrane suppression. In the Cre-knockin mice, the level of the threshold shift was negatively correlated to the level of pre-noise thresholds, suggesting that the OHC dysfunction leads to reduction in threshold shifts. This reduction in threshold shifts was correlated with the reduction in the molecular responses to the acoustic trauma.

Conclusion

OHC dysfunction reduces cochlear responses to acoustic overstimulation. Modulation of OHC function may serve as a therapeutic strategy for prevention of noise induced hearing loss.

PS - 586

Selective Loss of Inner Hair Cells in Ggt1dwg Mutant Mice

Dalian Ding¹; Haiyan Jiang¹; Chantal Longo-Guess²; Kenneth Johnson²; Richard Salvi¹

¹University at Buffalo; ²The Jackson Laboratory

Background

Dwarf grey *Ggt1dwg/dwg* mice have a spontaneous, loss of function mutation of the *Ggt1* gene. *Ggt1* codes for g-glutamyl transferase 1, a cell surface glycoprotein involved in the transfer of the glutamyl moiety of glutathione (GSH) to an acceptor molecule. Intracellular GSH, resynthesized through the g-glutamyl cycle, is critical for protecting cells from oxidative stress. The *Ggt1dwg/dwg* phenotype is characterized by gray coat, smaller body size, and early cataracts development. Since GSH plays an important role in reducing oxidative stress in the cochlea, we hypothesized that *Ggt1dwg/dwg* mice would be born with or develop age-related hearing loss and cochlear pathologies.

Methods

To test this hypothesis, we evaluated auditory function and cochlear in WT, *Ggt1+/dwg* and *Ggt1dwg/dwg* mice from 1 to 9 months of age.

Results

ABR thresholds (8-32 kHz) in WT mice remained largely unchanged between 1 and 9 months of age. ABR thresholds of Ggt1dwg/dwg mice were nearly the same as in WT mice from 1 to 3 months of age. However, hearing thresholds in Ggt1dwg/dwg mice increased rapidly and significantly (40-50 dB) between 3 and 6 months of age, but little increase was observed between 6 and 9 months of age. Mean cochleograms of WT and Ggt1+/dwg mice showed little hair cell loss between 1 and 9 months of age. Little hair cell loss was also observed in Ggt1dwg/dwg mice between 1 and 3 months of age. However, between 3 and 6 months of age, a massive loss of inner hair cells (IHC) was observed in Ggt1dwg/dwg mice. IHC losses were greatest (90% missing) in the apical third of the cochlea and tapered off to less than 10% loss near the base and less than 50% near the apex. Despite the massive loss of IHC, virtually all the outer hair cells were still present throughout the cochlea.

Conclusion

IHC and type I neurons provide the predominant if not exclusive pathway through which acoustic information is transmitted to the central auditory pathway. Ggt1dwg/dwg mice, which exhibit a selective loss of IHC represents an important new model for studying the functional consequence of a diminished neural input in the presence of outer hair cells.

PS - 587

Changes in Peroxisomes in COS7 Cells Following Gentamicin Treatment

Brian Carter¹; Takatoshi Karasawa²; Allan Kachelmeier²; Peter Steyger²; **Henry Adler**³

¹Oregon Health & Science University; ²Oregon Health & Science University, Oregon Hearing Research Center;

³Rochester Institute of Technology, National Technical Institute for the Deaf

Background

Ototoxic agents promote the genesis of intracellular free radicals, contributing to both cochlear and vestibular toxicity in vertebrates. However, gentamicin is preferentially cytotoxic to sensory cells compared to non-sensory cells. We hypothesize that gentamicin induce peroxisomal enzymes generate reactive oxygen species (ROS). In addition, cell culture facilitates the study of ototoxicity by allowing controlled exposure, clearance and recovery times. We treated COS7 cells with gentamicin to examine its effects on the number, size and distribution of peroxisomes in these cells.

Methods

COS7 cells were transfected with green fluorescent protein (GFP) specific for peroxisomes for 18 hours at 37°C, followed by treatment with or without gentamicin (5 mg/mL or 100 mg/mL) or gentamicin conjugated with Texas Red (GTTR; 5 mg/mL) at 22°C for one hour. Cells recovered at 37°C for 0, 1, 3, or 6 hours before fixation and confocal microscopy. Identical confocal settings were used for all groups. ImageJ was used to quantify puncta number and area per cell, followed by statistical analysis. Cell-free assays combining gentamicin and

the peroxisomal enzyme D-amino acid oxidase (DAAO) to assess ROS generation were also performed.

Results

DAAO generated ROS when exposed to gentamicin. In cells, GFP-conjugated peroxisomes were generally evenly dispersed throughout the cytoplasm. In many cells, a cluster pattern of peroxisomes appears to populate one side of the nucleus. Puncta number decreased following treatment with gentamicin (5 or 100 mg/mL), and returned to near baseline after 3 hours recovery. After GTTR exposure, puncta number increased following 3 hours recovery. All puncta numbers returned to baseline after 6 hours recovery, although, average and total peroxisomal puncta area decreased at 3 or 6 hours after gentamicin or GTTR exposure, respectively.

Conclusion

Changes in peroxisomal puncta number and area indicate that gentamicin affects peroxisomes within COS7 cells. The restoration to baseline levels in puncta number, followed by a decrease in puncta area following gentamicin treatment, suggests that affected cells compensate for decreased puncta area with increased puncta number, likely *de novo* genesis of peroxisomes. Whether these changes in peroxisomes are associated with peroxisomal generation of ROS remains to be determined. However, ROS are generated when peroxisomal enzymes encounter gentamicin. These studies bring additional insight into potential mechanisms of cytotoxicity as well as for new interventions to prevent ototoxicity.

PS - 588

Motor-Auditory Synchronization is Dependent on Degree of Fractal Structure in Auditory Sequences.

Summer Rankin; Charles Limb

Johns Hopkins University School of Medicine

Background

Visual examples of fractal structure (coastlines, trees) show repeating patterns that display properties of self-similarity (the parts resemble the whole)--a characteristic of fractals. Fractal ($1/f^\beta$) structure has also been observed in the statistics of temporal processes at different levels of organization, including rhythmic behavior, biology, and aspects of musical structure. Fractal analysis characterizes long-term correlation and self-similarity by taking sequential aspects of the time series into account. When coordinating finger taps with fluctuating auditory stimuli, participants were significantly better at predicting when the next beat would occur (resulting in successful coordination) when stimuli contained fractal structure compared to random stimuli.

Methods

We created 13 different stimuli that had a rhythm which contained systematically varying amounts of $1/f^\beta$ structure ($-1.21 < \beta < 1.21$), and an isochronous control sequence. The 13 sequences, each with a specific value of β , were created using the spectral synthesis method. The first 256 values of each sequence were treated as inter-onset intervals (IOIs) and cumulatively summed to create a series of events (a

rhythm). Stimuli consisted of 261 Hz pure tones that were 150 ms in duration. Sixteen volunteer participants were instructed to tap along with each event and to keep up with the rhythm to the best of their ability. The inter-tap intervals (ITIs) were analyzed using power spectral density.

Results

The structure of the stimuli was reflected in the participants' taps. The mean β values from each condition were fitted to the β values of the stimuli using a linear regression model ($R^2=0.843$, $p<.001$), showing that the structure of the participants' taps (ITIs) scaled with the structure of the stimuli (IOIs). As the amount of fractal structure in the stimuli increased or decreased, the structure of the taps did too.

Conclusion

Our results imply that humans are able to readily adapt to fluctuating stimuli rather than simply react to it (lagging behind by one event) as would be predicted from classical models of synchronization. This ability is helpful--even necessary--for engaging with the world.

PS - 589

The Psychophysics of Temporal Coherence in Budgerigars

Erikson Neilans; **Laurel A. Screven**; MichealL. Dent
University at Buffalo, SUNY

Background

Being able to hear and isolate communication signals in the environment is important for both humans and animals. In humans, we know that basic acoustic parameters such as frequency, loudness, and timing from different sound sources are important in the perceptual isolation or streaming of multiple auditory objects (Bregman, 1990). Relative to humans, little work has been devoted to figuring out how animals isolate sound sources to create auditory objects and even less is known about the comparative psychology of auditory stream segregation. Frequency separation of sounds is arguably the most common parameter studied in auditory scene analysis and has been shown to be an important feature for streaming auditory objects in both humans and birds. Frequency separation of sounds is not the only factor influencing auditory scene analysis, as the relative timing of sounds in the acoustic environment appears important as well (Elhilali, et al., 2009, van Noorden, 1975). Elhilali et al. (2009) found that, in humans, synchronous tones are heard as a single auditory stream, even at large frequency separations, compared to asynchronous tones with the same frequency separations, which are perceived as two sounds. These findings demonstrate how *both* timing and frequency separation of sounds are important for auditory scene analysis. It was unclear how animals such as budgerigars (*Melopsittacus undulatus*) would perceive synchronous and asynchronous sounds.

Methods

In the present study, budgerigars were trained and tested using operant conditioning procedures to investigate the perception of synchronous, asynchronous, and partially overlapping pure tones. Additionally, the order and number of synchronous and asynchronous tones were varied in order

to investigate how these parameters influenced stream segregation in budgerigars.

Results

Results illustrate that budgerigars segregate partially overlapping sounds in a manner predicted by computational models of streaming. Furthermore, perception of streams is affected by the ratio of overlapping synchronous tones versus non-overlapping asynchronous tones but not the serial position in the sequence.

Conclusion

These results support the idea that frequency has little influence on how overlapping pure tone stimuli are segregated, considering that the amount of frequency separation did not contribute to any noticeable differences in the collected psychometric functions. Furthermore, it appears that, at least in streaming of overlapping stimuli, location of the overlap has no influence on auditory perception.

PS - 590

The Effects of Age and Hearing Loss on the Temporal Modulation Transfer Function

Yi Shen

University of California, Irvine

Background

The temporal modulation transfer function (TMTF) is a common method to assess auditory temporal acuity. The TMTF is a function relating amplitude-modulation thresholds to modulation rates. Typically exhibiting a low-pass shape, TMTFs are often quantified by two parameters: sensitivity and cut-off frequency. Although being an established method for decades, the TMTF has not been widely adopted as a predominant way of accessing temporal acuity in clinical research, partly due to the time-consuming process needed for data collection. In a previous study, Shen and Richards [2013, J. Acoust. Soc. Am., 133(2), 1031-1042] developed a simplified procedure, the two-track procedure, for the estimation of the TMTF. Taking the advantage of this new procedure, the current study investigates (1) the effects of age and hearing loss on the TMTF, and (2) the agreement between the TMTF to another measure of auditory acuity, the gap detection threshold.

Methods

TMTFs and gap detection thresholds were measured from nine young and twenty-five older listeners. The older listeners had wide ranges of age (55- 88 years) and hearing loss (the averaged pure-tone threshold across 1, 2, and 4 kHz was between 0 and 55 dB HL). The stimuli were 500-ms, 85-dB SPL narrowband noise ranging from 1600 to 2400 Hz. For the TMTF measurements, listeners discriminated between noise stimuli that were either amplitude modulated (AM) or quasi-frequency modulated (QFM). The AM and QFM stimuli have the same power spectrum but differ in their amplitude-modulation depths. For the gap detection measurements, listeners detected the presence of a temporal gap imposed in the temporal center of the narrowband carrier.

Results

The TMTF sensitivity improved either with increasing hearing threshold or with decreasing age. No significant effect of age or hearing threshold was found for the TMTF cutoff frequency or the gap detection threshold. No significant correlation was found between the TMTF parameters and the gap detection threshold.

Conclusion

The estimates of the TMTF sensitivity suggests that hearing impairment leads to enhanced coding of low-rate amplitude modulation, while the sensitivity to amplitude modulation degrades as one ages. The effects of age and hearing loss on temporal acuity are difficult to discern from the TMTF's cutoff frequency or from gap detection threshold using naïve listeners.

PS - 591

Spectral and Temporal Cues for Recognition of Non-Harmonic Natural Sounds by Guinea Pigs

Hisayuki Ojima¹; Eriko Tachi¹; Junsei Horikawa²; Masato Taira¹

¹Tokyo Medical and Dental University; ²Toyohashi University of Technology

Background

Compared to harmonic sounds, it remains uncertain how animals rely on acoustic cues to recognize non-harmonic sounds. We successfully conditioned guinea pigs to a semi-natural noise-like sound (target, T) using food as reinforcer and have behaviorally examined this question by applying its spectrally and temporally modified versions as test sound.

Methods

Conditioning sound (5.7s in duration) comprised ten 80-ms segments of noise-like bursts. These segments were generated by variously amplifying a single footstep sound produced by an actual stepping motion. Power spectrum of individual segments showed 3 major energy peaks at 0.6, 1.8 and 3.0 kHz. Test sounds were generated by modifying the T sound digitally. Animals were trained in a group so that one was compelled to approach food earlier than others. Training took 14-16 days before animals reached >95% correct response rate and correct reject rate in 5 consecutive sessions.

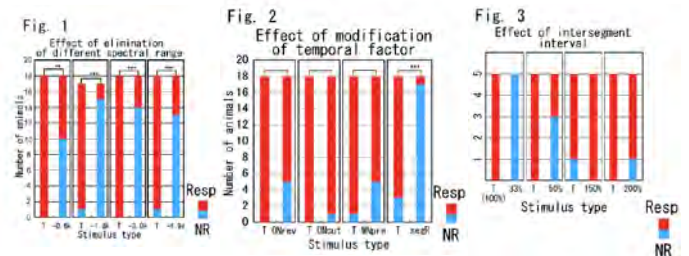
Results

Test 1 was designed to see importance of spectral position. A frequency range centered at 0.6, 1.8, or 3.0 kHz was eliminated from the T sound. Eliminated energy level was equalized among the sounds, and the remaining spectral component was amplified to adjust to the T sound energy level. For results, see Fig. 1. Test 2 was designed to see contribution of temporal factors. Every segment of a T sound was modified with their order unchanged in the following ways; full individual segments were locally time-reversed (segR), only a 16-ms onset portion was time-reversed (ONrev), a 1-ms surge-like transient occurring at the onset was eliminated (ONcut), and a 5-ms wideband noise was prefixed (WNpre). For results, see Fig. 2. In Test 3, to see importance of the overall rhythm,

time intervals of neighboring segments were changed to 33%, 50%, 150% or 200% of the original ones. For results, see Fig. 3.

Conclusion

Absence of dominant spectral positions, unlike the importance of the 1st and 2nd formants for human vowel perception, suggests that energy peaks may not be crucial for T sound recognition. Transient temporal disturbance such as elimination of a surge-like portion or prefixion of a short noise to the original sound does not seem to be destructive so much to the sound recognition. Since only the modified version of T sound with the shortest intervals was perceived differently, guinea pigs may need a minimum time window, slightly longer than 20 ms, for perceiving the T sound.



PS - 592

The Detection of Ultrasonic Calls by Adult CBA/CaJ Mice

Anastasiya Kobrina; Angela Calabrese; Erikson Neilans; Micheal Dent

University at Buffalo, SUNY

Background

Mice are frequently used as an animal model in auditory research, yet their hearing capabilities have not been fully explored. Previous studies (Radziwon et al., 2009; Henry, 2004) have examined auditory threshold sensitivity for pure tone stimuli in CBA/CaJ mice, but little is known about how they perceive their own ultrasonic vocalizations (USVs), and nothing is known about how aging influences this perception. These USVs are thought to be important for acoustic communication, with possible functions including mate attraction, courtship, and other social interactions. In order to determine how well mice detect these complex communication stimuli, several CBA/CaJ mice were tested at various ages in a detection task using operant conditioning procedures.

Methods

In the present study, mice were trained and tested using operant conditioning procedures with positive reinforcement to nose poke when they detected a USV. USVs were presented at various intensities according to the Method of Constant Stimuli. Several different naturally produced USVs were used. These communication signals included male sweep, 30 kHz harmonic, chevron, inverse chevron, complex, down sweep, and up sweep calls. Thresholds for detection of these calls were calculated using $d' = 1.5$. Mice were tested at various ages throughout their lifespan.

Results

Mice were able to detect USVs at a lower intensity than pure tones of the same frequency range (33-44 kHz). Not surprisingly, thresholds also differed for the different USV types. Finally, thresholds differed across the lifespan, but mice that were quite old were still able to detect USVs presented at a high intensity.

Conclusion

Results indicate that young and old CBA/CaJ mice are able to detect USVs at lower intensities than pure tones. The results suggest that mice are sensitive to their complex vocalizations even into old age, highlighting their importance for survival and communication, and laying the groundwork for future studies on acoustic communication and aging in this species.

PS - 593

Heart Rate and Respiratory Frequency Changes in Response to Diverse Musical Tempos Stimulation

Tamara Liberman¹; Eduardo Medina-Ferret²; Ricardo Velluti¹; Marisa Pedemonte¹

¹Facultad de Medicina CLAEH; ²Escuela Uruguaya de Tecnología Médica, Universidad de la República

Background

Human behavior responds to motivations such as music possesses the capability to provoke responses on the listener. Musical speed seems a relevant aspect when it comes to satisfying a motivation. Hence, elucidating the incidence that musical *tempo* may have on the listener is of interest since human bodies behave in rhythmic ways, and external rhythms may influence intrinsic rhythmical functions.

Our aim was explore the heart rate (HR) and respiratory rate (RR) by listening to musical pieces in different *tempos*, comparing musicians with non musicians.

Methods

Under electroencephalographically controlled quiet wakefulness, musicians and non musicians were presented with three musical pieces in three *tempo* versions each: original, increased and decreased tempo. The HR, HR variability (HRV) and RR were recorded by electrocardiogram and chest wall movements' belt respectively. Musics were separated by pink noise (control). On processing, the total length (2 minutes) was divided into first and second minute. All results were statistically analyzed.

Results

When comparing control with musics, non musicians show a higher HRV, while it decreases in musicians in presence of music. Higher HRV in musicians is observed when listening to higher *tempo* versions. Concerning the HR, it shows higher in the presence of music for both groups. The HR seems to accompany the musical tempo in musicians, increasing or decreasing along with the musical *tempo*. While in non musicians such correlation is not observed, although statistical significant changes in HR are found for the different *tempos*. All these findings concern the first minute processed; the sec-

ond minute shows more variable responses in general. Regarding RR, it was higher in non musicians than in musicians; it was slower in the control than when listening to music for non musicians, while in musicians the RR decreased during the slower versions, even slower than during control. When comparing *tempos*, non musicians held the same RR during original and slow versions while musicians decreased RR from original to slower versions.

Conclusion

The HR and RR react to music both in musicians and non musicians, although in musicians it would be in a more correlative manner. Furthermore, different musical *tempos* would influence the HR in singular ways and, since musicians show more consistent cardiac and respiratory changes than non musicians, it could be inferred that they are better at detecting musical changes and thus react to them. However, HR would decrease along time in both populations, probably due to habituation.

PS - 594

Cochlear Implant Users Rely on Tempo Rather Than Pitch For Perception of Musical Emotion

Meredith Caldwell³; Patpong Jiradejvong¹; Courtney Carver¹; Charles J. Limb^{1,2}

¹Department of Otolaryngology-Head and Neck Surgery;

²Peabody Conservatory of Music, Johns Hopkins University;

³Johns Hopkins University School of Medicine

Background

Music perception is difficult for cochlear implant (CI) users, primarily due to significant impairments in pitch perception. These impairments also lead to a reduced sense of enjoyment for many CI users when listening to music, which normally serves as an effective means of conveying emotion in normal hearing (NH) individuals. We sought to identify musical features that underlie perception of emotion in music in CI users, by creating musical melodies that were intended to convey emotions of both positive ("happy") and negative ("sad") valence. NH listeners utilize multiple musical cues to infer musical emotion, including pitch cues (tonality) and also rhythm cues (tempo), where major key and fast tempo stimuli are thought to be positive, and minor key and slow tempo are thought to be negative in emotional valence. In light of previous findings that CI users have largely intact rhythm perception but poor pitch perception, we hypothesized that CI users would rely on tempo cues rather than pitch cues to perform judgments of musical emotion.

Methods

A test battery of novel melodies was created that consisted of four-bar melodies with chordal accompaniment, played using piano tones. Each melody had four permutations, with alterations of tonality (major vs. minor) and tempo (presto vs. largo), in a 2x2 design that allowed us to present several versions of the same melody intended to provide either tempo or pitch information. The four versions included the following: major key/fast tempo, minor key/fast tempo, major key/slow tempo, and minor key/slow tempo. Three normal-hearing (NH) adults and one bilateral adult cochlear implant (CI)

user participated in the study. Participants were presented with each clip using free-field stimuli. After each stimuli, they were asked to provide ratings on a Likert scale of +5 (happy) to -5 (sad).

Results

Analysis of this pilot data revealed that CI users relied more heavily on tempo than on tonality, interpreting almost all fast-tempo clips as “happy” and all slow-tempo clips as “sad”, regardless of whether the melody was major or minor in key. In comparison, the NH group used both mode and tempo to drive ratings of emotion, with an even distribution of responses for ambiguous clips (minor/fast and major/slow). These findings suggest that CI users rely primarily on tempo rather than pitch to infer emotional valence of music.

Conclusion

CI users rely more heavily on tempo than tonality to determine musical affect, whereas NH individuals rely on both. These findings provide crucial information as to why CI users may not enjoy music following implantation. Furthermore, these results suggest that strategies for improvement of pitch perception should improve the ability of CI users to perceive musical emotion more accurately.

PS - 595

The Perception of Ultrasonic Tone Sweeps by Mice

Laurel Screven; David Holfoth; Katrina Toal; Micheal Dent
University at Buffalo, the State University of New York

Background

The ability to communicate with others implies a fundamental understanding of differences in the vocalizations that are created. In mice, acoustic communication includes vocalizations that differ in many characteristics, including frequency and duration. Mice are able to vocalize in ultrasonic frequency ranges, with many of their vocalizations in the 60-80 kHz range. The mice produce ultrasonic vocalizations (USVs) in social situations but their function is still somewhat unclear (Hanson & Hurley, 2012). Additionally, there has been little work done to show that mice are able to differentiate between their vocalizations. CBA/CaJ mice often produce upsweeping and downsweeping vocalizations (sweeps). Consequently, it is expected that the mice should not have difficulty differentiating between artificial pure tone stimuli within the same frequency range as their natural calls. Determining their ability to discriminate between these two artificially created stimuli will expand the current knowledge about acoustic communication in mice.

Methods

In the present study, the mice were trained and tested using operant conditioning procedures and positive reinforcement to discriminate between upsweeping and downsweeping pure tone stimuli. Multiple frequency ranges and temporal lengths of the stimuli were tested in a nose poking task. The animals were required to respond when they heard a change in the repeating background.

Results

The mice had difficulty discriminating between background and target upsweeps and downsweeps when the stimuli occupied the same bandwidths, even when the stimuli also differed in duration. However, when the sweeps occupied different frequency ranges, discrimination performance improved. For instance, when a repeating background downsweep ranging from 80 to 60 kHz was compared to a target upsweep ranging from 60 to 80 kHz, the mice could not discriminate between the two. On the other hand, when the target upsweep ranged from 50 to 80 kHz, discrimination was possible. Overall, bandwidth, not sweep direction or duration, appeared to be the primary cue for discrimination.

Conclusion

These results collected using artificial stimuli created to mimic natural USVs indicate that the bandwidth of vocalizations may be much more important for communication than the frequency contour of the vocalizations. This was surprising given the seeming complexity of many of the ultrasonic vocalizations of mice, and the many categories of vocalizations created by researchers attempting to understand acoustic communication in mice.

PS - 596

Temporal-Modulation Transfer Function of Bone-Conducted Ultrasonic Hearing in a Profoundly Hearing Impaired Patient

Takuya Hotehama; Seiji Nakagawa

National Institute of Advanced Industrial Science and Technology

Background

Ultrasound can be perceived via bone-conduction not only by the normal hearing but also by the profoundly hearing impaired. Thus, we have developed a novel hearing-aid using the bone-conducted ultrasonic (BCU) perception (BCU hearing aid: BCUHA) for the profoundly hearing impaired, which transmits a 30-kHz bone-conducted carrier that is amplitude-modulated by speech or environmental sounds. One of the most important problems for development of the BCUHA is to reveal how much information can be transmitted by the BCUHA to the profoundly hearing impaired patients.

Methods

In this study, to investigate the frequency characteristics of transmission of speech or environmental sounds by the BCUHA, we measured the temporal-modulation transfer functions (TMTFs) in a profoundly hearing impaired patient. TMTF shows the threshold of sinusoidal amplitude-modulation (SAM) detection as a function of modulation frequencies. The SAM detection threshold is determined systematically by measuring a detection of modulation depth. TMTF for 10, 20, and 30 kHz bone-conducted (BC) sounds were measured.

Results

The obtained TMTFs for all carriers commonly showed the low-pass characteristics in modulation frequency domain; the thresholds were low and roughly constant at low modulation frequencies from 10 to about 100 Hz and then begin to

increase at about 100-150 Hz as the modulation frequency increases. At the modulation frequency of about 800 Hz and higher, the detectability was disappeared. These findings indicate good agreement with the characteristics of temporal resolution of amplitude-modulated sound in the audio-sonic range.

Conclusion

Results of the TMTFs obtained from a profoundly hearing impaired patient indicated that substantial amount of information of the speech or environmental sounds in the low frequency can be transmitted by the BCUHA to the profoundly hearing impaired patients. And those results are useful information for further developments of the BCUHA.

PS - 597

Perception and Propagation Characteristics of Pinna-Conduction Hearing

Seiji Nakagawa¹; Takuya Hotehama²; Kazuhito Ito²

¹National Institute of Advanced Industrial Science and Technology (AIST) / Kansai University; ²National Institute of Advanced Industrial Science and Technology (AIST)

Background

Several mobile phones using a flat-panel loudspeaker that convey speech sound by vibrating the pinna have been commercialized (Fig. 1). In the pinna-conduction, it is thought that speech sounds are conveyed via both air- and bone-conduction pathways. Since the pinna consists of cartilage which shows strong non-linear properties, unique characteristics that differ from an ordinary bone-conduction may be observed in the pinna-conduction. To investigate peripheral mechanisms of the pinna-conduction, hearing thresholds, sound field in the outer ear canals, and vibrations of the head were measured when normal hearing subjects used pinna-conduction mobile phones.

Methods

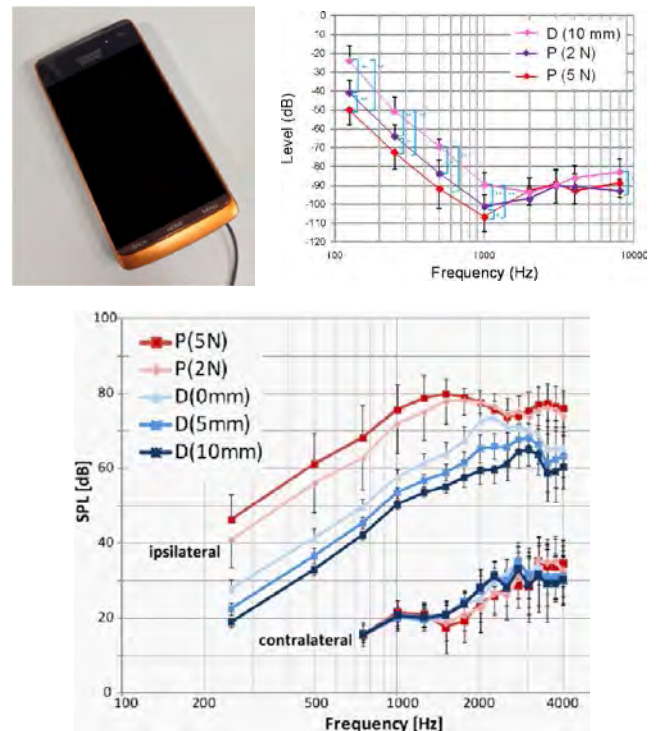
Hearing thresholds for tone bursts were measured by a three-alternative forced-choice procedure. Sound fields in the outer ear canals were measured using probe microphones, which is inserted into the both ear canals. Also, vibrations of the head were measured using accelerometers. In the contact conditions, contact pressures were set at 2 (pressed normally) or 5 N (pressed firmly). In the non-contact conditions, distances from the intertragal incisure were set at 0, 5, or 10 mm.

Results

Thresholds decreased linearly as the contact pressure increased below 1 kHz, whereas the contact pressure did not affect thresholds above 2 kHz (Fig. 2). Sound fields in the ipsilateral ear canal increased as the contact pressure increased or the distance decreased below 1 kHz, whereas the contact pressure did not affect sound fields above 2 kHz (Fig. 3). On the other hand no significant effects of the contact pressure or the distance were observed in the contralateral. In the vibration measurement, differences between the ipsi- and contra-lateral responses were smaller than the sound field measurement.

Conclusion

The results indicated that there are bone-conduction pathways from the pinna to the inner ear, which gets only sounds below 1 kHz through. Since similar characteristics were observed in the threshold and the sound field in the outer ear canal, it is suggested that the osseotympanic emission, sound emission into the ear canal from the inner wall, is a dominant component of the pinna-conduction. On the other hand, smaller inter-lateral differences of the vibration in the outer ear canal suggest an existence of significant amount of bone-conducted components other than the osseotympanic emission.



PS - 598

Acoustic Discrimination of Onset Rise Time Revisited

Björn Friedrich¹; Jesko L. Verhey²; Peter Heil¹

¹Leibniz Institute for Neurobiology, Magdeburg, Germany;

²Otto von Guericke University, Magdeburg, Germany

Background

Onsets are particularly salient features of sounds. The temporal shape of the onset contributes, among others, to its timbre. Previous studies suggest that just noticeable differences (JNDs) of rise times of pure tones and white noise are about 25–30% of the reference if the signals are clearly audible. For sound levels near threshold, JNDs increase. The notion that JNDs are a constant fraction of the reference (Weber's law) suggests that discrimination follows a multiplicative model, i.e. rise times should be analyzed on a logarithmic scale. The present study re-examines rise-time JNDs by measuring psychometric functions at three levels.

Methods

All stimuli had a fall time of 50 ms and a total duration of 400 ms and were presented at three different sound levels (10,

22, and 34 dB HL). They were either 3125-Hz sinusoids or broadband white noise. A method of adjustment was used with eight reference stimuli differing in their rise time (0.25–64 ms). The rise time of the test stimuli were adjusted to match that of the reference on a logarithmic scale (factor of $2^{1/6}$ between steps). For each of the 48 conditions (8 rise times \times 3 sound levels \times 2 carriers), 50 adjustments were made by every subject ($n = 10$), from which the psychometric functions were derived.

Results

The distributions of adjusted rise times are considerably better described by log-normal than by normal distributions. Therefore, the standard deviation was derived from a log-normal distribution fitted to the data. The JNDs estimated this way are (i) much larger than those in previous studies and (ii) depend on the reference rise time. This variation with reference times was most prominent for noise at low sound levels.

Conclusion

Rise-time equality judgments follow a log-normal distribution, which renders the arithmetic standard deviation, used as a proxy for the JND in previous studies, unsuited. JNDs for a change in rise time depend on the type of stimulus and sound level, and vary non-monotonically with reference rise time. Thus the data do not fulfill Weber's law. This suggests that listeners use multiple cues for rise-time discrimination and that their saliency depends on the stimulus parameters.

PS - 599

Human Pupil Dilation Responses to Auditory Stimulations: Effects of Stimulus Property, Context, Probability, and Voluntary Attention

Hsin-I Liao; Makoto Yoneya; Shunsuke Kidani; Makio Kashino; Shigeto Furukawa

NTT Communication Science Laboratories

Background

Pupil size is modulated by the locus coeruleus – norepinephrine (LC-NE) system, which is known to serve as an alert system that monitors salient and/or novel events in the environment. In the current study, we aim to examine whether pupil size can be used as a physiological marker for auditory salience, and if so, to investigate the factors determining auditory salience, such as stimulus properties, context, stimulus probability, and attention.

Methods

We measured participants' pupil size while they were given an auditory sequence with oddballs presented against repeated standard sounds. Stimuli were presented diotically for 50 ms in 300-ms inter-stimulus-intervals, and the interval between the oddballs was 9–12 s. In experiment 1, two types of oddballs, a white noise and a 2000-Hz tone, were used against repeated 1000-Hz standard tones. In experiment 2, only the white noise and the 1000-Hz tone were used, and they were interchanged as the oddballs and standards. The probability of the oddballs' occurrence was manipulated as 1%, 2%, or 10%. In experiment 3, the same procedure as experiment 1

was used, except that participants' attention was manipulated to be towards or away from the auditory stimuli.

Results

In all experiments, pupil size increased at the stimulus onset of the noise oddballs against the repeated 1000-Hz tones, and the effect of pupil dilation lasted about 4 s. In experiment 1, the pupil dilation to the oddball was larger for the noise than for the 2000-Hz tone against the background of 1000-Hz standard tones. In experiment 2, when the 1000-Hz tone were interchanged as the oddballs against the noise background, the pupil dilated to the 1000-Hz oddballs only when they appeared with about 1% chance, but not at 2% or 10% chance. The extent of pupil dilation to the noise oddballs did not differ among the probabilities we tested. In experiment 3, when attention was directed away from the auditory stimuli (i.e., engaged in a visual task), the dependence of pupil dilation on the stimulus property (i.e., larger pupil size for the noise than the 2000-Hz tone) remained as observed as when attention was directed to the auditory stimuli.

Conclusion

Pupil dilation can be used as a physiological marker for certain aspects of auditory salience. The interactions among stimulus properties, context, and stimulus probability are critical in determining the pupil dilation. The stimulus-dependent factor of pupil dilation appears to be independent of voluntary attention.

PS - 600

Change Detection in Multi-Speaker Scenes is Independent of Selective Attention

Christian Starzynski; Alexander Gutschalk
University of Heidelberg

Background

While we can follow one speaker among others, we may often miss the disappearance of another speaker from the same scene. Here, we tested the attention hypothesis of change deafness¹ using multi-speaker scenes where one speaker disappears in half of the trials. We expected enhanced MEG activity in auditory cortex when listeners are cued to one particular voice² and sought for similar enhancement in non-cued trials where speaker disappearance is detected, compared to trials where disappearance remains unnoticed.

Methods

Trials consisted of two 5-s scenes separated by a noise burst. Scene 1 comprised two male and two female speakers, drawn from a set of 24 speakers of German audiobooks. Scene 2 comprised either the same four speakers reading another passage, or only three of the four speakers. Listeners ($N=16$) indicated whether one speaker had disappeared. In another experiment, one of the speakers was played alone as a cue before each trial. Listeners ($N=12$) were instructed to attend to this speaker in scene 1 and indicate if the speaker disappeared in scene 2.

EG data were transformed into source space using dipoles fitted to a sine-tone localizer.

Speech-locked MEG signals were extracted by cross correlation between the MEG source signal and positive values of the first derivative of the target speakers' amplitude envelope.

Results

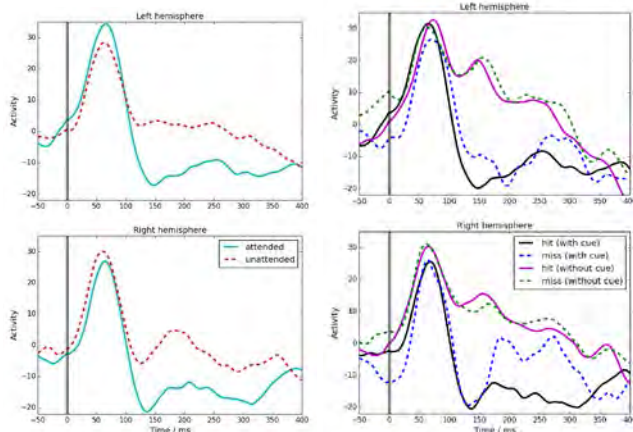
The hit rate (78.7% vs. 51.8%, $t=5.1$, $p=0.00003$) and the false alarm rate (30.4% vs. 12.7%, $t=2.9$, $p=0.012$) were higher for the cued experiment. The detectability (d') was not significantly different between cued and non-cued (1.5 vs. 1.45, $t=0.14$, $p=0.89$).

When listeners were cued to focus on one particular voice, the N1m response in auditory cortex was prominently enhanced for attended compared to unattended speakers². No significant activation difference was observed between hit and miss trials in both experiments. Comparison between the two experiments revealed a P2m that was only observed in the uncued experiment. It is unclear if this P2m is specific for the uncued experiment, or if attention driven negativity obliterates the P2m in the cued experiment.

Conclusion

These results suggest that selective attention as indexed by signal enhancement in auditory cortex does not support change detection. Potentially change detection can be alternatively based on speech or semantic² content, but this was difficult because the short segments were presented without context.

1. Eramudugolla et al. *Current Biology* 2005;15:1108–1113.
2. Ding & Simon. *J Neurophysiol* 2011;107:78–89.



PS - 601

Using Pupillometry to Measure Increases in Effort When Switching Attention Between Competing Streams of Degraded Speech

Eric Larson; Mihwa Kim; Adrian KC Lee
University of Washington

Background

Attention is a selective process that allows us to tune into one of potentially several possible sound sources of interest. The ability to intentionally redirect attention based on task goals and stimulus properties is critical to communication in many environments. However, such cognitive control mechanisms likely impose a cost (i.e., increased listening effort) on listeners. Here we examined how the cost of switching attention

changes when the auditory input is degraded via noise vocoding.

Methods

Subjects performed a task where they attended to one of two simultaneous auditory streams. Each stream consisted of four letters spoken by a male or female, and the subject was instructed to press a button any time the cued talker said the letter "O." The streams were processed using a noise vocoder with either 20 (easy) or 10 (hard) frequency bands to modulate the difficulty of stream segregation and selection. Within a given trial, the subject either maintained attention to the cued speaker over all four letters, or switched attention between the two talkers after the first two letters (e.g., attend male for the first two letters, then the female for the last two). On half of the trials, the duration of the silent gap between the second and third letter in the streams was decreased (600 ms to 200 ms) in order to increase the difficulty of attention switching. Eye tracking and pupil dilation measurements were performed concurrently, and pupil deconvolution was used to improve temporal analysis.

Results

Behavioral results suggest that, as expected, subject performance was substantially worse for the 10-band vocoder than the 20-band vocoder. Moreover, there was a clear cost of switching attention between the streams. Additional analysis of the pupillometry data also showed physiological evidence of these degradations in performance.

Conclusion

Behavioral and physiological results indicate increases in subject listening effort in challenging listening conditions.

PS - 602

Auditory Cortex is Highly Sensitive to Regularity in Sound Sequences

Nicolas Barascud¹; M. T. Pearce²; K. J. Friston³; T. D. Griffiths⁴; M. Chait¹

¹UCL Ear Institute, UK; ²Queen Mary University of London, UK; ³Institute of Neurology, University College London, UK;

⁴Newcastle University Medical School, UK

Background

A basic function of perception is to detect regularities in sensory input so as to facilitate the prediction, and hence processing, of future events. Here, we used psychophysics and magnetoencephalography (MEG) to investigate listeners' ability to detect the emergence of complex regularities (characterized by long repeating frequency patterns) in ongoing tone-pip sequences – and the degree to which this process is automatic or dependent on explicit attention.

Methods

Stimuli were sequences of 50 ms pure tones arranged according to four frequency patterns: **REG** – a regularly repeating pattern of R tones ($R=10, 15, 20$; new pattern for each trial). **RAND** – a sequence of tones of random frequencies. **REG-RAND** and **RAND-REG** sequences contained a transition between a **REG** and **RAND** patterns (transition time varying across trials). **CONTROL** stimuli consisting of a sim-

ple step change in frequency between two long pure tones were used to estimate basic response times (RT).

In the behavioural experiments ($N=16$), subjects actively detected the transitions in **REG-RAND**, **RAND-REG** and **CONTROL** stimuli (change occurred in 50% of the trials). The time required to detect the emergence and violation of regularity was estimated by subtracting the RT to **CONTROL** signals from that to **RAND-REG** and **REG-RAND**. In the MEG experiments ($N=16$; different subjects), naïve participants listened to the different stimuli while performing an incidental visual decoy task.

Results

Behavioural data reveal that listeners required about a cycle and a half to detect the emergence of regularity in **RAND-REG** signals. Since the transition is not detectable until at least one cycle has elapsed, this result suggests that the regularity pattern is acquired very rapidly, even before hearing two complete repetitions of the pattern. This behavioural performance closely resembles that of an ideal observer model with infinite memory. MEG data indicate that brain response latencies (when the subjects were *not* actively listening to the transitions) reliably match the RT data. A network of sources in Superior Temporal Gyrus and Inferior Frontal Gyrus are implicated in regularity extraction.

Conclusion

Our findings suggest that the auditory system is remarkably efficient at detecting the emergence of complex regularities in sound sequences, even for very long patterns. Furthermore, this detection does not appear to rely on explicit attention.

PS - 603

Effects of Reverberation During Attention Switching in Normal Hearing Listeners

Katherine Ingle; Eric Larson; Adrian KC Lee

University of Washington

Background

Humans are adept at understanding sound in complex acoustic environments, but we do not yet fully understand the listening effort (or cognitive load) associated with listening under different task demands or listening conditions. One non-invasive technique for quantifying cognitive load is to measure pupillometric responses during different tasks. The purpose of this experiment was to test whether increasing reverberation during a selective attention task could yield measurable increases in pupillometric responses indicative of increased cognitive load. We hypothesized that this may even occur if behavioral responses to reverberant and anechoic stimuli remained equivalent.

Methods

Subjects listened to male/male or female/female speaker pairs speaking four letters each (both talkers speaking simultaneously). The letter strings were modified to sound either reverberant or anechoic from the left and right hemifields (using HRTFs). They were cued at the start of each trial to either maintain attention to one of the speakers for all four letters (maintain-attention condition), or to switch attention between

the first two and last two letters (switch-attention condition). Subjects were instructed to press a button whenever they heard a specific target letter ("O") in the target stream. Eye position and pupil size were continuously recorded during the task.

Results

Subjects had a larger change in pupil diameter in the switch-attention condition compared to the maintain-attention condition in both reverberant and anechoic cases, and behavioral data showed a similar trend.

Conclusion

Cognitive load increases when listeners must switch attention between multiple talkers, and can be measured via pupillometry. This technique could prove useful in further research for hearing impaired or older listeners.

PS - 604

Listening Effort Measured Via Pupil Dilation: Outcome Measure of Cochlear Implant Frequency-Electrode Allocation Adjustment

Matthew Winn; Jan Edwards; Ruth Litovsky

University of Wisconsin-Madison

Background

Listening effort is elevated for people who have hearing loss, with consequences on health, occupational life, and social life. Clinical measures of speech recognition (e.g. accuracy scores for word and sentence identification) fail to quantify listening effort. Previous literature has shown that pupil dilation is a reliable, objective index of cognitive load during listening and is an extremely fine-grained measure. In this study, we aimed to establish pupillometry as a means to evaluate reductions in listening effort for people with bilateral cochlear implants (BiCIs).

Resolution in the spectral (frequency) domain remains a major problem for CIs. Complementary non-overlapping frequency-electrode allocation (e.g. "interleaved" or "zippered" channel maps) has been proposed as a means to increase bilateral cochlear implant (BiCI) signal clarity by reducing electrical current interaction in the implanted electrode arrays. Here, we obtain various measures to evaluate potential improvement from interleaved channel maps.

Methods

The main task was sentence recognition, which required no multitasking. Pupil diameter was measured during the sentence test using a Tobii60XL eye-tracker, filtered and normalized according to established techniques, and aggregated over the time between stimulus and response. Listeners also completed open-set word recognition and a test of spectral resolution using modified speech sounds. Ten BiCI listeners used their regular maps and the experimental interleaved maps for all tasks.

Results

Four of ten listeners showed reduced pupil dilation (less listening effort) when using interleaved maps compared to their everyday maps. Three listeners showed the opposite pattern

(greater effort), while three showed negligible difference between the two conditions. Results corroborate previous reports of wide group variability with interleaved maps, with relevant changes emerging at the individual level. Here, individual differences were revealed by patterns in pupil dilation, which was correlated with spectral resolution performance ($r^2 = 0.530$); individuals who showed increased resolution with the interleaved map also generally exhibited less listening effort with this map. However, word recognition did not predict improvements in spectral resolution or listening effort ($r^2 = 0.05$), underscoring the need for more direct sensitive measures.

Conclusion

Several BiCI listeners demonstrated reduced listening effort when using interleaved processing maps. Pupillometry can potentially serve as an outcome measure for clinical interventions on a group level or an individual level. In this case, effects emerged without elevation of task difficulty, such as masking or signal interruptions, and were generally not detected by word recognition alone.

PS - 605

Can You Divide Attention Across Two Streams or Are You Rapidly Switching Between Them?

Lindsey Kishline; Eric Larson; Adrian KC Lee
University of Washington

Background

When listeners divide their attention to multiple auditory objects, what strategy is deployed? Previously, divided attention has been looked at under the “spotlight” model of attention, borrowed from vision research, which predicts enhancement of specific spatial regions. However, the strategy used in attending to more than one spatial region is not definitively known. Recent behavioral studies on divided attention describe several models to account for divided attention, these include a rapid switching of attention, a broadening of the spotlight, and multiple spotlights in parallel Best et al (JASA ,2006; 120: 1506-16). In this study we investigate all three models and the behavioral performance associated with each.

Methods

In each trial listeners were presented with six repeating spoken letters [AUIOMB] distributed in azimuth [$\pm 90^\circ$, $\pm 30^\circ$, $\pm 10^\circ$], each trial lasts for 21 seconds with letters being presented with 1/6 of a second offset in rapid succession. Listeners were cued to attend to two of the letters and ignore the others on each trial, and to press a button when one of the target letters changed to an ‘R’. Listener’s had to discount distractor R’s that would occur in non target letter positions. In half the trials the temporal order of the two target letters were presented so that one target always preceded the second target, facilitating a rapid switching strategy. In the other half of the trials the target letters were presented in a random temporal order. There were two options for the spatial arrangement of the target letters; in half the trials the target letters were contiguous (had adjacent spatial locations), and the other half the target letters were separated by one or more

spatial locations. This allowed testing of a broadening versus parallel spotlight(s).

Results

We expect listeners will perform better when the temporal order of stream presentation can facilitate them in rapid switching between focus of attention amongst multiple streams compared to in conditions in which the temporal order of stream presentation is completely random.

Conclusion

Different performance was seen when target letters were contiguous.

PS - 606

Sounds in Sequence Modulate Dynamic Characteristics of Microsaccades

Makoto Yoneya; Hsin-I Liao; Shunsuke Kidani; Shigeto Furukawa; Makio Kashino

NTT Communication Science Laboratories

Background

Microsaccades are one component of fixational eye movements. Although microsaccades are not consciously perceived, they can be influenced by visual attention and even by auditory attention. In the current study, we used an auditory oddball paradigm to test our hypothesis that microsaccade behavior reflects the salience of auditory events. In addition to conventionally examined properties, such as amplitude and peak velocity, we computed damping factor and natural frequency by considering the response curve of a microsaccade as the step response of a second-order transfer function.

Methods

Participants were instructed to keep looking at the central fixation point on the computer screen, while listening to the auditory sequence with oddballs presented against repeated standard sounds. Auditory stimuli were presented diotically for 50 ms in 300-ms inter-stimulus-intervals. An auditory sequence consisted of 1000-Hz-tone standards with white-noise oddballs or of white-noise standards with 1000-Hz-tone oddballs. The probability of the oddballs was manipulated as 1%, 2%, or 10%. Eye movements were recorded using the Eyelink-CL system with a sampling rate of 1000 Hz and an instrument spatial resolution $< 0.01^\circ$. Microsaccades were determined with the algorithm reported in Engbert and Kliegl (2003). Based on the ballistic property of microsaccades, we calculated several dynamic characteristics (amplitude, peak velocity, overshoot, damping factor and natural frequency) from their shapes of the curves. The time evolution of each characteristic before and after presentation of auditory stimuli was examined.

Results

The presentation of noise oddballs induced a temporal decrease in the microsaccade rate, whereas the presentation of 1000-Hz standard tones did not. In addition, we confirmed a significant decrease in the damping factor of microsaccades with the presentation of noise oddballs. These effects of the noise oddballs did not differ among the probabilities we tested. In contrast, neither the standards nor the oddballs

induced any significant change in the dynamics of microsaccades when the 1000-Hz tones were used as oddballs.

Conclusion

The damping factor of microsaccades, which is an indicator of the accuracy in position control, temporally decreased with the presentation of a salient sound in a certain context. This result indicates that brain regions involved in microsaccade target selection, possibly the superior colliculus, could temporally lose control with changes in auditory inputs under a certain condition.

Reference: Engbert R, Kliegl R. Microsaccades uncover the orientation of covert attention. *Vision Res.* 2003; 43(9): 1035-45.

PS - 607

Auditory Context Effects in Normal-Hearing Listeners and Cochlear-Implant Users

Ningyuan Wang; Heather Kreft; Andrew Oxenham
University of Minnesota

Background

Auditory context effects, such as loudness recalibration and spectral contrast enhancement, have been observed in normal auditory and speech perception. These effects may help “normalize” the incoming sound and produce perceptual invariance in the face of the variable acoustics produced by different rooms, talkers, and backgrounds. Little is known about whether cochlear-implant (CI) users experience these effects. Discovering whether and how CI users experience auditory context effects should provide us with a better understanding of the underlying mechanisms, and may provide us with ways in which to improve CI processing to better approximate normal auditory perception.

Methods

We examined the effects of a long-duration precursor on the perception of both loudness and (spectral or place) pitch of a short-duration target stimulus, which followed the precursor after a 50-ms gap. In separate experiments, CI users were asked to compare the loudness or pitch of the brief target with that of a comparison stimulus of the same duration that was presented after a 2-s gap. The assumption was that the precursor may affect the perception of the target but not the comparison stimulus. The target stimulus was always presented to a middle electrode (electrode 8), and the position of the precursor was parametrically varied from electrode 2 through 14. The baseline comparison condition involved no precursor. When testing loudness, the current level of the precursor was set to 100% of the CI user’s dynamic range (DR), based on the maximum comfortable level and the target was set to 70% DR. The comparison stimulus was varied between 40% and 100% DR within each block of trials. When testing pitch, the current of the comparison stimulus was divided in differing proportions between electrodes 7 and 9 to vary its perceived pitch between the values obtained for electrode 7 alone and electrode 9 alone. Similar conditions were tested in normal-hearing listeners using a noise-vocoder simulation of CI processing.

Results

Preliminary data confirm effects associated with loudness recalibration and/or enhancement in normal-hearing listeners, with different patterns of results found in CI users. In contrast, no clear effects were observed on spectral pitch.

Conclusion

The outcomes so far suggest potential differences between normal-hearing listeners and CI users in their perception of context-induced effects. The results may provide a basis for signal-processing techniques that compensate for these perceptual differences.

PS - 608

Temporal Integration of Consecutive Tones Into Synthetic Vowels Demonstrates Perceptual Assembly in Audition

Jefta Saija¹; Tjeerd Andringa²; Deniz Başkent³; Elkan Akyürek⁴

¹University of Groningen, University Medical Center Groningen; ²University of Groningen, Faculty of Mathematics and Natural Sciences, Artificial Intelligence and Cognitive Engineering (ALICE); ³University of Groningen, University Medical Center Groningen, Department of Otorhinolaryngology / Head and Neck Surgery; ⁴University of Groningen, Department of Psychology, Experimental Psychology

Background

Temporal integration is the perceptual process where sensory stimulation is combined over time into longer percepts, which can span over ten times the duration of a minimally detectable stimulus. Particularly in the auditory domain, such “long-term” temporal integration has been characterized as a relatively simple function that acts chiefly to bridge brief input gaps, or as a perceptual grouping mechanism, which places integrated stimuli on temporal coordinates (i.e., preserving their temporal order information). These properties are not observed in visual temporal integration, suggesting that they might be modality-specific. The present study challenges that view.

Methods

Young normal hearing participants were presented with rapid series of successive tone stimuli, in which two separate, deviant target tones were to be identified. During the task, the targets were always sequential and never actually overlapping (ensured by a minimum inter-stimulus gap of 10 ms). Critically, the target tone pair could be perceived as a single synthetic vowel if they were interpreted to be simultaneous. Such an outcome indicates that during auditory temporal integration the order information of the target tone pair is lost.

Results

Despite the fact that the targets were always separated by silence, the listeners frequently reported hearing just one sound, the synthetic vowel. This was reported nearly as often as having heard both consecutive tones in the correct order.

Conclusion

These results demonstrate that auditory temporal integration, like its visual counterpart, truly assembles a percept from sensory inputs across time, and does not just summate or perceptually group time-ordered (identical) inputs, or fill gaps therein. This finding supports the idea that temporal integration is a universal function of the human perceptual system.

PS - 609

Neural Correlates of Auditory Streaming in Human Scalp Potentials Generated from the Brainstem and Thalamocortical Auditory Pathway

Shimpei Yamagishi¹; Sho Otsuka²; Shigeto Furukawa³; Makio Kashino³

¹Tokyo Institute of Technology; ²The University of Tokyo;

³NTT Communication Science Laboratories

Background

Neural correlates of auditory streaming have been reported both in subcortical and cortical sites. We have found the correlation between the auditory brainstem frequency-following response (FFR) and behavioral reports of subjective changes of perceived streams evoked by a prolonged exposure to a repeated acoustic pattern (Yamagishi et al., ARO 2013). To compare brainstem and higher sites, we examined how the middle latency response (MLR), which is generated from the thalamocortical auditory pathway, correlates with perceptual changes in auditory streaming.

Methods

The stimulus was a repeated triplet-tone sequence (ABA-ABA-...; A: 315-Hz tone, B: 400-Hz tone, -: silence). The duration of each tone was 50 ms, which included rising and falling cosine ramps of 10 ms. The duration of silence was 60 ms. The frequency difference between A and B tones was four semitones. Twenty-two normal-hearing adults participated in the experiment. The experiment consisted of 40 sessions. In each session, participants were presented with 200 repetitions of ABA- triplets. While listening, they pressed a button corresponding to one-stream or two-stream percepts whenever they experienced perceptual switching. At the same time, the scalp potential was recorded using a vertical one-channel electrode montage. The electrode placements were Cz (active), ipsilateral earlobe (reference), and forehead (ground). The recorded response was segmented at every onset of ABA- triplets and classified according to behavioral reports (one-stream or two-stream), then averaged within each perceptual category. The results were evaluated in terms of the peak of the averaged MLR waveform. The general waveform of the MLR has two negative peaks (Na, Nb) and two positive peaks (Pa, Pb). Peak-to-peak amplitudes (Na-Pa amplitude, Nb-Pb amplitude) were compared between perceptual categories (one-stream or two-stream).

Results

The Nb-Pb amplitude of MLR to the B tone in the triplet was significantly larger for two-stream than for one-stream percepts ($p=0.01$).

Conclusion

The MLR to the B tone reflects subjective changes of perceived streams. In our early study, a significant difference in the FFR between perceptual categories was observed at the A2 tone. This difference between the FFR and MLR suggests that processing in the brainstem and thalamocortical pathway differently contribute to auditory streaming.

PS - 610

The Role of Precursor in Tone Detection With Schroeder-Phase Complex Maskers

Hisaaki Tabuchi; Bernhard Laback; Piotr Majdak; Thibaud Necciari

Austrian Academy of Sciences, Acoustics Research Institute

Background

Phase effects with Schroeder-phase harmonic complex maskers have been attributed to the peakiness of envelope representation after passing the auditory filter. It has been proposed that fast-acting cochlear compression reduces the excitation level for peaky envelope representations, thus, reducing the amount of masking. To test this explanation based on compression, masker phase effects were measured with and without a precursor designed to elicit the medial olivocochlear reflex (MOCR). Activation of the MOCR is thought to reduce compression. To minimize across-channel processes, a narrow band Schroeder-phase complex was used.

Methods

The maskers were 40-ms harmonic complexes with 100-Hz fundamental frequency and frequency components from 3400 to 4600 Hz. The phase curvature C ranged from -1 to 1 with an increment of 0.25. The target was a 30-ms, 4000-Hz tone temporally centered at the masker. The precursor was a 400-ms, 800-Hz (off-frequency) or 4000-Hz (on-frequency) tone preceding the masker (precursor offset-to-masker onset gap = 0 ms). The precursor, masker, and signal were gated on and off with 5-ms cosine-squared ramps. Precursor and masker levels of 60 and 90 dB SPL were tested. Masking thresholds at 79 percent correct were estimated with an adaptive three-interval forced choice procedure from the right ears of six normal hearing listeners.

Results

There was no statistically significant difference between the off-frequency and no-precursor conditions. For both masker levels, masked thresholds decreased by about 10 dB as C varied from -1 to 0.5 and increased by the same amount as C varied from 0.5 to 1. The thresholds in the on-frequency precursor condition were relatively constant across different phase curvatures. Compared to the off-frequency and no-precursor conditions, the on-frequency precursor generally raised the thresholds; the greatest relative increases (about 10 dB) were found around C of 0, while the increase diminished as C approached +1 or -1.

Conclusion

The results for the off-frequency and no-precursor conditions are consistent with previous studies, showing a systematic masker phase effect. The overall smaller amount of masker phase effect in our study can be attributed to restricting the

spectral range of the harmonic complex to the width of one auditory filter. The lack of phase effect for the on-frequency precursor condition, presumed to activate the MOCR, supports an explanation of the masker phase effect relying on masker compression.

PS - 611

Auditory Perception of Statistically Blurred Sound Textures

Richard McWalter; Ewen MacDonald; Torsten Dau
Technical University of Denmark

Background

Sound textures have been identified as a category of sounds which are processed by the peripheral auditory system and captured with running time-averaged statistics [McDermott et al., 2011]. Although these sound textures are temporally homogeneous, they offer a listener with enough information to identify and differentiate sources. This experiment investigated the ability of the auditory system to identify statistically blurred sound textures and the perceptual relationship between sound textures.

Methods

Sound texture statistics for all samples were measured and the mean value for each statistic was computed across textures. This mean value represents the blurred state. Sound samples were then generated such that their statistics moved from the shared blurred state to the individual target statistics, or focused state, over the duration of 60 seconds. The subjects were asked to identify an image corresponding to the sound sample. Both the response selection and time selected were captured. The sound sample order and number of occurrences was randomized. The results from the first sound texture identification task were used to create a second identification task, where a 3 second duration blurred sound texture was presented. The degree of blur was selected as the point when the first quartile responded correctly. Additionally, a control test with the target sound texture statistics was conducted to ensure the subjects could perform the task.

Results

The results from 15 test subjects for the gradual blur experiment revealed that identification varied across textures, with the first quartile correct identification occurring between 73% blur for textures with strong low frequency modulation and 17% blur for textures with random sparse events. Correct identification of textures was achieved in 72% of presentations. The results for the second task show 53% correct identification, which suggests that the preceding greater blurred state has an effect on the identification of a sound texture. The control test showed a percent correct of 71, which suggests that the significance of the preceding blur reduced as the sound texture approached the target statistics.

Conclusion

The correct identification of sound textures depended on the preceding blurred state and varied significantly across textures, which draws parallels to visual recognition [Bruner et al., 1964]. The identification of sound textures with slow modulation was most robust to statistical blur, followed by high fre-

quency modulations and finally textures composed of sparse random events. These findings may aid in identifying how the auditory system groups different sound textures beyond their statistical properties.

PS - 612

Variable Time Courses in Auditory Space Shifts Induced by the Ventriloquism Aftereffect

Justin Fleming; Adam Bosen; Paul Allen; William O'Neill; Gary Paige
University of Rochester

Background

Persistent presentation of spatially offset auditory and visual targets causes a residual shift in the perception of auditory space toward the visual—a phenomenon known as the 'ventriloquism aftereffect.' Previous studies have shown that this shift can occur quickly, but the dynamics of the effect remain undetermined. The aims of this study were to characterize the ventriloquism aftereffect across and within subjects as well as the time-course of its acquisition.

Methods

We presented young adult subjects with exposure to a fixed audio-visual discrepancy while intermittently including sound localization trials to assess the effect of exposure on the perception of auditory space. Subjects first performed a block of sound localization trials to establish baseline performance. A set of 28 trials (50ms noise bursts) were presented across $\pm 30^\circ$ azimuth at 2m distance, each localized using a laser pointing task. Next, subjects completed two blocks of trials in which the sound localization task was interleaved with audio-visual exposure trials. Subjects were simultaneously presented with noise bursts paired with a flashing LED offset 8° to the left or right of the sound in different sessions, while covering the same $\pm 30^\circ$ field. The two exposure blocks were separated by a rest period, during which subjects were kept in darkness. Finally, subjects repeated the initial localization block. Throughout the experiment, subjects' heads were fixed and eye position was maintained centrally.

Results

All subjects showed a shift of auditory spatial localization toward the visual stimulus during exposure blocks that remained afterwards, albeit with reduced magnitude that differed among subjects. Sound localization trials within the exposure blocks revealed that the shift developed over time. Time constants varied widely by subject, from less than 10 exposure trials to over 50. For all subjects, maximum shifts during the second exposure block were larger than the mean shifts during the post-exposure block, suggesting a reversion toward baseline perception of auditory space. This residual shift averaged $\sim 3^\circ$, or about a third of the audio-visual offset during exposure. Further, if subjects showed a post-exposure shift in one direction, they shifted by a comparable magnitude in the opposite direction when retested with the opposite audio-visual discrepancy.

Conclusion

The ventriloquism aftereffect is a fast-acting form of auditory plasticity, the magnitude and time course of which vary sub-

stantially across subjects while remaining relatively uniform within individuals.

PS - 613

Temporal Coherence Leads to the Formation of Auditory-Visual Objects II: Detection of Auditory Timbre Deviants

Huriye Atilgan¹; Ross Maddox²; Adrian KC Lee²; Jennifer Bizley¹

¹University College London; ²University of Washington

Background

Everyday listening often requires that listeners are able to attend to some sound sources while ignoring others. Visual cues may provide an additional source of information that facilitates grouping of sound elements and enables listeners to successfully attend to target sounds. In this study we asked whether a temporally modulated visual stimulus (which itself contained no task-relevant information) could enhance the ability of listeners to detect brief timbre deviants occurring in a target stream.

Methods

Human listeners were presented with two simultaneous auditory stimuli and a visual stimulus of 14 s duration. The auditory stimuli were vowel sounds, which were modulated with uncorrelated low pass 7 Hz amplitude envelopes. Within each stream brief (100 ms) timbre deviants were inserted by morphing the reference vowel (/u/ or /a/) into a deviant vowel (/ε/ or /I/). A visual stimulus was presented centrally on a computer monitor and consisted of a gray disk with a white radius whose radius was also modulated by a low-pass envelope that either matched that of the target stream, the distractor stream, or was uncorrelated with either. Listeners were asked to report, by button press, timbre deviants that occurred in the target vowel, which started 1 s before the distractor stream. They were also required to press a button if the visual stimulus transiently changed color. Performance was assessed by calculating d' values from the observed hit rates and false alarm rates, where false alarms were button presses to deviants in the distractor stream

Results

Preliminary results (7 listeners) suggest that performance is significantly impaired when the visual stimulus has a modulation envelope that is temporally congruent with the distractor stream. In this condition hit rates were decreased and false alarms increased. Performance across subjects was statistically similar when the visual stimulus followed the same amplitude envelope as the target stream, and when the visual stimulus was independently modulated, although performance was variable across subjects.

Conclusion

A temporally modulated visual stimulus can influence the ability of listeners to segregate two concurrently presented competing auditory stimuli.

PS - 614

Visual Calibration of Auditory Distance Perception

Ľuboš Hládek¹; Christophe Le Dantec²; Aaron Seitz²; Norbert Kopčo³

¹P. J. Safarik University; ²University of California, Riverside, Department of Psychology; ³P. J. Safarik University, Kosice, Institute of Computer Science

Background

Ventriloquism effect (VE) occurs when a sound is perceived to originate from the location of a nearby visual stimulus. Ventriloquism aftereffect (VA) occurs if the shift in the perceived sound location persists even after the visual stimulus is removed. A recent study showed both these effects in the distance dimension [Hládek et al., (2013), Ventriloquism effect and aftereffect in the distance dimension, ICA Montreal, POMA Volume 19, pp. 050042]. A complex pattern of effects was observed, however, the baseline performance with no AV disparity was not measured in that study.

Methods

Two experiments were performed in a small reverberant room, similar to the previous study. Both experiments consisted of 2 sessions. In Experiment 1, listeners localized a 300-ms broad-band noise (A-only trials) coming from one of 8 loudspeakers placed in front of the listeners. On interleaved audio-visual (AV) trials, sounds were paired with visual signals (LEDs) that were aligned (AV-Aligned baseline) or displaced closer (AV-Closer condition) or farther (AV-Farther) from the sounds by 30%. The AV condition was kept constant throughout a session. In Experiment 2, subjects localized A-only stimuli without any interleaved AV trials.

Results

In Experiment 1, A-only performance differed from the AV performance even in baseline AV-Aligned sessions. As in previous study, VE was stronger in AV-Closer than AV-Farther condition, independent of the baseline used. However, VAs were very similar for both AV-Farther and AV-Closer conditions. Relative to AV-Aligned baseline, distance-dependence of the effects was smaller than in the previous study. In Experiment 2, learning effects were observed even without any visual stimulation.

Conclusion

The differences in the strength of VA and VE for AV-Closer vs. AV-Further conditions are in part due to differences in the baseline AV and A-only performances. However, given that the differences in relative effect sizes for VA-Closer vs. VA-Further conditions were observed even relative to the measured baselines, it is likely that different neural mechanisms underlie VE and VA in distance. In addition, when visual calibration of auditory distance occurs in reverberant space, spontaneous room learning occurs which is likely to interact with the effects of visually guided learning.

PS - 615

Deriving the “Salience Level” of a Target Sound Using a Tapping Technique

Shunsuke Kidani; Hsin-I Liao; Makoto Yoneya; Makio Kashino; Shigeto Furukawa

NTT Communication Science Laboratories, NTT

Background

Salience is an attribute of a sound related to the degree to which the sound captures attention. This study aimed to quantify the salience using a tapping technique. This technique is based on the assumptions that, when presented with a sequence of two alternating sound segments, a listener tends to tap on beat synchronously to the more salient sound of the two [Chon & McAdams (2012)], and that the presence of other loud sounds interferes with the tapping [Tsunoda (1975)].

Methods

The stimulus was a sequence of isochronously alternating tones (... RTRTRT...), where R is a reference sound (a pink noise burst) and T is a target sound to be evaluated. The stimulus was presented via a headphone. Ts included abstract sounds (e.g., white noise, tone) and environmental sounds (e.g., bell, animal call). The A-weighted sound pressure levels of T were always 65 dB. The listener's task was to tap with a button press on beat synchronously to the more salient sound of the two. The sound pressure level of R was decreased or increased when the listener tapped on R or T, respectively. An adaptive up-down method was used to find the level of R at which R and T were tapped at the same rate. This level of R was defined as the “salience level,” a higher salience level indicating the higher salience of T. The obtained salience levels were compared with the subjective rating values on salience and loudness scales (referred to as the salience and level values, respectively) derived through a paired comparison method.

Results

The obtained salience levels varied significantly among Ts (ANOVA; $p < 0.05$). There was a significant positive correlation ($p < 0.05$) between the salience level and the salience value, whereas no significant correlation was found between the salience level and the loudness value.

Conclusion

The salience level obtained by the tapping method reflects the subjective salience of T. The salience level is somewhat independent of subjective loudness of a sound, as indicated by the lack of correlation between the salience level and the loudness value.

PS - 616

The Influence of Task-Irrelevant Sounds and Images on Change Detection in Complex Acoustic Scenes

Ediz Sohoglu; Marjia Cauchi; Maria Chait

UCL Ear Institute

Background

The ability to detect sudden acoustic changes in the environment is critical for survival. Previous work has shown that

task-irrelevant sounds disrupt change detection performance in complex acoustic scenes, despite not physically masking the changes (Cervantes et al, 2012). In the current study, we asked whether change detection performance can be disrupted even when the task-irrelevant sound occurs after the critical time of change. In a second experiment, we asked whether detection performance can be disrupted crossmodally with visual images.

Methods

Listeners were presented with complex acoustic scenes containing four to fourteen pure-tone components, each with a unique frequency and amplitude rate (see Cervantes Constantino et al, 2012). Critically, components of each scene were separated by at least 2 Equivalent Rectangular Bandwidths to minimize physical masking.

There were two types of change for listeners to detect. In “change-appear” scenes, a new component was added to each scene after a variable period of time relative to scene onset. In “change-disappear” scenes, one component was removed from each scene. Performance was assessed relative to a control “no-change” condition.

In Experiment 1, we compared change detection performance when scenes were presented alone or in the presence of 20 ms task-irrelevant sounds (four-tone chords) occurring 0 to 150 ms after the time of change. In Experiment 2, the task-irrelevant events were single cartoon images taken from a previous study (Forster and Lavie, 2008). When present, these images appeared around a central fixation cross, either at the time of auditory change or at matched times in the “no-change” condition. In both experiments, listeners were told to focus on detecting scene changes and ignore the chords or cartoon images.

Results

We found that change detection performance was significantly reduced in the presence of the task-irrelevant sounds, even when presented up to 150 ms after the scene change. To our surprise, performance was *enhanced* (rather than disrupted) when the task-irrelevant events were cartoon images.

Conclusion

Our results suggest that task-irrelevant sounds need not occur precisely at the time of change to disrupt performance. Intriguingly, task-irrelevant images enhanced (rather than disrupted) performance. This visual effect is not easily attributable to general alerting because task-irrelevant sounds had the opposite effect. Instead, the auditory change transient might have perceptually fused with the visual signal and “popped out” of the scene (see Van der Burg et al., 2008). In ongoing experiments, we are further characterizing the origin of this crossmodal difference.

Temporal Coherence Leads to the Formation of Auditory-Visual Objects I: Detection of Auditory Frequency Excursions

Ross Maddox; Adrian KC Lee

University of Washington

Background

Listeners often need to listen to one sound source while ignoring another one. It is also common, such as in speech, that the source of a given sound is visible to the listener, and that features in both modalities change coherently. In this study we asked if a visual stimulus can lead to enhanced auditory perception, even if it offers no task-relevant information.

Methods

We presented listeners with two simultaneous auditory stimuli and one visual stimulus with a duration of 14 s. Each trial had two ongoing tone streams (440 and 565 Hz, counterbalanced) whose amplitudes were modulated by uncorrelated noise envelopes, low-pass filtered at 7 Hz. The target stream began 1 s before the distractor stream. The visual stimulus was a gray disc surrounded by a white ring whose radius also varied according to a low-pass noise envelope. The visual envelope matched either the i) target or ii) distractor tone stream, or iii) was uncorrelated to both. Listeners were instructed to respond by button press to brief (100 ms) up-down excursions (± 1.5 semitones) in the frequency of the target tone (ignoring those events when they occurred in the distractor stream). To encourage attention to the visual target, subjects were also required to respond to transient color changes in the outer ring of the visual stimulus. Performance was assessed by calculating d' from the observed hit and false alarm rates, where a false alarm was defined as a response to an event in the distractor stream.

Results

Results from 16 subjects show that performance is slightly but significantly better when the visual envelope matches the target audio stream versus the distractor. When all three envelopes are mutually uncorrelated, performance is not significantly different from either of the other two conditions.

Conclusion

Here we show that temporal coherence between a visual and auditory stimulus can influence auditory performance in the presence of a distractor. Crossmodal binding was created by co-modulating visual radius with auditory amplitude, but yielded enhanced performance in an auditory frequency-based task. This enhancement of an orthogonal stimulus dimension (about which no information was provided by the visual stimulus) suggests that subjects form audio-visual objects that allow distracting stimuli to be better ignored.

Audiovisual Speech Perception in 3-Year-Old Children: Effects of Competing Two-Talker Babble

Tina Grieco-Calub¹; Janet Olson²

¹*Northwestern University*; ²*Northern Illinois University*

Background

Speech perception is multimodal. Depending on the context, listeners can shift their perceptual weight to higher fidelity cues. For example, older children and adults derive benefit from congruent visual cues (i.e., lipreading) when listening to speech in the presence of acoustic competition (Sumby & Pollack, 1954; Sekiyama and Burnham, 2008). Although the ability to integrate auditory and visual speech cues is present in infancy, evidence suggests that younger children weight auditory cues. It is unclear, however, how the complexity of acoustic competition influences this behavior. This study tests the prediction that three-year-old children are sensitive to visual speech cues during language processing in quiet and in the presence of two-talker babble.

Methods

Spoken language processing was evaluated in real time using a 'looking-while-listening' task (Fernald et al., 1998). Participants were three-year-old, typically developing children ($N=20$). On each trial, children were shown two known objects on a large screen and instructed by a female speaker to look at one of the objects. Children listened either in the absence (quiet) or presence of two-talker babble (competitor; +10 dB or 0 dB signal-to-noise ratio). In each condition, children were either provided with auditory information alone or with audiovisual information via a video of the speaker (AV trials). Children's eye gaze was video recorded and coded offline (30 frames/sec) to determine eye position following the onset of the spoken label. Language processing was quantified by the time it took for children to identify the label (i.e., reaction time, RT) and overall accuracy of target-object fixation following the spoken label onset.

Results

Consistent with published data, children were proficient at visually identifying objects after hearing spoken labels in quiet. Children listening to target speech at +10 dB SNR were highly accurate; performance declined, however, in the more challenging competitor condition (0 dB SNR). Paired t-tests revealed significantly slower RTs in both the quiet and competitor conditions when visual cues were available (AV trials). Overall accuracy, however, was unchanged in the AV trials relative to auditory-alone trials. Slowed RTs suggest that children are attending to the visual speech signal; the absence of improved accuracy, however, suggests that this processing load is not aiding language processing.

Conclusion

Three-year-old children process visual cues on an audiovisual speech perception task in quiet and in the presence of two-talker babble. This additional processing load, however, does not result in improved accuracy. Findings have implica-

tions for audiovisual language intervention in preschool-aged children.

PS - 619

Induction of GATA3 and Brn3a Expression in Human Mesenchymal Stem Cells After Lentivirally Mediated Neurogenin-1 Expression

Athanasia Warnecke; Luisa Schäck; Stefan Budde; Henning Windhagen; Thomas Lenarz; Andrea Hoffmann
Hannover Medical School

Background

Human mesenchymal stem cells (huMSC) may be one source for the cell replacement therapy of degenerated neurons since they can be isolated from the bone marrow of the patient, their capacity for tri-lineage differentiation and their secretion for trophic factors. However, *in vitro* expanded huMSC did not integrate into the host tissue after transplantation to the inner ear. Thus, aim of this study was to pre-differentiate huMSC towards a neuronal fate *in vitro* prior to implantation for a better integration or prior to their use as biomimetic cell coating of electrodes.

Methods

In order to achieve these objects, the transcription factors neurogenin-1 or neuronal differentiation 1 were lentivirally overexpressed in huMSC isolated from bone marrow aspirates. For the induction of neuronal differentiation, incubation in neuronal medium was preceded by stimulation with neurotrophic factors, i.e. BDNF and GDNF/NT3 or retinoic acid.

Results

Using quantitative reverse transcription PCR, the increased expression of transcription factors expressed by developing primary auditory neurons, such as Brn3a (POU4f1) and GATA3, was detected after induction of Neurogenin-1 expression. In addition, the expression of the receptors TrkB and GFRa1 was induced by treatment with their specific ligands BDNF and GDNF. Immunocytochemically as well as by PCR, the expression of vesicular glutamate transporter 1 (VGLUT1) was also identified. Even though these changes in gene and protein expression were induced, alterations towards the typical bipolar or pseudomonopolar morphology were not observed as it would be expected in SGN.

Conclusion

The lentiviral modification of huMSC for the expression of neurogenin-1 as well as treatment with BDNF and GDNF were able to induce expression of some spiral ganglion specific genes/proteins. However, morphological changes were not observed under these conditions. Therefore, an optimization of the herein presented protocol is envisaged.

PS - 620

Merlin Supports Schwann Cell Proliferation and Axon Regeneration Following Nerve Injury

Kristy Truong; Iram Ahmad; Alison Seline; Tyler Bertroche; J. Jason Clark; Marlan R. Hansen

University of Iowa

Background

The role of merlin, the protein product of the *NF2* tumor suppressor gene, in Schwann cell (SC) neoplasia is well established, but its role in normal SCs homeostasis is less clear. As SCs support axon regeneration, including in spiral ganglion neurons (SGN), we used models of cochlear and sciatic nerve injury to explore the role of merlin in SC responses to nerve injury and their ability to support axon regeneration.

Methods

Rats were deafened by systemic kanamycin injection. Cochlear sections were immunostained with anti-phospho-specific merlin (p-merlin) and anti-neurofilament antibodies. Sciatic nerve axotomies were performed in P0Schdel39-121 mice, which harbor an inactivating merlin mutation in SCs, and in wild-type (WT) mice. Mice were injected with EdU to label proliferating cells. Cut and uninjured contralateral nerves were excised on days 7, 21, and 180 following axotomy and labeled for merlin, p-merlin, EdU and TUNEL (apoptosis). We also performed sciatic nerve crush in adult WT and P0Schdel39-121 mice. Recovery of nerve function at 7, 21, 60 and 90 days was assessed by measuring paw contact area and intensity on a pressure pad and by nerve conduction assays. A 2D dissector was used to quantify axon regeneration.

Results

As previously shown, treatment with kanamycin resulted in degeneration of SGN peripheral processes extending to the organ of Corti and merlin became phosphorylated in cochlear SCs correlated with the loss of nerve fibers. Likewise merlin became phosphorylated in sciatic nerve SCs following axotomy. Interestingly, P0Sch39-121 mice demonstrated a significantly lower rate of proliferation and apoptosis following sciatic nerve sectioning compared with WT mice. Functional studies showed decreased contact area and intensity of the injured paw 7, 21 and 60 days following nerve crush in P0SCHdel39-121 mice compared to the WT mice that recovered fully in both groups by 90 days post injury. This delayed nerve regeneration was correlated with a reduced density of regenerated axons and increased extracellular matrix deposition in P0SCHdel39-121 compared to WT mice.

Conclusion

Merlin becomes inactivated by phosphorylation in cochlear and sciatic SCs following nerve injury correlated with their re-entry into the cell cycle. Reduced proliferation of SCs and axon regeneration in P0SCHdel39-121 mice following nerve injury suggests a paradoxical role for merlin in supporting SC proliferation and axon regeneration following nerve injury.

Regeneration of Pre-Synaptic Sensory Functions May Not Restore Post-Synaptic Neurotransmission

Eric Mendonsa¹; Jinwei Hu²; Helen Xu²; O'neil Guthrie¹

¹Loma Linda Veterans Affairs Medical Center; ²Loma Linda University Medical Center

Background

Ablation of pre-synaptic sensory function is often followed by post-synaptic dysfunctions that cascade from the peripheral nerve to the central auditory nervous system. Therefore, regeneration of pre-synaptic sensory function is hypothesized to restore post-synaptic neurotransmission.

Methods

In the current study, we evaluate this hypothesis in a Long-Evans rat model of noise injury. The animals were exposed to a damaging level of noise and both pre and post synaptic cochlear functions were monitored at baseline and 1 day, 1 week and 1 month after the exposure.

Results

The results showed that the noise exposure was enough to suppress (relative to baseline) pre-synaptic sensory function as determined by distortion product otoacoustic emissions, cochlear microphonics and summing potentials. Additionally, post-synaptic neurotransmission was altered as revealed by auditory brainstem responses. However, during 1 month of recovery from the noise exposure, a given animal would exhibit regeneration of its pre-synaptic functions in the absence of post-synaptic neurotransmission. For instance, the temporal patterns and levels of pre-synaptic functional recovery showed no association with post-synaptic neurotransmission.

Conclusion

These results suggest that noise exposure may uncouple pre- and post-synaptic functions, such that post-synaptic activity suffers the greater loss. Additionally, the regeneration of pre-synaptic functions may not restore post-synaptic neurotransmission.

Serum-Free and Feeder-Free Derivation of Human Neural Progenitors With Fasciculated Architectures

Robert Duncan; Liqian Liu; Stacy Schaefer; Margaret Decker

University of Michigan

Background

Stem cell therapy holds the potential for a biological solution to hearing loss. While hair cell regeneration remains an exciting possibility, this area lags behind neural regeneration, where implantation of exogenous stem cell-derived neurons has already proven beneficial in some reports. Recent developments have made significant strides in auditory nerve fate specification using a variety of pluripotent stem cell types, but there is no current methodological consensus. We sought to establish serum-free and feeder-free culture conditions that

produced auditory-like neural progenitors from human embryonic stem cells (hESCs).

Methods

H7 hESCs were differentiated using a step-wise program for generating glutamatergic neurons, modified from Kim et al., PNAS, 2011. Embryoid bodies were pushed toward an ectodermal lineage with Noggin and dorsomorphin followed by rosette formation on Matrigel in the presence of retinoic acid and purmorphamine. Neural precursors were expanded and terminally differentiated in a Neurobasal-rich medium. Placodal marker expression was monitored by quantitative PCR and functional maturation examined with patch-clamp electrophysiology. To examine whether forced expression of Neurogenin-1 enhanced neurodifferentiation, hESCs and precursors were infected with adenovirus driving human Neurog1-2A-GFP. In some cases, infected cells were sorted by flow cytometry to obtain cultures with graded levels of Neurog1/GFP expression.

Results

Neural rosettes and progenitor cells exhibited upregulated expression of the proneural genes Neurog1-3 (~20-50-fold) and Ascl1 (>1000-fold) while downregulating the pluripotency genes Nanog and Pou5f1. Cells at these stages expressed otic markers Pax2/8, Pou4f1, and Gata3 as well as non-otic marker Pax6. Terminal differentiation of these precursors for 2 weeks produced cells exhibiting voltage-gated potassium and sodium currents. Forced overexpression of Neurog1 had no apparent impact on differentiation efficiency, assayed as %TUJ1+ cells. Interestingly, high density cultures of chemically-induced progenitors produced 3-dimensional aggregates with varying capacity for axon bundling. Fasciculated neurite projections varied from 0.1-1 mm and extended up to 1 cm in length.

Conclusion

A stepwise, serum-free, and feeder-free protocol was established in which otic markers were highly upregulated. The concomitant upregulation of other placodal markers suggests incomplete otic induction and heterogeneity in fate specification. Additional small molecules such as FGFs and Wnts may be required. Observation of thick axon bundles and tubular neural aggregates raises the possibility that ganglia-like architectures may be produced for whole-nerve replacement. Surprisingly Neurog1-overexpression had no apparent impact on differentiation efficiency, which may reflect limitations in the delivery vector or a fundamental difference between responses in mouse and human stem cells.

Transplantation of Terminally Differentiated Neurons Derived from IPS Cells Into Cochleae Using The 3D Collagen Matrix

Hiroe Ohnishi; Takayuki Nakagawa; Masaaki Ishikawa; Yousuke Tona; Nakarin Asaka; Juichi Ito
Kyoto University

Background

There are great expectations to pluripotent stem cells including iPS cells for clinical application and drug discovery. In the research area of inner ear biology, regeneration of spiral ganglion neurons using pluripotent stem cells have been investigated and the results indicate a possibility for functional recovery. In view of the translation such basic findings into the clinic, there are several issues to be resolved for the safety and efficacy as a therapeutic treatment. One of the issues is a risk of tumorigenesis, so we have to use terminally differentiated neuron for transplantation. However, terminally differentiated neurons are greatly damaged by detachment from culture surface. Therefore, in our study, in order to solve these problems, we established high-efficiency neural induction method, and prepared neuron on 3D collagen matrices.

Methods

Modifying to the method reported previously (Li et al., 2011, PNAS), human iPS cells were differentiated into neural stem cells (NSCs) without use of feeder cells and these NSCs were differentiated into neuron on matrigel coated culture vessels. We characterized these differentiated cells using immunostaining and RT-PCR and confirmed establishment high-efficiency neural induction method. Then, NSCs derived from human iPS cells were seeded on a 3D collagen matrix and differentiated into neurons on it using same method. We performed identification subtype of neurons on 3D collagen matrix using immunostaining. We also tested the survival of iPS cell-derived neurons cultured on a 3D collagen matrix after transplantation into guinea pig cochleae.

Results

Human iPS cell-derived NSCs showed expression of NSC markers and no expression of undifferentiated cell-markers. These iPS cell-derived NSCs enabled expansion without losing neuronal differentiation potency. After 14-day culture in a differentiation condition, the majority of cultured cells expressed a marker for glutamatergic neurons. iPS cell-derived NSCs seeded on a 3D collagen matrix were differentiated into neurons. After transplantation into normal guinea pig cochleae, we identified the survival of human iPS cell-derived neurons in the cochlea.

Conclusion

Our study revealed that our method for neural induction is highly efficient for generation of glutamatergic neurons from human iPS cells, and that culture of iPS cell-derived neurons on a 3D collagen matrix is a useful method for preparation of transplants.

Stem Cell-Derived Sensory Neurons: Electrophysiological Properties and High Frequency Stimulation

Karina Needham; Tomoko Hyakumura; Mirella Dottori; Bryony Nayagam
University of Melbourne

Background

In severe cases of sensorineural hearing loss where the numbers of auditory neurons are significantly depleted, stem cell-derived neurons may provide a potential source of replacement cells. The success of this therapy relies, among other things, upon producing electrically active neurons from stem cells that are able to correctly relay sound information to the brainstem. Here we examine the electrophysiological properties of stem cell-derived neurons and their ability to respond to the high frequency stimulation.

Methods

Using our published differentiation assay, whole-cell patch-clamp recordings were made from stem cell-derived sensory neurons displaying bipolar morphology (n=86), and cultured primary auditory neurons (n=17).

Results

Stem cell-derived neurons generated action potentials in response to membrane depolarization, and displayed voltage-gated sodium and potassium currents. General firing properties were considered relative to time in culture, and grouped into the following clusters on the basis of the mean number of days *in vitro* (DIV); 31 DIV (n=10), 35 DIV (n=29), 42 DIV (n=18), 48 DIV (n=15), and 53 DIV (n=14). There was no significant difference in resting membrane potential, threshold or firing latency over time. Stem cell-derived neurons reliably entrained to stimuli up to 20 pulses per second (pps), with 50% entrainment at 50 pps. A comparison with cultured primary auditory neurons indicated similar firing precision during low-frequency stimuli, but significant differences after 50 pps due to differences in action potential latency and width.

Conclusion

Stem cell-derived neurons did not entrain to high stimulation rates as effectively as cultured mammalian auditory neurons however their electrical phenotype is stable in culture and consistent with that reported for embryonic (day 15) auditory neurons.

Bone Marrow-Derived Stromal Cells Suppress Immune Responses Due to Xenografting in The Cochlea

Masaaki Ishikawa; Takayuki Nakagawa; Hiroe Onishi; Yousuke Tona; Nakarin Asaka; Yoshitaka Kawai; Juichi Ito
Kyoto University

Background

The ultimate goal of our project is to examine the efficacy of human iPS cells as a source for transplants aiming regeneration of spiral ganglion neurons. However, engraftment of hu-

man iPS cell-derived neurons or neural progenitors caused severe immune responses in grafted guinea pig cochleae. To resolve this problem, we examined the effects of systemic application of bone marrow-derived stromal cells (BMSCs) of guinea pigs on suppression of immune responses in cochleae due to transplantation of human iPS cell-derived cells.

Methods

Bone marrow was harvested from guinea pig femurs, and was seeded on tissue culture dish. Adherent cells were regarded as BMSCs, and prepared for administration at densities of 1.0×10^6 cells/ml in PBS after two passages. Human iPS cell-derived neural cells cultured on the collagen mesh were used as transplants. Guinea pigs were used as experimental animals. Before transplantation, spiral ganglion neurons of experimental animals were damaged by local application of ouabain. Human iPS-derived neural cells were transplanted into the scala tympani. All animals received intramuscular injections of tacrolimus during the survival period. On day 7 after transplantation, cochlear specimens were collected and provided for histological assessments. Four animals were treated with an intravenous injection of BMSCs immediately after transplantation, and other 3 animals without BMSC were served as controls.

Results

For infiltration of inflammatory cells, obvious infiltration of CD45-positive cells was identified in cochlear specimens without BMSCs treatment, suggesting that xenografts caused severe immune responses. In cochlear specimens with BMSCs treatment, infiltration of CD45 positive cells was limited. There was a significant difference in numbers of CD45 positive cells in the basal portion of the cochleae between two groups. Surviving transplants were identified in three out of four animals with BMSCs treatment, while no surviving transplants in animals without BMSCs treatment.

Conclusion

Present results indicate that systemic application of BMSCs has effects on suppression of immune responses in cochleae due to xenografting.

PS - 626

Cell Line Variability in the Differentiation of Human Pluripotent Stem Cells to an Otic Progenitor-Like Fate

Samuel Gubbels; Cynthia Chow; Su-Chun Zhang; Parul Trivedi

University of Wisconsin - Madison

Background

Pluripotent stem cells have the potential to generate any cell type in the body. Given this quality, human pluripotent stem cells can be used for developmental studies, disease modeling, drug discovery and potentially for therapeutic purposes. Notable progress has been made in applying human pluripotent stem cell technology towards these goals in organ systems such as the retina, central nervous system, peripheral nervous system and the cardiovascular system. Recently, several methods for the generation of inner ear hair cells

from mouse and human pluripotent stem cells have been described. Continued progress in this area of auditory research will require refinement of differentiation protocols to enrich the resultant otic progenitor and hair cell populations. One source of variability in human pluripotent stem cell differentiation can be an inherent predilection of each stem cell line to differentiate towards certain germ layer and progenitor cell derivatives. We hypothesize that different human pluripotent stem cell lines will have variable potency for generating otic progenitor-like cells upon differentiation under identical conditions.

Methods

Three commonly used and federally-approved human pluripotent stem cell lines were differentiated towards an otic progenitor-like lineage using a differentiation protocol we have developed through modification of an embryoid body-based neural differentiation protocol. We compared human pluripotent stem cell lines using a stepwise, longitudinal analysis of the expression of early otic gene and protein markers during the differentiation process using RT-PCR, q-PCR and immunocytochemistry.

Results

Individual human pluripotent stem cell lines demonstrated variability in their ability to differentiate towards an otic progenitor-like fate. The temporal pattern and level of expression of otic progenitor markers such as Pax2, Pax8, Six1, Eya1 and Dlx5 varied between cell lines upon differentiation under identical conditions. Individual cell lines demonstrated a high level of consistency in the expression of otic progenitor marker transcripts and proteins.

Conclusion

Human pluripotent stem cell lines appear to follow a similar transcriptional program upon otic differentiation, however there are important differences in the efficiency of individual lines in doing so. Our findings highlight the need to consider the effect of individual cell line variability in studies of Hu-PSC differentiation towards an otic progenitor and hair cell-like fate.

PS - 627

The Creation of a Hair Cell Line by Conditional Reprogramming of Otic-Stem Cells

Brandon Walters; Shiyong Diao; Jian Zuo
St. Jude Children's Research Hospital

Background

Hair Cells (HCs) are mechanosensory cells in the cochlea that detect sound and are responsible for our sense of hearing. There are only ~6,000 HCs in an entire ear and their low abundance impedes our ability to study them using many powerful modern techniques. A common approach for investigating cell types that are present in low abundance *in vivo* is to develop cell lines that can be grown and studied *in vitro*. Unfortunately, attempts to develop a cell line to study HCs *in vitro* have had only limited success, and thus far, no viable candidates have emerged. However, recent studies have identified a pool of stem cells within the cochlea (referred to as otic-stem cells) which can, under the right conditions, dif-

ferentiate into HCs *in vitro*. Unfortunately, these cells can only be isolated from neonatal cochlea and they stop dividing within 5-7 passages, thus preventing them from producing large numbers of HCs *in vitro*. Despite this limitation, otic-stem cells are an excellent candidate for creating a novel HC line if their senescence can be overcome

Methods

Otic-stem cells were harvested from postnatal day (P) P1-P4 mice, grown for 3-5 days in renewal media. Solid spheres were identified, harvested, and plated on a layer of mitomycin-C inactivated 3T3 cells, grown in F-media supplemented with rho-associated kinase inhibitors. Colonies were identified 5 days later, manually harvested, plated on coated plates, and allowed to differentiate for 14 days. If needed mRNA was harvested from the cultures, and HC associated genes were quantitated.

Results

The conditional reprogramming method for cell immortalization was first developed for epithelial stem cells from the breast and prostate. Here we applied this technique to otic-stem cells and demonstrate that otic-stem cells can be successfully conditionally reprogrammed, allowing them to grow exponentially, for at least 25 passages. Importantly the conditionally reprogramming technique did not appear to recruit non-otic stem cells to proliferate, as equal numbers of reprogrammed colonies or spheres form from the same population. Finally we demonstrated that conditionally reprogrammed cells retain the ability to form HC-like cells, as they up-regulated transcripts of several HC markers when differentiated.

Conclusion

Conditional reprogramming of otic-stem cells has allowed for the unlimited proliferation of these cells, and they appear to maintain the ability to form HC-like cells when desired. We hope to further characterize these cells to understand if they truly become HCs, and if they do so at similar rates to endogenous otic-stem cells.

PS - 628

Self-Assembling Peptide Amphiphile Nanogels Promote Grafted Stem Cell Differentiation Into Otic Neuronal Progenitors.

Augusta Fernando¹; Zafar Sayed¹; Chaoying Zhang¹; Eric Berns²; Nicholas Stephanopoulos²; John Kessler¹; Samuel Stupp²; Akihiro Matsuoka¹

¹Northwestern University; ²IBNAM

Background

Despite recent encouraging progress, the potential clinical use of human pluripotent stem cell (hPSC)-based therapies for regeneration of the inner ear is hindered by several critical hurdles—namely the long term survival of transplanted hPSCs and their effective neuronal differentiation. Recent studies have shown the survival and growth of transplanted stem cells are largely regulated by the recreated stem cell “niche” which is crucial to further stem cell therapies for the inner ear. The aim of this study was 1) to develop an appropriate

biochemical and biophysical “niche” for hPSCs with nanofiber-based peptide amphiphile (IKVAV-PA) gels both *in vitro* and in human cadaveric human temporal bones, 2) to be able to generate otic neuronal progenitors from human embryonic stem cells (hESCs) using growth factors and introduce them in the stem cell niche to support their survival.

Methods

Previously described hESC line WA07-Feeder dependent cell line was used in this study. Human ESCs were seeded on matrigel coated culture dishes and differentiated to otic neural progenitors (ONPs) by commercially available substrates. Following treatment with BMP4 and Noggin, immunocytochemistry and flow cytometry characterization produced a population of pre-placodal ectoderm (PPE), which was further differentiated to generate ONPs.

In vitro live/dead cell viability assays and EdU proliferation assays were performed in PA gels with cultured hPSCs and Matrigel was used as the control matrix. NESTIN was employed to confirm the presence of neuronal precursors. Two human cadaveric temporal bones were used to test the feasibility of using nanogels in a future clinical setting. The resultant vestibulocochlear nerve complex was harvested and sectioned for transmission electron microscopy.

Results

Cell viability assays in IKVAV-PA gels demonstrated adequate hPSC viability on days 5, 7, and 14 with minimal apoptosis. EdU cell proliferation assays on day 5 showed no proliferating cells, with NESTIN positivity on day 15 supporting hPSC maturation into a neuronal phenotype. All tests on the control Matrigel supported the generation of ONPs.

In a cadaveric temporal bone study, fluorescence corresponding to both IKVAV-PA gel and TRA 1-81 stained hPSCs was noted along the internal auditory canal following intracochlear injection.

Conclusion

Recreating a “stem cell niche” by providing self-assembling nanogels with the appropriate neurotrophins may be used to promote cell survival and neuronal differentiation in the future.

PS - 629

Micropatterned Silicone Substrates for Affordable and Reproducible Embryoid Body Formation

Stacy Schaefer; Sanskriti Varma; R. Keith Duncan
University of Michigan

Background

Stem cell differentiation protocols often begin with the formation of embryoid bodies, or EBs. These spherical cell aggregates are characterized by the expression of markers to all three embryonic lineages: ectoderm, endoderm, and mesoderm. Traditional methods for EB formation are marked by low reproducibility of EB size, a key factor in lineage specification. A more recent method that has improved reproducibility relies on forced aggregation in V-shaped microwells cast in polydimethylsiloxane (PDMS) culture-well inserts. The

commercially available AggreWell-800 format allows for tight control over EB size, and a single insert yields 300 EBs. However, while AggreWell plates are conveniently prefabricated, they are prohibitively expensive for many labs. We sought to duplicate AggreWell inserts in a simple and affordable way.

Methods

Negative casts from AggreWell inserts were created using 1.5% agarose. Agarose negatives were then filled with Sylgard 184 to create duplicates of the original inserts. Sylgard is an affordable, non-porous, non-toxic, and optically clear PDMS elastomer. Additionally, Sylgard can be coated with materials such as polyethylene glycol (PEG) and poly(2-hydroxyethyl methacrylate) (pHEMA) to further inhibit cell adhesion and thus promote EB formation. H7 human embryonic stem cells were seeded into AggreWell, uncoated Sylgard, PEG-Sylgard, or pHEMA-Sylgard inserts and cultured for 48 hours. Resulting EBs were examined for size, circularity, and differentiation potential.

Results

EB size was significantly larger on average between aggregates formed in PEG-Sylgard and AggreWell inserts ($P < 0.05$). No other statistically significant morphological differences were identified relative to AggreWell EBs. Moreover, expression of ectodermal, endodermal, and mesodermal markers (antibodies to Nestin, GATA6, and Brachyury, respectively) was detected in EBs from all three conditions. Semi-quantitative analysis of immunofluorescence levels in 20 EBs from each substrate group revealed no statistically significant bias towards any particular lineage.

Conclusion

Duplication of AggreWell inserts using Sylgard 184 is affordable, reproducible, and scalable in comparison to AggreWell. The inherently hydrophobic attributes of Sylgard 184 creates a low cell-attachment condition that does not require further modification by PEG or pHEMA. Sylgard microwells are capable of yielding EBs of comparable size and circularity to those formed by AggreWell, and the cells are capable of following all three lineages, including ectoderm, allowing for future use in differentiation of stem cells towards an otic fate.

PS - 630

The Controlled Generation of Otic Neuronal Progenitors from Human Embryonic Stem Cells

Chaoying Zhang; Augusta Fernando; Christopher Gouveia; John Kessler; Akihiro Matsuoka
Northwestern University

Background

Pluripotent stem cells are promising candidates for the regeneration of spiral ganglion neurons (SGNs), because they have the potential to increase the number of SGNs that are available for electrical excitation via a cochlear implant. The potential clinical use of pluripotent stem cell-based therapies for regeneration of SGNs is still hindered by a number of critical hurdles, including safety, dose of transplanted stem cells, tumorigenicity, efficacy of progenitor cell production, long term

survival in a supportive niche, appropriate and safe neuronal differentiation, cell delivery, integration at appropriate sites, immunorejection, and functional efficacy in hearing. The goal of this study is to elaborate on our current understanding/limitation of SGN regeneration through the controlled generation of functional human embryonic stem cell (hESCs) derived otic neuronal progenitors (ONPs) using diffusible ligands and the overexpression of relevant human transcription factors.

Methods

Cells from the H7/H9 hESC line were grown in hESC media on a feeder layer of irradiated murine fibroblasts and supplemented with 4 ng/ml of basic fibroblast growth factor (bFGF). Human ESCs were dissociated with 1% collagenase and plated on Matrigel-coated tissue culture plates as aggregates in N2B27 supplemented serum free medium (SFM). Combinations of various ligands (BMP4, Noggin, FGFs, WNT, and Sonic hedgehog) and neurotrophic factors (BDNF and NT-3) were used to promote stem cell differentiation. Nucleofection of hESC-derived pre-placodal ectoderm cells with PAX2 and PAX8 using an Amaxa® Cell Line Optimization Nucleofector® Kit (Lonza, Cologne, Germany) was also performed. Immunohistochemistry, RT-PCR, and q-PCR were used to characterize both the ligand-treated hESCs and the nucleofected hESCs.

Results

Immunohistochemical analyses indicated that ligand-treated hESCs expressed ONP transcription factors. In addition, extended treatment of these cells with FGF3, FGF10, and WNT1 in conjunction with BDNF/NT-3 for 14 days induced neurite formation indicating the morphologic change towards ONPs. Although a low efficiency of nucleofection was observed, several of the PAX2/PAX8 nucleofected hESCs expressed ONP transcription factors.

Conclusion

The controlled generation of hESC-derived ONPs can be successfully performed with diffusible-ligand treatments as well as nucleofection. Functional analysis of these cells could further advance stem cell replacement therapy of SGNs.

PS - 631

In Vitro Differentiation of Pluripotent Stem Cells With Co-Expression of MicroRNAs and Transcription Factors for Promoting Hair Cell Fate

Michael Ebeid; Prashanth Sripal; Jason Pecka; Timothy Hallman; Kirk Beisel; Garrett Soukup
Creighton University

Background

The mammalian inner ear lacks the capacity to regenerate hair cells (HCs). Strategies for guiding pluripotent stem cells (PSCs) differentiation into HCs represent a promising approach in regenerative research. An emerging paradigm in cell reprogramming is utilization of a combination of crucial factors regulating gene expression including transcription factors (TFs) and microRNAs (miRNAs). miRNA-183 family members (miR-183, miR-96, and miR-182) are required for

HC differentiation and maintenance. In addition, the TF Atoh1 is necessary and contextually sufficient for HC development. Other TFs including Pou4f3 and Gfi1 are also necessary for HC differentiation and survival. Our goal is to guide PSCs toward a HC fate by co-expression of HC specific microRNAs and TFs.

Methods

We have developed a series of plasmid vectors (pVs) for co-expressing various combinations of miR-183 family members, TFs (Atoh1, Pou4f3, or Gfi1), and red fluorescent protein (RFP) from a single open reading frame by ribosome-mediated cleavage of intervening viral 2A peptide elements. This series of pVs was converted to adenoviral vectors (AdVs) that can be used to efficiently transduce cells. HEK293 cells were used to validate protein expression by western blot (WB) analysis, RFP expression by fluorescence microscopy and flow cytometry, and miRNA expression by quantitative reverse transcription and PCR (qRT-PCR). Induced pluripotent stem cells (iPSCs) were transfected with pVs, and cellular morphology was assessed by fluorescence microscopy. Mouse embryonic stem cells (mESCs) were used to generate embryoid bodies (EBs) in suspension culture as a model that better recapitulates the embryonic microenvironment. EBs were transduced with AdVs to assess transduction efficiency by fluorescence microscopy, and to examine effects on cell morphology and differentiation.

Results

In HEK293 cells, vectors largely functioned as expected by yielding RFP expression and increased miRNA detection. Vectors encoding more factors yielded less RFP expression than simpler vectors, suggesting that protein expression is not equal among all vectors. However, WB analysis showed that Atoh1, Pou4f3, and Gfi1 are produced, although one viral 2A peptide element appeared to work inefficiently and may require redesign. Cytomorphological analysis of iPSCs transfected with pVs showed that miR-183 family in combination with Atoh1 uniquely produced some morphologically HC-like cells. EBs generated from mESCs were efficiently transduced with AdVs, and further analyses are pending.

Conclusion

Preliminary results suggest that combining HC-specific miRNAs and TFs may provide a more efficient means for differentiating HC in therapeutic strategies for HC repair.

PS - 632

Conditioning the Cochlea to Facilitate Survival and Integration of Exogenous Cells Into the Auditory Epithelium

Yong-Ho Park¹; Kevin F. Wilson²; Yoshihisa Ueda³; Hiu Tung Wong⁴; Lisa A Beyer⁴; Donald L Swiderski⁴; Yehoash Raphael⁴

¹Chungnam National University; ²University of Utah;

³Kurume University School of Medicine; ⁴The University of Michigan

Background

Inserting stem cells (SC) into the auditory epithelium (AE) of deaf ears is a complicated task due to the hostile, high potassium environment of the scala media (SM) and the robust junctional complexes between the epithelial cells which resist SC integration. To facilitate survival and integration of exogenous injected cells in the AE, it would be necessary to "condition" the cochlea: eliminate the high potassium concentration and reversibly open the cell-cell junctions of the AE. As a first step, we evaluated the survival of cells in artificial cochlear fluids *in vitro* and then conditioned the cochlea *in vivo* to facilitate survival and integration of exogenous cells into the auditory epithelium.

Methods

Cell survival in cochlear fluids was evaluated by monitoring fluorescence of mCherry labeled HeLa cells after adding artificial fluids (endolymph, perilymph or mixture of endolymph and perilymph) to the culture. *In vivo* experiments used neomycin-deafened guinea pigs. To render SM more hospitable to exogenous cells, we reduced potassium levels by (a) injecting furosemide intravenously, and (b) replacing endolymph with artificial perilymph. To disrupt adherens junctions in the AE, we injected sodium caprate via cochleostomy. We then injected HeLa cells into the SM. Changes of AE junctions were evaluated in whole-mounts stained for ZO-1. Presence of HeLa cells in the cochlea was evaluated by fluorescence stereomicroscopy followed by epi-fluorescence of AE whole-mounts. Effect of sodium caprate on spiral ganglion neuron survival was evaluated by assessing density of spiral ganglion neurons (SGNs) in Rosenthal's canal profiles.

Results

In culture experiments, cells exposed to artificial endolymph detached from the dish, became spherical and died within six hours. Cells cultured in perilymph or in the endolymph-perilymph mixture survived. *In vivo*, after introducing sodium caprate into the SM, gaps appeared between cells. Some transplanted HeLa cells appeared to adhere to the AE surface, but others appeared at the same focal plane as the native AE cells, suggesting that those exogenous cells integrated into the tissue. HeLa cells survived in the SM of conditioned cochleae for at least 7 days, but in un-conditioned (control) cochleae they died promptly. Transient opening of junctions in the AE with sodium caprate did not induce a drastic SGN degeneration throughout the entire cochlea.

Conclusion

With specially designed measures to condition the cochlea, the recipient tissue can be transiently modified to enhance survival and integration of exogenous cells after injection into SM.

PS - 633

A Coregulatory Network of NR2F1 and MicroRNA-140

David Cuthbertson; David Chiang; Fernanda Ruiz; Li Na; Fred Pereira

Baylor College of Medicine

Background

The orphan nuclear receptor NR2F1 is required for the development of the inner ear and cerebral cortex, as illustrated by (*Nr2f1*—/—) knockout mice in which neurogenesis, axonal guidance, neocortical patterning, and patterning of the cochlear sensory epithelium are affected. MicroRNAs (miRNAs) are small single-stranded RNAs that negatively regulate gene expression at the post-transcriptional level and have roles in the developing and functional inner ear, where their expression profiles change both temporally and spatially during embryogenesis and post-natal maturation. MiRNA mutations cause hearing loss and abnormal inner ear development. We investigated a proof-of-concept coregulation between NR2F1 and miRNAs to better understand the regulatory mechanisms of inner ear development and functional maturation.

Methods

A bioinformatic approach was used to identify miRNAs potentially targeted by NR2F1 (Montemayor et. al. 2010) and intersections with several online miR-target algorithms and databases to find the genes co-targeted by the miRNA and NR2F1. Target gene expression changes were validated by qRT-PCR analyses using inner ears from *Nr2f1*—/— and WT littermates. Cerebral cortex from C57Bl/6 mice were processed for chromatin immunoprecipitation (ChIP) assays to determine NR2F1 direct binding to target gene loci. Luciferase-Klf9-3'UTR reporter assays were performed to validate the regulation by miR-140.

Results

We identified 11 potential miRNAs that might co-regulate target genes with NR2F1. MiR-140 was found to be down-regulated by 4.5-fold ($P=0.004$) in the inner ear but not in the cerebral cortex of *Nr2f1*—/— mice compared to wild-type littermates. The *Klf9* gene was upregulated 2.9-fold ($p<0.01$) in the inner ear but not cerebral cortex of *Nr2f1*—/— mice and contains multiple binding sites for miR-140. We therefore focused our investigation on the coregulation of NR2F1 and miR-140 on the target gene *Klf9*. We determined that NR2F1 directly binds and regulates both *miR-140* and *Klf9* loci *in vivo* by ChIP and qRT-PCR analyses. By luciferase assay we showed that miR-140 directly regulates *Klf9* ($p=0.001$), implicating an example coregulatory network involving NR2F1, miR-140, and *Klf9*.

Conclusion

We have described and experimentally validated a novel tissue-specific coregulatory network between NR2F1, miR-140,

and *Klf9* in the inner ear and we propose the existence of many such coregulatory networks important for both inner ear development and function.

PS - 634

Effect of Visual Field Motion on Subsequent Perception of Self-Motion

Catherine O'Leary; Benjamin Crane; Shawn Olmstead-Leahey

University of Rochester

Background

When an object is moved in visual space there are two possible perceptions: 1) the viewer perceives external object motion or 2) the viewer perceives self-motion (vection). The latter occurs if the object motion involves a significant portion of the visual field. Thus perception of visual motion can be ambiguous. We aimed to expand the current understanding of vection by examining the effect of visual field movement (VFM) duration on the perception of subsequent self-motion. We hypothesized that longer duration VFM would produce greater vection and would thus require greater vestibular stimulation to null the perception of self-motion. To test this, we examined how VFM influenced vestibular threshold and bias.

Methods

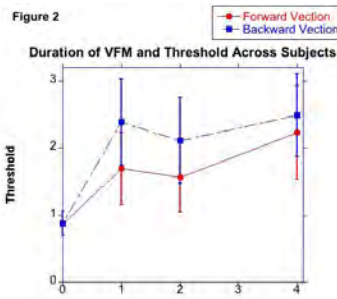
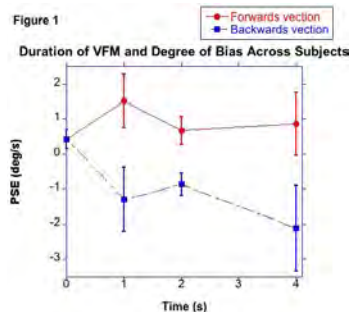
We recruited 8 subjects without previous history of vestibular symptoms and screened them to assure normal visual and vestibular function. Subjects sat on a hexapod motion platform. A visual star-field stimulus, filling 98° of the visual field, was presented at a constant velocity of 20 cm/s for 0 (no visual stimulus), 1, 2, or 4 seconds. Platform motion in the forward or backward direction occurred during the final 1s of the visual stimulus, during which subjects also heard an audible tone. The subjects reported the perceived direction of platform motion using a pushbutton device. The magnitude of platform motion was varied across trials in a staircase manner to determine the point of subjective equality (PSE). We calculated the peak velocity of the vestibular stimulus at the PSE to determine the degree of bias across different VFM durations. We examined the correlation of vection with platform peak velocity and VFM duration.

Results

In the absence of a visual stimulus, 7/8 subjects had little to no bias. Across subjects VFM significantly increased bias (ANOVA, $p=0.01$, Fig. 1) and threshold (ANOVA, $p=0.04$, Fig. 2) when compared to the control condition. When 1s or greater, the duration of VFM did not significantly increase bias (ANOVA, $p=0.33$) or threshold (ANOVA, $p=0.66$).

Conclusion

Perception of self-motion is biased by VFM. Longer duration VFM did not change bias or threshold. These results suggest that perception of vection is not a distinct form of multisensory integration.



PS - 635

The Influence of Target Distance on Dynamic Visual Acuity

Joshua Haworth¹; Kara Beaton²; Eric Anson³; Dale Roberts⁴; Michael Schubert¹

¹Johns Hopkins University School of Medicine; ²Johns Hopkins University Department of Biomedical Engineering;

³University of Maryland Department of Physical Therapy;

⁴Johns Hopkins University Department of Neurology

Background

During yaw head rotation while viewing near targets, the gaze stability required to overcome the translational motion induced from convergence of the eyes is greater than that required during pitch head rotation, as a result DVA may be worse for yaw vs pitch head rotation. The purpose of the study was to examine difference in DVA between yaw and pitch at near and far target distances.

Methods

We measured static (head still) and dynamic (sinusoidal pitch and yaw head movements) visual acuity with near (0.45m) and far (2m) targets in healthy individuals. During each test, subjects viewed a series of optotypes (letter "E" randomly rotated by 0, 90, 180, or 270 degrees) at Snellen acuity levels between 20/200 and 20/8(far) or 20/40(near). At each acuity level, subjects were presented with five force-choice trials in which they reported their perceived direction of the optotypes. In the dynamic tests, head movements between 120-180 deg/s triggered optotype presentation for 80ms. Display screen resolution was 1920x1200 (0.225mm/pixel, corresponding to angular resolutions of 8.73×10^{-6} deg/pixel at near viewing and 1.95×10^{-5} deg/pixel at far viewing). Scores were reported in logMAR units (logarithm of the minimal angle of resolution).

Results

We did not find any difference in DVA between pitch and yaw head rotation for near targets. However, DVA appeared to differ between near vs. far targets.

Conclusion

DVA appeared to be affected by near viewing in the manner we tested. This result, however, is limited by the differing acuity range we were able to produce for far and near testing. We are developing software to allow smaller optotypes for the near target distance. We expect this will lead to expanded findings on the impact of near viewing on DVA.

PS - 636

Vestibulo-Ocular Nulling: Quantifying Perceived Retinal Slip Without Recording Eye Movements

Kara Beaton¹; Ken Pierson²; Colleen McDermott²; Mark Shelhamer¹; David Zee¹; Michael Schubert¹

¹Johns Hopkins University School of Medicine; ²Johns Hopkins University

Background

We've recently developed an innovative approach to rapidly and unobtrusively quantify *perceived* retinal slip without recording eye movements. In the Vestibulo-Ocular Nulling (VON) test, head movement data controls the position of a visual target through a variable motion-gain in real-time. Subjects adjust this motion-gain until the target appears fixed-in-space with head movements (i.e., the subject "nulls" the target movement). By measuring the amount of illusory motion experienced for a given head movement, we can quantify the degree of perceptual impairment due to the VOR. The purpose of these experiments was to examine the perceptual vs. physiological differences in the vestibulo-ocular reflex by comparing our VON motion-gain to traditional VOR gain.

Methods

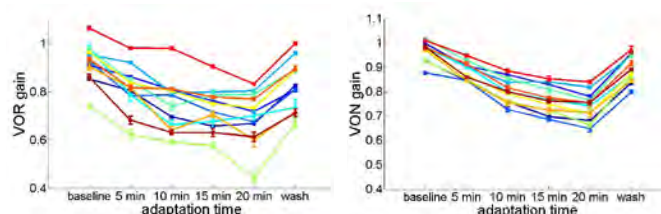
In this series of experiments, we compared VOR gain (measured via video-oculography) to VON motion-gain during a traditional lens-adaptation paradigm. Healthy subjects performed gaze-stability exercises (GSE) while wearing 0.5X minifying lenses to rapidly down-adapt their VOR gain. GSE were performed in the light during 5 minute blocks for 15 or 20 minutes total. VON motion-gain and VOR gain, measured in complete darkness, were recorded between blocks.

Results

During VON testing, subjects successfully nulled target motion rapidly (within several seconds) and consistently throughout adaptation. Both VON motion-gains and VOR gains showed adaptation, but VON motion-gains were considerably more consistent across subjects (Figs. 1 and 2); follow-on experiments indicated that this was due to the difficulty in imagining remembered targets in the dark during the VOR testing. Moreover, perceived retinal slip (VON motion-gain) was less than physiological retinal slip (VOR gain) throughout adaptation.

Conclusion

VON motion-gain provides a rapid, reliable measure of perceived retinal slip. By quantifying this perceptual deficiency in the VOR, we are able to define a 'real-world' performance metric that may have more utility than VOR gain alone.



Sensorimotor Assessment and Rehabilitation Apparatus (SARA): A Portable Device For Rapid Evaluation Of Sensorimotor Function

Michael Schubert¹; Kara Beaton¹; Dale Roberts¹; Mark Shelhamer²

¹Johns Hopkins University; ²National Aeronautics and Space Administration, Johnson Space Center

Background

Exposure to novel gravitational environments during space-flight elicits modulations in otolith signaling, disrupting multiple sensorimotor subsystems simultaneously. Functional consequences include disorientation, dizziness, postural and locomotor instabilities, motion sickness, and an impaired ability to read. We are interested in how these interdependent sensorimotor subsystems are functionally coordinated during adaptation to novel environments and in the development of portable technologies that can both rapidly evaluate these systems and be used as countermeasures to ameliorate related symptoms. The goal of our NASA-funded project is to develop a hand-held sensorimotor assessment to measure changes in sensorimotor function during and following space-flight. We call this device SARA: *Sensorimotor Assessment and Rehabilitation Apparatus*.

Methods

SARA incorporates a tablet computer, small (watch-size) three-axis wireless motion and surface EMG sensors, and a pair of red-blue eyeglasses (one lens is red and the other is blue). Combining this simple hardware with clever analytical algorithms, we can assess changes in multiple sensorimotor subsystems quickly, on the order of several seconds to minutes. Specifically, SARA evaluates the vestibulo-ocular reflex, ocular skew and torsional disconjugacy, spatial orientation, posture, and locomotion.

Results

SARA's operational capabilities have been validated during several rounds of parabolic flight testing over the past few years. To-date, we can measure changes in coordinated postural and locomotor movements during lunar-g and following altered g-level exposure (e.g., during 1g post-flight testing). The oculomotor tests in SARA show a clear increase in the variability in VON and skew responses in altered g-levels. Procedural and algorithmic modifications are currently ongoing to improve SARA's capacity to more explicitly show the characteristic changes in vestibulo-ocular reflex during different g-levels. SARA has also been used in ground-based laboratory experiments to track systematic changes in sensorimotor function during adaptation to externally-imposed perturbations, such as magnifying lenses or limb vibration.

Conclusion

Here we describe the development of a hand-held sensorimotor assessment tool (SARA) and describe its ability to measure changes in sensorimotor function in both parabolic flight and laboratory environments. SARA's portability and rapid assessment makes it an ideal tool for scientists, clinicians, and researchers to quickly quantify sensorimotor function

with minimal resources (time, equipment, personnel). Future work will include the development of individualized rehabilitation protocols, based on the assessment results output by SARA.

Relationship Between Visual Influence on Path Integration and Landmark Navigation Ability

Kishiko Sunami; Hidefumi Yamamoto; Yuki Koda; Hideo Yamane

Osaka City University Graduate School of medicine

Background

Our spatial perception consists of three parts: allocentric representation, cognition based on absolute position information such as direction and distance; egocentric representation, cognition based on self-centered relative position information such as front, back, right, and left; and path integration, one's own internal spatial perception. Egocentric representation mainly uses visual sense information, for which the parietal association area is mainly used. In order to construct egocentric representation as allocentric representation, which is an absolute spatial representation, experts believe that the functions of hippocampus and parahippocampal gyrus are necessary. We animals are constantly moving, so we need to perceive how we are moving and constantly update spatial cognition. This internal spatial cognition inside us is path integration. Animal experiments have reported that path integration is recognized through visual and olfactory information and vestibular stimulation. Of them, vestibular stimulation is considered to play a large role in path integration. This study investigated Landmark navigation, the ability to convert the function of path integration and egocentric spatial cognition to allocentric spatial information, and examined the association of these functions.

Methods

8 healthy adults without a history of vestibular or central disorder were reviewed for the following: 1) -1 Path integration (distance) a) walk 15 m with eyes closed, and return to the starting point with closed eyes; b) walk 15 m with eyes open, and return to the starting point with eyes closed. 1) -2 Path integration (angle) a) walk 1 m with closed eyes, rotate 60°, 90°, 120°, 240°, 270°, or 300°, walk 1 m again, and return to the starting point by following the last track with eyes closed; b) Move in the same manner with eyes open, and return to the starting point by following the last track with eyes closed; 2) Using a computer software on visual spatial cognition conversion ability on landmark navigation, the ability to convert egocentric spatial cognition to allocentric spatial cognition and vice versa were investigated.

Results

1) -1 Visual input helped improve path integration (distance). 1) -2 Visual input had no association with path integration (angle). 2) The ability to convert allocentric representation information to egocentric representation information tended to correlate with improvement in path integration using visual input.

Conclusion

In this study, distance path integration improved using visual input.

Previous studies have reported the effects of visual input in improving angular path integration. These experiments examined the reproducibility of path integration in the presence or absence of visual input. Visual input did not have an effect in improving angular path integration in this study. This may be attributed to a difficulty in reproducibility, because the examination method required the subjects to walk and turn repeatedly, thus demanding them to make several turns.

Based on the confirmation of a person’s current position by allocentric and egocentric representation and integrating this with information from his trajectory, namely path integration, a person can understand his movement and position in space. The ability to convert allocentric representation information to egocentric representation information tended to correlate with improvement in path integration using visual input. Experts have reported that this ability to convert allocentric representation information by visual input to egocentric representation information and vice versa, i.e., landmark navigation, is strongly associated with the hippocampus. It can be assumed that visual information processing during path integration is also related to the functions of the hippocampus.

PS - 639

Ocular Vestibular Evoked Myogenic Potentials Are Modulated by Increased Intracranial Pressure

Robert Gürkov; Reza Wakili; Klaus Bartl; Claudia Kantner
University of Munich

Background

Ocular vestibular evoked myogenic potentials (oVEMP) represent extraocular muscle activity in response to vestibular stimulation. We sought to investigate whether oVEMP are modulated by increasing intracranial pressure (ICP).

Methods

20 healthy subjects were enrolled in this study. Air-conducted sound was used to elicit oVEMP with the subjects lying supine on a tilt table. In order to elevate the ICP, the table was stepwise tilted from the horizontal plane to a 30-degree-declination, corresponding to a 0°, 10°, 20° and 30° head-down position. At each inclination angle, oVEMP recording was performed in two head positions: 1) the head in line with the body and 2) the body tilted while the head was positioned horizontally.

Results

When tilting both the body and head, oVEMP amplitudes gradually declined from 4.59 µV at 0° to 2.24 µV at 30° head-down position, revealing a highly significant reduction of amplitudes for the tilt angles of 10, 20 and 30° when compared to the baseline value (p < 0.001). In parallel, the response prevalence decreased and latencies prolonged. Similar effects were observed when the body was tilted but the head positioned horizontally, even though the decrease of oVEMP amplitudes was less pronounced. A gravito-inertial force effect upon the otolith organs could thereby be excluded as a possible confounder. According to a regression analysis, the dependence of amplitudes on the level of inclination can be expressed by the following formula: $y = -0.7848 \cdot x + 5.3951$ ($R^2 = 0.9995$). In the range of 0° to 30°, there was thus a linear correlation between tilt angle and oVEMP amplitudes.

fect upon the otolith organs could thereby be excluded as a possible confounder. According to a regression analysis, the dependence of amplitudes on the level of inclination can be expressed by the following formula: $y = -0.7848 \cdot x + 5.3951$ ($R^2 = 0.9995$). In the range of 0° to 30°, there was thus a linear correlation between tilt angle and oVEMP amplitudes.

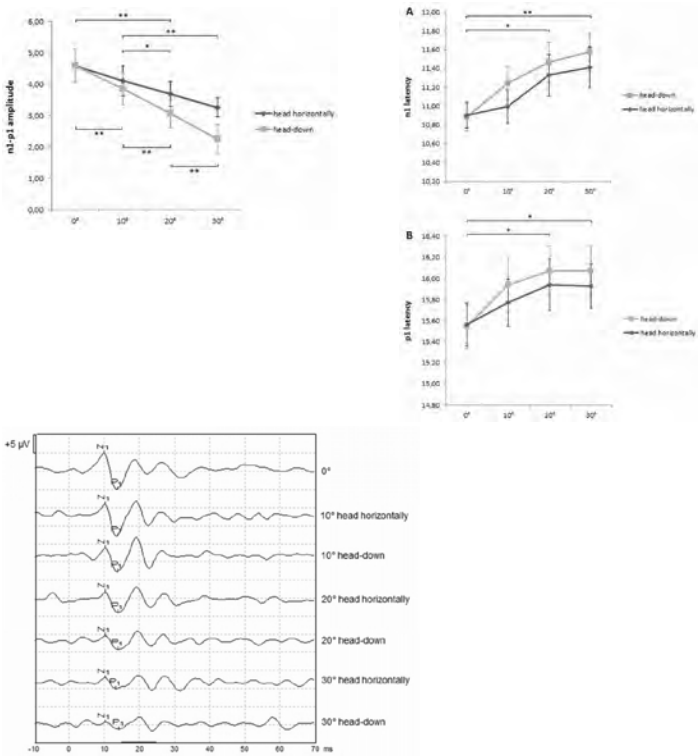
Conclusion

oVEMP were modulated in response to increasing intracranial pressure induced by head-down position. In the range of the horizontal plane to a 30° head-down tilt, there was a linear correlation between oVEMP amplitudes and the inclination angle. oVEMP are therefore in principle suitable as a new method of non-invasive ICP measurements.

Table 1: Amplitudes and latencies recorded in different positions (n = 40).

	n1-p1 amplitude (µV)	n1 latency (ms)	p1 latency (ms)	Response prevalence
Supine position				
10° head horizontally	4.59 ± 0.54	10.88 ± 0.15	15.54 ± 0.21	39 (98 %)
10° head-down	4.11 ± 0.53	10.99 ± 0.18	15.77 ± 0.22	39 (98 %)
20° head horizontally	3.85 ± 0.48	11.24 ± 0.18	15.94 ± 0.25	39 (98 %)
20° head-down	3.69 ± 0.45	11.33 ± 0.22	15.94 ± 0.24	39 (98 %)
30° head horizontally	3.25 ± 0.46	11.41 ± 0.22	15.93 ± 0.21	37 (93 %)
30° head-down	2.24 ± 0.30	11.58 ± 0.20	16.07 ± 0.23	35 (88 %)

Values are expressed as mean ± SE.



Head and Trunk Stability During Roll Motion With Galvanic Vestibular Stimulation

Miguel Pereira¹; William Paloski¹; Scott Wood²

¹University of Houston; ²Azusa Pacific University

Background

The purpose of this study is to characterize the influence that the vestibular system has on head and trunk stabilization during roll motion disturbances. It has been shown before that, with a visual reference, the head tends to deviate toward earth vertical during roll motion, presumably to stabilize gaze and spatial orientation. This study extends on those findings by adding an external vestibular stimulus during roll-motion disturbances with and without back support, and using both perceptual and functional tasks.

Methods

Perception and closed-loop nulling performance in the roll plane was measured in 11 healthy subjects inside a motion simulator. The simulator utilized a Stewart-type motion base (CKAS, Australia), single-seat cabin with triple scene projection covering 150° horizontal by 50° vertical, and joystick controller. The simulator's cabin moved following a sum-of-sinuosoids signal (0.02 Hz - 0.2 Hz), chosen to be within the range of otolith-mediated tilt responses. Subjects were instrumented with electrodes on the mastoid processes, which were connected to a current stimulator that produced pseudorandom Galvanic Vestibular Stimulation (GVS) during some trials (± 3.5 mA peak-to-peak). Subjects were also instrumented with inertial sensors on the head and trunk to measure their head and trunk motion relative to upright. During eyes open conditions subjects viewed an Earth-referenced visual scene (horizon and vertical lines). For the perception task, subjects were asked to report their perceived tilt during roll axis disturbances by maintaining the joystick aligned with Earth-vertical. For the nulling task, subjects were asked to null roll axis disturbances using the same joystick. Both tasks were presented with GVS on/off, with/without backrest support, and with eyes open/closed in a block-randomized manner.

Results

As expected, perceptual and nulling performance decreased with GVS on condition, and improved with a visual reference. Head and trunk movements were also less compensatory with GVS on. Subjectively, several subjects noted relying on somatosensory cues more during the removal of a back-rest.

Conclusion

We conclude that head stability during passive roll motion depends on the context and integration of multiple senses, with vestibular detection of head tilt providing a key reference. Head and trunk stability appears well correlated with both perceptual errors of tilt as well as functional performance in nulling tilt disturbances.

Influence of Head and Body Tilt on Perception of Fore-Aft Translation

Benjamin Crane

University of Rochester

Background

The otoliths equivalently sense gravity (tilt) or linear acceleration due to translation. Although the laws of physics do not permit any accelerometer to differentiate the two, they must be disambiguated to maintain orientation in space. The prior literature has implicated several factors in this disambiguation including stimulus frequency, semicircular canals, and extra-vestibular sensory cues. During ambulation, the head tilts during translation which adds additional complexity as the position of the head relative to the body must be determined. Effects of head/body orientation on translation perception have not previously been investigated.

Methods

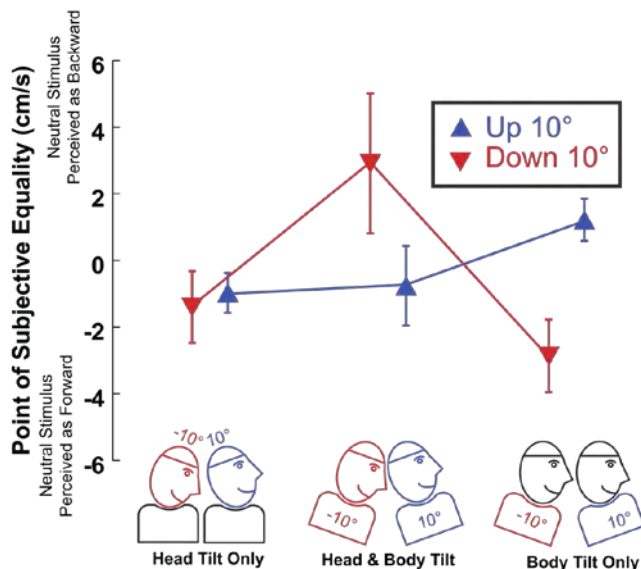
Eleven human subjects (7 female, age 41 ± 18 years, range 22 – 66) were tested during fore-aft (surge) motion. After each 2s translation subjects pressed a button to indicate the perceived motion as forward or backward. Stimuli were randomly interleaved in which subjects were tilted forward or backwards by 10°. In one block the subject tilted their own head $\pm 10^\circ$ while the body remained level, in another block the head and body tilted together, and in the final condition the body tilted while the subjects tilted the head in the opposite direction so the head remained level in space.

Results

Head tilt while the body remained upright did not influence perception of fore-aft motion ($p > 0.05$, Fig. 1). Tilting the body and head together biased the perception of fore-aft motion such that during pitch down (PD) a neutral movement was significantly ($p < 0.001$) more likely to be perceived as backward and during pitch up (PU) neutral motion was likely to be perceived as forward (Fig. 1). Thus during PD the point of subjective equality (PSE) at which motion was equally likely to be perceived as forward or backward was shifted forward and vice-versa for PU. When the body was tilted but the head remained stable in space the influence on perception was highly significant ($p < 0.001$) but opposite that which occurred during head and body tilt.

Conclusion

Tilt can be perceived as translation when the head and body are tilted together but not when only the head is tilted. Thus head-on-body position as determined through either proprioception or motor efferent copy is likely used to correct for the tilt-translation ambiguity. In the unnatural situation in which the body tilts but the head remains stable, this 'correction' works in an inappropriate direction.



PS - 642

Presynaptic Influence of Changes in Otolithic Drive on the Conditioned Soleus H-Reflex

Apollonia Fox; David Kocaja; Koichi Kitano

Indiana University

Background

The vestibular system has both direct and indirect connections to the soleus motor pool via the vestibulospinal and reticulospinal tracts. This vestibular information is one factor affecting sensorimotor integration within the spinal motor pool. Previous studies indicated a facilitation of the soleus H-reflex caused by tilting. While the mechanisms underlying spinal modulation are well established (eg. presynaptic inhibition), the connections from vestibular nuclei to the specific mechanisms within the spinal cord are not known. The purpose of this study was to identify whether tilt changes the amount of presynaptic inhibition in the soleus H-reflex.

Methods

Eight healthy subjects (3 male, 5 female) participated. H-reflex was elicited using a 1 ms square pulse. Stimulus intensity was adjusted to evoke an H-reflex with magnitude of 15% of Mmax. Common fibular nerve conditioning was administered using a 1 ms square pulse at 1.5 times the motor threshold, 100 ms prior to soleus H-reflex stimulation. Changes in static otolith drive were induced by suspending the subject on a tilt table at 60 degrees relative to supine. The ankle was held at 90 degrees with a flexible air cast and subjects wore a blindfold for the duration of the testing. EMG was recorded from soleus on the right leg. All EMG signals were amplified (1,000 gain), sampled at 2,000 Hz and bandpass filtered (20-450Hz). Standardized peak-to-peak amplitude of the soleus H-reflex was analyzed. A 2x2 repeated measures ANOVA (tilt x H-reflex conditioning) with $p \leq 0.05$ was employed.

Results

The means for the control non-tilted and tilted H-reflex were $0.145 (\pm 0.007)$ and $0.145 (\pm 0.009)$, respectively. The means for the non-tilted and tilted, common fibular nerve conditioned

H-reflex were $0.112 (\pm 0.029)$ and $0.050 (\pm 0.014)$, respectively. Omnibus ANOVA demonstrated a significant main effect of conditioning, $F(1,7) = 19.58$, $p < .05$. The mean difference between the control and the conditioned H-reflex without tilt was $0.031 (\pm 0.014)$. The mean difference between the control and conditioned H-reflex during tilt was $0.064 (\pm 0.015)$.

Conclusion

Consistent with previous data, the effect of common fibular nerve conditioning altered the amount of presynaptic inhibition in the soleus H-reflex. Tilt angle appears to have an impact on the magnitude of presynaptic inhibition. Further study is suggested.

PS - 643

Objective Measurements of Balance

Dysfunction in Children Who Are Deaf

Nikolaus Wolter¹; Karen A Gordon²; Luis D Vilchez-Madrigal³; Blake C Papsin²; Sharon L Cushing²

¹University of Toronto; ²University of Toronto, Hospital for Sick Children, Archie's Cochlear Implant Lab; ³University of Toronto, Hospital for Sick Children

Background

Vestibular end organ dysfunction occurs in <70% of children with deafness¹ and associated balance deficits can be measured using the balance subset of the Bruininks-Oseretsky Test of Motor Proficiency II (BOT-2)². Yet, the BOT-2 can only capture gross abnormalities in balance and may overlook subtle differences. Maintaining upright stance requires balancing individual body segments on top of one another. Adults with cochleovestibular loss do not do this normally³. It is not known if children born with cochleovestibular deficits develop similarly abnormal strategies to stay upright. Quantification of body segment position and posture may elucidate important differences between children's head and trunk movement in addition to assessing how they control their center of mass. Our objective in the present study was to detect and quantify abnormal balance in children with combined cochleovestibular deficits.

Methods

Balance was assessed in 36 children (18 children with cochleovestibular loss who use bilateral cochlear implants and 18 age and gender matched normal hearing children) by performing the BOT-2 within the Challenging Environmental Assessment Lab. Light emitting markers placed at the head and trunk were used to measure angular movements of the head and trunk segments and approximate the center of mass by comparison of the markers position to an upright neutral stance recorded at the start of each trial. Center of pressure area and sway velocity were obtained using forceplates in the floor which measure pressure changes by location. Postural control during BOT-2 Task 1 (tandem stance with eyes open) was quantified and compared between the 2 groups.

Results

Despite being able to perform the task, the BOT-2 scores were significantly worse in children with cochleovestibular loss using implants compared to normal hearing controls ($p < 0.01$). These children also had significantly worse postural control

as measured by center of pressure area and sway velocity($p=0.001$). Children with cochleovestibular loss had abnormally large angular movements of both the head and trunk segments($p=0.004$) which may contribute to less efficacious postural strategies measured by greater displacements of the center of pressure relative to the center of gravity during quiet stance($p=0.009$).

Conclusion

Quantification of the biomechanical properties of postural control while performing individual tasks of the BOT-2 is feasible. Although nearly all children with cochleovestibular loss were able to complete the task, they used different and less efficient strategies than normal. A better understanding of these postural strategies may aid in the development of rehabilitation options aimed at improving balance in this population.

References:

1. Buchman CA, Joy J, Telischi FF, Balkany TJ. Vestibular Effects of Cochlear Implantation. *Laryngoscope*. 2004;114(Suppl. 103):1–22.
2. Cushing SL, Chia R, James AL, Papsin BC, Gordon KA. A Test of Static and Dynamic Balance Function in Children With Cochlear Implants: The Vestibular Olympics. *Arch Otolaryngol Head Neck Surg*. 2008;134(1):34–38.
3. Creath R, Kiemel T, Horak F, Jeka JJ. The role of vestibular and somatosensory systems in intersegmental control of upright stance. *J Vestib Res*. 2008;18(1):39–49.

PS - 644

Single Unit Recording Suggests Complex Processing of Input from a Vestibular Prosthesis.

James Phillips; Leo Ling; Kaibao Nie; Amy Nowack; Christopher Phillips; Jay Rubinstein
University of Washington

Background

Electrical stimulation of ampullar nerve afferents in monkeys by a vestibular prosthesis can produce compensatory eye movements that are appropriately directed and scale with current and frequency of stimulation. Since the vestibular afferents typically modulate their firing rate based on the acceleration and velocity of the head, most devices are constructed to modulate the frequency of firing to provide a modulated motion signal to the brain. Previous experiments have shown that such frequency modulation produces a highly reliable frequency modulation of secondary vestibular neurons, while amplitude modulation produces recruitment of afferent fibers and vestibular neurons. In this study, we examine the activity of secondary vestibular neurons during both amplitude modulated and frequency modulated stimulation with a vestibular prosthesis, and suggest that the responses reveal complex relationships between stimulation, neural activity, and behavior.

Methods

5 rhesus monkeys were implanted with a vestibular receiver stimulator with stimulation sites in the semicircular canal perilymphatic space adjacent to the ampulla. The monkeys were also implanted with scleral coils, stabilization lugs and a recording chamber placed to access the vestibular nuclei. Biphasic pulse electrical stimulation was delivered to each canal to modulate eye movement behavior and during recording of secondary vestibular neurons with tungsten microelectrodes.

Results

Electrical stimulation of vestibular afferents produces phase locked driving of secondary vestibular neurons. However, the reliability of that driving, expressed as the percentage of stimuli to which a given neuron will respond, is highly idiosyncratic from neuron to neuron, and varies with current amplitude and with frequency of stimulation for a given neuron. Furthermore, many neurons which have high resting rates without stimulation, show primarily an intermittent reduction in discharge variability with sinusoidal amplitude modulated electrical stimulation, due to the time locked nature of their response to the afferent discharge entrained to the electrical stimulation. Therefore, for these neurons, amplitude modulation is modulating the recruitment of afferent fibers, but primarily modulating the synchrony of secondary vestibular neuron discharge.

Conclusion

These observations support a complex mechanism of vestibular prosthesis action where modulation of neural synchrony, combined with recruitment of individual neurons and phase locked frequency modulation, are affected by both stimulation frequency and current to produce the surprisingly normal behavioral outputs that are observed when vestibular function is restored with such a device.

PS - 645

Amplitude Modulation for Vestibular Prostheses

Christopher Phillips; Steven Bierer; Leo Ling; Kaibao Nie; Amy Nowack; James Phillips; Jay Rubinstein
University of Washington

Background

Electrical stimulation of the individual branches of vestibular nerve can produce a viable vestibular prosthesis. While pulse rate modulation stimulation strategies closely emulate the natural behavior of the afferent nerve, current amplitude modulated stimulation strategies can work by modulating the recruitment of individual afferents to a constant pulse rate. Here we examine the eye movements mediated by the vestibulo-ocular reflex (VOR) during current amplitude modulated (AM) stimulation of individual ampullary nerves in non-human primates.

Methods

3 rhesus macaques were implanted unilaterally with a vestibular prosthesis with an electrode array adjacent to each ampulla. We measured eye movements with scleral coils in response to AM stimulation trains of 300 pps biphasic pulses.

es delivered to each ampulla with the animal stationary, and during en-bloc sinusoidal rotation. Two AM stimulation strategies were employed: a linear relationship, where head velocity was directly mapped to stimulation current, and a 'feed-forward' relationship, which interposed the inverse of an empirically determined non-linear relationship between elicited eye velocity and stimulation current.

Results

Constant current stimulation trains elicited sustained nystagmus with a direction consistent with the orientation of the canal stimulated. Modulation of the current modulated the slow phase velocity of the eye movement in a highly non-linear fashion; sinusoidal current modulation produced non-sinusoidal velocity modulation. A feed-forward AM strategy was capable of eliminating some, but not all, asymmetries in the VOR response; there was always a velocity bias away from the implanted ear and the direction of eye movement was not in a constant plane through the entire sinusoidal eye movement.

Conclusion

The results suggest that AM modulation strategies can elicit eye movements comparable to those resulting from rate modulated stimulation. Such a stimulation strategy, combined with a head mounted rotation sensor, could produce a functional vestibular prosthetic for VOR. However, asymmetries in elicited VOR cannot be overcome by accounting for the non-linearity in the stimulation current versus eye-velocity relationship, and the vestibular system does not fully adapt to a baseline stimulation current and pulse rate, or current spread to adjacent ampullae.

PS - 646

The Frequency Responses of Irregular Primary Utricular Afferent Neurons to Bone-Conducted Vibration (BCV) and Air-Conducted Sound (ACS)

Ian Curthoys¹; Vedran Vulovic¹; Ljiljana Sokolic¹; Jacob Pogson¹; Mike Robins¹; Ann Burgess¹; Wally Grant²

¹University of Sydney; ²Virginia Tech, Blacksburg, Virginia

Background

Bone conducted vibration (BCV) and air-conducted sound (ACS) are now being widely used to test otolith function. The frequency responses of utricular afferents to these stimuli are not known. This study measured the frequency response of irregular primary utricular afferents to BCV and ACS.

Methods

Single primary vestibular neurons were recorded extracellularly of guinea pigs anesthetized with Ketamine and Xylazine. BCV stimulation was delivered either by a Radioear B-71 bone oscillator cemented to the skull or a Bruel and Kjaer 4810 Minishaker vibrating the stereotaxic frame. ACS stimulation of up to 140dB SPL was delivered by a TDH-49 headphone. Frequency responses were determined from objectively measured thresholds.

Results

Neurobiotin labelling showed that the neurons synapsed on type I receptors at the striola of the utricular macula but were dimorphic. Primary utricular neurons which are activated by both ACS and BCV have different frequency tuning - for BCV the afferents have very low thresholds from 50Hz up to 800-1000Hz. For ACS the neurons have a V-shaped tuning curve with lowest thresholds at 1000-2000Hz. Utricular neurons show phase locking for ACS up to 3000Hz (and possibly beyond), and to BCV up to 1500Hz. Phase-locking limits the maximum firing rate of the neuron. So to a stimulus of 50Hz, the maximum firing rate is just 50 spikes/s, even though testing with higher stimulus frequencies shows the cell can fire at much higher firing rates. Some irregular semicircular canal neurons were activated at 100Hz BCV and synchronized to the stimulus. They were not activated at 500Hz BCV.

Conclusion

The different frequency responses to BCV and ACS are most likely due to the different transduction mechanisms. Phase locking up to such high frequencies is probably due to the receptor hair cell being deflected once on each stimulus cycle. At low frequencies (<500 Hz), phase locking imposes a limit on the maximum firing rate of single neurons, the limit being the stimulus frequency. We think phase-locking is the cause of the very steep suprathreshold rate-intensity functions of these neurons.

Utricular afferents originating from the striola have lowest threshold to low frequency BCV (<1000Hz), but in contrast their lowest thresholds for ACS are from 1000-2000Hz. When activated, these neurons show tight phase locking up to high frequencies which indicates that these utricular afferents are activated by each cycle of the stimulating frequency.

PS - 647

Effects of Electron Irradiation on Vestibular Function in Rats

Jinghe Mao^{1,2}; Xuehui Tang¹; Jun Huang¹; Chunli Yang¹; Ansley Scott²; Margie Rayford²; Wu Zhou¹; **Hong Zhu¹**

¹University of Mississippi Medical Center; ²Tougaloo College

Background

The adverse effects of high energy radiation on astronaut health during long duration space missions are serious concerns of NASA. Radiation exposure may compromise vestibular function since nasopharyngeal cancer patients experience post-irradiation vertigo. However, little is known about the underlying mechanisms.

Methods

In the present study, we established a rodent model to study the effects of electron radiation exposure on the vestibular system by recording vestibular afferent responses to vestibular stimuli. Sprague-Dawley rats were exposed to unilateral cranial electron irradiation at dosage varying from 0 to 60Gy. Seven days following the exposure, single unit recording of vestibular afferent activity was performed on the side ipsilateral to the irradiation side under barbiturate anesthesia. A total of 309 horizontal semicircular canal afferents' responses

to sinusoidal earth-horizontal rotations (~1Hz) were recorded from 36 animals.

Results

Preliminary analysis shows that exposure to 30 and 60 Gy electron irradiation caused significant decreases in the gains of the irregular horizontal semicircular canal afferents but had no significant effect on the regular afferents.

Conclusion

These results indicate that irradiation exposure induces specific functional deficit of the vestibular system.

PS - 648

Effects of Antidepressant on The Vestibular System

Hiroaki Shimogori; Kazuma Sugahara; Makoto Hashimoto; Hiroshi Yamashita

Yamaguchi University Graduate School of Medicine

Background

Phosphorylation of the transcription factor cAMP responsive element-binding protein (CREB) is thought to play a key role in neurogenesis. In our previous study, phosphorylated CREB (p-CREB) -like immunoreactivities were observed in vestibular ganglion cells after unilateral labyrinthectomy (UL). In addition, another study was reported that, after UL, p-CREB-like immunoreactivities were also detected in bilateral vestibular nuclei. These results indicate that vestibular system may have a potential of neuronal plasticity. It is well known that antidepressant shows its effects by activating CREB-BDNF axis on hippocampal neurons. We thought the possibility that up-regulation of CREB-BDNF axis might facilitate neuronal plasticity in the vestibular system. The aim of the present study was to evaluate the effects of general application of antidepressant on vestibular system by analyzing BDNF mRNA.

Methods

Hartley white guinea pigs with normal tympanic membranes and normal Preyer reflexes were used in this study. Animals were divided into two groups. In one group, animals were applied normal food for 30 days (normal group), and in another group, animals were applied normal food with antidepressant (sertraline hydrochloride) in concentration with 0.01% for 30 days (sertraline group). Before and after feeding, from each group, tissues were removed and BDNF mRNA was extracted from hippocampus, vestibular nucleus, and vestibular ganglion. RT-PCR was conducted and BDNF mRNA was analyzed quantitatively.

Results

In the sertraline group, the amount of BDNF mRNA from the hippocampus was statistically larger than that in the normal group. However, in the vestibular nucleus and vestibular ganglion, no statistical difference was found between both groups.

Conclusion

Chronic application of antidepressant increased BDNF mRNA levels in the hippocampus, not in the vestibular system. The

possibility still remains that mRNA level may change before and after vestibular damage.

PS - 649

Using Transgenic Zebrafish to Understand Ribbon Synapse Function in Vivo

Katie Kindt¹; Teresa Nicolson²

¹*National Institute on Deafness and Other Communication Disorders*; ²*Oregon Health and Science University*

Background

Hair cells, photoreceptors and bipolar cells have a specialized presynaptic density, also known as the synaptic ribbon. The synaptic ribbon is an electron dense structure composed primarily of a protein called Ribeye. The synapse acts as a scaffold to tether vesicles adjacent to the presynaptic membrane near Ca²⁺ channels (Ca_v1.3). At synaptic ribbons exocytosis is coupled to graded changes in membrane potential that activate synaptic Ca²⁺ channels. Synaptic ribbons are able to encode the frequency, intensity and phase of stimuli. The size and shape of synaptic ribbons vary depending on the requirements of a given sensory cell, but how these variations enable diverse sound encoding requirements is not clear.

Methods

To study activity at ribbon synapses we have created a transgenic zebrafish that expresses a genetically-encoded Ca²⁺ indicator localized exclusively to the synaptic ribbon. This transgenic reliably measures presynaptic Ca²⁺ signals. In addition to this tool to examine synapse function *in vivo*, we have taken advantage the zebrafish system and manipulated synaptic ribbons genetically to understand how synapse size alters synapse function.

Results

Using this transgenic line we observe a heterogeneous range of Ca²⁺ signals at individual synaptic ribbons. The Ca²⁺ signals we measure are precise and local – in *caV1.3* mutants we observe no Ca²⁺ response at synaptic ribbons. Despite the heterogeneity in Ca²⁺ signals, within a hair cell Ca²⁺ signals are homogeneous. By pushing our system, either genetically or pharmacologically, we find that by increasing synapse size, we observed significant changes in the magnitude of the presynaptic calcium signal, distribution of Ca_v1.3, and unique changes to the properties of vesicle release.

Conclusion

Overall this data provides new and interesting insight on the how the physical properties of synaptic ribbons can generate the diverse coding requirements in different sensory cells.

Regional Differences in the Timing of Terminal Mitosis and Establishment of Stereocilia Polarity in Utricular Hair Cells.

Tao Jiang

NIDCD/NIH, University of Maryland

Background

The utricle macula, one of the five vestibular organs in the inner ear, responds to changes in horizontal linear acceleration of the head. Within the macula lies the striola, a distinct region that has atypical otoconia distribution and hair cell type. Based on the position of the kinocilium within the apical plane of the hair cell, the lateral extrastriolar region of the utricle has reversed hair bundle polarity relative to the rest of the organ. Thus, a line of polarity reversal can be drawn within the utricle, across which hair bundles point towards each other. Existing literature suggests that the establishment of hair cell polarity within the utricle and consequently the line of polarity reversal is initiated at embryonic day (E) 13.5 and completed by E18.5. During this developmental period, hair bundles within the medial utricle change their orientation much more significantly than their counterparts in the lateral utricle. Here, we investigated whether this establishment of hair cell polarity in the utricle is related to the timing of cell cycle exit of hair cell precursors.

Methods

To assess the timing of cell cycle exit, pregnant female mice were injected with EdU, an analog of thymidine, at different ages from E11.5 to E16.5. Then, embryos were harvested at E18.5 and processed for EdU labeling and anti-Myosin VI staining. The percentages of EdU-labeled hair cells were scored. In addition, hair bundle orientation was determined by using phalloidin, anti-spectrin and anti-Gai antibodies.

Results

- 1) Hair cell precursors in the striola are first to exit from cell cycle starting before E11.5, followed by precursors in the medial extrastriola. In contrast, hair cells precursors in the lateral extrastriola only undergo terminal mitosis starting after E13.5. Labeled hair cells are rarely detected in the striola after E14.5, but reduced number of labeled hair cells outside the striola is evident in specimens injected with EdU at E16.5 suggesting that new hair cells are still being generated beyond E16.5 in the extrastriolar regions.
- 2) Prior to distinct hair bundle formation, hair cell polarity is already evident in nascent hair cells based on anti-Gai antibody staining.
- 3) Based on phalloidin and anti-spectrin staining, hair bundle orientation only undergoes slight refinement after bundle formation.

Conclusion

In the developing utricle, hair cell polarity is evident soon after hair cell precursors undergo terminal mitosis and only minor adjustment in hair bundle orientation is observed subsequently.

The Primary Auditory Cortex in Learning and Memory

Norman Weinberger

University of California Irvine

Auditory comprehension is essential to hearing because it gives meaning to sounds, whether of natural or human origin. Yet, remarkably, relatively little effort has been devoted to the issue of how sounds gain behavioral meaning, in stark contrast to the extensive attention expended to understand the detection and perception of sound. Meaning is acquired through experience, i.e., learning, and retained through memory. Research during the past two decades has identified the primary auditory cortex (A1) of animals and humans as a site deeply engaged in the acquisition and storage of auditory information throughout lifespan, as opposed to the traditional belief that auditory cognition is produced only by "higher association areas". In general, the encoding of behaviorally relevant sounds in A1 is strengthened as part of a functional remodeling of acoustic processing, known as "representational plasticity" (RP). Whereas "plasticity" is very widely applied to almost any instance of non-transient neural change, representational plasticity consists of systematic modification of a parameter of sound, e.g., acoustic frequency. Representational plasticity can't be known during training trials but can only be detected by testing subjects after training with a wide range of acoustic stimuli, thus revealing its degree of specificity and domain of effect. The implications of representational plasticity transcend local plasticity because RP alters the processing of future sounds within the modified acoustic dimension. Whereas previously adult representational plasticity in A1 had been denied, a flourishing research initiative has revealed that it is ubiquitous across acoustic parameters, tasks and species. Whether any purely auditory-analytic cortical neurons exist is now open to question. Representational plasticity takes many forms, e.g., from reduced threshold and bandwidth through receptive field shifts to marked increases in area of preferred representation. It is affected by previously unsuspected factors, such as the particular strategy used to solve auditory problems, and has several identified functions, accounting for the importance of sound and the strength of auditory memory. The mechanisms of representational plasticity are now being pinpointed and include activation of the cholinergic system in A1 and selective increases in neuronal synchrony (gamma oscillations and neuronal spike co-variances). It is now possible to create "specific false auditory memory" by direct manipulation of acoustic representations in the primary auditory cortex. The implications for understanding normal hearing and translational applications are considerable. The need for a far more dynamic conceptualization of the auditory system is now required. *Supported by DC RO1-02938 and RO1-10013.*

SY - 061

Evanescent and Longer-Lasting Changes in Auditory and Prefrontal Cortices During Attention and Learning

Jonathan Fritz

University of Maryland, College Park

Rapid task-related receptive field plasticity (RFP) alters the tuning properties of A1 neurons in a task-specific fashion that may enhance their ability to encode the attended, task-relevant spectral and temporal features of the current task. The nature of adaptive task-related responses in A1 can be influenced by multiple factors including task stimuli, design, rewards, context, and animal motivation and task performance, but overall RFP enhances the contrast between foreground (task-relevant) and background (task-irrelevant) stimuli. RFP could be measured within 1-2 minutes of task onset, and in some A1 neurons, lasted only while the animal was engaged in task performance. However, in other A1 neurons, RFP persisted minutes or hours more after behavioral task completion. We compared task-related plasticity in A1 vs several secondary auditory cortical (AC) areas, in a simple task in which the animals learned to discriminate variable frequency tonal targets from noisy background stimuli. In secondary AC areas, we found relatively heightened responses to targets vs. background stimuli during behavior, compared to responses observed in passive listening. Cells in secondary AC also showed persistent effects of attention. Secondary AC is thus likely to play a key role in the transformation from sound to meaning, which includes multiple steps from an initial, faithful encoding of spectrotemporal acoustic pattern to further stages where the auditory scene is analyzed, relevant auditory objects are recognized, categorized and associated with task-specific behavioral meaning and appropriate responses. Auditory responsive cells in dorsal frontal cortex (dFC) showed gated, adaptive, highly selective encoding of task-relevant target stimuli in the tone detect task. We propose that dFC contributes to sensory discrimination by keeping track of task goals, selectively attending to the class of task-relevant stimuli, and biasing sensory cortex in favor of task-relevant stimuli by reshaping acoustic filter properties of AC neurons. The challenge for the future is to understand the mechanisms of top-down control by which the flow of incoming sensory information to AC is dynamically modulated during behavior, reflecting attentional focus. Stimulation of dFC, paired with pure tone presentation, elicits changes in A1 receptive fields that are similar to those observed in attention-driven behavior. Also, preliminary neuroanatomical results show reciprocal connections between dFC and some secondary auditory areas. These results support the idea that dFC and all AC are part of a larger broad network that uses neuromodulators and an array of plasticity mechanisms to optimize processing of relevant stimuli during auditory attention and beyond.

SY - 062

Neural Circuits Responsible for Auditory Spatial Learning

Andrew King

University of Oxford

There is growing evidence that the activity of neurons in both primary and non-primary auditory cortex can be modulated by a variety of task-related factors and by inputs from other sensory modalities, suggesting that neurons at this early level of cortical processing carry information about both the acoustical properties of sounds and their behavioral meaning. Moreover, plasticity in the cortical representation of behaviorally significant sounds, particularly in the primary auditory cortex (A1), has been shown to accompany auditory learning. Both short-term adaptation as well as longer lasting plasticity of neural coding are critical for maintaining perceptual abilities when auditory inputs change. This can be seen, for example, if the relationship between spatial cue values and sound source direction is altered as a result of a conductive hearing loss in one ear. Our studies in ferrets have demonstrated that the auditory system is able to accommodate these changes, both during development and in later life, and therefore maintains accurate sound localization in spite of the highly abnormal inputs available. The mechanism for adaptation to altered auditory spatial cues involves a reweighting of different cues, with localization judgments becoming more dependent on the monaural spatial cues provided to the intact ear and less on the binaural cues that are altered by the hearing loss. This plasticity is context specific, however, since changes in cue weighting can be reversed if normal hearing is restored, providing a basis for maintaining accurate perception in dynamic acoustic environments. In ferrets raised with an intermittent hearing loss in one ear, these behavioral findings are paralleled by a corresponding reweighting of auditory spatial cues in A1. It is likely that plasticity of cue integration in the cortex occurs throughout life since the ability of adult ferrets to relearn to localize sound accurately after occluding one ear depends on the integrity of both A1 and secondary cortical areas and is prevented by the selective loss of cholinergic neurons in the basal forebrain that target the cortex. These studies have also revealed, however, that descending projections from the auditory cortex to the midbrain are required for spatial learning, demonstrating that we need to look beyond the cortex to fully understand the adaptive capabilities of the auditory system. Supported by the Wellcome Trust and Action on Hearing Loss.

SY - 063

Learning-Related Neuroplasticity in the Human Auditory System

Nina Kraus

Northwestern University

Background

The previous speakers have focused on cortical neuroplasticity. Our research has focused on subcortical function, although I prefer to avoid such distinctions as our neural probe, although nominally of collicular origin, successfully serves as

a snapshot of the broader auditory system involving sensory, cognitive, and reward centers. With it, assessing subjects across the age span, in cross-sectional and longitudinal designs, and with intervention, we have uncovered some “neural signatures.”

Methods

Because of the close adherence to the evoking stimulus, and the fact that the stimulus is acoustically complex, the response can be thoroughly characterized in terms of timing, harmonics and phase. We can also examine its inter-trial consistency and phase locking.

Results

From this broad canvas, we have been able to discern neural signatures. We have found signatures of enhancement, such as seen in musicians and bilinguals; we have found signatures of deprivation such as seen in poverty and clinical conditions such as learning problems and difficulty hearing in noise. The effect on the response is not global; the response characteristics that are affected differ widely: sliders on a studio mixer rather than a volume knob. Given the known mutability of the auditory system, and starting from the grounding of the signature responses, we are able to investigate learning-related neuroplasticity in individuals. Interventional approaches we are investigating include amplification (e.g., classroom FM systems for dyslexic children), music instruction and software-based training. With each intervention, we have observed a change in response properties; older individuals regain a “young” response signature; poor readers’ responses look more like those of good readers.

Conclusion

The hope is that with such a measure, uniformity can be achieved—across populations, across species, and across labs—in the assessment of learning-related plasticity.

PD - 132

Effect of Resveratrol in Acute Cochlear Damage by 3-Nitropropionic Acid

Young Ho Kim¹; Ji Hye Lee¹; Kyung Tae Park¹; Yoon Chan Rah¹; Young Chul Kim²

¹Department of otorhinolaryngology, Seoul National University College of Medicine, Seoul National University Boramae Medical Center; ²Department of physiology, Chungbuk National University, College of Medicine

Background

3-Nitropropionic acid (3-NP) induces hearing loss by impairing mitochondrial energy generation. Resveratrol is known to be a potent anti-oxidant protecting organs from various injuries. The present study was designed to investigate the protective effect of resveratrol against acute 3-NP-induced cochlear damage.

Methods

Male Sprague-Dawley rats were divided into 3 groups. In group A, the 3-NP vehicle was injected (intratympanically), and in group B, only resveratrol (10 mg/kg, 5 days) was administered (intraperitoneally). 3-NP (500 mM, 4 µl, intratympanically) was administered with (group D) or without (group

C) resveratrol treatment (10 mg/kg, 5 days). The auditory brainstem response (ABR) was recorded at click and at 8, 16, and 32 kHz before and after injection. After cochlear harvest, hematoxylin/eosin staining was performed.

Results

3-NP exposure (group C) resulted in elevated ABR thresholds that exceeded the maximum recording limit, while resveratrol treatment before 3-NP exposure (group D) led to a significant decrease in hearing threshold shift. Histological analysis of group C revealed loss of fibrocytes in the spiral ligament, hair cells in the organ of Corti, stellate fibrocytes and interdental cells in the spiral limbus, and spiral ganglion cells, while in group D, these cells were relatively preserved. The injection of 3-NP vehicle (group A) or only resveratrol (group B) revealed normal ABR thresholds and cochlear structures.

Conclusion

These results suggest that resveratrol may protect 3-NP-induced acute cochlear injury.

PD - 133

Netrin-1 Protects Outer Hair Cells Against Aminoglycoside

Kohei Yamahara; Norio Yamamoto; Takayuki Nakagawa; Juichi Ito

Kyoto University

Background

We have demonstrated that insulin-like growth factor1 (IGF-1) protects cochlear hair cells of neonatal mice against aminoglycoside (Hayashi et al. Molecular and Cellular Neuroscience 2013). As effectors of IGF-1 signaling during hair cell protection against aminoglycoside, we have identified two kinds of genes, *Gap43* and *Ntn1* (netrin-1) using microarray and quantitative RT-PCR (qRT-PCR) (Hayashi et al., manuscript in submission). The netrins constitute a conserved family of secreted proteins related to laminins, with members involved in axon guidance and cell migration. In rodents, netrin-1 is expressed in many tissues outside the central nervous system including the inner ear. Recent work has identified other roles of NTN1 than axon guidance and cell migration, including tissue morphogenesis or an anti-apoptotic survival effect. The aim of this study is to identify the role of NTN1 during the protection of hair cells by IGF-1 against aminoglycoside.

Methods

We administered neomycin only, both neomycin and IGF-1, or both neomycin and NTN1 to the cochlear explant cultures of neonatal mice. We tried three different concentrations of NTN1 (50 ng/ml, 500 ng/ml or 5000 ng/ml). After 24 hours of treatment, we analyzed the difference in the numbers of surviving hair cells in the basal turn of each group. The hair cells with remaining stereocilia labeled with phalloidin were considered alive.

Results

500 ng/ml or 5000 ng/ml of NTN1 significantly attenuated the loss of the outer hair cells in neomycin-damaged cochle-

ar sensory epithelia compared with neomycin-only treated group.

Conclusion

NTN1 protects outer hair cells against neomycin. This effect of NTN1 was not completely comparable with that of IGF-1. Our results indicate that NTN1 plays a partial role during the protection of hair cells by IGF-1 against aminoglycoside.

PD - 134

Targeted Modifications to Aminoglycoside Structure Reduce Ototoxic Side Effects

Markus Huth; Kyu-Hee Han; Kayvon Soutadeh; Sarah Verhoeven; Andrew Vu; Robert Greenhouse; **Alan Cheng**; Anthony Ricci
Stanford University

Background

Aminoglycosides are antimicrobials with significant side effects, causing hearing loss through hair cell degeneration. However, their clinical application remains commonplace because of potent antibacterial activities and low costs. Several studies indicate that drug entry into hair cells requires patent mechanotransducer channels and that their blockage reduces ototoxicity. After entry into hair cells, it is poorly metabolized with a half-life of months. To prevent cochleotoxicity, we applied biophysical properties of mechanotransducer channels and crystallographic data on aminoglycoside binding sites on bacterial ribosome, and designed and modified the aminoglycoside, sisomicin.

Methods

Nine derivatives of the parent aminoglycoside sisomicin were synthesized and applied to rat cochlear cultures. Hair cell survival was assessed after treatment with new and parent compounds. New and parent compounds were tested in a bacterial (*E. Coli*) growth assay and minimal inhibitory and bacteriocidal concentrations measured. From these results, a lead compound (N2) was selected and further compared against sisomicin via dose-response experiments using cochlear cultures and bacterial growth assays using different bacterial strains. Next, N2 was tested in an *in vivo* mouse model of sisomicin/furosemide-induced hair cell loss and hearing loss, and ABR/DPOAEs were measured in injected animals prior to histologic analyses 1 week and 1 month after drug administration. Lastly, N2 was used to treat an *in vivo* mouse model of urinary tract infection that normally subsides upon sisomicin treatment. Antibacterial activities were measured by bacterial growth from collected urine, bladder and kidney tissues.

Results

Sisomicin causes hair cell loss in a basal-apical gradient and inhibits growth of *E. Coli*. All 9 derivatives exhibit less toxicity against hair cells *in vitro*, but only 3 maintain antimicrobial activities against *E. Coli*. Dose-response experiments show that the concentration causing 50% basal hair cell loss was 94 μ M for sisomicin and 3.5 mM for N2. N2 retains toxicity against *E. Coli*, *K. pneumonia*, but lost some activities towards *P. aeruginosa* and staphylococcal species. Whole animal assays demonstrate threshold shifts and outer hair cell loss in

animals injected with sisomicin/furosemide and significantly less in those injected with N2/furosemide. N2 yielded similar toxicity profiles only when injected at ~2.3 times the sisomicin dose. *In vivo* bladder infection model demonstrates comparable antimicrobial activities between sisomicin and N2 without causing kidney or hearing dysfunction.

Conclusion

Targeted modification of aminoglycosides is a feasible approach in reducing aminoglycoside toxicity, while maintaining antibacterial activities at the expense of spectrum of bacterial coverage. Further experiments aim to improve toxicities against multiple bacterial strains.

PD - 135

Hearing Loss and Otopathology Following Systemic and Intracerebroventricular Delivery of 2-Hydroxypropyl- β -Cyclodextrin

Scott Cronin¹; Kelsey Thompson²; Austin Lin³; Keith Duncan⁴

¹*University of Michigan*; ²*Northwestern University*;

³*University of Michigan Medical School*; ⁴*University of Michigan, Kresge Hearing Research Institute*

Background

Cyclodextrins are cyclic oligosaccharides that form a ring-like, water-soluble, structure with a hydrophobic pocket. Believed to be safe at even high doses, cyclodextrins are used extensively in the pharmaceutical industry as drug excipients. Recently, 2-hydroxypropyl- β -cyclodextrin (HPBCD), gained attention as a therapy for Niemann-Pick type C (NPC). Cyclodextrins mediate their effects through alterations in cell membrane and intracellular lipids, most notably cholesterol. Through this interaction with cholesterol and other cell lipids, they mediate changes in tight junctions, cellular transport, and cell signaling with potentially detrimental impact on cell function and viability. While cyclodextrins have been studied in multiple organ systems, little is known about their interaction with the cochlea or the mechanism of ototoxicity.

Methods

Multiple experimental groups were studied by varying injection route, dose, and time to reflect both published animal data and current human investigational drug dosing. One injection of either saline or HPBCD was given at P4-6 weeks in FVB/NJ mice either subcutaneously (SC) or intracerebroventricularly (ICV). Auditory brainstem responses (ABR) were measured at 4, 16, and 32 kHz corresponding to apical, mid, and basal segments of the organ of Corti. Whole mounts were prepared and stained with rhodamine-phalloidin and cytochrome c oxidase performed. The fraction of missing hair cells was calculated along the entire tonotopic axis.

Results

Both high dose SC and ICV administration of HPBCD caused significant hearing loss. Affected animals exhibited ABR threshold shifts of approximately 40-65 decibel (dB), regardless of delivery route (Figure 1). High dose SC (8000 mg/kg HPBCD) and high dose ICV (40mM HPBCD) caused similar hearing loss. The change in ABR thresholds were tightly cor-

related to outer hair cell (OHC) loss with no significant loss of inner hair cells. Low dose SC (4000 mg/kg HPBCD) did not cause a major ABR shift at any threshold, but low dose ICV (5mM HPBCD) caused an ABR shift at 32 kHz. Interestingly, combined low dose SC and ICV injection caused ABR threshold shifts in 4, 16, and 32 kHz of a magnitude similar to higher doses (Figure 2).

Conclusion

Hearing loss associated with HPBCD is mediated through OHC loss and independent of route of administration at high doses. At low doses, SC and ICV are synergistic leading to ABR shifts out of proportion to the hearing loss seen when administered independently. These doses may have clinical implications in NPC therapy.

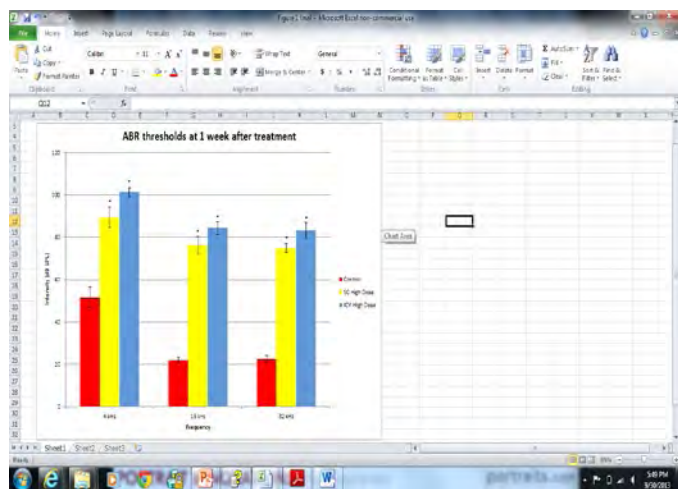


Figure 1: ABR threshold for control, subcutaneous (SC) high dose, and intracerebroventricular (ICV) high dose at 1 week after a single treatment. ABR threshold elevations between both treatment groups are similar but significantly different from control. Error bars represent standard error of the mean. $P < 0.05$ (*). Abbreviations: speech pressure level (SPL), auditory brainstem response (ABR), kilohertz (kHz).

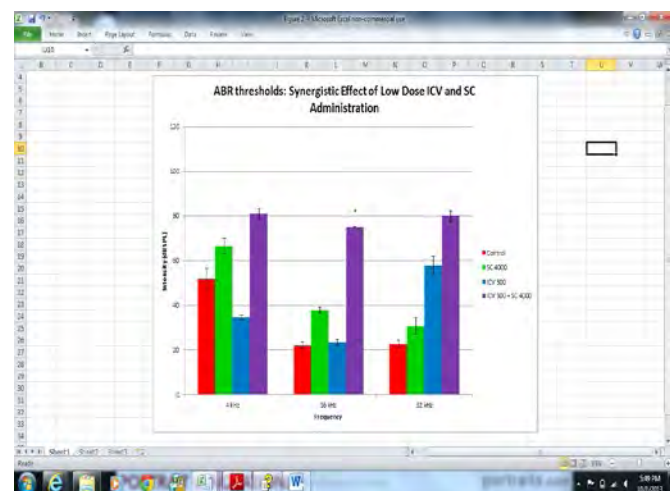


Figure 2: Figure 1: ABR threshold for control, subcutaneous (SC) low dose, and intracerebroventricular (ICV) low dose, and ICV with SC low dose at 1 week after a single treatment. When given together, ICV low dose and SC low dose act synergistically to cause significantly more hearing loss than either given individually.

Error bars represent standard error of the mean. $P < 0.05$ (*). Abbreviations: speech pressure level (SPL), auditory brainstem response (ABR), kilohertz (kHz).

PD - 136

Cyclin-Dependent Kinase 2 (CDK2) is Involved in Aminoglycoside Antibiotic-Induced Hair Cell Death

Litao Tao; Neil Segil

University of Southern California

Background

The molecular mechanisms of hair cell death caused by ototoxic aminoglycoside antibiotics have been studied and several biochemical pathways have been identified as important players involved in aminoglycoside-induced hair cell apoptosis. We have previously observed that when CDK inhibitors p19Ink4d and p21Cip1 are mutated, hair cells aberrantly re-enter cell cycle, and die through apoptosis. Similarly in neurons, loss of both p27Kip1 and p21Cip1 leads to aberrant cell cycle re-entry and death. In neurons, a number of studies have tied the initiation of apoptosis to aberrant CDK2 activation, and as a consequence cell cycle re-entry. These observations led us to test the role of CDK2 in gentamicin-induced hair cell death. In contrast to neurons, in this study we show that while CDK2 is involved in gentamicin-induced hair cell death, this process does not appear to involve cell cycle re-entry, but rather suggests a role for CDK2 in the regulation of downstream apoptotic factors stimulated by c-Jun.

Methods

Organotypic cultures of cochlea from neonatal wild type or CDK2 knockout mice were treated with gentamicin and several pharmaceutical CDK2 inhibitors. In addition, the potential downstream targets of CDK2 were investigated by qPCR, western blotting and immunofluorescence staining. Organotypic cultures of utricles from mature animals were used to investigate the role of CDK2 in mature hair cells after gentamicin treatment. Finally, ABR and immunohistochemistry were used to assess the sensitivity to gentamicin ototoxicity in CDK2 wildtype or knockout animals after trans-tympanic injection of gentamicin.

Results

Pharmacological inhibition of CDK2, as well as mutation of the CDK2 gene, attenuated hair cell death in response to gentamicin in organotypic culture of cochlea from neonatal mice. Similar protective effects by CDK2 inhibition or knockout were observed in utricular cultures from mature animals. In addition, *in vivo* animal experiments showed CDK2 knockout animals were significantly less sensitive to gentamicin ototoxicity. No evidence for aberrant cell cycle reentry of hair cells was observed. Further biochemical investigations indicated that phosphorylation of c-Jun at S63 and S73 was not affected by the inhibition of CDK2, but that gentamicin-induced expression of c-Jun target genes involved in apoptosis was suppressed when CDK2 was inhibited.

Conclusion

The results indicate that CDK2 activity facilitates gentamicin-induced hair cell death and that transcriptional activity of

c-Jun appears to be regulated by CDK2 during hair cell apoptosis after gentamicin treatment.

PD - 137

Trafficking Studies of Fluorescently Labeled Aminoglycosides Reveal Separate Intracellular Pools With Different Toxicity Profiles

Dale Hailey¹; Robert Esterberg²; Tor Linbo²; Edwin Rubel¹; David Raible²

¹University of Washington & Virginia Merrill Bloedel Hearing Research Center; ²University of Washington

Background

Inner ear mechanosensory hair cells are sensitive to many therapeutic agents including aminoglycoside antibiotics (AGs). The goals of our research program are to understand why aminoglycosides cause hair cell death and how this death might be prevented. Previous work has identified routes by which aminoglycosides enter hair cells, early subcellular changes they cause, and pro-death signaling cascades they activate. Our group previously showed that different AGs kill hair cells at different rates (Owens KN et al., *Hear Res* 2009). Hair cell death from neomycin is complete after a 30-min exposure. In contrast, a fraction of hair cells are resistant to a 30-min gentamicin exposure, but die with a 6-hour exposure. Here we report studies of intracellular trafficking of labeled AGs in hair cells in lateral line neuromasts of larval zebrafish, and identify intracellular loci that contribute to differential AG toxicity.

Methods

Texas Red has previously been used to label gentamicin (Steyger PS et al., *J Assoc Res Otolaryngol* 2003). We used this same labeling method to add fluorescent tags to a variety of structurally related AGs including gentamicin, neomycin, G418 and paromomycin. The labeled AGs kill zebrafish lateral line hair cells, and their fluorescent signals allow us to observe AG loading and trafficking in real time in the hair cells of sedated larvae. We can then correlate intracellular trafficking events with other markers of hair cell damage and death.

Results

All of the labeled AGs first enter the apical region of hair cells in a mechanotransduction-dependent manner. They then distribute into two visually separable pools—a diffuse signal present throughout the cell body, and bright membrane-bound punctae. Notably, AGs that rapidly kill hair cells distribute primarily to the diffuse pool. Those that kill hair cells more slowly distribute primarily to punctae, most of which colocalize with lysosomal markers. Interference with endocytic processes blocks formation of punctae and increases the diffuse signal. These changes coincide with increased aminoglycoside toxicity.

Conclusion

We show that trafficking studies of labeled AGs can indicate intracellular pools that differentially contribute to AG toxicity. Our results suggest that rapid damage from AGs likely comes from the diffuse pool, not the punctae. Delivery to the punctae may initially be cytoprotective by sequestering AGs. Further

studies of AG trafficking may be useful for identifying fluorescent signatures of altered AGs that are less toxic to hair cells.

PD - 138

Transfer of Calcium from Endoplasmic Reticulum to Mitochondria Underlies Aminoglycoside-Induced Hair Cell Death in the Zebrafish Lateral Line

Robert Esterberg; Dale Hailey; Edwin Rubel; David Raible
University of Washington

Background

The transfer of Ca²⁺ between endoplasmic reticulum (ER) and mitochondria is becoming increasingly recognized for its role in the regulation of multiple cellular processes, ranging from bioenergetics to cellular dysfunction and death. We recently demonstrated that disruption of intracellular Ca²⁺ homeostasis within mechanosensory hair cells is a critical signal and a reliable predictor of hair cell death following ototoxic aminoglycoside antibiotic exposure. Here we demonstrate that mitochondrial uptake of Ca²⁺ is central to toxicity. For these studies we employ the zebrafish lateral line system, as it provides an opportunity to directly monitor intracellular Ca²⁺ changes during ototoxin-induced cell death in an organismal context.

Methods

We have generated a number of transgenic zebrafish lines expressing the genetically encoded Ca²⁺ indicators, GCaMP3 and RGECCO, targeted to subcellular compartments specifically within hair cells. These domains include ER and mitochondria, the largest Ca²⁺ stores within the cell. We then exposed anesthetized larvae to concentrations of aminoglycoside that induce hair cell death within a subset of lateral line hair cells, allowing us to compare intracellular Ca²⁺ dynamics individually or simultaneously in both compartments between living and dying hair cells exposed to the same concentration of aminoglycoside.

Results

We demonstrate that efficient ER-mitochondrial Ca²⁺ flow in unperturbed zebrafish larvae drives mitochondrial activity. Following exposure to aminoglycosides, Ca²⁺ handling within the ER and mitochondria of dying hair cells is distinctly different than that of living cells. Within dying hair cells, fluorescence of ER-targeted Ca²⁺ indicators decreases in a manner consistent with efflux of Ca²⁺. This is followed by an increase in fluorescence of mitochondrial-targeted Ca²⁺ indicators consistent with mitochondrial Ca²⁺ uptake. Mobilization of Ca²⁺ from the ER is a reliable predictor of downstream mitochondrial changes and of cell death; such changes in organellar Ca²⁺ are not observed within hair cells that survive aminoglycoside exposure. Pharmacological agents that shunt ER-derived Ca²⁺ away from mitochondria and into cytoplasm mitigate aminoglycoside toxicity, while agents that promote mitochondrial Ca²⁺ accumulation exacerbate toxicity.

Conclusion

Our results demonstrate that mitochondrial calcium accumulation is central event underlying aminoglycoside toxicity. We

suggest that efficient ER-mitochondrial Ca^{2+} flow under physiological conditions occurs at the cost of increased susceptibility to ototoxins.

PD - 139

Damage-Induced Phagocytic Activity of Supporting Cells is Severely Impaired by Cisplatin

Elyssa Monzack¹; Lindsey May¹; Jonathan Gale²; Lisa Cunningham¹

¹NIDCD; ²UCL Ear Institute

Background

Hair cells are susceptible to death from aging, excessive noise, and exposure to ototoxic drugs, including the aminoglycoside antibiotics and platinum-based chemotherapy drugs such as cisplatin. Recent data from our labs and others indicate that supporting cells are active participants in hair cell survival, death, and phagocytosis and are major determinants of whether a hair cell under stress lives or dies. Here, we have examined the phagocytic activity of supporting cells in response to hair cell death caused by either aminoglycosides or cisplatin.

Methods

Utricles from adult Atoh1-Cre x Rosa26-tdTomato transgenic mice were cultured for up to 48 hours in 3 mM neomycin, 30 $\mu\text{g}/\text{ml}$ cisplatin, or control medium. For live imaging experiments, spinning disk confocal imaging of hair cells and supporting cells was used to examine the critical cell-cell interactions that take place during exposure to either of these ototoxic stresses.

Results

When hair cells are killed by aminoglycosides, supporting cells first constrict the apical portion of the hair cell until it separates from the cell body, then phagocytose the remainder of the hair cell, similar to the processes we have described in the chick utricle. In contrast, cisplatin results in significantly fewer supporting cell constrictions and accumulation of hair cell corpses in the sensory epithelium. Together, these data indicate that supporting cells in the mature mammalian inner ear efficiently phagocytose hair cells killed by aminoglycoside treatment, while cisplatin exposure results in a defect in this phagocytic activity.

Conclusion

Our data indicate that cisplatin causes a defect in the phagocytic removal of hair cells by supporting cells. These results are important from a basic science perspective in that they describe ototoxin-dependent differences in critical intercellular signaling events between stressed hair cells and their surrounding supporting cells. Additionally, the data are clinically relevant, as they suggest that supporting cells should be specifically targeted in the future development of therapies aimed at preventing hearing loss.

PD - 140

Epigenetic Regulation of Atoh1 Expression During Development of the Mouse Organ of Corti

Zlatka Stojanova¹; Tao Kwan²; Neil Segil¹

¹University of Southern California; ²House Research Institute

Background

Hearing loss is predominantly caused by the death of sensory hair cells in the inner ear. The *Atoh1* gene is necessary and sufficient in the context of the inner ear for sensory hair cell formation, and, as such, is a highly desirable therapeutic target for hearing restoration. Understanding the mechanisms controlling transcriptional activation and silencing of the *Atoh1* gene is thus a significant goal. An important mechanism of transcriptional regulation is through the reversible post-translational modification of proteins associated with DNA, such as the histones which form the nucleosome core and that can modulate transcription both positively and negatively.

Methods

To begin to understand the mechanisms of *Atoh1* gene transcriptional regulation in the mouse inner ear, we have developed tools for studying the epigenetic status of genes in the purified cell types of the perinatal organ of Corti. These techniques include a micro-chromatin immunoprecipitation (μChIP) assay from FACS-purified hair cells, supporting cells, and their progenitors.

Results

We have assessed some of the major, well-studied histone modifications at the *Atoh1* locus in the prosensory domain and during differentiation of the organ of Corti, as well as in perinatal hair cells and supporting cells. We have observed a developmental sequence of epigenetic changes that correlate with *Atoh1* expression in differentiating hair cells and supporting cells. One specific example is between the active transcriptional state of *Atoh1* in differentiating hair cells, and the presence of histone H3 acetylation at lysine K9 (H3K9ac), a hallmark of active gene expression. Blocking histone acetylation pharmacologically, blocks the appearance of H3K9Ac at the *Atoh1* locus, and blocks the timely appearance of hair cells in the developing organ of Corti.

Conclusion

In conclusion, we have analyzed the epigenetic state of the *Atoh1* locus in purified hair cells, supporting cells, and their progenitors, and correlated it with the expression status of the gene at different stages in the development of the organ of Corti.

Activated Notch Causes Deafness by Promoting a Supporting/Progenitor Cell-Like Phenotype in Developing Auditory Hair Cells

Grace Savoy-Burke; Felicia Gileles; Wei Pan; Patricia White; Amy Kiernan

University of Rochester Medical School

Background

Notch signaling is an essential pathway involved in the differentiation of hair cells and supporting cells via the mechanism of lateral inhibition. The lateral inhibitory model predicts that cells adopting the primary cell fate (the hair cell fate) will inhibit the surrounding cells from adopting the same cell fate, leading to the adoption of a secondary cell fate (the supporting cell fate). In the central nervous system, studies have shown that Notch not only prevents the adoption of the primary cell fate (neurons), but also actively promotes the adoption of the secondary cell fate (glia). Here, we investigated whether Notch similarly promotes a supporting cell fate during sensory differentiation in the inner ear.

Methods

To generate animals expressing activated Notch, we crossed mice containing a ubiquitously expressed conditional *NICD* allele to animals containing a *Gfi1-Cre* allele, which expresses *Cre* in all hair cells soon after they begin differentiating. Hearing was assessed at P35 by auditory brainstem responses (ABRs) and measuring distortion product otoacoustic emissions (DPOAEs). Morphological changes in *NICD*-expressing hair cells were analyzed at P6, P11 and P20 by immunohistochemistry in sections of the entire inner ear and wholemount preparations of the organ of Corti.

Results

Gfi1-Cre;NICD offspring were viable and healthy, although they exhibited no Preyer reflex, indicative of a hearing deficit. ABR and DPOAE measurements in *Gfi1-Cre;NICD* animals and their littermate controls showed that *NICD*-expressing animals had no responses to the highest sound levels, demonstrating profound deafness. Analyses of hair cell markers showed that Myo6, parvalbumin and calretinin expression were downregulated in the *NICD*-expressing hair cells in the cochlea. In contrast a number of progenitor/supporting cell markers were upregulated in the *Gfi1-Cre;NICD* hair cells, including P27^{KIP1}, Sox2, and Prox1. The *NICD*-expressing inner hair cells lost their normal flask-like shape and contacted the basement membrane, a morphology more consistent with supporting/progenitor cells. Interestingly, the *Gfi1-Cre;NICD* offspring showed no behaviors indicative of a vestibular disorder, and there were no morphological abnormalities in the vestibular region of the inner ear.

Conclusion

Taken together, these data indicate that in the early differentiating sensory epithelia, activation of Notch inhibits hair cell differentiation while promoting a supporting/progenitor cell-like phenotype.

The Lin28b/Let-7 Axis Regulates the Timing of Progenitor Cell Cycle Exit and Differentiation in the Mammalian Cochlea

Erin Golden; Angelika Doetzlhofer

Johns Hopkins University

Background

The prosensory cells of the mammalian cochlea undergo several critical steps as they progress from undifferentiated progenitor cells to the highly specialized hair cells and supporting cells that comprise the mature organ of Corti. These steps, which include cell cycle exit, cell type differentiation, and maturation, occur in a highly stereotyped order; however, the molecular mechanisms regulating their timing are largely unknown. We recently identified that the *Lin28/let-7* axis is active in the developing cochlea. *Lin28* and its homologue *Lin28b* encode for evolutionarily conserved RNA-binding proteins that play a critical role in maintaining stem cell pluripotency. They act through both enhancing the translation of growth-related genes and repressing the expression of the *let-7* family of microRNAs. We have found that within the undifferentiated cochlea, *Lin28b* is expressed throughout the prosensory domain and drastically decreases as prosensory progenitors differentiate. Conversely, *let-7* miRNA expression increases throughout cochlea differentiation. We hypothesize that this switch in expression of the *Lin28b/let-7* miRNA axis is playing an important role in the transition of cochlear progenitor cells to a differentiated state.

Methods

We used both in situ hybridization and quantitative PCR to characterize the temporal and spatial expression pattern of *Lin28b* and the *let-7* miRNAs during cochlea differentiation. In order to address the role of *Lin28b* in cochlea differentiation, we used both lentiviral-infected organotypic cochlea cultures and a doxycycline-inducible transgenic mouse line (*iLIN28B*) to overexpress *Lin28b* prior to hair cell differentiation. Microarray and qPCR were used to identify targets of *Lin28b* within the differentiating cochlea. In order to determine if *Lin28b* is acting through a *let-7* miRNA-dependent mechanism, we have used a second doxycycline-inducible mouse line (*iLet-7*) that specifically overexpresses the miRNA *let-7g* to rescue the *iLIN28B* phenotype.

Results

We have found that prolonged expression of *LIN28B* within the progenitor cells significantly delays their terminal mitosis and differentiation. Interestingly, in the *iLIN28B* transgenic cochlea overall hair cell patterning and total number are not significantly different from non-transgenic littermates; however, supporting cell number is significantly increased and ectopic supporting cells are observed. This striking effect of *iLIN28B* overexpression can be reversed by simultaneous overexpression of a *Lin28b*-insensitive form of *let-7*; suggesting that *Lin28b* regulates progenitor cell cycle and differentiation in a *let-7*-dependent manner. Experiments addressing the downstream mechanisms of this pathway are ongoing.

Conclusion

Our data indicate that the Lin28b/let-7 axis plays an important role in timing steps key to proper cochlea development, including progenitor cell cycle exit and differentiation

PD - 143

Map3k4 Signaling Governs Sensory Potential of Progenitors in the Mammalian Inner Ear

K. Haque; A Pandey; HW Zheng; Su-Hua Sha; Chandrakala Puligilla

Medical University of South Carolina

Background

The sense of hearing depends on the precise cytoarchitecture of the organ of Corti (oC) which contains sensory inner and outer hair cells and highly-specialized nonsensory support cells arranged in an organized pattern. Alterations to this cytoarchitecture including changes in the hair cell or support cell number or their alignment cause hearing deficits, emphasizing the importance of understanding the molecular events that regulate and coordinate cell cycle exit, fate-specification, and patterning. The mitogen-activated protein kinases (MAPKs) were shown to modulate tissue development, cell proliferation, and differentiation by regulating several signal transduction cascades. Previous work has implicated the role of MAPK signaling in cochlear development and function and that MAPK-mediated FGF signaling is required for otic induction. However, we do not have a full understanding of roles of specific MAPK molecules that comprise MAPK signaling cascades. In particular, MEKK4, which encodes MAPK kinase kinase is shown to function in neural tube closure and skeletal patterning. However, the functional role(s) for MEKK4 in the developing cochlea have not been examined.

Methods

To dissect MEKK4 function, we analyzed mice harboring a kinase-inactive MEKK4 mutation at different embryonic and postnatal stages.

Results

Using *in situ* hybridization we analyzed MEKK4 expression at different developmental stages. Based on our results, MEKK4 expression initiates in the prosensory domain of the cochlea as early as E13.5. As the cochlea develops, MEKK4 expression is maintained throughout the sensory epithelium until postnatal stages. We examined hearing by performing ABR measurements in mutants, heterozygotes and wild-type control littermates and found that ablation of MEKK4 activity leads to significant hearing loss. In addition, we observed no ABR responses at any tested frequency in these mice as early as 6 weeks. Consistently, at the cellular level we found dramatic perturbations in the cytoarchitecture of the developing oC, including drastic reduction in number of outer hair cells and Deiters' cells along with extra pillar cells. These data suggest that MEKK4 plays a direct role in specification of these cell types. Our data also indicates that MEKK4 is expressed in the developing spiral ganglion neurons which prompted us to investigate spiral ganglion neuron innervation in mutants. Our initial findings suggest diminished innervation along with defects in fasciculation of spiral ganglion neurons.

In particular, neurons seem less robust and type II neurons rarely formed synapse with outer hair cells and instead of fibers turning toward base as seen in wild-type controls, most of these didn't make turns but projected towards strial edge of the sensory epithelium.

Conclusion

Our study suggests that MEKK4 signaling plays a key role in fate specification of hair cells and support cells and is essential for hearing. Based on our data, we hypothesize that MEKK4 functions to instruct hair cell and support cell formation probably by interacting with Atoh1.

PD - 144

Otic Sensory Lineage Specification and Genetic Regulation of Fbxo2

Byron Hartman¹; Roman Laske¹; Stefan Heller²

¹Stanford University School of Medicine, Department of Otolaryngology-HNS; ²Stanford University School of Medicine, Department of Otolaryngology-HNS, Department of Molecular and Cellular Physiology

Background

The overall goal of this project is to improve our understanding of how transcriptional states and related cellular identities specific to the otic sensory lineage are initiated and maintained. We used a comparative microarray approach to identify otic-specific expression patterns, with a focus on genes that are active early and maintained in sensory progenitors throughout development and maturation.

Methods

Gene expression levels in mouse otic progenitor cells from different developmental stages were assayed and compared to non-otic populations, including whole embryos with otic regions removed. Among the most otic-specific genes identified was *Fbxo2*, which encodes the F-box protein, Fbx2, a glycoprotein specific ubiquitin ligase subunit originally identified as one of the most abundant proteins in the guinea pig organ of Corti (Thalmann et al. 1997). Fbx2 is also reportedly abundant in organ of Corti of juvenile and adult mice and deletion of *Fbxo2* results in progressive age-related hearing loss and hair cell degeneration beginning at two months of age, with no other detectable phenotype outside the ear (Nelson et al. 2007). We performed developmental qRT-PCR and immunofluorescence expression studies to determine onset and define spatio-temporal patterning of *Fbxo2*.

Results

Onset of *Fbxo2* expression occurs in the early otocyst and expression is maintained in mature hair cells and supporting cells. The highly specific expression pattern of *Fbxo2*, taken together with cochlear degeneration in null mice, suggests that *Fbxo2* activation is a specific transcriptional feature of the otic sensory lineage and dedicated machinery for ongoing protein quality control is essential for inner ear function. We are generating mouse and ES cell lines with a multifunctional knock-in cassette driving expression of fluorescent reporter, lineage tracing, and drug-selection tools from the *Fbxo2* locus. These will be used for *in vivo* and *in vitro* experiments

to investigate development and maintenance of otic sensory cells and *Fbxo2* expression.

Conclusion

We aim to identify functional cis-regulatory elements and transcription factors that regulate *Fbxo2*. Phylogenetic and transcription factor binding site analyses suggest that *Fbxo2* may be regulated by one or more cis-regulatory modules that integrate activity of multiple transcription factors, including Pax2 and Gata3. We are developing promoter-enhancer reporter mouse lines and *in vitro* assays to characterize the minimal promoter/enhancer elements and transcription factor interactions that regulate expression of this gene. Knowledge of otic transcriptional regulation and *Fbxo2* regulatory element reporters will be applied to stem cell based *in vitro* models of otic development.

PD - 145

The Usher 3A Product, Clarin-1, is Involved in Mechanotransduction Regulation and Ribbon Synapse Maturation in Zebrafish Hair Cells

Marisa Zallocchi; Olugwatobi Ogun

Boys Town National Research Hospital

Background

Mutations in *clarin1* cause Usher syndrome type 3 (USH3A) in humans which is characterized by hearing loss, vestibular dysfunction and retinitis pigmentosa. Mouse models for USH3A also show hearing impairment and mild stereocilia dysmorphology. Expression of *clarin1* has been described at the stereocilia level and synapses in both cochlear and vestibular hair cells. Recently a similar pattern of expression has been described in zebrafish hair cells.

Methods

RT-qPCR, immunohistochemistry, western blot and FM1-43 uptake in wild type, control and morphant animals.

Results

The conspicuous maternal transfer of the *clarin1* transcript (detected as early as 0.5hpf -hours post fertilization), demonstrates the importance of *clarin1* during early steps in development. By the time the maternal transcript abundance starts to decrease the zygotic gene activation begins (3.5hpf to 4hpf) and the *clarin1* transcript levels increase. At the protein level, we detect *clarin1* at 1dpf (days post fertilization) in the otic vesicle, where it can be seen at the apical region of the hair cell precursors. By 5dpf *clarin1* is expressed at the base of the hair bundle and at the point of insertion of the kinocilium. Western blot analysis demonstrates the expression of two specific bands at around 25kDa. Because of its presence at the apical aspect of hair cells we analyzed whether *clarin1* may be playing a role in mechanotransduction channel regulation. FM1-43 uptake was measured in 2dpf and 3dpf live fish injected with control or *clarin1*-specific morphants. Qualitative and quantitative analysis shows a dramatic decrease in dye uptake in the *clarin1* morphants. This effect can be reversed by co-injection of the specific morpholino with the *clarin1* coding transcript. Planar cell polarity was unaffected in these morphants. Because *clarin1* is involved in ribbon

synapse maturation in mice we examined the synapses and neuronal terminals. We observed a decrease in the number of synaptic ribbons (Ribeye immunostaining) and abnormalities in the neuronal terminals that contact the neuromast hair cells (GFP labeled afferent neurons).

Conclusion

Because *clarin1* is not at the tip of the stereocilia, the decrease in dye uptake suggests *clarin1* may be playing a role in the regulation (i.e. transport, complex formation, etc.) of particular components of the mechanotransduction machinery. Likewise, at the synapses it may be a facilitator of ribbon synapse assembly and/or transport. In summary, the results demonstrate the importance of *clarin1* function at both the apical and basal microdomains of zebrafish hair cells.

PD - 146

GPSM2/LGN Executes Polarity Cues in the Mammalian Inner Ear

Yoni Bhonker¹; Shaked Shvatzki¹; Tal Elkan¹; Sun Myoung Kim²; Fumio Matsuzaki³; David Sprinzak⁴; Ping Chen²; Karen B. Avraham¹

¹Department of Human Molecular Genetics and Biochemistry, Sackler Faculty of Medicine and Sagol School of Neuroscience, Tel Aviv University, Tel Aviv, Israel;

²Department of Cell Biology, Emory University, Atlanta, GA, USA; ³Laboratory for Cell Asymmetry, RIKEN Center for Developmental Biology, Kobe, Japan; ⁴Department of Biochemistry and Molecular Biology, Wise Faculty of Life Sciences, Tel Aviv University, Tel Aviv, Israel

Background

Planar cell polarity (PCP) is a pathway responsible for the polarization of stereocilia in the mammalian inner ear, an essential process for hearing. We have previously identified a pathogenic mutation in the gene *GPSM2/LGN* in a Palestinian family suffering from hearing loss and brain malformations (Walsh et al. *AJHG* 2010). *Lgn* is conserved in mitotic spindle orientation, and is regulated by the PCP pathway. It was recently shown to affect the structure of the hair bundle in an extensive characterization of its canonical binding partner *Gai*. Using a mouse model, *Lgn Δ C/ Δ C* mice lacking the C-terminal GoLoco domains of *LGN* (Konno et al. *Nat. Cell Bio.* 2007), we examined the effect of this mutation on the development of the inner ear. *Looptail*, a *Vangl2* PCP mutant, was examined for the effect of the PCP pathway on *Lgn* and associated proteins.

Methods

Auditory brainstem response was tested to evaluate hearing. Immunofluorescence was used to identify changes in hair cell morphology and protein localization.

Results

Lgn Δ C/ Δ C mice are profoundly deaf at the onset of hearing, tested at P17. At the molecular level, the localization of *Lgn* and *Gai3* was highly correlated with hair bundle orientation, basal body position and the kinocilium in both wild type and mutant mice. Mutant mice showed misoriented and flattened hair bundles. In addition, the microtubule network was abnormal in *Lgn* mutant mice. *Lgn* and *Gai3* localization were well

correlated with misoriented hair bundles in Looptail mutants. However, no change was observed in the polarized localization of core PCP proteins Vangl2 or Fz3, which relays the global cue(s) and couples coordinated polarization of neighboring cells in *LgnΔC/ΔC* mice.

Conclusion

We show that *LgnΔC/ΔC* mice are a profoundly deaf, similarly to humans with a mutation in the orthologous gene. *Lgn* polarizes to the lateral side of hair cells along with *Gai3* in a Vangl2-dependent manner, and affects the localization of the basal body, kinocilium and microtubule network. The kinocilium in turn is required to restrict the localization of *Lgn* to the cell periphery. In the inner ear, *Gai3* localization appears to be dependent on *Lgn* function. Together, our data suggests that *Lgn* acts in parallel or downstream of core PCP genes and is required for transduction of polarity instructions from polarized core PCP proteins

PD - 147

A Theoretical Model for Hair Bundle Morphogenesis

Adrian Jacobo; A. James Hudspeth
The Rockefeller University

Background

With the notable exception of those in the mammalian cochlea, the hair bundles of many species and receptor organs display a similar structure. Stereocilia arranged in a hexagonal pattern cover a portion of the apical surface of a hair cell, with stereociliary lengths that grow progressively in the direction of the kinocilium to form the characteristic staircase shape [Tilney 1983, Favre 1986, Jacobs 1990]. To organize stereocilia in this particular arrangement, a developing hair cell must convey the information necessary to define the boundary of the hair bundle, determine the hexagonal arrangement of the stereocilia, and produce a height gradient.

Methods

In this work we propose a variant of a reaction-diffusion model [Schnakenberg 1979] to explain how a hair cell might solve this problem (Figure 1a). The model proposes the existence of two morphogens **A** and **B**, which diffuse from the periphery of the apical surface and the kinocilium, respectively. These two molecules also have characteristic degradation rates. The combination of diffusion and degradation creates a concentration gradient for each morphogen, with the concentration decreasing away from the source. The model also proposes that **A** and **B** will serve as the substrates for the synthesis of two other morphogens **U** and **V**. Finally, **U** catalyzes its own formation in the presence of **V**.

Results

Under the right conditions this set of reactions is able to produce hexagonal Turing patterns [Turing 1952] for the concentrations of **U** and **V**, which can then be used by the cell to signal the positions where stereocilia will grow (Figure 1b). For the pattern to arise **A** and **B** must be present in the right proportions. Given the gradients that these two morphogens form across the cell surface, the conditions for the existence of the pattern will be fulfilled in only a small region. There-

fore, by adjusting these gradients the cell can tailor the region where the hair bundle will be created.

It can be seen that the gradients of **A** and **B** can also convey positional information to the stereocilia to establish the height gradient.

Conclusion

Using this model we predict that a hair cell needs at least two sources of morphogens, the cell boundary and the kinocilium, to produce the observed hair bundle. We are also able to predict how bundles will change under certain perturbations that might now be tested experimentally.

Favre D, Bagger-Sjöbäck D, Mbiene J, Sans A (1986). *Anatomy and Embryology Freeze-fracture study of the vestibular hair cell surface during development*. *Anat Embryol*, 176:69–76.

Jacobs RA, Hudspeth AJ (1990). *Ultrastructural Correlates of Mechano-electrical Transduction in Hair Cells of the Bullfrog's Internal Ear*. *Cold Spring Harb Symp Quant Biol*, 55:547–561.

Schnakenberg J (1979). *Simple chemical reaction systems with limit cycle behaviour*. *J Theor Biol*, 81:389–400.

Tilney LG, Saunders, JC (1983). *Actin filaments, stereocilia, and hair cells of the bird cochlea. I. Length, number, width, and distribution of stereocilia of each hair cell are related to the position of the hair cell on the cochlea*. *J Cell Biol*, 96(3):807–21

Turing AM (1952). *The Chemical Basis of Morphogenesis*, *Philos. Trans. R. Soc. London Ser. B*, 237(641):37-72.

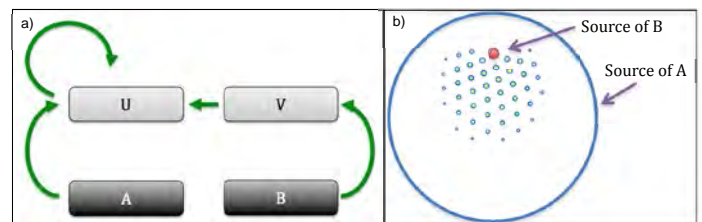


Figure 1: a) Schematic representation of the network of morphogen interactions. **A** and **B** act as substrates for the synthesis of **U** and **V**. In the presence of **V**, **U** self-catalyzes. The four morphogens can diffuse. b) Isoconcentration lines of **U** at the apical surface of a hair cell in the presence of the indicated sources of **A** and **B**. The hexagonal pattern created by peaks in the concentration of **U** acts as a signal to position the stereocilia.

SY - 064

Enduring Cortical Cellular Deficits Outlast Temporary Developmental Hearing Loss

Dan Sanes; Todd Mowery; Vibhakar Kotak
New York University

Background

A general principle of development holds that sensory experience during finite periods of maturation, called critical periods (CP), influences central nervous system (CNS) function, thereby shaping adult performance. Thus, the deficits that attend developmental hearing loss can be minimized when

hearing is restored before CPs close. However, children with transient hearing loss can display long-lasting deficits in perception, speech, or language skills. Therefore, it is possible that hearing loss can induce changes to the CNS that persist long after hearing has been restored. In this presentation, I will briefly review the impact of profound developmental hearing loss on auditory cortex cellular properties, and then ask whether similar effects are observed for much milder and briefer periods of deprivation.

Methods

Previously, we have examined the cellular effects resulting from sensorineural hearing loss (SNHL; bilateral cochlear removal), or moderate conductive hearing loss (CHL, bilateral malleus removal). More recently, we have begun to explore the effects due to mild and transient conductive hearing loss. Mild hearing loss was induced by implanting silicone earplugs bilaterally at the time of ear canal opening, leading to a ~25 dB shift in behavioral thresholds. This approach permitted the restoration of normal hearing by removing the earplugs, and allowed us to determine whether CPs had closed. To measure the effects induced by earplug insertion, or their removal, we performed whole-cell recordings from pyramidal neurons in layer 2/3 of thalamorecipient auditory cortex, and obtained measures of membrane properties (current clamp) and synaptic properties (voltage clamp).

Results

Most membrane and inhibitory synaptic properties failed to mature only when hearing loss was induced within a brief time window following ear canal opening. Some cellular properties did not recover when hearing was restored after only 2 weeks, even when the recovery period extended to adulthood.

Conclusion

These results demonstrate that even transient periods of mild hearing loss can derail central auditory maturation, and imply that the delays in acquiring perceptual skills, which persist long after peripheral transduction returns to normal, could result from long-term deficits in membrane and synaptic properties.

SY - 065

Cortical Reorganization Following Exposure to Traumatic and Non-Traumatic Noise

Martin Pienkowski

Salus University

Background

Following the demonstration that adult somatosensory cortex reorganizes after a peripheral nerve injury, Robertson and Irvine (1989) showed that mechanical lesions to the (high-frequency-tuned) base of the cochlea led to the over-representation of lesion-edge mid-frequencies in primary auditory cortex (A1). More recent work by Kamke et al. (2005) has suggested that cholinergic modulation of A1 by the basal forebrain, which appears necessary for plasticity driven by some forms of perceptual learning, is not required for lesion-induced reorganization in A1. Instead, such reorganization could be driven in purely bottom-up fashion, by a release from inhibition of the

lesion-edge A1 region, coupled with a Hebbian strengthening of excitatory connections from the lesion-edge to the deafferented region.

Methods

We have recently exposed groups of normal-hearing adult cats to various types of noise backgrounds at non-traumatic levels (~70 dB SPL) for several weeks to months.

Results

Persistent exposure to moderate-level, meaningless noise can induce reorganization in A1 reminiscent of that following hearing loss (Norena et al., 2006; Pienkowski and Eggermont, 2009; 2011). Specifically, frequencies outside of a sharply filtered noise exposure band become over-represented in A1 at the expense of frequencies within the noise band. These changes gradually reverse with the termination of exposure, but the reversal can be incomplete over a recovery period twice as long as the initial exposure duration.

Conclusion

I will discuss the potential mechanisms and clinical relevance of this new manifestation of long-term auditory cortical plasticity. Much remains to be learned, including whether or not noisy environments can lead to lasting "auditory processing disorders", including tinnitus, in the absence of any damage to the auditory periphery.

SY - 066

Cortical Cartography Following Deafness

Stephen Lomber¹; Carmen Wong¹; Daniela Kühne²; Andrej Kral²

¹University of Western Ontario; ²Hannover Medical University

Background

Sensory input is essential for the functional development of the cerebrum. A lack of acoustic experience in deaf individuals impairs maturation of auditory circuits and structures. Auditory cortical areas are differentially affected in cats deafened shortly after birth versus cats deafened in adulthood. Interestingly, the total volume of auditory cortex is positively correlated to the age of deafness onset, such that auditory cortex is more diminished in cats deafened earlier in life. To further understand the relationship between acoustic experience and cortical development, auditory cortex of congenitally deaf cats (CDC) was examined. In CDCs, a genetic defect causes inner ear degeneration during development, preventing any hearing experience.

Methods

Cerebral cytoarchitecture was revealed immunohistochemically using SMI-32, a monoclonal antibody used to distinguish auditory areas in many species. Auditory areas were delineated in coronal sections and their volumes measured.

Results

In CDCs, total auditory cortex volume was dramatically reduced in comparison to hearing animals. Total auditory cortex volumes were reduced, but to a lesser extent in early deafened and adult deafened cats, supporting the correlation between auditory cortex volume and hearing experience. While

all ten auditory areas were significantly diminished in deaf animals, some regions appeared to be more affected than others. Within auditory cortex of CDCs, the fractional volume of primary auditory cortex was significantly reduced in comparison to hearing cats, while second auditory cortex was expanded. In early deafened or adult deafened cats, primary auditory cortex and second auditory cortex were similarly reduced or expanded, but to a lesser extent. Anterior limits of rostral auditory areas were shifted posteriorly, suggesting expanded somatosensory cortex. Additionally, posterior limits of caudal auditory areas were shifted anteriorly, suggesting expanded visual cortex. Furthermore, a novel area with uniquely light SMI-32 labeling was discernible from the strongly immunoreactive anterior auditory field and adjacent somatosensory cortex. This new area may reflect underlying crossmodal plasticity following congenital deafness.

Conclusion

Overall, this study demonstrates the importance of sensory input during development to shape the overall cartography of the cerebrum.

SY - 067

Neural Coding of Binaural Cues With Bilateral Cochlear Implants: Effects of Duration and Onset-Time of Deafness

Bertrand Delgutte; Kenneth Hancock; Yoojin Chung
Massachusetts Eye and Ear Infirmary

Background

Although bilateral cochlear implants (CI) provide benefits for localizing sounds and speech reception in noise, binaural performance of CI users is still below normal, especially in tasks involving interaural time differences (ITD) such as binaural unmasking. This poor performance is surprising because the neural coding of ITD can be as precise as normal in animals with normal auditory development that are bilaterally implanted as adults (Smith and Delgutte, *J Neurosci* 27:6740). Unlike these animals, CI users often experience periods of auditory deprivation before implantation and, when deafness has an early onset, the deprivation may occur during a sensitive period for the experience-dependent maturation of binaural circuits. We therefore examined the effects of onset-time and duration of deafness on the ITD sensitivity of inferior colliculus (IC) neurons in animal models of bilateral CI.

Methods

We compared the ITD sensitivity of IC neurons in three groups of adult animals that were bilaterally implanted with intracochlear electrodes: (1) acutely deafened cats that were deaf for only 1-2 weeks, (2) long-term, deafened cats that were deaf for 6 months during adulthood, and (3) congenitally deaf white cats that became deaf before onset of hearing. Single-unit recordings were made under barbiturate/urethane anesthesia in response to periodic trains of biphasic pulses with varying ITD at low pulse rates (20-80 Hz).

Results

The incidence of ITD sensitive neurons was greatly reduced in congenitally-deaf cats compared to both groups of adult-deaf-

ened cats. In addition, the highest pulse rate for which IC neurons show sustained responses was lower in congenitally deaf cats than in the other two groups, thereby posing problems for encoding ITD at the high pulse rates used in CI processors. Long-term, adult deafened cats showed a milder deficit in which the distribution of best ITDs across the neural population was scattered and lacked the contralateral bias that is present in both normal-hearing and acutely deafened cats, and is essential for fine ITD acuity near the midline.

Conclusion

Congenital deafness causes more severe degradation of neural ITD coding than deafness of comparable duration occurring during adulthood. This finding argues for the importance of fitting deaf children with sound processors that provide reliable ITD cues at an early age. The milder deficits observed in adult deafened cats are similar to those observed in normal-hearing animals raised in altered auditory environments, and may be reversible if the CIs deliver appropriate binaural cues.

SY - 068

Cortical Consequences of Unilateral and Bilateral Deafness

Andrej Kral¹; Peter Hubka¹; Silvia Heid²; Jochen Tillein³

¹*Institute of Audioneurotechnology*; ²*Institute of Physiology III*; ³*Institute of Audioneurotechnology*

Congenitally deaf cats (CDCs) have been used as an animal model of prelingual deafness (Kral and Sharma, 2012, *TINS*). Microelectrode recordings were performed at the primary auditory cortex under stimulation at the hearing and deaf ear with bilateral cochlear implants in anesthetized adult animals. Local field potentials were compared at the cortex ipsilateral and contralateral to the hearing ear. Unit responses were investigated with respect to facilitating or suppressive binaural interactions. The contralateral aural preference has been shown to be reduced in bilaterally deaf CDCs (Kral et al., 2013, *Brain*), whereas the effect on response latencies was more extensive than on amplitudes. Developmental plasticity of aural preference in single-sided hearing (or single-sided cochlear implants in animals chronically electrically stimulated using portable signal processors) was observed with a sensitive period of first 3.5 months in the hemisphere ipsilateral to the hearing ear. Stimulation effects were more pronounced when recording responses to the hearing ear in both hemispheres. With respect to morphology of LFPs, pronounced hemisphere-specific effects were observed, with LFP morphology more similar for responses recorded at the same cortex (even though stimulation was at deaf and the hearing ear was compared). However, the responses recorded at the different hemispheres were more different, even though the same ear was stimulated. That demonstrates the hemispheric specificity of some cortical adaptations irrespective of the ear stimulated. Further, onset latencies revealed that in the same animals the sensitive period for the cortex ipsilateral to the trained ear is shorter than the one for the contralateral cortex. Binaural interactions in multiunit recordings confirmed a reduced suppressive interaction in unilaterally congenitally deaf cats at the hemisphere ipsilateral to the hearing ear, but

not at the hemisphere contralateral to the hearing ear. The results suggest a different adaptation process at the hemisphere ipsilateral to the hearing ear, involving down-regulated suppressive mechanisms not found in the contralateral hemisphere. Single-sided deafness leads to an asymmetric brain, with specific adaptations on the hemisphere ipsilateral and contralateral to the hearing ear. Aural preference for the first hearing ear results. It needs to be overcome when restoring hearing at the deaf ear later in life.

SY - 069

Developmental Consequences of Unilateral Stimulation/deprivation in Children Using One Cochlear Implant

Karen Gordon¹; Daniel Wong²; Salima Jiwani¹; Desiree de Vreede³; Blake Papsin¹

¹*The Hospital for Sick Children*; ²*University of Konstanz*;

³*University of Leiden*

Cochlear implants deliver electrical pulses to stimulate the auditory nerve in children with sensorineural hearing loss, restoring activity to the auditory pathways. Although we would ideally establish a normally mature auditory system in these children, this is not a realistic outcome of implantation at present. Auditory function along the pathways is altered by effects of deafness, including degenerative changes and cross-modal reorganization, and the abnormal input delivered by the implant. Present devices cannot accurately represent acoustic sounds such as speech and music and, because implants were traditionally provided in only one ear, binaural cues were not available. Using electrophysiological measures in children using cochlear implants, we found evidence of abnormalities in the caudal brainstem but normal-like rostral brainstem activity and cortical oscillation patterns. Rapid developmental plasticity was measured over the first year of implant use in both the brainstem and cortex, often before development of speech perception could be assessed with behavioral tests. Longer periods of unilateral implant use revealed atypical patterns of auditory activity; abnormal strengthening from the stimulated ear in both auditory cortices were found in children who used a right unilateral implant for > 1.5 years with no stimulation in their other ear. These children tended to have better speech perception in their first than second implanted ear. More normal patterns of activity were found in children who received bilateral implants simultaneously or < 1.5 years delay and they had similar speech perception abilities in each ear. The results suggest that both bilateral and unilateral auditory deprivation should be limited in children.

SY - 070

Effect of Asymmetric Hearing Loss and Considerations for Cochlear Implantation

Jill Firszt¹; Laura Holden¹; Ruth Reeder¹; Noel Dwyer¹; Sarah Zlomke²; Kristen Lewis²

¹*Washington University School of Medicine*; ²*Midwest Ear Institute*

Background

Traditionally, cochlear implant (CI) recipients have had moderate to profound hearing loss in both ears. Individuals with

asymmetric hearing loss; that is, moderate to profound hearing loss in one ear and better hearing in the other ear, have not been implanted routinely because of their better hearing ear. Often these individuals have discontinued amplifying the poorer ear due to lack of benefit and wear amplification only in the better hearing ear. They are therefore, unilateral listeners. Recent research at Washington University School of Medicine (St. Louis) has examined performance and outcome variables in adults with asymmetric hearing loss who received a CI in the poorer ear to determine whether this treatment improved communication function.

Methods

Adults with asymmetric hearing loss (one ear meeting CI candidacy criteria and the other ear with better hearing) were evaluated pre-implant and 6 months post-implant. The test protocol was designed to incorporate measures and conditions that simulated real-life listening challenges (e.g., background noise, varied speaker locations and loudness levels, and multiple talkers). Additionally, a self assessment of perceived communication function was completed at each interval.

Results

For adults with postlingual hearing loss, group mean results indicated significant open-set speech recognition in the implanted ear after 6 months for measures in quiet and noise. Furthermore, significant improvements in speech recognition and localization were observed when comparing the 6-month bimodal condition to the pre-implant, everyday listening condition. For adults with prelingual hearing loss, speech recognition was limited and localization abilities were not significantly improved. For all participants, mean questionnaire ratings indicated improved perceived communication function at 6 months post-implant compared to pre-implant.

Conclusion

Distinct patterns were observed for adults with postlingual versus prelingual hearing loss. All postlingual adults had speech recognition even with prolonged periods of deafness and no hearing aid use. In contrast, prelingual adults did not obtain similar results. Age at onset is a significant factor, despite substantial hearing levels in the non-implanted ear.

SY - 071

Consequences of Auditory Deprivation on Spatial Hearing Abilities of Cochlear Implant Users

Ruth Litovsky

University of Wisconsin - Madison

Background

Bilateral cochlear implants (BiCI) are provided to a growing population of children and adults, through simultaneous or sequential procedures. We are interested in the consequences of early vs. late implantation for the emergence of sound localization, spatial release from masking and for de-reverberation. Adults in our studies became deaf at various stages in life and underwent varied periods of auditory deprivation prior to implantation. Most children with BiCIs are congeni-

tally deaf, and have no exposure to acoustic hearing prior to being implanted. Comparing their spatial hearing abilities with those of post-lingually deaf children allows us to explore the significance of early acoustic exposure on the extent to which they develop sensitivity to the acoustic cues that are most relevant for spatial hearing: interaural difference in time and level (ITD and ILD).

Methods

Research processors are used to selectively present ITDs and ILDs in which timing of individual pulses are controlled. We study dependence of binaural sensitivity on interaural pitch-matching, and the extent to which mis-matched stimulation is tolerated. Data are considered in the context of spread of excitation along the basilar membrane in monopolar stimulation. Models with multi-channel vocoders that simulate spread of excitation in normal-hearing listeners explore healthy systems that receive degraded stimuli. Multi-electrode stimulation, more relevant for representing speech information, is used to study the effect of channel interaction on binaural sensitivity.

Results

Early auditory deprivation leads to severe reduction of sensitivity to ITDs, but not ILDs. In adults, multi-electrode stimulation with up to 8 binaural channels is successful in retaining binaural sensitivity that is at least as good as that seen in single-channel stimulation. In both adults and children, performance is typically better in NH vocoders than with true BiCI users, even when using multi-channel simulations that take into account spread of excitation.

Conclusion

Binaural sensitivity can rarely be restored to BiCI users with the same level of sensitivity seen in NH listeners. Some of these issues may be limited by the fact that the BiCI devices do not capture and present binaural cues with fidelity; thus, daily stimulation experience by patients are not maximized by clinical processors. Approaches to overcoming these limitations will be discussed. Finally, the effect of training may be an important aspect of clinical treatment after bilateral implantation.

PD - 148

A Non-Canonical Pathway for Auditory Nociception

Emma Flores

Northwestern University, Feinberg School of Medicine

Background

The mammalian cochlea contains two types of sensory receptors, inner and outer hair cells, and two classes of primary sensory neurons, type I and II afferents. Sound-stimulated IHCs synapse onto type I afferents and transmit sensory information to the brain (canonical auditory pathway); however, it remains unclear if the OHC/type II afferent connection is functional and what type of stimulus, if any, stimulates this alternative neural pathway. In addition, loud noise can stimulate saccular hair cells, and some saccular afferents connect to the cochlear nucleus, providing another potential pathway for sound perception. Here we use *Vglut3*^{-/-} mice, which do

not display any signs of hearing due to a silent canonical inner hair cell/type I pathway, and lack a presumed saccular auditory pathway, to determine whether painful or tissue-damaging noises are detected by the canonical, the saccular or a novel auditory pathway.

Methods

We developed two assays: a behavioral paradigm to test avoidance to acute, presumably painfully-loud noise (Loud Noise Avoidance), and a measure of neuronal activity in response to prolonged, tissue-damaging noise (Noxious-Noise neuronal Response). The LNA assay was designed to determine if and how rodents avoid acutely-applied noise of 100dB, 105dB, and 115dB. In the NNR assay we examined c-Fos immunoreactivity within the cochlear nucleus following sustained exposure to tissue-damaging (120dB, 1hr) versus innocuous (80dB, 1 hr) noise.

Results

Using the LNA assay, we find that control mice display nocifensive behavior by quickly avoiding 100, 105 and 115dB noise. This avoidance required cochlear function, as aged CD1 mice, which have degenerated cochleae but normal vestibular function, failed to avoid loud noise. Furthermore, this avoidance required the canonical auditory pathway, as *Vglut3*^{-/-} mice also failed to avoid loud noise. However, with the NNR assay we found that, while as expected both innocuous and tissue-damaging noise triggered neuronal activity in the cochlear nucleus of control mice, tissue-damaging (but not innocuous) noise also elicited such an activity in *Vglut3*^{-/-} mice.

Conclusion

Acute nocifensive behavior is mediated by the canonical (IHC/Type I afferent) auditory pathway, as it requires cochlear function and VGLUT3. In contrast, tissue-damaging noise detection does not require VGLUT3, implying the existence of an alternative mechanism that is probably different from the canonical or the saccular auditory pathways. We term this form of sensation, a hybrid of pain and hearing, auditory nociception.

PD - 149

Type I IFN is Produced in Supporting Cells Against Virus Infection of the Cochlear Sensory Epithelium Via RIG-I Like Receptor Signaling Pathway

Yushi Hayashi¹; Koji Onomoto²; Ryo Narita³; Mitsutoshi Yoneyama²; Hiroki Kato³; Akiko Taura³; Takayuki Nakagawa³; Juichi Ito³; Takashi Fujita³; Kimitaka Kaga¹

¹*Institute of Clinical Research of National Hospital*

Organization Tokyo Medical Center; ²Chiba University;

³Kyoto University

Background

The inner ear has been regarded as an immunoprivileged site like the central nervous system, the cornea or the retina of the eye because of isolation by the blood-labyrinthine barrier. Several studies have recently revealed the presence of immunocompetent cells in the inner ear, but there are no

reports which indicate that the cochlear tissue itself possesses immunocompetence. Retinoic acid inducible gene-I (RIG-I) like receptors (RLRs) including RIG-I and melanoma differentiation-associated gene 5 (MDA5) were identified as a sensor of viral double-stranded (ds) RNA. Activation of RLRs results in the up-regulation of transcription factors like interferon (IFN) regulatory factor (IRF)-3, which leads to transcription of type I IFN that is an anti-viral cytokine. This sequential signaling provokes innate immune reactions and contributes to triggering adaptive immunity. There are some diseases of the cochlea which are possibly related to viral infection such as sudden hearing loss. However, there are no reports which clarify the relationship between viral infection and inner ear disease. The aim of this study was to investigate whether the cochlea possesses immunocompetence against viruses through RLR signaling.

Methods

We used *ex vivo* system of the cochlear sensory epithelium infected with Theiler's murine encephalomyelitis virus (TMEV). The expression change of RLRs and type I IFN induced by virus infection was estimated using immunohistochemistry, western blotting and qRT-PCR.

Results

RIG-I and MDA5 were expressed weakly in Hensen's and Claudius' cells which are supporting cells outside of the outer hair cell area in the uninfected cochlear sensory epithelium, but their expression was absent in auditory hair cells. When infected with TMEV, dsRNA of viruses became detectable in the area of Hensen's and Claudius' cells. In these dsRNA-positive cells, the expression of RIG-I and MDA5 was dramatically increased as compared with uninfected cells. Results of histochemical analysis showed that IRF-3 is also detectable in Hensen's and Claudius' cells of the normal cochlea. Virus-infected cells exhibited nuclear accumulation of IRF-3, suggesting that TMEV infection activates IRF-3 in the cochlea. TMEV infection induced high levels of gene expression of IFN α 4 and IFN β 1 which are type I IFNs, suggesting that the cochlea recognizes viral infection and triggers an antiviral program.

Conclusion

This is the first report that the cochlear sensory epithelium expresses the RIG-I family and produces IFNs. Interestingly, not auditory hair cells but supporting cells like Hensen's and Claudius' cells play an important role in innate immunity against virus infection.

PD - 150

Selective Ablation of Hair Cells is Sufficient for the Recruitment of Macrophages Into the Inner Ear

Tejbeer Kaur¹; Melissa K. Strong²; Keiko Hirose¹; Edwin W Rubel²; Mark E. Warchol¹

¹Washington University; ²University of Washington

Background

Prior studies have demonstrated that macrophages are recruited into the cochlea after acoustic trauma or aminogly-

coside ototoxicity, but the signals that initiate macrophage recruitment have not been identified. Moreover, the precise function of macrophages in the injured ear is not known. We have used a novel mouse model to characterize the response of cochlear and vestibular macrophages to elimination of hair cells.

Methods

Mice expressing human diphtheria toxin receptor under control of the Pou4f3 promoter were crossed to CX3CR1-GFP mice, which express GFP in all macrophages. Mature mice (6-8 weeks postnatal) were given a single injection of diphtheria toxin (DT, 25ng/gm), which caused extensive loss of both inner and outer hair cells. After 1-56 days recovery, cochleae and vestibular organs were fixed, processed for immunohistochemistry, and imaged with confocal microscopy.

Results

Cochlear hair cell loss was first evident at 3 days after DT injection and nearly-complete ablation of inner and outer hair cells was observed after 14 days. Increased numbers of GFP-expressing macrophages was also noted at 3 days post-DT. The macrophages were particularly abundant below the basilar membrane and in close contact with neurons within the habenula perforata and the tunnel of Corti. Macrophages extended processes into the injured IHC and OHC regions. BrdU labeling studies suggested that the increase in macrophages was due to infiltration of circulating monocytes, rather than proliferation of resident macrophages. The numbers of macrophages associated with the sensory epithelium peaked at 7 day post-DT and declined at later survival times. In contrast, the spiral ganglion contained elevated numbers of macrophages as late as 56 days post-DT. Systemic treatment with minocycline did not affect macrophage numbers or cochlear pathology after DT injection. However, systemic treatment with liposomally-encapsulated clodronate caused a ~50% reduction in macrophage recruitment. The consequences of this depletion are currently under investigation. Treatment with DT also led to a partial loss of vestibular hair cells and entry of macrophages into the utricular sensory epithelium. These macrophages frequently extended processes that appeared to engulf entire hair cells and/or calyx nerve terminals.

Conclusion

Our results suggest that the death of hair cells - without any other evident otic pathology - is sufficient to recruit macrophages into the inner ear. Macrophages appear to phagocytose injured hair cells and interact with afferent neurons. Other functions of otic macrophages remains unknown.

Differences in Cochlear Sensory and Supporting Cell Mitochondrial Metabolism Bias Free Radical Production

Heather Jensen Smith; Lyandysha Zholudeva; Kristina Ward; Michael Nichols
Creighton University

Background

Although there are numerous causes of hearing loss and deafness, reactive oxygen species (ROS) are key regulators of multiple pathologies including: aminoglycoside-induced ototoxicity, noise-induced and age-related hearing loss. Unfortunately, the source of these cell-damaging ROS remains controversial. Given that ROS are normal byproducts of ATP synthesis that can rise to lethal levels when mitochondrial metabolism is perturbed, intrinsic differences in cochlear sensory (inner and outer hair cell, I/OHC) and supporting (pillar) cell mitochondrial metabolism may explain why high-frequency OHCs are profoundly sensitive to a host of challenges.

Methods

Mitochondrial metabolism was compared in apical, low-frequency (20% of cochlear length) and basal, high-frequency (80% of cochlear length) IHCs, OHCs and pillar cells obtained from acutely-cultured, intact cochlear (organ of Corti) explants harvested from mice (postnatal day 5±1). Intensity-based changes in the metabolic intermediate, nicotinamide adenine dinucleotide (NADH), were used to measure endogenous, mitochondrial inhibitor, mitochondrial uncoupler and GM-induced differences in sensory and supporting cell mitochondrial metabolism. Two-photon fluorescence lifetime imaging was also used to examine the distribution of distinct NADH fluorescence lifetime pools before and after treatment. The free radical probe DHR-123 was used to detect ROS production in sensory and supporting cells during GM exposure.

Results

In all regions of the cochlea, mitochondrial metabolism was significantly enhanced in sensory relative to supporting cells. NADH fluorescence lifetimes, a measure of the microenvironment of NADH, were also significantly different between sensory and supporting cells. Despite similar amounts of functional mitochondria in IHCs and OHCs, endogenous levels of NADH were greatest in high-frequency OHCs. GM significantly increased NADH intensity and concentration in high-frequency OHCs but not in IHCs or pillar cells. Within 30 minutes of GM application, ROS are dramatically and specifically increased in high-frequency sensory cells. High-frequency OHCs showed the largest increase in ROS with GM treatment.

Conclusion

Intensity- and fluorescence lifetime-based metabolic profiling of NADH metabolism revealed basal turn, high-frequency OHCs to be metabolically responsive to a number of changes in their microenvironment including metabolic toxins and GM. High-frequency IHCs, low-frequency IHCs and OHCs and, pillar cells are substantially less sensitive. Consistent

with the heightened susceptibility of high-frequency OHCs to undergo apoptosis after aminoglycoside exposure, GM-induced changes in mitochondrial metabolism and cell-damaging free radical production was greatest in high-frequency OHCs. This metabolic predisposition biases basal turn OHC responses to a variety of cochlear insults, particularly those involving energy metabolism and ROS production.

Purinergic Modulation of Type II Cochlear Afferents: Sensing Trauma in the Ear?

Chang Liu; Elisabeth Glowatzki; Paul Fuchs
Johns Hopkins University School of Medicine

Background

The mammalian cochlea is innervated by two groups of cochlear afferents. Type I afferents are well known for transmitting acoustic information with high fidelity and efficiency. In contrast, the function of type II afferents has remained mysterious for decades. In the present study, we asked whether type II afferents, in addition to glutamatergic excitation by OHCs, also may be driven by purines and pyrimidines released from damaged or stressed tissue, as might occur during acoustic trauma.

Methods

We performed whole-cell giga-ohm seal recordings from type II afferents near their terminal arbors under OHCs in excised cochlear turns from young rats (P7 – P9) while applying ATP or UTP. To study the function of type II afferents in damaged tissue, we recorded from type II afferents while OHCs were lysed mechanically with a sharp pipette. Cell rupture was confirmed by the loss of preloaded FM1-43 from the hair cell membrane.

Results

Both ATP and UTP depolarized all tested afferents. ATP-evoked currents reversed at 0 mV and could be blocked by the P2X receptor antagonist PPADS, suggesting the opening of ionotropic purinergic receptors. In contrast, UTP-evoked currents reversed at -70 mV and were antagonized by XE-991, an inhibitor of KCNQ channels, suggesting that UTP activates metabotropic P2Y receptors to close KCNQ channels through second messenger mediated pathways. The closure of KCNQ channels increased membrane resistance, and thus less current was necessary to activate action potentials. Finally, in order to study the effect of cell damage, we examined the responses of type II afferents while OHCs were acutely ablated with a sharp pipette. Strikingly, upon hair cell rupture, a large inward current was generated in the type II afferent, and a slower component of that current was blocked by P2X antagonist PPADS. Using extracellular loose-patch recording of the type II afferent, bursts of action potentials can be recorded when a single OHC was ablated.

Conclusion

Our results therefore suggest that type II cochlear afferents could respond to tissue damage caused by noxious levels of sound. The likely mechanism involves ATP, the common mediator of tissue damage, acting through ionotropic and metabotropic purinergic receptors. Activation of the ionotrop-

ic P2X receptor strongly depolarizes the type II afferents, whereas activation of the metabotropic P2Y receptor increases membrane resistance to facilitate firing.

PD - 153

Noise-Induced and Age-Related Functional and Structural Cochlear Alterations in *Igf1*^{-/-} Mice

Adelaida Celaya¹; Julio Contreras²; Lourdes Rodriguez-dela Rosa³; Jose Manuel Zubeldia⁴; **Isabel Varela-Nieto**⁵
¹CSIC; ²Facultad De Veterinaria, UCM, Madrid, ES.; ³Centro de Investigación Biomédica en Red de Enfermedades Raras, Madrid, ES; ⁴Hospital GU Gregorio Marañón, Madrid, ES.; ⁵Instituto de Investigaciones Biomédicas 'Alberto Sols' CSIC-UAM, Madrid, ES.

Background

The physiological age-related decrease in circulating IGF-I levels have been related to cognitive and brain alterations. Therefore, IGF-I is considered a neuroprotective agent. Human IGF-I deficiency is a rare disease associated with poor growth rates, mental retardation and syndromic hearing loss (OMIM608747). *Igf1*^{-/-} mice are dwarfs with poor survival rates and congenital profound deafness, which worsens with ageing. **Our objective was to compare the susceptibility of *Igf1*^{-/-} and *Igf1*^{+/+} mice to damage by using exposure to excessive noise at different ages.**

Methods

Animals. *Igf1*^{-/-} and *Igf1*^{+/+} mice were maintained in MF10-laHsd*129/Sv genetic background. **Hearing.** Auditory Brainstem Responses (ABR) was performed with a Tucker Davis Technologies workstation before (pre) and 3, 14 and 28 days after noise exposure. **Noise exposure.** Mice were exposed awake in a sound reverberant chamber to a violet swept sine noise enriched in high frequencies as reported⁵ at 105 dB SPL for 30 minutes. **Cochlear morphology and immunohistochemistry.** Cresyl-violet or hematoxylin-eosin staining of 10 mm cochlear paraffin and frozen sections. Serial frozen sections (10 mm) were collected to detect neurofilament and synaptophysin. **Hair-cell quantification.** Decalcified cochleae were mid-sectioned exposing ~80% of the whole extent of the basilar membrane. The organ of Corti (OC) was dissected and phalloidin-stained, and its total length was divided into equidistant 5% sectors as reported⁶ using stereological software (CAST®). The number of inner (IHC) and outer (OHC) hair cells in systematically randomly sampled areas were determined, and cell density (cells/1000 mm²) was estimated for each sector. **RT-qPCR.** RNA expression levels of cochlear genes involved in synaptogenesis, inflammation and cell cycle were analyzed by real time quantitative PCR using probes from TaqMan®. **Serum determinations.** IGF-I levels were determined using a specific ELISA assay (OCTEIA Rat/Mouse IGF-I kit, IDS Ltd.). **Statistical analysis.** A mixed model procedure with ANOVA or Student t-test was carried out with SPSS v19.0 software or with RealTime StatMiner® software for RT-qPCR data. Post hoc multiple comparisons included Bonferroni and Tamhane tests. Data are expressed as mean±SEM. The results were considered significant at p<0.05.

Results

Igf1^{+/+} and *Igf1*^{-/-} mice show an age-dependent decrease in IGF-I serum levels, especially from 6 months of age on, which correlates with the increase in ABR thresholds. Noise-exposure experiments with 1 and 3 months-old mice did not reveal differences between genotypes, both genotypes were equally sensible to NIHL. However, 6 month-old *Igf1*^{-/-} presented greater susceptibility to noise damage, with higher threshold shifts and a poorer recovery compared to noise-exposed *Igf1*^{+/+} mice. The cellular and molecular mechanisms underlying susceptibility to damage will be discussed.

Conclusion

These data suggest that IGF-I moderate deficit enhances otic sensibility to damage. Therefore, IGF-I-based therapies could contribute to prevent or ameliorate age-related and noise-induced hearing loss.

PD - 154

A Comparative RIP-Seq Approach Reveals Distinct Roles for Caprin-1 and TIA-1 in Regulating Protein Translation During Cochlear Stress.

Jonathan Gale; Emily Towers; Naila Haq; Sally Dawson
UCL Ear Institute

Background

The cochlea is exposed to a wide variety of stresses throughout life including noise damage, ototoxic drugs and the ageing process. Relatively little is known about the molecular mechanisms by which hair cells respond to damage. We previously demonstrated that stress granules form following oxidative stress and ototoxic damage in an inner ear cell line (OC-2 cells) and in hair cells *in vitro* respectively. Stress granules are aggregates of proteins that bind specific mRNAs preventing their translation and thereby regulating protein expression to promote cell survival during cellular stress. In OC-2 cells and hair cells stress granule formation involves TIA-1 and Caprin-1, the latter being a direct transcriptional target of the hair cell-specific transcription factor Pou4f3 (Towers et al, J Cell Sci. 2011).

Methods

To better understand the role of stress granule components TIA-1 and Caprin-1 in regulating RNAs we followed their expression using immunocytochemistry and evaluated the specific RNAs that they bind using a combined immuno-precipitation and next generation sequencing approach (RIP-seq) in the OC-2 cells after exposure to two different types of stress.

Results

Caprin-1 and TIA-1 are recruited to stress granules within 1 hour of the onset of either heat shock or arsenite. To determine which RNAs are bound by Caprin-1 and TIA-1 during heat shock and arsenite treatment immuno-precipitation was performed using Caprin-1, TIA-1 and control IgG antibodies to pull down the interacting RNAs from treated and untreated OC-2 cells. The resulting pools of pulled-down RNAs were identified by Illumina Next Generation Sequencing (HiSeq 2000, PE100). Comparative data analyses identified: (i) many

changes in the RNAs bound to Caprin-1 after heat shock and arsenite treatment are common to both stress paradigms and (ii) there is little overlap in the RNA pools bound to Caprin-1 and TIA-1 suggesting distinct binding properties. Pathway analysis (DAVID v6.7, NIAID, NIH) highlighted a number of different pathways being regulated at the RNA level by TIA-1 and/or Caprin-1 including cell death-related RNAs and calcium-binding RNAs.

Conclusion

Our data reveal that Caprin-1 and TIA-1 regulate different RNA pools during cellular stress. Elucidating the molecular components that are “triaged” by TIA-1 and Caprin-1 could identify novel therapeutic targets to enhance cell survival during cochlear stress.

PD - 155

Ultrastructural 3D Characterization of Wound Healing in Deafened Organ of Corti Powered by SBF-SEM

Tommi Anttonen; Ilya Belevich; Eija Jokitalo; Ulla Pirvola
University of Helsinki

Background

Our focus is to provide ultrastructural characterization of pathophysiological changes occurring in the organ of Corti acutely after trauma. This knowledge is essential for the design of repair and regenerative therapies for sensorineural hearing loss.

Methods

We have studied acute changes taking place in the ototoxically challenged murine organ of Corti *in vivo* with serial block-face scanning electron microscopy (SBF-SEM). This method can be used to generate 3D models from biological samples at ultrastructural level. It suits perfectly the research on the auditory organ that is characterized by cytoarchitectural complexity and intricate innervation pattern. In SBF-SEM, the surface of the fixed and resin-embedded tissue block is imaged by detecting back-scattered electrons. An ultramicrotome mounted inside SEM cuts the block with fixed step-size to reveal fresh block surface for imaging. With this setup, one can automatically acquire thousands of images in perfect alignment, from which fine-detailed 3D reconstruction of a biological sample can be segmented.

Results

In the non-traumatized cochlea, the cell bodies of Deiters' cells form distinct cups around the basal poles of outer hair cells (OHCs). The cups tightly insulate nerve endings that synapse on OHCs. Upon ototoxic challenge, OHCs show signs of apoptosis before scar formation by Deiters' cells at the epithelial surface is initiated. Concomitantly with apoptotic OHC condensation, the cups of Deiters' cells are replaced by prominent swelling of the cell bodies to fill luminal spaces. Nerve fibers show concurrent retraction. We provide direct evidence that Deiters' cells possess macrophage-like function, as they actively digest apoptotic OHC debris, including cell nuclei, thereby maintaining tissue homeostasis. We show that the two functions of Deiters' cells, i.e. scarring that is

based on remodeling of the actin cytoskeleton to fill the sites of lost OHCs, and clearance of degenerating OHCs are separate processes, as they are mainly performed by different supporting cells.

Conclusion

The close association of the Deiters' cells cup with nerve terminals suggests that Deiters' cells have a structural role in the maintenance of the synaptic area. The apical scar formation appears to be a late phase in the wound healing process, as OHC condensation and supporting cell swelling within the sensory epithelium precedes it. Taking into account this sequence of post-traumatic events, OHC protection from apoptosis appears to be a more feasible way to protect hearing than intervention with the process of scar formation.

PD - 156

Inhibition of Retinoic Acid Signaling Rescues Inner-Ear Defects in a Mouse Model of CHARGE Syndrome

Donna Martin¹; Jennifer Skidmore¹; Elizabeth Hurd²; Alina Saiakhova³; Donald Swiderski¹; Ethan Sperry¹; Peter Scacheri³; Yehoash Raphael¹

¹The University of Michigan; ²The University of Edinburgh;

³Case Western Reserve University

Background

Exposure to excess or insufficient vitamin A *in utero* poses increased risks for developmental anomalies in humans, including craniofacial dysmorphisms and olfactory, vision, and hearing deficits. Interestingly, these same disorders are observed in CHARGE syndrome, an autosomal dominant condition and leading cause of deafblindness. CHARGE is caused by mutations in the gene encoding CHD7, an ATP-dependent chromatin remodeling protein and epigenetic modifier that controls nucleosome sliding and transcriptional activation/elongation. The extensive phenotypic overlap between vitamin A excess or deficiency and CHARGE led us to hypothesize that CHD7 and retinoic acid, a vitamin A metabolite and important developmental morphogen, share common mechanistic pathways. Dissecting these pathways could help develop interventions for multiple sensory impairments.

Methods

We analyzed gene expression in *Chd7* wild type and mutant mouse inner ears using RNA-seq and quantitative RT-PCR. To test whether retinoic acid signaling during pregnancy influences *Chd7* deficiency phenotypes, we administered retinoic acid or citral (a retinoic acid inhibitor) to pregnant mice and analyzed inner ear structure by paint filling. Levels of retinoic acid activity were monitored in *Chd7* mutant and wild type embryos using RARE (retinoic acid response element) reporter mice, which express β -galactosidase in response to retinoic acid. Human induced pluripotent stem cells (iPSCs) were derived from *CHD7* mutation positive CHARGE patients to test for retinoic acid signaling effects.

Results

RNA-seq of microdissected e10.5 inner ears revealed 50% or greater up-regulation of 425 genes and down-regulation

of 146 genes in *Chd7* heterozygous null vs. wild type mice. Several genes are potential targets of CHD7, including genes encoding retinoic acid synthetic enzymes (*Aldh*), degradation enzymes (*Cyp26*), and receptors (*Rar*, *Rxr*). *Chd7* heterozygous null inner ear defects were unaffected or worsened by retinoic acid treatment, whereas citral treatment resulted in partial correction. *Chd7* mutant embryos exhibited mildly increased β -galactosidase staining in the developing cochleovestibular ganglion, consistent with enhanced retinoic acid signaling. Human iPSCs from *CHD7* mutation-positive patients exhibited normal differentiation into neuroectodermal lineages.

Conclusion

Disrupted retinoic acid signaling in the *Chd7* mutant cochleovestibular ganglion, and partial rescue of *Chd7* deficient inner ear defects by retinoic acid inhibition, suggest critical roles for vitamin A metabolism in the multiple sensory impairments observed in CHARGE. Further detailed analysis of these shared molecular pathways between retinoic acid and CHD7 in mouse and human stem cells could prove beneficial for developing treatments for sensory deprivation.

PD - 157

Combined Fgf9/20 Signaling is Necessary and Sufficient to Regulate Growth of Cochlear Progenitor Cells

Sung-Ho Huh; Mark Warchol; David Ornitz
Washington University School of Medicine

Background

The organ of Corti (OC) is a complex mechanosensory structure that transduces sound vibrations into neuronal signals. The OC contains one row of inner hair cells (IHC) and three rows of outer hair cells (OHCs), separated by pillar cells (PCs). In addition, each sensory hair cell is associated with an underlying supporting cell (SC). The mechanisms that regulate the formation of OHCs are significant, since the loss of OHCs is a leading cause of sensorineural deafness and age-related hearing loss. Although mouse mutants lacking fibroblast growth factor (FGF) receptor 1 suggest a role for FGF signaling in OHC development, the underlying mechanisms regulating OHC development are not known. Previously, we have generated *Fgf20* knockout mice and found out that mice lacking a functional *Fgf20* gene are viable and healthy but are congenitally deaf. Furthermore, we showed that *Fgf20* is required for OHC differentiation. The *Fgf20* paralog, *Fgf9*, is also expressed in the developing inner ear but alone has no known role in cochlear development.

Methods

To investigate potential functional redundancy, *Fgf9* and *Fgf20* double knockout mice were generated. In addition, to identify which cell type receives the FGF signal *Fgfr1* and 2 were inactivated in cochlear epithelium or associated mesenchyme. To determine whether FGF signaling is sufficient for sensory progenitor proliferation, a constitutively activated FGFR1 was induced in the developing inner ear. Immunostaining was used to assess the size and proliferation index of

the progenitor cell population, and sensory hair cell differentiation.

Results

In *Fgf9/20* double mutant mice, the cochlear length was decreased by 60% but the density of OHCs was comparable to *Fgf20* mutant cochlea. *Fgf9/20* double mutant showed decreased proliferation in sensory progenitor cells. Examination of potential receptor targets of *Fgf9/20* indicate that mesenchymal FGFRs phenocopy the cochlear length phenotype and regulate progenitor cell proliferation while epithelial FGFRs regulate epithelial differentiation and patterning. Ectopic activation of *Fgfr1* in mesenchymal cells resulted in increased sensory progenitor cell proliferation and increased cochlear length.

Conclusion

These data indicate that FGF9 and FGF20 function together to regulate the size of the cochlear progenitor cell population, ultimately regulating cochlear length, and FGF20 functions independently to induce OHC and outer SC differentiation.

PD - 158

Septin7 Regulates the Formation of Inner Ear During Early Developmental Stage

Hiroko Torii¹; Norio Yamamoto²; Atsuhiro Yoshida²; Takayuki Nakagawa²; Juichi Ito²

¹Graduate School of Medicine, Kyoto University;

²Department Otolaryngology, Head and Neck Surgery, Graduate School of Medicine, Kyoto University

Background

Septin proteins are GTP-binding proteins that are evolutionally conserved through eukaryotes except plants. Septin complex can interact with membrane, myosin and microtubules. Their functions include formation of the cortical rigidity, control of the vesicular transportation and compartmentalization within plasma membrane. These functions contribute to the formation of the cellular polarity that is important characteristics of epithelial cells. Our previous reports showed that Septin7, a core protein of multimeric Septin complex, was expressed in the embryonic cochlea (Yoshida et al. *Hear Res* 2012) and Septin7 conditional knockout (cKO) mice showed prominent inner ear hypoplasia by the time of embryonic day 13.5 (E13.5) (Torii et al., ARO meeting 2013).

Methods

To identify the roles of Septin7 in inner ear development, we analyzed the phenotypes of Septin7 cKO mice embryos (*Foxg1Cre+Septin7^{flxed/flxed}*) more precisely. We performed immunohistochemistry to characterize the cell proliferation, apoptosis, neural development and hair cell differentiation in the developing mice inner ear from -E8.5 to E18.5. We also investigated the macroscopic morphology of the inner ear by using paintfilling.

Results

Macroscopic morphology of the inner ear was normal until E10.5. But on E13.5, the inner ear became severely hypoplastic. This suggests that the development of the inner ear gross morphology was impaired between E10.5 and E13.5

in Septin7 cKO mice. Neither the promotion of apoptosis nor the decrease of cell proliferation was detected by immunohistochemistry between E12.5 and E16.5. Sox2 positive and Myo6 positive cells were detected within the remnant inner ears even on E17.5, suggesting that the differentiation of sensory epithelia happened in Septin7 cKO inner ears. These cell populations had innervation from the β 3-tubulin positive auditory nerves.

Conclusion

Our results indicate that Septin7 is involved in the development of inner ear, especially the formation of the inner ear gross morphology but not in the differentiation of the sensory epithelia.

PD - 159

RNA Microarray Analysis in Mouse Cochlea Reveals Hmga2, the High Mobility Group Transcription Factor, in the Developing and Mature Inner Ear Sensory Epithelia

Azel Zine¹; Arnaud Fontbonne¹; Ibtihel Smeti¹; Isabelle Watabe¹; Nesrine Abboud¹; Francois Feron²

¹LNIA - CNRS UMR 7260; ²NICN - CNRS UMR 7259

Background

Previous data show that early postnatal cochlea harbors stem/progenitor cells and shows a limited regenerative/repair capacity. These stem/progenitor cell properties are progressively lost later during the postnatal development and adult. Hair cell regeneration through stem cells might represent one route to generating new hair cells, but genes that govern inner ear stem cell properties including self-renewal and the capacity to become hair cells have not been identified.

Methods

We used microarrays analysis of gene expression patterns of the cochlear sensory epithelium (CSE) of the mouse at postnatal day-3 (P3) and adult to identify genes that would help us to characterize the origin of inner ear stem cells and to test the hypothesis that inner ear stem cells could be expanded *in situ* to generate new hair cells. Ingenuity Pathway Analysis (IPA) and David bioinformatics tools were used for networks analysis. Some genes related to stem cell signaling pathway or hair cell differentiation were confirmed by qRT-PCR and immunohistochemistry.

Results

The comparison between CSE of P3 and adult mice obtained using SAM software revealed about 5644 differentially expressed transcripts with a (FC) > 2. We focused on one of up-regulated genes in the P3 CSE, HMGA2, shown to promote the maintenance of different stem cell populations and proliferation of a variety of tissues and cell lineages. IPA analysis showed the most significant IPA network assembled around Hmga2 in P3 CSE included direct interactions with HDAC2 and MIR-Let7, two genes involved in the chick inner ear regeneration.

We observed a broad HMGA2 expression in E14.5 embryonic cochlea in developing hair and supporting cells, in addition to immature cells in the GER and LER areas. By P3, HMGA2

is predominantly expressed in the hair and supporting cells. By P12 and adult, Hmga2 decreased in the hair and supporting cells. Using qRT-PCR assays, we found a decrease in transcript level for HMGA2 comparable to other inner ear developmental genes (Sox2, Atho1, Jagged1 and Hes5) in the CSE of the adult relative to postnatal ears.

Conclusion

We have generated comprehensive measurements of the transcriptomic changes that occur between P3 and adult CSE. The insights gained from our database suggest that there are about 5644 differentially expressed transcripts between the two CSE. Among these genes, one-candidate such as HMGA2, which is important for the stem cell-renewal, is higher in the hair and supporting cells of P3 CSE. Future experiments will examine the role of HMGA2 during development and in the expansion of inner ear stem cells *in vitro* and *in vivo*.

PD - 160

The Zinc-Finger Protein Insm1, Expressed in Delaminating Neuronal Progenitors, Nascent Neurons and Nascent Outer Hair Cells, Promotes Neurogenesis and Neuron Survival in Spiral and Vestibular Ganglia

Sarah Lorenzen¹; Anne Duggan¹; Osipovich Anna²; Mark Magnuson²; Jaime García-Añoveros¹

¹Northwestern University; ²Vanderbilt University Medical Center

Background

Discussion of the development and differentiation of inner ear neurons and hair cells has centered on the bhlh transcription factors. These factors, while necessary, cannot alone account for proper differentiation of these cells. Furthermore, no factor has been described that can differentiate between inner and outer hair cells in early stages of development. Insm1 is a zinc-finger protein that is expressed throughout the developing nervous system in late neuronal progenitors and nascent neurons. In the embryonic cortex and olfactory epithelium, Insm1 promotes the transition of progenitors from apical, proliferative, and uncommitted (i.e., neural stem cells) to basal, terminally-dividing and neuron producing. Here we determined the expression and function of Insm1 in inner ear development.

Methods

Insm1 expression pattern was assessed by *in situ* hybridization and with an Insm1 reporter line. Insm1 lineage analysis was conducted with Insm1 GFP-Cre mouse crossed with reporter mice AI9 and NZG (Jackson) which express tdTomato or nuclear localized lacZ behind a floxed STOP cassette. Insm1 function was analyzed by comparing wild type and Insm1 knockout (KO) embryos. Immunohistochemistry was used to identify delaminating progenitors, nascent neurons, cells in mitosis, and cells undergoing apoptosis.

Results

In the otocyst, delaminating and delaminated progenitors express Insm1, whereas, apically dividing progenitors do not.

Lineage analysis confirms that nearly all of the auditory and vestibular neurons come from cells which have expressed *Insm1*. In the absence of *Insm1*, we observe fewer delaminated progenitors and an increase in apoptosis in nascent neurons. Accordingly, spiral and vestibular ganglia have a 40% reduction in neuron number. Unexpectedly, we also find that nascent, but not mature, OHCs express *Insm1*, whereas IHCs never express *Insm1* nor are they derived from progenitors that have expressed *Insm1*. To our knowledge, this is the earliest molecular distinction between OHCs and IHCs.

Conclusion

Insm1 plays a critical role in inner ear development similar to that of olfactory epithelium and cortex. *Insm1* is expressed in all neuronally committed progenitors and nascent neurons, and it regulates neurogenesis and survival of auditory and vestibular neurons. *Insm1* is also transiently expressed in nascent OHCs and not IHCs during embryogenesis. This unique expression, so early and only in OHCs, suggests a role of *Insm1* in their distinct differentiation from that of IHCs.

PD - 161

A Gata3-MafB Transcriptional Network Controls Auditory Synapse Development and Function

Wei-Ming Yu¹; Jessica Appler¹; Ye-Hyun Kim²; Allison Nishitani¹; Jeffrey Holt²; Lisa Goodrich¹

¹Harvard Medical School; ²Harvard Medical School and Children's Hospital Boston

Background

A promising future therapy to restore hearing is to stimulate hair cell regeneration. This approach requires spiral ganglion neurons (SGNs) to develop a normal ribbon synapse on the regenerated hair cells. Similarly, the cochlear implant, an effective current therapy for hearing loss, requires the maintenance of the integrity of SGNs and their synapses. Therefore, identification of the molecules that drive formation of hair cell ribbon synapses may lead to the development of new therapies and broaden opportunities for patient treatment.

Methods

Here, we show that the MafB transcription factor acts in SGNs to drive differentiation of the large postsynaptic density (PSD) characteristic of the ribbon synapse. We generated a floxed allele of *MafB* and specifically removed MafB protein from spiral ganglion neurons. We also created a strain of mice (*MafBCE*) that overexpress MafB upon Cre-mediated recombination.

Results

In *MafB* conditional knockout mice, SGNs fail to develop normal PSDs, leading to reduced synapse number and impaired auditory responses. Conversely, synapse development is accelerated in mice with precocious and excessive *MafB* expression (*MafBCE* mice). The onset of MafB production depends on the activity of Gata3, which is also required for synapse development. Moreover, restoration of MafB significantly rescues the ribbon synapse defect in *Gata3* mutants.

Conclusion

Our results demonstrated that MafB is a powerful regulator of synaptogenesis that offers a new molecular entry point for treating hearing loss.

PD - 162

Ephrin-A Proteins Promote Targeting of VCN Axons to Contralateral MNTB

Sofia Marshak; Mariam Abdul-Latif; Karina Cramer
University of California, Irvine

Background

Mammalian auditory brainstem nuclei compute interaural intensity and time differences, which are used in sound localization. A key component of the underlying circuitry is the strictly contralateral projection from the ventral cochlear nucleus (VCN) to the medial nucleus of trapezoid body (MNTB), where the VCN axon terminates in the calyx of Held. While VCN axons grow through the region of the ipsilateral MNTB, they terminate selectively on the contralateral side with remarkable precision. This selectivity likely results from the combined roles of axon guidance molecules. Candidate molecules include the Eph receptors and their ephrin ligands, which fall into the A and B subclasses. Previous studies in our laboratory demonstrated that mutations that reduce EphB signaling result in aberrant ipsilateral projections in addition to the normal pathway, suggesting that EphB signaling normally prevents ipsilateral terminations. Here we explored the role of EphA and ephrin-A proteins in the formation of this pathway.

Methods

We first conducted an immunohistochemical expression analysis to identify EphA and ephrin-A proteins expressed along the developing VCN-MNTB pathway from late embryonic ages until postnatal day 10. We then assessed the role of these molecules in directing formation of VCN-MNTB circuit. We applied vital or lipophilic tracer to trace VCN projections unilaterally in mutant mice that lack *ephrin-A2* and *ephrin-A5*. We quantified calyceal projections terminating in MNTB on both sides of the brainstem.

Results

Several EphA family proteins were expressed in the developing auditory pathway at the ages examined. Ephrin-A2 was expressed postnatally in the midline and just outside MNTB. Ephrin-A5 was expressed in MNTB principal neurons. We found that *ephrin-A2*^{null};*ephrin-A5*^{null} double knockout mice had a significant proportion of VCN projections that terminated aberrantly in ipsilateral MNTB in comparison to wild type littermates. In some cases these projections appeared to arise from abnormal axon growth trajectories.

Conclusion

Taken together, the results suggest that both EphA and EphB signaling are important for VCN axon targeting. The expression patterns of these proteins and the effects of mutations on axon growth suggest that the two subclasses may have distinct roles in assembly of this neural circuit.

En1 is Necessary for Specification and Survival of a Subset of Superior Olivary Complex Neurons

Stephen Maricich¹; Walid Jalabi²; Stefanie Altieri¹; Rita Digiacomo²

¹University of Pittsburgh; ²Case Western Reserve University

Background

The brainstem superior olivary complex (SOC) plays important roles in sound localization. However, little is known about the genetic pathways and transcription factors necessary for specification and maturation of SOC neurons. *En1*, a gene expressed by a subset of developing and mature SOC neurons, encodes a homeobox transcription factor important for neuronal development in the midbrain, cerebellum, hindbrain and spinal cord. We set out to determine *En1*'s role in early and later SOC neuron development.

Methods

We used conditional deletion strategies in mice to specifically delete *En1* in SOC neuron precursors at early embryonic or later ages. We then used basic histology, immunohistochemistry, *in situ* hybridization and axon tracing techniques to analyze the effects on SOC neuron development.

Results

Early *En1* function is critical for development of glycinergic neurons of the lateral superior olive (LSO) and all neurons of the medial (MNTB) and ventral (VNTB) nuclei of the trapezoid body. Interestingly, neurons of the lateral nucleus of the trapezoid body (LNTB), which also express *En1*, are unaffected by *En1* deletion. *En1* deletion results in the loss of nearly all cholinergic neurons of the VNTB, while those found in the medial and lateral olivocochlear systems are not affected. Surprisingly, crossed projections from the cochlear nucleus (CN) to the SOC are present in the absence of MNTB neurons, although their ultimate targeting is aberrant compared to control mice.

Conclusion

Our data define an important role for the *En1* gene in the development of SOC neurons with glycinergic and mixed neurotransmitter phenotypes. They also shed light on developmental processes that control axon targeting within the CN-SOC projection.

Supporting Cells Sense Noise-Induced Damage Via TRPA1 Channels and Protect the Cochlea by Actively Changing the Geometry of the Organ of Corti

A. Catalina Vélez-Ortega¹; Stephanie E. Edelmann¹; Channy Park²; Ruben Stepanyan¹; Kelvin Y. Kwan³; Ghanshyam P. Sinha¹; David P. Corey³; Gregory I. Frolenkov¹

¹University of Kentucky; ²UCLA; ³Harvard Medical School

Background

Acoustic overstimulation leads to an increase in oxidative stress that can remain for several days as measured by the

production of the lipid peroxidation byproduct 4-hydroxynonenal (4-HNE). Since TRPA1 channels can be directly activated by 4-HNE and they have been involved in sensing noxious stimuli by nociceptive neurons, we evaluated their role as damage sensors in the cochlea.

Methods

TRPA1 expression in the organ of Corti was evaluated with antibodies against the human PLAP reporter expressed in *TrpA1*^{-/-} mice. Functional TRPA1 channels were assessed by the uptake of FM1-43 in cultured cochlear explants stimulated with TRPA1 agonists. Whole cell patch-clamp recordings and bright-field and fluorescent Ca²⁺ imaging were performed to evaluate cell responses to the application of TRPA1 agonists. Active changes in cell shape were evaluated after UV stimulation of photo-activatable (caged) Ca²⁺ chelators. Auditory brainstem responses (ABR) before and after consecutive exposures to broadband noise were assessed in 3-week old wild type and *TrpA1*^{-/-} mice.

Results

PLAP labeling revealed that TRPA1 is highly expressed in the supporting cells of the organ of Corti. FM1-43 uptake confirmed the presence of functional TRPA1 channels in the wild type Hensen's cells (HeC), cells of the Kolliker's organ (CKO), epithelial cells near the spiral ligament, but not in the Claudius's cells. TRPA1-mediated inward currents were observed in wild type HeC, Deiters' (DC) and pillar cells (PC). The most robust and long-lasting Ca²⁺ responses to puff application of TRPA1 agonists were observed in HeC, suggesting that these cells act as the major sensor of oxidative damage. Ca²⁺ responses in HeC triggered Ca²⁺ waves that propagated toward CKO, sometimes triggering there a faster Ca²⁺ wave that required extracellular ATP. The propagation of TRPA1-mediated Ca²⁺ responses was accompanied by prominent tissue displacements that seemed to be originated at DC or PC. None of the responses to TRPA1 agonists described above were observed in *TrpA1*^{-/-} mice. Flash photolysis of caged Ca²⁺ compounds in individual PC confirmed that these cells possess Ca²⁺-dependent contractile machinery that is capable of changing the geometry of the organ of Corti. Finally, the ongoing ABR analysis shows that *TrpA1*^{-/-} mice seem to be more susceptible to noise-induced hearing loss than wild type controls.

Conclusion

We believe that TRPA1-initiated Ca²⁺-dependent active changes of the supporting cell shape represent a novel mechanism modulating the cochlear sensitivity. This mechanism seems to participate in the protection of the organ of Corti after noise exposure.

Glucocorticoids Protect Cochlea Against NIHL by Modulating Hes1 Expression

Bin Wang¹; Xiaoyan Zhu²; Fanglu Chi³

¹Eye, Ear, Nose and Throat Hospital, Fudan University, PR China; Johns Hopkins University; ²Second Military Medical University, PR China; ³Eye, Ear, Nose and Throat Hospital, Fudan University, PR China

Background

Glucocorticoids (GCs) have been widely used in the clinical treatment of inner ear diseases. The protective effects of GCs against acoustic injury have also been confirmed in various animal experiments. However, the molecular mechanisms where by GCs exert their benefit on noise-induced hearing loss (NIHL) remain largely unknown. The negative basic helix-loop-helix (bHLH) transcription factor, hairy and enhancer of split 1 (Hes1), has recently been described as one of the pivotal genes for the control of inner ear hair cell differentiation. Hes1 negatively regulates inner ear hair cell differentiation by antagonizing the action of the positive bHLH transcription factors such as Math1. It was reported that Hes1 protein expression was up-regulated in the aminoglycoside-damaged guinea pig organ of Corti. More recently, we found significant up-regulation of cochlear Hes1 expression following acoustic trauma. These findings suggest that the increase of Hes1 expression may be involved in the pathogenesis of both ototoxic and acoustic lesions. The purpose of the present study was to explore whether hairy and enhancer of split 1 (Hes1) was involved in the protective effect of dexamethasone against NIHL.

Methods

Guinea pigs, which were administered intraperitoneal injections of either saline, 1.0 mg/kg dexamethasone, 20.0 mg/kg RU38,486, or a combination of both drugs (dexamethasone plus RU38,486) for 5 consecutive days, were exposed to whiteband noise (115 dB sound pressure level). Auditory brainstem response (ABR) recordings were performed before and 24 h after noise exposure. Dehydrogenase (SDH) staining specimens were examined under a phase contrast microscope equipped with a digital camera to determine the number of missing inner hair cells (IHCs) and outer hair cells (OHCs). The expression level of Hes1 in cochleae was compared using real-time RT-PCR and Western blot analysis.

Results

Noise exposure for 3 h induced auditory brainstem response (ABR) threshold elevations, outer hair cell losses, and increase of Hes1 expression. Dexamethasone administration significantly decreased the noise exposure-induced ABR threshold shifts at the same level in all frequencies, the number of OHCs lost and the noise exposure-induced Hes1 expression compared with the saline-injected noise exposure group. Although RU38,486 alone had no significant effect on Hes1 expression, it could block the inhibitory effects of dexamethasone on both mRNA and protein expression of Hes1, suggesting that dexamethasone suppresses cochlear Hes1 expression in guinea pigs after noise exposure via a GR-dependent mechanism.

Conclusion

Dexamethasone provides protection against noise-induced hearing loss (NIHL) possibly by suppressing cochlear Hes1 expression via a glucocorticoid receptor (GR)-dependent mechanism.

Noise-Induced Necrotic Outer Hair Cell Death is Modulated by Receptor-Interacting Protein Kinases

Kayla Hill; Hong-Wei Zheng; Su-Hua Sha

Medical University of South Carolina

Background

Receptor-interacting protein (RIP) kinases promote the induction of necrotic cell death pathways. The interaction of RIP1 and RIP3 through the RIP homotypic interaction motif leads to cellular ATP depletion and necrotic cell death pathways. It is well known that traumatic noise induces both apoptotic and necrotic outer hair cell (OHC) death. Here, we investigated the role of RIP kinases in noise-induced necrotic OHC death pathways using adult CBA/J mice.

Methods

Broadband noise from 2–20 kHz at 106 dB SPL for 2 hours was used to induce permanent threshold shifts (PTS). Propidium iodide labeling of OHC nuclei allowed for determination of apoptosis and necrosis via morphological criteria. Anti-RIP3, anti-RIP1, and anti-phospho-AMPK α (p-AMPK α) labeling of cochlear surface preparations was used to determine expression of RIP3, RIP1, and p-AMPK α in OHCs. Delivery of necrosis inhibitor necrostatin-1 (Nec-1) to the round window via intra-tympanic application was used to determine the number of apoptotic and necrotic OHC nuclei. Intra-tympanic delivery of RIP3 siRNA was employed to detect the expression of p-AMPK α .

Results

One hour after noise exposure, OHCs in the basal region of the cochlea displayed apoptotic and necrotic features, increased RIP1 and RIP3 protein levels, and increased formation of RIP1/RIP3 complexes. Treatment with necrosis inhibitor Nec-1 or RIP3 siRNA (siRIP3) diminished noise-induced elevation of RIP1 and RIP3 levels and decreased the number of necrotic OHC nuclei. Noise-induced active AMPK α levels, commonly associated with necrotic cell death, decreased with Nec-1 or siRIP3 treatment, consistent with the reduction of levels of RIP1 and RIP3. Finally, morphological assessment of OHCs showed that siRIP3 treatment reduces noise-induced OHC death.

Conclusion

Our results suggest that noise-induced OHC necrosis is modulated by RIP kinases. Inhibition of RIP kinase levels by a necrosis inhibitor or by silencing RIP3 can reduce noise-induced necrotic OHC death.

Innate Immune System in Cochlear Resident Cells and its Responses to Acoustic Trauma

Bo Hua Hu; Qunfeng Cai

University of Buffalo

Background

Tissue immunity is an important defense mechanism in living organisms. It protects host tissues from not only foreign invaders, but also endogenous stress molecules released from or displayed on damaged cells. The cochlea responds to injury by activating inflammatory responses. While the contribution of circulating immune cells has been recognized, the role of cochlear resident cells in defense responses to stress remains unclear. The current study was designed to profile the expression pattern of immune response genes in the organ of Corti; to examine their roles in maintaining normal cochlear functions, and to examine their involvement in noise-induced cochlear pathogenesis.

Methods

Transcriptome of cochlear sensory epithelium was examined using Illumina RNA sequencing (RNA-seq). The results for selected genes were verified for the tissue of the organ of Corti using qRT-PCR arrays and immunohistology. To determine the gene function, auditory brainstem responses and distortion production otoacoustic emission were examined in three knockout mouse models (*CD14*, *Irf7* and *Tlr4*). To determine how the immune genes in cochlear local cells respond to acoustic overstimulation, temporal changes in expression patterns of selected genes were examined in the organs of Corti of the mice exposed to a broadband noise at 120 dB for 1 hour. The function of differentially expressed genes was analyzed using DAVID Bioinformatics Resources. Moreover, the roles of *CD14* and *Tlr4* in cochlear responses to acoustic trauma were examined in the knockout mice.

Results

RNA-seq analysis revealed constitutive expression of innate-response genes in cochlear sensory epithelium. Further screening of 84 genes associated with innate and adaptive systems revealed the expression of 39 genes in sensory and supporting cells of the organ of Corti. Immunohistology revealed that supporting cells and inner hair cells are the major cell populations for the expression of the innate response genes. Acoustic overstimulation resulted in the induction of expression of immune response genes, including *Trf7*, *CD14* and *Tlr4* that are related to Toll-like receptor pathway. *Irf7* knockout mice showed a mild threshold elevation at a low frequency (4 kHz, 9.4 dB). *CD14* and *Tlr4* knockout mice showed greater functional loss also in the low frequency range (4 and 8 kHz) after the acoustic trauma, although these mice exhibited the normal hearing sensitivity in the physiological condition.

Conclusion

Innate response genes are constitutively expressed in the cochlear resident cells, and their function is required for modulation of cochlear responses to acoustic trauma.

Antioxidant Response and Coincident Apoptosis Regulation in the Auditory Receptor After Noise Exposure

Pedro Melgar-Rojas¹; Juan C Alvarado²; Veronica Fuentes-Santamaria³; **Jose M. Juiz³**

¹Universidad de Castilla-La Mancha; ²IDINE/Med School/ Universidad de Castilla-La Mancha; ³IDINE/Med School/ UCLM

Background

Noise exposure is a common cause of hearing loss. Genetic and molecular studies have evidenced the central role of oxidative stress in the pathogenesis of noise-induced hearing loss (NIHL) [1]. Intense noise causes an excessive production of reactive oxygen species (ROS), leading to oxidative stress on hair cells and subsequent cochlear damage. In this regard, it is essential to elucidate the molecular mechanisms that underlie cochlear damage. This may impact the development of new therapeutic strategies for NIHL. Towards this goal, we are testing the involvement of oxidative stress and apoptotic pathways in NIHL by evaluating transcriptional levels of key genes by quantitative real time PCR (qRT-PCR).

Methods

Wistar rats were exposed to broadband noise (0.5-32 kHz, 118 dB SPL), for 4h/day during 4 consecutive days to induce permanent threshold shift (PTS). Auditory brainstem responses (ABR) were evaluated [2] prior to exposure and 1 day (d), 4d and 10d post-exposure. At each time point, cochleae were micro-dissected and qRT-PCR was performed in order to evaluate the expression levels of key genes related to oxidative stress [3] and apoptosis.

Results

PTS was confirmed by the auditory threshold shifts on ABR recordings up to 10d post-exposure. qRT-PCR revealed an up-regulation of antioxidant enzyme genes (*Sod1*, *Cat* and *GPx1*) at 1 day post-exposure. This was accompanied by increased expression of the anti-apoptotic *Bcl-2* gene and down-regulation of one of the pro-apoptotic *Bax* genes, suggesting an attempt to restore cellular stress-related damage. At 4d-postexposure expression levels of the three antioxidant enzyme genes decreased relative to 1d, whereas apoptotic death had likely been triggered, as seen by up-regulation of *Casp3* and down-regulation of *Bcl-2*. Finally, at 10d post-exposure, all tested genes, related either to antioxidation or apoptosis regulation, were intensely down-regulated.

Conclusion

qRT-PCR analysis allowed us to distinguish three phases of oxidative stress in noise-exposed cochleas: 1) Acute transcriptional response, characterized by up-regulation of the antioxidant cell machinery and blockade of apoptotic death. 2) Intermediate response, characterized by relative failure of antioxidant mechanisms and activation of apoptotic pathways. 3) Late response, characterized by complete failure of antioxidation mechanisms and execution of cell death programs.

Autophagy Defends Against Noise-Induced Hearing Loss

Su-Hua Sha; Hu Yuan

Medical University of South Carolina

Background

Autophagy is a self-degradation process involving lysosome-dependent turnover of cellular constituents and clearance of damaged cellular components. Because of its physiological function in sequestering damaged cellular components into membrane-bound autophagosomes and subsequent degradation via fusion with lysosomes, autophagy plays an important role in maintaining cellular homeostasis. Here, we investigated the function of autophagy in noise-induced temporary and permanent auditory threshold shifts (TTS and PTS, respectively), in adult CBA/J mice.

Methods

Broadband noise from 2–20 kHz at 98 dB SPL for 2 hours was used to induce permanent threshold shifts (PTS), 106 dB to induce severe PTS (sPTS), or 96 dB SPL to induce temporary thresholds shifts (TTS). Auditory brainstem responses were used to measure auditory function. Myosin VIIa and DAB staining of the cochlear epithelia was used to quantify outer hair cell (OHC) loss. Immunolabeling of cochlear surface preparations with the marker of autophagy (LC3B) or in combination with the lysosome marker (LAMP1) determined the expression of autophagosomes and the formation of autophagolysosomes in OHCs. GFP-LC3 transgene mice further confirmed the expression of LC3 in OHCs. Delivery of LC3B siRNA to the round window via intra-tympanic application was used to detect autophagy and hearing function. We treated with 3-methyladenine (3-MA) or rapamycin via intra-peritoneal injection to observe the influence of pharmacological regulators of autophagy on noise-induced hearing loss (NIHL).

Results

LC3B-associated immunofluorescence increased in OHCs 1 hour after either TTS- or PTS-noise exposure, but not after sPTS, with TTS exerting a significantly stronger effect than PTS. Consistent with these results, GFP fluorescence significantly increased in OHCs of GFP-LC3 transgene mice after TTS-noise exposure. In addition, the co-localization of LC3B and LAMP1 significantly increased in OHCs after TTS-noise exposure. Treatment with rapamycin significantly increased expression of LC3B and prevented noise-induced PTS. In contrast, treatment with 3MA resulted in down-regulation of LC3B expression, intensifying the magnitude of both TTS and PTS. Furthermore, silencing LC3B corroborated the results from 3MA treatment, blocking rapamycin-induced elevation of LC3B, and impeding its protection against NIHL.

Conclusion

Autophagy is a defense process in sensory hair cells and it protects against NIHL and hair cell death.

Accelerated Noise-Induced Hearing Loss and Audiogenic Seizure in Mice Lacking Thrombospondins

Diana Mendus¹; Felix Wangsawihardja¹; Srividya Sundaresan¹; Nicolas Grillet²; Elyse Rankin-Gee¹; Farhad Ghoddoussi³; Avril Genene Holt³; Ulrich Mueller²; Brenda Elaine Porter¹; Mirna Mustapha¹

¹Stanford University; ²The Scripps Research Institute;

³Wayne State University

Background

Thrombospondins released by glial cells in the central nervous system promote synapse formation during development and repair synaptic connectivity after injury. To identify genes that are involved in synaptopathy and neuropathy in the cochlea, we studied TSP1 and TSP2 role in cochlear synapse formation and stabilization. We also identified these genes to be important in cochlear maintenance by showing age-related effects in TSP mutants. Here we further elucidate the mechanisms by which TSPs help to maintain hearing in mice. We studied 1) whether TSPs play a protective role in high noise level environment; 2) whether lack of TSPs lead to accelerated hearing loss after noise insult; and 3) the behavioral consequences of TSP disruption in peripheral and central auditory system during noise-induced stress.

Methods

Using quantitative RT-PCR, we measured expression of TSPs at different developmental ages, and before and after noise exposure. *In situ* hybridization was used to identify cell types that express TSPs. We exposed mice to 30 minutes 100 dB SPL broad-band noise. Manganese-enhanced magnetic resonance imaging was used to examine auditory pathways in TSP mutants and their wild type controls. Auditory, brain and cardiac functions were assessed by electrophysiological tests.

Results

Analysis of TSP1 and TSP2 expression levels by qPCR revealed significant up-regulation in the mRNA of both of these genes during the critical window of postnatal inner ear development. Our *in situ* studies showed that TSPs are also expressed in the supporting cells of the organ of Corti. Noise exposure experiments revealed that TSP mutants initially have a higher sensitivity to noise-induced trauma and have higher rates of hearing loss upon noise exposure. Using transgenic TSP1, TSP2 and TSP1/2 KO mouse models, we show that absence of TSPs leads to noise-induced audiogenic seizures in TSP2 and TSP1/2 KO mice but not in TSP1 KO as compared to wild type control.

Conclusion

Based on our study, TSP1 and TSP2 genes are likely to be protective in high noise level environments. Exposure to noise in individuals carrying TSP mutations may predispose them to rapid hearing loss and audiogenic epilepsy.

Endocochlear Potential (EP) Reduction at Low Noise Exposure Levels in Mice

Kevin Ohlemiller

Washington University School of Medicine

Background

Loud noise (110-116 dB SPL, 2 hr) causes EP reduction in mice that may be temporary (Hirose and Liberman, JARO 2003) or permanent (Ohlemiller et al., JARO 2011), depending on genetic background. To date, it has been assumed that EP reduction will only result from high levels of noise. If that is true, then EP reduction is not commonly a factor in either temporary or permanent noise-induced threshold shifts (TTS, PTS). We have tested this explicitly.

Methods

We varied the level of a 2-hr OBN noise exposure from 92-119 dB SPL in young (1.5 mos) and older (4-24 mos) C57BL/6, CBA/J, and BALB/c inbred mice, then measured the basal turn EP 1-3 hrs after exposure.

Results

For all strains and ages, the EP fell to 10-30 mV for exposures above 110 dB. We interpret this as the point of reticular lamina rupture (Hirose and Liberman, JARO 2003) so that organ of Corti injury, not stria injury, dominates the EP reduction. Lower exposure levels yielded widely divergent effects by strain and age. B6 mice showed little effect of noise for exposures below 110 dB, irrespective of age. Young BALB mice showed EP reduction for exposure levels as low as 95 dB. Young and older CBA mice showed very different patterns. In young CBA, exposure levels as low as 92 dB caused EP reduction. In older CBA mice, clear EP reduction was seen at 98 dB.

Conclusion

These data suggest the following: 1. The 'EP profile' (acute EP versus noise level) reflects two injury processes: metabolic injury to the stria at lower exposure levels, and breach of the reticular lamina at high exposure levels. 2. The threshold exposure for reticular lamina rupture is largely independent of age or genetic background. 3. The EP profile of B6 mice is qualitatively different from that in CBA and BALB, in that B6 mice lack a metabolic injury component. 4. Lateral wall susceptibility may partly establish the early sensitive period to PTS. 5. Depending on age and genetic background, acute EP reduction can occur at surprisingly low noise levels (<92 dB SPL). Therefore, EP reduction may participate in some TTS, and acute lateral wall pathology may modulate PTS. Our data greatly extend the range of noise exposures over which EP reduction and lateral wall pathology occur, and suggest a profound influence of genetic background.

Probing Cochlear Amplification With Low Frequency Suppression of Voltage and Pressure Measured at the Cochlea's Basilar Membrane

Wei Dong¹; Elizabeth Olson²

¹*Loma Linda Veterans Association for Research and Education*; ²*Columbia University*

Background

A recent study showed that the activation of the cochlear amplifier depended on proper timing between the outer hair cell (OHC) extracellular voltage and basilar membrane (BM) velocity (Dong and Olson, 2013). Amplification occurred when the phase of OHC extracellular voltage (an approximate measure of OHC force) was ~ in phase with BM velocity. With this phasing, OHCs inject energy into the traveling wave. Therefore, the phase between OHC voltage and mechanical responses is a key factor controlling cochlear amplification. In the present study, a low-frequency suppressor tone was used to further explore this aspect of the operation of the cochlear amplifier.

Methods

A novel hybrid-sensor was positioned close to the sensory tissue to measure OHC extracellular voltage and intracochlear pressure responses simultaneously and at the same location. Experiments were performed in anesthetized young adult gerbils. The BM was accessed through a hand-drilled hole in scala tympani (ST) in the basal turn of the cochlea, where the best frequency is ~ 20 kHz. The hybrid-sensor was constructed in the lab, and was composed of our lab's standard micro-pressure sensor (OD 125 microns) with a 28 micron diameter, isonel-insulated platinum electrode adhered to its side. The hybrid-pressure sensor was calibrated post-construction and before and after the experiment. Pure tone stimuli (probe tones) were accompanied by a low frequency suppressor, typically at a frequency of 4 kHz. Both pure and suppressor tones were delivered over a range of sound pressure level (SPL).

Results

When pure tone stimulation was accompanied by a low-frequency suppressor tone at moderate SPL, OHC extracellular voltage and intracochlear pressure were both mildly suppressed in the peak region. When the low-frequency tone was increased to ~ 80 dB SPL, the voltage was almost saturated by the low frequency tone and responses at the probe tone frequencies were greatly reduced. At the same time the pressure response was reduced nearly to its passive state. On the other hand, the phase shift between pressure and voltage (of the probe tones) changed little.

Conclusion

These findings suggest that suppression is caused primarily by the saturation of OHC electrical responses and not by a change in the relative phasing of the underlying mechanics.

PD - 173

Simulating the Effect of Detaching the Tectorial Membrane from the Spiral Limbus on the Response of the Basilar Membrane to a Pure Tone and Two-Tone Suppression

Julien Meaud¹; Karl Grosh²

¹Georgia Institute of Technology; ²University of Michigan, Ann Arbor

Background

Recent experiments with genetically modified mice (Lukashkin et al., PNAS, 2012) have demonstrated that the attachment of the tectorial membrane (TM) to the spiral limbus is not necessary for normal cochlear amplification on the basilar membrane. Using computational models, we investigate here the effect of detaching the TM on the single tone response and on two-tone suppression (TTS).

Methods

Using a previously developed computational framework, we simulate the response of the cochlea to a pure tone and two-tone stimuli using two computational models. In the first model (TM-A), the TM is attached to the spiral limbus; in the 2nd model (TM-D), the TM is detached from the spiral limbus.

Results

With both models, the response to a pure tone is similar to experiments. However, while the simulations of TTS are similar to measurements with wild-type animals, the predictions obtained with the TM-D model are significantly different.

Conclusion

Our theoretical results demonstrate that altering the mechanical load applied by the TM on the outer hair cell hair bundles affects two-tone suppression. This conclusion could be tested by measuring TTS on the BM of mutant mice.

PD - 174

Similarities and Differences Between Backward and Forward Traveling Waves in the Cochlea

Yizeng Li; Karl Grosh

University of Michigan

Background

Acoustic signals are converted into electronic pulses in the hearing organ through a forward traveling wave that propagates from the cochlear base to the apex. This wave results from a coupling of the intracochlear fluid and the flexible hearing organ. Acoustic energy delivered from the stapes is carried by the forward traveling wave. In otoacoustic emissions, energy is generated inside the cochlea and emitted towards the ear canal. A backward traveling wave is hypothesized to carry this reverse energy flow. However, the characteristics of the backward traveling wave are less known compared to the knowledge on the forward wave. Structural acoustic reciprocity provides insights on energy transfer between any two given points in a passive cochlea; yet limited information can be derived from the reciprocity alone in terms of the actual spatial content of the response between the two locations on the traveling pathway. In this work, we investigate the differ-

ence between forward and backward wave propagation on the traveling path, not just at two locations. This work helps to understand how energy is carried during otoacoustic emissions.

Methods

A mathematical model of the cochlea is used to make predictions about wave propagation in the cochlea. To generate forward and backward traveling waves that originate at various longitudinal locations, the basilar membrane or the fluid pressure is excited at different positions. We primarily consider a passive cochlear model. Both numerical and analytical models will be used; the latter provides physical interpretations via the expressions of the solutions. Analytical solutions are obtained using a long wave cochlear model with WKB approximation.

Results

The spatial response of the BM basal to the forcing place is found to be predominantly a backward traveling wave and the response apical a forward traveling wave. However, the nature of an internally excited response is much different than that of an externally stimulated forward traveling wave. The waves on the backward path are dominated by the frequency corresponding to the characteristic frequency of the point being excited. This is very different from a stapes generated forward traveling wave which excites all frequencies along the cochlea. The phase and group delays of the backward traveling wave depend on the reflection condition at the base of the cochlea.

Conclusion

The backward traveling wave is not a reversed replica of the forward traveling wave.

PD - 175

A Mathematical Model of the Chan-Hudspeth Experiments

Amir Nankali; Karl Grosh

University of Michigan

Background

Hearing relies on a series of coupled electrical, acoustical and mechanical interactions inside the cochlea that enable sound processing. The local structure and electrical properties of the organ of Corti (OoC) and basilar membrane (BM) give rise to the global, coupled behavior of the cochlea. However, it is hard to determine the causes of important behavior, like the effect of active processes, in the coupled setting. Experiments, like Chan-Hudspeth (Chan, DK and Hudspeth AJ, *Biophys. J.*89 ,4382; Chan, DK and Hudspeth AJ, *Nat. Neurosci.*8,149), aim to keep the cochlea in as pristine state as possible – while still enabling local response determination. The purpose of this study is to replicate the experimental conditions by means of a computational model, in order to interpret the phenomena and explain mechanisms giving rise to the results. Moreover, we use these experiments to test models of cochlea function and activity.

Methods

We build a geometric model that simulates the experimental configuration. We use analytic and finite element methods to compute the response to acoustic stimulation. The model is based on a three dimensional representation of the fluid and structure, including the electrical domain and the outer hair cell somatic motility.

Results

We show that the length of the excised cochlea and its activity level determine whether the cochlea acts as simple harmonic oscillator or a traveling wave amplifier. The BM boundary conditions effect on its characteristic frequency (CF) of the excised segment is also explored. We find that for low frequency best places (apex) the effect is not significant. Moreover, it is shown that the constrained fluid mass on the scala tympani side of the OoC affects the CF of the segment, while the unconstrained fluid mass of the scala media side does not, matching the experimental data. Both guinea pig and gerbil models are utilized and the results are found to be qualitatively similar except that the length scales are different.

Conclusion

We show that even for segments of the cochlea only 2-3 wavelengths long, traveling waves may exist in an active, excised section of the cochlea.

PD - 176

Phase of Shear Vibrations Within Cochlear Partition Leads to Activation of the Cochlear Amplifier

Jessica Lamb; Lamb S. Jessica; **Richard S. Chadwick**
NIDCD

Background

Since Georg von Békésy laid out the place theory of the hearing, researchers have been working to understand the remarkable properties of mammalian hearing. Because access to the cochlea is restricted in live animals, and important aspects of hearing are destroyed in dead ones, models play a key role in interpreting local measurements. Interest in the role the tectorial membrane (TM) plays in cochlear tuning led us to develop models that directly interface the TM with the cochlear fluid. In this work we add an angled shear between the TM and reticular lamina (RL), which serves as an input to a nonlinear active force. This feature plus a novel combination of previous work gives us a model with TM-fluid interaction, TM-RL shear, a nonlinear active force and a second wave mode.

Methods

Wentzel-Kramers-Brillouin (WKB) models are attractive because they are analytically tractable, appropriate to the oblong geometry of the cochlea, and can predict wave behavior over a large span of the cochlea.

Results

The behavior we get leads to the result the phase between the shear and basilar membrane (BM) vibration is critical for amplification. We show there is a transition in this phase that occurs at a frequency below the cutoff, which is strongly influ-

enced by TM stiffness. We describe this mechanism of sharpened BM velocity profile, which demonstrates the importance of the TM in overall cochlear tuning and offers an explanation for the response characteristics of the *Tectb* mutant mouse. Also our model predicts that the optimal gain is obtained when the phase difference between the shearing displacement and the BM displacement differs by nearly a quarter cycle in agreement with previous experimental results.

Conclusion

Our model offers an intriguing possibility to explain the simultaneous increase in selectivity with loss of sensitivity of the *Tectb* mutant - a band pass filtering mechanism, with the low corner being determined by the TM-BM interaction.

PD - 177

Distribution of Intra-Cranial Sound Pressure During Bone Conduction Stimulation

Jae Hoon Sim¹; Christof Rösli¹; Rahel Gerig¹; Adrian Dalbert¹; Christian Fausch¹; Stefan Stenfelt²; Alexander Huber¹

¹University Hospital Zurich; ²Linköping University

Background

Recent studies proposed that non-osseous skull contents such as brain and cerebro-spinal fluid (CSF) contribute to bone conduction (BC) hearing as an important pathway of sound pressure. Some studies even indicate that this pathway is the dominant pathway when stimulation occurs on non-osseous sites such as the neck or the eye. However, the mechanism of sound propagation via this pathway is still controversial i.e. whether it is independent of skull-bone vibration. Further, its frequency dependency has not been investigated. The aim of this study is to investigate the spatial distribution of the intra-cranial sound pressure during BC stimulation at two positions on the skull bone, and thus the relationship between the BC excited intra-cranial sound pressure and the vibration of the bone encapsulating the cochlea.

Methods

Measurements were performed in three human cadaveric whole heads. A bone anchored hearing aid (BAHA) was attached to a percutaneously implanted screw at two positions (mastoid and forehead). Two stimulation signals were used: (1) a stepped-sine signal in the frequency range of 0.1 – 10 kHz for measurement in frequency domain, and (2) a two-cycle sine signal at frequencies between 0.5 and 8 kHz for measurements in time domain. A hydrophone was sequentially positioned intra-cranially in five positions (central, anterior, posterior, superior, and lateral) to map intra-cranial sound pressure during BC stimulation. The five positions of the hydrophone in the intra-cranial space were confirmed by X-ray.

Results

When stimulation was at the mastoid, the intra-cranial pressure in the ipsi-lateral position was larger than the intra-cranial pressures in the other positions at high frequencies; the intra-cranial sound pressures in all other positions had similar magnitudes in the measured frequency range. When the stimulation was at the forehead, the intra-cranial sound pressure magnitudes were similar for all five measurement

positions for the entire frequency range tested. For the lateral position of the hydrophone, stimulation at the ipsi-lateral mastoid resulted in larger intra-cranial sound pressure than stimulation at the forehead. For other positions of the hydrophone, the intra-cranial sound pressure magnitudes were similar for stimulation at the mastoid and forehead.

Conclusion

The spatial distribution of the intra-cranial sound pressure magnitudes were relatively uniform for stimulation with a bone transducer attached to the mastoid and forehead. Only the intra-cranial sound pressure in the ipsi-lateral position with stimulation at mastoid has larger magnitudes than the intra-cranial sound pressure in other position with other stimulation sites.

PD - 178

Mechanical Amplification by Non-Oscillating Saccular Hair Cell Bundles

Yuttana Roongthumskul; Dolores Bozovic
University of California, Los Angeles

Background

Spontaneous oscillations exhibited by hair bundles from the bullfrog sacculus suggest the existence of an active process that might underlie the sacculus' exquisite sensitivity to mechanical stimulations. However, it was shown that these bundles do not spontaneously oscillate under *in vivo* conditions: the overlying otolithic membrane applies not only elastic and mass loading, but also large mechanical offsets in the direction that opens the transduction channels (towards the kinocilium). While oscillating hair bundles were shown to amplify mechanical stimuli, it is still unknown whether or not a non-oscillating (quiescent) hair bundle benefits from its active process. Therefore, we focus on the response of individual hair bundles in the quiescent state due to mechanical deflections towards their kinocilia.

Methods

Bullfrog sacculi were excised and mounted into a two-compartment chamber, where the apical and basal side of the sacculus was exposed to artificial endolymph and perilymph, respectively. Hair bundle motions were recorded with a high-speed CMOS camera at 500 frames per second. Mechanical stimuli were applied to an individual hair bundle with a flexible glass probe of stiffness ~100 - 200 $\mu\text{N/m}$. Steady-state or ramp-type offsets were imposed towards its kinocilium. In some experiments, a small sinusoidal stimulus was simultaneously added.

Results

As the mechanical offset to the bundle is applied towards the kinocilium, the characteristic frequency of the spontaneous oscillation increases with the size of the offset, while oscillation amplitude slightly decreases. With increasing deflection, in the absence of sinusoidal stimulus, a number of hair bundles spend a longer fraction of time in the channel-open state and exhibit stochastic brief excursions (spikes) towards the channel-closed state. Sinusoidal stimulus evokes mechanical spikes at a particular phase of the ac component of the stimulus, leading to an amplified movement of the bun-

dle with respect to the passive response. Statistics of spike occurrence show higher vector strength as offset increases.

Conclusion

Mechanical offset drives hair bundles into a regime, where bundle spikes can be observed. Application of a small sinusoidal stimulus entrains the occurrence of these mechanical spikes. Non-oscillating hair bundles can therefore amplify applied mechanical stimulus.

PD - 179

Stationary Noise Responses and Equivalent Quasilinear Filters in a Model of Cochlear Mechanics: An Iterative Frequency-Domain

Approach

Yi-Wen Liu

National Tsing Hua University

Background

To argue that quasilinear filtering could result from instantaneous nonlinearities, Liu and Neely (2011) calculated equivalent linear filters of a nonlinear model of cochlear mechanics via time-domain simulation; pseudorandom stimuli were generated, and equivalent linear filters were obtained by cross-correlating the acoustic input and the cochlear output. This previous method encountered two problems. First, calculating the cross-correlation function required averaging across pseudo-random stimuli, and the rate of convergence was slow. Secondly, it was unclear whether the equivalent filters could be realized under the cascade structure that describes wave propagation in the cochlea. The realizability issue was of interest because it was part of the EQ-NL (equivalent nonlinearity) theorem proposed by de Boer (1997). The present work addresses both problems at once by calculating the noise responses iteratively in the frequency domain.

Methods

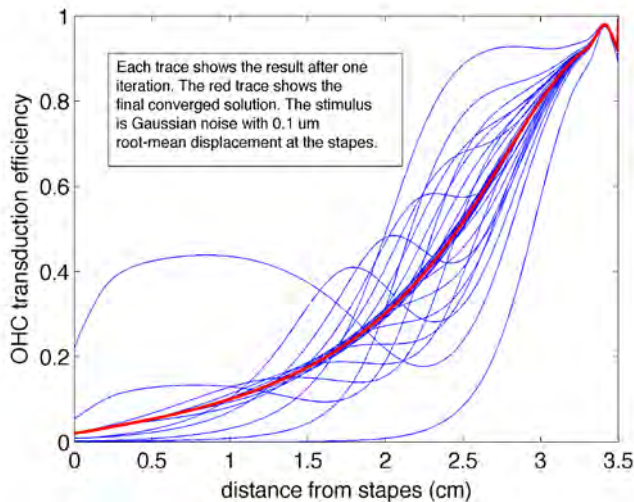
The cochlear model (Liu and Neely, 2010) consists of a transmission line with electromotile outer hair cells (OHCs) that are subject to saturation of mechano-electrical transduction currents. The iterative method consists of two steps --- prediction and update (Kanis and de Boer, 1993). In the prediction step, the cochlear responses are solved linearly, and the input to the instantaneous nonlinearity (IIN) at the OHCs is calculated. In the update step, the OHC transduction efficiency (TE) is adjusted based on how saturated the transduction current is. The two steps alternate and repeat until the solution converges. Being new here is an exact expression of TE as a function of IIN. The expression is derived by assuming that the equivalent gain of a nonlinear function is equal to the expected value of its slope. It turns out the expected value is straightforward to calculate when the stimulus is stationary Gaussian noise.

Results

As stimulus level increases, the TE of OHC decreases non-uniformly in the cochlea, the magnitude of the equivalent transfer function also decreases, and the latency of Wiener kernels drops. These results were obtained much more efficiently than by the time-domain approach.

Conclusion

A fast method to solve nonlinear cochlear mechanical equations is developed. For the first time, stationary noise responses in the nonlinear cochlear model can be calculated in the frequency domain. Numerically stable solution is obtained by assuming that the OHC transduction efficiency equals the expected value of the slope of the current saturation function. This last result provides clues on how to think of the nonlinear cochlea precisely as a quasilinear system.



PD - 180

Emphasis of Carrier ITD Information During the Rising Segments of Amplitude Modulated Sounds and its Absence for the Transposed Counterpart

Mathias Dietz¹; Torsten Marquardt²; David McAlpine²

¹Universität Oldenburg; ²University College London

Background

Recently, employing a novel stimulus in which sound amplitude and interaural phase difference (IPD) are modulated with a fixed mutual relation, we demonstrated that the human auditory system utilizes interaural timing differences in the temporal fine-structure only during the rising portion of each modulation cycle (Dietz et al., Proc. Natl. Acad. Sci., 2013). These stimuli, amplitude modulated binaural beats (AMBBs), possess temporal and interaural properties typical of reverberant speech, but are well parameterized, allowing for more systematic investigation of the dominance by, for example, the carrier or the modulation frequency. Our previous study examined sensitivity of human listeners to ITDs conveyed at a 500-Hz carrier frequency. The current study investigates from where ITD information is extracted when the AMBB is transposed to 4 KHz. Transposed AMBBs are expected to mimic the temporal and interaural cues accessible to cochlear implant users receive when listening to speech or music in reverberant environments.

Methods

Psychoacoustic procedures were identical to those described in Dietz et al. (2013). The carrier frequency of the low-frequency AMBB was 256 Hz. An IPD pointer was used to

match the intracranial percepts of AMBB stimuli and transposed AMBBs. Transposed AMBBs were generated by multiplying the half-wave rectified low-frequency AMBB to a 4 KHz carrier.

Results

Data from transposed AMBBs do not reveal a strong dominance of the rising slope segment, but rather an averaging of IPDs across the entire AM cycle.

Conclusion

At low carrier frequencies, adaptation prior to binaural interaction facilitates a mechanism of “glimpsing”, by which listeners strongly weight IPDs during the rising segment of ongoing envelopes. The effect has a strong contribution to listeners ability to localize sound sources in reverberation (Haas effect) - b the direct-to-reverberant ratio is optimal immediately following modulation minima. From the absence of any dominance of the rising slope dominance transposed AMBBs we conclude that fluctuating ITDs in the temporal envelope domain are less useable in sound-source localization tasks. With the temporal properties at the level of the auditory nerve expected to be very similar, different brainstem mechanisms seem to cause this deviation from the Colburn and Esqui-saud hypothesis. A consequence for cochlear implantees is that their interaural disparities may not facilitate the IPD glimpsing that underpins localization in many complex acoustic environments.

PD - 181

The Relations Among Center Frequency, Envelope Rate, and Sensitivity to Envelope-Based Ongoing Interaural Time Delays

Leslie Bernstein; Constantine Trahiotis

University of Connecticut Health Center

Background

The ability to perceive changes of interaural temporal disparities (ITDs) imposed on high-frequency complex stimuli has long been recognized as being mediated by the envelopes of such stimuli. Furthermore, the efficiency of such ITD-processing has been shown to be dependent on the rate of fluctuation of the envelope. At a previous meeting of this association, we presented new empirical data confirming some of our earlier research showing that, as center frequency is increased, the envelope-rate at which efficiency of envelope-ITD processing begins to degrade becomes lower and lower, both in absolute and relative terms.

Methods

Sensitivity to ongoing interaural temporal disparities (ITDs) was measured using a two-cue, two-alternative, forced choice, adaptive task. The stimuli were bandpass-filtered pulse trains centered at 4600, 6500, or 9200 Hz and were based on those used by Majdak and Laback (2009) [J. Acoust. Soc. Am. 125, 3903-3913]. Data were obtained at each center frequency while holding stimulus bandwidth constant or increasing it in a manner proportional to center frequency. At each center frequency, threshold ITD was measured for pulse repetition rates ranging from 64 to 609 Hz. In

order to preclude listeners' use of ITD-information conveyed by low-frequency distortion products, two types of continuous background noise were employed: 1) a continuous, diotic noise which was low-passed at 1300 Hz and presented at a spectrum level equivalent to 30 dB SPL (a noise routinely employed in our laboratory); 2) a continuous, interaurally uncorrelated, broadband noise (50 Hz to 20 kHz) presented at a spectrum level of about 9 dB (a noise employed by Majdak and Laback in their 2009 study).

Results

The results and quantitative predictions of them via a cross-correlation-based model that includes stages of peripheral processing indicated that: 1) overall, threshold ITDs increased with increases in center frequency; 2) as in earlier studies, the envelope-rate at which efficiency of envelope-ITD processing began to decline decreased as center frequency was increased; 3) threshold ITDs were accounted for quantitatively by assuming that listeners' decisions were based on the use of a single, criterion, change in normalized interaural correlation at all three center frequencies tested.

Conclusion

It appears that, even for relatively broadband "click" stimuli, the cutoff frequencies of the putative envelope low-pass filters that determine sensitivity to ITD at high envelope rates are inversely related to center frequency.

PD - 182

The Peak of Contralateral Masking is Predicted by Pitch Matching

Justin Aronoff¹; Monica Padilla²; David Landsberger²

¹University of Illinois at Urbana-Champaign; ²House Research Institute

Background

Bilateral cochlear implant users typically have different electrode insertion depths and cell survival in each ear, creating the challenge of determining how to perceptually align the left and right ear. One common approach to doing this is to use a pitch matching task where participants are asked to indicate whether stimulation on an electrode in one ear yields the same perceived pitch as stimulation on an electrode in the other ear. Although this approach is quick and simple, pitch matches change over time. Given its malleability, pitch matching may not provide results consistent with other measures of binaural integration such as contralateral masking. With contralateral masking, stimulation in one ear masks a stimulus in the opposite ear. This masking is place-specific, resulting in a peak of contralateral masking that varies depending on the masker location. This experiment investigated whether pitch matching predicts the location of the peak of contralateral masking.

Methods

Six bilateral cochlear implant users were tested. Pitch matching was performed by stimulating a reference site in one ear and adjusting the stimulation site of an equally loud probe in the opposite ear until the pitch was perceived to be the same across ears. Contralateral masking was measured using a modified Bekesy tracking procedure; a 20 ms probe was

temporally embedded in a 500 ms masker. Maskers were presented at the most comfortable loudness level. The peak of contralateral masking was indicated by the location of the largest masked threshold shift.

Results

The pitch matching data for each subject was fit based on a linear regression. This fit was compared to the peak of contralateral masking for each participant and location. Comparisons between the predicted and actual peak of contralateral masking indicated that, on average, the peak predicted by the pitch matching data was within one mm of the actual peak measured by the contralateral masking task.

Conclusion

The results suggest that the peak of contralateral masking can be predicted by pitch matching. Future experiments will investigate whether changes in pitch matching correlate with changes in the peak of contralateral masking.

PD - 183

Training Interaural Level Difference Discrimination Improves Spatial Release from Masking for Speech Identification

Yu-Xuan Zhang; Xiang Gao; Tingting Yan

Beijing Normal University

Background

Speech perception in noise gets better when the noise masker is spatially separated from the speech signal. This release from masking can be obtained using binaural cues such as interaural time and level differences. However, it is unclear whether the release can benefit from improved discrimination of these cues.

Methods

Normal-hearing adults (N=9) practiced on interaural level difference (ILD) discrimination with headphone-delivered 1-kHz low-pass noise, sinusoidally amplitude modulated at 8 Hz, for seven 30-minute sessions. Before and after training, these listeners and a no-contact control group (N=8) were tested on a speech identification task, in which spoken tokens of single-syllable Mandarin words were embedded within speech-shaped noise at multiple signal-to-noise ratios (SNRs). The speech signal was always presented with an ILD of 0 dB, while the noise ILD could be 0 (collocated with the signal), 3, or 6 dB (displaced from the signal). To reduce the influence of rapid learning with the speech task, a practice session was administered to all listeners before the experiment and different word lists were used in the pre- and post-training tests.

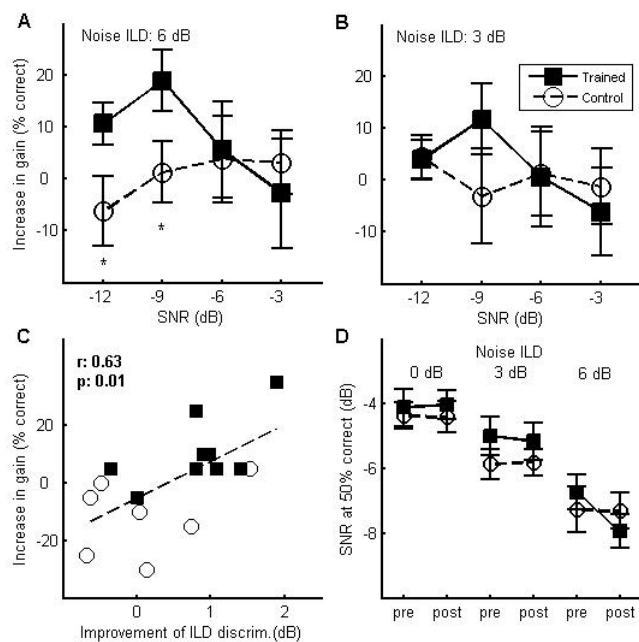
Results

Before training, speech identification in noise got better with masker displacement, indicating ILD-based release from masking (by 1.3 and 2.5 dB at 50% intelligibility for masker displacement of 3 and 6 dB). After training, the trained listeners improved more than controls on ILD discrimination with an untrained standard of 6 dB, but not with the trained standard of 0 dB. Correspondingly, they also showed a greater increase than controls in speech identification performance gain obtained with masker displacement of 6 dB (Fig. 1A),

but not with masker displacement of 3 dB (Fig. 1B). Moreover, the improvements for ILD-based release and for ILD discrimination were significantly correlated (Fig. 1C). At 50% intelligibility, the effect of ILD training on speech identification amounted to a 1.3-dB decrease in threshold SNR for noise ILD of 6 dB and no change under other conditions (Fig. 1D).

Conclusion

ILD discrimination learning transferred to ILD-based release from masking for speech identification in noise. The location specific manner of this transfer is incompatible with general learning mechanisms such as improved spatial attention or “better-ear” listening. Instead, the results suggest a direct link between discriminability of binaural cues and spatial release from masking. The study opens the possibility of improving speech perception in noise via psychoacoustic training.



PD - 184

Multi-Channel Processing of Inconsistent Interaural Time Differences

Matthew Goupell¹; Ruth Litovsky²

¹University of Maryland - College Park; ²University of Wisconsin - Madison

Background

When broadband sounds from the free field are analyzed by an auditory filterbank, they have consistent interaural-time-difference (ITD) information across channels. Multi-channel ITD just-noticeable differences (JNDs) can be predicted between two source locations, ITD1 and ITD2, by: (1) calculating cross-correlation functions across frequency (i.e., cross-correlogram), (2) multiplying the cross-correlation functions across frequency into a “lateralization function,” and (3) assuming ITD1 can be discriminated from ITD2 if the value of the lateralization function of ITD2 is adequately reduced at ITD1. This study explores applicability of information from cross-correlogram-based models to performance of bilateral cochlear-implant (BICI) users. Specifically, we sought to

model highly-variable ITD sensitivity across frequency seen in BICI users, which may result from asymmetrical neural degeneration. The purpose of this study was to begin developing a cross-correlogram-based model that would predict ITD JNDs in BICI users. JNDs were measured for stimuli designed to simulate an extreme form of variable ITD sensitivity across frequency in normal-hearing listeners.

Methods

We measured ITD JNDs in eight normal-hearing listeners. The stimuli were 300-ms, 65-dBA, 10-Hz narrowband noises with center frequencies of 300 to 1400 Hz. Stimuli contained either one or three bands. In the three-band stimuli, the center band was 750 Hz and the spacing between bands was varied ($\Delta=20, 50, 100, 250$, or 450 Hz). The ITDs were consistent across-frequency or made inconsistent by forcing one or two of the bands to have zero ITD in the presence of a non-zero ITD in the other band(s) [similar to Dye (1990, J.Acoust.Soc.Am.)].

Results

JNDs for multi-band stimuli that had consistent ITDs across frequency were smaller than JNDs for single-band stimuli. Increasing the number of zero-ITD bands in the multi-band stimuli generally increased JNDs. Multi-band JNDs were higher for smaller Δ s compared to larger Δ s if there was a zero-ITD band, which was a result of within-channel interaural decorrelation. The cross-correlogram model needed to be adapted to predict lower JNDs for multi-band stimuli with consistent ITDs and to accommodate decorrelated stimuli when there were inconsistent ITDs.

Conclusion

BICI users demonstrate highly-variable ITD sensitivity across frequency, which was simulated in this experiment by using multi-band stimuli with inconsistent ITDs across frequency. This produced decorrelated stimuli, which warranted some changes in the cross-correlogram model to accurately predict JNDs. Future studies will measure and predict ITD JNDs for more realistic CI simulations (e.g., high-frequency acoustic pulse trains that simulate current spread).

Directional Hearing in Single-Sided Deaf Patients: Contribution of Spectral Cues and High-Frequency Hearing Loss in the Hearing Ear

Martijn Agterberg¹; Myrthe Hol²; Marc Van Wanrooij³; John Van Opstal³; Ad Snik²

¹*Donders Institute for Brain, Cognition and Behaviour, Radboud University, Nijmegen, The Netherlands;*

²*Radboud university medical center, Donders Institute for Brain, Cognition and Behaviour, Department of Otorhinolaryngology, Nijmegen, The Netherlands;*

³*Department of Biophysics, Donders Institute for Brain, Cognition and Behaviour, Radboud University, Nijmegen, The Netherlands*

Background

Direction-specific interactions of sound waves with the head, torso and pinnae provide unique spectral-shape cues that are used for the localization of sounds in the vertical plane, whereas horizontal sound localization is based primarily on the processing of binaural acoustic differences in arrival time (interaural time differences, or ITDs) and sound level (interaural level differences, or ILDs). Because the binaural sound-localization cues are absent in listeners with single-sided deafness (SSD), their ability to localize sound is heavily impaired. However, some studies have reported that SSD listeners are able, to some extent, to localize sound sources in azimuth, although the underlying mechanisms used for localization are unclear.

Methods

The ability of SSD listeners to use monaural cues to localize sounds in the horizontal plane is tested in a completely dark sound attenuated room. Listeners pointed with a head-fixed laser pointer, which projected onto a small plastic plate positioned in front of the listener's eyes. Listeners were asked to point the laser dot as fast and as accurately as possible in the perceived sound direction after stimulus exposure. Listeners were asked to localize low-pass (LP; 0.5-1.5 kHz); high-pass (HP; 3-20 kHz) and broadband (BB; 0.5-20 kHz) filtered Gaussian white noises. We tested whether high-frequency hearing loss in the hearing ear affected the sound localization abilities. To investigate the possible use of spectral cues, a custom-made mold was inserted in the pinna of the hearing ear.

Results

Several listeners with SSD could localize high-pass and broadband sound sources in the horizontal plane, but inter-subject variability was considerable. Localization performance of SSD listeners further deteriorated when the pinna cavities of their hearing ear were filled with a mould that disrupted their spectral-shape cues. Our data indicate that the amount of high-frequency hearing loss greatly influences the directional hearing abilities of SSD listeners.

Conclusion

Our data demonstrate that inter-subject variability concerning directional hearing of SSD patients, can be, to a large

extent, explained by the severity of high-frequency hearing loss in their hearing ear. We suggest that before considering a bone-conduction device, localization abilities and hearing thresholds in the better ear of listeners with SSD should be thoroughly investigated. The capacities of listeners with SSD who are able to use monaural pinna-induced spectral-shape cues for localization of sounds in the horizontal plane, might be affected, or even deteriorate, with the offered bone-conduction device.

Head-Movement Compensation Results in a Slightly Moving Auditory World

W. Owen Brimijoin; Michael A. Akeroyd

MRC Institute of Hearing Research

Background

The vestibulo-ocular reflex counteracts head movements to stabilize the projection of the visual world onto the retina. It is not yet clear to what extent moving listeners arrive at a correspondingly stable percept of the auditory world. Here we present results suggesting that, for sounds presented over both headphones and loudspeakers, complete stabilization does not occur; rather, the most static-appearing sounds are ones that actually move slightly with the head.

Methods

Using motion tracking and manikin head-related transfer functions we created signals whose virtual locations were moved in real time so as to counteract a listener's head movements. Listeners were asked to turn their heads back and forth between $\pm 15^\circ$. While in motion, they were presented with 3 seconds of amplitude modulated noise and asked to report whether the signal moved or appeared static with respect to the world. The ratio at which the signals were moved (i.e., the rate of movement of the sound location versus the movement of the head) was varied. A ratio of 1.0 corresponds to a geometrically stable signal (i.e., an exact compensation for head movements). A ratio larger than 1.0 corresponds to a counter-rotating sound and any ratio smaller than 1.0 corresponds to a sound that moves with the head. An analogous experiment was conducted in a ring of 24 loudspeakers, but the signals were presented from three different center locations of 0, 45 and 90°.

Results

For the headphone and loudspeaker experiments, we found that listeners were more likely to report signals as being static when they moved with a ratio of approximately 0.8 (i.e., that moved slightly with the head) than when they were moved with the expected ratio of 1.0. The effect was smaller for signals located to the side of the listener than for signals in front.

Conclusion

Unlike the complete stabilization found in the visual system, acoustic signals that partially moved with the head were actually perceived as being the most static. These results suggest that real world signals should be perceived as rotating slightly opposite to head movements, likely reflecting a general phenomenon related to auditory coordinate transformation and dynamic spatial hearing.

Rate Effects in Interaural and Sequential Level Difference Perception

Bernhard Laback¹; Mathias Dietz²; Stephan D. Ewert²

¹Austrian Academy of Sciences; ²Universitaet Oldenburg

Background

Previous studies on human listeners' sensitivity to changes in the interaural level difference (ILD) reported increasing dominance of the onset with increasing modulation rate of a stimulus. Those studies left unclear whether this rate effect is also manifested as decrease in ILD sensitivity, particularly if the stimulus duration and loudness are kept constant across rates. Moreover, it is unclear if the reported modulation rate effect is specific to binaural hearing or if it arises also in monaural sequential level difference (SLD) discrimination

Methods

In experiment 1, ILD discrimination thresholds and SLD discrimination thresholds were measured in seven normal-hearing listeners using bandpass-filtered pulse trains (4 kHz) with rates of 100, 400, and 800 pulses/s. Experiment 2 compared ILD thresholds between unmodulated 4-kHz pure tones and pulse trains. It was hypothesized that amplitude modulation up to a certain rate enhances ILD perception and that ILD thresholds are highest for steady-state stimuli. The thresholds were predicted by a simple model, based on the "internal" ILD of the signal after passing left and right ear stages that mimic peripheral adaptation (Dau et al., 1996, JASA 99: 3615).

Results

For pulse trains from 100 to 400 pulses/s, both ILD and SLD thresholds decreased, contrary to the expectation of a rate limitation but consistent with temporal integration. However, from 400 to 800 pulses/s ILD thresholds increased while SLD thresholds remained constant. The ILD thresholds for unmodulated 4-kHz-tones were found to be higher than those for all pulse-trains. The model correctly predicted the increase of thresholds from 400 to 800 pulses/s and the even higher thresholds for tones.

Conclusion

The improvements in ILD/SLD sensitivity from 100 to 400 pulses/s can be understood in terms of integration of underlying cues over an increasing number of temporal windows ("looks"). The deterioration from 400 to 800 pulses/s, observed for ILD but not for SLD, is consistent with a specifically binaural rate limitation. The model results suggest that this deterioration with rate could be due to increasing compression of the internal ILD cue following peripheral adaptation. The correct model prediction of poorest ILD sensitivity observed for unmodulated tones can be understood by considering that such stimuli resemble the theoretical upper limit of modulation rate after cochlear filtering. Overall, low-rate amplitude modulation appears to enhance ILD discrimination.

A Novel Mechanism to Regulate the Cochlear Mechanotransduction Operating Point

Anthony Peng; Anthony Ricci

Stanford University

Background

To hear, animals rely on specialized mechanosensory hair cells. All hair cells feature a mechanosensory organelle called a hair bundle that is comprised of actin-filled microvilli, termed stereocilia, arranged in a staircase pattern. Deflection of the hair bundle causes activation of mechanoelectrical transduction (MET) channels. During constant hair bundle deflection, MET currents decrease by a process called adaptation. Previously, it was thought that calcium drives mechanotransduction adaptation, and low extracellular calcium levels shifted the operating point of the mechanotransduction channel through adaptation. Recently, we have shown that mammalian auditory mechanotransduction adaptation is not driven by calcium as previously thought. However, the operating point of the mammalian auditory mechanotransduction channel still shifts in the presence of low extracellular calcium. This effect is not due to intracellular calcium levels, indicating an external effect of calcium. Therefore, a new mechanism is required to explain how the mechanotransduction operating point is regulated by calcium, independent of adaptation.

Methods

Whole cell patch clamp recordings of rat outer hair cells were obtained. Hair cells were voltage clamped and mechanical stimuli were delivered via a piezo actuated glass probe or using a fluid-jet stimulator (ALA HSPC1). Solutions were delivered to the apical surface of hair cells via a perfusion manifold driven by a peristaltic pump or by gravity flow.

Results

To first characterize the low extracellular calcium effect, the calcium dependence of the extracellular effect was determined to have a half-activation for the operating point shift of 0.25mM. Using different external divalent ions show that the observed shifts in operating point were specific to particular divalent ions. Variability in the efficacy of the low external calcium effect suggests that the biochemical state of the cell is important. Sometimes two processes were observed in low calcium: one that increases resting open probability, and another that can decrease the resting open probability.

Conclusion

The cochlear mechanotransduction operating point is controlled via extracellular calcium through an unknown mechanism with two extracellular possibilities being the tip-link or a binding site along the lipid membrane.

Molecular Mechanics of Hair-Cell Tip Links

Marcos Sotomayor

The Ohio State University

The hair-cell tip link, an essential component of the transduction apparatus, is formed by two atypical cadherins: protocadherin-15 and cadherin-23. These two proteins are required

for mechanotransduction, are involved in hereditary deafness, and are thought to convey mechanical force directly to hair cell transduction channels. Here we use X-ray crystallography and molecular dynamics simulations to characterize the mechanical response of the extracellular domains of protocadherin-15 and cadherin-23. Our results provide a molecular view of tip-link mechanics and identify the molecular determinants of tip-link strength.

SY - 074

Dynamic Molecular Composition of Regenerating Tip Links in Mammalian Cochlear Hair Cells

Artur Indzhykulyan^{1,5}; Ruben Stepanyan¹; Anastasiia Nelina¹; Kateri Spinelli²; Zubair Ahmed³; Inna Belyantseva⁴; Thomas Friedman⁴; Peter Barr-Gillespie²; David Corey⁵; Gregory Frolenkov¹

¹University of Kentucky; ²Oregon Health & Science University; ³Cincinnati Children's Research Foundation; ⁴National Institute on Deafness and Other Communication Disorders; ⁵Harvard Medical School

Sound detection by inner ear hair cells requires tip links that interconnect mechanosensory stereocilia and convey force to the transduction channels. Current models postulate a static composition of the tip link with cadherin 23 (CDH23) at the upper and protocadherin 15 (PCDH15) at the lower end of the link. In terminally differentiated mammalian auditory hair cells, tip links are subjected to sound-induced forces throughout an organism's life. Hair cells can regenerate disrupted tip links and restore hearing, but the molecular details of this process are unknown.

We used a calcium chelator BAPTA to disrupt the tip links in the inner hair cells of the cultured postnatal mouse organ of Corti explants. We developed a novel implementation of backscatter electron scanning microscopy to visualize simultaneously immuno-gold particles and stereocilia links which allowed us to explore tip link molecular composition during the recovery process. To follow the recovery of hair bundle's mechanosensitivity, we used conventional whole cell patch-clamp technique and the tightly controlled bundle deflection with a rigid probe.

We show that functional, mechanotransduction-mediating tip links have at least two molecular compositions, containing either CDH23/PCDH15 or PCDH15/PCDH15. During regeneration, shorter tip links containing nearly equal amounts of PCDH15 at both ends appear first. Whole cell patch-clamp recordings demonstrate that these transient PCDH15/PCDH15 links mediate mechanotransduction current of normal amplitude but abnormal Ca²⁺-dependent decay (adaptation). The mature CDH23/PCDH15 tip link composition is re-established later, concomitant with complete recovery of adaptation.

Our findings provide a molecular mechanism for regeneration and maintenance of mechanosensory function in postmitotic auditory hair cells. Ongoing studies using fast calcium imaging could answer the question whether PCDH15 participates

in molecular remodeling of the tip links alone or in the complex with the transduction channel.

SY - 075

Effects of Lipid Bilayer Alterations on Transduction Currents of Mammalian Hair Cells

Thomas Effertz¹; Anthony Ricci²

¹Stanford University; ²Stanford University, Department of Otolaryngology, Department of Molecular and Cellular Physiology

Background

Sound reception requires specialized sensory cells, hair cells. Their sensory organelle, the hair bundle, consists of actin filled stereocilia, arranged in a stair case pattern. A deflection towards the tallest row increases the open probability of mechano-electrical-transduction (MET) channels residing at the tip of the shorter stereocilia rows. MET-currents decay over time during constant stimulation; the peak current can be recovered with increased stimulus intensity. This process, termed adaptation, was long thought to be driven by Ca²⁺ entry through MET-channels. Recent data from rat inner- and outer hair cells suggests that Ca²⁺ entry is not driving MET-current adaptation. This finding raises questions as to the molecular mechanisms of the MET-channel adaptation and how this channel senses force. One idea is that forces are relayed to the channel via the lipid bilayer. It is unknown if these forces are sufficient to gate the mammalian MET-channel. Studies on non-mammalian channels (MscL, TREK-1) indicate that alterations of the bilayer affects channel gating and open probability.

Methods

Whole cell voltage clamp recordings of inner hair cells (IHC) from P9-11 rats were performed. Hair bundles were actuated by a piezo driven, stiff glass probe. Experiments included alteration of the bilayer membrane by puffing different lipids onto the IHC hair bundle. The MET-current responses of a given IHC were recorded before and after treatment. Effects on dynamic and static parameters of MET-currents were investigated.

Results

Altering the membrane composition changed the measured MET-currents of IHCs. Treatment with conical and inverse conical lipids affected i.e. the channel resting open probability (ca. 3% in controls and ca. 0% after treatment), peak current amplitudes (reduction of ca. 80% from 1 nA to 200 pA) and the half activation point for current displacement plots shifted significantly to the right. Also the extent of adaptation to steps of increasing size was larger in lipid treated bundles compared with control measurement in the same cell. Those effects were irreversible during the duration of the experiment.

Conclusion

We have indications for the importance of the lipid bilayer to relay forces to the MET-channel. The composition and thus the mechanical properties of the membrane seem to affect channel gating and adaptation.

SY - 076

Could Ca²⁺ Release from Intracellular Stores Regulate Mechano-Electrical Transduction?

Ghanshyam Sinha; Gregory Frolenkov

University of Kentucky

Background

It is still unknown how exactly the function of mammalian cochlear outer hair cells (OHC) can be regulated by the release of Ca²⁺ from intracellular stores. Two types of Ca²⁺ stores have been proposed in the OHCs, the IP₃-gated stores activated downstream of many G-protein coupled receptors and ryanodine receptor stores typically responsible for Ca²⁺-induced Ca²⁺ release. So far, only IP₃-gated Ca²⁺ release has been demonstrated in OHCs while the evidence for Ca²⁺-induced Ca²⁺ release has been rather indirect. Similarly uncertain are the potential physiological effects of the increased intracellular Ca²⁺ on the OHC function. Besides obvious requirement of low intracellular Ca²⁺ for OHC survival, the only well-documented effects of intracellular Ca²⁺ were the changes of OHC longitudinal stiffness.

Methods

We used photo-activatable (caged) compounds to stimulate Ca²⁺ release from intracellular stores by liberating either IP₃ or free calcium within the OHC. We monitored the resulting Ca²⁺ transients and simultaneously measured the non-linear capacitance of OHCs. Changes of the stiffness of the hair bundles were monitored by measuring stereocilia deflections with fluid-jet.

Results

In OHCs of an acutely isolated organ of Corti explants loaded with 100 μM of caged IP₃, UV illumination led to a prominent but slow release of calcium, confirming the presence of IP₃-gated stores in these cells. UV flash-photolysis of the Ca²⁺-bound o-nitrophenyl-EGTA (NP-EGTA) produced instantaneous Ca²⁺ release followed by its propagation longitudinally along the OHC. This propagation is likely to be diffusive, because thapsigargin (50 μM), an inhibitor of the endo/sarco-plasmic reticulum ATPase, did not affect it. The Ca²⁺-induced Ca²⁺ release, if present, was difficult to resolve. Contrary to expectation, the OHC non-linear capacitance also did not change even after about one minute post-surge of intracellular calcium.

Conclusions

OHCs possess IP₃-gated stores and negligible amount of Ca²⁺-induced Ca²⁺ release stores. The most likely downstream target of the IP₃-gated Ca²⁺ increase is the cytoskeletal stiffness but not the plasma membrane motor machinery. Because the major IP₃-gated Ca²⁺ stores are localized beneath the cuticular plate, we believe that Ca²⁺ release from these stores modify the mechanical properties of the actin network in the cuticular plate, thereby regulating mechano-electrical transduction.

SY - 077

Changes in Mechano-Electrical Transduction and Calcium Overload in Overstimulated Outer Hair Cells

Ruben Stepanyan^{1,2}; Artur Indzhukulian¹; Ghanshyam Sinha¹; Julie McLean¹; Gregory Frolenkov¹

¹*University of Kentucky*; ²*Case Western Reserve University*

Background

Sound-induced mechanical vibrations of hair cell stereocilia activate mechano-electrical transduction (MET) channels. The MET channel is a non-selective cation channel with high Ca²⁺ permeability. During periods of excessive stimulation MET machinery is being exposed to intense mechanical forces. Here we investigate changes in the MET currents and Ca²⁺ load after mechanical overstimulation of hair bundles.

Methods

Whole cell patch clamp recording of young postnatal mouse cochlear hair cells was performed. Stereocilia were stimulated using a fluid jet or stiff glass probes driven by a piezo actuator. Intracellular Ca²⁺ was monitored using Fura 2, AM and RhodX, AM calcium indicator dyes. The morphology of stereocilia was examined by high resolution scanning electron microscopy.

Results

Large positive and negative deflections of stereocilia, as expected, resulted in a decrease in the amplitude of MET current. In addition, MET responses acquired pronounced tail currents and, most interestingly, both positive and negative stereocilia deflections began to evoke MET responses. Despite a reduction in the MET current amplitude, the adaptation of MET responses was not affected by overstimulation. High resolution scanning electron microscopy revealed normal morphology of the stereocilia bundles in the damaged hair cells with only minor loss of the tip links. Calcium imaging revealed that elevated Ca²⁺ was promptly removed from the cytosol, while Ca²⁺ accumulation sustained in mitochondria of basal, high frequency outer hair cells after the end of stimulation.

Conclusion

Mitochondrial Ca²⁺ overload is a common event leading to cell death, featured by the increase in production of mitochondrial reactive oxygen species. Future studies will explore whether a novel class of small peptide antioxidants, which concentrate to the inner mitochondrial membrane, will protect hair cells against overstimulation.

SY - 078

An Efficient Gene Delivery Method for the Annotation of Gene Function in Mechanosensory Hair Cells

Ulrich Mueller; **Wei Xiong**; Thomas Wagner; Ulrich Mueller
The Scripps Research Institute

Background

The hair cells of the mammalian inner ear are the mechanosensors for the detection of sound and head movement. Protruding from the apical surface of each hair cell is a hair

bundle that contains mechanotransduction machinery for converting sound-induced vibrations into electrical signals. The mechanisms that regulate the development of hair bundles and their function for mechanotransduction are poorly defined.

Methods

Here we describe a method that combines microinjection with electroporation to efficiently express cDNAs and shRNAs in hair cells followed by the analysis of mechanotransduction response.

Results

Using imaging and electrophysiology, we use this method to demonstrate that hair bundle proteins function in mechanotransduction in unexpected ways.

Conclusion

We predicted that our method will accelerate the study of gene function in hair cells, and will facilitate the elucidation of the mechanisms by which mutations in more than 100 genes cause deafness in humans.

SY - 079

A New Probe for Cochlear Hair Bundle Stimulation

Kiriaki Domenica Karavitaki; David P. Corey
Harvard Medical School

Background

Electrophysiological measurements of mechanotransduction require appropriate stimulus methods that mimic *in vivo* stimulation. In otolith organs where stereocilia are extensively cross-linked, moving the kinocilium is sufficient. Proper coupling to mammalian cochlear hair cells is more difficult: The tallest stereocilia of outer hair cells (OHCs) are firmly attached to the tectorial membrane—although shorter stereocilia must be coupled to taller in a column, stereocilia need not be coupled laterally. Inner hair cell (IHC) bundles are uniformly deflected by fluid movement so IHC bundles need no connections other than tip links. Indeed, we have shown that lateral coupling between tallest-row stereocilia is weak in both IHCs and OHCs. Therefore, uniform and simultaneous delivery of the stimulus to all the tallest stereocilia is challenging. Cochlear bundles have been experimentally stimulated by a fluid jet, but fluid jet is generally slow, it does not allow a precise displacement stimulus to the hair bundle, and does not permit stiffness measurements. The glass or silicon stimulus probes that fit inside the V shape of the bundle are large compared to the stereocilia in the bundle, raising questions about how the probe is coupled to shorter stereocilia; but they are often small compared to the width of the bundle, raising concern about the homogeneity of stimulation. Finally, for many experiments such as Ca^{2+} imaging, such probes obscure visualization of individual stereocilia.

Methods

We have developed silicon-based probes that mimic the *in vivo* stimulus delivery to cochlear hair bundles. The probes were designed to fit the bundle shape using a MEMS design software (L-edit, Tanner EDA) and manufactured from poly-

silicon at MEMSCAP using the POLYMUMPS process. The stiffness is much larger than that of hair bundles, so these probes deliver an effective displacement stimulus.

Results

The resulting probes improve the homogeneity of stimulation along the tallest stereociliary row; they allow visual access of the shortest stereocilia; they deliver stimuli in both the excitatory and the inhibitory directions; and they are easily adaptable to the different shapes of IHCs and OHCs.

Conclusions

Stimulus probes for cochlear hair cells that can deliver an *in vivo*-like stimulus will provide cochlear physiologists with tight mechanical stimulation for accurately characterizing cochlear mechanotransduction.

PS - 651

Precedence Based Speech Segregation in Bilateral Cochlear Implant Users

Shaikat Hossain¹; Vahid Montazeri¹; Peter Assmann²; Emily Tobey¹; Ruth Litovsky²

¹University of Texas at Dallas; ²University of Texas at Dallas;

²University of Wisconsin-Madison

Background

The precedence effect (PE) is a well-documented auditory phenomenon that enables the perceptual domination source (lead) over echo (lag) sounds in reverberant environments. In addition to localization, it has been previously found that the PE plays an important role for normal-hearing (NH) listeners in spatial unmasking of speech in situations where the PE introduces a perceived spatial separation between target and masker speakers. The present study focused on the PE in a unique, but rapidly growing, population of listeners who use bilateral cochlear implants (BiCIs). Very little is known about the PE, and in particular its relationship to speech segregation for BiCI users. BiCI users continue to face limitations in communicating effectively in reverberant environments and the findings from this research may lead to improvements in signal processing strategies for BiCIs.

Methods

Subjects include normal hearing (NH) listeners tested using binaural vocoder simulations and BiCI users. Subjects identified nonsense sentences in the presence of either speech-shaped noise or a competing talker at various signal-to-noise ratios (SNRs). Testing was conducted in sound field using two loudspeakers positioned at 0 and 60 degrees in the azimuthal plane in a soundproof booth. Three different spatial configurations were tested: F-F condition (baseline with target and masker presented from the same front loudspeaker); F-R (target was in front and masking signal was from the right side loudspeaker); F-RF (similar to the F-R condition, but with the addition of a copy of the masker from the front loudspeaker, after a 4ms delay relative to the side loudspeaker).

Results

Results from NH participants listening through CI simulations show reduced identification scores and higher variability across all three of the spatial configurations compared to a

NH control group. A benefit was exhibited in the F-RF condition as compared to the F-F condition, where the addition of a delayed copy of the masker led to spatial unmasking, likely due to the masker being perceived as spatially distinct from the target. This benefit was exhibited in the conditions where the interference was a competing talker at lower SNRs. Collection of data from BiCI users is ongoing.

Conclusion

Our findings from NH participants listening through CI simulations suggest that BiCI users may potentially be able to derive benefit from the PE in speech segregation. Ongoing testing will examine whether BiCI users can receive such a benefit in spatial unmasking or whether factors which limit binaural sensitivity reduce the potential benefit provided by the PE.

PS - 652

Listening Effort in Users of Bilateral Cochlear Implants and Bimodal Hearing

Matthew Fitzgerald; Sapna Mehta; E. Katelyn Glassman; Keena Seward; Arlene Neuman

New York University School of Medicine

Background

Many bilateral cochlear implant (CI) recipients, or users of bimodal hearing (CI + hearing aid in the contralateral ear) report that it is easier to listen when both devices are active than with only a single device. However, there is no established procedure to quantify listening effort in these individuals. Here we used a dual-task paradigm to measure listening effort in bilateral / bimodal and unilateral listening conditions. In a dual task paradigm, the listener divides attention between a primary and secondary task. As the primary task becomes more difficult, fewer cognitive resources are available for the secondary task, generally resulting in poorer performance.

Methods

Participants consisted of bilateral CI recipients, or were users of bimodal hearing. The primary task was to repeat AzBio sentences either in quiet, or with a + 10 dB signal-to-noise (SNR) ratio. The secondary task was to recall a string of digits presented visually before a set of two sentences. As a control, both the sentence-recognition and digit-recall tasks were tested by themselves in a single-task paradigm. Participants were tested both unilaterally and bilaterally / bimodally.

Results

On the primary sentence-recognition task, while performance decreased between the quiet and noise conditions, sentence-recognition scores did not on average differ between the single- and dual-task paradigms. Performance on the secondary digit-recall task was characterized by considerable variability. Nonetheless, on average digit-recall scores were lower in the quiet condition and even lower in noise, suggesting that 1) this task is sensitive to changes in listening effort, and 2) listening effort increases with noise. Digit-recall scores obtained bilaterally did not differ appreciably from those obtained unilaterally in either sequentially or simultaneously implanted bilateral CI recipients. There may be a small trend for better bilateral than unilateral digit-recall scores to be seen in noise for bilateral CI users who displayed bilateral

benefits to speech understanding. A similar trend for bimodal digit-recall scores to be higher than unilateral scores was also seen in two users of bimodal hearing.

Conclusion

A dual-task paradigm may be useful for quantifying listening effort because, on average, when compared to the single-task control 1) performance on the primary sentence-recognition task was not affected, but 2) performance on the secondary digit-recall task decreased. However, there is considerable variability on the digit-recall task with the present protocol, which hinders the ability to draw clear conclusions about listening effort in bilateral or bimodal vs. unilateral listening conditions.

PS - 653

Envelope Shape Affects Neural ITD Coding With Bilateral Cochlear Implants

Kenneth Hancock; Yoojin Chung; Bertrand Delgutte
Massachusetts Eye & Ear Infirmary

Background

Bilateral cochlear implant (CI) users receive minimal benefit from interaural time difference (ITD) cues, especially with present sound processors, which deliver ITDs only in the amplitude envelopes of high-rate pulse trains. The only previous single-unit study of neural envelope ITD coding with CI (Smith & Delgutte, *J Neurophysiol* 99:2390) used sinusoidal modulation, which poorly represents the diversity of envelope shapes contained in natural stimuli because it confounds repetition rate and the width of each envelope cycle. Here we used stimuli that allow independent manipulation of the two variables to measure ITD sensitivity of single neurons in the inferior colliculus (IC) of anesthetized, acutely-deafened, bilaterally-implanted cats.

Methods

Stimuli were amplitude-modulated, high-rate (1000 pulses/s) pulse trains. The envelope waveform interleaved single cycles of a sinusoid with silent intervals. Both the duration of each sinusoidal modulation burst (which determines the attack slope), and the repetition rate of the modulation bursts were systematically varied (range: from 20 to 250 Hz for rate, and from 4 to 48 ms for width). Each modulation waveform was presented with at least three different ITDs (0, ± 400 μ s) to assess neural ITD sensitivity. ITD was usually applied to the whole waveform; in some cases, the measurement was repeated with ITD applied only to the envelope.

Results

Neural ITD coding was relatively poor using continuous sinusoidal modulation, but was generally enhanced by insertion of silent intervals between modulation bursts. There was considerable variability among neurons with respect to the envelope parameters that maximized ITD sensitivity. In some neurons, ITD coding was best for low repetition rates with minimal dependence on envelope width. In other neurons, coding was best for brief envelope bursts (high attack slopes) with lesser sensitivity to repetition rate. All of the few neurons tested in both ITD conditions were sensitive to ITD in the

whole waveform but half were not sensitive to envelope-only ITD for any envelope shape.

Conclusion

Across our neuron sample, the main trends were consistent with human psychophysics (Laback et al. JASA 130:1515, Noel & Eddington JASA 133:2314, van Hoesel et al. JARO 10:557): ITD coding generally improved with longer silent intervals and briefer envelope bursts (i.e. increased attack slopes), and was best for repetition rates in the range of 50-125 Hz. Future CI processing strategies designed to enhance these envelope features are likely to improve coding of ITD for natural stimuli, including speech.

PS - 654

Neural Coding of Interaural Time Difference in an Awake Rabbit Model of Bilateral Cochlear Implants

Yoojin Chung; Kenneth Hancock; Bertrand Delgutte
Massachusetts Eye and Ear Infirmary

Background

Bilateral cochlear implants (CI) provide benefits over unilateral implants for sound localization and speech reception in noise. However, binaural performance of bilateral CI users is still substantially below normal, especially in tasks involving interaural time differences (ITD). Here, we characterize ITD sensitivity of inferior colliculus (IC) neurons in a novel awake rabbit model of bilateral CIs.

Methods

Four adult Dutch-belted rabbits were deafened and bilaterally implanted with 8-ring animal cochlear arrays. Single unit recordings were made from the IC during repeated sessions lasting 2 hours each from 4 up to 25 weeks after implantation. Stimuli were periodic trains of biphasic pulses with varying pulse rates (20-640 pps) and ITDs (~2000-2000 μ s).

Results

ITD tuning curves in awake rabbits were qualitatively similar to those previously observed in anesthetized cat, and could be peak-type, trough-type or sigmoid. However sustained, ITD-sensitive responses were observed at higher pulse rates compared to anesthetized cats, and, on average, ITD sensitivity was better in awake rabbit for pulse rates above 100 pps. Consistent with previous findings in normal hearing and unilaterally-deafened animals, there was strong spontaneous activity in awake rabbits. At low and intermediate pulse rates (20 - 160 pps), this background activity could mask ITD sensitivity in the overall firing rate. In such cases, however, selecting the spikes synchronized to individual stimulus pulses by temporal windowing revealed ITD sensitivity. Such windowing might be implemented more centrally by coincidence detection across multiple IC neurons with similar response latencies. Neurons tended to favor contralateral-leading ITDs, a trend that was most clear for the pulse-locked spikes.

Conclusion

ITD sensitivity was observed at higher pulse rates in awake animals compared to anesthetized animals. In addition, strong background activity could mask ITD sensitivity in the

overall firing rate at low and intermediate pulse rates. The neural pulse-rate limits of ITD sensitivity found in awake animals are more consistent with the perceptual rate limits in human CI users.

PS - 655

Measuring Binaural Integration in Children

Morrison Steel; Karen Gordon; Blake Papsin
The Hospital for Sick Children

Background

Bilateral cochlear implants (CIs) have been provided to children to promote binaural hearing and perhaps ease the increased effort required for listening shown by unilaterally implanted children (Pisoni et al., 2007). Unfortunately, it remains unclear whether these children have access to accurate binaural cues. In a previous study, we found children using bilateral CIs reported hearing from both devices simultaneously rather than one integrated image (Salloum, et al., 2010), suggesting abnormal perception of bilateral CI input. We aimed, in the present study, to measure: 1) binaural integration and 2) listening effort in children.

Methods

Thirty children participated in this study: 26 with normal hearing (mean age = 12.80 ± 3.24 years) and 4 with deafness and sequentially implanted bilateral CIs (11.30 ± 1.48 years). Stimuli were click trains presented through insert earphones for normal listeners and biphasic electrical pulses delivered from an apical electrode for children using CIs. Bilateral stimuli, presented in random order with unilateral controls, varied in interaural level, timing, and place. Pupil diameter was measured using an Interacoustics Videonystagmography system. While wearing video goggles, participants were instructed to choose a single circle or pair of circles to indicate whether they heard one or two sounds, respectively. Reaction time from stimulus onset to response was measured for each trial.

Results

Normal listeners perceived most bilateral stimuli as one sound with high accuracy ($87 \pm 16\%$). Their perception of single sounds decreased with the introduction of interaural timing differences of 2 ms with a concurrent increase in reaction time ($t(47.25) = -2.02$, $p < 0.05$). Reaction times were positively correlated with pupil diameter across groups (normal listeners: $R = 0.81$, $p < 0.01$; CI listeners: $R = 0.96$, $p < 0.05$). The 4 children using CIs had more variable responses to bilateral input and longer reaction times.

Conclusion

Children with normal hearing consistently hear bilaterally presented clicks as one sound. This integrated image deteriorates when the interaural timing difference is extended beyond the physiological range (> 1 ms). Reaction time and pupil diameter show agreement perhaps indicating listening effort. Children with bilateral CIs appear to integrate input from the two devices but perceive one image less frequently than normal.

Lateralization of Modulated- and Constant-Amplitude Pulse Trains in Normal-Hearing and Bilateral Cochlear-Implant Listeners

Kyle Easter; Matthew Goupell

University of Maryland - College Park

Background

Compared to normal-hearing (NH) listeners, bilateral cochlear-implant (BICI) users are worse at free-field sound localization and understanding speech in noise. However, NH and BICI listeners show more equitable binaural performance in highly-controlled direct stimulation experiments that use constant-amplitude pulse trains (CAPTs). It is possible that sounds with amplitude modulations reduce binaural performance for free-field stimuli in BICI users. We hypothesized that uncontrolled loudness growth between the ears causes interaural decorrelation, which in turn reduces binaural performance for modulated stimuli. To test this hypothesis, the lateralization of CAPTs and modulated stimuli was compared for NH and BICI listeners.

Methods

Data from ten NH listeners and preliminary data from five BICI listeners was collected. Stimuli were presented over headphones for the NH listeners and via direct stimulation for the BICI listeners. Stimuli were CAPTs or modulated-amplitude pulse trains (MAPTs). CAPTs were band-limited Gaussian acoustic pulses with a 4-kHz center frequency and a 1.5-mm bandwidth or monopolar electrical stimulation from a pitch-matched electrode pair for the NH and BICI listeners, respectively. The pulse rate of the CAPTs and the modulation rate of the MAPTs was varied between 10, 30, 100, and 300 Hz. MAPTs had a sine tone or 1000-Hz CAPT carrier for NH and BICI listeners, respectively. A control carrier condition was also tested. Listeners indicated the perceived lateralization for a range of interaural level and time differences (ILDs and ITDs, respectively).

Results

In NH listeners, ILD lateralization was independent of stimulus type or rate. ITD lateralization depended on stimulus type and rate. CAPTs produced a large lateralization range, which was independent of pulse rate. MAPTs produced an increasing lateralization range as the rate increased to 100 Hz and a decreased range at 300 Hz. BICI listeners showed broadly similar trends in ILD and ITD lateralization compared to the NH listeners. Differences included large lateralization offsets for assumed zero ILD and ITD and, in some BICI listeners, MAPTs produced more variable lateralization responses compared to CAPTs.

Conclusion

NH and BICI listeners lateralize ILDs and ITDs in broadly similar ways. However, lateralization for MAPTs was more variable than CAPTs in some BICI listeners. This indicates that modulations may introduce interaural decorrelation, which ultimately could reduce binaural benefits of BICIs. If the more variable responses are a result of interaural decorrela-

tion, this problem might be remediated through alternative CI mapping techniques.

Across-Electrode Integration of Interaural Time Difference in Bilateral Cochlear Implant Listeners

Katharina Egger; Piotr Majdak; Bernhard Laback

Acoustics Research Institute, Austrian Academy of Sciences

Background

Binaural hearing provides substantial cues essential for localization and segregation of sound sources. Despite bilateral implantation, cochlear implant (CI) listeners' performance in those everyday challenges is still rather limited compared to normal hearing listeners. It is assumed that those limitations are at least partly due to the CI listeners' low sensitivity to interaural time differences (ITDs) which is to some extent linked to the suboptimal encoding of ITD cues with current bilateral CI systems. ITD sensitivity of CI listeners stimulated at a single interaural electrode pair has been investigated intensively. This study addressed the CI listeners' sensitivity to ITD presented at multiple interaural electrode pairs.

Methods

Experiments were performed using direct stimulation via synchronized research interfaces. In pretests, up to four interaurally pitch-matched electrode pairs were identified. ITD just-noticeable differences (JNDs) for unmodulated 100-pulses-per-second pulse trains were measured in a constant stimuli paradigm. Measurements were performed using different tonotopic separations between electrode pairs and at different current levels. All pairs were tested using the same ITD, and the temporal offset across electrodes corresponded to half the interpulse interval. Multiple-pair JNDs were compared to single-pair JNDs at corresponding levels.

Results

The results mostly showed only small or even no decrease in JNDs for multiple-pair stimulation when compared to single-pair stimulation. If at all, then a decrease in JNDs was found more often for larger tonotopic separations and at constant current levels. When holding loudness constant, JNDs tended to be similar for single- and multiple-pair conditions. Substantial effects of current level were observed, showing increasing JNDs with decreasing level irrespective of electrode-pair configuration.

Conclusion

Improvements in ITD sensitivity due to across-electrode integration appear to be smaller than in acoustic hearing. The results show a complex interaction of the factors stimulation current level, tonotopic distance, and effective pulse rate received by the auditory nerve. Implications for the access to ITD cues with current stimulation strategies and its potential improvement with future systems are discussed.

Effects of Age at Deafness Onset on Neural Coding of Interaural Time Differences in Gerbil Auditory Brainstem and Midbrain

Maike Vollmer; Martin Kempe; Armin Wiegner
Comprehensive Hearing Center, University Hospital
Wuerzburg

Background

In acoustic hearing, interaural time differences (ITDs) are important cues for directional hearing and speech understanding in noise. Precise ITD discrimination in the microsecond range is assumed to be dependent on normal auditory experience during development. In contrast, to explore the effects of severely distorted auditory experience on neural ITD coding we used an animal model for bilateral deafness and cochlear implantation.

Methods

Specifically, to determine the effects of age at deafness onset on neural ITD coding, gerbils were bilaterally deafened either as juveniles around hearing onset (P12) or as adults (~10 wk of age). After deafness durations of ~8 weeks, animals were bilaterally implanted, and single neuron responses to electric ITDs were recorded in the dorsal nucleus of the lateral lemniscus and in the inferior colliculus. Adult gerbils with normal auditory experience prior to the electrophysiological experiment served as controls.

Results

The incidence of ITD-sensitive neurons in the two deafened groups was similar to that in normal hearing control animals. Independent of age at deafness onset, deafness resulted in greater variabilities for all ITD parameters tested (ITD at maximum spike rate, best ITD; ITD at maximum slope, ITDms; physiological modulation depth, PMD; half width; half rise). In contrast to the narrow distribution of best ITDs that are biased towards contralateral-leading in normal hearing animals, both deafened groups had broad distributions of best ITDs around the midline. These results were paralleled by a lower incidence of ITDms, thus a reduced sensitivity to changes in ITDs, within the physiological range. Moreover, both deafened groups demonstrated reduced sharpness in ITD tuning (broader halfwidth and half rise), lower PMD and higher neural ITD discrimination thresholds than normal hearing control animals. When compared across the two deafened groups, neurons in juvenile deafened animals revealed significantly poorer ITD sensitivities (ITD signal to total variance ratio) than those in adult deafened animals.

Conclusion

The results indicate that prolonged periods of both early- and late-onset deafness lead to various degradations in neural ITD coding that may help to explain the overall poor behavioral ITD discrimination performance in human bilateral cochlear implant (CI) users. In addition, the severely reduced ITD sensitivity of neurons in early-onset deafness may be a physiological correlate for the limited ability of most prelingually deaf CI subjects to utilize ITD cues for directional hearing if implanted later in life. These findings suggest the importance

of temporally correlated binaural hearing experience early in life in order to fully benefit from binaural stimulation.

Comparison Of Mono- And Binaural Activity Between Infra- And Supragranular Layers Of The Auditory Cortex In Congenitally Deaf And Hearing Control Cats

Jochen Tillein¹; Peter Hubka²; Andrej Kral²

¹J.W.Goethe University and Medel Starnberg; ²Experimental Otolology, ENT Clinics, Medical University Hannover, Germany

Background

Previous studies have demonstrated that congenital deafness in cats leads to a wide range of deficits or alteration in the adult auditory cortex. E.g. acute intracochlear electrical stimulation results in lower firing rates, lower numbers of responding neurons, a smaller dynamic range, lower cortical thresholds and a decreased sensitivity to binaural cues (Kral & Sharma 2012, Tillein et al., 2010). As these data have not been analyzed yet with respect to cortical depth the recent study focuses on the analysis of activity in infra- and supragranular layers, respectively. A former study has shown that synaptic activity is significantly decreased along cortical columns in infragranular layers in congenitally deaf cats (CDCs) compared to hearing cats (HCs) (Kral et al. 2005). We investigated neuronal activity after monaural and binaural stimulation using single- and multi unit responses.

Methods

Animals of the two groups (CDC and HC) were acutely stimulated with charge-balanced biphasic pulse trains (3 pulses, 200µs/phase, 500pps) in wide bipolar configuration through a custom made cochlear implant inserted into the scala tympani of the cochlea on either side. Control animals were acutely deafened by intracochlear application of neomycin. Multi-unit activity was recorded intracortically in regions which were most responsive as defined by local field potential surface mapping using 16 channel electrode arrays (Neuronexus probes) inserted perpendicular to the cortical surface. In each animal 1-3 tracks were stained by fluorescence dye (Dil) for later histological reconstruction. Animals were stimulated mono- and binaurally. In the binaural mode also time delays were introduced to measure sensitivity to interaural time delays (ITDs). Template ITD functions (Tillein et al., 2010) were fitted to the data and distribution of classified ITD functions were compared along cortical depth and between groups.

Results

Preliminary results revealed a significant reduction of spike activity within the infragranular layers of CDCs compared to HCs. The number of classified ITD functions was significant lower in CDCs with a maximum located in the supragranular and dorsal parts of the infragranular layers while in the HCs the highest numbers of classified ITD functions were most frequently found in deeper infragranular layers.

Conclusion

The decline of spike activity within the infragranular layers of CDCs confirms previous findings about decreased synaptic activity within these layers and might also cause the shift of classified ITD functions towards supragranular layers in CDCs. In conclusion, apart from a reduced ITD sensitivity in CDCs congenital deafness leads to distinct changes of neuronal responses along the depth of auditory cortex by mainly affecting the infragranular layers.

PS - 660

Short-Term Adaptation Improves Cochlear-Implant Speech Processing

Robert Smith; Mahan Azadpour

Syracuse University

Background

Neural systems typically display adaptation, a process that reduces responses to ongoing steady stimulation and enhances responses to changes in the input. In the auditory system adaptation occurs at many levels of processing presumably beginning with synaptic transmission from inner hair cells (IHCs). Since cochlear implants (CIs) bypass IHCs it was hypothesized that adding hair-cell type short-term adaptation to CI speech processors would improve speech intelligibility. The present study expands upon previous results (Smith et al, 2010 ARO midwinter meeting) showing that some improvements indeed occur.

Methods

Results are based on 6 subjects who had been using their Nucleus processor for at least 6 months, and their processor was simulated using their audiologist produced maps and the Nucleus MATLAB Toolbox and Implant Communicator. Short-term adaptation was applied to the stimulus envelope in each electrode channel by inserting a 1st order high-pass filter prior to modulating the pulse train output of the channel. Filters were normalized to the operating range of an individual channel and the time constant and amount of adaptation produced by the filter adjusted in an attempt to improve performance beyond that in the absence of filtering. The main tests involved perception of consonants in quiet and background noises without and sometimes with feedback and laboratory training. Some effects of the filter on single channel consonant perception were also obtained. Results were analyzed in terms of overall percent correct, confusion matrices and consonant features.

Results

The best filter was found for each subject and produced an improvement ranging between 5 and 10 percent in most subjects and tasks. Improvements were a nonmonotonic function of time constant with individual best time constants of 25 to 50 msec and best onset increase of 30% to 50% of a channel's dynamic range. Sentence comprehension tests in quiet were higher in all subjects for the adaptation-based strategy that was the "best" condition for consonant tests in quiet. Improvements also occurred with training and for low and medium level background babble noise. Single channel

performance also improved with filtering consistent with the full processor results.

Conclusion

Results show that adding short-term adaptation to CI envelope processing results in improved speech intelligibility but the optimum performance is yet to be determined. Improvements are presumed to occur because of increased emphasis on envelope variations leading to better access of within and across channel speech cues.

PS - 661

The Effect of Spread of Excitation on Phonemic Restoration in Cochlear Implants

Kristen Mills¹; Deniz Baskent²; Jong Ho Won¹

¹University of Tennessee Health Science Center; ²University of Groningen

Background

Background noise is an inevitable part of one's everyday auditory environment, but it is particularly challenging for cochlear implant (CI) users to correctly understand speech in the presence of noise. The degradations in the bottom-up speech cues by the CI processing may hinder the top-down compensation for speech degradation, such as phonemic restoration (PR). The PR effect can be measured by the increase in intelligibility when silent interruptions in a sentence are filled with noise, which presents an ambiguity to the brain and thus activates the top-down system for finding the right lexical filling, using linguistic rules, semantic context, and expectations. We hypothesized that spread of excitation (SOE) in the auditory nerve may degrade the representation of the bottom-up speech signals and result in the reduced top-down repair mechanism. To test this hypothesis, PR of interrupted sentences was measured in normal hearing listeners using vocoder simulations that are designed to test the effect of SOE.

Methods

Normal hearing listeners were presented with original or vocoded IEEE sentences with periodic silent intervals with and without a filler noise in the gaps. The noise vocoders of 16-channel processing (based on Baskent, 2012, JARO) simulated four different levels of SOE: -1, -2, -4, and -8 dB/mm (Bingabr et al., 2008, Hear Res). The size of PR was measured by an increase in speech identification scores after the addition of the filler noise.

Results

A significant effect of SOE was shown on the intelligibility of sentences with and without a filler noise, suggesting that different degrees of SOE in individual patients may affect variability in speech perception outcomes in CI users. PR was observed for the original sentences; however, subjects showed no PR when they were presented with vocoded sentences at any SOE level.

Conclusion

The absence of PR at all four SOE levels suggests that 16 channels of spectral resolution may be too sparse for listeners to extract the necessary speech cues from interrupted

sentences when the gaps were filled with filler noises. Alternatively, it is possible that other types of speech cues that are not adequately transmitted through CI speech processors may contribute to the inefficient use of top-down processing. We will discuss the potential effects of temporal fine structure on PR in CI users.

PS - 662

Assessment of Spectral and Temporal Resolution in Cochlear Implant Users: Speech and Psychoacoustic Approach

Il Joon Moon¹; Jong Ho Won²; Matthew Winn³

¹University of Washington; ²University of Tennessee Health Science Center; ³University of Wisconsin-Madison

Background

Spectral ripple discrimination (SRD) and temporal modulation detection (TMD) have been shown to significantly correlate with speech perception abilities in cochlear implant (CI) users. To evaluate speech perception outcomes, previous studies have generally utilized phoneme, word or sentence recognition. With such speech perception tasks, however, it is difficult to isolate the effect of specific cues on perception, because various components, such as spectral, temporal, linguistic, and contextual factors are combined in speech. It is not clear whether psychophysical abilities carry over to reflect abilities of listeners to glean specific cues in speech. Toward clarifying that relationship, we used speech perception measures where specific spectral or temporal cues were controlled exclusively, and measured the recovery of those cues vis a vis categorization.

Methods

Ten CI and 11 normal-hearing (NH) subjects participated. To evaluate the sensitivity to spectral cues in speech signals, we measured identification of a /ba/-/da/ continuum made from modified natural speech, featuring manipulation of formant transitions. To evaluate the sensitivity to temporal cues in speech, identification performance was measured using two continua (deer-tier, beer-pier) that varied in voice-onset time (VOT). Subjects' psychometric functions along the acoustic cue continua were modeled using logistic regression, and quantified using the model coefficients corresponding to the manipulated cues. The same group of subjects was also tested for SRD and TMD. Correlations between coefficients for the speech tasks and thresholds for SRD and TMD were computed.

Results

Coefficients from both the spectral and temporal speech tests in the NH group were higher than those for CI subjects, indicating that NH subjects were generally more efficient at utilizing the cues for categorization. A significant correlation was found between the SRD scores and formant coefficients (/ba/-/da/ identification) in CI subjects ($r = 0.84$, $p = 0.002$). However, while TMD thresholds were correlated with VOT coefficients of the temporal speech task, this relationship did not reach statistical significance.

Conclusion

The current paradigm underscores the relationship between speech perception and non-linguistic psychoacoustic measures. Although speech is a complex signal with multiple cues, the ability to recover those cues bears some relationship with basic psychophysical abilities. These speech perception tasks, in which spectral and temporal cues are manipulated orthogonally in speech stimuli, may be a useful tool to evaluate CI performance with different encoding strategies or mapping parameters.

PS - 663

Variation of Anatomical and Physiological Parameters Causes Inter-Individual Variances in the Neural Representation of Speech in Cochlear Implant Users.

Michele Nicoletti; Werner Hemmert

Technische Universität München

Background

Cochlear implant (CI) users show a huge variation in performance. It is therefore likely that they would benefit if their coding strategy could be adapted to their individual strengths and weaknesses. The studies published by Nelson et al. (2008, 2011) show huge differences in the spread of excitation (SOE) across CI users. Some subjects even show large variations in SOE for different electrode locations, where variations in SOE lobes between 0.5 dB / mm and 2.5 dB / mm are not uncommon. However, the development of strategies that are able to compensate individual differences requires a deep understanding of the physiological causes which limit performance in each patient.

Methods

To tackle this question, we have developed a model framework, which allows us to study how physiological variations in the implanted cochlea impact speech coding in the auditory nerve. The study presented here focuses on inter-individual differences observed in channel cross talk. This study investigates possible reasons that lead to SOE variations based on an electro-anatomical model (EAM) of an idealized human cochlea. The most important anatomical, physiological and operational parameter variations were covered and their influence on SOE evaluated. For the quantitative analysis of neurophysiological variations, such as the distribution of the nerve fibers and the formation of „dead regions zones“ (DRZ) (Moore and Glasberg 1997), this EAM model was combined with a nerve population model in which the number and the distribution of spiral ganglion cells along the cochlea was varied (Nicoletti et al. 2013).

Results

The model predicts that SOEs differ between near and far field (Briaire 2000) and shows which parameters influence SOEs most. Furthermore, the model quantifies the impact on the neural representation of speech. It demonstrates that with a decreasing number of nerve cells the probability of DRZs increases. With more than 5,000 nerve cells the cochlear spiral is covered sufficiently homogeneous with ganglion cells to represent spectral components relevant for speech coding.

Conclusion

For cell count of less than 5,000 randomly distributed nerve cells along the cochlea, the probability for the formation of DRZ increases, which is consistent with observations from Blamey et al. (1997) and Khan et al. (2005). Finally, our model shows that not the absolute number of spiral ganglion cells is important for the performance of a CI-user, but also how they are distributed across the cochlea.

PS - 664

Clinical Validation of Lately Developed Noise Reduction and Output Compression Algorithms

Dan Gnansia¹; Sonia Saaï¹; Bertrand Philippon¹; Alexis Bozorg-Grayelli²; Jean-Pierre Lavieille³

¹Neurelec - Oticon Medical; ²University hospital, Dijon; ³Noth hospital, Marseille

Background

Flexible programmable cochlear implant speech processors allow software updates and signal processing features development. All new developed functionalities have to be clinically relevant and should be tested. The goal of the present study is to present results from clinical validation of lately developed noise-reduction (VoiceTrack™) and output compression (XDP) algorithms in cochlear implant recipients.

Methods

VoiceTrack™ is a noise-reduction method using one microphone. This algorithm integrates noise estimation based on spectral minimum over a time-window, evaluating the steady background noise spectral profile. This profile is finally spectrally subtracted, taking into account the signal information in order to maintain overall loudness of target signal.

XDP output-compression function showed four frequency zones, with two linear parts (one knee-point) per zone. Specific presets adapted to sound presentation level were proposed for testing.

Both algorithms were tested on 20 cochlear implant recipients over 2 test sessions. For VoiceTrack™, speech perception was assessed through speech in quiet and in noise tests with two noise types: steady-state speech-shaped noise (5dB SNR) and multitalker babble (0, 5 and 10dB SNR). For XDP, tests in quiet at several intensities (40, 55, 70 and 85 dB SPL) and in babble noise (5dB SNR) were performed. Pure tone thresholds were also assessed. Finally, a questionnaire was used to evaluate sound quality and everyday life listening situations. Subjects were first tested immediately after noise reduction activation, then after one month of use.

Results

Results showed that VoiceTrack™ did modify neither pure-tone thresholds, nor speech intelligibility in quiet. Moreover, significant improvement in steady noise and in babble noise has been observed. XDP results showed no improvements in quiet for medium presets, but significant improvement in noise. Pure-tone thresholds were not affected. Listening quality testing for noise annoyance and overall preference also found significant improvements.

Conclusion

With regards to implementation hypothesis and results, both VoiceTrack™ and XDP algorithms can then be clinically validated. Those algorithms have shown significant outcomes and sound quality improvements compared to the standard processing. It is now proposed for clinical practice. Additional tests showed that noise-reduction level had to be set carefully not to affect speech in quiet. Output-compression preset had also major impact on speech in quiet. Fitting guidelines were then produced following this study.

PS - 665

Improving Speech Perception in Noise for Cochlear Implant Listeners by Combining Harmonic Regeneration With Noise Suppression

Qudsia Tahmina¹; Yi Hu¹; Christina Runge²; David Friedland²

¹University of Wisconsin-Milwaukee; ²Medical College of Wisconsin

Background

Several studies on the EAS benefits have shown that many postlingually deafened patients, fitted with the latest multichannel speech processors, perform very well in quiet listening situations. However, speech performance deteriorates rapidly with increased levels of background noise, even for the best CI users.

Although previous studies showed a significant improvement in the speech perception in noise for cochlear implant users by using single-channel noise-reduction algorithms, most noise reduction methods use preset optimization criteria and offer no remedy for the problem that the noise-suppressed speech may no longer possesses the properties mandated by the acoustic process of speech production (for instance, the harmonic structures in voiced segments of the noise-suppressed speech are usually severely distorted). The reduction in intelligibility by the logMMSE-SPU algorithm can be attributed to the corrupted envelopes and the lack of preservation of the F0 contour, which is needed for speech and language recognition.

The objective of this study is to integrate harmonic regeneration techniques in noise reduction to further improve the intelligibility of noise-suppressed speech for CI patients.

Methods

We propose a noise-reduction algorithm combined with a well-established acoustic model of voiced speech production: harmonic modeling of voiced speech.

The noisy input is first processed through the log-minimum mean square error algorithm to suppress the unwanted noise(A, in the attached block diagram) and the voiced frames are detected which are then modified using statistical-approach-based harmonic-regeneration algorithm(B, in the attached block diagram) that attempts to estimate the fundamental frequencies and magnitudes of the harmonics.

Subjects: 7 subjects that wear CI in one side and hearing aid in the contra-lateral side.

Materials: IEEE sentences produced by a male talker.

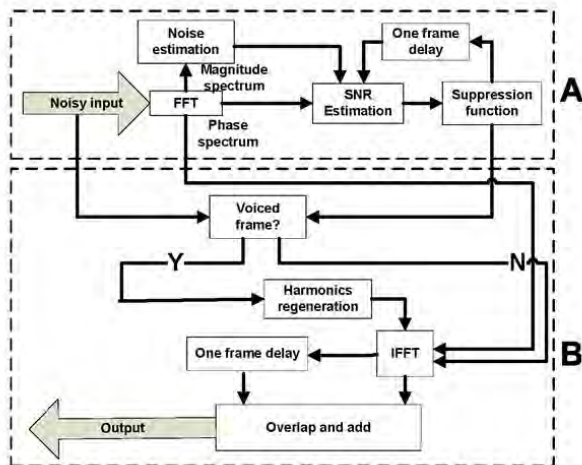
Results

Test results for speech recognition showed significant improvements compared to those obtained with unprocessed noisy speech and speech processed by the LogMMSE algorithm alone. Results showed a 15% improvement in intelligibility when compared to those obtained with noise suppression alone.

Conclusion

The present study examined the effect of applying Harmonic regeneration techniques to noise suppressed speech on speech perception with electric and acoustic stimulation.

Further research in improving the estimation of harmonic frequencies and magnitudes could enhance the perception by cochlear implant patients.



PS - 666

The Virtual Tripole: A New Stimulation Mode for Cochlear Implants

Monica Padilla¹; Justin Aronoff²; David Landsberger¹

¹House Research Institute; ²University of Illinois

Background

Spectral resolution is a limiting factor in performance with cochlear implants. Monopolar virtual channel (MPVC) stimulation (current steering) can be used to increase the number of channels beyond the number of electrodes but is limited by the broad spread of excitation. Tripolar (TP) stimulation (current focusing) reduces the spread of excitation improving performance (e.g. Srinivasan et al. 2013), but the number of possible channels is limited by the number of electrodes.

We propose a new stimulation mode called a virtual tripole (VTP). It is a modification of traditional TP stimulation to allow current steering. VTPs theoretically provide more channels and reduce spread of excitation relative to MP stimulation.

Methods

Six users of the Advanced Bionics CII or HiRes 90K cochlear implant participated in the study.

Spread of excitation for electrode 9 was measured using MP, TP, and VTP maskers and TP probes. Spread of excitation was also measured at location 8.5 using MPVC and VTP maskers and VTP probes. A 2AFC forward masking task was used.

MPVC and VTP speech processing strategies were implemented in sound processors using the same rate and phase duration for both maps, although parameters differed across subjects. Spectral resolution performance with the two strategies was tested using a modified spectral task, the SMRT (Spectro-temporal Modulated Ripple Test) task (Aronoff and Landsberger, 2013).

Results

VTP stimulation produces narrower spread of excitation for most subjects tested. Preliminary results suggest that VTP maps provide better spectral resolution than MPVC maps.

Conclusion

These preliminary results suggest that a VTP strategy may provide performance benefits relative to an MPVC strategy similarly to the benefit observed between TP and MP strategies (e.g. Srinivasan et al., 2013).

PS - 667

Spectral and Temporal Resolution of Information-Bearing Acoustic Changes in Vcoded Sentences

Christian Stilp¹; Matthew Goupell²

¹University of Louisville; ²University of Maryland

Background

Information-bearing acoustic changes in the speech signal are highly important for speech perception, demonstrated when acoustic changes were measured in full-spectrum sentences using cochlea-scaled entropy (CSE; Stilp & Kluender, 2010 *Proc Natl Acad Sci USA*) and later extended to vocoded sentences using an adapted metric (CSE_{CI}; Stilp, Goupell, & Kluender, 2013 *J Acoust Soc Am*). While information-bearing acoustic changes appear to underlie speech perception in acoustic and simulated electrical hearing, Stilp *et al.* simulated CI processing using a single set of vocoder parameters, obscuring the breadth and depth of perceptual reliance upon these acoustic changes to understand vocoded speech. Here, spectral and temporal resolutions of noise-vocoded sentences were manipulated to reveal the importance of information-bearing acoustic changes for understanding speech across wide ranges of signal quality.

Methods

TIMIT sentences were noise-vocoded with variable spectral resolution (4-24 spectral channels spanning 300-5000 Hz) or variable temporal resolution (4-64 Hz cutoff frequency for extraction of amplitude envelopes). Four 80-ms sentence intervals were replaced with speech-shaped noise on the basis of having high- or low-CSE_{CI}. Sentences with no noise replace-

ments were included as controls. The importance of information-bearing acoustic changes was gauged by the decrease in performance when high-CSE_{CI} intervals were replaced relative to other conditions.

Results

Preliminary results are consistent with previous literature: performance declined more when high-CSE_{CI} intervals were replaced with noise compared to when low-CSE_{CI} intervals were replaced. Information-bearing acoustic changes were more important for sentence understanding as spectral resolution decreased, producing the largest decrement at 6 spectral channels. At high spectral resolutions, performance nearly overcame replacement of low-CSE_{CI} intervals but not high-CSE_{CI} intervals. Conversely, these acoustic changes became more important as temporal resolution increased, with performance in all conditions plateauing between 16-32 Hz.

Conclusion

Information-bearing acoustic changes prove important for understanding vocoded speech across wide ranges of signal quality. Spectral and temporal resolutions are revealed to play complementary roles in information-bearing acoustic changes: replacing these changes with noise impaired performance most at lower spectral resolutions and higher temporal resolutions. Results inform speech perception by CI users: removing information-bearing acoustic changes impaired performance most when spectral resolution approximated the number of effective channels transmitted by CIs (typically 6-8 channels). Current CI processing strategies encode channel amplitudes, but results suggest potential for additional perceptual benefit by also incorporating changes in amplitude.

PS - 668

Responses of Midbrain Neurons to Cochlear-Implant Simulations in the Awake Rabbit

Tianhao Li; Laurel Carney

University of Rochester

Background

Improving cochlear implant (CI) users' performance within the current configuration of CI devices is challenging because of our limited knowledge of the mechanisms underlying neural coding of speech. Ranasinghe et al. (2012, JARO, 13:527) suggested that average rate across the midbrain population supported CI-like speech discrimination. However, the diversity of temporal modulation processing of midbrain neurons was not considered, nor was temporal response patterns analyzed. The present project investigated effects of spectral and temporal CI-like processing on neural coding in the midbrain across neurons with different spectral and temporal response characteristics.

Methods

Auditory midbrain responses were recorded from two awake Dutch-belted rabbits. Response maps and modulation transfer functions (MTFs) were measured to characterize neurons. The stimuli were acoustic CI simulations of four vowels (in "had," "heed," "whod" and "heard") produced by two talkers (1 male, 1 female), presented contra-laterally. Sine-wave and

noise-band vocoders were used to process natural vowels to simulate CI-like speech signals. To investigate the effect of spectral resolution and temporal modulation information, two numbers of spectral channels (4 and 16) and two temporal envelope cutoff frequencies (50 and 200 Hz) were used. The average response rate and shuffled auto-correlation were used to quantify neural responses.

Results

The responses of midbrain neurons to these stimuli were diverse. In particular, the type of MTF (i.e. band-pass, band-reject, or all pass) and the sensitivity of cells to changes in modulation frequency (i.e. the change in rate vs. modulation frequency) influenced the responses to CI-like speech sounds. For neurons with large changes in rate as a function of modulation frequency, the effects of the MTF dominated, and thus the averaged rates were strongly influenced by the temporal envelope cutoff frequencies. For neurons with relatively flat MTFs, spectral effects dominated, and response rates were strongly affected by the number of spectral channels. For intermediate neurons, combinations of spectral and temporal effects were observed. In addition, the temporal regularity of neurons that phase-locked to the envelope was more degraded for acoustic CI simulations than for natural vowels.

Conclusion

Given that some neurons were more affected by spectral profile, it is significant to improve functional spectral resolution for CI users, consistent with previous psychoacoustic studies. The degradation of temporal regularity in response patterns suggests that it is also critical to optimize temporal stimulation patterns for the recovery of temporal envelope information at higher levels of the auditory system.

PS - 669

The Effect of Spectral Manipulations on Spatial Release from Masking in Simulations of Cochlear Implants for Single-Sided Deafness

Jessica Wess¹; Douglas Brungart²; Joshua Bernstein²

¹University of Maryland; ²Walter Reed National Military Medical Center

Background

Communication in complex environments requires the listener to attend to the target speech of interest while ignoring background maskers. Normal-hearing (NH) individuals are able to capitalize on spatial separation to aid in target-masker stream segregation (i.e., "spatial release from masking," SRM). Although CI users are generally thought to benefit little from the binaural-difference cues that enhance stream segregation for NH listeners, our recent results suggest that CIs can facilitate SRM for single-sided-deaf (SSD) individuals in competing-talker situations where monaural cues fail to promote stream segregation. Preliminary results suggest that this SRM is robust to relatively large interaural delays, and that it does not depend on contextual cues provided by the content of the competing speech messages. However, little is known about the sensitivity of this SRM to interaural spectral

mismatches, which might occur accidentally due to incorrect placement of the CI on the basilar membrane or intentionally as a result of nonlinear spectral mapping in the CI processor. This study aimed to identify the portions of the spectrum responsible for the SRM and to determine the effects of spectral mismatch between the CI and NH ears on SRM.

Methods

Vocoder simulations with NH listeners provided an initial assessment of the spectral dependence of SRM in SSD patients with CIs. These listeners participated in a task based on the Coordinate Response Measure that required them to segregate a target talker from two same-gender maskers in the first (normal) ear while listening either to silence or a noise-vocoded mixture containing only the maskers in the second (CI) ear. Experiment 1 introduced spectral mismatch by frequency-shifting the synthesis filters in a six-channel vocoder upwards or downwards by 1, 2, 4 or 7 auditory-filter equivalent rectangular bandwidths (ERBs). Experiment 2 evaluated the frequency dependence of SRM, presenting the maskers to subsets of eight vocoder channels, while presenting the remaining channels with just noise.

Results

Preliminary results from Experiment 1 indicate that SRM was only somewhat affected by spectral mismatches, diminishing little for mismatches as large as 4 ERBs. Performance was impacted more by downward than by upward spectral shifts. Data collection for Experiment 2 is underway.

Conclusion

Although mild spectral dependence of SRM suggests some opportunity to optimize frequency allocation to improve binaural hearing capabilities for SSD CI users, the robustness of the SRM effect to spectral mismatches suggests that even with a basally-shifted frequency allocation, a CI should still facilitate substantial SRM.

PS - 670

Word Position Influences Recognition in Speech Intelligibility Tasks

Stefanie Keller

Technische Universität München

Background

Common tests for determining the speech reception threshold in noise of hearing impaired patients consist of grammatically correct but semantically empty sentences. It is already known, that in these tests memory effects speech recognition of the first and last words of the sentences; errors at these positions are minimal and in the middle they increase. But not only the position but also the grammatical class of a word causes different cognitive effort. This should be seen by the recall of sentences in a speech intelligibility test.

Methods

This study analyses the effect of different conditions on the comprehended words belonging to different grammatical classes and their position. So far, normal hearing subjects and subjects with cochlear implants were measured via headphones / audio cable with a German speech intelligibility

test (OLSA) with different binaural conditions. The measurement took place in an auditory booth (IAC 350). One list was presented for training and the different binaural conditions were randomized.

Results

The results do not only show the expected memory effects for the noun at the first and last position of the sentences. Errors for the comprehension of centered numerals were reduced. This is important because in the middle of a sentence, normally the attention of a listener is minimal, therefore one would expect larger error rates. But being a really closed set of words, it can explain the reduced errors. In contrast, the verbs, cognitive more complex, show neither significant in- nor decreasing error rates.

Conclusion

We conclude that careful analysis of speech reception tests can provide not only information of speech intelligibility but also of more cognitive aspects involved in speech intelligibility like memory effects.

PS - 671

Mandarin Tone Recognition in English-Speaking Normal Hearing Listeners and Cochlear Implant Subjects

Kaibao Nie¹; Sophia Hannaford²; Ward Drennan¹; Jay Rubinstein¹

¹University of Washington-Seattle; ²Whitman College

Background

In tonal languages such as Mandarin, tone pattern is highly associated with the lexical meaning of a spoken word. Most studies have focused on studying tone recognition performance in native speakers. The purpose of this study is to investigate whether non-native Mandarin speakers have the capability of recognizing tone patterns in tonal languages. The results will also demonstrate if they can potentially serve as a replacement subject pool when evaluating novel pitch coding strategies in cochlear implants.

Methods

Ten normal-hearing (NH) adult subjects who are native English speakers were recruited. Three cochlear implant (CI) subjects who are also native English speakers were pilot tested. None of the subjects had any language background in Mandarin Chinese or other tonal language. The tone stimuli used were adapted from a previous study (Wang, Zhou, & Xu, JASA, 2011). NH speakers were presented with unprocessed tone stimuli, simulated sounds of an 8-channel CIS (continuous interleaved sampling) coding strategy, and simulated sounds of the HSSE (harmonic single side-band encoding) coding strategy designed to improve pitch coding in cochlear implants. CI subjects were tested with their clinical speech processor, listening to unprocessed tone stimuli. Each subject was given 4 trial blocks in a training session, each containing 160 tone discriminations. The training was repeated on a second day.

Results

NH English speakers were able to achieve on average 87.7% of Mandarin tone recognition after training. The average performance was significantly better with HSSE than with CIS simulations (85.9% vs. 61.9%, $p < 0.001$) For the CI group, they were able to recognize 59.5% of the tonal patterns, which is comparable to the finding from Mandarin-speaking CI subjects (a mean of 58.3% in 19 CI subjects, Wang, Zhou, & Xu, JASA, 2011).

Conclusion

The present study demonstrates the remarkable ability of English-speaking subjects to recognize tonal patterns. Novel pitch coding strategies are currently being evaluated with these cochlear implant subjects.

PS - 672

Perception of Prosodic Boundaries in Cochlear Implants – an Eye-Tracking Study

Anita Wagner; Deniz Baskent
UMCG

Background

Lexical segmentation is essential for speech comprehension. Recognising word boundaries limits the simultaneous activation of words with similar acoustics: It resolves lexical embedding (e.g., 'pain' in 'champagne', or 'ham' in 'hamster'), and hinders activation of words that can be spuriously perceived across word boundaries (e.g., "cheese" in "much easier").

Cochlear-implant (CI) users have to make most of the linguistic cues embedded in the inherently degraded speech signal due to electric stimulation, and therefore it is especially important for them to be able to reliably use such mechanisms. This paper investigates speech segmentation in listeners with cochlear implants.

The speech signal contains various cues to word boundaries, e.g., F0 movement or lengthening of speech segments adjacent to word boundaries. The differences in duration between a syllable at a word boundary versus within a word can be as large as 20-40 ms. Dutch listeners have been shown to rely on such durational cues (e.g., Salverda, Dahan and McQueen, 2003). The signal transmitted via CI is limited in spectral resolution but the temporal structure of speech is well preserved. In an eye-tracking study we examine whether the temporal structure is enough to efficiently recognize word boundaries. Listeners' eye-movements reflect the time-course of speech processing and they capture how acoustic details affect listeners perception before the heard word was consciously recognised.

Methods

We adapted a design similar to Salverda, et al. (2003). Participants' eye movements to pictures on the screen are measured while they listen to auditory stimuli. The stimuli are recordings of sentences that contain a target word (e.g. zebra) recorded either as a (1) bisyllabic word (e.g. ... de zebra ontsnapt was), or (2) as a word crossing a word boundary accompanied by stress (e.g. ... de zee Brazilië omringt), or as word crossing a word boundary without lexical stress (e.g. ...

de zee brasems bevat). These sentences were cross-spliced leading to three versions, that are lexically identical but differ in phonetic details. On the display participants see pictures of the target (e.g. zebra), the competitor (e.g. zee), and two distractor pictures.

Results

Proportions of eye fixations to the competitor versus the target for CI listeners will be compared to normal hearing listeners in normal and CI-simulating conditions.

Conclusion

These results give insight into speech processing by CI users, and show how and if linguistic mechanisms of speech perception can compensate for the impoverished speech signal.

PS - 673

The Extracellular Matrix Component Brevican Affects High-Speed Synaptic Transmission at the Calyx of Held

Mandy Sonntag¹; Maren Blosa¹; Solveig Weigel¹; Rudolf Rübsamen²; Markus Morawski¹

¹University of Leipzig, Paul-Flechsig-Institute for Brain Research; ¹University of Leipzig, Paul-Flechsig-Institute for Brain Research; ²University of Leipzig, Institute of Biology

Background

Specific neuron types in the central nervous system are surrounded by specialized extracellular matrix (ECM) components classified as perineuronal nets (PN) or perisynaptic matrix of axonal coats (AC). PNs and ACs are discussed to be involved in the modulation of synaptic activity, but to date their specific function remains elusive. For three reasons the medial nucleus of the trapezoid body (MNTB) is a suitable model to investigate the respective functionality: (i) Virtually all neurons in the MNTB are associated with perineuronal and perisynaptic ECM. All principal neurons are targeted by huge axosomatic terminals, the calyces of Held, enabling (ii) experimental access to both the pre- and postsynaptic membrane and (iii) acquisition of both the presynaptic and the postsynaptic discharge activity. The ECM in the MNTB is characterized by a unique organization of the matrix component brevican, which forms a ring-like structure around presynaptic terminals potentially sealing the synaptic cleft, while other ECM components (like aggrecan) surround the entire cell body. Because of this close association with synaptic terminals, we hypothesize that brevican is essential for the fast and reliable synaptic transmission at the calyx of Held.

Methods

We performed extracellular single-unit recordings at the calyx of Held in the MNTB *in vivo* in subadult wildtype mice and transgenic mice lacking the ECM component brevican. Pre- and postsynaptic activity was acquired simultaneously which allowed for quantification of dynamics and reliability of synaptic transmission.

Results

We found a significant change in the dynamics of synaptic transmission at the calyx of Held in brevican-deficient mice

compared to wildtype animals. Specifically, the pre- to post-synaptic AP transmission delay was prolonged and the post-synaptic AP was broader in the knock-outs, but the reliability of synaptic transmission was not affected.

Conclusion

Our results indicate that the ECM component brevicin promotes fast synaptic transmission at the calyx of Held, which is essential for the function of the MNTB within the brainstem sound localization circuit. These findings are in agreement with our hypothesis that perineuronal and perisynaptic matrix vitally modulates synaptic activity.

PS - 674

Loss of Kv1.3 Potassium Channels Impairs Auditory Function

Lynda EL-HASSAR¹; **Lei Song**²; Vali Gazula³; Dhasakumar Navaratnam⁴; Joseph Santos-Sacchi²; Leonard Kaczmarek³
¹Neurobiology and Pharmacology, Yale University School of Medicine; ²Surgery, Yale University School of Medicine; ³Pharmacology, Yale University School of Medicine; ⁴Neurology, Yale University School of Medicine

Background

Kv1.3 is a low threshold voltage-dependent potassium channel involved in various physiological functions including cell volume regulation, proliferation, and insulin signaling. Within the central nervous system, deletion of Kv1.3 gene from mitral cells of the olfactory bulb dramatically increased the sensitivity of the olfactory system. Kv1.3 channels are also present in presynaptic terminals of the medial nucleus trapezoid body (MNTB) within the auditory brainstem and in the bouton-like structures on inner and outer hair cells within the cochlea. In this study, we have tested whether Kv1.3 channels contribute to auditory function.

Methods

We used both *in vivo* Auditory Brainstem Responses (ABR) and *in vitro* whole cell patch-clamp recordings of MNTB slices from Kv1.3 *-/-* knockout (KO) mice to investigate the role of KV1.3 channels in auditory function.

Results

We found that ABR thresholds are elevated in 2-4 months old Kv1.3^{-/-} KO mice over those in wild type (WT) mice. Latencies of peaks I, II and IV are prolonged in 4 month old Kv1.3^{-/-} KO mice. In addition, we have found a desynchronization of ABR waves in Kv1.3^{-/-} KO mice suggesting an alteration of synaptic transmission and changes in spike fidelity within auditory pathways. Our preliminary results from the high fidelity calyx of Held/MNTB synapse in young mice (P13-17) show that lack of Kv1.3 channels increases the spike frequency and the spike threshold at presynaptic terminals (Calyx of Held) in response to square pulses of injected currents.

Conclusion

Our preliminary data showing that loss of Kv1.3 channels primarily influences the properties of the presynaptic terminals and of the ABR waves strongly suggest that Kv1.3 channels are required for normal auditory function.

PS - 675

Activity-Dependent Regulation of the Probability of Neurotransmitter Release at the Endbulb of Held

Tenzin Ngodup¹; Jack Goetz²; Brian McGuire³; Wei Sun⁴; Amanda Lauer³; Matthew Xu-Friedman²

¹University at Buffalo, State University of New York; ²Dept. Biological Sciences, University at Buffalo, State University of New York; ³Department of Otolaryngology-HNS, Johns Hopkins University, Baltimore, MD; ⁴Center for Hearing and Deafness, Dept of Communicative Disorders and Sciences, University at Buffalo, State University of New York

Background

Synaptic transmission depends on the probability of neurotransmitter release (P_r), but it is unknown how the particular level of P_r is regulated. Synapses with high P_r depress during high levels of activity, which could reduce the faithful transfer of information between neurons. This is a major issue for auditory nerve synapses onto bushy cells (BC) in the antero-ventral cochlear nucleus. These synapses, called endbulbs of Held, normally show strong depression at physiologically-relevant rates of activity. This raises the question how BCs transmit information when activity levels are high.

Methods

Experiments were done using P15-50 CBA/CaJ mice, using voltage- and current-clamp recordings in brain slices. Synaptic activity was elicited by stimulating single auditory nerve fibers using pairs of pulses, or trains of activity.

Results

We hypothesized that neural activity could be an important factor in regulating P_r . To test this, we reared mice in constant, non-damaging noise for a week, and found that endbulbs change from depressing (high P_r) to facilitating (low P_r). After returning to control conditions, P_r recovered to high, suggesting these changes are a homeostatic response to activity. By contrast, there were no changes in the amplitude of the first EPSC or quantal size (Q), suggesting the number of release sites (N) must increase. To test this, we examined BC structure, and found noise-reared BCs had somewhat larger dendritic arborization, as well as increases in VGlut1-positive puncta around BC somata. In electron micrographs, endbulbs from noise-reared animals had larger profiles, more release sites per profile, and larger mitochondria than endbulbs from control animals. There was no evidence of degenerating nerve terminals. Functionally, these changes had the effect that noise-reared BCs showed higher spiking probability even during high rates of activity.

Conclusion

Our results suggest that experience-dependent activity is a crucial factor in regulating P_r at the endbulb of Held, and could have major effects on all downstream processing.

The Role of the Medial Olivocochlear Efferent Pathway in Noise Induced Hearing Loss in the VGLUT3 Knockout Mouse

Chi-Kyou Lee¹; Omar Akil²; Rebecca Seal³; Lawrence Lustig²

¹Cheonan Hospital, Soonchunhyang University School of Medicine, Cheonan, Korea; ²University of California San Francisco, San Francisco; ³University of Pittsburgh, Pittsburgh

Background

The efferent olivocochlear neuronal pathway from the brainstem has been hypothesized to improve signal detection in the presence of noise and contribute to protection from acoustic overexposure that would result in both temporary and permanent hearing loss. An interesting model in which to study this hypothesis is the mouse lacking vestibular glutamate transporter 3 (VGLUT3). This mouse has a normal afferent and efferent neuronal pathway but lacks an afferent signal due to loss of glutamate release at inner hair cell afferent synapse. In such a model, the relative contributions of afferent and efferent input to noise-induced hearing loss can be partially deduced, due to the efferent reflex in the absence of any afferent stimulation.

Methods

Ten 8-week old FVB wild type (WT) and 9 VGLUT3 knockout (KO) mice were tested. Pre-exposure auditory brainstem response (ABR) thresholds in a free field and DPOAE were determined. Mice were then exposed to a 105 dB SPL broad band of noise (4 to 20 kHz) for 32 minutes to create a temporary threshold shift (TTS). Auditory measures (click, 8k, 16k, 32k tone ABR and DPOAE) were performed at 1, 3, 7 and 14 days post-exposure. Histologic analysis was performed at each time point along with immunohistochemical staining of 8-isoprostane to evaluate the degree of damage from reactive oxygen species (ROS).

Results

As expected, VGLUT-3 KO mice had no measureable ABR responses. After noise exposure, WT mice showed elevated thresholds at day 1 and then slowly recovered to normal responses for both click and frequency specific ABR by 2 weeks.

Both groups had normal DPOAE responses before noise exposure. Following noise exposure, both groups had reductions in DPOAE levels, however the VGLUT-3 KO mice had a significantly smaller shift in DPOAEs than wild type. Further, while both groups demonstrated recovery of DPOAEs to normal levels, the recovery in the KO mice was significantly slower as compared to wild type {threshold shift; day 1(wild; 16.3 dB, KO; 6.4 dB), day 3(wild; 8.5 dB, KO; 6.1 dB), day 7(wild; 11.0 dB, KO; 4.3 dB)}.

Histologically, there was no differences noted in morphology, inner and outer hair cell numbers or 8-isoprostane staining levels.

Conclusion

Following noise exposure leading to a TTS, both WT and KO mice had reductions in DPOAE levels, though KO mice had a lower DPOAE shift and slower recovery as compared to WT mice. This data supports a role of the efferent auditory pathway in noise protection. In this model, loss of the afferent input leads to decreased OHC damage (DPOAEs) following noise exposure, and suggests that noise protection afforded by the afferent-efferent reflex arc is mostly mediated by the efferent system.

Staggered Development of SPON Neurons in Mice Lacking L-Type Ca²⁺-Channels

Sara Leijon; Neil Portwood; Anna K Magnusson
Karolinska Institutet

Background

Congenital hearing loss affects 2-3/1000 living newborns, making it a common hereditary disease. Although the underlying etiology is largely unknown, recent studies suggest that the gene regulation of the inner and outer hair cells in the hearing organ may be the cause. Detailed knowledge of how sensorineural hearing loss specifically affects the central auditory pathways involved in the processing of vocal communication, such as human speech or animal vocalizations, is scarce. Herein, we investigate the superior paraolivary nucleus (SPON) – an auditory brainstem nucleus recently implicated in conveying the coarse temporal sound structure, which is key for perceiving verbal communication to higher order auditory brain areas. To better understand how the biophysical properties of SPON neurons are shaped during postnatal development, we studied the SPON in a congenitally deaf mouse lacking cochlear-driven activity in the auditory nerve (Platzer et al. (2000) Cell:102:89-97).

Methods

Whole-cell patch-clamp recordings were performed on postnatal (P) mice lacking the alpha-1D subunit of the Cav1.3 ion channel. This calcium channel is essential for release of neurotransmitter onto auditory afferents of the inner hair cell (IHC), and the mice are consequently born deaf (Platzer et al. (2000) Cell: 102:89-97). For comparison, age-matched (P5-P12) wild type mice were used as controls in the electrophysiological characterization of the respective SPON neurons. We used immunocytochemistry to investigate the expression of membrane proteins, such as ion channel subunits, in the alpha-1D and WT mice.

Results

The results demonstrate that the intrinsic membrane properties of SPON neurons are significantly different in the alpha-1D mutant mice aged P5-P10 (pre-hearing) compared to age-matched controls. Specifically, the resting membrane potential (RMP) is more depolarized and the input resistance and membrane time constant are significantly higher than in WT animals. When measuring the voltage sag induced upon hyperpolarization, indicative of the h-current, this property was greatly reduced, or sometimes absent in SPON neurons compared to pre-hearing control animals. This was confirmed

by isolating inwardly rectifying currents, which were smaller and displayed slower kinetics in the mutant's SPON neurons. Surprisingly, this electrophysiological profile changed dramatically within one week in the mutant mice. In P10-P14 (post-hearing) animals the intrinsic membrane properties were indistinguishable, except that the RMP remained depolarized in SPON neurons from the alpha-1D mutant and WT mice. This was matched by an up-regulation of the h-current, which displayed significantly faster time constants, equally fast to the WT mice.

Conclusion

The results from this congenitally deaf mouse model show that SPON neurons develop differential intrinsic membrane properties, compared to pre-hearing WT mice. Surprisingly, the SPON neurons lacking cochlear-driven activity undergo a staggered development and when compared to post-hearing WT animals, the intrinsic properties are indistinguishable, presumably related to plasticity mechanisms compensating the de-afferented condition. This indicates that some of the unique electrical properties of brainstem neurons may be rescued in a congenitally deaf condition but it also highlights the importance of interpreting developmental data obtained in transgenic mouse models with caution.

PS - 680

GABAergic Inhibition and its Modulation by GABA Transporters in the Murine Lateral Superior Olive

Alexander Fischer¹; Jonathan Stephan¹; Matthew A. Xu-Friedman²; Désirée Griesemer¹; Eckhard Friauf¹

¹Animal Physiology Group, Department of Biology, University of Kaiserslautern, D-67653 Kaiserslautern, Germany; ²Department of Biological Sciences, University at Buffalo, NY, USA

Background

The glycinergic projection from the medial nucleus of the trapezoid body (MNTB) to the lateral superior olive (LSO) is an amenable inhibitory model system that can be driven very specifically, in contrast to diffuse inhibitory interneuronal connectivity in most other brain regions. In gerbils and rats, this projection shifts within the first two postnatal weeks from predominantly GABAergic to predominantly glycinergic (Kotak et al., 1998; Nabekura et al., 2004). However, in adult gerbils, LSO neurons still exhibit a decrease or increase in sound-evoked discharge rate due to presynaptic GABA_B receptor activation or inactivation, respectively (Magnusson et al., 2008). Hence, GABA still controls excitability in the mature LSO. We here investigated GABAergic signaling in the mouse LSO, including the role of GABA transporters 1 and 3 (GAT-1, GAT-3).

Methods

To assess the GABAergic contribution at MNTB-LSO synapses, patch-clamp recordings of primary LSO neurons were performed during electrical stimulation of MNTB fibers at postnatal day (P)4 and P11.

Results

In contrast to gerbils and rats, we found that the GABA-to-glycine shift is already complete by P4 in the mouse LSO, indicating interspecies differences. However, focal puffs of GABA at P11 still induced robust GABA_AR- and GABA_BR-mediated inhibitory currents in LSO neurons, pointing to an extrasynaptic location of these receptors. Further, the presence of presynaptic GABA_BRs at MNTB-LSO synapses was tested by presynaptic calcium imaging. Bath application of baclofen (100 µM) during electrical stimulation of MNTB fibers resulted in a 20% decrease of presynaptic calcium influx. Amplitude and kinetics of GABA-induced postsynaptic currents were markedly altered during pharmacological inhibition of the GABA reuptake transporters GAT-1 (NO711, 10 µM) and GAT-3 (SNAP5114, 40 µM), indicating a strict control of local GABA concentrations at the somata of LSO neurons beyond the GABA-to-glycine shift at the MNTB-LSO synapses. Recordings from LSO astrocytes revealed functional GAT-1 and GAT-3 in these cells. Upon focal GABA application (1 mM), LSO astrocytes displayed transporter currents of around 130 pA that could be partially inhibited by NO711 (36%) or SNAP5114 (34%).

Conclusion

Regarding the role of tonic inhibition by ambient transmitters (Farrant & Nusser, 2005), we propose a versatile function of GABA in the mouse LSO, which is not restricted to synapses, but also includes extrasynaptic sites. GATs appear to be good candidates to control such extrasynaptic GABA concentrations and thus modulate tonic inhibition.

PS - 681

Different Populations of Neurons With Distinct Membrane and Synaptic Properties in the Dorsal and Ventral Part of the Ventral Nucleus of the Lateral Lemniscus (VNLL) of Mice

Ursula Koch; Veronika Baumann; Franziska Caspari; Elisabet Garcia-Pino

FU Berlin

Background

Neurons in the ventral nucleus of the lateral lemniscus (VNLL) show mixed responses to sounds in terms of temporal response pattern and binaurality. Also, distinct biophysical neuron types have been found in the VNLL. Anatomical studies suggest that at least a subset of ventrally located VNLL neurons receives a major excitatory input that arises from the contralateral ventral cochlear nucleus and inhibitory inputs coming from the ipsilateral trapezoid body. To identify whether different neuron types and inputs are systematically distributed within the VNLL, we characterized the membrane and synaptic properties of VNLL neurons relative to their location within the VNLL.

Methods

Membrane and synaptic properties of VNLL neurons were characterized by patch-clamp recordings in acute brain slices from P22/23 C57Bl6J mice. Excitatory and inhibitory synaptic currents were evoked by stimulating the incoming fibers of the lateral lemniscus with a glass electrode placed ~50 µm

ventral to the recorded neuron. Differences of synaptic and membrane properties of VNLL neurons along the dorsal/ventral axis were compared. Additionally, standard immunohistochemistry of perfusion fixed brain sections including the VNLL was performed using antibodies against HCN1, VGluT1 and GlyT2.

Results

Based on the immunolabelling pattern against HCN1 and VGluT1, the VNLL could be divided into a ventral (vVNLL) and dorsal part (dVNLL). Neurons in these two parts of the VNLL also showed significant differences in membrane and synaptic properties. Neurons in the vVNLL predominantly displayed an onset-type firing pattern during depolarizing current injections and a small voltage sag during hyperpolarizing current injections. Moreover, these neurons had small Ih amplitudes and HCN1 immunostaining was much weaker compared to the dVNLL region. Fiber stimulation evoked extremely large excitatory synaptic currents that were all-or-none, resembling a single calyx-like synaptic input. In contrast, neurons in the dVNLL exhibited two types of firing patterns: onset-type and sustained firing pattern. Both neuron types had low input resistance, prominent voltage sag and significantly larger isolated Ih compared to vVNLL neurons. Moreover, dVNLL neurons received 2-7 relatively small excitatory inputs. Both, inhibitory and excitatory inputs to vVNLL neurons had much faster rise and decay times compared to dVNLL neurons.

Conclusion

Our results show two distinct areas in the VNLL based on membrane and synaptic properties. This suggests that vVNLL and dVNLL might play different roles in respect to auditory information processing.

PS - 682

The Naked Mole Rat Auditory Brainstem: An Anatomical and Neurochemical Description

Elisabet Garcia-Pino¹; Nikodemus Gessele¹; Thomas J Park²; Ursula Koch¹

¹Institute of Biology, Freie Universität Berlin; ²Department of Biological Sciences, University of Illinois at Chicago

Background

Although the African naked mole rat (*Heterocephalus glaber*) uses a fairly large vocal repertoire for communication, these subterranean animals display surprisingly high auditory thresholds (~40-50 dB) and poor performance in sound localization. Their hearing is also predominantly sensitive to low frequency sounds. We were interested whether these poor hearing abilities are correlated with a rudimentary auditory anatomy. To address this question we used immunohistochemical procedures to study the morphology of auditory structures and the neurochemical phenotypes of synaptic inputs in the adult naked mole rat.

Methods

We performed standard immunohistochemistry on fixed brain sections of the auditory brainstem and midbrain. We used antibodies raised against vesicular glutamate transporter 1 (VGluT1) and glycine transporter 2 (GlyT2) to label both excitatory and inhibitory boutons. We also immunostained the

hyperpolarization-activated cyclic nucleotide-gated channel HCN1 and the microtubule associated protein 2 (MAP2) to further characterize the auditory structures.

Results

All the prominent nuclei of the auditory brainstem are present. The major subdivisions of the cochlear nucleus (CN) can be clearly identified. In the superior olivary complex (SOC) the lateral superior olive (LSO) is large and elongated, in contrast to a small medial superior olive (MSO). The medial nucleus of the trapezoid body (MNTB) consists of only a low number of neurons scattered within the trapezoid body. Still, both LSO and MSO neurons receive prominent glycinergic inputs. In contrast, the ventral and dorsal nucleus of the lateral lemniscus (VNLL; DNLL) and the inferior colliculus are of comparable size to other rodents. Interestingly, only VNLL but not LSO and MSO neurons display strong HCN1 immunolabelling.

Conclusion

Despite their poor hearing abilities, all structures of the auditory brainstem are well preserved. These animals have a large LSO and a small MSO, which was surprising considering their low frequency hearing range. Moreover, HCN1 labeling, which is an indicator of temporally precise integration of synaptic inputs, is, unlike in other rodents, almost completely missing in the LSO and MSO. We speculate that this missing HCN1 labeling contributes to the sluggish sound localization abilities of these animals.

PS - 683

Airborne and Underwater Hearing in the Great Cormorant (*Phalacrocorax Carbo*) Studied With ABR and Laser Vibrometry

Ole Larsen; Tina Huulvej; Magnus Wahlberg; Jakob Christensen-Dalsgaard

University of Southern Denmark

Background

Numerous studies have mapped the hearing abilities of birds in air, but currently there is little or no data, physiological, psychophysical or behavioral, on how diving birds hear or react to sound under water. Therefore, it is unknown whether the ears of diving birds are adapted to hearing under water and to what extent anthropogenic noise influences their hearing during a dive. In the present study, we measured the audiogram of cormorants in air and under water and compared the results to biophysical measurements of eardrum vibrations.

Methods

We obtained audiograms from wild-caught Great Cormorants (*Phalacrocorax carbo*) using auditory brainstem response (ABR) and measured eardrum vibrations using laser Doppler vibrometry (LDV). The ABR was measured first in a (150x100x80 cm) sound attenuated and anechoic box using three subdermal electrodes and, secondly, with its head and neck submerged approximately 10 cm under water in a (90x100x60 cm) water filled tank while being artificially ventilated. The ABR-response to calibrated tone bursts was measured at different intensities and frequencies (500, 1000, 2000, 4000, and 6000 Hz) to obtain hearing threshold values

in air and under water. The bird was overdosed immediately after the last ABR. LDV measurements were obtained from reflecting foil on the eardrum first in an anechoic room and finally in the tank with the laser beam focused on the tympanic membrane placed 25 cm under water, and we obtained transfer functions of tympanic membrane motion in the frequency range 200 Hz to 10 kHz.

Results

The shape of the ABR audiogram follows the eardrum vibration transfer function. Both methods showed a clear peak with highest sensitivity at 1-2 kHz in air, while the most sensitive response was displaced towards lower frequencies (about 1 kHz) under water. In addition, the bandwidth of the water audiogram was only about half of that of the air audiogram.

Conclusion

The results suggest that cormorants have less sensitive in-air audiograms compared to other similar-sized birds. The hearing abilities in water are better than what would have been expected for a purely in-air adapted ear.

PS - 684

Deafness Related to Hyperbilirubinaemia is Associated With Endoplasmic Reticulum Stress and Transmission Failure at Central Auditory Synapses

Ian Forsythe; **Emanuele Schaivon**; Joshua L. Smalley
University of Leicester

Background

Bilirubin encephalopathy and kernicterus are serious neurological conditions associated with Jaundice, which have specific effects on synaptic transmission in the auditory brainstem. When plasma bilirubin concentration is high, it crosses the blood-brain-barrier and causes neuronal damage in the CNS by unknown mechanisms. Previously we have shown that bilirubin causes destruction of the calyx of Held synapse in the medial nucleus of the trapezoid body (MNTB) Hausteijn M.D. et al, *J Physiol* 588:4683-93 (2010) 4693. Here we present data on a mouse model of hyperbilirubinaemia and on microarray analysis of the changes in gene expression following exposure to high bilirubin concentrations.

Methods

A single intraperitoneal injection of bilirubin (0.5 mg/g) and sulfadimethoxine (0.3mg/g) was administered to CBA/Ca mice (11-20 days old). Auditory brainstem responses (ABRs) were monitored *in vivo* using click stimulation under Hypnorm/Midazolam anesthesia. Electron microscopy (EM) and patch clamp recording were made from MNTB neurons. Under voltage clamp miniature excitatory postsynaptic currents (mEPSCs) were recorded at -80 mV. Additionally brainstem and cerebellum global gene expression were measured using Illumina mouseRef-8 BeadChips in control and bilirubin exposed mice and compared with gene expression in cell lines exposed to bilirubin.

Results

ABRs were largely abolished 4h after bilirubin injection, but they had recovered 24h and 5 days later. An EM study

showed two changes at the calyx of Held synapse: the presynaptic terminals were packed with vesicles, and were partially detached from the postsynaptic membrane. After 24h the presynaptic terminals partially recovered, but were still abnormally overfilled with vesicles. Whole cell experiments validated the damage to the Calyx of Held synapse, showing a significant decrease in the mEPSC amplitude (control 83.4 ± 7.3 pA, $n = 6$ vs bilirubin 2.3 ± 3.5 pA, $n = 7$) and in the frequency of spontaneous events, (control 7.2 ± 1.1 Hz, $n = 6$ vs bilirubin 2.5 ± 0.4 Hz, $n = 7$) that had recovered after 24h (amplitude in control 62.3 ± 3.5 pA vs bilirubin 84.4 ± 8.2 pA, frequency in control 7.2 ± 1.1 Hz vs bilirubin 5.4 ± 0.9 Hz, $n = 4$ and 6 , respectively). Bilirubin exposure in cell lines induced gene-expression changes consistent with endoplasmic reticulum (ER) stress. A similar gene expression pattern was observed in the brainstem and cerebellum of bilirubin-exposed mice.

Conclusion

We conclude that acute injection of bilirubin causes short-term, reversible damage to synapses in the auditory system and provides a good model for further study of the mechanisms of bilirubin toxicity in the auditory system which may be mediated in part by ER stress pathways.

PS - 685

Detecting the Early Effects of Noise Exposure

Daphne Barker; **Chris Plack**; Kathryn Hopkins; Richard Baker

The University of Manchester

Background

Previous research in rodents has found that noise exposure produces striking and permanent damage to low spontaneous rate fibers in the auditory nerve that is not accompanied by a decrease in sensitivity to low-level sounds. Previous research with humans has indicated that listeners exposed to occupational or recreational noise but with normal audiograms have deficits in some supra-threshold discrimination tasks, but the link to the animal results is unclear.

Methods

The experimental group contained volunteers exposed to high levels of recreational noise. The volunteers in the control group were matched as closely as possible in terms of age and educational background but were not exposed to high levels of recreational noise. Both groups had clinically normal hearing. Volunteers were tested in two separate strands: psychophysical and electrophysiological. The psychophysical strand included measurement of interaural phase difference (IPD) thresholds to test temporal processing and notched noise thresholds to test detection efficiency (which was expected to be related to the number of low spontaneous-rate fibres). In the electrophysiological strand, the auditory brainstem response (ABR) was measured as a function of level and neural phase locking was assessed using the frequency-following response (FFR) for pure and transposed tones.

Results

Analysis of the psychophysiological tests did not reveal any significant differences between noise-exposed and non-

noise-exposed volunteers in the IPD nor the notched-noise tests. For the electrophysiological strand, there was a statistically significant difference between the two groups for the FFR measure but no significant difference between groups for the ABRs.

Conclusion

Although there were no significant deficits on the psychophysical tests related to noise exposure, a significant difference in the FFR measure between groups suggests that exposure to high levels of recreational noise can result in a deficit in neural temporal coding without affecting the audiogram. This could result from a reduction in auditory nerve function similar to that observed in the animal models.

PS - 686

The Effect of Carboplatin Induced Ototoxic Hearing Loss on Evoked Potentials in Chinchillas

Taylor Remick; David R. Axe; Michael G. Heinz
Purdue University

Background

Sensorineural damage in the periphery can cause changes within the central auditory pathway. Noninvasive evoked potentials provide a system wide physiological response to stimuli across different levels of the auditory pathway. Using these measures, the effects of peripheral sensorineural damage on temporal coding is assessed in both the periphery and more central levels.

The effects of ototoxic hearing loss on peripheral and central auditory centers was measured non-invasively in anesthetized chinchillas. The chemotherapy drug carboplatin has been shown to induce IHC specific lesions causing a disruption of signal transduction in the periphery without altering the mechanical properties of the basilar membrane or the functional characteristics of the cochlear amplifier.

Methods

Non-invasive measures were recorded in chinchillas before carboplatin exposure and across a 4-week time course following exposure. DPOAEs were collected as a measure of OHC function, ensuring that observed changes were from damage to the IHCs. Auditory Brainstem Response (ABRs) from short pure-tone bursts were used to determine threshold and to monitor suprathreshold function at different stages of the auditory pathway. Frequency-Following Responses (FFRs) were recorded using amplitude modulated tones at varying modulation frequencies to assess changes in temporal coding following hearing loss.

Results

Preliminary findings following carboplatin exposure suggested no change in OHC function (no change in DPOAE amplitudes) and no significant change in ABR thresholds. In contrast, ABR wave-I showed reduced amplitudes and increased latencies following exposure. Later waves also showed decreased amplitudes and increased latencies, however the magnitude of these changes differed from the peripherally based wave-I showing less change in amplitude and more

change in latency. FFRs showed a reduction in envelope coding within a few days of injection, with preliminary data suggesting a partial recovery of envelope coding as the time course progresses.

Conclusion

Carboplatin induced changes in peripheral coding follow many of the same trends observed following exposure to moderate noise levels that produce synaptic degeneration without permanent threshold shift. Intuitively this makes sense as both exposures cause a decrease in the total auditory signal that is transmitted through the auditory nerve (through deafferentation following noise and through destruction of the IHCs following carboplatin). Both cases results in a loss of total AN fibers able to convey information to the CNS. Studying time course effects allows for the possibility of gaining insight into the potential mechanisms underlying changes in central responses following peripheral damage.

PS - 687

Measurements of Auditory Evoked Responses by Bone-Conducted Ultrasound in the Complete Hearing-Impaired

Seiji Nakagawa

National Institute of Advanced Industrial Science and Technology (AIST) / Kansai University

Background

Bone-conducted ultrasound (BCU) is perceived even by those who are profoundly sensorineural hearing-impaired, and a novel hearing-aid using BCU perception (BCU hearing-aid, BCUHA, Fig. 1), which transmits amplitude-modulated ultrasound by bone-conduction, has been developed for the profoundly hearing-impaired. To improve the BCUHA, the characteristics and mechanisms of BCU perception need to be better specified. We previously reported that BCU activates the auditory nerve, the brainstem pathway, and the auditory cortex in both normal-hearing and hearing-impaired subjects and hypothesized that the cochlea inner hair cells respond to ultrasound itself with a peculiar vibration mode of the basilar membrane. On the other hand, persistent refutation exists that BCU perception depends on generation of audible frequency components in the transmission path by non-linearity of biological tissue. Various unique characteristics of BCU perception and results of our previous physio-acoustical measurements on/around the living human head denied this idea, however, more straightforward neurophysiological evidence is needed. Auditory brainstem responses (ABRs) and auditory evoked brain magnetic fields (AEFs) were measured in the "complete" hearing-impaired subjects who show no measurable hearing sensitivity by the ordinary audiometry.

Methods

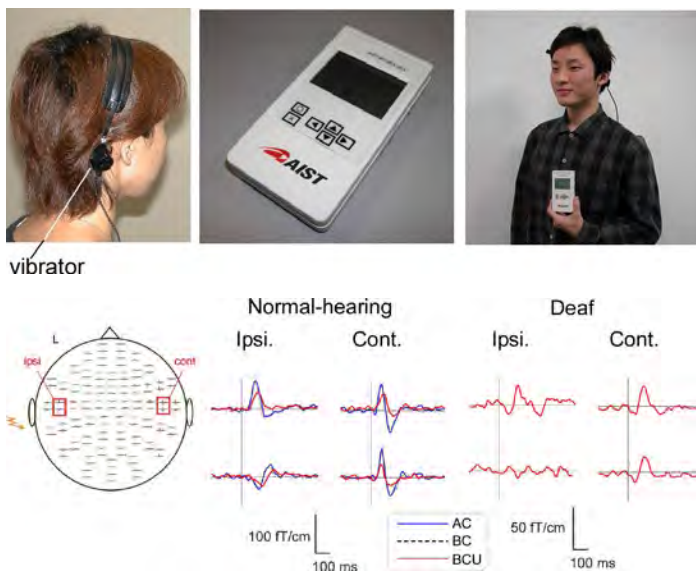
ABR and AEF were recorded in 6 complete hearing-impaired and 10 normal-hearing subjects. As BCU stimuli, a 30-kHz tone pip with duration of 1.0 ms and a 30-kHz tone burst with duration of 100 ms were used in ABR and AEF measurements, respectively.

Results

ABRs and AEFs were clearly elicited even in the hearing-impaired who had no measurable hearing sensitivity (Fig.2). In the ABR measurements, waves-I, which indicates compound action potential of the auditory nerve, were clearly elicited even in some complete hearing-impaired subjects. In the AEF measurements, in terms of the effects of stimulation side, same phenomena as air-conducted sounds were observed for BCU perception in both complete hearing-impaired and normal-hearing subjects.

Conclusion

The results obtained strongly indicate that BCU perception does not depend on the generation of audible frequency components by non-linearity of biological tissue. Also, the results push our hypothesis that BCU goes through the normal auditory pathway even though unique processes may exist in the cochlea. Additionally, same effects of stimulation side as air-conducted sound indicate that left and right BCU channels were separately localized, i.e, each BCU entered the ipsilateral auditory pathway before branching to the contralateral at the superior olivary nucleus.



PS - 688

GABAergic and Glycinergic Inhibitory Synaptic Transmission in the Cochlear Nucleus Studied in VGAT Channelrhodopsin-2 Mice

Ruili Xie; Paul Manis

University of North Carolina at Chapel Hill

Background

Both glycine and GABA mediate inhibitory synaptic transmission in the ventral cochlear nucleus (VCN). In mice, the time course of glycinergic inhibition is slow in bushy cells and fast in multipolar (stellate) cells, and is proposed to contribute to the processing of temporal cues in both cell types. Much less is known about GABAergic synaptic transmission, since electrical stimulation of the auditory nerve or the tuberculoventral pathway evokes little GABAergic synaptic current in brain slice preparations, and spontaneous GABAergic miniature

synaptic currents occur infrequently. On the other hand, direct application of GABA *in vitro*, and GABA and its antagonists *in vivo* demonstrated the existence of functional receptors. However, these studies provided little insight into the origin and time course of natural synaptic inputs.

Methods

We used transgenic mice in which channelrhodopsin-2 and EYFP is driven by the vesicular GABA transporter (VGAT-EYFP-ChR2) so that the light-activated ion channel channelrhodopsin-2 is expressed in VGAT positive neurons. In the cochlear nucleus, VGAT expression, detected by EYFP fluorescence, occurs in both GABAergic and glycinergic neurons in all divisions. We performed whole-cell patch clamp recording in both bushy and multipolar cells from parasagittal brain slices containing only cochlear nucleus. VGAT-expressing neurons were excited with brief flashes of light from a 473 nm LED using epifluorescent illumination in an upright microscope.

Results

Light stimulation evoked action potentials in presynaptic cells, which in turn generated inhibitory postsynaptic potentials (IPSPs) onto both bushy and planar multipolar cells. Two μM strychnine blocked only $\sim 40\%$ of the IPSP amplitude in planar multipolar cells, but blocked over 90% of the IPSPs in bushy cells. The remaining IPSPs in both cell types were completely blocked by the addition of 10 μM SR95531, a GABA(A) receptor antagonist. In multipolar cells, a substantial fraction of the evoked IPSP is GABAergic. In the absence of receptor blockers, repetitive light stimulation at 20 Hz evoked repeated IPSPs that depressed in multipolar cells, but which also summated to generate a sustained hyperpolarization and a similar response pattern is seen in the presence of strychnine. In bushy cells, the same stimulation pattern in the absence of strychnine evoked IPSPs that depressed rapidly after the onset of the train.

Conclusion

We conclude that local GABAergic release within the CN differentially influences bushy and multipolar cells, and that, like glycinergic inhibition, GABAergic inhibition may have cell-type specific functions in VCN principal neurons.

PS - 689

Glutamate Transporters Differentially Shape Synaptic Responses in the Developing Auditory Brainstem

Jason Sanchez; Seema Ghelani; Sedona Speedy; Sebastian Otto-Meyer

Northwestern University

Background

Glutamate transmission is tightly regulated at mature synapses throughout the brain. Features that regulate glutamate transmission include (1) transmitter release at presynaptic terminals, (2) transmitter action on postsynaptic receptors, and (3) transmitter clearance from the synaptic cleft by transporters. Neuronal and glial transporters clear glutamate from mature auditory synapses, which increases synaptic efficiency.

cy, the recycling of transmitter, and the prevention of excitotoxic damage. Less clear is the relationship between glutamate transporters and synaptic response properties in the developing auditory system.

Methods

The purpose of this study was to characterize the developmental profile of glutamate clearance from the synaptic cleft in the chicken cochlear nucleus magnocellularis (NM). Here, two to three synaptic contacts from the auditory nerve result in large and fast excitatory postsynaptic currents (EPSCs) mediated by AMPA-type glutamate receptors (AMPA-Rs). At different developmental time periods, we pharmacologically blocked neuronal and glial transporters to investigate the effect on EPSCs mediated by AMPA-Rs using whole cell voltage-clamp methods.

Results

We found a developmental difference in the properties of glutamate clearance from NM synapses. Around synaptogenesis, prior to the onset of hearing (embryonic days 11-12), blocking transmitter clearance with TBOA had no effect on AMPA-R response properties, suggesting that glutamate transporters are neither effective or present at early developing NM synapses. In contrast, after the onset of hearing and during a period of early synaptic refinement (E15-16), we observed a significant effect of glutamate transport blockade on the amplitude, kinetics and paired-pulse ratio of AMPA-R mediated EPSCs. During transport blockade at this age, peak amplitudes were smaller, kinetics were slower and paired pulse ratios changed from depression to facilitation, suggesting that the accumulation of transmitter alters both pre- and postsynaptic properties. At functionally mature synapses (E19-20), EPSCs decayed slowly when clearance was blocked with TBOA, but only when trains of rapid pulses were used as stimuli. The slower decay of EPSCs occurred despite a reduction in released transmitter and increased synaptic depression. This result was magnified when desensitization was relieved from AMPA-Rs with cyclothiazide, suggesting a progressive accumulation of transmitter and its subsequent rebinding to AMPA-Rs.

Conclusion

The findings show that glutamate transporters differentially regulate both pre- and postsynaptic glutamate transmission in the developing auditory brainstem. In addition, the effect of glutamate clearance from the synaptic cleft elucidates the action of transporters in the context of different developmental time periods.

PS - 690

Golgi Cells Provide Feedback Inhibition to Granule Cells in Dorsal Cochlear Nucleus

Daniel Yaeger; Laurence Trussell
Oregon Health & Sciences University

Background

The dorsal cochlear nucleus (DCN) integrates auditory and non-auditory information. Although the function of the non-auditory input is not understood, it may provide information key in the DCN's function as a sound localization circuit. Non-au-

ditary information is relayed to the DCN by mossy fibers, which make potent excitatory synapses onto granule cells. Granule cells synapse onto the principal cells in this circuit. Principal cells integrate inputs from granule cells and auditory nerve, and project to inferior colliculus. Given the significance of the mossy fiber-granule cell synapse, we determined how inhibition regulates mossy fiber-evoked granule cell firing.

Methods

We used paired whole-cell recordings in mouse DCN brain slices and computational modeling to address this question.

Results

Based on previous work suggesting that Golgi cells provide inhibition to granule cells, we used a mouse line labeling Golgi cells to perform paired recordings between Golgi and granule cells. Golgi cells made inhibitory synapses onto granule cells with a connection probability of 22%. We then investigated what synaptic input drives Golgi cell firing. In paired recordings between nearby granule cells and Golgi cells, granule cells made excitatory synapses onto Golgi cells with a connection probability of 31%. Excitatory currents at the granule-Golgi cell synapse showed prominent facilitation. In 50% of granule-Golgi cell pairs in which the Golgi cell was held in current clamp, individual granule cells firing at 100 Hz were able to evoke spikes in the Golgi cell. The probability of Golgi cell spiking increased throughout the train, suggesting that synaptic facilitation may underlie this effect. We also observed that 13% of granule-Golgi pairs were reciprocally connected, which was slightly higher than expected from the product of the unidirectional connection probabilities. We used a Neuron model of the mossy fiber-granule cell-Golgi cell microcircuit to determine how feedback inhibition from Golgi cells regulates mossy fiber-evoked granule cell firing.

Conclusion

We show that Golgi cells provide feedback inhibition to granule cells. Reciprocally connected granule-Golgi cell pairs provide a way for Golgi cell spiking to be self-limiting, as Golgi cell spiking will turn off granule cell spiking and thus limit excitation of Golgi cells. This circuit arrangement may allow granule cells to respond only to the onset of a period of mossy fiber activity.

PS - 691

Modulation of Gerbil Spherical Bushy Cell Excitability by Local Acetylcholine Application

David Goyer; Thomas Kuenzel
Institute for Biology 2, RWTH Aachen University

Background

In low frequency hearing mammals, spherical bushy cells (SBC) receive direct input from the auditory nerve via specialized axosomatic synapses, the Endbulbs of Held. Recent data have shown [Kuenzel et al., 2011] that inhibition changes SBC input-output function by tuning excitability in a stimulus-dependent manner. Furthermore, the existence of modulating neurotransmitters in the cochlear nucleus have been shown before [Klepper & Herbert, 1991; Happe & Morley, 1998], but not investigated on an electrophysiological level for SBC. We hypothesize that these modulatory systems play

an additional role in fine-tuning of SBC input-output function. Here, we show the influence of locally applied Acetylcholine (ACh) on SBC by simultaneously applying ACh and electrically stimulating the auditory nerve.

Methods

In frontal and parasagittal auditory brainstem slices of P14-20 gerbils (*Meriones unguiculatus*), whole cell patch clamp recordings from SBC were obtained in the presence of strychnine and GABA receptor antagonists. First, auditory nerve fibers were electrically stimulated with a bipolar tungsten electrode to evoke Endbulb inputs. Then, 1mM ACh (in ACSF) was locally applied onto the SBC with a Picospritzer. The combination of auditory nerve shocks with pharmacological stimulation was then used to assess the effect of ACh on the SBC firing probability. An in-silico model of SBC was implemented in NEURON to explore the impact of ACh effects on sound coding.

Results

We show that ACh causes a depolarization of 3.23 mV (+/- 1.7 mV), relaxing back to rest with a weighted-tau of 282 ms (+/- 311ms). Additionally, repeated ACh applications (10sec interval) tonically shift the RMP towards depolarized values from $RMP \pm std$ to $RMP+1.34$ mV (+/- 1.66mV). The combined electrical and pharmacological stimulation revealed a profound effect of ACh on the SBC's firing probability. By analyzing the responses of a model SBC to simulated auditory nerve inputs during long-lasting depolarizations, we explored the interaction of low-voltage activated potassium conductances with the effects described here.

Conclusion

We could demonstrate that the local application of ACh has a transient effect as well as a long-term effect on the SBC resting membrane potential. Further studies will shed light on the effect the altered membrane potential has on SBC excitability. We hypothesize that low voltage activated potassium channels are activated by the depolarized membrane potential, lowering SBC excitability. The duration of both effects we describe here indicate that ACh acts in a non-stimulus dependent manner, suggestive of roles in context-dependent changes of coding.

PS - 692

Consequences of Genetic Alterations of Electrical Properties of Neurons in the Ventral Cochlear Nucleus

Xiao-Jie Cao; Donata Oertel

University of Wisconsin School of Medicine and Public Health

Background

The ability of octopus and bushy cells in the ventral cochlear nucleus to convey precise timing information depends on the presence of opposing low-voltage-activated K^+ (g_{KL}) and hyperpolarization-activated conductances (g_h). Mice that lack HCN1, a subunit of the channels that mediate g_h , have not only slower and smaller Ih but also smaller I_{KL} (Cao and Oertel, 2011), raising the question how I_h and I_{KL} are altered by

the elimination of Kv1.1 (KCNA), one of the subunits of the shaker K^+ channels.

Methods

We compared whole-cell patch-clamp recordings from bushy and octopus cells in brain slices from mice that contain Kv1.1 (Kv1.1^{+/+}) with those that lack Kv1.1 (Kv1.1^{-/-}) that were kindly provided by Dr. Bruce Tempel (Smart et al., 1998).

Results

As in other mouse strains, the three groups of principal cells, octopus, bushy and stellate cells, were distinguishable by their responses to current pulses. Input resistances, resting potentials, and number of action potentials evoked by current were not measurably different. Threshold rates of depolarization were, however, different in Kv1.1^{+/+} and Kv1.1^{-/-} octopus cells and also in bushy cells. Under voltage-clamp we found that in octopus cells, the magnitude of the peak I_{KL} , but not the steady state, is reduced in Kv1.1^{-/-} cells. In bushy cells the magnitude of I_{KL} currents was not significantly different in Kv1.1^{+/+} and Kv1.1^{-/-} cells. The magnitude and kinetics of Ih were similar in mutants and wild type. A surprising observation from these experiments was the dramatic difference in the magnitudes of g_h and g_{KL} between wild type strains. In Kv1.1^{+/+} octopus cells, g_{KL} max was 50% as large as in HCN1^{+/+} and less than 20% that in ICR mice. Threshold rates of depolarization were roughly correlated with maximal g_{KL} and also varied widely between wild type strains.

Conclusion

Our results indicate that the differences in the intrinsic electrical properties of octopus and bushy cells in mouse strains that have Kv1.1 and those that lack Kv1.1 are subtle. Slightly smaller peak outward currents are associated with decreases in the threshold rates of depolarization. We have also observed large differences in the properties of principal cells between wild type strains: inbred Kv1.1^{+/+}, inbred HCN1^{+/+}, and outbred ICR mice.

PS - 693

Inhibition Dynamically Shapes the Acoustic Responsiveness in Spherical Bushy Cells

Christian Keine; Rudolf Rübsamen

University of Leipzig

Background

Spherical bushy cells (SBC) of the anteroventral cochlear nucleus (AVCN) provide temporally precise input to nuclei of the superior olivary complex involved in binaural computation necessary for sound source localization. Despite the very strong excitatory auditory nerve fiber input provided by the endbulb of Held, the SBCs do not act as a pure relay. Instead they show considerable integration of acoustically evoked excitatory and inhibitory inputs. Both, glycine and GABA receptors are expressed by SBCs and allow for a powerful inhibition. However, their specific functional role in signal transmission *in vivo* is still inconclusive.

Methods

Effects of acoustically evoked inhibition on signal transmission at the endbulb of Held-SBC synapse were assessed with

in vivo extracellular recordings in P25-P32 gerbils. Voltage signals were decomposed into APs and isolated EPSPs (iEPSPs) allowing for an analysis of the input-output relationship under varying stimulus conditions: absence of acoustic stimulation, stimulation at the unit's characteristic frequency, within the inhibitory sideband, and outside the receptive field.

Results

In none of the above conditions did the ANF input generate reliable SBC spiking; even in the absence of acoustic stimulation SBCs show spike failures. Under acoustic stimulation the rate of spike failures were either increased or reduced in a frequency- and level-dependent manner. A considerable number of cells show non-monotonic rate-level functions and pronounced inhibitory sidebands. Acoustic stimulation within the excitatory response area can increase the presynaptic firing rate more strongly than the postsynaptic one as seen from an increase in failure fraction. Stimulation within the unit's inhibitory sideband does not change the ANF input rate, but considerably reduces the success rate of postsynaptic AP generation. Activation of inhibitory inputs can also prolong the EPSP-AP transition time and the time course of the inhibitory effects outlasts the excitatory effects in the millisecond range. Both processes modulate the temporal precision of acoustically evoked SBC firing. Ionophoretic application of glycine supports the notion that higher sound pressure levels activate more glycinergic inputs leading to a more efficient postsynaptic AP suppression.

Conclusion

Inhibitory inputs on SBCs can be activated by acoustic stimulation and are strong enough to considerably change the input-output function. The inhibition-induced changes in SBC spike rates and timing are likely to play a crucial role in signal processing in mammalian brainstem sound localization circuitry.

PS - 694

Auditory Experience Regulates the Expression of AMPA Receptors and VGLUT1 in Auditory Nerve-Bushy Cell Synapses and GLT1 in Astrocyte Processes

Cheryl Clarkson; Maria Rubio

University of Pittsburgh

Background

In vivo changes in response to sensory experience regulate postsynaptic glutamate receptors (Quinlan et al., 1999). Therefore, changes in auditory experience could induce experience-dependent plasticity in auditory synapses. The synapse of the auditory nerve onto Bushy cells (AN-BCs) is biophysically and anatomically specialized for the fast conduction of excitatory currents in the auditory pathway (Trussell 1999). Previously, we showed that short-term (1 day) conductive hearing loss (CHL) reversibly scales up GluA3 AMPAR subunits in AN-BC synapses (Whiting et al., 2009), indicating that these synapses are sensitive to changes in auditory experience. However, we do not know 1) whether similar changes in AMPAR scaling occurs after long periods of sound reduction; and 2) whether auditory experience also

alters the expression of neuronal and glial glutamate transporters, which are essential for maintaining fast synaptic transmission.

Methods

To address these questions, we used a 10 day CHL model (~45 dB sound reduction) in adult rats, followed by earplug removal after 10 days. Hearing thresholds were assessed by ABRs, and the expression levels for GluA2, GluA3 and GluA4 AMPAR subunits in AN-BCs were determined by postembedding immunogold labeling after freeze-substitution. Similarly, expression levels of glutamate transporters in the AN terminals and in the enwrapping astrocyte processes were analyzed with antibodies for synaptic vesicular glutamate transporter 1 (VGLUT1) and glial glutamate transporter 1 (GLT1).

Results

Data from animals earplugged for 10 days showed that the interpeak ABR latencies (I-III waves) were prolonged by 0.51 ms. Analyses of AMPAR subunits at AN-BCs synapses showed a significant increase in the number and density of gold particles for GluA2/3, but not for GluA2, implying that GluA3 is responsible for the detected GluA2/3 increase. Interestingly, the gold labeling for GluA4 was significantly decreased. Gold labeling for VGLUT1 and GLT1 was also significantly decreased.

Conclusion

We conclude that AMPAR scaling at AN-BCs synapses differs between short- and long-term CHL, suggesting that AMPAR transmission at AN synapses is auditory experience-dependent. AMPAR scaling was accompanied by a decrease in neuronal and glial glutamate transporter expression. This decrease suggests that less glutamate is available for release from AN endings, as well as less clearance of glutamate at the synaptic cleft. All together our data show that CHL might alter the temporal precision of AN synapses.

PS - 695

Glycine and GABA Shape the Inhibitory Synaptic Response of Spherical Bushy Cells in an Activity Dependent Manner

Jana Nerlich¹; R. Michael Burger²; Beatrice Dietz¹; Rudolf Rübsamen¹; Ivan Milenkovic¹

¹University of Leipzig, Institute of Biology; ²Lehigh University, Dept. of Biological Science

Background

In the auditory brainstem of mature altricial rodents, inhibition contributes to accurate AP timing necessary for sound source localization. The interaction of excitation and inhibition at spherical bushy cells in the anteroventral cochlear nucleus (AVCN) attunes output AP timing by controlling the fidelity of well-timed, large EPSPs. Inhibitory transmission on mature spherical bushy cells is mediated by both glycine and GABA. The function of their action and the advantages of such a two-transmitter based system beyond early development are still poorly understood. In slice recordings, evoked inhibitory postsynaptic currents (eIPSCs) exhibit a slow synaptic decay to pulse train stimuli depending both on stimulus duration and

input rate. Glycinergic transmission largely determines the amplitude of inhibitory postsynaptic responses, yet a simultaneous activation of GABA_A receptors enhances and prolongs the inhibitory effect. Here we investigated the synaptic mechanisms utilized by the synergistic glycine/GABAergic transmission.

Methods

Pharmacologically isolated, synaptically evoked IPSCs were measured from SBCs at postnatal days P22-30 by means of whole cell recordings. The contributions of glycine- and GABA-mediated synaptic transmission to IPSC properties were assessed by manipulating glycine or GABA release and clearance in the synaptic cleft.

Results

The weighted time constant of evoked IPSCs was dependent on the presynaptic activity, specifically, it was prolonged at higher input frequencies and longer stimulus duration. The synergistic glycine (fast) and GABA (slow) signaling determined the IPSC decay time. While isolated glycinergic currents were faster than the control IPSCs, the slow GABAergic component most prominently prolonged decay times at higher input frequencies. GABA spillover and activation of extrasynaptic GABA_A receptors were unlikely to underlie this effect, as the low affinity GABA_A antagonist TPMPA (200μM) did not influence the prolonged decay. However, GABA clearance possibly contributed to the slow kinetic of IPSCs because the pharmacological blockade of GABA uptake (NO711 20μM, SNAP5114 100μM) lengthened the decay time constant. Additionally, glycine accumulation in the synaptic cleft contributed to the activity dependent prolongation of inhibition. Inhibition of the neuronal glycine uptake transporter (ORG25543, 20μM) significantly increased the IPSC decay time. The effect of glycine rebinding to its receptors was abolished by the low affinity competitive GlyR antagonist SR95531 (200μM).

Conclusion

Our data suggest that the slow inhibition on SBCs is shaped by the activity of respective glycine/GABA uptake transporters. The slow transmitter clearance and repetitive receptor binding, rather than spillover of transmitter to extrasynaptic receptors contribute to prolongation of decay times at higher input rates.

PS - 696

Synaptic Plasticity Interacts With Postsynaptic Membrane Kinetics in the Chick Cochlear Nucleus

Stefan Oline; R. Michael Burger

Lehigh University

Background

Auditory stimuli are processed in parallel frequency-tuned circuits, beginning in the cochlea. Auditory nerve fibers (nVIII) share this topographic pattern, known as tonotopy, and impart frequency tuning onto their postsynaptic targets in nucleus magnocellularis (NM). Though all NM neurons perform similar computational functions, physiological specializations exist along the tonotopy that reflect the characteristic frequency

(CF) of their nVIII inputs. High CF neurons have low input resistance and receive few (1-3) large inputs. Low CF neurons receive more than eight small inputs each, yet are more excitable with a higher input resistance. These tonotopic input and membrane properties are likely to confer computational specificity along the tonotopy. Unlike high CF NM cells, low CF NM neurons improve output jitter relative to their inputs, perhaps by averaging the timing of many inputs. An experimentally efficient way to relate membrane properties to computation is by examining responses to injected current ramps of varying slopes. Ramps create systematically changing PSPs from which spike responses can be evaluated.

Methods

Synaptic and current ramp evoked responses were recorded in current clamp from tonotopically localized NM neurons from aged E 19-P1 chicks. Spike threshold was evaluated with respect to PSP slope. Slope threshold was defined as the lowest membrane voltage slope to result in a spike.

Results

Ramp injection revealed that low CF neurons had lower slope thresholds and longer integration periods than high CF neurons. Synaptic train stimulation evoked spikes with latencies that increased following each pulse. Output jitter and latency were larger in low CF cells at all stimulus frequencies, expanding upon a previously observed difference in output jitter for single pulses.

Conclusion

Low CF neurons were shown to be more tolerant of a prolonged depolarization preceding a spike than high CF neurons. Additionally, depressed synaptic inputs to NM drove spikes with greater jitter and latency in low CF neurons. A tradeoff may exist between an NM neuron's synaptic input characteristics and membrane excitability. Low excitability in high CF neurons in combination with few inputs may allow the neuron to function as a relay with a strong refractory period between cycles. In contrast, greater excitability in low CF neurons allows for summation of many small inputs to improve output timing. Importantly, this property may act as a physiological form of dithering, where noise is added to a system to increase precision.

PS - 697

The Novel Presynaptic Protein Mover Contributes to Molecular Heterogeneity in the Rodent Ventral Cochlear Nucleus

Friederike Wetzel; Thomas Dresbach

University of Goettingen Medical School

Background

Bushy cells in the anterior part of the ventral cochlear nucleus are the postsynaptic targets of auditory nerve fibres. At the bushy cell soma, these fibres form a small number of large, excitatory nerve endings called endbulbs of Held. Due to their remarkable size these terminals are a useful model to investigate the molecular architecture underlying signal transmission at these specialized synapses. Bushy cell somata also receive a number of inhibitory inputs from different

origins, which is thought to contribute to signal processing at bushy cells. We had previously identified Mover, a vertebrate-specific synaptic vesicle protein that binds to the active zone scaffolding protein Bassoon, as component of rat AVCN synapses.

Methods

To characterize the expression of Mover in the cochlear nucleus in more detail, we have used confocal microscopy analysis of immunostained brain sections.

Results

Here, we show that Mover colocalizes with the synaptic vesicle marker Synapsin in the ventral cochlear nucleus, consistent with its association with synaptic vesicles in biochemical fractions. At bushy cell somata, we detected Mover both at endbulbs of Held and at inhibitory synapses using confocal microscopy. Quantitative fluorescence analysis revealed that Mover colocalized more extensively with VGAT-positive than with VGlut1-positive synapses. Moreover, fluorescence intensity levels of Mover varied between endbulbs, and were below detection limit at some, whereas Mover was detected at the majority of inhibitory terminals.

Conclusion

Thus, Mover may contribute to molecular and functional heterogeneity in the cochlear nucleus. We are currently analyzing Mover knockout mice generated in the lab to test this hypothesis.

PS - 699

Connexin Expression in the Bat and Mouse Cochlear Nucleus

Alyssa Wheeler; Mark Johnson; James Simmons
Brown University

Background

Gap junctions make up electrical synapses in the nervous system, particularly to confer temporal precision on neuronal circuits. The time-sensitivity of hearing, and particularly echolocation, makes the auditory system an obvious candidate for having electrical synapses, which have been identified in the cochlear nucleus (CN) of the rat and monkey at an ultrastructural level. But, the protein composition of these channels is still unknown. Previous research from our lab has shown that neuronal connexin (CX)-36 is expressed in the bat CN. Initially, no expression was found in the mouse. Due to the potentially greater demand for temporal precision in bat echolocation than mouse hearing, we hypothesized that there should be connexin expression in more bat CN neurons than in mouse CN neurons. We confirmed the expression of CX-36 in the bat CN and reexamined its expression in the mouse CN, where it also was found. An additional gap-junction protein, CX-45, often is found in association with CX-36. We found this protein, too, in the bat and the mouse CN. The function of electrical synapses in the bat's auditory brainstem is not clear; but we think that they are involved in detecting coincident arrival of different frequencies in FM biosonar stimuli.

Methods

We performed immunohistochemistry in the bat and mouse CN to determine if CX-36 and CX-45 are expressed. Additionally, we sought to develop an *in situ* hybridization (ISH) protocol for neuroanatomical work in the big brown bat (*Eptesicus fuscus*). We performed *in situ* hybridization for both CX isoforms in the bat CN to determine where CX mRNA was expressed. We also used LacZ and PLAP reporter genes from heterozygous CX-36 knockout mice to re-evaluate CX-36 expression in the mouse CN.

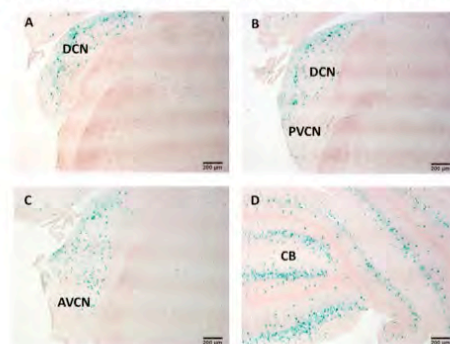
Results

We found that both CX-36 and CX-45 are expressed in the bat and the mouse CN, but we did not find that CX protein is expressed by more bat CN neurons than mouse CN neurons. However, we observed differences between globular bushy neuron cytoarchitecture in the bat and mouse that suggest echolocation demands extreme temporal precision in the bat CN. We developed ISH as a method that can be successfully utilized in our model species.

Conclusion

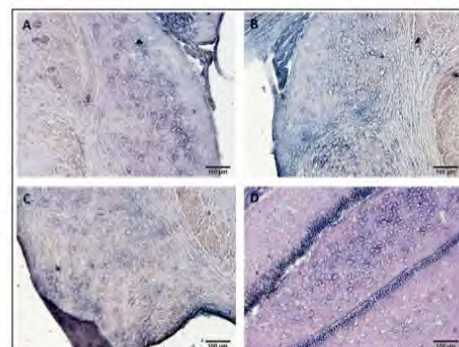
We conclude that electrical synapses may play a temporal coincidence-detecting role in auditory processing across mammals.

CX-36 expression in the mouse cochlear nucleus



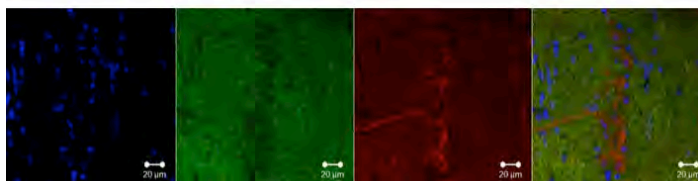
Cx36^{LacZ/+} mice (generously provided by Gilad Barnea) showed CX-36 gene expression in the **A**) dorsal cochlear nucleus (DCN), **B**) posterior-ventral cochlear nucleus (PVCN), and **C**) anterior-ventral cochlear nucleus (AVCN), but not in adjacent auditory brainstem nuclei. **D**) The cerebellum (CB) is shown as a positive control. Age-matched wild type controls show no LacZ expression (not shown).

CX-36 *in situ* hybridization in the bat cochlear nucleus



For the first time ever, we performed *in situ* hybridization in the big brown bat brain. Results show CX-36 mRNA expression in the **A**) dorsal cochlear nucleus (DCN), **B**) DCN and its border with the posterior-ventral cochlear nucleus (PVCN), and **C**) anterior-ventral cochlear nucleus (AVCN). **D**) The hippocampus is a positive control. Sense probe controls show background-level expression (data not shown).

Globular bushy neuron cytoarchitecture in the bat AVCN



Immunofluorescence in the bat anterior ventral cochlear nucleus shows the configuration of globular bushy neurons (GBNs) along the root of the auditory nerve. Blue = DAPI nuclear stain; Green = AlexaFluor 488 secondary antibody background stain for fiber visualization; Red = MapII neuron marker protein. In the merged image, GBNs align themselves to the auditory nerve in long chains rather than the clusters observed in the rat and monkey. GBNs have been shown to express gap junctions on an ultrastructural level; and in this work (data not shown) we show that they also express CX-36 and CX-45 protein and mRNA.

PS - 700

Perinatal Expression of *Erb4* Is Required For Normal Ventral Cochlear Nucleus Organization

Kathleen Yee

University of Mississippi Medical Center

Background

A critical locus for hearing is the cochlear nucleus (CN), the first auditory synaptic site in the brain. Studies of the CN during functional hearing, including hearing onset and decline, has yielded an extensive literature of CN anatomy and physiology; in contrast, relatively less is known about the CN during development. Laboratory interest in elucidating molecules that contribute to mature CN organization has prompted study of the tyrosine kinase receptor *Erb4* and its neuregulin (Nrg)-1 ligands for several reasons. During development, *Erb4* and Nrg-1 are critical for events, including migration and differentiation and under disease states, both molecules have been shown to be schizophrenia susceptibility genes.

Methods

Methods employed include in situ hybridization, general histological staining, histochemistry and immunohistochemistry. Normal expression data was obtained from wild type CN and loss of function studies were performed on age-matched wild type and *Erb4* mutant mice.

Results

The laboratory has previously shown that perinatal *Erb4* expression is spatiotemporally dynamic. *Erb4* mRNA is expressed in the dorsal and ventral CN at E16.5 and molecular/granule cell layer, deep dorsal and ventral CN at postnatal day 0. General histological staining shows perturbations within the CN including altered organization within the posteroventral cochlear nucleus (PVCN). Reported here is that vesicular glutamate transporter 1 (vGlut1; Millipore) which labels auditory nerve fiber terminals in the CN (Zhou et al., 2007) shows a decrease in vGlut1 staining in the octopus and stellate region of the PVCN in *Erb4* null mice compared to wild-type controls, raising the possibility that one or both of these cell types may be compromised in the absence of *Erb4* function. Normal octopus cell markers, potassium channels (HCN-1 and $K_v1.1$) are detected in *Erb4* $-/-$ CN, providing evidence that octopus cells are present. However, the average volume occupied by perineuronal net-stained

octopus cells and their dendrites in *Erb4* $-/-$ mice is smaller than in wild type controls.

Conclusion

These data show that developmental expression of the receptor tyrosine kinase *Erb4* contributes to the normal anatomical organization of the PVCN. Differences in vGlut1 localization and perineuronal net-staining, respectively, may be important for the positioning of glutamatergic neurons and/or regulation of their afferents and contributing to the morphological features of octopus cells in *Erb4* null versus wild type mice. These data suggest that circuitry underlying sound localization may be critically dependent on CN *Erb4*-Nrg signaling and may be an early stage of aberrant auditory processing in certain schizophrenia patient populations.

PS - 701

The Diversity and Fidelity of Temporal Coding of Amplitude Modulation in the Cochlear Nucleus

Chris Scholes¹; Robert Mill¹; Alan Palmer¹; Stephen Coombes²; William Rhode³; **Christian Sumner¹**

¹MRC Institute of Hearing Research; ²School of Mathematical Sciences, University of Nottingham;

³Department of Psychology, University of Wisconsin, Madison, WI, USA

Background

The timing of spikes is important in representing rapid fluctuations in sound energy. We have previously shown that some units in the cochlear nucleus (CN) show complex patterns of spike timing in response to even sinusoidal stimulus envelopes (Laudanski et al, 2010). Here, we examine the nature of the temporal coding of amplitude modulation (AM) in all types of cochlear nucleus neurons, and the impact this has on the fidelity with which AM frequency is encoded

Methods

We re-analysed previously published data, describing the responses of ~400 cochlear nucleus neurons to AM tones. Three novel analysis methods were applied: 1. We measured spike train complexity by the number of delay peaks in the shuffled autocorrelation. 2. We determined whether the observed spike trains were consistent with either a pure Poisson process or one modified by refractoriness. 3. We used a spike train classifier to quantify the ability of CN neurons to accurately signal the modulation frequency. We also subjected models of cochlear nucleus neurons to the same analysis.

Results

Unit types (e.g. choppers) that showed complex patterns of spike timing, beyond that expected from refractoriness, provided excellent discrimination of modulation frequencies. Primary-like units, whose behaviour approximated modulated Poisson processes, exhibited poor discrimination performance. For all unit types, at any given modulation frequency, discrimination correlated well with spike train complexity. The dependency of the fidelity of temporal coding on unit type and spike train complexity can be explained by known biophysi-

cal processing in CN neurons, and provides insights into how these differences in coding arise.

Conclusion

CN neurons employ multiple temporal coding strategies to represent AM. Modulation frequency is best encoded by complex spike trains that are highly non-linear functions of the stimulus fluctuations. The improved, complex temporal coding arises from the interaction between the integration of multiple auditory nerve fibre inputs and the non-linear 'resetting' following an action potential.

PS - 702

Efficient Envelope Extraction by Adaptive Spiking in the Owl's Cochlear Nucleus

Bertrand Fontaine¹; Katrina MacLeod²; Louisa Steinberg¹; Christine Köppl³; José Pena¹

¹Albert Einstein College of Medicine; ²University of Maryland; ³Carl von Ossietzky Universität Oldenburg

Background

Efficiently encoding the temporal fine structure or envelope of sound is critical for perceptual tasks such as sound localization and identification. In the barn owl, two functional pathways, which start already at the cochlear nuclei, encode these features differently. Nucleus Angularis (NA) is thought to encode envelope information more reliably whereas Nucleus Magnocellularis is specialized for encoding temporal fine-structure information. Here we compare the envelope encoding in the auditory nerve (AN) and NA and show that a cellular mechanism is sufficient for efficient envelope extraction in NA.

Methods

In vivo extracellular recording were performed in AN and NA of 9 owls. Their ability to encode envelope was compared using coherence analysis of the responses. The envelope filtering properties were estimated by deriving modulation transfer functions (MTFs) at different sound levels. *In vitro* somatic recordings were performed in chicken AN with current inputs mimicking AN afferents. A spiking neuron model consisting of a leaky integrate and fire neuron with an adaptive threshold that depended both on the membrane potential and the history of spiking was fitted to the *in vivo* data.

Results

NA cells, while losing ability to encode sound fine-structure, encoded the envelope better than individual AN fibers. While AN MTFs were always low-pass NA MTFs became band-pass as the level increased. This behavior is also seen in *in vitro* somatic recordings in NA. The origin of the band-pass filter was not sub-threshold (the membrane voltage is still low-pass) but was correlated with threshold variation. We successfully fitted a spiking neuron model with threshold adaptation based on sodium inactivation to the *in vivo* data and showed that the threshold steady-state function could explain the MTF change as a function of input level.

Conclusion

NA cells encoded the envelope more efficiently and reliably the envelope than AN fibers consistent with NA being involved

in coding sound identity. While most of the models of rate band-pass filtering are based on delayed inhibition we conclude that in the avian NA MTF properties can be explained by threshold adaptation. Thus cellular mechanism based on spike initiation non-linearity could account for the emergent selectivity without any need for network mechanisms.

PS - 703

Neural Correlates of the Detection of Tones in Noise in the Cochlear Nucleus of Nonhuman Primates

Margit Dylla; Peter Bohlen; Ramnarayan Ramachandran
Vanderbilt University

Background

An essential function of the auditory system is the ability to detect sounds in the presence of noise. Previous studies in the inferior colliculus (IC) and the cochlear nucleus (CN) provide information that is necessary to better understand this process. For tones presented alone, individual IC neurometric thresholds and slopes closely matched psychometric (behavioral) thresholds and slopes. While IC neurometric thresholds matched psychometric thresholds, response thresholds of CN neurons were, on average, 19 dB higher than behavioral thresholds. CN neurometric slopes were also shallower than psychometric slopes. In further studies, results showed that the addition of noise shifted IC neurometric thresholds to higher sound pressure levels, matching the shift of psychometric thresholds. This correlation suggests that the IC plays an important role in processing signals in noise. Here we report results of experiments designed to evaluate the threshold shifts of CN neurons of awake and behaving animals during detection of tones in noise. This current study tests the hypothesis that the neuron-behavior response correlations found in the IC are different than the responses of neurons in the CN.

Methods

Two nonhuman primates (*Macaca mulatta*) were trained in a reaction time lever release task with appropriate catch trials to report the detection of tones in noise. Single units with characteristic frequencies ranging up to 32 kHz were recorded from the CN (n=55) while monkeys performed the detection task. Most of the units were classified as type I, type I/III or type III, based on the excitation and inhibition present in responses to tones as a function of frequency and sound pressure level. Psychometric and neurometric functions were created using signal detection theory and Receiver Operating Characteristic (ROC) analyses.

Results

The results show that background noise caused an increase in the baseline firing rate of CN neurons. The dynamic range of CN neurometric functions shifted to higher sound pressure levels in the presence of noise. However, neurometric functions showed lower shifts when compared with simultaneously measured psychometric functions. On the average, neurometric functions shifted at a rate of .7 dB per 1 dB of psychometric shift.

Conclusion

These results, that the magnitude of CN thresholds and threshold shifts in noise did not match with behavioral thresholds and threshold shifts in noise, suggest that the CN responses are transformed by the level of the IC to produce strong neuron-behavior correlations.

PS - 704

Estimating Spectral-Temporal Receptive Fields in the Cochlear Nucleus

Arkadiusz Stasiak¹; Thomas Blumensath²; Jessica Monaghan²; Matthew Wright²; Stefan Bleack²; Ian Winter³

¹University of Cambridge; ²Institute of Sound and Vibration Research, University of Southampton, SO17 1BJ; ³Department of Physiology, Development and Neuroscience, University of Cambridge, CB2 3EG

Background

The spectro-temporal receptive field (STRF) has been extensively used to characterise the responses of neurons at higher levels of the auditory pathway. This approach has been less frequently used in the auditory brainstem. In this study we compare the STRFs of single units of the cochlear nucleus in response to a variety of complex stimuli, including synthetic signals (closely based on those used to estimate STRFs in the cortex) and conspecific vocalisations.

Methods

Single units have been recorded extracellularly from the cochlear nucleus of normal-hearing urethane anaesthetised guinea pigs. The stimuli were pure tones (to measure conventional receptive fields), complex synthetic signals (static and dynamic ripples, dynamic random chords and white noise) and conspecific animal vocalisations (chirp, purr, chatter and whistle). We selected a variety of signals to provide a variation in temporal envelope and spectral range. The synthetic signals were 15s long and presented 5 times; the conspecific vocalisations were no longer than 1s and presented 25 times; all stimuli within a category were presented in a random order.

Results

The STRFs patterns observed were restricted in frequency and time precedence; they were largely neuron specific. The precedence time usually was no longer than 10 ms (measured up to 40 ms). The maximum STRF peak agrees very well with the unit's BF. Peak regions in the STRFs are likely to represent afferent excitatory inputs. It is less obvious what the trough regions indicate; they could reflect suppression or more indirect, inhibitory inputs. The STRF pattern showed some correlation with unit classification with onset and pause/build units showing the greatest diversity in their responses.

Conclusion

These experiments are intended to identify dictionary elements that may be used by adaptive sparse coding algorithms aimed at improving the detectability of signals in noise. Crucially we now need to explore the level-dependency of these dictionary elements.

PS - 705

Neural Selectivity to Vocalizations in the Dorsal Cochlear Nucleus

Christine Portfors¹; Patrick Roberts²

¹Washington State University; ²Oregon Health & Science University

Background

Many animals use vocalizations to communicate and consequently an important function of the auditory system is to detect and discriminate different vocalizations. The neural mechanisms underlying this task are not well understood. Neural selectivity to vocalizations is known to occur at the level of the auditory midbrain and it is currently thought that selectivity emerges there. However, few studies have examined selectivity to vocalizations in auditory brainstem nuclei. The dorsal cochlear nucleus (DCN) is a cerebellum-like structure that integrates direct auditory nerve input with multimodal inputs, including descending input from auditory nuclei, and thus has circuitry that potentially could create selectivity to vocalizations. The purpose of this study was to investigate whether responses in DCN are selective to different natural vocalizations that share similar frequency spectra characteristics.

Methods

We recorded single unit responses in the DCN of awake, restrained mice. We presented pure tones and broad-band noise to identify the well-described physiological response types found in DCN. We then presented a large repertoire of social vocalizations at different intensities. We used the pure tone responses to predict the responses to vocalizations.

Results

Neurons in DCN responded to vocalizations in a heterogeneous manner. Some neurons responded to many of the vocalizations but some neurons were highly selective and only responded to a subset of the vocalizations. In some neurons, the pure tone frequency tuning curve did not predict the responses to vocalizations.

Conclusion

Selectivity to vocalizations occurs in the DCN, and the way that a neuron in DCN responds to complex sounds cannot always be predicted by its responses to pure tone stimuli.

PS - 706

Monaural Cross-Frequency Coincidence Detection in Noise-Induced Hearing Loss

Mark Sayles; Ann Hickox; Michael Heinz

Purdue University

Background

The spatio-temporal pattern of auditory-nerve activity is characterized by rapid across-frequency phase changes near distinct spectral components. These phase changes give cues to important perceptual features of sound. Spatio-temporal cues could be extracted by a monaural cross-frequency coincidence detection mechanism in neurons receiving inputs from an array of neighboring ANFs. Some cochlear nucleus (CN) neurons act as monaural coincidence detectors. Here,

we examine the effect of sensori-neural hearing loss on the monaural phase sensitivity of model coincidence detector neurons operating on the output of a model of the auditory periphery. We compare the model responses to those of ANFs and CN single units.

Methods

We used signals known as Huffman sequences. These are broadband clicks with a flat magnitude spectrum, and a phase spectrum characterized by a 2π transition centered at F_t . The phase transition slope is controlled by a parameter, r . We co-varied r and F_t with r -values of [0.85, 0.9, 0.92, 0.95, 0.98], and F_t varied in 1/25th octave steps over 0.5 octaves around the neuron's best frequency. We refer to stimuli with $r = 0.85$ as the "broad" phase transition, and $r = 0.98$ as the "sharp" phase transition. Responses to Huffman sequences from a model of the auditory nerve (Zilany et al., 2013) were used as input to a monaural coincidence-detector model (Krips & Furst, 2009) to simulate the responses of CN units behaving as idealized coincidence detectors which spike when at least L of their N inputs with CFs within W octaves of F_t spike within a coincidence window of duration Δ . We systematically varied the degree of simulated hearing impairment in the auditory nerve model by varying the hair cell coefficients C_{OHC} and C_{IHC} . Responses to the same stimulus set as used with the computational model were recorded from ANFs and CN units in both normal-hearing and hearing-impaired (noise-exposed) anesthetized chinchillas.

Results

Comparing the responses to the "broad" and "sharp" stimuli, we find a greater relative difference in firing rate between the two stimuli for impaired than for normal model ANFs. This effect is reflected in the output of the coincidence detector model.

Conclusion

The results support the hypothesis that broadened peripheral filters in noise-induced hearing loss result in an increased sensitivity to local phase changes along the basilar membrane. This has functional consequences for the representation of complex sounds in hearing impairment as well as for novel amplification strategies aimed to restore normal spatio-temporal response patterns.

PS - 707

Acoustic Trauma Upregulates Pain Associated Proteins in Rat Cochlear Nucleus

Senthilvelan Manohar¹; Francesca Yoshie Russo²; Robert Dingman¹; Richard Salvi¹

¹University at Buffalo; ²University of Rome

Background

Chronic tinnitus, which often arises from cochlear damage, shares many similarities with phantom limb pain. Recent studies suggest a causal link between increased expression of activated microglia in CNS and the development of neuropathic pain following peripheral nerve injury. To preserve function and promote survival of denervated nerves in the CNS, neurotrophic factors are secreted from the local environment. Unfortunately, changes in protein expression of these neuro-

trophic factors and its receptors can induce severe pain. To determine if cochlear damage alters neurotrophic factor receptors and activated microglia, we exposed rats to unilateral acoustic trauma and looked for changes in the expression of relevant genes and proteins in the cochlear nucleus.

Methods

We examined the expression of TrkA gene and protein and activated microglia in the rat cochlear nucleus 2, 14 and 28 days after a unilateral noise-exposure (2 h, narrow band noise at 12 kHz, 126 dB SPL). Western blots were used to study TrkA protein expression at 2, 14 and 28 days post-exposure and immunolabeling with a MHC class II protein marker was used to study activated microglia 14 and 28 days post-exposure. Hearing loss and cochlear damage were evaluated using the ABR and cochleograms.

Results

Unilateral noise exposure caused significant hearing loss and massive cochlear damage in the exposed ear, but no hearing loss or damage in the unexposed ear. Two bands (77 kDa and 140 kDa) of TrkA protein were observed on western blots; one was an unglycosylated 77 kDa protein and the other was a glycosylated extracellular domain 140 kDa protein. The unglycosylated TrkA band was downregulated at 2 and 14 days, but was upregulated at 28 days. Glycosylated band was downregulated at all the time points studied. The number of MHC Class II immunoreactive microglia cells was significantly higher in the ventral cochlear nucleus, but not the dorsal cochlear nucleus, on the noise exposed side compared to the unexposed side.

Conclusion

Previous studies on facial and spinal cord injury have shown a strong correlation between changes in expression of TrkA protein and hypersensitivity to pain. Similarly, an increased numbers of activated microglia cells have been associated with neuropathy. The noise-induced upregulation of activated microglia and changes in TrkA protein expression in the cochlear nucleus following cochlear damage may provide new insights on the molecular mechanisms that lead to spontaneous hyperactivity in the cochlear nucleus, chronic tinnitus and new therapeutic strategies for treating tinnitus.

PS - 708

Manipulations of Dexamethasone Kinetics in Perilymph

Alec Salt¹; Jared Hartsock¹; Ruth Gill¹; Fabrice Piu²; Stefan Plontke³

¹Washington University School of Medicine; ²Otonomy Inc, California; ³University of Halle, Halle, Germany

Background

We have previously reported that dexamethasone (Dex) applied locally to inner ear perilymph of guinea pigs is rapidly lost with an elimination half time from scala tympani of around 22 min. In the present study, we investigated manipulations of the perilymph kinetics for Dex. We studied whether Dex was metabolized in the ear through cellular pathways comparable to those in the liver, in which cytochrome P450 CYP3A4 and CYP17A (known to be present in the cochlea) dominate. In

addition, the kinetics of FITC-labeled dexamethasone was compared with that of native Dex.

Methods

The perilymphatic compartment of the ear was filled with Dex-containing solution injected for 1 hr from a pipette sealed into the lateral semi-circular canal (SCC). Sequential samples of perilymph were taken from the lateral SCC 2 hr after injection finished. Measured concentrations of Dex were used as an index of Dex retention. Retention of Dex was compared when specific antagonists of CYP3A4 (ketoconazole: 10 μ M) and CYP17A (abiraterone: 10 μ M), were included in the medium, together with DMSO controls. The retention of FITC-labeled dexamethasone (Invitrogen) was also assessed.

Results

The amount of Dex retained in perilymph was not influenced significantly by inhibitors of CYP3A4 or CYP17A activity. In contrast, FITC-labeled Dex (FW 841) was retained in perilymph substantially longer than native Dex (FW 392). The mean concentration of the first 3 perilymph samples (reflecting perilymph originating in the LSCC, the vestibule and part of scala vestibuli) averaged 79.4 % (SD 8.0, n=6) of the injected concentration for FITC-labeled Dex compared to 29.3 % (SD 4.5, n=4) for native Dex.

Conclusion

Specific inhibitors for CYP3A4 and CYP17A had no significant influence on Dex retention in the ear, showing that metabolism through these pathways makes a negligible contribution to Dex loss from perilymph. FITC labeling of Dex, which more than doubles the formula weight and may change other properties, dramatically reduces the rate at which Dex is eliminated from the ear. The rapid elimination of native Dex from perilymph is a serious problem as it reduces both the duration and the spatial extent of local Dex therapy. Modification of the Dex molecule in a manner that leaves binding to the receptor intact may solve the unfavorable kinetic characteristics of Dex, allowing the drug to remain there for a longer period following IT application and to spread further up the cochlea.

PS - 709

Recovery of Hearing After Local Glucocorticoid Therapy of Sudden Sensorial Hearing Loss – a Meta-Analysis by Mathematical Simulations of Clinical Protocols

Arne Liebau¹; Alec Salt²; Olivia Pogorzelski¹; Stefan Plontke¹

¹University of Halle (Saale), Department of Otorhinolaryngology - Head and Neck Surgery; ²Washington University School of Medicine, St. Louis, Department of Otolaryngology

Background

During the last two decades, there is an increasing interest in local therapy of inner ear diseases. Results of a recent Cochrane meta-analysis comparing the effectiveness of local (intratympanic) glucocorticoid therapy in sudden sensorial hearing loss, showed a significant higher odds ratio for hearing improvement in comparison to both, no further or

placebo therapy, and to continuation of systemic treatment in a “salvage” situation (after insufficient hearing recovery by systemic treatment) but not for primary intratympanic therapy. However, there are no data available of the quantitative correlation between the used application protocols (e.g. applied concentration, volume, numbers of application etc) and the changes in hearing thresholds. The aim of this meta-analysis was to reveal the distinctions between different application schemes, application systems, drug concentrations, and glucocorticoids used.

Methods

In the present meta-analysis, intra cochlea drug concentration (C_{max}) and dose (AUC, area under the curve) at different sites along the cochlea was calculated with a validated computer simulation program for intra cochlea drug dispersion (Cochlear Fluids Simulator V 3.081). The simulations were based on the application protocols in published controlled and uncontrolled clinical studies, and on pharmacokinetic data derived from experiments in animals and humans. The calculated doses were related to the mean change in hearing thresholds in the respective studies.

Results

The results showed a higher maximum of intra cochlea glucocorticoid concentration after both a longer retention time of the drug solution at the round window niche and the use of higher concentrations of the applied substance. Furthermore, after preliminary calculations, a trend became apparent that increasing maximum glucocorticoid concentration is accompanied with less hearing improvement in patients.

Conclusion

This knowledge could in the future support the choice of appropriate therapy protocols and drugs. However, evaluation of available studies was difficult because many confounding variables may influence the mean therapy outcome in patients such as age, clinical history, time of start of treatment, initial hearing loss etc. but are impossible to individually reconstruct based on the data in published studies. The study thus also points out the importance of reporting individual patient data in clinical studies allowing a comparison of different therapy strategies instead of pooled data masking the effects of individual patient characteristics.

PS - 710

Sodium-Glucose Transporter-2 (SGLT2; SLC5A2) Enhances the Cellular Uptake of Gentamicin

Meiyan Jiang; Takatoshi Karasawa; Qi Wang; Hongzhe Li; Peter Steyger
Oregon Health and Science University

Background

The aminoglycoside antibiotic gentamicin continues to be clinically essential, and is frequently used worldwide to treat bacterial sepsis. However, the nephrotoxic and ototoxic side-effects remain serious complications. The electrogenic SGLT2 is primarily expressed in kidney proximal tubules, a major site

of gentamicin toxicity. We hypothesized that SGLT2 traffics gentamicin, and promote cellular toxicity.

Methods

SGLT2 expression *in vitro* and *in vivo* was examined by immunofluorescence. To determine if *in vivo* inhibition of SGLT2 reduces cellular uptake of gentamicin, SGLT2 heterozygous or null mice were pre-treated with an SGLT2 inhibitor – phlorizin, or vehicle alone. Mice then received gentamicin-Texas Red (GTTR; 2 mg/kg, pH 7.4; i.p.). After 30 minutes, serum and kidney were collected from anesthetized mice prior to cardiac perfusion and fixation. To determine if SGLT2 can traffic GTTR *in vitro*, stable cell lines were generated by retroviral gene expression using SGLT2-pBabe construct in KDT3 cells (KDT3-SGLT2).

Results

SGLT2 was robustly expressed in kidney proximal tubule cells of heterozygous, but not null mice. SGLT2 expression was confirmed in proximal tubule derived KPT2 cells but not in distal tubule derived KDT3 cells. In mice, phlorizin decreased GTTR uptake by kidney proximal tubule cells in SGLT2^{+/+} mice, but not in SGLT2^{-/-} mice. Serum GTTR levels were elevated in SGLT2 null mice, and in phlorizin-treated wildtype and SGLT2 heterozygous mice, compared to untreated mice. D-glucose competitively decreased the uptake of 2-NBDG, a fluorescent analog of glucose, by KPT2 cells. Phlorizin strongly inhibited 2-NBDG uptake by KPT2 cells. Pre-treatment with phlorizin (20, 50 or 100 ug/ml) also reduced GTTR uptake by KPT2 cells in a dose- and time-dependent manner. KDT3-SGLT2 cells demonstrated elevated GTTR uptake compared to control cell lines (KDT3-pBabe).

Conclusion

SGLT2 facilitates gentamicin entry into kidney proximal tubule cells *in vivo* that is acutely inhibited by phlorizin. However, phlorizin does not inhibit renal uptake of GTTR in SGLT2^{-/-} mice, indicating phlorizin specificity for SGLT2, and that compensatory factors enable SGLT2-independent uptake of GTTR in these mice. Loss of SGLT2 function, by antagonism or by gene deletion increases gentamicin serum levels, and potentially gentamicin toxicity, a concern for anti-diabetes drug development based on SGLT2 antagonism.

PS - 711

Endotoxemia-Induced Cochlear Innate Immune Cytokine and Fluorescently-Tagged Gentamicin Levels Are Attenuated in Hypo-Responsive TLR4 C3H/HeJ Mice.

Zachary Urdang; Jianping Liu; Barbara Larrain; Meiyan Jiang; Dennis Trune; Peter Steyger
Oregon Health and Science University

Background

Sepsis is the coincident diagnosis of Systemic Inflammatory Response Syndrome and active infection. Treatment options for gram-negative sepsis includes aminoglycoside therapy which carries the risk of acute renal failure, and/or permanent ototoxicity. We have observed synergistic ototoxicity between endotoxemia (as a model for gram-negative induced SIRS)

and aminoglycoside therapy in mice. In this study, we used the C3H/HeJ mouse that has an SNP mutation in Toll-like-receptor-4 (TLR4) that reduces its inflammatory response to endotoxin agonism as a means to investigate the role of TLR4 in endotoxemia-enhanced aminoglycoside ototoxicity.

Methods

Mice received lipopolysaccharides (LPS) or DPBS intravenously 24 hours prior to tissue collection and processing. Some mice received gentamicin-Texas Red (GTTR) following intraperitoneal injection 1 hour prior to tissue collection. Using quantitative-multi-plex ELISA we simultaneously measured 8 acute phase cytokines (mIL-1a, mIL-1b, mIL-6, mIL-10, mKC (i.e. IL-8), mMIP-1a, mMIP-2, and mTNFa) in whole cochlear homogenates in C57/Bl6, C3H/HeOuJ as controls, and C3H/HeJ mice as a negative control. The fluorescence intensity of GTTR was quantified in cochlear lateral wall wholemounts in fibrocyte, basal, intermediate, and marginal cell layers. The fold change in signal for each strain was calculated by normalizing the means each LPS cohort was versus the DPBS cohort; relative percent error students' t 95% confidence intervals were propagated, and non-overlapping confidence intervals between amongst strains were considered significant.

Results

Acute phase cytokine concentrations in LPS-treated C3H/HeJ cochleae were attenuated compared to C3H/HeOuJ and C57/Bl6 wild-type controls similarly treated with LPS. GTTR quantification in cochlear lateral wall whole mounts revealed statistically significant (p<0.05) reductions in GTTR fluorescence in LPS-treated C3H/HeJ mice compared to endotoxemic C3H/HeOuJ mice in the fibrocyte and marginal cell layers. GTTR fluorescence was also reduced in basal and intermediate cell layers, yet did not reach statistical significance in LPS-treated C3H/HeJ mice compared to LPS-treated C3H/HeOuJ mice.

Conclusion

In mice, endotoxemia elevates whole cochlear homogenate levels of acute phase cytokines at the protein level. This is accompanied by an increase in cochlear loading of gentamicin-Texas Red. In C3H/HeJ mice this cytokine response is attenuated and coincides with decreased GTTR fluorescence in the lateral wall. Together these results suggest that TLR4 signaling may play a key role in synergistic endotoxin-aminoglycoside ototoxicity.

Evaluation of the Systemic and Intratympanic Application of the Selective Glucocorticoid Receptor Agonist Compound-A for Ototoxic Effects

Christoph Arnoldner¹; Markus Krause²; Elisabeth Engleder³; Hanna Schöpfer⁴; Lukas Landegger²; Franz Gabor³; Wolfgang Gstöttner²; Clemens Honeder²

¹Medical University of Vienna; ²Department of Otorhinolaryngology, Medical University of Vienna, Austria; ³Department of Pharmaceutical Technology and Biopharmaceutics, University of Vienna, Austria; ⁴Department of Pathobiology, Institute of Anatomy, Histology and Embryology, University of Veterinary Medicine Vienna, Austria

Background

Glucocorticoid therapy is used for many conditions affecting the inner ear. The systemic application of glucocorticoids causes side effects like hyperglycemia or osteoporosis, especially if the drugs are given for a longer period of time. To counteract these problems, the topical application of glucocorticoids has been evaluated in various conditions affecting the inner ear. Another possibility to improve therapy of the inner ear is the use of novel compounds. Selective glucocorticoid receptor agonists like Compound-A are potent anti-inflammatory drugs, but show a reduction in side effects. As this novel class of drugs has never been used for inner ear therapy, we evaluated the topical and the systemic application of Compound-A for ototoxic effects.

Methods

Pigmented guinea pigs were used as animal model. The total 24 animals were grouped as follows: 1) Systemic application of Compound A (1,5mg/kg; n=6); 2) systemic application of Compound A (4,5mg/kg; n=6); 3) intratympanic application of Compound A (1mM; n=6); 4) intratympanic application of Compound A (10mM; n=6). Contralateral ears in the topically treated animals were used as controls. Hearing thresholds were determined by the measurement of auditory brainstem responses to clicks and noise bursts between 1 and 32 kHz. ABRs were measured before and directly after the application as well as on days three, seven, 14, 21 and 28. After the final audiometry, animals were euthanized and temporal bones were harvested for the preparation of organ of Corti wholemounts and histological slides.

Results

Systemic administration of Compound A (1,5 mg/kg & 4,5 mg/kg) did not result in hearing threshold shifts. In contrast, the intratympanic application of Compound A (1mM & 10mM) resulted in a hearing loss, which was more pronounced in the high frequencies. The histological evaluation of the inner ears showed, that the application of Compound A via both routes did not result in a haircell loss.

Conclusion

Selective glucocorticoid receptor agonists like Compound A could provide novel therapeutic options for the treatment of inner ear disorders, but extensive testing for ototoxic effects

prior to evaluation of otoprotective effects is warranted. Systemic application of Compound A merits evaluation for otoprotective effects in trauma models.

Prevention of Hearing Loss Due to Physical Trauma in the Cochlea by an Intracochlear Drug Delivery Implant

Erik Pierstorff¹; Mariana Remedios Chan¹; Yen-Jung Angel Chen²; Federico Kalinec²; William Slattery¹

¹O-Ray Pharma, Inc; ²House Research Institute

Background

Cochlear implants have restored hearing in thousands of patients over the past two decades. However, because residual hearing is damaged in the process of cochlear implantation, this valuable procedure has been restricted to those patients with profound or total deafness. Many patients with severe hearing loss, a far larger group, are not currently implanted for fear of losing their residual hearing. As of December 2010, approximately 219,000 people worldwide had received cochlear implants. However, these numbers are increasing rapidly each year; Should a method be developed to allow implantation in patients with severe hearing loss but who retain some residual hearing, it is possible that as many as 10 times the number of patients might benefit from cochlear implantation. For this reason many investigators and the manufacturers of cochlear implants are investigating the possibility of developing implants to be used in the setting of residual hearing. There is evidence that the addition of a steroid at the time of implantation may allow preservation of residual hearing.

Methods

We have developed multiple extended release steroid formulations in various dose-ranges utilizing sustained release polymer formulations. To test their activity, our sustained release steroid formulations were implanted directly into the cochleae of guinea pigs in a cochlear implant trauma model sufficient to induce hearing loss.

Results

Pre- and post- treatment otoacoustic emissions and ABRs were performed to assess hearing. In all cases, significant hearing improvement was observed in ears administered steroid implants. Scanning electron microscopy was performed to determine if there were any effects of the drug on the structures of the cochlea.

Conclusion

These results demonstrate that our sustained release steroid formulations are safe and effective in preserving hearing from trauma induced in the cochlea. It is interesting to note that the drug treatment was added following the induction of trauma. Thus this drug formulation may be used in a cochlear implant to prevent hearing loss associated with implantation.

In Vivo Delivery of Atoh1 Gene to Rat Cochlea Using a Dendrimer-Based Nanocarrier

Nan Wu¹; Shi-ming Yang¹; Yan Wu²

¹Institute of otolaryngology, Chinese PLA general hospital;

²National center for nanoscience and technology

Background

Gene therapy is a promising clinical solution to hearing loss. However suitable gene carriers for the auditory system are currently unavailable. Given the unique structure of the inner ear, the route of delivery and gene transfer efficiency are still not optimal at present.

Methods

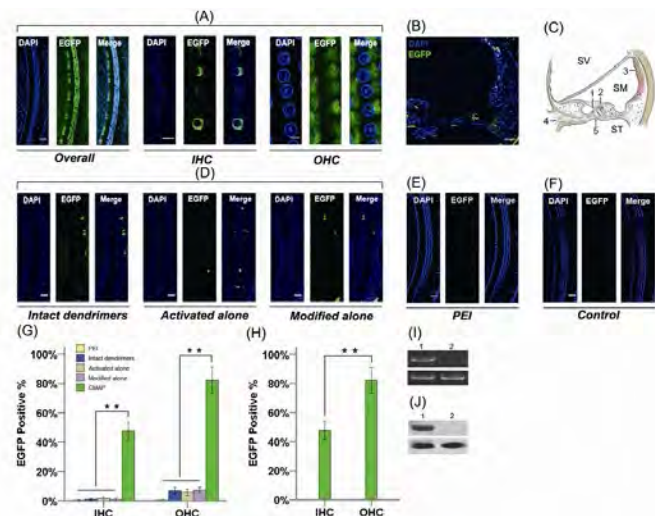
We treated polyamidoamine (PAMAM) dendrimers by activating and modifying with Na-carboxymethyl- β -cyclodextrins (CM- β -CD) in sequence. A novel gene carrier (CM- β -CD modified activated PAMAM dendrimers, CMAP) was then constructed. CMAP nanoparticles could bind pRK5-Atoh1-EGFP plasmids to form vector-DNA complexes (dendriplexes). Then these dendriplexes were locally applied on the round window membrane to *in vivo* deliver Atoh1 gene to rat cochlea. The results of transfection were determined by detecting green fluorescence seven days after inoculation. At the same time, auditory brainstem response (ABR) was determined to evaluate the safety.

Results

The dendriplexes (CMAP-pRK5-Atoh1-EGFP) has a mean particle size of 132 ± 20 nm and zeta potential of 31 ± 3 mV. These dendriplexes could be delivered to the inner ear by passive gradient permeation through intact round window membrane. A relatively selective gene transfer with high efficiency was achieved in the auditory hair cells but not much in other cell types in the cochlea. The transfection efficiencies in IHCs and OHCs were $47.57 \pm 6.68\%$ and $82.14 \pm 9.67\%$, respectively. ABR determination indicates good tolerance.

Conclusion

In this study, a novel CMAP nanocarrier based on PAMAM dendrimers was constructed and used to deliver Atoh1-EGFP genes to rat cochlea by topical administration *in vivo*. The results indicated that this non-viral delivery system was highly efficient and exhibited low toxicity to auditory epithelia. The strategies of constructing a CMAP nanocarrier, together with an atraumatic delivery route of permeation through intact RWM, provided a potential solution to transfect auditory system.



Gene expression in the cochlea seven days after introduction. Group of CMAP dendriplexes treatment (A-B): (A) Representative confocal fluorescence microscopy images of the basilar membrane in the surface mount samples. Scale bar = 50 μ m for overall; 10 μ m for IHC and OHC. (B) A typical image of gene expression in the whole cochlea in cryosection samples. Scale bar = 50 μ m. (C) Schematic diagram of gene expression in the cochlea: (1) IHCs; (2) OHCs; (3) stria vascularis; (4) spiral ganglion cells; (5) mesothelial cells beneath Corti's organ; (SV) scala vestibule; (SM) scala media; (ST) scala tympani. (D) Groups of intact/activated/modified PAMAM dendriplexes treatments. Scale bar = 50 μ m. (E) Group of PEI polyplex treatment. Scale bar = 50 μ m. (F) Control group (inoculation of artificial perilymph using the same method). Scale bar = 50 μ m. (G) Comparison of transgenic efficiency among PEI (n=5), intact PAMAM dendrimers (n=5), activated only (n=5), modified only (n=5), and CMAP (n=7, ** p<0.01). (H) Difference in transgenic efficiencies between IHCs and OHCs treated with CMAP dendriplexes (n=7, ** p<0.01). (I) RT-PCR tests: CMAP dendriplex treatment (lane1); negative control (lane2). (J) Western blot analysis: CMAP dendriplex treatment (lane1); negative control (lane2).

Evaluation of the impact on hearing function. ABR thresholds were monitored before and after inoculation (seven days) of artificial perilymph (control group), PEI polyplexes, and CMAP dendriplexes. CMAP group (n=7) shows a significantly smaller increase than PEI (n=5, * p<0.05). PEI group shows a significant increase in ABR threshold (n=5, ** p<0.01) compared with the control group (n=5), whereas CMAP group shows no difference (n=7, p>0.05). No significant increase in post-operative ABR threshold was detected in the control group (n=5, p>0.05).

Dose Dependent Threshold Rescue Using Antisense Oligonucleotides in Usher Mice

Abhilash Ponnath¹; Francine Jodelka²; Anthony Hinrich²; Hamilton Farris¹; Nicolas Bazan¹; Frank Rigo²; Michelle Hastings²; Jennifer Lentz¹

¹LSUHSC; ²RFU

Background

Combined deaf-blindness is a hallmark of Usher syndrome (Usher). Patients with type 1 Usher suffer congenital sensorineural hearing impairment, vestibular dysfunction, and

adolescent-onset of retinitis pigmentosa. A cryptic splice site mutation (216G>A) in *USH1C*, which encodes the protein harmonin, is responsible for Usher in Acadian patients. Mutant mice carrying two copies of the 216G>A mutation (216AA) are profoundly deaf, and have vestibular and retinal dysfunction similar to patients. Treatment with a single systemic dose of antisense oligonucleotides (ASOs) a few days after birth partially corrects splicing and protein expression in the cochlea, improves OHC stereocilia organization and rescues cochlear hair cells, vestibular function and hearing function.

Methods

Varying concentrations ASOs were administered five days after birth and responses to acoustic stimuli were measured by auditory-evoked brainstem response (ABR) at 1 month of age.

Results

Although hearing thresholds at low frequencies (8 kHz) were the same for all concentrations tested, they were significantly lower than mutant control mice. However, a dose dependent threshold rescue was observed for mid (16 kHz) and high (32 kHz) frequencies. Circling behavior was not observed at all ASO concentrations tested. Longevity of therapeutic effect, as well as, correlations to *Ush1c* splicing and protein expression will be determined.

Conclusion

These results show that ASO technology may become a major therapeutic strategy for congenital hearing impairment.

PS - 716

A Fully Integrated Inner Ear Drug Delivery System With Programmable Reciprocating Flow for Timed Dosage

Vishal Tandon¹; Wooseok Kang¹; Ernest Kim²; Abigail Spencer²; Erin Pararas²; Michael McKenna¹; Sharon Kujawa¹; Mark Mescher²; Jason Fiering²; William Sewell¹; Jeffrey Borenstein²

¹Massachusetts Eye and Ear Infirmary; ²Draper Laboratory

Background

Sensorineural hearing loss is the most prevalent auditory disorder, often treated with cochlear prostheses that can only partially restore hearing function. Advances in the molecular biology of hearing show promise for drug-based approaches to treating and preventing hearing loss, with potential for regeneration of hearing function. Due to the toxicity, instability, and poor targeting associated with these drugs when delivered systemically, methods for long-term local delivery with an implantable device will likely be necessary. Here we report on advances in our micromechanical system for intracochlear delivery that integrate microfluidics and control hardware in a miniaturized package.

Methods

We previously presented a drug delivery platform comprising a micropump designed to be worn by guinea pigs for acute and chronic experiments. Our next generation miniaturized system integrates microfluidic channels patterned in lam-

inated layers of polyimide films, valves consisting of membranes that are deflected to block or actuate flow, miniaturized electromagnetic actuators that operate the valves and pumps, and control circuitry. The platform is arranged with a pumping chamber connected fluidically to four ports with normally-closed valves; a drug reservoir, a fluid source, and a cannula that is implanted in the cochlea. The pumping chamber is actuated in a peristaltic sequence with any two valves, resulting in controlled flow along a chosen path. This push-pull system is highly adaptable, enabling modes of direct drug infusion, reciprocating flow, and drug dilution. In addition to push-pull delivery, we are also developing simpler direct infusion systems constructed from commercially available micropumps for some of the animal studies.

Results

The platform is ultimately intended to be implantable in humans for treatment of auditory disorders. It is currently designed as a head mount for guinea pigs, and has a footprint of 30 mm x 40 mm x 9 mm. Laboratory testing confirms that the system delivers precise, reciprocating flow to the cochlea apically at rates that avoid damage to hair cells. DNQX, a glutamate receptor antagonist that affects compound action potentials but not distortion product otoacoustic emissions, provides a tool to examine efficacy and safety of drug delivery.

Conclusion

Further miniaturization of our system will bring it closer to the requirements for a human implant. Such a platform enables pharmacokinetic characterization of acute and chronic effects of biomolecular reagents on hearing function *in vivo*, ultimately leading to hearing loss treatment strategies for humans.

PS - 717

Impact of Kv3 Channel Modulator AUT3 on Auditory Temporal Resolution in Rats

Natalia Rybalko¹; Jiri Popelar¹; Daniel Suta¹; Charles H. Large²; Josef Syka¹

¹Institute of Experimental Medicine ASCR; ²Autifony Therapeutics, Imperial College Incubator, London, UK

Background

Voltage-gated K⁺ channels of the Kv3 subfamily enable fast firing of many central neurons and are strongly expressed in the central auditory system. However, they have been shown to decline with age (von Hehn et al., 2004), which could contribute to age-related auditory processing disorders including temporal auditory resolution deficits. In the present study, the effect of AUT3 (a novel drug positively modulating Kv3 channels) on auditory temporal resolution was examined in Fischer 344 (F344) rats. F344 rats are known to suffer an accelerated age-related decline in hearing performance (Syka, 2010). Evaluation of the temporal resolution was based on the measurement of ability to detect silent gaps in noise using a behavioral gap-prepulse inhibition paradigm.

Methods

The effect of AUT3 was examined in aged (19-21-month-old) and young adult (3-4 month-old) F344 rats, using the acoustic startle response (ASR) recording. Amplitude of ASR and pre-

pulse inhibition of ASR induced by gap (gap-PPI) were measured before and after AUT3 administration (30 or 60 mg/kg or vehicle, i.p.) using a cross-over design with at least 7 days between dosing sessions. 110 dB SPL broad-band noise bursts were used as startling stimuli; gaps from 5 to 50 ms, embedded in 65dB broad-band noise, served as prepulse stimuli. Hearing thresholds were assessed prior to the first drug administration and at the end of the study from auditory brainstem responses.

Results

In the control condition aged rats showed significantly smaller ASR amplitudes and weaker gap-PPI compared to the young-adult rats. The effect of AUT3 on the ASR depended on AUT3 dose. AUT3 at 60mg/kg significantly reduced ASR amplitude in both age groups while neither vehicle nor 30mg/kg dose of AUT3 affected ASR. The effect of AUT3 on gap-PPI was determined by age. Both tested doses of AUT3 significantly, but temporarily, increased the gap-PPI efficiency in aged rats, but did not alter gap-PPI in young rats. Hearing thresholds were unaffected by AUT3 administration.

Conclusion

The deficit of gap-PPI indicates worsening of temporal resolution in aged F344 rats, similar to the deficits seen in aged humans. AUT3 significantly improved auditory temporal processing in the aged rats. These results suggest that AUT3, via positive modulation of Kv3 channels, has potential in the treatment of age-related hearing impairment.

PS - 718

AAV1-Mediated Postnatal Pendrin Expression in the Scala Media of *Slc26a4* Null Mice Partially Restores Hearing Thresholds in the Mutant Mice

Jianjun Wang; Qing Chang; Qi Li; Binfei Zhou; Susan Wall; Xi Lin

Emory University School of Medicine

Background

Mutations in the *SLC26A4* gene (coding for Pendrin protein) is the cause of the most common form of human syndromic deafness, the Pendred syndrome, accounting for 5-10% of all cases of congenital deafness. Major symptoms are congenital bilateral sensorineural hearing loss and goiter. Currently no treatment is available. We used *Slc26a4*^{-/-} mouse model to test a promising new gene therapy approach for this disease.

Methods

Slc26a4 genetagged with myc tag was inserted into adeno-associated virus (AAV) backbone plasmid with chicken- β -actin promoter. The AAV plasmids were packaged into AAV2/1 viruses (AAV2/1-*Slc26a4*-myc). About 1.0 μ l virus solution of AAV2/1-*Slc26a4*-myc was injected into the scala media of the left cochlea of newborn mice (P0-P2), while the right cochlea was injected with 1.0 μ l AAV2/1-GFP virus solution. We confirmed that the injection procedures we used didn't damage hearing in wild type mice. Whole-mount immunostaining in the cochlea of *Slc26a4*^{-/-} mice was performed to find out the cellular expression of *Slc26a4* at 8, 30 and 60 days after in-

jections. Auditory brainstem response (ABR) was measured to determine the hearing thresholds at various frequencies ranging from 4 to 32 kHz.

Results

AAV viruses were prepared with a high titre (1.50×10^{13} genome copy/ml). Immunolabeling revealed that the virally-mediated expression of *Slc26a4* in the *Slc26a4*^{-/-} mice was in the Deiters' cells, Hensen's cells, Claudius cells, outer sulcus cells and spindle-shaped cells, and the expression lasted for at least two months. Measured at one and two months after injections, we found that the ABR thresholds of the ears injected with AAV2/1-*Slc26a4*-myc was significantly lower than the ears injected with AAV2/1-GFP. At 4 and 8 kHz, the hearing improvement was about 10 dB. Near the injection site the injected ear showed about 20 dB improvement in the ABR threshold at 12 kHz.

Conclusion

Gene transfer of AAV2/1-mediated *Slc26a4* partially rescued the hearing in the *Slc26a4*^{-/-} mice. We are currently performing viral injections at embryonic stages to test if the hearing could be further improved by making the exogenous *Slc26a4* gene transfer earlier.

PS - 719

Neurotrophin Delivery Using Nanoengineered Mesoporous Silica Particles for Spiral Ganglion Neuron Survival in the Deaf Cochlea

Andrew Wise¹; Justin Tan¹; Yajun Wang²; Frank Caruso²; Robert Shepherd¹

¹Bionics Institute; ²University of Melbourne

Background

Spiral ganglion neurons (SGNs) in the deafened cochlea undergo continual degeneration ultimately leading to cell death. The exogenous application of neurotrophins can prevent SGN loss. However, a significant barrier to the potential clinical translation of neurotrophin-based therapies is the lack of a clinically relevant delivery technique that is safe and effective. We have examined the use of mesoporous silica particles to deliver Brain Derived Neurotrophic Factor (BDNF) at therapeutically effective levels necessary for SGN survival in the deafened guinea pig.

Methods

Adult guinea pigs (n=11) were deafened with ototoxic aminoglycosides and, one week later, bilaterally implanted with drug-delivery particles via a cochleostomy into the scala tympani. One ear received particles (n=7) that were loaded with BDNF (~1.33 μ g per particle) and the other ear received control (unloaded) particles. Two animal cohorts were used. One cohort was implanted for four weeks and the other cohort for eight weeks. Cochleae were collected and sectioned for histological analysis. The density of SGNs throughout the cochlea was determined in mid modiolar sections. The extent of fibrotic tissue response within the scala tympani was also measured.

Results

Analysis of SGN density showed a significantly greater density of SGNs in cochleae that were implanted with BDNF-loaded particles compared to the contralateral cochleae that were implanted with control (unloaded) particles (repeated measures ANOVA, $p < 0.05$). Analysis of the tissue response to implantation of particles showed a small but significant increase in the extent of fibrotic tissue in cochleae implanted with BDNF-loaded particles compared to cochleae implanted with control particles (repeated measures ANOVA, $p < 0.05$).

Conclusion

This study has shown that the use of nanoengineered mesoporous silica particles for BDNF delivery was effective in protecting SGNs from deafness-associated degeneration in the deafened guinea pig. The particles were well tolerated when chronically implanted for a period of up to eight weeks, with a small but significant increase in tissue response observed in the neurotrophin-treated cochlea. The outcome of this study indicates that mesoporous silica particles can provide therapeutic levels of neurotrophins for nerve survival in a safe and effective manner and has the potential to be used in a clinical setting to protect SGNs and/or residual hearing following cochlear implantation.

PS - 720

Development of Cartilage Conduction Hearing Aid (4) –Electromagnetic Cartilage Conduction Transducer–

Ryota Shimokura¹; Hiroshi Hosoi¹; Tadashi Nishimura¹; Takashi Iwakura²; Toshiaki Yamanaka¹

¹Nara Medical University; ²Rion Co., Ltd.

Background

In 2004, professor Hosoi found that clear sound can be heard when a transducer touches softly on an aural cartilage. From the basis for the idea, a trial model of the cartilage conduction hearing aid has been completed. The cartilage conduction hearing aid is suitable for patients who can not insert an existing earplug of a hearing aid in his/her ear canal because of particular disorders such as atresia of the canal, severe otorrhea, and so on.

In the basic and clinical researches, the a piezoelectric bimorph covered by elastic material has been used as a transducer because of the high crashworthy. However, the bimorph transducer consumes much electric power in the control circuit and restricts flexural amplitude. Therefore, to resolve the disadvantages, our research group has developed an electromagnetic cartilage conduction transducer. Consequently, the power consumption could be reduced in the same standard as general speakers, and the high input voltage realizes the larger driving amplitude. In this study, the vibration and acoustical properties were compared among the previous bimorph transducer and new electromagnetic transducer.

Methods

For the vibration, the outputs from an artificial mastoid (Type 4930, B&K, Denmark) were compared. An oscillator and amplifier generated a swept sine signal, and it input to the bi-

morph or electromagnetic transducer. The output convolved with the inversed swept signal showed the spectral characteristics of the vibration.

For the acoustic, the generated sounds in the external auditory canal were compared. The measurement in the canal was carried out using a small microphone introduced in general hearing aids (FC-23453-C05, Knowles Electronics, US). The input signal and generators were same as the vibration measurements.

Results

The vibration of the electromagnetic transducer was much larger than that of the bimorph transducer especially in the lower frequency range than 2 kHz. The peak of vibration was around 500 Hz, and the difference was about 50 dB in this frequency range. Consequently, the sound generated in the canal was also much larger for the electromagnetic transducer below 2 kHz. The difference was about 30 dB around 500 Hz. The battery life of one zinc-air battery (PR44, Rion, Japan) was much expanded until 120 hours for the electromagnetic transducer compared with the bimorph transducer (3 hours).

Conclusion

The electromagnetic transducer was superior according to the vibration, acoustical and battery life performances. The next challenge for the practical use is to improve the crashworthy of it.

PS - 721

Effect of Middle-Ear Pathology on High-Frequency Ear-Canal Reflectance Measurements in the Frequency and Time Domains

Gabrielle Merchant¹; Jonathan Siegel²; Stephen Neely³; John Rosowski⁴; Hideko Heidi Nakajima⁴

¹Speech and Hearing Bioscience and Technology, Harvard-MIT Division of Health Sciences and Technology; ²Northwestern University; ³Boys Town National Research Hospital; ⁴Massachusetts Eye and Ear Infirmary, Harvard Medical School

Background

Wideband acoustic immittance measurements are non-invasive measures of middle-ear mobility over a wide frequency range. These measurements allow for the calculation of ear-canal pressure reflectance or directly related quantities such as absorbance. These quantities have been characterized in a variety of patient populations as well as in temporal bone experiments. Collectively, these data suggest that wideband reflectance shows potential utility in the non-invasive differential diagnosis of middle-ear and some inner-ear pathologies. However, due to frequency limitations in commercially available devices, immittance and reflectance have not been well described at frequencies above 6-8 kHz. Additionally, analyses of these measurements have focused on the responses to stimulus frequencies below 3-4 kHz, while ignoring high-frequency or time-domain information. This work uses a novel approach to measure reflectance that utilizes

high-frequency signals and analyzes reflectance in both the frequency and the time domains.

Methods

To accomplish these tasks we used a custom built sound source (the HARP system designed by author JHS) in consort with an ER-10B probe tube microphone (Etymotic Research). This custom acoustic system delivers stable high-frequency sounds with little crosstalk between the stimulus generator and the microphone signals. Experiments were performed with fresh normal human temporal bones before and after simulating various middle-ear pathologies. This preparation allowed for the serial introduction of well-controlled pathologies whose effects could be readily compared to the initial normals. Several of the pathologies could also be reversed.

Results

Reflectance measurements were made at frequencies as high as 20 kHz, and our time domain analysis allowed us to inspect the impulse response of the reflectance over the initial few milliseconds of the response with a temporal resolution of 0.025 ms. Preliminary data analyses show consistent results below 4 kHz with similar data acquired with a commercially available reflectance system. Additionally, there are changes at higher frequencies that seem to be real and reversible, but that vary between specimens. Finally, time domain data for normal middle ears appear to be quite consistent across specimens.

Conclusion

High-frequency measurements improve temporal resolution of reflectance measurements. The utility of the high-frequency measurements and temporal analysis in diagnosis of pathology will be assessed.

PS - 722

Effect of Ossicular Discontinuity on Mechanics and Audiometry

Rosemary Farahmand¹; Sarah Lookabaugh¹; Gabrielle R. Merchant²; Christof Roosli³; Cagatay H. Ulku⁴; Christopher H. Halpin¹; John J. Rosowski¹; Hideko Heidi Nakajima¹

¹Massachusetts Eye and Ear Infirmary, Harvard Medical School; ²Speech and Hearing Bioscience and Technology, Harvard-MIT Division of Health Sciences and Technology;

³Clinic of Otorhinolaryngology-Head and Neck Surgery, University Hospital Zurich, Zurich, Switzerland; ⁴Department of Otorhinolaryngology - Head and Neck Surgery, Meram School of Medicine, Necmettin Erbakan University, Konya, Turkey

Background

Ossicular discontinuity may be complete, with no contact between the disconnected ends, or "partial," where normal contact at an ossicular joint or along a continuous bony segment of an ossicle is replaced by soft tissue. These soft tissue connections vary widely from flaccid mucosal bands to stiffer, fibrotic connections. Because of the proximity of the disconnected ends and the space-filling soft tissue, identification of partial disarticulations may be difficult during surgery, and other means of diagnosis would be valuable.

It has been proposed that the two types of ossicular discontinuity result in different frequency-dependences of ossicular output, and different patterns of audiometrically determined conductive hearing loss. We wish to determine the validity of this proposal, and better understand the mechanics underlying conductive hearing loss.

Methods

We analyzed audiograms from patients with various forms of surgically-confirmed ossicular discontinuity. We also analyzed umbo velocity and reflectance measurements from a subset of these patients. Finally, we performed experiments on fresh temporal bone specimens to study the differing mechanical effects of complete and partial discontinuity. We simulated partial discontinuity using a compliant material to reunite the disconnected chain. The mechanical effects of these lesions were assessed via laser-Doppler measurements of stapes velocity.

Results

(1) Calculations comparing the air-bone gap (ABG) at high- and low-frequencies show that when high-frequency ABGs are larger than low-frequency ABGs, the surgeon usually reported soft tissue bands at the point of discontinuity. However, some partial discontinuities as well as complete discontinuities were reported in cases with larger low-frequency ABGs and flat ABGs across frequencies. (2) Analysis of umbo velocity in patients reveals no significant difference in magnitude and phase across frequencies between the two types of ossicular discontinuity. (3) On average, surgically-described complete ossicular discontinuity ears tend to have a larger energy reflectance notch (narrow-band decrease) in the 600-800 Hz frequency range than partial discontinuity ears. (4) Temporal bone experiments reveal that partial discontinuity results in a greater loss in stapes velocity at high frequencies as compared to low frequencies, whereas with complete discontinuity, large losses in stapes velocity occur at all frequencies.

Conclusion

Our findings suggest that when patients have a larger ABG at high frequency as compared to low frequency, partial ossicular discontinuity should be considered in the differential diagnosis.

PS - 723

Round Window Velocity by Bone Conduction in Cadaveric Specimens With Simulated Otosclerosis

Jeremie Guignard¹; Andreas Arnold²

¹Artificial Hearing Research, ARTORG Center, University of Bern, Switzerland and Eaton Peabody Lab, Mass. Eye and Ear Infirmary, Harvard Medical School, Boston MA.;

²Department of Otorhinolaryngology, Head and Neck Surgery, Inselspital, University of Bern, Switzerland

Background

Stapes fixation due to otosclerosis results in conductive hearing loss, and a loss in bone conduction (BC) hearing thresholds at certain frequencies (known as the Carhart's notch).

Previous reports suggest that there is a purely mechanical component in the worsening of the BC thresholds, in addition to sensorineural components. Middle ear surgery, and in particular fenestration of the bony cochlea wall (e.g. the stapes) is known to increase the BC thresholds in otosclerotic patients. The mechanisms of the influence of stapes fixation, stapedotomy/stapedectomy and stapes prostheses are still a subject of speculation. Objective measurements of the mechanical phenomena in whole cadaver heads might give new cues on the matter.

Methods

Laser Doppler vibrometry (LDV) was used to measure the velocity of the cochlear promontory (CP) and the surface of the round window (RW) in 5 ears of 4 embalmed whole-head specimens. The ears were stimulated with a Baha Intenso® BC hearing aid, with pure sinus tones logarithmically spread between 0.1 and 10kHz, repeated twice at -20, -30, and -40 dBVrms. Small patches of reflective tape were used to improve LDV signal. A complete set of measurements was made after each of the following manipulations: fixation of the stapes with bone cement, stapes fenestration (stapedotomy), insertion of a piston stapes prosthesis, stapedectomy, and insertion of a steel-wire connective tissue (Schuknecht) prosthesis. To reduce the variability due to change in laser beam angle between repeated measurements, the velocity of the RW was normalized to the one of the CP.

Results

Changes in average RW velocity could be observed for frequencies between 1 and 3 kHz, and especially near 2 kHz. Stapedotomy increased the average RW velocity by up to 5dB when compared to the fixed stapes situation, whether the piston prosthesis was inserted or not. Stapedectomy lowered the average RW and brought it back to the level of the fixed stapes. The insertion of the Schuknecht prosthesis lowered the average RW velocity of up to 3dB below the fixed stapes situation.

Conclusion

Our preliminary results suggest that variations in the amplitude of cochlear fluid motion may explain the improvement of the BC thresholds seen after stapes fenestration in otosclerotic patients.

PS - 724

Efficiency of Cochlear's Direct Acoustic Cochlear Stimulator (Codacs) Actuator in Different Coupling Modes

Martin Großhörmichen; Rolf Salcher; Robert Schuon; Thomas Lenarz; Hannes Maier
Hannover Medical School

Background

The Codacs (Cochlear's Direct Acoustic Cochlear Stimulator, Cochlear) is an actuator which is intended for inner ear stimulation with a K-Piston through the stapes footplate (SFP) after a stapedotomy. However, further application, stimulating middle ear structures are possible. Here, the actuator applicabil-

ity and efficiency under alternative coupling conditions was investigated

Methods

Beside the standard K-Piston application (N = 11) three alternative stimulation sites were tested with the Codacs in cadaveric human temporal bones. These included stapes head stimulation with a "Bell prosthesis" (N = 9), SFP stimulation with an "Omega connector" (N = 8) and reverse round window (RW) stimulation (N = 11). In all alternative conditions the axial coupling force was adjusted to ~ 5 mN. TB selection and actuator output determination were conducted in analogy to the ASTM standard F2504-05. Stimulation responses were measured at the SFP and the RW with a Laser Doppler Velocimeter. Based on the obtained response the Codacs equivalent sound pressure output level [dB SPL] was calculated.

Results

Over the entire investigated frequency range (0.125 to 10 kHz) the average outputs in all conditions were flat within a range of maximally 23.5 dB (Figure 1), usually having a peak at the actuator resonance (~ 2 kHz). The mean (0.5, 1, 2, 3, 4 kHz) outputs at 1 V_{RMS} were 117 dB SPL (RW), 141 dB SPL (Bell (SFP)), 133 dB SPL (Bell (RW)), 134 dB SPL (Omega) and 115 dB SPL (K-Piston). Whereas RW stimulation provided an output similar to the standard K-piston application, the other stimulations modes using the SFP as input site were more efficient. Comparing results of the "Bell coupling" measured at both reference sites (SFP and RW) were in good accordance to each other with a maximum difference of ~ 11 dB.

Conclusion

All sites investigated for alternative coupling possibilities provided sufficient output for hearing aid applications when the stimulation was performed at controlled axial force. The results demonstrate the possibility of using the Codacs at alternative stimulation sites with sufficient output, provided experimental conditions are adapted to the "real" situation including geometric issues and the constant force condition. The similarity of both "Bell coupling" results shows that the RW as well as the SFP are adequate references to estimate the equivalent output in stapes stimulations.

Codacs Equivalent Soundpressure Mean Values in Different Conditions

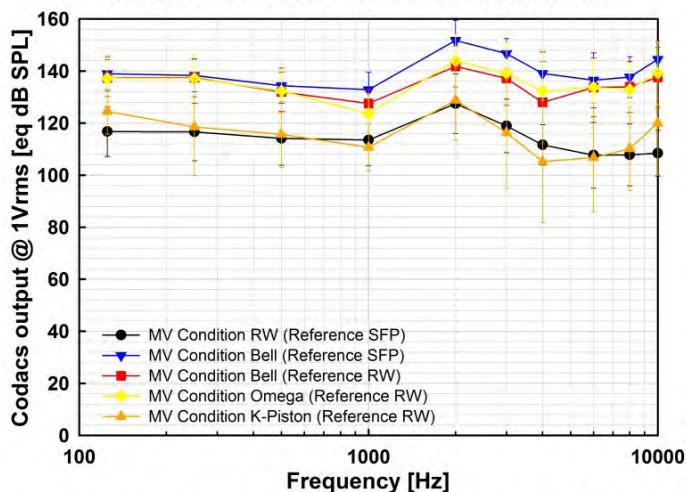


Figure 1: Mean values (MVs) of the Codacs output @1V_{RMS} [equivalent dB SPL] in the four different conditions. Output references are given in the legend. The error bars represent the standard deviations.

PS - 725

Does Eustachian Tube Angulation Correlate With Otitis Media?

N Wendell Todd; Celsha Ukatu

Emory University

Background

The route of the Eustachian tube lumen is described as straight in patients with otitis media, but angulated in persons without otitis media. The description is from studies that utilized luminal cast impressions, with subsequent tissue removal.

Methods

From a group of 41 clinically ear-normal cadavers, the five crania with the largest mastoid pneumatization and the five with smallest mastoid pneumatization were selected for clinical CT imaging. To contrast these extremes of nil otitis media in childhood versus those quite likely to have had otitis media in childhood, Eustachian angulations were determined in the plane defined by the ends of the bony and cartilaginous lumina.

Results

The bony-cartilaginous Eustachian tube intercept angle was not related to the mastoid size indicator of childhood otitis media: large mastoids, right side, median 18.3 degrees, range 15.0 to 43.8; small mastoids, right side, median 23.4, range 11.3 to 30.6; large mastoids, left side, median 17.9, range 8.8 to 28.0; small mastoids, left side, median 22.0, range 13.4 to 26.4. Bilateral symmetry of angulations was found: Spearman $r = .91$ (95% confidence interval .64 to .98).

Conclusion

Angulation of the lumina of the Eustachian tube seems unrelated to otitis media.

PS - 726

Positive Middle Ear Pressure Versus Ear Canal Pressure Variations: A Preliminary Study With Wideband Power Absorbance in Humans

Xiao-Ming Sun; Laina M. Burdick

Wichita State University

Background

Recent studies demonstrated differences and similarities between negative middle ear pressure (nMEP) and positive and negative ear canal pressure (pECP and nECP) in effect on otoacoustic emissions (Sun, 2012, *Ear Hear*) and wideband power absorbance (PA) measured in the ear canal (Sun & Shaver, 2013, ARO). We postulate that there are difference and similarity between positive middle ear pressure (pMEP) and ECP in effect on wideband PA.

Methods

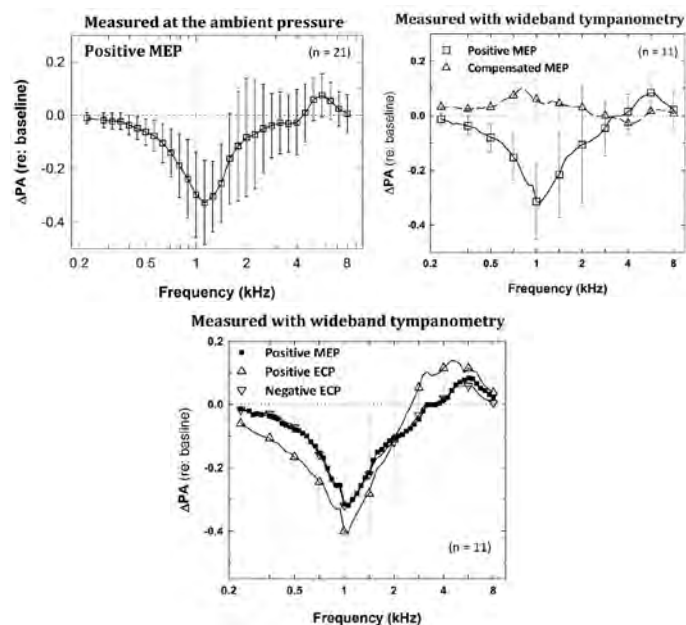
Data were collected from 23 normal-hearing adults using a wideband tympanometry research system (Interacoustics). Wideband PA was measured from ~0.223 to 8 kHz with two procedures: (1) at the ambient pressure ($n=21$); (2) with a tympanometry procedure, i.e., ECP swept from +200 to -300 daPa ($n=11$), under normal and pMEP conditions, respectively. Subjects produced pMEP by performing the Valsalva maneuver. MEP was estimated by a bandpass tympanogram peak pressure (BTPP). The effect of pMEP was defined as difference in PA between normal and pMEP conditions. Tympanometry data at BTPP under normal MEP was also subtracted from data with ECP manipulations under two MEP conditions to define three effects: compensation effect (PA at BTPP under pMEP) and pECP and nECP effects (PA at ECP = \pm pMEP, respectively, under normal MEP).

Results

Under pMEP (mean: 109.5 daPa), PA measured at the ambient pressure decreased for frequencies below 2 kHz (~0.33 at 1.1 kHz) and increased (up to 0.08) at 5 to 6 kHz. Similar PA changes by pMEP were shown when measured with the tympanometry procedure. The transition frequency for PA decrease and increase was at around 4 kHz. Difference in PA between the compensated and normal MEP conditions was small (<0.1). The PA changes by nECP and pMEP were similar for all frequencies. In contrast, pECP resulted in a larger reduction for low frequencies and larger enhancement for high frequencies (differences up to 0.1).

Conclusion

Positive MEP substantially alters PA in a frequency-specific pattern. Compared with nMEP data previously reported, pMEP produces slightly less (~0.05) changes of PA for both low and high frequencies. Both pMEP and nMEP are common in individuals and their effects should be accounted for in establishing clinical PA norms. Compensation of pMEP with an equivalent ECP effectively rectifies the altered PA. This procedure may help achieve a more reliable diagnosis of middle ear diseases in ears with a concurrent MEP. The effects of nECP and pMEP are comparable, whereas the pECP effect is larger for both low and high frequencies.



PS - 727

Test-Retest Reliability of Wideband Middle Ear Absorbance and Wideband Acoustic Stapedius Reflex Measures in Adults With Normal Hearing

M. Feeney¹; Douglas Keefe²; Lisa Hunter³; Denis Fitzpatrick²; Angela Garinis¹; Daniel Putterman¹; Garnett McMillan¹

¹Portland VA Medical Center; ²Boys Town National Research Hospital; ³Cincinnati Childrens Hospital

Background

Recent studies have demonstrated that wideband acoustic immittance (WAI) measures of middle ear function are more sensitive to middle ear disorders than traditional 226 Hz tympanometry in adults. Several studies have addressed test-retest reliability of WAI, but there have been no reports of test-retest reliability for measurements obtained at peak tympanometric pressure. The present study was part of a larger study evaluating a WAI test battery for the evaluation of middle ear and cochlear function in adults and children. Wideband absorbance was measured at ambient pressure (*Aa*) and at peak tympanometric pressure (*At*) for down-swept (*AtD*) and up-swept (*AtU*) absorbance tympanograms in adults with normal hearing. Test-retest reliability was also evaluated for a wideband absorbance measurement of the ipsilateral acoustic stapedius reflex threshold (ASRT) for broadband noise at peak tympanometric pressure in comparison with a clinical ASRT.

Methods

Thirty adults with normal hearing were recruited for the study. All subjects had normal puretone thresholds with air-bone gaps ≤ 10 dB and normal 226 Hz tympanometry. The experimental system consisted of an Interacoustics wideband tympanometry research system running custom software. *Aa*, *AtD*, *AtU* and ipsilateral ASRTs for broadband noise were

obtained for each subject on two visits separated by approximately 1 month.

Results

Test-retest repeatability was estimated for *Aa* and *AtD* and *AtU* by fitting a linear mixed model with measurement-type as a 3-level, categorical fixed effect and subject and subject-ear as hierarchical random effects. Residual variance, which estimates repeatability, was estimated separately for each measurement type. Models were fit separately to measurements taken at each test frequency. *AtD* tended to have the smallest residual variance (highest repeatability) across test frequency, although there was no statistically significant difference in repeatability compared to *Aa* or *AtU* at any frequency when corrected for multiple comparisons.

The same methodology was used to compare the repeatability of wideband ASRT to the clinical ASRT. Mean ASRTs were about 11 dB higher using the clinical method ($p < 0.001$). The residual variance of the wideband ASRT was significantly higher (i.e. lower repeatability) than the clinical ASRT ($p < 0.0001$). However, the clinical ASRT resulted in an absent reflex in 17% of ears compared to only 9% for the wideband ASRT.

Conclusion

In normal hearing subjects, the repeatability of *AtD* and *AtU* was comparable to that of *Aa*. The ipsilateral wideband ASRT for broadband noise was significantly lower than the clinical ASRT and resulted in fewer absent reflexes.

PS - 728

Gene Expression Studies: Correlation of Affymetrix® Gene Chip to QRT-PCR Results in the Mouse Middle and Inner Ear

Fran Hausman; Carol MacArthur; J Beth Kempton; Dongseok Choi; Katherine D Shives; Dennis Trune OHSU

Background

The qRT-PCR technique and, more recently, microarray gene chips are often used to assess gene expression in tissues of interest. However, few studies exist that compare PCR gene expression results with those from gene chip technology. Therefore, we performed a comparison of fold change results in murine inner and middle ear tissues in three groups of animals from our Affymetrix® and PCR libraries: A) Inner ear gene fold change after transtympanic steroid treatments (dexamethasone - Dex or prednisolone - Pred); B) inner and middle ear gene fold change after bacterial (*Hemophilus influenza*) challenge to the middle ear; and C) inner ear gene fold change in autoimmune mice with and without prednisolone treatment.

Methods

For each method of analysis of fold change, tissue was harvested for mRNA using the identical protocol from middle and inner ear tissues at 6 hours after steroid or bacterial treatment. Untreated mice were used as controls. A total of 8-16 mice were used for each group. Middle ear and inner ear mRNA was processed for quantitative analysis of 8 inflam-

matory cytokine genes (IL-1 α , IL-1 β , IL-6, IL-10, Ccl3, Cxcl2, TNF α , Cxcl1), and 24 ion homeostasis genes (Slc12a2, Atp1b2, Atp1b1, Clcnka, Atp1a1, Cldn3, Cldn4, Cldn14, Gjb2, Gja1, Gjb3, Gjb6, Aqp1, Aqp2, Aqp3, Aqp5, Kcne1, Kcnq1, Kcnq4, Kcnj10, Scnn1a, Scnn1b, Scnn1g, Tmprss3). The method utilized custom PCR arrays, or, the Affymetrix® 430.2 Gene Chip. Fold change of these cytokine and ion homeostasis genes obtained by Affymetrix® and PCR methods were compared. Statistical correlations of gene expression between the two methods were determined by regression analysis for middle and inner ear results.

Results

Comparison of the Affymetrix® and qRT-PCR results showed high correlation between the two methods of gene analysis: A. Inner ear tissues after steroid treatments (Dex: R = 0.878, prob = 0.0000000017; Pred: R = 0.989, prob = 2.49 e-22); B. Middle and inner ear tissues after bacterial exposure (Middle ear R = 0.988, prob = 6.9 e-26; Inner Ear: R = 0.9658, prob = 3.89 e-19); C. Autoimmune mouse inner ear tissues (no treatment: R = 0.894, prob = 5.39 e-12; prednisolone treatment: R = 0.8259, prob = 5.83 e-9).

Conclusion

These results reveal a strong correlation between the two methods of assessing gene expression in the middle and inner ear. These findings support the validity of the gene chip technology when compared to the more traditional qRT-PCR.

PS - 729

Non-Typeable Hemophilus Influenza (NTHi) Bacteria Induces Early Inflammation and Potent Mucin Gene Expression in Mouse Middle Ear Epithelial Cells

Stéphanie Val; Katelyn Burgett; Humaira Mubeen; Mary Rose; Diego Preciado

Children's National Medical Center

Background

Otitis Media (OM) is one of the most common conditions characterized by middle ear infectious inflammation that leads to persistent mucoid effusions, characteristic of chronic OM. Non-typeable Hemophilus influenza (NTHi) is the most common pathogen cultured in middle ear disease progression.

This study aims at investigating the mechanisms of Muc5b mucin induction in middle ear epithelium in response to NTHi infection, focusing on NF- κ B transcription factor activation as a potential mediator.

Methods

We used proteomics in children ear effusions, mouse trans-tympanic inoculation experiments and cultures of transformed mouse middle ear cells (mMEEC) in submerged or air liquid interface (ALI) conditions. RNAs were assayed with RT-qPCR, histology was performed with mouse middle ear, immunofluorescence, Western Blot and ELISA for p65 localization. Promoter activation was evaluated using a reporter plasmid containing Muc5b, Muc5ac or 3 NF- κ B binding domains.

Results

Previous results from our group showed that ear effusions from chronic OM patients were characterized by an overproduction of MUC5B whereas MUC5AC was less predominant. *In vivo* experiments showed that mice inoculated with NTHi lysates in the ear have a mucosal metaplasia of the middle ear observed in histologic sections, associated with a high upregulation of Cxcl2 mRNA when live NTHi are inoculated. *In vitro* challenge of mMEEC in submerged or ALI conditions with NTHi lysates during 24hrs and 48hrs demonstrated dose and time dependent upregulation of Cxcl2 and Muc5b mRNA using qPCR. Interestingly, the expression of the other mucin Muc5ac, and an NF- κ B oxidative stress response enzyme, Ho-1, are also markedly up-regulated by NTHi lysates in these cells. Investigations into the mechanisms underlying these effects revealed that NTHi lysates potently induce the Muc5b and Muc5ac promoters, and that NF- κ B translocated into the nucleus from 30 min to 6 hrs after NTHi lysates exposure, effect verified by western blot analysis and p65 subunit ELISA assay in nuclear and cytoplasmic extracts. An experiment using a reporter plasmid containing 3 NF- κ B binding domains showed that NTHi lysates increase NF- κ B binding to its responsive elements in the nucleus.

Conclusion

In conclusion, NTHi induces Muc5b and Cxcl2 expression and protein production in different biological models, and NF- κ B is implicated in this effect: it translocates to the nucleus in response to NTHi lysates at early times of exposure and binds to its specific DNA sequence. This work is being developed to better understand the mechanisms leading to OM induced by NTHi bacteria.

PS - 730

Localization and Proliferation of Lymphatic Vessels in the Tympanic Membrane

Takenori Miyashita¹; James L. Burford²; Young-Kwon Hong³; Haykanush Gevorgyan²; Lisa Lam²; Nozomu Mori¹; Janos Peti-Peterdi²

¹Department of Otolaryngology, Faculty of Medicine, Kagawa University; ²Department of Physiology and Biophysics and Department of Medicine, Zilkha Neurogenetic Institute, Keck School of Medicine, University of Southern California; ³Department of Surgery and Department of Biochemistry and Molecular Biology, Norris Comprehensive Cancer Center, Keck School of Medicine, University of Southern California

Background

Lymphatic vessels are an important part of the immune system, and the presence of abundant lymphatic vessels in the auricle and external auditory canal has been reported. Lymphatic vessels drain interstitial fluid and thereby guide interstitial flow, which has been identified as an important organizing factor in lymphangiogenesis, and lymphatic circulation is important for wound healing and prevention of edema and infection. Although lymphatic vessels have been suggested as an important organizing factor in pathological conditions of the tympanic membrane, localization in the tympanic membrane has not been established.

In this study, we focused on localization of the lymphatic vessels in the tympanic membrane, and the regenerative response after perforation of the tympanic membrane, by using whole-mount imaging of the tympanic membrane of Prox1 GFP mice.

Methods

Prox1-GFP BAC transgenic mice were deeply anesthetized using ketamine and xylazine and perfused via the left ventricle with a fixative solution (4% paraformaldehyde in PBS). The tympanic membrane on both sides was dissected carefully under a stereomicroscope. The brain and cochlea were also collected. The tympanic membrane and the cochlea were then decalcified. The tympanic membrane and the cochlea were examined using a 2-photon laser scanning fluorescence microscope. Images were collected as a z-series file and analyzed with Leica LCS imaging software.

Results

Many lymphatic vessel loops were detected in the pars flaccida, whereas no lymphatic vessel loops were observed in the greater part of the pars tensa in the normal tympanic membrane. In the pars tensa, lymphatic vessel loops were located around the malleus handle and annulus tympanicus. Lymphatic vessel loops surrounding the malleus handle were connected to the lymphatic vessel loops in the pars flaccida. Lymphatic vessel loops in the pars flaccida were connected to the lymphatic vessel loops surrounding the tensor tympani muscle or annulus tympanicus.

To observe lymphatic regeneration in the healing tympanic membrane, we used an animal model of acute tympanic membrane perforation. Almost no lymphatic regeneration was observed at day 1 and day 4. At day 7, abundant lymphatic regeneration was observed in the pars tensa, where almost no lymphatic vessels were observed in the normal tympanic membrane.

Conclusion

We demonstrated localization of the lymphatic vessels of the tympanic membrane, and lymphatic vessel response during regeneration of the tympanic membrane. These results suggest that site-specific lymphatic vessels play an important role in the integrity of the tympanic membrane.

PS - 731

Genomic-Based Identification of Novel Potential Biomarkers and Molecular Networks in Response to Diesel Exhaust Particles in Human Middle Ear Epithelial Cells

Moo Kyun Park¹; Jee Young Kwon²; Jae-Jun Song³; Byung Don Lee¹

¹Soonchunhyang University College of Medicine;

²Department of Life Science, Institute of Environmental Science for Green Chemistry, Dongguk University;

³Department of Otolaryngology-Head and Neck Surgery, Dongguk University Ilsan Hospital

Background

Recent epidemiologic studies showed that ambient particulate matter is associated with increases in the morbidity

and daily mortality caused by respiratory diseases. Among diverse constituents of ambient particulate matters, diesel exhaust particles (DEPs) have been recognized as a main constituent. A number of studies associated between exposures to DEPs and increased risk of respiratory diseases have been reported for the last decade. Otitis media (OM), the most common inflammatory disease of the middle ear cavity, has also been known to occur by DEPs. However, scientific evidences for DEPs-induced inflammation are not sufficient yet. In this study, we firstly identified novel biomarkers and potential molecular signaling networks induced by DEPs in human middle ear epithelial cells (HMEECs).

Methods

The HMEEC was treated with DEP (60µg/ml) for 6h. Total RNA was extracted and used for microarray analysis. Molecular pathways among differentially expressed genes were further analyzed by using Pathway Studio 9.0 software

Results

Total 254 genes were differentially expressed in DEPs-exposed HMEECs. Among them, 86 genes and 168 genes were up-and down-regulated, respectively. In order to verify reliable biomarker and define meaningful signaling networks among the entire genome profiling, *in silico* approach was applied. We found several novel biomarkers such as SRC, MMP14, TP53, and EIF2AK3 as well as putative molecular signaling networks.

Conclusion

Our findings provide scientific evidences for establishment of novel mechanisms associated with DEPs-induced inflammation in airway HMEECs. These expression profile may provide a useful clue for the understanding of environmental pathophysiology of otitis media.

PS - 732

Visualizing Soft-Tissue in Human Temporal Bones Using MicroCT and PTA Staining

Jan Buytaert; Daniel De Greef; Johan Aerts; Joris Dirckx
University of Antwerp

Background

MicroCT is a very suitable and capable method for imaging the middle and inner ear morphology; that is, of the bony structures at least. Soft tissue however features a limited X-ray absorbance in comparison to bone, yielding low contrast in CT-reconstructions. The recent introduction of heavy element staining (Metscher et al. 2009) provides a possible remedy for this generic issue in high resolution imaging of biological tissue.

Methods

7 human temporal bones were obtained through collaboration with Cochlear, Belgium; stained with PhosphoTungstic Acid (PTA) and scanned with a custom-made high-resolution X-ray micro-Computed Tomograph.

2D image segmentation and 3D triangulation of the X-ray image datasets was achieved in the Amira 5.2 software package (Visualization Sciences Group, an FEI Company).

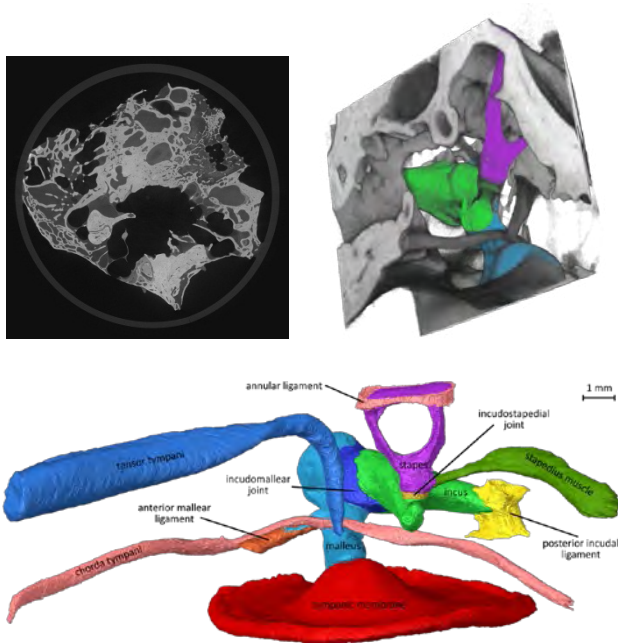
Results

From the 3D volume renderings of the 7 temporal bones with segmented structures, statistical data emerges with respect to:

- the existence, volume/shape and orientation of ligaments and muscles, some of which that are still under debate;
- the determination of hydraulic lever ratio of tympanic membrane surface area versus footplate surface area;
- the dimensions and thickness of the tympanic membrane and round window;
- the volume ratio of internal fluid filled channels versus the total ossicle volume;
- determination whether the ossicular joints have a fluid-filled joint cleft (and whether they are synovial, cartilaginous or fibrous);
- insights on the detailed structure of the lenticular process (blood vessel, debate around the 4th ossicle ...);
- the thickness of annular ligament in between the oval window and stapes footplate;
- estimates of the mucosa thickness on top of the ossicles and tympanic membrane;
- the shape and interspecimen variability of the manubrial fold or plica mallearis;

Conclusion

Through heavy element staining of soft tissue, microCT achieves high-resolution and contrast on mixed tissue type samples; here applied on 7 human temporal bones. Thus, unprecedented detail and quantified data becomes available on essential middle and inner ear features.



PS - 733

Effect of Mutations of PspA and PspC Proteins on Viability and Virulence of *Streptococcus Pneumoniae* in the Chinchilla Ear

Patricia Schachern Schachern¹; Vladimir Tsuprun¹; Patricia Ferrieri¹; David Briles²; Sarah Goetz¹; Sebahattin Cureoglu¹; Michael Paparella¹; Steven Juhn¹

¹University of Minnesota Medical School; ²University of Alabama

Background

There are approximately 13 million episodes of otitis media in the United States in children under five years of age and *Streptococcus pneumoniae* continues to be the most common bacterial agent. Bacterial resistance to antibiotics underscores the need for better vaccines. Pneumococcal conjugate vaccines are modestly protective against otitis media; however, limited serotype coverage and serotype replacement have led to the investigation of pneumococcal proteins as potential vaccine candidates. Two proteins, pneumococcal surface proteins A (PspA) and C (PspC), are important virulence factors and are expressed by virtually all strains. Although a number of pneumococcal proteins have been investigated in other organs, we previously found that they may have diverse organ-specific effects on the viability and virulence of pneumococci. In this study, we investigated the viability and virulence of single (PspA⁻ and PspC⁻) and double (PspA⁻/PspC⁻) mutant strains of pneumococcal PspA and PspC proteins in the chinchilla ear.

Methods

Chinchilla middle ears were inoculated with 0.5 ml of bacteria: 6 chinchillas with 2.3×10^6 CFU/ml wild-type; 6 with 3.5×10^6 CFU/ml PspC⁻; 6 with 1.6×10^6 CFU/ml PspA⁻; and 6 with 1.4×10^6 CFU/ml PspA⁻/PspC⁻. Bacterial colony forming unit (CFU) levels in middle ear effusions and light microscopic analysis of the number of inflammatory cells in the round window membrane were compared 48 hours after inoculation.

Results

At 48 hours, CFUs in middle ears were increased for wild-type and PspC⁻ strains compared to corresponding inoculum levels; however, no bacteria were detected in the PspA⁻ and PspA⁻/PspC⁻ groups. Significant differences in CFUs were seen between the wild-type and each of the mutant strains and between PspC⁻ and the other mutants. The number of inflammatory cells in the round window membrane was significantly higher in the wild-type compared to the PspA⁻, PspC⁻, and PspA⁻/PspC⁻ groups. No significant difference in the number of inflammatory cells was observed between any pairs of mutant groups.

Conclusion

These results indicate that single PspA⁻ and double PspA⁻/PspC⁻ mutants were highly attenuated in the ear. They were much less viable and less virulent than wild-type and PspC⁻ strains. This makes both PspA and PspC proteins potential candidates for a vaccine design against pneumococcal otitis media.

A Mouse Model With Fibrous Dysplasia of the Bone Exhibits Progressive Hearing Loss Caused by Cochlear Overgrowth

Omar Akil¹; Faith Hall-Glenn²; Jolie Chang³; Alfred Li⁴; Wenhan Chang⁴; Tamara Alliston²; Edward Hsiao⁵; Lawrence Lustig³

¹University of California San Francisco; ²University of California, San Francisco, Department of Orthopaedic Surgery; ³University of California, San Francisco, Department of Otolaryngology, Head & Neck Surgery; ⁴University of California, San Francisco, Endocrine Unit, San Francisco VA Medical Center; ⁵University of California, San Francisco, Division of Endocrinology and Metabolism, Institute for Human Genetics, Department of Medicine

Background

Several developmental bone disorders such as osteogenesis imperfecta, skeletal dysplasias, craniosynostoses and fibrous dysplasia (FD), are associated with hearing loss. However, the pathogenesis of these bone diseases in the cochlea and how they cause hearing loss is poorly understood. FD is a rare bone disorder in which local areas of bone show fibrocellular infiltration leading to trabecular overgrowth, bone pain, deformity, and fragility. Dysplastic lesions in the temporal bone can be variable in severity and location and are associated with both conductive and sensorineural hearing loss depending upon what part of the auditory pathway is affected.

Methods

In this study, we investigate the cause and nature of hearing loss using a mouse model with severe bony changes reminiscent of FD. Col1^{+/}/Rs1⁺ mice express an engineered Gs-coupled G-protein coupled receptor with constitutive activity, which in turn leads to severe bony overgrowth similar to that observed in FD patients. Hearing was studied with auditory brainstem response (ABR), distortion product otoacoustic emissions (DPOAE), histology, immunofluorescence, immunohistochemistry, microcomputed tomography (micro CT) and Quantitative PCR (QPCR).

Results

The auditory function and the associated anatomic and histologic changes within the temporal bone were examined. Hearing tests revealed progressive hearing loss in Col1^{+/}/Rs1⁺ mice but highly variable ABR thresholds. At P10-12 weeks Col1^{+/}/Rs1⁺ mice do not show DPOAE responses above background noise when compared to WT. This suggested a defect in the delivery of sound to the cochlea that could be due to conductive hearing loss or to defects in outer hair cell (OHC) function. Histological analysis of the cochlea of Col1^{+/}/Rs1⁺ mice showed bony and fibrous overgrowths that affected the outer cortex of the otic capsule and the adjacent labyrinth compared to WT controls. Though the FD-like lesions often increased the thickness of the cochlear walls, no lesions were observed in the cochlea mid-modular bone. The stria vascularis, organ of Corti, spiral ganglion and cochlea nerve fibers were normal. Myosin7a immunofluorescent and rhodamine phalloidin imaging of whole mount cochlea revealed no OHC loss in the Col1^{+/}/Rs1⁺. These results, combined with the loss

of DPOAE responses, suggested the hearing loss is conductive in nature. This finding is supported by microCT analysis of the FD mice temporal bones which showed that the FD lesions impinged upon the ossicles. To determine the effect of FD on cochlear bone remodeling, we examined the expression of sclerostin (SOST), a key bone regulatory factor, in cochlea from WT and Col1^{+/}/Rs1⁺ mice. We observed high expression in WT cochlea, with a significant decrease in expression that correlated to the severity of Col1^{+/}/Rs1⁺ cochlear overgrowth. Taken together, these data suggest that Col1^{+/}/Rs1⁺ cochlea exhibit increased bone remodeling due in part to decreased SOST expression by osteocytes, which may activate osteoblast-mediated bone remodeling.

Conclusion

The progressive hearing loss observed in the Col1^{+/}/Rs1⁺ mice is conductive, caused at least in part by impingement of the ossicles by the exuberant FD lesions. The loss of SOST expression in the cochlea of the FD mice results in increased bone formation. Our findings indicate that strategies that manipulate bone remodeling may be useful for treating FD patients with conductive hearing loss.

PS - 735

Fetal Development Of The Elastic-Fiber-Mediated Entesis In The Human Middle Ear

Yoshitaka Takanashi¹; Yukio Katori¹; Gen Murakami²; Tetsuaki Kawase¹

¹Tohoku University Graduate School of Medicine;

²Iwamizawa Kojin-kai Hospital

Background

In the human adult middle ear the annular (collateral) ligament of the incudostapedial joint and the bony insertions of the tensor tympani and stapedius muscles are composed of elastic fibers rather than collagen fibers. Colocalization of elastic elements and matrix substances, including elastin and hyaluronan are composed predominantly of elastin and oxytalan fibers. The present study was performed to clarify the distribution of elastin in the three middle ear joints of fetuses as well as those in adults.

Methods

The study was performed in accordance with the provisions of the Declaration of Helsinki 1995 (as revised in Edinburgh 2000). We examined paraffin-embedded sections of the ear ossicles obtained from 5 donated cadavers (75–90 years old; mean age, 81years; 4 males and 1 female) and the heads of 11 fetuses (4 at approximately 15–16 weeks of gestation, crown rump length(CRL) 115–127 mm, and; 7 at approximately 25–30 weeks, CRL200–250 mm). We performed observation by the immunohistochemistry for these specimens. Furthermore, we added observations with transmission electron microscopy performed on 2 adult specimens of the incudostapedial joint.

Results

In the present study using immunohistochemistry, we demonstrated the distribution of elastin in all three joints of the auditory ossicles in adults and fetuses. In adults, the expression of elastin did not extend out of the annular ligament composed

of mature elastic fibers but clearly overlapped with it. Electronmicroscopic observations of the annular ligament demonstrated a few microfibrils along the elastic fibers. Thus, in contrast to the vocal cord, the middle ear entheses seemed not to contain elaunin and oxytalanfibers. In midterm fetuses (at approximately 15–16 weeks of gestation) before opening of the external auditory canal, the incudostapedial joint showed abundant elastic fibers, but the incudomalleolar and stapediovestibular joints did not. At this stage, hyaluronan was not colocalized, but distributed diffusely in loose mesenchymal tissues surrounding the auditory ossicles. Therefore, fetal development of elastin and elastic fibers in the middle ear entheses is unlikely to require acoustic oscillation. In late-stage fetuses (25–30 weeks), whose auditory ossicles were almost the same size as those in adults, we observed bundling and branching of elastic fibers. However, hyaluronan expression was not as strong as in adults. Colocalization between elastic fibers and hyaluronan appeared to be a result of postnatal maturation of the entheses.

Conclusion

The middle ear entheses contained abundant elastic elements. They were not elaunin or oxytalan fibers, but elasticfibers because of sparse content of microfibrils.

PS - 736

Development of the Mucosa in the Eustachian Tube of Neonatal Gerbils

Yi Li¹; Huizhan Liu²; Jun Li³; David He²

¹Beijing Tongren Hospital, and Creighton University;

²Creighton University; ³Shanghai Qingpu Hospital, and Creighton University

Background

The Eustachian tube is a small canal that connects the tympanic cavity with the nasal part of the pharynx. The epithelial lining of the Eustachian tube contains a ciliated columnar epithelium at the tympanic cavity and pseudostratified, ciliated columnar epithelium with goblet cells near the pharynx. The tube serves to equalize air pressure between the atmosphere and the middle ear across the eardrum. Additionally, it drains mucus away from the middle ear into the nasopharynx. Abnormal or impaired function(s) of the Eustachian tube may cause pathological changes in the middle ear. Blockage of the Eustachian tube is the most common cause of all forms of otitis media, which is common in children, partly because the Eustachian tube is not completely developed. In the present study, we examined development of the Eustachian tube in neonatal gerbils with focus on the morphological and functional development of ciliated cells in the mucosa.

Methods

Neonatal gerbils ranging in age between postnatal day 0 (P0) and 2 months after birth were used for the experiments. Conventional microscopy was used to examine the anatomical changes of the Eustachian tube. During development, morphological changes in the cilia of the mucosa were examined using scanning electron microscopy. Ciliary motion (beat frequency) was measured using a photodiode-based displacement measurement system.

Results

The length of the Eustachian tube increased significantly between P0 and P12. At P0, scanning electron microscopy showed that the mucosa contained a high density of ciliated cells with a few goblet cells on the pharynx side. During development, the number of ciliated cells decreased while the number of goblet cells increased. At P12, the mucosa looked adult like. The ciliary beat frequency increased from 8 Hz to 12 Hz between P0 and P8, at which time the ciliary beat frequency was not statistically different from that measured from adult animals.

Conclusion

The Eustachian tube undergoes significant anatomical changes between P0 and P12. The mucosa is morphologically and functionally mature at P12 when onset of hearing starts.

PS - 737

Role of the PI3K/PTEN/AKT Pathway in Otitis Media

Hwan-Ho Lee¹; Anthony Chin¹; Kwang Pak²; Stephen Wasserman³; Allen Ryan²

¹Departments of Surgery/Otolaryngology, UCSD;

²Departments of Surgery/Otolaryngology, UCSD and San Diego Veterans Administration Medical Center La Jolla;

³Departments of Medicine, School of Medicine, UCSD

Background

Hyperplasia of the middle ear mucosa is a hallmark of otitis media (OM), the most common disease of childhood. However, the intracellular pathways that mediate growth of the mucosa remain poorly understood. The PI3K/PTEN/AKT pathway is an important mediator of cell growth in many systems, which remains largely unexplored in the middle ear (ME). To explore its role in OM, we assessed the expression of genes encoding the members of this pathway during a ME infection, and evaluated the effects of inhibitors on mucosal growth *in vitro*.

Methods

Whole-genome gene arrays were generated from the MEs of mice undergoing OM induced by nontypeable *Haemophilus influenzae* (NTHi). Relative expression of PI3K/PTEN/AKT genes was assessed prior to ME infection, and at intervals that captured the entire course of an acute OM episode. In addition, inhibitors of AKT and PTEN were used to block signaling in this pathway, in ME mucosal explants from animals previously infected with NTHi.

Results

Genes encoding the PI3K delta and gamma subunits were upregulated 8.5- and 3.5-fold, respectively, 24 hours after ME inoculation with NTHi. Similarly, the *PTEN* gene was upregulated 6.1-fold at the same time. The genes encoding AKT1, AKT2 and AKT3 were upregulated 9.0-, 3.0- and 2.6-fold, respectively, also peaking at 24 hours. The growth of ME mucosal explants in culture was significantly reduced by the AKT inhib9tor MK2206 and the PTEN inhibitor BPV.

Conclusion

During OM, genes encoding the protein substrates of the PI3K/PTEN/AKT pathway are upregulated just prior to the period of intense mucosal hyperplasia. Combined with growth reduction by pathway inhibitors, the data suggest that PI3K/PTEN/AKT signaling plays a significant role in regulating growth of the ME mucosa during OM.

PS - 738

The Inflammasome Adaptor ASC Contributes To Multiple Innate Immune Processes In The Resolution Of Otitis Media

Arwa Kurabi¹; Kwang Pak¹; Jasmine Lee¹; Chelsea Wong¹; Harold Hoffman¹; Stephen Wasserman²; Allen Ryan¹

¹UCSD; ²UCSD medicine

Background

The inflammasome complex and its activation of inflammatory cytokines by proteolytic cleavage play a crucial role in host defense and have been implicated in the pathogenesis of several inflammatory diseases. The current study was designed to understand the contribution of the inflammasome and IL-1 β (interleukin-1 β) activation in an animal model of otitis media (OM), a common pediatric disease.

Methods

We examined the middle ear (ME) response to Nontypeable *Haemophilus influenzae* (NTHi) in wild-type (WT) mice, using gene microarrays and our established murine model of acute OM. The expression of 45,000+ transcripts representing essentially all mouse genes were compared between NTHi-infected and sham MEs using Affymetrix gene chip. In addition, OM was induced by NTHi inoculation into the MEs of WT versus ASC-deficient mice.

Results

Expression of members of the NALP family of inflammasome receptor genes was significantly up-regulated early in NTHi infection of the ME, potentially resulting in the activation of specific down-stream regulatory cascades that contribute to the proliferative inflammatory response observed during OM. In addition, expression of the pro-forms of the inflammasome targets IL-1 β and IL-18 were also up-regulated. To evaluate the role of inflammasome-mediated cytokine maturation, NTHi-induced Mice lacking the ASC gene showed near absence of IL-1 β maturation in the ME and a reduction in leukocyte recruitment and infiltration to the cavity. In addition, macrophages from ASC-deficient mice exhibited reduced phagocytosis of NTHi. These inflammatory defects were linked to an increase in the degree and duration of mucosal epithelial hyperplasia in the ME of ASC-/- mice, as well as a delay in ME bacterial clearance.

Conclusion

These data demonstrate an important role for the inflammasome and cytokine processing in the course and resolution of OM. This is mediated by the participation of cleaved target molecules in multiple processes in the response to infection of the ME.

PS - 739

Is the 3D Sound-Induced Motion of the Tympanic Membrane Consistent With Thin-Shell Theory?

Morteza Khaleghi¹; Cosme Furlong¹; Jeffrey Cheng²; John Rosowski²

¹Worcester Polytechnic Institute; ²Massachusetts Eye & Ear Infirmary

Background

The acousto-mechanical-transformer behavior of the tympanic membrane (TM) is determined by its shape and mechanical properties. Holographic studies of 1D vibrations of the TM have been reported by several groups; however, 3D measurements of TM displacement are few. In this study, we will use full-field-of-view holographic techniques to near simultaneously measure the shape and 3D sound-induced displacement of cadaveric TMs.

Methods

The geometrical constraints imposed by the ear canal make 3D measures of TM displacement in intact ears difficult. However, we can, even in such a confined geometry, measure both a 1D component of sound-induced displacement and the shape of the membrane through the intact ear canal. Then by considering the TM as a thin-shell, in which the principal components of vibration are parallel to vectors normal to the surface of the TM, we can calculate the motion in 3D. To address a basic question concerning the applicability of the thin-shell approximation to the TM, we directly measure the 3D motion of a TM, using a multiple sensitivity vector technique, together with its shape, in a widely exposed chinchilla TM model after removing the ear canal. We then compare the theoretically-computed components of displacement with the experimentally determined displacement components.

Results

Preliminary analyses suggest the thin-shell hypothesis is applicable for excitation frequencies up to 4 kHz, with correlation coefficients between theory and measurement of >0.90. This result suggests that in this range of excitation frequencies, the displacement vectors on the surface of the TM are mainly out-of-plane (parallel to the normal vector of the TM), and displacement components tangential to the TM surface are negligible.

Conclusion

Due to the particular geometry of the TM in which the maximum ratio of the thickness to the radius of curvature is less than 0.05, the TM can be modeled as a thin-shell. In this circumstance, the principal component of the displacement vector is normal to the shape of the membrane. Based on this assumption, a miniaturized holographic otoscope capable of measuring shape and 1D sound-induced displacement of the TM can be used to estimate 3D motion of the TM inside the ear canal.

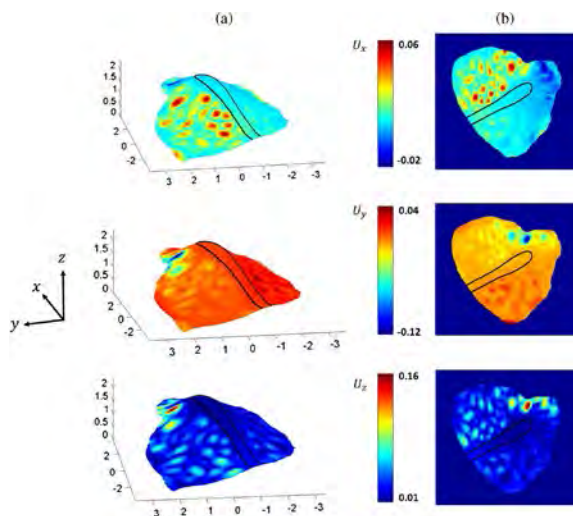


Fig.1. Principal components of displacement along three orthogonal axes of the TM as obtained by application of our approach. TM was subjected to sound stimuli of 5730 Hz and sound pressure level of 101 dB: (a) 3-D view. (b) 2-D top view. The z axis corresponds to the lateral-medial direction with medial as positive, which was defined by the longitudinal axis of the illuminating and reflected laser beam. The x direction is approximate to the rostral (anterior)-caudal (posterior) axis with rostral positive. The y direction is approximate to the dorsal (superior)-ventral (inferior) direction with ventral positive. Displacements are in the unit of μm .

References

[1] J.J. Rosowski, I. Dobrev, M. Khaleghi, W. Lu, J.T Cheng, E. Harrington, and C. Furlong, "Measurements of three-dimensional shape and sound-induced motion of the chinchilla tympanic membrane," *Hearing research*, 301, 44-52, 2012.

[2] M. Khaleghi, W. Lu, I. Dobrev, J.T Cheng, C. Furlong, and J.J. Rosowski, "Digital holographic measurements of shape and three-dimensional sound-induced displacements of tympanic membrane," *Optical Engineering* 52, 101916-101916, 2013.

[3] M. Khaleghi, C. Furlong, J.T. Cheng, and J.J. Rosowski, "3-Dimensional quantification of surface shape and acoustically-induced vibrations of TM by digital holography," *Proc. Fringe 2013*, pp. 599-602. Springer Berlin Heidelberg, 2014.

PS - 740

A Three Dimensional Volumetric Study of the Epitympanum in Human Temporal Bones

Kyoko Shirai¹; Monika Schachern²; Pat Schachern²; Michael Paparella³; Sebahattin Creoglu²
¹Research fellow of department of Otolaryngology at University of Minnesota, Resident of department of Otorhinolaryngology at Tokyo Medical University; ²University of Minnesota; ³University of Minnesota, Paparella Ear Head and Neck Institute, Minneapolis, MN, USA

Background

The pathophysiology of chronic otitis media requires a proper understanding of the disease. Three-dimensional evaluation allows us to see the changes in ventilation pathways in pathologic conditions. Restoration of the ventilation will be the main focus of treatment in order to prevent any recurrences or re-

sidual problems. The aeration pathway from the Eustachian tube leads directly to the mesotympanic and hypotympanic space, whereas the epitympanum is away from the direct air stream and not aerated.

The epitympanic diaphragm consisting of the incus, malleus, and their folds, is described as the floor of the epitympanum, which is the dividing structure from the mesotympanum. It is believed that epitympanum and mastoid aeration occurs through the tympanic isthmus.

It has been suggested that a reduced volume of the bony boundaries of the epitympanum is related to a selective attic disventilation syndrome and chronic otitis media.

The purpose of this study is to compare the volume of the epitympanum between the groups of normal and chronic otitis media (COM).

Methods

Six children's temporal bones that presented with chronic otitis media (COM group) and 3 normal children's temporal bones as a control group from the human temporal bone (HTB) collections of the University of Minnesota were examined.

The epitympanum was divided into 5 different compartments: anterior area(A), lateral area(L), medial area(M), posterior area(P) and Malleus-Incus area(MI).

Three-dimensional models were generated from HTB histopathologic slides with reconstruction software (Amira®). Measurements of the bony volumes of each compartment, total epitympanum (E) volume, and the ratio of the malleus and incus to the total epitympanum (MI/E) were taken.

Results

There were no differences of the bony volumes of each compartment or of the total epitympanum volume between the COM group and the control group. There were also no differences in MI/E between the two groups.

Conclusion

The evidence supports that no relationship exists between epitympanic volume and COM. Further studies are necessary to clarify what kind of differences in anatomical features could be found between COM and the control groups.

Our next study will focus on the evaluation of the soft tissue blockage of the tympanic isthmus in cases with chronic otitis media.

	Anterior	Posterior	Lateral	Medial	Malleus-Incus	MI/total	total	total-MI
Normal	2.36	3.47	11.17	17	10.56	0.23	46.7	36.32
COM	2.66	2.74	10.42	16.22	9.86	0.23	41.71	31.85
(median)								(mm ³)

Mechanical Properties of the Incudo-Malleolar Joint: Measurements of Quasi-Static and Dynamic Behavior

Rahel Gerig¹; Sebastian Ihrle²; Albrecht Eiber²; Christof Rösli¹; Jae Hoon Sim¹; Alexander Huber¹

¹University Hospital Zurich, Division of Otorhinolaryngology, Head and Neck Surgery; ²University of Stuttgart, Institute of Engineering and Computational Mechanics

Background

The incudo-malleolar joint (IMJ) is the diarthrodial joint connecting malleus and incus of the middle-ear ossicular chain in mammals. In humans, this joint contains synovial fluid which presumably causes a viscoelastic behavior. Under static loads, occurring for example with the influence of air pressure fluctuations, the IMJ is expected to show a mainly elastic compliance. Under dynamic excitation, additionally the influence of the viscosity of the synovial fluid in the IMJ is supposed to increase as the frequency increases. This viscoelastic characteristic of the IMJ can be integrated into a comprehensive mechanical model to answer questions about anatomical features and function of the IMJ, and to serve as a base for the development and optimization of middle-ear implants. However, the mechanical properties of the IMJ have not been measured, and its role in sound transmission and/or possible protection mechanism is still open.

Methods

To determine the mechanical properties of the IMJ under static and dynamic excitation, the malleus-incus complex was isolated from fresh human temporal bones. For measurements of the *static behavior* of the IMJ, the malleus was fixed to a custom-made frame, and the incus was excited by applying a quasi-static force while measuring the resulting spatial displacement subsequently at several points on the incus. For measurements of the *dynamic behavior*, the isolated malleus-incus complex was excited by an electrodynamic shaker using different test signals and 3-D velocity components were measured at several points on the malleus-incus complex. The measurements were performed using a 3-D Laser Doppler Vibrometry (LDV) system with three independent LDVs. The relative motion between the malleus and incus was calculated, and spatial behavior of the IMJ was characterized. Different intensities and directions of excitation were used, and their influence on the IMJ motion was analyzed as well.

Results

The force deflection curves obtained from the static measurement show a significant hysteresis loop and a nonlinear characteristic. Both depend on the excitation direction and position of the force application point, i.e. the spatial force and torque. In case of the dynamic measurement, the incus exhibits a spatial relative motion depending on the excitation amplitude, direction and frequency. A state dependent stiffness and damping matrix, describing the behavior of the IMJ, can be derived from those measurements.

Conclusion

The IMJ shows a viscoelastic and nonlinear behavior under quasi-static and dynamic excitation.

Pulsed Digital Holographic Methods for Transient Acoustic Measurements and Characterization of the Mechanical Properties of the Human Tympanic Membrane

Ivo Dobrev¹; Cosme Furlong¹; Jeffrey Cheng²; John Rosowski²

¹Worcester Polytechnic Institute; ¹Worcester Polytechnic Institute; ²Massachusetts Eye & Ear Infirmary

Background

Our research is focused on the tympanic membrane (TM) and its role in transforming sound energy in the ear canal into mechanical vibrations of the ossicles. Past work has concentrated on the TM's response to continuous tonal stimuli. Here we describe methods to investigate the transient response of the TM after excitation by a brief pulse.

Methods

We develop digital holographic systems (DHS) for the quantification of the sound induced response of the TM. These systems have already been used in temporal-bone testing. We are now optimizing the system for rapid *in-vivo* and transient measurements. The new DHS system incorporates double pulsed (<20µs pulse separation) image gathering methods that allow quantification of the transient displacement time-waveform on the TM surface excited with a sharp click. The optimized system allows for precise (<1ms jitter) synchronization between the camera acquisition, laser illumination and acoustic excitation for a temporal resolution of <20 µs while using a regular frame rate (<20fps) camera.

Results

The DHS system measures instantaneous response of >500k data points on the TM surface, which allows observations of spatially-dependent motion parameters such as modal frequencies, time constants, damping ratios, Q-factors, etc. This allows us to infer local material properties along the TM. The DHS performance was tested against Laser Doppler Vibrometer (LDV) measurements; the displacements measured by the two methods were highly correlated ($r > 0.95$); estimates of above motion parameters based on the two methods were within 5%. We recorded the displacements of a human cadaveric TM in response to a transient acoustic stimulus produced by a 100µs square wave excitation signal. The measured time constants of decay were in the 500-1000µs range, dominant modal frequencies were at 1.1, 1.8 and 3.7 kHz (within 20dB of the peak), and Q-factors were in the 7-12 range.

Conclusion

The DHS is a new and versatile means to quantitatively characterize the transient dynamics of the human TM. Future work will focus on development of methods to analyze the transient response of the TM, including the measurement of its spatially varying mechanical and dynamic properties in-vivo.

Pathways for Bone Conducted Sound in Chinchilla

David Chhan¹; John Rosowski²; Melissa McKinnon³

¹MIT-Harvard Health Science and Technology;

²Massachusetts Eye and Ear Infirmary, Harvard Medical School; ³Massachusetts Eye and Ear Infirmary

Background

Bone conduction (BC) testing is performed in the audiology clinic to help differentiate conductive from sensorineural hearing loss. In air conduction (AC), sound is conducted from the outer ear, through the middle ear to the inner ear. The simple view of BC sound is that it directly stimulates the inner ear, and bypasses the outer and middle ear. In reality, BC is a complicated phenomenon that involves different sound pathways, including the external and middle ear. However, not all of these pathways are well understood. The goal of this work is to define the different pathways and quantify their contribution to bone conduction hearing in chinchilla.

Methods

We measured intracochlear sound pressure (**P_{sv}** in the vestibule near the oval window and **P_{st}** in scala tympani near the round window) and cochlear potential (**CP**) in response to AC and BC stimulation in anesthetized chinchillas. We introduced four manipulations: occlusion of the ear canal, interruption of the incudo-stapedial (**IS**) joint, fixation of the stapes and fixation of the round window.

Results

Both ear canal sound pressure (**P_{ec}**) and cochlear responses, (**CP** and scala vestibule pressure **P_{sv}**) increase on average by 10 dB for frequencies less than 2 kHz after the ear canal was occluded. In addition, when the ear canal is occluded, the ratio of cochlear responses to ear canal sound pressure in BC is very similar to the ratio of these variables during AC at frequencies below 2 kHz. A further finding is that interruption of the ossicular chain when the ear canal is occluded reduces the response to BC stimuli at low frequencies, by about 10 dB, an amount consistent with the removal of the occlusion induced increase, while reducing the response to AC sound stimulation by more than 40 dB.

Conclusion

The data suggest that compression of the occluded ear canal is a major contributor to BC stimulation in chinchilla at frequencies less than 2 kHz. The lack of an additional effect after ossicular interruption suggests that ossicular inertia is not a major contributor to BC stimulation. The effect of stapes and round window fixation on the BC response will also be described.

Tympanic Membrane Surface Motion and Near-Field Sound Pressure With Open or Occluded Ear Canal by Forward or Reverse Stimulation

Jeffrey Cheng¹; Michael Ravicz²; Cosme Furlong³; John Rosowski¹

¹Massachusetts Eye and Ear Infirmary, Harvard Medical School; ²Massachusetts Eye and Ear Infirmary; ³Worcester Polytechnic Institute

Background

We have quantified tympanic membrane (TM) surface motion using digital opto-electronic holography while the TM was stimulated by ear-canal sound pressures ("forward stimulation") or by motion of the ossicles ("reverse stimulation"). Under either stimulation, the TM moves with a complex pattern at frequencies above a few kHz. Previous comparisons show no connection of this complex motion pattern to the sound field recorded in the plane of the tympanic ring, which is 2-4 mm from the apex of the conical shaped TM. A possible explanation is that sound pressure variations due to non-uniform TM motion dissipate by the time they reach the tympanic ring plane. Here we compare TM surface motion to sound pressures measured within 0.5 mm of the TM surface.

Methods

Sound for forward stimulation was generated by a speaker attached to the lateral end of an artificial ear canal (EC). Reverse stimulation was provided by a piezoelectric stimulator contacting the incus body near the long process. TM motion was measured by stroboscopic holography with the laser illuminating the TM via a transparent window in the artificial EC wall; sound pressure was measured with a probe tube microphone advanced down the EC opening and positioned within 0.5 mm of the TM surface. The position of the probe was varied in 3 dimensions in 0.3-0.5 mm increments. We compare pressure distribution near the TM surface with TM displacement over the 0.25 to 18.5 kHz range with both forward and reverse stimulation. We also made measurements after occluding the ear canal.

Results

In forward stimulation, the sound pressure near the TM surface is fairly uniform up to 15 kHz, which is inconsistent with the non-uniform TM motion pattern that appears above a few kHz. While reverse stimulation produces an increase in sound pressure spatial variation, these variations are not consistent with spatial variations of the reverse-driven TM motion. In general, TM displacement patterns from forward and reverse stimulation differ at most measurement frequencies (below 15 kHz), but shows more similarity at the highest frequencies (17~18.5 kHz). Whether the EC is open or occluded has no significant effect on the sound field and TM motion above 1 kHz.

Conclusion

TM motion and sound pressure near the TM surface differ between forward and reverse stimulation, and in neither case does the pressure profile match the TM motion pattern.

Sound Pressure Distribution in the Human Ear Canal for Sound Emanating from the Middle Ear

Michael Ravicz; Jeffrey Tao Cheng; John Rosowski
*Eaton-Peabody Lab., Mass. Eye & Ear Infirmary and
 Harvard Medical School*

Background

Sound pressure variations with location within the human ear canal (EC) for sound entering the EC at the opening have been fairly well described; however, little information is available about the sound pressure distribution within the EC for sound emanating from the middle ear (for instance, otoacoustic emissions conducted laterally from the inner ear). We have shown that the pattern of tympanic membrane (TM) motion is much different when the TM is driven from the middle ear ("reverse stimulation") than when it is driven by EC sound ("forward stimulation"). It is therefore likely that the sound field within the EC is different as well. Such differences have implications for the measurement of otoacoustic emissions within the EC.

Methods

Sound fields were measured in real and artificial ear canals of human temporal bones with a microphone and narrow (0.5 mm inner diameter) probe tube mounted on a 3-axis micro-manipulator and advanced medially down the EC from the opening. Sound pressure in response to broadband chirps was measured in four anatomically-defined regions: (1) within 0.5 mm of the conical TM surface; (2) in the plane of the tympanic ring; (3) in a plane perpendicular to the EC axis at the posterior edge of the tympanic ring; and (4) along the EC axis between the TM and the EC opening. Sound for forward stimulation was generated by a small speaker attached to the EC near its lateral end. Reverse stimulation was provided by a piezoelectric stimulator contacting the incus body near the long process. Measurements were repeated with the lateral end of the EC blocked with a clear plastic window with a hole for the microphone probe tube.

Results

The EC sound field emanating from the TM with reverse stimulation is much different from that present during forward stimulation. With reverse stimulation, the sound field shows substantial transverse variations at the TM and larger variations at the tympanic ring plane but is approximately uniform at the EC perpendicular plane. The sound distribution along the EC shows some similarities whether the EC is open or blocked. The nonrigid ear canal termination provided by the TM affects the global EC sound field for both forward and reverse stimulation.

Conclusion

The EC sound field for reverse stimulation shows similarities and differences with that for forward stimulation. These differences have implications for the measurement of otoacoustic emissions.

Proposal of New Classification of Sound Conduction Pathway - Air, Bone and Cartilage Conductions -

Hiroshi Hosoi; Tadashi Nishimura; Ryota Shimokura
Nara Medical University

Background

Hosoi found in 2004 that a clear sound can be heard when a vibration signal is delivered to the aural cartilage from a transducer. This form of signal transmission is referred to as "cartilage conduction (CC)". After that we have examined its mechanism, application and superiority over the air or bone conduction.

Methods

(Experiment 1) For the comparison with the air conduction, we measured sound pressure level (SPL) in the auditory external canal for two conditions: the transducer touching the aural cartilage (touching condition) and the transducer in essentially the same position but not touching the aural cartilage (non-touching condition).

(Experiment 2) For the comparison with the bone conduction, we conducted the SPL measurement in the canal and an loudness matching test at the same time, stimulating at aural cartilage and skull bone (i.e., mastoid).

Results

(Experiment 1) In the frequency range below 3 kHz, the aural cartilage was vibrated strongly, and then the SPLs for the touching condition were substantially higher than those for the non-touching condition.

(Experiment 2) The loudness induced by the cartilage conduction was determined dominantly by the SPL in the canal, while the loudness of bone conduction was much higher than the SPL in the canal.

Conclusion

As we obtained the results which suggest that cartilage conduction is hard to categorize in the air and bone conductions, we propose new classification in consideration of cartilage conduction (Table 1).

- 1) Air conduction pathway: sound emitted from a sound source outside of the ear enters into the external auditory canal, and reaches the inner ear passing through the middle ear.
- 2) Bone conduction pathway: sound information in the form of vibration is input to bone tissue and reaches the inner ear conducting through the temporal bone.
- 3) Cartilage conduction pathway: sound information in the form of vibration enters the aural cartilage (e.g., tragus), thereby generating sound in the canal, and reaches the inner ear passing through the middle ear.

Table1 Classification of the three pathways in terms of two respects

Pathway	Transmission media	Skull bone
Air	Sound	immobile
Bone	Vibration	vibrated
Cartilage	Vibration	immobile

PS - 747

Eye Position Influences on Auditory Processes Measured from Within the External Ear Canal

Kurtis Gruters¹; Christopher Shera²; Jennifer Groh¹

¹Duke University; ²Harvard Medical School

Background

Coordination between vision and hearing in the spatial domain requires that both the visual eye-centered and auditory head-centered reference frames share information about eye position with respect to the head. Previous research has found that the position of the eyes in their orbits can modulate the firing rates and response patterns of auditory cells in the inferior colliculus (e.g. Groh et al. 2001, Zwiers et al. 2004), primary auditory cortex (Werner-Reiss et al., 2003; Fu et al. 2004), lateral/medial banks of the intraparietal sulcus (e.g. Mullette-Gillman et al., 2005, 2009), and superior colliculus (e.g. Jay and Sparks, 1984, Lee & Groh, 2012). However, it is not clear at what level of the system eye position begins to influence auditory processes. We sought to test this question by determining whether eye position affects the collection of gain control mechanisms that act on auditory signals within the ear itself.

Methods

We measured sound pressure level in response to brief clicks in the external ear canal of monkeys (n=3) and humans (n=7) as they fixated various locations along the horizontal azimuth. Sound pressure measured in this fashion reflects both oto-acoustic emissions generated by outer hair cells and the action of middle ear muscular reflexes.

Results

All three monkeys and four of seven humans exhibited statistically significant effects of eye position on the sound pressure level recorded in at least one of their ear canals during a period of time after the stimulus (ANOVA, $p < 0.05$). The time course of the effect varied across subjects.

Conclusion

These preliminary results indicate that eye position influences auditory activity even at the very periphery of the auditory system. Regardless of where eye position signals first “enter” the auditory pathway in a neuroanatomical sense, their presence at this early stage of processing suggests that they then have the potential to ramify throughout the system from the periphery and support a variety of interactions between vision and audition.

PS - 748

Wave Propagation in the Skull Bone During Bone Conduction Stimulation

Christof Roosli¹; Jae Hoon Sim¹; Rahel Gerig¹; Adrian Dalbert¹; Bjoern Christian Fausch¹; Stenfelt Stefan²; Alexander Huber¹

¹Department of Otorhinolaryngology, Head and Neck Surgery, University Hospital Zurich, Switzerland; ²Linköping University, Sweden

Background

Bone conduction (BC) hearing aids are used for patients with conductive or mixed hearing losses who cannot wear conventional hearing aids, or for patients with single sided deafness. Some BC hearing aids stimulate the skull directly, while others are placed on the skin covering the skull. The latter way of stimulation is also used as preclinical assessment of BC hearing aids and to determine BC hearing thresholds. The propagation of skull-bone vibration with different modes of stimulation may vary. This study aims to investigate on wave propagation in the skull bone during bone conduction stimulation, for different stimulation sites and stimulation modes.

Methods

Measurements were performed in three human cadaveric whole heads. A bone anchored hearing aid (BAHA) was attached to a percutaneously implanted screw or positioned with a steel headband at two positions (mastoid and forehead) using a static force of 5 Newtons. The transferring force with the two interfaces was calibrated using a skull simulator and an artificial mastoid. Two stimulation signals were used: (1) a stepped-sine signal in the frequency range of 0.1 – 10 kHz for measurement in frequency domain, and (2) a two-cycle sine signal at frequencies between 0.5 and 8 kHz for measurements in time domain. Simultaneously, skull bone vibrations were measured at multiple points on the skull using a Laser Doppler Vibrometer system.

Results

While the magnitude of the transferred force was similar for both the BAHA “coupled to the screw” and “positioned with the headband”, the phase with “positioned with the headband” showed larger phase delay than with “coupled to the screw” above 1 kHz. Skull bone vibrations showed near rigid-body motion at low frequencies below 0.5 kHz, and clear traveling waves were observed at high frequencies above 2 kHz, for both conditions. The speed of wave propagation was of a similar magnitude and only the direction of the wave propagation changed for the two stimulation sites. Significant attenuation with distance from the bone vibrator was not observed.

Conclusion

Stimulation on the skin covering the skull seems to be a reasonable way of preclinical assessment of BC hearing aids directly attached to the skull in regard to wave propagation. The propagation speed was similar without attenuation of the magnitude for the two stimulation sites of the mastoid and the forehead.

A High-Frequency Finite-Element Model of the Gerbil Middle Ear

Nima Maftoon¹; W. Robert J. Funnell¹; Sam J. Daniel¹; Willem F. Decraemer²

¹McGill University; ²University of Antwerpen

Background

Although most middle-ear finite-element models have been developed for the human ear, thorough validation of models requires the higher-quality experimental data that can be collected in other species. This study investigates the response of the gerbil middle ear using a finite-element model. The calculated responses are compared with our multipoint vibrometry measurements in the frequency range of 0.2 to 10 kHz.

Methods

The geometry of the model is based on a reconstruction of the gerbil middle ear using a microCT dataset, supplemented by histological and orthogonal-plane fluorescence optical sectioning images. The model includes the pars tensa, pars flaccida, malleus, incus, stapes, anterior malleolar fixation, posterior incudal ligament, incudomalleolar joint, incudostapedial joint, annular ligament, and a discrete treatment of the cochlear load. The eardrum was modelled using second-order shell elements with variable thickness. Second-order tetrahedral solid elements were used to model the ossicles and ligaments. The cochlear load was considered to be purely resistive. Material properties were defined based on *a priori* estimates from the literature. After obtaining model results with baseline material properties, we performed sensitivity analyses to explore the effects of different material parameters on the model results.

Results

We present the effects of various model states and parameter values on response features such as low-frequency magnitude, resonance frequencies, pars-tensa break-up frequency and frequency-response smoothness. We modelled two pars-flaccida conditions, when it is naturally flat and when it is retracted inside the middle-ear cavity, and studied the different effects of the two states on the manubrium and pars-tensa responses. We explored different methods to model frequency-dependent damping, including Rayleigh damping and hysteretic damping. We also investigated the effects that the nature of the anterior malleolar fixation to the air-cavity wall has on the results. Elsewhere we have proposed a method for estimating ideal open-cavity responses from measurements with partial opening in the cavity wall. Here we use that method to compare our modelling results (without the tympanic cavity) with experimental results.

Conclusion

The model will be useful for interpreting experimental observations and for addressing open questions about how the eardrum and the rest of the middle ear function.

Finite-Element Modelling of the Newborn Ear Canal and Middle Ear

Hamid Motallebzadeh; Nima Maftoon; Robert Funnell; Sam Daniel

McGill University

Background

Available hearing-screening procedures cannot distinguish clearly between conductive and sensorineural hearing loss in newborns, and the results of available diagnostic tests in very young infants are difficult to interpret. Admittance measurements can help to detect conductive losses but do not provide reliable results for newborns. The newborn ear is anatomically very different from the adult one; for example, the newborn's canal wall is not yet fully ossified and has a much lower stiffness than that of the adult. At last year's meeting, preliminary results of finite-element models of the newborn ear canal and middle ear were reported. Since then, more investigation of the model parameters has been done and results have been compared with more sets of clinical measurements.

Methods

Finite-element models of the newborn ear canal and middle ear were developed and their responses were studied for frequencies up to 2000 Hz. Material properties were taken from previous measurements and estimates, and the sensitivities of the models to these different parameters were examined. In addition, mesh-resolution effects were also studied. The simulation results were validated through comparison with previous experimental measures.

Results

Simulations indicate that at frequencies up to 500 Hz the admittance of the canal wall is comparable to that of the middle ear in the newborn. Above 500 Hz the admittance of the canal wall remains almost constant but the middle-ear admittance increases. For some ranges of material parameters, a broad resonance peak is observed with the maximum admittance at 1200–1500 Hz. For some values of the damping ratio, multiple resonance peaks appear which are consistent with some reported clinical measurements. Within this frequency range, the admittance of the middle ear is much larger than that of the canal wall.

Conclusion

Given the large amount of inter-subject variability present in the admittance data of newborns, and the uncertainty in the model parameters, it appears that for plausible parameters these models produce results that are within the range of measured data. Our model predicts that at the conventional tympanometric frequency of 226 Hz the newborn canal-wall admittance is comparable to that of the middle ear, so the canal-wall admittance is not negligible as it is in adults. In addition, this model suggests that tympanometry with probe tones in the vicinity of the middle-ear resonance frequency, where the middle-ear admittance dominates, improves the chance that the measured admittance will give useful information about the middle ear.

The Effects of Cytosolic Glutamate on Synaptic Transmission at Auditory Hair Cell Synapses

Soyoun Cho; Henrique von Gersdorff

The Vollum Institute, Oregon Health & Science University

Background

To manage an uninterrupted flow of auditory signals, hair cell synapses continuously release glutamate, the neurotransmitter stored in vesicles. Vesicular glutamate transporter 3 (VGLUT3) fills vesicles with glutamate in hair cells and mice lacking VGLUT3 show no glutamate release and are deaf. At the calyx of Held synapse and at cone synapses in the retina, increasing intracellular glutamate concentration enhances glutamate transport into vesicles. We studied how cytosolic glutamate affects spontaneous and evoked release at the adult bullfrog auditory hair cell synapses.

Methods

Amphibian papillae were carefully dissected from adult bullfrogs. Semi-intact preparations of hair cells and their connecting afferent fibers were obtained as described by previous studies. Paired whole-cell voltage-clamp recordings were performed.

Results

We measured EPSCs from corresponding postsynaptic afferent fibers by depolarizing hair cells using a pair of 20 ms-long pulse from -60 mV to -30 mV with 20 ms inter-stimulus interval. To examine the effect of additional glutamate on synaptic transmission, we compared EPSCs within 2 minutes after break-in as a control and after more than 4 minutes of whole-cell configuration to allow extra glutamate to diffuse into the hair cell and be transported into vesicles. The paired-pulse ratio (PPR; $\text{EPSC}_2/\text{EPSC}_1$) was calculated using both peak amplitude and charge of EPSCs. PPR was significantly increased by 40 mM glutamate both with EPSC peaks (48%) and charges (25%). Besides the changes in PPR, the amplitudes of the first EPSCs were significantly increased after more than 4 minutes of glutamate diffusion.

Using intracellular 40 mM glutamate in hair cells, we measured membrane capacitance (C_m) from presynaptic hair cells simultaneously with EPSCs from connected afferent fibers. We compared the ratio of EPSC charge to changes in presynaptic C_m evoked by a 100 ms and 500 ms pulse. The ratio (EPSC/C_m) of later recordings significantly increased by additional 40 mM glutamate in comparison with early recordings. This suggests the additional glutamate in the cytosol eventually loaded the released vesicles and this increased the amount of evoked release without increasing the number or the size of presynaptic vesicles. After holding hair cells at -90 mV, the average amplitude of spontaneous EPSCs without additional glutamate in the presynaptic patch pipette was about 60 pA and this was significantly increased by 40 mM glutamate (105pA).

Conclusion

The cytosolic glutamate in hair cells can alter spontaneous and evoked release. Individual vesicles in hair cells are not fully loaded with glutamate in physiological conditions.

Deconvolution Analysis of the Instantaneous Rate of Neurotransmitter Release from Auditory Hair Cells

Owen Gross; Henrique von Gersdorff

Vollum Institute

Background

Synaptic ribbons at the terminals of auditory hair cells facilitate inexhaustible, low-latency release of neurotransmitter when nearby voltage-gated calcium channels are opened. Individual neurotransmitter release events, observable as miniature excitatory post-synaptic currents (mEPSCs) in afferent nerve fibers projecting to the brain, are uniform in shape but exhibit a wide range of amplitudes. Interestingly, the statistics of mEPSC amplitude distributions are significantly different for hair cells near the resting membrane potential (-60 mV) compared to hyperpolarized hair cells (-90 mV). Here we describe a method for studying the instantaneous rate of neurotransmitter release from depolarized hair cells (-30 mV), for which rapid, evoked exocytosis tends to obfuscate the specific contribution of individual fusion events in the EPSC.

Methods

Whole cell calcium currents and EPSCs were measured for auditory hair cells and afferent fibers of the bullfrog amphibian papilla as previously described (Cho et al., 2011). The change in the hair cell membrane capacitance (ΔC_m) caused by fusion of vesicles during exocytosis was estimated using the simulated lock-in amplifier method. The instantaneous rate of neurotransmitter release was calculated for afferent fiber EPSCs using Wiener deconvolution and a subsequent filtering procedure tailored to the statistical properties of afferent fiber signals and noise.

Results

Deconvolution analysis was successfully used to discriminate exocytotic events separated by intervals smaller than 100 μ s, allowing precise calculations of the instantaneous neurotransmitter release rate even when evoked EPSCs exhibit complex forms associated with high rates of exocytosis. The vesicular content determined for individual events during evoked exocytosis was typically larger than for spontaneous events, suggesting either a greater concentration of neurotransmitter per vesicle or a greater likelihood of multivesicular release for evoked events. To distinguish between these two interpretations, we integrated the instantaneous release rate during evoked exocytosis and compared this value to the number of fused vesicles estimated from ΔC_m , assuming an average single-vesicle capacitance of 40 aF. Close agreement between these two values favors the conclusion that a larger proportion of events are multivesicular during evoked exocytosis.

Conclusion

Our findings are consistent with previous hair cell studies reporting larger individual exocytotic events associated with more depolarized membrane potentials. To date, the mechanisms that underlie multivesicular release remain largely unknown, although prior experimental results and simulations indicate an important role for Ca^{2+} nanodomains at hair cell terminals.

PS - 753

Optical Approaches to Studying the Physiology of Hair Cell Ribbon Synapses

Aaron Wong¹; Kirsten Reuter¹; Carolin Wichman¹; Sebastian Kügler²; Tobias Moser¹

¹University of Goettingen Medical School; ²University of Göttingen

Background

Each cochlear inner hair cell is contacted by multiple post-synaptic spiral ganglion neurons through a specialized ribbon synapse. Previous work in our lab has shown marked heterogeneity in the size of Ca^{2+} -channel cluster and amplitude and voltage dependence of synaptic Ca^{2+} signal (Frank *et al.* 2009; Meyer *et al.*, 2009) at active zones within single inner hair cell. Such heterogeneity of presynaptic Ca^{2+} signaling is potentially relevant for explaining large dynamic range of sound encoding. However, its underlying mechanisms and the link to transmitter release are not well understood, due to the difficulty in single synapse measurement through electrophysiological techniques. Recent advances in optogenetics and microscopic techniques allow us to better dissect the function of individual IHC synapses.

Methods

Experiments were performed on freshly dissected mouse organs of Corti first apical coil. Synaptic activity in IHCs was measured by both classical electrophysiological measurements (patch-clamp: Ca^{2+} current and capacitance measurement) and recently developed genetically-encoded reporters for Ca^{2+} and exocytosis. High resolution fluorescence microscopy was used to measure fluorescence change of the reporters. For optical stimulation, channelrhodopsin variants (ChETA and Ai32) were expressed in IHC by crossing conditional expression mouse line with a Cre expression line driven by parvalbumin-promotor. Photoablation was performed by introducing a fluorescein-conjugated ribbon-binding peptide (Francis *et al.*, 2011) into IHCs through whole cell patch-clamp.

Results

We present preliminary results along with potential caveats. Spatially resolved imaging techniques was used to discretely study the function of individual IHC synapses. Localized exocytosis at different active zones in an IHC were measured quantitatively and compared with the heterogeneity of Ca^{2+} signal and simultaneously recorded capacitance changes. To explore putative function of synaptic ribbon in vesicle priming/replenishment in IHCs, we tested photoablation with on wild-type mice and a bassoon mutant, in which a large portion of IHC active zones lack a synaptic ribbon (Khimich *et al.*, 2005).

Lastly, current clamp measurements are underway to test the light responses of IHCs expressing the channelrhodopsins for use in optical stimulation.

Conclusion

Employing optical methods in studying hair cell synapse function adds to the knowledge base already acquired using whole-cell techniques. Specifically, the ability to distinguish among different synapses within an electrically compact IHC is critical in understanding the segregation of auditory information at this synapse. Moreover, genetically encoded reporters and effectors (optical stimulation) of IHC can potentially be used in applications where structural preservation of tissue is critical (e.g. electron microscopy).

PS - 754

Intensity Coding at the Inner Hair Cell Ribbon Synapse is Supported by a Highly Efficient Mechanism of Vesicle Pool Refilling

Juan Goutman

Instituto de Investigaciones en Ingeniería Genética y Biología Molecular (CONICET - UBA)

Background

At the onset of an acoustic stimulus, spike rate in auditory nerve neurons increases abruptly and then decays into a steady-state phase, of up to hundreds of hertz. This rate can be maintained as long as the stimulus duration, determining a high demand of activity at the inner hair cell (IHC) ribbon synapse. In this work, we investigated how synaptic responses recovered after prolonged stimulation of the IHC. Also, we sought for causes of the decay in synaptic responses.

Methods

Explants of the organ of Corti from neonatal rats were used for experiments (apical region). Simultaneous pre- and post-synaptic patch-clamp recordings at the IHC ribbon synapse were performed. The intracellular calcium concentration was measured with ratiometric fluorescent indicators, introduced in the IHC through the recording electrode. Fluorescence intensity was detected with a CCD camera. The series of differential equations corresponding to a model of the IHC ribbon synapse were solved numerically.

Results

We observed a fast recovery process with an average rate per second of 0.25 of the onset response, when using pulses at -20 mV. A faster rate was observed after pulses at -30/-40 mV (0.48 s⁻¹). Depletion of synaptic vesicles was consistently higher as presynaptic Vm increased, and so was the global $[\text{Ca}^{2+}]_i$ at the IHC, as expected for larger calcium currents. Therefore, recovery rate would not depend on presynaptic calcium concentration, but on vesicle availability. This conclusion was further confirmed by evaluating recovery at individual time points after depleting pulses of different Vm. Deconvolution analysis of ensemble responses at different IHC Vm indicated an onset component, followed by a steady state release that is < 10% of peak. Synaptic depression occurred regardless of the number of vesicles released at the onset. Simulations with a ribbon synapse model did not show equal-

ly adapting release rates. Instead, moderate or low peak release rates were followed by sustained components.

Conclusion

Fast recovery of synaptic responses is observed after prolonged stimulations at the IHC ribbon synapse. This process would ensure sustained activity for long periods of time. Less intense stimuli allow for faster recovery, possibly due to remaining vesicles in reserve pools. Unlike shown before, calcium would not modulate recovery. Synaptic depression at sub-maximal stimuli suggest that vesicles are not the sole limiting factor, but other mechanisms may apply.

PS - 755

Ca²⁺ Sensitivity of Otoferlin-Dependent Exocytosis at Cochlear and Vestibular Hair Cell Ribbon Synapses

Philippe Vincent¹; Yohan Bouleau¹; Saaid Safieddine²; Christine Petit²; Didier Dulon¹

¹Inserm and University of Bordeaux; ²Institut Pasteur

Background

Otoferlin, a C2 domain Ca²⁺ binding protein, plays a key role as calcium sensor in presynaptic exocytosis of cochlear inner hair cells (IHCs) and vestibular hair (VHCs). Johnson and Chapman (2010) showed, using SNARE-bearing liposomes *in vitro*, that the recombinant otoferlin six-C2 domains accelerate membrane fusion with a rather high Ca²⁺ sensitivity ($K_D \sim 2 \mu\text{M}$). However, *in situ* in hair cells, the real Ca²⁺ sensitivity of the otoferlin-dependent exocytosis still remains to be determined.

Methods

We used gradual caged Ca²⁺ photolysis experiments combined with patch clamp membrane capacitance measurement to determine the Ca²⁺ sensitivity of VHCs (type I) and IHCs exocytosis in both wild-type and otoferlin deficient mice at the age of balance (P5) and hearing (P14) onset. Patch clamp recordings were performed using EPC10 Heka amplifier. A C2 confocal microscope system (*Nikon*) was used to record the changes in intracellular Ca²⁺ during UV-photolysis of DM-nitrophen with a high power collimated UV light source.

Results

In wild-type mice, we found that, during voltage activation of Ca²⁺ channels, exocytosis of VHC-ribbons has an apparent higher Ca²⁺ efficiency than IHCs (2.99 fF/pC vs 0.49 fF/pC). Quantitative confocal imaging analysis using Imaris software indicated a larger non-overlapping surface area of individual CaV1.3 patches with CtBP2 patches in IHCs, CaV1.3 patches in IHCs being nearly two times larger than in VHCs. To directly probe the intrinsic Ca²⁺ sensitivity of the Ca²⁺ sensor, sequential gradual photo-released of intracellular Ca²⁺ were applied to voltage-clamped VHCs and IHCs loaded with DM-nitrophen and Ca²⁺ indicators. The rate of capacitance rise as a function of intracellular uncaged Ca²⁺ was found to be half-maximal at $4.3 \pm 0.1 \mu\text{M}$ and $4.0 \pm 0.7 \mu\text{M}$ in VHCs and IHCs, respectively. In otoferlin deficient mice, the rate of exocytosis was largely reduced by a factor of 20 (at $[\text{Ca}^{2+}]_i =$

$10 \mu\text{M}$) and showed poor Ca²⁺ dependence in both VHCs and IHCs.

Conclusion

The intrinsic Ca²⁺-sensor for exocytosis has a similar high Ca²⁺ affinity in IHCs and VHCs. The apparent higher Ca²⁺ efficiency of voltage-evoked exocytosis in VHCs is due a different CaV1.3 channel organization at their synaptic ribbons.

PS - 756

Involvement of ATP in Vesicle Pool Replenishment and Exocytosis in Auditory Hair Cell Synapse

Karina Leal; Henrique von Gersdorff

Vollum Institute, Oregon Health and Science University

Background

The hair cell afferent synapses are specialized for fast and precise synaptic transmission and have an unusual rapid ability to recruit new vesicles with little fatigue in response to continuous stimulation. At the presynaptic terminal, ATP consumption and production is highly regulated in response to synaptic activity. Previously, ATP has been shown to be essential for the preliminary stages of exocytosis but not for vesicle fusion in rod bipolar ribbon synapses. Here we address the requirements for ATP in exocytosis and regulating the recruitment kinetics of synaptic vesicles in the bullfrog amphibian papilla.

Methods

Amphibian papillae were dissected from adult bullfrogs. The amphibian papilla were stretched out and split with fine microtools to expose hair cells and afferent fibers perfused with artificial perilymph. Whole-cell patch clamp recordings and membrane capacitance measurements were performed with a double EPC9/2 patch-clamp amplifier. Data analysis was performed with Igor Pro software and Excel.

Results

Our results indicate that ATP is a necessary component for continuous vesicle release at hair cell synapses. We dialyzed hair cells with ATP or the non-hydrolyzable analogue, ATP- γ -S, and examined the whole-cell calcium current and capacitance jumps. In hair cells, ATP- γ -S does not affect calcium current amplitude, but does significantly decrease capacitance jumps with increasing stimulus depolarization. At short depolarizations durations, capacitance jumps with ATP- γ -S had the same average size as ATP controls, suggesting ATP- γ -S does not affect the immediate releasable pool. In contrast, at depolarizations of 100 ms and greater, capacitance jumps are significantly decreased suggesting recruitment of vesicles is impaired. Additionally, in the presence of ATP, successive depolarizations of 200 ms, which deplete the releasable pool of vesicles, the capacitance jump remained constant at 30 s intervals suggesting full recovery of the vesicle pool. In contrast, although substitution of ATP- γ -S for ATP had no effect on exocytosis triggered by the first initial stimulus, subsequent capacitance jumps were significantly reduced. Additionally, a decrease in the calcium current was not observed and was comparable

to control ATP conditions. Overall, at hair cell synapses these data suggest that ATP hydrolysis is necessary for vesicle replenishment.

Conclusion

ATP is required for vesicle recruitment and plays a role in maintaining the readily releasable pool of synaptic vesicles at hair cell synapses.

PS - 757

Quantal Release at the Auditory Hair Cell Synapse in the Turtle

Anthony Ricci; **michael schnee**
Stanford University

Background

Ribbon synapses of auditory hair cells are specialized to respond to graded changes in receptor potential with varying levels of vesicle release. Ribbon synapses differ from conventional synapses in the ability to maintain a high release rate of multiple vesicles from each active zone to ensure continued transmission of sound signals to the cochlear nucleus. The quantal hypothesis proposed by Katz¹ in 1954 demonstrated that the postsynaptic response is composed of quantal units resulting from the fusion of single vesicles. Each presynaptic active zone contains a single or a few vesicles whose release probability is low and independent of other vesicles. Release at the hair cell is composed of a wide range of EPSC amplitudes (up to 15×2.4) with similar kinetics that produce broad Gaussian amplitude histograms and led to the proposal of multivesicular release (MVR). MVR might involve the release of multiple vesicles near simultaneously which sum to produce a large range of EPSCs or might come from vesicles fusing with each other pre release³.

Methods

Paired voltage clamp recordings of the hair cell and afferent fiber in the turtle auditory papilla.

Results

Here paired recordings from turtle auditory hair cells and primary afferent fibers show that amplitude histograms vary depending on the presynaptic calcium load. Holding potentials eliciting <5% of the I_{Ca} revealed a single Gaussian peak with mean and variance of 61 ± 13 pA ($n=13$) while stimulations eliciting 10-30% of I_{Ca} produce multi-peaked Gaussian distributions with peaks that scaled with the smallest amplitude. The number of peaks per stimulation varied from 3 to 9 with a mean of 5.2 ± 2.1 SD. Depolarizations evoking I_{Ca} of 40-60% were broad with much less discernable peaks. Depolarizations eliciting >60% of I_{Ca} produced largely complex events. For depolarizations eliciting <10% of I_{Ca} EPSC amplitude did not change with increasing depolarization rather the frequency increased similar to results obtained with afferent recordings and high K^{+5} .

Conclusion

Data are analyzed to determine if classical quantal release mechanisms can account for measured responses at reduced stimulation.

¹J. Physiology (1954) 124: 560-573

²Nat Neurosci (2002) 5: 147-154

³J Neurosci (2008) 28: 5403-5411

⁴J. Neuroscience (2009) 29(23):7558-7566

⁵J. Neurophysiol (2013) 110:204-220

PS - 758

Spatial-Temporal Maturation of Inner Hair Cell's Ribbon Synapses Molecular Elements

Felipe Salles; Jee-Hyun Kong; Anthony Ricci
Stanford University

Background

The ribbon synapse is a challenging structure for molecular/morphological characterization, as it is composed of multiple proteins confined to a small compartment. A proper molecular profile becomes relevant because little is known on how this molecular machinery is assembled and what the specific functions are of each component. Functional studies alone cannot separate molecular components and need a molecular backbone upon which to base interpretations. This study aimed to generate a comprehensive temporal panel of structural and vesicle-related synaptic proteins of rat inner hair cells' as a means of identifying important molecules throughout synaptic maturation.

Methods

We performed immunohistochemistry in freshly dissected and fixed whole mounts of rat tissue at ages P3, P8, P14 and adult. At P3 the hearing system is still immature, although synaptic proteins are already expressed. At P8, calcium currents peak and action potentials in inner hair cells drive transmitter release (Beutner and Moser, 2001; Johnson et al., 2005). At P14, after hearing onset, inner hair cells exhibit close to mature synaptic responses, and adults have fully mature synaptic properties. We then analyzed the expression of ribeye and piccolo (structure), bassoon (anchoring), otoferlin, VGlut3 (vesicles), $Ca_v1.3$ (channel), PSD95, homer1a (post-synaptic structure), RIM1/2 (vesicle release), SERCA2, PMCA and mitochondria (calcium metabolism) under confocal microscopy. Quantification, co-localization and volume measurements were performed in 3D rendered images using Volocity software and plotted in Excel or Origin softwares.

Results

We observed a quantitative decrease for all the structural markers, and a pronounced co-localization of ribbons, PSD 95, homer 1a, piccolo, bassoon and RIM 1/2. However, piccolo, bassoon and RIM1/2 were always expressed at higher counts than the other components, possibly as a reserve for protein turnover. The calcium channels show pronounced clustering and consequent co-localization with the ribbons and the post-synaptic structures throughout development. The vesicle associated proteins, VGlut 3 and otoferlin show a diffuse distribution in the cell bodies. VGlut 3 is strongly expressed at all ages, and otoferlin has a low expression at early age, suggesting timed expression these proteins has an impact in vesicle release properties and consequent synaptic maturation. The immunoexpression of PMCA, SERCA2 and

mitochondria did not exhibit direct co-localization or evident relationship with the ribbons.

Conclusion

Results show clustering of calcium channels and temporal expression of structural proteins happen along with synaptic maturation and suggest an inter-dependable structural/functional relation in development.

PS - 759

Exogenous Ribeye B-Domain Localizes to Synaptic Ribbons and Disrupts Ribbon Stability in Zebrafish Hair Cells

Lavinia Sheets¹; Matthew Hagen²; Teresa Nicolson²

¹Harvard Medical School, Massachusetts Eye and Ear Infirmary; ²Oregon Health & Science University

Background

Synaptic ribbons are formed by the self-association of Ribeye — a unique and important structural component of ribbon synapses. Ribeye consists of two subdomains: an N-terminal, proline rich A-domain and a C-terminal B-domain. Previous *in vitro* studies have shown that Ribeye A-domain alone forms ribbon-like aggregates and that both A- and B- domains form homo- and heteromeric interactions. As these interactions are likely the basis for ribbon-synapse assembly, we wanted to examine how Ribeye A- and B- domains behave *in vivo*. To that end, we characterized the interactions of endogenous full-length Ribeye with exogenous truncated forms of Ribeye in the hair cells of stable transgenic zebrafish larvae.

Methods

Stable transgenic lines of *ribeye a (A-domain)-6xmyc*, *ribeye b (A-domain)-gfp*, *ribeye a (B-domain)-6xmyc*, and *ribeye a (B-domain)-gfp* driven by the hair cell specific promoter *myo6b* were generated in TU and TLF wild-type backgrounds. Zebrafish larvae were fixed at 2-, 3-, and 5-days-post fertilization in 4% paraformaldehyde, then processed for whole-mount immunohistochemical labeling of hair-cell synaptic proteins. Z-stack images of neuromasts were acquired with a confocal microscope using a 60X/1.5 N.A. oil immersion lens. *ribeye b* expression levels in posterior lateral line hair cells were measured using qPCR.

Results

Unexpectedly, exogenously expressed Ribeye A-domain generally failed to aggregate or localize to synaptic ribbons, even in the presence of endogenous Ribeye. By contrast, Ribeye B-domain robustly aggregated in the presence of endogenous Ribeye and localized to synaptic ribbons. Moreover, the B-domain preferentially localized to the basal end of ribbons adjacent to the postsynaptic density. Overexpression of Ribeye B-domain also appeared to affect synaptic-ribbon stability; endogenous Ribeye immunolabel was significantly reduced in 5-day-old B-domain transgenic larvae while relative expression of *ribeye* transcript in B-domain expressing hair cells was comparable to wild-type.

Conclusion

Our data reveals that exogenously expressed Ribeye domains behave differently *in vivo* than they do *in vitro*, and

suggests a potential substructural organization of elements within synaptic ribbons.

PS - 760

Developmental Changes in the Voltage-Gated Ca²⁺ Channels (VGCC) That Mediate Acetylcholine (ACh) Release at the Transient Efferent-Inner Hair Cell Synapse

Graciela Kearney; Javier Zorrilla San Martín; Carolina Wedemeyer; Ana Belén Elgoyhen; Eleonora Katz
Instituto de Investigaciones en Ingeniería Genética y Biología Molecular (INGEBI-CONICET)

Background

Since birth until the onset of hearing (postnatal day (P) 12 in mice), inner hair cells (IHCs) are innervated by medial olivocochlear (MOC) efferent fibers. At P9-11, ACh release is supported by both P/Q and N-type VGCCs and negatively regulated by L-type VGCC, coupled to BK potassium channel activation. We previously reported that at P5-7, P/Q- but not N-type VGCC partially support ACh release and that blocking BK channel increases the quantum content of evoked release (*m*) (Zorrilla de San Martín et al., ARO Abstracts 2012). Our goal is now to determine which other type/s of VGCCs mediate ACh release at this (P5-7) and earlier stages (P3) and whether BK channels and L-type VGCCs are functionally coupled.

Methods

Postsynaptic responses were monitored in whole-cell voltage-clamped IHCs while electrically stimulating the efferent fibers in P3 and P5-7 mouse cochleas.

Results

At P5-7, SNX-482, the R-type VGCC antagonist, significantly reduced *m* (control: 0.84±0.01; 500 nM SNX: 0.37±0.05, n=2; *p*<0.05). Surprisingly, both the L-type VGCC antagonist nifedipine and the agonist Bay-K enhanced *m* (%increment = 161±21, 3 mM Nife; 294±26, 10 mM Bay-K). This suggests that at P5-7, Ca²⁺ entry through L-type VGCC might be both supporting release and activating BK channels. However, occlusion experiments showed that IbtX had no effect on *m* after incubation with L-type VGCC modulators (*m* = 0.56±0.18 control; 1.64±0.86 Nife; 1.85±1.02 Nife+IbtX; n=2, *p*>0.50 and *m* = 1.10±0.42 control; 2.67±0.80 Bay-K; 2.23±0.16 Bay-K+IbtX; n=3; *p*>0.2). Moreover, nifedipine had no effect on *m* after blocking both P/Q-type VGCC and BK channels with 200 nM ω-AgaIVA and 100 nM IbtX, respectively (*m* = 0.91±0.25 ω-Aga+IbtX and 1.08±0.29 for ω-Aga+IbtX+Nife; *p*>0.5, n=3). In addition, Bay-K had no effect on *m* after blocking BK channels (control: 0.95, IbtX: 2.7, IbtX+Bay-K: 2.8). Altogether, these results show that L-type VGCCs do not support, but negatively modulate release by activating BK channels at P5-7. Preliminary experiments show that at P3, ω-AgaIVA, does not affect *m* (control: 0.54±0.06; ω-AgaIVA 0.62±0.25; n=2; *p*>0.5), suggesting that P/Q-type VGCCs do not support ACh release at this early stage. Bay-K significantly enhanced *m* by 382±120%; n=2), indicating that L-type VGCCs also modulate ACh release at P3.

Conclusion

Our results show that there are significant changes in the VGCC types that support neurotransmitter release at the transient MOC-IHC synapse during postnatal development.

PS - 761

Syntaxin-1B Binding Partners in Hair Cells

Tyson Fisher; Neeliyath Ramakrishnan; Dennis Drescher
Wayne State University School of Medicine

Background

While the exact identities of hair cell SNARE proteins are still unknown, experimental evidence suggests that syntaxin-1, SNAP-25 and synaptobrevin-1/2 may form the core SNARE complex of the hair cell. Of syntaxin isoforms, we have detected only syntaxin-1B in trout hair cells. Syntaxin 1B has also been identified in rat organ of Corti, pointing to a possible involvement of this syntaxin isoform in the hair cell synaptic complex. Whereas in mouse, the syntaxin-1B knockout is lethal, the syntaxin-1A knockout is little affected. Cultured neurons from the former show severe deficits in fast exocytosis. Our current investigation examined binding partners of syntaxin-1B in trout hair cells, using a yeast two-hybrid screening protocol.

Methods

Syntaxin-1B was amplified by PCR and cloned in yeast bait vector pGBKT7. Two syntaxin-1B bait constructs were used in yeast strain Y187 and mated with a trout hair cell cDNA prey library, created using the pGADT7 Rec vector, in yeast strain AH109. One syntaxin-1B bait construct contained the syntaxin N-terminal helix, encompassing regions Ha, Hb and Hc, while the second construct covered the SNARE domain as well as portions of the Hc helix. Colonies obtained after selection in a quadruple dropout medium were used for PCR amplification. The PCR products were sequenced and identified via an NCBI BLAST search.

Results

Of 54 different positive prey clones, we identified four sequences of particular synaptic interest: calmodulin, Tax1 binding protein, disks large associated protein 1-like protein, and protein tyrosine phosphatase receptor type U (PTPRU). The PTPRU sequence comprised a short cytoplasmic region which, in the complete protein, is flanked on the N- and C-terminal sides, respectively, by a transmembrane domain protruding extracellularly and a pair of intracellular tyrosine phosphatase domains. Using cloned rat sequences, we detected positive interaction between syntaxin-1B and GST-PTPRU by pull-down assay. We further performed immunoprecipitation using specific anti-syntaxin-1 antibody and detected a band corresponding to PTPRU, not detected in the negative control. Conversely, using anti-PTPRU, we detected syntaxin 1 in immunoprecipitation reactions, clearly demonstrating a direct interaction between syntaxin-1B and PTPRU.

Conclusion

Our results showed that syntaxin-1B interacts with many novel proteins in saccular hair cells. Some isoforms of receptor-type protein tyrosine phosphatase are known to be required for proper synapse formation via interaction with

pre-synaptic and post-synaptic proteins. The role of PTPRU in hair cells and its possible function within the synaptic complex are subjects of ongoing investigation.

PS - 762

Molecular Characterization of Ribeye and the GABAA Alpha 1 Receptor Subunit in Hair Cells

Zachary VandeGriend; Marian Drescher; Neeliyath Ramakrishnan; Dennis Drescher

Wayne State University School of Medicine

Background

Ribeye, the primary protein of the synaptic body in ribbon synapses of hair cells, retinal photoreceptors and bipolar cells, interacts with synaptic complex proteins anticipated to impact exocytosis (Uthiah and Hudspeth, 2010; Kantardzhieva et al., 2011). There are three described variants of human C-terminal binding protein 2 (CTBP2) including ribeye (variant 2, isoform 2), differing with respect to their amino-terminus half as opposed to the highly conserved carboxy-terminus half, which exhibits high identity to a transcriptional corepressor. We now report the molecular characteristics of the form of ribeye and its non-conserved amino terminus specifically expressed in hair cells, accomplished with a purified preparation of hair cells isolated from the trout sacculus with $> 1 \times 10^6$ hair cells, uniquely robust in expression of hair cell transcripts and proteins. In addition, we examined the question of whether GABAA alpha 1, immunoprecipitated with ribeye in a retina preparation, suggested to result from the inclusion of bipolar cells (Kantardzhieva et al., 2011), is actually expressed in hair cells, consistent with the possibility that GABA is a transmitter in efferents and in a subpopulation of vestibular hair cells (Holstein et al., 2004).

Methods

Degenerate primers were designed with Accelrys software targeting cDNA for CTBP2 isoforms and GABAA alpha 1 expressed across teleosts. The primers, applied in PCR to trout saccular hair-cell cDNA, crossed introns, and all products were sequenced.

Results

The saccular hair cell ribeye sequence (GenBank Accession No. KF644437) overall was 65% identical, 74% positive to human ribeye. The conserved carboxy-terminus half was 94% identical and 97% positive to CTBP2 isoform 1, whereas the amino-terminus half was 40% identical, 52% positive to CTBP2, isoform 2-ribeye. Compared to teleost sequence, the amino terminus of trout saccular hair cell ribeye was closer to zebrafish *ribeye a* (54% identity, 65% positive) required for photoreceptor function than *ribeye b* (44% identity, 57% positive).

Degenerate primers for GABAA alpha 1 have elicited amplification of 80% of full-length cDNA from trout saccular hair cells (GenBank Accession No. KF644440) with 90% identity, 93% positive amino acid sequence relative to human.

Conclusion

Molecular analysis of CTBP2 transcript obtained directly from hair cells indicates expression of the long form, ribeye, with

an extended amino terminus supporting formation of protein aggregates potentially underlying synaptic vesicle tethering. Further, we have identified in hair cells for the first time transcript expression of the GABAA alpha 1 subunit immunoprecipitated with ribeye.

PS - 763

The Role of Ca²⁺ Binding Protein 2 (CaBP2) in Synaptic Sound Encoding and Hearing

Maria Picher¹; Alexandra Ivanovic²; Guy VanCamp³; Tobias Moser¹

¹University of Goettingen Medical Center; ²Max Planck Institute of experimental Medicine; ³University of Antwerp

Background

Ca_v1.3 Ca²⁺ channels are L-type voltage gated Ca²⁺ channels expressed at inner hair cell (IHC) ribbon synapses in the cochlea. In IHCs Ca_v1.3 channels show a fast activation at relatively negative voltages and slow inactivation kinetics, two crucial characteristics to enable precise sound encoding over prolonged periods of time. Ca²⁺ dependent inactivation (CDI) is a Calmodulin (CaM) dependent feature of voltage gated Ca²⁺ channels and is generally weak in IHCs. Ca²⁺ binding proteins (CaBPs), members of the EF-hand Ca²⁺ binding protein family are closely related to CaM, expressed in neurons and sensory cells and were suggested to antagonize CDI in IHCs by competing with calmodulin.

Methods

In this study we investigate to which extent CaBP2 could be responsible for a proper Ca_v1.3 channel gating in IHCs. To address this question we performed experiments in HEK293/SK3-1 cells to study the interaction between various mutants of CaBP2 and the Ca²⁺ channel. In another set of experiments we characterized a CaBP2 knock out mouse model by examining the auditory function of these mice with auditory brainstem recordings (ABR) and distortion product otoacoustic emission measurements (DPOAEs). To identify changes in the synaptic function of IHCs we used whole cell patch clamp recordings and focused on protocols identifying changes in the biophysical properties of the Ca_v1.3 Ca²⁺ channels in the presence and absence of CaBP2.

Results

Experiments with HEK293/SK3-1 cells reproduced the effect of CaBP2 in preventing CDI and in addition, revealed a significant shift of V_h to more hyperpolarized potentials. No reduction of Ca_v1.3 current was observed when co-expressing CaBP2. The truncated CaBP2, thought to occur in human DFNB93, showed less potent inhibition of CDI and did not cause the V_h shift, observed with wild-type CaBP2.

A mouse mutant expressing LacZ in the CaBP2 locus was generated and revealed expression in IHCs and to a lesser extent in outer hair cells. ABR and DPOAE measurements checking in these CaBP2 loss of function mouse mutants demonstrated the signature of an auditory synaptopathy in IHCs with impaired ABR despite normal DPOAE. Preliminary whole cell patch clamp recordings indicate an enhanced CDI of Ca_v1.3 Ca²⁺ channels in IHCs lacking CaBP2.

Conclusion

This study provides evidence, that CaBP2 is crucial for a precise regulation of Ca_v1.3 channels in IHCs, synaptic sound encoding and hearing.

PS - 764

Ribbon Synapse Domains in Development and Noise Exposure

Steve Paquette; Felicia Gilels; Patricia White

University of Rochester

Background

Rates of spontaneous potential generation in dendritic fibers comprising the cochlear nerve appear to be set within three different sub-classes: (1) low rate, high threshold, (2) mid-level rate and threshold, and (3) high rate, low threshold [1]. Retinal ganglion neurons have also been observed to generate spontaneous action potentials as a module to guide development and maturation [2]. Here we assess the model that fiber sub-type is dependent upon organization of synaptic components. This model is tested here as a developmental series in FVB/n mice. The degree to which hearing is affected in normal aging and in response to noise-induced excitotoxic stress in the FVB/n line is also examined.

[1] Liberman CM. *J. Acoust. Soc. Am.* **1978**, 63, 2, 442-455.

[2] Meister M, Wong ROL, Baylor DA, Shatz CJ. *Science*. **1991**, 252, 939-943.

Methods

Development of hearing in the FVB/n strain is examined using auditory brainstem response (ABR) data. Organization of cochlear inner hair cell (IHC) synapses is then examined using a custom algorithm for determination of paired pre- and post-synaptic domains. A Bayesian population cluster analysis is then performed on synapse domain size and position obtained from reconstructions of confocal microscopy data.

Results

Animals with noise-damaged hearing showed similar ABR traces to those of 1-year old wild-type animals. Clustering analysis of synaptic components showed that in noise-damaged animals, a visible distinction could be made between modiolar and pillar synapses relative to the unexposed animals. Basal to apical determinations on synapse localization throughout development reflected a maturation of IHCs at 4 months of age. Analysis of synapse component sizes yielded significant differences between noise-damaged animals and those seen in the normal developmental progression.

Conclusion

The developmental series ABR data show that FVB/n mice initially have incomplete hearing at 2 months and show a progressive IHC maturation, ending in deafness at 1 year. While ABRs are similar in noise-damaged and aged animals, the spatial distribution of synapses is largely different between the two groups in animals 3-days post-deafening and 1 year respectively. The difference between noise damage and normal aging is further characterized by examining the positions of pillar and modiolar synapses at identical time points.

PS - 765

Endocochlear Potential (EP) Reduction is Irrelative to Connexin26 (GJB2) Deficiency Induced Congenital Deafness

Jin Chen; Jing Chen; Yan Zhu; Chun Liang; Hong-Bo Zhao
University of Kentucky Medical Center

Background

Connexin 26 (Cx26, *GJB2*) mutations are a major genetic cause of hearing loss and responsible for 50% of nonsyndromic deafness. Mouse models show that Cx26 deficiency can cause congenital deafness with cochlear development disorders, hair cell degeneration, and the reduction of endocochlear potential (EP) and active cochlear mechanics. However, the detailed mechanism still remains unclear. Our previous studies demonstrated that hair cell degeneration is not a primary cause for hearing loss. In this study we investigate the role of EP reduction in Cx26 deficiency-induced deafness. We found that the EP reduction is not directly relative to Cx26 deficiency induced deafness.

Methods

Cx26 in the inner ear was conditionally deleted by loxP-Cre technique. EP was directly recorded. Hearing function was assessed by ABR and DPOAE measurements. Cochlear morphology and Cx26 expression were examined by confocal microscopy.

Results

Deletion of Cx26 in the inner ear caused congenital, complete deafness. EP was reduced. However, the degree of EP reduction is irrelative to deafness. Different from complete deafness, the EP was not completely abolished in Cx26 knockout (KO) mice and could still retain at the high level (> 70 mV). We further found that deletion of Cx26 before postnatal day 5 (P5) could result in congenital, profound hearing loss. The cochlea had development disorders. The EP could still retain at higher levels. However, deletion of Cx26 expression after P5 could result in hearing loss but not complete deafness. The cochlea had normal development.

Conclusion

EP reduction is not associated with congenital deafness in Cx26 deficient mice. Cx26 deficiency induced congenital deafness may mainly result from cochlear developmental disorders.

PS - 766

SLC26A4 p.T410M Homozygous Mutation Found in a Cystic Cochlea With an Enlarged Vestibular Aqueduct Which is Different from IP-II With Respect to the Lack of a Bony Modiolus

Hiroshi Yamazaki¹; Yasushi Naito²; Juichi Ito¹

¹Kyoto University; ²Kobe City Medical Center General Hospital

Background

Mutations in the *SLC26A4* gene are the second leading cause of deafness in autosomal recessive inheritance and highly

associated with incomplete partition type II (IP-II) or isolated enlarged vestibular aqueduct (EVA). The former is the most common inner ear malformation which is defined by the middle and apical turns coalesce to form a cystic apex with a dilated vestibule and EVA. There are over 160 reported mutations in *SLC26A4* and analysis of the common types of mutations demonstrated that biallelic mutations in *SLC26A4* were associated with EVA, but severity of a cochlear malformation as well as a presence of a thyroid disease varied between the types of mutations. Among the mutations in *SLC26A4*, p.T410M was relatively rare, but found in both European and Asian populations. Clinical features and radiographic findings of patients with the p.T410M homozygous mutation have not been investigated well.

Methods

A retrospective case review

Results

A 1-year-old boy presented with profound sensorineural hearing loss and was diagnosed with nonsyndromic sensorineural hearing loss. He had neither family history of hearing loss nor perinatal problem. His genetic testing for hearing loss using Invader assay identified a *SLC26A4* p.T410M homozygous mutation. CT images identified a bilaterally symmetrical inner ear malformation, in which a cystic cochlea without a bony cochlear modiolus, dilated vestibule, and EVA were observed. MRI suggested a cerebrospinal fluid (CSF) communication between the malformed cochlea and the IAC on the left side. These radiographic findings did not entirely match with the definition of IP-II, but rather met the criteria for cochlear hypoplasia type II defined by Sennaroglu. This patient underwent sequential bilateral cochlear implantation. No specific problem was observed during the implantation on the right side, while a severe CSF gusher occurred during the implantation on the left side. His CI-aided speech discrimination score of infant words was 90% and he could orally communicate at 2 years after implantation.

Conclusion

Mutations in *SLC26A4* were found in all reported types of inner ear malformations with EVA, including IP-II, isolated EVA, and cochlear hypoplasia type II. Severity of a cochlear malformation might be different between the types of the mutations and p.T410M homozygous mutation was associated with a most severe type of malformations, a cystic cochlea without a bony modiolus. Genetic diagnosis of the exact type of *SLC26A4* mutations might be useful to predict CSF gusher during implantation.

Generation and Phenotype Assessment of an Slc44a2 Knockout Mouse on the FVB/NJ Background

Thankam Nair; Pavan Kommareddi; Irina Laczkovich; Bala Naveen Kakaraparthi; Ariane Kanicki; Lisa Kabara; David Dolan; Thomas E Carey

KHRI, University of Michigan

Background

SLC44A2/CTL2 (choline transporter-like protein 2), was discovered in the inner ear. It is abundantly expressed in lung, leukocytes, kidney and testis. CTL2 is implicated in immune-mediated hearing loss and transfusion-related acute lung injury (TRALI). Exons 3-10 spanning the *Slc44a2* first extracellular loop were targeted for deletion in strain C57BL/6J, a strain subsequently shown to carry the *Ahl Cdh23753A* allele. The knockout was backcrossed to the ARHL-resistant FVB/NJ strain (*Cdh23753G*) and hearing was evaluated in this genetic context.

Methods

B6.129-*Slc44a2*^{del-ex3-10/Tec} mice were backcrossed to FVB mice and progeny were PCR genotyped for *Cdh23753G* and the *Slc44a2* deletion. After backcross five (97% FVB background), intercross progeny were ABR tested at 1.5 and 3.5 months of age at 12, 24, and 48 kHz, and at 4.5 and 6 months at 12, 24, and 32 kHz.

Results

Fourteen mice from backcross five - intercross one (6 *Slc44a2*^{del-ex3-10/del-ex3-10}, 2 *Slc44a2*^{del-ex3-10/+}, and 6 *Slc44a2*^{+/+}) were evaluated. All progeny mice were ARHL-resistant *Cdh23753G/753G*, but we found that all FVB mice including wild-type mice have 60-80 dB SPL hearing loss at 48 kHz. One male *Slc44a2*^{del-ex3-10/del-ex3-10} mouse died after the first ABR. At 4.5 months, all five *Slc44a2*^{del-ex3-10/del-ex3-10} mice (3 males, 2 females) had mild to profound hearing loss (40-75 dB SPL) at 12, 24 and 32 kHz. Two *Slc44a2*^{del-ex3-10/+} male mice and six (4 male, 2 female) *Slc44a2*^{+/+} mice had no hearing loss at any frequency. A second male *Slc44a2*^{del-ex3-10/del-ex3-10} mouse was found dead after the third ABR. At 6 months, all four remaining *Slc44a2*^{del-ex3-10/del-ex3-10} mice had persistent hearing loss and the 2 males had progressive loss (55-105 dB SPL) at all three frequencies. The two *Slc44a2*^{del-ex3-10/+} mice and 5/6 *Slc44a2*^{+/+} mice had normal hearing (one had 40 dB at 32 kHz). Curiously, in the next generation of homozygous *Slc44a2*^{del-ex3-10/del-ex3-10} mice there were fewer than expected males (4/22). This generation is 1.5 months old and being tested.

Conclusion

Wildtype FVB/NJ mice have normal hearing thresholds at 32kHz but not at 48 kHz. Mice with a 97% FVB background homozygous for the *Slc44a2*^{del-ex3-10/del-ex3-10} but not *Slc44a2*^{+/+} and heterozygous *Slc44a2*^{del-ex3-10/+} exhibit mild to profound hearing loss at 12, 24 and 32 kHz from 4.5 months onwards, with evidence of progressive hearing loss. Hints of greater effects in males must be confirmed. These data indicate that the *Slc44a2* gene is important for normal auditory function.

Stria Vascularis Dysfunction in a Mouse Model of Mitochondrial Hearing Loss

Sharen McKay¹; Wayne Yan²; **Lei Song**²; Nuno Raimundo³; Joseph Santos-Sacchi²; Gerald Shadel⁴

¹*Yale University School of Medicine*; ²*Surgery, Yale*

University School of Medicine; ³*University of Goettingen*;

⁴*Pathology and Genetics, Yale university School of Medicine*

Background

Hearing loss caused by degeneration of the stria vascularis is characterized by a flat audiogram, loss of endocochlear potential and atrophy of the stria epithelium. Strial hearing loss constitutes a significant proportion of human presbycusis cases and is implicated in other forms of deafness. We recently described a transgenic mouse model of hearing loss induced by over-expression of the mitochondrial ribosomal RNA (rRNA) methyltransferase, TFB1M (Tg-TFB1M). These mice recapitulate maternally inherited deafness caused by the human A1555G mtDNA mutation, which results in increased methylation of the 12S rRNA in mitochondrial ribosomes and tissue-specific susceptibility to apoptosis. In this study we characterize the tissue specific origin of hearing loss in this particular mouse model.

Methods

We measured ABR and EP and subsequently fixed cochlear tissue for histological observation. Whole cell patch clamp was also used to measure motility and nonlinear capacitance of the mouse outer hair cells.

Results

We observe hearing loss progressing from three months of age to one year and subsequent histological analysis revealed apoptosis in the stria vascularis. Consistent with strial dysfunction, there is a significant reduction in the endocochlear potential in Tg-TFB1M mice compared to littermate controls. However, stria atrophy, as measured by the width of the stria at the middle turn using 5 um hematoxylin stained FFPE histological sections through the cochlea, is not evident. Outer hair cells show normal motility and nonlinear capacitance.

Conclusion

We conclude that the mechanism of hearing loss in this mouse model is likely due to strial dysfunction, but does not conform to the classical atrophic model of strial hearing loss. Studies are underway to identify the precise mechanism of the strial dysfunction to provide new insight into how mitochondrial dysfunction contributes to deafness pathology in a tissue-specific manner.

Identification and Validation of a Novel POU4F3 Mutation in a Hearing-Impaired Family by Massively Parallel Sequencing and Functional Genetic Study in Cell-Lines

Chuan-Jen Hsu¹; **Chen-Chi Wu**^{1,2}; Yin-Hung Lin³; Ying-Chang Lu¹; Hsiao-Chun Lin¹; Yi-Tsen Lin¹; Pei-Lung Chen^{2,4}

¹Department of Otolaryngology, National Taiwan University Hospital, Taipei, Taiwan; ²Department of Medical Genetics, National Taiwan University Hospital, Taipei, Taiwan;

³Graduate Institute of Molecular Medicine, National Taiwan University College of Medicine, Taipei, Taiwan; ⁴Graduate Institute of Medical Genomics and Proteomics, National Taiwan University College of Medicine, Taipei, Taiwan

Background

Hearing impairment is a genetically heterogeneous condition with > 100 deafness genes identified thus far. Recent studies have confirmed the utility of massively parallel sequencing (MPS) in addressing the genetically heterogeneous hereditary hearing impairment. In our previous study, we used MPS to sequence 80 genes in 12 multiplex families, and identified 2 known mutations and 2 novel mutations as the causative mutations in 4 families. Recently, we further upgraded the screening panel to include 131 deafness genes, and applied the panel to another 12 multiplex families.

Methods

Twelve unrelated multiplex families with idiopathic sensorineural hearing impairment were enrolled and subjected to the MPS panel. Criteria for data filtering included: allele frequencies <5%, both PolyPhen2 and SIFT scores >0.95, Sanger sequencing, segregation pattern, and evolutionary conservation of amino acid residues. To determine the effects of missense mutations on the subcellular localization of POU4F3, COS-1 cells were transiently transfected with constructs encoding either the wild-type or the mutant protein fused to an HA-tag C-terminally.

Results

In the proband of an autosomal dominant family with 5 affected members, we found a novel missense mutation, p.K328E (c.982A>G), in exon 2 of *POU4F3*. The pathogenicity of p.K328E was supported by its high SIFT (1) and PolyPhen2 (0.998) scores, as well as its absence in the 5400 NHLBI exomes, 1000 Genomes, and the 100 normal hearing controls. Furthermore, heterozygosity for p.K328E co-segregated with the phenotype of hearing impairment in the affected members of the family, and the amino acid residue p.K328 was evolutionarily conserved. The proband of the family was a 45-year-old female with profound hearing loss which developed since around 30-years old. Her grandfather, her mother and her mother's two half sisters (with the same father) also revealed progressive hearing impairment of late onset. All the affected patients exhibited normal temporal bone imaging results. Transfection studies in COS-1 cells showed that whereas the wild-type POU4F3 is located almost exclusively in the nucleus, part of the mutant proteins was also present in

the cytoplasm, indicating the localization ability of the mutant protein was compromised.

Conclusion

We identified a novel *POU4F3* p.K328E mutation in a hearing-impaired Taiwanese family by using a MPS screening panel, and then confirmed its pathogenicity in COS-1 cells. The application of MPS screening followed by functional genetic study in cell-lines facilitates a fast genetic diagnosis and a deep comprehension of the molecular pathology in families with hearing impairment.

Drastic Disruption of Gap Junction Plaque in Brn4 Deficient Mouse, a Model for DFN3 Nonsyndromic Deafness

Yoshinobu Kidokoro¹; Kazusaku Kamiya²; Osamu Minowa³; Katsuhisa Ikeda²

¹Juntendo University Faculty of Medicine; ²Juntendo University School of Medicine, Department of Otorhinolaryngology; ³BioResource Center, RIKEN

Background

Congenital hearing deafness is occurred proportion of 1 in 2000 birth, and it is the most number of congenital diseases. In human, X chromosomelinked nonsyndromic hearing loss, deafness type 3 (DFN3) is the most popular nonsyndromically hering loss. Brn4, which encodes a POU transcription factor, is the gene responsible for DFN3. To investigate the function of Brn4 in cochlea, we have developed Brn4 deficient mice as a model of DFN3 nonsyndromic deafness (Minowa O et al., Science, 1999) . These mice show low endocochlear potential (EP), hearing loss and severe ultrastructural alterations in spiral ligament fibrocytes (Minowa O et al., Science, 1999) . In humans, mutations in the connexin26 (Cx26) and connexin 30 (Cx30) genes, which encode gap junction proteins and are expressed in cochlear fibrocytes and nonsensory epithelial cells (cochlear supporting cells) to maintain proper EP, are well known to be responsible for hereditary sensorineural deafness. Although, the molecular pathologies of Brn4 deficiency causing low EP are still unclear. In this study, we analyzed the formation of gap junction plaques (GJP), the functional molecular complex of the gap junction of Brn4 KO mice in different stages by confocal microscopy and three dimensional graphic constructions to determine the association between the Connexins and Brn4.

Methods

It has been hypothesized that gap junction in the cochlea provide an intercellular passage by which K⁺ are transported to maintain high levels of the endocochlear potential essential for sensory hair cell excitation. In this study, we analyzed the formation of gap junction plaques in cochlear supporting cells of Brn4 KO mice in different stages by confocal microscopy and three dimensional graphic constructions. Immunofluorescence staining with antibodies against Cx26 and Cx30 was performed on whole-mount preparations of finely dissected organ of Corti that included inner sulcus cells (ISCs). Fluorescence confocal images were obtained with a LSM510-META confocal microscope (Carl Zeiss). Cx30 was immunola-

belled by red fluorescence, Cy3 and observed 543nm laser at confocal microscopy. Cx26 was immunolabelled by green fluorescence, Alexa488 and observed 488nm laser. Three-dimensional images were constructed with z-stacked confocal images by IMARIS. We also investigated ultra-structures of gap junctions in 6-week-old mice by scanning electron microscope photography, and measured protein levels of Cx26 in Brn4-KO mice in 6-week-old by western blotting.

Results

Gap junctions composed of mainly of Cx26 and Cx30 in wild type mice showed horizontal linear gap junction plaques along the cell-cell junction site with the adjacent cells and these formed pentagonal or hexagonal outlines of normal inner sulcus cells and border cells. However, the gap-junction plaques in Brn4 KO mice did not show normal linear structure, but the round small spots were observed around the cell-cell junction site. The size of gap junction units of Brn4 KO mice was significantly shorter than control mice. In 2-week-old, wild type and Brn4-KO mouse, gap junction plaque forms linear units regularly around the cells. In 4-week-old Brn4-KO mouse also forms linear structure of gap junction plaque, although a part of them are disrupted and scattered. In 6-week-old Brn4-KO mouse, a number of small gap junction plaques composed of Cx30 scattered around cell-cell junction sites were observed. The length of each GJPs were notably shorter than the littermate control. In a detailed analysis with three-dimensional graphic construction of the GJP structure in the ISCs, wild-type adult mouse cochlear showed large, planar GJPs at the cell border that formed orderly pentagonal or hexagonal outlines around normal ISCs. In contrast, cochlear from Brn4-KO mice showed drastically fragmented small vesicle-like GJPs, resulting in an extremely diminished total plaque area as compared with control mice. Ultra structures of gap junctions were observed in 6-w-old wild type and Brn4-KO mice by scanning electron microscope photography. Horizontal ultrathin sections of ISCs showed the gap junctions in Brn4-KO mice as in control mice. Western blotting analysis showed that decreased protein expression was observed for Cx26 in Brn4-KO mice. The protein levels of Cx26 were normalized to the corresponding β -actin levels and expressed relative to the amount present in each littermate controls.

Conclusion

In this study, we demonstrated the drastic disruption of GJP occurred as an initial pathology of the hearing impairment caused by Brn4 deficiency and suggested the pathological association with the hearing loss caused by the mutations of connexins such as Cx26 and Cx30 which is most frequently detected in hereditary deafness. The disruption of GJP observed after 4w were also observed in our two Connexin26 mutant mice. This indicates that Brn4 expressions directly or indirectly affect on gap junction formation in ISCs. The loss of GJP area may then abolish the proper biophysical potential needed for intercellular communication in the cochlea. This may explain why Brn4-KO mice showed significantly decreased EP in our previous study (Minowa O et al., Science, 1999). Currently, downstream targets of POU3F4 including gap junction genes and their estimated transcription factors

in the cochlear supporting cells are unknown. Although the whole molecular pathway between Brn4 and cochlear gap junction have not been found yet, our data clearly demonstrated that POU3F4 affects the expression and assembly of gap junction proteins, Gjb6 (Cx30) and Gjb2 (Cx26) in cochlear supporting cells. These findings may explain the decrease of EP and the severe hearing loss in Brn4 deficient mice and DFN3 patients. Our results demonstrated that Brn4 gene mutation affects on the accumulation and localization of gap junction proteins at the cell border among cochlear supporting cells. It may suggest that Brn4 significantly associates with cochlear gap junction properties to maintain proper EP in cochlea as well as the mutations of Cx26 or Cx30.

PS - 771

Connexin 26 Null Mice Exhibit Spiral Ganglion Degeneration That Can Be Blocked by BDNF Gene Therapy

Yohei Takada¹; Lisa Beyer¹; Donald Swiderski¹; Diane Prieskorn¹; Shaked Shivatzki²; Karen Avraham²; Yehoash Raphael¹

¹University of Michigan; ²Tel Aviv University

Background

Mutations in the connexin 26 gene (*GJB2*) are the most common genetic cause of deafness, leading to congenital bilateral nonsyndromic sensorineural hearing loss. Here, we report the generation of a mouse model for a connexin 26 (Cx26) mutation, in which cre-Sox10 drives excision of the Cx26 gene from supporting cells of the auditory epithelium. We determined that the conditional knockout mice (generated on a C57BL/6 background) designated *Gjb2-CKO*, have severe hearing loss at P28. The goal of the experiments was to characterize the progression of structural and functional deficits over time, and to determine if BDNF gene therapy can influence the condition of the ear and hearing.

Methods

Hearing thresholds were measured using ABR audiometry at ages 1 and 3 months of age. Cx26-specific immunocytochemistry was performed on whole mounts. Histology on mid-modiolar plastic sections was performed at ages 1, 3, or 6 months. Ad.BDNF gene therapy was performed at 1 month of age by adenovirus injection into the scala media or scala tympani at the cochlear base.

Results

In wild-type mice, immunoreactivity of Cx26 appears as a dotted line along the perimeter of nonsensory cells. *Gjb2-CKO* auditory epithelium lacked Cx26 staining. *Gjb2-CKO* mice exhibit significant threshold shifts compared to wild-type mice at all frequencies tested. At 24 kHz, the wild-type mice also exhibited elevated thresholds related to the C57BL/6 background. Degeneration in the cochlea included loss of hair cells with a gradient beginning from the basal turn and progressing to the apex. Similarly, SGN density in Rosenthal's canal decreased rapidly along a gradient from the base of the cochlea to the apex. Few SGNs survived until 6 months of age, and often clustered in clumps. Ad.BDNF treatment res-

cued SGNs in the basal cochlear turn but had no protective effect on the organ of Corti.

Conclusion

We have characterized a *Gjb2*-CKO mouse and determined that degenerative changes occur in the organ of Corti and in SGNs. In both structures, degeneration progressed from base to apex. Ad.*BDNF* gene therapy via the scala media or scala tympani rescued SGNs in the base of the cochlea but had no influence on hair cells.

PS - 772

Cochlear Abnormalities in Mice on a Low-Thiamine Diet

Stéphane Maison; Yanbo Yin; M. Charles Liberman
Harvard Medical School

Background

Targeted deletion of *Slc19a2*, the high-affinity thiamine transporter, causes selective IHC loss (Liberman et al., JARO 7:211-7, 2006), an unusual feature also observed in temporal bones of premature infants (Amatuzzi et al., JARO 12:595-604, 2011). To probe whether thiamine deficiency is key to the genesis of selective IHC loss, mice were maintained on a low-thiamine diet during fetal development and/or early post-natal life.

Methods

Dietary thiamine concentration (normally 22 mg/kg) was decreased to 0-2 mg/kg in different groups. Cochlear function was characterized at 5 wks of age by measuring ABRs and DPOAEs. Histopathology was assessed by immunostaining cochlear whole mounts for synaptic markers (CtBP2 and GluA2) and an efferent-terminal marker (VAT).

Results

In all thiamine-deprived groups, cochlear thresholds were unchanged re age-matched controls, and DPOAE suprathreshold amplitudes were also normal. In contrast, supra-threshold neural responses (ABR Wave 1) were depressed by ~30% for frequencies ≥ 16 kHz. No significant loss of sensory cells or synapses was observed, and the density of medial olivocochlear innervation of outer hair cells was normal. However, the density of lateral olivocochlear terminals was significantly altered: mice deprived of thiamine during gestation showed a ~20% decrease; whereas post-natal deprivation caused a ~40% increase.

Conclusion

These results do not support a direct role of thiamine in selective IHC loss; however, they are consistent with a role in development of the lateral olivocochlear innervation.

PS - 773

Activation of Stem Cell Homing Promotes the Cochlear Invasion of Bone Marrow Mesenchymal Stem Cells

Kazusaku Kamiya¹; Keiko Karasawa¹; Asuka Miwa¹; Takashi Anzai¹; Megumi Funakubo¹; Osamu Minowa²; Katsuhisa Ikeda¹

¹*Juntendo University*; ²*BioResource Center, RIKEN*

Background

Congenital deafness affects about 1 in 1000 children and more than half of them have genetic background such as Connexin26 (Cx26) gene mutation. The strategy to rescue such heredity deafness has not been developed yet. Recently, a number of clinical studies for cell therapy have been reported and clinically used for several intractable diseases. Inner ear cell therapy for sensorineural hearing loss also has been studied using some laboratory animals, although the successful reports for the hearing recovery accompanied with supplementation of the normal functional cells followed by tissue repair, recovery of the cellular/molecular functions were still few. Previously, we developed a novel animal model for acute sensorineural hearing loss due to fibrocyte dysfunction and performed cell therapy with bone marrow mesenchymal stem cells (MSC) as supplementation of cochlear fibrocytes functioning for cochlear ion transport.

Methods

We transplanted the MSCs to the lateral semicircular canal after the induction of stem cell homing factors (SDF1, MCP1) in the host cochlear tissue, and their receptors in transplant MSCs.

Results

We applied our previous strategy for inner ear MSC transplantation to Cx26cKO mice which we developed as a model for hereditary hearing loss and confirmed that our MSC transplantation was safety and useful for the replacement of the Cx26-mutated cochlear mesenchymal cells functioning for the ion transport. To enhance the efficiency, we analyzed the machinery of the stem cell induction to the targeted site in cochlea and found that monocyte chemotactic protein 1 (MCP1:CCL2) and stromal cell-derived factor-1 (SDF-1:CXCL12) played important roles for this cell induction as stem cell homing factors. To enhance MSC invasion to cochlea tissue, we developed a novel transplant strategy by induction of MCP1 /SDF1 expression in host cochlear tissue and enhanced expression of their receptors, chemokine (C-C motif) receptor 2 (CCR2) and C-X-C chemokine receptor type 4 (CXCR4) in MSC.

Conclusion

With this strategy, we induced efficient invasion of MSC to inner ear tissue and differentiation to form gap junctions with Cx26 among transplanted MSCs in Cx26-deficiente mouse inner ear.

PS - 774

Mechanotransducer Current in Beethoven Mice

Laura Corns; Walter Marcotti

University of Sheffield

Background

The mechanotransducer channel opens in response to stereociliary bundle deflection resulting in an inward current, the role of which is to depolarize hair cells and drive synaptic transmission at their basolateral membrane. Despite the importance of this channel the molecular identity is still unknown, although a strong candidate is TMC1. *Tmc1* mutations in humans cause either profound congenital deafness or progressive hearing loss, the latter of which can be modelled by the mutant mouse, *Beethoven* (*tmc1^{bth/bth}*). *Beethoven* mice have a single point mutation in *tmc1*; this mutation is semi-dominant as deafness phenotypes are observed in both *tmc1^{bth/+}* mice and *tmc1^{bth/bth}* mice. Studying the mechanotransducer channel properties in these mice could provide evidence as to whether TMC1 is a component of the mechanotransducer channel. It is particularly pertinent to explore calcium permeability within the *Beethoven* mice, as this property can be attributed to the channel itself as oppose to properties that could be attributed to accessory proteins.

Methods

We made whole cell patch clamp recordings from outer hair cells (OHCs) of the apical coil in acutely dissected organs of Corti from *Beethoven* mice and their wild-type littermates between postnatal day 4 (P4) and P9. To elicit the mechanotransducer current, a piezoelectric driven fluid jet was placed close to the hair bundles and sinusoidal stimuli applied.

Results

The amplitude of the mechanotransducer currents recorded in apical OHCs from *tmc1^{Bth/+}* and *tmc1^{Bth/Bth}* mice aged P4 to P9 were similar to those observed in wild-type littermates, confirming previous reports (Marcotti *et al.*, 2006, J Physiol, 574:677). Despite this lack of change in the maximal current amplitude, there appeared to be differences in the calcium permeability of the mechanotransducer channel in both *tmc1^{Bth/+}* and *tmc1^{Bth/Bth}* compared to their wild-type littermates in OHCs at P6-P8.

Conclusion

Our results indicate that TMC1 could be a component of the transducer channel, substantiating recent results in inner hair cells of *tmc1^{Bth/+}/tmc2^{-/-}* mice (Pan *et al.*, Neuron, 79:1) and OHCs in *deafness* (*tmc1^{-/-}*) mice (Kim & Fettiplace, 2012, 141:1).

PS - 775

Systemic Endotoxin Enhances Entry of Fluorescein Into Perilymph Through Compromise of the Blood-Labyrinth Barrier

Keiko Hirose¹; Jared Hartsock¹; Shane Johnson²; Peter Santi²; Alec Salt¹

¹Washington University School of Medicine; ²University of Minnesota School of Medicine

Background

The blood labyrinth barrier (BLB) tightly regulates the circulation of blood in the inner ear such that cells, proteins, ions, and fluid that pass through the inner ear remain within blood vessels and limit entry into the inner ear under normal conditions. The blood labyrinth barrier is analogous to the blood brain barrier (BBB) although the cellular components of the BLB are different.

Methods

We injected mice with sodium-conjugated fluorescein, which was avidly absorbed in the serum, and collected perilymph samples in sequential aliquots from the posterior semicircular canal of mice. We compared the perilymph of control mice with perilymph from mice pretreated with lipopolysaccharide (LPS, 1mg/kg x2 days).

Results

The concentration of sodium-conjugated fluorescein was significantly higher in the perilymph of mice pretreated with LPS when compared with controls. The normalized fluorescein concentration in perilymph from control mice was **7%** (SD:5% n=5), while in LPS-treated mice, the average was **19%** (SD:7% n=8). Sodium concentrations of the collected fluid samples confirmed that the sampled fluid was perilymph and not endolymph.

Conclusion

This work is the first demonstration of perilymph sampling and pharmacokinetic studies in the mouse inner ear and the first to use perilymph sampling to quantify the integrity of the blood labyrinth barrier in a rigorous fashion. Systemic inflammation results in increased permeability of small molecules through vessels of the inner ear and compromises the blood labyrinth barrier.

PS - 776

Effects of Artificial Endolymph Injection on Inner Ear Function and Morphology in Guinea Pigs

Daniel Brown¹; Yasuhiro Chihara²; Ian Curthoys¹

¹The University of Sydney; ²Singapore University

Background

Vertigo attacks in Ménière's Disease are often thought to be caused by endolymphatic hydrops producing a sudden rupture of the membranous labyrinth. However, the details of changes in cochlear and vestibular function during hydrops development, and how a sufferer may recover from a labyrinth rupture are poorly understood.

Methods

We slowly (40 nl/minute) injected artificial endolymph into the membranous labyrinth of anaesthetized guinea pigs while continuously monitoring several objective measures of cochlear and vestibular function, including Compound Action Potential thresholds, Summating Potential ratios, Cochlear Microphonic, low-frequency biased DPOAEs, Endocochlear Potential and the Vestibular Evoked Potential. Temporal bones were subsequently analysed using X-ray micro-tomography (Micro-CT).

Results

Endolymph injection caused a slow decline in cochlear sensitivity, particularly to low-frequency sounds, and a displacement of the hair cells towards scala tympani. After 3 ml of injection, cochlear sensitivity and hair cell displacement suddenly recovered, followed several minutes later by a transient change (usually a loss) in vestibular sensitivity to bone-conducted vibration. Vestibular sensitivity often recovered several 30-40 minutes after the abrupt loss of function. Consecutive endolymph injections in the same animal often produced multiple episodes of cochlear function loss with abrupt recovery, and multiple episodes of sudden vestibular sensitivity loss. Micro-CT results demonstrated an increased endolymph volume during the injection, with a slight decrease in endolymph volume following the abrupt episodes of cochlear recovery. Micro-CT failed to demonstrate any labyrinth ruptures.

Conclusion

These results suggest that cochlear hydrops gradually increases endolymph pressure causing a displacement of the organ of Corti and a low-frequency hearing loss, until some phenomenon suddenly alleviates the hydropic pressure. Given that this series of events occurred several times in the same acute animal experiment suggests either that the pressure-relief is not caused by a rupture of the labyrinth but rather by some other mechanism, or that a tear of the labyrinth is able to heal within 40 minutes to allow endolymph pressure to increase again with consecutive fluid injections. These results support the theory that hydrops causes the symptoms of Meniere's Disease. It is possible that differences in inner ear morphology between people may allow some people to develop hydrops but not experience the sudden relief of pressure, likely to underlie the vertigo attacks in Meniere's.

PS - 777

The Effects of Vasopressin Type 2 Receptor Antagonist (OPC-41061) on Endolymphatic Hydrops

Naoya Egami¹; Akinobu Kakigi¹; Taizo Takeda²; Tatsuya Yamasoba¹

¹University of Tokyo; ²Kochi Medical School

Background

Meniere's disease (MD) is histologically characterized by endolymphatic hydrops (EH) in the inner ear. EH is considered to be the result of dysfunction of inner ear water homeostasis, which involves excessive production of endolymph and/or reduced absorption of endolymph. There is considerable

evidence that water homeostasis in the inner ear is regulated partly via the vasopressin-aquaporin2 (VP-AQP2) system.

Treatment of this disease principally aims at a reduction in excess water retention in the endolymphatic compartment. Since the mal-regulation of the VP-AQP2 system in the inner ear is thought to play an important role in the pathogenesis of MD, application of an inhibitor of the VP-AQP2 system seems to be a rational treatment strategy for MD. In the present study, we investigated whether systemic administration or local application from the round window (RW) of vasopressin type 2 receptor antagonist; V2 antagonist (OPC-41061), an inhibitor of the VP-AQP2 system reduced the endolymphatic space.

Methods

Hartley guinea pigs with a positive Preyer's reflex weighing about 300 g underwent surgical obliteration of the endolymphatic sac (ES) and duct of the left ear. All animals were allocated to survive for 4 weeks after electrocauterization of the ES and were divided into four groups of saline application (control), systemic application of OPC-41061, RW application of xanthan gum and RW application of OPC-41061. We quantitatively assessed the increase ratios of the cross-sectional area of scala media (IR-S) and examined the proportion of the area of the saccule relative to that of the vestibule.

Results

In control and RW application of xanthan gum, moderate EH were seen in both the cochlea and the saccule. In contrast, both systemic and RW applications of OPC-41061 significantly reduced EH in both the cochlea and the saccule compared to those of control and RW application of xanthan gum.

Conclusion

Systemic or local application of OPC-41061 reduced endolymphatic hydrops in the cochlea and the saccule. These results suggest that VP-AQP2 system plays an important role in the pathogenesis of MD and an inhibitor of the VP-AQP2 system will be a promising drug in the treatment of MD.

PS - 778

The Quantitative Analysis of Aquaporin Expression Levels in the Inner Ear

Takushi Miyoshi¹; Norio Yamamoto¹; Taro Yamaguchi²; Yosuke Tona¹; Kiyokazu Ogita²; Takayuki Nakagawa¹; Juichi Ito¹

¹Graduate School of Medicine, Kyoto University; ²Faculty of Pharmaceutical Sciences, Setsunan University

Background

The inner ear is a fluid-filled sensory organ, whose function depends on strict volume regulation of the two major extracellular fluid domains, the perilymph and the endolymph. Aquaporins (AQPs) are water channel proteins, which are considered to be major candidates for water regulation. Although previous studies reported the expression of several subtypes of AQPs in the inner ear, their functions remain unclear. To elucidated functions of AQPs in the inner ear, we measured the change of mRNA expression levels of all AQP subtypes using quantitative reverse transcription polymerase chain re-

action (qRT-PCR) in two situations. First, the quantification was longitudinally performed at several time points during the maturation of inner ear functions. Second, we compared AQP mRNA expression levels between normal inner ears and those with endolymphatic hydrops which will cause the disruption of the water homeostasis. As a genetic model of endolymphatic hydrops, we used *Slc26a4* knockout mice that also have sensorineural hearing loss.

Methods

Whole inner ears were dissected from C57BL6/J mice at postnatal days (P) 3, 10, and 21 and total RNA was extracted. The expression level of each AQP subtype was determined by qRT-PCR. The expression level of each AQP subtype was also compared between *Slc26a4*^{-/-} and *Slc26a4*^{+/-} mice.

Results

The expression levels of AQP0, AQP1, AQP8, AQP9, and AQP12 increased prominently in the inner ear from P3 to P21. Especially, AQP9 expression level increased about 70-fold from P3 to P21. In *Slc26a4*^{-/-} mice inner ears, AQP4, AQP6 and AQP11 expression were increased compared to that in *Slc26a4*^{+/-} mice inner ears at P21.

Conclusion

AQP genes whose expression levels increased during the functional maturation of inner ears are considered to be involved in the establishment of inner ear functions. These results should be confirmed in the future by morphological studies using immunohistochemistry. AQP genes whose expression levels increased in *Slc26a4* knockout mice might be up-regulated to keep the water homeostasis stable or might be a cause of endolymphatic hydrops. These results will contribute to the elucidation of the mechanisms how AQPs are involved in the pathogenesis of sensorineural hearing loss.

PS - 779

Developmental Changes of ENaC Expression and Function in the Inner Ear of Pendrin Knock-out Mouse as a Perspective of Development of Endolymphatic Hydrops

Bo Gyung Kim; Jin Young Kim; Sung Huhn Kim; Jae Young Choi

Yonsei University College of Medicine

Background

Pendrin mutation causes enlarged vestibular aqueduct, which is one of the findings of dilatation of membranous labyrinth, and various degrees of sensorineural hearing loss. Selective abolition of pendrin causes dilatation of membranous labyrinth that called as endolymphatic hydrops, loss of endocochlear potential, and consequently hearing and vestibular function loss. Because Na⁺ transport is one of the most important driving forces for fluid transport, epithelial Na⁺ channel (ENaC) is thought to play an important role in fluid volume regulation in the inner ear. Therefore, dysfunction of Na⁺ transport through ENaC by acidification of endolymph in the pendred syndrome can be one of the causes of endolymphatic hydrops in pendred syndrome. We tried to investigate

the changes of ENaC transcript expression and its function according to development of pendrin knock-out mouse.

Methods

Pds^{+/+} and *Pds*^{-/-} mice ranging from postnatal (P) day 0 to P56 (P0, P6, P15, P56) were used for the present study. After determining genotypes of each mouse, comparisons were made between the *Pds*^{+/+} and *Pds*^{-/-} mice for experiment. The membranous portion of cochlea and vestibule were separated and each was used for real-time RT-PCR. Real-time RT-PCR was performed to identify the changes of ENaC transcript expression level according to the development (P0, P6, P15, P56) of pendrin knock-out mouse. For the measurement of ENaC-dependent transepithelial current, we used two representative epithelial tissues of cochlear and vestibular compartment; Reissner's membrane and non-sensory roof epithelium of saccule which were reported to show mostly ENaC-dependent transepithelial current in their apical side. The membranous tissue of Reissner's membrane and non-sensory roof epithelium of saccule in P0 and P56 mice was dissected off in perilymph-like physiologic saline solution and folded for measuring transepithelial current using vibrating probe.

Results

We investigated the changes of ENaC transcript expression and its function according to development of pendrin knock-out mouse. In the cochlea, transcript expression of β and γ ENaC was significantly increased at P56 in *Pds*^{-/-} mouse, when compared to *Pds*^{+/+} mouse ($p < 0.05$). In the vestibule, transcript expression of β ENaC was significantly increased at P56 and γ ENaC from P6 to P56 in *Pds*^{-/-} mouse ($p < 0.05$). The ENaC-dependent transepithelial current was not significantly different between *Pds*^{+/+} mouse and *Pds*^{-/-} mouse in the Reissner's membrane and saccular extramacular non-sensory epithelium at P0, but the current was significantly increased in *Pds*^{-/-} mouse at P56, when compared to *Pds*^{+/+} mouse.

Conclusion

Both transcriptional expression and function of ENaC in the cochlea and vestibule tended to be increased in *Pds*^{-/-} mouse than *Pds*^{+/+} mouse from P6, which finally significantly increased at P56. It is tempting to speculate that increased Na⁺ concentration in the endolymph caused endolymphatic hydrops in *Pds*^{-/-} mouse, and ENaC expression and function was likely to be increased for the compensation of increased Na⁺ concentration of the endolymph in the cochlea and vestibule postnatally. Based upon these findings, the cochlea and the vestibule can be the main regulatory site of Na⁺ concentration in the inner ear postnatally, and this result provide insight into the role of ENaC in regulating fluid volume and Na⁺ homeostasis during the development.

Immunohistochemical Localization of Natriuretic Peptide Receptor A Within Cells of the Potassium Cycling Pathway in the Cochlea

Sara Prince; George Trachte; Janet Fitzakerley

University of Minnesota Medical School

Background

In the cardiovascular and renal systems, natriuretic peptides and their receptors regulate sodium/potassium concentrations, blood volume, and blood pressure. The three receptors for natriuretic peptides --- NPR-A, NPR-B, and NPR-C --- are located in the inner ear. Previous work in our laboratory has shown that administration of atrial natriuretic peptide (ANP) significantly improves thresholds in normal mice and that NPRA knockout mice exhibit an early onset, high frequency hearing loss. In the kidney, one hypothesis is that ANP acts via NPR-A to activate the sodium, potassium, 2 chloride transporter NKCC1, resulting in natriuresis. It is unknown whether the relationship of NPRA and NKCC1 is similar in the cochlea. The experiments in this study were designed to test the hypotheses that NPRA 1) is located in regions of the cochlea important for the regulation of endolymph ion composition and 2) is co-localized with NKCC1.

Methods

The location of NPRA and NKCC1 within the cochlea was determined using standard immunohistochemical techniques. CBA/J mice under 100 days old with normal hearing were perfused with a 4% paraformaldehyde/0.05% picric acid solution and cochlear sections were cut at a thickness of 10 microns on a cryostat. Commercially available antibodies against NPRA and NKCC1 were used and visualized via confocal microscopy. Kidney tissue was used as a positive control for both NPRA and NKCC1, while skeletal muscle acted as a negative control.

Results

Co-localization of NPRA and NKCC1 occurred in a non-uniform pattern throughout the marginal cell layer of the stria vascularis (StV), but the two proteins were found separately elsewhere. NPRA staining was found ubiquitously in the basal cells, while NKCC1 was found in more superficial layers of the StV as described in other studies. In the spiral ligament, NPRA was expressed in root cells, while NKCC1 was found in fibrocytes. These proteins were not co-localized in the spiral limbus, as NPRA was found in interdental cells whereas NKCC1 was found diffusely throughout the remaining regions. NPRA was found in spiral ganglion cells and co-localized with NKCC1 in the tectorial membrane, but was not found within any other cells in the organ of Corti.

Conclusion

These results support the hypothesis that NPRA is found in many cells of the cochlear potassium recycling pathways, although NKCC1 is not always the effector protein. Therefore, specific manipulations of NPRA pathways could be effective treatments for conditions such as Meniere's disease.

Expression of TRPM4 in the Mouse Cochlea and its Putative Roles in the Potassium Ion Transport and the Inner Hair Cell Repolarization

Junko Murata¹; Mayumi Sakuraba¹; Ryoichi Teruyama²; Kazusaku Kamiya¹; Junji Yamaguchi¹; Hideyuki Okano³; Yasuo Uchiyama¹; Katsuhisa Ikeda¹

¹Juntendo University School of Medicine; ¹Juntendo

University School of Medicine; ²Louisiana State University;

³Keio University School of Medicine

Background

The present study was conducted to elucidate the presence and function of the melastatin-related subfamily of transient receptor potential channels, TRPM4, in the mouse inner ear. For the first step for it, we tried to clarify the spatio-temporal expression pattern of the TRPM4 in the mouse inner ear, and the changes of TRPM4 expression level during the development.

Methods

We did immunohistochemistry via the customized anti-TRPM4 antibody in the inner ear of mice from the embryonic day 15.5 (E15.5) to 20-week-old. We also performed the semi-quantitative real-time PCR assay by using the samples from the Organ of Corti and the stria vascularis of the different embryonic and postnatal developmental stages.

Results

Immunoreactivity (IR) was found in: (a) the basolateral portion of inner hair cells (IHCs), (b) the apical side of stria marginal cells, (c) the apical portion of the dark cells of the vestibular labyrinth, and (d) a part of the type II neurons in spiral ganglion. Subsequently, changes in the distribution and expression of TRPM4 during inner ear development were also evaluated from samples from various embryonic and postnatal stages. Immunohistochemical localization demonstrated that the emergence of the TRPM4-IR in IHCs occur shortly before the onset of hearing, while that in the marginal cells happens earlier at the time of birth coinciding with the onset of endolymph formation. Furthermore, semi-quantitative real-time PCR assay showed that expressions of TRPM4 in the Organ of Corti and in the stria vascularis increased dramatically at the onset of hearing.

Conclusion

Because TRPM4 is a Ca²⁺-activated monovalent selective cation channel, these findings suggest that TRPM4 is involved in K⁺ transport that is essential for signal transduction in IHCs and for the formation of the endolymph by marginal cells. More specifically, TRPM4 in the basolateral portion of the IHCs contribute to repolarization during signal transduction, while that in the marginal cells play a role in the formation and maintenance of the high K⁺ concentration that uniquely exists in endolymph.

Adrenergic and Cholinergic Stimulation-Mediated Changes of Transepithelial Current from Human Endolymphatic Sac Epithelium

Sung Huhn Kim¹; Bo Gyung Kim¹; Jin Young Kim²; Won-Sang Lee¹; Jae Young Choi¹

¹Yonsei University College of Medicine; ²Research Center for Human Natural Defense System, Yonsei University College of Medicine

Background

Endolymphatic sac (ES) epithelium consists of heterogeneous cell types and various ion transports occurred through the epithelium to maintain the inner ear ion homeostasis and fluid volume. So far, there has been no functional study about the ion channel activity of human ES epithelium. We measured the net physiologic current from human ES epithelium through specific ion channels and investigated the effect of adrenergic and cholinergic stimulation on the transepithelial current using electrophysiologic and pharmacologic methods.

Methods

Human endolymphatic sac was harvested during acoustic tumor surgery via translabyrinthine approach. The luminal side of ES was exposed and folded for current measurement. Scanning vibrating electrode technique was used to measure transepithelial current under short-circuit condition. Specific ion-dependent current was measured using electrophysiological and pharmacological method. Ion channel expression was also investigated using microarray and proteomics.

Results

The vector of net transepithelial current was various and the net current from ES epithelium was very tiny. In the cystic portion of the ES, small cation absorption/anion secretion current or cation secretion/anion absorption current was observed depending on the area of the ES. However, net current from epithelium ductal portion showed cation absorption/anion secretion current. The cation secretion current was inhibited by 100 μ M and 1 mM Ba²⁺, 1 mM 4-AP, 10 μ M DIDIS, 100 nM apamin, and 10 μ M amiloride in the cystic portion. But the current from the ductal portion was inhibited only by 10 μ M amiloride. The current of the cystic portion was significantly changed by the application of adrenergic stimulator (10 μ M isoproterenol and 100 μ M epinephrine) and/or cholinergic stimulator (10 μ M substance P and 10 μ M carbachol). Adrenergic stimulation induced cation absorption/anion secretion current or cation secretion/anion absorption current depending on the area of ES. The isoproterenol-dependent cation absorption current, cation secretion current, and anion secretion current was blocked by bumetanide (10 μ M), Ba²⁺ (1 mM), and DIDS (10 μ M) respectively. Substance P increased anion secretion current. Various K⁺ channels, ENaC, Cl⁻ channels, adrenergic receptors, and cholinergic receptors were detected in the microarray and proteomic analysis.

Conclusion

These results suggest that transepithelial current from ES epithelium of cystic portion is nearly neutral in physiologic condition, which means cation secretion and absorption is

balanced, however, ductal portion has more cation secretion activity than cystic portion. The ion transport in human ES epithelium of cystic portion was regulated by adrenergic and cholinergic stimulation.

Improved Inner Ear RNA Extraction and Quantification

Beth Kempton; Fran Hausman; Teresa Wilson; Carol MacArthur; Dennis Trune

Oregon Health & Science University

Background

The extraction of high quality RNA from the inner ear is necessary for qRT-PCR, Affymetrix Gene Arrays, etc., but often yields are reduced due to small tissue amounts, prolonged dissection times for tissue isolation, etc. Furthermore, some experimental treatments (e.g., steroid treatments) induce unusual variability of housekeeping genes that increases their statistical variance and potentially masks real treatment effects. Thus, maximizing RNA extraction is critical for quantitative comparisons of gene function and the initial handling of tissues can significantly impact the quality and quantity of the isolated RNA.

Methods

Therefore, alternative methods of inner ear tissue dissection and preparation were examined to a) improve RNA yield, b) improve RNA quality, c) reduce variability of housekeeping gene RNA yields to improve statistical power. We employed steroid treatment of mice that we previously determined induces considerable variance in housekeeping gene RNA yield. BALB/c mice were injected transtympanically with PBS, prednisolone, or dexamethasone, inner ear tissues harvested at 6 hours, and RNA extracted by two different techniques. The first was dissection of tissues in cold phosphate buffer with storage in RNeasy lysis buffer at -20 degrees. The second technique was to dissect tissues in RNeasy lysis buffer, blot off any excess RNeasy lysis buffer, then flash freeze in liquid nitrogen and store at -80 degrees.

Results

The second method was far superior. a) We obtained a higher yield of RNA. b) The 260/230 ratio was improved, indicating less salt contamination in the final sample. c) The housekeeping gene values were lower and less variable, implying no treatment effects on their measurement.

Conclusion

Adaptation of this alternative method should provide improved yields of inner ear RNA and benefit experimental studies requiring assessments of gene activity. The higher RNA quality achieved also will reduce variability for statistical comparisons between experimental groups.

Age Related Shifts Of Absolute Pitch Judgment And Their Relation To The Hearing Impairment.

Minoru Tsuzaki¹; Toshie Matsui²; Toshio Irino³; Chihiro Takeshima⁴

¹Kyoto City University of Arts; ²University of Tsukuba;

³Wakayama University; ⁴J. F. Oberlin University

Background

There have been several personal reports that judgments of absolute pitch (AP) possessors shifted upwards by one or two semitones due to aging. The phenomenon has been confirmed by a web-based pitch naming task with more than two thousand participants. Its physiological cause, however, has not been clarified.

Methods

To approach this problem, an AP naming task were performed for 73 AP possessors whose age ranged from 19 to 63. Audiometric data were also measured for each participants. In the pitch labeling task, sampled sounds of 88 keys of an acoustic grand piano were presented in a random order. Each participant was required to label the pitch class with 12 buttons on a GUI to each sample sound disregarding its register. Their hearing levels were also measured for 6 frequencies ranging from 250 Hz to 8 kHz.

Results

The performance of the AP naming task deteriorated as a function of the participants' age. A strong asymmetry was observed for this age-related deterioration. The tendency for the participants to judge that the piano sounds were one or two semitone higher than the correct pitch class was more obvious than that for the lower direction. This asymmetry became more salient for the aged group. The hearing levels for the frequencies higher than 1 kHz significantly deteriorated as a function of the ages. To investigate a relation between the age-dependent AP shift and the hearing level, a regression analysis between the individual, average hearing level above 1 kHz and the individual, average AP shift was performed. No clear dependency of the degree of AP shift on the ages was observed.

Conclusion

It has been assumed that the pitch class judgment requires the temporal information based on the phase locked neural firings. For example, it has been reported that the response patterns of the AP possessors tend to unstable and inaccurate above about 4 kHz, where the phase locking becomes uncertain. Although hearing level data obtained by the air-conducted audiometry might not represent age-related hearing deficit solely due to the change in the cochlear mechanical filtering, the current observation suggests that it is necessary to inquire factors of aging other than the age related changes in the cochlear mechanism to explain the age-dependent AP shift.

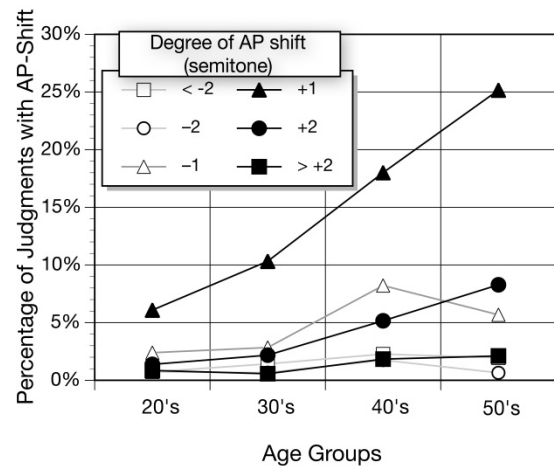


Fig. 1 Percentage of AP shift for each of the age groups. The parameters are the degree of AP shift in semitones. The positive values (closed symbols) correspond to the case where the judgments were "higher" than the correct answers.

Infant Missing Fundamental Pitch Sensitivity and Melody Discrimination

Bonnie Lau; Lynne A. Werner

University of Washington

Background

Previous studies from the lab have demonstrated that 3-month-old infants are able to discriminate harmonics on the basis of missing fundamental (MF) pitch like adult listeners. Two additional studies were conducted to further compare the ability of adults, 7- and 3-month-olds on their sensitivity to pitch changes and ability to discriminate MF pitch in a melody using an observer-based method.

Methods

In Experiment I, MF harmonic complex discrimination thresholds were obtained for a fundamental frequency (F0) of 200 Hz using an adaptive method that presented $\Delta F0$'s of 5, 2.5, 1.5, 1.0, 0.5, and 0.025% in a series of 6 test phases. In Experiment 2, the ability to use pitch in melody discrimination was tested. Participants were presented with the first 7 notes of "Twinkle, Twinkle, Little Star" as a background melody and learned to respond when a change in the melody (i.e., a wrong note) occurred. To ensure that participants were responding on the basis of the MF of each note in the melody, the stimuli consisted of 5 variations of the background melody and 5 variations of the change melody. In each variation of the melodies, the harmonic composition of each note differed, such that the upper and lower edge frequencies as well as the spectral centroid did not change in the same direction as the pitch contour of the melody. Participants were therefore required to ignore the spectral changes and respond based only on the MF of each note in order to complete the task.

Results

In Experiment I, while adult thresholds ranged between 1.5 - 0.025% $\Delta F0$, almost all infants at both ages had thresholds of 0.025% $\Delta F0$. In Experiment II, almost all adults and infants

tested successfully completed the MF melody discrimination task.

Conclusion

Infant performance on both MF pitch discrimination tasks was comparable to adult participants.

PS - 786

Ferret Pitch Perception is Dominated by Temporal Cues, Unlike That of Humans

Kerry Walker¹; Josh McDermott²; Joe Kang¹; Andrew King¹
¹University of Oxford; ²MIT

Background

Psychophysical studies indicate that humans can use both the spacing of resolved harmonics (i.e. spectral cues) and the envelope periodicity of unresolved harmonics (i.e. temporal cues) to determine pitch (Carlyon & Shackleton, 1994). However, spectral cues tend to dominate pitch perception in humans. Ferrets are a common animal model in auditory research. Although these animals can make a variety of pitch discrimination judgments (Walker *et al.*, 2009; Yin *et al.*, 2010), the roles of spectral and temporal pitch cues remains unclear.

Methods

Four ferrets were trained, using water rewards and time-outs, to lick at a spout to their left or right depending on whether a harmonic tone complex was low (500 Hz) or high (1000 Hz) in pitch. This “standard” tone contained all the harmonics falling between 1 – 10 kHz. Once the ferrets learned the task, “probe” click trains were presented on a random subset of trials to investigate the cues underlying discrimination. The probe stimuli contained either: low numbered harmonics (1 – 4 kHz), presumed to be at least partially resolved on the ferret cochlea, and thus to contain spectral cues; high numbered harmonic (4 – 10 kHz), presumed to be unresolved, and to thus contain mostly temporal cues; high harmonics with randomized phase; high harmonics with alternating phase; and all harmonics from the standard (1 – 10 kHz) with randomized phase. Four humans were also tested on a pitch discrimination task that was designed to match the ferrets’ behavioral task as closely as possible.

Results

Ferrets chose correctly when temporal cues were preserved, but their performance was near chance when only spectral cues were available. Randomizing harmonic phases impaired performance in both the high- and all-harmonics conditions, consistent with responses based on temporal envelope periodicity. Human listeners, on the other hand, were most impaired when spectral cues were removed, and were less reliant on temporal cues, consistent with prior work.

Conclusion

In contrast to humans, ferrets discriminate pitch based primarily on temporal periodicity from unresolved harmonics. Previous results suggest that gerbils (Klinge & Klump, 2009) and marmosets (Bendor, Osmanski & Wang, 2012) may also rely more strongly on temporal cues than do humans. Spectral pitch perception in humans may therefore be unique to

our species, perhaps a result of the superior spectral resolution of human hearing.

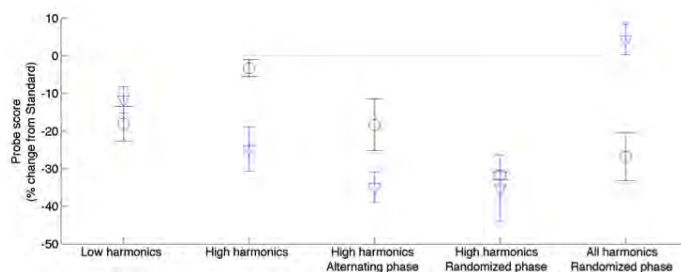


Figure 1: Performance of ferrets (black circles) and humans (blue triangles) across 5 different probe stimuli. Performance is calculated as a fraction of the percent correct achieved by each subject on wideband standard click trains: $(\text{Score}_{\text{Probe}} - \text{Score}_{\text{Standard}}) * 100 / \text{Score}_{\text{Standard}}$.

PS - 787

Formant-Frequency Discrimination for Synthetic Single-Formant Vowel-Like Sounds: Comparison of Budgerigar and Human Thresholds

Laurel Carney¹; Kristina S. Abrams¹; Joyce M. McDonough¹; Douglas M. Schwarz¹; Fabio Idrobo²
¹University of Rochester; ²Boston University

Background

Vowel contrasts are primarily determined by the lowest two formant frequencies (Fant, 1960). We are exploring the coding and processing of formants in the central nervous system. In this study, discrimination thresholds of the budgerigar were estimated for comparison to human thresholds (Lyzenga and Horst, 1997, JASA 102:1755).

Methods

Stimuli were harmonic complexes shaped with a triangular spectral envelope centered on the formant frequency. Stimulus conditions followed those in Lyzenga and Horst's (1997): the fundamental frequency (F0) was 100 or 200 Hz, the slope of the spectral envelope was 100 or 200 dB/octave, components were in sine phase or random phase. Stimuli were presented at 60 dB SPL. Operant conditioning and a two-alternative choice task were used to train and test three birds. The bird initiated each trial by pressing a center switch and responded by pressing a switch to the left or right. Reinforcement was a millet seed after each correct trial. Just-noticeable-differences (JNDs) in formant frequency were estimated using a two-down-one-up tracking procedure. The target formant frequency was either aligned with the harmonic at 2000 Hz, or it was placed midway between two harmonics, at 2050 or 2100 Hz. Each bird's threshold was based on five stable estimates.

Results

Formant-frequency discrimination thresholds and trends in threshold across conditions were similar for budgerigars and humans. The strongest trend in the results was that the JNDs were smaller when the formant peak was between harmonics than when it was aligned with a harmonic. JNDs were also

smaller for the lower F0, for the steeper spectral slope, and for stimuli with components in sine phase.

Conclusion

The similarity in thresholds and in trends across stimulus conditions between budgerigar and human JNDs for formant frequency discrimination suggests that similar cues may be used by both species for this task. The largest difference in JND across conditions was related to the alignment of the formant with a harmonic; aligned and mis-aligned stimuli differ substantially in their amplitude envelopes, which are encoded by auditory-nerve timing patterns (Tan and Carney, 2005, JASA 117:1210). The similarity between budgerigar and human thresholds across these stimulus conditions may reflect the fact that they have similar thresholds for amplitude modulation detection. Future work will explore the ability of models for amplitude modulation processing in the auditory pathway to predict the trends in thresholds (Carney and McDonough, 2012, IEEE CISS Proc.).

PS - 788

Human Time-Frequency Acuity Beats the Fourier Uncertainty Principle

Jacob Oppenheim; Marcelo Magnasco
Rockefeller University

Background

The time-frequency uncertainty principle states that the product of the temporal and frequency extents of a signal, as measured by the second moments, cannot be smaller than $1/(4\pi)$. This limit applies to all linear operators in signals analysis, most notably, the Fourier Transform, and the closely related correlation function. By measuring the precision with which subjects can determine the frequency and timing of notes, we present a direct test of the applicability of the theorem to human auditory processing, helping to narrow the space of algorithms that could be used in auditory processing.

Methods

We study human ability to simultaneously judge the frequency and the timing of a sound, the auditory equivalent of a Vernier task. Subjects are presented with a test note and asked to compare its frequency with a reference note and its timing with a second, anharmonic note. Using standard psychophysical methods, we quantify their performance, extracting the second moments of their psychometric curves for both timing and frequency, the equivalent of the quantities in the uncertainty principle.

Results

Our subjects often exceeded the uncertainty limit, sometimes by more than tenfold, mostly through remarkable timing acuity. When we repeated the test with theoretically less optimal (non-Gaussian) pulses, we found no decrease in performance, which implies an even greater violation of the theorem. These results may be used to rule out several well-known algorithms as models for auditory processing, and for the analysis of auditory data.

Conclusion

Our results establish a lower bound for the complexity of the algorithms employed by our brains in parsing transient sounds, ruling out simple "linear filter" models of early auditory processing. The violation of the uncertainty limits suggests that Fourier transform-based algorithms, such as reverse correlation, may be ill-suited to the analysis of auditory data, being unable to account for the amazing precision of human hearing. We additionally highlight timing acuity as a central feature in auditory object processing.

PS - 789

Psychometric Functions for Pure-Tone Frequency Discrimination by Aged Listeners

Huanping Dai¹; Emily Buss²; Michael Primus³

¹University of Arizona; ²Department of Otolaryngology, University of North Carolina at Chapel Hill; ³Division of Communicative Disorder, University of Wyoming

Background

Our purpose is to measure psychometric functions (PFs) for frequency discrimination by aged listeners and compare the functions with those measured for young listeners [Dai and Micheyl (2011) *J. Acoust. Soc. Am.* 130, 263-271]. PFs describe the relationship between the signal strength and the proportion of correct responses (PC). PFs contain detailed information about the subjects' perceptual processing; such information can be significant for both theoretical and practical purposes. To our knowledge, there has been no report of PFs for frequency discrimination in aged listeners. These data provide a more complete characterization of the effect of advanced age on frequency discrimination than discrimination thresholds at a single PC.

Methods

Five listeners (64-69 yrs) participated, each with normal low-frequency hearing and mild to moderately severe high-frequency hearing loss. PFs were measured at 250, 1000, and 4000 Hz using an adaptive tracking procedure combined with a 2IFC paradigm. Responses obtained in these tracks were fitted with the following function: $PC = L/2 + (1-L) \Phi(d'/2^{1/2})$, in which L denotes the attention-lapse rate, Φ denotes the cumulative-normal function, and $d' = [\Delta f/f] / \alpha^\beta$, where α represents the threshold, and β the slope of PFs.

Results

The PFs of aged listeners were parallel to those of young listeners; aged listeners' functions were shifted by a factor of four in frequency compared to those of young listeners, independent of frequency. At 4 kHz, where aged listeners differed most in terms of pure-tone sensitivity, there was no significant correlation between the hearing loss and frequency-discrimination thresholds; indeed, these thresholds were nearly identical. Aged listeners collectively showed a higher rate of attention lapse than young listeners.

Conclusion

In theory, aging can impair frequency discrimination through peripheral or central mechanisms. Frequency discrimination is often argued to rely on temporal processing at low frequen-

cies and spectral cues at high frequencies. If aging affected the peripheral encoding of these cues, then the finding of a uniform age effect across frequency would imply parallel degradation of temporal and spectral cue encoding. Alternatively, aging could degrade frequency discrimination via a central mechanism, which applies consistently across frequency. This interpretation is consistent with the higher lapse rate in aged listeners, showing the effect of aging on attention.

PS - 790

Auditory-Tactile Integration in Temporal Frequency Discrimination

Juan Huang¹; Alex Forrence¹; Yang Zhang²; Steven Hsiao³; xiaoqin wang⁴

¹*Johns Hopkins University*; ²*Tsinghua University, Beijing, China*; ³*Mind and Brain Institute, Johns Hopkins University*;

⁴*Department of Biomedical Engineering, Johns Hopkins University*

Background

In the present study we investigate the integration of auditory and tactile inputs in humans performing a frequency discrimination task.

Methods

Subjects were presented with either periodic or aperiodic click trains delivered through the skin (tactile channel) or through the ear (auditory channel) alone (unimodal) or in various combinations (bimodal). Subjects were given two click trains and were asked to indicate which click train contained the higher frequency. There were four testing conditions: (1) unimodal (auditory or tactile alone) (2) cross modal; (3) unimodal/bimodal; and (4) bimodal/bimodal.

Results

Results show that human subjects can integrate click train stimuli from audition and touch to form an integrated perception of temporal frequency for frequencies below 100 Hz. (The performance deteriorated at temporal frequencies between 60 and 100 Hz). The results also show that human subjects can discriminate the repetition rate of click trains between auditory and tactile channels, regardless of whether the click trains are periodic or aperiodic, over the same frequency range (15-100 Hz). The performance in unimodal temporal frequency perception tasks was better for auditory than for tactile stimuli. Results also show that when auditory and tactile clicks were presented interleaved, subjects tended to perceive higher temporal frequency than when the auditory and tactile clicks were presented simultaneously.

Conclusion

We conclude that low frequency tactile and auditory click trains are integrated to produce a single cross-modal percept and further that the perception of temporal frequency in the auditory and tactile systems operate on similar neural mechanisms. Since neurons in both audition and touch show phase locked responses to vibratory and auditory stimuli, temporal codes may play a role in vibratory frequency perception in both sensory systems.

PS - 791

Vowel Segregation Using Inharmonic Stimuli

Eugene Brandewie; Andrew Oxenham

University of Minnesota

Background

Previous research has shown that small differences in fundamental frequency (F0) can be used to perceptually segregate two simultaneously presented vowels with equal duration. This study tests whether harmonicity is required, or whether segregation can be based on average component spacing within each vowel, by jittering the harmonics frequencies of the vowels.

Methods

Listeners were presented with two simultaneously presented Klatt-synthesized vowels with equal duration, with a nominal F0 of 130 Hz. Four values of F0 differences between the vowels were tested (0, 1, 2, and 4 semitones) in both a control and a jittered condition in which individual harmonics for each vowel were independently varied by as much as 30% from their nominal frequency. Listeners reported both vowels on each trial.

Results

Results from the harmonic control conditions show improvements in vowel identification performance with F0 differences, with a performance asymptote at 1 semitone difference, consistent with previous research. Performance in the jittered conditions show no effect of F0 differences, or average component spacing. However performance was significantly better than in the harmonic condition with no F0 difference.

Conclusion

Jittering the harmonic frequencies eliminates the benefits of F0 differences between two simultaneously presented vowels, but having the two vowels presented via different component frequencies, even with the same average F0, provides a small but significant advantage in perceptual segregation.

PS - 792

The Effect of Preceding Stimulation on a Broadband Measure of Frequency Resolution

Evelyn Davies-Venn; Elizabeth Strickland

Purdue University

Background

The threshold for detection of spectral modulation is a broadband measure of frequency resolution, which has been found to correlate with speech perception in quiet and in noise by listeners with normal hearing and listeners with hearing aids or cochlear implants (e.g. Henry et al., 2005; Saoji et al., 2009). Previous studies using narrowband measures of frequency resolution in simultaneous masking have shown that preceding stimulation may change frequency selectivity. If the preceding stimulation has the same spectrum as the masker, frequency selectivity may increase (e.g. Strickland 2004, 2008), while if the preceding stimulation is broadband frequency selectivity may decrease (e.g. Strickland, 2001). In the present study, detection of spectral modulation was mea-

sured as a function of stimulus duration, with and without a precursor that was either spectrally modulated or flat.

Methods

A within-subject repeated measures design was used to measure broadband frequency resolution in listeners with normal hearing using spectral ripple stimuli. This was done as a function of stimulus duration, with and without a precursor of varying intensities and durations. The spectral modulation detection task (Litvak et al., 2007) was used to measure listeners' detection thresholds for a flat versus spectrally modulated signal at a fixed spectral ripple density. The spectral modulation detection threshold (SMT) was determined by varying the spectral contrast (i.e. peak-to-trough) of the test signal. In the precursor condition, a spectral ripple noise with a flat (i.e. 0 dB spectral contrast) or a modulated spectrum was used as the precursor. It was presented ipsilaterally, contralaterally and bilaterally.

Results

Preliminary results show that spectral modulation detection thresholds increase with decreasing ripple stimulus duration. For the short-duration ripple stimuli, a flat-spectrum precursor presented ipsilaterally or contralaterally decreases behavioral measures of listeners' broadband frequency resolution, i.e. increases the SMT.

Conclusion

Preceding stimulation changes frequency resolution. Results will be considered in the framework of cochlear gain reduction by the preceding stimulation.

PS - 793

Context Effects in Pitch Discrimination

Coral Dirks; Andrew Oxenham

University of Minnesota, Twin Cities

Background

The terms time-order error and contraction bias refer to the phenomenon that stimuli are judged closer in magnitude to the mean of the overall stimulus range than their actual magnitude. One explanation relies on Bayesian inference, whereby sensory information is combined with a prior, based on the expected (mean) magnitude. A recent auditory example using simple frequency discrimination found large bias effects, with better performance when the first tone was closer to the mean than the second tone, and poorer performance when the second tone was closer to the mean. The results suggested a very large sensory bias, because the mean just-noticeable difference (JND) was over 13%, and thus nearly an order of magnitude higher than those found in most other studies. Large JNDs can also signify confusion on the part of subjects, and so in this study we measured the effects of practice on the size of the JND and on the size of the bias. We also included control conditions to test for potential response biases in addition to sensory biases.

Methods

Twenty normal-hearing listeners participated in a 2-alternative forced-choice frequency-discrimination experiment, where the 70-ms tones were selected from a range between

800 and 1200 Hz. The frequency difference between two tones in a pair ranged between 0.5 and 5%. Feedback was provided. In one set of experiments, listeners were asked to select the higher of the two tones. In the other set (presented in counterbalanced order across listeners), they were asked to select the lower of the two tones. Thus, the stimuli were the same in the two sets, just the mode of judgment differed.

Results

Even with no prior practice, the average JND in the first block of trials was 1.16%. This decreased to 1.04% after additional practice. A marked bias was observed, consistent with the earlier study, even after practice. Neither the JND nor the amount of bias was affected by the mode of judgment.

Conclusion

A significant contraction bias was found in a simple frequency-discrimination task, even when listeners displayed high sensitivity to frequency differences, and the bias did not diminish substantially after practice. In addition, because it remained the same, regardless of mode of judgment, the bias appears to be sensory in nature. The outcomes support the original findings and generalize them to the range of JNDs more typically found in the literature.

PS - 794

Frequency Discrimination Assessed by a Modified Startle Response in Adult Rats Exposed to Noise as Juveniles

Daniel Suta¹; Da-Wei Shen²; Natalia Rybalko¹; Jiri Popelar¹; Paul W.F. Poon²; Josef Syka¹

¹Institute of Experimental Medicine, Academy of Sciences of the Czech Republic, Prague, Czech Republic; ²National Cheng Kung University, Tainan, Taiwan

Background

The auditory system of rats undergoes extensive refinement during the early postnatal period. It has been demonstrated many times that sound stimulation experienced during this so called 'critical period' may significantly influence the state of the auditory system in the adult animal. Recent recordings of neuronal activity in the inferior colliculus of adult rats exposed briefly to noise as juveniles revealed impaired neuronal frequency tuning and sound intensity processing without influencing their hearing thresholds (Grecova et al., 2009; Bures et al., 2010). The aim of this study was to behaviorally assess frequency discrimination in adult animals exposed to noise as juveniles.

Methods

Experiments were performed on Long-Evans rats. Three groups of animals were exposed as juveniles (P14) to broadband noise (125 dB SPL); each group was exposed for a different period: 8 min, 12 min or 25 min. The fourth group consisted of control animals without any noise exposure. At the age of 3-6 months a modified method of measuring the prepulse inhibition of the acoustic startle response was used to analyze frequency discrimination: the animals were continuously stimulated with a pure tone, the frequency of which was changed during a short period preceding the startling

stimulus. The frequency resolution was tested at intensities of 70-90 dB SPL for frequencies of 4kHz and 16kHz.

Results

Animals exposed for 12 or 25 min had elevated auditory thresholds throughout the whole frequency range, while animals exposed for 8 min had auditory thresholds similar to control animals. Animals exposed for 12 or 25 min showed substantially worse frequency resolution, but also animals exposed for 8 min demonstrated impaired frequency resolution in comparison with controls. An improvement of frequency discrimination with increasing sound intensity was observed to a different extent in animals of all groups.

Conclusion

We demonstrated the use of a modified measurement of the prepulse inhibition of the acoustic startle response for evaluating frequency resolution in the rat. We conclude that a brief noise exposure during the critical period can result in an alteration of frequency discrimination in adult rats, which may appear even in individuals with normal hearing thresholds.

PS - 795

Human Pitch Perception in Real-World Conditions is Spectral Pattern Recognition, Not Periodicity Detection

Samuel Norman-Haignere; Josh McDermott
Massachusetts Institute of Technology

Background

Pitch is typically defined as the perceptual correlate of acoustic periodicity, and is thought to be a fundamental component of auditory perception. Pitch is often most important in contexts in which it changes over time, with the pattern of changes conveying prosody and emotion in speech, and structure in music. How are such changes detected? For most real-world sounds, changes in periodicity produce approximate translations of the pattern of excitation along the cochlea (because of the approximate logarithmic representation of frequency), providing a cue that the auditory system could potentially use to detect pitch changes. The cue provided by spectral pattern translation is notably distinct from that of periodicity in that spectral pattern matching could also be used to detect log-frequency shifts of aperiodic (inharmonic) sounds. Here we test the contribution of spectral pattern matching to human pitch judgements by measuring performance on a standard pitch discrimination task, as a function of whether the sounds to be compared are 1) periodic (manipulated by mistuning harmonics) and 2) similar in their spectral excitation profiles modulo translation (manipulated by adjusting the relative amplitudes of different harmonics).

Methods

Subjects were presented with two pairs of alternating tones on every trial, and judged which of the two pairs contained a pitch change. Discrimination thresholds were measured using an adaptive procedure. Across adaptive runs, we manipulated the periodicity and the spectral similarity of the tones in each pair.

Results

Surprisingly, aperiodicity had no effect on discrimination thresholds for tones so long as the spectral variation between tones was modest. In contrast, increasing the amount of spectral variation between tones substantially increased discrimination thresholds for both periodic and aperiodic tones, even when listeners were given extensive feedback and training (and even though the spectral variation did not affect periodicity). Substantial effects of periodicity were only observed when the tones in each pair had fully non-overlapping frequencies, preventing subjects from using a spectral pattern matching strategy.

Conclusion

The results suggest that the auditory system is able to use periodicity information to some extent when spectral pattern cues are absent, but that spectral pattern matching dominates pitch perception under conditions of modest note-to-note spectral variation, as is typical of real-world conditions. We illustrate how a simple model based on spectral cross-correlation can explain the observed results, as well as classic periodicity-based findings.

PS - 502

Effect of Renal Failure on Voice

Zaahir Turfe¹; Abdul Latif Hamdan²; Doja Saredidine³

¹*Michigan State University College of Human Medicine;*

²*American University of Beirut Medical School;* ³*American University of Beirut Medical Center*

Background

This study aimed to assess the prevalence of phonatory symptoms in patients with chronic renal failure.

Methods

A total of 20 patients with chronic renal failure and 18 healthy controls were recruited. Subjects were asked about the presence or absence of hoarseness, vocal effort and vocal fatigue. Vocal effort and vocal fatigue were graded for 0 to 3. The mean score of vocal effort and fatigue were compared in both groups. Acoustic analysis using Visi Pitch IV was performed. Fundamental Frequency, habitual pitch, Shimmer, Relative Average perturbation, Harmonic to noise ratio, Voice turbulence Index and the maximum phonation time (MPT) were reported. The recording of the patients were evaluated blindly using the GRABS classification.

Results

There was no significant difference in the prevalence of any of the phonatory symptoms in patients with renal failure vs. controls. Patients with renal failure were twice more likely to have hoarseness compared to controls with an odds ratio of 2.7. There was also no significant difference in any of the acoustic parameters between patients and controls except for a borderline significance in the maximum phonation time (9.93 vs. 13.6 seconds in controls) with a p value of 0.055. There was no significant difference in the mean score of any of the perceptual evaluation parameters between patients and control.

Conclusion

Patients with renal failure do not have a significantly higher prevalence of phonatory symptoms compared to controls but are twice more likely to have hoarseness.

PS - 796

Formant Frequency in Relation to Hyoid Bone Position

Zaahir Turfe¹; Abdul Latif Hamdan²

¹Michigan State University College of Human Medicine;

²American University of Beirut Medical Center

Background

This study aimed to examine the correlation between the position of the hyoid bone on lateral cephalographs and formant frequencies, F1, F2, F3 and F4 during sustained vowels /a/, /i/, /o/, /u/.

Methods

Fifty two consecutive patients between the age of 9 years and 38 years presenting to the Orthodontics were invited to participate in this study. Lateral cephalographs were analyzed using the digital cephalostat in a standardized fashion. Linear measurements included: H-S: linear vertical distance from Hyoid bone to Sella Turcica, H-PNS: linear vertical distance from hyoid bone to posterior nasal spine, H-C3: linear measure from hyoid bone to the most anterior point of cervical vertebra C3, H-MP, linear vertical distance from hyoid bone to mandibular plane. All subjects underwent acoustic analysis using Visi-Pitch IV. Average fundamental frequency and formant frequencies were recorded. Pearson's correlation was calculated to estimate the strength of the relationship between the measurement parameters of the hyoid cartilage and acoustic parameters.

Results

There was a moderate correlation that was statistically significant between the average Fundamental frequency for the vowel /a/ and all the three cephalo-caudal parameters for hyoid position, namely H-S, H-PNS and H-C3 (r 0.596, 0.445, and 0.481 respectively with p values of 0, 0.001 and 0 respectively). There was a moderate negative correlation between F3, F4 and the vertical position of the hyoid bone as shown with r values for H-C3, H-S (r >0.30 and p value <0.05). There was also a moderate negative correlation between F2 and H-S (r of -0.406 and p value of 0.003) and between F1 and H-C3 (r 0.366 and p value 0.008). There was a moderate negative correlation between F1, F3 and F4 and H-S (all r>0.30) that was statistically significant (p values < 0.005). There was also a negative correlation between F3, F4 and H-C3 (r 0.392 and 0.309 respectively) that was statistically significant (p values < 0.005). For the vowel /o/ there was a moderate negative correlation between F4 and H-S and H-PNS (r values of -0.364 and -.0373 respectively) that was statistically significant (p values of 0.008 and 0.006 respectively). For the vowel /u/, F4 correlated moderately and significantly with H-S (r of 0.371 and p value of 0.014).

Conclusion

There is moderate correlation between the high formants, namely F4, and the cephalo-caudal position of the hyoid

bone in relation to the base of the skull and the third cervical vertebra C3.

PS - 797

Physiological Analysis of Double Vowel Perception in Listeners With Normal Hearing

Mark Hedrick; Jong Ho Won

The University of Tennessee Health Science Center

Background

Previous research has shown that perception of double vowels improves with increasing temporal onset asynchrony of the vowels, even if the vowels have the same fundamental frequency and amplitude (Hedrick & Madix, 2009). We sought to determine whether such improvements can be simulated using an auditory nerve model, and whether this model can be used to explain vowel confusion matrices constructed from the Hedrick & Madix (2009) data from normal-hearing listeners.

Methods

The peripheral auditory model of Zilany & Bruce (2006, 2007) was employed using 30 characteristic frequencies and a frequency range of 100-5000 Hz. Auditory neurograms were then made for each vowel for references. The following simulation procedure consisted of a single trial: a double vowel pair and asynchrony value (from 0 to 150 ms) was presented as the target; the model response was determined for the target; the NeuroSimilarity Index Measure (NSIM, Hines & Harte, 2012) was used to compare the model response to the references; the two references with the largest NSIM values were then selected as the predicted vowels. If both the predicted vowels were the actual vowels in the double vowel target, then this trial was counted as a correct response. To more accurately mimic the human data, the model was ran without noise, and with a Gaussian noise added, using S/N ratios of 5, 6, 7, 8, 9, or 10 dB.

Results

With the addition of noise, the model was able to mimic human performance when improvement in onset asynchrony is modeled as a change in S/N ratio. For example, a model S/N ratio of 5 dB mimicked human data for 0 ms onset asynchrony, and a model S/N ratio of 9 to 10 dB mimicked human data for 125 and 150 ms onset asynchrony. Some selections contributing to the confusion matrix data in humans was also mimicked by the model, but some aspects of the confusion matrix data was not simulated by the model.

Conclusion

The peripheral auditory model was able to mimic improvement in double vowel identification as temporal onset asynchrony of the vowels increased by representing the asynchrony as changes in S/N ratio. Whether these changes in S/N ratio would reflect either peripheral neural encoding mechanisms or cognitive decision processes will be explored in future studies. The inability of the model to mimic some vowel confusions suggests further modeling may need to employ decision processes.

Periodicity and Aperiodicity in the Perception of Speech in Both Steady-State and Fluctuating Maskers

Kurt Steinmetzger; Stuart Rosen
University College London

Background

Hearing-impaired listeners and cochlear implant (CI) users experience great difficulties in speech perception in all types of background noise, and unlike normal-hearing listeners show little benefit from fluctuations in the masker. One popular (if partial) explanation for these difficulties proposes a key role for temporal fine structure (TFS) cues which are severely limited by CI speech processing. However, there is controversy over whether TFS has a special role in allowing fluctuating masker benefit or whether its contribution to speech perception is just as important for steady maskers. We investigated the abilities of normal-hearing listeners to perceive speech targets in the background of noise maskers in a variety of conditions mixing presence and absence of periodicity in both target and masker.

Methods

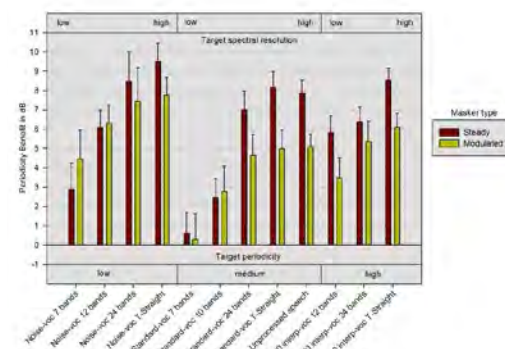
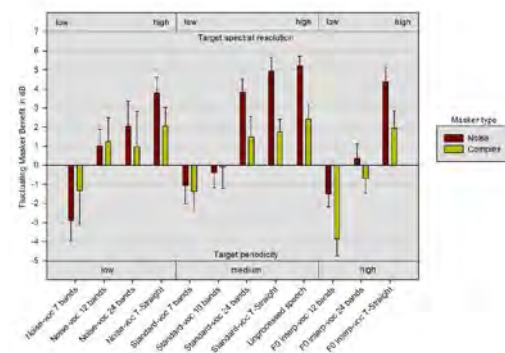
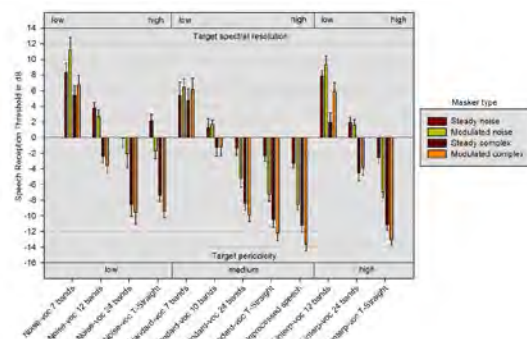
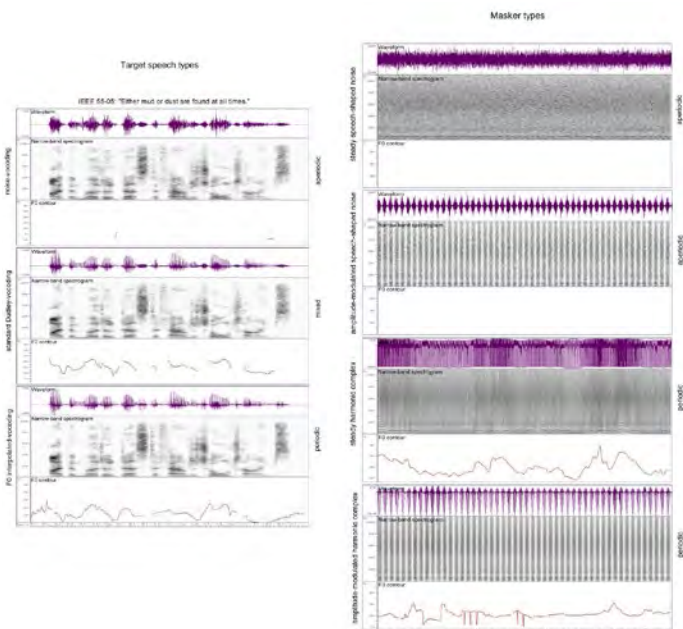
Speech Reception Thresholds (SRTs) were measured adaptively for IEEE sentences processed to change their source characteristics (and hence their periodicity). The sentences were embedded in four different maskers: speech-shaped noise and harmonic complexes with a dynamically varying fundamental frequency, that were either steady or fluctuating at 10 Hz. Additionally, we varied the spectral resolution of the target speech over a wide range. In two separate experiments 16 and 12 normal-hearing subjects were tested.

Results

It was found that increasing the amount of periodicity in masker and target greatly aids speech intelligibility across all levels of spectral resolution. In line with previous findings, the effectiveness of a masker was found to be strongly reduced when it was periodic. We also observed an effect of periodicity for the target speech, with fully periodic speech at a high spectral resolution being more intelligible than any other processing condition. Contrary to what was been believed previously, we found that the fluctuating-masker benefit (FMB) is markedly smaller for periodic than for aperiodic maskers, and that a substantial FMB requires a high spectral resolution of the target speech.

Conclusion

Our results show the importance of periodicity in tracking a speech signal through a background noise and suggest that the inability to exploit periodicity in segregating masker and target speech may be an even more important factor in the limitations of CI speech perception than the inability to benefit from fluctuations in a masker.



Comprehension of Degraded Speech Becomes Less Effortful but not More Automatic With Training

Julia Huyck¹; Ingrid Johnsrude²

¹Kent State University; ²Queen's University, Kingston, ON, Canada

Background

Perceptual learning is an important determinant of the intelligibility of degraded or accented speech. Attention to degraded speech appears necessary for such learning (Huyck and Johnsrude, 2012), and is required for degraded (but not clear) speech to be processed as language by the brain. Left inferior frontal cortex (LIFG) activity appears to be a marker of such effortful listening (Wild et al., 2012). This raises the question: after learning, is degraded speech processed more like clear speech, requiring less attention and less LIFG engagement during perception?

Methods

We conducted an fMRI experiment with 42 young adult listeners in which comprehension (word report) of degraded (6-channel noise-vocoded) sentences was assessed before and after “attended” and “unattended” training. All participants received both training types, in counterbalanced order. Clear and unintelligible (rotated noise-vocoded) sentences were included as within-subject controls. Test blocks consisted of 5 sentences of each speech type. Training blocks consisted of 18 sentences of each type, each sentence presented simultaneously with a sequence of AM noise bursts. During “attended” training, listeners made a binary intelligibility judgment for each sentence. During “unattended” training, listeners made a binary target detection judgment for each AM sequence. After the session, we assessed recognition memory for the sentences presented during training. Imaging during training was accomplished on a Siemens 3T MR system (sparse imaging: TR = 9 sec).

Results

Word-report scores during tests confirmed that attention is required for learning of degraded speech. Whereas clear sentences presented during training were equally well remembered regardless of attentional state, memory of unattended degraded sentences was significantly worse than that of attended degraded sentences, indicating that the unattended ones were processed less completely. Furthermore, the magnitude of this difference did not depend on training order, suggesting that learning of degraded speech does not lead to greater processing of it when unattended. Activity in the LIFG was specific to the attended degraded speech condition, as predicted, but this interaction effect was significantly smaller when “attended” training was second compared to when it was first.

Conclusion

Since recognition of unattended sentences did not improve after effective training, processing does not appear to become more automatic with learning. However, the effort required to comprehend attended degraded speech, as indicated

by LIFG activation, does seem to decrease with increased experience (testing and/or “unattended” exposure).

Effects of Lexicality and Attention on the Auditory Streaming of Speech

Alexander Billig; Matthew Davis; Robert Carlyon

MRC Cognition and Brain Sciences Unit

Background

The sensitivity of auditory streaming to a large number of stimulus parameters has been explored extensively. However, the role played by higher-level factors in streaming is less well understood, particularly for speech. We investigate the effects of lexical knowledge and attention on the perceptual organization of syllables, the initial fricatives of which stream apart under repetition.

Methods

Both experiments required the detection of targets – syllables containing a gap after the initial /s/. This task provides an objective measure of streaming as listeners are better at judging the relative timing of sounds falling within the same stream than of those in separate streams. *Lexicality experiment*: Listeners heard sequences of repeated words (“stem”, “stone”) or acoustically matched nonwords (“sten”, “stome”). They reported their percept throughout, and detected occasional targets in the penultimate syllable. The lexicality of the targets was manipulated independently of that of the preceding syllables. *Attention experiment*: Listeners were presented with long and short sequences of the repeated nonword “sti” in one ear, and a concurrent frequency-modulated tone in the other, which ended before the final two syllables. In the “attend” condition, listeners attended to the speech throughout and continuously reported their percept. In the “switch” condition, they identified attenuations in the tone. In both conditions, listeners also detected occasional targets in the final two syllables.

Results

When speech was attended in both experiments, the initial /s/ sound in each syllable formed a separate stream after several presentations. The percept then fluctuated between streamed and fused states in a bistable manner. *Lexicality experiment*: Gap detection was better when streaming caused the syllables preceding the target to transform from words into nonwords, rather than from nonwords into words, and did not depend on the lexicality of the target. *Attention experiment*: Preliminary data indicate a marginal effect of task on gap detection (Switch > Attend) for long sequences.

Conclusion

Auditory streaming not only depends on the acoustic characteristics of speech sounds, but is also influenced by lexical knowledge. Initial results suggest that attention may affect streaming of syllables in a similar way to that of pure tones. Further work will use objective measures to probe the nature of these attentional effects, and will study their dependence on the acoustic and linguistic characteristics of stimuli used in the competing task.

The Effect of Audibility on Spatial Release from Masking

Helen Glyde; Joerg M. Buchholz; Lillian Nielsen; Virginia Best; Harvey Dillon

National Acoustic Laboratories

Background

Speech intelligibility is typically improved when target speech is spatially separated from distracting speech. This difference in speech intelligibility between spatially separated and co-located target and distracting speech is termed spatial release from masking (SRM). The Listening in Spatialized Noise Sentences (LiSN-S) test is a headphone-based test which can be used to assess SRM with symmetrically separated maskers. Normative data in hearing-impaired (HI) listeners shows a monotonic decrease in SRM with increasing hearing loss. Since the LiSN-S incorporates linear amplification according to NAL-RP, which only partly restores audibility, it is unclear how far the observed reduction in SRM can be explained by limited audibility. The present study therefore investigates the effect of limited audibility on SRM for this test paradigm.

Methods

SRM was measured with a research version of the LiSN-S in 16 HI listeners as well as in 16 normal-hearing (NH) listeners with a simulated hearing loss. All HI subjects had a moderate sloping hearing loss and their average hearing loss was simulated in the NH group by pre-filtering (attenuating) the speech material. Three different linear amplification schemes were applied to provide different levels of audibility: NAL-RP as well as two amplification schemes that provided increased gain to compensate for an additional 25% and 50% of the considered hearing loss.

Results

The HI listeners showed an average SRM of 5.1 dB for NAL-RP amplification, which increased to 6.6 dB and 8.4 dB when an extra 25% and 50% of amplification was applied. This significant increase in SRM with increasing amplification was purely due to increased intelligibility in the spatially separated condition; the co-located condition was unaffected. The simulated HI group showed a similar increase in SRM with increasing amplification, but their overall scores were consistently better by approximately 3dB. When normal speech levels (100% extra amplification) were applied to NH listeners a further increase in SRM of about 3 dB was observed.

Conclusion

The decrease in SRM with increasing hearing loss, as measured by the LiSN-S, can be largely explained by reduced audibility and can be partly restored by increased amplification. This general behaviour is confirmed in NH listeners with a simulated hearing loss. However, HI listeners show an overall decrease in SRM that seems independent of amplification and may be explained by differences such as in age, cognitive ability, frequency resolution, or binaural processing.

Timing and Specificity of Preparatory Attention in Cocktail-Party Listening

Emma Holmes¹; Padraig Kitterick²; A. Quentin Summerfield¹

¹University of York; ²NIHR Nottingham Hearing Biomedical Research Unit

Background

Individual differences in cocktail-party listening could arise from differences in either central attention or peripheral transduction. We have developed a technique which isolates one aspect of attention, based on a procedure devised by Hill and Miller (2010, Cerebral Cortex). On each trial, they presented three simultaneous voices differing in fundamental frequency and spatial location. In advance of the acoustic stimuli, participants were cued visually to either the location or the pitch of the voice which was to receive attention. Functional magnetic resonance imaging revealed a distinct cortical network, in which levels of activity depended on whether pitch or location was cued, in preparation for the acoustic stimuli. Potentially, therefore, brain activity recorded before acoustic stimuli are presented could reveal differences in the control of attention without being confounded by differences in transduction. In the current experiments, we applied this principle to compare the time course of preparatory attention between adults and children.

Methods

Participants were 24 children aged 7-16 years and 16 adults aged 18-27 years, all with normal hearing. We recorded brain activity using 64-channel electroencephalography. On each trial, two sentences spoken by adult talkers (one male and one female) were presented simultaneously from loudspeakers at two spatial locations (one left and one right of fixation). Participants were cued, in advance of the acoustic stimuli, to either the location (left/right) or the gender (male/female) of the target talker. The task was to report key words spoken by that talker. A control condition, in which the visual cues did not have implications for attention, allowed cortical activity evoked by the configurational properties of the cues to be distinguished from activity evoked by attentional processes.

Results

Event-related potentials (ERPs) differed between trials on which participants were cued to the location compared to the gender of the target talker. Evidence of cue-specific preparatory attention, manifest as more positive ERPs evoked by the cue to location than gender in posterior scalp locations, started 60 ms after the onset of the visual cue in adults and 72 ms in children.

Conclusion

Adults and – more surprisingly – children display distinct cortical activity very soon after the onset of a visual cue that directs auditory attention to the location or gender of one talker in a mixture of talkers. This technique has the potential for increasing understanding of the contribution of central impairments to difficulties in cocktail-party listening.

PS - 804

Ear Dominance in a Dichotic Cocktail Party

Eric Thompson¹; Nandini Iyer²; Brian D. Simpson²; Griffin Romigh²

¹Ball Aerospace & Technologies Corp.; ²Air Force Research Lab

Background

Cherry (1953) reported that when listeners were presented with a dichotic signal over headphones, they could reliably report words presented to the attended ear with very few errors, while only being aware of gross properties of the talker in the unattended ear. More recently, Gallun et al. (2007) showed that there were large differences in performance on a dichotic listening task depending on the ear of presentation. The number of errors was significantly larger when the target was presented to the left rather than to the right ear.

Methods

Phrases selected from the Coordinate Response Measure (CRM) corpus were presented to listeners over headphones in three listening conditions: a) Target+Noise presented to left or right ear with no contralateral masker; b) Target+Noise presented to either ear with noise in the contralateral ear; and c) Target+Noise presented to either ear with a contralateral Speech+Noise masker, where the speech masker is a different, same-sex talker CRM phrase. Other independent variables were target ear (left or right), type of cuing (cuing target ear before or after stimulus presentation), type of listening condition within a block (random ear-of-presentation vs. fixed), and signal-to-noise ratio (-18 to -6 in 3-dB steps). The dependent variable was percent correct target color-number identification.

Results

Listeners showed ear dominance in that target identification was significantly better when the target signal was presented in the right ear than in the left ear. The right ear advantage was only evident in conditions with a contralateral speech masker. There was no difference in performance between the ears for the noise-only or no-masker contralateral conditions. Performance was worse for fixed blocks in which all targets were in the left ear than in the right ear. Trial-to-trial target-ear uncertainty reduced performance, but more for left-ear than for right-ear presentations. The largest right-ear advantage was seen with the postcue condition, in which the target ear was only known after stimulus presentation.

Conclusion

When two speech inputs are presented simultaneously, one to each ear, the signal in the right ear appears to be preferentially processed, even when the listener is instructed to attend to the signal in the left ear for an entire block of trials. This suggests some limitations in the brain that cannot be overcome through modulation of attention.

PS - 805

Binaural Glimpses at the Cocktail Party?

Stephan Ewert¹; Andrea Lingner²; Lisa Benda²; Sven Schoernich²; Lutz Wiegrebe²

¹Universitaet Oldenburg; ²Ludwig-Maximilians-Universitaet Munich

Background

In everyday situations, like the infamous cocktail party, humans need to focus on a single sound source while ignoring competing sources: In situations where target and masker are maximally separated, speech intelligibility (SI) is improved compared to situations where target and masker are co-located. Such asymmetric configurations of target and masker lead to a 'better-ear effect' with improved signal-to-noise ratio (SNR) at one ear. However, in everyday situations interfering sounds are often surrounding the listener. In such symmetric configurations, better-ear effects are absent in a long-term, wideband sense, while they might persist in the form of 'glimpses' distributed across frequency and time. It has been shown that also in symmetric conditions a spatial separation of the maskers from the target lead to improved SI.

Methods

This study aims to quantify SI in a paradigm closely matching the cocktail party situation: Listeners were surrounded by a frontal target speaker and eight masking speakers. Eight maskers (running single talker speech) were presented in five spatial configurations. In the reference condition, all eight maskers coincided with the target direction. In the test conditions, maskers were all presented from the loudspeaker in the back of the listener or distributed on either two, four, or eight loudspeakers, symmetrically placed around the listener. SI was assessed using an adaptive matrix sentence test.

Results

In all of the test conditions, SI was substantially improved compared to the reference condition; the strongest improvement was observed for four loudspeakers each playing two maskers (at azimuths of -140, -40, +40, and +140°). Interestingly, the improved SI persisted in a control experiment where the frequency range of the maskers above 1500 Hz was replaced with speech-shaped noise. In this condition the potential for better-ear glimpses in the form of short-time SNR improvements was limited. First simulations show that the directionality of the subjects' outer ears contributes very little to the improved SI.

Conclusion

The data show that better-ear glimpses in the form of short-time SNR improvements may not be solely responsible for the improved SI at the Cocktail Party. Instead we hypothesize that fast sampling of fluctuating interaural time differences (ITD) of the maskers and target underlie the improved SI ('ITD glimpses'). This hypothesis will be evaluated in a state-of-the-art binaural SI model.

Adaptation to Room Reverberation in Nonnative Phonetic Training

Eleni Vlahou¹; Aaron Seitz¹; Norbert Kopčo²

¹University of California, Riverside; ²Safarik University, Košice

Background

Speech communication often occurs in adverse listening conditions, such as noisy and reverberant environments. Room reverberation distorts the speech signal and hampers intelligibility, an effect particularly pronounced for nonnative listeners (e.g., Nábelek and Donahue, 1984, *J. Acoust. Soc. Am.* 75: 632-634). There is evidence that prior exposure to consistent reverberation is beneficial for native listeners, resulting in improved speech intelligibility (Brandewie & Zahorik, 2010, *J. Acoust. Soc. Am.* 128: 291-299), but less is known about the patterns of interference and adaptation to room reverberation for nonnative listeners during the acquisition of novel phonetic categories. In the present study we investigate these issues, addressing in particular the differential effects of phonetic training in multiple reverberant rooms versus a single anechoic environment on the perception of nonnative phonemes in anechoic and reverberant conditions.

Methods

Listeners were trained on a difficult dental-retroflex phonetic distinction. Stimuli were CV syllables coming from a Hindi speaker and were presented in anechoic space or in simulated reverberant environments, crossed with supervised and unsupervised training. Supervised training consisted of a 2AFC task with trial-by-trial performance feedback. Unsupervised training employed a videogame which promoted stimulus-reward contingencies. Before and after training, participants were tested using the trained voice and trained rooms, as well as using an untrained voice and untrained rooms.

Results

When tested with the trained voice, participants showed significant improvements for trained and untrained stimuli and rooms. Exposure to the stimuli in three different rooms vs. exposure only in anechoic room resulted in similar amounts of learning and generalization to untrained rooms. Supervised training resulted in larger improvements than unsupervised training. No generalization of learning to an untrained voice was observed for either type of room simulation.

Conclusion

The results show that phonetic categorization training of the dental-retroflex distinction in nonnative listeners is robust against variation in room characteristics, but also that it does not benefit from exposure to the stimuli in different reverberant environments. The lack of generalization of learning to an untrained voice suggests that listeners encoded talker-specific, non-phonetic details. While these results confirmed that acquisition of novel phonetic categories for nonnative listeners is robust against reverberation variations, it is likely that the extent to which phonetic learning and reverberation adaptation interact depends on the specific acoustic and phonetic features important for the trained discrimination.

Learning an Invented Auditory Non-Linguistic Rule: Children Versus Adults

Liat Kishon-Rabin; Shira Cohen; Sara Ferman; Daphne Ari-Even Roth

Tel-Aviv University

Background

Learning of a language involves both implicit and explicit processes that are considered memory-based learning mechanisms. The memory systems involved in the acquisition of the different elements of the language differ depending on the element and age at acquisition. For example, learning of grammar in early childhood uses implicit processes that allow unconscious effort of automatic identification of patterns of regularities and extraction of rules from linguistic sequences. In contrast, learning grammar in adulthood is known to involve explicit processes including conscious use of knowledge that can be supplemented and enhanced by implicit learning. In a previous study we showed that in 5 training sessions, 5/10 adults were able to extract rules from auditory non-linguistic sequences supporting the hypothesis that rule learning is not specific to language. The purpose of the present study was to compare the process of rule extraction from a sequence of non-linguistic auditory stimuli by children to that found in adults.

Methods

A total of 18, 12-year old boys and girls participated in learning an invented 'Dolphin language'. Ten of the children trained for five sessions and eight trained for 10 sessions using the same training protocol as the adults. In each session, each child listened twice to a modeling list of 12 sequences that consisted each of the same four different sounds (pure-tones and narrow bands) but in a different order according to an invented rule. The children were then presented with 24 sequences, half of which were from the modeling list. They were asked to judge the correctness of these sequences and to complete the last signal in 12 more sequences. Transfer of learning was tested with new sequences.

Results

Results showed that: (1) similar to adults, children were grouped to "learners" and "non/hard-learners"; (2) in the "learners" group, children required twice as much training as adults in order to reach comparable performance; (3) in contrast to adults, children showed no transfer of learning but made attempts to verbalize the rule; and (4) reaction time decreased for the children "learners" on both tasks, but increased for the adults on the judgment task.

Conclusion

Over all our data support the notion that children learn auditory sequential patterns via implicit memory processes. The fact that only adults showed transfer of learning to new stimuli, were able to verbalize the rule and showed faster improvement compared to children may be ascribed to the maturity of their explicit and implicit mechanisms.

Auditory-Neurophysiologic Responses to Speech in Pre-Readers: The Search for a Reading Biomarker

Travis White-Schwoch; Nina Kraus

Northwestern University

Background

Learning to read builds upon the development of basic language skills. One of these skills is phonological awareness (PA), the knowledge of the sound structure of spoken language. Children with developmental dyslexia have poor PA, and in school-aged children PA and reading vary systematically with the neural precision of speech encoding, as observed in auditory midbrain and cortex. Little is known, however, about the development of these neural systems with respect to early language skills.

Methods

We recorded auditory brainstem responses to the speech sounds [ba], [da], and [ga] in pre-school aged children. We considered three aspects of the auditory-neurophysiologic responses: the stability of the response, a measure of trial-by-trial synchronous firing in auditory midbrain; the physiologic distinction between speech syllables, a timing-based measure of speech discrimination; and neural timing for fast-changing speech elements in noise. All of these are established 'neural signatures' of reading ability in school-aged children.

Results

Pre-readers with good phonological awareness had more consistent neural responses to speech. These children also had superior temporal coding of fast-changing speech elements (i.e., consonant-vowel transitions) reflected in enhanced physiologic speech discrimination and resilience to background noise.

Conclusion

The neural hallmarks of reading are closely linked to phonological skills in children not yet old enough to read. Reduced subcortical phase locking at high rates (> 100 Hz) may diminish the precision of speech encoding, causing some children difficulty learning to read. These results highlight the role of the central auditory system in developing language-based skills. Identifying objective neurophysiologic correlates of poor PA in pre-readers may inform the design of biomarkers for reading and auditory processing (dis)ability.

Correlations Between Lip Contours and Modulation Envelopes in Speech

Arun Palghat Udayashankar¹; Meghan Stansell²; Gabreille Saunders²; Peter Jacobs¹

¹Oregon Health and Science University, National Center for Rehabilitative Auditory Research; ²National Center for Rehabilitative Auditory Research

Background

Showing a speaker's face is known to improve speech recognition in noise performance compared with the audio-alone condition. We explore how modulation frequency envelopes

correlate with lip motion. Modulation filtering of speech involves decomposing the signal into frequency bands and then dividing each band into a high frequency carrier and a low frequency modulation envelope. The modulation envelope temporally shapes the carrier frequency in a way that is similar to the way the lips shape sound energy during speech production. We present the relationship between lip contour movements and modulation envelopes as recorded during audio-visual speech at the sentence, word, and simple-sound level.

Methods

Two subjects were asked to speak 400 sentences from the revised speech-in-noise (R-SPIN) corpus and from the CUNY nonsense-syllable test (NST) corpus. A commercial face tracker (Luxand Inc.) was used to extract 66 points from the face during articulation with a high speed camera (96 fps). The coordinates of the outer lips were fit to an ellipse for each video frame and the area of the ellipse was tracked over time. Modulation envelopes with a ~500 Hz bandwidth were extracted. Correlations between the area of the ellipse and the modulation envelope of the lowest frequency band were calculated for words, sentences, and simple sounds. Preliminary speech intelligibility tests were done on audio signals which were recomposed with the audio carrier and the visual envelope to determine the intelligibility of visually-augmented speech.

Results

The correlation of the lowest frequency modulation band was 0.38 +/- 0.07 (N=400) for sentences, 0.45 +/- 0.08 (N = 727) for words and 0.64 +/- 0.12 for simple sounds. The delay of the audio relative to the lips ranged from 5 to 15 ms depending on the speaker. When the lip contour was used instead of the modulation envelope, the sentences and words were intelligible, but there did not appear to be a benefit of swapping the lip contours for the modulation envelope under low SNR conditions.

Conclusion

Despite having found that the lips correlate with the modulation envelope, we found that replacing the lowest modulation envelope with the lip contour did not provide an improvement in intelligibility; hence more sophisticated algorithms are required to augment the audio using the visual features. Several algorithms will be presented. Results from this work could motivate future development in integrating visual cues into hearing aid signal processing.

Modifications in Stimulus Timing Dependent Plasticity Mediated Learning Rules in Dorsal Cochlear Nucleus Following NMDA Receptor Blockade

Roxana Stefanescu; David T Martel; James A. Wiler; Sanford Bledsoe; Susan E. Shore
University of Michigan

Background

The dorsal cochlear nucleus (DCN) is the first somatosensory integration brain station in the auditory pathway, receiving auditory input from the cochlea and somatosensory input from the spinal trigeminal nucleus (Sp5) via parallel fibers. Stimulus timing dependent plasticity (STDP), the macroscopic correlate of spike timing synaptic plasticity, can be induced in DCN following a bimodal (auditory-somatosensory) stimulation protocol in which auditory and Sp5 electrical stimulation are presented at various onset difference intervals. *In vitro* studies in DCN (Tzounopoulos et al. Nat Neurosci., 7(7):719-25, 2004) have shown that spike timing dependent plasticity modifications take the form of a Hebbian "learning rule" in fusiform cells but are anti-Hebbian in cartwheel cells. More recent studies (Koehler and Shore, PLoS One, 8(3):e59828, 2013) demonstrated that *in vivo*, fusiform cells may exhibit different learning rules depending on their degree of inhibition. Moreover, the cell population learning rule may be different in normal and tinnitus animals (Koehler and Shore, ARO abstracts, 2014). These results suggest complex underlying synaptic plasticity mechanisms, which may play an important role in normal DCN function as well as pathological changes associated with tinnitus. A major contribution to these plastic modifications could be the NMDA receptor (NMDAR) which has been previously implicated in spike timing dependent plasticity at the parallel fibers in DCN (Fujino and Oertel, PNAS 100(1):265-70, 2003). With this motivation, we investigated the contribution of the NMDA receptor (NMDAR) to the stimulus timing dependent learning rule in the guinea pig DCN.

Methods

In vivo, sound-evoked and spontaneous extracellular electrophysiological responses were obtained from fusiform cells in the guinea pig DCN before and after bimodal stimulation to determine the stimulus time dependent learning rule of each cell. The evaluation of the learning rule was performed again after an NMDA blocker has been infused into the fusiform-cell layer of DCN.

Results

Blocking NMDARs had mostly a suppressive effect, depressing the learning rule for most of the bimodal intervals. In certain cells however, blocking NMDARs resulted in a complete "switch" of the learning rule from a Hebbian to anti-Hebbian configuration. Other modifications were also induced in the rate level functions of the DCN cells.

Conclusion

We conclude that similar to other brain structures, NMDARs contribute significantly to stimulus timing dependent synap-

tic plasticity in the DCN. The effects observed when blocking this receptor may suggest possible new avenues of modulation and control of plasticity mechanisms in normal and pathological systems.

Sound Loudness Affected by High Doses of Salicylate and Noise Exposure

Chao Zhang^{1,2}; Wei Sun¹; Elizabeth Flowers¹; Qiuju Wang²

¹State University of New York at Buffalo; ²Chinese PLA

General Hospital

Background

Hyperacusis is a subjective phenomenon which refers to a marked intolerance to ordinary environmental sounds. Hyperacusis is typically associated with sensorineural hearing loss caused by noise or ototoxic drug exposure. However, the cause of hyperacusis is not clear. Our previous studies suggest that noise exposure and high doses of salicylate can induce exaggerated startle reflex in rats, suggesting hyperacusis behavior. However, there is no direct measurement for loudness change caused by salicylate or noise exposure to verify this model.

Methods

To further establish and validate this model for hyperacusis, we established an operant conditioning based behavioral task to measure changes in the loudness of rats before and after inducing hyperacusis. This paradigm was designed based on human's psychoacoustic task of loudness (Cox et al. 1997). During this task, food-restricted rats were reinforced by palatable food pellets to nose-poke the right or left food-dispensers upon perceiving a loud or a soft sound. After the correct rates reached ~95%, the loudness response curve was determined by measuring the percentage response on one side of the food dispenser when a sound from 40 to 110 dB SPL (10 dB step) was presented. We hypothesize that rats with hyperacusis will show a rapidly increasing loudness growth function and a reduced dynamic range of the loudness response curve.

Results

The loudness response was measured before and after the treatment of high doses of salicylate or noise exposure. We found that the loudness response curves were significantly affected after salicylate injection (250 mg/kg, intraperitoneally). In about one-third of rats, the loudness curve shift dramatically to the left which change is consistent with our hypothesis and the loudness change in hyperacusis patients. In about one-third of rats, the loudness change was similar to recruitment and some others showed a loudness change may be affected by tinnitus. Noise exposure (105 dB SPL, 1 hour) induced a revisable loudness change similar to recruitment and hyperacusis. More intense noise exposure is current used for this model.

Conclusion

The loudness response test is very sensitive to the sound intensity change. A stable and reliable curve can be achieved in rats before and after rats were treated with salicylate and noise exposure. This test method, which mimics the loudness

response measurement reported in humans, can be very useful to evaluate loudness change in animal models.

PS - 811

Possible Contribution of Non-Classical Auditory Centers to Salicylate-Induced and Noise-Induced Tinnitus and Hyperacusis

Richard Salvi; Guang-Di Chen

SUNY at Buffalo

Background

Regions of the CNS outside the classical auditory pathway have been proposed to play a role in tinnitus and hyperacusis; however, there is a paucity of experimental data addressing this issue. Tinnitus- and hyperacusis-like behaviors can be reliably induced with a high dose of salicylate whereas the effects of intense noise exposure are more variable. To determine the extent to which areas outside the classical auditory pathway might contribute to tinnitus and hyperacusis, we compared the electrophysiological changes occurring in the amygdala, striatum, hippocampus and cingulate cortex after salicylate treatment or intense noise exposure.

Methods

Rats were exposed to a sodium salicylate (SS, 250 mg/kg) or intense high-frequency narrowband noise (noise-induced hearing loss assessed with ABR). Sound evoked multiunit activity and local field potential (LFP) were recorded in the amygdala and the striatum at different frequencies and intensities. Peristimulus time histograms from all the units studied were used to construct a frequency-intensity matrix representing the neural population response. Similar measurements were obtained from rats before and after salicylate treatment, but in addition to amygdala and striatum, additional measurements were obtained from the hippocampus and cingulate.

Results

SS induced shifts in the frequency receptive fields (FRF) of neurons in the amygdala such that neurons with low and high characteristic frequencies (CF) shifted their CFs towards the mid-frequencies, resulting in an expanded population of neurons with CFs between 10-20 kHz, a frequency that matches the pitch of salicylate-induced tinnitus. The SS-induced hyperactivity was also observed in the striatum and hippocampus, but not in the cingulate cortex. The intense noise exposures enhanced the responses of neurons in the amygdala to frequencies below the noise band, while the responses to frequencies within and above the noise damaged area were attenuated or abolished. Interestingly, in a few animals, the enhancement of sound evoked activity was observed at frequencies near edge of the hearing loss reflecting plastic reorganization. In contrast to SS, the noise-induced enhancement of the auditory response was not observed in the striatum.

Conclusion

For SS-treatment, three areas outside the classical auditory pathway, the amygdala, striatum, hippocampus, but not the cingulate, undergo significant physiological changes that may contribute to tinnitus. For high-frequency noise exposures, the amygdala undergoes physiological changes being

related to the noise-induced tinnitus and hyperacusis. However, noise exposure does not affect the striatum in the same way as SS suggesting that the striatum may not be involved in noise-induced tinnitus and/or hyperacusis.

PS - 812

Behavioral Assessment of Salicylate-Induced Hearing Loss and Gap Detection Deficits in Rats

Kelly Radziwon¹; Daniel Stolzberg²; Richard Salvi¹

¹*University at Buffalo*; ²*University of Western Ontario*

Background

Many researchers use gap prepulse inhibition of the acoustic startle reflex (GPIAS) to screen animals for tinnitus. Presumably, tinnitus fills in the silent gap in the background noise resulting in the reduction of GPIAS. However, recent research in humans has called the tinnitus-gap filling hypothesis into question. The purpose of this experiment was to test this hypothesis by determining gap detection thresholds in rats.

Methods

Six Sprague Dawley rats were used in the gap detection experiment; five of these rats were used to obtain broadband noise thresholds. The stimulus used in the gap detection experiment was a continuous broadband noise presented at 20, 30, 40, or 60 dB SPL. The rats were tested using a go/no-go operant conditioning procedure to detect a silent gap embedded within the broadband noise. The go/no-go procedure with the psychophysical Method of Constant Stimuli was also used to determine broadband noise thresholds in quiet. After baseline gap detection thresholds were collected, the rats were tested once per week with either a single injection of sodium salicylate (200 mg/kg IP), previously shown to induce tinnitus in rats, or an equivalent volume of saline. The injections were administered 2 h before testing gap thresholds or broadband noise thresholds. Mean *hit* and *false alarm* rates were used to calculate thresholds using signal detection theory. Mean gap thresholds decreased from approximately 2 ms for stimuli presented at 60 dB to approximately 5 ms at 20 dB. Salicylate had little or no effect on gap thresholds at high stimulus levels (30-60 dB SPL).

Results

Although sodium salicylate increased gap thresholds at the lowest sound level (20 dB SPL), the rats could always detect gaps longer than 10 ms at the higher sound levels. Since salicylate produced a mean hearing loss of 17 dB SPL in the broadband noise detection experiment, the effects of salicylate seen in the gap detection experiment is most parsimoniously explained by hearing loss alone.

Conclusion

Hearing loss impairs temporal resolution at low sensation levels. Since most instances of tinnitus involve moderate to substantial hearing loss, separating the effects of tinnitus from the effects of hearing loss on gap detection performance becomes difficult. Our results suggest that any gap detection deficits from salicylate are the result of hearing loss alone and not caused by tinnitus filling in the silent gaps.

High Doses of Salicylate Causes Prepulse Facilitation of Offset-Gap Induced Acoustic Startle Response

Wei Sun; Lauren Doolittle; Elizabeth Flowers; Chao Zhang
State University of New York at Buffalo

Background

Prepulse inhibition of acoustic startle reflex (PPI), a well-established method for evaluating sensorimotor gating function, has been used to detect tinnitus in animal models. Reduced gap induced PPI (gap-PPI) was considered as a sign of tinnitus. Since a silent gap with a rapid raising/fall time contains both onset and offset stimuli, these stimuli may play as a separate cue to induce PPI. It is not clear which signals are affected by tinnitus or hearing loss.

Methods

We tested the PPI using three different shapes of gaps: an onset-gap which has a rapid onset-time and a long offset-time (Figure 1A), an offset-gap which has a rapid offset-time and a slow onset-time (Figure 1B), and an onset-offset-gap which has both rapid onset and offset time (Figure 1C). Tinnitus was induced by high doses of salicylate (250 mg/kg, i.p.) and gap-PPI was recorded before and after salicylate treatment.

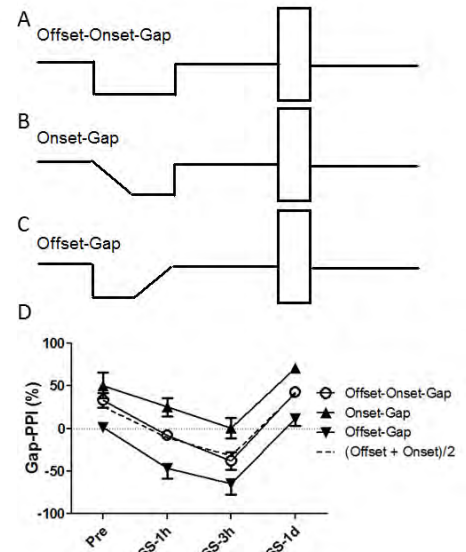
Results

The onset-gaps caused stronger inhibitions than the offset-gaps. Gap-PPI induced by onset-offset-gaps, equals to the averaged gap-PPI induced by the onset- and offset-gaps. The onset-gap induced PPI was significantly reduced one to three hours after salicylate treatment (Figure 1D). Surprisingly, the offset-gap caused a facilitation of startle response. Treatment of vigabatrin (60 mg/kg/day, 14 days), an anti-seizure drug that elevates central GABA levels, blocked salicylate induced the startle facilitation induced by offset-gap.

Conclusion

Salicylate induced reduction of gap-PPI was not only caused by decrease of the onset-gap induced PPI, but also by the facilitation induced by the offset-gaps. Enhancing GABAergic activities can alleviate salicylate induced tinnitus.

Figure 1. Sun et al.[^]



The Effects of Cholecystokinin (CCK) on Auditory Responses

Guang-Di Chen; Adam Sheppard; Richard Salvé
SUNY at Buffalo

Background

Cholecystokinin (CCK), a gastrointestinal hormone released during feeding, is responsible for gallbladder contraction, secretion of pancreatic enzymes and insulin secretion, and regulating bowel motility. The octapeptide CCK (CCK8) is also produced and released in the cerebral cortex, hippocampus, striatum, and the amygdala. While CCK in the periphery acts via CCK-A receptors, centrally, CCK acts as a co-transmitter or modulator of neuronal activity via CCK-B receptors. CCK in the central nervous system facilitates glutamate release from neurons by increasing the number of vesicles released and the probability of release. It also induces depolarization of neurons by suppressing potassium conductance. Besides controlling food intake, CCK in the brain is implicated in other functions such as exploratory, anxiety, learning, and memory. Interestingly, preliminary studies suggest that brain CCK may be involved in neural plasticity.

Methods

To test the hypothesis that CCK8 regulates excitability and plasticity in the auditory cortex, microelectrodes were inserted into the auditory cortex for recording sound-evoked local field potential (LFP) and neuronal discharges. CCK8 was locally infused into the recording region using a fluidic, silicon multichannel electrode. In experiment-1, we investigated the effect of CCK8 on auditory-evoked responses. Experiment-2 investigated the effect of CCK8 on modulating plasticity of auditory neurons.

Results

CCK8 induced a dose-dependent enhancement of auditory-evoked LFPs and sound-evoked neuronal discharges. The LFP-enhancement was level-dependent with greater increases seen at higher stimulation intensities. The maximal

increase was ~70%. Neuronal discharge rate, except the early component (~10 ms), was significantly enhanced. Interestingly, our preliminary data showed that repetitive acoustical stimulation (tone bursts) combined with CCK8 application induced a shift of the neuron's frequency receptive field (FRF) towards the frequency of the repeated acoustic stimulus.

Conclusion

The data suggest that CCK8 can increase sound-evoked activity in auditory cortex and that the combination of CCK8 plus repetitive acoustic stimulation can modify the receptive fields of neuron in the auditory cortex. Thus, CCK8 could conceivably be used with sound therapies to modify abnormal auditory perceptions such as tinnitus and/or hyperacusis.

PS - 815

Two-Alternative Forced Choice Task for Assessing Noise-Induced Tinnitus in Rats

Nina Kashanian¹; Kelly Radziwon¹; Richard Salvi¹; Daniel Stolzberg²

¹University at Buffalo; ²University of Western Ontario

Background

Tinnitus, the persistent perception of a phantom sound, can be a debilitating condition and is the second highest complaint among veterans. In order to determine possible treatments and to investigate the underlying mechanisms of tinnitus, a reliable animal model is required that can clearly dissociate the presence of tinnitus and hearing loss. Previously, we have demonstrated that a two-alternative forced choice behavioral paradigm can detect salicylate-induced tinnitus in rats. Here, we present a modified version of this paradigm which is suitable for the detection of noise-induced tinnitus in rats.

Methods

Rats (N=4) were trained in a two-alternative forced choice paradigm to activate a left feeder in the presence of a steady-state narrowband noise (NBN: 1/8 of an octave band, center frequencies randomized across trials: 4, 5, 6, 8, or 11kHz at 70 dB SPL), and to activate a right feeder in the presence of an amplitude-modulated noise (AM: broad-band noise, 100% modulation depth, 5kHz at 70dB) or no sound (Quiet). Rats were trained to a >85% hit rate criteria for each stimulus. They were tested after (1) an acute exposure (continuous 16 kHz NBN at 110 dB while awake for 30 or 40 minutes) and then (2) long-term noise exposure (continuous 16-20 kHz NBN at 84 dB for 7 days, then at 90 dB SPL for 5 days). The presence of noise-induced tinnitus was judged by a significant shift in responses on Quiet trials from the right feeder (associated with Quiet) to left feeder (associated with a steady NBN). Such a shift would indicate that the rat was experiencing a steady phantom sound on Quiet trials.

Results

Compared to sham, rats showed evidence of tinnitus following most acute and all long-term noise exposures by switching their response behavior only during quiet trials from the feeder associated with Quiet to the feeder associated with a steady-state NBN. This implies that rats perceived a steady-state sound after noise exposure. The long-term, lower inten-

sity exposures seemed to produce greater and longer evidence of tinnitus than acute exposures.

Conclusion

Since there was only a noise-induced change in performance on Quiet trials, but not AM and NBN trials, the data suggest that this paradigm is testing for the presence of tinnitus and is not confounded by hearing loss. These results demonstrate that this is a reliable method for assessing acute tinnitus in rats.

PS - 816

Tinnitus-Related Changes in GABAA Receptor Inhibition in Auditory Thalamus of Rats.

Evgeny Sametsky; Jeremy Turner; Deb Larsen; Lynne

Ling; Donald Caspary

SIU School of Medicine

Background

Inhibition plays a critical role in shaping responses in auditory thalamus or medial geniculate body (MGB). Tinnitus-related inhibitory dysfunction has not been examined in MGB. Two competing hypotheses exist regarding a putative role for GABAergic inhibition in pathogenesis of tinnitus in MGB. Increased spontaneous activity and abnormal neuronal hyperactivity has been observed in dorsal cochlear nucleus (DCN) and inferior colliculus (IC) in sound exposure animal models of tinnitus suggesting a **down-regulation of inhibitory neurotransmission** within central auditory system circuits. A competing thalamocortical dysrhythmia hypothesis (Llinas and Steriade, 2006) suggests that tinnitus pathology is linked to **elevated tonic inhibition** in a subset of thalamocortical neurons resulting in their abnormal bursting activity.

Methods

To test these competing hypotheses, we examined GABAergic inhibition in MGB of three groups of rats: control (C) (n=11), sound exposed with behavioral evidence of tinnitus (T) (n=14) and sound exposed animals showing no behavioral evidence of tinnitus (NT) (n=4). Sound-exposure and tinnitus screening approximated the methods described by Turner et al., 2006. Using *in vitro* whole-cell recordings of MGB thalamocortical neurons, extrasynaptic tonic GABA_A receptor (GABA_AR) currents were evoked by bath application of the subunit selective agonist, gaboxadol (0.1-10 μ M), in the presence of glutamatergic blockers.

Results

Two months following tinnitus-inducing sound exposure, significant ($p = 0.02$) increases in tonic GABA_AR currents were observed in MGB neurons from tinnitus compared to control animals contralateral to the exposure (maximal current density at 10 μ M (C: 1.83 ± 0.11 pC, n = 32 cells; T: 2.18 ± 0.08 pC, n = 43 cells; NT: 2.09 ± 0.10 pC, n = 11 cells). Larger tonic currents were recorded from T neurons in both dorsal and ventral MGB subdivisions. NT neurons were not statistically different from C or T neurons. Pharmacokinetics of evoked extrasynaptic GABA_AR currents were not different between experimental groups, suggesting that GABA_AR extrasynaptic subunit composition was not altered by tinnitus pathology. Patch-clamp findings were supported by *in situ* hybridization

studies showing increased message levels for subunits (α_4 and δ) associated with extrasynaptic GABA_AR tonic inhibition. Analysis of spontaneous inhibitory postsynaptic potentials (sIPSPs) revealed no differences in measured parameters implying that synaptic GABA transmission in MGB is not affected by tinnitus-related pathology.

Conclusion

Collectively these data show no net down-regulation of inhibitory GABA transmission in MGB associated with tinnitus. The data rather suggest the tonic GABA_AR current component is elevated in the tinnitus group lending some support to the thalamocortical dysrhythmia model of tinnitus.

PS - 817

Effects of Furosemide on Central Hyperactivity and Tinnitus After Acoustic Trauma in Guinea Pig

Wilhelmina Mulders; Kristin Barry; Courtney McMahan; Donald Robertson

University of Western Australia

Background

Acoustic trauma can cause hearing loss and is also known to increase spontaneous activity (hyperactivity) in central auditory structures. Hyperactivity has been suggested to play a role in the generation of tinnitus. Using a guinea pig model we have previously demonstrated that for some time after trauma, central hyperactivity is due to hyperexcitability of central neurons and is, at that stage, still dependent on peripheral afferent drive. At later time-points the central hyperactivity becomes independent of primary afferent activity and is generated intrinsically. This suggests a possible therapeutic window for early-onset tinnitus using treatments that reduce primary afferent firing. Furosemide, a loop diuretic, reduces spontaneous firing of auditory afferents and may therefore be clinically relevant.

Methods

We investigated in our guinea pig model of acoustic trauma and hearing loss, the efficacy of an acute dose of furosemide in reducing spontaneous firing of auditory afferents, using the spectrum of neural noise (SNN) from round window recording, hyperactivity in inferior colliculus, using extracellular single neuron recordings, as well as tinnitus at early time-points after cochlear trauma. Tinnitus was assessed using gap prepulse inhibition of acoustic startle (GPIAS) and prepulse inhibition of acoustic startle (PPI). We also investigated the effects of chronic (7 days, once daily) administration of furosemide or saline on hyperactivity in inferior colliculus, measured 24 hrs after the last injection.

Results

Acute furosemide administration caused a strong decrease in SNN. Both acute and chronic administration of furosemide caused a marked statistically significant decrease in central hyperactivity compared to saline control injections. In animals for which GPIAS and PPI measurements suggested the presence of tinnitus (reduced GPIAS, unaltered PPI), GPIAS

reductions could be reversed with an acute injection with furosemide but not saline.

Conclusion

Our results suggest that furosemide reduced central hyperactivity as a result of decreased spontaneous firing of auditory afferents. Additionally, we have shown that acute furosemide suppresses behavioural signs of tinnitus in our animal model. These data support the notion that hyperactivity is involved in the generation of tinnitus and further suggest that there may be a therapeutic window some time after cochlear trauma for drug treatments that target peripheral spontaneous activity. Our results from chronic administration of furosemide suggest a long-term effect on hyperactivity, which may be important for clinical translation.

PS - 819

Impulse Noise Effects on ABR, Pre-Pulse Inhibition, Gap Detection, and Auditory Nerve Connections

Karin Halsey; David Dolan; Josef Miller; Susan Shore; Jennifer Eberle; Ariane Kanicki; Susan DeRemer; Diane Prieskorn; Richard Altschuler

University of Michigan

Background

Tinnitus due to noise over-exposure is a condition that affects a significant portion of the population, especially people exposed to damaging noise, impulse noise, or blast events.

Methods

N = 54 Sprague Dawley rats were unilaterally exposed to impulse noise designed to simulate small arms fire, and compared to matched sham-exposed animals (N=18). In life assessments included Auditory Brainstem Responses (ABRs), Pre-Pulse inhibition (PPI) and Gap inhibition (GI) of the acoustic startle reflex. After perfusion and fixation there was assessment for hair cell loss and loss of CTBP2 immunostaining, a marker for Inner Hair Cell (IHC) auditory nerve connections.

Results

The sham noise exposure group had no change in any of the in-life assessments. Impulse noise-exposed animals had variable final ABR shifts ranging from none to 65 dB, and many (but not all) showed changes in GI that could be interpreted as evidence of tinnitus. Care was taken to exclude data from any animals with an ABR loss in the unexposed ear, as correlations were found between unexposed ear ABR losses and GI performance. A correlation was found between reduced PPI performance and a noise-induced reduction in CTBP2 immunolabeled IHC - auditory nerve connections. Hair cell loss, ABR I/O and latency results will also be discussed.

Conclusion

Impulse noise resulted in physiological and morphological changes in rats. Reductions in CTBP2 staining had correlations to performance on physiological assessments, especially in PPI. Bilateral hearing loss should be avoided in GI experimental designs.

PS - 820**Bimodal Stimulus Timing Dependent Plasticity in Primary Auditory Cortex is Altered After Noise-Induced Tinnitus**Gregory Basura¹; Seth Koehler²; James Wiler¹; Susan Shore¹¹University of Michigan; ²Johns Hopkins University**Background**

Primary auditory cortex (A1) neurons demonstrate bimodal (auditory-somatosensory) integration that is stimulus-timing dependent, as demonstrated in dorsal cochlear nucleus (Koehler and Shore, PLoS One, 2013), with Hebbian and anti-Hebbian timing rules analogous to *in vitro* spike-timing dependent plasticity (STDP). After noise exposure, and tinnitus, there are changes in bimodal integration and plasticity in DCN. The rationale for the present study was to determine if tinnitus-associated changes in STDP principles like those found in DCN also exist in A1 after noise-induced tinnitus.

Methods

Four-shank, 32-channel silicon electrodes were placed in A1 of sham and noise-exposed guinea pigs with and without evidence of tinnitus as indicated by gap-induced pre-pulse inhibition of the acoustic startle. Stimulus-timing dependent plasticity was measured by comparing tone-evoked responses and spontaneous activity before, 5 and 15 minutes after bimodal (tone-spinal trigeminal nucleus; Sp5) stimulation with alternating pairing orders (tone-Sp5 or Sp5-tone) and intervals (40, 20, 10 and 0ms).

Results

Bimodal stimulation in sham controls and in noise-exposed animals without tinnitus induced suppression or facilitation of tone-evoked firing rates 5 min after pairing, and predominantly Hebbian-like timing rules 15 minutes after pairing. In contrast, noise-exposed animals with tinnitus showed Hebbian timing rules 5 min after pairing and predominantly anti-Hebbian-rules 15 min after pairing.

Conclusion

The present findings demonstrate that, like the DCN, A1 responses following bimodal stimulation reflect STDP. Moreover, noise-induced tinnitus can modify multisensory integration in A1 and influence temporal relationships of converging auditory and non-auditory sensory systems. This effect on sensory processing may improve the understanding of mechanisms driving neural changes in A1 and ultimately lead to treatments for tinnitus.

PS - 821**Therapeutic Effect of Sildenafil on Blast-Induced Tinnitus and Auditory Impairment**Houmeir Hojjat¹; Gulrez Mahmood²; Jinsheng Zhang²¹Wayne State University School of Medicine; ²Department of Otolaryngology-Head and Neck Surgery, Wayne State University School of Medicine**Background**

Blast induced auditory impairment and tinnitus, described as "ringing" in the ears, is a primary concern affecting 62%

of military service members following traumatic brain injury. Currently there is no definite treatment for tinnitus, leading to lifelong patient struggles with significant neurological, social, and physical sequelae of this disease. To search for treatment, we studied the therapeutic effects of sildenafil, a phosphodiesterase-5 inhibitor, on blast-induced tinnitus and hearing impairment. Sildenafil modulates cGMP and nitric oxide synthase enzymes, causing vasodilatation and potential benefit to noise-induced hearing loss.

Methods

In this study, 14 Sprague Dawley rats were exposed to three consecutive blast exposures at 22 psi and tested for tinnitus using a gap-detection acoustic startle reflex paradigm. Hearing thresholds and detectability were measured using auditory brainstem responses and prepulse inhibition, respectively. Blasted rats were either treated with sildenafil or tap water following exposure, while 8 age-matched sham-blast control rats were treated with sildenafil.

Results

Our results showed that while sildenafil did not prevent acute tinnitus onset, it significantly suppressed high-frequency tinnitus from 3 to 6 weeks post-blast and reduced hearing impairment during the first week post-blast. Complex results were observed in the startle force data, where sildenafil-treated rats displayed significantly reduced startle force, suggesting involvement of traumatic brain injury.

Conclusion

Taken together, our data indicate that sildenafil has a therapeutic effect on blast-induced tinnitus and hearing impairment in a time-dependent manner. For future experiments, higher sildenafil dosage prior to blast exposure and combination with other treatments should be investigated.

PS - 822**Sodium Salicylate Modulates Excitability of Dopaminergic Neurons Derived from Human IPS Cells**Xiping Zhan¹; Mingyao Ying²; Jonathan Sagal²; Werner Graf¹¹Howard University; ²Johns Hopkins University**Background**

Dopaminergic neurons have diverse targets in the brain providing a major projection to the nucleus accumbens, a structure in the ventral striatum implicated in tinnitus. Yet the roles of dopaminergic transmission in tinnitus generation or modulation are still elusive. Sulpiride, a D2 antagonist, blocks dopaminergic activity and has been shown to alleviate tinnitus, but use of dopamine or its agonist failed to improve the condition. Some dopamine reuptake inhibitors, such as Nortriptyline and Venlafaxine can suppress tinnitus, but others can not. These findings seem to be contradictory.

Methods

Following a modified protocol with proneural transcription factor Atoh1, dopaminergic neurons were generated from human inducible pluripotent stem cells (iPS). High-performance liquid chromatography (HPLC), immunohistochemistry and *in*

vitro patch-clamp neurophysiology were used to characterize the induced dopaminergic neurons (iDA). SS was used as a neuroactive reagent that putatively induces tinnitus in human and animals.

Results

iDA cells appeared to release dopamine as assayed by HPLC. They were positively labeled for Tyrosine Hydroxylase, a marker of dopaminergic neurons. In addition, they have identical physiological properties as neurons derived from human embryonic stem cells and primary neurons from the ventral tegmental area and the substantia nigra in animals. We found that a higher concentration (1.4 mM), but not a lower one (0.7 mM) of SS produced a complete and reversible block of spontaneous activity of iDA neurons. We further found that SS dampens the hyperpolarization sag in voltage and blocks the late events of hyperpolarization-dependent rebound spikes but not the early ones. Hyperpolarization dependent rebound spikes were not affected by ML218 (1 μ M), a Type-T current blocker. The rebound events can not be attenuated by apamin (0.2 μ M), but can be blocked by ML252 (5 μ M), a KCNQ2 potassium channel inhibitor.

Conclusion

Our findings suggest that KCNQ2 potassium is a potential target of SS which is the underlying mechanism of iDA neuronal spontaneous activity suppression. Since KCNQ2 receptors are distributed in the auditory brainstem, they may be affected directly by SS as well. Taken together, SS can generate tinnitus by the convergent effects on multiple neuronal targets, either in the auditory or non-auditory systems. The involvement of dopaminergic neurons in tinnitus also provides a clue to the complexity of tinnitus associated distress and potential avenues for treatment.

PS - 823

Effects of Unilateral Acoustic Trauma on Neural Activity in the Ipsilateral Inferior Colliculus of Unanesthetized Rats

Stefanie Kennon-McGill; Hongyu Zhang; Christopher Neal; Hinrich Staecker; Dianne Durham; Thomas Imig
University of Kansas Medical Center

Background

Previous studies have shown alterations in neural activity in auditory structures, such as the inferior colliculus (IC), following unilateral acoustic trauma, which is often used as a model for tinnitus. However, the majority of these studies have been performed solely in the IC contralateral to the damaged ear, which is thought to receive the majority of the input from the damaged cochlea. We previously discovered changes in both the ipsilateral and contralateral IC by using 2-deoxyglucose (2DG) as a metabolic measure of activity. It is possible that this increase in metabolic activity observed in the ipsilateral IC following acoustic trauma might correspond with a possible increase in single-unit activity in the ipsilateral IC of awake, freely moving rats.

Methods

Male Long Evans rats were unilaterally exposed to a 118 dB SPL, 16 kHz tone for 4 hours while under isoflurane anesthesia. The rats (n=9 damage, n=14 control) were implanted with a permanent recording chamber above the IC ipsilateral to the damaged ear. A minimum of 7-10 days following acoustic trauma, single-unit data were collected from the awake, freely moving rats. Spontaneous activity (SA), response to noise, and characteristic frequency (CF) were collected from each cell. Cells were categorized according to location in the IC and CF. These data were then compared with recordings from the contralateral IC.

Results

There is not an overall significant difference in SA between either the ipsilateral damaged group (13.9 spikes/sec, n=135 units) and the control group (14.15 spikes/sec, n=158 units), or the ipsilateral and contralateral group (11.62 spikes/sec, n=209 units). The units in the external nucleus of the ipsilateral damaged group display higher levels of activity (16.5 spikes/sec, n=32 units) compared to the contralateral group (10.73 spikes/sec, n=55 units), although the difference is not statistically significant. No other changes between the ipsilateral damaged group and control, or ipsilateral and contralateral groups were observed.

Conclusion

These data do not correspond with the 2DG studies, in which we saw a robust increase in activity in the ipsilateral IC, compared to both controls and the contralateral IC. The difference in outcome is most likely due to 2DG and single-unit recording measuring two different parameters of neural activity, which could reveal more about the mechanisms by which tinnitus is induced following acoustic trauma.

PS - 824

An Improved Approach to Measure Acoustic Startle Reflex in a Tinnitus Mouse Model

Calum Grimsley¹; Jesse Young¹; Jasmine Grimsley²; Ryan Longnecker¹; Brad Chadwell¹; Olga Galazyuk¹; Alexander Galazyuk¹

¹Northeast Ohio Medical University; ²NEOMED

Background

Developing an effective animal model has become critical to the advancement of tinnitus research. A popular technique for tinnitus assessment in laboratory animals utilizes prepulse inhibition of the acoustic startle reflex. The waveform of a startle response recorded from a pressure sensor contains multiple positive and negative peaks. Little is known as to which of these peaks should be measured to accurately assess the magnitude of a startle response. Furthermore, current measurements of the acoustic startle do not take the animals mass into account, which is critical for accurate startle assessment. A larger animal will show a larger force, for the same startle magnitude.

Research into animal kinetics utilizes high speed camera recordings combined with pressure sensor recordings to assess animal locomotion. We adopted this approach to address: 1) which component of a complex startle waveform

best represents the startle response, and 2) how to accurately calculate this peak magnitude.

Methods

Adult CBA/CaJ mice were placed upon a force plate in a small acoustic chamber (Kinder Scientific). A twenty milliseconds 120 dB SPL broadband noise was used to elicit an acoustic startle. The high speed camera (HiSpec Lite, Fastec Imaging Corp) recording identified the movements correlating with the various positive and negative peaks collected from the force plate. Force data were then analyzed using the 'flight-time method' (Linthorne, 2001). This method mathematically converts the 'force-time' data into 'height-time' data, resulting in a value of vertical displacement of the center of mass of the animal (i.e., the height jumped).

Results

Using high speed video we show that the first and largest negative peak of the force plate waveform correlates to the peak jump height of the animal during a startle. Mathematical transformation of force data into displacement using the 'flight time method' produced reliable evaluation of the startle response magnitude.

Conclusion

A major advantage of this proposed method is the incorporation of the mass of the animal into an empirical calculation of the 'height jumped' following the startle stimulus. This allows for repeatable and comparable analysis of the same animal over time, pre- and post-experimental condition, regardless of changes to the animal's mass. Additionally, our method extracts the most mechanical relevant information (i.e., height jumped) from the raw force data provided by the pressure sensor.

PS - 825

Sound-Triggered Suppression of Neuronal Firing in the Auditory Cortex: Implication to the Residual Inhibition of Tinnitus

Alexander Galazyuk; Calum Grimsley; Ryan Longenecker
Northeast Ohio Medical University

Background

Tinnitus can be suppressed briefly following the offset of an external sound. This phenomenon, termed "residual inhibition," has been known for almost four decades, although its underlying cellular mechanism remains unknown. In our previous work we have shown that the majority of neurons in the inferior colliculus (IC) exhibit long lasting suppression of spontaneous activity following the offset of an external sound. The time course of suppression corresponded to the time course of residual inhibition in tinnitus patients. Tinnitus patients often report an increased effect of tinnitus-matched pure tones on the duration of their residual inhibition. Our data show pure tones induce longer suppression than wideband noise. If the suppression is an underlying mechanism, the auditory cortex (AC) neurons should also exhibit suppression because residual inhibition of tinnitus is a perceptual phenomenon. To test this hypothesis, we studied sound evoked suppression in

auditory cortex neurons of awake mice. Animals with behavioral signs of tinnitus and control unexposed mice were used.

Methods

Experiments were conducted on adult CBA/CaJ mice. For tinnitus induction mice were exposed to a narrowband noise centered at 12.5 kHz presented at 116 dB SPL unilaterally for 1 hour under general anesthesia (Ketamine/Xylazine). Tinnitus was then assessed utilizing gap-induced prepulse inhibition of the acoustic startle reflex. Extracellular recordings were performed in auditory cortex contra- and/or ipsilateral to the exposed ear in awake restrained animals. Pure tones at neurons' characteristic frequency and/or wideband noise stimuli 30 sec duration were delivered in the free-field.

Results

We found that auditory cortex neurons in control mice exhibited sound-triggered suppression of their spontaneous firing. Similar to the IC, the duration of this suppression after sound offset in AC neurons roughly corresponded to the stimulus duration (about 30 s). AC neurons also showed longer suppression to tones at their characteristic frequency than to wideband noise stimuli. Unlike the IC, in addition to the suppression after stimulus offset, the majority of AC neurons also showed suppression during stimulus presentation.

Conclusion

Similar to the IC, AC neurons exhibit long lasting suppression of their spontaneous firing following sound offsets. The time course of this suppression corresponds to the time course of residual inhibition in tinnitus patients. These data further suggest that suppression may be a neural correlate of the residual inhibition of tinnitus in humans.

PS - 826

Reflex Modification Audiometry as a Tool to Assess Hearing in CBA/CaJ Mice

Ryan Longenecker; Fuad Alghamdi; Alexander Galazyuk
Northeast Ohio Medical University

Background

Traditional methods for measuring animal hearing performance can be invasive and time consuming. A behavioral test that does not require formal operant training would be useful to quickly measure an animal's hearing. In our previous work we have demonstrated that continuous narrowband noise suppresses startle responses in mice, to startle stimuli, embedded in that noise. Furthermore, this suppression was sound level and frequency dependent. The frequency-dependent suppression curve approximated the known behavioral audiogram. The goal of this study was to develop a reliable method for assessment of hearing performance in normal animals and possibly hearing deficits in the animals exposed to loud sounds.

Methods

Initial acoustic startle performance was assessed for each CBA/CaJ mouse by producing a startle input/output function. To effectively alter a startle with background noise, the startle value was set to 75% of the maximum startle response. Narrowband noise ranging in center frequency from 4 to 22

kHz (in one third octave steps) were presented at 10 to 80 dB SPL. For acoustic trauma induction, a group of mice were exposed to a narrowband noise centered at 12.5 kHz presented at 116 dB SPL unilaterally for 2 hour under general anesthesia (Ketamine/Xylazine).

Results

Prior to sound exposure, all mice showed thresholds similar to that of an audiogram for CBA/CaJ mice. Although there was some variance between mice, the greatest degree of startle masking was achieved by 12.5 and 16 kHz background noise. The startle reflex was masked the least by 4kHz and 22kHz background noise. Following sound exposure the input/output curve was altered, showing higher thresholds at 12.5 and 16kHz, reflecting damage at the frequency range of the exposure. Masking thresholds at this range increased significantly compared to the pre-exposure thresholds.

Conclusion

Reflex modification audiometry could be a useful tool for fast assessing animals' audiometry.

PS - 827

Induction of Enhanced Acoustic Startle Responses Following Intense Noise Exposure: Dependence on the Degree of Threshold Shift.

Christopher Yurosko; Rony Salloum; Lia Santiago; Sharon Sandridge; James Kaltenbach
Cleveland Clinic

Background

Several previous studies have reported that intense sound exposure results in decrements in the amplitude of the acoustic startle response (ASR). However, a recent study from our laboratory showed that intense sound exposure induces enhancements of the ASR, and this has been interpreted as evidence that the animals may have hyperacusis. We performed 4 rounds of experiments in succession to test the consistency of enhanced startle after noise exposure across experiments.

Methods

In each round, we compared startle amplitudes vs. startle stimulus levels in control animals with those obtained from animals that had previously been exposed to an intense tone (10 kHz tone 115 + 6 dB SPL) for 4 hours. Startle amplitudes were measured for startle stimulus levels ranging from 57 to 120 dB SPL. Such measures were obtained daily beginning 1 day post-exposure and continuing for the next 2-3 weeks. At the end of this period, auditory response thresholds were determined by measuring auditory brainstem responses (ABR) with tone pips varied from 4 to 16 kHz. The data from each experiment were analyzed separately to assess whether the direction and/or degree of startle amplitude change was consistent, and if not, whether the differences might be related to differences in the degree of threshold shift induced by the sound exposure.

Results

All sound exposed animals showed decreased ASR amplitudes within the first two-three days post-exposure. In-

terestingly, beginning on the third or 4th day post-exposure, the direction of change in the ASR amplitudes reversed in three of the 4 exposed animal groups. Startle amplitude increased above control levels, and the degree of the increase was in proportion to the degree of maximal threshold shift, which varied across groups between 36 and 62 dB. However, one of the 4 exposed animal groups showed no reversal on the 3rd or 4th day post-exposure, but remained decreased throughout the 3 weeks of startle testing. The latter group of animals showed the severest maximal threshold shift, which exceeded 75 dB. The results suggest that noise exposure induces hyperacusis-like enhancements of startle with moderate threshold shift (up to 62 dB), but severe threshold shift (75 dB or more) may result in a decrease in startle amplitude.

Conclusion

These findings could potentially explain why different investigators have reported seemingly opposite effects of noise exposure on acoustic startle responses, with some reporting noise-induced decrements and some reporting noise-induced enhancements of ASR.

PS - 828

Suppressive Effect of the M3-Selective Muscarinic Acetylcholine Receptor Agonist, Pilocarpine, on Noise Induced Hyperactivity in the Dorsal Cochlear Nucleus

Rony Salloum
Cleveland Clinic

Background

It is widely believed that tinnitus is caused by a state of neuronal hyperactivity in the central auditory system (Roberts et al., 2010; Kaltenbach et al., 2011). We previously showed that hyperactivity induced in the dorsal cochlear nucleus (DCN) by intense sound exposure can be suppressed by applying the acetylcholine receptor agonist, carbachol, to the surface of the DCN. However, because carbachol acts non-selectively on a wide range of cholinergic receptor subtypes, the subtypes mediating carbachol's suppressive effect on hyperactivity are unknown. Since M3 muscarinic receptors have been shown previously to modulate spontaneous activity in normal hearing animals (Koszeghy et al., 2012), we set out to determine whether an agonist of this receptor subtype, pilocarpine, would have a similar suppressive effect on hyperactivity as carbachol.

Methods

To test our hypothesis, we used two groups of adult Syrian hamsters, one of which was exposed to a 10 kHz tone at 115 dB for 4 hours, the other served as unexposed controls. Multiunit recordings from the DCN were performed 2 to 3 weeks post exposure or post-control treatment with the electrode placed in the fusiform cell layer at the tonotopic locus showing highest activity. Baseline recordings of spontaneous activity were performed for 8 minutes. Then, 200 μ M pilocarpine or control solution (aCSF) was applied to the DCN surface and measurements were continued for at least another 8 minutes. Changes in the mean level of spontaneous activity induced by each test solution were then calculated.

Results

Noise-exposed hamsters exhibited a baseline of spontaneous activity in the fusiform cell layer that was clearly elevated above the levels observed in controls, consistent with the induction of hyperactivity by the intense sound exposure. Application of 200 μ M pilocarpine to the DCN surface of exposed animals was effective in suppressing the induced hyperactivity by 40 to 70% below the predrug baseline. In contrast, aCSF alone had only minor effects on hyperactivity, changing it by \pm 20%. In some cases, we observed a partial recovery of activity following pilocarpine administration, although the recovery never reached the pre-drug baseline.

Conclusion

Noise-induced hyperactivity in the fusiform cell layer of the DCN can be effectively suppressed with the application of 200 μ M Pilocarpine to the DCN surface. These results suggest that M3 receptors may have potential to become important targets for drug therapy aimed at abolishing the abnormal activity underlying tinnitus.

PS - 829

Use of the Zebrafish for Testing Drugs to Treat Tinnitus

Catherine Pham¹; Meshell Bellah¹; Daniel Ledee¹; Calvin Wu¹; Thomas Lukas²; Ernest Moore¹

¹University of North Texas; ²Northwestern University

Background

The rising incidence of tinnitus in returning armed forces personnel from several Middle Eastern conflicts is a cause for grave concern. Coupled with a lack of effective pharmaceutical agents to prevent or treat tinnitus has led to a renewed sense of urgency. One approach that has been championed is the re-purposing of already approved FDA drugs that have been used to treat other medical conditions such as epilepsy or pain (Wu et al., 2011; Gopal et al., 2012). Developing drugs solely to treat tinnitus has been challenging to pharmaceutical companies due to a limited understanding of the underlying pathophysiology, problems creating models of the tinnitus-like condition *in vitro* and *in vivo*, the heterogeneity of tinnitus symptoms, as well as the paucity of effective clinical trials. Within the last decade or so, however, these challenges do not seem totally formidable due to the introduction of the zebrafish as a tractable model to evaluate drug regimens.

Methods

We employ in the zebrafish combined studies of (a) behavioral swimming activity, (b) auditory startle response, (c) auditory brain stem responses, (d) microelectrode arrays, and (e) forward genetic screens, in an attempt to better understand the underlying correlates of tinnitus.

Results

So far, we have profiled four classes of potential tinnitus drugs including anti-epileptics, antioxidants, calcium channel blockers, as well as potassium channel openers, and quantified their results. The behavioral and electrophysiologic assays provide a correlate of tinnitus, e.g., increased swimming activity, changes in membrane properties, or up-regulation in gene transcripts, and potential "tinnitus" drugs are used to

down-regulate the "aberrant" activity. In aggregate, the results indicate that KCNQ-type channel openers such as retigabine are the most effective at reducing tinnitus-like responses.

Conclusion

These studies have begun to address key underlying mechanisms that yield additional insight into the conundrum of tinnitus. Our conceptual framework encompassing possible target identification perhaps shows promise for the prevention and the treatment of the annoying manifestations of tinnitus.

PS - 830

Associations Between Tinnitus, Neuroticism, Depression and Anxiety in a Large UK Population Aged 40 to 69 Years

Abby McCormack¹; Mark Edmondson-Jones¹; Heather Fortnum¹; Piers Dawes²; Hugh Middleton³; Kevin Munro⁴; David Moore⁵

¹NIHR Nottingham Hearing Biomedical Research Unit;

²University of Manchester; ³The University of Nottingham;

⁴The University of Manchester; ⁵Cincinnati Children's Hospital Medical Center

Background

Previous research has suggested that a proportion of the population are severely affected by tinnitus. Clinical studies indicate increased risk for depression and anxiety among tinnitus patients. Furthermore, there is growing evidence that the experience of severity is closely related to personality factors such as neuroticism. Results from general population data are limited. The aim was to examine the association between tinnitus severity and a putative predisposing personality factor, neuroticism, and to further explore associations between tinnitus severity and symptoms of depression and anxiety, while controlling for neuroticism. Our hypothesis was that if neuroticism conveys vulnerability to psychological distress associated with symptoms of being unwell, then neuroticism would substantially mediate the association between tinnitus and anxiety/depression.

Methods

This research was conducted using the UK Biobank dataset (a cross-sectional design study of >500,000 people from across Britain aged between 40-69 years). Participants were recruited through National Health Service registers and the study aimed to be inclusive and as representative of the UK population as possible. A single assessment included subjective questions concerning hearing and tinnitus. Symptoms of depression and anxiety were examined, along with health-related quality of life. Neuroticism was self-rated on 13 questions from the Eysenck Personality Inventory (EPI). While controlling for demographic factors and hearing difficulty, the associations between depression and anxiety symptoms, neuroticism, and tinnitus were tested with regression analyses in a subset (N=172,621) of the population that answered the tinnitus questions.

Results

Neuroticism was significantly associated with current tinnitus (OR=2.11, 95% CI=2.0-2.2) and bothersome tinnitus

(OR=4.1, 95% CI=3.7-4.6), and neuroticism had a stronger effect on the perceived severity of tinnitus than did subjective hearing difficulty. The individual items: 'loneliness', 'mood swings', 'worrier/anxiousness' and 'miserableness', were the strongest predictors of bothersome tinnitus. After controlling for neuroticism, bothersome tinnitus was significantly associated with depression symptoms (OR=1.15, 95% CI=1.12-1.18) and anxiety symptoms (OR=1.05, 95% CI=1.02-1.07).

Conclusion

Clinicians treating tinnitus patients should consider treatment for anxiety and depression which then may reduce the severity of tinnitus. Likewise, clinicians treating people for anxiety and/or depression should bear in mind that tinnitus may be a contributing factor. Additionally, tinnitus patients with higher levels of neuroticism may be more likely to experience bothersome tinnitus, possibly as a reflection of greater sensitivity to intrusive experiences. Therefore, psychological interventions tailored to different personality types may be beneficial for tinnitus patients over the long-term.

PS - 831

Relationship Among Tinnitus Intensity Reduction and Improvement in the Patients' Quality of Life, Achieved Through Sound Stimulation During Sleep.

Daniel Drexler¹; Matías Lopez¹; Silvana Rodio¹; Manuela Gonzalez¹; Darío Geisinger¹; Marisa Pedemonte²

¹Centro Tinnitus Montevideo; ²Centro de Medicina del Sueño, Facultad de Medicina Claeh

Background

Different types of sound treatments had been developed to improve tinnitus patients' quality of life. In a previous pilot study by our group, a maintained intensity reduction (averaged 14 dB SPL) was achieved using a treatment protocol with customized sound stimulation during sleep (Pedemonte et al., International Tinnitus Journal, 16: 37-43, 2010). Psychological questionnaires are widely used in clinical trials to evaluate evolution. The aim of the present study was to compare the relationship between intensity reduction of tinnitus and the results of psychological tests.

Methods

Twelve patients with subjective idiopathic tinnitus, treated with sound stimulation during sleep, were studied. A customized sound that matches the tinnitus spectral and intensity characteristics was created for each patient. Taking into account that most of the tinnitus is complex sounds, specific software was designed with the aim of being able to match the patients' perception. This software was loaded on an iPad for the physicians' use, and another software capable of reproducing the created sounds was loaded into the patients' iPods. Customized ear buds with flat response in the range 0.125-16 kHz were created. Assessment of the results was performed considering tinnitus intensity decrease, and comparing this improvement with scores in three different psychological tests: Tinnitus Handicap Inventory (THI), Tinnitus Reaction Questionnaire (TRQ) and Tinnitus Functional Index (TFI). Also a visual analogic scale (VAS) for tinnitus annoyance was per-

formed. All the tests were done at the beginning, middle and end of a period of three months of daily stimulation.

Results

After three months of treatment, 11 out of 12 patients stopped being aware of the tinnitus in the daytime for long periods. In this stage, an overall intensity decrease average of 14.1 dB (statistically significant, $p < 0.001$ Wilcoxon test) was observed. This improvement was followed by statistically significant decrements of 78% for the TRQ, 65% for THI and 77% for the TFI. Also, all subscales of TFI showed score improvements. The VAS for tinnitus annoyance results presented a statistically significant improvement of 61% of the pre-treatment scores.

Conclusion

Those results demonstrate that a reduction in the intensity of 14.1 dB SPL (which implies a reduction of 62% of the pre-treatment perceived intensity) has a correlation in the observed psychological tests scores improvement. Customized sound treatment applied during sleep is beneficial both in the achievement of intensity reduction and in the improvement of psychological impact of tinnitus.

PS - 832

Changes on Electroencephalographic Waves During Sleep in Tinnitus Patients Treated With Sound Stimulation at Night

Marisa Pedemonte; Martín Testa

Centro de Medicina del Sueño. Facultad de Medicina CLAEH

Background

Auditory processing occurs during sleep (Velluti, 2008, The auditory system in sleep. Elsevier-Academic Press, Amsterdam). Based on this knowledge, we have applied a new strategy for the treatment of idiopathic subjective tinnitus: sound stimulation during sleep. This treatment provoked a maintained decrement in the tinnitus intensity (Pedemonte et al., 2010, The International Tinnitus Journal, 16: 37-43). However, we can recognize different stages of sleep (with spindles, N2; with slow waves, N3; and with Rapid Eyes Movements, REM) where several functions related to learning and memory have different relevance. In this work we attempted to determine the impact of sound in the different sleep stages.

Methods

Ten patients with idiopathic tinnitus, treated with sound stimulation mimicking tinnitus during sleep were studied. Polysomnographies were recorded during the night with electroencephalography from frontal and temporal electrodes. Patients started the night with the usual sound stimulation for the tinnitus treatment which was stopped after at least one pass through each of the sleep. Data processing was carried out fixing twenty temporal windows (1 sec duration each one) selected in each sleep stage; 10 of them during silence and the other 10 during the sound stimulation. The researchers analyzed the power spectra and the coherence in electroencephalographic waves recorded, comparing values during noiseless versus sound stimulation, exploring dif-

ferent electroencephalographic frequency ranges (delta: 0,5-3,5 cps; theta: 4-7,5 cps; alpha: 8-12 cps) in the same sleep stage. The wave coherence intra and inter-hemispheric data was analyzed with the results statistically validated (Student t test).

Results

Most patients showed changes in all sleep stages with nine out of ten patients showing some degrees of inter-hemisphere differences without relationship with the stimulation side. Sound stimulation increased power spectra of delta, theta and alpha frequencies; however, theta rhythm was the most changed. These changes happen in all sleep stages with a slight predominance in N2. Changes are greater in temporal than in frontal areas being independent from the stimulated side and brain dominance. The coherence analysis showed that both inter and intra-hemispheric coherences changed during sound stimulation; most of the time the percentage of coherence decreased in N2 and N3 increasing in REM sleep. Delta and theta rhythms were the most changed.

Conclusion

The results demonstrate that during sleep the auditory information enters and generates electrophysiological changes, therefore, we can assume that sound input is being processed. All stages of sleep seem involved in the processing.

PS - 833

Long-Latency Auditory Evoked Potentials in Unilateral Tinnitus Patients in Wakefulness Compared With Normal Subjects

Matías López-Paullier¹; Eduardo Medina-Ferret¹; Marisa Pedemonte²; Ricardo Velluti²

¹Clinicas Hospital; ²CLAEH

Background

Unilateral subjective tinnitus is a very frequent condition characterized by a phantom auditory perception in only one ear. Many levels of the auditory processing could participate in its generation introducing changes in the evoked responses. We have demonstrated (ARO 2012) differences in the auditory brainstem evoked potentials in unilateral tinnitus patients comparing pathological side (tinnitus) versus normal hearing side. Since tinnitus is a conscious perception, our aim was to explore higher auditory regions studying the long latency auditory potentials (LLAP, 500ms) in patients suffering unilateral tinnitus, comparing the result with LLAP in normal subjects.

Methods

Five patients with unilateral subjective idiopathic tinnitus and five normal controls without tinnitus were studied during wakefulness. LLAP were recorded with two different sound intensities -high and low- at 70 and 55 dB over the patient specific threshold respectively, during electroencephalographically (EEG) controlled wakefulness, exhibiting alpha rhythm. The LLAP was analyzed in their wave's latency and amplitude, and also the power spectra (Fast Fourier Transform, FFT) of every case. Statistical analyses were applied, comparing right and left responses in the same patient and with the normal controls ones.

Results

The LLAP did not show differences between both sides neither in latencies nor in amplitude in studied populations: control and unilateral tinnitus patients.

Two studied groups showed asymmetries between right and left sides in the power spectra at lower frequencies (4, 6, 8 and 10 Hz) stimulating with both low and high intensity. However, the relative distributions of power spectra were similar between the two sides -with high or low stimulating intensities- in both studied populations.

Conclusion

LLAP showed inconclusive changes in tinnitus patients compared to normal controls. The variability found in the power spectra of both populations would be determined by other influences that may not depend on the presence of tinnitus (changes in attention to stimuli, current EEG brain waves, brain dominance, etc.).

However, further research is needed to find new electrophysiological tools in order to objectify the presence of tinnitus, e.g., wavelets analysis.

PS - 834

Implementation of Auditory Late Latency Response Measurement System and Investigation of Gap Prepulse Inhibition of N1-P2 Amplitudes

Il-Yong Park¹; Bong Jik Kim¹; Myung-Whan Suh²; Jae Yun Jung¹; Seung-ha Lee¹; Phil-Sang Jung¹

¹Dankook University; ²Seoul National University

Background

Although an objective tinnitus detection method for animals, the gap prepulse inhibition of acoustic startling (GPIAS), was reported, the method for human has not been established. In our study, we have implemented the auditory late latency response (ALLR) measurement system which can apply the gap prepulse paradigm to human. Based on the system, we investigated the inhibition of N1-P2 amplitude of the measured auditory late latency responses. The aims of this study are to show if the gap prepulse prior to main pulse stimulation can inhibit the N1-P2 amplitude like GPIAS and the implemented system can detect the gap prepulse inhibition (gPPI) of N1-P2 in normal subjects. Ultimately, we try to demonstrate the possibility of the objective tinnitus detection by showing the differences of the gPPI of N1-P2 between tinnitus patients and normal controls.

Methods

Our implemented ALLR measurement system is composed of a wireless EEG acquisition headset, a signal DAQ, an insert earphone, a sound amplifier, and our developed LabVIEW GUI program for creating sound stimulus and analyzing the measured ALLRs. At first, for verifying the performance of the implemented system to detect the gPPI, N1-P2 amplitudes evoked by gap prepulse paradigm stimuli were measured for 8 persons with normal hearing level. Then, 15 tinnitus patients and 15 normal control subjects have been recruited for the comparative measurement using our implemented sys-

tem. Patients with tinnitus being matched with 4 kHz or 8 kHz on psychoacoustic tinnitus test have been recruited for identifying the effect on gPPI of tinnitus.

Results

The gap prepulse inhibitions were observed in all of the 8 normal control subjects' measured ALLRs and the value of gPPI was $43 \pm 8.7\%$ in case of the background sound level of 40 dB SPL. And the compared gPPI results between tinnitus patients and normal subjects are presenting on the poster after completing our clinical trial by the use of our implemented ALLR measurement system.

Conclusion

The results show that the gap prepulse can inhibit the N1-P2 amplitude evoked by the main pulse stimulus and our implemented system can detect the gPPI. The comparison of gPPIs between tinnitus patients and normal controls using our implemented system shows if the gPPI of N1-P2 can be used as an important index for the objective tinnitus detection.

PS - 835

Increased Contralateral Suppression of DPOAEs in Humans With Chronic Tinnitus and Hyperacusis Suggests Hyperactivity of the Medial Olivocochlear Pathway

Jennifer Melcher; Inge Knudson; Christopher Shera
Massachusetts Eye and Ear Infirmary

Background

Studies examining effects of contralateral noise on otoacoustic emissions in tinnitus are numerous, but spotty in their incorporation of crucial controls and conflicting in their results. Some studies report less noise-induced OAE suppression than normal while others report no difference between tinnitus and control subjects. Here, we present a stringently controlled study comparing effects of contralateral noise on DPOAEs in people with tinnitus and without. In contrast to most previous OAE/tinnitus studies, diminished tolerance of sound on the basis of level (hyperacusis) was taken into account.

Methods

40 ears in 23 men (30-54 yrs) with clinically normal or near-normal audiograms underwent DPOAE measurement in the presence and in the absence of broadband noise to the contralateral ear ($L1=55$; $L2=40$ dB SPL; $f1/f2=1.2$; $f2=1-5.6$ kHz; 60 dB SPL noise; ~ 28 f2 points per octave). Multiple noise/no noise measurements were made for each ear. Separate measurements of ear canal pressure during noise and no noise demonstrated that activation of middle ear muscles was not a factor in the results. Loudness discomfort level and a three-item questionnaire were used to classify ears as hyperacusis or not and thus form four groups: tinnitus/hyperacusis (TH; 13 ears; mean age: 41), tinnitus only (T; 7; 47), hyperacusis only (H; 10; 43), no tinnitus/no hyperacusis (nTnH; 10; 46). Mean behavioral threshold from 0.125-16 kHz for DPOAE-recorded ears was matched across groups, as was threshold for the noise-stimulated, contralateral ears. Mean DPOAE magnitude was also matched. Slight differences in

age between groups were regressed out. Noise-induced effects were quantified as the difference in DPOAE magnitude averaged over half-octave f2 bands.

Results

All groups showed, on average, suppression of DPOAE magnitude by contralateral noise, but TH, T and H showed slightly greater suppression. Because of this similarity, TH, T and H were combined and compared with nTnH in a two-way ANOVA (group x f2 band). There was a significant effect of group ($p = 0.03$) and no interaction (consistent with greater suppression in TH/T/H across f2 bands). The effect of group for 1-1.4 kHz remained significant after correction for multiple comparisons ($p = 0.03$).

Conclusion

These results suggest that the medial olivocochlear pathway mediating contralateral suppression can be hyperactive in those with tinnitus and/or hyperacusis. The results provide further evidence for hyperactive function of the auditory brainstem of humans with tinnitus and/or hyperacusis.

PS - 836

Acoustic Startle Response in Humans With Tinnitus and Hyperacusis

Inge Knudson; Jennifer Melcher
Massachusetts Eye and Ear Infirmary

Background

It has been hypothesized that elevated acoustic startle response (ASR) in animal models is a marker for hyperacusis (i.e., diminished tolerance of sound on the basis of level). The present study begins to test this hypothesis by comparing measurements of ASR amplitude and behavioral measures of hyperacusis in the same human subjects.

Methods

Subjects were 22 men (34 - 61 yrs.) with clinically normal or near-normal hearing who were not taking medications known to suppress ASR. Based on loudness discomfort level (LDL) and responses to a three-item questionnaire, subjects were classified as hyperacusis or not using previous criteria (Gu et al. *J Neurophysiol.* 104: 3361-70, 2010). They were further divided into four groups: tinnitus/hyperacusis (8 subjs.), tinnitus only (5), hyperacusis only (3), no tinnitus/no hyperacusis (6). Audiometric thresholds at half-octave intervals 0.125-8 kHz did not differ significantly between the four groups ($p > 0.05$). Electromyographic (EMG) activity was recorded from electrodes near the eye during presentation of progressively more intense broadband noise bursts (75 - 110 dBA in 5 dB steps; burst duration: 40 ms; time between burst presentations: 11 - 19 s). ASR magnitude was quantified as the root-mean-squared (RMS) EMG over a post-stimulus interval (20 - 100 ms after stimulus onset) minus the RMS pre-stimulus.

Results

ASR magnitude increased with increasing intensity of the ASR stimulus in all groups. The increase was most pronounced in the two groups with tinnitus. A two-way ANOVA (tinnitus x hyperacusis) showed a significant effect of tinnitus, at 100 and 105 dBA ($p = 0.02, 0.007$), but not hyperacusis

(and no interaction). Scores on an inventory of anxiety did not differ systematically between groups, so it is unlikely that anxiety, a factor known to influence ASR, accounts for the intergroup differences. ASR showed no correlation with LDL.

Conclusion

These preliminary data add to growing evidence – from fMRI and auditory brainstem potentials - for ubiquitous hyperactivity in the lower auditory system of humans with tinnitus. They also suggest that elevated ASR may not be a reliable marker for hyperacusis.

PS - 837

Atlas-Based Single Subject Functional MRI Study of Tinnitus

J. Tilak Ratnanather; Xiaoying Tang; Angela F. Koenig; Patpong Jiradejvong; Andreia V. Faria; Charles J. Limb
Johns Hopkins University

Background

Neuroimaging studies of tinnitus in humans have generally used voxel based morphometry methods but with conflicting results. An alternative is based on pre-defined regions of interest that carry both spatial and anatomical meaning (atlas-based analysis – ABA). These structures are defined in a common template and automatically warped to the subject space, allowing for whole brain 3D segmentation. This approach is illustrated by a single subject study of tinnitus in which the functional activity was measured in response to two different stimuli: the first in response to pitched-matched frequency of the subject's tinnitus and the second to jaw manipulation that suppresses tinnitus. Anatomical connectivity of significantly activated regions is indirectly measured by ABA with diffusion tensor images (DTI).

Methods

For pure tone stimulus (EXP1), an acquisition cycle consisted of three phases of pitch-matched frequency (S1), set pure tone (S2) and baseline and was repeated 10 times. Stimulus at 55db SPL was delivered to the left ear. For jaw modulation (EXP2), the cycle consisted of jaw manipulation (S1), mouth opening (S2) and baseline. DTI and fMRI volumes were co-registered to the structural MPRAGE scan. Deconvolution analysis yielded beta coefficients used in linear regression comparing S1 with S2 in EXP1 and EXP2 separately and S1 in EXP1 with S2 in EXP2. Activation was defined according to t-statistics thresholded at 2.012 ($p < .05$) with cluster sizes of at least 200 and 50 voxels for EXP1 and EXP2 to correct for multiple comparisons ($p < .01$). DiffeoMap was used to parcellate the scans in 156 regions.

Results

In EXP1, cortical activation was observed in right superior temporal gyrus, right inferior temporal gyrus, left inferior orbital gyrus, left fusiform in S1 but not in S2; in contrast left middle temporal gyrus and right supramarginal gyrus were activated in S2 but not S1. In EXP2, right and left superior orbital gyrus were activated in S1 but not in S2 while the right angular gyrus was activated in S2 but not S1. Mean diffusivity of white matter areas subjacent to activated structures in EXP1 tended to be lower than that averaged from 10 controls.

Conclusion

Parcellation maps may help to identify anatomical and functional connectivity in regions activated or suppressed in functional tasks in the same framework. Results suggest that there are changes in neural activity during tinnitus suppression which suggests additional analyses.

PS - 838

Influence of Tinnitus on Auditory Spectral and Temporal Resolution, and Speech Perception Ability in Tinnitus Patients

Hyun Joon Shim¹; Hyun Woo Kang²; Yong-Hwi An²; Jong Ho Won³

¹*Eulji Medical Center, Eulji University School of Medicine;*

²*Department of Otorhinolaryngology, Eulji Medical Center, Eulji University School of Medicine, Seoul, KOREA;*

³*Department of Audiology and Speech Pathology, University of Tennessee Health Science Center, Knoxville, TN 37996, USA*

Background

The aims of this study were to investigate 1) the influence of tinnitus upon the auditory spectral and temporal resolution and 2) the effect of tinnitus on speech perception ability in noise.

Methods

To exclude the effect of decreased hearing threshold, unilateral idiopathic tinnitus patients with symmetric hearing thresholds were enrolled in this study. Subjects were 13 patients who have symmetric hearing loss > 20 dB HL and a binaural difference < 10 dB at 0.25, 0.5, 1, 2, 3, 4, and 8 kHz, or who have normal hearing thresholds and a binaural difference < 10 dB at 0.25, 0.5, 1, 2, 3, 4, and 8 kHz, and threshold discrepancies < 15 dB at 9, 11.2, 12.5, 14, 16, 18 and 20 kHz. Thirteen normal hearing subjects without tinnitus were enrolled as a control group. Four different psychoacoustic measurements were performed: 1) spectral-ripple discrimination, 2) temporal modulation detection, 3) Schroeder-phase discrimination, and 4) word recognition in noise.

Results

There were no significant differences in spectral-ripple thresholds, temporal modulation detection thresholds, and Schroeder-phase discrimination scores between affected sides and non-affected sides of unilateral tinnitus patients. For the word in noise test, affected sides showed significantly worse performance compared to non-affected sides ($p < 0.05$).

Conclusion

We could not find any evidence that the tinnitus-affected ears show worse spectral and temporal processing compared to non-tinnitus ears in unilateral tinnitus patients. The spectral ripple discrimination data suggests that the tinnitus-affected ears may not have broader auditory filters compared to non-affected ears with the same hearing thresholds. However, the difference in speech perception ability in noise suggests that tinnitus might have a masking effect when subjects try to understand target speech. These results imply that the occurrence of tinnitus does not depend upon the degree of

cochlear damage, but upon the change of central auditory pathway by deafferentation.

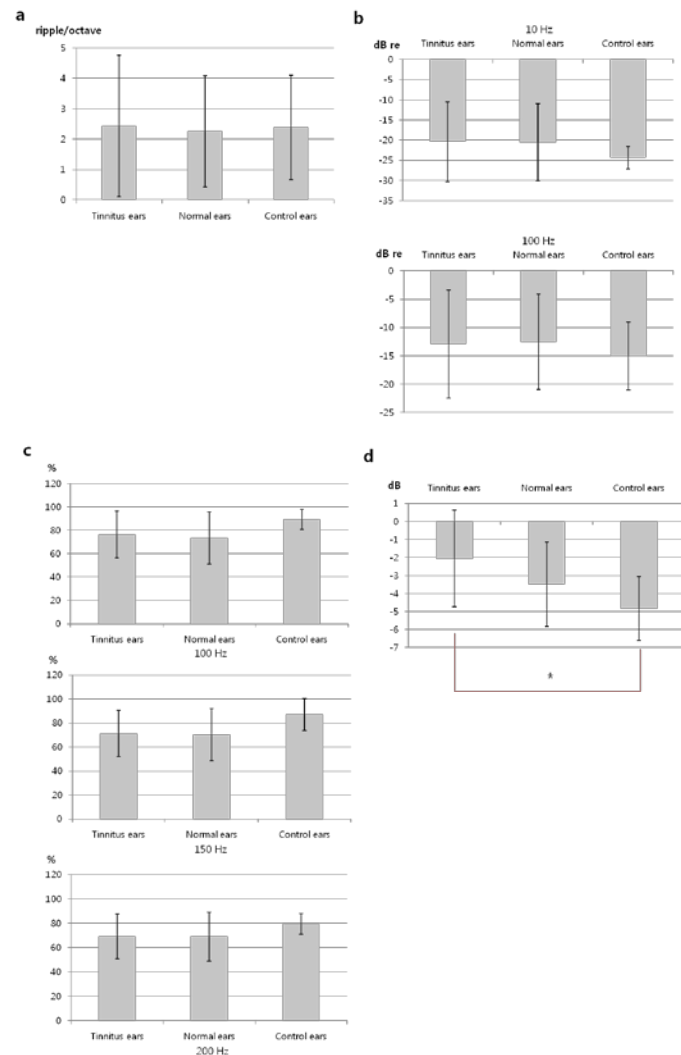


Figure 1. Comparisons of psychoacoustic results among tinnitus ears, normal ears of tinnitus patients and control ears

There are no significant difference among 3 groups in Spectral-ripple thresholds (a), temporal modulation detection thresholds (b) and Schroeder-phase discrimination scores. Only signal-to-noise ratio (d) is significant different between tinnitus ears and control ears.

* <0.05

PS - 839

A Cueing Experiment in Tinnitus Patients to Assess Auditory Attention

Gijsbert Van Zanten¹; Anne-Marie Keuning¹; Inge Wegner¹; Carlijn Hoekstra¹; Tobias Borra²; **Huib Versnel¹**

¹University Medical Center Utrecht; ²Utrecht University

Background

Attention is thought to play a prominent role in tinnitus. Attention towards tinnitus enhances its severity. A measure of auditory attention is provided by a probe-signal method, in which attention is drawn by a cue frequency. In norma-hear-

ing subjects, detection of a tone in a background of noise is enhanced when the tone has the attended frequency while detection of other tones is decreased. In the current study we examine whether this cueing experiment can be applied in tinnitus patients in order to assess their attention to a cue frequency and also to their tinnitus frequency. If indeed this is feasible, the question is whether a cue at an appropriate distance from the tinnitus frequency can reduce the attention towards the tinnitus.

Methods

Experiments were performed in normal-hearing controls without tinnitus and in tinnitus patients who could match their tinnitus to a frequency (between 3 and 9 kHz). Tones were presented in continuous broad-band white noise in one of two intervals. Detection was measured using a two-alternative forced choice paradigm. In a baseline experiment, signal-to-noise ratios were assessed in which a tone was detected with 80% correct scores. Three experiments were then performed on separate days. First, without an external cue tone, detection was measured for probe tones below and around the tinnitus frequency; in this case the tinnitus provides an internal cue. Second, a cue of 1 kHz (well below tinnitus frequency) was presented 1.25 s before the two detection intervals, and probe tones were varied around the cue frequency. The third experiment was as the first, but with an added cue tone about half an octave below the tinnitus frequency.

Results

A minority of tinnitus patients demonstrated enhanced attention for a cue of 1 kHz. Only a few patients showed a clear attention peak at their tinnitus frequency and/or at one octave below. In those cases this peak was not reduced by an external cue. The patients indicated on a visual analog scale that the tinnitus severity did not change in the course of the experiments.

Conclusion

Tinnitus patients can show normal auditory attention in the low-frequency region well below their tinnitus frequency. However, attention to tinnitus is not convincingly demonstrated using the cueing experiment. Therefore, we conclude that this method is not appropriate for clinical use to quantify attention to tinnitus.

PS - 840

Acoustic Analysis of the Sounds of Objective Tinnitus

Shinjiro Fukuda¹; Takenori Miyashita²; Toshihiro Mori³; Ryuhei Inamoto²; Hiroshi Hoshikawa²; Nozomu Mori²

¹Faculty of Medicine, Kagawa University; ²Department of Otolaryngology, Faculty of Medicine, Kagawa University;

³Department of Otolaryngology, Takamatsu Red Cross Hospital

Background

The aim of this study is to record and analyze the sound of objective tinnitus acoustically. Objective tinnitus can be perceived as an actual sound emanating from the patient's ears. Objective tinnitus can arise from muscle spasms, blood flow, and respiratory problems (Guen-Ho Lee et al., 2012). It is

important to analyze the distinctive sound to diagnose it as objective tinnitus. The sounds of objective tinnitus are different according to the site of genesis (Klockhoff I et al., 1971; Watanabe I et al., 1974; East CA et al., 1987). We recorded and analyzed the sounds of objective tinnitus.

Methods

The subjects were three patients complaining of tinnitus. Two patients perceived the tinnitus only during eyelid blinking, which was audible with otoscope and synchronized with the motion of eardrum. Stapedius reflex test was performed to identify the pattern of the static compliance changes during eyelid blinking. Objective tinnitus was recorded with commercial stereo microphone (RP-VC201 : Panasonic, Japan) and commercial dictaphone (Voice-Trek V22 : OLYMPAS, Japan). Acoustic analysis of the recorded objective tinnitus was performed with the sound analyzer (MDVP Model 5105 :KayPENTAX, USA)and free software (SoundEngine Free).

Results

The sound of tinnitus in two patients contained a wide-frequency band, whereas the sound of tinnitus in another one contained high frequency band with the peaks of 2kHz and 6kHz. The spike response around 1 Hz was obtained by stapedius reflex test in the former two patients, whereas the change in the small baseline of the amplitude was observed in the latter patient.

Conclusion

The results of sound analysis and stapedius reflex test demonstrated that the frequency distribution was different according to the site of genesis. The spike response around 1 Hz in stapedius reflex test suggests that the sound with a wide-frequency band may be caused by muscular contraction of the stapedius or tensor tympani. The change in the small baseline of the amplitude in stapedius reflex test suggests that the sound with high frequency band may be caused by palatal muscle. Recording objective tinnitus and its acoustical analysis are useful to diagnose the genesis site of tinnitus.

PS - 841

Middle Ear Myoclonus Cured by Selective Tenotomy of the Tensor Tympani: Strategies for Targeted Intervention for Middle Ear Muscles

Hiroshi Hidaka¹; Youhei Honkura²; Jun Ota³; Shigeki Gorai³; Tetsuaki Kawase²; Toshimitsu Kobayashi²

¹Tohoku University Graduate School of Medicine;

²Department of Otolaryngology-Head and Neck Surgery, Tohoku University Graduate School of Medicine;

³Department of Otolaryngology, Iwaki Kyoritsu General Hospital, Iwaki, Fukushima, Japan

Background

Myoclonus is a sudden, involuntary jerking of a muscle or group of muscles. Middle ear myoclonus is a rare disorder produced by repetitive contractions of the middle ear muscles. Bhiarmco et al. (2007) recently conducted a systematic review of management strategies for middle ear myoclonus, and stated that differentiating between the diagnoses of sta-

pedial myoclonus and tensor tympani (TT) myoclonus has not been described in detail in the literature, and definitive, objective methods of separating one from the other are currently lacking. Other than the present lack of consensus regarding treatment, no previous studies showed objective changes in outcome by assessing responses to intervention before and after treatment.

We firstly describe a case of middle ear myoclonus that was successfully cured by selective transection of the tensor tympani (TT) without sectioning the stapedius tendon (ST), and then review previously reported cases, elucidating precipitating factors for interventions targeting middle ear muscles.

Methods

In addition to our case, 23 cases were identified by the previous systematic review published in 2012 regarding middle ear myoclonus in which surgical interventions were conducted. Outcomes for selective tenotomy of TT or ST were analyzed focusing on the following six preoperative factors: 1) history of facial palsy; 2) provoking factors for tinnitus; 3) auscultation of the ear; 4) movement of the ear drum; 5) complication with palatal myoclonus; and 6) confirmation of myoclonus during surgery.

Results

Factors related to history of facial palsy and provoking factors for tinnitus represented significant factors for selective tenotomy of ST ($p<0.05$ and $p<0.01$, respectively). Furthermore, no auscultation of the ear was significant for selective tenotomy ($p<0.01$), specifically for ST. Confirmation of muscle contraction during surgery contributed significantly ($p<0.01$) to targeted intervention, but selective tenotomy of TT was successfully performed in three cases without such confirmation by confirming variations in compliance with tympanometry.

Conclusion

Assessment of the history of facial palsy, provoking factor of tinnitus, auscultation of the ear, and confirmation of myoclonus during surgery appear helpful in predicting which middle ear muscle is undergoing myoclonus. Furthermore, long-time-based tympanometry offers objective information for planning targeted intervention for middle ear muscles and clarifying clinical outcomes.

PS - 842

Changes of Tinnitus in Sudden Sensorineural Hearing Loss: Relationship Between Tinnitus Pitch and Audiometric Shape

Hong Ju Park¹; Tae Su Kim²; Kyoung Ho Park³; Jong Woo Chung¹

¹Asan Medical Center; ²Kangwon National University; ³the Catholic University of Korea

Background

Different mechanisms, such as lateral inhibition and homeostatic plasticity, are proposed to be involved in tinnitus generation. The aims of this study were to evaluate the changes of the acute and 1-month follow-up tinnitus pitch in patients with idiopathic sudden sensorineural hearing loss (SSNHL) and to explore the mechanisms of tinnitus generation.

Methods

Thirty-six patients with SSNHL with new-onset tinnitus who underwent audiological tests, including pure-tone audiometry and pitch-matching and loudness balance tests, at both initial and follow-up examinations were included. The relationship between tinnitus pitch and the maximum hearing loss or edge frequency was evaluated.

Results

The initial mean tinnitus pitch (2.9 kHz), which was close to the initial edge frequency (2.7 kHz), increased to a significantly higher frequency (4.6 kHz) at the 1-month follow-up, which was close to the frequency of maximum hearing loss (5.6 kHz). There were no significant differences in the frequency of maximum hearing loss, edge frequency, and loudness of tinnitus between initial and follow-up examinations. The tinnitus pitch had a more significant correlation with the edge frequency ($r=0.46$, $p=0.005$) than the frequency of maximum hearing loss ($r=0.33$, $p=0.047$) at initial examination; however, at the 1-month follow-up, the tinnitus pitch showed a significant correlation only with the frequency of maximum hearing loss ($r=0.52$, $p=0.001$), not the edge frequency.

Conclusion

Our findings suggest that there may be diverse mechanisms by which tinnitus can occur in patients with SSNHL. The change in the tinnitus pitch from the edge frequency at initial examination towards the frequency of maximum hearing loss at follow-up suggests that tinnitus is generated mostly by reduced lateral inhibition at the acute stage and that a homeostatic mechanism plays a major role in tinnitus generation at the chronic stage.

PS - 843

Alterations of the Limbic System Associated With Tinnitus May Maintain Rapid Reaction Time to Affective Stimuli.

Jake Carpenter-Thompson; Kwaku Akrofi; Sara Schmidt; Fatima Husain

University of Illinois Urbana-Champaign

Background

Tinnitus, also known as “ringing in the ears”, occurs in 10-15% of the population. The subjective form is characterized by the perception of an internal noise in the absence of an external sound source. Tinnitus may result from neuroplasticity associated with alterations in central auditory structures and associated brain regions. In recent years, the limbic system has been implicated in the development of intrusive tinnitus; however, the neural bases of tinnitus remain unknown. Therefore, we investigated the effect of tinnitus on the emotional processing system in middle-aged adults.

Methods

Alterations of the limbic system were investigated using functional magnetic resonance imaging and stimuli from the International Affective Digital Sounds database. There were three groups of participants: bilateral hearing loss with tinnitus (TIN), age- and gender-matched controls with bilateral

hearing loss without tinnitus (HL) and matched normal hearing controls without tinnitus (NH). Subjects rated sounds as pleasant (P), unpleasant (U), or neutral (N) in the scanner.

Results

Elevated response was obtained in bilateral parahippocampus and right insula for the TIN>NH ($P>N$) comparison. Similarly, increased left parahippocampus response was observed for the TIN>HL ($P>N$) comparison. A region-of-interest analysis detected elevated right amygdalar response in the NH control group for the $P>N$ and $U>N$ contrasts, but did not detect an elevated amygdalar response in the TIN or HL group for the same comparisons. Faster reaction time was observed for affective sounds relative to neutral sounds in the TIN and NH groups, but not in the HL group.

Conclusion

The fMRI results indicate the emotional processing system in tinnitus may be re-routed to avoid the amygdala, and instead rely on the parahippocampus and insula during affective sound processing. The behavioral results demonstrate that these changes may preserve the speed advantage for the processing of affective stimuli despite hearing loss. Our results build on past tinnitus research by including a hearing loss group to better parse out the effects of tinnitus from hearing loss on emotional processing. The finding of the present study should be accounted for in current and future management strategies.

PS - 844

Multiple Electro-Stimulation Treatments to the Promontory for Tinnitus

Ronen Perez¹; Chanan Shaul¹; Michael Vardi²; Nidal Muhanna¹; Paul Kileny³; Jean-Yves Sichel¹

¹Shaare Zedek Medical Center; ²ESimME; ³University of Michigan Health System

Background

First reports of suppressing tinnitus using electro-stimulation go back as early as 1801. Increased interest in this treatment modality has been seen in the past decades with the development of cochlear implants which have been shown to relieve tinnitus in a high percentage of implanted patients. Recent clinical trials demonstrated the beneficial effect in some patients of applying electro-stimulation at different peripheral sites, from the tympanic membrane to the cochlear nerve. The objective of the current study was to assess the safety and efficacy of multiple sessions of electro-stimulation by a trans-tympanic needle electrode on the promontory for tinnitus relief.

Methods

Ten patients (8 males, 2 females), mean age 50.1 ± 12 years (range 34-67) with severe unilateral tinnitus completed all stages of the study. Patients with tinnitus duration between 6 months to 3 years were included. The patients underwent three consecutive, alternate day, 30 minute sessions of bi-phasic charge balanced electro-stimulation pulses to the promontory near the round window. The stimulation was delivered by a trans-tympanic needle electrode. The main outcome measures included: 1) Tinnitus loudness reported by

visual analog scale (VAS) between 1-10, at baseline, before and after each treatment, and 1, 2, 3 and 4 weeks following the last treatment. 2) Tinnitus Handicap Inventory (THI) questionnaire at baseline and 4 weeks after treatment. 3) Tinnitus specific audiometric tests which included minimum masking level, dominant pitch match and tinnitus loudness at baseline and 4 weeks after treatment. 4) Repeat physical examination throughout the duration of the experiment and basic audiometry testing at baseline and 4 weeks after treatment (for safety assessment).

Results

No long term adverse safety outcomes were noted in physical examination or audiological evaluation. VAS levels decreased by ≥ 2 levels in 5 patients (50%). The statistically significant ($p < 0.05$) VAS level decrease in comparison to baseline began from the second treatment up to three weeks after, suggesting residual inhibition. A statistically significant correlation ($p < 0.01$, correlation coefficient 0.787) was observed between VAS level decrease and the patients' tinnitus duration. In addition, a significant decrease in THI total score as well as in all three sub-categories of the questions (functional, emotional and catastrophic) ($p < 0.05$) was noted 4 weeks after treatment. Tinnitus specific tests at that time were unchanged from baseline.

Conclusion

Multiple sessions of electro-stimulation to the promontory appear to be safe and may be beneficial for some tinnitus patients. Further clinical trials are warranted.

PS - 845

Hyperacusis is a Theoretical Construct; not a Behavior: Reconciling Human and Animal Data

Anthony Cacace¹; Dennis McFarland²

¹Wayne State University; ²Wadsworth Labs, NYS Health Department

Background

Hyperacusis is a suprathreshold perceptual phenomenon characterized by adverse reactions of acoustic stimuli at sound levels typically considered normal to others. Herein, we argue that hyperacusis is a theoretical construct that is *not* directly observable; it represents an explanatory variable that can be estimated by psychoacoustic metrics, questionnaire-based assessments, and person-to-person interviews. When recent documents refer to hyperacusis as a "behavior;" i.e., based on a motor activity observed during selected animal experiments studying tinnitus, vis-à-vis the gap detection startle reflex, it creates a quagmire in terms of conceptualizing, identifying, and diagnosing this anomaly.

Methods

Literature review.

Results

By itself, the use of observable sound-evoked motor activity in small rodents is inadequate to identify hyperacusis because it does not rule out other intervening variables or explanations for exaggerated motor-response behaviors. The

development of a multimethod technique would be necessary for construct validation.

Conclusion

Hyperacusis is a theoretical construct that is *not* directly observable. Furthermore, if hyperacusis falls under the rubric of hyperactive sensory-system states, then consideration should be given to whether it represents an auditory modality-specific entity or is part of a more generalized "supramodal" or "polysensory" dysfunction which might include adverse responses to other types of sensory stimuli such as light, smell, and taste.

PS - 846

Acute Effects of Transcutaneous Vagus Nerve Stimulation on Tinnitus-Related Mental Stress

Jukka Ylikoski¹; Jarmo Lehtimäki¹; Ulla Pirvola²; Antti Aarnisalo²; Antti Mäkitie²

¹Helsinki Ear Institute; ²University of Helsinki

Background

Mental stress is associated with imbalance of the autonomous nervous system, leading to reduced parasympathetic activity. Therefore, treatment of choice of tinnitus-related mental stress (TRMS) would be vagus nerve stimulation (VNS). Also, VNS paired with appropriate sound therapy might reduce the tinnitus sensation itself, as shown in a rat tinnitus model. However, conventional VNS with an implanted electrode is an invasive procedure and is therefore less suitable for tinnitus treatment. It has been recently shown by functional MRI, MEG and EEG recordings that transcutaneous VNS (tVNS) of the auricular branch of the vagus nerve activates the central vagal pathways in a similar way as implanted VNS. The aim of the present study is to investigate acute effects of tVNS on TRMS, as measured by heart rate variability (HRV).

Methods

The left auricular branch of the vagus nerve of 24 patients with moderate or severe TRMS was stimulated with tVNS continuously for 60 min. HRV parameters were calculated on the basis of the heartbeat measured with a HRV scanner over a 5-min-period before and immediately after stimulation. Heart rate was continuously monitored during the treatment session.

Results

tVNS consistently reduced TRMS. tVNS had a clearcut beneficial effect on tinnitus-related distress, increasing significantly patients' coherence and subjective well-being. Heart rate monitoring during tVNS treatment showed no cardiac or circulatory effects (e.g. bradycardia) in any of the patients.

Conclusion

One of the most important strategic goals for successful tinnitus therapy is to diminish TRMS. The present study shows that tVNS can reduce the severity of subjective TRMS in patients and that this treatment is safe.

Purinergic Modulation of Firing Activity in the Cochlear Nucleus is Developmentally and Tonotopically Determined

Tamara Radulovic¹; Sasa Jovanovic²; Rudolf Rübsamen²; Ivan Milenkovic²

¹University of Leipzig; ²Faculty of Biosciences, Pharmacy and Psychology, UNiversity of Leipzig

Background

In the developing auditory system, purinergic signaling attunes activity in the cochlea and in the brainstem. Endogenous release of ATP contributes to action potential generation in the inner hair cells and enhances glutamate-driven firing of bushy cells (BCs) in the ventral cochlear nucleus (VCN). These modulatory effects of ATP diminish with maturity, both in the periphery and in the central auditory neurons. In VCN bushy cells, activation of P2X2/3 receptors enhances AP firing through cytosolic calcium signaling and protein kinase C activity. Here we determined the developmental time course of purinergic modulation referring to the tonotopic organization of the cochlear nucleus.

Methods

We used *in vivo/ex vivo*-electrophysiology to examine the responsiveness of CN neurons to P2X2/3R agonists and antagonists at topographically distinct positions during early postnatal development. Experiments were performed on Mongolian gerbils, aged P13-23 for *in vivo*-, and P4-16 for slice recordings.

Results

In vivo extracellular recordings conducted from hearing onset in combination with iontophoretic drug applications revealed that P2X2/3 receptors mediate the enhancement of spontaneous and sound evoked activity of BCs only in the low-frequency regions, i.e. at the rostral pole of the VCN. Bushy cells with high characteristic frequencies (CF > 15 kHz) did not show significant responses to the pharmacological manipulations of P2X2/3R. Slice recordings displayed positive responses of BCs to puff application of P2X2/3R agonists throughout the anterior VCN shortly before hearing onset P10-12. During early auditory experience (P13-16), the population of BCs reacting to P2X2/3R stimulation becomes progressively constrained to a narrow low-CF isofrequency region at the anterior VCN. Notably, the stellate cells were not subject to purinergic modulation.

Conclusion

We conclude that purinergic modulation of BCs' action potential firing and resulting Ca²⁺ signaling conveyed by the heteromeric P2X2/3R is active during the critical, early postnatal period of auditory circuit development. The P2X2/3R-mediated effects are extended to the period of early auditory experience specifically in the low-frequency region of the anterior VCN. These results suggest a general role of purinergic signaling in early establishment of the tonotopic gradient and, at later stages, more specific effects on low-frequency neurons possibly mediating processes such as pruning and synaptic strengthening.

Tonotopy and Periodotopy in Human Auditory Cortex

Gijs Hoskam¹; Cris Lanting¹; Dave Langers²; Pim van Dijk¹

¹University Medical Center Groningen, Groningen, the Netherlands; ²NIHR Nottingham Hearing Biomedical Research Unit, School of Clinical Sciences, University of Nottingham, Queen's Medical Centre, Nottingham, United Kingdom

Background

In recent years advances have been made in mapping the tonotopic organization in human auditory cortex (Saenz & Langers, Hearing Research, 2013). It has been hypothesized that the cortical representation of other stimulus features, such as amplitude modulation rate, may also form an orderly map in auditory cortex. The exact organization of both maps remains debated (Barton et al., PNAS, 2012; Herdener et al., Cortex, 2013). The goal of this study was to study the tonotopic organization, the representation of amplitude modulation rate (periodotopy), and assert whether these maps are task dependent.

Methods

Subjects were normal hearing adults (n=19). Functional MRI experiments were performed on a Philips 3T scanner. A scanning session consisted of three separate runs (with a visual, auditory or no task) lasting 45 minutes in total, during which 3x52 scans were obtained (sparse scanning, TR=10s). During each of the runs, amplitude modulated tones (100% modulation depth, rates 0-54 Hz) of various frequencies (250-8000 Hz) were presented at 60 phon level. A group-level GLM was used to assess the relative contribution of each of the conditions to the measured response. Tonotopic maps were obtained by determining for each voxel the best-frequency, defined as the weighted average of the relative contribution of the sound frequencies. A similar approach was used to determine a map reflecting the amplitude modulation tuning, or a periodotopy map. The results were visualized on an inflated brain.

Results

Preliminary analyses show that both tonotopic and periodotopic gradients can be obtained. A tonotopic gradient was found, with low frequencies predominantly anteromedially and high frequencies posterolaterally in the auditory cortex. A periodotopic gradient was found with low modulation rates predominantly anterolaterally and high modulation rates more posteromedially. These gradients appear to be approximately perpendicular to each other.

Conclusion

Both a tonotopic organization as well as a periodotopic organization can be found in human auditory cortex. The orientations of the main gradients in both maps appear to have an almost perpendicular angle, similar to findings by Herdener et al. Further analyses will be carried out on the relation of these maps and the task performed.

Changes in Brain Networks Detected by Resting State Functional MRI in Subjects With Long-Term Unilateral Sensorineural Hearing Loss

Guangyu Zhang¹; Jian Wang²

¹Zhong-Da Hospital, Medical School of Southeast University; ²SHCD, Dalhousie University, Halifax, Canada

Background

It has been recognized that the impact of sensorineural hearing loss (SNHL) is not limited in the loss of auditory sensitivity but rather extended to the changes in many aspects of brain functions such as the decline of cognitive functions. Previous study has shown that unilateral hearing loss is an attractive model for investigating the functional reorganization.

Methods

In this study, we evaluated how unilateral SNHL (USNHL) impacted the functional organization of the whole-brain network seen by resting state functional MRI (rs-fMRI). This was done by comparing the results of rs-fMRI between normal hearing subjects (n=14) and patients with long-term USNHL (total n=30, 16 and 14 for left and right deafness respectively). The functional network of the brain is analyzed using seeding method for connectivity as well as topographic analyses on three nodal topological properties.

Results

Subjects with USNHL, especially those with left deafness, showed significant differences from the control in many aspects of rs-fMRI results in many brain regions, including those that were well recognized for cognitive functions. Moreover, the changes in rs-fMRI were correlated with the results of many behavior tests in which subjects with USNHL generally performed worse than the normal control, although the cross-group difference did not reach significance.

Conclusion

These results demonstrate the value of the rs-fMRI for evaluating brain plasticity related to SNHL-induced decline in cognitive function.

Figure Legends

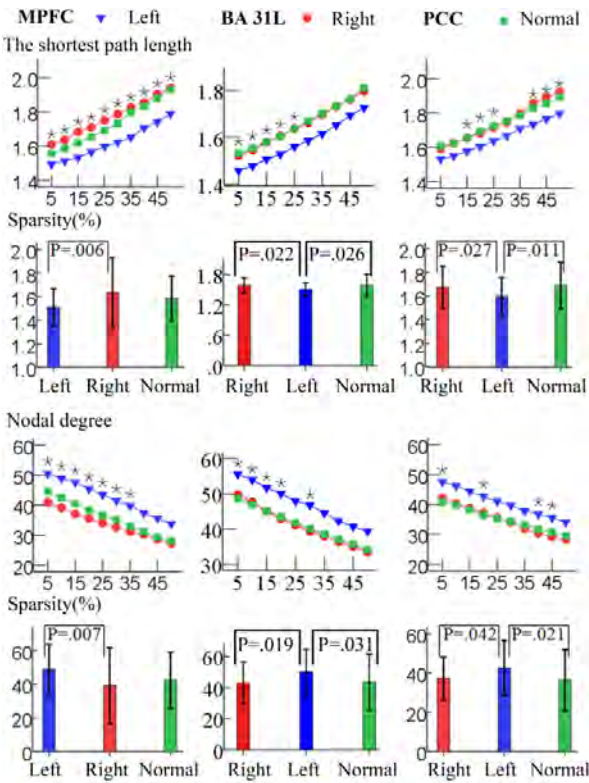


Fig. 1. Graph theoretical measures of nodal topological properties for MPFC, BA 31L and PCC. Asterisks indicate the points at which a significant difference is seen ($p < 0.05$) between the USNHL group and the control. Error bars: \pm 2SEs. Abbreviations (see Table S5).

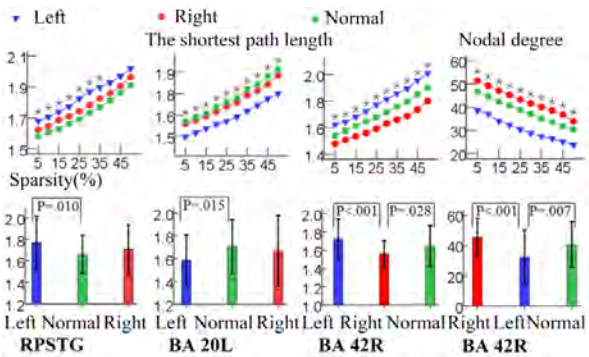


Fig. 2. Graph theoretical measures of nodal topological properties for BAs 20L, 42R, and RPSTG. The asterisks marked the points of significance ($p < 0.05$) among the three groups. The bar graphs showed the values obtained at the sparsity threshold of 20%. The significant differences were verified by the P values obtained in the post hoc tests after one way ANOVAs. Error bars: \pm 2SEs. Abbreviations (see Table S5).

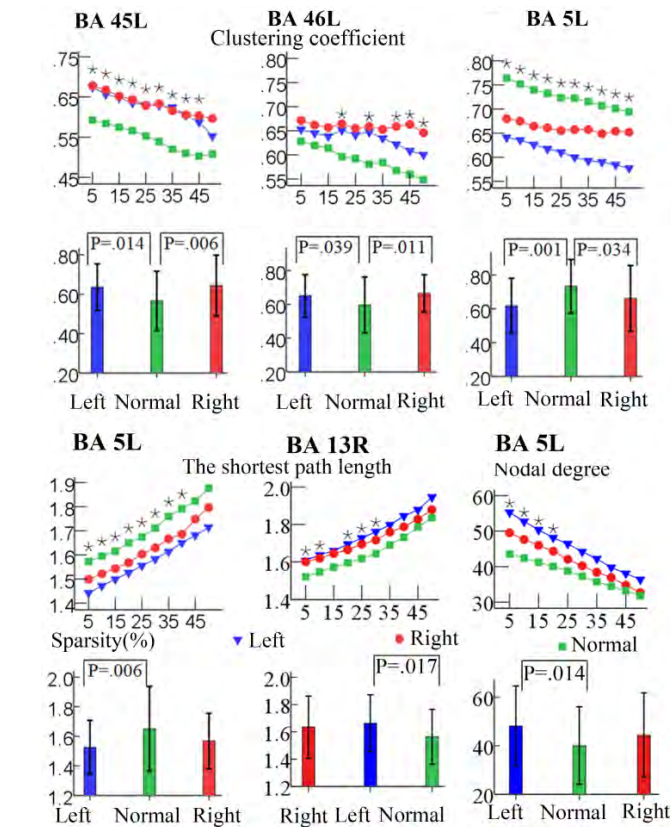


Fig. 3. Graph theoretical measures of nodal topological properties for BAs 45L, 46L, 13R and 5L. The asterisks marked the points of significance ($p < 0.05$) among the three groups. The bar graphs showed the values obtained at the sparsity threshold of 20%. The significant differences were verified by the P values in those graphs and were obtained in the post hoc tests after one way ANOVAs. Error bars: ± 2 SEs (standard errors). Abbreviations (see Table S5).

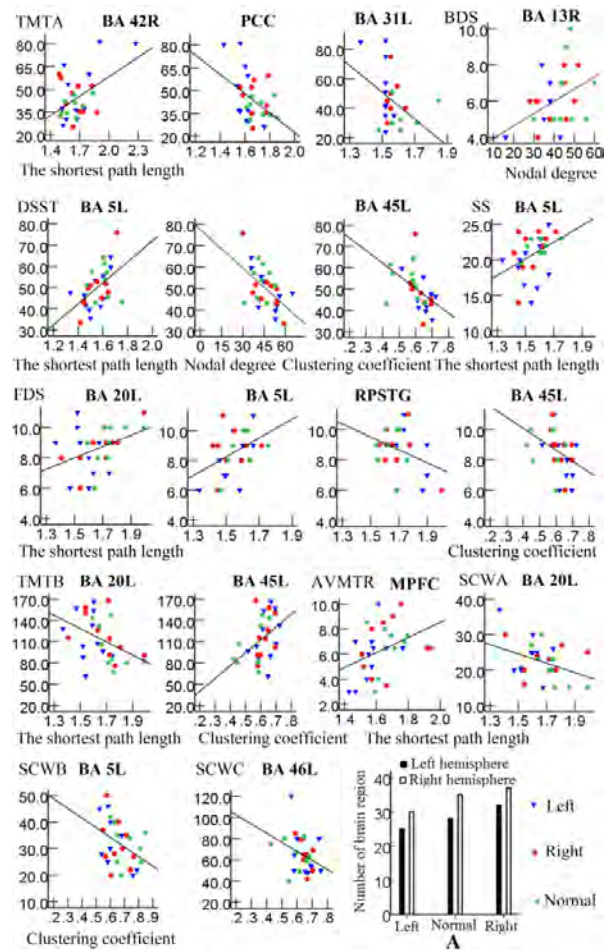


Fig. 4. Correlations between nodal topological properties and performance scores of neuropsychological tests. Only regions that showed significant correlations were shown. TMTA, trail making test part A; DSST, digit symbol substitution test; SS, semantic similarity; FDS, forward digit span; BDS, backward digit span; TMTB, trail making test part B; AVMT, auditory verbal memory test-delayed recall; SCWA, stroop color-word A; SCWB, stroop color-word B; SCWC, stroop color-word C. (A), the correlation analysis between cognitive performance scores and nodal topological properties in all of BAs. Transverse axis is the brain hemisphere in the three groups including LUSNHL, normal hearing and RUSNHL groups, and longitudinal axis indicates the number of brain regions that are significantly correlated with cognitive performance scores. Left: LUSNHL group; Normal: normal hearing group; Right: RUSNHL group. Abbreviations (see Table S5).

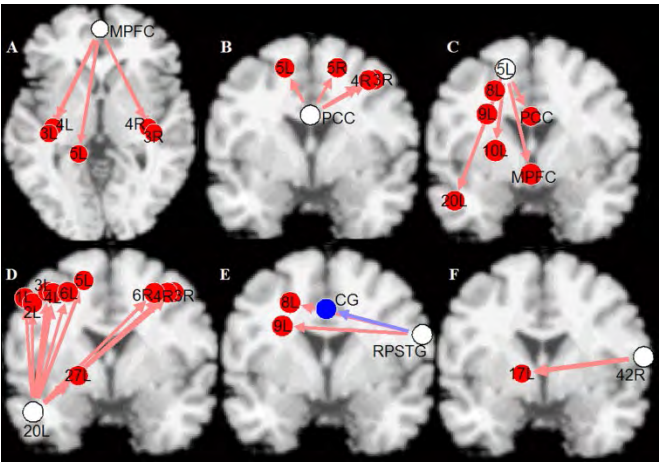


Fig. 5. Functional connectivity diagrams developed by CONN toolbox ($p < 0.05$, FDR corrected) for post hoc t-tests between the USNHL group and the control. A-E indicate significant changes in functional connectivity in the LUSNHL group. F indicates significant changes in the RUSNHL group. The seeds are represented by white circles, and the number in the circle indicates the index of the BA-based ROIs. The red line indicates an increase in functional connectivity, while the blue line indicates a decrease. Arrow-widths represent T-values. See CONN toolbox manual for details. Abbreviations (see Table S5).

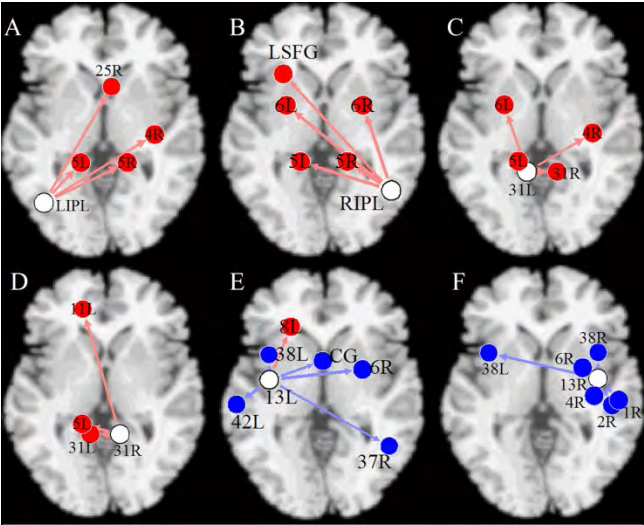


Fig. S1. Functional connectivity diagrams developed by CONN toolbox ($p < 0.01$, uncorrected) for post hoc t-tests between the USNHL group and the control. A-F indicate significant differences of functional connectivity between the left USNHL (LUSNHL) group and the control. The seeds are represented by white circles, and the number in the circle indicates the index of the BA-based ROIs. The red line indicates an increase in functional connectivity, while the blue line indicates a decrease. Arrow-widths represent T-values. See CONN toolbox manual for details. Abbreviations (see Table S5).

Table 1. Summary for significant differences in rs-fMRI observations for USNHL groups compared with the control

Brain region	Connectivity		Shortest path length	Nodal degree	Co-efficiency
Changes	targets				
LUSNHL					
Enhanced	↑		↓	↑	
			↓	↑	
	↑		↓	↑	
	↑		↓		
					↓
					↑
					↑
Deteriorated	↓	Cingulate gyrus	↑	↓	
	↓	Frontoparietal	↑	↓	
	↓	temporal network			
RUSNHL					
Enhanced	↑	BA 17L	↓		

PD - 198
Ginkgo Biloba Extract EGb 761® Has a Protective Effect Against Noise Induced Hearing Loss and Tinnitus Development in the Mongolian Gerbil

Konstantin Tziridis; Sabine Korn; Sönke Ahlf; Holger Schulze
University of Erlangen-Nuremberg
Background

In modern societies an increasing number of people suffer from hearing disorders that result from an over-exposure to noise, i.e. noise induced hearing loss (NIHL). This NIHL may be etiologically responsible for the development of a number of secondary diseases, like hyperacusis, tinnitus or depression due to social isolation. Against this background, effective strategies to take protective measures against the development of NIHL are gaining increasing relevance in health care policy. Two strategies are being pursued, first, reducing noise exposure by technical measures or, second, preventing the development of NIHL via pharmacological interventions. A substance that has been shown to protect against NIHL in guinea pigs is the Ginkgo biloba plant extract EGb 761® that provides a number of different mechanisms that may counteract the development of NIHL and its consequences which may include the development of a tinnitus percept.

Methods
 In a previous study (Ahlf et al., 2012) we have described the development of noise trauma induced tinnitus in the Mongolian gerbil both on a behavioral and neurophysiological level. Here we tested the effectiveness of a prophylactic EGb 761® treatment in the context of NIHL and tinnitus development in this animal model.

Ahlf S, Tziridis K, Korn S, Strohmeyer I, Schulze H (2012) Predisposition for and prevention of subjective tinnitus development. PLoS One 7: e44519.

Results

We found a strong reduction in NIHL and tinnitus development in the 17 EGb 761® treated animals (group E) compared to the 19 vehicle treated control animals (group V). On the electrophysiological level we identified a strong stabilizing effect of EGb 761®, especially in the E animals without tinnitus, not only on the evoked rate in auditory cortex but also in the local field potentials and auditory brainstem responses when comparing these data sets with V animals with and without tinnitus percept.

Conclusion

With this work, we present a possible protectional mechanism against NIHL and tinnitus. Additionally, we present a model of the function of the Ginkgo biloba extract on animal neurophysiology.

PD - 199

Noise Trauma Induced Development of Subjective Tinnitus: Predisposition and Prevention

Holger Schulze; Sönke Ahlf; Konstantin Tziridis
University of Erlangen-Nuremberg

Background

Dysfunction of the inner ear as caused by presbycusis, injuries or noise traumata may result in subjective tinnitus, but not everyone suffering from one of these diseases develops a tinnitus percept and vice versa. The reasons for these individual differences are still unclear and may explain why different treatments of the disease are beneficial for some patients but not for others. In a hearing impaired animal model we here for the first time compare behavioral and neurophysiological data in specimen with (T) and without (NT) a tinnitus percept that may elucidate this question.

Methods

An acoustic trauma in 35 anesthetized Mongolian gerbils was used to induce frequency specific hearing loss (HL) in all animals and the subsequent development of a tinnitus percept in most animals. We demonstrated the existence of possible tinnitus percepts and roughly estimated the perceived tinnitus frequencies. Responses of single and multi-units in primary auditory cortex field AI to tones were recorded before and during multiple recording sessions after the acoustic trauma.

Results

Although noise trauma induced a similar permanent HL in all animals, tinnitus did develop only in about 75% of these animals. NT animals showed higher overall cortical and auditory brainstem activity before noise trauma compared to T animals; that is, animals with low overall neuronal activity in the auditory system seem to be prone to develop tinnitus after noise trauma. Furthermore, T animals showed increased activity of cortical neurons representing the tinnitus frequencies after acoustic trauma, whereas NT animals exhibited an activity decrease at moderate sound intensities by that time. Plastic changes of tonotopic organization were transient, only seen in T animals with complex temporal dynamics and vanished by the time the tinnitus percept became chronic. As

these tonotopic changes in AI and changes in evoked rates at BF were transient in the T animals whereas the increases in spontaneous discharge rate and discharge rate at high, tinnitus-related frequencies persisted beyond one week post trauma, we believe that the latter are the neurophysiological correlates of the tinnitus percept rather than the former.

Conclusion

We propose a model for tinnitus prevention that points to a global inhibitory mechanism in auditory cortex that may prevent tinnitus genesis in animals with high overall activity in the auditory system, whereas this mechanism seems not potent enough for tinnitus prevention in animals with low overall activity.

PD - 200

Cortical Processing of the Syllable Rate of Speech in Musician and Nonmusician Children

Dana Strait¹; Daniel Abrams²; Samantha O'Connell³; Nina Kraus³

¹*University of Maryland*; ²*Stanford University*; ³*Northwestern University*

Background

Speech processing at syllabic rates (~2-5 Hz) has received considerable attention in recent years, possibly due to reported relationships between language-related learning disabilities and aspects of auditory perception and neurophysiology that occur at this time scale. In contrast to the left-lateralized cortical processing at millisecond-level phonemic rates, cortical processing of the syllable rate of speech is right-lateralized¹. While it has been reported that syllable-rate lateralization is diminished in the presence of reading impairments², we do not know whether this deficiency can be remediated nor whether remediation would correspond to improved reading performance. We assessed the experience-related malleability of this mechanism with music training and its implications for reading proficiency in musician children. We predicted that musicians, who regularly attend to and manipulate rhythms that unfold at the syllable rate, would demonstrate increased rightward laterality in syllable-rate processing concurrent with improved reading performance and beat synchronization at this rate.

Methods

We recorded cortical evoked potentials to speech in 29 musician and nonmusician children using a 32-channel silver-electrode cap, in addition to assessing reading ability and beat synchronization abilities. Consistent with previous reports^{1,2}, the stimulus was the sentence "The young boy left home." The stimulus envelope was extracted by performing a Hilbert transform on the speech stimulus. The amplitude envelope was then low-pass filtered to isolate the speech envelope. Cross-correlations between the speech envelope and cortical responses yielded information on cortical response timing (lag) and envelope-tracking precision (correlation strength). Cortical response timing and envelope-tracking precision were compared across right and left electrode sites and be-

tween musicians and nonmusicians to quantify their laterality and group distinctions.

Results

Musicians demonstrated increased precision in cortical speech envelope-following responses over right-hemisphere temporal sites and indicated strengthened rightward laterality in processing the syllabic rate of speech. Musicians also outperformed nonmusicians on beat synchronization and reading. Musicians' improved reading fluency may stem in part from improved syllable-rate processing, exhibited by cortical envelope-following responses.

Conclusion

These data provide neurophysiological evidence that musicians have more precise representations of the speech envelope, the acoustical cue that provides syllable pattern information in speech. Musicians' increased laterality in syllable-rate processing may indicate increased efficiency in speech processing, with implications for auditory-related tasks that depend on sensitivity to syllabic cues such as reading.

REFERENCES

¹Abrams, et al. (2008) *J Neurosci*.

²Abrams, et al. (2009) *J Neurosci*.

PD - 201

Structural and Functional Analysis of Auditory Cortex in a Mouse Model of Fragile X Syndrome

Teresa Wen; Khaleel Razak; Iryna Ethell
University of California, Riverside

Background

Fragile X Syndrome (FXS) is a leading inherited intellectual disability that affects 1 in 4000 males and 1 in 8000 females. FXS is a known genetic cause of autism. Structural and functional studies of humans with FXS indicate auditory cortical deficits. Most notable is hypersensitivity to sounds. Early cortical deficits may lead to deficits in higher auditory functions such as language reception. The *Fmr1* knockout (KO) mouse is a well characterized mouse model for FXS. The KO mice also show increased acoustic startle and audiogenic seizures.

In vivo electrophysiological recordings from single neurons in the KO mouse auditory cortex conducted in our lab show four main processing deficits: 1. Hyper-responsiveness to tones, 2. broad frequency receptive fields, 3. altered spectrotemporal processing and 4. increased variability in responses. These functional deficits may arise from the development of abnormal connections in the auditory cortex.

In the present study, we analyzed development of dendritic spines in excitatory cortical neurons and the association of perineuronal nets (PNN) with Parvalbumin (PV) positive interneurons in wild-type (WT) and KO mice. These two measures examine possible deficits in excitatory and inhibitory processes that may cause hyper-responsiveness in auditory responses. In addition, we examined stimulus specific adaptation in the cortex using an auditory odd-ball paradigm in

which a broad-band noise stimulus acted as a deviant stimulus in a train of standard tones.

Methods

The presence of PV-positive interneurons and PNNs was determined using immunohistochemistry and confocal imaging. *In vivo* electrophysiology was performed in the auditory cortex to evaluate auditory response properties in both KO and WT mice.

Results

Preliminary data suggest abnormal dendritic spine development in the auditory cortex of KO mice. Electrophysiology data indicate a larger increase in response to the deviant stimulus in KO mice, suggesting abnormal adaptation processes as observed in humans with FXS.

Conclusion

These data indicate significant auditory processing deficits in FXS model mice that can be useful outcome measures for preclinical testing of potential therapies in FXS.

PD - 202

Direct Electrophysiological Recording of Human Auditory Cortex Responses to Different Pitch Values

Phillip Gander¹; Sukhbinder Kumar²; Kirill Nourski¹; Hiroyuki Oya¹; Hiroto Kawasaki¹; Matthew Howard¹; Timothy Griffiths²

¹University of Iowa; ²Newcastle University

Background

Mechanisms of pitch representation and analysis in human auditory cortex remain elusive and continue to be debated (Barker et al., *Cereb Cortex* 22:745-53, 2012; Griffiths & Hall, *J Neurosci* 32:13343-7, 2012). The current investigation extended the work of Griffiths et al. (*Curr Biol* 20:1128-32, 2010) exploring pitch-related activity in human auditory cortex using electrocorticographic recordings.

Methods

Experimental subjects were six neurosurgical patients undergoing diagnostic epilepsy monitoring. Experimental stimuli were 1 s bursts of broadband noise followed by 1.5 s regular interval noise (RIN), presented at rates below and above the lower limit of perceived pitch (8, 16, 32, 64, 128, 256 Hz). Local field potentials were recorded from Heschl's gyrus (HG) and lateral superior temporal gyrus (STG) using multichannel depth electrodes and subdural grid arrays, respectively.

Results

Evoked responses from the noise to RIN transition emerged as the pitch salience increased and reached its maximum for the 256Hz rate. Similarly, induced responses in the high gamma range (60 - 200Hz) emerged as the rate crossed the lower limit of pitch and were most robust for the 128 and 256Hz rates, with typical onset latencies of approximately 70 ms. RIN-induced responses were sustained for a longer duration than to broadband noise, and, in some electrodes, for the entire duration of the stimulus. The location of pitch-associated high gamma responses in HG was found to vary across

subjects, but this was more pronounced on sites within medial two thirds of the HG. Similar to induced responses along HG, focal regions of posterior lateral STG also showed more robust and longer duration responses for pitch-evoking stimulus rates in each subject.

Conclusion

These data are consistent with previous work (Griffiths et al., 2010) and also provide information about the variability across subjects that exist in pitch-evoked response properties and location along HG. Responses on lateral STG suggest a network of activity in response to pitch stimuli.

PD - 203

Lip Reading May Prevent Visual Reorganization of Auditory Phonological Areas in Post-Lingual Deaf Adults

Diane Lazard¹; Anne-Lise Giraud²

¹*Institut Arthur Vernes;* ²*Department of Neuroscience, University Medical Centre*

Background

When one sense is defective at birth, the intact senses take over and become more efficient. Things are not so clear in acquired sensory loss, particularly when it happens in late childhood or adult age.

Methods

Using fMRI and behavioral tests, phonological processing from written material of 18 post-lingually deafened subjects, candidate for a cochlear implantation, and 17 matched hearing controls was investigated. Results were interpreted with regards to cochlear implant outcome.

Results

We found that the adults with acquired profound deafness processed phonology from written material faster than hearing controls, without systematic accuracy loss. This paradoxical cognitive gain was mediated by a functional interaction between early visual cortex and the left inferior prefrontal cortex, which by-passed the graphemic and phonological steps usually taking place in left fusiform gyrus and superior temporal cortex. Accelerated phonological processing was accounted for by a phonological reorganization of the right superior temporal sulcus, yet it negatively predicted the proficiency with which post-lingual deaf individuals understood speech once they got a cochlear implant.

Conclusion

These data suggest that maintaining active auditory-based phonology through lip-reading is a costly adaptation to deafness, which nonetheless may preserve the possibility to revert to hearing, whereas optimizing written communication (reading) may compromise future auditory restoration by visual take over.

PD - 211

Categorization of Speech and Non-Speech Sounds in the Human Auditory Cortex Revealed by Intracranial Recordings

Mitchell Steinschneider¹; Kirill Nourski²; Hiroto Kawasaki²; Hiroyuki Oya²; Matthew Howard²

¹*Albert Einstein College of Medicine;* ²*University of Iowa*

Background

There is controversy as to what level in the auditory pathways speech is transformed from acoustic representations to speech-related auditory objects. Some investigators postulate that activity in primary auditory cortex is directly involved in the representation of sound objects (see Nelken, Curr Opin Neurobiol 2008). An alternative view is that the activity in primary auditory cortex is dominated by the representation of acoustic sound attributes (e.g. Steinschneider et al., Hear Res 2013). This controversy persists with regard to activity in the non-primary auditory cortex located on the posterolateral superior temporal gyrus (PLST). While selective attention strongly modulates activity elicited by speech on PLST (Mesgarani & Chang, Nature 2012), PLST also maintains a representation of acoustic features (e.g. Leaver & Rauschecker, J Neurosci 2010). Further, prefrontal cortex has been implicated in the formation of auditory objects (e.g. Russ et al., Hear Res 2007).

Methods

To help clarify the respective roles of auditory and auditory-related cortex in the generation of sound objects, we examined the electrocorticogram simultaneously recorded from Heschl's gyrus (HG), the putative location of primary auditory cortex in humans, as well as PLST and prefrontal cortex. Experimental subjects were neurosurgical patients undergoing evaluation for treatment of medically intractable epilepsy. The subjects were engaged in target detection tasks using a variety of non-speech and speech sounds as both background and target stimuli. Analysis of electrophysiological recordings focused on high gamma (70-150 Hz) cortical activity, which had been shown to correlate with both neuronal firing rate and hemodynamic responses (Nir et al., Curr Biol 2007).

Results

We found that posteromedial HG strongly responded to all forms of sound stimuli regardless of their context. Likewise, early high gamma activity on PLST strongly represented both target and background stimuli. In contrast, later activity on PLST exhibited a differential representation of the stimuli depending on whether they were background or targets. Activity in prefrontal cortex overlapped in time with later portions of activity on PLST and was primarily restricted to the targets.

Conclusion

We propose that high gamma activity in primary auditory cortex as well as earlier activity on PLST primarily reflect the representation of sound attributes. In contrast, later activity on PLST and that emanating from prefrontal cortex are involved in object formation necessary for successful performance in target detection tasks, including those utilizing speech.

Figure-Ground Segregation in Complex Acoustic Scenes: An MEG Study

Sundeep Teki¹; Christopher Payne¹; Timothy Griffiths²; Maria Chait¹

¹University College London; ²Newcastle University

Background

The acoustic environment consists of multiple temporally overlapping sound sources which makes it hard for the listener to segregate particular sounds of interest. Although much research has been done on this 'cocktail party problem', the underlying brain mechanisms are still unclear.

Methods

We used a stochastic figure-ground (SFG) stimulus to investigate the temporal dynamics of auditory segregation using Magnetoencephalography (MEG). The stimulus consists of a series of chords containing a random number of pure tone components, some of which are randomly selected (this number defines the 'coherence' of the figure) to repeat over a certain number of chords. These synchronous frequency components pop out of the background as a distinct 'figure' and can be used to study the brain bases of segregation in complex acoustic scenes (Teki, Chait et al., 2011, 2013). Here, naïve listeners were instructed to perform an incidental visual task whilst passively listening to SFG signals that comprised a transition from background to figures with different levels of coherence (0, 2, 4, or 8).

Results

Two separate experiments with different SFG stimuli were conducted: the basic SFG stimulus and a variant with white noise between successive stimulus chords (Teki, Chait et al., 2013). Robust evoked transition responses were elicited whose amplitude increased with the coherence of the figure and consisted of an early peak and a later sustained component. Source reconstruction of evoked power revealed that auditory cortex as well as the intraparietal sulcus (IPS) responded to the emergence of salient figure segments in both stimulus conditions. Analysis of the sustained phase of the transition response to the basic SFG stimulus revealed activity in IPS that was not present during the early phase, suggesting a specific role for IPS in the perceptual representation of coherent figures after initial encoding in the auditory cortex.

Conclusion

The MEG data suggest that the brain can parse complex acoustic signals even in the absence of focused attention as indicated by the robust transition responses obtained during passive listening conditions. The sources underlying this transition were found to be localized in the auditory cortex as well as the IPS, thus extending a role for non-auditory areas in auditory perceptual organization (Cusack, 2005; Teki, Chait et al., 2011; Dykstra et al., 2012).

Preserved Responsiveness and Reduced Intracortical Connectivity in the Auditory Cortex After Congenital Deafness

Peter Hubka¹; Jochen Tillein²; Andrej Kral¹

¹Medical University Hannover, Germany; ²ENT Department, J.W.Goethe University Frankfurt, Germany and Medel Starnberg, Germany

Background

Congenital sensory deprivation was shown to cause substantial changes in neural network function and deficits in perception after a peripheral activation of deprived afferent pathways. Despite these deficits, peripheral electrical stimulation of auditory nerve is still able to reliably activate the primary auditory cortex (field A1). Further spread of activation to non-primary auditory fields has not been studied yet. The present study is aimed on the functional analysis of the activation of the primary auditory cortex and the posterior auditory field (PAF) evoked by mono- and binaural electrical stimulation using cochlear implants.

Methods

Multiunit activities from six congenitally deaf cats (CDC) and five hearing controls were recorded simultaneously in A1 and PAF by means of 16 channel microelectrode arrays (Neuronexus probes). All animals were electrically stimulated; mono- and binaural responses were evoked by pulse trains (500Hz, 3 pulses) at intensities of 0-10 dB above response thresholds. Effective connectivity between the simultaneously recorded positions in the fields A1 and PAF was computed using transfer entropy approach. Connectivity results were then further analyzed and visualized by means of visualization of similarity (VOS) and clustering technique.

Results

Activation of PAF was repeatedly found in all adult CDCs, which responses exhibited typical deficits related to the auditory deprivation (shorter response duration, sharp onset responses and fewer spikes). The response pattern in PAF, both in hearing controls and CDC, showed typical characteristics of PAF responses previously described in hearing cats (peak latencies in the range of 15-30 ms, longer duration). Effective connectivity analysis among the cortical responses from both fields revealed two major differences between groups. First, connectivity strength between neurons in A1 and PAF was significantly decreased in CDCs. Second, cluster analysis of connectivity distributions revealed two clusters corresponding to positions located in A1 and PAF in both groups. In CDCs, connectivity distributions of positions located in A1 were additionally divided into two distinct clusters corresponding to the positions in supra- and infragranular layers. This reflects disrupted columnar connectivity pattern within A1 in CDCs. In contrast, activations recorded in A1 of hearing controls formed one single connectivity cluster indicating that the neurons from all layers constitute one computational unit.

Conclusion

These results demonstrate preservation of responsiveness of PAF to peripheral electrical stimulation after long-term con-

genital deafness. Cortical connectivity is, however, significantly decreased between the positions in A1 and PAF, as well as between the supragranular and infragranular layers of A1 in deprived animals.

PD - 215

Rhythms and the Brain: Analysis of Neural Dynamics Accompanying Musical Beat Perception

John Iversen¹; Aniruddh Patel²; Scott Makeig¹

¹University of California, San Diego; ²Tufts University

Background

Perception is jointly shaped by external stimulus characteristics and internal cognitive interpretation. Where and how do bottom-up (stimulus-driven) and top-down (cognitive) influences on perception converge in the brain? We explore this question via the auditory perception of ambiguous rhythms. We employ rhythms in which the perceptual organization of repeating rhythm can be manipulated at will by a listener. Specifically, we use rhythms in which listeners can voluntarily alter where they hear the 'downbeat' (the most salient beat in a repeating rhythm pattern), thus influencing the perceived meter of the phrase. Such manipulation has profound consequences on the perception of the same physically invariant rhythmic phrase, but the mechanism for this dynamic perceptual change has not been characterized.

Methods

We use magnetoencephalography (MEG) to address whether bottom-up and top-down influences on rhythm perception converge in auditory cortex or also in other brain areas. In separate trials, 16 listeners were instructed to mentally impose different metrical organizations on the repeating stimulus, specifically by hearing the downbeat at one of three different places in the rhythmic phrase. Crucially, the imagined beat could coincide with a note onset or could occur at a silent moment in the pattern (producing a syncopated rhythm percept). This allowed disentangling neural processes related to sound processing *per se* and to organization of the endogenous beat / meter percept.

Results

For a subset of participants for which head geometry was available ($n=6$) the data were decomposed by independent component analysis (ICA) to identify maximally independent sources of MEG activity. An average of 12 (± 5) sound-related and 5 (± 2) beat-related component processes were returned by ICA per person. The majority of 'sound-related' components were localized to temporal and parietal cortex, while the majority of beat-related components were localized to pre-motor and parietal regions. Results for the participants without individual geometry, using a generic head model, were consistent.

Conclusion

The presence of beat-related responses in motor structures is consistent with past findings of motor system involvement during listening to beat-evoking rhythms. Localization of both sound- and beat-related components within parietal cortex

suggests it is a locus for interaction of bottom-up and top-down processes in rhythm perception.

PD - 188

Middle-Ear Atlas Registration Method for Surgical Simulation

Guillaume Kazmitcheff^{1,2}; Yann Nguyen^{1,3}; mathieu miroir¹; Evelyne Ferrary^{1,3}; Alexis Bozorg-Grayeli⁴; Stéphane Cotin²; Christian Duriez²; Olivier Sterkers^{1,3}

¹UMR-S 867, Inserm / Université Denis Diderot, Paris 7; ²Equipe Shacra Inria Lille Nord Europe / Université Lille 1, Lille; ³AP-HP, Hôpital Pitié Salpêtrière, Service d'ORL et de Chirurgie cervico-faciale, Paris; ⁴Service ORL, Hôpital Général, Dijon

Background

A middle-ear microsurgery simulator is being developed for training and rehearsal purpose. The identification of the surgical approach or contraindications is mainly due to the anatomical configuration of the ear. The middle-ear anatomy differs between patients. To improve teaching and to provide a rehearsal tool, the simulator should take into account for the patient imaging. Manual segmentation and parameterization of the model is a laborious work. Thus, we propose a semi-automated algorithm to perform a quick and precise registration of our validated mechanical atlas to match the patient dataset.

Methods

A precise mechanical atlas of the left middle-ear is implemented in a medical simulation software, sofa-framework (INRIA, France) and based on a finite element model (FEM). The mechanical behavior of the atlas was previously evaluated in dynamic and static (Kazmitcheff et al., 2013). The registration algorithm consist in, first, a semi-automated rigid registration of our atlas based on the selection of three anatomical targets, followed by deformable registration to fit with accuracy the middle-ear components pictured on the Dicom files. Spring forces are used to deform our validated finite element model. Thus parameterization of the mechanical atlas is conserved. This registration accuracy is compared to a manual process using MeshDev (Roy et al., 2002). A NewTom 5G Cone Beam Computed Tomography (QR SRL, Verona, Italy) is used for the acquisition of height human ears imaging.

Results

The presented registration method supplies a result in 110 seconds, and 260 seconds with the selection of the three anatomical targets by the surgeon. In comparison, a manual segmentation, parameterization and evaluation require 3 man-days. A mean error of 0.201 mm is obtained using our semi-automated method and 0.187 mm for the manual segmentation. The errors are within the imaging resolution of the Dicom files, 0.26 mm, corresponding to the diagonal of the voxel.

Conclusion

Registration algorithm of the middle-ear is a complicated task since it is performed on the smallest human bones. Currently available methods yield to unsatisfactory results or require a manual intervention. The presented algorithm allows per-

forming a registration in less than 260 seconds with accuracy close to a manual process and within the imagery resolution. The main advantage is it avoids a time-consuming work of manual segmentation, parameterization, and evaluation. This algorithm will be used in our surgical simulator to take into account for the patient anatomy in order to provide a complete training and rehearsal tool.

PD - 190

Virtual Simulation of Stapedotomy and Stapedioplasty Surgery

Yann Nguyen^{1,3}; Guillaume Kazmitcheff^{1,2}; Mathieu Miroir¹; Evelyne Ferrary^{1,3}; Stéphane Cotin²; Christian Duriez²; Olivier Sterkers^{1,3}

¹UMR-S 867, Inserm / Université Denis Diderot, Paris 7;

²Equipe Shacra Inria Lille Nord Europe / Université Lille 1, Lille; ³AP-HP, Hôpital Pitié Salpêtrière, Service d'ORL et de Chirurgie cervico-faciale, Paris

Background

Stapedotomy and stapedioplasty are two challenging procedures of the middle ear microsurgery, since the surgeons is in direct contact with sensitive structures such as the ossicular chain. Those procedures are taught and performed in the last phase of the surgical apprenticeship. Training and practices are essential to master those techniques in order to assure safety and surgical outcome for the patient. Today only the dissection of temporal bone allows a realistic practice. However, it is expensive, and it requires administrative authorization. To improve surgical teaching, we propose to use a virtual surgical simulator based on a finite element model of the middle ear, which is being developed. The objective of this study is to simulate the stapes footplate drilling and the placement of an ossicular prosthesis.

Methods

A mechanical model of the ossicular chain is implemented in a medical simulation software, sofa-framework (INRIA, France). The mechanical behavior of the model was previously evaluated in both dynamic and static, and was successfully confronted to temporal bone experiments. A Phantom Omni haptic device (Sensable, Wilmington, Ma) allows interaction with the simulation. A surgical hand piece with a 0.6 mm diameter burr and a conventional micro-forceps are modeled in Sofa. Collisions responses, mechanical deformations, and carving algorithms are optimized in order to reach real-time computation, require for interactive simulation.

Results

Both procedures are successfully simulated. An average frame rate of 60 Hz is observed when no interaction between the surgical instruments and the anatomical structures is observed. This rate drops to 20 Hz at a minimum when components collide. Using a simulation time step set to 0.4 seconds, we are able to run the simulation in real-time allowing interactive simulation.

Conclusion

Results have shown that the mechanical model implemented and the presented computation algorithms, allowing carving and collision response, are compatible with a real-time inter-

active simulation of a stapedotomy and a stapedioplasty surgery. The simulator also provides an interesting feedback to analyze the surgical gesture, drilling volume or incus motion and the by a comparison to expert performance.

PD - 191

Dynamic Properties of Tympanic Membrane in a Chinchilla Otitis Media Model

Zachary Yokell; Xiyang Guan; Rong Gan

University of Oklahoma

Background

Otitis media is known to cause changes to both the thickness and mechanical properties of the tympanic membrane (TM). Our previous studies have reported the static and dynamic properties of the human TM, but there are no published data for the dynamic properties of chinchilla TM in otitis media (OM). In fact, the chinchilla OM model is a popular middle ear infection model in hearing research with clinical applications. This paper reports our current investigation on changes of mechanical properties between the healthy/normal and OM ears in chinchillas over the auditory frequencies. Information about the dynamic properties of infected ears will enhance understanding of the otitis media induced hearing loss.

Methods

Four chinchillas were inoculated with *Haemophilus influenzae* in both ears for 4 days and three chinchillas were left untreated as control/normal ears. After euthanizing the animal, the TMs were harvested and a rectangular strip with the annulus attached was cut from the posterior side of each TM. Each sample was then mounted in MTS (material testing system) and subjected to acoustic stimuli over 200-8000 Hz. A laser Doppler vibrometer was used to measure the sample vibration induced by acoustic driving. The experiment was simulated in a finite element model and the inverse problem solving method was applied with the viscoelastic constitutive equations to derive the dynamic properties of each specimen.

Results

The results include the complex moduli (storage modulus and loss modulus) over the frequency domain and the relaxation moduli over the time domain for 6 control and 8 OM ears. Both storage modulus and loss modulus were higher in the otitis media case than in the control case over the frequency range.

Conclusion

Acoustic driving successfully simulated the motion of the TM over a range of frequencies. The application of the inverse problem solving method was effective in generating data about the changes in the storage modulus and loss modulus over the frequencies that was tested. Otitis media was shown to consistently have an effect on dynamic properties of the chinchilla tympanic membrane. The data reported here have furthered our understanding of the impact of otitis media on the properties of mammalian tissues.

Effects of Middle Ear Condition on Intracochlear Pressure in Human Temporal Bones With Bone Conduction Excitation

Christof Stieger¹; Defne Abur²; Julie P. Merchant³; Kourosh Roushan⁵; Rosemary Farahmand⁴; John J. Rosowski⁴; Hideko Heidi Nakajima⁴

¹University Hospital Basel and University Bern, Inselspital, Switzerland; ²Smith College; ³Massachusetts Eye and Ear Infirmary; ⁴Massachusetts Eye and Ear Infirmary, Harvard Medical School; ⁵Dept. of ORL, University Hospital Basel, Switzerland

Background

Key questions regarding fundamental mechanisms underlying bone conduction (BC) hearing have eluded investigators in the past. For example, experimental studies on BC on human specimens have generally been limited to measuring the velocity or acceleration of the bone outside the cochlea in response to BC stimulation.

We developed new methods that enable measurement of BC-evoked intracochlear pressures while suppressing artifacts that arise from relative motion between the cochlear bone and sensors. This new technique enables quantification of the intracochlear pressures and cochlear input drive (differential pressure across the cochlear partition) produced by BC. Our goal is to determine the contributions of different BC mechanisms, such as the inertial effects of ossicular motion to BC.

Methods

Fiberoptic pressure sensors (diameter of 200 μm) were inserted into the scala vestibuli (SV) and scala tympani (ST) through cochleostomies near the oval and round windows. The sensors were sealed with dental impression material (Jeltrate) and firmly fixed with additional dental cement to prevent fluid and air leaks and allow for similar vibration of the sensor and surrounding promontory bone. Precautions were taken to ensure no leakage of air and fluid near the sensor tips. Pressures in SV and ST, as well as the cochlear drive were compared between BC and AC under three different conditions of the middle ear: 1) normal intact ossicular chain, 2) disarticulated incudo-stapedial joint, and 3) fixed stapes. The temporal bone was stimulated by a commercially available bone-anchored hearing aid (Cochlear).

Results

BC stimulation generally resulted in frequency-dependent SV pressures slightly higher or similar to ST pressures. In contrast, air-conduction (AC) stimulation generally resulted in SV pressures substantially higher than ST pressures for most frequencies. On the other hand, BC can stimulate a cochlear drive that is of similar magnitude to the AC-evoked cochlear drive. With BC, ossicular disarticulation resulted in small changes in scalae pressures and cochlear drive, while fixation of the stapes tended to decrease scalae pressures and cochlear drive at mid-frequencies.

Conclusion

BC stimulation can produce cochlear drive magnitudes similar to that obtained by AC. However, unlike AC, which results in SV pressure substantially higher than ST pressure, BC results in SV pressure only slightly higher than or approximately equal to ST pressure. Ossicular discontinuity has only small effects on BC induced scalae pressures, while stapes fixation results in decreased scalae pressures and cochlear drive.

PD - 193

The Utility of Animal Models in the Study of Bone Conduction

John Rosowski; David Chhan; Melissa McKinnon; Hideko Nakajima

Massachusetts Eye & Ear Infirmary

Background

Animals have been used to study the multiple mechanisms that stimulate the inner ear during bone conducted (BC) sound presentation for many years. The pioneering work of Wever, Tonndorf and others in cats and guinea pigs first documented many of the signal pathways, which are known to contribute to this complex phenomenon.

Methods

We will review some of the classic and recent animal work describing different pathways for sound stimulation of the inner ear that results from vibration of the head and body. Our own methods include measurements of cochlear potential (CP), intracochlear sound pressures in scala vestibuli and scala tympani (**Psv** and **Pst**), and laser vibrometer measurements of the motion of the skull and ossicles. We discuss the possible relationships between these quantities and describe possible artifacts associated with their use.

Results

Older and more recent results that help distinguish the contribution of the different stimulus paths to the BC response will be reviewed. Comparisons to results from humans will be made.

Conclusion

Animal models of bone conduction allow a unique combination of measurements of sensory potentials as well as multiple physical parameters associated, e.g. ossicular velocity and intracochlear sound pressures, with cochlear stimulation. While differences between the size and structure of human and animal heads and bodies introduce differences in BC stimulus paths and responses, the ability to investigate all of the different pathways in a single preparation has benefits over the mixture of multiple live and cadaveric human measurements used in the study of the human response to BC stimuli.

PD - 194

Novel Auditory Test Curves Derived from 3D Finite Element Models of Human Ear

Rong Gan; Xiao Ji; Xiangming Zhang

University of Oklahoma

Background

Two 3-dimensional (3D) finite element (FE) models of the human ear based on histological sections of an adult ear (52

years old) and a pediatric ear (4 years old) were developed in our lab. Each model consists of the ear canal, tympanic membrane (TM), ossicles, middle ear cavity, and spiral cochlea. The middle ear tissues are assumed as nonlinear viscoelastic materials and the model has multi-physics (acoustic, structure, and fluid) coupled FE analysis capability. In this paper, we report the clinically relevant applications of the FE models by developing the auditory test modeling system (ATMS) software with four novel "auditory test curves" named as the middle ear transfer function (METF), energy absorbance (EA), admittance tympanogram (AT), and TM vibration holography. Each curve is correlated to the disease or parameters of the middle ear structure. ATMS can assist physicians and audiologists to interpret the diagnostic test results with the specific type of middle ear disorders.

Methods

Validations of the adult and pediatric models with experimental measurements in human temporal bones and the clinical test data were conducted first. A JAVA software package, including two normal models and two diseased models: "general middle ear disorders" and "otitis media" for adult and pediatric ears, was then established. The tools to simulate middle ear disorders and output the novel auditory test curves were created in ATMS.

Results

Users can input the patient information and clinical observations into ATMS and select the function they want to check, such as the METF, EA, AT, or TM holography. For example, for observations of "TM stiffness increase", the stiffness change of the TM (pars tensa and flaccida), or incus-stapes joint, or stapedial annular ligament can be selected separately or together. For observations of "otitis media", the middle ear pressure, fluid, and ossicular stiffness changes can be selected. The curves of METF, EA, AT and TM holography from ATMS reflect the consequence caused by each entity users selected.

Conclusion

The ATMS software has made encouraging progress with the auditory test curve database. Users can compare the curves from ATMS with their clinical test results and make the quantitative analysis or diagnosis on middle ear disorders which cannot be seen through the TM.

PD - 195

Simultaneous Measurement of Differential Intracochlear Pressure and Ossicular Velocity by Scanning Vibrometry During Very High Intensity Sound Presentation

Nathaniel Greene¹; Herman Jenkins²; Mario Pineda³; Daniel J. Tollin⁴; James Easter⁵

¹University of Colorado Anschutz Medical Campus;

²Department of Otolaryngology, University of Colorado School of Medicine, Aurora, CO 80045 USA; ³Polytec Inc. Irvine, CA 92618 USA; ⁴Neuroscience Training Program, Department of Physiology and Biophysics, Department of Otolaryngology, University of Colorado Anschutz Medical Campus, Aurora, CO 80045 USA; ⁵Cochlear Boulder LLC, Boulder, CO 80301 USA

Background

High intensity sounds, as occur during a blast event, can cause profound sensorineural hearing loss. Measurements of both ossicular motion and differential intracochlear pressure have proven to be useful techniques for the exploration of normal and pathological processes of ossicular transmission; however, previous studies have either relied upon measurements in animal models or measurements at more moderate sound intensities. In this study, we recorded intracochlear pressure, via fiber optic pressure sensors placed in both scala vestibuli (SV) and tympani (ST), while simultaneously measuring ossicular velocity with a scanning laser Doppler vibrometer (SLDV) in human cadaveric temporal bones, during presentation of harmonic and impulsive stimuli with peak pressures in excess of 3 PSI in the ear canal (180dB SPL).

Methods

Three human cadaveric temporal bones were prepared by mastoidectomy and extended facial recess to expose the ossicular chain. Harmonic stimuli, with frequencies between 20Hz and 2.5kHz, and simulated blast waveforms of short (40 msec) and long (400 msec) duration were presented using a custom-built concentrating horn (~12m in length) driven by a 12" subwoofer and 1000W amplifier. Measurements of pressures in the SV and ST (in one specimen) and external auditory canal (EAC) were made concurrently with SLDV measurements of the malleus head (M), incus body (I), incus long-process (ILP), stapes capitulum (S), stapes footplate (SFP) and round window (RW) velocity. Ossicular displacements were analyzed in time and frequency domains.

Results

Simultaneous measurements allowed estimates of SV/EAC and ST/EAC transfer functions, middle ear gain and group delay along the ossicular chain, as well as cochlear fluid volume velocity and cochlear impedance during intense acoustic stimulation. Phase relationships between the motion of ossicular components were consistent with published reports. Peak intracochlear pressure increased with the sound pressure level in the ear canal, such that SV/EAC and ST/EAC transfer functions were comparable at moderate (~114 dB SPL) and intense (~160 dB SPL) sound presentation levels. High intensity impulses drove the ossicular chain to extreme

displacements in both directions, and the maximum observed out of plane stapes displacement exceeded 50 μm , consistent with previous estimates from single-axis LDV measurements.

Conclusion

Consistent with previous results at extremely high sound pressures, maximum stapes displacements in human cadaveric specimens were substantially greater than previous estimates from animal models. These results provide further evidence suggesting that currently accepted models of acoustic hazard do not fully capture the ossicular displacement response to high-intensity impulse in humans.

PD - 204

Spiral Ganglion Degeneration and Hearing Loss as a Consequence of Satellite Cell Death in Saposin B Knockout Mice

Lawrence Lustig¹; Omar Akil¹; Ying Sun²; Chi-Kyou Lee¹; Wujuan Zhang³; Tiffany Ku¹; Greg Grabowski⁴

¹University of California San Francisco; ²Department of Pediatrics, University of Cincinnati College of Medicine;

³Division of Pathology and Laboratory Medicine University of Cincinnati College of Medicine; ⁴Division of Human Genetics and Cincinnati Children's Hospital Medical Center and the Department of Pediatrics, University of Cincinnati College of Medicine

Background

Saposins (Sap) are a family of four small glycoproteins, termed Sap A-D, that are generated in lysosomes from a single precursor protein, prosaposin. Genetic deficiencies of individual saposins or the precursor prosaposin leads to lysosomal storage diseases, highlighting their physiological importance in glycosphingolipid (GSL) degradation. Each of the four saposins is necessary for the activity of one or more lysosomal GSL hydrolases. Saposin B (Sap B), is an essential activator protein for arylsulfatase A in the hydrolysis of sulfatide, a lipid component of myelin. To study Sap B's role in hearing and balance, a Sap B knockout (KO) mouse was evaluated.

Methods

A mouse model of Sap B deficiency was previously generated by introducing a point mutation into the Sap B domain of prosaposin, destroying one of the three essential disulfide bonds of Sap B. Auditory measures including acoustic brainstem responses (ABR) and distortion product otoacoustic emissions (DPOAE) and contralateral suppression of DPOAEs (CS-DPOAE). Vestibular assessment was performed with a swimming test. Histologic analysis included light and electron microscopy (EM) and immunofluorescence and Alcian blue staining with mass spectrometry to detect acidic sulfated lipids.

Results

At both light and EM levels, inclusion body accumulation was seen in the KO mouse in Satellite cells surrounding spiral ganglion (SG) neurons from P1 month (P1 mo) onward, progressing into large vacuoles preceding satellite cell degeneration,

and followed by SG degeneration. EM also revealed reduced or absent myelin sheaths in SG neurons from P8mo onwards in these mice. Hearing loss was initially seen at P6mo and progressed thereafter for frequency specific stimuli while click responses became abnormal from P13mo onward. The progressive hearing loss correlated with the accumulation of inclusion bodies in the satellite cells and their subsequent degeneration. Outer hair cell numbers and efferent function measures (DPOAE and CS-DPOAE) were normal in the KO mice throughout this period. Alcian blue staining of the SG demonstrated that these inclusion bodies corresponded to sulfatide accumulation. In contrast, changes in the vestibular system were much milder and no physiologic deficits were seen.

Conclusion

These results demonstrate that loss of Saposin B function leads to progressive sulfatide accumulation in Satellite cells surrounding the SG neurons, leading to Satellite and Schwann cell degeneration, and subsequent SG degeneration with a resultant loss of hearing. Relative sparing of the efferent auditory and vestibular neurons suggest alternate glycosphingolipid metabolic pathways predominate in these other systems relative to the afferent auditory neuronal pathways.

PD - 205

Progressive Hearing Loss in Mice With a Mutation Affecting the Ubiquitin-Proteasome Pathway

Martin Schwander¹; Ulrich Mueller²; Suzan Harris¹

¹Rutgers University; ²The Scripps Research Institute

Background

Once damaged, auditory hair cells and neurons cannot be renewed and thus require a special maintenance strategy to protect themselves during pathological stress situations including mechanical and oxidative stress. As one possibility, they may maintain their functionality by constantly turning over their proteins. The regulated non-lysosomal degradation of proteins occurs via the ubiquitin-proteasome pathway and is essential for many cellular processes including the cell cycle, the regulation of gene expression, and responses to oxidative stress. Deregulation of the ubiquitin-proteasome system leads to loss of cellular homeostasis and has been implicated in age-associated illnesses ranging from cancer to neurodegenerative disorders. Comparatively little is known about the role of protein quality control in the function and dysfunction of the auditory system.

Methods

In a genetic screen, we have identified *ENU796* mice, which carry a missense mutation in Mambo, a putative component of the ubiquitin-proteasome pathway.

Results

We found that Mambo is expressed in cochlear hair cells, supporting cells, and spiral ganglion neurons. Measurement of the auditory brainstem response revealed that hearing loss in *ENU796* mutant mice is progressive in nature. While hair

cell development is unaffected in *mutant* mice, outer hair cell function is perturbed and hair cells eventually degenerate. In a yeast two-hybrid screen we identified putative interacting proteins for Mambo including components of the ubiquitin pathway.

Conclusion

In summary, our studies demonstrate a novel function for Mambo in maintaining the integrity of the neurosensory epithelium in the mammalian cochlea and suggest a function for the ubiquitin-proteasome pathway in this process.

PD - 206

Infrared Stimulation of the Ear Depends on Intact Hair Cells

Peter Baumhoff¹; Michael Schultz²; Nicole Kallweit²; Mika Sato¹; Alexander Krüger²; Tammo Ripken²; Thomas Lenarz¹; Andrej Kral¹

¹Institute of Audioneurotechnology (VIANNA), ENT Clinics, Hannover Medical School; ²Laser Zentrum Hannover e. V.

Background

In recent years, laser stimulation of the auditory system has attracted attention as a potential, more focused, alternative for conventional cochlear implants. The absorption of pulsed laser energy also induces sound waves in the absorber, an effect e.g. applied in optoacoustic imaging.

Methods

For a better understanding of laser induced sound within the auditory periphery, we utilized two pulsed laser sources (434 - 1961 nm, 5 ns, 6µJ; 1860nm, 20µs - 20 ms, 6 - 500 µJ) to perform ex-vivo and in-vivo experiments.

We investigated potential acoustic resonances caused by pulsed laser stimulation of the guinea pig tympanic bulla ex-vivo. An optical fiber was inserted into the tympanic bulla of a macerated skull through a bullotomy. The laser beam aimed at the basal cochlear turn. A calibrated Brüel&Kjaer microphone placed on the outer ear canal was used to record the sound generated by laser irradiation.

Multiunit responses of the Inferior colliculus (IC) were recorded in-vivo from 15 normal hearing ketamine-anesthetized guinea pigs. An optical fiber was positioned into a cochleosotomy or into the bulla. A 32channel Neuronexus-probe was stereotactically inserted into the IC and characteristic frequencies were determined with tonal stimulation.

Results

Fourier transform of ex-vivo acoustic recordings had distinct peaks at 5 kHz (resonance of the bulla) and smaller peaks at 8 and 13 kHz. For wavelengths absorbed in bone, the frequency spectrum was largely independent of pulse duration and wavelength.

Interestingly, IC activation by inner ear laser stimulation was strong at units with characteristic frequencies below 6 kHz for intra cochlear laser stimulation, but less for extra cochlear irradiation. The general activation pattern in the IC did not depend on wavelength, pulse duration or intra cochlear fiber orientation. This suggests an excitation by sound generated

within the auditory apparatus rather than an additional, neuronal mechanism of excitation. No responses to laser stimulation could be recorded from the IC of completely deafened animals, but the IC remained responsive to electric intra cochlear stimulation at normal thresholds in all cases tested.

Conclusion

We propose residual hearing as the most parsimonious explanation for any auditory response to laser pulses in the cochlea. Hearing status has to be precisely controlled in laser stimulation experiments, particularly at low frequencies. Laser induced sound within auditory structures seems to have strong low frequency content due to resonance, even though the short pulse duration could suggest otherwise.

PD - 207

Infrared Radiation Modulates Mitochondrial Membrane Potential in Cultured Neonatal Spiral and Vestibular Ganglion Neurons

Vicente Lumbreras; Suhrud Rajguru

University of Miami

Background

Previous studies have shown that infrared-evoked intracellular calcium transients in excitable cells may be driven by mitochondrial calcium cycling. The total force driving protons into the mitochondria is a combination of the mitochondrial membrane potential and the mitochondrial pH gradient. The membrane component of the electrochemical potential provides the charge gradient required for mitochondrial Ca²⁺ regulation and may explain the observed responses. In the present study, we analyzed pulsed infrared radiation (IR) evoked changes in the mitochondrial membrane potential of cultured neonatal spiral and vestibular ganglion neurons.

Methods

Experiments were performed on cultured spiral and vestibular ganglion neurons isolated from p2-p3 rat pups. After 4 days in culture, the neurons were loaded and incubated for 30 minutes with mitochondrial membrane potential sensors JC-1 (1.5 µM) or rhodamine 123 (10 µM). Oligomycin A and FCCP were used as positive controls. Pulsed IR (0.25-2 pulses/s) was delivered to the neurons using a 400 µm optical fiber connected to a Capella laser (wavelength = 1863 nm). Image sequences of the neurons under IR stimulation were collected using a confocal microscope. Image processing was done using ImageJ and Matlab to study whether the probes used increased or decreased their fluorescence intensity proportional to a stimulus that modulates the levels of mitochondrial membrane potential or ROS.

Results

The spiral and vestibular ganglion neurons responded with a pulse-by-pulse response in rhodamine 123 fluorescence synchronized with the low frequency IR pulses applied. In addition, the ratio of red/green fluorescence of JC-1 changed significantly with IR, suggesting an increase in the mitochondrial membrane potential. Positive control cultures incubated with FCCP and oligomycin showed similar changes in mitochondrial membrane potential.

Conclusion

Our results suggest that IR changed the mitochondrial membrane potential in the neurons. Changes in the mitochondrial membrane potential were synchronized with the applied IR pulses. Resultant reversible mitochondrial Ca^{2+} cycling is likely the primary source of the $[\text{Ca}^{2+}]_i$ transients evoked by IR. The results suggest that IR can be utilized to study the role of presynaptic mitochondria on Ca^{2+} dynamics, respiratory metabolism and events controlling synaptic transmission in the inner ear.

PD - 208

Elementary Properties of Potassium Channels Responsible for Potassium Extrusion in the Endolymphatic Sac

Maria Perez-Flores¹; Jun Zhou¹; H Dou¹; Hyo Jeong Kim¹; Choong ryoul Sihn¹; Ning Li¹; Andrea L Meredith²; Karl Pfeifer³; Ebenezer N Yamoah¹

¹University of California Davis; ²University of Maryland;

³NICHD

Background

The endolymphatic sac (ES) is an intracranial extension of the labyrinthine epithelium and has been demonstrated to serve as a secretory as well as a resorption porch. Thus, alterations of its functions induce distension of the compartment (hydrops), as seen in several inner ear diseases. The ES and inner ear are uniquely endowed with a specialized electrochemical milieu (high K^+ and 80 mV extracellular potential) not known in any other organ in mammals. While the cellular structures in the lateral wall of the cochlear duct have been identified to be the site for the generation of this "privileged" environment, the mechanisms underlying its formation remain unknown.

Methods

We isolated the ES from C57 mice, and performed high-resolution cell-attached single-channel and whole-cell configuration recording techniques.

Results

We found that ES cells expressed a large K^+ conductance (~ 230 pS), which was insensitive to the large conductance Ca^{2+} -activated K^+ channel ($\text{BK}/\text{IK}_{\text{Ca}}$) blockers (Paxilline, IbTx and ChTx). Additionally, the channel was expressed in ES cells of $\text{BK}^{-/-}$ mice. The channel was blocked when TEA and the KCNQ (Kv7) channel blocker, linopirdine, was applied and it was absent in ES cells of $\text{Kv7.1}^{-/-}$ mice. These data suggest that the channel may consist of the α -subunit of Kv7.1 subtype. We observed that high extracellular $[\text{K}^+]$ decreases the P_{open} of the channel, probably modifying the number of open and closed states. These findings and predictions were confirmed using mathematical simulations.

Conclusion

Here, we have identified a large conductance K^+ channel current at the apical aspects of the ES cells that confers K^+ extrusion into the endolymph. Using pharmacology and genetics, we demonstrate that Kv7.1 , with startlingly large conductance, is responsible for K^+ -diffusional potential in the ES.

Moreover, the gating of the K^+ channel is dependent on external K^+ , making it immaculately suitable to extrude K^+ into high K^+ endolymph. The exceptional features of Kv7.1 in the ES and the cochlear duct confer K^+ -diffusional potential necessary to establish and maintain the endocochlear potential.

PD - 209

Functional Role of the Glutamic Acid Residue (E290) in the Extracellular S5-Pore Linker of the Kv7.1 Channel

Karen Doyle¹; **Wenyang Wang²**; Hyo Jeong Kim²; Ebenezer Yamoah²

¹General Otolaryngology Clinic; ²UCDAVIS

Background

The endolymph of the scala media consists of a high K^+ concentration (~150 mM) and an extracellular potential of ~80 mV, making it an unfavorable environment for the flow of K^+ ions from marginal cells (MCs). Kv7.1 (KCNQ1) channels are localized at the apical aspects of the MC membrane, and the channel is the main diffusional pore responsible for K^+ export from MCs. The objective of this study is to identify features of Kv7.1 that allow it to operate in a less permissive environment. We identified Glutamic acid (E) residues at position 290, which lies in the S5-pore linker of the extracellular domain as a potential site for channel modulation. To explore the function of E290, we examined effects of cysteine-modifying reagents on channel gating.

Methods

Human Kv7.1 (hKv7.1) or hKv7.1 mutant DNA was transiently transfected in CHO cells. Whole-cell voltage clamp recordings were performed at room temperature. After control data were obtained, MTS reagent stock solutions were diluted with bath solution and applied immediately, or discarded if they were not used within 5 min.

Results

hKv7.1 currents were inhibited significantly more than expected from theoretical calculations based on the GHK flux equation by the elevation of extracellular K^+ . Higher levels of K^+ increased the fraction of channels in the inactivated state and decreased the fraction of channel recovery from the inactivated state. hKv7.1 LQT1-associated mutations E290K and E290A did not produce measurable currents. The E290C mutation dramatically decreased the effect of elevated extracellular K^+ . MTS reagents modified the mutated cysteine without altering channel functions. MTSES and MTSPeS increased the K^+ current and shifted the $G_{\text{K}}\text{-V}$ relationship to more negative voltages, whereas MTSEA and MTSET decreased the current and shifted the $G_{\text{K}}\text{-V}$ in the opposite direction.

Conclusion

Differences in the effects of MTS reagents can be attributed primarily to differential ionization and binding size. These results suggest that physiological changes in potassium concentrations may directly control the function of Kv7.1 and that E290 represents an essential role in the phenotypic properties of the channel in the cochlear duct.

Slow-Cycling Cells in Tympanic Border Cells Mostly Distribute Beneath Organs of Corti

Norio Yamamoto; Mirei Taniguchi; Takayuki Nakagawa; Juichi Ito

Graduate School of Medicine, Kyoto University

Background

Mammalian cochlear sensory epithelial cells are believed to possess minimal regenerative potential because they halt proliferation during late stage of embryogenesis and never regenerate after birth. This means that sensorineural hearing loss caused by the death of cochlear sensory epithelial cells is a permanent condition. However, stem or progenitor cells were recently identified in neonatal mice following dissociation of their inner ear organs. This suggests that regenerative therapy for sensorineural hearing loss may be possible. Unfortunately, dissociation distorts the microanatomy of the inner ear, making it difficult to determine the precise location of stem or progenitor cells in unaltered specimens. To develop new therapeutic approaches based on sensory epithelial cell regeneration, the location of these stem or progenitor cells must be elucidated.

Stem cells normally proliferate at a slow rate in adult organs. In fact, so-called label-retaining cells, or slow-cycling cells, of the brain and skin are recognized as stem cells. In previous study, using the exogenous proliferation marker, 5'-bromo-2'-deoxyuridine (BrdU) in combination with the endogenous proliferation marker Ki-67, we found that tympanic border cells (TBCs) contained BrdU-Ki67 double positive cells. Hence, TBCs, which are located beneath the basilar membrane *in vivo*, represent slow-cycling cells of the murine cochlea.

In this study, we tried to identify more specific location of slow-cycling cells within tympanic border cells.

Methods

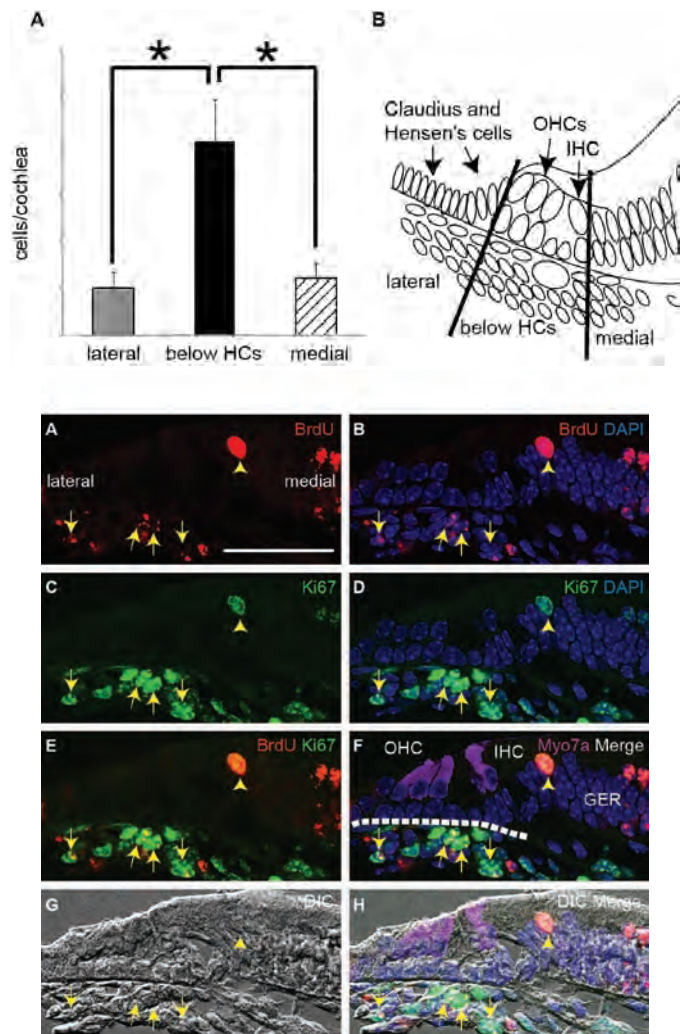
To label slow-cycling cells, we dissected the murine cochlea five days after injection of BrdU. Sectioned cochleae were immunostained with BrdU and Ki67. To determine which tympanic border cell populations contained the greatest numbers of slow-cycling cells, we divided the TBCs into three regions (a region below hair cells, a medial region, and a lateral region) based on their location within the basilar membrane.

Results

Roughly 66% of the slow-cycling cells were located in the region below the hair cells where both a vascular structure (i.e., a cochlear spiral modiolar artery) and the basement membrane of the basilar membrane exist.

Conclusion

The result suggests the possibility of stemness of the slow-cycling cells in the TBCs because the location of the slow-cycling cells resembles the microenvironment of stem cells, "stem cell niche".



Hair Cell Specific Expression of Clarin-1 is Sufficient to Prevent Auditory and Vestibular Dysfunction in the Mouse Model for Ear Disease in Usher Syndrome III

Ruishuang Geng¹; Suhasini Gopal¹; Daniel Chen¹; David Furness²; Kumar Alagramam¹

¹Case Western Reserve University; ²Keele University

Background

Usher syndrome III (USHIII) is an autosomal recessive disorder caused by mutation in the human Clarin-1 gene and characterized by progressive loss of hearing and vision. Previously, we showed that, in the mouse, 1) Clarin-1 mRNA is expressed as early as embryonic day 17 (e17), and its expression is restricted to ganglion and hair cells of the inner ear, 2) Clarin-1 mRNA is expressed in the inner ear during embryonic, neonatal and postnatal periods, 3) mutation in Clarin-1 affects hair cell function and bundle morphology as early as postnatal day 2 (P2), and 4) mutation in Clarin-1 results in profound hearing loss and variable degree of vestibular dysfunction by P21. In this project, we tried to answer two important questions: Is the expression of Clarin-1 in ganglion cells and hair cells necessary for hearing and balance? Is the ear dependent on postnatal expression of Clarin-1, or is Clar-

in-1 required only during ear development? Answers to these questions are important to understand the role of Clarin-1 in the inner ear and guide our efforts to develop therapies for USHIII patients.

Methods

A transgenic line was generated to limit expression of mouse Clarin-1 to hair cells between e12.5 and P0-3. The transgene construct, TgAC1, is composed of Atoh1 enhancer::beta-globin basal promoter fused to mouse Clarin-1 cDNA. We then generated mice carrying TgAC1 in the Clarin-1 knockout background. Offspring of this cross were designated 'KO-TgAC1.' Hearing (ABR), balance (VsEP) and hair cell morphology were evaluated in KO-TgAC1 mice at various time points.

Results

KO-TgAC1 mice displayed wild-type hearing and balance function at weaning age (P21). However, longitudinal evaluation showed progressive loss of function, starting around P25-30. At a young age (<P15), hair cells from the KO-TgAC1 mice are comparable to wild-type hair cells. However, stereocilia begin to show signs of degeneration by P21. Examination of older mice (>P21) showed that hair cells fail to maintain their stereocilia, and this is consistent with the phenotype observed in KO-TgAC1 mice. Our investigation also revealed potentially critical 5' and 3' untranslated sequence associated with mouse Clarin-1 mRNA.

Conclusion

The inner ear is dependent on prenatal and postnatal expression of Clarin-1. Specifically, maintenance of stereocilia in the mature ear depends on Clarin-1. Expression of Clarin-1 in the ganglion cells is not necessary for the development of hearing or balance in the mouse.

PD - 218

Mink (KCNE1) and MiRP2 (KCNE3) Modulate Large-Conductance Ca²⁺-Activated K⁺ Channel Gating

Sonja Pyott¹; **Wenyang Wang**²; Choong-Ryoul Sihm²; Hyo Jeong Kim²; Yoshihisa Sakai³; Bernd Sokolowski³; Ebenezer Yamoah²

¹University of North Carolina at Wilmington; ²UCDAVIS;

³University of South Florida

Background

Large-conductance voltage- and Ca²⁺-activated K⁺ (BK) channels are involved in the regulation of neurotransmitter release and neuronal excitability. In many neurons, the influx of Ca²⁺ through Ca²⁺ channels together with membrane depolarization promotes rapid activation of BK channels, making them well suited for a role in rapid repolarization during action potentials and in generation of brief afterhyperpolarizations. Previous studies have demonstrated that BK channels in hair cells exhibit rapid inactivation, but the mechanism remains unknown. The KCNE genes encode Mink-related peptides, which are small, single transmembrane domain peptides that associate with pore forming K⁺ channel subunits to form mixed complexes with unique characteristics. Here, we in-

vestigated the functional interaction between Mink-BK and MiRP2-BK, *in vitro* and *in vivo*.

Methods

Using channel subunits cloned from mouse and human, we expressed them in Chinese hamster ovary (CHO) cells. Whole-cell and cell-attached single channel voltage clamp recordings were performed on CHO cells, hair cells (HCs) and spiral ganglion neurons (SGNs) at room temperature. Mink, MiRP2 and BK channel expressions were examined using immunostaining in CHO cells, as well as HCs and SGNs.

Results

- 1) Mink and MiRP2 both modulate current density of the BK channel by reducing the whole-cell current magnitude.
- 2) Co-expression of MiRP2 and BK produced rapid inactivation of ensuing currents.
- 3) BK channels expressed alone revealed characteristic large conductance (> 200 pS) events with sustained openings.
- 4) Examination of the elementary properties of the BK-MiRP2 channel currents showed robust reduction in the P_{open} of the channel, with no apparent change in the unitary current amplitude.
- 5) Mink and MiRP2 co-localize with BK channels in plasma membranes and cytoplasm in CHO cells, HCs and SGNs.

Conclusion

We demonstrated that BK channels co-assemble with Mink or MiRP2, and serve as a mechanism to diversify the gating properties of BK currents. We surmise that BK channel subunit association with MiRP2 may underlie the inactivation mechanisms in HCs and SGNs.

PD - 219

Acf7 is a Hair-Bundle Antecedent, Positioned to Integrate Cuticular Plate Actin and Somatic Tubulin

Lana Pollock¹; Patrick Antonellis¹; Shih-Wei Chou¹; Ahmed Hassan²; Ruishuang Geng¹; Xi Chen¹; Elaine Fuchs³; Kumar Alagramam¹; Manfred Auer²; Brian McDermott¹

¹Case Western Reserve University; ²Lawrence Berkeley National Laboratory; ³The Rockefeller University

Background

The precise morphology of the mechanosensitive hair bundle requires seamless integration of actin and microtubule networks.

Methods

Here, using RNA-seq and *in situ* hybridizations, we identify *macf1* (encoding Acf7) as a gene whose cognate protein is positioned to bridge these distinct cytoskeletal networks in hair cells. We determined the hair-cell-localization pattern of Acf7 protein by imaging an Acf7-Citrine fusion protein in zebrafish and by immunolabeling of vestibular and cochlear mouse hair cells. To determine whether there are linkers that

join the CP actin to the microtubules near the apical surface of the hair cell, we used electron tomography.

Results

We show that Acf7 circumscribes, underlies, and is interwoven into the cuticular plate (CP), and it also encircles the basal body. In cochlear hair cells, ACF7 localization is graded, with the highest concentration near each fonticulus. During development and hair-cell regeneration, Acf7 precedes formation of the hair bundle and CP. Finally, electron tomography demonstrates that the ends of microtubules insert into the CP and are decorated with filamentous linkers connecting microtubules to the CP.

Conclusion

These observations are consistent with Acf7 being a linker protein, which may shape the hair cell's cytoskeleton early during ensemble genesis.

PD - 220

Inner Hair Cell Membranes in Three Dimensions: Links Between Membranes, Mitochondria and Vesicles

Anwen Bullen¹; Timothy West¹; Roland Fleck²; Jonathan Ashmore¹; Carolyn Moores³; Andrew Forge¹

¹*UCL Ear Institute*; ²*National Institute for Biological Standards and Control*; ³*Institute of Structural and Molecular Biology, Birkbeck College*

Background

The ribbon synapse is a specialised structure that allows for rapid and sustained release of neurotransmitter from inner hair cells (IHCs). The ribbon body is anchored to the membrane near the synapse, and vesicles are tethered to it. Those vesicles on the side of the ribbon facing the synapse form the readily releasable pool, which can be quickly released at the onset of stimulus. This pool is then replenished from other vesicles tethered to the ribbon. However, how the vesicles tethered to the ribbon are themselves replenished is not well understood. Previous work has suggested that the generation of synaptic vesicles may involve a membrane system linked to mitochondria, observed in the basal cytosol of the IHC. The aim of this work was to examine the three dimensional structure of this membrane system, to establish the potential roles it may play in neurotransmitter synthesis and transport.

Methods

Serial block face scanning electron microscopy (SBF-SEM) was used to examine the membrane system in IHCs from mice, and electron tomography was used for high-resolution characterisation of the membrane and its association with organelles.

Results

The membrane system was shown to be a large asymmetric structure that traversed the cell from the apical region to the base. The membranes were mainly concentrated at the periphery of the cell. Nearly every mitochondrion present in the infra-nuclear portion of the IHC was associated with these membranes. Electron tomography revealed links tethering the mitochondria to rough endoplasmic reticulum (RER)

membranes, and links between vesicles at the synaptic ribbon. Links between vesicles and between vesicles and RER were also observed both close to and distant from the ribbon.

Conclusion

These results show that an organised system of membrane and mitochondria traverses the IHC from the synthetic machinery at the apical end of the cell to its base. Mitochondria and vesicles are tethered to this membrane system by linkages both close to and distant from synaptic ribbons. These linkages may have both structural and functional significance. Vesicles were linked to each other at these membranes and at the synaptic ribbon; these linkages may be significant in directing the path of vesicles to the synapse and in orientation of vesicles for docking.

Author Index

(Indexed by abstract number and page number)

Author Index

Name	Abstract No.	Page No.
A., Robert	SY-036	130
Aarnisalo, Antti	PS-846	538
Abavisani, Ali	PS-142	79
Abboud, Nesrine	PD-159	423
Abdelhamed, Zakia	PS-184	99
Abdul-Latif, Mariam	PD-162	424
Abernathy, Matthew	PS-584	369
Abrams, Daniel	PD-200	543
Abrams, Kristina S.	PS-787	509
Abur, Defne	SY-015, PD-192	118, 549
Adams, Michelle	PD-081	268
Adamsky, Svetlana	PD-035	136
Adler, Henry	PS-580, PS-587	367, 371
Adunka, Oliver F	PS-247	171
Adunka, Oliver	PS-317, PS-559	207, 356
Aedo, Cristian	PS-087	52
Aerts, Johan	PS-732	480
Agrawal, Sumit	PS-506	331
Agrawal, Yuri	PS-425	260
Agterberg, Martijn	PD-185	436
Aguilar, Carlos	PD-131	294
Aguillon-Hernandez, Nadia	PS-468	313
Ahlf, Sönke	PD-198, PD-199	542, 543
Ahlstrom, Jayne B.	PS-221	158
Ahmad, Iram	PS-620	387
Ahmed, Sameer	PS-347	221
Ahmed, Zubair	SY-074	438
Ahn, Joong Ho	PS-202, PS-567	109, 360
Aiken, Steven	PS-055	36
Akanyeti, Otar	PD-022	125
Akeroyd, Michael A.	PD-186	436
Akil, Omar	PS-395, PS-676, PS-734, PD-204	245, 453, 482, 551
Akin, Faith	SY-039	263
Akinpelu, Olubunmi	PS-121	69
Akram, Sahar	PS-274	184
Akrofi, Kwaku	PS-843	537
Akyürek, Elkan	PS-608	381
Al-Malky, Ghada	PS-037	27
Alafuzoff, Irina	PS-302	198
Alagramam, Kumar	PS-379, PD-216, PD-219	237, 554, 555
Alain, Claude	PS-001	11
Alamilla, Javier	PS-307	201
Albrecht, Otto	PS-459	308
Alexander, Joshua	PS-048	32
Alghamdi, Fuad	PS-826	528
Alinaghikhani, Mahdieh	PD-129	293
Allan, Chris	PS-513	335
Allen, Paul	PS-412, PS-414, PS-612	254, 255, 383
Allen, Prudence	PS-513	335
Alliston, Tamara	PS-734	482
Allman, Brian	PS-280	187
Aloni, Ishita	PS-316	206
Alsamri, Jamal	PS-440	299
Altieri, Stefanie	PS-308, PD-163	202, 425

Name	Abstract No.	Page No.
Altman, Russ	PS-531	343
Altschuler, Richard	PS-017, PS-584, PS-819	18, 369, 525
Alvarado, Juan C	PD-168	427
Amr, Sami S.	PS-296	195
An, Yong-Hwi	PS-838	534
Ananthakrishnan, Saradha	PS-056, PS-444	37, 301
Anbuhl, Kelsey	PS-413, PS-414	254, 255
Andeol, Guillaume	PS-406	251
Anderson, Jeffrey	PD-130	293
Anderson, Paul	PS-151, PS-165	83, 90
Anderson, Samira	PS-010, PD-125	15, 291
Andringa, Tjeerd	PS-608	381
Anna, Osipovich	PD-160	423
Anson, Eric	PS-635	395
Anton, Alexander	PS-573	363
Antonellis, Patrick	PD-219	555
Anttonen, Tommi	PD-155	421
Anzai, Takashi	PS-773	502
Aoki, Mitsuhiro	PS-179	97
Applegate, Brian	PS-334	215
Appler, Jessica	SY-009, PD-161	2, 424
Arnold, Andreas	PS-723	475
Arnoldner, Christoph	PD-112, PS-712	285, 470
Aronoff, Justin	PD-182, PS-666	434, 448
Arshian, Milad	PS-210	113
Arweiler, Iris	PS-492	325
Asaka, Nakarin	PD-061, PS-623, PS-625	149, 389, 389
Ashida, Go	PS-452, PS-456	305, 307
Ashmore, J.F.	PS-073	44
Ashmore, Jonathan	PD-220	556
Ashush, Hagit	PD-035	136
Askew, Charles	PD-045	141
Asp, Filip	PS-410, PS-514	253, 335
Asprey, Joanna	PS-191	103
Assmann, Peter	PS-651	440
Atilgan, Huriye	PS-613	384
Au, Adrian	PS-379	237
Auduong, Priscilla	PD-130	293
Auer, Manfred	PD-219	555
Aushana, Yonane	PS-265	180
Avan, Paul	PD-065	151
Avci, Ersin	PD-026	132
Avkin-Nahum, Sharon	PD-035	136
Avraham, Karen B.	PD-007, PD-146	6, 412
Avraham, Karen	PD-098, PS-771	278, 501
Awad, Bshara	PS-267	181
Axe, David R.	PS-686	457
Ayala, Yaneri	PS-061	39
Aytekin, Murat	PS-415	255
Azadpour, Mahan	PS-660	445
Azaiez, Hela	PD-010, PS-286	8, 191
Başkent, Deniz	PD-028, PD-029, PS-490, PS-494, PS-608	133, 133, 324, 326, 381
Baasov, Timor	PS-374	235
Babcock, Thomas	PS-025	21
Back, Sang A	PS-561	357
Bae, Mi Ran	PS-251	173

Name	Abstract No.	Page No.
Bagger-Sjöbäck, Dan	PD-116	287
Bai, Jun-Ping	PS-547, PS-548	351, 351
Bai, Xiaohui	PS-288	192
Bailey, Erin	PS-369	233
Bair, Thomas	PS-300	197
Baird, Andrew	PD-110	284
Baird, Theodore	PS-584	369
Bakay, Warren	PS-073	44
Baker, Richard	PS-685	456
Bakhos, David	PS-263, PS-468	179, 313
Balaban, Carey	SY-042	263
Baldwin, Emily	PD-033	135
Ballester, Jimena	PS-458	308
Ballo, Aleksander	PD-022	125
Banai, Karen	PD-086	273
Bandyopadhyay, Sharba	PS-076, PS-220	46, 157
Bang, Mi-Young	PS-251	173
Banks, Matthew	PS-271	183
Bao, Jianxin	PS-283, PS-333	189, 214
Barascud, Nicolas	PS-602	378
Barbour, Dennis	PS-516	336
Barclay, Meagan	SY-010	3
Bardsley, Rhian	PS-167	91
Baris, Hagit	PD-007	6
Barker, Daphne	PS-685	456
Barnstedt, Oliver	PS-068	42
Barr-Gillespie, Peter	PS-183, SY-074	99, 438
Barrott, Darrell	PD-056	146
Barry, Kristin	PS-817	525
Barth, Jeremy	PS-304	200
Bartl, Klaus	PS-639	397
Bartles, James	PD-044	141
Bartlett, Edward	PS-022, PS-023, PD-128	20, 20, 292
Bartsch, Dusan	PD-105	282
Bas, Esperanza	PD-035, PS-386, PS-556, PS-566	136, 241, 355, 360
Basch, Martin	PS-191	103
Basinou, Vasiliki	PS-014	17
Baskent, Deniz	SY-050, PD-090, PS-474, PS-491, PS-661, PS-672	270, 275, 316, 324, 445, 451
Basta, Dietmar	PS-091, PS-422, PD-127	54, 258, 292
Basura, Gregory	PS-820	526
Batra, Ranjan	PS-461	309
Batrel, Charlene	PS-244	169
Baudo, Robert	PS-109	62
Baumann, Veronika	PS-681	454
Baumgartner, Robert	PS-171	93
Baumhoff, Peter	PD-206	552
Baxter, Michael	PS-429	261
Bazan, Nicolas	PS-715	471
Beaton, Kara	PS-635, PS-636, PS-637	395, 395, 396
Beckert, Michael	PS-105	60
Bee, Mark A.	PS-230	162
Beeler, Dina	PD-044	141
Behrens, Derik	PS-408	252
Beim, Jordan	PS-128	73
Beisel, Kirk	PS-631	392
Belakhov, Valery	PS-374	235

Name	Abstract No.	Page No.
Belding, Heather	PD-092	276
Belevich, Ilya	PD-155	421
Bellah, Meshell	PS-829	530
Belyantseva, Inna A.	PS-535	345
Belyantseva, Inna	SY-074	438
Ben-Shachar, Dorit	PS-374	235
Benard, Michel	PD-090	275
Benda, Lisa	PS-805	518
Bensaid, Mariem	PS-295	195
Bergevin, Christopher	PD-017, PD-077	123, 157
Berggren, Per-Olof	PD-001	4
Bermingham-McDonogh, Olivia	PD-047	142
Bernard, Abigail	PS-147	81
Bernhardt, Marlen	PD-110	284
Berninger, Erik	PS-410, PS-514	253, 335
Berns, Eric	PS-628	391
Bernstein, Joshua	PS-669	449
Bernstein, Leslie	PD-181	433
Bertroche, Tyler	PS-620	387
Best, Virginia	PS-149, PS-802	82, 517
Beurg, Maryline	PD-039	138
Beutelmann, Rainer	PS-063, PS-166	40, 90
Beyer, Lisa A.	PD-098	278
Beyer, Lisa A	PS-632	393
Beyer, Lisa	PS-358, PS-771	228, 501
Bharadwaj, Hari	PS-050, PS-054, PS-057, PS-088	33, 35, 37, 52
Bhatta, Puspanjali	PS-367, PS-563, PS-578	232, 358, 366
Bhonker, Yoni	PD-146	412
Bian, Shumin	PS-547	351
Bidelman, Gavin	PS-001, PS-049	11, 33
Bie, Xi	PS-460	309
Bieber, Rebecca	PS-194	104
Bierer, Julie	PS-473	315
Bierer, Steven	PS-473, PS-645	315, 400
Billig, Alexander	PS-801	516
Bing, Dan	PD-129, PS-554	293, 354
Bird, Jonathan	PS-303	199
Birkenhaefer, Ralf	PS-133	75
Bishop, Brian	PS-170	92
Bishop, Deborah	PS-061	39
Bitsche, Mario	PS-302	198
Bizley, Jennifer	PS-102, PS-268, PS-613	59, 181, 384
Black, Jennifer	PS-137	76
Blankenship, Chelsea	PS-488, PS-493	323, 325
Bledsoe, Sanford	PS-136	521
Bleeck, Stefan	PS-152, PS-400, PS-704	83, 248, 466
Bloomberg, Jacob	PS-420	257
Blosa, Maren	PS-673	451
Blum, Kerstin	PS-849	163
Blumensath, Thomas	PS-152, PS-704	83, 466
Blumer, Michael	PS-302	198
Boatman-Reich, Dana	PS-081	49
Boger, Erich	PS-303	199
Bohlen, Peter	PS-147, PS-160, PS-411, PS-703	81, 87, 253, 465
Bohorquez, Jorge	PS-556	355

Name	Abstract No.	Page No.
Bohuslavova, Romana	PS-178	96
Bok, Jin Woong	PS-370	233
Bok, Jinwoong	PS-313	204
Bonanni, Rossana Claudia	PS-504	330
Bonnet-Brilhault, Frédérique	PS-263	179
Booth, Kevin	PS-286	191
Boothalingam, Sriram	PS-125	71
Borck, Guntram	PS-299	197
Borenstein, Jeffrey	PS-716	472
Borland, Michael	SY-048	265
Borra, Tobias	PS-839	535
Borse, Vikrant	PS-563, PS-578	358, 366
Bosen, Adam	PS-612	383
Bosnyak, Daniel	PS-082	49
Böttger, Erik C.	PS-376	236
Botti, Teresa	PS-118, PS-120	67, 68
Botty, Astrid	PS-042	30
Boukari, Heithem	PS-376	236
Bouleau, Yohan	PD-102, PS-755	280, 493
Bourien, Jérôme	PS-243, PS-244, PS-354	169, 169, 226
Boven, Christopher	PS-240	168
Bowen, Macarena	PS-087	52
Bowl, Michael	PD-131	294
Boyden, Edward	PD-025, PS-257, PS-498	131, 176, 178
Bozorg-Grayeli, Alexis	PD-188	547
Bozorg-Grayelli, Alexis	PS-664	447
Bozovic, Dolores	PD-040, PD-041, PD-066, PD-178	139, 139, 151, 432
Braasch, Jonas	PS-168	91
Bradfield, Colby	PS-185	100
Brafman, Anat	PD-035	136
Braida, Louis D.	PS-142	79
Branchcheck, Joseph	PS-351	224
Brand, Yves	PD-018	123
Brandewie, Eugene	PS-791	511
Brantley, Jennifer	PD-035	136
Brecht, Elliott	PS-060	39
Breglio, Andrew	PS-042	30
Breinbauer, Hayo	PS-260	177
Bremen, Peter	PS-080, PS-084	48, 50
Brenowitz, Stephan	PS-239	167
Brewton, Dustin	PS-007	14
Briles, David	PS-733	481
Brimble, Mark	PD-034	136
Brimijoin, Owen	PS-161	87
Brimijoin, W. Owen	PD-186	436
Brossard, Julien	PS-252	173
Brown, Andrew	PS-104	60
Brown, Chris	PD-025, PS-498	131, 178
Brown, Christian	PS-250	172
Brown, Daniel	PS-776	503
Brown, Steve	PD-131	294
Brown, William	PS-231	163
Browne, Lorcan	PS-338, PS-339	217, 217
Brownell, William E.	PD-001	4
Brownstein, Zippora	PD-007	6
Bruce, Ian	PS-082	49

Name	Abstract No.	Page No.
Brugeaud, Aurore	PS-557	355
Bruneau, Nicole	PS-263	179
Brunette, Katyarina	PS-573	363
Brungart, Douglas	PS-149, PS-517, PS-669	82, 337, 449
Buchholz, Joerg M.	PS-802	517
Buchholz, Jörg	PD-091	275
Buchman, Craig A.	PS-247	171
Buchman, Craig	PS-317, PS-559	207, 356
Büchner, Andreas	SY-054	271
Buckey, Jay	PD-075	156
Buckiova, Daniela	PS-178	96
Budde, Stefan	PS-619	387
Budenz, Cameron L.	PS-253, PS-471	174, 314
Budenz, Cameron	PD-062	149
Buell, Elizabeth	SY-048	265
Buelles, Kerstin	PS-099	58
Buggins, Sarah-Louise	PS-167	91
Bullen, Anwen	PD-220	556
Buniello, Annalisa	PS-298	196
Burdiek, Laina M.	PS-726	477
Burford, James L.	PS-730	479
Burger, R. Michael	PS-106, PS-695, PS-696	61, 461, 462
Burgess, Ann	PS-646	401
Burgess, Martin	PS-405	250
Burgett, Katelyn	PS-729	479
Burghard, Alice	PS-075	45
Burianek, Brooke	PS-489	323
Burt, Rachel	PD-014	10
Buss, Emily	PS-789	510
Butler, Blake	PS-130	74
Buytaert, Jan	PS-732	480
Byun, Hayoung	PS-523	339
Cacace, Anthony	PS-845	538
Cacace, Anthony	263	
Cacace, Tony	SY-040	263
Cai, Qunfeng	PS-385, PS-582, PS-585, PD-167	240, 368, 370, 427
Cai, Rui	PS-079	48
Calabrese, Angela	PS-592	373
Caldwell, Meredith	PS-594	374
Calton, Melissa	PS-232	164
Campanelli, Dario	PS-554	354
Campbell, Kathleen	PS-028	23
Camper, Sally	PD-021	125
Canlon, Barbara	PS-014	17
Cao, Xiao-Jie	PS-692	460
Caras, Melissa	PS-524	206
Cardenas, Elena	PD-103	281
Carey, John	PS-216, PS-429	115, 261
Carey, Thomas E	PS-767	499
Carlile, Simon	PS-404, PS-405, PS-409	249, 250, 252
Carlyon, Robert	PD-024, PS-801	131, 516
Carney, Laurel H.	PS-077	46
Carney, Laurel	PS-170, PS-668, PS-787	92, 449, 509
Carpenter-Thompson, Jake	PS-843	537
Carr, Catherine	PS-452, PS-453, PS-456	305, 305, 307
Carr, Kali Woodruff	PS-528	341

Name	Abstract No.	Page No.
Carraro, Mattia	PS-340	218
Carter, Alexander	PS-429	261
Carter, Brian	PS-587	371
Cartwright, Daniel	PS-385	240
Caruso, Frank	PS-719	473
Carver, Courtney	PS-481, PS-482, PS-594	319, 320, 374
Case, Benjamin	PS-358	228
Caspari, Franziska	PS-681	454
Caspary, Donald	PS-079, PS-816	48, 524
Castellucci, Gregg	PS-024	21
Catanzaro, Michael	PS-210	113
Catherine, Connelly	SY-011	3
Cauchi, Marjia	PS-616	385
Cazettes, Fanny	PS-101	58
Cederroth, Christopher	PS-014	17
Celaya, Adelaida	PD-153	420
Chabot, Nicole	PS-130	74
Chadwell, Brad	PS-824	527
Chadwick, Richard S.	PD-176	431
Chait, M.	PS-602	378
Chait, Maria	PS-616, PD-213	385, 546
Chakchouk, Imen	PS-295	195
Chalupper, Josef	PS-492	325
Chambers, Claire	PS-274	184
Chan, Mariana Remedios	PS-713	470
Chandler, Helena	PS-430	262
Chandra, Rashmi	PS-535	345
Chang, Jiwon	PS-555	354
Chang, Jolie	PS-734	482
Chang, Qing	PS-384, PS-718	240, 473
Chang, So-Young	PS-392	243
Chang, Wenhan	PS-734	482
Charaziak, Karolina	PS-114, PS-115, PS-119, PD-071	65, 65, 68, 154
Chatterjee, Monita	PD-083, PS-489	269, 323
Chatterton, Paul	PD-067	152
Chavez, Eduardo	PS-189, PD-018	102, 123
Cheatham, Mary Ann	PS-327, PS-328, PS-366	211, 212, 231
Chen, Ai-Ting	PD-085	270
Chen, Aiting	PS-475	316
Chen, Brian	SY-012	3
Chen, Collin	PS-324	210
Chen, Daniel	PS-379, PD-216	237, 554
Chen, Fangyi	PS-539	347
Chen, Guang-Di	PS-027, PS-811, PS-814	23, 522, 523
Chen, Jenny	PS-257	176
Chen, Jin	PD-120, PS-765	289, 498
Chen, Jing	PD-120, PS-765	289, 498
Chen, Joseph	PD-080	267
Chen, Jun	PS-359, PS-360, PS-375	228, 229, 235
Chen, Kejian	PS-041	29
Chen, Leon	PS-576	365
Chen, Pei-Lung	PS-769	500
Chen, Ping	PD-146	412
Chen, Taosheng	PD-034, PS-378	136, 237
Chen, Tsung-Yu	PS-336	216
Chen, Wei Chun	PS-336, PD-122	216, 290

Name	Abstract No.	Page No.
Chen, Xi	PD-219	555
Chen, Yen-Jung Angel	PS-713	470
Chen, Zheng-Yi	PD-032, PD-068	135, 152
Cheng, Alan	PS-193, PD-134	104, 406
Cheng, Jeffrey Tao	PS-745	488
Cheng, Jeffrey	PS-739, PS-742, PS-744	484, 486, 487
Cheng, Weihua	PS-043, PS-270	30, 182
Cheng, Yen-fu	PS-194	104
Chertoff, Mark	PS-019, PS-236, PS-318	19, 166, 207
Chessum, Lauren	PD-131	294
Cheung, Linda	PS-301	198
Cheung, Steven	SY-005	1
Chhan, David	PS-743, PD-193	487, 549
Chi, Fang-Lu	PD-060	148
Chi, Fanglu	PS-533, PD-165	344, 426
Chiamvimonvat, Nipavan	PS-336	216
Chiang, David	PS-633	394
Chickov, Boris	PS-249	172
Chidavaenzi, Robstein	PD-048	143
Chihara, Yasuhiro	PS-776	503
Chin, Anthony	PS-737	483
Chintanpalli, Ananthakrishna	PS-221	158
Chiu, May S.	PS-421, PS-520	258, 338
Cho, Hyong-Ho	PS-181	98
Cho, Soyoun	PS-751	491
Cho, Sung-Il	PS-029	24
Cho, Yang-Sun	PS-523	339
Cho, Yong-Beom	PS-181	98
Cho, Young Mi	PS-294	194
Choi, Ah-Nam	PS-032	25
Choi, Byung Yoon	PS-294	194
Choi, Chul-Hee	PS-020, PS-571	19, 362
Choi, Dongseok	PS-728	478
Choi, Inyong	PS-088	52
Choi, Jae Young	PS-188, PS-251, PS-313, PS-370, PS-779, PS-782	101, 173, 204, 233, 505, 507
Choi, Yang Sun	PS-032	25
Choi, Young-Ho	PS-181	98
Chou, Shih-Wei	PD-219	555
Choung, Yun-Hoon	PS-372	234
Chow, Cynthia	PS-626	390
Choy, Kristel	PS-574	363
Christensen-Dalsgaard, Jakob	PS-683	455
Christensen, Anders	PD-072	154
Christensen, Julie	PD-083	269
Christianson, Bjorn	PS-447	302
Christianson, Gestur	PS-095	55
Chumak, Tetyana	PS-178	96
Chung, Jong Woo	PS-428, PS-567, PS-842	261, 360, 536
Chung, Juyong	PS-372	234
Chung, Phil-Sang	PS-392	243
Chung, Won-Ho	PS-523	339
Chung, Yoojin	SY-067, PS-653, PS-654	415, 441, 442
Churchill, Tyler	PS-175	95
Ciullo, Marina	PS-284	189
Clark, Brian	PS-416	256
Clark, J. Jason	PS-620	387

Name	Abstract No.	Page No.
Clarke, Jeanne	PS-491	324
Clarkson, Cheryl	PS-694	461
Clavier, Odile	PD-075	156
Cloninger, Christina	PS-412	254
Coates, Harvey	PD-080	267
Coffey, Bethany	PS-377	236
Coffin, Allison	PS-381, PS-383	238, 239
Cohen, Bernard	PS-207, SY-025	111, 122
Cohen, David	PS-387	241
Cohen, Helen	PS-420, PS-421	257, 258
Cohen, Shira	PS-807	519
Cohn, Edward	PS-573	363
Colburn, Steven	PS-045	31
Cole, Stacey	PS-303	199
Coleman, John	PS-041	29
Colesa, Deborah J.	PS-253, PS-471	174, 314
Coling, Donald	PS-582	368
Conaway, LaShardai N.	PD-099	279
Conaway, LaShardai	PS-304	200
Concas, Maria Pina	PS-284	189
Cone, Barbara	PS-093	54
Congdon, Sharon	PS-420	257
Contreras, Julio	PD-153	420
Convertino, Victor	SY-023	121
Cook, Rebecca	PS-332	214
Coombes, Stephen	PS-701	464
Cooper, Alan	PS-307	201
Cooper, Morris	PS-028	23
Coppola, Giovanni	PS-557	355
Corey, David P.	PD-164, SY-079	425, 440
Corey, David	PD-042, PD-067, PD-068, PD-069, SY-074	140, 152, 152, 153, 438
Corfas, Gabriel	SY-033	129
Corns, Laura	PS-774	503
Corsten-Janssen, Nicole	PD-012	9
Cosentino, Stefano	SY-051, PS-483	271, 320
Cosgrove, Dominic	PS-301	198
Cotin, Stéphane	PD-188, PD-190	547, 548
Cotter, Lucy	PS-210	113
Coventry, Brandon	PS-022	20
Cox, Brandon	PS-192, PS-200, PS-201, PS-215, PS-351	103, 108, 108, 115, 224
Cox, Weston	PS-174	94
Cramer, Karina	PD-162	424
Crane, Benjamin	PS-634, PS-641	394, 398
Crawley, Jacqueline	PS-074	45
Creoglu, Sebahattin	PS-740	485
Crone, Nathan	PS-081	49
Cronin, Scott	PD-135	406
Cummins, Graham	PS-065	262
Cunningham, Lisa L.	PS-042	30
Cunningham, Lisa	PS-390, PD-139	242, 409
Cureoglu, Sebahattin	PS-733	481
Curral, Benjamin	PD-013	10
Curthoys, Ian	PS-646, PS-776	401, 503
Cushing, Sharon L	PS-643	399
Cuthbertson, David	PS-633	394
D'Alessandro, Lisa	PS-058	38

Name	Abstract No.	Page No.
D'Amato, Luisa	PS-120	68
Dahmen, Johannes	PS-068, PS-096, SY-044	42, 56, 264
Dai, Chenkai	PS-202	109
DAI, Chunfu	PS-203, PS-223	109, 159
Dai, Huanping	PS-789	510
Dai, Lengshi	PS-052	34
Dai, Mike Jau Jiing	PS-534	345
Dai, Pu	PS-281, PS-297, PD-085, PS-475	188, 196, 270, 316
Dai, Qinglei	PS-281	188
Dalbert, Adrian	PS-477, PD-177, PS-748	317, 431, 489
Dalhoff, Ernst	PS-112, PS-123	64, 70
Dallos, Peter	PS-327, PS-328	211, 212
Dan, Ki Soon	PS-032	25
Danesh, Ali	PS-510	333
Daniel, Sam J.	PS-749	490
Daniel, Sam J	PS-121	69
Daniel, Sam	PS-750	490
Darbro, Benjamin	PS-300	197
Darrow, Keith	PS-062, PD-025, PS-250, PS-498	40, 131, 172, 178
Darville, Lancia	PS-176	95
Dau, Torsten	PS-492, PS-509, PS-611	325, 333, 383
David, Alais	PS-404	249
David, Stephen	PS-097, PS-277, PS-278, PS-279, PS-445	56, 186, 186, 187, 301
Davies-Venn, Evelyn	PS-792	511
Davis, Matthew	PS-801	516
Davis, Robin	SY-036	130
Dawes, Piers	PS-830	530
Dawson, Sally	PS-037, PD-131, PD-154	27, 294, 420
de Boer, Egbert	PS-539	347
De Greef, Daniel	PS-732	480
De Jongh, Miranda	PS-037	27
de Monvel, Jacques Boutet	PD-102	280
De Ridder, Dirk	SY-048	265
De Spirito, Marco	PS-382	239
de Vreede, Desiree	SY-069	416
Dean, Clare	PS-576	365
Decker, Margaret	PS-622	388
Decraemer, Willem F.	PS-749	490
Deeks, John	PD-024	131
Deerinck, Tom	SY-012	3
dela Rosa, Lourdes Rodriguez	PD-153	420
Delano, Paul H	PS-087	52
Delgutte, Bertrand	PS-465, SY-067, PS-653, PS-654	311, 415, 441, 442
Delimont, Duane	PS-301	198
Della Santina, Charles	PS-202, PS-216, PS-261	109, 115, 177
Della Santina, Charley	PS-429	261
Dent, Micheal	PS-148, PS-592, PS-595	81, 373, 375
Dent, MichealL.	PS-589	372
Depireux, Didier	PD-113	285
DeRemer, Susan	PS-819	525
derNederlanden, Christina Vanden Bosch	PD-088	274
Deroche, Mickael	PD-083, PS-489	269, 323
Derudas, Marco	PD-064	150

Name	Abstract No.	Page No.
Desloge, Joseph G.	PS-142	79
Desmadryl, Gilles	PS-243	169
Desmonds, Terri	PD-064	150
Dewan, Isha	PS-185	100
Dewey, James	PS-127	72
Dewey, Rebecca	PS-134	76
Dhar, Sumitrajit	PS-127	72
Dhooge, Ingeborg	SY-054	271
Di Stazio, Mariateresa	PD-008	7
Diao, Shiyong	PD-034, PS-627	136, 390
Diaz, Rodney	PD-058, PD-100	147, 279
Dickinson, Danielle	PS-167	91
Diedesch, Anna	PS-401	248
Dietz, Beatrice	PS-695	461
Dietz, Mathias	PS-457, PD-180, PD-187	307, 433, 437
Digiacomo, Rita	PD-163	425
Dillon, Harvey	PS-802	517
Dimitrijevic, Andrew	PD-082, PS-440	268, 299
Dimitrov, Alexander	PS-065	262
Ding, Bo	PS-008, PS-009	14, 14
Ding, Dalian	PS-157, PS-342, PS-361, PS-362, PS-363, PS-582, PS-586	86, 219, 229, 229, 230, 368, 370
Ding, Nai	PS-437, PS-441	297, 299
Dingman, Robert	PS-131, PS-707	74, 467
Dirckx, Joris	PS-732	480
Dirks, Coral	PS-793	512
Dobrev, Ivo	PS-742	486
Dodd, Nicole	PS-178	96
Doesburg, Sam M.	PS-472	315
Doetzlhofer, Angelika	PD-142	410
Doherty, Joni	PS-344	220
Doi, Katsumi	PS-426	260
Dolan, David	PS-017, PS-767, PS-819	18, 499, 525
Dolležal, Lena-Vanessa	PS-154	84
Dolmetsch, Ricardo	PS-074	45
Donato, Roberta	PS-059, PS-458	38, 308
Dondzillo, Anna	PS-459	308
Dong, Jing	PS-281	188
Dong, Wei	PS-116, PD-172	66, 429
Doolittle, Lauren	PS-813	523
Dorning, Joanne	PD-131	294
Dos Santos, Aurélie	PS-527	341
Dottori, Mirella	PS-030, PS-624	24, 389
Dou, H	PD-208	553
Dougherty, Brian	PS-258	176
Doyle, Karen Jo Doyle	PS-352	225
Doyle, Karen	PS-336, PD-124, PD-209	216, 290, 553
Doyle, Philip	PS-506	331
Dragicevic, Constantino	PS-087	52
Dreisbach, Laura	PS-113	64
Drennan, Ward	PS-671	450
Dresbach, Thomas	PS-697	462
Drescher, Dennis	PD-107, PS-761, PS-762	283, 496, 496
Drescher, Kristen	PS-573	363
Drescher, Marian	PD-107, PS-762	283, 496
Drex1, Markus	PS-110, PS-117	63, 66
Drexler, Daniel	PS-831	531

Name	Abstract No.	Page No.
Drga, Vit	PS-146	80
Druckenbrod, Noah	PS-309	202
Drummond, Meghan	PS-303	199
Du, Xiaoping	PS-043, PS-270, PS-571	30, 182, 362
Duan, Chongwen	PS-366	231
Dubno, Judy R.	PS-221	158
Dubno, Judy R	PS-006	13
Duggan, Anne	PD-160	423
Duifhuis, Hendrikus	PD-071	154
Dulon, Didier	PD-102, PS-755	280, 493
Dumont, Rachel	PS-183	99
Duncan, Keith	PD-135	406
Duncan, R. Keith	PS-629	391
Duncan, Robert	PS-622	388
Duret, Guillaume	PD-005, PS-551	5, 352
Durham, Dianne	PS-019, PS-391, PS-823	19, 243, 527
Duriez, Christian	PD-188, PD-190	547, 548
Durruthy-Durruthy, Robert	PS-531	343
Duscha, Stefan	PS-376	236
Dutta, Jyotishka	PD-128	292
Dutta, Kelsey	PS-061	39
Dwyer, Noel	SY-070	416
Dylla, Margit	PS-147, PS-160, PS-411, PS-703	81, 87, 253, 465
Earl, Brian	PS-236, PS-318	166, 207
Easter, James	PD-195	550
Easter, Kyle	PS-656	443
Easwar, Vijayalakshmi	PS-055	36
Eatock, Ruth Anne	PD-036, PS-242	137, 169
Ebeid, Michael	PS-631	392
Eberle, Jennifer	PS-017, PS-819	18, 525
Eckert, Mark A.	PS-006	13
Eckhard, Andreas	PS-527	341
Eckrich, Stephanie	PD-105	282
Eckrich, Tobias	PS-849	163
Ed, Hight	PD-025	131
Edeline, Jean-Marc	PS-265, PS-507	180, 332
Edelmann, Stephanie E.	PD-164	425
Edge, Albert S. B.	PS-557	355
Edge, Albert	PS-190, PS-194, PD-036, PD-059, PS-242, PS-538, PS-570	102, 104, 137, 148, 169, 346, 361
Edge, Roxanne	PS-366	231
Edmondson-Jones, Mark	PS-830	530
Edwards, Jan	PS-604	379
Effertz, Thomas	SY-075	438
Egami, Naoya	PS-418, PS-777	257, 504
Egger, Katharina	PS-657	443
Eggermont, Jos	SY-029	127
Eggleston, Jessica	PD-079	267
Eiber, Albrecht	PS-741	486
Eipert, Lena	PS-072	44
Eisenman, David J.	PD-010	8
Eisenman, David	PD-011	9
El-Amraoui, Aziz	PD-065	151
EL-HASSAR, Lynda	PS-674	452
Elgoyhen, Ana Belén	PS-760	495
Elgueda, Diego	PS-277, PS-431	186, 294

Name	Abstract No.	Page No.
Eliades, Steven	PS-081	49
Elkan, Tal	PD-146	412
Elkon, Ran	PD-010, PD-011	8, 9
Ellerbee, Audrey	PS-334	215
Ellinger, Chris	PS-209	112
Elliott, Maxwell	PS-128	73
Ellisman, Mark	SY-012	3
Engdahl, Bo	PS-520	338
Engel, Jutta	PS-849, PD-104, PD-105	163, 281, 282
Engleder, Elisabeth	PD-112, PS-712	285, 470
Englitz, Bernhard	PS-274, PS-435	184, 296
Epp, Bastian	PS-509, PS-545	333, 350
Epstein, Michael	PS-159	87
Eramo, Sara L.M.	PS-382	239
Erath, Sebastian	PS-402	249
Erdogmus, Deniz	PS-441	299
Ernst, Arne	PS-422, PD-127	258, 292
Ernst, Arneborg	PS-091	54
Ervasti, James	PD-067	152
Erwood, Andrew M.	PD-078	266
Eshraghi, Adrien	PS-259, PS-386, PS-388, PS-556	177, 241, 242, 355
Eshtan, Sarah Jacob	PD-056	146
Esposito, Elise	PS-106	61
Esser, Karl-Heinz	PS-564	359
Esterberg, Robert	PD-137, PD-138	408, 408
Ethell, Iryna	PD-201	544
Eversole, Robert	PS-584	369
Ewert, Donald	PS-270	182
Ewert, Donalt	PS-043	30
Ewert, Stephan D.	PD-187	437
Ewert, Stephan	PS-805	518
Fabiani, Monica	PS-137	76
Fadeeva, Elena	PS-249	172
Falchier, Arnaud	PS-255	175
Faletra, Flavio	PD-008	7
Fallon, James	PS-254, PS-478	174, 318
Fang, Jie	PD-001, PS-582, PS-585	4, 368, 370
Fang, Qing	PD-021	125
Farahmand, Rosemary B.	SY-015	118
Farahmand, Rosemary	PS-722, PD-192	475, 549
Faria, Andreia V.	PS-837	534
Farris, Hamilton	PS-715	471
Fathabad, Somayeh	PD-124	290
Fausch, Bjoern Christian	PS-748	489
Fausch, Christian	PD-177	431
Feeney, M.	PS-727	478
Feeney, Patrick M.	PS-387	241
Feinstein, Elena	PD-035	136
Fekete, Donna M.	PD-099	279
Felix, Sarah	PS-246	170
Fell, Barbara	PD-104	281
Fellows, Abigail	PD-075	156
Ferber, Alexander	PS-413, PS-414	254, 255
Ferger, Roland	PS-098	57
Ferman, Sara	PS-807	519
Fernandez, Katharine A.	PS-570	361

Name	Abstract No.	Page No.
Fernandez, Katharine	PS-560	357
Fernando, Augusta	PS-310, PS-628, PS-630	203, 391, 392
Feron, Francois	PD-159	423
Ferrary, Evelyne	PD-188, PD-190	547, 548
Ferrieri, Patricia	PS-733	481
Fetoni, Anna	PS-382	239
Fettiplace, Robert	PD-039	138
Fiebig, Pamela	PS-258	176
Fiering, Jason	PS-716	472
Figacz, Alex	PS-293	194
Finkbeiner, Steven	SY-058	272
Fiorillo, Benjamin	PS-225	160
Firpo, Matt	PS-389	242
Firszt, Jill	SY-070	416
Fischer, Alexander	PS-680	454
Fischer, Brian	PS-101, PS-174	58, 94
Fischer, Nathalie	PS-364	230
Fisher, Tyson	PS-761	496
Fishman, Yonatan	PS-443	300
Fitzakerley, Janet	PS-780	506
Fitzgerald, Matthew	PS-652	441
Fitzgerald, Tracy S.	PS-042	30
Fitzgerald, Tracy	PS-535	345
Fitzpatrick, Denis	PS-727	478
Fitzpatrick, Douglas C.	PS-247	171
Fitzpatrick, Douglas	PS-317, PS-559	207, 356
Fleck, Roland	PD-220	556
Fleming, Justin	PS-412, PS-612	254, 383
Flores, Emma	PD-148	417
Flowers, Elizabeth	PS-810, PS-813	521, 523
Floyd, Robert	PS-270	182
Folmer, Robert	PS-518	337
Fontaine, Bertrand	PS-702	465
Fontbonne, Arnaud	PD-159	423
Forge, Andrew	PD-220	556
Forgues, Mathieu	PS-559	356
Forgues, Matthieu	PS-317	207
Formby, Craig	SY-031	127
Formeister, Eric	PS-247, PS-317, PS-559	171, 207, 356
Forrence, Alex	PS-790	511
Forsythe, Ian	PS-449, PS-684	303, 456
Fortnum, Heather	PS-830	530
Foster, Nichole	PS-071	43
Foster, Norman	PD-130	293
Foster, Sarah	PS-568	360
Fox, Alex	PS-404	249
Fox, Apollonia	PS-642	399
Fox, Daniel	PS-028	23
Francis, Nikolas	PS-431	294
Francis, Shimon	PD-070, PS-562	153, 357
Frank, Thomas	SY-007	2
Franken, Tom	PS-455	306
Free, Rolien	PD-028, PD-029, PS-490	133, 133, 324
Fregia, Melody	PS-420	257
Freyman, Richard	PS-399	247
Friauf, Eckhard	PS-450, PS-680	304, 454
Frick, Claudia	PS-226	160

Name	Abstract No.	Page No.
Fridberger, Anders	PD-001, PD-002, PD-116, PS-521, PS-539	4, 4, 287, 339, 347
Fridman, Gene	PS-261	177
Fiedl, Karl E.	PS-572	362
Friedland, David	PS-665	447
Friedman, Thomas B.	PS-535	345
Friedman, Thomas	PS-303, SY-074	199, 438
Friedrich, Björn	PS-598	376
Friedrich, Jr., Victor L.	PS-206	111
Frisina, Robert D.	PS-008, PS-009, PS-011	14, 14, 15
Frisina, Robert	PS-283	189
Friston, K. J.	PS-602	378
Fritz, Jonathan	PS-097, PS-277, PS-431, PS-446, SY-061	56, 186, 294, 302, 404
Fritzsche, Bernd	PS-312, PS-529	204, 342
Fritzsche, Bernd	128	
Fröhlich, Felix	PS-091	54
Frolenkov, Gregory I.	PD-164	425
Frolenkov, Gregory	SY-074, SY-076, SY-077	438, 439, 439
Frolov, Daniil	PS-331	213
Frydman, Moshe	PD-007	6
Fu, Qian-Jie	PS-474	316
Fu, Qiang-jie	PS-493	325
Fuchs, Elaine	PD-219	555
Fuchs, Paul	PD-108, PD-119, PD-152	283, 288, 419
Fuentes-Santamaria, Veronica	PD-168	427
Führ, Hartmut	PS-464	311
Fuhr, Martin	PS-450	304
Fuji, Hironori	PS-427	261
Fujii, Hironori	PS-036, PS-423	27, 259
Fujimoto, Chisato	PS-199, PS-418	107, 257
Fujita, Takashi	PD-149	417
Fujita, Takeshi	PS-015, PS-343	17, 219
Fujita, Tomoki	PS-394	244
Fukuda, Fumi	PS-526	340
Fukuda, Shinjiro	PS-840	535
Fukuda, Yuriko	PS-343	219
Fukushima, Hisaki	PS-505	331
Fuller, Christina	PD-028, PD-029	133, 133
Funabiki, Kazuo	PS-219, PS-456	117, 307
Funakubo, Megumi	PS-773	502
Funnell, Robert	PS-750	490
Funnell, W Robert J	PS-121	69
Funnell, W. Robert J.	PS-749	490
Furlong, Cosme	PS-739, PS-742, PS-744	484, 486, 487
Furness, David	PD-039, PS-380, PS-583, PD-216	138, 238, 369, 554
Furrer, Stephanie	PS-200, PS-215	108, 115
Furukawa, Shigeto	PS-143, PS-264, PS-599, PS-606, PS-609, PS-615	79, 180, 377, 380, 382, 385
Gabor, Franz	PD-112, PS-712	285, 470
Gabrielaitis, Mantas	SY-007	2
Gabriele, Mark	PS-070	43
Gadziola, Marie	PS-089	53
Gagner, Christine	PS-113	64
Galazyuk, Alexander	PS-824, PS-825, PS-826	527, 528, 528
Galazyuk, Olga	PS-824	527
Gale, Jonathan	PD-064, PD-139, PD-154	150, 409, 420

Name	Abstract No.	Page No.
Gallun, Frederick G.	PD-092	276
Gallun, Frederick	PS-518	337
Galvin, John J	PD-029	133
Galvin, John	PS-474	316
Gan, Rong	PD-191, PD-194	548, 549
Gander, Phillip	PS-275, PD-202	185, 544
Gandolfi, Michele	PS-576	365
Gandour, Jackson	PS-444	301
Gao, Xiang	PD-183	434
García-Añoveros, Jaime	PD-160	423
Garcia-Lazaro, Jose'	PS-059	38
Garcia-Pino, Elisabet	PS-681, PS-682	454, 455
Garinis, Angela	PS-727	478
Garinis, Angie	PS-387	241
Garnham, Carolyn	PS-388, PS-556	242, 355
Garret, Goss	PS-566	360
Gasparini, Paolo	PD-008, PS-284, PS-285, PD-131	7, 189, 190, 294
Gater, Rachel	PS-583	369
Gatto, Maria Pia	PS-504	330
Gattu, Tilak	SY-040	263
Gaudrain, Etienne	PS-491, PS-494	324, 326
Gazula, Vali	PS-674	452
Geary, Robert	PS-425	260
Gebhart, Mathias	PD-105	282
Geisinger, Darío	PS-831	531
Geisler, C. Daniel	PS-544	349
Geleoc, Gwenaelle	PD-063	150
Geng, Ruishuang	PD-216, PD-219	554, 555
George, Sahara	PS-440	299
Georgescu, Maria-Magdalena	PD-065	151
Gerig, Rahel	PD-177, PS-741, PS-748	431, 486, 489
Gerka-Stuyt, John	PS-379	237
Gessele, Nikodemus	PS-682	455
Gevorgyan, Haykanush	PS-730	479
Ghelani, Seema	PS-689	458
Gherardi, Monica	PS-504	330
Ghoddoussi, Farhad	PD-170	428
Ghosh, Sumana	PS-563, PS-578	358, 366
Gileles, Felicia	PD-141	410
Gilels, Felicia	PS-287, PS-764	191, 497
Gilkey, Robert	PS-396	245
Gill, Ruth	PS-708	467
Gillespie, Deda	PS-307	201
Giraud, Anne-Lise	PD-203	545
Giraudet, Fabrice	PD-065	151
Girotto, Giorgia	PD-008, PS-284, PS-285, PD-131	7, 189, 190, 294
Glassman, E. Katelyn	PS-652	441
Glassman, Elizabeth	PS-480	319
Gloeckner, Cory	PS-132	75
Glowatzki, Elisabeth	PS-213, PS-224, PD-152	114, 159, 419
Glueckert, Rudolf	PS-302, PS-364	198, 230
Glyde, Helen	PS-802	517
Gnansia, Dan	PS-664	447
Goebel, Joel	PS-416	256
Goeckel, Tom	PS-398	247
Goetz, Jack	PS-675	452

Name	Abstract No.	Page No.
Goetz, Sarah	PS-733	481
Goktug, Asli	PS-378	237
Gold, Jeff	PS-387	241
Golden, Erin	PD-142	410
Golding, Nace L.	PS-451, PS-455	304, 306
Golding, Nace	PS-462	310
Goldstein, Bradley	PD-081, PS-566	268, 360
Goldwyn, Joshua	PS-454	306
Goman, Adele	PS-167	91
Gomez-Casati, Maria Eugenia	SY-033	129
Goncalves, Stefania	PS-515	336
Gondo, Yoichi	PS-289	192
González, Antonia	PS-337	216
Gonzalez, Manuela	PS-831	531
Goodman, Shawn	PS-124, PS-126	71, 72
Goodman, Spencer	PS-303	199
Goodrich, Lisa	SY-009, PS-309, PD-161	2, 202, 424
Goodyear, Richard	PD-064, PS-327, PS-328	150, 211, 212
Gopal, Suhasini	PD-216	554
Gorai, Shigeki	PS-841	536
Gordon, Brian	PS-137	76
Gordon, Karen A.	PS-472	315
Gordon, Karen A	PS-643	399
Gordon, Karen	SY-069, PS-655	416, 442
Goren, Alison	PS-489	323
Goto, Akihiro	PS-219	117
Göttfert, Fabian	SY-007	2
Gottlieb, Assaf	PS-531	343
Gottshall, Kim	PS-417	256
Goupell, Matthew	PS-485, PS-495, PD-184, PS-656, PS-667	321, 326, 435, 443, 448
Gourévitch, Boris	PS-507	332
Goutman, Juan	PS-754	492
Gouveia, Christopher	PS-630	392
Goyer, David	PS-691	459
Grabowski, Greg	PD-204	551
Graf, Werner	PS-822	526
Grant, Ken	PS-517	337
Grant, Wally	PS-646	401
Grati, M'hamed	PS-295, PS-353	195, 225
Gratton, Gabriele	PS-137	76
Gratton, Michael Anne	PS-324	210
Gray, Lincoln	PS-070	43
Green, Glenn	PD-012, PS-503	9, 330
Green, Steven H	PS-369	233
Green, Steven	SY-035, PS-227	129, 161
Greenberg, David	PS-457	307
Greenberg, Robert	SY-002	1
Greene, Nathaniel	PS-413, PS-414, PD-195	254, 255, 550
Greenhouse, Robert	PD-134	406
Gregg, Melissa	PD-088	274
Grieco-Calub, Tina	PS-618	386
Grienwald, John	PD-082	268
Griesemer, Désirée	PS-680	454
Griffin, Amanda	PS-399	247
Griffith, Andrew J.	PD-063	150
Griffiths, T. D.	PS-602	378

Name	Abstract No.	Page No.
Griffiths, Timothy	PS-275, PD-202, PD-213	185, 544, 546
Grillet, Nicolas	PD-170	428
Grimsley, Calum	PS-824, PS-825	527, 528
Grimsley, Jasmine	PS-824	527
Groh, Jennifer	PS-747	489
Grolman, Wilko	PS-234, PS-245	165, 170
Gröschel, Moritz	PS-091, PD-127	54, 292
Grosh, Karl	PD-173, PD-174, PD-175	430, 430, 430
Gross, Benjamin	PS-060	39
Gross, Owen	PS-752	491
Großhörmichen, Martin	PS-724	476
Grothe, Benedikt	PS-407, PS-449, PS-466	251, 303, 312
Grover, Mary	PD-019	124
Groves, Andrew	PS-191	103
Grush, Leslie	PS-518	337
Gruters, Kurtis	PS-747	489
Gstoettner, Wolfgang	PD-112, PS-712	285, 470
Guan, Xiyang	PD-191	548
Gubbels, Samuel	PS-626	390
Guenther, Frank H	PS-021	19
Guérit, François	PS-492	325
Guerkov, Robert	PS-110	63
Guex, Amelie	PS-250	172
Guignard, Jeremie	PS-723	475
Guinan, John	PS-141, PD-015, PS-419	78, 122, 257
Gummer, Anthony	PS-112, PS-123	64, 70
Gunewardene, Niliksha	PS-030	24
Guo, Ben	PS-480	319
Guo, Jing	PS-551	352
Guo, Wei-wei	PD-101	280
Guo, Wei	PS-062, PS-257	40, 176
Guo, Weiwei	PD-038	138
Gupta, Chhavi	PS-259, PS-386, PS-388, PS-556	177, 241, 242, 355
Gurgel, Richard	PD-130	293
Gürkov, Robert	PS-117, PS-639	66, 397
Gurumurthy, Channabasavaiah	PS-197	106
Guthrie, O'Neil	PS-033, PS-621	26, 388
Gutschalk, Alexander	PS-273, PS-600	184, 377
Guymon, Allan	PS-350	224
Guymon, C. Allan	PD-078	266
Haacke, Ewart	SY-040	263
Haber, Yaa	PS-430	262
Hackett, Troy	PS-255, PS-276	175, 185
Hacking, Adam	PD-115	286
Hackney, Carole	PD-039	138
Haehnel, Melanie	PD-022	125
Hageman, Kristin	PS-202	109
Hagen, Matthew	PS-759	495
Hahnewald, Stefan	PS-252	173
Hailey, Dale	PD-137, PD-138	408, 408
Hajicek, Joshua	PS-129	73
Hakizimana, Pierre	PD-001, PD-002, PD-116	4, 4, 287
Hall-Glenn, Faith	PS-734	482
Hallman, Timothy	PS-631	392
Hallworth, Richard	PS-269	182
Halonon, Joshua	PS-002	11

Name	Abstract No.	Page No.
Halpin, Christopher H.	PS-722	475
Halsey, Karin	PS-017, PS-819	18, 525
Hamacher, Volkmar	PD-026	132
Hamdan, Abdul Latif	PS-502, PS-796	513, 514
Hamlet, William	PS-107	61
Hammershøi, Dorte	PD-072	154
Han, Chul	PS-004, PS-013	12, 16
Han, Dong-Yi	PD-085	270
Han, Emily	PS-022	20
Han, Helen	PS-162	88
Han, JiHye	PD-082	268
Han, Kyu-Hee	PD-134	406
Han, Min A	PS-561	357
Han, Mingyu	PS-475	316
Han, Wei-Ju	PD-085	270
Han, Yu	PS-375	235
Han, Zhao	PS-533	344
Hancock, Kenneth	SY-067, PS-653, PS-654	415, 441, 442
Hannaford, Sophia	PS-671	450
Hansen, John	PS-487	322
Hansen, Marlan R.	PS-241, PD-078, PS-620	168, 266, 387
Hansen, Marlan	PS-300, PS-350	197, 224
Hao, Qing-qing	PD-101	280
Haq, Naila	PD-154	420
Haque, K.	PD-143	411
harada, tamotsu	PS-505	331
Harding, Joseph	PS-383	239
Hare, Joshua M.	PS-566	360
Hargrove, Tim	PS-028	23
Harper, Elizabeth	PS-041	29
Harris, Kelly C	PS-006	13
Harris, Suzan	PD-205	551
Harrison, Robert V.	PS-058, PS-340	38, 218
Harrison, Robert	SY-032	128
Hartley, Douglas	PS-134, PS-433	76, 295
Hartman, Byron	PS-531, PD-144	343, 411
Hartmann, Thomas	SY-047	265
Hartsock, Jared	PS-708, PS-775	467, 503
Hasegawa, Shingo	PS-015, PS-343	17, 219
Hashimoto, Makoto	PS-036, PS-368, PS-423, PS-427, PS-648	27, 232, 259, 261, 402
Hashino, Eri	PD-055	146
Hassan, Ahmed	PD-219	555
Hastings, Michelle	PS-715	471
Hausman, Fran	PD-126, PS-496, PS-728, PS-783	291, 327, 478, 507
Haworth, Joshua	PS-635	395
Hayasaka, Takahiro	PS-499, PS-501	328, 329
Hayashi, Hisamitsu	PS-179	97
Hayashi, Lauren	PS-381	238
Hayashi, Yushi	PD-149	417
Hayes, Sarah	PS-280	187
Hazrati, Oldooz	PS-487	322
He, Christy	PS-333	214
He, David	PS-529, PS-736	342, 483
He, Lifan	PD-053	145
He, Wenxuan	PS-543	349
Hecker, Dietmar	PD-104, PD-105	281, 282

Name	Abstract No.	Page No.
Hedrick, Mark	PS-797	514
Heid, Silvia	SY-068	415
Heil, Peter	PS-222, PS-598	158, 376
Heinz, Michael G.	PS-229, PS-686	162, 457
Heinz, Michael G	PS-237	166
Heinz, Michael	PS-706	466
Hell, Stefan	SY-007	2
Heller, Stefan	PS-190, PD-037, PS-531, PD-144	102, 137, 343, 411
Hellström, Sten	PD-116	287
Hemmert, Werner	PS-169, PS-470, PS-486, PS-663	92, 314, 322, 446
Hempel, John-Martin	PS-470	314
Hendriks, Petra	PS-490	324
Hendriksen, Ferry	PS-234	165
Henin, Simon	PS-129	73
Henry, Kenneth	PS-237	166
Heo, Ji Hye	PS-251	173
Herrmann, Barbara	PS-419	257
Hertzano, Ronna	PD-010, PD-011	8, 9
Hesse, L.L.	PS-073	44
Heyd, Julia	PS-432	295
Hickox, Ann E	PS-237	166
Hickox, Ann	PS-229, PS-706	162, 466
Hidaka, Hiroshi	PS-841	536
Hideaki, Moteki	PD-094	277
Higgins, Nathan	PS-103	59
Highstein, Stephen	PD-051, PD-052	144, 144
Hight, Ariel	PS-250, PS-257, PS-498	172, 176, 178
Hildebrandt, Heika	PS-133	75
Hill, Kayla	PD-166	426
Hillas, Elaine	PS-389	242
Hinrich, Anthony	PS-715	471
Hinton, Ashley	PS-002	11
Hirano, Shigeru	PS-499, PS-501	328, 329
Hirose, Keiko	PS-040, PD-150, PS-775	29, 418, 503
Hirose, Yoshinobu	PS-036, PS-365, PS-368	27, 231, 232
Hirota, Koichi	PS-143	79
Hisa, Yasuo	PS-357, PS-394	227, 244
Hittle, Bradley	PS-500	328
Hládek, Luboš	PS-614	384
Hmani-Aifa, Mounira	PS-295	195
Hoa, Michael	PS-344	220
Hoekstra, Carlijn	PS-839	535
Hoffer, Michael	PS-041	29
Hoffman, Harold	PS-738	484
Hoffman, Howard J.	PS-421	258
Hoffman, Howard	PS-520	338
Hoffman, Larry	PS-218, PS-574	116, 363
Hoffmann, Andrea	PS-619	387
Hohmann, Volker	PS-173	94
Hojjat, Houmeh	PS-821	526
Hol, Myrthe	PD-185	436
Holcomb, Paul	SY-012	3
Holden, Laura	SY-070	416
Holfoth, David	PS-148, PS-595	81, 375
Holmes, Emma	PS-803	517
Holstein, Gay R.	PS-206	111

Name	Abstract No.	Page No.
Holstein, Gay R	PD-051	144
Holstein, Gay	SY-020	120
Holt, Avril Genene	PD-170	428
Holt, Jeffrey R.	PD-063	150
Holt, Jeffrey R	PD-055	146
Holt, Jeffrey	SY-009, PD-045, PD-161	2, 141, 424
Homma, Kazuaki	PS-327, PS-328, PS-366	211, 212, 231
Honeder, Clemens	PD-112, PS-712	285, 470
Hong, Bo	PS-438	298
Hong, Meng-Di	PD-085	270
Hong, Mengdi	PS-475	316
Hong, Seong Ah	PS-522	339
Hong, Sung Hwa	PS-469, PS-523	313, 339
Hong, Young-Kwon	PS-730	479
Honkura, Youhei	PS-841	536
Hopkins, Kathryn	PS-685	456
Hori, Takeshi	PS-036, PS-368	27, 232
Horikawa, Junsei	PS-264, PS-591	180, 373
Horn, David	PS-314	205
Hornak, Aubrey	PS-534	345
Hoshikawa, Hiroshi	PS-840	535
Hoskam, Gijs	PD-196	539
Hosoi, Hiroshi	PS-525, PS-526, PS-720, PS-746	340, 340, 474, 488
Hosokawa, Kumiko	PS-345, PS-346	220, 220
Hosokawa, Seiji	PS-345, PS-346, PS-347	220, 220, 221
Hossain, Shaikat	PS-651	440
Hotehama, Takuya	PS-596, PS-597	375, 376
Hou, Zhao-Hui	PD-085, PD-101	270, 280
Housley, Gary	SY-010	3
Houston, Lisa	PD-082	268
Howard, Matthew	SY-003, PS-275, PS-436, PD-202, PD-211	1, 185, 297, 544, 545
Hoyos, Tatiana	PD-013	10
Hsiao, Edward	PS-734	482
Hsiao, Steven	PS-790	511
Hsu, Chuan-Jen	PS-579, PS-769	366, 500
Hu, Bo Hua	PS-297, PS-371, PS-385, PS-582, PS-585, PD-167	196, 233, 240, 368, 370, 427
Hu, Jinwei	PS-033, PS-621	26, 388
Hu, Juan	PS-288	192
Hu, Lingxiang	PD-059, PS-538	148, 346
Hu, Ning	PS-043, PS-227	30, 161
Hu, Yi	PS-665	447
Hu, Zhengqing	PD-057	147
Huang, Chengcheng	PS-435	296
Huang, De-Liang	PD-085	270
Huang, Juan	PS-790	511
Huang, Jun	PS-647	401
Huang, Lin-Chien	SY-010	3
Huang, Shasha	PS-475	316
Huber, Alexander M	PS-477	317
Huber, Alexander	PD-177, PS-741, PS-748	431, 486, 489
Hubert, Nikolai	PD-127	292
Hubka, Peter	SY-068, PS-659, PD-214	415, 444, 546
Hudspeth, A. James	PD-147	413
Huet, Antoine	PS-243	169
Huetz, Chloe	PS-265	180

Name	Abstract No.	Page No.
Huh, Sung-Ho	PD-157	422
Hultcrantz, Malou	PD-116	287
Huma, Andreea	PS-298	196
Hunter, Lisa	PS-727	478
Huq, Farhan	PS-503	330
Hurd, Elizabeth	PD-012, PD-156	9, 421
Huriye, Atilgan	PS-102	59
Hurley, Robin	SY-041	263
Husain, Fatima	PS-843	537
Huth, Markus	PD-134	406
Hutson, Ken	PS-247, PS-317	171, 207
Hutter, Michele	PS-518	337
Huulvej, Tina	PS-683	455
Huyck, Julia	PS-800	516
Hyakumura, Tomoko	PS-624	389
Ibrahim, Mohannad	PS-503	330
Iconaru, Luigi	PD-034	136
Idrobo, Fabio	PS-787	509
Ihlefeld, Antje	PS-155	85
Ihrle, Sebastian	PS-741	486
III, William Merwin	PS-247, PS-317	171, 207
Iizuka, Takashi	PD-095	277
Ikedo, Katsuhisa	PD-095, PS-770, PS-773, PS-781	277, 500, 502, 506
Ikedo, Ryoukichi	PS-189	102
Ikedo, So	PS-264	180
Ikedo, Takuo	PS-423, PS-427	259, 261
Illing, Robert-Benjamin	PS-133	75
Im, Gi Jung	PS-555	354
Im, Gi-Jung	PD-108	283
Imayoshi, Itaru	PS-182	98
Imig, Thomas	PS-391, PS-823	243, 527
Inamoto, Ryuhei	PS-840	535
Indzhukulian, Artur	SY-074, SY-077	438, 439
Infante, Esperanza Bas	PD-081	268
Ingham, Neil	PS-298, PS-299	196, 197
Ingle, Katherine	PS-603	379
Inoguchi, Fuduki	PS-066	41
Inokuchi, Go	PS-343	219
Inoue, Maki	PS-289	192
Irino, Toshio	PS-784	508
Irsik, Vanessa	PD-088	274
Irvine, Dexter	PS-222, PS-478	158, 318
Irving, Sam	PS-254, PS-478	174, 318
Ise, Momoko	PD-096	277
Iseli, Claire	PS-317	207
Ishchanov, Anvarbek	PS-260	177
Ishikawa, Masa-aki	PD-061	149
Ishikawa, Masaaki	PS-623, PS-625	389, 389
Ishikawa, Seiji	PS-499, PS-501	328, 329
Ishiyama, Akira	PS-031, PS-345, PS-346, PS-347	25, 220, 220, 221
Ishiyama, Gail	PS-031, PS-345, PS-346, PS-347	25, 220, 220, 221

Name	Abstract No.	Page No.
Ito, Juichi	PS-217, PD-046, PD-061, PS-499, PS-501, PS-530, PS-623, PS-625, PD-133, PD-149, PD-158, PS-766, PS-778, PD-210	116, 142, 149, 328, 329, 342, 389, 389, 405, 417, 422, 498, 504, 554
Ito, Kazuhito	PS-597	376
Ito, Rindy	PD-079	267
Ito, Yatsuji	PS-179	97
Ivanovic, Alexandra	PS-763	497
Iversen, John	PD-215	547
Ives, David Timothy	PS-172	93
Iwakura, Takashi	PS-720	474
Iwasa, Kuni	PS-355	226
Iwasaki, Shinichi	PS-418	257
Iyer, Nandini	PS-092, PS-149, PS-804	54, 82, 518
Jabeen, Talat	PS-542	348
Jackson, Dakota	SY-012	3
Jackson, Ronald	PS-041	29
Jacob, Stefan	PD-001	4
Jacobo, Adrian	PD-147	413
Jacobs, Peter	PS-113, PS-809	64, 520
Jacques, Steven S.	PS-540	347
Jackel, Brittany N.	PS-158	86
Jagger, Dan	PS-184	99
Jagger, Daniel	PS-338, PS-339	217, 217
Jahan, Israt	PS-312	204
Jain, Ritu	PS-220	157
Jajoo, Sarvesh	PS-563	358
Jakobsson, Anne-Marie	PS-514	335
Jalabi, Walid	PS-308, PD-163	202, 425
Jamshid, Temirov	PD-001	4
Jang, Jeong Hun	PS-294	194
Jang, Ki-Hyeon	PS-020	19
Jaumann, Mirko	PS-536	346
Javier, Lauren	PS-403	249
Jedrzejczak, Wiktor	PD-073	155
Jeffers, Penelope WC	PS-560	357
Jeffers, Penelope	PS-577	365
Jenkins, Herman	PD-195	550
Jenkins, Kimberly	PD-125	291
Jennings, Todd	PS-466	312
Jensen-Smith, Heather	PS-537	346
Jeong, Joonsoo	PS-248	171
Jeong, Junhui	PS-251	173
Jessica, Lamb S.	PD-176	431
Ji, Fei	PD-101	280
Ji, Haiting	PD-009	7
Ji, Xiao	PD-194	549
Jiang, Haiyan	PS-342, PS-361, PS-362, PS-586	219, 229, 229, 370
Jiang, Linjia	PD-031	134
Jiang, Meiyuan	PS-580, PS-710, PS-711	367, 468, 469
Jiang, Tao	PS-650	403
Jiang, Zhi-Gen	PS-552, PS-569	353, 361
Jiao, Qing-Shan	PD-085	270
Jin, Sun Hwa	PS-523	339
Jing, Zhizi	SY-007	2

Name	Abstract No.	Page No.
Jiradejvong, Patpong	PS-481, PS-482, PS-594, PS-837	319, 320, 374, 534
Jiwani, Salima	PS-472, SY-069	315, 416
Jodelka, Francine	PS-715	471
Johannesen, Peter T.	PS-144	80
Johannesen, Peter	PD-074	155
Johansson, Ann	PD-116	287
John, Sasha	PS-440	299
Johnson, Ann-Christin	PS-521	339
Johnson, Colin	PS-184	99
Johnson, Kenneth	PS-183, PS-586	99, 370
Johnson, Mark	PS-699	463
Johnson, Shane	PS-775	503
Johnson, Tiffany	PS-039	28
Johnsrude, Ingrid	PS-800	516
Jokitato, Eija	PD-155	421
Jones, Heath	PS-175	95
Jones, Sherri	PS-193	104
Jones, Simon	PS-439, PS-447	299, 302
Jones, Timothy	PS-211, PS-214	113, 114
Jorgensen, Erik	PD-106	282
Joris, Philip X.	PS-455	306
Joris, Philip	PS-235	165
Josupeit, Angela	PS-173	94
Jou, Ilo	PS-581	367
Jovanovic, Sasa	PS-847	539
Juhn, Steven	PS-733	481
Juiz, Jose M.	PD-168	427
Jun, Sang Beom	PS-262	179
Jung, David	PD-115	286
Jung, Enja	PS-172	93
Jung, Hak Hyun	PS-555	354
Jung, Jae Hoon	PS-428	261
Jung, Jae Yun	PD-035, PS-392, PS-834	136, 243, 532
Jung, Martin	PD-104	281
Jung, Phil-Sang	PS-834	532
Kabara, Lisa L.	PS-471	314
Kabara, Lisa	PS-017, PS-767	18, 499
Kachelmeier, Allan	PS-580, PS-587	367, 371
Kaczmarek, Leonard	PS-674	452
Kaf, Wafaa	PS-510	333
Kaga, Kimitaka	PD-149	417
Kageyama, Ryoichiro	PS-182	98
Kajikawa, Yoshinao Kajikawa	PS-255	175
Kajikawa, Yoshinao	PS-276	185
Kakaraparthi, Bala Naveen	PS-767	499
Kakigi, Akinobu	PS-199, PS-777	107, 504
Kale, Sushrut	PS-256	175
Kalinec, Federico	PD-006, PS-565, PS-713	6, 359, 470
Kalinec, Gilda	PS-565	359
Kalinski, Hagar	PD-035	136
Kalluri, Radha	PS-205, PS-238	110, 167
Kallweit, Nicole	PD-206	552
Kaltenbach, James	PS-827	529
Kamerer, Aryn	PS-318	207
Kamiya, Kazusaku	PD-065, PD-095, PS-770, PS-773, PS-781	151, 277, 500, 502, 506
Kamogashira, Teru	PD-076	156

Name	Abstract No.	Page No.
Kampangkaew, June	PS-420	257
Kan, Alan	PS-175, PS-495	95, 326
Kan, Lixin	PS-310	203
Kanaan, Moien	PD-007	6
Kandler, Karl	PS-448	303
Kane, Catherine	PS-227	161
Kaneda, Hideki	PS-289	192
Kang, Dongyang	PS-297, PS-475	196, 316
Kang, Hyun Woo	PS-838	534
Kang, Joe	PS-786	509
Kang, Sujin	PS-469	313
Kang, Woo Seok	PD-115	286
Kang, Wooseok	PS-716	472
Kanicki, Ariane	PS-017, PS-767, PS-819	18, 499, 525
Kanold, Patrick	PS-139, PS-311	77, 203
Kantner, Claudia	PS-639	397
Kanzaki, Ryohei	PS-016, PS-083, PS-086	47, 50, 51
Kappy, Michelle	PS-209	112
Kararo, Evan	PS-261	177
Karasawa, Keiko	PS-773	502
Karasawa, Takatoshi	PS-587, PS-710	371, 468
Karavitaki, Kiriaki Domenica	SY-079	440
Karino, Shotaro	PD-076	156
Karmarkar, Sumedha	PS-201	108
Kashanian, Nina	PS-815	524
Kashino, Makio	PS-143, PS-599, PS-606, PS-609, PS-615	79, 377, 380, 382, 385
Kashio, Akinori	PS-199	107
Kasini, Kamyar	PS-536	346
Kastl, Daniel	PS-132	75
Kataoka, Kazunori	PD-109	284
Kato, Hiroki	PD-149	417
Katori, Yukio	PS-005, PS-038, PS-348, PS-735	13, 28, 223, 482
Katsuno, Tatsuya	PD-046	142
Katz, Eleonora	PS-760	495
Kaur, Tejbeer	PS-305, PS-563, PD-150	200, 358, 418
Kawai, Yoshitaka	PS-625	389
Kawas, Leen	PS-383	239
Kawasaki, Hiroto	PS-275, PS-436, PD-202, PD-211	185, 297, 544, 545
Kawase, Tetsuaki	PS-005, PS-038, PS-348, PS-735, PS-841	13, 28, 223, 482, 536
Kawauchi, Satoko	PS-373	234
Kayla, Hill	PS-360	229
Kazmitcheff, Guillaume	PD-188, PD-190	547, 548
Kearney, Graciela	PS-760	495
Keating, Peter	PS-068, PS-096	42, 56
Keefe, Douglas	PS-727	478
Keine, Christian	PS-693	460
Keith, Robert	PS-488	323
Keller, Stefanie	PS-670	450
Kempe, Martin	PS-658	444
Kempter, Richard	PS-452, PS-453	305, 305
Kempton, Beth	PD-126, PS-783	291, 507
Kempton, J Beth	PS-496, PS-728	327, 478
Kendall, Ann	PS-374	235
Kennon-McGill, Stefanie	PS-391, PS-823	243, 527

Name	Abstract No.	Page No.
Keppner, Herbert	PS-252	173
Kersigo, Jennifer	128	
Kessler, John	PS-310, PS-628, PS-630	203, 391, 392
Kettler, Lutz	PS-100	58
Keuning, Anne-Marie	PS-839	535
Khaja, Ameenuddin	PS-049	33
Khaleghi, Morteza	PS-739	484
Khoury, Leila	PS-267	181
Ki, Mia	PS-370	233
Kiaci, Shayesteh	PS-153	84
Kidani, Shunsuke	PS-599, PS-606, PS-615	377, 380, 385
Kidd, Jr., Gerald	PS-149	82
Kidokoro, Yoshinobu	PS-770	500
Kiernan, Amy	PD-141	410
Kikic, Merijam	PS-037	27
Kileny, Paul	PS-844	537
Kilgard, Michael	SY-048	265
Kim, Ah Reum	PS-294	194
Kim, Ana	PS-576	365
Kim, Bo Gyung	PS-251, PS-779, PS-782	173, 505, 507
Kim, Bong Jik	PS-834	532
Kim, Dong Kee	PS-561	357
Kim, Doo Hee	PS-262	179
Kim, Duck	PS-170	92
Kim, Ernest	PS-716	472
Kim, Hak-Young	PS-512	334
Kim, Hey-Su	PS-020	19
Kim, Hong Lim	PS-561	357
Kim, Hyo Jeong	PS-306, PS-336, PS-352, PD-122, PD-123, PD-124, PD-208, PD-209, PD-218	201, 216, 225, 290, 290, 290, 553, 553, 555
Kim, Jin Young	PS-779, PS-782	505, 507
Kim, Kyu-Sung	PS-424	259
Kim, Kyunghee	PD-039	138
Kim, Mi-Jung	PS-004, PS-013	12, 16
Kim, Mihwa	PS-601	378
Kim, Min Young	PS-294	194
Kim, Minbum	PS-424	259
Kim, Namkeun	SY-016	119
Kim, Soo	PS-468	313
Kim, Su-Jin	PS-020	19
Kim, Sun Keum	PS-522	339
Kim, Sun Myoung	PD-146	412
Kim, Sung Huhn	PS-779, PS-782	505, 507
Kim, Sung June	PS-248	171
Kim, Tae Su	PS-842	536
Kim, Ted	PS-328, PS-366	212, 231
Kim, Ye-Hyun	SY-009, PD-161	2, 424
Kim, Yeon Ju	PS-372	234
Kim, Young Chul	PD-132	405
Kim, Young Ho	PD-132	405
Kim, Young Sun	PS-372	234
Kimura, Ryuichi	PS-005	13
Kimura, Tomoko	PS-066	41
Kindt, Katie	PS-649	402
King, Andrew	PS-068, PS-096, SY-062, PS-786	42, 56, 404, 509

Name	Abstract No.	Page No.
King, Ruairidh	PD-131	294
Kinoshita, Makoto	PS-199, PS-418	107, 257
Kirjavainen, Anna	PS-186	100
Kirkwood, Nerissa	PD-064	150
Kishline, Lindsey	PS-605	380
Kishon-Rabin, Liat	PS-807	519
Kita, Tomoko	PD-061	149
Kitajiri, Shin-ichiro	PD-046, PS-530	142, 342
Kitamura, Morimasa	PS-499, PS-501	328, 329
Kitano, Koichi	PS-642	399
Kitterick, Padraig	PS-803	517
Klapoetke, Nathan	PS-257	176
Kline-Schoder, Robert	PD-075	156
Klinge-Strahl, Astrid	PS-063, PS-072	40, 44
Klis, Sjaak	PS-234, PS-245	165, 170
Klug, Achim	PS-459	308
Klump, Georg M.	PS-072, PS-154	44, 84
Klump, Georg	PS-044, PS-063, PS-408	31, 40, 252
Knipper, Marlies	SY-034, PD-129, PS-536, PS-554	129, 293, 346, 354
Knudson, Inge	PS-835, PS-836	533, 533
Knudson, Kevin	PS-300	197
Ko, Kwang Woo	PS-451	304
Kobayashi, Takamitsu	PS-426	260
Kobayashi, Toshimitsu	PS-005, PS-038, PS-841	13, 28, 536
Kobrina, Anastasiya	PS-592	373
Koceja, David	PS-642	399
Koch, Ursula	PS-681, PS-682	454, 455
Kochanek, Krzysztof	PD-073	155
Kocher, Acadia A.	PS-164	89
Koda, Yuki	PS-638	396
Koehler, Karl	PD-055	146
Koehler, Seth	PS-140, PS-820	78, 526
Koenig, Angela F.	PS-837	534
Koeppl, Christine	PS-452	305
Koeritzer, Margaret	PS-040	29
Kohrman, David	PS-293	194
Kokkinakis, Kostas	PS-397	246
Kolbe, Diana	PD-010	8
Kommareddi, Pavan	PS-767	499
Kondo, Kenji	PS-199	107
Kong, Jee-Hyun	PS-758	494
Kong, JeeHyun	PS-355	226
Kong, Ying-Yee	PS-437, PS-441	297, 299
Konrad-Martin, Dawn	PS-113	64
Koo, Ja-Won	PS-032	25
Kopčo, Norbert	PS-614, PS-806	384, 519
Kopco, Norbert	PS-173	94
Kopelovich, Jonathan C.	PS-241	168
Kopke, Richard	PS-043, PS-270, PS-571	30, 182, 362
Kopp-Scheinpflug, Conny	PS-449	303
Koppl, Christine	PD-077	157
Köppl, Christine	PS-702	465
Korchagina, Julia	PS-327, PS-328	211, 212
Korn, Sabine	PD-198	542
Koschak, Alexandra	PD-105	282
Kössl, Manfred	PS-432	295

Name	Abstract No.	Page No.
Kotak, Vibhakar	PS-078, PS-272, SY-064	47, 183, 413
Koussa, Mounir	PD-042	140
Kowalski, Tomasz	PS-282	188
Kozin, Elliott	PD-025, PS-242, PS-250, PS-498	131, 169, 172, 178
Kral, Andrej	PS-075, PD-026, SY-066, SY-068, PS-659, PD-214, PD-206	45, 132, 414, 415, 444, 546, 552
Kramer, Benedikt	PS-226	160
Kramer, Richard H.	PS-451	304
Kranebitter, Veronika	PD-037	137
Kraus, Nina	PS-010, PS-046, PS-047, PS-138, PS-315, PS-528, SY-063, PS-808, PD-200	15, 32, 32, 77, 205, 341, 404, 520, 543
Krause, Bryan	PS-271	183
Krause, Eike	PS-110, PS-117	63, 66
Krause, Markus	PS-712	470
Kreeger, Lauren	PS-462	310
Kreft, Heather	PS-473, PS-607	315, 381
Kretzberg, Jutta	PS-456	307
Krey, Jocelyn	PS-183	99
Krishnan, Ananthanarayan	PS-048, PS-056, PS-444	32, 37, 301
Kristiansen, Arthur G.	PS-577	365
Krizman, Jennifer	PS-046	32
Kros, Come	PD-064	150
Krüger, Alexander	PD-206	552
Ku, Tiffany	PD-204	551
Kubli, Lina	PS-517	337
Kudo, Motoi	PS-066	41
Kuenzel, Thomas	PS-691	459
Kugler, Kathrin	PS-110	63
Kügler, Sebastian	PS-753	492
Kühne, Daniela	SY-066	414
Kujawa, Sharon G.	PS-560, PS-570, PS-577	357, 361, 365
Kujawa, Sharon	SY-030, SY-056, PS-716	127, 272, 472
Kum, Jason	PS-196	106
Kumar, Sukhbinder	PD-202	544
Kunisada, Takahiro	PS-179	97
Kuo, Bryan	PD-033, PS-261	135, 177
Kuokkanen, Paula	PS-452, PS-453	305, 305
Kurabi, Arwa	PS-738	484
Kurgan, Lukasz	PS-356	227
Kurima, Kiyoto	PD-063	150
Kurioka, Takaomi	PS-026, PS-373	22, 234
Kurrabi, Arwa	PD-110	284
Kurt, Simone	PS-292	193
Kuthubutheen, Jafri	PD-080	267
Kuwada, Shigeyuki	PS-170	92
Kuze, Bunya	PS-179	97
Kwan, Kelvin Y.	PD-164	425
Kwan, Tao	PD-140	409
Kwon, Bomjun	PD-030	134
Kwon, Hyo Kyoung	PS-567	360
Kwon, Jee Young	PS-731	480
Kymissis, Ioannis (John)	PS-256	175
Laback, Bernhard	PS-171, PS-610, PD-187, PS-657	93, 382, 437, 443
Lackner, Christina	PS-486	322

Name	Abstract No.	Page No.
Lacour, Stephanie	PS-250	172
Laczkoich, Irina	PS-767	499
Ladak, Hanif	PS-506	331
LaFaire, Petrina	PS-258	176
Lagarde, Marcia M Mellado	PS-215	115
Lai, Jesyin	PS-023	20
Lakemeyer, Gerhard	PS-398	247
Lall, Kumud	PS-560, PS-570	357, 361
Lam, Lisa	PS-730	479
Lamb, Jessica	PD-176	431
Land, Rüdiger	PS-075	45
Landegger, Lukas	PS-712	470
Landsberger, David	PD-182, PS-666	434, 448
Lang, Dustin	PS-388	242
Lang, Hainan	PS-304, PS-341, PD-099	200, 218, 279
Langers, Dave	PD-196	539
Lanting, Cris	PD-196	539
Laos, Maarja	PS-198	107
Large, Charles H.	PS-717	472
Larrain, Barbara	PD-126, PS-711	291, 469
Larsen, Deb	PS-816	524
Larsen, Ole	PS-683	455
Larson, Eric	PS-601, PS-603, PS-605	378, 379, 380
Larsson, Christina	PD-116	287
Laske, Roman	PD-144	411
Lau, Bonnie	PS-785	508
Laudanski, Jonathan	PS-507	332
Lauer, Amanda	SY-011, PS-225, PS-675	3, 160, 452
Laumen, Geneviève	PS-044	31
Lavieille, Jean-Pierre	PS-664	447
Lavner, Yizhar	PD-086	273
Layman, Wanda	PS-291	193
Lazard, Diane	PD-203	545
Le Dantec, Christophe	PS-614	384
Le Prell, Colleen	PS-025, PS-034	21, 26
Leake, Patricia	PS-395	245
Leal, Karina	PS-756	493
Ledbetter, Noah	PS-516	336
Ledee, Daniel	PS-829	530
Lee, Adrian KC	PS-601, PS-603, PS-605, PS-613, PS-617	378, 379, 380, 384, 386
Lee, Amy	PD-105	282
Lee, Byung Don	PS-731	480
Lee, Chi-Kyou	PS-676, PD-204	453, 551
Lee, Choongheon	PS-211	113
Lee, Dan	PS-498	178
Lee, Daniel J.	PS-242, PS-257	169, 176
Lee, Daniel	PS-062, PD-025, PS-250, PS-350	40, 131, 172, 224
Lee, Dasom	PD-021, PS-232	125, 164
Lee, Hee Yoon	PS-334	215
Lee, Ho Sun	PS-248	171
Lee, Ho-Sun	PD-114	286
Lee, Hwan-Ho	PS-737	483
Lee, Jae Hee	PS-522	339
Lee, Jae Wook	PS-392	243
Lee, Jae-Hun	PS-020	19
Lee, Jasmine	PS-738	484

Name	Abstract No.	Page No.
Lee, Jeong Han	PS-306, PD-121, PD-122	201, 289, 290
Lee, Jeong-Han	PS-336, PS-352, PD-124	216, 225, 290
Lee, Ji Hye	PD-132	405
Lee, Ji Won	PS-567	360
Lee, Ji Young	PS-555	354
Lee, Jun Han	PS-029	24
Lee, Jun Ho	PD-114	286
Lee, Min Young	PS-262	179
Lee, Se Hee	PS-555	354
Lee, Seonjoo	PS-520	338
Lee, Seung-ha	PS-834	532
Lee, Sungsu	PS-181	98
Lee, Sze Chim	PD-129, PS-554	293, 354
Lee, Won-Sang	PS-782	507
Lee, Yoojin	PS-035	26
Leek, Marjorie	PD-092, PS-518	276, 337
Legan, Kevin	PS-327, PS-328	211, 212
Léger, Agnès	PS-142	79
Lehmann, Ashton	PD-025, PS-498	131, 178
Lehmann, Jessica	PS-464	311
Lehtimäki, Jarmo	PS-846	538
Leibiger, Barbara	PD-001	4
Leijon, Sara	PD-001, PS-679	4, 453
Leiter, Andrew	PS-312	204
Leman, Marc	SY-054	271
Lenarduzzi, Stefania	PD-008	7
Lenarz, Thomas	PD-026, PS-249, PS-564, PS-619, PS-724, PD-206	132, 172, 359, 387, 476, 552
Lenoir, Marc	PS-244	169
Lentz, Jennifer	PS-715	471
León, Alex	PS-087	52
Lescanne, Emmanuel	PS-263, PS-468	179, 313
Lesica, Nicholas	PS-059	38
Leu, Rose	PD-021, PS-232	125, 164
Leung, Johahn	PS-404, PS-405, PS-409	249, 250, 252
Levi, Rafi	PD-022	125
Lewis, James	PS-126	72
Lewis, Kristen	SY-070	416
Lewis, M. Samantha	PS-518	337
Li, Alfred	PS-734	482
Li, Carol	PS-425	260
Li, Chuan-Ming	PS-421, PS-520	258, 338
Li, Dengke	PD-038	138
Li, Gang Q.	PS-242	169
Li, Geng-Lin	PS-330, PS-331	213, 213
Li, Hongzhe	PS-323, PS-380, PS-393, PS-476, PS-710	210, 238, 244, 317, 468
Li, Huawei	PD-009, PD-032	7, 135
Li, Hui	PS-283	189
Li, Jia-na	PD-101	280
Li, Jia-Nan	PD-085	270
Li, Joyce	PS-312	204
Li, Jun	PS-736	483
Li, Na	PS-067	42
Li, Ning	PD-208	553
Li, Qi	PS-384, PS-718	240, 473
Li, Song-Zhe	PS-040	29
Li, Tianhao	PS-668	449

Name	Abstract No.	Page No.
Li, Wei	PS-043, PS-270	30, 182
Li, Wenyan	PD-032	135
Li, Yi	PS-529, PS-736	342, 483
Li, Yizeng	PD-174	430
Liang, Chun	PD-120, PS-765	289, 498
Liang, Ruqiang	PS-283, PS-333	189, 214
Liao, Eric	PD-013	10
Liao, Hsin-I	PS-599, PS-606, PS-615	377, 380, 385
Liao, James	PD-022	125
Lieberman, Charles	PD-013	10
Lieberman, M. Charles	SY-030, SY-033, SY-055, PS-560, PS-772	127, 129, 272, 357, 502
Lieberman, Tamara	PS-593	374
Lichtenhan, Jeffery	PD-015, PS-510	122, 333
Liddle, Rodger A.	PS-535	345
Liebau, Arne	PS-709	468
Lieberman, Rachel	PD-125	291
Lim, David	PS-035	26
Lim, Hubert	PS-132	75
Lim, Hye Jin	PS-372	234
Limb, Charles J.	PS-164, PS-594, PS-837	89, 374, 534
Limb, Charles	PD-027, PD-083, SY-054, PS-481, PS-482, PS-489, PS-588	132, 269, 271, 319, 320, 323, 371
Lin, Angela E.	PS-296	195
Lin, Austin	PD-135	406
Lin, Hsiao-Chun	PS-579, PS-769	366, 500
Lin, Nan	PS-204	110
Lin, Shuh-Yow	PD-103	281
Lin, Vincent	PD-080	267
Lin, Wenwei	PD-034	136
Lin, Xi Erick	PD-009	7
Lin, Xi	PS-281, PS-353, PS-384, PS-718	188, 225, 240, 473
Lin, Yi-Tsen	PS-769	500
Lin, Yin-Hung	PS-579, PS-769	366, 500
Lin, Yung-Song	PD-083	269
Linbo, Tor	PD-137	408
Linden, J.F.	PS-073	44
Ling, Leo	PS-644, PS-645	400, 400
Ling, Lynne	PS-816	524
Lingner, Andrea	PS-407, PS-805	251, 518
Linke, Ines	PS-249	172
Linser, Paul	PS-004, PS-013	12, 16
Linthicum, Jr., Fred H.	PS-344	220
Litovsky, Ruth Y.	PS-158	86
Litovsky, Ruth	PS-175, PS-485, PS-495, PS-604, SY-071, PD-184, PS-651	95, 321, 326, 379, 416, 435, 440
Little, David	PS-162	88
Liu, Chang	PD-152	419
Liu, Dan	PS-333	214
Liu, Huizhan	PS-529, PS-736	342, 483
Liu, Jianping	PS-323, PS-711	210, 469
Liu, Jianzhong	PS-041	29
Liu, Jun	PD-085, PS-475	270, 316
Liu, Ke	PD-101	280
Liu, Liqian	PS-622	388

Name	Abstract No.	Page No.
Liu, Qiang	PD-106	282
Liu, Wei	PS-302	198
Liu, Xiao-Ping	PD-045, PD-055	141, 146
Liu, Xue Zhong	PS-295, PS-353	195, 225
Liu, Yi-Wen	PS-546, PD-179	350, 432
Liu, Yu-Wei	PS-107	61
Liu, Zhandong	PS-191	103
Llomas, Gerard Encina	PS-509	333
Lobarinas, Edward	PS-034, PS-157	26, 86
Locke, Shannon	PS-409	252
Lomber, Stephen	PS-130, SY-066	74, 414
Long, Glenis R.	PS-129	73
Longenecker, Ryan	PS-825, PS-826	528, 528
Longenecker, Ryan	PS-824	527
Longo-Guess, Chantal	PS-586	370
Lonsbury-Martin, Brenda L.	PS-111	63
Lookabaugh, Sarah	PS-722	475
López-Paullier, Matías	PS-833	532
Lopez-Poveda, Enrique A.	PS-144, PD-074	80, 155
Lopez, Ivan	PS-031, PS-218, PS-345, PS-346, PS-347, PS-574	25, 116, 220, 220, 221, 363
Lopez, Matías	PS-831	531
Lorenzen, Sarah	PD-160	423
Lorenzi, Christian	PS-172, PS-265	93, 180
Low, Jacob	PD-118	288
Löwenheim, Hubert	PS-226, PS-527	160, 341
Lu, Hui-Ping	PD-083	269
Lu, Jingqiao	PD-009, PS-281	7, 188
Lu, Thomas	PS-519	338
Lu, Ying-Chang	PS-579, PS-769	366, 500
Lu, Yong	PS-107	61
Lu, Zhongmin	PS-353	225
Lubianski, Troy	PS-387	241
Lucertini, Marco	PS-122	69
Luk, Lauren	PS-393	244
Lukas, Thomas	PS-829	530
Lumbreras, Vicente	PS-259, PS-566, PD-207	177, 360, 552
Lundberg, Yunxia	PD-054	145
Lundkvist, Gabriella Schmitz	PS-014	17
Luo, Wen-Wei	PD-060	148
Luo, Wenwei	PS-533	344
Luo, Xin	PD-084	269
Lustig, Lawrence	SY-019, PS-676, PS-734, PD-204	120, 453, 482, 551
Luu, Ngoc-Nhi	PS-527	341
Lv, Ping	PS-336, PD-123, PD-124	216, 290, 290
Lysaght, Andrew	PS-575	364
Lysakowski, Anna	PS-214, PD-048, PD-049	114, 143, 143
Ma, Rui	PD-060	148
Maass, Juan	PS-191	103
Maat, Bert	PD-028	133
MacArthur, Carol	PD-126, PS-496, PS-728, PS-783	291, 327, 478, 507
MacDonald, Ewen	PS-611	383
MacLeod, Katrina	PS-702	465
MacIin, Ed	PS-137	76
Macpherson, Ewan	PS-406	251
Maddox, Ross	PS-613, PS-617	384, 386

Name	Abstract No.	Page No.
Maftoon, Nima	PS-749, PS-750	490, 490
Magnasco, Marcelo	PS-788	510
Magnuson, Mark	PD-160	423
Magnusson, Anna K	PS-679	453
Mahendrasingam, Shanthini	PD-039, PS-583	138, 369
Mahmood, Gulrez	PS-821	526
Mahrt, Elena	PS-074	45
Maier, Hannes	PS-724	476
Maison, Stéphane	PS-772	502
Majdak, Piotr	PS-171, PS-610, PS-657	93, 382, 443
Makashay, Matthew	PS-517	337
Makeig, Scott	PD-215	547
Makishima, Tomoko	PS-212, PS-332	113, 214
Mäkitie, Antti	PS-846	538
Mallet, Adeline	PD-102	280
Malmierca, Manuel	PS-061	39
Mangosing, Sara	PD-103	281
Manis, Paul	SY-045, PS-688	264, 458
Manley, Geoffrey	PD-077	157
Mann, Mary Anne	PD-051	144
Mann, Mary	PD-052	144
Manohar, Senthilvelan	PS-280, PS-361, PS-362, PS-707	187, 229, 229, 467
Manohar, Senthivelan	PS-131	74
Mao, Beatrice	PS-415	255
Mao, Jinghe	PS-647	401
Marcotti, Walter	PS-774	503
Maricich, Stephen	PS-308, PD-163	202, 425
Markovitz, Craig	PS-132	75
Marnell, Daniel	PS-542	348
Marquardt, Torsten	PS-483, PD-180	320, 433
Marrone, Nicole	PS-109, PS-162	62, 88
Marshak, Sofia	PD-162	424
Martel, David T	PS-136	521
Martel, David	PS-818	117
Martin, Brett	PS-480	319
Martin, Donna	PD-012, PD-156	9, 421
Martin, Glen K.	PS-111	63
Martín, Javier Zorrilla San	PS-760	495
Martineau, Joëlle	PS-468	313
Martinelli, Giorgio P	PS-207	111
Martinelli, Giorgio	PS-206	111
Martinez-Vega, Raquel	PS-298	196
Masaki, Noritaka	PS-499	328
Masmoudi, Saber	PS-295	195
Mason, Christine	PS-149	82
Masud, Salwa	PS-054	35
Masuya, Hiroshi	PS-289	192
Mathias, Samuel	PD-087	273
Matsui, Toshie	PS-784	508
Matsumoto, Yu	PD-109	284
Matsunobu, Takeshi	PS-026, PS-373	22, 234
Matsuoka, Akihiro	PS-310, PS-628, PS-630	203, 391, 392
Matsuzaki, Fumio	PD-146	412
Mattiace, Linda	PS-576	365
Mattiaccio, Jonelle	PS-195	105
Maulucci, Giuseppe	PS-382	239

Name	Abstract No.	Page No.
May, Lindsey	PS-390, PD-139	242, 409
Mayer, Florian	PS-459	308
Mayko, Zachary	PS-065	262
McAlpine, D.	PS-073	44
McAlpine, David	PS-059, PS-095, PS-338, PS-339, PS-400, PS-439, PS-447, PS-457, PS-458, PS-483, PD-180	38, 55, 217, 217, 248, 299, 302, 307, 308, 320, 433
McCall, Andrew	PS-210	113
McClellan, Joseph H	PS-247	171
McClellan, Joseph	PS-317, PS-559	207, 356
McColgan, Thomas	PS-452, PS-453	305, 305
McCormack, Abby	PS-830	530
McCormick, David	PS-024, PS-445	21, 301
McDermott, Brian	PD-219	555
McDermott, Colleen	PS-636	395
McDermott, Josh	PS-150, PS-278, PD-089, PS-786, PS-795	82, 186, 274, 509, 513
McDermott, Joshua H.	PS-156	85
McDonough, Joyce M.	PS-787	509
McFarland, Dennis	PS-845	538
McGee, JoAnn	PS-573	363
McGinley, Matthew	PS-024, PS-445	21, 301
McGuire, Brian	PS-225, PS-675	160, 452
McGuire, Elizabeth	PS-403	249
McGuire, Tammy	PS-310	203
McIntosh, Michael	PS-213	114
McKay, Colette	PD-024	131
McKay, Sharen	PS-768	499
McKenna, Charles	PD-115	286
McKenna, Michael J.	PS-577	365
McKenna, Michael	PD-115, PS-716	286, 472
McKinley, Gareth	PD-118	288
McKinnon, Melissa	PS-743, PD-193	487, 549
McLaughlin, Christopher	PS-559	356
McLean, Julie	SY-077	439
McLean, Will	PD-036	137
McMahon, Courtney	PS-817	525
McMillan, Garnett	PS-727	478
McWalter, Richard	PS-611	383
Meadows, Marc	PS-228, PS-233	161, 164
Measor, Kevin	PS-090	53
Meaud, Julien	PD-173	430
Medina-Ferret, Eduardo	PS-593, PS-833	374, 532
Meech, Robert	PS-028	23
Meenderink, Sebastiaan W.F.	PD-041, PD-066	139, 151
Mehraei, Golbarg	PS-054, PS-057	35, 37
Mehta, Anahita	PS-848	57
Mehta, Sapna	PS-652	441
Meinke, Deanna	PD-075	156
Meiser, Carina	PS-536	346
Melcher, Jennifer	PS-835, PS-836	533, 533
Melchionna, Teresa	PS-556	355
Melgar-Rojas, Pedro	PD-168	427
Mellado-Lagarde, Marcia	PD-001	4
Mellott, Jeffrey	PS-069	42
Meltser, Inna	PS-014	17
Menapace, Deanna	PS-214	114

Name	Abstract No.	Page No.
Mendonsa, Eric	PS-621	388
Mendus, Diana	PD-021, PS-232, PD-170	125, 164, 428
Meng, Xiangying	PS-139	77
Meng, Xiankai	PS-242	169
Mensink, Jorien	PD-090	275
Merchant, Gabrielle R.	PS-722	475
Merchant, Gabrielle	PS-721	474
Merchant, Julie P.	SY-015, PD-192	118, 549
Meredith, Andrea L	PD-208	553
Meredith, Frances	PD-050	143
Mertes, Ian	PS-124	71
Merwin, William	PS-559	356
Merzenich, Michael	SY-028	127
Mescher, Mark	PS-716	472
Mesgarani, Nima	PS-097	56
Mett, Igor	PD-035	136
Meyer, Martin	PS-376	236
Meyron-Holtz, Esther G.	PS-374	235
Micco, Alan	PS-258	176
Michalka, Samantha W	PS-021	19
Michanski, Susann	SY-007	2
Michel, Vincent	PD-065	151
Micheyl, Christophe	PD-087, PS-443	273, 300
Micucci, Joseph	PD-012	9
Middlebrooks, John C	PS-084	50
Middlebrooks, John	PS-080, PS-403, PS-467	48, 249, 312
Middleton, Hugh	PS-830	530
Mikosz, Andrew M	PD-055	146
Milenkovic, Ivan	PS-695, PS-847	461, 539
Mill, Robert	PS-701	464
Millard, Rodney	PS-254	174
Miller, Daniel	PS-210	113
Miller, Josef	PS-584, PS-819	369, 525
Mills, Kristen	PS-661	445
Min, Kyou Sik	PS-248	171
Mina, Amir	PD-037	137
Minich, Rebecca	PS-290	193
Minoda, Ryosei	PD-096	277
Minowa, Osamu	PS-289, PD-095, PS-770, PS-773	192, 277, 500, 502
Mintz, Matti	PS-208	111
miroir, mathieu	PD-188, PD-190	547, 548
Misurelli, Sara M.	PS-158	86
Mittal, Jeenu	PS-386	241
Mittal, Rahul	PS-295, PS-353	195, 225
Miwa, Asuka	PS-773	502
Miwa, Julie	PS-106	61
Miwa, Toru	PD-096	277
Miyashita, Mie	PS-426	260
Miyashita, Takenori	PS-730, PS-840	479, 535
Miyazaki, Hiromitsu	PS-348	223
Miyoshi, Takushi	PS-778	504
Mizuta, Keisuke	PS-179	97
Mlynarczyk, Gregory	PS-442	300
Möhrle, Dorit	PD-129	293
Moleti, Arturo	PS-118, PS-120, PS-122	67, 68, 69
Molis, Michelle R.	PD-092	276

Name	Abstract No.	Page No.
Monaghan, Jessica	PS-152, PS-400, PS-704	83, 248, 466
Monroe, David	PS-187	101
Montazeri, Vahid	PS-651	440
Montgomery, Johanna	SY-010	3
Monzack, Elyssa	PD-139	409
Moon, Il Joon	PS-523, PS-662	339, 446
Moon, In Seok	PS-188	101
Moon, Sung	PS-035	26
Moore, Brian	PS-515	336
Moore, David	PS-830	530
Moore, Ernest	PS-829	530
Moores, Carolyn	PD-220	556
Mora, Emanuel C.	PS-432	295
Morawski, Markus	PS-673	451
Moreno, Sylvain	PS-001	11
Morgan, Anna	PD-008	7
Mori, Nozomu	PS-730, PS-840	479, 535
Mori, Toshihiro	PS-840	535
Morioka, Shigefumi	PS-357	227
Morley, Barbara	PS-214	114
Morozko, Eva	PS-535	345
Morris, David	SY-053	271
Morrison, Laura	PD-011	9
Morse-Fortier, Charlotte	PS-399	247
Morse, Sue	PD-131	294
Morton, Cynthia	PD-013	10
Moser, Tobias	SY-007, PS-299, PS-753, PS-763	2, 197, 492, 497
Moskovitz, Jakob	PS-019	19
Moskowitz, Howard	PD-108	283
Mosrati, Mohamed Ali	PS-295	195
Moss, Cynthia	PS-415	255
Motallebzadeh, Hamid	PS-750	490
Motegi, Hiromi	PS-289	192
Moteki, Hideaki	PS-286	191
Motley, Samantha	PS-305	200
Motohashi, Tsutomu	PS-179	97
Motwani, Kartik	SY-012	3
Mountain, David	PS-541	348
Mowery, Todd	PS-272, SY-064	183, 413
Mubeen, Humaira	PS-729	479
Mueller, Ulrich	PD-170, SY-078, SY-078, PD-205	428, 439, 439, 551
Muhanna, Nidal	PS-844	537
Mühler, Roland	PS-511	334
Mukherjee, Debashree	PS-367, PS-563, PS-578	232, 358, 366
Mulavara, Ajitkumar	PS-420	257
Mulders, Wilhelmina	PS-817	525
Mullangi, Ala	PS-437, PS-441	297, 299
Müller, Marcus	PS-226, PS-527	160, 341
Müller, Peter Paul	PS-564	359
Müller, Susanne	PD-127	292
Mullins, Cody	SY-012	3
Munjal, Tina	PS-481	319
Münkner, Stefan	PS-849, PD-104, PD-105	163, 281, 282
Munnamalai, Vidhya	PD-099	279
Munro, Kevin	PS-830	530
Murakami, Gen	PS-735	482

Name	Abstract No.	Page No.
Murata, Junko	PS-781	506
Mustapha, Mirna	PD-021, PS-232, PD-170	125, 164, 428
Muthaiah, Vijaya Prakash Krishnan	PS-362	229
Na, Li	PS-633	394
Nacev, Alek	PD-113	285
Nadol, Joseph	SY-059	273
Nagatani, Yoshiki	PS-525	340
Naghani, Iman	PS-548	351
Naghibolhosseini, Maryam	PS-129	73
Nagode, Daniel	PS-311	203
Nahm, Edmund	PS-576	365
Nair, Thankam	PS-767	499
Naito, Yasushi	PS-766	498
Nakagawa, Seiji	PS-596, PS-597, PS-687	375, 376, 457
Nakagawa, Takayuki	PS-217, PD-061, PS-530, PS-623, PS-625, PD-133, PD-149, PD-158, PS-778, PD-210	116, 149, 342, 389, 389, 405, 417, 422, 504, 554
Nakahara, Haruka	PS-016, PS-083	47, 50
Nakahara, Ichiro	PS-219	117
Nakajima, Hideko Heidi	PS-721, PS-722, PD-192	474, 475, 549
Nakajima, Hideko	SY-015, PD-193	118, 549
Nakamura, Takashi	PS-357	227
Nam, Jong-Hoon	PS-542, PS-544	348, 349
Nankali, Amir	PD-175	430
Narayanan, Praveena	PD-067	152
Narita, Ryo	PD-149	417
Naskar, Souvik	PS-327, PS-328	211, 212
Nauwelaers, Tim	PD-026	132
Nava, Casey	PS-288	192
Navaratnam, Dhasakumar	PS-547, PS-548, PS-549, PS-674	351, 351, 351, 452
Nayagam, Bryony	PS-030, PS-231, PS-624	24, 163, 389
Nayak, Shruti	PD-053	145
Neal, Christopher	PS-391, PS-823	243, 527
Necciari, Thibaud	PS-610	382
Needham, Karina	PS-030, PS-231, PS-624	24, 163, 389
Neely, Stephen	PS-546, PS-721	350, 474
Neilans, Erikson	PS-589, PS-592	372, 373
Nelina, Anastasiia	SY-074	438
Nelken, Israel	PS-267	181
Nelson, Paul	PS-076	46
Nelson, Rick	PS-300	197
Neng, Lingling	PS-018, PS-325, PS-326	18, 211, 211
Nerlich, Jana	PS-695	461
Neuman, Arlene	PS-652	441
Neusius, Daniel	PS-407	251
Newlands, Shawn	PS-204	110
Newman, Dina	PS-283	189
Ng, Sum-yan	PS-553	353
Ng, Zheng Yen	PS-490	324
Ngodup, Tenzin	PS-675	452
Nguyem, Tot Bui	PS-208	111
Nguyen-Huynh, Anh	PS-476	317
Nguyen, Kimanh	PS-031	25
Nguyen, Tot Bui	PS-200, PS-215	108, 115
Nguyen, Yann	PS-507, PD-188, PD-190	332, 547, 548

Name	Abstract No.	Page No.
Ni, Amy	PS-187	101
Nibu, Ken-ichi	PS-015, PS-343	17, 219
Nicholas, Brian	PS-562	357
Nichols, David	PS-529	342
Nichols, Michael	PD-151	419
Nicoletti, Michele	PS-169, PS-663	92, 446
Nicolson, Teresa	SY-008, PS-649, PS-759	2, 402, 495
Nie, Kaibao	PS-644, PS-645, PS-671	400, 400, 450
Nie, LiPing	PD-058	147
Nielsen, Lillian	PS-802	517
Nik, Atefeh Mousavi	PS-335	215
Nishimura, Tadashi	PS-525, PS-526, PS-720, PS-746	340, 340, 474, 488
Nishio, Ayako	PS-535	345
Nishitani, Allison	PD-161	424
Niwa, Katsuki	PS-026, PS-373	22, 234
Noda, Takahiro	PS-016, PS-083, PS-085, PS-086	47, 50, 51, 51
Noda, Tetsuo	PS-289, PD-095	192, 277
Noftz, William	PS-070	43
Nopp, Peter	PS-169	92
Noreña, Arnaud	SY-026	126
Norman-Haignere, Samuel	PS-795	513
Norris, Jesse	PD-075	156
Nouaille, Sylvie	PD-102	280
Nourski, Kirill	PS-436, PD-202, PD-211	297, 544, 545
Nouvian, Régis	PS-243, PS-354	169, 226
Novak, Michael	PS-137	76
Nowack, Amy	PS-644, PS-645	400, 400
Numata, Ryota	PS-264	180
Nutile, Teresa	PS-284	189
Nuttall, Alfred L.	PS-539, PS-540	347, 347
Nuttall, Alfred L.	PS-568	360
Nuttall, Alfred	PS-552	353
O'Beirne, Greg A.	PS-145	80
O'Brien, Daniel	PS-322	209
O'Connell, Samantha	PD-200	543
O'Leary, Catherine	PS-634	394
O'Leary, Stephen	SY-037	130
O'Neill, William	PS-412, PS-612	254, 383
Oba, Sandy	PS-474	316
Ober, Thomas	PD-118	288
Obermair, Gerald J.	PD-104	281
Ochi, Shohei	PS-530	342
Oertel, Donata	PS-692	460
Oesterle, Elizabeth	PS-190	102
Offutt, Sarah	PS-132	75
Oghalai, John	PS-334, PS-550	215, 352
Ogita, Kiyokazu	PS-778	504
Ogun, Olugwatobi	PD-145	412
Oh, Hun Jae	PS-029	24
Oh, Sejo	PS-035	26
Oh, Seung Ha	PS-248, PD-114	171, 286
Oh, Seung-Ha	PS-262, PS-512	179, 334
Ohlemiller, Kevin	PS-534, PD-171	345, 429
Ohnishi, Hiroe	PS-623	389
Oishi, Naoki	PS-376	236
Ojemann, Jeff	SY-006	2

Name	Abstract No.	Page No.
Ojima, Hisayuki	PS-591	373
Okano, Hideyuki	PS-781	506
Okayasu, Tadao	PS-525, PS-526	340, 340
Okunade, Oluwarotimi	PD-004	5
Oline, Stefan	PS-696	462
Oliver, Douglas	PS-061, PS-064, PS-460	39, 41, 309
Olmstead-Leahey, Shawn	PS-634	394
Olofsson, Åke	PS-410	253
Olson, Elizabeth	PS-256, PD-172	175, 429
Olson, Janet	PS-618	386
Olszewski, Łukasz	PD-073	155
Omelchenko, Irina	PS-190, PS-568	102, 360
Ong, H.C.	PS-073	44
Onishi, Hiroe	PS-625	389
Ono, Kazuya	PD-046	142
Ono, Munenori	PS-064	41
Onomoto, Koji	PD-149	417
Oppenheim, Jacob	PS-788	510
Orchard-Mills, Emily	PS-404	249
Ordoñez, Rodrigo	PD-072	154
Orestes, Peihan	PS-574	363
Ornitz, David	PD-157	422
Ortega, Aída	PS-337	216
Oshima, Hidetoshi	PS-038	28
Oshima, Kazuo	PD-037	137
Oshima, Takeshi	PS-005, PS-038	13, 28
Osumi, Noriko	PS-005, PS-348	13, 223
Ota, Jun	PS-841	536
Otsuka, Sho	PS-143, PS-609	79, 382
Otsuki, Naoki	PS-343	219
Otto-Meyer, Sebastian	PS-689	458
Otto, Larissa	PS-117	66
Ou, Henry	PS-558	356
Ouda, Ladislav	PS-266	181
Owada, Yuji	PS-005	13
Owoc, Maryanna	PS-062, PD-025, PS-498	40, 131, 178
Oxenham, Andrew J.	PS-128, PS-153	73, 84
Oxenham, Andrew J	PS-051	34
Oxenham, Andrew	PD-017, PS-473, PS-607, PS-791, PS-793	123, 315, 381, 511, 512
Oya, Hiroyuki	PS-275, PS-436, PD-202, PD-211	185, 297, 544, 545
Paasche, Gerrit	PS-249	172
Paciello, Fabiola	PS-382	239
Padilla, Monica	PD-182, PS-666	434, 448
Paige, Gary	PS-412, PS-612	254, 383
Pak, Kwang	PS-189, PD-018, PD-110, PS-737, PS-738	102, 123, 284, 483, 484
Pak, Natalie	PS-397	246
Palmer, Alan	PD-017, PS-701	123, 464
Paloski, William	PS-640	398
Pals, Carina	SY-050	270
Paludetti, Gaetano	PS-382	239
Pan, Bifeng	PD-045, PD-063	141, 150
Pan, Ning	PS-312, PS-529	204, 342
Pan, Wei	PD-141	410
Pandey, A	PD-143	411
Pangrsic, Tina	SY-007	2

Name	Abstract No.	Page No.
Pannu, Satinderpall	PS-246, PS-478	170, 318
Paparella, Michael	PS-733, PS-740	481, 485
Papesh, Melissa	PS-518	337
Papsin, Blake C.	PS-472	315
Papsin, Blake C	PS-643	399
Papsin, Blake	SY-069, PS-655	416, 442
Paquette, Stephen	PS-287	191
Paquette, Steve	PS-764	497
Pararas, Erin	PS-716	472
Parbery-Clark, Alexandra	PS-010	15
Park, Ah Young	PS-522	339
Park, Albert	PS-389	242
Park, Channy	PD-006, PD-164	6, 425
Park, Heesung	PS-523	339
Park, Hong Ju	PS-428, PS-842	261, 536
Park, Hun Yi	PS-372	234
Park, Hyo-Jin	PS-013	16
Park, Il Yong	PS-392	243
Park, Il-Yong	PS-834	532
Park, Jae Hong	PS-032	25
Park, Jung-sub	PS-581	367
Park, Kyoung Ho	PS-842	536
Park, Kyung Tae	PS-032, PD-132	25, 405
Park, Mi Na	PD-114	286
Park, Min-Hyun	PS-248	171
Park, Moo Kyun	PS-731	480
Park, Raekil	PS-035	26
Park, Sang Myun	PS-581	367
Park, Sera	PS-313	204
Park, Shi-Nae	PS-561	357
Park, So Young	PS-561	357
Park, Su Kyoung	PS-262	179
Park, Su-Kyoung	PS-512	334
Park, Thomas J	PS-682	455
Park, Yong-Ho	PS-632	393
Park, Yunea	PS-025	21
Parker, Andrew	PD-131	294
Parker, B. Eugene	PS-416	256
Parker, Luke	PS-132	75
Parker, Mark	PS-194	104
Parmar, Hemant	PS-503	330
Parthasarathy, Aravindakshan	PS-022, PD-128	20, 292
Pastore, M. Torben	PS-168	91
Patel, Aniruddh	PD-215	547
Patel, Chirag	PS-463	310
Patrick, Jim	SY-001	1
Patterson, Jessica	SY-012	3
Paul, Brandon	PS-082	49
Pavlik, Valory	PS-420	257
Pavlinkova, Gabriela	PS-178	96
Pawelczyk, Malgorzata	PS-282	188
Payne, Christopher	PD-213	546
Pearce, M. T.	PS-602	378
Pearl, Monica	PD-027	132
Pecka, Jason	PS-631	392
Pecka, Michael	PS-407	251

Name	Abstract No.	Page No.
Pedemonte, Marisa	PS-593, PS-831, PS-832, PS-833	374, 531, 531, 532
Pena, Jose L	PS-101	58
Peña, José Luis	PS-105	60
Pena, José	PS-702	465
Peng, Anthony	SY-072	437
Peng, You-Wei	PS-301	198
Peng, Zhenling	PS-356	227
Penninger, Richard	SY-054	271
Peppi, Marcello	PS-019, PS-318	19, 207
Perachio, Adrian	PS-212, PS-332	113, 214
Pereira, Fred	PD-005, PS-633	5, 394
Pereira, Frederick	PS-551	352
Pereira, Miguel	PS-640	398
Perez-Flores, Maria Cristina	PD-121	289
Perez-Flores, Maria	PD-208	553
Pérez-González, Patricia	PS-144, PD-074	80, 155
Perez, Ronen	PS-844	537
Perrin, Benjamin	PD-067	152
Perry, Trevor	PD-030	134
Peters, Brian	PS-420	257
Peterson, Adam	PS-222	158
Peterson, Diana	PS-442	300
Peti-Peterdi, Janos	PS-730	479
Petit, Christine	PD-065, PD-102, PS-755	151, 280, 493
Petrie, Tracy	PS-540	347
Pfeifer, Karl	PD-208	553
Pfingst, Bryan E.	PD-062, PS-471	149, 314
Pfingst, Bryan	PS-253, PS-484	174, 321
Pham, Catherine	PS-829	530
Phatak, Sandeep	PS-517	337
Philippon, Bertrand	PS-664	447
Philips, Amanda	PS-503	330
Phillips, Christopher	PS-644, PS-645	400, 400
Phillips, James	PS-208, PS-644, PS-645	111, 400, 400
Phillips, Jim	SY-004	1
Picher, Maria	PS-763	497
Pienkowski, Martin	SY-027, SY-065	126, 414
Pierce, Marsha	PS-185, PS-537	100, 346
Pierre, Pernilla Videhult	PS-521	339
Pierson, Ken	PS-636	395
Pierstorff, Erik	PS-713	470
Pineda, Mario	PD-195	550
Pinggera, Leyla	PS-364	230
Piotrowska, Anna	PD-073	155
Piotrowski, Tatjana	PD-031	134
Pirastu, Mario	PS-284	189
Pirvola, Ulla	PS-186, PS-198, PD-155, PS-846	100, 107, 421, 538
Piu, Fabrice	PS-708	467
Plack, Chris	PS-685	456
Plack, Christopher	PS-146	80
Plontke, Stefan	PS-708, PS-709	467, 468
Plue, Jan	PD-116	287
Pogorzelski, Olivia	PS-709	468
Pogson, Jacob	PS-646	401
Pollak, George	PS-067	42
Polley, Daniel B.	PS-257	176

Name	Abstract No.	Page No.
Polley, Daniel	PS-062	40
Pollock, Lana	PD-219	555
Ponnath, Abhilash	PS-715	471
Poon, Paul W.F.	PS-794	512
Popelar, Jiri	PS-717, PS-794	472, 512
Popelka, Gerald	SY-018	120
Porter, Brenda Elaine	PD-170	428
Portfors, Christine	PS-074, PS-065, PS-705	45, 262, 466
Portmann, Thomas	PS-074	45
Portwood, Neil	PS-679	453
Potter, Paul	PD-131	294
Powell, Kimerly	PS-500	328
Praetorius, Mark	PS-260	177
Preciado, Diego	PS-729	479
Presacco, Alessandro	PD-125	291
Pressnitzer, Daniel	PS-274	184
Price, Steven D.	PS-214, PD-048, PD-049	114, 143, 143
Prieskorn, Diane	PS-771, PS-819	501, 525
Primus, Michael	PS-789	510
Prince, Sara	PS-780	506
Pritchett, Cedric	PS-503	330
Pritz, Christian	PS-364	230
Prolla, Tomas	PS-361	229
Prosolovich, Ksenia	PS-480	319
Puel, Jean-Luc	PD-020, PS-243, PS-244, PS-354, SY-057	124, 169, 169, 226, 272
Pujol, Remy	PS-200	108
Puligilla, Chandrakala	PD-143	411
Pulliam, Nicole	PS-369	233
Purcell, David	PS-055, PS-125, PS-440	36, 71, 299
Puria, Sunil	SY-016, PD-117	119, 287
Purwar, Shalini	PS-441	299
Putterman, Daniel	PS-387, PS-727	241, 478
Puvvada, Krishna	PS-094	55
Puwol, Brenda	PS-386	241
Pyott, Sonja	PD-218	555
Qiu, Hong	PD-100	279
Quatieri, Thomas F.	PS-572	362
Quesnel, Alicia	PD-115	286
Quiñones, Patricia M.	PD-041, PD-066	139, 151
Rabbitt, Richard D	PD-051, PD-052	144, 144
Rabbitt, Richard	PD-106	282
Rabinowitz, Neil	PS-161	87
Radtke-Schuller, Susanne	PS-277, PS-449	186, 303
Radulovic, Tamara	PS-847	539
Radziwon, Kelly	PS-148, PS-812, PS-815	81, 522, 524
Rah, Yoon Chan	PS-032, PD-132	25, 405
Rahman, Irfan	PS-287	191
Rahmat, Sarah	PS-145	80
Rahne, Torsten	PS-511	334
Raible, David	PD-137, PD-138	408, 408
Raimundo, Nuno	PS-768	499
Rainey, Robert	PS-553	353
Rajguru, Suhrud	PS-259, PS-479, PS-566, PD-207	177, 318, 360, 552
Rajkowska, Elzbieta	PS-282	188
Rakhmankulova, Malika	PS-559	356

Name	Abstract No.	Page No.
Ramachandran, Ramnarayan	PS-147, PS-160, PS-411, PS-703	81, 87, 253, 465
Ramakrishnan, Neeliyath	PS-761, PS-762	496, 496
Ramamoorthy, Sripriya	PS-540	347
Ramekers, Dyan	PS-234, PS-245	165, 170
Ramkumar, Vickram	PS-367, PS-563, PS-578	232, 358, 366
Randle, Michelle	PS-192	103
Rankin-Gee, Elyse	PD-170	428
Rankin, Summer	PS-588	371
Raphael, Patrick	PS-334	215
Raphael, Robert	PD-005, PS-551	5, 352
Raphael, Yehoash	PS-209, PD-035, PD-062, PS-253, PS-358, PD-098, PS-471, PS-632, PD-156, PS-771	112, 136, 149, 174, 228, 278, 314, 393, 421, 501
Raphan, Theodore	PS-207	111
Rasetshwane, Daniel	PS-546	350
Rask-Andersen, Helge	PS-302	198
Rassendren, François	PS-354	226
Ratnanather, J. Tilak	PS-837	534
Rauch, Steven	PS-419	257
Ravicz, Michael	PS-744, PS-745	487, 488
Ray, Chester	SY-024	122
Rayford, Margie	PS-647	401
Rayyan, Amal Abu	PD-007	6
Razak, Khaleel	PS-007, PS-090, PD-201	14, 53, 544
Rebscher, Stephen	PS-395	245
Reed, George W.	PS-520	338
Reeder, Ruth	SY-070	416
Rehm, Heidi L.	PS-296	195
Rehman, Zarin	PS-227, PS-369	161, 233
Reini, Seth	PS-417	256
Reiss, Lina	PD-079, PS-476	267, 317
Remick, Taylor	PS-686	457
Remme, Michiel	PS-458	308
Ren, Chongyu	PD-045	141
Ren, Dong-Dong	PD-060	148
Ren, Tianying	PS-543	349
Renaud, Philippe	PS-250	172
Rennie, Katherine	PD-050	143
Reuter, Kirsten	PS-753	492
Reznicek, Gottfried	PD-112	285
Rhee, Chung-Ku	PS-392	243
Rhode, William	PS-701	464
Rhone, Ariane	PS-436	297
Ricci, Anthony J.	PD-117	287
Ricci, Anthony	PS-329, PS-355, PS-550, PD-134, SY-072, SY-075, PS-757, PS-758	212, 226, 352, 406, 437, 438, 494, 494
Ricci, Natalia	PS-420	257
Richardson, Ben	PS-079	48
Richardson, Guy	PD-064, PS-327, PS-328	150, 211, 212
Richardson, Matthew	PS-519	338
Richardson, Neal	PS-416	256
Richter, Claus Peter	PS-328	212
Richter, Claus-Peter	PS-258, PS-319, PS-320, PS-321, PS-322, PS-327	176, 208, 208, 209, 209, 211
Rieger, Brian	PS-053	35

Name	Abstract No.	Page No.
Rielo, Diego	PS-013	16
Rigo, Frank	PS-715	471
Rine, RoseMarie	PS-421	258
Rinzel, John	PS-435, PS-438, PS-454, PS-458	296, 298, 306, 308
Ripken, Tammo	PD-206	552
Rivera, Ileana	PS-388	242
Rivolta, Marcelo	PD-056	146
Roark, Kelly	PS-573	363
Roberson, Efreem	PS-479	318
Roberts, Dale	PS-216, PS-635, PS-637	115, 395, 396
Roberts, Larry	PS-082	49
Roberts, Larry	126	
Roberts, Melissa	PS-028	23
Roberts, Michael T.	PS-455	306
Roberts, Michael	PS-462	310
Roberts, Patrick	PS-705	466
Robertson, Donald	PS-817	525
Robins, Mike	PS-646	401
Robinson, Alan	PS-320	208
Robinson, Barbara	PS-241	168
Robles, Luis	PS-087	52
Roccio, Marta	PS-252	173
Rocha-Sanchez, Sonia	PS-196, PS-197	106, 106
Rodio, Silvana	PS-831	531
Rodrigues, Helio	PS-386, PS-388	241, 242
Rodriguez-Contreras, Adrian	SY-013	4
Roehm, Pamela	PD-053	145
Rogers, Amanda Mahoney	PS-177	96
Romero-Carvajal, Andres	PD-031	134
Romigh, Griffin	PS-804	518
Roongthumskul, Yuttana	PD-040, PD-178	139, 432
Röösli, Christof	PD-177	431
Roosli, Christof	PS-722	475
Röösli, Christof	PS-741	486
Roosli, Christof	PS-748	489
Rose, Mary	PS-729	479
Rosen, Stuart	PS-003, PS-798	12, 515
Rosowski, John J.	SY-015, PS-722, PD-192	118, 475, 549
Rosowski, John	SY-017, PS-721, PS-739, PS-742, PS-743, PS-744, PS-745, PD-193	120, 474, 484, 486, 487, 487, 488, 549
Ross, Deborah	PS-255, PS-276	175, 185
Rosskoth-Kuhl, Nicole	PS-133	75
Roth, Daphne Ari-Even	PS-807	519
Roth, Jerome	PS-363	230
Rothwell, Clayton	PS-396	245
Roushan, Kourosh	PD-192	549
Roux, Sylvie	PS-263	179
Roverud, Elin	PS-108	62
Roy, Alexis	PD-027, PS-481, PS-482	132, 319, 320
Roy, Soumen	PS-042	30
Rubel, Edwin W	PD-150	418
Rubel, Edwin	PS-190, PS-208, PS-305, PD-137, PD-138	102, 111, 200, 408, 408
Ruben, Robert	PS-497	327
Rubinato, Elisa	PD-008	7

Name	Abstract No.	Page No.
Rubinstein, Jay	PS-314, PS-644, PS-645, PS-671	205, 400, 400, 450
Rubio, Maria	PS-694	461
Rübsamen, Rudolf	PS-673, PS-693, PS-695, PS-847	451, 460, 461, 539
Rudnicki, Anya	PD-098	278
Rudnicki, Marek	PS-486	322
Ruggles, Dorea	PS-051	34
Ruiz, Fernanda	PS-633	394
Runge, Christina	PS-665	447
Rupp, Anna Sartori	PD-102	280
Rupprecht, Laura	PS-541	348
Russo, Francesca Yoshie	PS-707	467
Russo, Francesca	PS-131	74
Rutherford, Mark A	SY-007	2
Rüttiger, Lukas	PD-129, PS-536, PS-554	293, 346, 354
Ryals, Matthew M.	PS-042	30
Ryan, Allen F	PS-189	102
Ryan, Allen	PD-110, PS-737, PS-738	284, 483, 484
Rybak, Leonard P	PS-367, PS-578	232, 366
Rybak, Leonard	PS-028, PS-563	23, 358
Rybalko, Natalia	PS-717, PS-794	472, 512
Ryu, Nam Gyu	PS-523	339
Ryugo, David	SY-011, PS-225	3, 160
Saaï, Sonia	PS-664	447
Sabin, Andrew	PS-406	251
Sadeghi, Soroush	PS-213	114
Safieddine, Saaïd	PD-102, PS-755	280, 493
Sagal, Jonathan	PS-822	526
Sah, Anupam	PD-105	282
Saiakhova, Alina	PD-156	421
Saija, Jefta	PS-608	381
Saito, Kazuya	PS-426	260
Saito, Naohisa	PS-357	227
Saito, Osamu	PS-526	340
Sajani, Ravin	PS-259	177
Sakaguchi, Hirofumi	PS-357, PS-394	227, 244
Sakai, Yoshihisa	PS-356, PS-532, PD-218	227, 343, 555
Sakamoto, Takashi	PS-199	107
Sakamoto, Tatsunori	PS-217	116
Sakuraba, Mayumi	PS-781	506
Salcher, Rolf	PS-724	476
Salles, Felipe	PS-758	494
Salloum, Rony	PS-827, PS-828	529, 529
Salminen, Nelli	PS-095	55
Salt, Alec	PS-708, PS-709, PS-775	467, 468, 503
Salvi, Richard	PS-027, PS-131, PS-280, PS-342, PS-361, PS-362, PS-363, PS-586, PS-707, PS-811, PS-812, PS-814, PS-815	23, 74, 187, 219, 229, 229, 230, 370, 467, 522, 522, 523, 524
Saman, John	PS-388	242
Sametsky, Evgeny	PS-816	524
Samy, Ravi	PD-082	268
Sanchez, Jason	PS-689	458
Sanders, Holden	PS-093	54
Sandridge, Sharon	PS-827	529
Sanes, Dan H.	PS-316	206

Name	Abstract No.	Page No.
Sanes, Dan	PS-078, PS-155, PS-272, PS-524, SY-064	47, 85, 183, 206, 413
Sangi-Haghpeykar, Haleh	PS-420	257
Sanjust, Filippo	PS-120	68
Santi, Peter	PS-775	503
Santiago, Lia	PS-827	529
Santos-Sacchi, Joseph	PD-003, PD-004, PS-547, PS-548, PS-549, PS-674, PS-768	5, 5, 351, 351, 351, 452, 499
Santos, Sona	PD-058	147
Santurette, Sébastien	PS-492	325
Sarampalis, Anastasios	SY-050	270
Sarieddine, Doja	PS-502	513
Sarwar, Azeem	PD-113	285
Sasson, Yonatan	PS-159	87
Sato, Mika	PD-206	552
Sato, Mitsuo	PS-426	260
Satoh, Shun-ichi	PS-373	234
Satoh, Yasushi	PS-026	22
Saunders, Gabreille	PS-809	520
Savelyev, Sergey Savelyev	PS-014	17
Savoy-Burke, Grace	PD-141	410
Saxena, Renu	PS-296	195
Saxena, Udit	PS-513	335
Sayed, Zafar	PS-310, PS-628	203, 391
Sayles, Mark	PS-237, PS-706	166, 466
Sayyid, Zahra	PS-193	104
Scacheri, Peter	PD-156	421
Schachern, Monika	PS-740	485
Schachern, Pat	PS-740	485
Schachern, Patricia Schachern	PS-733	481
Schacht, Jochen	PS-374, PS-376	235, 236
Schäck, Luisa	PS-619	387
Schad, Maggie	PS-236	166
Schaefer, Stacy	PS-622, PS-629	388, 391
Schaette, R.	PS-073	44
Schaivon, Emanuele	PS-684	456
Scharinger, Anja	PD-105	282
Scheffer, Deborah	PD-068	152
Schemitsch, Michael	PS-161	87
Scheper, Verena	PS-249, PS-564	172, 359
Scheuer, Veronika	PS-849	163
Schick, Bernhard	PD-104, PD-105	281, 282
Schimmang, Thomas	PS-554	354
Schleich, Peter	PS-169	92
Schmidt, Sara	PS-843	537
Schmutzhard, Joachim	PS-364	230
Schnee, Michael	PS-329, PS-757	212, 494
Schoernich, Sven	PS-805	518
Schofield, Brett R	PS-071	43
Schofield, Brett	PS-069	42
Scholes, Chris	PS-701	464
Schönig, Kai	PD-105	282
Schoof, Tim	PS-003	12
Schöpfer, Hanna	PD-112, PS-712	285, 470
Schrode, Katrina	PS-230	162
Schroeder, Charles	PS-255, PS-276	175, 185
Schrott-Fischer, Annelies	PS-364	230

Name	Abstract No.	Page No.
Schrott-Fischer, Anneliese	PS-302	198
Schubert, Michael	PS-635, PS-636, PS-637	395, 395, 396
Schularick, Nathan	PS-300	197
Schulte, Bradley	PS-341	218
Schultz, Michael	PD-206	552
Schulze, Holger	PD-198, PD-199	542, 543
Schumacker, Paul	PS-366	231
Schuon, Robert	PS-724	476
Schuster, Maria	PS-470	314
Schwander, Martin	PD-205	551
Schwarz, Douglas M.	PS-787	509
Schweizer, Felix	PS-218	116
Schwieger, Jana	PS-564	359
Scollie, Susan	PS-055	36
Scott, Ansley	PS-647	401
Scott, Michael	PD-082	268
Screven, Laurel A.	PS-589	372
Screven, Laurel	PS-595	375
Seal, Rebecca	PS-676	453
Sedlacek, Miloslav	PS-239	167
Sedley, William	PS-275	185
Segawa, Kohei	PD-046	142
Segil, Neil	PS-553, PD-136, PD-140	353, 407, 409
Sehrawat, Kamini	PS-220	157
Seidman, Christine	PS-575	364
Seidman, Jonathan	PS-575	364
Seitz, Aaron	PS-614, PS-806	384, 519
Seline, Alison	PD-078, PS-620	266, 387
Selvakumar, Dakshnamurthy	PD-107	283
Selwood, David	PS-338	217
Sendin, Gaston	PS-354	226
Senn, Pascal	PD-037, PS-252	137, 173
Seo, Jin Young	PS-188	101
Seo, Toru	PS-426	260
Serrador, Jorge	PS-430	262
Sessoms, Pinata	PS-417	256
Setou, Mitsutoshi	PS-499, PS-501	328, 329
Seward, Keena	PS-480, PS-652	319, 441
Sewell, William	PD-115, PS-716	286, 472
Sha, Su-Hua	PS-359, PS-360, PS-375, PD-143, PD-166, PD-169	228, 229, 235, 411, 426, 428
Shadel, Gerald	PS-768	499
Shah, Kedar	PS-246	170
Shalev, Stavit	PD-007	6
Shamma, Shihab	PS-051, PS-097, PS-848, PS-274, PS-277, PS-431, PS-435, PS-446	34, 56, 57, 184, 186, 294, 296, 302
Shamsil, Arefin	PS-506	331
Shanbhag, Sharad	PS-089	53
Shanthakumar, Prashanthini	PD-131	294
Shapiro, Ben	PD-113	285
Shapiro, John	PS-461	309
Shaul, Chanan	PS-844	537
Shearer, A. Eliot	PD-010, PS-286	8, 191
Sheehan, Kelly	PS-367, PS-563, PS-578	232, 358, 366
Sheets, Kristopher	PS-218	116
Sheets, Lavinia	PS-759	495
Sheffield, Benjamin	PS-517	337

Name	Abstract No.	Page No.
Sheft, Stanley	PS-172	93
Shelhamer, Mark	PS-636, PS-637	395, 396
Shen, Da-Wei	PS-794	512
Shen, Jun	PD-068, PD-069, PS-296	152, 153, 195
Shen, Li	PS-438	298
Shen, Yi	PS-590	372
Shepherd, Robert	PS-254, PS-478, PS-719	174, 318, 473
Sheppard, Adam	PS-027, PS-814	23, 523
Shera, Christopher	PS-050, PS-118, PD-017, PS-747, PS-835	33, 67, 123, 489, 533
Sheth, Heeral	PS-246	170
Sheth, Meghal	PS-381	238
Sheth, Sandeep	PS-563	358
Sheykholeslami, Kianoush	PS-288	192
Shi, Fuxin	PD-059, PS-538	148, 346
Shi, Xiaorui	PS-018, PS-325, PS-326	18, 211, 211
Shibata, Seiji	PD-094	277
Shim, Dae Bo	PS-370	233
Shim, Hyun Joon	PS-838	534
Shim, Hyun-Yong	PS-523	339
Shim, Katherine	PS-177	96
Shim, Myung Joo	PS-561	357
Shimizu, Naoki	PS-212	113
Shimogori, Hiroaki	PS-036, PS-368, PS-423, PS-427, PS-648	27, 232, 259, 261, 402
Shimokura, Ryota	PS-720, PS-746	474, 488
Shin, Jung-Bum	PD-070, PS-562	153, 357
Shinn-Cunningham, Barbara G.	PS-257	176
Shinn-Cunningham, Barbara G	PS-021, PS-054	19, 35
Shinn-Cunningham, Barbara	PS-045, PS-050, PS-052, PS-057, PS-088, PD-087	31, 33, 34, 37, 52, 273
Shinomiya, Hitomi	PS-343	219
Shiotani, Akihiro	PS-026, PS-373	22, 234
Shirai, Kyoko	PS-740	485
Shiramatsu, Tomoyo	PS-016, PS-086	47, 51
Shiramatsu(Isoguchi), Tomoyo	PS-083	50
Shivatzki, Shaked	PD-098, PD-146, PS-771	278, 412, 501
Shives, Katherine D	PS-728	478
Shomron, Noam	PD-007	6
Shore, Susan E.	PS-136	521
Shore, Susan	PS-140, PS-818, SY-046, PS-819, PS-820	78, 117, 265, 525, 526
Shorter, Heidi	PS-041	29
Shu, Yilai	PD-032	135
Shull, Gary	PD-122	290
Shulman, Eli	PS-374	235
Shumway, Rylee J.	PD-041	139
Sichel, Jean-Yves	PS-844	537
Siegel, Jonathan	PS-114, PS-115, PS-119, PD-071, PS-721	65, 65, 68, 154, 474
Sihn, Choong Ryoul	PD-208	553
Sihn, Choong-Ryoul	PS-352, PD-122, PD-124, PD-218	225, 290, 290, 555
Silipino, Lorna	PD-010, PD-011	8, 9
Sim, Jae Hoon	PS-477, PD-177, PS-741, PS-748	317, 431, 486, 489
Simhadri, Sravanthi	PD-093	276

Name	Abstract No.	Page No.
Simmons, Caitlin	PS-025	21
Simmons, Dwayne	PS-534	345
Simmons, James	PS-699	463
Simon, Jonathan Z.	PS-094	55
Simon, Michelle	PD-131	294
Simoncelli, Eero	PS-161	87
Simpson, Brian D.	PS-804	518
Simpson, Brian	PS-092	54
Singer, Wibke	PS-554	354
Singewald, Nicolas	PD-105	282
Singheiser, Martin	PS-098	57
Sinha, Ghanshyam P.	PD-164	425
Sinha, Ghanshyam	SY-076, SY-077	439, 439
Sinks, Belinda	PS-416	256
Sinnegger-Brauns, Martina	PD-105	282
Sisto, Renata	PS-118, PS-120, PS-122	67, 68, 69
Skarzynski, Henryk	PD-073	155
Skidmore, Jennifer	PD-156	421
Skoe, Erika	PS-046	32
Slater, Jessica	PS-047, PS-138	32, 77
Slattery, William	PS-713	470
Sliwiska-Kowalska, Mariola	PS-282	188
Sloan, Christina	PD-010	8
Slowik, Amber	PD-047	142
Smalley, Joshua L.	PS-684	456
Smalt, Christopher	PS-572	362
Smeds, Henrik	PD-116	287
Smeets, Emma	PS-234	165
Smeti, Ibtihel	PD-159	423
Smith, Benjamin	PS-132	75
Smith, Heather Jensen	PD-151	419
Smith, Katie	PS-338, PS-339	217, 217
Smith, Michael	PS-187, PS-377	101, 236
Smith, Richard JH	PD-010, PS-286	8, 191
Smith, Richard	PD-094	277
Smith, Robert	PS-660	445
Smith, Spencer	PS-093	54
Smyth, Brendan	PS-324	210
Smythe, Nancy	PS-341	218
Snik, Ad	PD-185	436
Snyder, Joel	PD-088	274
Sohoglu, Ediz	PS-616	385
Soken, Hakan	PS-241	168
Sokolic, Ljiljana	PS-646	401
Sokolowski, Bernd	PS-176, PS-356, PS-532, PD-218	95, 227, 343, 555
Solomon, David	PS-425	260
Somers, David C	PS-021	19
Someya, Shinichi	PS-004, PS-013	12, 16
Sommers, Mitchell	PS-516	336
Son, Eun Jin	PS-522	339
Song, Chan Il	PS-428	261
Song, Jae June	PS-555	354
Song, Jae-Jun	PS-731	480
Song, Lei	PD-003, PS-674, PS-768	5, 452, 499
Song, Sang Hoon	PS-032	25
Song, Xinyu	PS-516	336

Name	Abstract No.	Page No.
Song, Yohan	PS-550	352
Sonja, Karg	PS-486	322
Sonntag, Mandy	PS-673	451
Soons, Joris	PD-117	287
Soto, Enrique	PS-337	216
Sotomayor, Marcos	PD-042, SY-073	140, 437
Soukup, Garrett	PS-185, PS-537, PS-631	100, 346, 392
Souluka, Athena	PD-100	279
Soutadeh, Kayvon	PD-134	406
Spankovich, Christopher	PS-025, PS-034	21, 26
Spear, Kayce	PS-476	317
Speedy, Sedona	PS-689	458
Spencer, Abigail	PS-716	472
Sperry, Ethan	PD-012, PD-156	9, 421
Spinelli, Kateri	SY-074	438
Spirou, George	SY-012	3
Spitsbergen, John	PS-584	369
Sprinzak, David	PD-146	412
Sripal, Prashanth	PS-631	392
Srivastava, Hemant	PS-076	46
Staecker, Hinrich	PS-019, PD-035, PS-391, PS-823	19, 136, 243, 527
Stagner, Barden B.	PS-111	63
Stamper, Greta	PS-039	28
Stankovic, Konstantina M.	PS-557	355
Stankovic, Konstantina	PD-118, PS-575	288, 364
Stansell, Meghan	PS-809	520
Stark, Gemaine	PS-476	317
Starzynski, Christian	PS-600	377
Stasiak, Arkadiusz	PS-152, PS-704	83, 466
Steadman, Mark	PS-434	296
Stecker, G. Christopher	PS-103, PS-401	59, 248
Steel, Karen P.	PS-299, PD-099	197, 279
Steel, Karen	PS-298	196
Steel, Morrison	PS-655	442
Steele, Charles R.	PD-117	287
Steele, Charles	SY-016	119
Steenon, Sharalyn	PS-185	100
Stefan, Stenfelt	PS-748	489
Stefanescu, Roxana	PS-818, PS-136	117, 521
Steinberg, Louisa	PS-702	465
Steinmann, Iris	PS-273	184
Steinmetzger, Kurt	PS-798	515
Steinschneider, Mitchell	PS-436, PS-443, PD-211	297, 300, 545
Stenfelt, Stefan	SY-014, PD-177	118, 431
Stepanyan, Ruben	PD-164, SY-074, SY-077	425, 438, 439
Stephan, Jonathan	PS-680	454
Stephani, Friederike	PS-849	163
Stephanopoulos, Nicholas	PS-628	391
Stepp, Cara E	PS-021	19
Sterkers, Olivier	PS-507, PD-188, PD-190	332, 547, 548
Steyger, Peter S.	PS-393	244
Steyger, Peter	PS-323, PS-380, PS-387, PS-569, PS-580, PS-587, PS-710, PS-711	210, 238, 241, 361, 367, 371, 468, 469
Stieger, Christof	SY-015, PD-192	118, 549
Stilp, Christian	PS-151, PS-667	83, 448
Stoddart, Paul	PS-231	163

Name	Abstract No.	Page No.
Stoelb, Corey	PS-158	86
Stojanova, Zlatka	PD-140	409
Stoller, Michelle L.	PD-099	279
Stolzberg, Daniel	PS-812, PS-815	522, 524
Stone, Jennifer S.	PS-215	115
Stone, Jennifer	PS-200, PS-208	108, 111
Strahl, Stefan	PS-245	170
Strait, Dana	PS-315, PS-528, PD-200	205, 341, 543
Stredney, Don	PS-500	328
Streit, Jürg	PS-252	173
Strenzke, Nicola	SY-007	2
Strickland, Elizabeth	PS-108, PS-141, PS-792	62, 78, 511
Striessnig, Joerg	PD-105	282
Strömbäck, Karin	PD-116	287
Strong, Melissa K.	PD-150	418
Strong, Melissa	PS-305	200
Stupp, Samuel	PS-628	391
Su, Gina L.	PS-253	174
Sugahara, Kazuma	PS-036, PS-365, PS-368, PS-423, PS-427, PS-648	27, 231, 232, 259, 261, 402
Sugimoto, Shunji	PS-264	180
Suh, Myung-Whan	PS-392, PD-114, PS-834	243, 286, 532
Sullivan, Sarah	PS-092	54
Summerfield, A. Quentin	PS-803	517
Summerfield, A. Quentin	PS-167	91
Sumner, Chris	PS-434	296
Sumner, Christian	PD-017, PS-701	123, 464
Sun, Hong	PS-342	219
Sun, Jian-he	PD-101	280
Sun, Jianhe	PD-038	138
Sun, Li	PD-085	270
Sun, Shuting	PD-115	286
Sun, Wei	PD-101, PS-675, PS-810, PS-813	280, 452, 521, 523
Sun, Xiao-Ming	PS-726	477
Sun, Ying	PD-204	551
Sunami, Kishiko	PS-638	396
Sundaresan, Srividya	PD-021, PS-232, PD-170	125, 164, 428
Sung, Michael	PD-018	123
Suri, Ranjan	PS-037	27
Suta, Daniel	PS-717, PS-794	472, 512
Suzuki, Hirokazu	PS-040	29
Suzuki, Jun	PS-005, PS-348	13, 223
Suzuki, Mitsuya	PS-012	16
Suzuki, Tomohiro	PS-289	192
Svirsky, Mario	PS-480, PS-515	319, 336
Swaminathan, Jayaganesh	PS-142	79
Swedenborg, Britta	PS-138	77
Swiderski, Donald L.	PS-632	393
Swiderski, Donald S.	PD-062	149
Swiderski, Donald	PS-209, PS-358, PD-156, PS-771	112, 228, 421, 501
Syka, Josef	PS-178, PS-266, PS-717, PS-794	96, 181, 472, 512
Tabuchi, Hisaaki	PS-610	382
Tachi, Eriko	PS-591	373
Tahmina, Qudsia	PS-665	447
Taira, Masato	PS-591	373

Name	Abstract No.	Page No.
Takada, Yohei	PD-098, PS-771	278, 501
Takahashi, Hirokazu	PS-016, PS-083, PS-085, PS-086	47, 50, 51, 51
Takahashi, Kazusa	PS-016, PS-083	47, 50
Takanashi, Yoshitaka	PS-735	482
Takata, Iori	PS-348	223
Takata, Yusuke	PS-005, PS-348	13, 223
Takeda, Taizo	PS-777	504
Takeshima, Chihiro	PS-784	508
Taketo, Makoto	PD-033	135
Taki, Kousuke	PS-066	41
Tambs, Kristian	PS-520	338
Tamura, Atsushi	PS-026, PS-373	22, 234
Tan, Chin-Hong	PS-137	76
Tan, Chin-Tuan	PS-480	319
Tan, Grace	PS-216	115
Tan, Justin	PS-719	473
Tan, Xiaodong	PS-319, PS-320, PS-321, PS-322	208, 208, 209, 209
Tanaka, Chiemi	PS-476	317
Tandon, Vishal	PS-716	472
Tang, Xiaoying	PS-837	534
Tang, Xuehui	PS-647	401
Tang, Zheng-Quan	PS-107	61
Taniguchi, Mirei	PD-210	554
Tao, Litao	PD-136	407
Tarang, Shikha	PS-197	106
Tarsha, Amir	PS-386	241
Tass, Peter	SY-049	266
Tateya, Ichiro	PS-182, PS-499, PS-501	98, 328, 329
Tateya, Tomoko	PS-182	98
Taura, Akiko	PS-217, PD-061, PS-530, PD-149	116, 149, 342, 417
Teitz, Tal	PS-378	237
Teki, Sundeep	PD-213	546
Telian, Steven	PS-503	330
Telisch, Fred	PS-386	241
Tellers, Philipp	PS-099, PS-464	58, 311
Tempel, Bruce	PD-043, PS-290, PD-123	140, 193, 290
Terreros, Gonzalo	PS-087	52
Teruyama, Ryoichi	PS-781	506
Testa, Martín	PS-832	531
Thein, Pru	PS-565	359
Thimmappa, Vikrum	PS-288	192
Thomas, Andrew	PS-558	356
Thompson, David	PS-082	49
Thompson, Elaine	PS-315	205
Thompson, Eric	PS-092, PS-804	54, 518
Thompson, Kelsey	PD-135	406
Thorne, Marc	PS-503	330
Thorne, Peter	SY-010	3
Thornton, Jennifer	PD-043	140
Thorson, Daniela	PS-278	186
Thorson, Ivar	PS-279	187
Tian, Chunjie	PS-372	234
Tian, Mei	PS-301	198
Tideholm, Bo	PD-116	287
Tierney, Adam	PS-046, PS-047, PS-528	32, 32, 341

Name	Abstract No.	Page No.
Tillein, Jochen	SY-068, PS-659, PD-214	415, 444, 546
Timms, Courtney	PS-160, PS-411	87, 253
Tlili, Abdelaziz	PS-295	195
Toal, Katrina	PS-148, PS-595	81, 375
Tobey, Emily	PS-487, PS-651	322, 440
Todd, Ann	PS-485	321
Todd, N Wendell	PS-725	477
Toh, Kazuko	PD-109	284
Toki, Hideaki	PS-289	192
Toler, Tomi L.	PS-296	195
Tollin, Daniel J.	PS-104, PS-413, PD-195	60, 254, 550
Tollin, Daniel J	PS-414	255
Tollin, Daniel	PS-044	31
Tolnai, Sandra	PS-154	84
Tolosa, Vanessa	PS-246	170
Tona, Yosuke	PS-217, PS-778	116, 504
Tona, Yousuke	PS-623, PS-625	389, 389
Tong, Mingjie	PS-570	361
Tooker, Angela	PS-246, PS-478	170, 318
Torii, Hiroko	PD-158	422
Toth, Peter	PS-173	94
Towers, Emily	PD-154	420
Town, Stephen	PS-102, PS-268	59, 181
Trachte, George	PS-780	506
Traer, James	PS-156	85
Trahiotis, Constantine	PD-181	433
Tranebjaerg, Lisbeth	PS-302	198
Tranfo, Giovanna	PS-504	330
Trevino, Carolina	PS-429	261
Trivedi, Parul	PS-626	390
Troiani, Diana	PS-382	239
Tropitzsch, Anke	PS-226	160
Trotter, Mathew	PS-254	174
Trujillo, Michael	PS-007	14
Trune, Dennis R	PS-496	327
Trune, Dennis	PD-126, PS-711, PS-728, PS-783	291, 469, 478, 507
Truong, Kristy	PS-620	387
Trussell, Laurence	PS-690	459
Tscherter, Anne	PS-252	173
Tse, Chun-Yu	PS-137	76
Tsuda, Junko	PS-368	232
Tsuprun, Vladimir	PS-733	481
Tsuzaki, Minoru	PS-784	508
Tuan, Tan Chin	PS-515	336
Tuft, Bradley	PS-350, PD-078	224, 266
Turfe, Zaahir	PS-502, PS-796	513, 514
Turner, Jeremy	PS-163, PS-816	88, 524
Tye-Murray, Nancy	PS-516	336
Tziridis, Konstantin	PD-198, PD-199	542, 543
Uchiyama, Yasuo	PS-781	506
Udayashankar, Arun Palghat	PS-809	520
Udeh, Adanna	PS-061	39
Ueda, Yoshihisa	PS-632	393
Ueyama, Takehiko	PS-357	227
Ukatu, CeIsha	PS-725	477
Ulku, Cagatay H.	PS-722	475

Name	Abstract No.	Page No.
Urdang, Zachary	PS-323, PS-711	210, 469
Uribe, Phillip	PS-383	239
Usami, Shin-ichi	PS-286	191
Uversky, Vladimir	PS-356	227
Vaillencourt, Dwayne	PS-209	112
Val, Stéphanie	PS-729	479
Valiyaveetil, Manoj	SY-043	263
van de Velde, Daan	SY-052	271
Van De Water, Thomas R.	PS-386	241
Van De Water, Thomas R	PD-035, PD-081, PS-566	136, 268, 360
Van De Water, Thomas	PS-388, PS-556	242, 355
van Dijk, Pim	PS-545, PD-196	350, 539
van Netten, Sietse	PD-064	150
Van Opstal, John	PD-185	436
van Ravenswaaij-Arts, Conny	PD-012	9
van Rij, Jacolien	PS-490	324
van Tilburg, Mark	PS-419	257
Van Wanrooij, Marc	PD-185	436
Van Zanten, Gijsbert	PS-839	535
VanCamp, Guy	PS-763	497
VandeGriend, Zachary	PS-762	496
Vander Werff, Kathy	PS-053	35
Vanneste, Sven	SY-048	265
Varakina, Ksenia	PD-129	293
Varakina, Ksenya	PS-554	354
Vardi, Michael	PS-844	537
Varela-Nieto, Isabel	PD-153	420
Varghese, Lenny	PS-021	19
Varma, Sanskriti	PS-629	391
Vater, Marianne	PS-432	295
Vazquez-Lopez, Sebastian	PS-096	56
Vega, Rosario	PS-337	216
Vélez-Ortega, A. Catalina	PD-164	425
Velluti, Ricardo	PS-593, PS-833	374, 532
Ventura, Christopher	PS-205	110
Vera, Krystal	PS-582, PS-585	368, 370
Verhagen, Justus	PS-024	21
Verhey, Jesko L.	PS-511, PS-598	334, 376
Verhoeven, Sarah	PD-134	406
Verhulst, Sarah	PS-050, PS-054, PS-057	33, 35, 37
Verhulst, Steven	PS-028	23
Verma, Ishwar	PS-296	195
Verma, Rohit	PS-250	172
Vernikos, Joan	SY-023	121
Verschooten, Eric	PS-235	165
Versnel, Huib	PS-234, PS-245, PS-839	165, 170, 535
Vetter, Douglas E.	PS-393	244
Vetter, Douglas	PS-349	223
Vigeant, Michelle	PS-164	89
Vijayakumar, Sarath	PS-214	114
Vijayaraghavan, Venkat	PS-444	301
Vilchez-Madrigal, Luis D	PS-643	399
Villafuerte, Joshua	PS-001	11
Vincent, Philippe	PD-102, PS-755	280, 493
Vlahou, Eleni	PS-806	519
Volkenstein, Stefan	PD-037	137
Vollmer, Maike	PS-658	444

Name	Abstract No.	Page No.
von Gersdorff, Henrique	PS-751, PS-752, PS-756	491, 491, 493
von Trapp, Gardiner	PS-316	206
Vorasubin, Nopawan	PS-347	221
Vozzi, Diego	PD-008	7
Vrabec, Jeffrey	PS-420	257
Vu, Andrew	PD-134	406
Vuckovic, Dragana	PD-008, PS-284, PS-285	7, 189, 190
Vulovic, Vedran	PS-646	401
Wagner, Anita	PS-672	451
Wagner, Hermann	PS-098, PS-099, PS-398, PS-452, PS-453, PS-464	57, 58, 247, 305, 305, 311
Wagner, Kay-Uwe	PS-196	106
Wagner, Thomas	SY-078	439
Wahlberg, Magnus	PS-683	455
Wakana, Shigeharu	PS-289	192
Wakaoka, Takanori	PS-179	97
Wakili, Reza	PS-639	397
Waldhaus, Joerg	PS-190	102
Waldhaus, Jörg	PS-527, PS-531	341, 343
Walker, Emily	PD-079	267
Walker, Kerry	PS-786	509
Walker, Logan	PS-004, PS-013	12, 16
Wall, Susan	PS-718	473
Wallmeier, Ludwig	PS-402	249
Walsh, Edward	PS-573	363
Walters, Brandon	PD-034, PS-627	136, 390
Walton, Joseph P.	PS-008, PS-009, PS-011	14, 14, 15
Walton, Joseph	PS-002, PS-060	11, 39
Wan, Guoqiang	SY-033	129
Wan, Ying-Wooi	PS-191	103
Wang, Angela	PD-130	293
Wang, Bin	PD-165	426
Wang, Bo	PS-582, PS-585	368, 370
Wang, Guojian	PS-475	316
Wang, Jian	PD-197	540
Wang, Jianjun	PS-384, PS-718	240, 473
Wang, Jing	PS-244	169
Wang, Jue	PD-057	147
Wang, Le	PS-045, PS-088	31, 52
Wang, Lu	PS-363	230
Wang, Ningyuan	PS-607	381
Wang, Qi	PS-710	468
Wang, Qian	PD-085	270
Wang, Qiuju	PS-810	521
Wang, Rosalie	PS-550	352
Wang, Ruikang	PS-540	347
Wang, Tian	PS-193	104
Wang, Wei-min	PS-301	198
Wang, Wenying	PS-306, PS-336, PD-123, PD-124, PD-209, PD-218	201, 216, 290, 290, 553, 555
Wang, Xiao-yu	PD-101	280
wang, xiaoqin	PS-790	511
Wang, Yajun	PS-719	473
Wang, Yong	PD-045	141
Wang, Zhengmin	PD-032	135
Wangemann, Philine	PS-535	345
Wangsawihardja, Felix	PD-021, PS-232, PD-170	125, 164, 428
Warchol, Mark E.	PD-150	418

Name	Abstract No.	Page No.
Warchol, Mark	PS-305, PD-157	200, 422
Ward, Bryan K.	PS-421	258
Ward, Bryan	PS-216, PS-429	115, 261
Ward, Kristina	PD-151	419
Ward, Simon	PD-064	150
Warnecke, Athanasia	PS-619	387
Wasserman, Stephen	PS-737, PS-738	483, 484
Watabe, Isabelle	PD-159	423
Waters, Michael F	PS-467	312
Watson, Claire	PD-043, PS-290	140, 193
Watts, Melissa M.	PS-253	174
Watts, Melissa	PS-471	314
Wedemeyer, Carolina	PS-760	495
Wegner, Inge	PS-839	535
Wei, Dongguang	PD-058, PD-100	147, 279
Wei, Eric	PD-018	123
Wei, Gao	PS-374, PS-376	235, 236
Wei, Min	PS-204	110
Weigel, Solveig	PS-673	451
Weimann, Sonia	PS-106	61
Weinberger, Norman	SY-060	403
Weisz, Catherine	PS-448	303
Wells, Sara	PD-131	294
Wells, Toby	PD-017	123
Wen, Teresa	PD-201	544
Wendel, Jillian	PS-048	32
Weng, Cindy	PD-130	293
Wenstrup, Jeffrey	PS-089	53
Werner, Lynne A.	PS-785	508
Werner, Lynne	PS-314	205
Wess, Jessica	PS-669	449
West, Matthew	PS-043, PS-270	30, 182
West, Timothy	PD-220	556
Westermann, Adam	PD-091	275
Wetzel, Friederike	PS-697	462
Wheeler, Alyssa	PS-699	463
White-Schwoch, Travis	PS-315, PS-528, PS-808	205, 341, 520
White, Karessa	PS-025	21
White, Patricia	PS-195, PS-287, PD-141, PS-764	105, 191, 410, 497
Whitlon, Donna	PD-019	124
Whitman, Gregory	SY-021	120
Wichman, Carolin	PS-753	492
Wichmann, Carolin	SY-007	2
Wickens, Brandon	PS-506	331
Wickesberg, Robert	PS-240	168
Widmer, Hans Rudolf	PS-252	173
Wiegner, Armin	PS-658	444
Wiegrebe, Lutz	PS-110, PS-117, PS-402, PS-407, PS-805	63, 66, 249, 251, 518
Wiet, Gregory	PS-500	328
Wiggins, Ian	PS-433	295
Wiler, James A.	PS-136	521
Wiler, James	PS-820	526
Wilkerson, Brent	PD-058, PD-100	147, 279
Williams, Anedra	PS-420	257
Williamson, Rachel	PS-167	91
Williamson, Robert	PS-420	257

Name	Abstract No.	Page No.
Williamson, Tanika	PS-011	15
Wilson, Elizabeth	PS-535	345
Wilson, Kevin F.	PS-632	393
Wilson, Teresa	PS-568, PS-783	360, 507
Wilson, Uzma	PD-015, PS-510	122, 333
Windhagen, Henning	PS-619	387
Winkels, Jessica	PS-293	194
Winn, Matthew	PS-604, PS-662	379, 446
Winter, Ian	PS-152, PS-704	83, 466
Wirtz, Christian	PS-169	92
Wisby, Laura	PD-131	294
Wise, Andrew	PS-254, PS-478, PS-719	174, 318, 473
Wisniewski, Matthew	PS-092	54
Wit, Hero P.	PS-545	350
Wojtczak, Magdalena	PS-128, PS-153	73, 84
Wolf, Fred	SY-007	2
Wolter, Nikolaus	PS-643	399
Won, Jong Ho	PS-469, PS-661, PS-662, PS-797, PS-838	313, 445, 446, 514, 534
Wong, Aaron B	SY-007	2
Wong, Aaron	PS-753	492
Wong, Carmen	SY-066	414
Wong, Chelsea	PS-738	484
Wong, Daniel	SY-069	416
Wong, Hiu Tung	PS-632	393
Wong, Hui Tui	PD-062	149
Wong, Kristen	PD-013	10
Wong, Victor	PS-228	161
Wong, Wesley	PD-042	140
Woo, Jeong-Im	PS-035	26
Woo, Ji-Yeon	PS-020	19
Woo, Jihwan	PS-469	313
Wood, Katherine	PS-102, PS-268	59, 181
Wood, Scott	PS-212, PS-640	113, 398
Woods, Kevin	PD-089	274
Wozny, David	PD-079	267
Wright, Beverly A.	PS-109	62
Wright, Beverly A	PS-162	88
Wright, Kevin	PS-177	96
Wright, Matthew	PS-152, PS-704	83, 466
Wu, Calvin	PS-829	530
Wu, Chen-Chi	PS-557, PS-579, PS-769	355, 366, 500
Wu, Ching-Chih	PD-084	269
Wu, Hao	PS-538	346
Wu, Jingjing	PS-224	159
Wu, Nan	PS-714	471
Wu, Patricia	PS-558	356
Wu, Xudong	PD-069	153
Wu, Yan	PS-714	471
Wu, Ying	PS-548	351
Xi, Xin	PD-085	270
Xiang, Jing	PS-493	325
Xiang, Yongqing	PS-207	111
Xiao Xia Zhu;	PS-002	11
Xie, Bingbin	PS-223	159
Xie, Jing	PS-376	236
Xie, Ruili	PS-688	458

Name	Abstract No.	Page No.
Xing, Yazhi	PS-304, PS-341, PD-099	200, 218, 279
Xiong, Wei	SY-078	439
Xu-Friedman, Matthew A.	PS-680	454
Xu-Friedman, Matthew	PS-148, PS-675	81, 452
Xu, Chongfeng	PS-281	188
Xu, Helen	PS-033, PS-621	26, 388
Xu, Linjing	PS-350, PD-078	224, 266
Xu, Wenhao	PD-070	153
Xu, Yinfang	PD-054	145
Xu, Yingyue	PS-114, PS-115	65, 65
Xue, Xijun	PS-281	188
Yaeger, Daniel	PS-690	459
Yahata, Izumi	PS-348	223
Yakushin, Sergei	PS-207, SY-025	111, 122
Yamada, Takao	PD-096	277
Yamagishi, Shimpei	PS-143, PS-609	79, 382
Yamaguchi, Junji	PS-781	506
Yamaguchi, Taro	PS-778	504
Yamahara, Kohei	PD-133	405
Yamamoto, Hidefumi	PS-638	396
Yamamoto, Norio	PD-061, PD-133, PD-158, PS-778, PD-210	149, 405, 422, 504, 554
Yamanaka, Toshiaki	PS-720	474
Yamane, Hideo	PS-638	396
Yamashita, Akinori	PS-525, PS-526	340, 340
Yamashita, Daisuke	PS-015, PS-343	17, 219
Yamashita, Hiroshi	PS-036, PS-365, PS-368, PS-423, PS-427, PS-648	27, 231, 232, 259, 261, 402
Yamashita, Tetsuji	PD-001	4
Yamasoba, Tatsuya	PS-199, PD-076, PS-418, PD-109, PS-777	107, 156, 257, 284, 504
Yamazaki, Hiroshi	PS-766	498
yamazaki, Muneharu	PS-038	28
Yamoah, Ebenezer N	PD-208	553
Yamoah, Ebenezer	PS-228, PS-233, PS-306, PS-335, PS-336, PS-352, PD-121, PD-122, PD-123, PD-124, PD-209, PD-218	161, 164, 201, 215, 216, 225, 289, 290, 290, 290, 553, 555
Yan, Denise	PS-295, PS-353	195, 225
Yan, Tingting	PD-183	434
Yan, Wayne	PS-768	499
Yan, Xu-kun	PD-101	280
Yan, Xukun	PS-281	188
Yanai, Shuichi	PS-526	340
Yang, Chanhee	PS-512	334
Yang, Chunli	PS-647	401
Yang, Guan	PD-101	280
Yang, Hyejin	PS-469	313
Yang, Ju	PS-325	211
Yang, Juan-Mei	PD-060	148
Yang, Juanmei	PS-533	344
Yang, Jun	PD-045	141
Yang, Liping	PD-054	145
Yang, Mu	PS-074	45
Yang, Shi-Min	PS-360	229
Yang, Shi-Ming	PD-085, PD-101, PS-714	270, 280, 471
Yang, Shiming	PD-038, PS-582, PS-585	138, 368, 370

Name	Abstract No.	Page No.
Yang, Shuzhi	PS-297	196
Yang, Ting-Hua	PS-579	366
Yang, Wei-Yan	PD-085, PD-101	270, 280
Yang, Xiao-Yu	PD-060	148
Yang, Xiao	PD-101	280
Yang, Yu-Qin	PS-552	353
Yang, Yuqin	PS-569	361
Yanik, Susan	PS-028	23
Yao, Justin	PS-080	48
Yaron, Orly	PD-007	6
Yasin, Ifat	PS-848, PS-146	57, 80
Yassin, Lina	PS-449	303
Yates, Bill	PS-210, SY-022	113, 121
Yazdanbakhsh, Arash	PS-021	19
Ye, Keqiang	SY-038	130
Yee, Kathleen	PS-349, PS-700	223, 464
Yeo, Sang Won	PS-561	357
Yin, Pingbo	PS-446	302
Yin, Yanbo	PD-013, PS-772	10, 502
Ying, Howard	PS-425	260
Ying, Mingyao	PS-822	526
Yizhar-Barnea, Ofer	PD-007	6
Ylikoski, Jukka	PS-846	538
Yokell, Zachary	PD-191	548
Yonemura, Sigenobu	PS-394	244
Yoneya, Makoto	PS-599, PS-606, PS-615	377, 380, 385
Yoneyama, Mitsutoshi	PD-149	417
Yong, Jiawey	PS-231	163
Yoo, Myung Hoon	PS-567	360
Yoon, Yang-soo	PD-082	268
Yoshida, Atsuhiko	PD-158	422
Yoshida, Naohiro	PS-005	13
Yoshizaki, Kaichi	PS-005	13
Young, Eric	PS-076, PS-224	46, 159
Young, Hunter K	PS-322	209
Young, Hunter	PS-319, PS-320, PS-321	208, 208, 209
Young, Jesse	PS-824	527
Young, Stephen	PS-316	206
Yu, Fei	PS-475	316
Yu, Heping	PS-288	192
Yu, Jintao	PS-342, PS-362	219, 229
Yu, Ning	PD-101	280
Yu, Wei-Ming	SY-009, PD-161	2, 424
Yu, Zhou	PS-213	114
Yu, Zitian	PS-438	298
Yuan, Hu	PS-360, PD-169	229, 428
Yuan, Huijun	PS-297	196
Yuan, Yongyi	PS-281, PS-475	188, 316
Yumoto, Eiji	PD-096	277
Yurosko, Christopher	PS-827	529
Zaar, Simon	PS-364	230
Zachary, Stephen	PD-119	288
Zahorik, Pavel	PS-165	90
Zallocchi, Marisa	PS-301, PD-145	198, 412
Zee, David	PS-216, PS-425, PS-636	115, 260, 395
Zelle, Dennis	PS-112, PS-123	64, 70
Zeng, Fan-Gang	PD-082, PS-440, PS-519	268, 299, 338

Name	Abstract No.	Page No.
Zha, Dingjun	PS-539	347
Zhan, Xiping	PS-822	526
Zhang, Andy	PS-256	175
Zhang, Chao	PS-810, PS-813	521, 523
Zhang, Chaoying	PS-628, PS-630	391, 392
Zhang, Duan-Sun	PD-068	152
Zhang, Fawen	PS-488, PS-493	323, 325
Zhang, Fei	PS-018, PS-325, PS-326	18, 211, 211
Zhang, Guangyu	PD-197	540
Zhang, Hongyu	PS-823	527
Zhang, Hongzheng	PS-476	317
Zhang, Huiming	PS-463	310
Zhang, Jingyuan	PS-195, PS-287	105, 191
Zhang, Jinhui	PS-018, PS-325, PS-326	18, 211, 211
Zhang, Jinsheng	PS-821	526
Zhang, Lichun	PS-241	168
Zhang, Ming	PS-508	332
Zhang, Qian	PS-196, PS-529	106, 342
Zhang, Su-Chun	PS-626	390
Zhang, Ting	PS-203	109
Zhang, Tracy	PD-040	139
Zhang, Wujuan	PD-204	551
Zhang, Xiangming	PD-194	549
Zhang, Xiao-Dong	PS-336	216
Zhang, Xin	PS-297	196
Zhang, Yan	PD-054	145
Zhang, Yanbin	PS-353	225
Zhang, Yang	PS-790	511
Zhang, Yifan	PS-548	351
Zhang, Yu-Xuan	PD-183	434
Zhang, Yuan	PS-540	347
Zhao, Hong-Bo	PD-097, PD-120, PS-765	278, 289, 498
Zhao, Hui	PD-085, PD-101	270, 280
Zhao, Lidong	PD-038	138
Zhao, Wei	PS-141	78
Zheng, Guiliang	PS-371	233
Zheng, Hong-Wei	PS-359, PD-166	228, 426
Zheng, Hongliang	PS-371	233
Zheng, HW	PD-143	411
Zheng, Jing	PS-293, PS-327, PS-328, PS-366	194, 211, 212, 231
Zheng, Lili	PD-044	141
Zheng, Qing	PS-288	192
Zheng, Tihua	PD-045, PS-288	141, 192
Zholudeva, Lyandysha	PD-151	419
Zhong, Sheng	PS-549	351
Zhou, Binfei	PS-718	473
Zhou, Chengyong	PS-297	196
Zhou, Jun	PD-208	553
Zhou, Ning	PS-484	321
Zhou, Wu	PS-647	401
Zhou, Yi	PD-093	276
Zhou, Yide	PS-371	233
Zhu, Hong	PS-647	401
Zhu, Juhong	PS-341	218
Zhu, Xiaoxia	PS-008, PS-009, PS-011	14, 14, 15
Zhu, Xiaoyan	PD-165	426

Name	Abstract No.	Page No.
Zhu, Yan	PD-097, PD-120, PS-765	278, 289, 498
Zhu, Yu-hua	PD-101	280
Zielinski, Brandon	PD-130	293
Zilany, Muhammad	PS-077	46
Zimmerman, Benjamin	PS-137	76
Zine, Azel	PD-159	423
Zion, Danielle	PS-489	323
Zirn, Stefan	PS-470	314
Zlomke, Sarah	SY-070	416
Zosuls, Aleks	PS-541	348
Zou, Junhuang	PD-045	141
Zou, Yi-Hui	PD-085	270
Zubeldia, Jose Manuel	PD-153	420
Zuccotti, Annalisa	PS-554	354
Zuk, Nathaniel	PS-465	311
Zuniga, Geraldine	PS-429	261
Zuo, Jian	PD-001, PS-192, PD-033, PD-034, PS-291, PS-378, PS-582, PS-585, PS-627	4, 103, 135, 136, 193, 237, 368, 370, 390
Zurek, Patrick	PS-399	247
Zwolan, Teresa	PS-503	330

